UNIVERSITY OF EAST SARAJEVO

FACULTY OF MECHANICAL ENGINEERING

6th INTERNATIONAL SCIENTIFIC CONFERENCE

COMETa 2022

„Conference on Mechanical Engineering Technologies and Applications“

PROCEEDINGS

17th-19th November

East Sarajevo, RS, B&H

COMETa 2022

6th INTERNATIONAL SCIENTIFIC CONFERENCE

17th - 19th December 2022

Jahorina, B&H, Republic of Srpska

University of East Sarajevo

Faculty of Mechanical Engineering

Conference on Mechanical Engineering Technologies and Applications

Z B O R N I K R A D O V A

P R O C E E D I N G S

Istočno Sarajevo, BiH, RS
17 - 19. novembar 2022.

East Sarajevo, B&H, RS
17th – 19th November, 2022

ZBORNIK RADOVA SA 6. MEĐUNARODNE NAUČNE KONFERENCIJE
”Primijenjene tehnologije u mašinskom inženjerstvu”
COMETa2022, Istočno Sarajevo, 2022.

PROCEEDINGS OF THE 6th INTERNATIONAL SCIENTIFIC CONFERENCE
”Conference on Mechanical Engineering Technologies and Applications”
COMETa2022, East Sarajevo, 2022

Organizator:	Univerzitet u Istočnom Sarajevu Mašinski fakultet Istočno Sarajevo
Organization:	University of East Sarajevo Faculty of Mechanical Engineering East Sarajevo
Izdavač:	Univerzitet u Istočnom Sarajevu Mašinski fakultet Istočno Sarajevo
Publisher:	University of East Sarajevo Faculty of Mechanical Engineering East Sarajevo
Za izdavača: *For publisher:*	PhD Milija Kraišnik, associate professor
Urednici: *Editors:*	PhD Dušan Golubović, full professor PhD Miroslav Milutinović, associate professor PhD Saša Prodanović, associate professor
Tehnička obrada i dizajn: *Technical treatment and desing:*	PhD Aleksije Đurić, senior assistant MSc Jovana Blagojević, senior assistant MSc Milica Bošković, senior assistant Krsto Batinić, assistant
Izdanje: *Printing:*	Prvo 1st
Register: *Register:*	ISBN 978-99976-947-6-8 COBISS.RS-ID 137162497

REVIEWERS

PhD Dušan Golubović, FME UES (B&H)
PhD Dušan Gordić, FE Kragujevac (Serbia)
PhD Ljubiša Dubonjić, FMCE Kraljevo (Serbia)
PhD Mirko Blagojević, FE Kragujevac (Serbia)
PhD Miroslav Stanojević, FME Belgrade (Serbia)
PhD Adisa Vučina, FMEC Mostar (B&H)
PhD Aleksandar Jovović , FME Belgrade (Serbia)
PhD Aleksandar Košarac , FME UES (B&H)
PhD Aleksandar Živković, FTS Novi Sad (Serbia)
PhD Biljana Marković, FME UES (B&H)
PhD Bogdan Marić, FME UES (B&H)
PhD Branimir Krstić , University of Difence, Military Academy (Serbia)
PhD Damjan Klobčar , FME Ljubljana (Slovenia)
PhD Darko Bajić , FME Podgorica (MNE)
PhD Dejan Jeremić , FME UES (B&H)
PhD Dragan Milčić, FME Nis (Serbia)
PhD Dragan Pršić, FMCE Kraljevo (Serbia)
PhD Goran Orašanin, FME UES (B&H)
PhD Jasmina Pekez, TF “Mihajlo Pupin” Zrenjanin (Serbia)
PhD Jelena Jovanović, FME Podgorica (MNE)
PhD Lozica Ivanović, FE Kragujevac (Serbia)
PhD Milan Banić , FME Niš (Serbia)
PhD Milan Rackov, FTS Novi Sad (Serbia)
PhD Milan Tica, FME Banja Luka (B&H)
PhD Milan Zeljković, FTS Novi Sad (Serbia)
PhD Milija Kraišnik , FME UES (B&H)
PhD Milomir Šoja, FEE UES (B&H)
PhD Miloš Milovančević, FME Nis (Serbia)
PhD Miodrag Žigić, FTS Novi Sad (Serbia)
PhD Mirko Dobrnjac , FME Banja Luka (B&H)
PhD Miroslav Milutinović, FME UES (B&H)
PhD Mladen Josijević, FE Kragujevac (Serbia)
PhD Mladen Tomić, FTS Novi Sad (Serbia)
PhD Mladomir Milutinović, FTS Novi Sad (Serbia)
PhD Nebojša Radić, FME UES (B&H)
PhD Nenad Grahovac , FTS Novi Sad (Serbia)
PhD Nikola Tanasić, FME Belgrade (Serbia)
PhD Nikola Vučetić, FME UES (B&H)
PhD Ranka Gojković , FME UES (B&H)
PhD Ranko Antunović , FME UES (B&H)
PhD Saša Prodanović, FME UES (B&H)
PhD Saša Živanović, FME Belgrade (Serbia)
PhD Silva Lozančić , Faculty of Civil Engineering Osijek (Croatia)
PhD Slaviša Moljević, FME UES (B&H)
PhD Slobodan Lubura, FEE UES (B&H)
PhD Slobodan Tabaković, FTS Novi Sad (Serbia)
PhD Snežana Nestić, FE Kragujevac (Serbia)
PhD Spasoje Trifković, FME UES (B&H)
PhD Srđan Vasković, FME UES (B&H)
PhD Stojan Simić, FME UES (B&H)
PhD Uroš Karadžić , FME Podgorica (MNE)

PhD Vladimir Milovanović, FE Kragujevac (Serbia)
PhD Vladimir Stojanović, FMCE Kraljevo (Serbia)
PhD Vlado Medaković, FME UES (B&H)
PhD Zdravko Pandur, FFWT UZ (Croatia)

INTERNATIONAL SCIENTIFIC COMMITTEE

PhD Dušan Golubović, FME UES (B&H) – president
PhD Adisa Vučina, FMEC Mostar (B&H)
PhD Aleksandar Aleksić, FE Kragujevac (Serbia)
PhD Aleksandar Jović, FME Belgrade (Serbia)
PhD Aleksandar Košarac, FME UES (B&H)
PhD Balasaheb M. Patre, SGGS IET (India)
PhD Biljana Marković, FME UES (B&H)
PhD Bogdan Marić, FME UES (B&H)
PhD Borut Kosec, NTF Ljubljana, (Slovenia)
PhD Božidar Rosić, FME Belgrade (Serbia)
PhD Branimir Krstić, Military academy, University of Defence in Belgrade (Serbia)
PhD Branko Vučijak, FME Sarajevo (B&H)
PhD Bratislav Blagojević, FME Niš (Serbia)
PhD Damjan Klobčar, FME Ljubljana (Slovenia)
PhD Danijela Tadić, FE Kragujevac (Serbia)
PhD Darko Knežević, FME Banja Luka (B&H)
PhD Dejan Jeremić, FME UES (B&H)
PhD Dragan Milčić, FME Niš (Serbia)
PhD Dragan Spasić, FTS Novi Sad (Serbia)
PhD George Nenes, UOWM (Greece)
PhD Goran Janevski, FME Niš (Serbia)
PhD Goran Orašanin, FME UES (B&H)
PhD Goran Putnik, University of Minho, (Portugal)
PhD Goran Šimunović, MEFSB (Croatia)
PhD Indiran Thirunavukkarasu, Manipal Institute of Technology, Indija
PhD Isak Karabegović, FTS Bihać (B&H)
PhD Ivan Samardžić, MEFSB (Croatia)
PhD Izet Bjelonja, FME Sarajevo (B&H)
PhD Jozsef Nyers, The Obuda University Budapest (Hungary)
PhD Kyros Yakinthos, AUTH, (Greece)
PhD Lozica Ivanović, FE Kragujevac (Serbia)
PhD Ljubodrag Tanović, FME Belgrade (Serbia)
PhD Ljubomir Miladinović, FME Belgrade (Serbia)
PhD Mathias Liewald, IFU, (Germany)
PhD Milan Rackov, FTS Novi Sad (Serbia)
PhD Milan Rakita, Purdue Univerzitet, SAD
PhD Milan Tica, FME Banja Luka (B&H)
PhD Milan Zeljković, FTS Novi Sad (Serbia)
PhD Mile Savković, FMCE Kraljevo (Serbia)
PhD Milorad Milovančević, FME Belgrade (Serbia)
PhD Milosav Ognjanović, FME Belgrade (Serbia)
PhD Mirko Blagojević, FE Kragujevac (Serbia)
PhD Mirko Dobrnjac, FME Banja Luka (B&H)
PhD Mirko Ficko,UM FPME, (Slovenia)
PhD Miroslav Stanojević, FME Belgrade (Serbia)

PhD Miroslav Živković, FE Kragujevac (Serbia)
PhD Mladen Tomić, FTS Novi Sad (Serbia)
PhD Mladomir Milutinović, FTS Novi Sad (Serbia)
PhD Nebojša Lukić, FE Kragujevac (Serbia)
PhD Nebojša Radić, FME UES (B&H)
PhD Nenad Pavlović, FME Niš (Serbia)
PhD Nikola Vučetić, FME UES (B&H)
PhD Nina Anđelić, FME Belgrade (Serbia)
PhD Novak Nedić, FMCE Kraljevo (Serbia)
PhD Obrad Spaić, UES PFM, (B&H)
PhD Pavel Kovač, FTS Novi Sad (Serbia)
PhD Ranislav Bulatović, FME Podgorica (MNE)
PhD Radivoje Mitrović, FME Belgrade (Serbia)
PhD Radoslav Tomović, FME Podgorica (MNE)
PhD Radovan Radovanović, The Academy of criminalistic and police studies Belgrade (Serbia)
PhD Ranko Antunović, FME UES (B&H)
PhD Risto Ciconkov, FME Skopje (Macedonia)
PhD Saša Ranđelović, FME Niš (Serbia)
PhD Sergej Alexandrov, Institute for Problems in Mechanics (Russia)
PhD Siniša Kuzmanović, FTS Novi Sad (Serbia)
PhD Slaviša Moljević, FME UES (B&H)
PhD Slavko Arsovski, FE Kragujevac (Serbia)
PhD Snežana Nestić, FE Kragujevac (Serbia)
PhD Spasoje Trifković, FME UES (B&H)
PhD Srđan Vasković, FME UES (B&H)
PhD Sreten Perić, Military academy, University of Defence in Belgrade (Serbia)
PhD Stanislav Karapetrović, University of Alberta (Canada)
PhD Stevan Stankovski, FTS Novi Sad (Serbia)
PhD Stojan Simić, FME UES (B&H)
PhD Strain Posavljak, FME Banja Luka (B&H)
PhD Velimir Stefanović, FME Niš (Serbia)
PhD Vencislav Grabulov, Institut IMS, Srbija
PhD Vladimir Popović, FME Belgrade (Serbia)
PhD Vlado Medaković, FME UES (B&H)
PhD Vojislav Miltenović, FME Niš (Serbia)
PhD Zdravko Krivokapić, FME Podgorica (MNE)
PhD Zorana Tanasić, FME Banja Luka (B&H)

ORGANIZING COMMITTEE

PhD Milija Kraišnik, FME UES – president
PhD Miroslav Milutinović, FME UES
PhD Saša Prodanović, FME UES
PhD Nikola Vučetić, FME UES
PhD Davor Milić, FME UES
PhD Aleksije Đurić, FME UES
Krsto Batinić, FME UES - Technical Secretary
Milica Bošković, ma, FME UES - Technical Secretary
Stanišić Vera – Secretary

GENERAL SPONSOR

**Ministry of Scientific and Technological Development,
Higher Education and Information Society
Republic of Srpska**

SPONSORS

Veritas
Automotive d.o.o.

TRB MILKUS

PMP
INDUSTRIES
PMP JELŠINGRAD - FMG A.D. Gradiška

САРАЈЕВО-ГАС А.Д.

РУДНИК И
ТЕРМОЕЛЕКТРАНА
ГАЦКО

РУДНИК И ТЕРМОЕЛЕКТРАНА УГЉЕВИК

TERMOELEKTRO

GRIJANJEINVEST

Ella Textile
d.o.o. Gradiška, Nova Topola

KOLEKTOR

The conference has been supported by:

International Federation for the Promotion of Mechanism and Machine Science

Association for Design, Elements and Constructions

Union of Mechanical Engineers and Technicians of Republic of Srpska

Countries from which conference participants come

PREFACE

The economic power of a society can be expressed by different indicators. However, it is certain that the competitiveness of the economy is one of the most important. In this sense, it is necessary for industrial production to follow modern development trends, which are based on current scientific achievements. Only a holistic approach in the application of knowledge in various engineering fields, and especially in the field of mechanical engineering, is a guarantee of economic progress, which enables long-term stability and prosperity of each country. Precisely for these reasons, the Faculty of Mechanical Engineering of the University of East Sarajevo organized the 1st International Scientific Conference COMETa in 2012, and this year is its 6th edition.

The main goal of the conference is to strengthen cooperation with the academic community, scientific-research institutions and, above all, with business entities. Conference COMETa 2022 is an opportunity for all participants to offer guidelines and create a better environment for more intensive industrial development through the exchange of knowledge and experience. That is going to have impact to increasing the competitiveness of national economic entities on the foreign market. The participation of a significant number of domestic and foreign scientists and researchers strengthens our conviction that in the near future we will be able to overcome challenges that are present in the technical-technological development of an advanced society in the 21st century, mainly through the generation of new ideas and the introducing of modern approaches to solving complex tasks in the field of mechanical engineering. In this sense, all your proposals and suggestions are more than welcome and will be carefully considered by the Scientific and Organizing Committee in order to improve the organization of the next conferences. Acknowledging the importance of the wide field of mechanical engineering for the overall industrial development of society, the work of the conference will take place through 7 sections, including the Student section. The program is focused on the following thematic areas:

- Manufacturing technologies and advanced materials,
- Applied mechanics and mechatronics,
- Machine design, simulation and modeling,
- Product development and mechanical systems,
- Energy and thermotechnic,
- Renewable energy and environmental protection,
- Maintenance and technical diagnostics,
- Quality, management and organization.

At this year's conference COMETa 2022, 105 papers including 4 plenary lectures will be published in the Proceedings.

We are specially looking forward that conference registered a record number of participants from abroad. Namely, 300 authors come from 25 countries. This is certainly the result of strenuous activities that were aimed at raising the international reputation and visibility of the conference in the regional, but also in the wider academic and scientific research space, which will be one of the primary goals in the future.

On behalf of the Organizing Committee of the conference COMETa 2022, we express our great gratitude to all the authors of the papers, reviewers, universities, faculties, business entities, national and international institutions and organizations that supported the conference. Without their help the organization and work of the conference would certainly not be at the level that its status deserves.

East Sarajevo, November 14th, 2022.

President of the Scientific Committee

PhD Dušan Golubović,
Full Professor

President of the Organizing Committee

PhD Milija Kraišnik,
Associate Professor

C O N T E N T

PLENARY LECTURES

MANUFACTURING TECHNOLOGIES AND ADVANCED MATERIALS

MACHINE DESIGN, SIMULATION AND MODELING

PRODUCT DEVELOPMENT AND MECHANICAL SYSTEMS

ENERGY AND THERMOTECHNIC

PLENARY LECTURES

COMETa 2022
6th INTERNATIONAL SCIENTIFIC CONFERENCE
17th - 19th November 2022
Jahorina, B&H, Republic of Srpska
University of East Sarajevo
Faculty of Mechanical Engineering
Conference on Mechanical Engineering Technologies and Applications

MICROSTRUCTURE-BASED ENGINEERING OF SOFT BIOLOGICAL MATERIALS

Alkiviadis Tsamis[1,2]

Abstract: Aortic disease (AoD) is a leading cause of mortality in developed countries. Two of the most common forms of AoD are aneurysm (widening) and dissection (tear in inner wall). Aneurysm and dissection often associate with bicuspid aortic valve (BAV) instead of the normal tricuspid aortic valve, and BAV aneurysms of ascending thoracic aorta have the tendency to bulge asymmetrically towards the greater curvature of aorta. Multiphoton microscopy can help us image collagen and elastin fibres, which are considered as main load-bearing constituents of the aortic wall, in order to investigate potential role of fibre microstructure in ascending thoracic aortic aneurysm or dissection. Regional differences in fibre microstructure may be driven by distinct mechanisms of vascular remodelling, and, combined with mechanical tests, could improve our understanding of the biomechanical mechanisms of aortic aneurysm and dissection potential. Should we wish to investigate the effect of microstructure in soft tissue formation and organ development, we would have to consider a rapidly growing process. In that process, the cells are the main load-bearing components, which cooperate to produce tissue-level forces that shape tissue formation. Our understanding of this phenomenon, called mechanotransduction, has advanced significantly over the past years, to the point where it is now clear that nearly every biological process is modulated by how these forces are decoded intracellularly. It is therefore important to create our own fluorescently-labeled matrix that could integrate into the tissue and enable tracking of these forces in-vivo. A new 3D optical nanomechanical biosensor (NMBS) based on fluorescent fibronectin fibres was developed based on integrated photolithography and micro-contact printing technology. NMBS was successfully validated under uniaxial tensile test of biologically relevant materials for microscopic vs. macroscopic mechanical strains. In the future, biomimetic 3D scaffolds could be fabricated by assembly of 2D fibre constructs based on the NMBS technology, in order to analyse the effect of selected set of load-bearing

[1] Asst. Prof. Dr. Alkiviadis Tsamis, Department of Mechanical Engineering, University of Western Macedonia, Kozani, Greece, atsamis@uowm.gr

[2] Hon. Lecturer Dr. Alkiviadis Tsamis, School of Engineering, University of Leicester, Leicester, United Kingdom, at441@leicester.ac.uk

microstructural components on both mechanical and functional response of soft biological materials.

Key words: Aortic aneurysm, Biosensor, Cell, Fibre microstructure, Soft tissue formation

1 AORTIC DISEASE: A LEADING CAUSE OF MORTALITY

Aortic disease is currently a large health concern because it is both common and can lead to fatal outcomes [1]. These consist of a variety of conditions targeting the aorta, with the most common forms being aneurysm [2, 3], dissection [4, 5], occlusion owing to atherosclerosis [6, 7] and a general stiffening of the normally elastic aorta that is thought to be a natural consequence of ageing [8-12]. There are many co-morbid abnormalities that can lead to or be associated with one or more of these conditions, including hypertension [13-15], genetic mutations (such as Marfan syndrome [16, 17]), developmental defects (such as bicuspid aortic valve (BAV) [18-20]), connective tissue disorders (such as Ehler-Danlos disorder [21, 22], scleroderma [23, 24], osteogenesis imperfecta [25, 26], polycystic kidney disease [27, 28] and Turner syndrome [29, 30]), as well as injury. All aortic diseases are associated with microstructural changes, either to the content or architecture of the connective fibres elastin or collagen.

2 ANEURYSM AND DISSECTION OFTEN ASSOCIATE WITH BICUSPID AORTIC VALVE

Bicuspid aortic valve is the most common congenital heart defect, arising in 1% to 2% of the general population, and along with predisposing to valvular dysfunction the defect is frequently associated with the development of ascending aortopathy and aneurysm [18-20, 31-33]. Patients with BAV uniformly have a large-diameter ascending thoracic aorta (ATA), indicative of the aortopathy, compared with age- and sex-matched controls (CTRL) [34]. Consequently, patients with BAV are at significant risk of aortic dissection [33, 35-37]. There is a bimodal age distribution among ascending thoracic aortic aneurysms (ATAAs), with patients with BAV presenting an average of 10 to 15 years earlier than the degenerative ATAAs that form in patients with tricuspid aortic valve (TAV) [32]. Furthermore, many BAV-associated ATAAs tend to dilate asymmetrically toward the greater curvature of the ascending aorta (extending from the right and noncoronary sinuses) compared with a more symmetric dilatation pattern that occurs in patients with TAV [38-41].

3 COLLAGEN AND ELASTIN FIBRES: MAIN LOAD-BEARING CONSTITUENTS OF THE AORTIC WALL

The aorta, the blood vessel responsible for delivering blood from the heart to the systemic circulation, normally possesses a high degree of elasticity, which aids in the propulsion of blood downstream to the systemic vasculature [1, 42], and a microstructure that supports this function [43, 44]. It is the connective fibres within this microstructure, elastin and collagen, which impart the elastic properties and strength of the aorta, respectively. Often, it is alteration of the quantity and/or architecture of these fibres that leads to the mechanical, and hence functional, changes associated with aortic disease [10, 15, 45-53]. For example, structural alterations in the walls of large arteries with progressing age cause a decrease in the total arterial compliance [10, 11,

54-57], which in turn leads to both a decreased distal blood flow and an increase in aortic pulse pressure [42]. This increased pulse pressure has been shown to be the strongest predictor of cardiovascular mortality, because it increases the mechanical load on the left ventricle [58].

4 MULTIPHOTON MICROSCOPY IMAGING ANALYSIS

Use of multi-photon microscopy [59-61] allows for imaging of collagen and elastin fibres in fresh tissue specimens without the need for pre-processing (staining) the tissue. The technique is based on wavelength analysis of the excitation light coming from auto-fluorescence of elastin fibres (wavelength: 525 ± 25 nm), and birefringence and periodicity in the molecule of collagen (2^{nd} harmonic, wavelength: 400 ± 50 nm). Multi-photon microscopy can image deep (>100μm), because long wavelength photons penetrate better into biological specimens. The excitation is limited to the focal plane and for this reason there is no need for pinhole. Therefore, it is not a light rejection technique and allows more emitted photons to be detected. On the contrary, one-photon microscopy does not image deep (<100 μm) because it uses short wavelength light. Also, one-photon microscopy is a light rejection technique because the light must go back through a pinhole.

Imaging could be performed using an Olympus multiphoton microscope (Model FV10, Olympus, Center Valley, Pa) to visualize elastin and collagen fibre architecture in 18 locations of the ATAA wall, namely 3 radial (RAD) locations and three circumferential (Θ) regions in both longitudinal-radial (Z-RAD) and Θ-RAD planes for all specimens [31, 60, 61]. During imaging, the Z-RAD or Θ-RAD planes of the samples could face the microscope lens to allow for visualization of RAD-oriented collagen and elastin fibres. Elastin and collagen fibres could be automatically detected according to intrinsic fluorescence and 2^{nd} harmonic generation, respectively. After acquiring images with multiphoton microscopy, the percent of fibres (elastin and collagen) oriented in the RAD direction, the average amplitude of angular undulation and the orientation index of the fibres could be quantified using an image-based analysis tool. A custom automated image-based analysis tool developed in MATLAB (MathWorks, Inc, Natick, Mass) based on image background removal [62] and on fibre detection algorithm [63] could be used to process the multiphoton images, in order to reveal the collagen and elastin fibre architecture in both Z-RAD and Θ-RAD planes of BAV-ATAA and TAV-ATAA in 3 RAD-locations within the aortic wall thickness.

5 REGIONAL DIFFERENCES IN FIBRE MICROSTRUCTURE: ASSOCIATIONS WITH BIOMECHANICAL MECHANISMS OF AORTIC ANEURYSM AND DISSECTION POTENTIAL

Reduced undulation of fibres about Θ-axis in inner wall layers of BAV-ATAA relative to TAV-ATAA may compromise the ability of inner wall layers of BAV-ATAA to resist to RAD loads and predispose to inner wall micro-tears in BAV-ATAA [64]. Increased undulation of elastin fibres about the Θ-axis and increased amount of RAD-oriented elastin and collagen fibre components in the outer wall layers of BAV-ATAA compared to non-aneurysmal CTRL-ATA is compatible with increased tensile stretch at the inflection point of Θ-strips of outer wall half of BAV-ATAA when compared with CTRL-ATA, since more undulated fibres permit increased stretch before all fibres become engaged (straightened) [10]. It can be suggested that fibre micro-architecture differs in the various tissue planes among patients grouped by valve phenotype, and could explain observed differences in biomechanical properties in BAV-ATAA vs. TAV-

ATAA [65, 66]. The discrepancy in fibre micro-architecture with fibres in inner layers being more stretched and with disrupted RAD-oriented components than fibres in outer layers may contribute to distinct mechanisms mediating development, progression and vascular remodeling associated with aneurysms arising in TAV vs. BAV patients.

ATAAs arising in patients with BAV versus TAV involve distinct mechanisms of extracellular matrix (ECM) remodeling indicative of differing vessel wall strength and dissection potential that are likely due to microarchitectural changes among collagen and elastin fibres [31]. Distinctions noted in ECM microarchitecture may form the basis of differing aneurysm geometries and aortic wall integrities in ATAAs arising in these two different valve morphologies. The finding of less RAD-oriented elastin fibres in region N (with respect to noncoronary sinus) and region R (with respect to right coronary sinus) of BAV-ATAA may directly correlate with earlier finding of decreased delamination strength (an ex-vivo measure of aortic dissection potential) in BAV-ATAA compared with TAV-ATAA [65], and may explain the asymmetric dilatation pattern commonly seen in patients with BAV-ATAA compared with those with TAV-ATAA. The region-specific architectural profile in BAV-ATAA may be driven by distinct mechanisms of vascular remodeling that are a consequence of valve morphotype-specific hemodynamic stresses/forces (e.g., blood flow-induced shear stress acting on the luminal surface) and contribute to an asymmetric dilatation pattern and/or convey a different regional propensity for delamination. When combined with additional region-specific (across the wall circumference and thickness) delamination or tensile biomechanical testing, our understanding of the biomechanical mechanisms of aortic aneurysm and dissection potential could be improved. There is a hope that a patient-specific simulation tool could be developed for enabling the prediction of aortic remodeling and disease progression. Such a tool could improve risk assessment for aortic catastrophe and direct therapy for patients with ATAA.

Decrease of elastin percentage distal to the suprarenal aorta within the arterial wall may suggest that beyond the suprarenal aorta, which is an arterial region with different predisposition to aneurysmal disease, arterial elastance is reduced [42, 67]. Future analysis could extend employing both second harmonic generation imaging analysis and uni-axial extension tests [64, 65] to investigate associations between the nondiseased/healthy aortic tissue microstructure and aortic tissue biomechanical properties, respectively [68]. This could provide insight into structure-associated biomechanical mechanisms of aortic aneurysm potential, and whether anatomic location influences arterial function as well as the effects of transluminal pressures and mechanical load on arterial wall connective tissue proteins. Future mechanical test information about the compliance of the aortic wall would also help draw conclusions about effect of mechanical properties on dedicated endovascular devices.

6 TRACKING CELL-GENERATED MICROSCOPIC STRAINS

Cell-generated mechanical forces transmitted via cell-cell and cell-ECM interactions are integral to a wide range of processes, from cell migration [69-74] and contractility [75] to tissue morphogenesis [76-82] and regeneration [83-86]. Our understanding of this phenomenon, called mechanotransduction, has advanced significantly over the past years, to the point where it is now clear that nearly every biological process is modulated by how these forces are decoded intracellularly. In most cases the underlying mechanobiology is not well understood, in part because direct measurement of forces in living tissue during dynamic processes has proved difficult, as well as forces generated on the cellular scale combine to drive macroscale tissue formation [87, 88]. A comprehensive approach to tissue engineering would entail

a combination of advanced in-silico and ex-vivo mechanotransduction assays to identify the magnitude of loads and strains that cells, or cell-seeded scaffolds are exposed to in a clinical scenario. This would facilitate the evaluation of bio-realistic loads in a bioreactor/3D cell culture, as to their effect on proliferation and differentiation. How these loads are transduced into cellular structures could be evaluated either through advanced numerical techniques or nanomechanical biosensors. There is a need to develop both in-vitro and in-vivo measurement tool, for cellular and tissue-level mechanical forces in 3D, that can span multiple length scales to enable force tracking, while minimally perturbing the biology of interest.

A fibronectin (FN) based nanomechanical biosensor (NMBS) can be developed to provide the capability to quantify the location, direction, and magnitude of strain on a 3D surface over time, from subcellular to tissue length scales [83]. The NMBS can be fabricated using an adaptation of surface-initiated assembly (SIA), which is a technique to microcontact print ECM proteins onto a thermo-responsive poly(N-isopropylacrylamide) (PIPAAm) surface and then release the ECM proteins (e.g., FN, laminin, collagen type IV, and fibrinogen) as an assembled, insoluble network with defined geometry [89]. Briefly, the NMBS can be designed in CAD (for example line width and spacing of 2 μm × 2 μm, 20 μm × 20 μm, 10 μm × 100 μm, and 100 μm × 100 μm to measure strain from the subcellular to multicellular length scales), transferred to a transparency photomask, and used to photolithographically pattern a photoresist-coated glass wafer. A polydimethylsiloxane (PDMS) elastomer stamp can be formed by casting on the patterned wafer and then inked with fluorescently-labeled FN. The PDMS stamp can then be used to microcontact print the FN onto a PIPAAm-coated glass coverslip and then removed to leave the NMBS on the PIPAAm surface. The NMBS can then be transferred to another surface, including tensile test strips, by adding room temperature water to dissolve the PIPAAm. The thickness of the dry NMBS is in the order of ~4 nm.

To validate and benchmark the NMBS as a microscopic strain sensor, controlled mechanical testing can be performed while visualizing microscopic deformations through fluorescence microscopy [83]. For example, a PDMS “dog bone” shaped tensile test strip can be designed and molded and NMBS with 10 μm wide lines and 100 μm spacing can be transferred across the gauge length. The test strip can then be mounted in a custom-designed uniaxial testing system that enables simultaneous microscopic imaging of the NMBS and macroscopic imaging of the PDMS. Elongation of the PDMS test strip can be measured by an increased distance between fiducial marks (small black dots on the PDMS in the gauge length). Time-lapse fluorescence imaging of the NMBS can provide tracking of both tensile and compressive strain at the microscopic scale based on mesh deformation. Quantification of strain can be performed using custom MATLAB software by converting the NMBS fluorescence image into global map of tensile and compressive strains with respect to undeformed reference length of NMBS mesh segments. To validate the accuracy of the NMBS strain mapping during uniaxial tensile testing, the average tensile and compressive strain observed via fluorescence microscopy can be correlated to the measured macroscopic distances between fiducial marks on the surface of the PDMS test strip. The overall width and thickness of the test strip can also be measured throughout tensile testing. Agreement between microscopic and macroscopic strains can establish that the NMBS accurately tracks strain of PDMS and indicate that PDMS behaves as an isotropic incompressible material in agreement with literature [90]. The validation experiment can be repeated by using the NMBS to track strain of a fibrin tensile test strip as a model of a biologically-derived compressible hydrogel. Agreement between microscopic and macroscopic strains can establish that

the NMBS accurately tracks strain of fibrin and indicate that fibrin behaves as an anisotropic compressible material in agreement with literature [91].

In the future, biomimetic 3D scaffolds could be fabricated by assembly of 2D fibre constructs based on the NMBS technology, in order to analyse the effect of selected set of load-bearing microstructural components on both mechanical and functional response of soft biological materials. NMBS tracking with more sophisticated point-cloud analysis would allow for a more detailed analysis of the strains and a better understanding of the stresses driving processes such as developmental morphogenesis and disease progression [83].

REFERENCES

[1] Tsamis, A., Krawiec, J.T., Vorp, D.A. (2013). Elastin and collagen fibre microstructure of the human aorta in ageing and disease: a review. *Journal of The Royal Society Interface*, 10/83, p.p. 20121004(1-22).

[2] Takigawa, M., Yoshimuta, T., Akutsu, K., Takeshita, S., et al. (2012). Prevalence and predictors of coexistent silent atherosclerotic cardiovascular disease in patients with abdominal aortic aneurysm without previous symptomatic cardiovascular diseases. *Angiology*, 63/5, p.p. 380-385.

[3] Jondeau, G., Boileau, C. (2012). Genetics of thoracic aortic aneurysms. *Current Atherosclerosis Reports*, 14/3, p.p. 219-226.

[4] Matsushita, A., Manabe, S., Tabata, M., Fukui, T., et al. (2012). Efficacy and pitfalls of transapical cannulation for the repair of acute type A aortic dissection. *The Annals of Thoracic Surgery*, 93/6, p.p. 1905-1909.

[5] Lu, S., Sun, X., Hong, T., Yang, S., et al. (2012). Bilateral versus unilateral antegrade cerebral perfusion in arch reconstruction for aortic dissection. *The Annals of Thoracic Surgery*, 93/6, p.p. 1917-1920.

[6] Momiyama, Y., Ohmori, R., Fayad, Z.A., Tanaka, N., et al. (2012). The LDL-cholesterol to HDL-cholesterol ratio and the severity of coronary and aortic atherosclerosis. *Atherosclerosis*, 222/2, p.p. 577-580.

[7] Momiyama, Y., Ohmori, R., Fayad, Z.A., Tanaka, N., et al. (2012). Associations between serum lipoprotein(a) levels and the severity of coronary and aortic atherosclerosis. *Atherosclerosis*, 222/1, p.p. 241-244.

[8] Fleenor, B.S., Sindler, A.L., Eng, J.S., Nair, D.P., et al. (2012). Sodium nitrite de-stiffening of large elastic arteries with aging: role of normalization of advanced glycation end-products. *Experimental Gerontology*, 47/8, p.p. 588-594.

[9] Sekikawa, A., Shin, C., Curb, J.D., Barinas-Mitchell, E., et al. (2012). Aortic stiffness and calcification in men in a population-based international study. *Atherosclerosis*, 222/2, p.p. 473-477.

[10] Tsamis, A., Rachev, A., Stergiopulos, N. (2011). A constituent-based model of age-related changes in conduit arteries. *American Journal of Physiology - Heart and Circulatory Physiology*, 301/4, p.p. H1286-1301.

[11] Zulliger, M.A., Stergiopulos, N. (2007). Structural strain energy function applied to the ageing of the human aorta. *Journal of Biomechanics*, 40/14, p.p. 3061-3069.

[12] Greenwald, S.E. (2007). Ageing of the conduit arteries. *Journal of Pathology*, 211/2, p.p. 157-172.

[13] Lionakis, N., Mendrinos, D., Sanidas, E., Favatas, G., et al. (2012). Hypertension in the elderly. *World Journal of Cardiology*, 4/5, p.p. 135-147.

[14] Palatini, P. (2012). Cardiovascular effects of exercise in young hypertensives. *Intenational Journal of Sports Medicine*, 33/9, p.p. 683-690.

[15] Tsamis, A., Stergiopulos, N., Rachev, A. (2009). A structure-based model of arterial remodeling in response to sustained hypertension*. Journal of Biomechanical Engineering*, 131/10, p.p. 101004(1-8).
[16] Lavall, D., Schafers, H.J., Bohm, M., Laufs, U. (2012). Aneurysms of the ascending aorta*. Deutsches Arzteblatt International*, 109/13, p.p. 227-233.
[17] Jondeau, G., Michel, J.B., Boileau, C. (2011). The translational science of Marfan syndrome*. Heart*, 97/15, p.p. 1206-1214.
[18] Bilen, E., Akcay, M., Bayram, N.A., Kocak, U., et al. (2012). Aortic elastic properties and left ventricular diastolic function in patients with isolated bicuspid aortic valve*. Journal of Heart Valve Disease*, 21/2, p.p. 189-194.
[19] Ikonomidis, J.S., Ruddy, J.M., Benton, S.M., Jr., Arroyo, J., et al. (2012). Aortic dilatation with bicuspid aortic valves: cusp fusion correlates to matrix metalloproteinases and inhibitors*. Annals of Thoracic Surgery*, 93/2, p.p. 457-463.
[20] Plaisance, B.R., Winkler, M.A., Attili, A.K., Sorrell, V.L. (2012). Congenital bicuspid aortic valve first presenting as an aortic aneurysm*. American Journal of Medicine*, 125/4, p.p. e5-7.
[21] Hamaoui, K., Riaz, A., Hay, A., Botha, A. (2012). Massive spontaneous diaphragmatic rupture in Ehlers-Danlos syndrome*. Annals of the Royal College of Surgeons of England*, 94/1, p.p. e5-7.
[22] Chu, L.C., Johnson, P.T., Dietz, H.C., Brooke, B.S., et al. (2012). Vascular complications of Ehlers-Danlos syndrome: CT findings*. American Journal of Roentgenology*, 198/2, p.p. 482-487.
[23] Leask, A. (2012). Emerging targets for the treatment of scleroderma*. Expert Opinion on Emerging Drugs*, 17/2, p.p. 173-179.
[24] Attaran, R.R., Guarraia, D. (2007). Ascending aortic aneurysm in a man with scleroderma*. Clinical Rheumatology*, 26/6, p.p. 1027-1028.
[25] van Dijk, F.S., Cobben, J.M., Kariminejad, A., Maugeri, A., et al. (2011). Osteogenesis imperfecta: a review with clinical examples*. Molecular Syndromology*, 2/1, p.p. 1-20.
[26] McNeeley, M.F., Dontchos, B.N., Laflamme, M.A., Hubka, M., et al. (2012). Aortic dissection in osteogenesis imperfecta: case report and review of the literature*. Emergency Radiology*, 19/6, p.p. 553-556.
[27] Fukunaga, N., Yuzaki, M., Nasu, M., Okada, Y. (2012). Dissecting aneurysm in a patient with autosomal dominant polycystic kidney disease*. Annals of Thoracic and Cardiovascular Surgery*, 18/4, p.p. 375-378.
[28] Kim, J., Kim, S.M., Lee, S.Y., Lee, H.C., et al. (2012). A case of severe aortic valve regurgitation caused by an ascending aortic aneurysm in a young patient with autosomal dominant polycystic kidney disease and normal renal function*. Korean Circulation Journal*, 42/2, p.p. 136-139.
[29] Mortensen, K.H., Hjerrild, B.E., Stochholm, K., Andersen, N.H., et al. (2011). Dilation of the ascending aorta in Turner syndrome - a prospective cardiovascular magnetic resonance study*. Journal of Cardiovascular Magnetic Resonance*, 13/1, p.p. 24(1-9).
[30] Maureira, J.P., Vanhuyse, F., Lekehal, M., Hubert, T., et al. (2012). Failure of Marfan anatomic criteria to predict risk of aortic dissection in Turner syndrome: necessity of specific adjusted risk thresholds*. Interactive Cardiovascular and Thoracic Surgery*, 14/5, p.p. 610-614.
[31] Tsamis, A., Phillippi, J.A., Koch, R.G., Chan, P.G., et al. (2016). Extracellular matrix fiber microarchitecture is region-specific in bicuspid aortic valve-associated ascending aortopathy*. Journal of Thoracic and Cardiovascular Surgery*, 151/6, p.p. 1718-1728 e5.

[32] Gleason, T.G. (2005). Heritable disorders predisposing to aortic dissection. *Seminars in Thoracic and Cardiovascular Surgery*, 17/3, p.p. 274-281.
[33] Ward, C. (2000). Clinical significance of the bicuspid aortic valve. *Heart*, 83/1, p.p. 81-85.
[34] Keane, M.G., Wiegers, S.E., Plappert, T., Pochettino, A., et al. (2000). Bicuspid aortic valves are associated with aortic dilatation out of proportion to coexistent valvular lesions. *Circulation*, 102/19 Suppl 3, p.p. III35-III39.
[35] Davies, R.R., Goldstein, L.J., Coady, M.A., Tittle, S.L., et al. (2002). Yearly rupture or dissection rates for thoracic aortic aneurysms: simple prediction based on size. *Annals of Thoracic Surgery*, 73/1, p.p. 17-27.
[36] Svensson, L.G., Adams, D.H., Bonow, R.O., Kouchoukos, N.T., et al. (2013). Aortic valve and ascending aorta guidelines for management and quality measures: executive summary. *Annals of Thoracic Surgery*, 95/4, p.p. 1491-1505.
[37] Nishimura, R.A., Otto, C.M., Bonow, R.O., Carabello, B.A., et al. (2014). 2014 AHA/ACC guideline for the management of patients with valvular heart disease: a report of the American College of Cardiology/American Heart Association Task Force on practice guidelines. *Circulation*, 129/23, p.p. e521-643.
[38] den Reijer, P.M., Sallee, D., 3rd, van der Velden, P., Zaaijer, E.R., et al. (2010). Hemodynamic predictors of aortic dilatation in bicuspid aortic valve by velocity-encoded cardiovascular magnetic resonance. *Journal of Cardiovascular Magnetic Resonance*, 12/1, p.p. 4(1-13).
[39] Hope, M.D., Hope, T.A., Crook, S.E., Ordovas, K.G., et al. (2011). 4D flow CMR in assessment of valve-related ascending aortic disease. *Journal of the American College of Cardiology: Cardiovascular Imaging*, 4/7, p.p. 781-787.
[40] Hope, M.D., Hope, T.A., Meadows, A.K., Ordovas, K.G., et al. (2010). Bicuspid aortic valve: four-dimensional MR evaluation of ascending aortic systolic flow patterns. *Radiology*, 255/1, p.p. 53-61.
[41] Weigang, E., Kari, F.A., Beyersdorf, F., Luehr, M., et al. (2008). Flow-sensitive four-dimensional magnetic resonance imaging: flow patterns in ascending aortic aneurysms. *European Journal of Cardio-Thoracic Surgery*, 34/1, p.p. 11-16.
[42] Westerhof, N., Stergiopulos, N., Noble, M.I.M. (2005). *Snapshots of hemodynamics: an aid for clinical research and graduate education*, Springer Science + Business Media, Inc., New York.
[43] Halloran, B.G., Davis, V.A., McManus, B.M., Lynch, T.G., et al. (1995). Localization of aortic disease is associated with intrinsic differences in aortic structure. *Journal of Surgical Research*, 59/1, p.p. 17-22.
[44] Holzapfel, G.A., Sommer, G., Auer, M., Regitnig, P., et al. (2007). Layer-specific 3D residual deformations of human aortas with non-atherosclerotic intimal thickening. *Annals of Biomedical Engineering*, 35/4, p.p. 530-545.
[45] Zulliger, M.A., Fridez, P., Hayashi, K., Stergiopulos, N. (2004). A strain energy function for arteries accounting for wall composition and structure. *Journal of Biomechanics*, 37/7, p.p. 989-1000.
[46] Holzapfel, G.A., Gasser, T.C., Ogden, R.W. (2000). A new constitutive framework for arterial wall mechanics and a comparative study of material models. *Journal of Elasticity*, 61/1-3, p.p. 1-48.
[47] Hariton, I., de Botton, G., Gasser, T.C., Holzapfel, G.A. (2007). Stress-driven collagen fiber remodeling in arterial walls. *Biomechanics and Modeling in Mechanobiology*, 6/3, p.p. 163-175.
[48] Tsamis, A., Stergiopulos, N. (2007). Arterial remodeling in response to hypertension using a constituent-based model. *American Journal of Physiology - Heart and Circulatory Physiology*, 293/5, p.p. H3130-3139.

[49] Alford, P.W., Humphrey, J.D., Taber, L.A. (2008). Growth and remodeling in a thick-walled artery model: effects of spatial variations in wall constituents. *Biomechanics and Modeling in Mechanobiology*, 7/4, p.p. 245-262.
[50] Gleason, R.L., Humphrey, J.D. (2005). A 2D constrained mixture model for arterial adaptations to large changes in flow, pressure and axial stretch. *Mathematical Medicine and Biology*, 22/4, p.p. 347-369.
[51] Hu, J.J., Fossum, T.W., Miller, M.W., Xu, H., et al. (2007). Biomechanics of the porcine basilar artery in hypertension. *Annals of Biomedical Engineering*, 35/1, p.p. 19-29.
[52] Hu, J.J., Ambrus, A., Fossum, T.W., Miller, M.W., et al. (2008). Time courses of growth and remodeling of porcine aortic media during hypertension: a quantitative immunohistochemical examination. *Journal of Histochemistry and Cytochemistry*, 56/4, p.p. 359-370.
[53] Rachev, A., Gleason, R.L., Jr. (2011). Theoretical study on the effects of pressure-induced remodeling on geometry and mechanical non-homogeneity of conduit arteries. *Biomechanics and Modeling in Mechanobiology*, 10/1, p.p. 79-93.
[54] London, G.M., Marchais, S.J., Guerin, A.P., Pannier, B. (2004). Arterial stiffness: pathophysiology and clinical impact. *Clinical and Experimental Hypertension*, 26/7-8, p.p. 689-699.
[55] MacSweeney, S.T., Young, G., Greenhalgh, R.M., Powell, J.T. (1992). Mechanical properties of the aneurysmal aorta. *British Journal of Surgery*, 79/12, p.p. 1281-1284.
[56] Wuyts, F.L., Vanhuyse, V.J., Langewouters, G.J., Decraemer, W.F., et al. (1995). Elastic properties of human aortas in relation to age and atherosclerosis: a structural model. *Physics in Medicine and Biology*, 40/10, p.p. 1577-1597.
[57] Langewouters, G.J., Wesseling, K.H., Goedhard, W.J. (1984). The static elastic properties of 45 human thoracic and 20 abdominal aortas in vitro and the parameters of a new model. *Journal of Biomechanics*, 17/6, p.p. 425-435.
[58] Benetos, A., Safar, M., Rudnichi, A., Smulyan, H., et al. (1997). Pulse pressure: a predictor of long-term cardiovascular mortality in a French male population. *Hypertension*, 30/6, p.p. 1410-1415.
[59] Cahalan, M.D., Parker, I., Wei, S.H., Miller, M.J. (2002). Two-photon tissue imaging: seeing the immune system in a fresh light. *Nature Reviews Immunology*, 2/11, p.p. 872-880.
[60] Jiang, X., Zhong, J., Liu, Y., Yu, H., et al. (2011). Two-photon fluorescence and second-harmonic generation imaging of collagen in human tissue based on multiphoton microscopy. *Scanning*, 33/1, p.p. 53-56.
[61] Konig, K., Schenke-Layland, K., Riemann, I., Stock, U.A. (2005). Multiphoton autofluorescence imaging of intratissue elastic fibers. *Biomaterials*, 26/5, p.p. 495-500.
[62] D'Amore, A., Stella, J.A., Wagner, W.R., Sacks, M.S. (2010). Characterization of the complete fiber network topology of planar fibrous tissues and scaffolds. *Biomaterials*, 31/20, p.p. 5345-5354.
[63] Karlon, W.J., Covell, J.W., McCulloch, A.D., Hunter, J.J., et al. (1998). Automated measurement of myofiber disarray in transgenic mice with ventricular expression of ras. *Anatomical Record*, 252/4, p.p. 612-625.
[64] Tsamis, A., Phillippi, J.A., Koch, R.G., Pasta, S., et al. (2013). Fiber micro-architecture in the longitudinal-radial and circumferential-radial planes of ascending thoracic aortic aneurysm media. *Journal of Biomechanics*, 46/16, p.p. 2787-2794.

[65] Pasta, S., Phillippi, J.A., Gleason, T.G., Vorp, D.A. (2012). Effect of aneurysm on the mechanical dissection properties of the human ascending thoracic aorta. *Journal of Thoracic and Cardiovascular Surgery*, 143/2, p.p. 460-467.
[66] Pichamuthu, J.E., Phillippi, J.A., Cleary, D.A., Chew, D.W., et al. (2013). Differential tensile strength and collagen composition in ascending aortic aneurysms by aortic valve phenotype. *Annals of Thoracic Surgery*, 96/6, p.p. 2147-2154.
[67] Liyanage, L., Musto, L., Budgeon, C., Rutty, G., et al. (2022). Multimodal structural analysis of the human aorta: from valve to bifurcation. *European Journal of Vascular and Endovascular Surgery*, 63/5, p.p. 721-730.
[68] Sherifova, S., Sommer, G., Viertler, C., Regitnig, P., et al. (2019). Failure properties and microstructure of healthy and aneurysmatic human thoracic aortas subjected to uniaxial extension with a focus on the media. *Acta Biomaterialia*, 99, p.p. 443-456.
[69] Bleaken, B.M., Menko, A.S., Walker, J.L. (2016). Cells activated for wound repair have the potential to direct collective invasion of an epithelium. *Molecular Biology of the Cell*, 27/3, p.p. 451-465.
[70] Boucher, E., Mandato, C.A. (2015). Plasma membrane and cytoskeleton dynamics during single-cell wound healing. *Biochimica et Biophysica Acta*, 1853/10 Pt A, p.p. 2649-2661.
[71] Rolin, G.L., Binda, D., Tissot, M., Viennet, C., et al. (2014). In vitro study of the impact of mechanical tension on the dermal fibroblast phenotype in the context of skin wound healing. *Journal of Biomechanics*, 47/14, p.p. 3555-3561.
[72] Basan, M., Elgeti, J., Hannezo, E., Rappel, W.J., et al. (2013). Alignment of cellular motility forces with tissue flow as a mechanism for efficient wound healing. *Proceedings of the National Academy of Sciences of the USA*, 110/7, p.p. 2452-2459.
[73] Wiegand, C., White, R. (2013). Microdeformation in wound healing. *Wound Repair and Regeneration*, 21/6, p.p. 793-799.
[74] Valero, C., Javierre, E., Garcia-Aznar, J.M., Gomez-Benito, M.J. (2014). A cell-regulatory mechanism involving feedback between contraction and tissue formation guides wound healing progression. *PLoS One*, 9/3, p.p. e92774(1-10).
[75] Kim, Y., Hazar, M., Vijayraghavan, D.S., Song, J., et al. (2014). Mechanochemical actuators of embryonic epithelial contractility. *Proceedings of the National Academy of Sciences of the USA*, 111/40, p.p. 14366-14371.
[76] Munjal, A., Lecuit, T. (2014). Actomyosin networks and tissue morphogenesis. *Development*, 141/9, p.p. 1789-1793.
[77] Munjal, A., Philippe, J.M., Munro, E., Lecuit, T. (2015). A self-organized biomechanical network drives shape changes during tissue morphogenesis. *Nature*, 524/7565, p.p. 351-355.
[78] Kiehart, D.P. (2015). Epithelial morphogenesis: apoptotic forces drive cell shape changes. *Developmental Cell*, 32/5, p.p. 532-533.
[79] Petridou, N.I., Skourides, P.A. (2014). FAK transduces extracellular forces that orient the mitotic spindle and control tissue morphogenesis. *Nature Communications*, 5, p.p. 5240(1-16).
[80] Martin, A.C., Goldstein, B. (2014). Apical constriction: themes and variations on a cellular mechanism driving morphogenesis. *Development*, 141/10, p.p. 1987-1998.
[81] Heller, E., Kumar, K.V., Grill, S.W., Fuchs, E. (2014). Forces generated by cell intercalation tow epidermal sheets in mammalian tissue morphogenesis. *Developmental Cell*, 28/6, p.p. 617-632.

[82] Aguilar-Cuenca, R., Juanes-Garcia, A., Vicente-Manzanares, M. (2014). Myosin II in mechanotransduction: master and commander of cell migration, morphogenesis, and cancer. *Cellular and Molecular Life Sciences*, 71/3, p.p. 479-492.
[83] Shiwarski, D.J., Tashman, J.W., Tsamis, A., Bliley, J.M., et al. (2020). Fibronectin-based nanomechanical biosensors to map 3D surface strains in live cells and tissue. *Nature Communications*, 11/1, p.p. 5883(1-15).
[84] Paez-Mayorga, J., Hernandez-Vargas, G., Ruiz-Esparza, G.U., Iqbal, H.M.N., et al. (2019). Bioreactors for cardiac tissue engineering. *Advanced Healthcare Materials*, 8/7, p.p. e1701504.
[85] Freytes, D.O., Wan, L.Q., Vunjak-Novakovic, G. (2009). Geometry and force control of cell function. *Journal of Cellular Biochemistry*, 108/5, p.p. 1047-1058.
[86] Liu, W.F. (2012). Mechanical regulation of cellular phenotype: implications for vascular tissue regeneration. *Cardiovascular Research*, 95/2, p.p. 215-222.
[87] Navis, A., Nelson, C.M. (2016). Pulling together: tissue-generated forces that drive lumen morphogenesis. *Seminars in Cell and Developmental Biology*, 55, p.p. 139-147.
[88] Campas, O., Mammoto, T., Hasso, S., Sperling, R.A., et al. (2014). Quantifying cell-generated mechanical forces within living embryonic tissues. *Nature Methods*, 11/2, p.p. 183-189.
[89] Feinberg, A.W., Parker, K.K. (2010). Surface-initiated assembly of protein nanofabrics. *Nano Letters*, 10/6, p.p. 2184-2191.
[90] Nunes, L.C.S. (2011). Mechanical characterization of hyperelastic polydimethylsiloxane by simple shear test. *Materials Science and Engineering: A*, 528/3, p.p. 1799-1804.
[91] Brown, A.E., Litvinov, R.I., Discher, D.E., Purohit, P.K., et al. (2009). Multiscale mechanics of fibrin polymer: gel stretching with protein unfolding and loss of water. *Science*, 325/5941, p.p. 741-744.

Ph.D. Alkiviadis Tsamis was born in 1979 in Athens, Greece. He is an Assistant Professor at the Department of Mechanical Engineering of the University of Western Macedonia (Kozani, Greece) and Honorary Lecturer at the School of Engineering of the University of Leicester (Leicester, United Kingdom). Prior to that, he was a Lecturer at University of Leicester's School of Engineering and Postdoctoral Research Fellow at Carnegie Mellon University's Department of Biomedical Engineering. Also, he was a Postdoctoral Research Scholar at University of Pittsburgh's Department of Bioengineering and Postdoctoral Research Fellow at Stanford University's Department of Mechanical Engineering under a fellowship by the Swiss National Science Foundation. He completed his Ph.D. in Biotechnology and Bioengineering at École Polytechnique Fédérale de Lausanne and obtained a Diploma in Mechanical Engineering from the National Technical University of Athens. His work has been published in a variety of journals, including Nature Communications, Materials Science and Engineering, Aging Cell, Journal of Thoracic and Cardiovascular Surgery, Journal of the Mechanical Behavior of Biomedical Materials, Journal of Biomechanics, and American Journal of Physiology. His research focuses on integration of multi-scale experimental and computational techniques to investigate structural mechanisms which are indicative of development of damage in fibre-reinforced soft biological materials.

COMETa 2022
6th INTERNATIONAL SCIENTIFIC CONFERENCE
17th - 19th November 2022
Jahorina, B&H, Republic of Srpska
University of East Sarajevo
Faculty of Mechanical Engineering
Conference on Mechanical Engineering Technologies and Applications

DIFFERENT WAYS FOR HAZ MICROSTRUCTURE PREPARATION AND TESTING ON HIGH ALLOY STEEL

Tomaž Vuherer[1]

Abstract: The heat-affected zone (HAZ) is the part of the weld that is affected by the heat generated by the welding process during welding. The microstructure of the HAZ is very heterogeneous and consists of different zones such as the coarse-grained HAZ, the fine-grained HAZ, the intercritical HAZ, and the over-tempred HAZ [1]. All these zones are very narrow and their properties are slightly different. These properties affect the integrity of the entire weld, so in many cases the HAZ may be the worst part of the weld. Another challenge is determining the properties of the individual HAZ regions, since the entire HAZ is very narrow and inhomogeneous. For this reason, many properties cannot be determined accurately, with the exception of a few, such as hardness, for which only a small region is sufficient for measurement. Therefore, it is important to know how to produce the individual microstructure of a HAZ in a wider range of the material in order to determine the actual properties of such a HAZ. One of the ways is to measure the welding parameters during welding to determine the actual influence of the thermal cycle on the formation of the invidual microstructure of HAZ in the weld. Moreover, it is crucial to repeat this weld thermal cycle in an unaffected base metal on a thermal welding simulator to obtain a suitable microstructure of the HAZ [1,2]. The second option is to prepare the microstructure in the furnace by slow heating which is followed by rapid cooling [1,3]. Both processes must be precise and accurate to obtain suitable HAZ microstructures. This article addresses the challenges of producing HAZ microstructures on the high-alloy steel CT781, which is widely used in the automotive industry for parts subjected to high dynamic loads.

Key words: Fatigue growt test, Heat Affected Zone, Mechanical testing, Welds

[1] Dr. Tomaž Vuherer, University of Maribor, Faculty of Mechanical Engineering, Maribor, Slovenia, tomaz.vuherer@um.si

1 INTRODUCTION

Welded joints made by fusion welding consist of weld metal, heat-affected zone and base material. The heat-affected zone (HAZ) is very narrow and has very different microstructures. There are different zones such as the coarse-grained grain HAZ (CG HAZ), the fine-grained grain HAZ (FG HAZ), the inter-critical HAZ (IC HAZ) and over-tempered HAZ (OT HAZ). Figure 1 shows the individual zones of the HAZ as a function of the maximum temperature reached during welding.

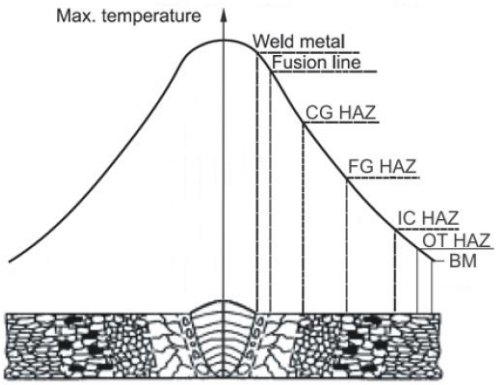

Figure 1. *Weld joint and its different regions*

Since the distance of each HAZ from the fusion line is different, the weld thermal cycle affects each HAZ differently. Figure 2 and Figure 3 show the effects of the weld thermal cycle on the individual HAZs to which they are exposed during welding and how this affects the process of microstructure formation of the HAZs.

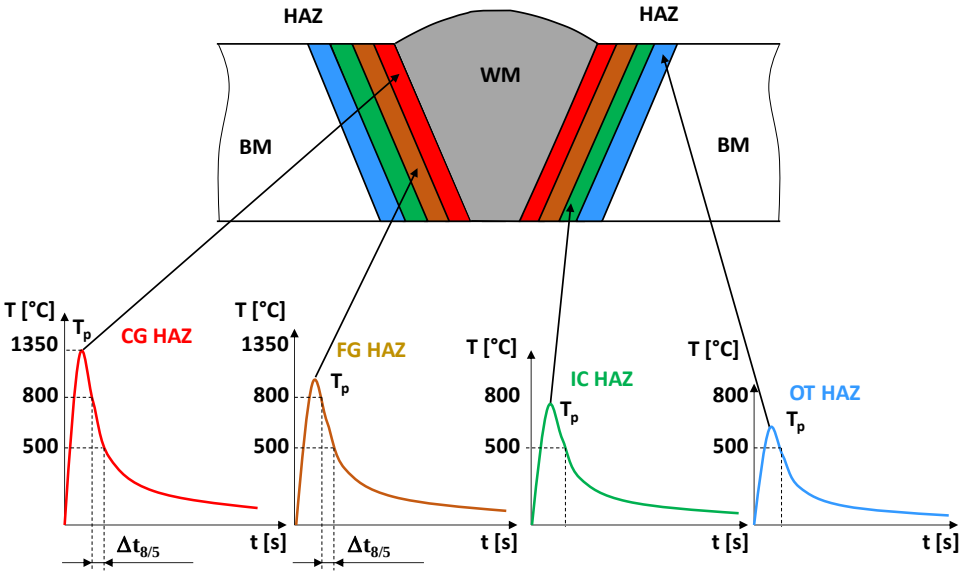

Figure 2. *Influence of the weld thermal cycle to individual HAZ*

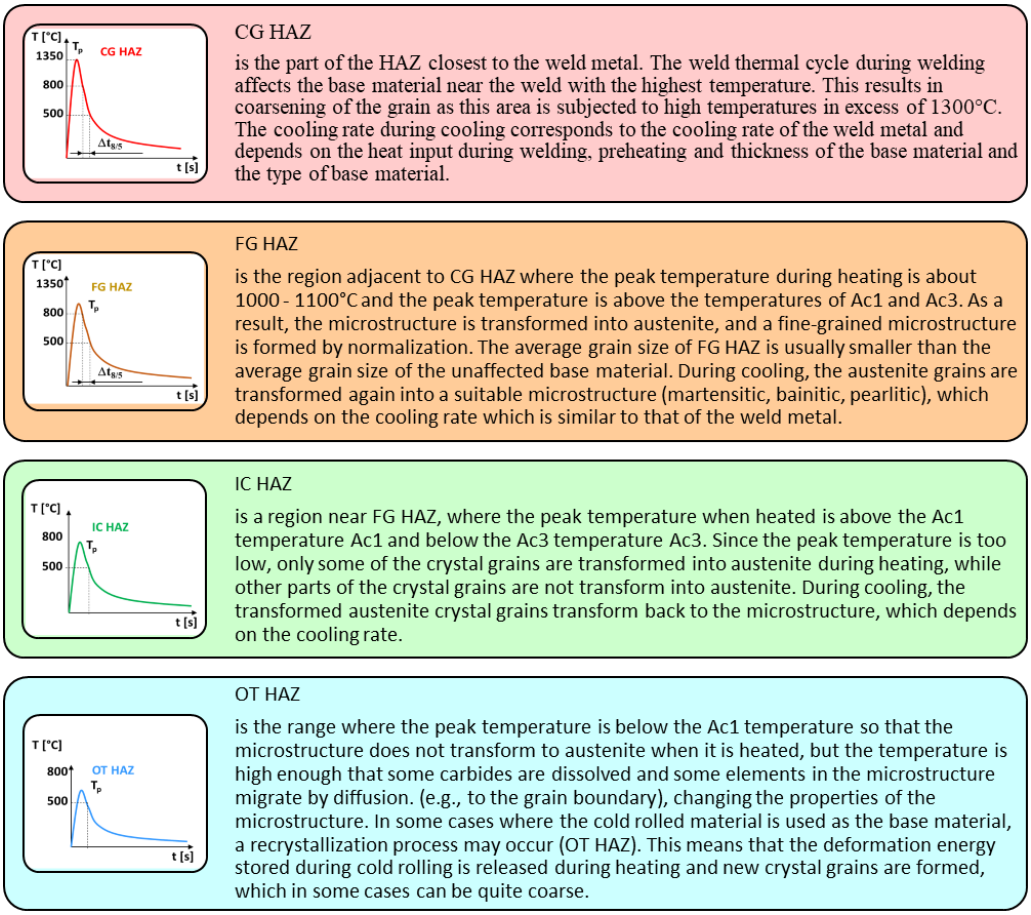

Figure 3. *Different HAZ in the welded joint*

For the integrity of the entire welded joint, it is important that each part of the welded joint has the appropriate properties that exceed the minimum requirements. This also applies to individual HAZs, where in some cases high hardness and low impact toughness can be a problem due to rapid cooling after welding [1-4].

2 MATERIAL

The 17CrNiMo7 steel was used for this investigation. This steel has good weldability and is suitable for various heat treatments. For this reason, it is suitable for parts and components subjected to high dynamic loads in the construction and automotive industries. The chemical composition of 17CrNiMo7 steel is shown in Table 1 and its mechanical properties are shown in Table 2.

Table 1. *Chemical composition of the 17CrNiMo7 steel (weight %)*

C	Si	Mn	Cr	Ni	Cu	Mo	Al	P	S
0.18	0.22	0.43	1.56	1.48	0.15	0.28	0.023	0.012	0.028

Table 2. *Mechanical properties of the steel in as delivered condition*

$R_{P0.2}$ (MPa)	R_m (MPa)	A_5 (%)
484	634	26

3 CG HAZ MICROSTRUCTURE PREPARATION USING WELDING SIMULATOR

The artificial HAZ microstructure can be prepared by various methods, e.g. by preparing the microstructure using a welding simulator or by producing the microstructure in a furnace with appropriate quenching. For the formation of the HAZ microstructure, it is important to know the welding process, the heat input during welding (welding parameters) and the thickness of the base material. All these parameters affect the width of HAZ. Since most of the transformations in this steel take place between 800 °C and 500 °C, the cooling time $\Delta t_{8/5}$ is crucial for the microstructure formation. The cooling time $\Delta t_{8/5}$ can be easily measured or it can be calculated from the welding parameters using the standard procedure EN ISO 1011-2. The other important parameters for simulating the specific part of the HAZ on the welding simulator are: the peak temperature reached in the HAZ during welding, the preheating temperature, the holding time at the peak temperature, and the final temperature at the end of the simulation. All these parameters can be measured during welding or calculated using the standard procedure EN ISO 1011-2. The procedures for determining the welding diagram and the influence of the weld thermal cycle are shown schematically in Figure 4 and Figure 5 for the 2D and 3D heat transfer during welding, while Figure 6 shows the procedure for evaluating the limiting thickness of both heat transfers.

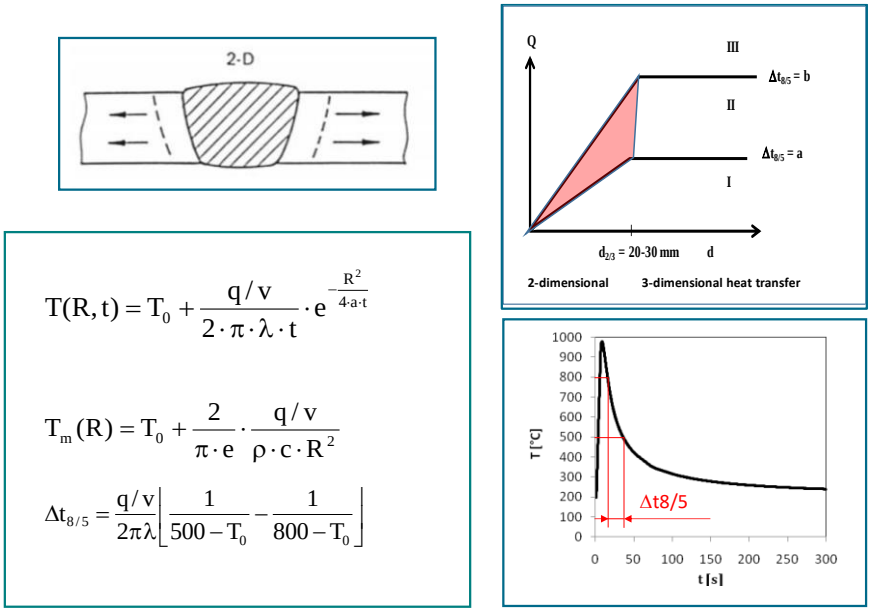

Figure 4. *Determination of welding diagram and the influence of weld thermal cycle for 2-D heat transfer during welding*

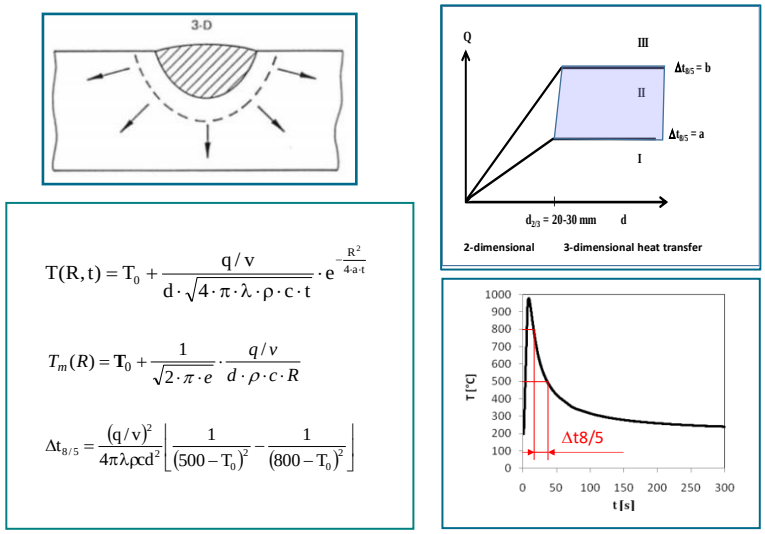

Figure 5. *Determination of welding diagram and the influence of weld thermal cycle for 3-D heat transfer during welding*

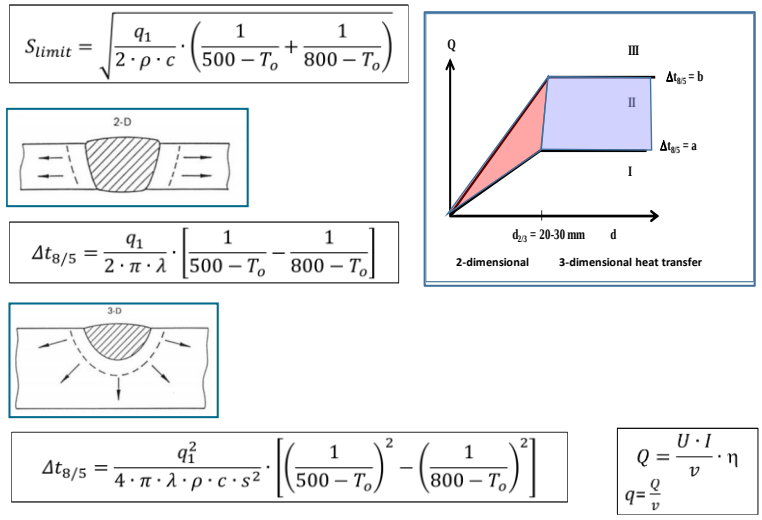

Figure 6. *Determination of the limiting thickness between 2-D and 3-D heat transfer during welding*

In these cases, the Rycalin equations of the moving heat source are used to construct the influence of the weld thermal cycle during welding on the material CG HAZ. These data are used for the simulation performed on the unaffected base material (upper parts on the left side of Figure 7). In the case of CGHAZ made of 17CrNiMo7 steel, the parameters were measured during real welding, where the cooling time $\Delta t_{8/5}$ was 5 s and the peak temperature was 1300°C. All parameters required for the simulation are listed in Table 3, and the overall influence of weld

thermal cycle used to formation of the CG HAZ microstructure is shown on the right side of Figure 7.

Table 3. *Parameters for CGHAZ simulation by using weld thermal simulator*

Preheating temp. (°C)	Heating rate (°C/s)	Peak temperature (°C)	Holding time at peak temperature (s)	Cooling time $\Delta t_{8/5}$ (s)	Finish time (s)
50	200	1300	3	5	70

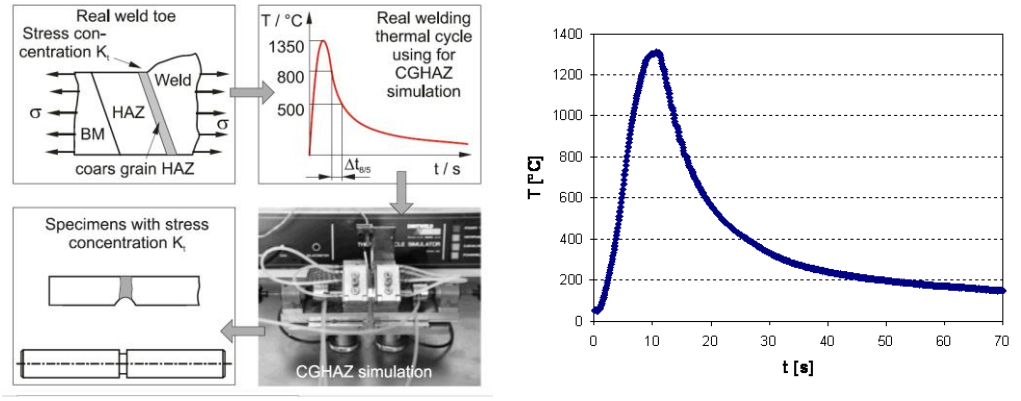

Figure 7. *HAZ preparation by using weld thermal simulator with influence of weld thermal cycle of the CG HAZ*

4 CG HAZ MICROSTRUCTURE PREPARATION IN FURNACE

The preparation of CG HAZ in the furnace is more complicated than by using a welding simulator, but it has the advantage that the whole sample has the CG HAZ microstructure and not only a part of the sample as in the HAZ preparation on the welding simulator. Therefore, the preparation of the microstructure in the furnace must be precise and accurate to obtain a suitable CG HAZ microstructure.

The first step is to coarsen the austenite grains, and the coarsening of the grain can be achieved by high temperatures over a short period of time or by lower temperatures over a longer period of time. In our case, the target size of the crystal grains that occur during real welding of the CG HAZ was 200 □m. The temperature of 1100°C was chosen to achieve the size of the grains. The duration of the holding time at this temperature was determined experimentally. Different samples of the base material were heated and held in the furnace at a temperature of 1100°C for different periods of time and cooled by quenching in water. During this process, martensite microstructures with grains of different sizes were formed. The results of the experiments are shown in Figure 8. The target holding time at 1100°C for the formation of the martensite microstructure with an average size of 200 μm is 3 hours. This holding time was chosen for the further investigations.

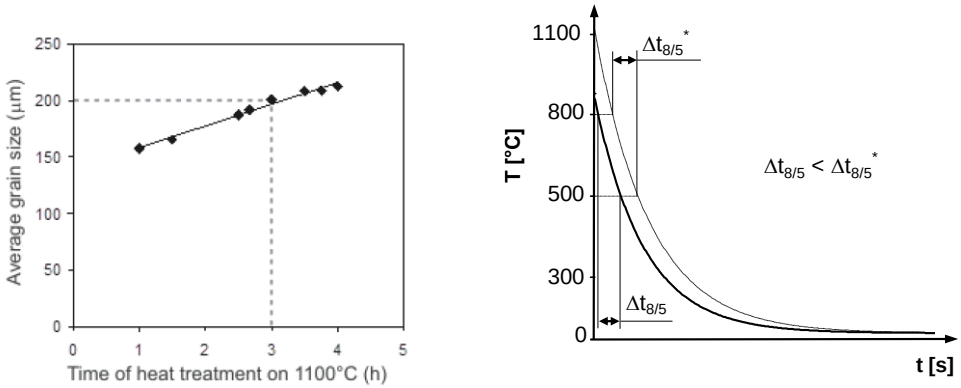

Figure 8. *Average size of crystals grain versus holding time in furnace at 1100°C (left) and $\Delta t_{8/5}$ measurements at quenching in water (right).*

In For proper CG HAZ microstructure formation, the cooling rate during quenching should be the same as during welding. This means that the cooling time $\Delta t_{8/5}$ must also be the same. The cooling time during quenching was measured experimentally. It was found that when quenching in water at a temperature of 870 °C, a cooling time $\Delta t_{8/5}$ of 5 s can be achieved, while this time is longer when quenching in water at a temperature of 1100 °C. The reason for this is the accumulation of heat in the sample, which does not allow such a fast cooling of the sample in contact with the water. See results in Figure 8.

The final heat treatment to produce the microstructure CG HAZ in the furnace is shown in Figure 9. The first part is held at a temperature of 1100 °C for three hours to achieve grain coarsening. Then the temperature is lowered to 870 °C, followed by water quenching to achieve an appropriate cooling rate and the correct CG HAZ microstructure.

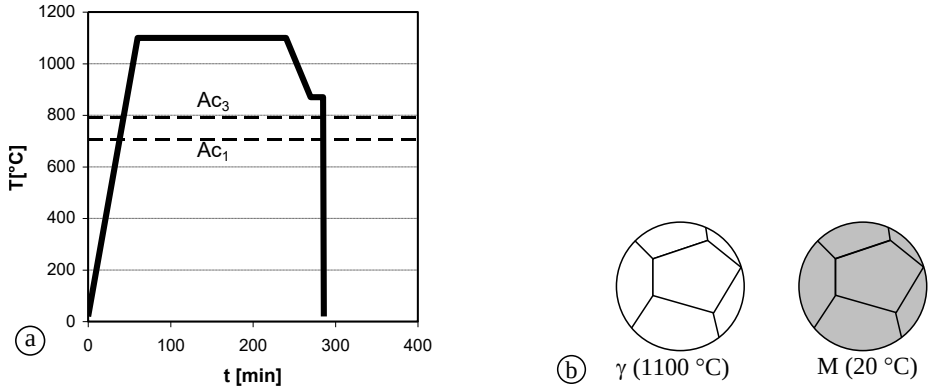

Figure 9. *CG HAZ microstructure preparation regime in furnace*

5 RESULTS AND DISCUSSION

The microstructure of CG HAZ, produced with the Smitweld 1405 weld thermal simulator, was imaged with the Epiphot300 optical microscope at two different magnifications. Figure 10 (left) shows the CGHAZ microstructure (100x) and Figure 10 (right) shows the CGHAZ microstructure at (200x). The average grain size is 200 μm. The microstructure consists of lath martensite.in water at a temperature of 870 °C,

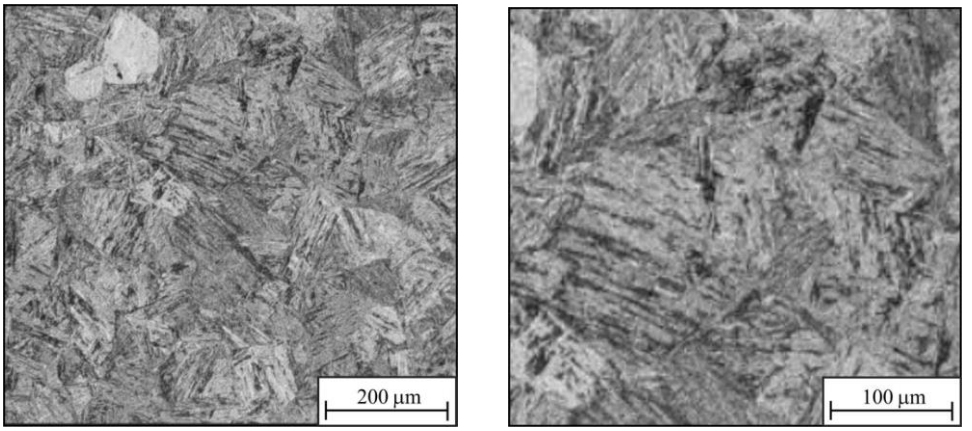

Figure 10. *CG HAZ prepared by weld thermal cycle simulator at different magnification (left 100 x and right 200 x)*

The furnace-produced CG HAZ microstructure was photographed with the same Nikkon Ephiphot 300 light microscope at two different magnifications. Figure 11 (left) shows the microstructure of CG HAZ (100x) and (200x). The average size of the crystal grains is 200 μm, and the microstructure consists of lath martensite.

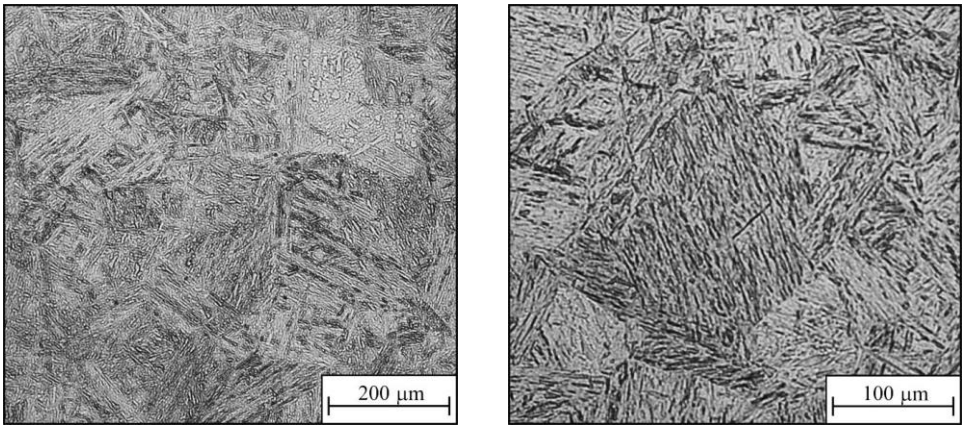

Figure 11. *CG HAZ prepared in furnace at different magnification (left 100x right 200 x).*

Hardness measurements were carried out by Vickers method, by using diamond pyramid with angle 136° and load 10 kg. Average hardness in both CG HAZ microstructures was approximately 388 HV. Scatter of the measurements was around 18 HV in both cases.

The tensile test from the CG HAZ, which was prepared using weld thermal simulator, could not be performed because this area is too narrow to machine the tensile specimens. However, there are the following correlations according to BSI 7448 part 2 to predict the estimated values for the yield strength at room temperature and the tensile strength.

R_{p02}= 3.28 HV – 221 valid for 165 < HV < 495 (1)

R_m = 3.15 HV + 93 valid for 250 < HV < 400 (2)

The tensile test was performed only on the microstructure CG HAZ, which was produced in the furnace. A cylindrical specimen was milled from the material. Table 4 shows the results of the tensile test, which was carried out on a servo-hydraulic 200 kN AMSLER machine.

Table 4. *Results of tensile tests*

Material	R_{p02} (MPa)	R_m (MPa)	σ_u (MPa)	A_g (%)	A_5 (%)	Z (%)	n (-)
CG HAZ simulator	1090*	1315*	-	-	-	-	-
CG HAZ furnace	1021	1366	1089	3,6	11,4	45,4	0,23

*Calculated from hardness by using BS 7448 part 2.

Standardised Charpy specimens with ISO -V notch were prepared from CG HAZ in an oven. Specimens were tested at various temperatures (-40, -20, 0, +20, and +50°C) on an instrumented Charpy pendulum AMSLER RPK 300. During the test, plots of force versus time and energy versus time were recorded. The results of the Charpy test at room temperature are shown in Figure 12 (left). The fracture surface of the specimen is shown in the same figure (right) and was photographed using a microscope SEM.

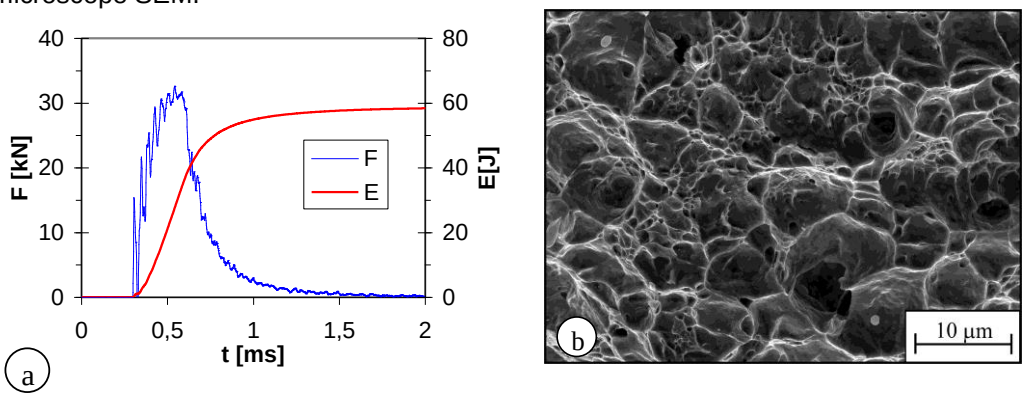

Figure 12. *Results of instrumented Charpy test at +20°C (a), fractured surface-SEM (b)*

Other results are shown in figure 13. The total energy for fracture decreases with test temperatures. In instrumented Charpy testing, the total energy for fracture can be divided into energy for crack initiation and energy for fracture propagation. The results described above are shown in Figure 14, where the energy for crack initiation remains almost independent of the test temperature, but the energy for crack propagation increases with test temperature.

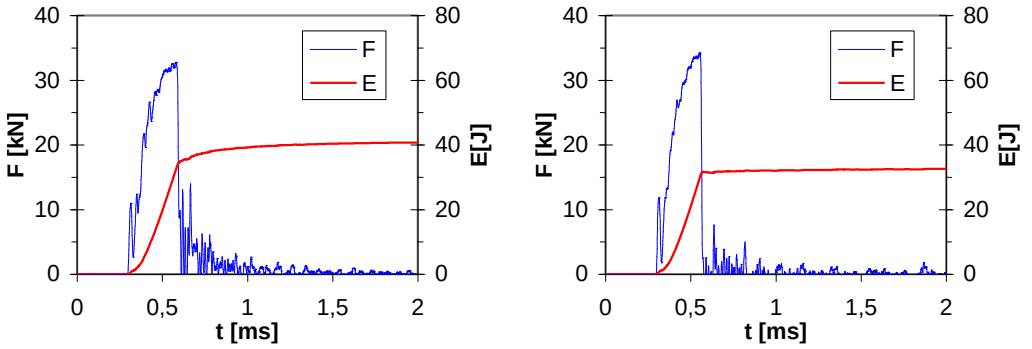

Figure 13. *Results of instrumented Charpy tests at -20 (a) and at -40°C.*

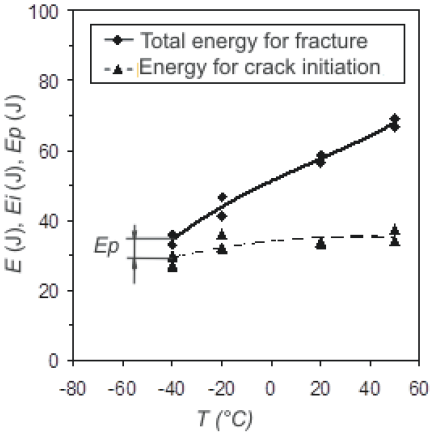

Figure 14. *Total energy for fracture, and split energy for initiation and energy for propagation.*

The crack growth tests and fracture mechanics tests were performed on unilaterally notched flexural specimens. Details of the tests and the geometry of the specimens are shown in Figure 15 and their results are in Figure 16.

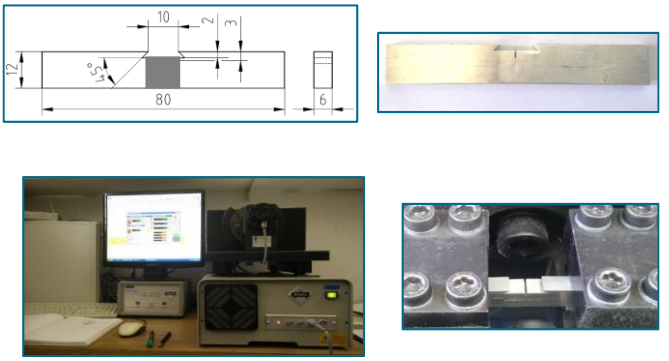

Figure 15. *Details from SENB fracture mechanics tests and fatigue growth tests.*

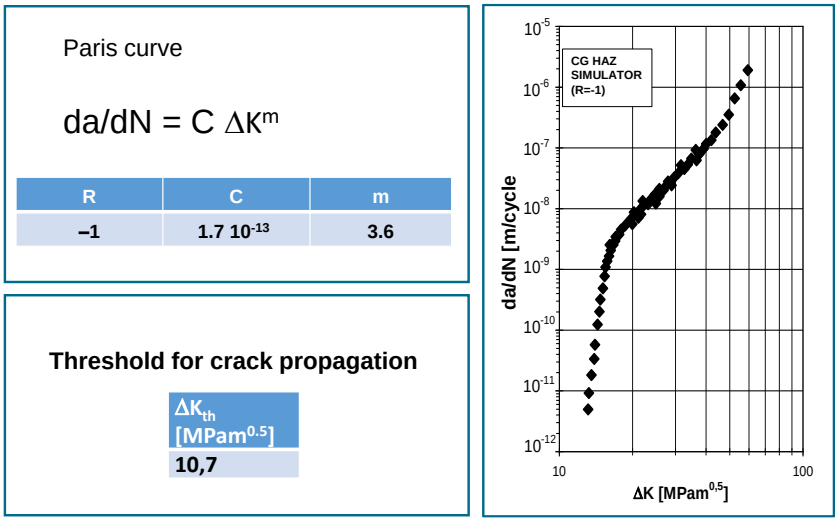

Figure 16. *Results of fracture mechanics tests.*

6 CONCLUSION

The HAZ region of the weld is very narrow and therefore does not allow specimens to be processed for testing. Moreover, this region is very heterogeneous, it consists of different types of microstructures and consequently has very different mechanical properties. To determine the properties of such HAZ regions, an artificial preparation of the HAZ macrostructure is required

In this article, two different methods of producing an artificial CG HAZ structure are presented. It can be produced by using a weld thermal simulator or by using a furnace and water quenching. Such an artificial HAZ microstructure is now present in a larger area (production of HAZ using weld thermal simulator); therefore, it is possible to machine the specimens for testing while the CG HAZ microstructure is distributed over the entire specimen (production of HAZ in a furnace).

Various properties have been successfully tested on artificially produced CG HAZ on steel CT 781, e.g. hardness test, tensile test, Charpy test, fracture mechanics tests and fatigue growth tests.

REFERENCES

[1] Vuherer, T. (2008). Analysis of influence of micro defects on fatigue strength of coarse grain HAZ in welds - *PhD Thesis, University of Maribor, Faculty of Mechanical Engineering.*

[2] Vuherer, T., Maruščak, P.O., Samardžić, I. (2012). Behaviour of coarse grain heat affected zone (HAZ) during cycle loading. Metalurgija 51/3, p.p. 301–304.

[3] Vuherer, T., Dunđer, M., Milović, Lj., Zrilić, M., Samardžić, I. (2013), Microstructural investigation of the heat-affected zone of simulated welded joint of P91 steel. Metalurgija 52/3, p.p. 317–320.

[4] Vuherer, T., Milović, Lj., Gliha, V. (2011). Behaviour of small cracks during their propagation from Vickers indentations in coarse-grain steel: an experimental investigation. *International journal of fatigue* 33/12, p.p. 1505–1513.

Tomaž Vuherer is full professor on University of Maribor, Faculty of Mechanical Engineering. He is head of Laboratory for Welding. Tomaž does research in Industrial Engineering, Materials Engineering and Mechanical Engineering

COMETa 2022
6th INTERNATIONAL SCIENTIFIC CONFERENCE
17th - 19th November 2022
Jahorina, B&H, Republic of Srpska
University of East Sarajevo
Faculty of Mechanical Engineering
Conference on Mechanical Engineering Technologies and Applications

POSSIBILITIES FOR THE APPLICATION OF REVERSIBLE PLANETARY TWO-SPEED GEARBOXES

Sanjin Troha[1], Željko Vrcan [2], Milan Tica[3], Miroslav Milutinović[4]

Abstract: Planetary gear trains (PGTs) present an improvement in relation to conventional gear trains, as several transmission ratios may be achieved by providing links between different elements of the component, and the transmission ratio can be varied under load by means of a brake or friction clutch acting on a PGT component. It is known that ships and boats must be able to perform a crash stop without stalling the engine or damaging the transmission, and rail vehicles have to go in both directions at the same speed while developing the same tractive effort. PGTs for this application must provide two equal transmission ratios, however with the output shaft rotating in different directions. This paper deals with two-carrier, two-speed PGTs having two coupling shafts and four external shafts, designed in a way to be able to change gears under load. A method to quickly determinate the structure and basic parameters of two-speed planetary gear trains that meet the application demands is presented in this paper, followed by an overview of the computer program DVOBRZ purposefully developed for this matter. A numerical example is provided, complete with an overview of the shifting capabilities of the studied PGTs.

Key words: marine reduction and reverse gearbox, mechanical power transmission, planetary gearbox, railway vehicle transmission

1 INTRODUCTION

The application of planetary gear trains (PGTs) presents considerable advantages in relation to the application of conventional gear trains. Therefore, there has been a significant expansion of their applications in various areas of mechanical engineering, e.g., machine tools, robot drives, fishing boats, railway vehicles etc. [1-6].

[1] Associate Professor, University of Rijeka, Faculty of Engineering, Rijeka, Croatia sanjin.troha@riteh.hr (ORCID 0000-0003-2086-372X)
[2] Associate Professor, University of Rijeka, Faculty of Engineering, Rijeka, Croatia zeljko.vrcan@riteh.hr
[3] Associate Professor, University of Banja Luka, Faculty of Mechanical Engineering, Banja Luka, Bosna i Hercegovina milan.tica@mf.unibl.org
[4] Associate Professor, University of East Sarajevo, Faculty of Mechanical Engineering, East Sarajevo, Bosniaa and Herzegovina, miroslav.milutinovic@ues.rs.ba

For example, machine tools such as linear planers and shapers have a slow, high load working motion, while the return motion is fast and has virtually no load except the internal resistances of the tool. As the machine usually incorporates a flywheel, reversing the main drive may become impractical, so a planetary gearbox capable of providing both transmission ratios may be used due to its capability to change ratios under load.

Modern railway vehicles are required to move in directions with the same speed. Both straight hydrodynamic and combined hydrodynamic/PGT transmissions are in common use in these vehicles, however an additional mechanical stage is required to reverse. A planetary gearbox providing two equal transmission ratios, however with the output shaft rotating in different directions can be used as an output stage.

Marine propulsion is also an important area for the application of PGTs as reverse and reduction gear trains. Marine gearboxes must be built for extreme reliability and ease of servicing at sea. Low speed diesel engines must be reversed or fitted with a controllable pitch propeller, while medium and high-speed engines can be fitted with a reversing planetary gearbox with two equal transmission ratios, however with the output shaft rotating in alternate directions to drive a considerably simpler fixed pitch propeller.

This can all be achieved by the application of compound two-speed PGTs obtained by linking the shafts of different component planetary gear trains. This paper deals with two speed PGTs, notably two-speed, two-carrier PGTs with four external shafts composed of two PGTs of the basic type.

A layout of the internal structures of compound gear trains is given, as the significant number of all possible schemes requires a systematization of the variants, as well as their labelling.

The procedure for the determination of the structure and important basic parameters of the gear train is followed by a numerical example in which the optimal two-speed planetary gear train configuration that meets predefined transmission requirements is selected. This is defined by the numbers of teeth of the central gears, their gear modules, and the ideal transmission ratios of the component gearsets. The position of the application and working conditions of the transmission determine the input data required for the computer program to define the structure and important internal parameters of the component planetary gear trains. The program will calculate several valid variants within the application parameters. However, the best solution must be determined by comparative analysis of the solutions [7,8].

2 PLANETARY GEARBOXES WITH MULTIPLE EXTERNAL SHAFTS

The two-component compound PGT is the simplest form of compound PGT. A PGT with four external shafts is created when two shafts of one component PGT are connected to two shafts of the other component PGT (Fig. 1). Of these four external shafts, two are coupled shafts and two are single external shafts. The component PGTs will be referred to as the component trains, while the complex geartrain with four external shafts will be referred to as the compound train.

The component PGTs are planetary gear trains of the basic type, as they consist of a sun gear 1, planet gears 2, ring gear 3 and planet carrier h, as shown in Fig. 2. This type of PGT is commonly used in engineering applications. Usually, it can be found as a single stage transmission, or as an integral part of compound PGTs. The primary advantage of this PGT over other PGT types lies in its efficiency and ease of calculation. Manufacturing is relatively easy, and the PGT is relatively small and

lightweight in comparison to the transmitted power. Wolf-Arnaudov symbols (Fig. 2) will be used for the description of both the simple and compound PGTs discussed in this paper [1,9].

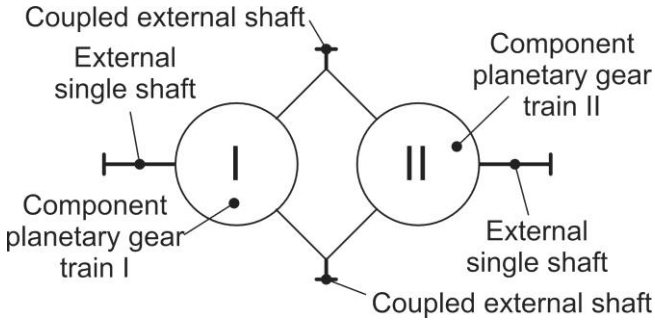

Figure 1. *Compound planetary gear train with four external (two single and two coupled) shafts*

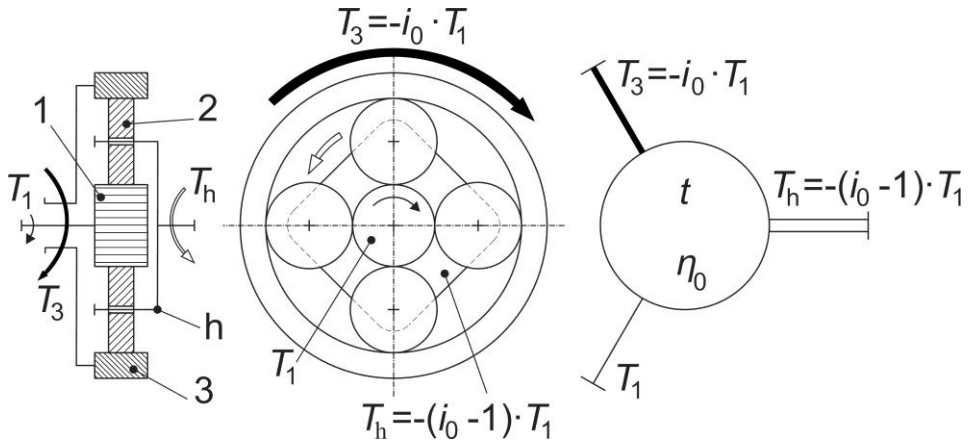

Figure 2. *Overview of torques on the shafts of a basic PGT*

The ideal torque ratio of the component PGT is given by Eq. 1:

$$t = \frac{T_3}{T_1} = \left|\frac{z_3}{z_1}\right| = -i_0 > 1 \tag{1}$$

Where i_0 is the basic transmission ratio, z_1 is the number of teeth of the sun gear and z_3 is the number of teeth of the ring gear. The actual transmission ratio depends on whether the sun gear, ring gear or planet carrier are the locked element.

Two component PGTs can be joined in a total of 36 possible ways [10], however only 12 different PGTs with four external shafts are possible due to isomorphism, as shown in Fig. 3.

All schemes have the possibility for a brake to be placed or the driving or operating machine to be connected to any external shaft in 12 different ways (V1…V12). These possibilities are referred to as the layout variants (Fig. 4). The placement of brakes on different shafts makes it possible to influence the flow of power flow and the kinematic characteristics of the PGT. This is a very important advantage, as these transmissions can then be used as multiple-speed gearboxes.

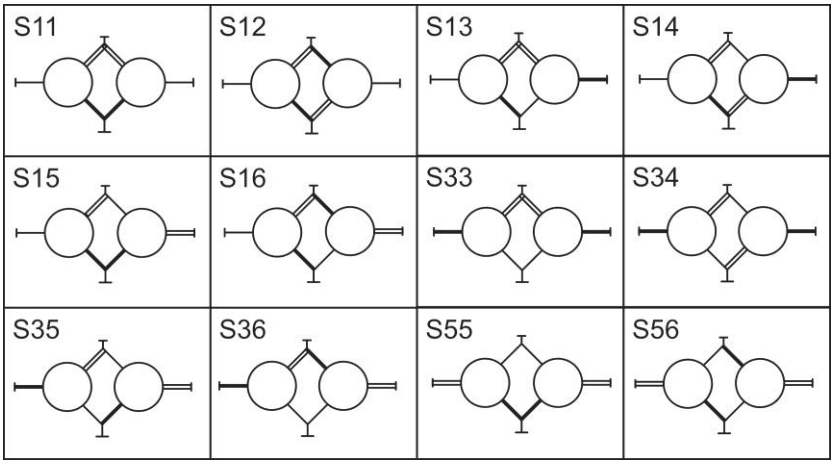

Figure 3. *All possible schemes of two-carrier planetary gear trains with four external shafts [1,10]*

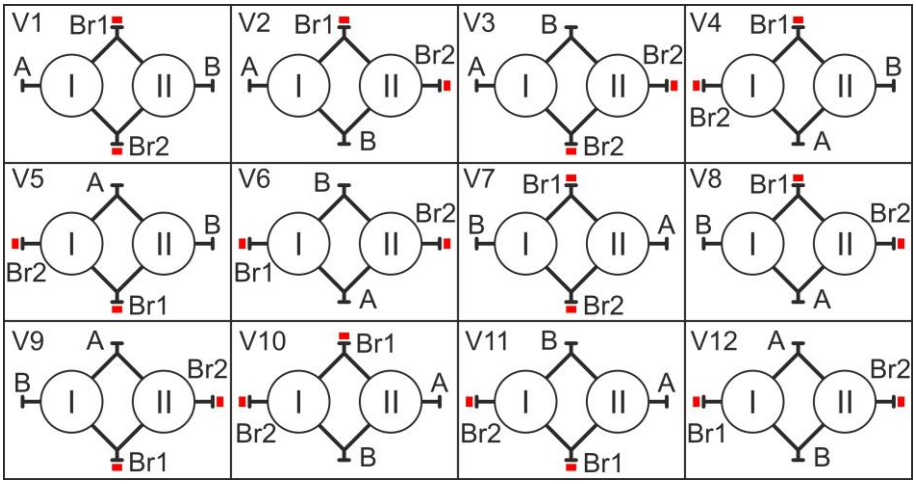

Figure 4. *Variants of two-carrier PGTs with four external shafts [11,13]*

3 NUMERICAL EXAMPLE AND DISCUSSION OF RESULTS

DVOBRZ is a computer program developed to synthetize two-speed PGTs [10]. It is also used to select the optimal variant from similar multi-speed PGTs.

The transmission ratio achieved with brake Br1 on is designated i_{Br1} while the transmission ratio achieved with brake Br2 on is marked as i_{Br2}, and all valid solutions are finally stored. The program can compare and sort all valid solutions according to the defined relevant criteria, such as minimal radial dimensions, maximum equivalent efficiency, minimum weight etc. [10].

The transmission of a railway vehicle will be used as a practical example for the selection of two-speed PGTs, although the same procedure would be applied in other occasions, such as a fishing boat transmission, a machine tool gearbox, a conveyor main drive etc.

In this case, the required transmission ratios are i_1 = -4,5 and i_2 = 4,5.

Solutions have been found with transmission ratios in the ranges -4,6 ≤ i_1 ≤ -4,4 and 4,4 ≤ i_2 ≤ 4,6. The frequency of working with each transmission ratio also provides important input data: α_{i1} = 0,5 (50%) and α_{i2} = 0,5 (50%). Now the optimal solution must be chosen according to the criteria of maximum efficiency while taking into consideration the operating conditions of the railway vehicle [12]. Six possible solutions for two-speed PGTs will be listed by the DVOBRZ program based on the requirements and assumptions listed above.

The summary of the main parameters is given in Table 1 while the kinematic schemes of acceptable solutions are displayed in Figure 5. The main parameters that have been provided include the numbers of teeth for all gears and ideal torque ratios for both component gear trains. All gearsets use three planet gears, except for the solution in bold using four. The program DVOBRZ was used to determine the ideal torque ratios for both gear trains. These ideal torque ratios were used to adopt the tooth numbers of all gears [13], the values of which have been presented in Table 1.

Table 1. *Main parameters of component PGTs*

	t_I	t_{II}	z_{1I}	z_{2I}	z_{3I}	z_{1II}	z_{2II}	z_{3II}
S36V6	3,5	4,555	14	17	49	20	35	92
S16V1	1,714	1,604	42	15	72	53	16	85
S33V4	1,714	4,437	42	15	72	16	27	71
S13V3	3,5	1,553	14	17	49	47	13	73
S12V2	4,55	1,553	20	35	91	47	13	73
S55V5	1,714	3,4	42	15	72	15	18	51

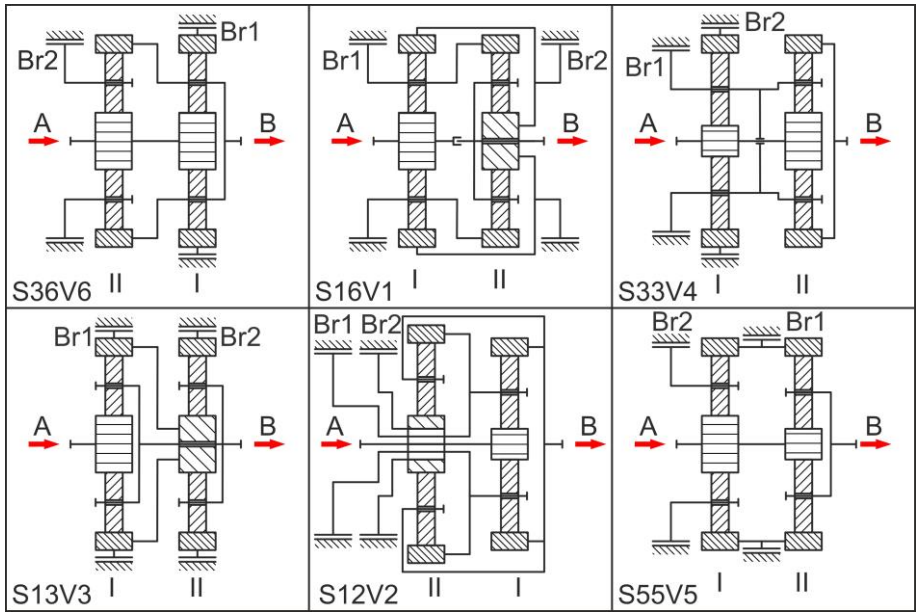

Figure 5. *Kinematic diagrams of acceptable PGT layouts*

The tooth numbers of the component PGTs respect the assembly conditions of coaxiality, adjacency and conjunction. The transmission ratios and efficiencies have been calculated for all acceptable solutions in both cases: with brake Br1 active, and with brake Br2 active.

The transmission ratio with brake Br1 on, i_{Br1} and the transmission ratio with brake Br2 on, i_{Br2}, are defined by using the adopted tooth numbers from Table 1. The basic efficiency was calculated as a function of the tooth numbers of all gears [10, 15], and the results presented in Table 3. The efficiency with brake Br1 on, η_{Br1} and the efficiency with brake Br2 on, η_{Br2}, were calculated as a function of ideal torque ratios and basic efficiencies [9].The results are presented in Table 2.

Table 2. *Transmission ratios and efficiencies*

	i_{Br1}	i_{Br2}	η_{0I}	η_{0II}	η_{Br1}	η_{Br2}
S36V6	4,5	-4,55	0,973	0,985	0,979	0,985
S16V1	-4,464	4,407	0,976	0,978	0,962	0,976
S33V4	-4,438	4,422	0,976	0,980	0,980	0,959
S13V3	4,5	-4,436	0,973	0,973	0,979	0,934
S12V2	-4,55	4,573	0,985	0,973	0,985	0,969
S55V5	4,4	-4,475	0,976	0,974	0,980	0,924

All solutions provide the required transmission ratios while also providing the high efficiency values in both directions of rotation of the output shaft. The designer then selects the optimal solution according to technological and economical demands of the PGT target application.

The selection is performed by analyzing the kinematic diagrams as given in Figure 5. Priority is given to designs which do not require drilled shafts. This is achieved with layout S36V6. This layout is shown kinematically in Fig. 6 and symbolically in Fig. 7. The direction of the power flow through this transmission solution is also shown in Figs. 6 and 7.

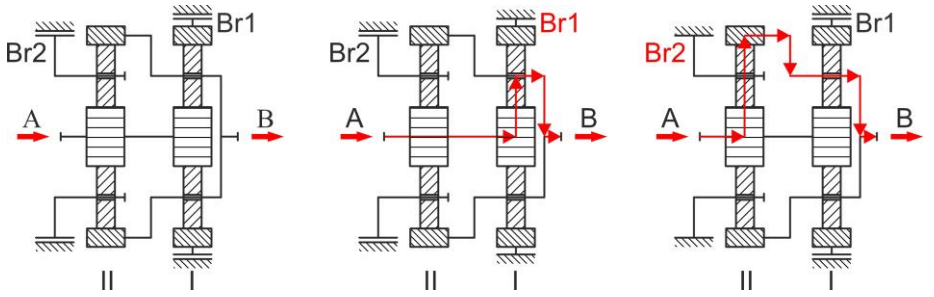

Figure 6. *Left: Kinematic scheme of transmission S36V6. Center: Power flow with brake Br1 on. Right: Power flow with brake Br2 on.*

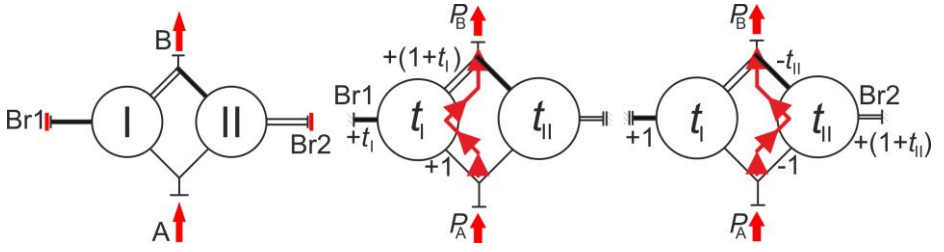

Figure 7. *Left: Symbolic view of transmission S36V6. Center: Symbolic view of power flow with brake Br1 on. Right: Symbolic view of power flow with brake Br2 on.*

The transmission ratio for solution S36V6 with brake Br1 on is given by Eq. 2, while the ratio with brake Br2 on is given by Eq. 3.

$$i_{\mathrm{Br1}} = -\frac{T_{\mathrm{B}}}{T_{\mathrm{A}}} = 1 + t_{\mathrm{I}} \tag{2}$$

$$i_{\mathrm{Br2}} = -\frac{T_{\mathrm{B}}}{T_{\mathrm{A}}} = -t_{\mathrm{II}} \tag{3}$$

With this design, both brakes are acting on single external shafts. It should be noted that in both situations, i.e., by activating any brake, only one stage remains operational (two-shaft operating mode), while the other revolves idly. Because of that, power is wasted in only one PGT stage and there is only one power output.

4 SHIFTING CAPABILITIES

The sets of achievable combinations of transmission ratios of a selected compound train, are represented as sets of points in Figs. 8-13. Every combination of transmission ratios corresponds to only one combination of ideal torque ratios, which can also be reviewed as an ordered pair. Every graph is provided with the appropriate expression for determining the ordered pair of the ideal torque ratios that corresponds to the pair of the required transmission ratios. The first member of the ordered pair is the ideal torque ratio of the first component train, while the second member of the ordered pair is the ideal torque ratio of the second component train. The required gear tooth numbers can be determined on the basis of the determined ordered pair of the ideal torque ratio. The number of teeth of the ring gear and sun gear is usually determined by taking into account the assembly conditions of the respective component train.

The ordered pairs for gearset S36V6 (Fig. 8) are defined by Equation 4:

$$(t_{\mathrm{I}}, t_{\mathrm{II}}) = \left(i_{\mathrm{Br1}} - 1, -i_{\mathrm{Br2}}\right) \tag{4}$$

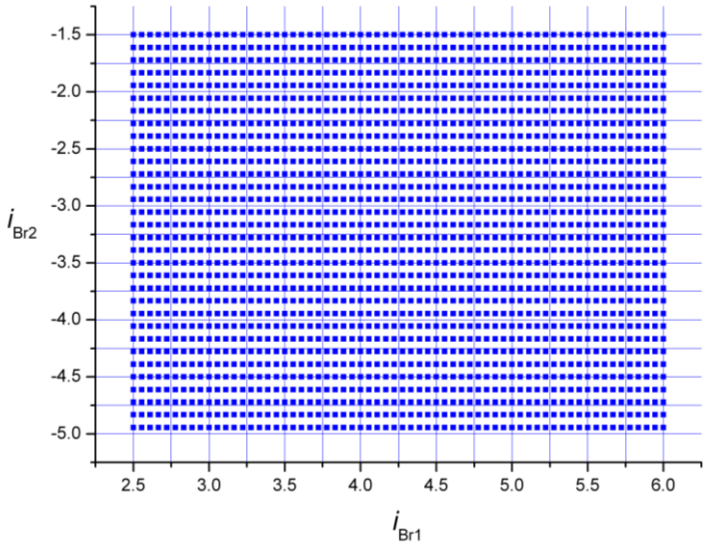

Figure 8. *Shifting capabilities of gearset S36V6*

The ordered pairs for gearset S16V1 (Fig. 9) are defined by Equation 5:

$$(t_{\mathrm{I}}, t_{\mathrm{II}}) = \left(\frac{i_{\mathrm{Br1}}(i_{\mathrm{Br2}} - 1)}{i_{\mathrm{Br1}} - i_{\mathrm{Br2}}}, \frac{1 - i_{\mathrm{Br1}}}{i_{\mathrm{Br2}} - 1} \right) \tag{5}$$

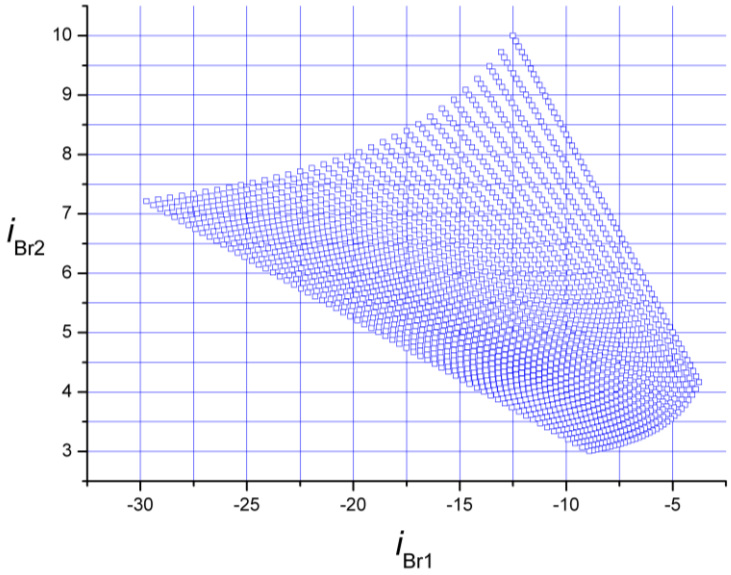

Figure 9. *Shifting capabilities of gearset S16V1*

The ordered pairs for gearset S12V2 (Fig. 10) are defined by Equation 6:

$$(t_{\mathrm{I}}, t_{\mathrm{II}}) = \left(-i_{\mathrm{Br1}}, \frac{1 - i_{\mathrm{Br1}}}{i_{\mathrm{Br2}} - 1} \right) \tag{6}$$

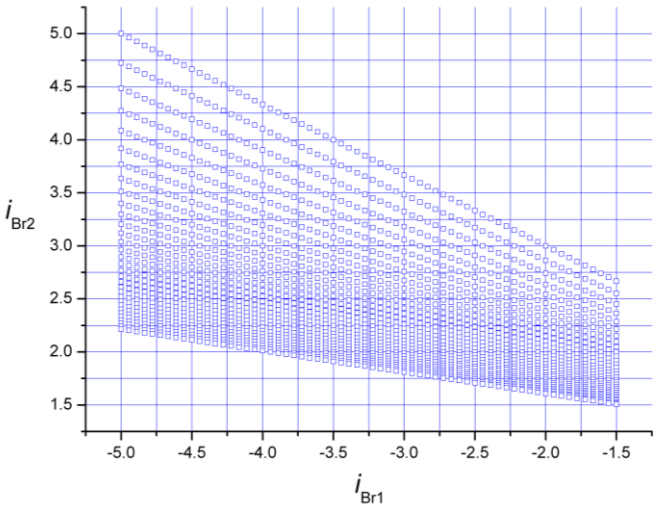

Figure 10. *Shifting capabilities of gearset S12V2*

The ordered pairs for gearset S13V3 (Fig. 11) are defined by Equation 7:

$$(t_{\mathrm{I}}, t_{\mathrm{II}}) = \left(i_{\mathrm{Br1}} - 1, \frac{1 - i_{\mathrm{Br2}}}{i_{\mathrm{Br1}} - 1} \right) \tag{7}$$

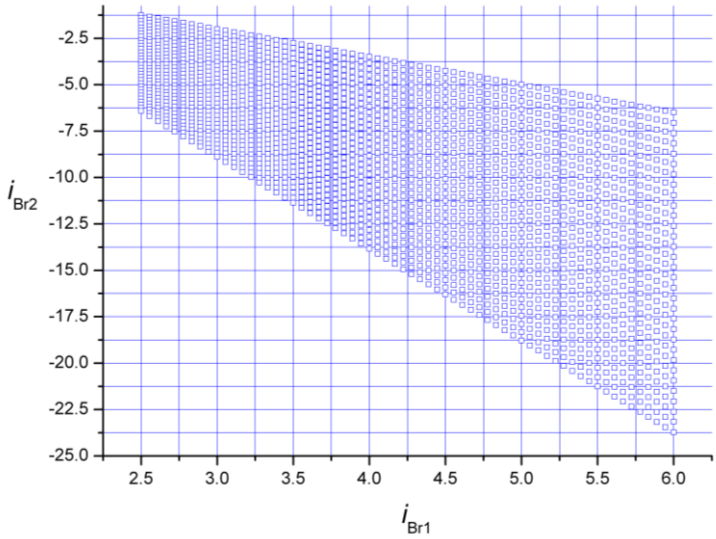

Figure 11. *Shifting capabilities of gearset S13V3*

The ordered pairs for gearset S33V4 (Fig. 12) are defined by Equation 8:

$$(t_{\mathrm{I}}, t_{\mathrm{II}}) = \left(\frac{i_{\mathrm{Br1}}(i_{\mathrm{Br2}} - 1)}{i_{\mathrm{Br1}} - i_{\mathrm{Br2}}}, -i_{\mathrm{Br1}} \right) \tag{8}$$

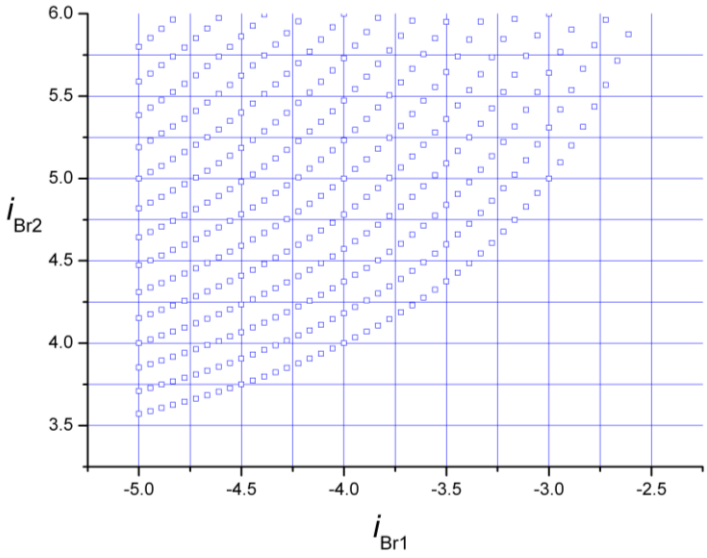

Figure 12. *Shifting capabilities of gearset S33V4*

The ordered pairs for gearset S55V5 (Fig. 13) are defined by Equation 9:

$$(t_{\mathrm{I}}, t_{\mathrm{II}}) = \left(\frac{i_{\mathrm{Br2}}(i_{\mathrm{Br1}} - 1)}{i_{\mathrm{Br2}} - i_{\mathrm{Br1}}}, i_{\mathrm{Br1}} - 1 \right) \tag{9}$$

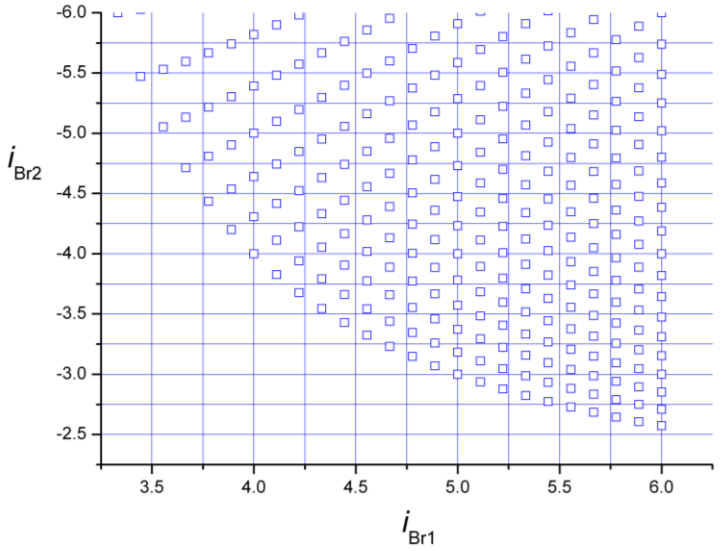

Figure 13. *Shifting capabilities of gearset S55V5*

5 CONCLUSION

This paper deals with two-speed planetary gear trains with four external shafts, composed of two simple planetary gear trains, including a systematization of their kinematic structure and layout variants. Due to their characteristics, such gear trains are applicable in systems which require the transmission ratio to change under load.

A quick overview of the structure and determination of basic parameters of two-speed planetary gear trains by means of the DVOBRZ computer program has been presented. The DVOBRZ program was developed for the examination and design of two-speed planetary gear trains. Afterwards, a numerical example dealing with the application to a railway vehicle where two directions of rotation at the same speed are necessary is given.

All the possible schemes obtained by program have realized and the main parameters defined. The most appropriate scheme was chosen by analyzing the obtained schemes according to application target demands, the additional demand being ease of manufacturing with no hollow shafts. Finally, the shifting capabilities of all examined gearsets and their variants are examined.

LITERATURA

[1] Stefanović-Marinović, J., Troha S., Milovančević, M. (2017). An Application of Multicriteria Optimization to the Two-Carrier Two-Speed Planetary Gear Trains. *FACTA UNIVERSITATIS Series: Mechanical Engineering*, vol. 15 vo. 1 p.p. 85-95.

[2] Penčić, M., Čavić, M., Borovac, B. (2017). Development of the low Backlash Planetary Gearbox for Humanoid Robots. *FME Transactions*, vol. 45, p.p. 122-129.

[3] Miloradović, N., Stojanović, B., Ćatić, D. (2009). Application of Planetary Reduction Gear in Operation of the Two Rope Grab. *FME Transactions*, vol. 37, p.p. 137-141.
[4] Troha, S., Vrcan, Ž., Karaivanov, D., Isametova, M. (2020). The Selection of Optimal Reversible Two-speed Planetary Gear Trains for Machine Tool Gearboxes. *FACTA UNIVERSITATIS Series: Mechanical Engineering,* vol. 18, no 1, p.p. 121 – 134.
[5] Troha, S., Stefanović-Marinović, J., Vrcan, Ž., Milovančević, M. (2020). Selection of the optimal two-speed planetary gear train for fishing boat propulsion. *FME Transactions*, no. 48 vol. 2, p.p. 397-403.
[6] Troha, S., Karaivanov, D., Vrcan, Ž., Marković, K., Šoljić, A. (2021). Coupled two-carrier planetary gearboxes for two-speed drives. *Machines, Technologies, Materials*, vol. 15 no. 6, p.p. 212-218.
[7] Vrcan, Ž., Stefanović-Marinović, J., Tica, M., Troha, S. (2022). Research into the Properties of Selected Single Speed Two-Carrier Planetary Gear Trains. *Journal of Applied and Computational Mechanics*, vol. 8 no. 2, p.p. 699–709.
[8] Pavlović, A., Fragassa A. (2020). Geometry optimization by FEM simulation of the automatic changing gear. *Reports in Mechanical Engineering*, vol. 1 no. 1, p.p. 199-205.
[9] Arnaudov, K., Karaivanov, D. (2013). The torque method used for studying coupled two-carrier planetary gear trains. *Transactions of FAMENA* no. 37 vol. 1, p.p. 49-61.
[10] Troha, S. (2011). *Analysis of a planetary change gear train's variants*. (in Croatian), PhD Thesis, Faculty of Engineering, University of Rijeka, Rijeka, Croatia.
[11] Troha, S., Lovrin, N., Milovančević, M. (2012). Selection of the two–carrier shifting planetary gear train controlled by clutches and brakes. *Transactions of FAMENA*, vol. 36 no. 3, p.p. 1-12.
[12] Stefanović-Marinović, J., Petković, M., Stanimirović, I., Milovančević, M. (2011). A model of planetary gear multicriteria optimization. *Transactions of FAMENA*, vol. 35 no. 4, p.p. 21-34.
[13] Troha, S., Žigulić, R., Karaivanov, D. (2014). Kinematic Operating Modes of Two-Speed Two-Carrier Planetary Gear Trains with four External Shafts. *Transactions of FAMENA*, vol. 38 no. 1, p.p. 63-76.
[14] Orlić, Ž., Orlić, G. *Planetary Transmissions* (2006) (in Croatian), Faculty of Engineering, University of Rijeka, 2006.
[15] Stefanović-Marinović, J. *Multicriterion optimization of planetary power transmission gear pairs*, (in Serbian), PhD Thesis, University of Niš, Faculty of Mechanical Engineering, Niš, Serbia, 2008.

BIOGRAPHY OF THE PRESENTING AUTHORS

Sanjin Troha is an Associate Professor with the Faculty of Engineering at the University of Rijeka. He teaches several courses for undergraduate and graduate students with backgrounds in mechanical engineering, naval archtecture, and electrical engineering background. He is also the lecturer of the course in multi-speed mechanical converters at the doctoral studies of mechanical engineering at the Faculty of Engineering of the University of Rijeka. He has authored and co-authored over 60 scientific papers published in domestic and international journals and proceedings. His scientific interest is primarily in the fields of complex gearboxes. He has been a collaborator on several domestic and foreign scientific research projects.

Željko Vrcan is an Associate Professor with the Faculty of Engineering at the University of Rijeka. He teaches several courses for undergraduate, graduate and PhD students with backgrounds in mechanical engineering, naval archtecture, and electrical engineering background. He has authored and co-authored more than 20 scientific papers published in domestic and international journals and proceedings. His scientific interests are the fields of complex gearboxes, materials transport and compliant mechanisms. He has been a collaborator on several domestic and international scientific research projects.

Milan Tica is an Associate Professor with the Faculty of Mechanical Engineering at the University of Banja Luka. He teaches several courses for undergraduate and graduate students with backgrounds in mechanical engineering. He is head of the Department of mechanics and construction at the Faculty of Mechanical Engineering of the University of Banja Luka. He has authored and co-authored over 35 scientific papers published in domestic and international journals and proceedings. His scientific interest is primarily in the fields of complex gearboxes, product development. He has been a collaborator on several domestic and foreign scientific research projects.

Miroslav Milutinović is an Associate Professor with the Faculty of Mechanical Engineering at the University of East Sarajevo. He teaches several courses for undergraduate and graduate students with backgrounds in mechanical engineering. He has authored and co-authored over 38 scientific papers published in domestic and international journals and proceedings. His scientific interest is primarily in the fields of complex gearboxes, reliability gearbox, product development, CAD tehnology. He has been a collaborator on several domestic and foreign scientific research projects. It is the holder of over 120 professional projects.

MANUFACTURING TECHNOLOGIES AND ADVANCED MATERIALS

COMETa 2022
6th INTERNATIONAL SCIENTIFIC CONFERENCE
17th - 19th November 2022
Jahorina, B&H, Republic of Srpska
University of East Sarajevo
Faculty of Mechanical Engineering
Conference on Mechanical Engineering Technologies and Applications

INVESTIGATING MECHANICAL RESPONSE AND COLLAGEN STRUCTURE IN THE INTESTINAL WALL

Panagiotis Chatzisavvas[1], Stefanos Gerardis[2], Alkiviadis Tsamis[3,4]

Abstract: Intestine is one of the most important organs playing a vital role in the normal function of the human body. It is divided into two major parts with different structures, the small and the large bowel. From a mechanical point of view, the ways the intestine accomplishes its functions are extremely complicating and hard to understand. The movements that have been observed serve a number of functions such as the propulsion of the chyme (Peristaltic movements), the cleaning of the tube (Migrating motor complex), the defecation (High amplitude propagating contractions), etc. The wall itself is a complex and composite material, consisting of four layers, with different structures among the layers. To manage the mechanical stresses, the intestine uses the submucosal layer that mainly consists of collagen fibers, which are considered as main load-bearing constituents. The structure of collagen fibers inside the wall resembles a double-oriented net, which "hugs" the tube. The structure of this net is affected in many ways by clinical conditions such as illness, aging, surgeries, etc. This paper reviews the existing information about the movements and mechanical response of the intestine, as well as the role of collagen in the corresponding operations. Our hope is that our study will encourage more rigorous interrogation of the structural changes within the intestinal wall, which could ultimately provide a better insight into the mechanics of the intestine and the pathophysiology of intestinal disease.

Key words: collagen structure, intestinal wall, movements, tensile strength

[1] Mr. Panagiotis Chatzisavvas, Department of Mechanical Engineering, University of Western Macedonia, Kozani, Greece, mech02518@uowm.gr
[2] Asst. Prof. Dr. Stefanos Gerardis, Department of Mechanical Engineering, University of Western Macedonia, Kozani, Greece, sgerardis@uowm.gr
[3] Asst. Prof. Dr. Alkiviadis Tsamis, Department of Mechanical Engineering, University of Western Macedonia, Kozani, Greece, atsamis@uowm.gr
[4] Lecturer Dr. Alkiviadis Tsamis, School of Engineering, University of Leicester, Leicester, United Kingdom, at441@leicester.ac.uk

1 INTRODUCTION

The gastrointestinal (GI) tract is a system of interconnected organs that work together in perfect harmony to ensure the smooth functioning of the body. It starts in the oral cavity and ends in the anus [1]. Throughout this route, the food undergoes a multitude of processes to extract the necessary substances and release the ones that are unnecessary. To serve this purpose, many organs and mechanisms are used (Figure 1A). For the support and development of cellular structures in mammalian tissues, a protein of particular mechanical interest, collagen, is produced. The GI tract needs large amounts of collagen to cope with the stresses, because many forces with different directions and intensities act on it [2]. Several scientists have linked collagen to diseases that occur in the gut and are still trying to sort out the exact mechanism of this linkage.

2 INTESTINAL MOVEMENTS

The GI tract has been a tissue of interest to both health scientists and engineers. Dynamic analysis with finite element method (FEM), response of the walls to tensile and bending experiments, fluid dynamics approach to the flow of chyme in the tube, and many others, are subjects of engineering applications [3]. Samples for *in vitro* or *in vivo* experimental investigations have been taken either from animals, such as rats, mice and Guinea pigs, or from human tissue, cadaveric or fresh.

2.1 Intestinal Wall

The intestinal wall is divided into 4 basic layers (as shown in Figure 1B). First layer is the mucosa. The mucosa is in contact with the contents and its role is to absorb the essential substances from the chyme. Next layer is the submucosa containing the collagen network, which represents the skeleton of the wall. Third layer of the intestinal wall is the muscularis. This layer contains two muscle layers, circular and longitudinal. The last layer is the outermost layer and is called the serosa [4].

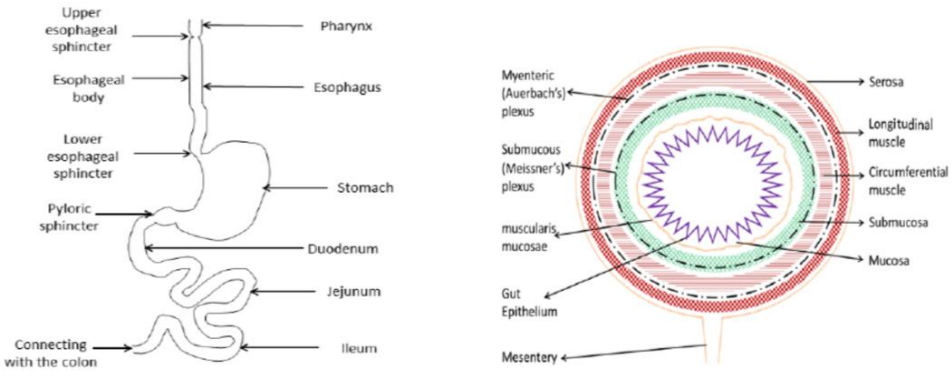

Figure 1. *Schematic diagram of : (A) the upper GI tract, including the esophagus, stomach and small intestine, (B) the typical four-layered structure of the GI tissue i.e. mucosa, submucosa, muscularis and serosa. (Adapted from* [1]*)*

2.2 Peristaltic Movements

The purpose of the peristaltic movements, the most basic type of motion, is to transport the contents along the length of the tube [5]. In the intestinal tract, this motion is achieved using progressive wave-like contractions [1]. The circular muscle tissue contracts progressively (i.e. towards the exit - anus) while at the same time the longitudinal muscle tissue relaxes. In this way, the pressure difference (about 20 mmHg) propels the chyme towards the exit [6].

2.3 Segmental-Mixing Movements

The scientific community has concluded that segmental-mixing movements' predominant role is to mix the chyme to make digestion easier and faster [5]. Certain variations in the literature appear. In terms of analysis, some scientists support that mixing is achieved by a progressive contraction (i.e. towards the exit - anus) but the flow is interrupted by a retrograde contraction (i.e. opposite to the exit - anus), and thus ensures that the chyme moves towards the exit and back again [5,7]. Others report that movement is achieved by partial-segmental contraction of the circular muscle tissue and that the juice is thus mixed in the vertical axis (transverse or radial plane) [5]. On the other hand, some scientists argue that the movement associates with slight or no displacement of the contents along the tube [5,6]. Moreover, it has been reported that the motion clearly displaces the chyme towards the exit, while some have documented that the displacement that occurs has no specific direction [1]. The frequency of the movements ranges from 7-20 contractions/min in the small intestine and 2-13 contractions/min in the large intestine, with no information about intensity [6].

2.4 Pendular Movements

Pendular movements aim to move the contents back and forth to achieve better mixing. However, there are no detailed reports on their characteristics. The longitudinal muscle tissue contracts, expands and perhaps propels the contents along the tube [7]. As in the previous movement, some scientists report that the contents is displaced, while others disagree with this claim [8].

2.5 MMC-Migrating Motor Complex

MMC is a special and very useful movement, occurring in the stomach and intestine only when both are empty (fasting state). Its purpose is to clear the lumen of microorganisms and food debris. It is mainly divided into 3 stages [9]:

- 1st stage: calm period without the occurrence of contractions.
- 2st stage: low-frequency contractions begin/appear with unsettled continuity.
- 3rd stage: the most obvious and characteristic stage of the movement (every 90-120 min). High-frequency contractions about 11-12 contractions/min occur at a relatively low speed of 6-10 cm/min [9].

2.6 Gastrocolic Reflex

The gastrocolic reflex is a complex function that is very much linked to the neurological system. Specifically, between the end of the small intestine (ileum) and the beginning of the large (colon), there is a valve (ileocecal valve) that prevents the passage of chyme [10]. When food is consumed, the stomach alerts the valve which seals. At the same time, the mechanism for moving chyme into the ascending colon (HAPC, see 2.7 below) is activated to make space available for the new chyme [11].

2.7 HAPC-High Amplitude Propagating Contractions

HAPC movement is found only in the large intestine, mainly in ascending and transverse colon [12]. Progressive high-pressure wave-like contractions of 120 mmHg aim at mass transport of contents towards the exit and directly relate to evacuation [5,13]. HAPC's incidence ranges at ~6 times/day mainly on awakening and after eating. Colon kinesiology differs from that of the small intestine, as it depends on some stimulation such as food ingestion [14].

2.8 LAPC-Low Amplitude Propagating Contractions

LAPC also occurs only in the large intestine (84.5% daily) [12,13]. Progressive low-pressure wave-like contractions of 5-40 mmHg occur [5,13]. LAPC not only maintains the tone of the colon and lengthens the intestinal wall to store stool [12], but also propels gases towards the exit and squeezes stools together [5]. It also occurs in retrograde direction in descending/sigmoid colon for more efficient dewatering [2,15].

2.9 RMC-Rectal Motor Complex

Successive retrograde contractions in the rectum serve to retent the feces until evacuation [16]. Contractions' pressure ranges from 15-45 mmHg with frequency of ~139 times/day [17]. Movement duration varies between 3-10 min and contractions' frequency is 3 and 6 contractions/min in upper and lower rectum, respectively [17]).

3 STRENGTH EXPERIMENTS IN GI WALL

Static/dynamic tensile [18–20], compression and *in silico* experiments have served to investigate the material response to stresses. Few experiments, however, have used healthy human tissue (fresh, cadaveric) [21,22] and fewer were *in vivo* [23]. It has been concluded that mechanical stresses are mainly born by two wall layers (submucosa, mucosa), with the other two being mechanically insignificant.

3.1 Static Tensile Strength Experiments In Small Bowel

3.1.1 Samples Along The Longitudinal Muscle Tissue Direction

The characteristic stress-stretch ratio curve (Figure 2) demostrating two peaks was derived for samples along longitudinal muscle tissue direction (cadaveric, fresh). For the fresh tissue (1st peak: 1.368 MPa, 2nd peak: 0.548 MPa), it was observed that the serosa and muscalaris layers were destroyed first, with the remaining two layers bearing the stresses, until destruction of the submucosa and eventual failure of the wall (145.88% for the total strain to failure) [22]. For cadaveric tissue, the stresses were 1st peak: 1.472 MPa, 2nd peak: 0.586 MPa, and the total strain to failure: 153.14% [22].

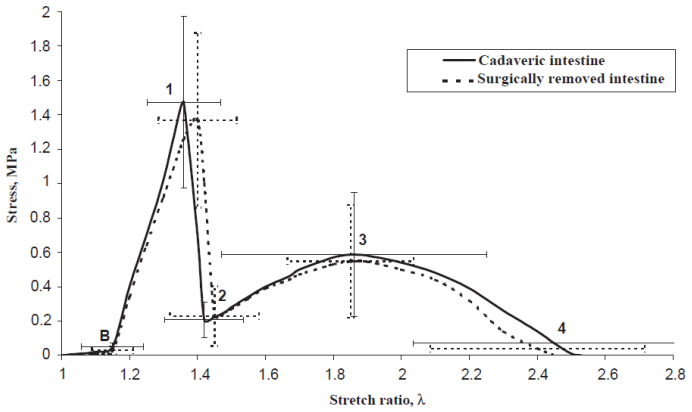

Figure 2. *Stress-stretch ratio curve in human fresh and cadaveric small intestinal tissue. Samples along the longitudinal muscle tissue direction. (Adapted from* [22]*)*

3.1.2 Samples Along The Circular Muscle Tissue Direction

The characteristic stress-stretch ratio curve demostrating one peak was derived for samples along the circular muscle tissue direction (cadaveric, fresh). For the fresh tissue (peak: 0.92 MPa), it was observed that the serosa and muscalaris layers were destroyed first, with the remaining two layers bearing the stresses, until destruction of the submucosa and eventual failure of the wall (138.39% for the total strain to failure) [22]. For cadaveric tissue, the peak stress was 0.83 MPa, and the total strain to failure was 138.9% [22]. All experiments in section 3.1 were conducted uniaxially (without accounting for material anisotropy) in a limited number of human tissue samples [22].

3.2 Static Tensile Strength Experiments In Large Bowel

Cadaveric tissue samples of human colon with varied characteristics were employed. Samples from all parts of the colon (ascending, transverse, descending, sigmoid), with or without smooth muscle fiber (tenia coli), were used in longitudinal and circumferential muscle direction. Stress-strain curves showed that the colon wall is viscoelastic, contractile and anisotropic, with tenia coli playing role in deformation [24].

4 COLLAGEN STRUCTURE

Collagen protein is an important structural element of the extracellular matrix [25]. It is mainly found in the submucosa and mucosa layers of the intestinal tract. The submucosa is responsible for receiving tensions in the intestinal tract and maintaining its geometry [2]. There is a huge lack of literature describing the structure of collagen in healthy human intestinal tissue, with the majority of reports focusing on animal tissue.

4.1 Collagen Structure In Small Bowel

4.1.1 Collagen Structure

Collagen in the small intestine is divided into two networks. In the first, there are collagen fibers (4-6μm diameter) with varied geometric characteristics in the literature [26,27]. In the submucosa of the small intestine, collagen structure is divided

into 3 non-crossed layers that are parallel to the longitudinal muscle tissue with deviations of -30° to 30° [27]. More predominantly, it has been reported that collagen structure consists of two crossed layers (60°-70°), with one clockwise and the other counterclockwise. Both layers are oriented 35°-40° with respect to circular muscle [28].

In the second network, microscopic fibrils (~0.2 μm diameter) of irregular arrangement and random orientation act as a net for attachment of first network fibers. The second network is presumed to transmit the stresses across the fibers [26,27].

4.1.2 Collagen Function

Collagen fibers in tissues have a wavy shape with inconsistent wavelength. The fiber intersections appear to mainly occur with a spatial spacing of about one period. Number/density of crossings and how these affect the material elasticity are not reported [26,29]. The reason why collagen fibers maintain their wavy shape under normal conditions is to impart elasticity of the tissue under stretched conditions [28]. However, since fibers deviate ±30° from the tube axis, their orientation can also change by circumferential stress [30] as shown in uniaxial/biaxial tests on animal tissue [30]. Collagen of the second network [26] and other layers of the intestinal tract (mucosa, muscalaris and serosa) does not show mechanical interest [31].

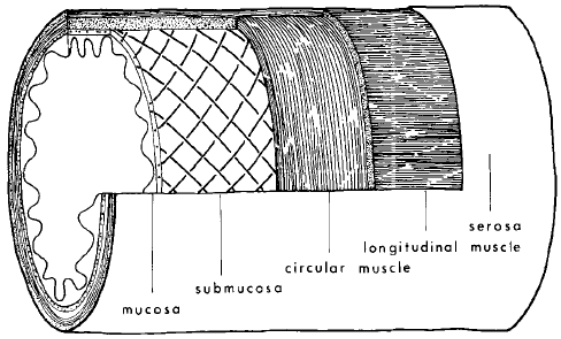

Figure 3. *Representation of intestinal tube and collagen structure. (Adapted from* [28]*)*

4.1.3 Factors That Affect Collagen Structure

One factor that affects the structure of collagen is ageing, with collagen fiber diameter being increased from birth to tissue maturation (adulthood). However, in senescence, the diameter of the fibers and fibrils decreases [26,31], collagen contracts resulting in structure densifications and thinning [32], and the elasticity of the tissue is compromised due to decreased undulations [29].

Diseases is another factor affecting the collagen structure. In bowel cancer, collagen becomes stiffer [32], and in systemic sclerosis, an amount of collagen penetrates the smooth muscle structure and makes the tissue considerably stiffer. In diseases such as GI scleroderma, the amount of collagen increases while fiber orientation changes [2]. Collagen structure is affected by many other diseases.

4.2 Collagen Structure In Large Bowel

The structure of collagen in the submucosa of the colon resembles that of the small intestine. The diameter of the fibers and fibrils remains the same along the length of the colon, with a slight reduction occurring in the last parts of the colon (descending, sigmoid colon and rectum). Also, the number of fibers and fibrils increases in the last

compared to the other parts of the colon. As a result, the last parts of the colon have a more rigid structure [33]. The factors that can affect the structure of collagen in the colon are the area where the collagen is found, age and finally the health of tissue.

5 REFERENCES

[1] Liao, D., Mark, E.B., Zhao, J., Drewes, A.M., and Brock, C. (2020). Modeling and measurement of the mechano-physiological function of the gastrointestinal organs. *Physiological Measurement*. 41 /11.

[2] Siri, S., Zhao, Y., Maier, F., Pierce, D.M., and Feng, B. (2020) .The macro-and micro-mechanics of the colon and rectum I: Experimental evidence. *Bioengineering*. 7/4, p.p. 1–16.

[3] Grønlund, D., Poulsen, J.L., Sandberg, T.H., Olesen, A.E., Madzak, A., Krogh, K., et al. (2017). Established and emerging methods for assessment of small and large intestinal motility. *Neurogastroenterology and Motility*. 29/7.

[4] Ødegaard, S., Nesje, L.B., Lærum, O.D., and Kimmey, M.B. (2012). High-frequency ultrasonographic imaging of the gastrointestinal wall. *Expert Review of Medical Devices*. 9/3, p.p. 263–273.

[5] Kumral, D. and Zfass, A.M. (2018). Gut Movements: A Review of the Physiology of Gastrointestinal Transit. *Digestive Diseases and Sciences*. 63/10, p.p. 2500–2506.

[6] Gayer, C.P. and Basson, M.D. (2009.) The effects of mechanical forces on intestinal physiology and pathology. *Cellular Signalling*. 21/8, p.p. 1237–1244.

[7] Fullard, L., Lammers, W., Wake, G.C., and Ferrua, M.J. (2014). Propagating longitudinal contractions in the ileum of the rabbit-Efficiency of advective mixing. *Food and Function*. 5/11, p.p. 2731–2742.

[8] Seerden, T.C., E P Lammers, W.J., de Winter, B.Y., de Man, J.G., Pelckmans, P.A., and Pelckmans Spatiotemporal, P.A. (2005). Spatiotemporal electrical and motility mapping of distension-induced propagating oscillations in the murine small intestine. *Am J Physiol Gastrointest Liver Physiol*. 289, p.p. 1043–1051.

[9] Deloose, E. and Tack, J. (2016). Redefining the functional roles of the gastrointestinal migrating motor complex and motilin in small bacterial overgrowth and hunger signaling. *Am J Physiol Gastrointest Liver Physiol*. 310, p.p. 228–233.

[10] Simrén, M., Abrahamsson, H., and Björnsson, E.S. (2001). An exaggerated sensory component of the gastrocolonic response in patients with irritable bowel syndrome. *Gut*. 48/1, p.p. 20–27.

[11] Roland, B.C., Ciarleglio, M.M., Clarke, J.O., Semler, J.R., Tomakin, E., Mullin, G.E., et al. (2014). Low ileocecal valve pressure is significantly associated with small intestinal bacterial overgrowth (SIBO). *Digestive Diseases and Sciences*. 59/6, p.p. 1269–1277.

[12] Bassotti G, Clementi M, Antonelli E, et al. (2001). Low-amplitude propagated contractile waves: a relevant propulsive mechanism of human colon. *Digestive and Liver Diseases* 33, p.p. 36-40.

[13] Bassotti, G., de Roberto, G., Castellani, D., Sediari, L., Morelli, A., Section, H., et al. (2005). Normal aspects of colorectal motility and abnormalities in slow transit constipation. *World J Gastroenterol*. 11/18, p.p. 2691–2696.

[14] Bharucha, A.E. (2012). High amplitude propagated contractions. *Neurogastroenterology and Motility*. 24/11, p.p. 977–982.

[15] Zhao, Y., Siri, S., Feng, B., and Pierce, D.M. (2020). The macro-and micro-mechanics of the colon and rectum II: Theoretical and computational methods. *Bioengineering*. 7/4, p.p. 1–15.

[16] Prior A, Fearn UJ, Read NW (1991). Intermittent rectal motor activity: A rectal motor complex. *Gut*. 32/11, 1360–1363.
[17] Auwerda, J.J.A., Bac, D.J., and Schouten, I.-W.R. (2001). Circadian Rhythm of Rectal Motor Complexes. *Diseases of the Colon and Rectum*. 44, p.p. 1328-1332.
[18] Massalou, D., Masson, C., Foti, P., Afquir, S., Baqué, P., Berdah, S. v., et al. (2016). Dynamic biomechanical characterization of colon tissue according to anatomical factors. *Journal of Biomechanics*. 49/16, p.p. 3861–3867.
[19] Bourgouin, S., Bège, T., Masson, C., Arnoux, P.J., Mancini, J., Garcia, S., et al. (2012). Biomechanical characterisation of fresh and cadaverous human small intestine: Applications for abdominal trauma. *Medical and Biological Engineering and Computing*. 50/12, p.p. 1279–1288.
[20] Gao, C. and Gregersen, H. (2000). Biomechanical and morphological properties in rat large intestine. *Journal of Biomechanics*. 33.
[21] Sokolis, D.P. (2021). Variation of passive biomechanical properties of the small intestine along its length: Microstructure-based characterization. *Bioengineering*. 8/3, p.p. 1–18.
[22] Egorov VI, Schastlivtsev I v, Prut E v, et al. (2002). Mechanical properties of the human gastrointestinal tract. *Journal of Biomechanics.* 35, p.p. 1417–1425.
[23] Bharucha AE, Hubmayr RD, Ferber IJ, et al. (2001). Viscoelastic properties of the human colon. *American Journal of Physiology-Gastrointestinal and Liver Physiology*. 281, p.p. G459–G466
[24] Massalou, D., Masson, C., Afquir, S., Baqué, P., Arnoux, P.J., and Bège, T. (2019). Mechanical effects of load speed on the human colon. *Journal of Biomechanics*. 91, p.p. 102–108.
[25] Badylak, S.F., Freytes, D.O., and Gilbert, T.W. (2015). Reprint of: Extracellular matrix as a biological scaffold material: Structure and function. *Acta Biomaterialia*. 23/5, p.p. S17–S26.
[26] Orberg, J.W., Klein, L., and Hiltner, A. (1982). Scanning electron microscopy of collagen fibers in intestine. *Connective Tissue Research*. 9/3, p.p. 187–193.
[27] Klein, L., Eichelberger, H., Mirian, M., and Hiltner, A. (1983). Ultrastructural properties of collagen fibrils in rat intestine. *Connective Tissue Research*. 12/1, p.p. 71–78.
[28] Gabella G (1987) The cross-ply arrangement of collagen fibres in the submucosa of the mammalian small intestine. *Cell Tissue Research*. 248, p.p. 491-497.
[29] Orberg, J., Baer, E., and Hiltner, A. (1983). Organization of collagen fibers in the intestine. *Connective Tissue Research*. 11/4, p.p. 285–297.
[30] Gilbert, T.W., Sacks, M.S., Grashow, J.S., Woo, S.L.Y., Badylak, S.F., and Chancellor, M.B. (2006). Fiber kinematics of small intestinal submucosa under biaxial and uniaxial stretch. *Journal of Biomechanical Engineering*. 128/6, p.p. 890–898.
[31] Yu, J., Zeng, Y., Zhao, J., Liao, D., and Gregersen, H. (2004). Quantitative analysis of collagen fiber angle in the submucosa of small intestine. *Computers in Biology and Medicine*. 34/6, p.p. 539–550.
[32] Despotović, S.Z., Milićević, Đ.N., Krmpot, A.J., Pavlović, A.M., Živanović, V.D., Krivokapić, Z., et al. (2020). Altered organization of collagen fibers in the uninvolved human colon mucosa 10 cm and 20 cm away from the malignant tumor. *Scientific Reports*. 10/1.
[33] Thomson HJ, Busuttil A, Eastwood MA, et al. (1987). Submucosal collagen changes in the normal colon and in diverticular disease. *International Journal of Colorectal Diseases.* 2, p.p. 208-213.

COMETa 2022
6th INTERNATIONAL SCIENTIFIC CONFERENCE
17th - 19th November 2022
Jahorina, B&H, Republic of Srpska
University of East Sarajevo
Faculty of Mechanical Engineering
Conference on Mechanical Engineering Technologies and Applications

KONFIGURISANJE I VERIFIKACIJA REKONFIGURABILNE MAŠINE SA HIBRIDNOM KINEMATIKOM MOMA V3

Saša Živanović[1], Goran Vasilić[2], Branko Kokotović[3], Nikola Vorkapić[4], Zoran Dimic[5], Nikola Slavković[6]

Rezime: U ovom radu je predstavljeno konfigurisanje troosne rekonfigurabilne mašine sa hibridnom kinematikom MOMA V3 koja predstavlja jednu edukacionu stonu glodalicu sa horizontalnim položajem glavnog vretena. U radu se predstavlja prototip mašine, njeno konfigurisanje, sistem za programiranje i upravljanje i verifikacija rada.

Ključne riječi: konfigurisanje, rekonfigurabilna mašina alatka, LinuxCNC, simulacija, programiranje, verifikacija

CONFIGURING AND VERIFICATION OF A RECONFIGURABLE MACHINE WITH HYBRID KINEMATICS MOMA V3

Abstract: This paper presents configuring a 3-axis reconfigurable machine with hybrid kinematics MOMA V3, which represents an educational desktop milling machine with a horizontal position of the main spindle. The paper consider the machine's prototype, its configuring, the system for programming and control and verification of work.

Key words: configuring, reconfigurable machine tool, LinuxCNC, simulation, programming, verification

[1]Prof. dr Sasa Zivanovic, University of Belgrade, Faculty of Mechanical Engineering, Serbia, szivanovic@mas.bg.ac.rs (CA)
[2] Goran Vasilic, Akademija tehničkih strukovnih studija Beograd, Odsek za saobraćaj, mašinstvo i inženjerstvo zaštite, gvasilic@atssb.edu.rs
[3]Doc. dr Branko Kokotovic, University of Belgrade, Faculty of Mechanical Engineering, Serbia, bkokotovic@mas.bg.ac.rs
[4]Nikola Vorkapic, University of Belgrade, Faculty of Mechanical Engineering, Serbia, nvorkapic@mas.bg.ac.rs
[5]Dr Zoran Dimic, Lola Institute, Belgrade, Serbia, zoran.dimic@li.rs
[6]Prof. dr Nikola Slavkovic, University of Belgrade, Faculty of Mechanical Engineering, Serbia, nslavkovic@mas.bg.ac.rs

1 UVOD

Intenzivan razvoj numerički upravljanih mašina alatki (NUMA) predstavlja osnovu savremenih industrijskih tehnoloških sistema. U doba Industrije 4.0 aktuelni trendovi unapređenja industrijske proizvodnje se ogledaju i kroz pravce razvoja savremenih mašina alatki kao što su [1,2]: usvajanje koncepta digitalizacije i integrisanja virtuenih mašina alatki sa sistemima za njihovo programiranje i upravljanje, uvođenje novih koncepcija mašina alatki baziranih na paralelnoj i hibridnoj kinematici, prilagođavanje specifičnim potrebama pojedinih grana industrije, uvođenje rekonfigurabilnih [3] i prilagodljivih mašina alatki, dalji razvoj nadzora i dijagnostike procesa obrade na mašinama alatkama, itd.

U radu se razmatra konfigurisanje mašine na bazi dvoosnog rekonfigurabilnog paralelnog mehanizma [4,5], koji pripada generaciji rekonfigurabilnih tehnoloških modula, koji može egzistirati samostalno ili u kombinaciji sa drugim mehanizmima, gradeći nove mašine alatke. Rezultat konfigurisanja je projekat i realizacija jedne rekonfigurabilne troosne glodalice sa upravljanjem otvorene arhitekture koja u osnovi ima rekonfigurabilni dvoosni paralelni mehanizam MOMA (MOdularna MAšina alatka sa upravljanjem otvorene arhitekture) [4,5]. Sa još jednom dodatnom serijskom traslatornom osom čini troosnu mašinu sa hibridnom kinematikom. Prve varijante ove mašine pokazane su na slici 1.

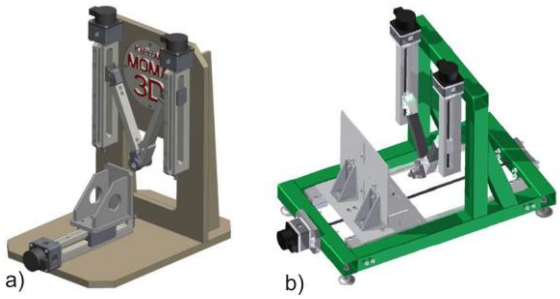

Slika 1. *Prikaz polaznih varijanti 3-osne rekonfigurabine mašine MOMA*

MOMA je uspostavljena kao sistem sastavnih elemenata (modularni sistem), na osnovu koga se može vršiti rekonfigurisanje i hardverskog i softverskog dela sistema [4]. MOMA je u osnovi namenjena za edukaciju u: (i) konfigurisanju i rekonfigurisanju novih mašina alatki, (ii) programiranju i (iii) upravljanju na bazi softvera otvorene arhitekture LinuxCNC [6].

U nastavku se daje opis strukture razmatrane mašine MOMA V3, dok je u trećem poglavlju predstavljeno konfigurisanje virtuelnog prototipa mašine. U četvrtom poglavlju predstavljen je sistem za programiranje i upravljanje mašinom, sa upotrebom virtuelne mašine za potrebe verifikacije programiranja. Poglavje 5 pokazuje ekeprimentalnu verifikaciju mašine kroz njen probni rad.

2 OPIS REKONFIGURABILNE MAŠINE MOMA V3

Ravanski rekonfigurabilni paralelni mehanizam MOMA je mehanizam sa dva stepena slobode, koji se sastoji od dve identične pogonske translatorne ose, po kojima se kreću dva klizača. Maksimalan hod kliazača duž pogonskih osa iznosi 200 mm. Klizači su pomoću dve spojke povezani u paralelni mehanizam. Spojke su sa klizačima i međusobno povezane obrtnim zglobovima, obrtna veza između spojki je ujedno i pokretna platforma paralelnog mehanizma. Dvoosni rekonfigurabilni paralelni mehanizam se konfiguriše prema programu gradnje [4]. Prikaz osnovnih pet tipova (M1 do M5) iz plana gradnje stone dvoosne rekonfigurabilne mašine MOMA je dat na slici 2.

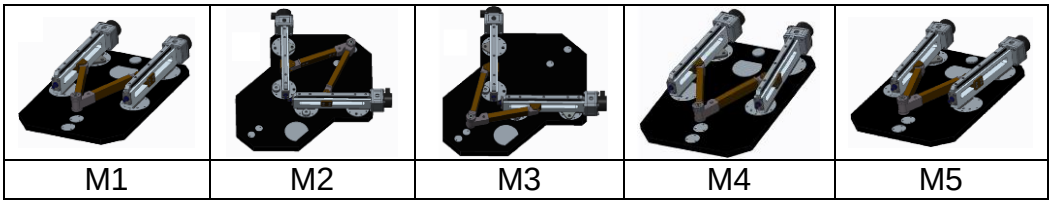

Slika 2. *Osnovni tipovi dvoosnog paralelnog mehanizma MOMA*

Paralelni mehanizam je baziran na modularnom principu, dok se njegova rekonfigurabilnost ogleda u tome što se međusobni položaj pojedinih modula translatornih osa može menjati, a takođe je moguće izvršiti promenu dužina spojki, pošto postoji familija različitih dužina spojki u tri nazivne veličine (200, 195 i 180 mm). Konfiguracija paralelnog mehanizma se može lako i brzo menjati prema programu gradnje [4,5,7,8]. Programom gradnje je definisana svaka od mogućih konfiguracija paralelnog mehanizma. Kao osnova za gradnju troosne rekonfigurabilne mašine sa hibridnom kinematikom koriste se izabrana tri tipa mašine i to M1, M4 i M5, sa slike 2, uz dodatnu serijsku translatornu osu, što je pokazano na slici 3.

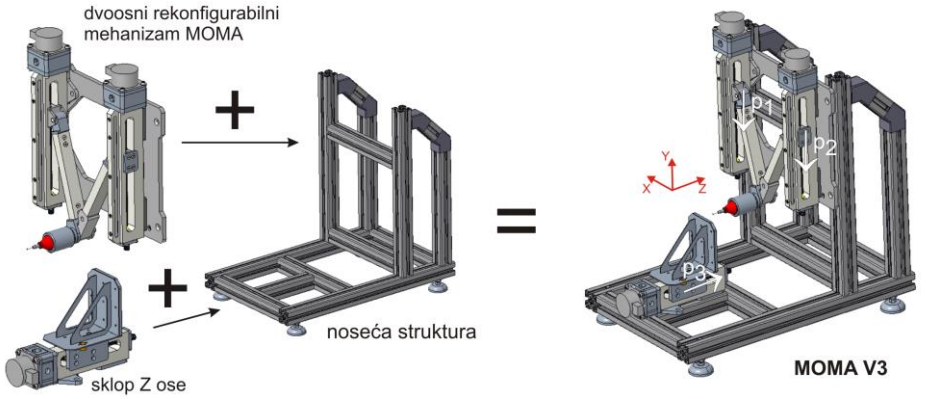

Slika 3. *Mašina MOMA V3 sa hibridnom (paralelno-serijskom) kinematikom*

CAD model virtuelnog prototipa mašine sa hibridnom kinematikom MOMA V3 je prikazan na slici 3 i predstavlja troosnu horizontalnu glodalicu sa glavnim vretenom koje se pokreće paralelnim mehanizmom po osama X i Y dok se pomeranje obratka ostvaruje po Z osi (p3). Paralelni mehanizam ima dve pogonske translatorne ose sa klizačima p1 i p2. Paralelni mehanizam čine dve spojke koje su obrtnim zglobovima povezane prvo međusobno a potom i za dva klizača (p1 i p2). Osa obrtnog zgloba, gde su povezane spojke čini pokretnu platformu mehanizma i u ovoj osi se postavlja glavno vreteno. Analiza kinematičkog modela, rešenje inverzne i direktne kinematike, radni prostor i analiza singulariteta dati su u radu [7].

3 KONFIGURISANJE VIRTUELNOG PROTOTIPA

Kao glavni rezultat konfigurisanja dobijaju se, konfiguracije mašine MOMA V3. Tokom konfigurisanja bilo je potrebno preći put, od geometrijskih i kinematičkih modela, preko Jakobijana, inverzne i direktne kinematike, analize singulariteta, analize

radnog prostora, optimizacije nekih elemanta mašine (npr. dužina spojki), do dobijanja virtuelnog prototipa, simulacija na virtuelnim prototipovima i konfigurisanja hardvera mašine na bazi raspoloživog fonda modula i testiranja upravljanja za konačnu verifikaciju konfigurisane nove mašine alatke [7,8].

Varijantnost strukture već prikazanog osnovnog rekonfigurabilnog dvoosnog paralelnog mehanizma omogućava, po definiciji, široku primenljivost ovog mehanizma kao tehnološkog modula za vertikalne i horizontalne troosne mašine alatke sa hibridnom (paralelno-serijskom) kinematikom. Za konfigurisanje razmatrane mašine uspostavljen je sistem sastavnih elemenata, ili modularni sistem, sa bazom raspoloživih modula i pravilima pomoću kojih je moguće njeno rekonfigurisanje [4,8].

Konfigurisanje virtuelnog prototipa mašine MOMA V3 je realizovano u okviru CAD/CAM sistema PTC Creo. Sve komponente i kompletiranje glavnog sklopa mašine su realizovani u CAD/CAM okruženju, pri čemu je iskorišćena mogućnost sklapanja mašine sa odgovarajućim kinematičkim vezama. Ovo omogućava korišćenje opcije simulacije rada kompletnog virtuelnog prototipa po zadatom programu. Potrebne kinematičke veze za razmatranu troosnu mašinu sa hibridnom kinematikom su tri translacije (p1, p2 i p3) koje koriste vezu tipa klizača (Slider), i 3 rotacije, koje koriste obrtne veze (Pin), na mestima veze spojki paralelnog mehanizma sa klizačima i međusobno, slika 4a.

Nakon definisanja kinematičkih veza pokretnih delova mašine, potrebno je napraviti vezu između koordinatnih sistema na obratku i alatu sa jedne strane i virtuelne mašine sa druge strane u okviru korišćenog CAD/CAM sistema PTC Creo [9]. Na virtuelnoj mašini alatki se definišu koordinatni sistem MACH_ZERO, na radnom stolu i TOOL_POINT na glavnom vretenu, slika 4b. Koordinatne sisteme sa istim nazivima imaju i obradak i alat. Ovi koordinatni sistemi se koriste tako da se njihovim poklapanjem ostvaruje postavljanje virtuelnog alata na virtuelnu mašinu i virtuelnog obratka sa pripremkom, na radni sto virtuelne mašine. Nakon ovako izvedenog virtuelnog baziranja obratka i postavljanja alata, moguće je pokrenuti simulaciju rada virtuelne mašine alatke po zadatom programu, opcijom Machine Play [9].

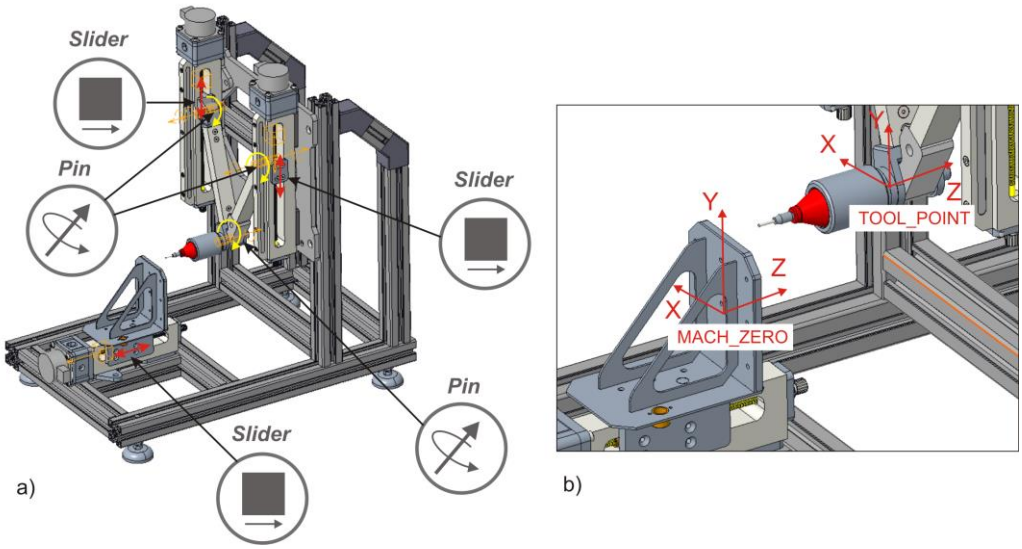

Slika 4. *Prikaz kinematičkih veza i koordinatnih sistema na virtuelnom prototipu mašine*

4 SISTEM ZA PROGRAMIRANJE I UPRAVLJANJE

Kao sistem za programiranje planirano je korišćenje raspoloživog CAD/CAM sistema PTC Creo, u kome je i konfigurisan virtueni prototip, dok je u pogledu realizacije sistema upravljanja izabran sistem otvorene arhitekture baziran na LinuxCNC sistemu koji je od ranije poznat i kao EMC2 (Enhanced Machine Control) [6,9]. U ovom poglavlju su date osnovne informacije o okruženju za programiranje, koje uključuje i virtuelnu mašinu za verifikaciju putanje alata, kao i informacije o konfigurisanju upravljanja otvorene arhitekture na bazi LinuxCNC sistema.

4.1 Sistem za programiranje

Kao sistem za programiranje razmatraju se dva pristupa. Prvi klasičan koji se odnosi na programiranje primenom G koda, odnosno prema standardu ISO6983, i novi pristup programiranju NUMA, poznatiji kao objektno orijentisano programiranje ili programiranje primenom STEP-NC protokola [10,11].

4.1.1 Programiranje primenom CAD/CAM sistema

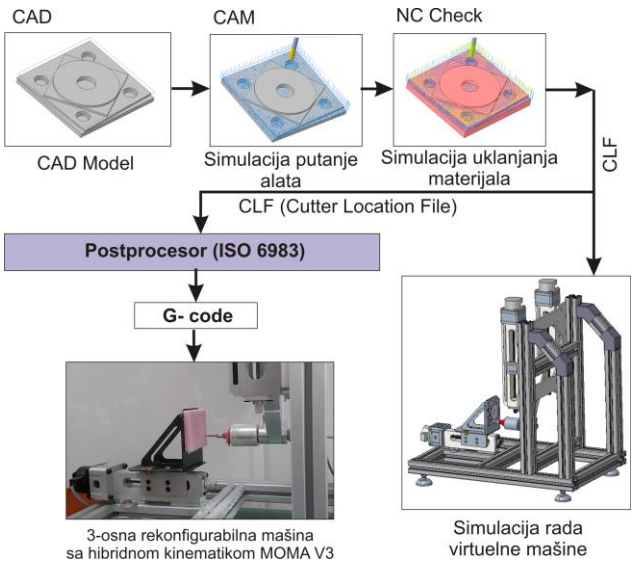

Slika 5. *Osnovna struktura sistema za programiranje prienom CAD/CAM sistema*

Na slici 5 je prikazana osnovna struktura sistema za programiranje. Verifikacija programa je moguća simulacijom putanje alata, simulacijom uklanjanja materijala i simulacijom rada virtuelne mašine koja radi po zadatom programu u CLF formatu. Postprocesiranje se vrši kao za troosnu glodalicu, gde se dobija G kod prema standardu ISO6983, koji je u ovom slučaju po formatu sličan programima za Fanuc CNC sisteme. Za prikazani primer test probnog dela sa slike 5, u poglavlju 5 je pokazana i obrada ovog dela.

4.1.2 Programiranje primenom protokola STEP-NC

Za pripremu uvođenja novog metoda programiranja primenom STEP-NC standarda, takođe je razmatrano konfigurisane i inegrisanje virtuelne mašine koja radi po programu u STEP-NC formatu u okruženju softvera STEP-NC Machine, slika 6.

Danas mali broj mašina može direktno interpretirati STEP-NC program. S tim u

vezi, za direktnu verifikaciju STEP-NC programa korisno je koristiti konfigurisane virtuelne mašine koje mogu raditi u okruženju STEP-NC Machine i izvršavati programe u *.stpnc formatu, slika 6. Razmatrana mašina MOMA V3 je konfigurisana i integrisana u okruženje STEP-NC Machine, prema metodologiji koja je detaljno data u [11]. Za programiranje je primenjen indirektni metod programiranja [10,11], dok je prilikom obrade STEP-NC program preveden u G kod, pošto razmatrana mašina može da interpretira samo G kod.

Kao primer za obradu iskorišćen je tipičnan STEP-NC probni deo. Za obradu ovog dela korišćeno je čeono vretenasto glodalo prečnika 3mm i obradak od stirodura. Pri obradi dela izvršena su tri zahvata (workingsteps – WS): WS_1 glodanje ravne površine, WS_2 glodanje cilindričnog džepa i WS_3 glodanje pravougaonog džepa, slika 6. Na slici 6 pokazana je simulacija obrade dela na mašini MOMA V3 koja je učitana iz baze mašina kao nova dodata mašina, koja je prethodno konfigurisana u STEP-NC Machine okruženju. Nakon simulacije na virtuelnoj mašini u STEP-NC Machine okruženju, izvršeno je prevođenje programa na G kod korišćenjem exoprt opcije za generisanje Fanuc G koda koji je učitan u upravljanje mašine nakon čega je realizovana i obrada dela, što je pokazano u poglavlju 5.

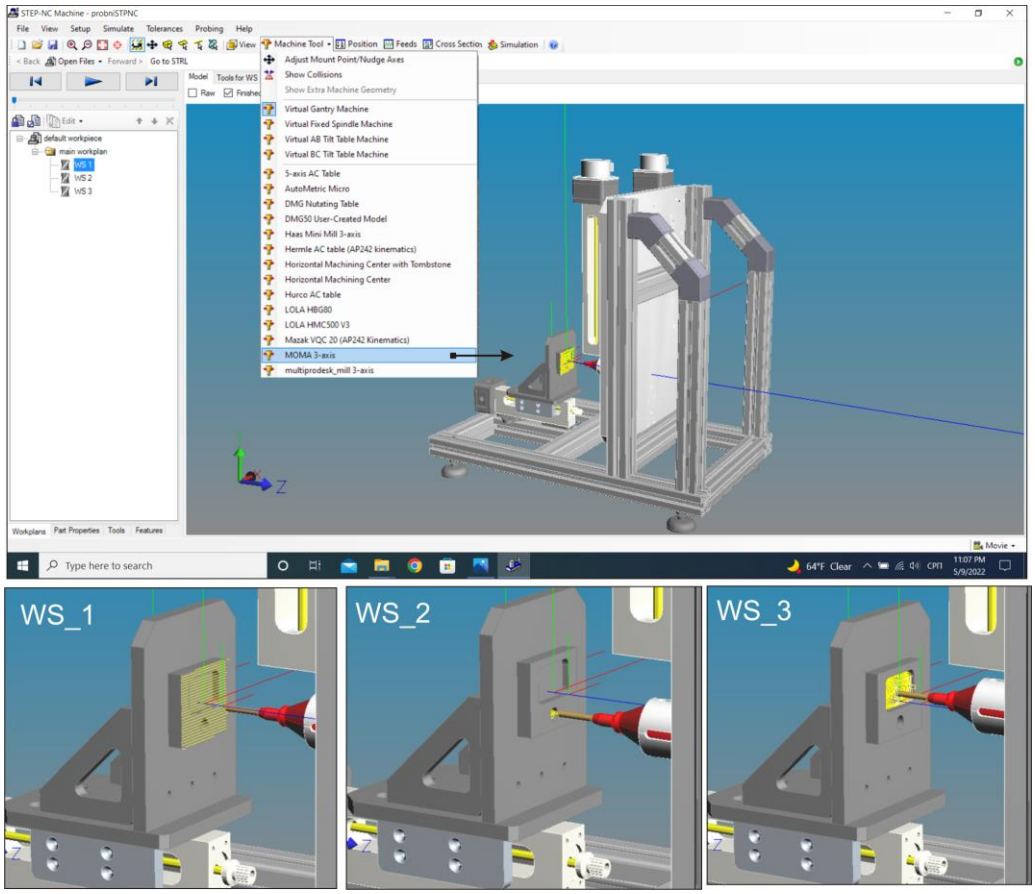

Slika 6. *Simulacija rada integrisane virtuelne mašine u okruženju STEP-NC Machine*

4.2 Sistem za upravljanje

Za razmatranu rekonfigurabilnu mašinu sa hibridnom kinematikom, čije se konfigurisanje razmatra u ovom radu kao sistem za upravljanje izabran je LinuxCNC koji predstavlja real-time softver za upravljanje mašinama alatkama i robotima, čiji se kod može slobodno koristiti, modifikovati i distribuirati (GNU-General Public License) [6].

Softverska struktura LinixCNC-a sadrži četiri osnovna programska modula i to: kontroler kretanja (EMCMOT), kontroler diskretnih ulaznih/izlaznih signala (EMCIO), kontroler procesa koji ih koordiniše (EMCTASK) i kolekciju grafičkih korisničkih inerfejsa (GUI). Detaljnije o ovoj strukturi se može videti u [12].

S obzirom da kinematika razmatrane mašine nije trivijalna, neophodna je bila zamena funkcija trivijalne kinematike, kinematikom za mašinu MOMA V3 u kojoj su implementirana rešenja i inverzne i direktne kinematike [7,8] u C jeziku. Prilikom integrisanja modela upravljanja, definišu se i parametri mašine, kao i referentni položaji svih osa, a na kraju se realizuje prevođenje i povezivanje softvera.

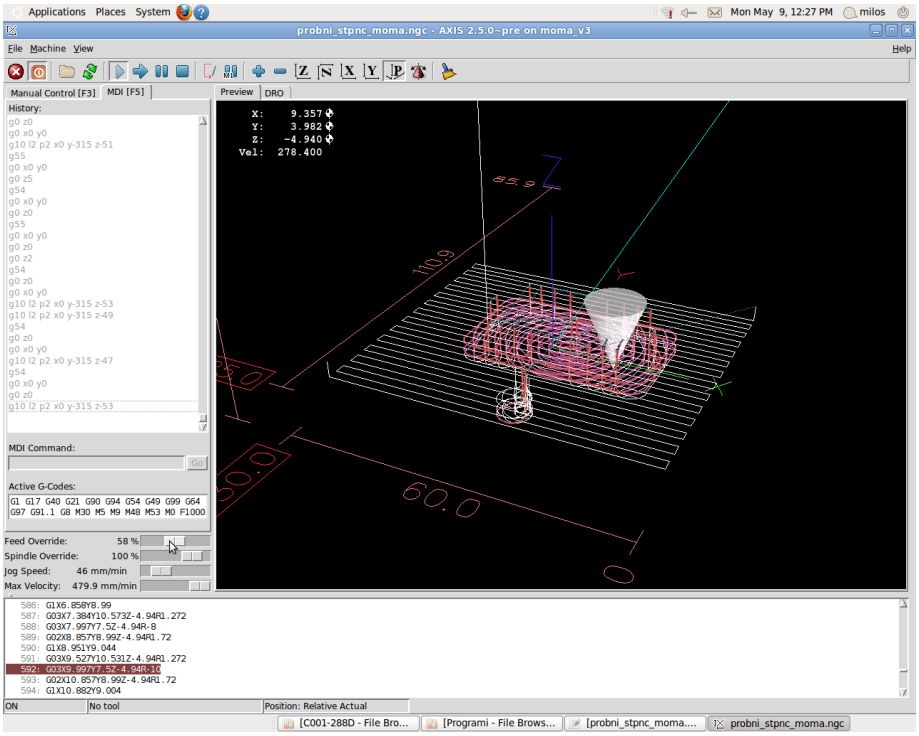

Slika 7. *Grafički korisnički interfejs AXIS*

Grafički korisnički interfejs - GUI (Graphical User Interface) predstavlja eksterni program koji komunicira sa LinixCNC-om slanjem komandi kao što su: uključenje mašine, prelazak na automatski režim rada, start programa, isključenje. GUI može slati i manuelne poruke, inicirane od operatera, kao što su: pomeranje osa mašine u ručnom režimu (JOG) ili slanje svih osa u referentnu poziciju (HOME AXES). Najčešće je u upotrebi Axis korisnički grafički interfejs, koji je korišćen za pokazano upravljanje mašinom MOMA V3 i prikazan je na slici 7, sa učitanim programom za programiranu

test konturu, koja je analizirana u prethodnom poglavlju. Ovo okruženje je vrlo intuitivno za rad, sa prepoznatljivim ikonicama koje olakšavaju rad operatera. Pored toga, pogodnost Axis okruženja je i mogućnost integracije sa virtuelnom mašinom, što je za sada realizovano za dvoosni paralelni mehanizam [12], a u planu je da se realizuje i za kompletnu mašinu sa hibridnom kinematikom.

5 VERIFIKACIJA PROTOTIPA – PROBNI RAD

Verifikacija prototipa mašine MOMA V3 realizovana je tokom probnog rada obradom izabranih radnih predmeta. Prvi se odnosi na test radni predmet za ispitivanje radne tačnosti NUMA, koji je skaliran i prilagođen merama radnog prostora mašine. Na ovaj način se postavlja prvo i najvažnije ispitivanje: provera da li sistem za upravljanje korektno interpolira putanju alata i da li alat zaista vodi po toj putanji. Pošto se u radu predstavljeni klasičan i novi metod programiranja razmatrane mašine pripremljeni su i programi za dva primera.

Prvi je primer sa slike 5, koji se odnosi na skalirani i prilagođeni test radni premet za ispitivanje geometrijske tačnosti NUMA, koji je obrađen i pokazan na slikama 8a,b. Materijal obratka je mekani materijal stirodur, a alat veretenasto ravno glodalo prečnika 3 mm.

Drugi primer se odnosi na verifikaciju indirektnog metoda programiranja primenom STEP-NC protokola obradom odgovarajućeg probnog dela, čija je simulacija obrade pokazana na slici 6, a simulacija putanje u sistemu za upravljanje na slici 7.
Ovo je uobičajeni probni deo koji se sastoji od tri osnovna zahvata i čija je obrada, takođe vršena na pripremku od stirodura alatom prečnika 3 mm, pokazana na slikama 8c,d.

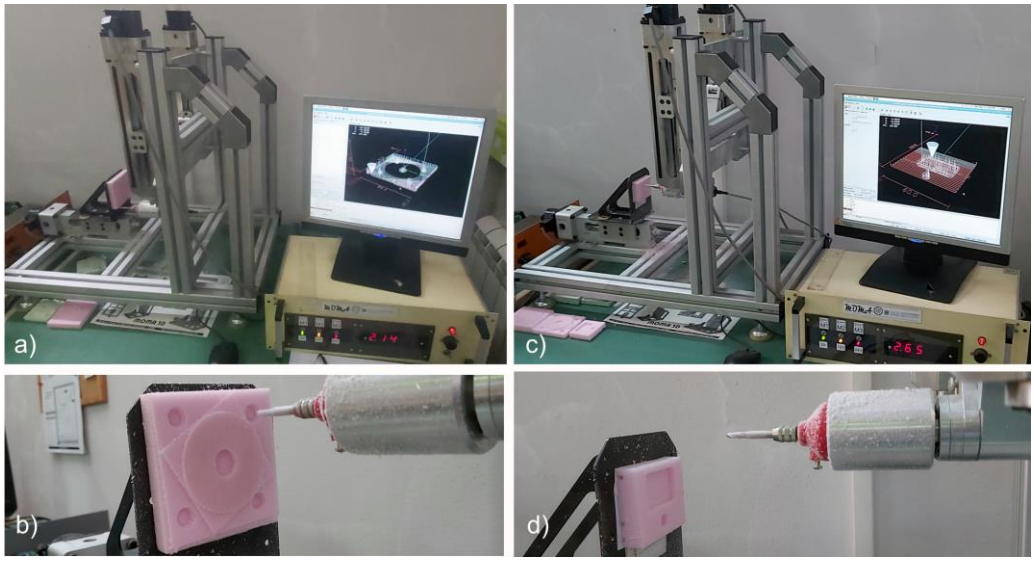

Slika 8. *Obrada test probih delova*

Na osnovu realizovanih eksperimenata obrade tokom probnog rada mašine može se zaključiti, da je konfigurisanje virtuelnog i stvarnog prototipa, kao i odgovarajućeg upravljanja za mašinu korektno, odnosno virtuelna mašina daje veran prikaz rada i iscrtanu test konturu kao i na stvarnoj mašini. Ovo može biti od značaja

za: (i) uvežbavanje rada na rekonfigurabilnim obradnim sistemima, (ii) verifikaciju programa obrade pre njegovog izvršenja na stvarnoj mašini, (iii) rekonfigurisanje upravljanja prilikom promene konfiguracije mašine, (iv) edukaciju za programiranje postojećim (G kod) i novim metodama programiranja (STEP-NC), itd.

6 ZAKLJUČCI

U radu je prikazano konfigurisanje jedne horizontalne 3-osne mašine sa hibridnom kinematikom, koja sadrži rekonfigurabilni paralelni mehanizam koji u kombinaciji sa serijskom translatrnom osom može da predstavlja realnu koncepciju za gradnju industrijskih mašina ovog tipa. Mašina predstavjena u ovom radu je edukaciona, laboratorijskog tipa sa konceptom CNC upravljanja otvorene arhitekture za mašine alatke specifične konfiguracije.

Razmatrana mašina MOMA V3 prati aktuelne trendove u razvoju savremenih mašina alatki kao što su: (i) osavremenjavanje mehaničke strukture u smislu uvođenja novih koncepcija mašina alatki baziranih na paralelnoj i hibridnoj kinematici; (ii) prilagođavanje specifičnim potrebama pojedinih grana industrije, uvođenjem rekonfigurabilnih i prilagodljivih mašina alatki; (iii) razmatranje novih metoda u programiranju NUMA, na bazi protokola STEP-NC; (iv) usvajanje pristupa digitalizacije i virtuelizacije u skladu sa, u svetu usvojenim, strategijama unapređenja industrijske proizvodnje pod paradigmom Industrije 4.0.

Pravci daljeg razvoja mašine MOMA V3 podrazumevaju dalje unapređenje sistema za upravljanje i integraciju virtuelne mašine u sistem upravljanja.

ZAHVALNOST

U okviru ovog rada saopštavaju se rezultati istraživanja koja su realizovana u okviru projekta “Integrisana istraživanja u oblasti makro, mikro i nano mašinskog inženjerstva“ i podprojekta TR35022 „Razvoj nove generacije domaćih obradnih sistema“, koji finansijski podržava Ministarstvo prosvete, nauke i tehnološkog razvoja Vlade Republike Srbije po Ugovoru 451-03-68/2022-14/200105, od 4.02.2022. godine.

LITERATURA

[1] Živanović, S., Tabaković, S., Zeljković, M. (2018). Machine tools and industry 4.0 - trends of development, Invited paper - Plenary lectures, Proceedings of the 4th international scientific conference ”Conference on Mechanical Engineering Technologies and Applications” COMETa2018, University of East Sarajevo Faculty of Mechanical Engineering, East Sarajevo-Jahorina, RS, B&H.

[2] Tabaković, S., Zeljković, M., Živanović, S. (2017). Savremene mašine alatke – trendovi u edukaciji, Konferencija sa međunarodnim učešćem - Primena novih tehnologija i ideja u školskom inženjerskom obrazovanju, Zbornik radova, Rad po pozivu, str. 9-17, Tehnička škola Požega.

[3] Koren Y., Heisel U., Jovane F., Moriwaki T., Pritschow G., Ulsoy G., Brussel H.V. (1999). Reconfigurable Manufacturing Systems, *Annals of the CIRP*, 48/2, pp. 527-540.

[4] Živanović S., Vasilić, G. (2014). Variants of configuring the 2-axis reconfigurable parallel mechanism - MOMA, Proceedings of 2nd International Scientific Conference Conference on Mechanical Engineering Technologies and

Applications COMETa 2014, pp.33-40, University of East Sarajevo, Faculty of Mechanical Engineering, Jahorina, RS, B&H.

[5] Vasilic, G., Živanović, S. (2016). Modelling and analysis of 2-axis reconfigurable parallel mechanism MOMA with translatory actuated joints. *TECHNICS special edition*, pp. 59-66.

[6] Linux CNC, Enhanced Machine Control - EMC2, http://www.linuxcnc.org/ , pristupljeno 17.10.2020.

[7] Vasilic, G., Zivanovic, S., Kokotovic, B. (2017). Modelling and analysis of 3-axis reconfigurable hybrid kinematics mechanism with translatory actuated joints, Proceedings of 5th International Conference on Advanced Manufacturing Engineering and Technologies, NEWTECH 2017, Editors: Majstorovic, V., Jakovljevic, Z., Lecture Notes in Mechanical Engineering, pp. 429-441, 5th – 9th June 2017, Belgrade, Serbia, Springer International Publishing AG 2017.

[8] Živanović, S., Glavonjić, M., Kokotović, B., Dimić, Z. (2014). Stona dvoosna rekonfigurabilna mašina sa paralelnom kinematikom – MOMA, Tehničko rešenje (Novi laboratorijski proizvod, M82), Univerzitet u Beogradu, Mašinski fakultet.

[9] Tabakovic, S., Zivanovic, S., Zeljkovic, M., Dimic, Z. (2021). Konfigurisanje nove edukacione mašine alatke na bazi mehanizma sa hibridnom kinematikom, Časopis *Tehnika,* Vol. 71, No. 5, str 603-612.

[10] Zivanovic, S., Vasilic, G. (2017). A New CNC Programming Method using STEP-NC Protocol, Faculty of Mechanical Engineering, Belgrade, *FME Transactions*, ISSN 1451-2092, Vol. 45, No. 1, pp. 149-158.

[11] Zivanovic, S., Slavkovic, N. (2021). Programming of machine tools and robots for machining using STEP-NC in the era of Industry 4.0, Keynote Lecture, Proceedings of the 15th International Conference on Accomplishments in Mechanical and Industrial Engineering DEMI 2021, pp. 3-26.

[12] Živanović, S., Dimić, Z., Vasilić, G., Kokotović, B. (2018). Konfigurisanje virtuelne rekonfigurabilne dvoosne mašine sa paralelnom kinematikom integrisane sa CNC sistemom otvorene arhitekture na bazi EMC2 softvera, *TEHNIKA,* Časopis saveza inženjera i tehničara Srbije, Vol. 4, str 519-526.

COMETa 2022
6th INTERNATIONAL SCIENTIFIC CONFERENCE
17th - 19th December 2022
Jahorina, B&H, Republic of Srpska
University of East Sarajevo
Faculty of Mechanical Engineering
Conference on Mechanical Engineering Technologies and Applications

KOLABORATIVNI ROBOTI U ZADACIMA MAŠINSKE OBRADE PRIMENA I PROGRAMIRANJE

Slobodan Tabaković [1], Saša Živanović [2]

Rezime: Aktuelne strategije razvoja industrije u pravcu digitalizacije u koje spadaju Industrija 4.0 i 5.0 obuhvataju automatizaciju industrijske proizvodnje i u operacijama izrade proizvoda koji obuhvataju neposredno učešće čoveka. To se najčešće odnosi na procese manipulacije i montaže. U radu se analzira mogućnost primene kolaborativnih robota u segmentu industrijske proizvodnje koji pored neposrednog učešća čoveka zahteva i mašinsku obradu materijala. To se pre svega odnosi na obradu materijala skidanjem ili dodavanjem materijala.

Ključne riječi: kolaborativni roboti, programiranje, mašinska obrada

COLLABORATIVE ROBOTS IN MACHINING TASKS APPLICATION AND PROGRAMMING

Abstract: Modern strategies for developing the industry in the direction of digitization, such as Industry 4.0 and 5.0, include the automation of industrial production in manufacturing operations that include direct human participation. This most often refers to the processes of manipulation and assembly. The paper analyzes the possibility of using collaborative robots in the segment of industrial production, which, in addition to direct human participation, also requires machining materials. It primarily refers to the processing of the material by removing or adding material.

Key words: collaborative robots, robot programming, machining

1 UVOD

Najvažnija merila razvoja ljudskog društva u poslednjih dve stotine godina obuhvataju stanje industrijskog sektora i trendove njegovog usavršavanja. Samim tim su se za ključne promene u industrijskoj proizvodnji vezivali periodi značajnog

[1] prof. dr Slobodan Tabaković, Univerzitet u Novom Sadu, Fakultet tehničkih nauka Novi Sad, tabak@uns.ac.rs (CA)
[2] prof dr Saša Živanović, Univerzitet u Beogradu, Mašinski fakultet, Beograd, Srbija, szivanovic@mas.bg.ac.rs

unapređenja kvaliteta ljudskog života [1]. Tako se mehanizacija proizvodnje (I industrijska revolucija) vezuje za razvoj modernog društva, a digitalizacija proizvodnje za društvo zasnovano na Internet tehnologiji. Savremeni trendovi koji se poslednjih godina javljaju kao nastavak procesa digitalizacije u industriji i posledica globalne pandemije ukazuju na potrebu za istraživanjima u pravcu stvaranja humano organizovane proizvodnje koja obuhvata integraciju ljudskog rada sa savremenim proizvodnim sistemima [2].

Slika 1. *Kolaborativni roboti u procesu montaže*

Jednu od karika ovakve proizvodnje predstavljaju nove generacije robota koncipiranih i projektovanih za rad u ljudskom okruženju čime se omogućava da savremeni roboti pored jednog od osnovnih sredstava fleksibilne automatizacije u industriji postanu i činioci koji direktno pomažu ljudima u pojedinim fazama proizvodnje koja je bazirana na manualnom ljudskom radu. Tu se pre svega misli na aktivnosti dodavanja delova u procesu montaže i pojedinim operacijama izrade proizvoda [3]. Na slici 1 je prikazan primer saradnje čoveka i robota. Ovako koncipirani, kolaborativni roboti prema specifikacijama mogu da se koriste kao automatizovani sistemi koji omogućuju delimičnu automatizaciju ljudskog rada u operacijama: mašinske obrade ivica radnih predmeta (obaranje ivica), merenja i kontrole, zakivanja i aditivnih tehnologija kao što su nanošenje materijala kao i površinske zaštite.

U radu se opisuje deo istraživanja sprovedenog sa ciljem analize mogućnosti primene kolaborativnih robota u operacijama mašinske obrade materijala rezanjem sa stanovišta programiranja i tačnosti.

2 KOLABORATIVNI ROBOTI

Koncept industrijskih robota sposobnih za rad u ljudskom okruženju je nastala iz potrebe za proširenjem oblasti automatizacije. Time je omogućena fleksibilna automatizacija i na radnim mestima koja podrazumevaju učešće ljudskog rada [4] što se primenjuje u manjim i srednjim serijama.

Značaj kolaborativnih robota u industriji danas raste vrlo brzo. Oni imaju nekoliko prednosti u odnosu na klasične industrijske robote: mogu da rade zajedno sa ljudima, njihovom okruženju je potrebno manje prilagođavanja, mogu se lako transportovati itd. S obzirom da su njihovi zglobovi elastičniji od onih kod klasičnih industrijsih robota, ovi roboti su manje pogodni za zadatke mašinske obrade. Međutim, kolaborativni roboti mogu biti opremljeni, senzorom sila i fleksibilnim glavnim vretenom kao end-efektorom, koji se može koristiti i za obrade glodanjem na mekim materijalima [5].

Slika 2. *Senzor sile za Fanuc robote*

Bezbednost učesnika proizvodnje u okružanju robota se obezbeđuje ugradnjom odgovarajućih davača sposobnih da detektuju kretanja, kontakte i sile koje su po pravcu i intenzitetu van očekivanih za kretanje predviđenog tereta po programiranoj putanji. Karakteristike komercijalnih robota su definisane ISO-TS 15066 standardom [6]. Komercijalne verzije kolaborativnih robota najčešće koriste senzore sile ili momenta (slika 2) uz moguće dodatne elemente u vidu lidar sistema ili kamera.

3 METODE PROGRAMIRANJA KOLABORATIVNIH ROBOTA

Metode programiranja industrijskih robota se usavršavaju od početka njihovog razvoja. U tom, skoro sedamdeset godina dugom periodu je razvijen veći broj različitih pristupa definisanju putanje izvršnog organa (end-efektora), funkcije kretanja kao i komunikacije sa drugim, automatizovanim, sistemima u proizvodnji [7-12]. Metode programiranja se najčešće dele na direktne i indirektne koji se realizuju u blizini robota uz primenu jedinice za obučavanje ili na udaljenim računarima primenom odgovarajućeg softvera.

Razlog za složenost programiranja robota za zadatke mašinske obrade je u tome što svaki proizvođač robota uglavnom koristi svoj sopstveni programski jezik robota, jer ne postoji industrijski standard [13,14,15]. Programiranje robota u zadacima mašinske obrade može se vršiti na nekoliko načina [9]: (i) korišćenjem CAD/CAM sistema za programiranje višeosnih mašina alatki uz korišćenje odgovarajućih translatora CAM podataka (Cutter Location File – CLF i G-kod) na jezik robota, (ii) postprocesiranjem CLF-a, od trenutnih CAD/CAM sistema za višeosnu obradu do G-koda ako kontroler robota može direktno da interpretira G-kod [13], (iii) korišćenjem novog metoda programiranja primenom protokola STEP-NC za zadatke mašinske obrade uz upotrebu razvijenih translatora za prevođenje u G kod ili jezik robota [9] (iv) koristeći specijalizovani CAM softver za programiranje robota za obradu koji generiše direktno jezik robota koristeći odgovarajuće postprocesore za robote (RoboGuide, RobotStudio, itd.).

Programiranje kolaborativnih robota se sprovodi na isti način uz uvođenje dodatnih naredbi kojima se reguliše ponašanje robota u slučajevima kontakta sa subjektima u okolini. Ovo je naročito važno u pripremi aktivnosti kao što je mašinska obrada. Prilikom kretanja alata osim neželjenog kontakta sa ljudskim subjektima postoji značajna mogućnost kolizije sa steznim priborom kao i pojave porasta opterećenja na vretenu usled promene dubine rezanja ili nehomogenosti materijala obrade. Kod većine komercijalnih robota lokalne promene nosivosti robota (odnosno granicu pojave kontakta) obezbeđuje uvođenjem sigurnosnih naredbi u programske rečenice. Japanski proizvođač Fanuc omogućava uvođenje PAYLOAD funkcije kojom se reguliše dozvoljeno opterećenje robota prilikom kretanja po programiranoj putanji. Ova funkcija preuzima vrednosti iz odgovarajuće matrice čime se omogućava definisanje različitih vrednosti preopterećenja različitim programskim rečenicama. Pri tome se preopterećenja definišu kao vektorske veličine što omogućava predviđanje potencijalnih kolizija. Na slici 3 je prikazan primer dela programa za kolaborativni robot sa definisanim lokalnim naredbama koje određuju nosivost.

```
  1:  !SimPRO Auto-Generated TPP ;
  2:  !test_komad, Zljeb ;
  3:  COL DETECT ON ;
  4:  UFRAME_NUM[GP1]=1 ;
  5:  UTOOL_NUM[GP1]=2 ;
  6:  PAYLOAD[1:EOAT w/o part] ;
  7:  MESSAGE[...] ;
  8:  ;
  9:  !Segment1 ;
 10:J P[1] 100% FINE    ;
 11:  PAYLOAD[1:EOAT w/o part] ;
 12:L P[3] 50mm/sec CNT100    ;
.....................................................................
.....................................................................
P[7]{
   GP1:
            UF : 1, UT : 2,                    CONFIG : 'N U T, 0, 0, 0',
            X =   700.000  mm,    Y =   -82.668  mm,    Z =    24.997  mm,
            W =  -180.000 deg,    P =   -90.000 deg,    R =     0.000 deg
};
/END
```

Slika 3. *Primer dela programa za kolaborativni robot*

4 PRIMER PRIMENE

Iz predhodno navedenog može da se zaključi da je primena kolaborativnih robota u fazama mašinske obrade moguća ali se primenjuje kod obrada kod kojih se stvaraju manje i predvidive sile otpora rezanjem kao što su obaranje ivica, izrada i obrada jednostavnijih otvora kao i završna obrada brušenjem mekih materijala (šmirglanje). Razlozi za to su neposredno prisustvo ljudskih subjekata i problemi koji nastaju usled uticaja subjektivnih faktora u definisanju preopterećenja. Takođe, moguća je primena kod obrade glodanjem mekih materijala kao što je stirodur, i lakše obradivi modelarski materijali, pri izradi modela složene geometrije. Kolaborativni roboti se uspešno primenljuju u realizaciji obrade beskontaktnim metodama kao što su lasersko graviranja (ne postoji mehaničko opterećenje kinematske strukture robota) i procesima dodavanja materijala aditivnim tehnologijama [12].

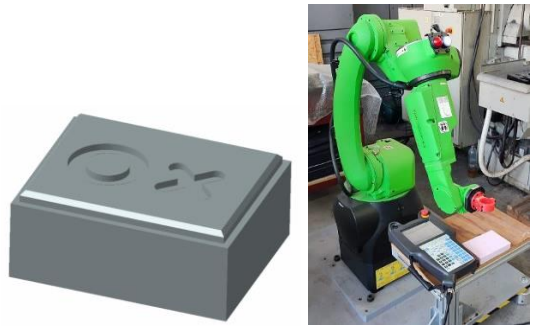

Slika 4. *Test radni predmet i priprema za verifikaciju*

Imajući u vidu postojeća ograničenja a u cilju provere jednostavnosti i tačnosti opisa putanje alata prilikom programiranja definisan je test radni predmet od mekanog materijala stirodur. Na slici 4 je prikazan izgled test radnog predmeta kao i robot pripremljen za obradu u Laboratoriji Fakulteta tehničkih nauka.

Test radni predmet se sastoji od ravnih površina orijentisanih u ortogonalnim pravcima, kosih površina (sa nagibom od 45°), jednog cilindričnog i dva ukrštena linearna žljeba. Ovakvim radnim

predmetom se testira mogućnost programiranja robota da izvrši linearne i kružnu interpolaciju kao i obradu površina pod nagibom u cilju simulacije 3+2 osne obrade tokom obaranja ivica.

Postupak programiranja i izrade odgovarajućih upravljačkih programa je realizovan za kolaborativni robot Fanuc CR 15-iA sa upravljačkim sistemom R-30iB instaliranom u Laboratoriji za mašine alatke Fakulteta tehničkih nauka u Novom Sadu. Programiranje robota je realizovano primenom dve metode:

- automatizovano, primenom softvera RoboGuide i
- ručno primenom Teching Pendant jedinice.

U prvom slučaju je programiranje robota u automatizovanom režimu realizovano definisanjem putanje alata na površinama CAD modela test radnog predmeta. Programski sistem RoboGuide omogućava simulaciju okruženja robota sa funkcijama interaktivnog definisanja putanje izvršnog organa uz simulaciju jedinice za obučavanje (slika 5).

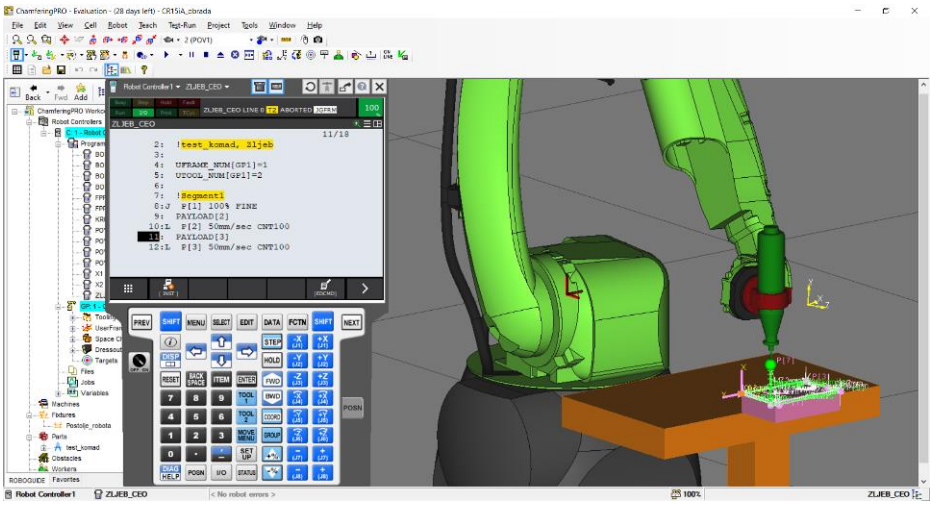

Slika 5. *Programski sistem za automatizovano programiranje robota sa definisanim putanjama neophodnim za obradu test radnog predmeta*

Slika 6. *Programiranje kolaborativnog robota u laboratorijskim uslovima*

Drugi metod izrade programa je realizovan primenom jedinice za obučavanje na robotu uz definisanje geometrijskih parametara i kolaborativnih funkcija. Ovaj postupak podrazumeva definisanje korisničkog koordinatnog sistema prema procedurama proizvođača, formiranje programa u skladu sa geometrijskim karakteristikama pojedinih površina koje se obrađuju. Ovakav postupak ručnog programiranja na samom robotu je primaran kod mašinske obrade skidanjem materijala (obezbeđuje geometrijski tačnu putanju alata), slika 6.

5 DISKUSIJA I ZAKLJUČCI

Definisanje područja primene kolaborativnih robota u zadacima mašinske obrade skidanjem materijala se može ostvariti kompleksnom analizom koja obuhvata: mogućnosti preciznog definisanja putanje alata postupcima programiranja, kompleksnost pripreme robota za proizvodnju sa stanovišta definisanja koordinatnih sistema kao i očekivanih rezultata sa stanovišta kvaliteta obrade.

Primenom pomenutih metoda programiranja može se zaključiti da je precizno definisanje putanje alata moguće za jednostavnije radne predmete. Pre svega se misli na putanje koje obuhvataju većim delom linearne segmente. Ovu informaciju treba uzeti sa određenom rezervom budući da CAM programski sistemi i za robotske sisteme omogućuju definisanje kompleksnijih putanja ali ovom fazom istraživanja oni nisu obuhvaćeni.

Priprema robotskih sistema za obradu koja podrazumeva definisanje lokalnih koordinatnih sistema. Zbog otvorene kinematske strukture, većeg broja stepeni slobode (6 i više DOF) i različite orijentacije izvršnih organa u odnosu na primarni koordinatni sistem podrazumeva kompleksne postupke definisanja pozicije i orijentacije. Samim tim ovo je izvor potencijalnih grešaka u procesu obrade.

Smanjena krutost kolaborativnih robota usled kinematske strukture uz dodatna ograničenja uslovljena bezbednosnim protokolima svakako ih ne preporučuje za zadatke mašinske obrade, mada je njihova primena i u ovoj oblasti moguća. Tu se pre svega misli na završne obrade mekših materijala niže klase tačnosti, kao što je na primer obrada modela od stirodura ili mekog drveta.

ZAHVALNOST

U okviru ovog rada saopštavaju se rezultati istraživanja koja su realizovana u okviru projekta „Inovativna naučna i umetnička istraživanja iz domena delatnosti FTN" na Fakultetu Tehničkih Nauka Univerziteta u Novom Sadu i projekta "Integrisana istraživanja u oblasti makro, mikro i nano mašinskog inženjerstva" i podprojekta TR35022 „Razvoj nove generacije domaćih obradnih sistema" na Mašinskom fakultetu Univerziteta u Beogradu, koje finansijski podržava Ministarstvo prosvete, nauke i tehnološkog razvoja Vlade Republike Srbije.

LITERATURA

[1] ElMaraghy, H., Monostori, L., Schuh, G., ElMaraghy, W. (2021). Evolution and future of manufacturing systems, *CIRP Annals*, 70/2, p.p.635-658.
[2] Bisen, A. S., Payal, H. (2022). Collaborative robots for industrial tasks: A review. Materials Today: Proceedings, 52, p.p. 500-504.
[3] Matthews, P., Greenspan, S.(2020) Automation and Collaborative Robotics: A Guide to the Future of Work, Apress, ISBN: 1484259645, 97814842596
[4] Krüger, J., Lien, T., & Verl, A. (2009). Cooperation of human and machines in assembly lines, *CIRP Annals*, Vol.: 58/2, p.p.628-646.
[5] Perez-Ubedaa, R. Gutierreza, S.C., Zotovicb, R., Lluch-Cerezoa, J. (2019). Study of the application of a collaborative robot for machining tasks, *Procedia Manufacturing* 41, p.p. 867–874.
[6] El Zaatari, S., Marei, M., Li, W., Usman, Z. (2019). Cobot programming for collaborative industrial tasks: An overview, *Robotics and Autonomous Systems*, 116, p.p.162-180.

[7] Pizá, R., Hermida, N. (2007). Programming and simulation of robotic systems for machining operations, IFAC Proceedings, 40/3, p.p. 36-41.
[8] Zivanovic, S., Slavkovic, N., & Milutinovic, D. (2018). An approach for applying STEP-NC in robot machining, *Robotics and Computer-Integrated Manufacturing*, 49, p.p.361-373.
[9] Slavkovic, N., Zivanovic, S., Milutinovic, D. (2018) An indirect method of industrial robot programming for machining tasks based on STEP-NC, *International Journal of Computer Integrated Manufacturing*, 32/1, p.p.43-57.
[10] Fogli, D., Gargioni, L., Guida, G., Tampalini, F. (2022). A hybrid approach to user-oriented programming of collaborative robots, *Robotics and Computer-Integrated Manufacturing,* 73, 102234.
[11] Hocken, R., Morris, G. (1986). An Overview of Off-Line Robot Programming Systems, *CIRP Annals,* 35/2, p.p. 495-503.
[12] Verl, A., Valente, A., Melkote, S., Brecher, C., Ozturk, E., Tunc, L. T. (2019). Robots in machining, *CIRP Annals*, 68/2, p.p.799-822.
[13] Milutinovic, D., Glavonjic, M, Slavkovic, N., Dimic, Z., Zivanovic, S., Kokotovic, B., Tanovic, Lj. (2011). Reconfigurable robotic machining system controlled and programmed in a machine tool manner, *International Journal of Advanced Manufacturing Technology*, 53/9-12, p.p.1217-1229
[14] Li, W., E. Red, G. Jensen, and M. Evans. (2007). Reconfigurable Mechanisms for Application Control (RMAC): Applications. *Computer-Aided Design and Applications*,4/1–4,p.p.549–556. https://doi.org/10.1080/16864360.2007.10738574
[15] DePree, J., and C. Gesswein. (2008). Robotic Machining White Paper project-Halcyon Development. Robotic Industries Association, October 31. https://www.robotics.org/robotic-content.cfm/Robotics/Halcyon-Development-RIA/id/43

COMETa 2022
6th INTERNATIONAL SCIENTIFIC CONFERENCE
17th - 19th November 2022
Jahorina, B&H, Republic of Srpska
University of East Sarajevo
Faculty of Mechanical Engineering
Conference on Mechanical Engineering Technologies and Applications

O TAČNOSTI MAŠINA ALATKI – TAČNOST POZICIONIRANJA

Milan Zeljković[1], Slobodan Tabaković[2]

Rezime: Tačnost je osnovna eksploataciona karakteristika mašina alatki koja se tokom vremena stalno povećava i praktično ilustruje istoriju razvoja mašina. Razvoj mašina alatki zahteva i razvoj metoda i instrumentacije za merenje i ispitivanje njihove tačnosti, obzirom da tačnost merne instrumentacije treba da je bar 5 do 10 puta veća od tačnosti merene veličine. Geometrijska tačnost je ključni segment u okviru tačnosti mašina alatki. Pored povećanja tačnosti mehaničkih komponenti, kod savremenih mašina alatki se tačnost postiže i numeričkom kompenzacijom. Numerička kompenzacija netačnosti ima veliki značaj za preciznu obradu. Ovaj rad razmatra metode za merenje geometrijskih netačnosti mašina. Kao poseban segment geometrijske tačnosti je prikazano ispitivanje tačnosti pozicioniranja numerički upravljanih mašina alatki prema, u Evropi vrlo često korišćenoj preporuci (smernici) VDI/DGQ 3441. Kroz zaključna razmatranja je pored ostalog, ukazano na neke od pravaca razvoja ove problematike. Na osnovu razvoja tržišta i tehnologija, jedan od ciljeva ovog rada je da ukaže na ulogu stručnjaka iz naših instituta i fakulteta pri povećanju tačnosti mašina alatki u eksploataciji.

Ključne riječi: mašine alatke, geometrijska tačnost, tačnost pozicioniranja,

ABOUT ACCURACY OF MACHINE TOOL – ACCURACY OF POSITIONING

Abstract: Accuracy is the basic exploitation characteristic of machine tools that have constantly been increasing over time and practically illustrates the history of machine development. The development of machine tools also requires the development of methods and instrumentation for measuring and testing their accuracy, considering that the accuracy of the measuring instrumentation should be at least 5 to 10 times greater than the accuracy of the measured quantity. Geometric accuracy is a key segment within machine tool accuracy. In addition to increasing the accuracy of mechanical components, with modern machine tools, accuracy is also achieved through numerical compensation. Numerical inaccuracy compensation is of great

[1] prof. dr Milan Zeljković, Univerzitet u Novom Sadu, Fakultet tehničkih nauka Novi Sad, milanz@uns.ac.rs (CA)
[2] prof. dr Slobodan Tabaković, Univerzitet u Novom Sadu, Fakultet tehničkih nauka Novi Sad, tabak@uns.ac.rs

importance for precision machining. This paper discusses methods for measuring the geometric inaccuracies of machines. As a particular segment of geometric accuracy, the examination of the positioning accuracy of numerically controlled machine tools according to the often-used recommendation (guideline) VDI/DGQ 3441 in Europe is presented. Based on the development of markets and technologies, one of the goals of this work is to point out the role of experts from our institutes and faculties in increasing the accuracy of machine tools in exploitation.

Key words: machine tools, geometric accuracy, accuracy of positioning,

1 UVODNA RAZMATRANJA

Eksploatacija mašina alatki, u užem smislu, obuhvata usklađenost rada mašine sa proizvodnim zadatkom i ponekad se naziva mikroeksploatacija. Eksploatacione karakteristike predstavljaju svojstva mašine alatke pri njenom radu - eksploataciji. Obzirom na osnovnu funkciju, tj. zadatak mašine alatke: transformacija pripremka u izradak, prvi zahtev je da on bude prema zahtevima definisnim konstrukcionom dokumentacijom, pa je osnovna eksploataciona karakteristika tačnost.

U industriji prerade metala neprekidno postoji zahtev za većom dimenzionalnom i geometrijskom tačnošću i manjom površinskom hrapavošću proizvedenih izradaka. Među industrijama koje zahtevaju postizanje strožijih tolerancija, tipični primeri su automobilska, vazduhoplovna i medicinska industrija, uključujući i trendove u proizvodnji poput automatske montaže i izrade mikro obradaka. Postizanje željene tačnosti izradaka predstavlja osnovni kriterijum pri izboru mašine alatke.

Tačnost izradka je usko povezana sa sposobnostima obradnog sistema, što je određeno interakcijom između mašine alatke i procesa obrade. Sposobnost mašina alatki se obično odražava na vezu alat-obradak u smislu geometrijske i kinematičke tačnosti, kao i uticaja statičkog, dinamičkog i toplotnog opterećenja.

Da bi odgovorili na izazov povećanja performansi i poboljšanja sposobnosti mašina alatki, proizvođači uvode nove optimizacione tehnike projektovanja, primenu nekonvencionalnih materijala i koncepcionih rešenja za filozofiju precizne proizvodnje. Međutim, proizvodni troškovi uključeni u takav poduhvat su veliki i često se promene kojima su mašine alatke izložene (npr. deformacije usled sila rezanja ili toplotnih opterećenja) ne mogu u potpunosti predvideti tokom faze projektovanja.

Drugi način povećanja performansi je stalno poboljšanje i razvoj novih metoda identifikacije i procene karakteristika mašina alatki [1]. Tokom godina, oblast metrologije[3] i ispitivanja mašina alatki dobijaju sve veći značaj za industriju. Na raspolaganju je veliki izbor metrološke opreme i metoda ispitivanja za procenu performansi mašina alatki. Međunarodni standardi za ispitivanja (npr. serija ISO 230), čiji je cilj da pokriju sve aspekte ispitivanja mašina alatki su podigli svest i donekle ispunili zahteve. Standardi za ispitivanje su od suštinskog značaja ako se performansama mogu zadovoljiti potrebe i proizvođača i krajnjih korisnika mašina alatki. Da bi se zadovoljile ove potrebe, standardi su u određenoj meri kompromis u smislu ekonomskih i aspekata kvaliteta. Ekonomski razlozi znače da se neproduktivno vreme mora svesti na minimum, dok razmatranje kvaliteta znači da kalibracija treba biti dovoljno detaljna da pruži značajne rezultate. Pronalaženje optimuma između ova dva zahteva je ključno pitanje pri razvoju ili poboljšanju metoda ispitivanja.

[3] Metrologija mašina alatki može se definisati kao aktivnost koja se odnosi na disciplinu merenja karakteristika mašina alatki, kao što su geometrijske greške u statičkim i dinamičkim uslovima [55]

Razvoj tačnijih mašina ne zavisi samo od jednog napretka već i od primene određenih tehnika tokom veka eksploatacije mašine. Polazeći od koncepcionog rešenja, delovi strukture mašina alatki danas su projektovani uzimajući u obzir niz pojava, kao što su elastične deformacije izazvane spoljnim silama ili gravitacijom, moguće habanje pokretnih delova, pojava toplotnih deformacija ili odgovori mašine na spoljne faktore [2]. Kao ilustracija se može navesti primer elemenata za linearno vođenje. Pored postizanja maksimalne ekonomične tačnosti izrade svakog vitalnog elementa mašine alatke, uvedene su posebne tehnike za proizvodnju i montažu linearnih vođica. Kompanije koje proizvode visoko tačne mašina alatki procenjuju da je potrebno više od 400 sati rada „tuširanja“ linearnih vođica na svakoj mašini kako bi se osigurala ravnost i upravnost svake ose. S druge strane, modularnost, zamenljivost delova i lako održavanje takođe moraju biti povezani sa tačnošću. Iz tog razloga, danas primena linearnih kotrljajućih vođica koje su unapred podešene od dobavljača čini ponovljivost i lakšu montažu mašina alatki i predstavljaju ekonomično rešenje.

Polazeći od stanja u proizvodnji mašina alatki u našoj zemlji i ne malog akumulisanog znanja u našim institutima i fakultetima cilj ovor rada je da ukaže na mogućnost povećanja performansi mašina alatki u eksploataciji kroz razvoj metoda ispitivanja i numeričke kompenzacije tačnosti. Rad je koncipiran kroz nekoliko celina. Nakon uvodnih razmatranja, u okviru drugog poglavlja su definisani pojmovi i izvršena je sistematizacija netačnosti mašina alatki. Treće poglavlje je posvećeno ispitivanju geometrijske tačnosti, kao osnovnom pokazatelju početnog kvaliteta mašina alatki. Kao poseban segment geometrijske tačnosi je prikazano ispitivanja tačnosti pozicioniranja mašina alatki prema, u Evropi vrlo često korišćenoj preporuci (smernici) VDI/DGQ 3441, u okviru četvrtog poglavlja. Kroz zaključna razmatranja, peto poglavlje, je pored ostalog, ukazano na neke od pravaca razvoja ove problematike.

2 OSNOVNI POJMOVI, IZVORI I SISTEMATIZACIJA GREŠAKA MAŠINA ALATKI

Tačnost je zapravo indirektni pokazatelj jedne od karakteristika mašina alatki, jer je u pitanju tačnost obrađenih izradaka. Razvoj i istorija razvoja mašina alatki su usko povezani sa njihovom tačnošću, odnosno sa tačnošću obradaka koji se na njima izrađuju. Kao ilustracija prethodnog Vilkinson – ova mašina za bušenje velikih otvora (1774. god.) ostvarivala je tačnost izrade prečnika 1 [mm], dok NU mašine alatke normalne tačnosti početkom dvadesetprvog veka imaju tačnost oko 10 [μm].

Da bi se što bolje razumeli pojmovi povezani sa tačnošću mašina alatki u nastavku se navode njihove definicije i daje kratko objašnjenje, pri čemu treba naglasiti da su pojmovi definisani onako kako se koriste u oblasti mašina alatki.

Tačnost predstavlja bliskost između izmerene i referentne vrednosti merene veličine. Kod mašina alatki tačnost se može definisati kao maksimalna translatorna ili rotaciona greška između bilo koje dve tačke u radnoj zapremini mašine [3]. ili, u smislu obrade, bliskost slaganja između stvarne vrednosti koja je rezultat operacije obrade i ciljne vrednosti veličine. Imajući u vidu prethodno može se konstatovati da je mašina alatka tačnija kada je odstupanje između ciljnog i stvarnog položaja u radnoj zapremini manje.

Ponovljivost predstavlja odstupanje uzastopnih merenja iste veličine izvedenih pod istim uslovi (zbog izvora slučajnih grešaka). U literaturi se pojam ponovljivost sreće i kao preciznost. Kod mašina alatki, ponovljivost se može shvatiti kao greška između višestrukih ponovljenih pokušaja pomeranja klizača mašine u isti položaj i pod istim uslovima [3]

Rezolucija je najmanja veličina koja se može uočiti ili izmeriti, a prouzrokuje primetnu promenu. Kod mašina alatki rezolucija se obično odnosi na najmanji

mehanički korak koji mašina može izvršiti tokom kretanja od tačke do tačke [3]. Kao opšte pravilo važi da rezolucija treba da bude za jedan red veličina manja od željene tačnosti mašine.

Nesigurnost (U), karakteriše rasipanje dobijenih vrednosti izmerene veličine koje se može sa dovoljno sigurnosti pripisati ovoj vrednosti. U literaturi nesigurnost se naziva i maksimalna očekivana netačnost merenja sa datom verovatnoćom [4]. Poznato je da svako merenje sadrži određenu netačnost, koja nije uvek ista. Nesigurnost je kombinacija više uticaja poput nesigurnosti mernog instrumenta, uticaja okoline, nesigurnost uzrokovana samom mašinom, kao i nesigurnost zbog pogrešne primene mernog instrumenta. Može se proceniti statističkim metodama, koje karakteriše standardno odstupanje distribucije ponovljenih merenja ili pretpostavljenom distribucijom. Na primer, ako skup različitih merenja rezultira srednjom vrednošću „k“, može se tvrditi da je „stvarna vrednost“ izmerene veličine unutar intervala ,,k ± kU“ sa utvrđenom verovatnoćom (obično je verovatnoća 95%, a tada je k = 2).

Tipičan primer postupka procene i izveštavanja o nesigurnosti za linearnu osu mašine alatke, dat je u aneksu A ISO 230-2 (2014) [5].

Pri ispitivanju tačnosti mašina alatki, a posebno pri ispitivanju geometrijske tačnosti, važno je konstatovati da su ove greške definisane i merene u položaju ili na putanji funkcionalne tačke. Standard ISO 230-1: 2012 (2012) [4] definiše funkcionalnu tačku kao „pridruženu središnju tačku ili tačku rezanja sa komponentom na mašini alatki, u kojoj bi alat za obradu bio u kontaktu sa obradkom u procesu obrade" (centralna tačka - TCP)). Ovo je tačka koja se nalazi na komponenti mašine alatke koja se može kretati unutar radne zapremine mašine. Iako se ispitivanje geometrijske tačnosti može obaviti bilo gde u radnom prostoru, smatra se dobrom praksom da se merna tačka podudara sa funkcionalnom tačkom, jer povezuje izmerenu netačnost direktno sa geometrijskim karakteristikama mašine alatke. Pored toga, pomeranje između funkcionalne tačke i merne tačke ima efekat povećanja nesigurnosti predviđene tačnosti, usled efekta poluge zbog ugaonih grešaka. Na taj način, minimiziranje udaljenosti između dve tačke minimizira uticaj nesigurnosti. Primena postavki merenja koje predstavljaju putanju alata za obradu omogućava da izmerene netačnosti uključuju doprinos ugaonih grešaka (naginjanje, talasanje i skretanje) u pravcu ispitivane ose.

Osnovni izvori grešaka, koji utiču na tačnost mašine alatke, mogu se grupisati na sledeći način [6]:

- koncepciono rešenje;
- geometrijske netačnosti vitalnih elemenata i sklopova;
- montaža;
- kretanje vitalnih komponenti;
- nestabilnost materijala;
- statičko opterećenje (gravitaciona opterećenja – masa radnog predmeta, masa sklopova mašine, sile rezanja, ….) ;
- toplotno opterećenje (unutrašnji izvori: glavno vreteno, zavojno vreteno sa recirkulacijom kuglica; motori; trenje, …; spoljašnji izvori: temperature okoline; grejna tela, …;);
- dinamičko opterećenje (promenljivost sila rezanja, inercijalne sile, habanje alata, vibracije,)
- upravljački sistem (greške interpolacije, …)

Ako se razmatranje proširi na obradni sistem pojavljuju se i ugib i habanja alata, pribora za stezanje i sile stezanja.

Poznato je da projektovanje preciznih mašina alatki ne bazira na tačnijoj izradi

elemenata mašine, već na koncepcionom rešenju. Pri tome kod mašina normalne tačnosti, posebno sa ručnim upravljanjem, je vrlo teško zadovoljiti Abeov princip, što predstavlja jedan od čestih izvora netačnosti. Kod savremenih numerički upravljanih mašina alatki je moguće zadovoljiti generalizovani Abeov princip – Brajanov princip [7]; „ako nije moguće ispoštovati Abeov princip, ili klizači koji prenose pomeranje moraju biti oslobođeni ugaonog pomeranja ili se podaci o ugaonom pomeranju moraju koristiti za izračunavanje posledica pomeranja.“ Poslednji deo rečenice predstavlja ključ za pristup problemu obezbeđivanja tačnosti mašina alatki, posebno numerički upravljanih. Ako je moguće izračunati posledice kada Abeovog princip nije zadovoljen kod projektovanja, navedene netačnosti je moguće kompenzovati. Upravljačkom sistemu NU mašine alatke se može naložiti da primeni kompenzacione parametre u softveru zasnovane na izračunatim netačnostima. Ovo je uslovilo da se u početku koristio naziv “softverska kompenzacija” a danas se, skoro isključivo, koristi “numerička kompenzacija”. Pri projektovanju preciznih mašina alatki, kako je poznato i kod konvencionalnih mašina, unutrašnji izvori toplote se ugrađuju što je moguće dalje od zone obrade, i na taj način smanjuje uticaj toplotnih deformacija. Ovo je lako izvodljivo sa elementima kao što su električni sistemi, rashladni sistemi ili servo pogoni. Međutim, elementi kao što su sklop glavnog vretena i zavojna vretena sa recirkulacijom kuglica, generišu toplotu i povećavaju njihovu temperaturu i toplotne deformacije, a praktično ih je nemoguće udaljiti iz zone obrade.

Pri diskusiji o greškama koncepcionog rešenja može se uočiti pojam, precizne mašine alatke, što ukazuje na razliku u odnosu na mašine alatke normalne tačnosti (za ove mašine se ponekad u literaturi sreće i naziv produkcione mašine alatke). Potrebno je konstatovati da, ako se posebno ne naglašava, misli na mašine alatke normalne tačnosti. Takođe treba ovde razjasniti i drugi pojam. Ako se posebno ne naglašava sem što se misli na mašine normalne tačnosti misli se na srednjeteške (eventualno lake i srednje teške mašine alatke), koje su najzastupljenije u pogonima i čija je kinematska struktura različita u odnosu na teške. Nasuprot tome neophodno je naglasiti kada su u pitanju ostali tipovi mašina kao što su: teške, midi, mini ili mikro mašine alatke.

Sistematizacija grešaka mašina alatki se najčešće vrši prema izvorima grešaka:

- geometrijske (geometrijsko/kinematičke),
- kinematičke,
- usled destva statičkog opterećenja,
- usled dejstva toplotnog opterećenja,
- usled dejstva dinamičkog opređenja,
- upravljačkog sistema.

Navedena sistematizacija je najčešće prisutna u okviru istraživačkih radova, ali je pri eksperimentalnom ispitivanju vrlo teško razdvojiti ostale greške od geometrijskih, odnosno u rezultatu se pojavljuje superponiranje grešaka. Primenom odgovarajućih programskih sistema razmatrane greške se mogu manje ili više uspešno modelovati i na taj način smanjiti njihov uticaj. Zbog toga se pojavljuje i sistematizacija koja greške grupiše na :

- geometrijske i
- operativne greške (greške pri eksploataciji usled toplotnog, statičkog, dinamičkog opterećenja i drugih izvora) mašina alatki.

U literaturi [9] tačnost mašina alatki se sistematizuje u tri grupe:

- geometrijska,
- kinematička i

- radna tačnost,

a odnosi se i na mašine alatke sa ručnim i numeričkim upravljanjem.

Prema teoriji sistema, prve dve navedene tačnosti se mogu posmatrati kao početni pokazatelji kvaliteta mašina alatki, a prethodno navedeni izvori grešaka predstavljaju poremećajne podsisteme. Sa stanovišta ovog rada, a i pri izučavanju navedene problematike autori smatraju pogodnu poslednju sistematizaciju. Mnogi autori se slažu da geometrijske i kinematičke greške čine osnovu netačnosti mašina alatki. Želeći da se izvrši uporedno razmatranje i konvencionalno i numerički upravljanih mašina alatki, u radu je akcenat na geometrijskoj tačnosti sa posebnim osvrtom, u okviru nje, na tačnost pozicioniranja. Jedan od razloga ovakog pristupa počiva na činjenici da se ispitivanje kinematičke tačnosti konvencionalno upravljanih mašina alatki vrši samo kod mašina gde je potrebna stroga zavisnost između pojedinih kretanja, pa se isto ređe vrši, a kod numerički upravljanih, takođe, ovo ispitivanje, sem jednog, nije još uvek standardizovano i za konkretne slučajeve definiše se i metodologija i odgovarajući pribori za merenje.

3 GEOMETRIJSKA TAČNOST MAŠINA ALATKI

Kako je prethodno konstatovano tačnost mašina alatki predstavlja temelj za definisanje mogućnosti mašine alatke i direktno utiče na tolerancije obrađenih delova. Kod savremenih mašina alatki se veća tačnost može realizovati kroz dva pravca. Jedan pravac je poboljšanje performansi mašina alatki koncipiranjem i projektovanjem boljih, krućih i tačnijih mašina alatki. Drugi je razvoj metoda za procenjivanje i merenje tačnosti mašina alatki i, kod mašina gde je to moguće, “numeričkom kompenzacijom” povećati tačnost.

U literaturi se sreće više definicija geometrijske tačnosti, odnosno geometrijskih netačnosti – grešaka. Neke od njih se navode u nastavku.

To su greške zbog nesavršene geometrije mašine alatke tokom izrade i montaže [6], [9]. One se manifestuju kao odstupanja u krajnjem položaju i orijentaciji alata i obradka u obliku ravnosti, paralelnosti, i sl. Sistemski karakter tih grešaka može varirati usled habanja komponenti tokom vremena i rezultirati promenama geometrija mašine. Geometrijske greške se ponekad mogu teško izmeriti pojedinačno zbog njihove prirode i nepristupačnosti. Međutim, oni se mogu prepoznati po njihovom uticaju na kinematičku strukturu mašine alatke i tačnost pozicioniranja. Danas se obično određuju laserskom interferometrijom [6], [9].

Geometrijske greške su one koje nastaju na mašini zbog njenog koncepcionog rešenja, netačnosti ugrađenih tokom montaže i kao rezultat komponenti koje se ugrađuju. Kao takve, one predstavljaju jedan od najvećih izvora netačnosti. Ove greške se odnose na kvazistatičku tačnost površina koje se kreću jedna u odnosu na drugu. Geometrijske greške mogu biti glatke i kontinualne ili imati histerezis ili slučajno ponašanje. Na ove greške utiču faktori kao što su ravnost i hrapavost površine, prednaprezanje ležaja itd. Geometrijske greške imaju različite uzroke kao što su greška linearnog pomeranja (tačnost pozicioniranja), pravost i ravnost kretanja ose, ugao nagiba vretena, greška normalnosti, greška zazora itd. [10].

Geometrijske greške nastaju zbog nesavršene geometrije vođica mašina alatki i drugih komponenti strukture, kao što su postolje, vođice, klizači, ležaji, zavojna vretena sa recirkulacijom kuglica, itd. i njihovog nesklada u konstrukcijskom konfiguracijom mašine [6], [9], [10], [11]. Sistemski karakter ovih grešaka može se promeniti zbog povremenih kolizija, kao i habanja komponenti, što rezultira promenom geometrije mašine [6]. Geometrijske greške je ponekad nemoguće pojedinačno izmeriti

zbog problema s pristupačnošću. Međutim, one se mogu odrediti uticajem na kinematičku strukturu mašine i rezultirajućom greškom kretanja osa.

Geometrijske netačnosti su odstupanja u obliku i položaju pojedinih komponenata mašine (stolovi, nosači, klizači, pinole). Ovde su od interesa samo one komponente koje obavljaju funkcije kretanje, vođenje i stezanja (nošenja - držanja). Kretanja na mašini se po pravilu odvijaju u nekoliko osa (do pet ili više), tako da se pored odstupanja u geometriji komponenata i kretanju komponenata u pravcu pojedinih osa mašine, geometrijska odstupanja su važni ciljni položaj međusobnih osa mašine.

Geometrijska tačnost mašina alatki je rezultat koncepcionog rešenja, tačnosti izrade pojedinih komponenti i sklopova, kao i montaže mašine alatke, a određuje (definiše) se nizom merno-kontrolnih operacija merenjem tačnosti: 1) veličine, oblika i položaja vitalnih elemenata; 2) trajektorije pri kretanju vitalnih elemenata (koji obezbeđuju relativno kretanje alata i obradka); 3) međusobnog položaja vitalnih elemenata (koji utiču na tačnost obradka pri eksploataciji mašine). Ovde se pod vitalnim elementima i sklopovima podrazumevaju elementi koji obezbeđuju funkciju kretanja, vođenja i oslanjanja, kao i stezanja.

Iz prethodnog se vidi da su neke od definicija posledica izvora geometrijskih grešaka, a neke određivanja – merenja navedenih grešaka. Poslednja definicija, koju predlažu i autori, objedinjuje oba pristupa. Kako se iz navedene definicije može videti neke geometrijske greške se definišu na bazi kretanja vitalnih elemenata pa se otuda u literaturi, kako je prethodno navedeno, ove greške grupišu u geometrijsko/kinematičke. Ovakva sistematizacija može dovesti do zabune vezano za „čisto“ kinematičke greške, odnosno kinematičku tačnost.

Ranije je već naglašeno da se elementi mašina alati izrađuju sa ekonomičnim tolerancijama, koje su, ponekad, veće od zahtevane tačnosti mašine alatke. Veličina ekonomičnih tolerancija se smanjuje vremenom, ali raste i zahtevana tačnosti mašina alatki. Imajući u vidu da se ovo razmatranje odnosi i na mašina sa ručnim i numeričkim upravljanjem (prema određenim studijama vrednost godišnje proizvodnje, u svetu, ručno i numerički upravjanih mašina alatki danas je podjednaka 50%, što zahteva još uvek ne malu pažnju u proizvodnji ručno upravljanih mašina). Da bi se obezbedila potrebna tačnost mašina alatki koristi se teorija mernih lanaca, i to u proizvodnji metoda podešavanja i metoda regulacije, a u pogonima održavanja, najčešće, metoda regulacije. Ako se zna da je veća tačnost numerički od ručno upravljanih mašina alatki, pored užih tolerancija izrade elemenata to se postiže i numeričkom kompenzacijom grešaka, što još dodatno ukazuje na potrebu ispitivanja geometrijske i ostalih tačnosti, posebno kod numerički upravljanih mašina alatki. Numerička kompenzacija grešaka NU mašina alatki je, kako je već i ranije naglašeno jedan od pravaca razvoja preciznih mašina.

Ispitivanje geometrijske tačnosti podrazumeva završno ispitivanje montirane mašine u neopterećenom i stacionarnom temperaturnom stanju. Praktično, reč je o ispitivanju pri primopredaji mašina alatki i obično se izvodi u pogonu proizvođača i sa njegovim priborima za merenje, ukoliko veličina mašine to dozvoljava (lake i srednje teške mašine). U slučaju teških mašina alatki, primopredaja mašina se često vrši u pogonu kupca pod originalnim uslovima ugradnje. Pored primopredaje, ispitivanja se mogu koristiti i u druge svrhe, proveru projektovanih preformansi, poređenje između sličnih mašina, a posebno za periodične provere mašina tokom veka eksploatacije, itd. Ispitivanje mašina alatki treba omogućiti ne samo proizvođačima, već i krajnjim korisnicima, posebno u savremenim uslovima kada se primenom numeričke kompenzacije mogu ostvariti bolje performanse na ekonomičan način.

Metode ispitivanja i pribori za merenje geometrijskih netačnosti razvijani su i uspostavljani tokom više decenija i dokumentovani su nacionalnim i međunarodnim standardima, a bazirani su na metodama i principima koje je razvio još prof. Schlesinger [8] 30-ih godina dvadesetog veka. Jedan od primera je međunarodni standard ISO 230-1 [12] koji sadrži opšte smernice za procenu geometrijske tačnosti mašina u uslovima bez opterećenja. Pored osnovnih standarda za ispitivanje geometrijske tačnosti mašina alatki serije ISO 230 [14-17] postoji i niz drugih standarda. U nastavku se navode neki od njih. Osnovni standard za pozicioniranje linearnih i rotacionih NU osa je [16], za ispitivanja geometrijske tačnosti osa rotacije [17], za ispitivanja kružnim testom [15], za ispitivanja pomeranja u pravcu dijagonale [16]. Ovi standardi se mogu primeniti na bilo koju mašinu alatku. Međutim, za neke tipove mašina postoje specifični standardi. Serija specifičnih standarda ISO 10791 je za obradne centre, sa ispitivanjima geometrijske tačnosti horizontalnih , vertikalnih obradnih centara [5] i za vertikalne obradne centre sa univerzalnim glavama [19], sa ispitivanjima tačnosti pozicioniranja [18], testovi za interpolaciju [20], za karakteristike kretanja po konturi [20]. Druga serija ISO 13041 je za NU strugove i strugarske obradne centre, sa ispitivanjima geometrijske tačnosti horizontalnih [21] i vertikalnih strugova [22], sa ispitivanjem tačnosti pozicioniranja [23], testovi za interpolaciju [24], za karakteristike kretanja po konturi [25]. Navedeni standardi definišu tačnost merenja u pravcu jedne ose ili u ravni.

Standardi predlažu principe merenja i odgovarajuće pribore za merenje. Ovi pribori su obično deo osnovne opreme svakog proizvodnog pogona. Međutim, standardi dozvoljavaju upotrebu bilo kog drugog mernog pribora, pod uslovom da je njihova tačnost najmanje jednaka metodi predloženoj u standardu. Ova mogućnost korišćenja metoda merenja koje nisu navedene u standardima često se mora koristiti kada mašine ili delovi mašina koji se mere imaju vrlo velike dimenzije ili se postavljaju vrlo visoki zahtevi za tačnost mašine.

Prvo ispitivanje, pri ispitivanju geometrijske tačnosti mašina alatki, je kontrola položaja površina. Postavljanje mašine, odnosno njenih osnovnih površina u horizontalan – vertikalan položaj predstavlja deo pripreme mašine za ispitivanje. Drugo, pri merenju geometrijskih odstupanja mašine, potrebno je proveriti tačnost tačaka kontakta nosača alata i obradka, njihov međusobni položaj kao i ose mašina. Pri merenju se razlikuje:

- relativno ili apsolutno merenje,
- merenje sa fiksnim merenim mestom u funkcionalnoj tački alata ili merenje sa pokretnim mernim mestom (stolom),
- merenje pokretnim stolom ili merenje pokretnim mernim priborom.

Da bi se odredila tačnost mašine, treba težiti relativnom merenju, odnosno određivanju relativnih odstupanja između držača alata i nosača obradka.

Metode merenja i analize tačnosti mašine alatke zavisi od namene i vrste netačnosti koja se meri i odgovarajuće komponente mašine i njene konfiguracije u strukturi mašine. Otuda se, metode merenja mogu grupisati u neposredne (direktne) i posredne (indirektne) u odnosu na dobijene rezultate o mašini alatki.

Neposredno merenje omogućava utvrđivanje jedne netačnosti pojedinačne komponente mašine, isključujući uticaje drugih komponenti. Neposredna merenja se mogu klasifikovati u tri podgrupe na osnovu njihove metrološke baze (reference): metode zasnovane na materijalnom telu (koriste artefakte), npr. provost, ravnost itd. Laserska metode koriste linearnost prostiranje laserske svetlosti i talasnu dužinu kao referencu. Gravitacione metode merenja baziraju na gravitacionom polju zemlje, [6].

Procena i merenje tačnosti mašine alatke pomoću kalibrisanih etalona (artefakata) i kalibrisanih izradaka poznatih dimenzija korišćeno je pre razvoja laserskih mernih instrumenata. Kalibrisani etaloni za određivanje grešaka prvenstveno su podložni promeni dimenzija i starenju materijala, dolazi do ugiba mernog lenjira usled gravitacije, što utiče na nesigurnost rezultata merenja [6,9]. U cilju minimiziranja ugiba lenjira potrebno je isti oslanjati u Beselovim (Friedrich Wilhelm Bessel) tačkama (Slika 1.). Na slici 2a prikazan je precizni granitni kvadrat za procenu normalnosti i merni lenjir (Slika 2b) za procenu pravosti linearnih osa mašine.

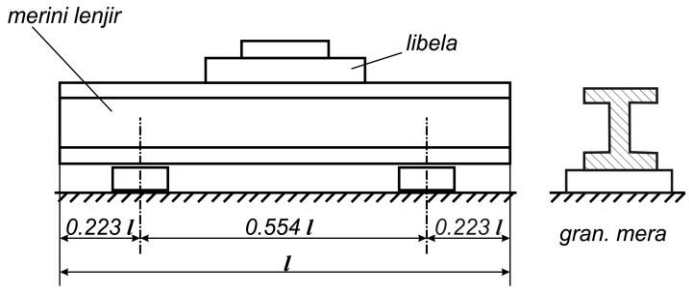

Slika 1. *Tačke oslanjanja mernog lenjira*

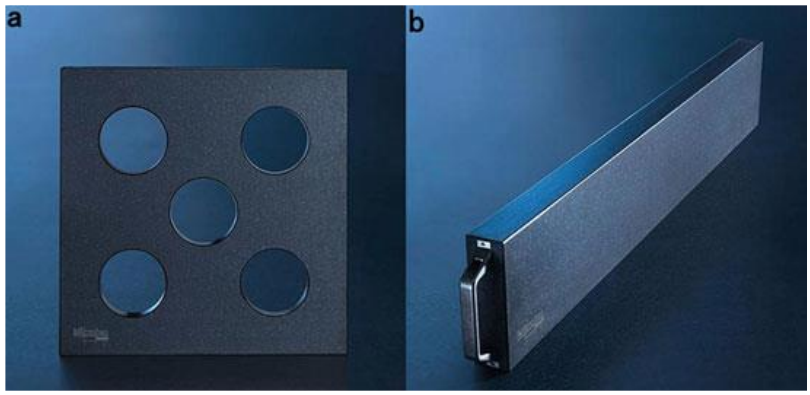

Slika 2. *Precizni granitni kvadrat za procenu normalnosti (a) i granitni merni lenjir za procenu pravosti linearne ose (b)*

Višedimenzionalni artefakti, poput ploča sa kalibrisanim sferama, se relativno često primenjuju poslednjih godina [9]. Primer kalibrisane ploče sa preciznim sferama prikazan je na slici 3.

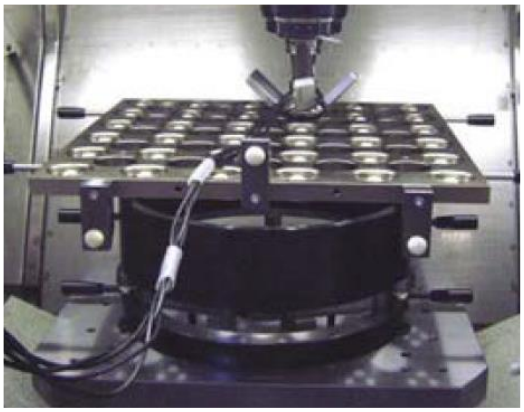

Slika 3. *Kalibrisana ploča sa preciznim sferama*

Jedna od najčešće korišćenih metoda za merenje geometrijskih netačnosti mašina alatki je laserska interferometrija, koja u kombinaciji sa specijalnim optičkim komponentama omogućava merenje skoro svake geometrijske netačnosti linearne ose uz visoku preciznost merenja i ocenjivanje tačnosti. Takođe, pošto se fokusiraju na jednu po jednu komponentu greške, omogućuju bolju identifikaciju pojedinačnih grešaka. Zbog koherentnosti, upotreba laserske interferometrije za merenje visoke preciznosti moguća je čak i za dugačke ose. Ovim metodama se uglavnom mere svojstva pozicioniranja mašina u pravcu pojedinih osa. Neki merni sistemi kombinuju više senzora za simultano merenje grešaka pozicioniranja, normalnosti i ugla [26]. I pri primeni laserske interferometrije uticaji grešaka se moraju uzeti u obzir kada se ispituju mašine alatke. Greške u talasnoj dužini lasera prenose se direktno na greške u merenju dužine [9]. Talasna dužina lasera može se promeniti ili se razlikovati od nominalne zbog grešaka u stabilizaciji frekvencije [27]. Faktori okoline, temperatura, pritisak, gustina i vlažnost vazduha, imaju zanemarljiv uticaj, obzirom da merna instrumentacija sadrži uređaje za automatsko kompenzovanje navedenih uticaja. Kod malih visoko preciznih mašina toplotna snaga laserskog sistema može uticati na merenja, jer tipični gasni helijum-neonski laseri emituju preko 5W toplote što može dovesti do lokalnog zagrevanja delova mašine i rezultirati odstupanjima i samim tim greškama pri ispitivanju mašine [16].

Metode zasnovane na gravitaciji koriste smer vektora gravitacije kao metrološku bazu. Tipični primeri takvih mernih pribora su libele (mehaničke ili elektronske). Omogućavaju merenje grešaka ugaonog pomeranja oko horizontalne ose. Nisu merljiva ugaona pomeranja oko vertikalne ose.

Posredne (indirektne) metode merenja otkrivaju netačnosti povezane sa istovremenim kretanjem dve ili više osa. Omogućavaju brz način za procenu sposobnosti pozicioniranja i tačnosti konture koja se realizuje na mašini, delimično ili u potpunosti identifikujući sve geometrijske netačnosti osa mašine alatke. Kao i kod neposrednih metoda dostupne su različite tehnike merenja, uključujući i korišćenje artefakata (delimično ili potpuno kalibrisanih ili nekalibrisanih) i konturnih merenja [23]. Druga grupa posrednih metoda merenja, takozvana konturna merenja, koriste istovremeno kretanje dve ili više osa za kretanje po posebnim linijama, npr. ravne linije u prostoru [6], kružne putanje nastale kretanjem dve linearne ose [6] ili kružne putanje kao rezultat dve linearne i jedne rotacione ose [6]. Odstupanja od nominalnih linija mere se posebnim mernim priborom ili u odnosu na neki artefakt.

Zbog određenih poteškoća i relativno dugog vremena merenja, zajedno sa potrebom za iskusnim inženjerima - operaterima, posredne metode se smatraju lakšim i bržim za izvođenje. Ipak, identifikovanje različitih grešaka nije uvek izvodljivo, jer na rezultat merenja utiče kombinovani efekat različitih izvora grešaka.

Kod mašina alatki sa paralelnom i hibridnom kinematikom, neposredna merenja ili nisu primenljiva ili mogu biti opravdana samo za određivanje nekih geometrijskih grešaka. Prethodno ukazuje da se kod ovih mašina uglavnom moraju koristiti posredne metode merenje [6].

Kako je ranije konstatovano završna tačnost NU mašina alatki se postiže numeričkom kompenzacijom grešaka. U cilju numeričke kompenzacije potrebno je izmeriti geometrijske greške i primenom homogene matrice transformacija (HMT) u upravljačkom sistemu mašine memorisati određene kompenzacije, prema procedurama karakterističnim za dati upravljački sistem. Na osnovu izmerenih vrednosti svih komponenata grešaka u merenim tačkama, primenom homogene matrice transformacije, se iste preračunavaju u komponente grešaka u funkcionalnoj tački. U tom cilju je potrebno poznavati kinematsku strukturu i geometrijske karakteristike mašine alatke [28].

U nastavku se daje primer geometrijskih grešaka mašine alatke sa tri linearne ose definisane u Dekartovom koordinatnom sistemu. Kretanje svake linearne ose je ograničeno vođicama u smeru koji određuju spojevi u kinematičkoj strukturi, dopuštajući samo jedan stepen slobode nominalnog kretanja. Dakle, idealno je da se opis položaja i kretanja klizača u odnosu na referentni koordinatni sistem ili koordinatni sistem prethodne ose može izraziti čistim prevođenjem koje utiče samo na poslednju kolonu HTM -a. Međutim, zbog geometrijskih netačnosti, kretanje i položaj klizača može se opisati sa šest stepeni slobode u obliku geometrijskih i kinematičkih grešaka. Geometrijske greške linearne ose odnose se na grešku svake ose pojedinačno i greške između osa. One su grupisane u greške komponenti (povezane sa geometrijom) i greške položaja (kinematičke). Greške u komponentama predstavljaju odstupanja šest izmerenih vrednosti koje zavise od ose kretanja. Za linearnu osu identifikovane su 3 linearne i 3 greške rotacije komponente mašine - klizača povezane sa njenim nominalnim pomeranjem. Linearne greške predstavljaju grešku linearnog pozicioniranja i dve greške normalnosti (vertikalna i horizontalna), a greške rotacije su: talasanje, skretanje i naginjanja pri kretanju [28, 29, 30]. Na slici 4 je prikazan primer šest komponenti grešaka horizontalnog klizača duž nominalnog linearnog kretanja u pravcu ose "X". Kod mašina alatki sa 3 ose postoji ukupno 18 grešaka komponenata i 3 greške položaja, kao što je prikazano u Tabeli 1.

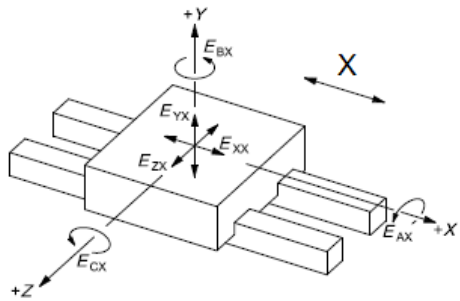

Slika 4. *Komponente grešaka linearne ose „X" [ISO 230-1 (2012)][12]*

Tabela 1. *Komponente i greške u položaju troosne mašine alatke*

Osa	Linearne greške			Ugaone greške		
	Pozicioniranje	Normalnost		naginjanje	talasenje	skretanje
X	E_{XX}	E_{YX}	E_{ZX}	E_{AX}	E_{BX}	E_{CX}
Y	E_{YY}	E_{XY}	E_{ZY}	E_{BY}	E_{AY}	E_{CY}
Z	E_{ZZ}	E_{XZ}	E_{YZ}	E_{CZ}	E_{BZ}	E_{AZ}
Gršeke položaja		E_{AOZ} , E_{COY} , E_{BOX}				

Napomena:

- E_{XX} (greška linearnog pozicioniranja): može se definisati kao greške kretanje pri translaciji komponente mašine duž svoje ose kretanja
- E_{YX}, E_{ZX} (greške normalnosti): translatorna greška komponente mašine koja se može pojaviti u bilo kom od dva pravca normalna na osu kretanja
- E_{AX}, E_{BX}, E_{CX} (ugaone greške): greške u rotaciji pokretnih komponenti mašine (klizanja) oko ose kretanja (naginjanje) ili oko dve ose koje su normalne prema osi nominalnog kretanja (talasanje i skretanje).

(Konvencija o imenovanju usvojena je iz ISO 230-1 [12] i zasnovana je na kombinaciji tri slova za opis grešaka. Slovo E potiče od greške reči (eláttoma- ελάττωμα), iza njega sledi slovo ose koje odgovara pravcu kretanja, a drugo slovo odgovara nazivu ose kretanja.)

Pored odstupanja kretanja linearno vođenih komponti mašine alatke, moraju se proveriti i odstupanja kretanja rotacionih osa, s obzirom da elementi mašine sa obrtnim kretanjem takođe imaju značajan uticaj na tačnost. Na primer, grešaka kretanja ose glavnog vretena, tačnost pozicioniranja obrtnog stola ili odstupanja položaja i oblika površina spajanja. Primeri površine spajanja su konus držača alata, konus za centriranje i pričvršćivanje steznih glava ili oslona površina obrtnih stolova. Za proveru netačnosti rotacionih osa mogu se koristiti različite metode i merni pribor. Analogno šest odstupanja kod pravolinijskog kretanja, rotaciono kretanje takođe ima šest pojedinačnih odstupanja od idealnog (bez grešaka) rotacionog kretanja (Slika 5.). Ako se uzmu u obzir greške kretanja rotacione ose za određeni proces obrade, nijedna od šest komponenti greške nema isti efekat na rezultujuću obrađenu površinu. Za slučaj obrade uzdužnim struganjem, sva relativna kretanja između alata i obratka sa komponentom u pravcu ose “X”, imaju direktan uticaj na odstupanje prečnika, grešku položaja, odstupanja od kružnog oblika ili hrapavost. Način na koji se određeno odstupanje kretanja odražava na geometriju obratka direktno zavisi od frekvencije ovog kretanja. Netačnosti u pravcu osa “Y” i “Z” imaju mali uticaj na prečnik i mogu se posmatrati kao odstupanja drugog reda. To ukazuje da se kod rotacionog kretanja mogu razlikovati osetljivi i neosetljivi pravci kretanja. Bez obzira na postupak obrade, osetljivi pravci se mogu definisati kao oni koji imaju komponentu u pravcu spojne linije između vrha alata i normale na površinu obrade. Odstupanja u pravcu tangente na površinu obratka imaju mali uticaj. Stoga se ovi pravci kretanja nazivaju neosetljivim pravcima. Sledeći ova razmatranja, jasno je da pri ispitivanju rotacionih osa treba odrediti samo komponente netačnosti koje su važne za odgovarajuću obradu (greške u osetljivim pravcima). Greške u neosetljivom pravcu mogu se zanemariti kao izvor grešaka drugog reda, jer one imaju efekat drugog reda na rezultat obrade. Pored razlike između osetljivog i neosetljivog, u zavisnosti od tehnologije obrade, mora se praviti razlika između fiksnih i obrtnih osetljivih pravaca. Ova razlika određuje vrstu merenja i merne pribore koji se mogu koristiti. Odstupanja kretanja ose obrtanja glavnog vretena se određuju tokom nekoliko obrtaja vretena tako da se mogu utvrditi različite komponente grešaka kretanja. Ukupna greška kretanja vretena u jednom pravcu sastoji se od ponovljive i neponovljive komponente. Ponovljive ili sinhrone komponente kretanja se ponavljaju na isti način sa svakim obrtom, odnosno na celobrojnim umnoščima frekvencije obrtanja. Neponovljiva ili asinhrona odstupanja pri obrtanju su odstupanja koja se javljaju na necelim umnoščima frekvencija obrtanja.

Asinhrone greške uključuju stohastička pomeranja kao i komponente sa fiksnim frekvencijama kretanja. Merenjem se može odrediti kriva unutrašnjeg i spoljašnjeg omotača odstupanja rotacionog kretanja. Podela ukupne greške na sinhrone i asinhrone se koristi za procenu uticaja kretanja glavnog vretena na rezultujuću tačnost obradka. Na primer, pri uzdužnom struganju, sinhrona greška utiče na odstupanje oblika (odstupanje kružnosti), a asinhrona utiče na hrapavost.

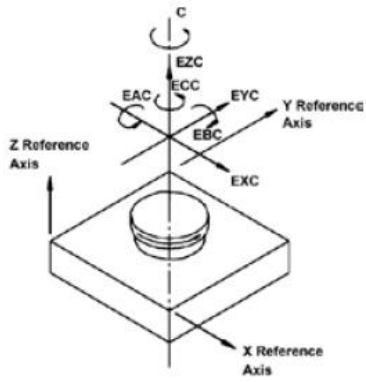

Slika 5. *Komponenta greške ose „C“ prema ISO 230-7 [17].*
EXC: radijalna greška kretanje ose „C“ u „X“ pravcu;
EYC: radijalna greška kretanje ose „C“ u „Y“ pravcu;
EZC: aksijalna greška kretanja ose „C“;
EAC: greška ose „C“ usled obrtanja oko ose „X“;
EBC: greška ose„C“ usled obrtanja oko ose„Y“ i
ECC: ugaona greška pozicioniranje.

Već je više puta naglašeno da sve oštrija konkurencija zahteva tačnije delove što se, praktično manifestuje u potrebi za tačnijim mašinama alatkama. Poslednje navedeno je, između ostalog, iniciralo potrebu razvoja metoda i mernog pribora za ispitivanja tačnosti savremenih mašina alatki. Može se konstatovati da je kraj dvadesetog veka omogućio postizanje zadovoljavajuće geometrijske tačnost mašina alatki u pravcu jedne ose numeričkom kompenzacijom netačnosti pozicioniranja, pa je, nakon toga, najveća netačnost parametara pravosti i normalnosti, što je dovelo da potrebe za definisanjem zapreminske tačnosti. Zapreminska tačnost preciznije odražava tačnost mašine alatke nego bilo koje drugo merenje koje se može izvršiti. “Konvencionalna“ (prava) definicija tačnosti 3D zapreminskog pozicioniranja (zapreminska tačnost) je kvadratni koren srednje tačnosti pomeranja (RMS) u pravcu tri ose. Ispitivanje zapreminske tačnosti primenom uobičajene laserske interferometrije je dosta skupo i naporno. Potrebno je više dana zastoja mašine i iskusan operater da bi se izvršila merenja. Zbog toga se razvijaju i predlažu druge metode za ispitivanje zapreminske tačnosti. Definicija ili metoda aproksimacije „prave“ zapreminske tačnosti treba da je u dobroj koleraciji sa istom, ali da je manje zahtevna za merenje tako da bi bila prihvaćena od strane proizvođača mašina alatki, i da postane praksa i obaveza da se rezultati zapreminske tačnosti dostavljaju korisniku [31].

Zapreminska tačnost V(XYZ) je maksimalni opseg relativnih odstupanja između stvarnog i idealnog položaja između alata i obradka mašine alatke pri kretanju X, Y, Z i orijentaciji u A, B, C u zapremini radnog prostora. Pod pretpostavkom da se kreće kruto telo, jednačine za šest grešaka u pravcima linearnih X, Y i Z, i rotacionih osa, A, B i C su [32]:

$$V(XYZ,X) = \text{deviations in } X \text{ at } XYZ = EXX + EXY + EXZ$$

$$V(XYZ,Y) = \text{deviations in } Y \text{ at } XYZ = EYX + EYY + EYZ$$

$$V(XYZ,Z) = \text{deviations in } Z \text{ at } XYZ = EZX + EZY + EZZ$$

$$V(XYZ,A) = \text{angular deviations around } X \text{ at } XYZ = EAX + EAY + EAZ$$

$$V(XYZ,B) = \text{angular deviations around } Y \text{ at } XYZ = EBX + EBY + EBZ$$

$$V(XYZ,C) = \text{angular deviations around } Z \text{ at } XYZ = ECX + ECY + ECZ$$

Ovde su greške normalnosti uključene u greške pravosti. Ugaone greške su male i mogu se tretirati kao skalarne.

Amplituda zapreminske greške može se definisati kao RMS tri linearna odstupanja, a amplituda zapreminske ugaone greške može se definisati kao RMS tri ugaona odstupanja.

$$V(XYZ,R) = \text{SQRT}\{V(XYZ,X)*V(XYZ,X)+V(XYZ,Y)*V(XYZ,Y)+V(XYZ,Z)*V(XYZ,Z)\}$$

$$V(XYZ,W) = \text{SQRT}\{V(XYZ,A)*V(XYZ,A)+V(XYZ,B)*V(XYZ,B)+V(XYZ,C)*V(XYZ,C)\}$$

Zapreminska tačnost i zapreminska ugaona tačnost se mogu definisati kao maksimalni domet u radnom prostoru.

$$R_{\max} = \text{Max}\{V(XYZ,R)\}$$

$$W_{\max} = \text{Max}\{V(XYZ,W)\}$$

Druga definicija zapreminske tačnosti matematički se definiše kako je prikazano u nastavku. Maksimalni opseg greške u svakom pravcu može se izraziti kao

$$X_{\max} = \text{Max}\{V(XYZ,X)\} - \min\{V(XYZ,X)\}$$

$$Y_{\max} = \text{Max}\{V(XYZ,Y)\} - \min\{V(XYZ,Y)\}$$

$$Z_{\max} = \text{Max}\{V(XYZ,Z)\} - \min\{V(XYZ,Z)\}$$

$$A_{\max} = \text{Max}\{V(XYZ,A)\} - \min\{V(XYZ,A)\}$$

$$B_{\max} = \text{Max}\{V(XYZ,B)\} - \min\{V(XYZ,B)\}$$

$$C_{\max} = \text{Max}\{V(XYZ,C)\} - \min\{\text{V}(XYZ,C)\}$$

Zapreminska tačnost i zapreminska ugaona tačnost se mogu definisati kao RMS maksimalnog opsega greške u svakom pravcu :

$$R_{\max} = \mathrm{SQRT}\{X_{\max} * X_{\max} + Y_{\max} * Y_{\max} + Z_{\max} * Z_{\max}\}$$

$$W_{\max} = \mathrm{SQRT}\{A_{\max} * A_{\max} + B_{\max} * B_{\max} + C_{\max} * C_{\max}\}$$

Gornje dve jednačine su na bazi validne definicije zapreminska tačnost, a da bi se ona odredila potrebno je opsežno i dugotrajno merenje.

Na kraju se prikazuje metoda definisanja zapreminske tačnosti na bazi grešaka dijagonalnog pomeranja tela (Ed) predložena u stadnardu ASME B5.54 i ISO 230-6 kao mera zapreminske greške. Neophodno je ovde objasniti oznake: ppp/nnn označava dijagonalni smer tela sa priraštajima u pravcu osa X, Y i Z i to: sve pozitivno/negativno; npp/pnn označava priraštaje u X, Y i Z koji su negativni/pozitivni, pozitivni/negativni i pozitivni /negativna, itd. Greške dijagonale tela u svakom pravcu su Dr(r) ppp/nnn, Dr(r) npp/pnn, Dr(r) pnp/npn i Dr(r) ppn/nnp. Na osnovu standarda ISO 230-6, dijagonalne greške E su definisane kao

Na osnovu prethodnog zapreminska greška je

$$\mathrm{Ed} = \max[\mathrm{E}_{\mathrm{ppp/nnn}}, \mathrm{E}_{\mathrm{npp/pnn}}, \mathrm{E}_{\mathrm{pnp/npn}}, \mathrm{E}_{\mathrm{ppn/nnp}}]$$

Ova definicija ne uključuje greške normalnosti. Da bi se uključila greška normalnosti, zapreminska greška se definiše kao

$$\mathrm{ESd} = \mathrm{Max}[\mathrm{Dr(r)ppp/nnn}, \mathrm{Dr(r)npp/pnn}, \mathrm{Dr(r)pnp/npn}, \mathrm{Dr(r)ppn/nnp}] - \min[\mathrm{Dr(r)pp/nnn}, \mathrm{Dr(r)npp/pnn}, \mathrm{Dr(r)pnp/npn}, \mathrm{Dr(r)ppn/nnp}]$$

Verifikacija metode dijagonalnog pomeranja je izvršena poređenjem sa razultatima konvencionalnog merenja. „Konvencionalnim merenjem“ 3D zapreminske tačnosti 10 srednje teških NU obradnih centara i prema metodi dijagonalnog pomeranja ASME B5.54, odnosno ISO 230-6, konstatovano je da navedena metoda dijagonalnog pomeranja i vrednost ESd predstavlju zadovoljavajuće dobru meru zapreminske tačnosti [32].

U cilju što sveobuhvatnijeg razmatranja tačnosti mašina alatki u nastavlu će se dati kratak prikaz i kinematičke i radne tačnosti.

Kinematičke greške mašina alatki se odnosi se na relativna odstupanja kretanja nekoliko pokretnih komponenti mašine, čija bi kretanja trebala da su u skladu sa strogim funkcionalnim zahtevima. Ove greške su posebno značajne tokom kombinovanog kretanja različitih osa, kao u slučaju izrade zupčanika relativnim kotrljanjem (koordinacija rotacionih kretanja), izrade profila gde je potrebna koordinacija rotacione u odnosu na linearnu ili linearne u odnosu na linearnu osu. Navedene greške se javljaju prilikom izvršavanja linearnih, kružnih ili drugih tipova interpolacionih algoritama. Merenja se, najčešće, izvode u neopterećenom stanju, iako su greške izraženije tokom obrade. Ove greške su blisko povezane sa geometrijskim greškama komponenti strukture mašine alatke pa se mogu delimično smatrati rezultujućim efektom geometrijskih grešaka tokom koordinatnog kretanja funkcionalnih komponenti. Da bi se izmerila kinematička odstupanja mašina, kretanje pojedinih osa mora se meriti sa najvećom mogućom rezolucijom i tačnošću. Iz tog razloga, linearna kretanja se često mere pomoću laserskog interferometra. Za merenje rotacionog kretanja mogu se koristi ugaoni optički enkoderi. Merenje odstupanja od ugaone brzine i neujednačenosti prenosa mogu se izvršiti pomoću seizmičkih torzionih senzora vibracija. Najčešće se za konkretna merenja definiše i metodologija merenja i merni pribor.

Jedina šire rasprostranjena metoda za ispitivanje kinematičkih (i geometrijskih) grešaka mašina alatki je test kružnosti u kome se meri apsolutna tačnost kružne putanje interpolirane numeričkim upravljanjem. Ispitivanja kružnih oblika sa velikim radijusima pružaju informacije o geometriji mašine, dok se uticaj dinamike pogonskih sistema procenjuje malim kružnim radijusima. Merenje se vrši pomoću dvostruke kugle (ball-bar), čiji nominalni radijus se može menjati u rasponu od 150 do 300 mm uz pomoć produžetaka. U teleskopsku mernu šipku integrisan je sistem za merenje položaja koji beleži promenu rastojanja između dve kugle tokom merenja. Apsolutna dužina merne šipke se kalibriše pre merenja pomoću merila ili na mernoj mašini.

Greške mašine se ogledaju u tipičnim odstupanjima zapisa merenja od idealnog kružnog oblika. Pošto se različita odstupanja na dijagramu preklapaju i različite greške ponekad dovode do sličnih odstupanja, jedna od mogućnosti kvalitativne evaluacije je upoređivanje zapisa merenja sa tipičnim karakteristikama pojedinačnih uzroka. Na taj način se mogu identifikovati dominirajuće greške u mašini. Prethodno ukazuje da test kružnosti spada u grupu posrednih merenja.

Najčešće primenjivan i tipični primer posrednog merenja, u skladu s ranijom sistematizacijom, je obrada test izradka (npr. ISO 10791-7 (2014)) koja povezuje dimenzije izradka sa netačnostima mašina alatki – ispitivanje radne tačnosti. Kada su u pitanju obradni centri za glodanje ISO standard definiše samo test izradak za troosne centre (Slika 6.). Obzirom da uslovi procesa rezanja (materijal, habanje alata, …) uvek utiču na rezultate ovih ispitivanja, to odstupanja izazvana tehnologijom se ne mogu odvojiti od odstupanja koja su posledica netačnosti mašine. Zbog toga se mora uvek obratiti posebna pažnja pripremi test izradaka i tumačenju rezultata merenja. Rezultati meranja test izradaka korisno dopunjuju rezultate direktnih merenja, prvenstveno geometrijske tačnosti.

Za ispitivanje radne tačnosti obradnih centara sa pet osa još uvek nisu standardizovani izradci, tako da kupci sami moraju da definišu test izradke da bi verifikovali mašinu koja ih zanima.

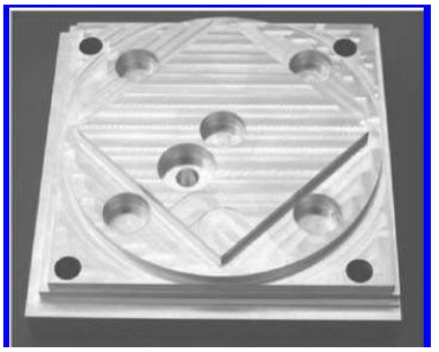

Slika 6. *Test izradak za troosne obradne centre za glodanje*

Prethodno je više puta naglašeno da operater treba da ima značajno znanje i iskustvo pri ispitivanju tačnosti mašina alatki. Kvalitet kompenzacije grešaka umnogome zavisi od operatera, njegovog razumevanja mogućih doprinosa mernoj nesigurnosti i neophodno je temeljno znanje o kompenzaciji grešaka za rešavanje problema i neočekivanih rezultata. Iskusni operateri predstavljaju veliku vrednost za proizvođača mašina alatki ili dobavljača usluga merenja i numeričke kalibracije.

Vreme potrebno za merenje svih sistemskih grešaka jedna je od glavnih prepreka za rasprostranjeniju primenu numeričke kompenzacije grešaka mašina alatki [6]. Sve procedure ispitivanja uključuju tri faze:

(A) Faza podešavanja. Ovo je potpuno ručna aktivnost. U zavisnosti od metode, može biti potrebno fino podešavanje instrumenata i vešt operater.

(B) Faza prikupljanja podataka (neposrednog merenja). Mašina obično radi u CNC režimu. U zavisnosti od metode i interfejsa, ova faza može zahtevati različit obim interakcije operatera.

(C) Faza evaluacije. Rezultati se tumače i kombinuju da bi se dobila kompletna mapa grešaka.

Slika 7 prikazuje tipične opšte sekvence ovih faza za neposredne (direktne) i posredne (indirektne) metode. Razvoj kombinovane merne instrumentacije značajno je smanjio ukupno vreme za neposredna merenja.

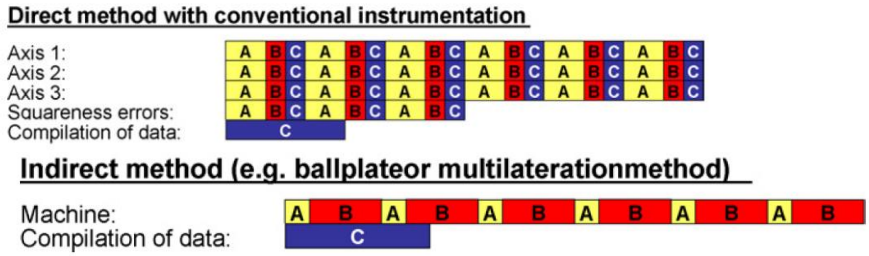

Slika 7. *Poređenje metoda mapiranja grešaka za 3-osnu mašinu: (A) faza podešavanja, (B) faza prikupljanja podataka i (C) faza evaluacije*

4 TAČNOST POZICIONIRANJA MAŠINA ALATKI

U cilju ilustracije određenih tvrdnji prikazanih u prethodnom poglavlju u nastavku se prikazuje ispitivanje tačnosti pozicioniranja troosnog NU obradnog centra, pri čemu se, iako je ispitivanje definisano određenim standardima i preporukama (smernicama) ukazuje na postojanje određenih nedorečenosti. Prethodno, pored ostalog, zahteva vrlo dobro poznavanje problematike koja se ispituje i veštog operatera sa iskustvom.

4.1 Merenje tačnosti pozicioniranja

Kod numerički upravljanih mašina alatki odstupanje položaja izvršnog organa za pomoćno kretanje ima poseban značaj za tačnost. Odstupanje od položaja predstavlja razliku između stvarne i nominalne vrednosti pozicije za sve koordinate. Ovo odstupanje zavisi od više uticajnih faktora, kao što su rezolucija i tačnost sistema za merenje položaja, elastične deformacije elemenata pogonsko-prenosnog sistema, inercijalne sile tokom ubrzanja i kočenja, efekati trenja ili klizanja po vođicama, stick-slip efekat, pomeranje klizača ili klizanje usled stezanja nakon pozicioniranja itd. Tačnost pozicioniranja je dodatno narušena kod NU mašina zbog kvaliteta upravljačkog sistema, a kod ručno upravljanih mašina zbog greške rukovaoca koja se ne može proceniti.

I ovde kao kod geometrijske tačnosti, u literaturi postoji više definicija tačnosti pozicioniranja, a u nastavku se navodi sledeća „Tačnost pozicioniranja se definiše kao odstupanje stvarnog od programiranog položaja izvršnog organa mašine alatke, pri

njegovom višestrukom dvosmernom zauzimanju pozicije u različitim položajima po svakoj od koordinatnih osa (pri nezavisnom kretanju duž ose - nezavisne ose)".

Za određivanje tačnosti pozicioniranja ose kretanja može se koristiti nekoliko mernih metoda: merač koraka sa mernom sondom, inkrementalna skala za poređenje i laserski interferometar, koji se posebno koristi za duge hodove. Postupak ispitivanja tačnosti pozicioniranja numerički upravljanih mašina alatki je definisan standardima npr. ISO 230-2, ASME B5.54, DIN ISO 230-2, NMTBA, BS3800, JIS-B6330, kao i preporukama (smernicama) VDI/DGQ 3441:1982, VDI 2617, i sl.

U nastavku se prikazije ispitivanje tačnosti pozicioniranja mašina alatka u skladu sa preporukom VDI/DGQ 3441 [33] i primenom laserske interferometrije.

Kod srednjeteških mašina alatki, obrtno kretanje pogonskog motora se pretvara u pravolinijsko izvršnog organa, posredstvom zavojnog vretena i navrtke sa recirkulacijom kuglica. Pri kretnju se zavojno vreteno zagreva usled trenja, što dovodi do njegovog izduženja, koje se menja tokom vremena i može se odraziti na rezultat merenja kada se koriste sistemi za indirektno merenje pomeranja. Zbog toga su definisane tri različite metode kretanja za dolaženje u mernu poziciju - tačku pri ispitivanju tačnosti pozicioniranja (Slika 8.).

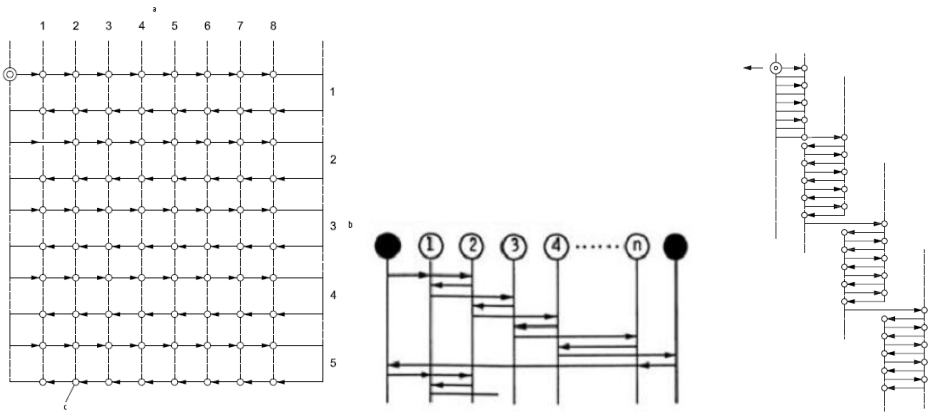

a) c)

Slika 8. *Limearna metoda kretanja (a); metoda kretanja hodočasnika (b); matoda kretanja klatna (c)*

Linearnu metodu kretanja, koja se njašće koristi, karakteriše kratka dužina putanje merenja i kratko vreme merenja za ceo postupak. Zbog velikog vremenskog kašnjenja između približavanja prvom mernom položaju (tački) iz različitih smerova, izduženje zavojnog vretena, kao rezultat zagrevanja, kako u opsegu promene smera tako i u širenju položaja je primetno. Ovu metodu kretanja karakteriše najkraće vreme merenja, ali i najveći vremenski interval između prvog i poslednjeg merenja u prvom mernom položaju.

Metoda kretanja klatna predstavlja drugu krajnost po tome što se sve izmerene vrednosti dobijaju jedna za drugom u svakom mernom položaju. To znači da je najveća moguća vremenska razlika između prikupljanja izmerenih vrednosti na prvom i poslednjem položaju, a najkraće vreme za pribavljanje izmerenih vrednosti na jednom položaju. Uticaj temperature se pojavljuje kao sistematska komponenta greške pozicioniranja, dok na opseg promene smera i raspon položaja gotovo ne utiče zagrevanje mašine.

Kod metode koraka hodočasnika, vremenski razmak pri pristupanju svim mernim položajima iz različitih smerova je mali, ali zbog veće dužine merne putanje vreme merenja za ceo postupak merenja je duže. Efekti temperature na mestu promene smera se nadoknađuju, ali se promene dužine zbog porasta temperature javljaju primetno u delu sistematske greške. Metoda koraka hodočasnika predstavlja kompromis između prethodne dve metode.

Za sve metode kretanja važno je da se evidentira što više mernih tačaka (položaja) i da se svakoj mernoj tački pristupi najmanje pet puta iz oba smera. Da bi se izbegle periodične greške, razmaci mernih tačaka trebaju biti različiti.

Kao i kod drugih ispitivanja parametara geometrijske tačnosti mašina alatki i ispitivanja tačnosti pozicioniranja se najčešće vrši metodom laserske interferometrije. Ova metoda predstavlja popularnu „neposrednu“ metodu merenja veoma velike tačnosti i preciznosti. Jedan od nedostataka metode je što zahteva mnogo vremena i značajno iskustvo operatera u cilju uspešne primene.

Pri ispitivanju tačnosti pozicioniranja obradnog centra H&H FM38 instalisanog na Fakultetu tehničkih nauka u Laboratoriji za mašine alatke u Novom Sadu laserskim interferometrom u pravcu ose “X” raspored komponenti merne opreme je prikazan na slici 9. Sistemi za merenje, koji se baziraju na principu laserske interferometrije imaju svojstvo, da je potrebno određeno vreme, da bi iskazali tačne i pouzdane podatke meranja. Za automatsko prikupljanje podataka pri merenju razvijeno je sopstveno programsko rešenje, kao i veza sa laserskom mernom instrumentacijom. Vreme mirovanja u mernoj tački (položaju) prema preporuci [8] treba da je 3 do 7 [s] (Slika 10). Program za “prikupljanje podataka” proverava da li je stvarna pozicija unutar postavljenog prozora greške oko ciljne pozicije. Ako je ovaj uslov ispunjen, pokreće se kontrola mirovanja koja nadgleda da li je promena položaja u određenom vremenskom ciklusu manja od dozvoljene vrednosti. Nakon mirovanja, merni sistem omogućava da vreme čekanja protekne, što bi trebalo da iznosi oko 70% vremena zadržavanja mašine T_W dok se ne zabeleži izmerena vrednost. Da bi se obezbedio visok nivo tačnosti merenja, merni računar neprekidno nadgleda parametre okoline i koriguje njihov uticaj na talasnu dužinu lasera. Takođe se meri temperatura mašine koja se ispituje i koriguju rezultati merenja.

Slika 9. *Prikaz postavljanja merne opreme pri ispitivanju tačnosti pozicioniranja ose “X” troosnog NU obrdnog centra*

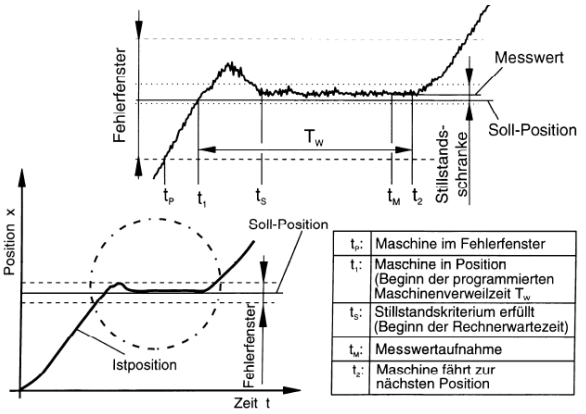

Slika 10. *Kontrola zaustavljanja za automatsko prikupljanje podataka pri merenju tačnosti pozicioniranja*

4.2 Statistička analiza rezultata

Za opisivanje tačnosti pozicioniranja za ciljnu tačku (položaj) potrebno je više karakterističnih vrednosti. Na slici 11 prikazana je raspodela izmerenih vrednosti u obliku Gausovih krivih za mernu tačku iz različitih smerova kretanja.

Izmerene vrednosti se matematički sračunavaju u skladu sa zakonitostima statistike:

- Srednja vrednost srednjih verednosti (centralna vrednost) u mernoj poziciji "j" (sistematsko odstupanje od ciljne vrednosti):

$$\overline{\overline{x}}_i = \frac{\left(\overline{x}_i \uparrow + \overline{x}_i \downarrow\right)}{2}$$

- Srednja vrednost izmerenih vrednosti u smeru pozitivnog kretanja:

$$\overline{x}_i \uparrow = \frac{1}{n} \sum_{j=1}^{n} x_{ij} \uparrow$$

- Srednja vrednost izmerenih vrednosti u smeru negativnog kretanja:

$$\overline{x}_i \downarrow = \frac{1}{n} \sum_{j=1}^{n} x_{ij} \downarrow$$

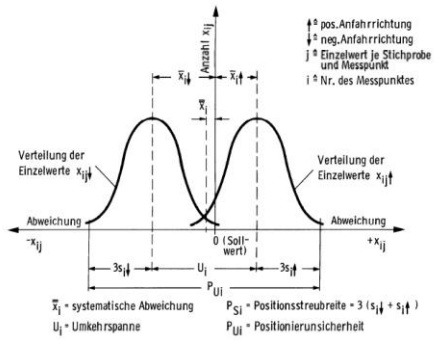

Slika 11. *Raspodela izmerenih vrednosti u mernoj tački*

- Raspon odstupanja srednjih vrednosti na mernoj poziciji "j" -U_j

$$U_j = \left| \bar{x}_j\uparrow - \bar{x}_j\downarrow \right|$$

- Maksimalni raspon odstupanja srednjih vrednosti - U_{max}

$U_{max} = U_{jmax}$

- Srednja vrednost raspona odstupanja srednjih vrednosti - $\bar{U}$

$$\bar{U} = \frac{1}{m}\sum_{j=1}^{m} U_j$$

- Standardno odstupanje (standardna devijacija) izmerenih vrednosti na mernoj poziciji "j" pri pozicioniranju iz (↑) pozitivnog, odnosno (↓) negativnog smera - $S_j\uparrow$, $S_j\downarrow$

$$S_j\uparrow = \sqrt{\frac{1}{n-1}\sum_{i=1}^{n}\left(x_{ij}\uparrow - \bar{x}_{ij}\uparrow\right)^2}$$

$$S_j\downarrow = \sqrt{\frac{1}{n-1}\sum_{i=1}^{n}\left(x_{ij}\downarrow - \bar{x}_{ij}\downarrow\right)^2}$$

- Srednje standardno odstupanje izmerenih vrednosti na mernoj poziciji "j" - $\bar{S}_j$

$$\bar{S}_j = \frac{1}{2}\left(S_j\uparrow + S_j\downarrow\right)$$

- Raspon odstupanja pojedinačnih vrednosti pozicioniranja na mernoj poziciji "j" -P_{sj}

$$P_{sj} = 6\,\bar{S}_j$$

- Maksimalni raspon odstupanja pojedinačnih vrednosti pozicioniranja - P_{smax}

$P_{smax} = P_{sjmax}$

- Srednja vrednost raspona odstupanja pojedinačnih vrednosti pozicioniranja - $\bar{P}_s$

$$\bar{P}_s = \frac{1}{m}\sum_{j=1}^{m} P_{sj}$$

Sada je moguće definisati i ostale statističke veličine:

- Raspon odstupanja centralnih vrednosti pozicioniranja - P_a

$$P_a = \left| \bar{\bar{x}}_{jmax} - \bar{\bar{x}}_{jmin} \right|$$

- Raspon odstupanja pozicioniranja - P

$$P = \left[\bar{\bar{x}}_j + \frac{1}{2}\left(U_j + P_{sj}\right) \right]_{max} - \left[\bar{\bar{x}}_j - \frac{1}{2}\left(U_j + P_{sj}\right) \right]_{min}$$

Ovako matematički definisane vrednosti pojedinih parametara kojima se definiše tačnost pozicioniranja mogu se iskazati i u vidu definicija.

Raspon odstupanja pozicioniranja - (P) je ukupno odstupanje pozicioniranja duž ispitivane ose obzirom na dobijene vrednosti u pojedinim mernim položajima (pozicijama), i obuhvata:

- raspon odstupanja centralnih vrednosti pozicioniranja (P_a),
- raspon odstupanja srednjih vrednosti dvosmernog pozicioniranja (U),
- raspon odstupanja pojedinačnih vrednosti pozicioniranja (P_s).

Raspon odstupanja centralnih vrednosti pozicioniranja - (P_a) predstavlja sistematsko odstupanje i njime je obuhvaćena najveća razlika srednjih vrednosti (aritmetičkih sredina) pozicioniranja u svim mernim pozicijama duž ispitivane ose.

Raspon odstupanja srednjih vrednosti dvosmernog pozicioniranja - (U) je razlika srednjih vrednosti (aritmetička sredina) pojedinačnih izmerenih veličina za oba smera ulaska u definisanu poziciju. Ovo odstupanje predstavlja sistematsko odstupanje.

Raspon odstupanja pojedinačnih vrednosti pozicioniranja - (P_s) opisuje slučajno odstupanje u svakoj mernoj poziciji duž ispitivane ose izraženo utvrđenom statističkom verovatnoćom.

Kao ilustracija tačnosti pozicioniranja jedne ose, na slici 12 dat je grafički prikaz tačnosti pozicioniranja NU struga za osu “X”. Na osnovu ovog prikaza mogu se otkriti sistematske greške u mernom ili sistemu pogona, npr.

- greška promene smera u položajima 2, 4 i 8 (relativno male) zbog grešaka u zavojnom vretenu ,
- povećavanje sistematske greške u svim pozicijama zbog ukupne greške zavojnog vretena.

Ako se merne pozicije ose koja se ispituje odaberu dovoljno blizu, tada je moguće otkriti komponente grešaka, kao što su greška nagibe ose zavojnog vreteno. Na osnovu rezultata merenja tačnosti pozicioniranja u pojedinim mernim pozicijama, kod savremenih upravljačkih jedinica moguće je izvršiti numeričku korekciju u cilju smanjenja netačnosti promene smera i centralnih vrednosti u pojedinim mernim pozicijama.

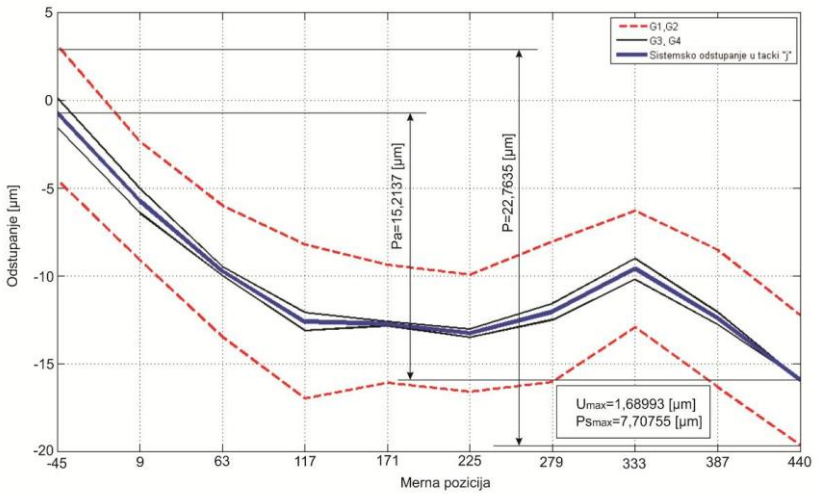

Slika 12. *Grafički prikaz statističkih parametara u mernim pozicijama duž “X”ose NU struga*

Vreme potrebno za ispitivanje tačnosti pozicioniranja NU struga pri linearnoj metodi kretanja, traje oko 10 sati, primenom metode koraka klatna, vreme merenja je 9 sati i nešto manje nego kod linearne metode [8]. Navedeni podaci ilustruju tvrdnje o potrebnom vremenu za ispitivanje geometrijskih grešaka mašina alatki.

4.3 Analiza uticaja brzine kretanja, vremena mirovanja i metode kretanja na tačnost pozicioniranja

U cilju upotpunjavanja znanja o ispitivanju tačnosti pozicioniranja mašina alatki ovde se razmatra uticaj brzine kretanja, vremena mirovanja u zaustavnoj poziciji i metode kretanja na tačnost. Da bi se ovo realizovala korišćena je metoda Taguchi. Metode kretanja i vreme mirovanja su prethodno rauzmatrani, tako da se u nastavku navode određeni komentari vezani za brzinu kretanja. Na osnovu dostupnih podataka u literaturi [34], brzina kretanja pri pozicioniranju najčešće iznosi 1000 [mm/min]. Prethodno kao i dosadašnje ne malo iskustvo autora pri eksperimentalnom ispitivanja tačnosti pozicioniranja uticalo je da se definiše maksimalna brzina 1200 [mm/min], a u skladu sa tim i minimalna i srednja vrednost. Mašina čija tačnost je ispitivana spade u srednjeteške (donja granica). Faktori ispitivanja i njihovi nivoi su dati u tabeli T.1.

Tabela 2. *Faktori ispitivanja i njihovi nivoi*

Faktori	Nivoi		
	1	2	3
v - brzina klizača [mm/min]	200	500	1200
t - vreme zaustavljanja [s]	3	5	7
c - metod kretanja	Linearni	Hodočasnika	Klatna

Ukupni podaci merenja se ovde ne navode, već se samo ilustruje obrada rezultata. Rangiranje faktora za pojedine parametre ispitivanja kojima se definiše tačnost pozicioniranja prema preporuci VDI/DGQ 3441 prikazani su na slikama od 13 do 17. Pri tome je na levom delu slike data tabela sa rangiranjem parametara, a na desnom odzivni S/N grafici.

	Faktor		
Nivo	1-v	2-t	3-c
1	-16,3	-15,7	-11,2
2	-14,0	-16,2	-20,0
3	-12,2	-10,6	-11,2
Δ	4,2	5,6	8,8
Mesto	3	2	1

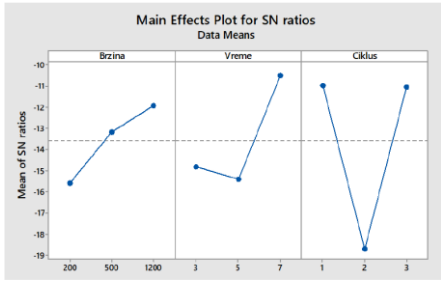

Slika 13. *Rangiranje uticaja pojedinih parametara i S/N grafici za maksimalni raspon odstupanja pojedinačnih vrednosti pozicioniranja (P_{smax})*

	Faktor		
Nivo	1-v	2-t	3-c
1	-14,53	-14,28	-14,23
2	-13,97	-14,12	-13,11
3	-13,13	-13,23	-14,29
Δ	1,40	1,05	1,19
Mesto	1	3	2

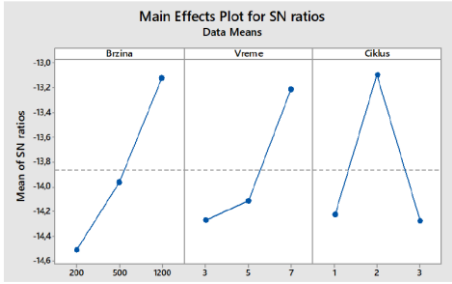

Slika 14. *Rangiranje uticaja pojedinih parametara i S/N grafici za raspon odstupanja srednjih vrednosti dvosmernog pozicioniranja (U)*

	Faktor		
Nivo	1-v	2-t	3-c
1	-23,72	-22,94	-25,75
2	-26,42	-27,34	-23,14
3	-26,91	-26,77	-28,16
Δ	3,19	4,40	5,02
Mesto	3	2	1

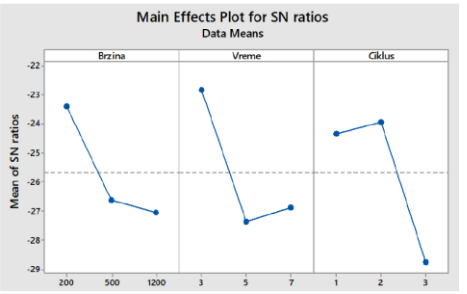

Slika 16. *Rangiranje uticaja pojedinih parametara i S/N grafici za raspon odstupanja centralnih vrednosti pozicioniranja (Pa)*

	Faktor		
Nivo	1-v	2-t	3-c
1	-29,18	-28,42	-28,75
2	-30,07	-31,15	-29,13
3	-29,76	-29,45	-31,14
Δ	0,89	2,73	2,39
Mesto	3	1	2

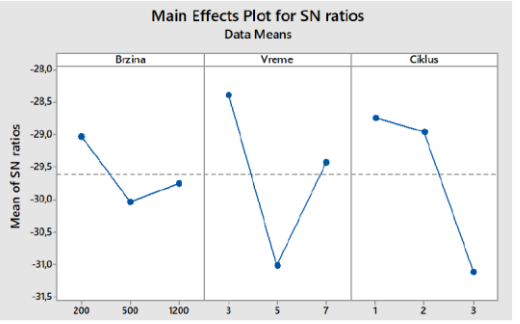

Slika 17. *Rangiranje uticaja pojedinih parametara i S/N grafici za raspon odstupanja pozicioniranja (P)*

Rangiranja S/N odnosa faktora je pokazalo, da na maksimalni raspon odstupanja pojedinačnih vrednosti pozicioniranja (P_{smax}) i raspon odstupanja centralnih vrednosti pozicioniranja (Pa) najveći uticaj ima metoda kretanja, na raspon odstupanja srednjih vrednosti dvosmernog pozicioniranja (U) brzina kretanja klizača, a na raspon odstupanja pozicioniranja (P) vreme mirovanja.

ANOVA analiza za iste parametre P_{smax}, U , Pa i P je prikazana u tabelama T.3, T.4, T.5 i T.6. Iz ovih tabela, na osnovu F testa, se zaključuje o signifikantnosti svakog pojedinačnog faktora. Faktor čija je F-vrednost veća od F=2,21, se smatra signifikantnim. Rezultati određeni primenom Taguči metoda su najvećim delom u saglasnosti sa rezultatima ANOVA analize.

Tabela 3. *Vrednosti ANOVA analize za maksimalni raspon odstupanja pojedinačnih vrednosti pozicioniranja (P_{smax})*

	Pmax			
Фактор	Стеоен слободе	Сума квадрата	Варијације	F-test	Процентуално учешће
v	2	17.53058665	8.765293	0.7936	12%
t	2	25.60551377	12.80276	1.1591	17%
c	2	81.88348382	40.94174	3.7066	56%
Грешка	2	22.0910031	11.0455		15%
Укупно	8	147.1105873			

Tabela 4. *Vrednosti ANOVA analize za raspon odstupanja srednjih vrednosti dvosmernog pozicioniranja (U)*

Фактор	Степен слободе	Сума квадрата	Варијације	F-test	Процентуално учешће
v	2	0,836140954	0,418070477	125,3487652	38%
t	2	0,508034868	0,254017434	76,16125375	23%
c	2	0,726236746	0,363118373	108,8726474	33%
Грешка	38	0,126739806	0,003335258		6%
Укупно	44	2,197152374			

Tabela 5. *Vrednosti ANOVA analize za raspon odstupanja centralnih vrednosti pozicioniranja (Pa)*

Фактор	Степен слободе	Сумаквадрата	Варијације	F-test	Процентуално учешће
v	2	59,4066	29,7033	0,1677	9%
t	2	67,2531	33,6265	0,1899	10%
c	2	208,1018	104,0509	0,5875	30%
Грешка	2	354,2066	177,1033		51%
Укупно	8	688,9680			

Tabela 6. *Vrednosti ANOVA analize za raspon odstupanja pozicioniranja (P)*

Фактор	Степен слободе	Сума квадрата	Варијације	F-test	Процентуално учешће
v	2	4,256433692	2,128217	0,0078	1%
t	2	82,03981859	41,01991	0,1507	11%
c	2	91,77787884	45,88894	0,1686	13%
Грешка	2	544,3322261	272,1661		75%
Укупно	8	722,4063572			

Na osnovu sprovedenih istraživanja i realizovane serije eksperimentalnih merenja moguće je definisati određene zaključke o uticaju razmatranih faktora (brzine kretanja klizača, vremena mirovanja i metode kretanja) na parametre kojima se prema VDI/DGQ 3441 definiše tačnost pozicioniranja.

Brzina kretanja klizača ima najveći uticaj na raspon odstupanja srednjih vrednosti dvosmernog pozicioniranja (U), i svi faktori su signifikantni.

Vreme mirovanja ima najveći uticaj na raspon odstupanja pozicioniranja (P), ali razmatrani faktori nisu signifikantni.

Metode kretanja imaju najveći uticaj na raspon odstupanja centralnih vrednosti pozicioniranja (Pa) i maksimalni raspon odstupanja pojedinačnih vrednosti pozicioniranja (P_{smax}). Takođe se može zaključiti da razmatrani faktori nemaju signifikantan uticaj na Pa, a pri definisanju P_{smax} je signifikantan samo factor metoda kretanja.

Ako se greške pozicioniranja grupišu prema karakteru na slučajne i sistematske, onda se može konstatovati da na greške slučajnog karaktera ima uticaj

samo metod kretanja, dok postoji signifikantnost razmatranih faktora samo na grešku sistemskog karaktera - raspon odstupanja srednjih vrednosti dvosmernog pozicioniranja (U). Vrednost navedenog parametra se može smanjiti numeričkom kompenzacijom.

Na kraju, imajući u vidu da je merilo tačnosti pozicioniranja NU mašine alatke raspon odstupanja pozicioniranja (P), može se konstatovati da razmatrani faktori nemaju signifikantan uticaj na isti. Prethodno predstavlja, između ostalog, obrazloženje zašto u standardima i preporukama (smernicama) za ispitivanje tačnosti pozicioniranja NU mašina alatki se ne navode vrednosti za razmatrane faktore.

Slična ispitivanja su izvedena i prema standard ISO 230- 2, i dobijeni su vrlo slični rezultati, da razmatrani faktori nemaju signifikantan uticaj na maksimalnu dvosmernu grešku pozicioniranja – M i dvosmernu grešku pozicioniranja – A.

I na kraju, prethodna razmatranja su samo potvrdila validnost desetina ispitivanja tačnosti pozicioniranja i numeričke korekcije NU mašina alatki u pogonima industrije prerade metala Srbije koje su autori realizovali poslednjih dvadesetak godina.

5 ZAVRŠNA RAZMATRANJA

Nepobitna je činjenica ta se tačnost mašina alatki sa vremenom povećava, kao odgovor na zahteve industrije za potrebom izrade što tačnijih izradaka sa ekonomičnim tolerancijama. Nakon izrade i montaže mašine alatke, potrebno je izvršiti temeljnu verifikaciju tačnosti i performansi mašine. U tu svrhu su standardima definisana određena ispitivanja. Važan rezultat ovih ispitivanja je i određivanje parametara numeričke kompenzacije za pojedine ose mašine. Praktično, ispitivanja se mogu koristiti u više svrha; kao ispitivanja u cilju prihvatanja mašine od strane kupaca, za proveru projektovanih performansi, za poređenje između sličnih mašina, za periodične provere mašina u toku eksploatacije, itd. U principu su najčešće izvode tri vrste ispitivanja.

Prvo, ispitivanja geometrijske tačnosti merenjem grešaka u ravni, paralelnosti ili koncentričnosti, kao i ispitiavnje tačnosti pozicioniranja numerički upravljanih osa (linearnih i rotacionih) mašine alatke neposrednim merenjem. Ova ispitivaja su definisana odgovarajućim standardima i preporukama,

Druga grupa uključuje postupke za proučavanje interpolacionog upravljanja, zasnovane na laserskim interferometrima, uređaju „Ball-Bar“ za relativno kretanje dve Dekartove ose. Prethodno predstavlja tipičnu metodu posrednog merenja.

Poslednja grupa ispitivanja predstavlja posredno merenje izradom “test izradaka”, odnosno proveru radne tačnosti mašina alatki.

Jedan od pravaca postizanja što veće tačnosti u montaži mašina alatki i mogućnost zadržavanja te tačnosti u eksploataciji je numerička kompenzacija. Numerička kompenzacija grešaka je jedna od važnih oblasti istraživanja u sadašnjem trenutku jer se kroz ovaj proces može postići povećanje tačnosti mašine alatke. Upravo su to neki od pravaca budućih istraživanja u oblasti razvoja metrologije i ispitivanja mašina alatki.

Trenutna merna instrumentacija omogućava precizno merenje odstupanja od nominalne geometrije mašine alatke, a cilj je razviti, jednostavnije i jeftinije metode, da bi zauzetost mašine pri ispitivanju bila što kraća.

Potrebno je razviti metode i softver za smanjenje velikih količina podataka prikupljenih prilikom kalibracije mašine, kao i grafičko predstavljanje i redukciju skupova parametara na nekoliko reprezentativnih karakteristika mašine koje imaju suštinski značaj za tačnost.

Neophodno je razviti metodologiju ispitivanja u cilju kombinovanja pojedinačnih odstupanja mašina kako bi se formirala slika ukupne tačnosti u trodimenzionalnom prostoru (zapreminske tačnosti).

LITERATURA

[1] Archenti A., 2011, A computational framework for Control of Machining System Capability, Stockholm, Sweden, KTH Royal Institute of Technology, Doctoral Thesis

[2] Theodoros, L.: Master Thesis; Royal Institute of Technology, School of Industrial Engineering and Management ; Department of Production Engineering,

[3] Slocum, H. A.: Precision machine design. Prentice Hall, Englewood Cliffs, NJ, 1992.

[4] Lopez de Lacalle, L., Lamikiz, A.: Machine tools for high performance machining. Springer, London, 2009.

[5] ISO 230-2:2014 E. Test code for machine tools part 2: Determination of accuracy and repeatability of positioning of numerically controlled axes. Standard, International Organization for Standardization, Geneva, CH, May 2014

[6] Schwenke H., Knapp W., Haitjema H., Weckenmann A., Schmitt R., Delbressine F., 2008, Geometric error measurement and compensation of machines—An update, CIRP Annals - Manufacturing Technology, vol.57, pp. 660–675

[7] Bryan B. J.: The Abb´e principle revisited: An updated interpretation. Precision Engineering, 1(3), 1979

[8] Weck, M., Brecher, C.: Werkzeugmaschinen 5 Messtechnische Untersuchung und Beurteilung, dynamische Stabilität. Springer, Berlin, 2006.

[9] Weckenmann A, Petrovic N(2005) Comparison ofCMMLength Measurement Tests Conducted with Different 1D, 2D and 3D Standards. Proceedings of 2nd International Scientific Conference Metrology in Production Engineering, Poland, 113–117

[10] Knapp W, Tschudi U, Bucher A (1990) Vergleich von Pru¨fko¨rpern zur Abnahme von Koordinatenmessgera¨ten, Technische Rundschau TR20/1990, Hallwag, Bern

[11] Bewoor A.K., Kulkarni V.A., 2009, *Metrology and Measurement*, Tata McGraw-Hill Education

[12] ISO 230-1:2012 E. Test code for machine tools part 1: Geometric accuracy of machines operating under no-load or quasi-static conditions. Standard, International Organization for Standardization, Geneva, CH, March 2012.

[13] ISO 230-1:1996, Test Code for Machine Tools. Part 1. Geometric Accuracy of Machines Operating Under No-Load or Finishing Conditions, ISO, Geneva.

[14] ISO 230-2:2006(E), Test Code for Machine Tools. Part 2. Determination of Accuracy and Repeatability of Positioning of Numerically Controlled Axes, ISO, Geneva.

[15] ISO 230-4:2005, Test Code for Machine Tools. Part 4. Circular Tests for Numerically Controlled Machine Tools, ISO, Geneva.

[16] ISO 230-6:2002, Test Code for Machine Tools. Part 6. Determination of Positioning Accuracy on Body and Face Diagonals (Diagonal Displacement Tests), ISO, Geneva.

[17] ISO 230-7:2006(E), Test Code for Machine Tools. Part 7. Geometric Accuracy of Axes of Rotation, ISO, Geneva

[18] ISO 10791-3:1998, Test Conditions for Machining Centres. Part 3. Geometric Tests for Machines with Integral Indexable or Continuous Universal Heads (Vertical Z-axis), ISO, Geneva.

[19] ISO 10791-6:2001(E), Test Conditions for Machining Centres—Accuracy of Feeds, Speeds and Interpolations, ISO, Geneva
[20] ISO 10791-8:2001, Test Conditions for Machining Centres. Part 8. Evaluation of Contouring Performance in the Three Coordinate Planes, ISO, Geneva
[21] ISO 13041-1:2004, Test Conditions for Numerically Controlled Turning Machines and Turning Centres. Part 1. Geometric Tests for Machines with a Horizontal Workholding Spindle, ISO, Geneva
[22] ISO/FDIS 13041-2:2008, Test Conditions for Numerically Controlled Turning Machines and Turning Centres. Part 2. Geometric Tests for Machines with a Vertical Workholding Spindle, ISO, Geneva
[23] ISO 13041-4:2004, Test Conditions for Numerically Controlled Turning Machines and Turning Centres. Part 4. Accuracy and Repeatability of Positioning of Linear and Rotary Axes, ISO, Geneva.
[24] ISO 13041-7:2004, Test Conditions for Numerically Controlled Turning Machines and Turning Centres. Part 7. Evaluation of Contouring Performance in the Coordinate Planes, ISO, Geneva
[25] ISO 230-1:1996, Test Code for Machine Tools. Part 1. Geometric Accuracy of Machines Operating Under No-Load or Finishing Conditions, ISO, Geneva
[26] Knapp W (2005) Machine Tool Testing Methods: Overview over ISO Standards and other Special Tests for Machine Tool Performance Evaluation and Interim Checking. Proceedings of METROMEET 05, Bilbao, Spain
[27] Castro HIF (2008) Uncertainty Analysis of a Laser Calibration System for Evaluating the Positioning Accuracy of a Numerically Controlled Axis of Coordinate Measuring Machines and Machine Tools. Precision Engineering 32(2):106–113.
[28] Bhattacharyya, A., Schmitz, T.L.., Payne, S.W.T. et al., Introducing engineering undergraduates to CNC machine tool error compensation. Advances in Industrial and Manufacturing Engineering (2022), doi: https://doi.org/10.1016/j.aime.2022.100089.
[29] Theodoros, L.: Master Thesis; Royal Institute of Technology, School of Industrial Engineering and Management ; Department of Production Engineering,
[30] Archenti A., 2011, A computational framework for Control of Machining System Capability, Stockholm, Sweden, KTH Royal Institute of Technology, Doctoral Thesis
[31] Smith, S.T. and Chetwynd, D.G., *Development in Nanotechnology*, Volume 2: Foundations of Ultraprecision Mechanism Design, ISBN: 2881248403, 1992
[32] Ramesh, R., Mannan, M.A., and Poo A.N., Error compensation in machine tools—a review. Part II: thermal errors. *Int. J. Mach. Tool Manu*., 40, 1257–1284, 2000.
[33] VDI/DGQ 3441 – 3445: Statistische Prüfung der Arbeits- und Positionsgenauigkeit von Werkzeugmaschinen
[34] Pfeifer T (2002) Production Metrology. Oldenbourg Verlag

COMETa 2022
6th INTERNATIONAL SCIENTIFIC CONFERENCE
17th - 19th November 2022
Jahorina, B&H, Republic of Srpska
University of East Sarajevo
Faculty of Mechanical Engineering
Conference on Mechanical Engineering Technologies and Applications

UTJECAJ NANOŠENJA PVD PREVLAKA NA OTPORNOST ADHEZIJSKOM TROŠENJU KONSTRUKCIJSKOG ČELIKA 45S20

Ivica Kladarić[1], Stjepan Golubić[2], Goran Šimunović[3], Katica Šimunović[4], Slavica Kladarić[5], Tomislav Šarić[6]

Rezime: PVD prevlake tvrdih spojeva smanjuju adhezijsko i abrazijsko trošenje, a pojedine vrste prevlaka također smanjuju faktor trenja. Temperatura PVD postupka je niža od temperature popuštanja čelika za poboljšavanje, nema deformacija dijelova i unošenja novih naprezanja. Tijekom toplinske obrade, PVD postupak se izvodi na kraju jer PVD prevlaka ne zahtijeva naknadnu toplinsku obradu. U radu je ispitan utjecaj nanošenja PVD prevlaka (cVIc i nACVIc) na otpornost adhezijskom trošenju konstrukcijskog čelika 45S20. Uzorci su prije postupka prevlačenja toplinski obrađeni normalizacijom, poboljšavanjem i kaljenjem. Rezultati mjerenja su obrađeni statistički. Na temelju provedenih eksperimentalnih ispitivanja utvrđeno je da otpornost adhezijskom trošenju PVD prevlaka u većoj mjeri ovisi o vrsti prevlake, a manje o prethodnoj toplinskoj obradi čelika.

Ključne riječi: PVD (Physical Vapour Deposition) prevlake, adhezijsko trošenje

THE INFLUENCE OF APPLYING PVD COATINGS ON ADHESION WEAR RESISTANCE OF STRUCTURALS STEEL 45S20

Abstract: PVD coatings of hard compounds reduce adhesion and abrasion wear, and some types of coatings also reduce the friction factor. The temperature of the PVD process is lower than the tempering temperature of quenched and tempered steels;

[1] Prof. dr. sc. Ivica Kladarić, Sveučilište u Slavonskom Brodu, Strojarski fakultet u Slavonskom Brodu, Slavonski Brod, Republika Hrvatska, ikladaric@unisb.hr (CA)
[2] Dr. sc. Stjepan Golubić, Sveučilište u Slavonskom Brodu, Strojarski fakultet u Slavonskom Brodu, Slavonski Brod, Republika Hrvatska, sgolubic@vub.hr
[3] Prof. dr. sc. Goran Šimunović, Sveučilište u Slavonskom Brodu, Strojarski fakultet u Slavonskom Brodu, Slavonski Brod, Republika Hrvatska, gsimunovic@unisb.hr
[4] Prof. dr. sc. Katica Šimunović, Sveučilište u Slavonskom Brodu, Strojarski fakultet u Slavonskom Brodu, Slavonski Brod, Republika Hrvatska, ksimunovic@unisb.hr
[5] Slavica Kladarić, dipl. ing. stroj., v. pred. Sveučilište u Slavonskom Brodu, Tehnički odjel, Slavonski Brod, Republika Hrvatska, skladaric@unisb.hr
[6] Prof. dr. sc. Tomislav Šarić, Sveučilište u Slavonskom Brodu, Strojarski fakultet u Slavonskom Brodu, Slavonski Brod, Republika Hrvatska, tsaric@unisb.hr

there is no deformation of the parts and no additional stresses. In the case of heat treatment, the PVD process is carred out at the end, since the PVD coating does not require subsequent heat treatment. In this work, the influence of PVD coatings (cVIc and nACVIc) on the adhesive wear resistance of structural steel 45S20 was investigated. Before the coating process, the samples were heat treated by normalizing, hardening and tempering, and hardening. Measurement results were statistically evaluated. Based on the experimental tests performed, it was found that the adhesive wear resistance of PVD coatings depends more on the type of coating and less on the previous heat treatment of the steel.

Key words: PVD (Physical Vapour Deposition) coatings, Adhesion Wear

1 UVOD

Zahtijevana svojstva strojnih dijelova i alata ostvaruju se izborom odgovarajućeg materijala te primjenom različitih postupaka klasične toplinske obrade i toplinske obrade površinskih slojeva.

Jedan od postupaka toplinske obrade površinskih slojeva je fizikalno prevlačenje u parnoj fazi, odnosno PVD postupak (*eng. Physical Vapour Deposition*). Kod postupaka prevlačenja u parnoj fazi stvara se površinski sloj koji je drugačijeg sastava od materijala podloge pri čemu nema difuzije u površinske slojeve podloge. Stvaranje prevlaka se ostvaruje transportom čestica, tj. atoma, molekula i iona u vakuumu. Kod PVD postupaka metalna komponenta prevlake se fizikalnim načinom prevodi iz čvrste u parnu fazu. Pomoću PVD postupka moguće je postići vrlo tanke tvrde ili zaštitne prevlake različitih kemijskih spojeva. PVD prevlake tvrdih spojeva smanjuju abrazijsko trošenje, a sniženje faktora trenja utječe na smanjenje adhezijskog trošenja [1, 2]. Prevlake nastale PVD postupkom u pravilu imaju dobru prionjivost na osnovni materijal i smanjuju njegovu površinsku hrapavost. PVD postupak se izvodi kao završna obrada jer PVD prevlaka ne zahtijeva naknadnu toplinsku obradu. Ovaj postupak provodi se pri temperaturama ispod 500 °C te su za njega prikladni i čelici koji se visoko temperaturno popuštaju (brzorezni čelici, alatni čelici za topli rad, čelici za poboljšavanje) [3].

PVD postupci se primjenjuju za izradu dijelova u brojnim industrijama; automobilska, vojna, tekstilna, prehrambena, drvna, kemijska, industrija papira, kao zaštitne i dekorativne prevlake za opremu u medicini te različite proizvode izrađene od metala, stakla, keramike itd. Zbog ekoloških razloga PVD postupak uvodi se i kao zamjena za galvansko nanošenje prevlaka kadmija, cinka, tvrdog kroma, nikla i sl. [4].

2 EKSPERIMENTALNI RAD

U okviru istraživanja primjenjivosti PVD prevlaka na konstrukcijskim čelicima eksperimentalno je istražen utjecaj nanošenja PVD prevlaka na otpornost adhezijskom trošenju konstrukcijskog čelika 45S20. Ispitivanje je provedeno na 18 ispitnih uzoraka izrađenih prema crtežu prikazanom na slici 1.

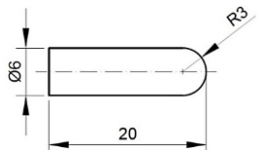

Slika 1. *Uzorak za mjerenje otpornosti trošenju*

Tri skupine po šest uzoraka su prije postupka prevlačenja toplinski obrađene normalizacijom, poboljšavanjem i kaljenjem. Nakon toplinske obrade pojedine skupine, dva uzorka su prevučena s prevlakom tipa cVIc, dva uzorka su prevučena s prevlakom tipa nACVIc, a dva su ostala bez prevlake.

Čelik 45S20 pripada skupini konstrukcijskih čelika poboljšane rezljivosti koji su namijenjeni za obradu na automatima velikim brzinama rezanja. Koristi se u velikoserijskoj proizvodnji različitih sitnih dijelova koji su slabije mehanički opterećeni, kao npr. vijaka, matica, osovinica, zatika, odstojnika i sl. [5].

Izabrani parametri toplinske obrade normalizacije, poboljšavanja i kaljenja za spomenute tri skupine ispitnih uzoraka navedeni su u tablici 1.

Tablica 1. *Parametri toplinske obrade za čelik 45S20 [6]*

Normalizacija	Poboljšavanje		Kaljenje
ϑ_N = 840 °C	ϑ_a = 840 °C	ϑ_P = 560 °C	ϑ_a = 840 °C
t_N = 1 h	t_a = 1 h	t_P = 2 h	t_a = 1 h
hlađenje na zraku	gašenje u vodi	hlađenje na zraku	gašenje u vodi

Prevlake tipa cVIc i nACVIc izabrane su na osnovi zahtjeva za visokom tvrdoćom površinskog sloja i niskim faktorom trenja koji se postavljaju pri izboru čelika za izradu strojnih dijelova. Temperatura primjene je u području uporabe konstrukcijskih čelika za poboljšavanje.

Prevlaka tipa cVIc je dvostruka prevlaka s nanostrukturom koja nastaje kombinacijom TiCN + CBC prevlake. TiCN prevlaka je konvencionalna prevlaka, a CBC (*eng. Carbon Based Coating*) je osnovna ugljična prevlaka. CBC komponenta koristi se kao suho mazivo s ciljem smanjenja faktora trenja.

Prevlaka tipa nACVIc je dvostruka prevlaka s nanostrukturom koja nastaje kombinacijom nACRo + CBC prevlake. nACRo (nc AlCrN/a-Si_3N_4) je nanokompozitna prevlaka, a CBC komponenta koristi se kao suho mazivo s ciljem smanjenja faktora trenja. Kod nACVIc prevlake za poboljšanje veze s osnovnim materijalom nanosi se sloj titana.

U tablici 2. navedena su osnovna svojstva izabranih prevlaka.

Tablica 2. *Svojstva izabranih PVD prevlaka [7]*

Prevlaka	Boja	Nanotvrdoća GPa	Debljina µm	Faktor trenja (na čeliku)	Max. tempe. uporabe °C
cVIc	siva	25	1 - 2	0,15	400
nACVIc	plavosiva	40-25	1 - 10	0,15	450

2.1 Prevlačenje uzoraka

Prevlačenje uzoraka PVD prevlakama provedeno je u tvrtki Gazela-Platit (Krško, Slovenija). Parametri prevlačenja izabrani su prema vrstama pojedinih prevlaka. Za prevlaku tipa cVIc temperatura postupka je iznosila 450 °C, a za prevlaku tipa nACVIc temperatura postupka je iznosila 460 °C. Trajanje oba postupka bilo je jednako. Prva faza postupka je ugrijavanje predmeta na temperaturu prevlačenja u trajanju od 1 h. U drugoj fazi provedeno je elektronsko čišćenje u trajanju od 15 min. Treća faza postupka je prevlačenje u trajanju od 3 h. Prevođenje metala koji se taloži iz čvrstog u plinovito stanje provedeno je pomoću električnog luka. Prije vađenja uzorci su hlađeni u peći 1 h do temperature od 100 °C.

2.2 Ispitivanje otpornosti adhezijskom trošenju

Tribološka ispitivanja provedena su metodom Pin-on-Disc na uređaju Taber-abrazer (model 503) u Laboratoriju za ispitivanje materijala Strojarskog fakulteta u Slavonskom Brodu.

Ispitni uzorak bio je u tarnom paru s pločom od nodularnog lijeva EN-GJS-400-12S. Nodularni lijev je izabran zbog toga što se pokazao kao optimalan materijal tribološkog para za izradu dijelova izloženih adhezijskom trošenju [8]. Ispitivanje je provedeno s po dva ispitna uzorka za svako stanje obrade. Mjerenje promjera površine trošenja na ispitnim uzorcima provedeno je pomoću svjetlosnog digitalnog mikroskopa nakon čega su izračunati gubici volumena i indeksi trošenja.

Prije pojedinog ispitivanja ploča je prebrušena brusnim papirom granulacije 320 što odgovara klasi hrapavosti N4, tj. Ra je od 0,1 µm do 0,2 µm i očišćena alkoholom kako bi se otklonio utjecaj prethodnog ispitivanja. Pregled ispitnih uzoraka i mjerenje promjera površine trošenja provedeno je nakon 10, 20, 30, 40, 50, 60, 70, 80, 90, 100, 200, 300, 400, 500, 600, 700, 800, 900 i 1000 okretaja. Svakim okretajem uzorak prelazi put od 257,6 mm, a nakon 1000 okretaja pređeni put je iznosio 257,6 m.

U skladu sa standardom ASTM G99 ispitni uzorak je opterećen silom od 9,81 N [8]. Gubitak volumena izračunat je na osnovi srednje vrijednosti dva mjerenja promjera površine trošenja pojedinog ispitnog uzorka prema jednadžbi (1) [9].

$$\Delta V = \frac{\pi \cdot d^4}{64 \cdot R} \tag{1}$$

gdje je: ΔV - gubitak volumena, mm^3
d - promjer površine trošenja, mm
R - polumjer kalote ispitnog uzorka, mm (R = 3 mm)

Primjeri mjerenja promjera površine trošenja i izgled uzoraka nakon 1000 okretaja ploče prikazani su na slikama 2., 3. i 4.

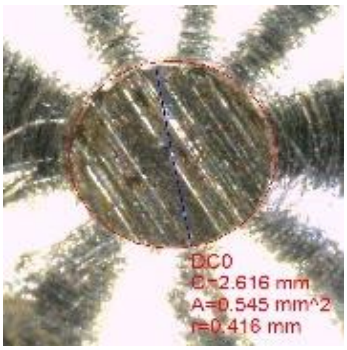

Slika 2. *Tragovi trošenja na normaliziranom čeliku 45S20 nakon 1000 okretaja*

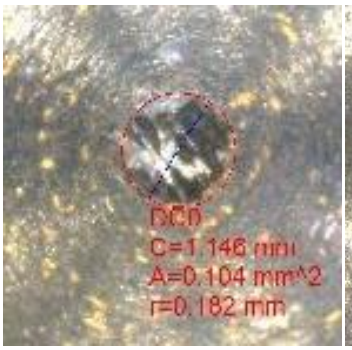

Slika 3. *Tragovi trošenja na normaliziranom čeliku 45S20 s prevlakom cVIc nakon 1000 okretaja*

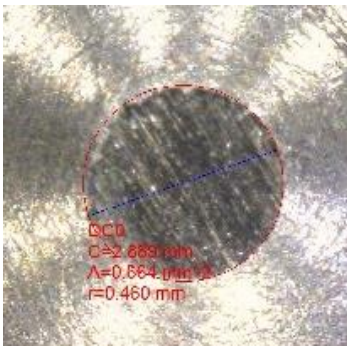

Slika 4. *Tragovi trošenja na normaliziranom čeliku 45S20 s prevlakom nACVIc nakon 1000 okretaja*

Dijagramski prikaz vrijednosti izračunatih gubitaka volumena čelika 45S20 za normalizirano, poboljšano i kaljeno stanje, bez prevlake, s prevlakom tipa cVIc i s prevlakom tipa nACVIc, prikazan je na slikama 5., 6. i 7.

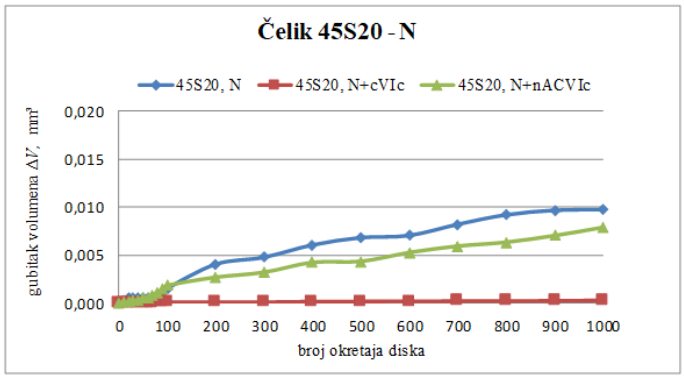

Slika 5. *Dijagramski prikaz izračunatih gubitaka volumena na normaliziranom čeliku 45S20 bez prevlake, s prevlakom tipa cVIc i s prevlakom tipa nACVIc*

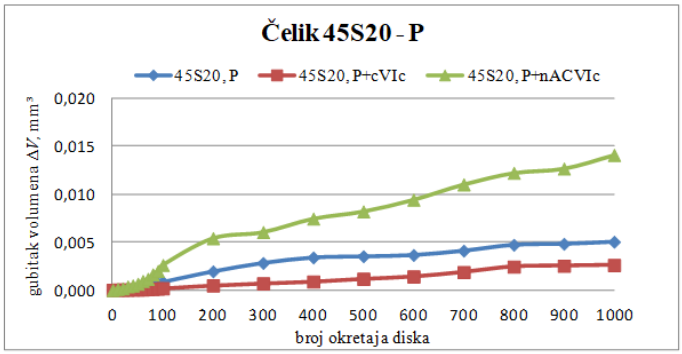

Slika 6. *Dijagramski prikaz izračunatih gubitaka volumena na poboljšanom čeliku 45S20 bez prevlake, s prevlakom tipa cVIc i s prevlakom tipa nACVIc*

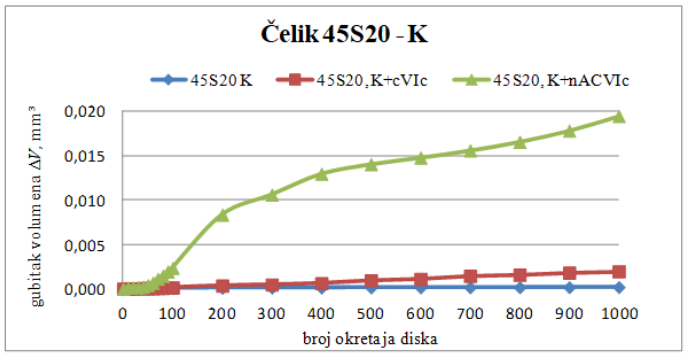

Slika 7. *Dijagramski prikaz izračunatih gubitaka volumena na kaljenom čeliku 45S20 bez prevlake, s prevlakom tipa cVIc i s prevlakom tipa nACVIc*

2.3 Indeks trošenja

Uspoređivanje utjecaja nanošenja PVD prevlaka na otpornost trošenju normaliziranog, poboljšanog i kaljenog konstrukcijskog čelika 45S20 provedeno je uspoređivanjem indeksa trošenja. Indeksi trošenja koriste se za kvantificiranje otpornosti trošenju različitih materijala. Bolju otpornost trošenju imaju materijali s nižim indeksom trošenja. Indeksi trošenja izračunati su prema metodi gubitka volumena nakon 1000 okretaja diska. Indeks trošenja gubitka volumena se računa po jednadžbi (2) [10].

$$i_{\Delta V} = \frac{\Delta V \cdot 1000}{n} \tag{2}$$

gdje je: $i_{\Delta V}$ = indeks trošenja gubitka volumena
ΔV = gubitak volumena, mm^3
n = broj okretaja diska

U tablici 3. navedeni su izračunati indeksi trošenja gubitka volumena ispitnih uzoraka nakon 1000 okretaja diska.

Tablica 3. *Indeksi trošenja gubitka volumena ispitnih uzoraka nakon 1000 okretaja diska*

Čelik	Toplinska obrada	Tip prevlake	Oznaka uzorka	Indeks trošenja gubitka volumena
45S20	Normalizirano	Bez prevlake	1.1.1	0,01157
			1.1.2	0,007878
		cVIc	1.2.1	0,000341
			1.2.2	0,00029
		nACVIc	1.3.1	0,010688
			1.3.2	0,005095
	Poboljšano	Bez prevlake	2.1.1	0,004065
			2.1.2	0,005995
		cVIc	2.2.1	0,00266
			2.2.2	0,002513
		nACVIc	2.3.1	0,014545
			2.3.2	0,013553
	Kaljeno	Bez prevlake	3.1.1	0,000204
			3.1.2	0,000153
		cVIc	3.2.1	0,002711
			3.2.2	0,001196
		nACVIc	3.3.1	0,010312
			3.3.2	0,028618

2.4 Analiza rezultata

Za utvrđivanje utjecaja toplinske obrade i vrste prevlake na adhezijsko trošenje konstrukcijskog čelika 45S20 provedena je statistička obrada indeksa trošenja gubitka volumena nakon 1000 okretaja diska, prema podacima navedenima u tablici 3. pomoću programa Design Expert 8.0.7.

Na slici 8. dan je grafički prikaz ovisnosti indeksa trošenja gubitka volumena o toplinskoj obradi čelika po vrsti prevlake, a na slici 9. dan je grafički prikaz ovisnosti indeksa trošenja gubitka volumena o vrsti prevlake po toplinskoj obradi čelika.

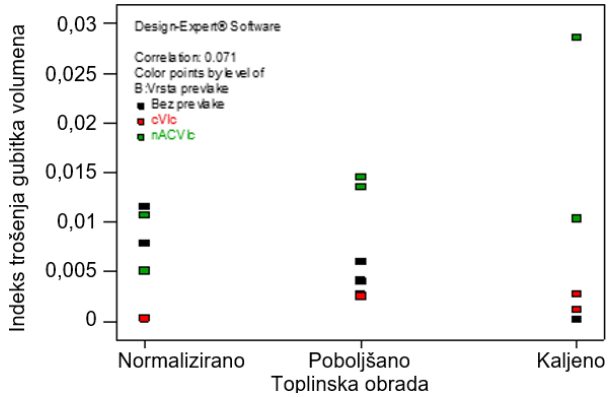

Slika 8. *Ovisnost indeksa trošenja gubitka volumena o toplinskoj obradi čelika, s rezultatima obojanima po vrsti prevlake*

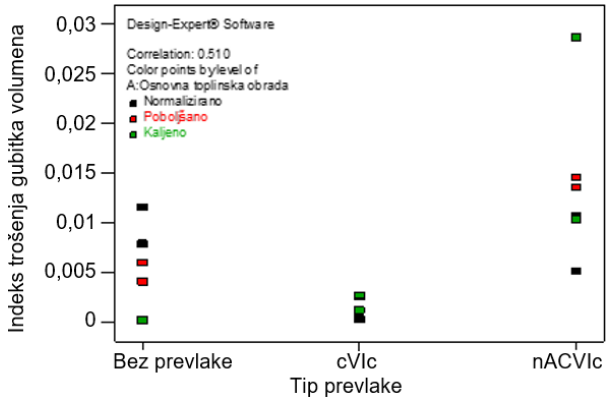

Slika 9. *Ovisnost indeksa trošenja gubitka volumena o vrsti prevlake, s rezultatima obojanima po toplinskoj obradi čelika*

U tablici 4. navedeni su rezultati statističke obrade podataka indeksa trošenja gubitka volumena ispitnih uzoraka za konstrukcijki čelik 45S20 koji su prije postupka prevlačenja PVD prevlakama tipa cVIc i nACVIc toplinski obrađeni normalizacijom, poboljšavanjem i kaljenjem.

Tablica 4. *Analiza varijance indeksa trošenja gubitka volumena ispitnih uzoraka za vjerojatnost pogreške prve vrste od 5 %*

Izvor varijabilnosti	Suma kvadratnih odstupanja, SS	Broj stupnjeva slobode, df	Prosječno ili srednje kvadratno odstupanje, MS	F omjer, F	Vjerojatnost F omjera, P-value	Kritična vrijednost F varijable za α=0,05, Fcrit
A - Toplinska obrada	$6{,}08683 \cdot 10^{-6}$	2	$3{,}04 \cdot 10^{-6}$	0,141535	0,86992	4,256495
B - Tip prevlake	0,000475171	2	0,000238	11,04896	0,003774	4,256495
Interakcija AB	0,000224661	4	$5{,}62 \cdot 10^{-5}$	2,611982	0,106628	3,633089
Pogreška	0,000193527	9	$2{,}15 \cdot 10^{-5}$			
Ukupno	0,000899445	17				

Analizom varijance podataka indeksa trošenja gubitka volumena ispitnih uzoraka konstrukcijskog čelika 45S20, prikazanoj u tablici 4. može se tvrditi, uz pouzdanost od 95 % (vjerojatnost pogreške prve vrste α = 5 %), da:

- toplinska obrada čelika nema značajan utjecaj na otpornost na adhezijsko trošenje (F < Fcrit ili vjerojatnost P-value > 0,05)
- tip prevlake ima značajan utjecaj na otpornost na adhezijsko trošenje (F > Fcrit ili vjerojatnost P-value < 0,05)
- ne postoji značajna interakcija između toplinske obrade čelika i vrste prevlake (F < Fcrit ili vjerojatnost P-value > 0,05).

3 ZAKLJUČAK

Povišenje otpornosti na trošenje jedan je od razloga primjene PVD prevlaka. Analizom rezultata ispitivanja otpornosti na adhezijsko trošenje uočena je značajna razlika trošenja u ovisnosti o vrsti prevlake kod konstrukcijskog čelika 45S20.

Kod čelika 45S20 u normaliziranom i poboljšanom stanju najmanje trošenje je bilo nakon prevlačenja s prevlakom tipa cVIc. Iako obje prevlake imaju jednak faktor trenja, otpornost adhezijskom trošenju čelika 45S20 je veća s prevlakom tipa cVIc u odnosu na prevlaku tipa nACVIc. Razlog tome treba tražiti u prionjivosti prevlaka cVIc i nACVIc.

Kod čelika 45S20 u kaljenom stanju najmanje trošenje je bilo bez prevlake, a najveće kada su prevučeni s prevlakom tipa nACVIc. Kaljeni uzorci s prevlakom tipa cVIc malo su se više trošili od uzoraka bez prevlake. Razlog postignutog najmanjeg trošenja u kaljenom stanju čelika 45S20 bez prevlake treba tražiti u izostanku moguće pojave ljuštenja tvrde PVD prevlake pri adhezijskom trošenju što bi tada uzrokovalo i trošenje abrazijskog tipa jer odvojene čestice djeluju kao abrazivi.

Otpornost adhezijskom trošenju PVD prevlaka prvenstveno ovisi o vrsti prevlake, a manje o vrsti čelika i prethodnoj toplinskoj obradi.

LITERATURA

[1] Filetin, T., Grilec, K. (2004). *Postupci modificiranja i prevlačenja površina*, HDMT, Zagreb.
[2] Burakowski, T., Wierzchoń, T. (1999). Surface Engineering of Metals Principles, *Equipment, Technologies, CRC Press*, London (New York).
[3] Krumes, D. (2004). *Površinske toplinske obrade i inženjerstvo površina,* Strojarski fakultet u Slavonskom Brodu, Slavonski Brod.
[4] Gojić, M. (2010). *Površinska obradba materijala*, Sveučilište u Zagrebu, Sisak.
[5] Filetin, T., Kovačiček, F., Indof, J. (2007). *Svojstva i primjena materijala*, Sveučilište u Zagrebu, Fakultet strojarstva i brodogradnje, Zagreb.
[6] Novosel, M., Krumes, D., Kladarić, I. (2013). *Željezni materijali Konstrukcijski čelici,* Strojarski fakultet u Slavonskom Brod, Slavonski Brod.
[7] Gazela-Platit, Katalog tvrdih prevlaka, Interni katalog tvrtke Gazela d.o.o., Krško.
[8] Golubić, S. (2004). *Primjena triboloških prevlaka na dijelovima vijčanih pumpi*, Magistarski rad, Fakultet strojarstva i brodogradnje, Zagreb.
[9] ASTM G99-17, (2017). Standard Test Method for Wear Testing with a Pin-on-Disk Apparatus, *ASTM International.*
[10] Golubić, S. (2018). *Utjecaj nanošenja PVD prevlaka na svojstva konstrukcijskih čelika za poboljšavanje*, Doktorska disertacija, Strojarski fakultet u Slavonskom Brod, Slavonski Brod.

COMETa 2022
6th INTERNATIONAL SCIENTIFIC CONFERENCE
17th - 19th November 2022
Jahorina, B&H, Republic of Srpska
University of East Sarajevo
Faculty of Mechanical Engineering
Conference on Mechanical Engineering Technologies and Applications

MAG WELDING OF DUPLEX STEEL FOR THE CONSTRUCTION OF ANTENNA MOUNTS

Tomasz Węgrzyn[1], Bożena Szczucka-Lasota[2], Wojciech Tarasiuk[3], Piotr Cybulko[4], Adam Jurek[5], Adam Döring[6], Aleksandar Kosarac[7]

Abstract: The stainless steel must be treated as good material used to construction of antenna mounts. The duplex steel 1.4462 steel has a very good resistance to corrosion in an ambient and also in an elevated temperatures. The duplex steel is rather good weldable, although it is prone to various types of welding incompatibilities. Many factors influence quality of the weld. The goal of the paper is to study of the influence of main MAG welding parameters on creation of proper welds. A novelty in an article is the use of shielding gas mixtures with a very limited amount of oxygen (below 1% O_2) in MAG welding. Welding duplex steels with a shielding gas mixture with a very low oxygen concentration was difficult until recently. It could be expected that new technological solution will allow to obtain a duplex joint with good corrosion resistance and good mechanical properties, which is important in antenna structures. The mechanical properties of several tested joints were investigated and the relationship between the oxygen content in the gas mixture and the oxygen content in the weld was determined.

Key words: welding, MAG, 1.4462 steel, experiment, thermal conditions

1 INTRODUCTION

The paper presents the results of investigation leading to the selection of the correct MAG welding parameters of a thin-walled structure made of 1.4462 duplex steel (stainless material). Duplex steel could be treated as an important material in the

1 Prof. dr hab. inż. Tomasz Węgrzyn, Silesian University of Technology, Katowice, Poland, tomasz.wegrzyn@polsl.pl
2 Dr hab inż. Bożena Szczucka Lasota, prof. PŚ, Silesian University of Technology, Katowice, Poland, bozena.szczucka-lasota@polsl.pl
3 Dr inż. Wojciech Tarasiuk, Bialystok University of Technology, Bialystok, Poland, w.tarasiuk@pb.edu.pl
4 Dr inż. Piotr Cybulko, Institute of Power Engineering in Białystok, Bialystok, Poland, p.cybulko@iezd.pl
5 Adam Jurek, Novar Sp. z o. o., Gliwice, Adam.Jurek@novar.com
6 Adam Döring, mgr inż. WSB University, Gdansk,
7 Prof. Aleksandar Kosarac, University of East Sarajevo, Sarajevo, BiH, Aleksandar Kosarac aleksandar.kosarac@ues.rs.ba

construction of antenna means. Duplex steel is especially very proper material for antenna holders and towers due to their very high strength and anti-corrosive properties [1-2]. Other applications in the main industrial sectors are also popular. The weldability of duplex steel is still not well recognized [3-4]. Initially, these steels were welded using low-oxygen welding process and low nitrogen process welding processes (basic coated electrodes and TIG welding processes) [6]. Currently, thanks to the use of modern gas mixtures of argon, it is possible to weld these steels with MAG processes with gas mixtures of argon with oxygen or nitrogen below 1% of each gas. In order to get good quality of weld, it is necessary to carefully determine all welding parameters.

The most important welding parameters in MAG process are [6-7]:

- type of filler materials,
- composition of shielding gas,
- beveling method,
- welding current,
- arc voltage,
- welding speed,
- additional thermal conditions.

Welding of 1.4462 duplex steel is rather more complicated task compared to austenite steel welding [8-9]. Welding of duplex stainless steel is slightly different from welding of austenitic stainless steel due to the bi-phase nature of duplex steel. This results in different principles leading to a properly made joint due to different metallurgical processes in the weld and different welding technology [10-11, 14].

Thicker duplex steel structures (above 4 mm) could have tendency to welding cracks. Incorrect selection of linear energy during duplex steel welding (especially above 1.3 kJ/mm) can contribute to forming different not beneficial inclusions, especially carbides and nitrides. To limit those negative structure in 1.4462 duplex steel (containing 0.034% C) in the MAG process, electrode wire are applied with a carbon content reduced to approx. 0.022% [6, 12, 13]. At the same time, it is recommended that the amount of carbide forming elements, especially such as Cr, must not increase in the electrode wire [13]. It is advantageous if there are more Ni and Mo in the electrode than the base material, as both elements are responsible for good plastic properties of the joint [6].

2 TESTED MATERIAL

Duplex sheet 1.4462 was chosen to create elements of an antenna mounts. The selection of process parameters included influencing of type of shielding gas mixture, welding current and speed. The main properties of the duplex steel and weld metal deposit (WMD) of the electrode wire MIGWELD 2209 (EN ISO 14343-A G 22 9 3 NL) is presented in the Table 1.

Table 1. *Mechanical properties of duplex steel*

Material	*Yield strength (YS), MPa*	*Tensile strength (UTS), Mpa*	*Elongation, %*
Duplex 1.4462	*430*	*670*	*24*
Wire	*560*	*720*	*25*

The composition of the duplex steel and the weld metal of tested electrode wire are presented in the Table 2.

Table 2. *Chemical composition of duplex steel 1.4462 and weld metal deposit of wire*

Chemical composition	*C, %*	*Mn, %*	*Cr, %*	*Mo, %*	*Ni, %*	*Si, %*	*P, %*	*S, %*
1.4462 duplex steel	*0.035*	*1.9*	*21.8*	*2.8*	*6.4*	*0.9*	*0.029*	*0.019*
Wire MIGWELD 2209	*0.022*	*1.6*	*21.6*	*3*	*9*	*0.5*	*0.021*	*0.018*

The table 2 shows that, apart from the carbon content, the chemical composition of the duplex steel and the wire is really similar. Shielding gas according to EN ISO 14175 standard should contain pure Ar or argon-oxygen mixtures up to max. 3% oxygen. In the article, it was decided to analyze the effect of very low oxygen content in shielding mixtures (below 1% O_2), which so far were unattainable, because for a long time gas producers were not able to create mixtures with such small and precise additions of the second component of the gas mixture.

3 RESEARCH METHODS

The joints were made from duplex steel with a thickness of 3 mm in a flat position with standard V bevelling (Fig. 1).

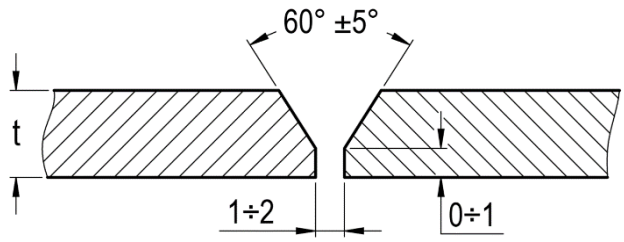

Figure 1. *Method of preparing metal sheets for welding*

After welding with various parameters, the samples for various tests were carried out. The joints were then assessed by certain NDT (non-destructivetest) and destructive testing. Visual tests and ultrasonic tests were carried out in accordance respectively with the EN:970/1999 and EN:1714/2002 standards. After that, the welded joints were checked also with the use of some destructive tests. A bend test was realized in accordance with EN:ISO-5173-201 standard, and the tensile test was done with PN-EN:ISO-6892-1/2020 standard. A hardness test was checked according to the EN:ISO 9015-1/2011 standard. The following duplex steel welding parameters have been selected:

- U_w = 18.5 V,
- I_w = 132 A,
- v_w = 317 mm/min.

The bending test was performed based on the EN-ISO-5173-2010 standard. For the bending tests prepared 10 samples with a thickness of 3 mm, width of 6 and length of mm 10 mm. The mandrel diameter was 33 mm and a roll distance was 56

mm. The bending angle was 180°. Five measurements of joint bending from the face side of the weld and also 5 measurements of the weld from the root size.

The next point of the research included joint tensile tests. The measurements were carried out on the ZWICK 100N5A machine. The microstructure of welded joints was tested by Olympus microscopy (Light microscopy – LM). The analysis of the oxygen (as well as nitrogen) content in the weld was performed on the ON 736 Leco device.

4 RESULTS AND ANALISYS

The NDT results are presented in the Table 3. This table is summarizing sample observations as a first part of the tests.

Table 3. *NDT observations*

Specimen mark	*Gas mixture*	*NDT results,*	*Observations*
D1	*Ar*	*No cracks*	*the shape of the weld is too flat*
D2	*Ar + 0.25 % O_2*	*No cracks*	*the convexity of the weld curve increases as a function of the oxygen content*
D3	*Ar +0.5% O_2*	*No cracks*	*the convexity of the weld curve increases as a function of the oxygen content. Good weld shape.*
D4	*Ar +0.75% O_2*	*No cracks*	*optimal weld shape*
D5	*Ar +1% O_2*	*Small cracks*	*the weld is too narrow*

The oxygen content in the Ar-O_2 shielding mixture was gradually increased. The oxygen content at the level of 1% O_2 was too high as there were small cracks in the weld. The joint shape was most appropriate when 0.5 O_2 or 0.75% O_2 was added to the argon gas mixture. The next stage of the research were bending tests, which were performed according to EN-ISO-5173-2010 standard. Bending tests results are presented in Tab. 4.

Table 4. *Bending test observations*

Specimen mark	*Gas mixture*	*Results*
D1	*Ar*	*small cracks*
D2	*Ar + 0.25 % O_2*	*No cracks*
D3	*Ar +0.5% O_2*	*No cracks*
D4	*Ar +0.75% O_2*	*No cracks*
D5	*Ar +1% O_2*	*small cracks*

The bending test results clearly show that the welded joints (tested samples D2, D3, D4) were made correctly, and that the welding parameters generally were correctly chosen. Minor cracks were observed in sample D1, which proves that the

addition of oxygen to the argon shielding mixture is necessary. Cracks were again observed in sample D5. Only those samples with the best results after the bending test observations were selected for the next stage of research. Thus, In the next point of the investigation the samples (D2, D3, D4) were tested on the ZWICK 100N5A machine. The tensile strength results for the joints are presented in the Table 5.

Table 5. *Tensile strenght of the joints*

Specimen	*UTS, MPa*	*Elongation, %*
D2	*585*	*23*
D3	*593*	*24*
D4	*602*	*24.5*

The results of the tensile strengths were positive. Tested joints were characterized with a high value of ultimate tensile strength, much above the recommended value of 500 MPa (for antenna structures). In one case (D4), the result was even above 600 MPa, which proves perfectly selected welding parameters. The last stage of the work was to check the content of both occurring phases in the welded joint and compare this content with the base material (fig 2).

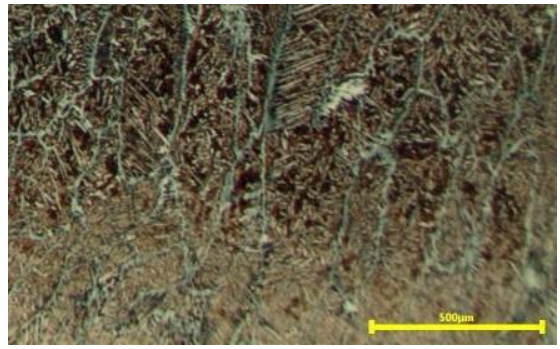

Figure 2. *Structure of the duplex connector (sample D4)*

The figure shows that the base material (lighter shade) and weld have very similar contents of both phases (austenite and delta ferrite). The austenite grains in the base material and in the weld are also of a similar level. No welding defects and non-conformities were found, which proves a good welding process. Finally, it was decided to check the oxygen content in the weld metal depending on the type of gas mixture used. The oxygen content in the alloy was checked on a ON 736 Leco device. The test results are presented in Table 6.

Table 6. *Oxygen content in WMD*

Specimen mark	*Gas mixture*	*O in WMD*
D1	*Ar*	*455 ppm*
D2	*Ar + 0.25 % O_2*	*460 ppm*
D3	*Ar +0.5% O_2*	*470 ppm*

D4	*Ar +0.75% O_2*	*485 ppm*
D5	*Ar +1% O_2*	*510 ppm*

By analyzing the table data, it can be easily noticed that with increasing oxygen content in the shielding gas mixture, there is a non-linear increase in the oxygen content in the weld metal deposit.

These results inspired the authors to check whether the relationship will be similar when nitrogen is added to the shielding argon gas mixture in similar contents. For this purpose, similar joints were made as in the part of the research on the influence of various small oxygen-containing mixtures.

In this part of the research, it was decided to focus only on the relationship between the nitrogen content in the argon mixture and the nitrogen content in the weld metal. The test results are presented in Table 7.

Table 7. *Nitrogen content in WMD*

Specimen mark	*Gas mixture*	*N in WMD*
N1	*Ar*	*55 ppm*
N2	*Ar + 0.25 % N_2*	*56 ppm*
N3	*Ar +0.5% N_2*	*59 ppm*
N4	*Ar +0.75% N_2*	*64 ppm*
N5	*Ar +1% N_2*	*65 ppm*

By analysing the table data, it can be easily noticed that with increasing nitrogen content in the argon shielding gas mixture, there is a non-linear increase in the oxygen content in the weld metal deposit.

Adding nitrogen to argan is highly recommended as nitrogen is an austenitic factor and allows to control the relationship between the austenite and delta ferrite content in the base material and in the weld. This article only focuses on the presence of oxygen and gas mixtures. Tests on nitrogen content are only comparisons in the last point of the research.

5 CONCLUSIONS

Duplex steel structures are more and more often used for various antenna elements due to their high strength and good anti-corrosion properties. The paper analyses the weldability of duplex steel with the modern MAG process. The article focuses on the selection of shielding gas mixtures with very small amount of second component. Due to the possibility of obtaining mixtures with a very low content of the second component, the influence of oxygen (in the range of 0 to 1% O_2, stroke 2.5% O_2) on the weldability of duplex steels was checked. NDT studies have shown that oxygen should be introduced into the argon shielding mixture. Further destructive tests (bending, tensile strength, microscopic tests) showed that the most advantageous was the use of argon mixture containing 0.75% O_2.

Based on the results of all tests, the main conclusions were formed:

- The MAG process is correct for welding duplex steels

- the best mechanical properties of the joint were obtained when a gas mixture containing 0.75% O_2 was used
- It has been presented that good duplex steel couplings can be obtained that can be used in the construction of antenna mount components
- It was noticed that even an unknown increase in the oxygen content in the shielding gas mixture leads to a noticeable increase in the oxygen content in the weld metal.
- Similarly, it was found that an unknown increase in the nitrogen content in the argon shielding gas mixture leads to a noticeable increase in the nitrogen content in the weld metal.
- Welded joints made of duplex steel are perfect for the construction of antenna elements and their assemblies

ACKNOWLEDGMENT

This paper is a part of the COST project, CA 18223.

REFERENCES

[1] Jaewson, L., Kamran, A., Jwo, P. (2011). Modeling of failure mode of laser welds in lap-shear speciments of HSLA steel sheets. Engineering Fracture Mechanics, Vol 1, p.p. 347-396.
[2] Darabi, J., Ekula, K. (2016). Development of a chip-integrated micro cooling device. Microelectronics Journal, Vol 34, Issue 11, pp. 1067-1074, https://doi.org/10.1016/j.mejo.2003.09.010.
[3] Hadryś, D. (2015). Impact load of welds after micro-jet cooling. Archives of Metallurgy and Materials, Vol. 60, Issue 4, p.p. 2525-2528, https://doi.org/10.1515/amm-2015-0409.
[4] Golański, D., Chmielewski, T., Skowrońska, B., Rochalski, D., (2018). Advanced Applications of Microplasma Welding. Biuletyn Instytutu Spawalnictwa w Gliwicach, Vol. 62, Issue 5, p.p. 53-63. http://dx.doi.org/10.17729/ebis.2018.5/5.
[5] Skowrońska, B., Szulc, J., Chmielewski, T., Golański, D. (2017). Wybrane właściwości złączy spawanych stali S700 MC wykonanych metodą hybrydową plazma + MAG. Welding Technology Review, Vol. 89 (10), p.p. 104-111. http://dx.doi.org/10.26628/ps.v89i10.825.
[6] Silva, A., Szczucka-Lasota, B., Węgrzyn, T., Jurek, A., (2019). MAG welding of S700MC steel used in transport means with the operation of low arc welding method. Welding Technology Review, Vol. 91 Nr 3, PL ISSN 0033-2364, 23-30.
[7] Krupicz, B., Tarasiuk, W., Barsukov, V.G., Sviridenok, A.I. (2020). Experimental Evaluation of the Influence of Mechanical Properties of Contacting Materials on Gas Abrasive Wear of Steels in Sandblasting Systems. Journal of Friction and Wear, Vol. 41, Issue: 1, p.p. 1-5.
[8] Shwachko, V. I. (2000). Cold cracking of structural steel weldments as reversible hydrogen embrittlement effect. International Journal of Hydrogen Energy, no. 25.
[9] Fydrych, D., Łabanowski, J., Rogalski, G., (2013). Weldability of high strength steels in wet welding conditions. Polish Maritime Research, Vol 20(2(78), p.p. 67-73. https://doi.org/10.2478/pomr-2013-0018.
[10] Kosarac, A., Mladenovic, C., Zeljkovic, M., Tabaković, S., Knezev, M. (2022). Neural-Network-Based Approaches for Optimization of Machining Parameters Using Small Dataset. Materials 15 (3):700. DOI: 10.3390/ma15030700.

[11] Ramon, J., Basu, R., Voort, G. V., Bola, G. A. (2021). Comprehensive study on solidification (hot) cracking in austenitic stainless steel welds from a microstructural approach, International Journal of Pressure Vessels and Piping, 2021. Vol. 194. Part B. P.104-560. ISSN 0308-0161, https://doi.org/10.1016/j.ijpvp.2021.104560.
[12] Rogalski, G., Świerczyńska, A., Landowski, M., Fydrych, D., (2020). Mechanical and microstructural characterization of TIG welded dissimilar joints between 304L austenitic stainless steel and Incoloy 800HT nickel alloy. Metals. Vol. 10. No. 5. P. 559-570.
[13] Niedzielska, M., Chmielewski, T. (2017). HVOF spraying process conditions of coating Cr3C2-NiCr deposited onto 316L steel. Welding Technology Review. Vol. 89, No. 3. Mar. 2017.
[14] Szymczak, T., Makowska K., Kowalewski, Z.L., (2020). Influence of the welding process on the mechanical characteristics and fracture of the S700MC high strength steel under various types of loading. Materials, 13; 5249:1-17.10.3390/ma13225249.

COMETa 2022
6th INTERNATIONAL SCIENTIFIC CONFERENCE
17th - 19th December 2022
Jahorina, B&H, Republic of Srpska
University of East Sarajevo
Faculty of Mechanical Engineering
Conference on Mechanical Engineering Technologies and Applications

PREDICTION OF THE WEAR CHARACTERISTICS OF ZA-27/SiC NANOCOMPOSITES USING THE ARTIFICIAL NEURAL NETWORK

Aleksandar Vencl[1], Blaža Stojanović[2], Slavica Miladinović[3], Damjan Klobčar[4]

Abstract: The zinc-aluminium casting alloy ZA-27 is well-established and is a frequently used material for plain bearing sleeves. It has good physical, mechanical and tribological properties. Its tribological properties can be improved further by adding hard ceramic particles to the alloy. The tested nanocomposites were produced by the compocasting process with mechanical alloying preprocessing (ball milling). Three different amounts of SiC nanoparticles, with the same average size of 50 nm, were used as reinforcement, i.e. 0.2, 0.3 and 0.5 wt. %. Tests were performed on a block-on-disc tribometer (line contact) under lubricated sliding conditions, at two sliding speeds (0.25 and 1 m/s), two normal loads (40 and 100 N) and a sliding distance of 1000 m. The prediction of wear rate was performed with the use of an artificial neural network (ANN). After training the ANN with architecture 3-4-1, the regression coefficient for the network was 0.99973. The experimental values and values obtained by applying the Taguchi method were compared with the predicted values, showing that ANN is more efficient in predicting wear.

Key words: Artificial neural network, Nanocomposites, Nanoparticles, Wear, ZA-27 alloy

1 INTRODUCTION

The ZA-27 alloy [1] is a zinc-aluminium casting alloy which is a frequently used material for plain bearing sleeves. Although it has good physical, mechanical, corrosion and tribological properties, it can be improved further by adding hard ceramic particles to the alloy [2-6]. Nanocomposites are a relatively new kind of material that is made up of a matrix and nano-size reinforcements with substantially distinct physical and

[1] Full professor, Aleksandar Vencl, University of Belgrade, Faculty of Mechanical Engineering, Belgrade, Serbia, avencl@mas.bg.ac.rs (CA)
[2] Full professor, Blaža Stojanović, University of Kragujevac, Faculty of Engineering, Kragujevac, Serbia, blaza@kg.ac.rs
[3] Research assistant, Slavica Miladinović, University of Kragujevac, Faculty of Engineering, Kragujevac, Serbia, slavicam@kg.ac.rs
[4] Associate professor, Damjan Klobčar, University of Ljubljana, Faculty of Mechanical Engineering, Ljubljana, Slovenia, damjan.klobcar@fs.uni-lj.si

mechanical characteristics from the matrix. They can be made using a variety of processing techniques [7,8]. Due to the size of the reinforcement, surface characteristics rather than bulk qualities dominate the properties of nanocomposite materials. Furthermore, the nano-scale reduction in the size of the reinforcement phase increases the importance of particle interaction with dislocations, which, when combined with other strengthening effects found in microcomposites, results in improved mechanical properties.

The artificial neural network (ANN) is a computer programme that can simulate relationships between a set of input and output variables. Numerous ANNs have been used to solve challenging scientific and engineering issues in a variety of domains [9]. The ANN tends to mimic the operations of the human brain and transmits information via mutually connected nodes called neurons. It employs the black-box modelling principle, which, in contrast to white and grey-box modelling, permits the exclusion of physical information or equations that relate the relationship between the input and matching output without the loss of accuracy. Each ANN is made up of three layers: the input layer, the hidden layer, and the output layer. The number of neurons in the input layer is the same as the number of input factors, and the number of neurons in the output layer is the same as the number of output factors. The hidden layer, however, can have many layers and can have different numbers of neurons in each layer [10]. ANN is usually used with a high amount of input data, but it can be used successfully for small data sets as well. For example, the application of ANN for the prediction of the wear rate of vacuum casted ZA-27 alloy composites reinforced with marble dust was done based on 25 experiments [11], while in another example, the prediction of wear and coefficient of friction of ZA/ZrB_2 composite was done based on only 20 experiments [12]. For both investigations, ANN gave a good correlation between predicted and experimental values.

Our previous study [13] demonstrated that nano-size reinforcement led to a finer structure in the nanocomposites matrix and improvement of basic mechanical properties (hardness and compressive yield strength). Erosive wear properties were also slightly improved due to the increase in ductility of nanocomposites [14], as well as the sliding wear resistance in lubricated conditions [15]. In this paper, we apply ANN to the experimentally acquired wear values to see if it can predict them with acceptable accuracy.

2 EXPERIMENTAL DETAILS

2.1 Materials and wear testing

The chemical composition of the matrix material, zinc-aluminium alloy ZA-27, was according to the ASTM standard [1]. Three nanocomposites with 0.2, 0.3, and 0.5 wt. % SiC (particle size < 50 nm) were produced through the compocasting process with mechanical alloying pre-processing (ball milling). Prior to the compocasting technique, ball milling was used to mechanically alloy matrix alloy metal chips with nanoparticles. The apparatus used for semi-solid processing is described elsewhere [15], as well as the production process parameters and a detailed description of the experimental procedure [13,14].

Experimental research of the wear characteristics was carried out under lubricated sliding conditions, on a tribometer with a block-on-disc contact geometry. Lubrication was provided by gear oil (ISO VG 220, ISO L-CKC/CKD). The blocks were produced from tested nanocomposites, while the discs were made of hardened and tempered steel 42CrMo4. The tests were conducted over a 1000 m sliding distance at

sliding speeds of 0.5 and 1 m/s and normal loads of 40 and 100 N. The wear scars on the blocks were measured after each test to calculate the wear volume.

2.2 Artificial neural network (ANN) model

The ANN simulation starts with a "training" process in which a set of inputs are applied to the network and the resulting set of outputs is compared to known values. The training is performed until the error between the output and known values reach some predefined value. This means that ANN may take a long time to be ready for use. Once it has been trained, the network can be used to predict the output for inputs that were not in the training data set. ANNs are reliable for prediction within the trained data range, but not for prediction beyond the trained data range [17].

In this study, a feed-forward backpropagation multilayer ANN is employed. Training and testing of the ANN are conducted using the software MATLAB R2016a. The logarithmic sigmoid transfer function (logsig) and linear transfer function (purelin) are used as activation transfer functions, while the Levenberg-Marquardt backpropagation algorithm (trainlm) is used as the training algorithm. Several ANN architectures have been tested (3-3-1, 3-4-1 and 3-10-1) in order to get the one with the best prediction accuracy. One hidden layer was chosen due to a small data set and low complexity of the experiment (investigation) [18]. Ultimately, the developed ANN had architecture 3-4-1 (Fig. 1), which means it had three inputs (SiC amount, sliding speed, and normal load), 4 neurons in one hidden layer, and one output (wear rate).

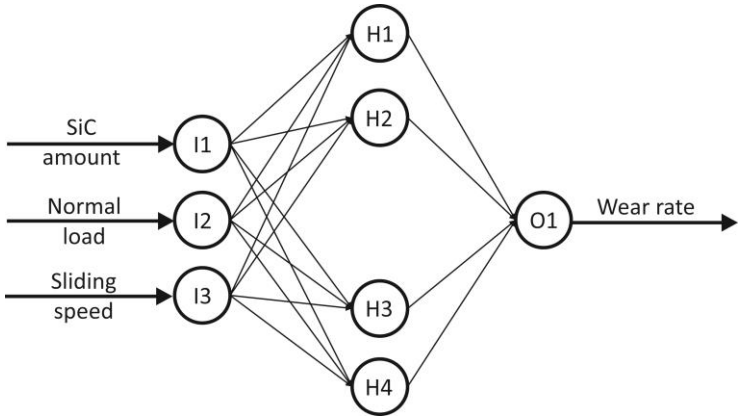

Figure 1. *Architecture of the developed feed-forward backpropagation multilayer ANN*

3 RESULTS AND DISCUSSION

The values of the used parameters in the input layer of the modelled ANN were shown in Table 1. The experimental output values [15], which were used for training, validation and testing of the ANN, are also shown in Table 1. An ANN was trained using 70 % of the data, while 15 % was used for testing and 15 % for validation. The performance and accuracy of the used ANN model are evaluated through statistical indicators such as mean square error (MSE) and regression coefficient (*R*) [17,19]. The closer the MSE value gets to zero, the better the accuracy of the model is. On the other hand, the ideal value for *R* is 1, and the closer it gets to one, the better correlation between the two groups of data (target and output values) is.

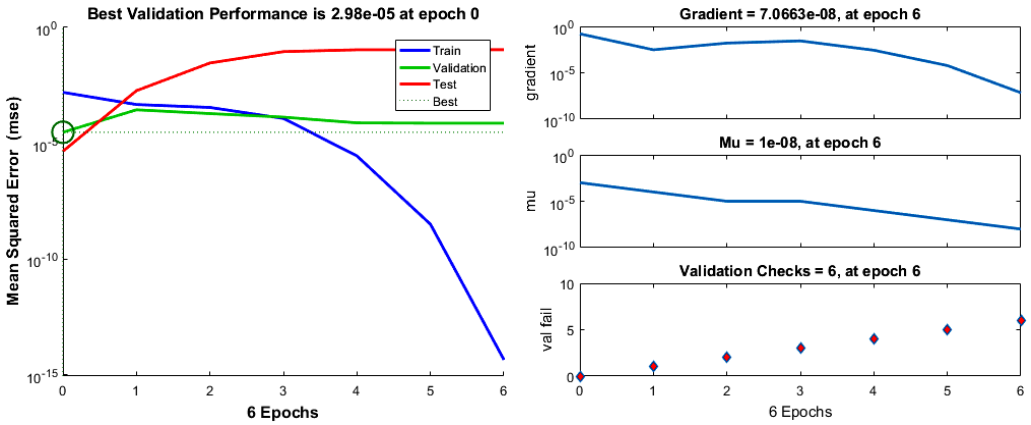

Figure 2. *Performance of the modelled ANN – mean square error and training state plots*

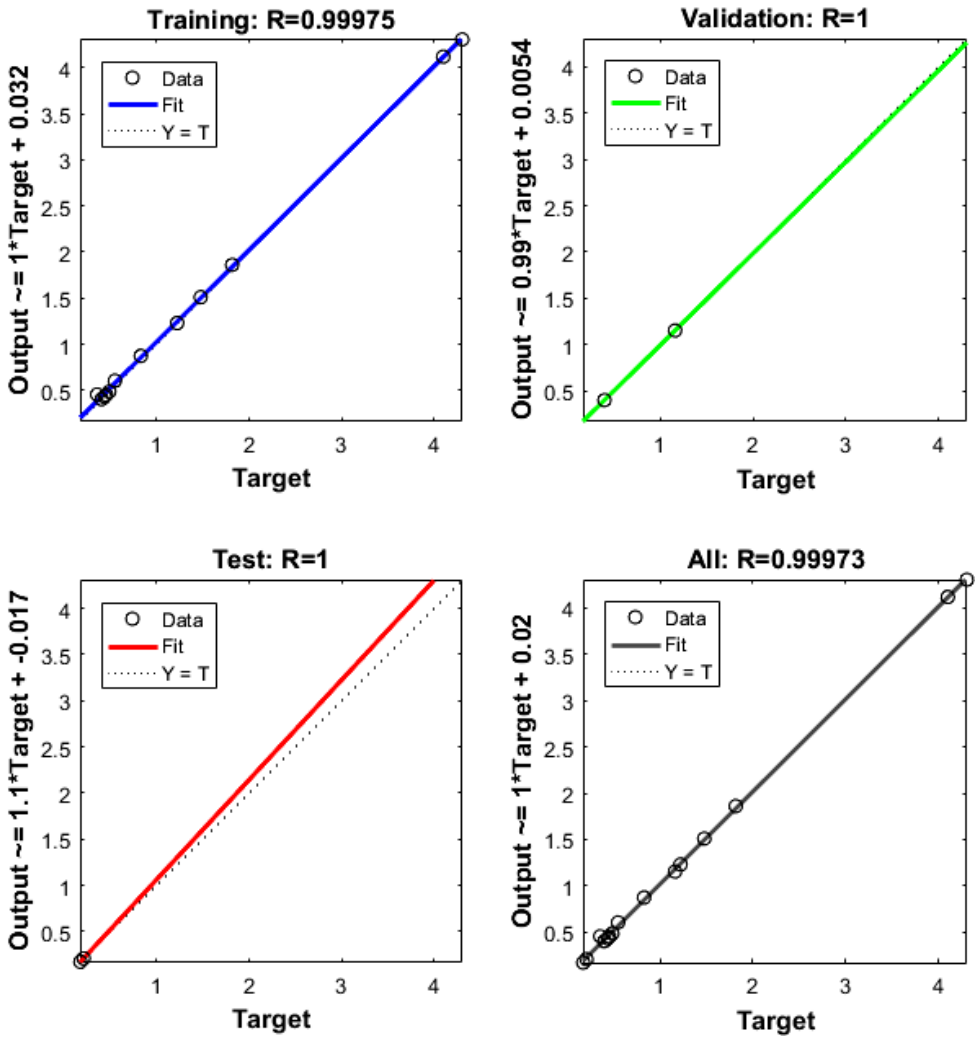

Figure 3. *Accuracy of the modelled ANN – regression analysis of different phases*

The performance of the modelled ANN is shown in Figure 2, and it can be noticed that the mean square error (MSE) for training initially has a high value and then decreases to a very small value as the number of epochs increases. This means that the ANN's training process is being performed correctly. Even though training continues until epoch 6, the best validation performance is achieved at epoch 0 with a value of 0.0000298. The training state of ANN (Fig. 2) shows that the final value of the gradient coefficient at epoch 6 is very close to zero, i.e. 7.0663×10^{-8}.

Regression analysis of the modelled ANN is performed and the regression coefficient for training, validation and testing, as well as the overall regression coefficient of the network, was obtained and shown in Figure 3. The overall regression coefficient of the network was very close to 1 (R = 0.99973), indicating a good fit and good agreement between the experimental results and the ANN model prediction.

Based on the developed mathematical model, using modelled ANN, it is possible to predict the wear rate of the nanocomposites within the limits of the experiment (trained data range). The values of the wear rate predicted with ANN are presented in Table 1 and compared with the experimental data. The deviation (error) of the predicted values from the experimentally measured values is expressed through their difference, which is also calculated as the percentage increase/decrease. Although there was a small number of data for ANN training (only 12 data), these differences were very small and the average error was only 3.38 %.

Table 1. *Input layer values, experimental data and predicted ANN output values of the composite wear rate*

Sample no.	*SiC amount, wt. %*	*Sliding speed, m/s*	*Normal load, N*	*Wear rate x 10^{-4}, mm^3/m*			
				experimentally measured	*predicted with ANN*	*error*	*± error, %*
1	*0.0*	*0.25*	*40*	*1.815*	*1.861*	*-0.045*	*2.49*
2	*0.0*	*0.25*	*100*	*4.304*	*4.303*	*0.000*	*0.01*
3	*0.0*	*1.00*	*40*	*1.476*	*1.510*	*-0.034*	*2.30*
4	*0.0*	*1.00*	*100*	*4.099*	*4.117*	*-0.018*	*0.44*
5	*0.2*	*0.25*	*40*	*0.436*	*0.432*	*0.004*	*0.87*
6	*0.2*	*0.25*	*100*	*1.221*	*1.230*	*-0.009*	*0.78*
7	*0.2*	*1.00*	*40*	*0.486*	*0.487*	*-0.001*	*0.15*
8	*0.2*	*1.00*	*100*	*0.548*	*0.606*	*-0.058*	*10.53*
9	*0.3*	*0.25*	*40*	*0.402*	*0.403*	*-0.001*	*0.22*
10	*0.3*	*0.25*	*100*	*1.162*	*1.154*	*0.008*	*0.66*
11	*0.3*	*1.00*	*40*	*0.356*	*0.456*	*-0.099*	*27.80*
12	*0.3*	*1.00*	*100*	*0.452*	*0.451*	*0.001*	*0.20*
13	*0.5*	*0.25*	*40*	*0.209*	*0.209*	*0.000*	*0.08*
14	*0.5*	*0.25*	*100*	*0.828*	*0.874*	*-0.046*	*5.55*
15	*0.5*	*1.00*	*40*	*0.174*	*0.171*	*0.003*	*1.72*
16	*0.5*	*1.00*	*100*	*0.404*	*0.405*	*-0.001*	*0.25*
						Average ± error, %	*3.38*

The accuracy of the ANN prediction was compared with the prediction obtained with the Taguchi method [15], for the same experimental set of data, and presented in Figure 4. It can be noticed that, in both cases, there is a good correlation between experimental and predicted values and both prediction methods can be used with high reliability. However, values obtained by the modelled ANN are closer to experimental values; therefore, it can be concluded that in this case, the ANN is more efficient in predicting wear rate.

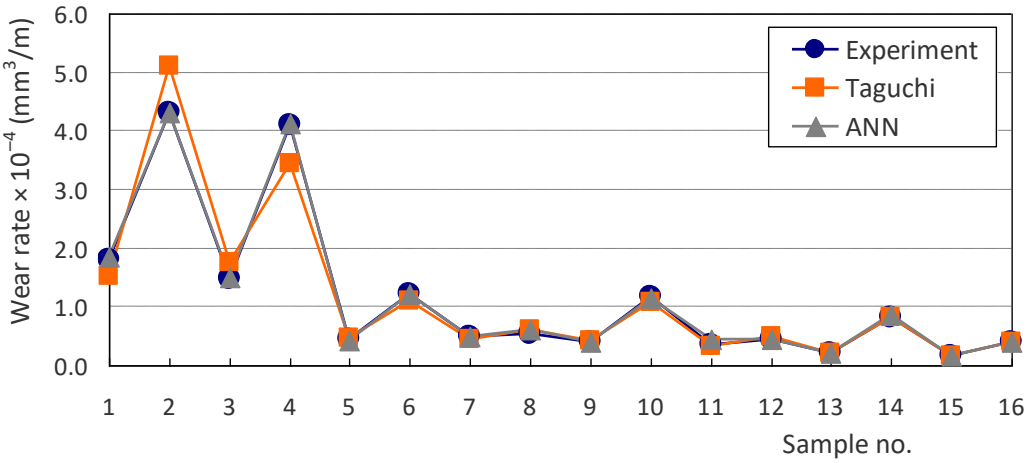

Figure 4. *Comparison of experimental, Taguchi and ANN results*

4 CONCLUSIONS

In this study, ANN was used to investigate and predict how the SiC nanoparticles, sliding speed and normal load affect the wear rate of ZA-27/SiC nanocomposites. The optimal architecture for the modelled ANN was 3-4-1, i.e. the one with three inputs (SiC amount, sliding speed, and normal load), 4 neurons in one hidden layer, and one output (wear rate). The ANN model was developed using the software MATLAB R2016a.

When compared to the experimental measurements, the results predicted by the ANN model are adequate, i.e. the regression coefficient was very close to 1 (R = 0.99973), and the average error was less than 3.38 %. Therefore, testing time and cost can be reduced by obtaining satisfactory results using the developed ANN rather than measuring them.

By comparing the two predicting methods (Taguchi and ANN), it can be concluded that ANN, in this case, is more efficient in the prediction of wear rate since their predicted values are closer to the experimentally measured values. In future research, some other machine learning techniques like random forest, gradient boosting and decision trees could be applied and then compared to ANN, because these techniques are suitable for small data sets.

ACKNOWLEDGEMENT

This work has been performed as a part of activities within the projects 451-03-68/2022-14/200105 and TR 35021, supported by the Republic of Serbia, Ministry of Education, Science and Technological Development, and its financial help is gratefully acknowledged. Collaboration through the bilateral Project 337-00-00111/2020-09/50 and BI-RS/20-21-047 between Republic of Serbia and Republic of Slovenia is also acknowledged.

REFERENCES

[1] ASTM B 86 (2013). Standard specification for zinc and zinc-aluminum (ZA) alloy foundry and die castings.

[2] Gervais, E., Barnhurst, R.J., Loong, C.A. (1985). An analysis of selected properties of ZA alloys. *Journal of Metals (JOM)*, vol. 37, no. 11, p.p. 43-47.
[3] Prasad, B.K., Yegneswaran, A.H., Patwardhan, A.K. (1996). Characterization of the wear response of a modified zinc-based alloy vis-à-vis a conventional zinc-based alloy and a bearing bronze at a high sliding speed. *Metallurgical and Materials Transactions A*, vol. 27, no. 11, p.p. 3513-3523.
[4] Vučetić, F., Veličković, S., Milivojević, A., Vencl, A. (2017). A review on tribological properties of microcomposites with ZA-27 alloy matrix. *Proceedings od the 15th International Conference on Tribology – SERBIATRIB '17*, Kragujevac (Serbia), 17-19.05.2017, p.p. 169-176.
[5] Bobić, B., Mitrović, S., Babić, M., Vencl, A., Bobić, I. (2011). Corrosion behaviour of the as-cast and heat-treated ZA27 alloy. *Tribology in Industry*, vol. 33, no. 2, p.p. 87-93.
[6] Bobić, B., Bobić, I., Vencl, A., Babić, M., Mitrović, S. (2016). Corrosion behavior of compocasted ZA27/SiC_p composites in sodium chloride solution. *Tribology in Industry*, vol. 38, no. 1, p.p. 115-120.
[7] Rohatgi, P.K., Schultz, B. (2007). Lightweight metal matrix nanocomposites – Stretching the boundaries of metals. *Material Matters*, vol. 2, no. 4, p.p. 16-20.
[8] Hebatalrahman, H.A. (2022). Hardness and tribological properties of laser irradiated PMMA based nano-microcomposites. *Tribology and Materials*, vol. 1, no. 1, p.p. 21-26.
[9] Yusri, I.M., Abdul Majeed, A.P.P., Mamat, R., Ghazali, M.F., Awad, O.I., Azmi, W.H. (2018). A review on the application of response surface method and artificial neural network in engine performance and exhaust emissions characteristics in alternative fuel. *Renewable and Sustainable Energy Reviews*, vol. 90, p.p. 665-686.
[10] Stojanović, B., Gajević, S., Kostić, N., Miladinović, S., Vencl, A. (2022). Optimization of parameters that affect wear of A356/Al_2O_3 nanocomposites using RSM, ANN, GA and PSO methods. *Industrial Lubrication and Tribology*, vol. 74, no. 3, p.p. 350-359.
[11] Gangwar, S., Pathak, V.K. (2020). Dry sliding wear characteristics evaluation and prediction of vacuum casted marble dust (MD) reinforced ZA-27 alloy composites using hybrid improved bat algorithm and ANN. *Materials Today Communications*, vol. 25, paper 101615.
[12] Kumar, V., Gautam, G., Singh, A., Singh, V., Mohan, S., Mohan, A. (2022), Tribological behaviour of ZA/ZrB_2 in situ composites using response surface methodology and artificial neural network. *Surface Topography: Metrology and Properties*, vol. 10, no. 4, paper 045001.
[13] Bobić, B., Vencl, A., Ružić, J., Bobić, I., Damnjanović, Z. (2019). Microstructural and basic mechanical characteristics of ZA27 alloy-based nanocomposites synthesized by mechanical milling and compocasting. *Journal of Composite Materials*, vol. 53, no. 15, p.p. 2033-2046.
[14] Vencl, A., Bobić, I., Bobić, B., Jakimovska, K., Svoboda, P., Kandeva, M. (2019). Erosive wear properties of ZA-27 alloy-based nanocomposites: Influence of type, amount and size of nanoparticle reinforcements. *Friction*, vol. 7, no. 4, p.p. 340-350.
[15] Vencl, A., Stojanović, B. et al. (2022). Enhancing of ZA-27 alloy wear characteristics by addition of small amount of SiC nanoparticles and its optimisation applying the Taguchi method, *Tribology and Materials*, article in press, DOI: 10.46793/tribomat.2022.014
[16] Vencl, A., Bobić, I., Jovanović, M.T., Babić, M., Mitrović, S. (2008). Microstructural and tribological properties of A356 Al-Si alloy reinforced with Al_2O_3 particles. *Tribology Letters*, vol. 32, no. 3, p.p. 159-170.

[17] Canakci, A., Ozsahin, S., Varol, T. (2012). Modeling the influence of a process control agent on the properties of metal matrix composite powders using artificial neural networks. *Powder Technology*, vol. 228, p.p. 26-35.
[18] Heaton, J. (2008). *Introduction to Neural Networks for Java*, Heaton Research, Inc., Chesterfield.
[19] Yankov, E., Minev, R., Tonchev, N., Lazov, L. (2022). Determination of the optimal mode of laser surface marking of aluminium composite panels with CO_2 laser, *Tribology and Materials*, article in press, DOI: 10.46793/tribomat.2022.011

COMETa 2022
6th INTERNATIONAL SCIENTIFIC CONFERENCE
17th - 19th November 2022
Jahorina, B&H, Republic of Srpska
University of East Sarajevo
Faculty of Mechanical Engineering
Conference on Mechanical Engineering Technologies and Applications

ANALYSIS OF MACHINE TOOLS DYNAMIC STABILITY BY APPLICATION OF VIBRATION TIME SIGNAL DECOMPOSITION

Cvijetin Mlađenović[1], Aleksandar Košarac[2], Aleksandar Živković[3], Miloš Knežev[4], Dejan Marinković[5], Robert Čep[6]

Abstract: Self-excited vibrations represent one of the most unfavorable phenomena in the cutting process, which can result in accelerated wear or breakage of the tool, sudden deterioration of the machined surface quality, increased noise and energy consumption, etc. To avoid these negative influences, special diagrams are used to define the cutting regimes, which, depending on the main spindle RPM and the depth of cut, show the border between the stable and unstable working areas of the machine tool from the self-excited vibrations point of view. These diagrams, called - stability lobe diagrams, can be defined by applying mathematical models or experimental tests This paper presents the definition of the stability lobe diagram of the machining system by experimental identification of self-excited vibrations. Limiting cutting depths, required for defining the stability map, were determined by the self-excited vibrations time signal decomposition.

Keywords: dynamic behavior of machine tools; self-excited vibrations; stability lobe diagram

1 INTRODUCTION

Self-excited vibrations represent the most unfavorable type of vibrations during cutting, which draw energy for their origin and amplitude growth from the processing process itself. These vibrations often lead to unstable operation of the machine tool,

[1] Dr Cvijetin Mlađenović, University of Novi Sad, Faculty of Technical Sciences, Novi Sad, Serbia, mladja@uns.ac.rs
[2] Dr Aleksandar Košarac, University of East Sarajevo, Faculty of Mechanical Engineering, East Sarajevo, RS, B&H, aleksandar.kosarac@ues.rs.ba
[3] Dr Aleksandar Živković, University of Novi Sad, Faculty of Technical Sciences, Novi Sad, Serbia, acoz@uns.ac.rs
[4] Miloš Knežev, University of Novi Sad, Faculty of Technical Sciences, Novi Sad, Serbia, knezev@uns.ac.rs
[5] Dejan Marinković, University of Novi Sad, Faculty of Technical Sciences, Novi Sad, Serbia, dejan.marinkovic@uns.ac.rs
[6] Dr Robert Čep, VSB – Technical University of Ostrava, Faculty of Mechanical Engineering, Ostrava-Poruba, Czech Republic, robert.cep@vsb.cz

resulting in a reduction in the quality of the machined surface, the appearance of noise, accelerated wear of tools and machine tool elements [1], etc.

To avoid these negative influences, special diagrams are used to define the cutting regimes, which, depending on the main spindle RPMs and depth of cut, show the boundary between a stable and unstable working area of the machine tool from the self-excitation vibrations point of view. These diagrams, called - stability lobe diagrams (SLD), can be defined by applying mathematical models (analytical, numerical ...) or experimental tests (tangent method, sound mapping ...).

Research on mathematical modeling of self-excited vibrations was among the first carried out by Tobias [2] and Tlusty [3], who identified the regenerative mechanism of self-excited vibrations and developed a mathematical model for defining the stability lobe diagrams in the form of differential equations with delay [4]. In addition to the previous one, the second most commonly applied method for defining the stability lobe diagram was proposed by Altintas and Budak [5]. This method, called the zero-order approximation, is based on the prediction of system stability using the zero-order Fourier expression for approximation of the change in the cutting force and to form a stability lobe diagram for processes where the cutting force varies relatively little, e.g. machining of the flat surfaces with end mills.

As modeling the dynamic behavior of the machining system is a complex procedure, as an alternative to mathematical methods for defining the stability lobe diagram, an approach based on experimental examination is proposed. With this approach, a more accurate stability lobe diagram is defined because certain approximations are not taken into account, as is the case when modeling the dynamic behavior of the machining system [4]. Experimental tests of self-excited vibrations were among the first carried out by Koenigsberger and Tlusty [6] and V.A. Kudinov [7]who defined a stability lobe diagram for turning and proposed the appropriate experimental methodology.

With the development of computer technologies, more sophisticated methods of examination and analysis of self-excited vibrations have been made possible, and thus the definition of the stability lobe diagram by experimental methods has become simpler. Thus, Quintana et all. [7] proposed a method of defining the stability lobe diagram using the sound mapping technique. To define the stability lobe diagram, the authors conducted 600 experiments, varying 30 different speeds and 20 cutting depths. For each of these experiments, the noise level was measured and entered into a 3D sound map. Based on this map and the FFT analysis of the sound signal, the authors defined a stability lobe diagram, which showed satisfactory accuracy compared to the one defined by the analytical method.

The paper presents the definition of the stability lobe diagram of the machining system by experimental identification of self-excited vibrations for the milling process. Limiting cutting depths, required for defining the stability lobe diagram, were determined by a new method based on the decomposition of the self-excited vibrations time signal. The proposed method was applied to determine the limit depths of cut when milling aluminum Al7075 on the EMCO ConceptMill 450 machining center. These limit depths were used to define the experimental stability lobe diagram which, for verification, was compared with the stability lobe diagram defined by the Fourier series method [5].

2 DETERMINATION OF LIMITING DEPTH OF CUTTING USING THE VIBRATION SIGNAL DECOMPOSITION METHOD

Self-excited vibrations in machining occur when the excitation frequency (forced vibrations, variation of cutting force due to the regenerative effect, or some other form of external excitation) coincides with the self-frequency of the so-called critical element of the machining system. When machining robust workpieces, the critical element of the machining system is most often the assembly tool-tool holder-main spindle, while when machining thin-walled workpieces, the critical element is the workpiece. Considering the above, when analyzing self-excited vibrations, it is necessary to know the natural frequencies of the characteristic elements of the machine tool, which are most often determined by experimental modal analysis.

Experimental testing of self-excited vibrations is most often performed by machining with a continuously variable cutting depth, whereby the vibration signal is collected in the time domain with appropriate sensors. During these tests, the workpiece, thanks to its inclined shape, enables a continuous increase of the cutting depth in the feed direction, while the RPMs of the main spindle increase with each subsequent pass of the tool. The cutting process is stopped at the moment of intense noise occurrence in the working space of the machine, which is usually accompanied by self-excited vibrations. The exact moment of vibration occurrence is determined based on the recorded signals. The signal of self-excited vibrations in the time domain, recorded during experimental tests, does not provide much information about the characteristics of the vibrations, so it is necessary to transform it into the frequency domain by applying a fast Fourier transformation.

When machining with a continuously variable depth of cut, the time signal contains information about the tool vibration for a wide range of depths of cut. If the entire vibration signal, from the beginning to the end of the cutting, is transformed into the frequency domain, it is possible to determine the frequency of self-excited vibrations, but it is not possible to detect the depth at which they occurred.

To obtain information about the cutting depth at which self-excited vibrations occur, the total time signal must be divided into a certain number of equal time parts that, depending on the expected accuracy, correspond to the desired change in the cutting depth. The accuracy of determining the limit cutting depth directly depends on the increment of the division of the time signal, so that increment should be as small as possible. With a fast Fourier transformation, each segment of the time signal is transformed into the frequency domain, and in the segment in which the frequencies of self-excited vibrations occur, the limiting depth of the cut is determined.

The limiting depth of cut depends on feed during the experiment (v_p), the inclination angle of the workpiece (α_0), and the moment of self-excited vibrations occurrence (T_{spv}). The moment of occurrence of self-excited vibrations is determined as the geometric mean of the initial and final time of the signal segment in which there was a jump in the amplitude of self-excited vibrations, measured from the cutting beginning (Tstart) (1). Calculation of the limit cutting depth is performed according to expression (2).

$$T_{SPV} = \sqrt{T_{seg\_start} \cdot T_{seg\_emd}} - T_{start} \tag{1}$$

$$b_{lim} = v_p \cdot \tan \alpha_0 \cdot T_{SPV} \tag{2}$$

Figure 1 shows an example of a time signal of self-excited vibrations divided into three equal segments. A fast Fourier transform was performed on each of these three signal segments and corresponding plots were obtained, also shown in Figure 1.

In the first image, which corresponds to the stable part of the signal, the basic rotation frequency of the main spindle can be distinguished at 70 [Hz] (≈4250 [rpm]) with its harmonics. In the remaining two images also appears a frequency close to the own frequency of the main spindle-tool holder-tool assembly (≈1090 [Hz]), which represents the frequency of self-excited vibrations. In addition, comparing the signals in the frequency domain with the signal in the time domain, it is noticeable that with the increase in the amplitude of the time signal, the amplitude of the frequency of self-excited vibrations also increases. By analyzing Figure 1, it is concluded that the self-excited vibrations occurred in the second segment of the time signal, whose initial time is T_{seg_start}=13[s], and final T_{seg_end}=13.5[s]. Taking into account the feed during the experimental test (v_p=336[mm/min]), the angle of inclination of the workpiece (α_0=11º), as well as the time of the start of cutting (T_{start}=10.1[s]), using expressions 1 and 2, the cutting depth was determined for a specific case, which is b_{lim}=3.42 [mm]. In addition, by analyzing the third segment of the time signal, it can be confirmed that the amplitude of self-excited vibrations is the highest in this segment and that these vibrations occurred earlier, i.e. in the second segment.

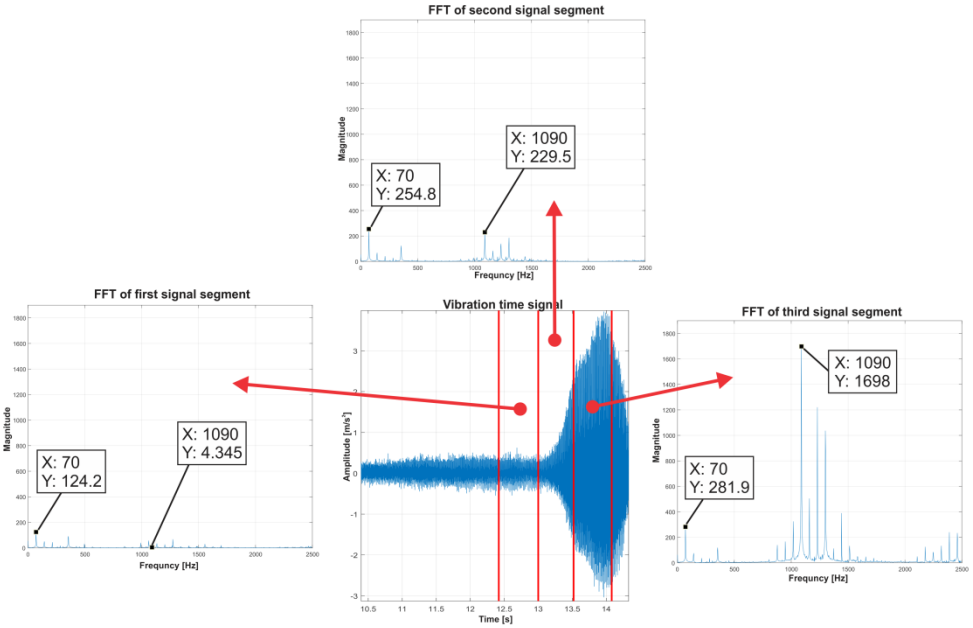

Figure 1. *Example of decomposed vibration signal FFT in machining with continuous change of cutting depth*

3 EXPERIMENTAL DEFINITION OF THE STABILITY LOBE DIAGRAM FOR THE EMCO CONCEPTMILL450 MACHINING CENTER

The experimental definition of the stability lobe diagram was carried out by the method of the self-excited vibrations time signal decomposition, on the EMCO ConceptMill450 machining center (Figure 2a), while milling a workpiece made of aluminum Al7075 with an inclined upper surface (Figure 2b), using an HSS end-mill with a diameter of ϕ10 [mm].

The main goal of this experimental test is to analyze the applicability of determining the limit cutting depths by the proposed method of the self-excited vibrations time signal decomposition. For this purpose, 29 experiments were conducted in which the main spindle RPM was varied in the range from 3000 [rpm] to 10000 [rpm], while the feed was constant at 0.02 [mm/thoot]. The workpiece, thanks to its inclined shape, enables a continuous increase of the cutting depth in the feed direction (Y axis of the machine tool), while the main spindle RPM increases with each subsequent pass of the tool in increments of 250 [rpm]. At the moment of occurrence of self-excited vibrations, the feed is stopped, the tool is moved in the direction of the X-axis of the machine and the experiment is repeated for the next main spindle RPM. During each experiment, the vibrations of the main spindle were recorded using diagnostic instrumentation, consisting of a PCB 352C33 acceleration sensor (accelerometer) and a National Instruments USB-4432 A/D card. To better detect the occurrence of self-excited vibrations, the acceleration sensor is placed as close as possible to the cutting zone, and in this case, it is fixed on the outer sleeve of the main spindle of the machining center.

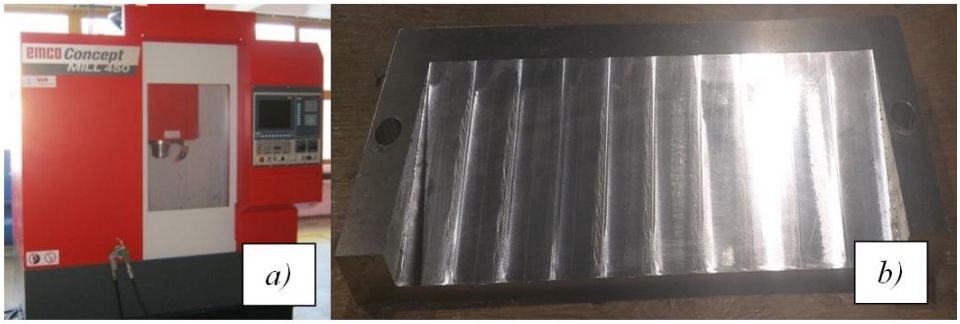

Figure 2. *a) EMCO Concept Mill 450 machining center; b) aluminum workpiece Al7075;*

To prevent damage to the machining center elements, the maximum cutting depth is limited to 8 [mm]. Therefore, for some values of the main spindle RPM, it is not possible to determine the exact value of the limit cutting depth if it is greater than 8 [mm].

The vibrations time signal, recorded during machining with a continuously variable depth of cut, contains information about the tool vibration for the wide range of cutting depths, i.e. from the beginning to the end of the cut. To obtain information about the limit cutting depth at which self-excited vibrations occur, the time signal for each performed experiment was divided into n equal parts with an increment of 0.25 [s], and then each of those parts was transformed into the frequency domain, using fast Fourier transformations. In this way, vibration frequencies are observed for each defined time range, and it is possible to detect the occurrence and increase in the amplitude of the frequency of the self-excited vibrations.

As already mentioned, self-excited vibrations occur at a frequency close to the natural frequency of the critical element (assembly) of the machining system. Therefore, it is necessary to mention that the natural frequency of the tool-tool holder-main spindle assembly is 1038 [Hz] and that it was determined in previous research.

Figure 3a shows the time signal of vibrations during machining with 6500 [rpm] of the main spindle, where, for the sake of clarity of the diagram, only four segments are separated in the region of the vibration amplitude sudden jump. A fast Fourier

transformation was performed on each of those four signal segments and corresponding diagrams were obtained (Figure 3b).

In the first two diagrams of Figure 3b, which are defined by applying the fast Fourier transformation to the first two segments of the vibration signal, the fundamental frequency of the tool rotation at 109 [Hz] (≈6500 [rpm]) and its harmonics are distinguished. In the remaining two diagrams, in addition to the basic frequency of rotation of the tool, a frequency close to the natural frequency of the tool appears, which also represents the frequency of self-excited vibrations (≈1060 [Hz]). By analyzing the amplitudes at the frequency of 1060 [Hz], it can be concluded that the self-excited vibrations occur in the third separated segment of the vibration time signal. The moment of vibrations occurrence is determined from expressions (1) and (2), based on the known time of the beginning (T_{seg_start}=8.836[s]) and the end (T_{seg_end}=9.086[s]) of the third separated vibration segment, taking into account the known time of the cutting start (T_{start}=6.439[s]), the feed during machining (v_p) and the angle of the workpiece inclined surface (α_0).

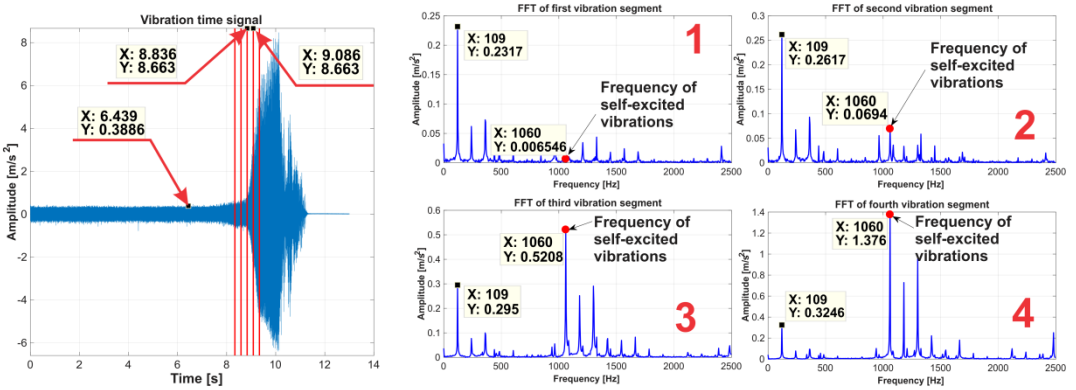

Figure 3. *a) Vibration time signal for machining at 6500 [rpm] with separated segments; b) FFT of vibration signal isolated segments*

The vibrations time signals for all performed experiments were analyzed in the same way, and the results are shown in Table 1.

Table 1. *Experimental limit cutting depths determined by the vibration signal decomposition method*

Exp. no.	Main spindle RPM	Feed [mm/min]	Limit depth of cut [mm]	Exp. no.	Main spindle RPM	Feed [mm/min]	Limit depth of cut [mm]
1	3000	240	5,23	16	6750	540	5,25
2	3250	260	4,01	17	7000	560	7,43
3	3500	280	3,28	18	7250	580	8
4	3750	300	5,91	19	7500	600	7,83
5	4000	320	8	20	7750	620	8
6	4250	340	3,75	21	8000	640	8
7	4500	360	3,31	22	8250	660	5,75
8	4750	380	4,96	23	8500	680	4,9
9	5000	400	8	24	8750	700	4,54
10	5250	420	8	25	9000	720	3,83
11	5500	440	6,3	26	9250	740	3,51

12	5750	460	3,67	27	9500	760	3,18
13	6000	480	3,17	28	9750	780	3,04
14	6250	500	3,47	29	10000	800	3,07
15	6500	520	4,15				

To define the stability lobe diagram based on the experimental values obtained by the self-excited vibrations time signal decomposition method, it is necessary to approximate the curve through the values shown in Table 1. Approximation, i.e. curve fitting was performed by creating an algorithm in the Matlab software environment, which defined the stability lobe diagram shown in red color in Figure 4. To verify the proposed experimental method, Figure 4 shows the mathematically defined stability lobe diagram obtained using the Fourier series method [5]. This stability lobe diagram is depicted in blue color. The Fourier series method has been analyzed in previous research and is not in detail described in this work.

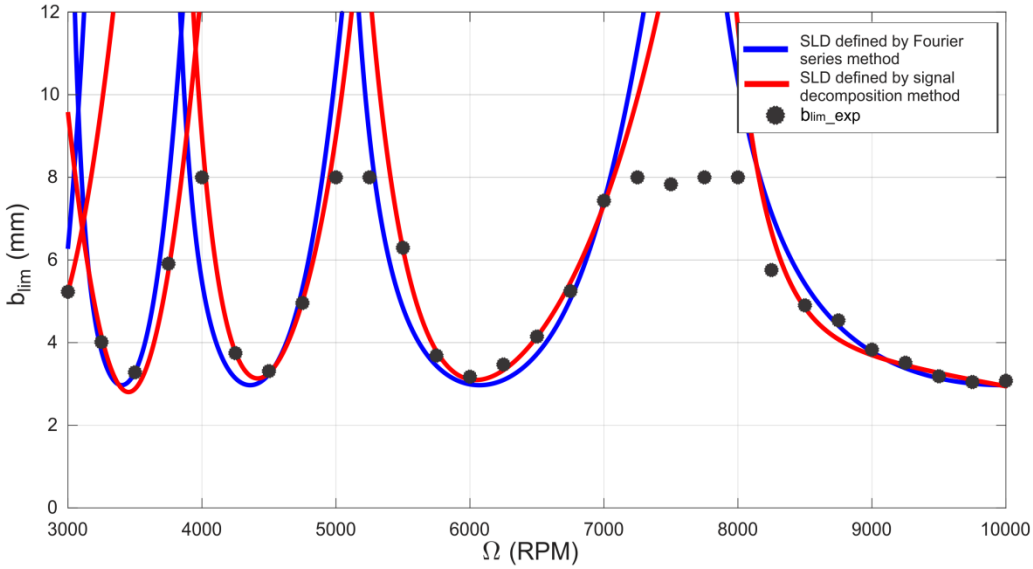

Figure 4. *Stability lobe diagram defined by the self-excited vibrations time signal decomposition method (red line) and by Fourier series method (blue line)*

4 CONCLUSION

The paper presents the definition of the stability lobe diagram of the machining system by experimental identification of self-excited vibrations. Limit cutting depths, required for the diagram defining, were determined by the self-excited vibrations time signal decomposition method.

Using the proposed method, the limit cutting depths was determined in machining aluminum Al7075 on the EMCO ConceptMill 450 machining center, and the stability lobe diagram of this machining system was defined.

Verification of the stability lobe diagram obtained by the proposed new experimental method was carried out by comparing it with a mathematically defined stability lobe diagram, created by the application of the Fourier series method. Based on this verification, it was concluded that the self-excited vibrations time signal decomposition method gives very good results in the experimental determination of the limit cutting depths and that it can be effectively applied for the verification of

mathematical models for the prediction of the occurrence of the self-excited vibration.

In addition, to fully complete the methodology of the stability lobe diagram experimental definition, which is presented in this paper, it is necessary to compare the obtained results with other experimental methods of defining the machining system stability lobe diagram (analysis of the roughness of the machined surface, tangent method, etc.). This comparison of the mentioned experimental methods represents the direction of future research within the milling process stability analysis.

REFERENCES

[1] Quintana, G., Ciurana, J.: Chatter in machining processes: A review, International Journal of Machine Tools and Manufacture, 2011. 51(5): pp. 363-376.
[2] Tobias, S., Fishwick, W.: Theory of regenerative machine tool chatter, The engineer, 1958. 205(7): pp. 199-203.
[3] Tlusty, J., Polacek, M.: The stability of machine tools against self-excited vibrations in machining, International research in production engineering, 1963. 1(1): pp. 465-474.
[4] Mlađenović, C., Košarac, A., Zeljković, M., Knežev, M.: Experimental Definition Of Machining Systems Stability Lobe Diagram, in XIII International Scientific Conference MMA 2018 – Flexible Technologies 2018. Novi Sad, Srbija: University of Novi Sad, pp. 95-98.
[5] Altintaş, Y., Budak, E.: Analytical prediction of stability lobes in milling, CIRP Annals-Manufacturing Technology, 1995. 44(1): pp. 357-362.
[6] Koenigsberger, F., Tlusty, J.: Machine Tool Structures. Vol. 1. 1970: Pergamon Press. 528.
[7] Kudinov, V.A., ed.: Dinamika stankov. 1967, Mašinostroenie, Moskva.
[8] Quintana, G., Ciurana, J., Ferrer, I., Rodríguez, C.A.: Sound mapping for identification of stability lobe diagrams in milling processes, International journal of machine tools and manufacture, 2009. 49(3): pp. 203-211.
[9] Zhu, L., Liu, C.: Recent progress of chatter prediction, detection and suppression in milling, Mechanical Systems and Signal Processing, 2020. 143: pp. 106840.
[10] Košarac, A., Šikuljak, L., Obradović, Č., Mlađenović, C., Zeljković, M.: Cutting parameters influence on surface roughness in AL 7075 milling, in 19th International Symposium INFOTEH-JAHORINA (INFOTEH), 2020. Jahorina, East Sarajevo, Bosnia and Hercegovina: IEEE.pp. 1-6.
[11] Košarac, A., Mlađenović, C., Zeljković, M., Šikuljak, L.:Experimental method for defining the stability lobe diagram in milling Č4732 (42CRMO4) steel, Acta Technica Corviniensis-Bulletin of Engineering, 2019. 12(2): pp. 31-34.
[12] Mlađenović, C., Košarac, A., Zeljković, M., Knežev, M., Živković, A.: Analytically-experimental definition of the machining systems stability lobe diagram, 37th International Conference on Production Engineering, Faculty of Engineering, Kragujevac, Serbia, Str. 316-321, 2018, ISBN 978-86-7083-893-2.

COMETa 2022
6th INTERNATIONAL SCIENTIFIC CONFERENCE
17th - 19th November 2022
Jahorina, B&H, Republic of Srpska
University of East Sarajevo
Faculty of Mechanical Engineering
Conference on Mechanical Engineering Technologies and Applications

NUMERICAL ANALYSIS OF PLANE STRAIN MULTI-DIRECTIONAL UPSETTING OF PRISMATIC SAMPLES

Nemanja Dačević[1], Marko Vilotić[2], Mladomir Milutinović[3], Luka Sevšek[4], Ljiljana Stefanović[5], Dragiša Vilotić[6]

Abstract: The plane strain multi-directional upsetting process, a severe plastic deformation (SPD) method, is used for the production of ultra-fine grained metals. Since the value and distribution of accumulated plastic strain and stress directly influence the microstructure, understanding of stress-strain state during the process is of utmost importance. Today, the finite element method (FEM) is one of the most used tools for stress-strain analysis of metal forming processes. In this paper, effective strain and stress distribution, determined by FEM, throughout six upsetting passes is presented. The material of prismatic samples is high-alloyed austenitic steel X2CrNiMo17-12-2, widely used for medical implants. Material characteristics and necessary boundary conditions are experimentally determined. Simulation results are verified comparing force and dimensional measurements from experiment and simulation.

Key words: finite element method, plane strain upsetting, severe plastic deformation

1 INTRODUCTION

In his paper [1] Valiev defined severe plastic deformation (SPD) as metal forming technology used for producing ultra-fine grained (UFG) bulk materials by imposing very high strains without major changes to the sample geometry. UFG materials are defined as materials with an average grain size of less than 1μm [2]. Compared to conventional materials, these materials exhibit superior mechanical characteristics, primarily strength, hardness, and ductility. The improvement of these properties makes it possible to reduce the dimensions and weight of structural and

[1] MSc, Nemanja Dačević, Faculty of Technical Sciences, Novi Sad, Serbia, dacevic@uns.ac.rs
[2] PhD, Marko Vilotić, Faculty of Technical Sciences, Novi Sad, Serbia, markovil@uns.ac.rs
[3] PhD, Mladomir Milutinović, Faculty of Technical Sciences, Novi Sad, Serbia, mladomil@uns.ac.rs
[4] MSc, Luka Sevšek, Faculty of Mechanical Engineering, Ljubljana, Slovenia, luka.sevsek@fs.uni-lj.si
[5] MSc, Ljiljana Stefanović, Faculty of Technical Sciences, Novi Sad, Serbia, ljiljanastefanovic@uns.ac.rs
[6] PhD, Dragiša Vilotić, Faculty of Technical Sciences, Novi Sad, Serbia, vilotic@uns.ac.rs

equipment parts. In addition, UFG metals can replace alloyed metals of similar characteristics, reducing the consumption of "rare" metals. Furthermore, the development of micro and nano-components is directly dependent on the availability of suitable materials. For a material to acquire these new properties, the UFG structure must consist of predominantly high-angle grain boundaries and be uniformly distributed throughout the bulk of the material [3].

Valiev also formulated primary conditions that any SPD method should fulfill[4]:

- Even if the considerable refinement of the microstructure already occurs at strains of 1 - 2 [3], the formation of the UFG structure is possible only after exceeding values of 6 - 8. Imposed large strains should not lead to the formation of defects in the material.
- SPD processes should be carried out at temperatures lower than 0.4 of the melting temperature of the material. Processing at higher temperatures leads to a reduction in accumulated dislocation density and an increase in grain size.
- For SPD processes, a high hydrostatic pressure greater than 1 GPa is desirable as it contributes to the deformability of the material, and therefore allows higher straining.
- Formation of equiaxed ultrafine grains depends on the vorticity of the metal flow which is at the macro level related to the non-monotonous character of the deformation.

If we take a closer look at the given SPD definition and primary conditions, we see that most of the mentioned requirements can be analysed using FEM software. Effective plastic strain and stress are the main results of almost any metal forming process simulation. The distribution of UFG in the sample is directly related to the stress and strain distribution, so to some extent, we can predict the grain refinement after the process by analysing the stress-strain state in the sample. If we include some damage models in the simulation, we can predict the maximum possible strain or the number of stages in repetitive processes. Hydrostatic pressure and material flow are also results that are easy to acquire and analyse. In addition, knowledge of the specific pressure is of great importance for the design of SPD tools due to the high forces in SPD processes. Furthermore, in repetitive methods, such as the one that is the subject of this article, FEA is useful to predict the necessary stroke to achieve the desired dimension after the process.

Today, there is a wide selection of FEM software specialized for metal forming simulations. For sheet metal forming, there is Stampack, Pam-Stamp, and AutoForm, while for the bulk metal forming simulation Q-Form, Deform, and Simufact.forming are the most popular choices. For the purposes of the research presented in this article, the Q-Form UK 10.2.1 software was used.

2 MULTI-DIRECTIONAL PLANE STRAIN UPSETTING

Because of the many advantages offered by ultrafine-grained metals, much research has been conducted to develop new SPD methods or to modify existing ones. As a result, it is now possible to induce SPD using different processing methods on a variety of metallic materials with different geometries and shapes. In their review paper [5], Bagherpour et al. classify SPD techniques based on the processing method as follows:

- SPD techniques based on equal-channel angular pressing,
- SPD techniques based on torsion under high pressure,
- SPD techniques based on direct/indirect extrusion,

- SPD techniques based on pressing/forging,
- SPD techniques based on rolling,
- Combined SPD techniques.

The common characteristic of all SPD techniques based on pressing is achieving extreme values of strain through repetitive compression using flat or profiled punches on different sides of the specimens. Among all of the methods based on pressing most attention attracted multi-directional forging in open [1] or closed die [6]. Multi-directional forging was first applied for the formation of UFG microstructure in relatively large, bulk billets made of rather brittle metals, because of the relatively low specific load at the tooling and elevated process temperature. The main disadvantages of this method are the lower strain homogeneity compared to the equal-channel angular pressing and high-pressure torsion, the occurrence of tensile stresses on the free surface, and difficulties in achieving the desired geometric accuracy. When the process is carried out in a closed die, greater hydrostatic stress is applied and geometric accuracy is significantly improved [6]. It is worth noting that the SPD method V-shape die compression [7] was developed in the Department of Mechanical Engineering at the Faculty of Technical Sciences in Novi Sad as part of a larger, decade-long research on SPD methods.

In the plane strain compression method, the prismatic sample is upset in the axial direction with a flat punch for the defined value of stroke. Plane strain compression die (Figure 1) restricts the flow of material in the lateral direction, while the material flows freely along the mould in the longitudinal direction. Since the width of the sample is constant, the state of plane strain is present in the sample. After the first stage, the sample is removed from the dies, rotated for 90 degrees, reinserted into the die and upset again [8]. The dies are mounted on a Sack & Kiesselbach 6.3 MN hydraulic press and the process is carried out at room temperature (Figure 1. b). In order to decrease the friction MoS2 lubrication manufactured by Valvoline, Germany, was used.

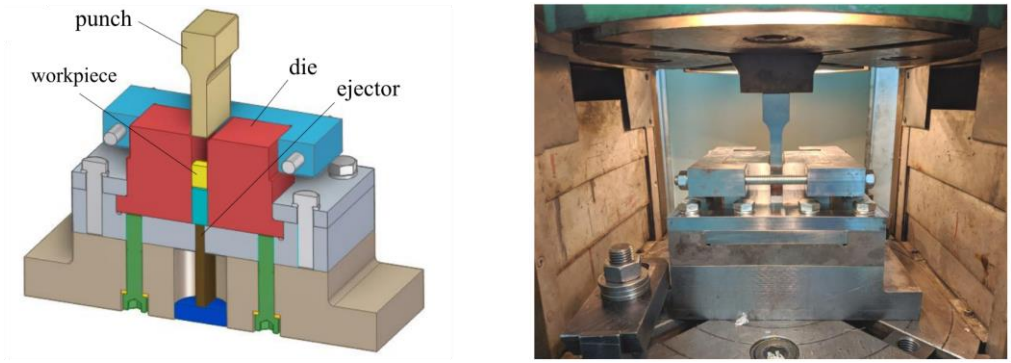

(a) *(b)*

Figure 1. *Plane strain compression die: (a) a cross-section of the CAD model, (b) a photo of the die attached to the hydraulic press [9]*

Prismatic samples were made of high-alloy, low-carbon steel X2CrNiMo17-12-2. The main characteristics of this steel are austenite microstructure, high strain hardening and high corrosion resistance. The results of tensile tests [9] have shown that this steel has excellent mechanical properties: relatively low yield strength, high strength, high elongation at fracture and extremely high uniform deformation. The

uniform elongation and the low value of the ratio between the yield strength and the strength of the material indicate a very pronounced tendency of the steel to strengthen during cold forming. The dimensions of the samples before upsetting were 20x20x13.5 mm. Figure 2 shows a prismatic sample after each of the six stages.

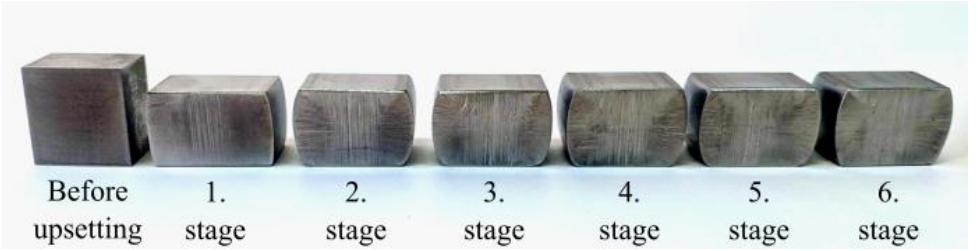

Figure 2. *Prismatic sample after each of the six upsetting stages [9]*

In the FEM analysis setup, dies were modelled as rigid. The material of the sample was modelled as plastic with a modulus of elasticity of 200GPa and a Poisson's ratio of 0.27. The stress-strain curve was determined experimentally by upsetting Rastagaev specimens [9]. The Coulomb friction coefficient was used to describe the contact conditions. A value of 0.075 was determined by the ring compression test [9]. Based on preliminary simulations, it was concluded that a coefficient of friction of 0.1 on the contact surface between the upper tool and the sample better describes the actual conditions. A friction coefficient of 0.075 was used for all other contact surfaces. The finite element mesh was defined by the maximum dimension of an element of 1 mm. For the type of FEM element, tetrahedral ones were chosen. In table 1 dimension and force measurements from the simulation and experiment are compared.

Table 1. *Force and dimension measurements from experiment and simulation*

Stage number:	Longitudinal dimension of the sample (mm):		Height of the sample (mm):	Effective strain:	Force (kN):	
	Experiment:	Simulation:			Experiment:	Simulation:
0	20.06	20	20.03	/	/	/
1	24.71	25.02	15.5	0.29	359	366
2	24.46	24.89	16.05	0.5	488	495
3	24.64	25.40	15.84	0.5	558	587
4	24.39	24.32	16.1	0.49	588	632
5	24.44	24.24	16.08	0.48	588	604
6	24.35	24.12	16.13	0.48	598	634

If we compare the data from the previous table, we see a good correlation between the experimental and simulation results. This verifies the simulation setup is verified and further analysis is possible.

Figure 3 shows the effective strain distribution in longitudinal and cross-section. The distribution is not completely uniform over either the longitudinal or the lateral cross-section, but a certain gradient can be seen. The maximum strain occurs in the centre of the sample and along the diagonals with values between 3.6 and 4.4. The

average effective strain over the entire volume of the sample is 2.66, while the accumulated effective strain calculated from the experiment is 2.74.

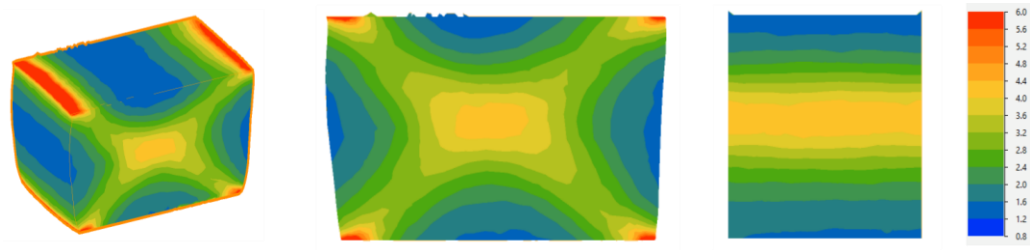

(a) *(b)* *(c)*

Figure 3. *Effective strain distribution (a) in the sample, in his (b) longitudinal and (c) lateral cross-section*

The mean, hydrostatic stress has only negative values in the sample, which means that a state of compressive stress is present. The average value of the mean stress was 997 MPa, the maximum was close to 1400 MPa, while the minimum was around 700 MPa.

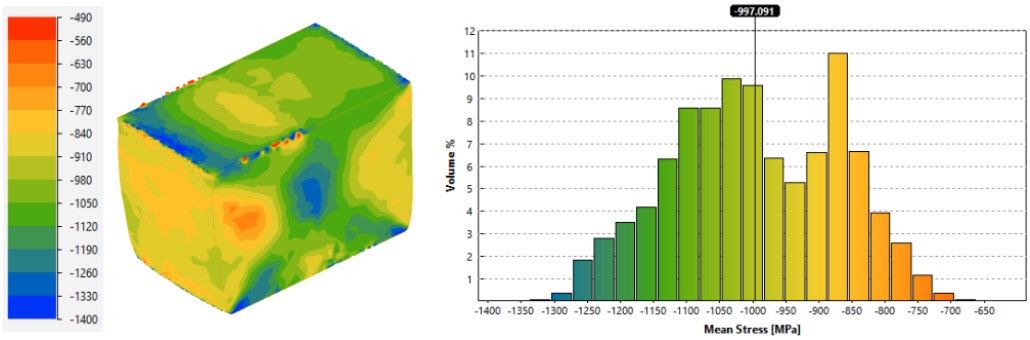

Figure 5. *Mean stress distribution and statistics*

Figure 4. shows the effective stress distribution after third and sixth upsetting pass. As we can see, the central zone with maximum effective stress from the third phase expanded across almost the entire cross-section after the sixth stage.

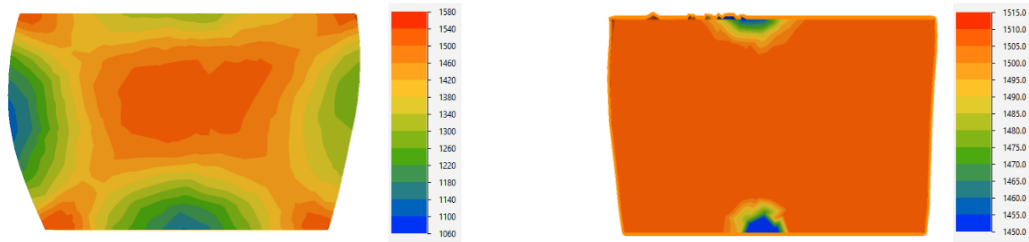

(a) *(b)*

Figure 4. *Effective stress distribution after (a) the third and (b) the sixth stage*

3 CONCLUSIONS

Following conclusions can be drawn from the previous findings.

1. The simulation setup was verified by comparing the force and dimensions of the sample from the experiment and the simulation
2. The simulation predicts the longitudinal dimension quite well, which is important, given that it represents the height of the sample in the next stage.
3. The average value of the effective strain was 2.66. To satisfy the Valiev condition, at least 7 additional phases must be performed.
4. The average value of the mean stress was 997 MPa, which means that in the next stage Valiev condition will be fulfilled.
5. After the sixth stage, the maximum effective stress was achieved over the entire cross-section of the sample.

ACKNOWLEDGEMENT

This research was made possible by grant BULKSURFACE-359 funded by the Ministry of Education, Science, and Technological development of the Republic of Serbia. The authors thank the CEEPUS programme that allowed them to be mobile within the CII-HR -0108 network. The authors also thank Micas Simulations Ltd. in the United Kingdom and their representatives PhD. Nikolay Biba and Paul Mordvintsev for the academic use of the QForm programme at the Faculty of Mechanical Engineering in Ljubljana, Slovenia.

LITERATURE

[1] R. Valiev, Zhilyaev A. and Langdon T. (2013). Bulk nanostructured materials: Fundamentals and Applications.
[2] Huang Y., Langdon T. (2013). Advances in ultrafine-grained materials, Materials Today, vol. 16, no. 3, pp. 85-93.
[3] Valiev, R.., Islamgaliev, R.K., Alexandrov, I.V., Zufarovich Valiev, R., Islamgaliev, R.K. and Alexandrov, I.V. (2000). Bulk nanostructured materials from severe plastic deformation, Progress in Material Science, vol. 45, p.p. 103–189.
[4] Valiev, R. (2009). Nanostructuring of metallic materials by SPD processing for advanced properties, International Journal of Materials Research, vol. 100, p.p. 757 – 761.
[5] Bagherpour E., Pardis N., Reihanian M. and Ebrahimi R., (2018). An overview on severe plastic deformation: research status, techniques classification, microstructure evolution, and applications, The International Journal of Advanced Manufacturing Technology, vol. 100, no. 5- 8, pp. 1647-1694.
[6] Ghosh A. (1985). Method of producing a fine grain aluminum alloy using three axes deformation, US4721537A.
[7] Vilotić M. (2015). Intenzivna plastična deformacija u procesima višefaznog sabijanja materijala, Doctoral disertation, Faculty of Technical Sciences, University of Novi Sad.
[8] Vilotić M., Dačević N., Milutinović M., Movrin D. and Šidjanin L. (2020). New severe plastic deformation method for 316l medical grade steel processing new spd method for 316l steel processing, Acta Technica Corviniensis - Bulletin of Engineering, Hunedoara, Vol. 13, Iss. 1.
[9] Project work report (2019-2020), Development of a method for improving material properties by combined bulk and surface plastic – BULKSURFACE.

COMETa 2022
6th INTERNATIONAL SCIENTIFIC CONFERENCE
17th - 19th November 2022
Jahorina, B&H, Republic of Srpska
University of East Sarajevo
Faculty of Mechanical Engineering
Conference on Mechanical Engineering Technologies and Applications

MAŠINA ALATKA SA PARALELNIM MEHANIZMIMA NAMENJENA ZA SEČENJE PENASTIH MATERIJALA USIJANOM ŽICOM

Goran Vasilić[1], Saša Živanović[2], Milan Milutinović[3], Zoran Dimić[4]

Rezime: U okviru ovoga rada je prikazana mašina alatka koja u svojoj strukturi sadrži dva ravanska paralelna mehanizma. Prikazana mašina alatka je namenjena za sečenje penastih materijala usijanom žicom. Platforme paralelnih mehanizama nose po jedan kraj žice a kretanja platformi su uslovljena kretanjem žice po konturama na obratku. Upotrebljeni paralelni mehanizmi su nezavisni, tako da mašina alatka omogućava translatorno kretanje žice u pravcu dve ose kao i obrtno kretanje žice oko istih osa.

Ključne riječi: Kompleksne mašine alatke, Nekonvencionalne metode obrade, Paralelni mehanizmi, Rekonfigurabilne mašine alatke

MACHINE TOOL WITH PARALLEL MECHANISMS INTENDED FOR CUTTING FOAM MATERIALS WITH HOT WIRE

Abstract: In this paper, a machine tool is presented, which in its structure contains two planar parallel mechanisms. The shown machine tool is intended for cutting foam materials with a hot wire. At the displayed machine tool, the platforms of the parallel mechanisms carry one end of the wire each, and the movements of the platforms are determined by the desired movement of the wire along the contours of the workpiece. The parallel mechanisms used are independent, so that the machine tool enables translational movement of the wire in the direction of two axes as well as rotary movement of the wire around the same axes.

Key words: Complex machine tools, Unconventional machining processes, Parallel mechanisms, Reconfigurable machine tools

[1] Goran Vasilić, Akademija tehničkih strukovnih studija, Odsek za saobraćaj, mašinstvo i inženjerstvo zaštite, Beograd, Srbija, gvasilic@atssb.edu.rs
[2] prof dr Saša Živanović, Univerzitet u Beogradu, Mašinski fakultet, Beograd, Srbija, szivanovic@mas.bg.ac.rs
[3] dr Milan Milutinovič, Akademija tehničkih strukovnih studija, Odsek za saobraćaj, mašinstvo i inženjerstvo zaštite, Beograd, Srbija, mmilutinovic@atssb.edu.rs
[4] dr Zoran Dimić, Lola institut, Beograd, Srbija, zoran.dimic@li.rs

1 UVOD

Mašine alatke zasnovane na paralelnim mehanizmima su u sve većoj meri predmet mnogih istraživanja iz razloga što paralelni mehanizmi poseduju izvesne prednosti u odnosu na tradicionalne serijske mehanizme [1]. Kao rezultat mnogih istraživanja, autori predlažu mašine alatke različitog koncepta, različitih konfiguracija i različite namene [2][5]. Navedeni ali i mnogi drugi naučni radovi uglavnom predlaži koncept hibridnih mašina alatki koje su zasnovane na kombinaciji paralelnih i serijskih mehanizama. Mašine alatke [2][5] zasnovane na hibridnim mehanizmima su u najvećoj meri namenjene za proces obrade glodanjem, za "Pick & Place" operacije i u nešto manjoj meri za procese zavarivanja. U grupu hibridnih mehanizama spadaju i mehanizmi dobijeni serijskim povezivanjem najmanje dva mehanizma sa paralelnom kinematikom [6][8]. Proces obrade sečenje penastih materijala usijanom žicom je do sada razmatran i primenom industrijskih robota [9][10].

U okviru ovoga rada je prikazana mašina alatka koja se po svom konceptu razlikuje od većine poznatih mašina alatki koje u svojoj strukturi sadrže bar jedan paralelni mehanizam. Prema dostupnoj literaturi, autori ovog naučnog rada zaključuju da se prikazana mašina alatka i prema strukturi i mogućoj nameni razlikuje od svih poznatih mašina alatki zasnovanih na paralelnim mehanizmima što je bio dovoljan razlog za njen razvoj.

2 OPIS KOMPLEKSNE MAŠINE ALATKE

Mašina alatka koju autori predstavljaju u ovom radu spada u do sada nedovoljno istraženu grupu mašina koje u svojoj strukturi sadrže više od jednog mehanizma sa paralelnom kinematikom. Mašina alatka namenjena za proces obrade sečenja žicom (slika 1.a) sadrži dva ravanska dvoosna mehanizma sa paralelnom kinematikom prikazanih na slici 1.b. Kao što je već rečeno platforme paralelnih mehanizma nose po jedan kraj usijane žice kojom se tokom procesa obrade seku penasti materijali poput stiropora, stirodura itd. Na ovaj način je omogućeno translatorno kretanje krajeva žice i to u pravcu osa "*x*" i "*y*", a slaganjem translatornih kretanja krajeva žice se realizuje promena orijentacije žice i to obrtanjem oko osa "*x*" i "*y*". Osim kretanja alata, omogućeno je i kretanje radnog stola na koji se postavlja obradak i to duž ose "*z*" koja je upravna na ravni paralelnih mehanizama "Oxy".

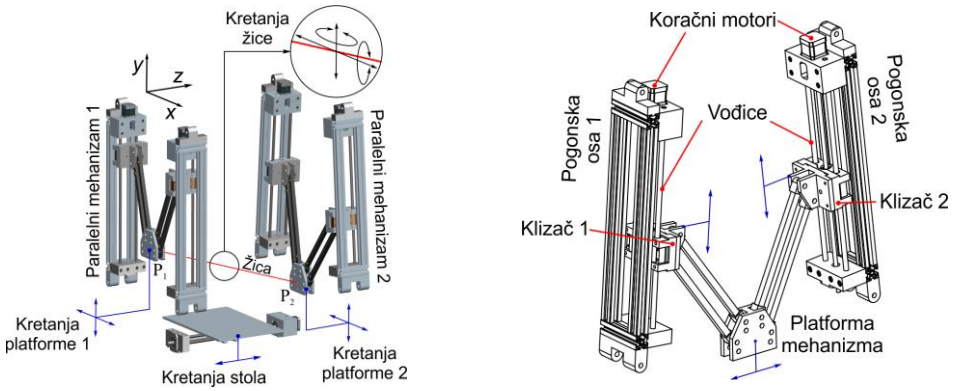

(a) (b)

Slika 1. *CAD model: a)Mašine alatke za sečenje žice; b)Dvoosnog ravanskog mehanizma sa paralelnom kinematikom (preuzeto i dorađeno [11])*

Paralelni mehanizmi koji su korišteni za gradnju mašine alatke sa slike 1.a su konfigurisani prema uzoru na rekonfigurabilni dvoosni mehanizam sa paralelnom kinematikom "MOMA" koji je bio predmet nekih ranijih istraživanja autora [12],[13],[14]. Ravanski paralelni mehanizam sa slike 1.b. je kao i mehanizmam "MOMA" rekonfigurabilnog tipa pa se njegova konfiguracija može brzo i lako promeniti u skladu sa trenutnim potrebama [15]-[17] koje proizvodni proces nalaže. Konfiguracija dvoosnog mehanizma sa paralelnom kinematikom sa slike 1.b se kao i u slučaju mehanizma "MOMA" može menjati promenom orijentacije pogonskih osa kao i upotrebom spojki različitih dužina. Glavna razlika između dvoosnog rekonfigurabilnog mehanizma "MOMA" i dvoosnog rekonfigurabilnog mehanizma sa slike 1.b je u tome što mehanizam sa slike 1.b poseduje fizičku platformu. Uvođenjem fizičke platforme su se obezbedile dodatne mogućnosti za upotrebu mehanizma. Za ispravan rad mehanizma je neophodno obezbediti da orijentacija platforme zadržava konstantnu orijentaciju tokom rada mehanizma pa se iz tog razloga umesto dve (što je slučaj kod mehanizma "MOMA") koriste četiri spojke. Iz tog razloga je mehanizmu sa slike 1.b dodeljen naziv "MOMA 4S". Za sada je definisano pet osnovnih konfiguracija mehanizma "MOMA 4S" od kojih je jedna polazna konfiguracija (Slika 2. "MOMA 4S-P") kod koje su pogonske ose mehanizma paralelne i vertikalne. Ostale četiri konfiguracije se dobijaju obrtanjem pogonskih osa oko tačaka O_1 i O_2 za ugao od 5° ili 10° stepeni na spoljašnju ili unutrašnju stranu. U skladu sa tim, konfiguracije i nose nazive "MOMA 4S–S_" i "MOMA 4S–U_" u kojima je prema slici 2. naveden i ugao rotacije pogonskih osa čije su moguće vrednosti već navedene. Zauzeta orijentacija pogonskih osa se zadržava učvršćivanjem pogonskih osa za nepokretne delove mehanizma nazvanih "Blok 1" i "Blok 2".

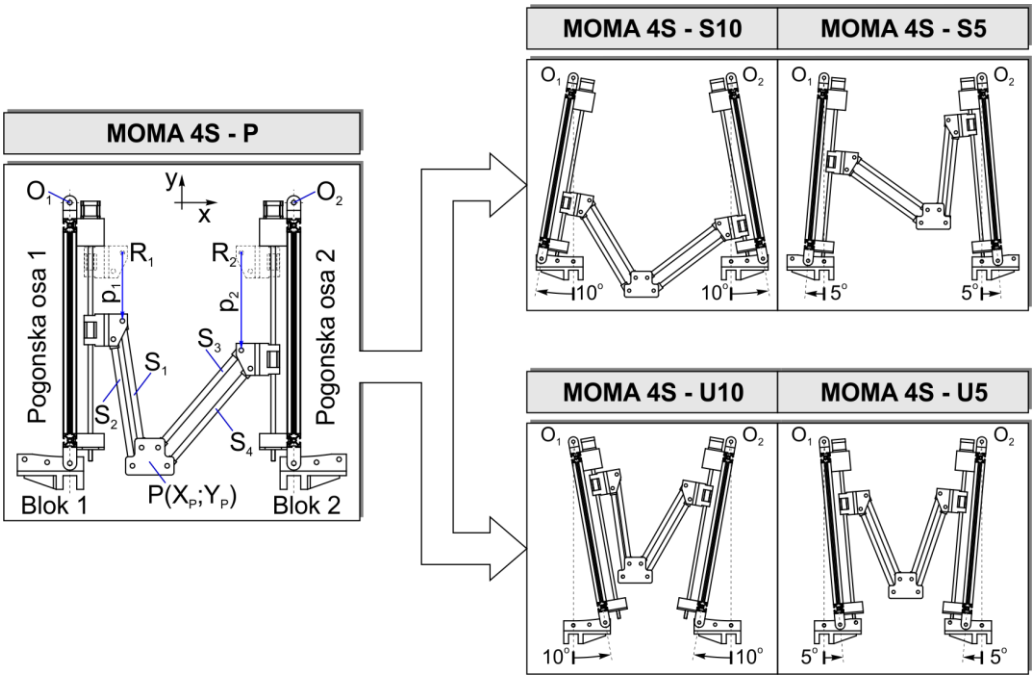

Slika 2. Osnovne *konfiguracije dvoosnog rekonfigurabilnog mehanizma MOMA 4S*

Upotrebom dva paralelna mehanizma *MOMA 4S* i povezvanjem njihovih platformi žicom kako je prikazano na slici 1, dobija se kompleksna mašina alatka

namenjena za obradu penastih materijala usijanom žicom. Ovakva konfiguracija mašine alatke podseća na neke već analizirane mašine sa tri i više stepeni slobode [18],[19]. Međutim, prikazana mašina alataka (slika 1) se razlikuje od navedenih i drugih sličnih mašina po tome što su upotrebljeni mehanizmi nezavisni i rade sinhronizovano tokom obrade pri čemu se dužina žice između dve platforma menja tokom procesa obrade usled promene orijentacije žice. Zbog promene dužine žice tokom procesa obrade, žica se ne može posmatrati kao platforma četvoroosnog paralelnog mehanizma već se ceo mehanizam, kao što već je rečeno mora posmatra kao mehanizam sastavljen od dva nezavisna dvoosna paralelna mehanizma. Sa druge strane, mehanizam mašine alatke sa slike 1 se razlikuje i od drugih mehanizma sastavljenih od dva ili više paralelna mehanizma [20],[21] po tome što su u navedenim radovima upotrebqeni paralelni mehanizmi međusobno zavisni a celokupni mehanizam čini jedan hibridni mehanizam dobijen serijskim povezivanjem dva paralelna mehanizma. Prema datom opisu mehanizma mašine alatke namenjene za proces obrade sečenja žicom i upoređivanjem, sama mašina alatka se svrstava u grupu kompleksnih mašina alatki. Prema procesu obrade za koji je mašina alatka namenjena, dodeljen joj je naziv MOMA-W (W-wire).

3 PROGRAMIRANJE MAŠINE ALATKE MOMA-W

Mašina alatka MOMA-W je konfigurisana tako da se programiranje vrši na isti način kao i programiranje višeosnih mašina alatki namenjenjenih za nekonvencionalnu metodu obrade W-EDM (Wire - Electrical Discharge Machining). Prema standardu ISO-6983 [22], kretanje alata se za navedenu metodu obrade definiše pomoću koordinata *x*, *y*, *u* i *v*. Prema slici 2, tokom realizacije procesa obrade, alat (žica) se kreće po dve zadate konture pri čemu se svaka od kontura sastoji od niza tačaka. U skladu sa standardom ISO-6983, koordinate tačaka "Konture 1" su definisane koordinatama *x i y* dok su koordinate tačaka "Konture 2" definisane *koordinatama u* i *v.*

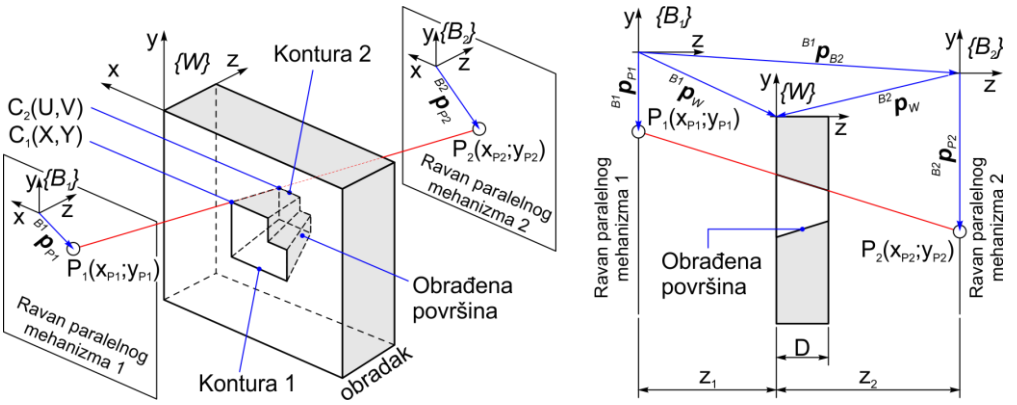

Slika 3. *Uprošten geometrijski model kompleksne mašine alatke MOMA-W*

Koordinate tačaka *x*, *y*, *u* i *v* su definisane u koordinatnom sistemu obratka *{W}* dok su koordinate platformi paralelnih mehanizama "P_1" i "P_2" definisane u nepokretnim koordinatnim sistemima *{B_1}* i *{B_2}* koji su vezani za "Paralelni mehanizam 1" i "Paralelni mehanizam 2" respektivno.

4 KINEMATIKA OBRADNOG PROCESA KOMPLEKSNOM MAŠINOM ALATKOM MOMA-W

Kao što je već rečeno u prethodnom poglavlju, kretanje alata (žice) tokom procesa obrade kompleksnom mašinom alatkom MOMA-W je određeno koordinatama tačaka koje definišu dve konture. Kako svaka od platformi kompleksne mašine alatke nosi po jedan kraj žice, zadatak mašine je da na osnovu programiranih koordinata tačaka obe konture (x, y, u i v) dovede platforme oba mehanizma u određenu poziciju kako bi se ostvarila željena pozicija i orijentacija žice. Pozicija nepokretnog koordinatnog sistema $\{B_2\}$ u odnosu na koordinatni sistem $\{B_1\}$ kompleksne mašine alatke MOMA-W je definisana vektorom ${}^{B1}\boldsymbol{p}_{B2}$ i poznata je na osnovi konfigurisanog hardverskog dela mašine alatke. Pre samog procesa obrade, obradak sa slike 3 se može postaviti i pozicionirati na bilo kom mestu na radnom pokretnom radnom stolu mašine sa slike 1. Pozicija koordinatnog sistema obratka $\{W\}$ u odnosu na nepokretni koordinatni sistem $\{B_1\}$ je definisana vektorom ${}^{B1}\boldsymbol{p}_{W}$. Kako je vektor ${}^{B1}\boldsymbol{p}_{B2}$ poznat, prema slici 3 se određuje i pozicija koordinatnog sistema obratka $\{W\}$ u odnosu na nepokretni koordinatni sistem $\{B_2\}$ prema vektorskoj jednačini ${}^{B2}\boldsymbol{p}_{W} = {}^{B1}\boldsymbol{p}_{W} - {}^{B1}\boldsymbol{p}_{B2}$. Koristeći prethodno definisane vektore, koordinate platformi "P_1" i "P_2" i koordinate tačaka programiranih kontura "C_1" i "C_2" se mogu posmatrati u odnosu na nepokretni koordinatni sistem $\{B_1\}$. U tom slučaju, pozicije platformi "P_1" i "P_2" u koordinatnom sistemu $\{B_1\}$ su određene vektorskim jednačinama (1)

$$\begin{aligned} {}^{B1}\boldsymbol{p}_{P1} &= [{}^{B1}X_{P1}\ {}^{B1}Y_{P1}\ 0]^{T} \\ {}^{B1}\boldsymbol{p}_{P2} &= [{}^{B1}X_{B2}\ {}^{B1}Y_{B2}\ {}^{B1}Z_{B2}]^{T} + [{}^{B2}X_{P2}\ {}^{B2}Y_{P2}\ 0]^{T} \end{aligned} \tag{1}$$

dok su koordinate tačaka programiranih kontura "C_1" i "C_2" u koordinatnom sistemu $\{B_1\}$ određene vektorskim jednačinama (2)

$$\begin{aligned} {}^{B1}\boldsymbol{p}_{C1} &= [{}^{W}X_{C1}\ {}^{W}Y_{C1}\ 0]^{T} + [{}^{B1}X_{W}\ {}^{B1}Y_{W}\ {}^{B1}Z_{W}]^{T} \\ {}^{B1}\boldsymbol{p}_{C2} &= [{}^{W}X_{C2}\ {}^{W}Y_{C2}\ D]^{T} + [{}^{B1}X_{W}\ {}^{B1}Y_{W}\ {}^{B1}Z_{W}]^{T} \end{aligned} \tag{2}$$

Koristeći jednačine (1) i (2), na osnovu poznatih (programiranih) koordinata tačaka "C_1" i "C_2", koordinate platforme "P_1" u koordinatnom sistemu $\{B_1\}$ se određuju na osnovu jednačine (3). Na isti način se prema jednačini (4) određuju koordinate platforme "P_2" u koordinatnom sistemu $\{B_2\}$.

$$\begin{aligned} {}^{B1}X_{P1} &= -{}^{B1}Z_{C1}\cdot({}^{B1}X_{C2} - {}^{B1}X_{C1}) / ({}^{B1}Z_{C2} - {}^{B1}Z_{C1}) + {}^{B1}X_{C1} \\ {}^{B1}Y_{P1} &= -{}^{B1}Z_{C1}\cdot({}^{B1}Y_{C2} - {}^{B1}Y_{C1}) / ({}^{B1}Z_{C2} - {}^{B1}Z_{C1}) + {}^{B1}Y_{C1} \end{aligned} \tag{3}$$

Na isti način se prema jednačini (4) određuju koordinate platforme "P_2" u koordinatnom sistemu $\{B_2\}$.

$$\begin{aligned} {}^{B2}X_{P2} &= -{}^{B2}Z_{C1}\cdot({}^{B2}X_{C2} - {}^{B2}X_{C1}) / ({}^{B2}Z_{C2} - {}^{B2}Z_{C1}) + {}^{B2}X_{C1} \\ {}^{B2}Y_{P2} &= -{}^{B2}Z_{C1}\cdot({}^{B2}Y_{C2} - {}^{B2}Y_{C1}) / ({}^{B2}Z_{C2} - {}^{B2}Z_{C1}) + {}^{B2}Y_{C1} \end{aligned} \tag{4}$$

U prehodnim jednačinama, koordinate tačaka "C_1" i "C_2" tj. koordinate ${}^{W}X_{C1}$,

${}^{w}Y_{C1}$, ${}^{w}X_{C2}$ *i* ${}^{w}Y_{C2}$ odnosno *X*, *Y*, *U* i *V* respektivno, predstavljaju spoljašnje koordinate kompleksne mašine alatke MOMA-W i one se realizuju dovođenjem platformi upotrebljenih paralelnih mehanizama u pozicije koje su određene jednačinama (3) i (4). Koordinate platformi "P_1" i "P_2" u koordinatnim sistemima *{B_1}* i *{B_2}* predstavljalju spoljašnje koordinate upotrebljenih paralelnih mehanizama i realizuju se dovođenjem klizača pogonskih osa u određenu poziciju. Pozicije klizača na vođicama pogonskih osa se posmatra u odnosu na referentnu tačku (na slici 2 - R_i) a rastojanja klizača od odgovarajućih referentnih tačaka nose oznake p_i. Veličine p_i su unutrašnje koordinate upotrebljenih paralelnih mehanizama a ujedno i kompleksne višeosne mašine alatke MOMA-W. Na osnovu datog opisa, može se konstatovati da kompleksna mašina alatka MOMA-W, programiranu poziciju i orijentaciju alata (žice) realizuje dovođenjem klizača pogonskih osa u određene pozicije kojima se ostvaruju koordinate platformi paralelnih mehanizama datih jednačinama (3) i (4). Postupak određivanje vrednosti unutrašnjih koordinata p_i (i=1-4) je prikazan u ranije objavljenim naučnim radovima autora [12][13],[23] kao i u [11] te se ne prikazuje u okviru ovoga rada.

5 EKSPERIMENTALNA POSTAVKA I VERIFIKACIJA RADA KOMPLEKSNE MAŠINE ALATKE MOMA-W

Eksperimentalnu postavku kompleksne višeosne mašine alatke MOMA-W namenjene za sečenje penastih materijala usijanom žicom je prikazana na slici 4. Eksperimentalnu postavku čine: i) Hardverski deo mašine; ii) Upravljački deo mašine i iii) Laboratorijsko napajanje. Laboratorijsko napajanje se koristi za grejanje žice kojom se seče materijal, ovde stirodur. Hardver mašine čiji je 3D-CAD model prikazan na slici 1, je sačinjen od noseće konstrukcije na koju su pričvršćena dva ravanska rekonfigurabilna mehanizma sa paralelnom kinematikom. Upravljački deo mašine alatke MOMA-W čini softverski sistem otvorene arhitekure LinuxCNC u koji je implementirana kinematika mašine alatke. Deo upravljačkog sistema i drajveri kojima se na osnovu signala iz softverskog dela upravljačkog sistema upravlja radom koračnih motora pogonskih osa, takođe je pokazan na slici 4.

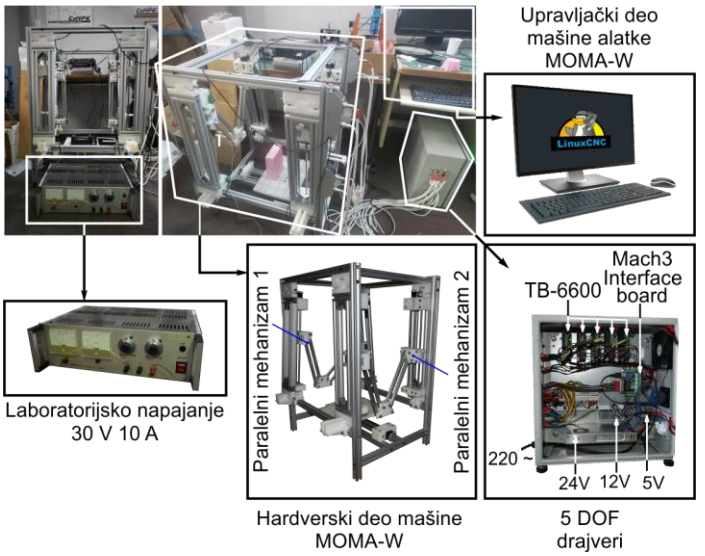

Slika 4. *Eksperimentalna postavka kompleksne mašine alatke MOMA-W namenjena za proces obrade sečenja žicom penastih materijala*

Primenjujući metod ručnog (manuelnog) programiranja kao i upotrebom dostupnog CAD/CAM softverskih paketa, izarđeno je više delova sa postavljenim različitim zahtevima kako bi se prvenstveno potvrdila ispravnost izvedenih jednačina na osnovu kojih se upravlja mašinom alatkom MOMA-W a potom i da bi se utvrdile mogućnosti koje mašina alatka pruža. Rad mašine je prikazan na slici 5, dok su izrađeni delovi podeljeni po grupama i prikazani na slikama 6-9.

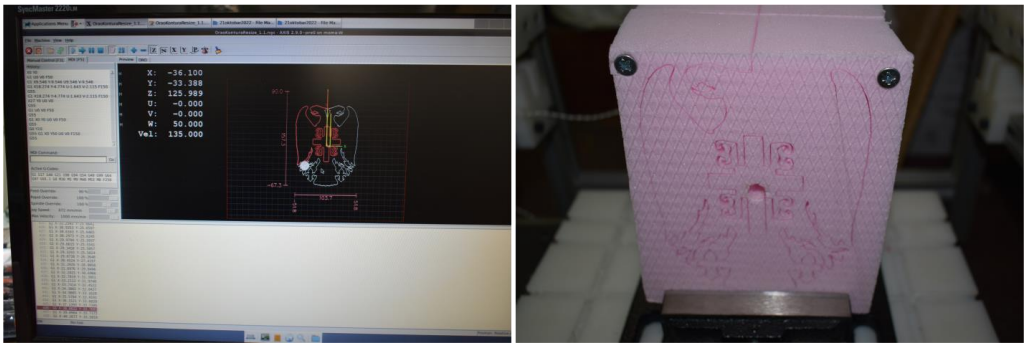

Slika 5. *Mašina alatka MOMA-W tokom procesa obrade*

(a) *(b)*

Slika 6. *Tankozidi delovi: a) Logo centra za nove tehnologije (CeNT) Mašinskog fakulteta u Beogradu; b) Logo MOMA mašina alatki zasnovanih na ravanskom rekonfigurabilnom mehanizmu sa paralelnom kinematikom*

(a) (b)

Slika 7. *Delovi složene geometrije: a)Grb Reublike Srbije; b)Lavlja glava*

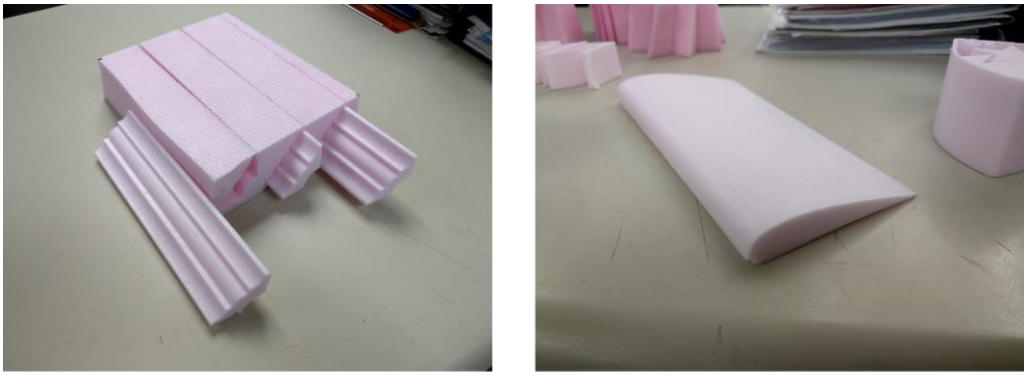

(a) (b)

Slika 8. *Delovi većih dužina: a)Ukrasna lajsna; b)Aero profil*

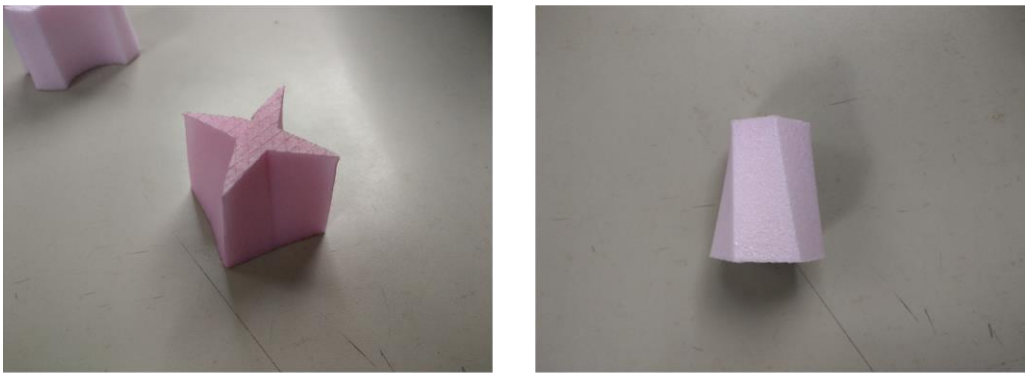

(a) (b)

Slika 9. Delovi *izrađeni sa velikim promenama nagiba žice: a)Četvorokraka zvezda; b)Šestougaona uvijena zarubljena piramida*

6 ZAKLJUČCI

Kompleksna višeosna mašina alatka MOMA-W prikazana u ovom radu je jedna od retkih mašina alatki koju čine dva paralelna mehanizma koja su međusobno nezavisna i povezana žicom promenljive dužine koja predstavlja alat, pa se mašina alatka može svrstati u klasu kompleksnih mašina alataki koja pripdada grupi mašina alatki nove generacije. Dosadašnje analize i ispitivanja prikazane mašine alatke su dala dobre rezultate na osnovu kojih se može zaključiti da postoji opravdanost za gradnjom i upotrebom mašine sa ovakvim konceptom. Takođe, dobijeni rezultati su pokazali da postoje mogućnosti za daljim unapređenjem i usavršavanjem kompleksne višeosne mašine alatke MOMA-W kao i drugih mašina alatki zasnovanih na istom ili sličnom konceptu što će i biti predmet budućih istraživanja autora.

Verifikacijom rada mašine alatke MOMA-W su se stekli uslovi da se mašina alatka MOMA-W koristi u edukacione svrhe na visoko školskim ustanovama pri čemu bi se akcenat stavio prvenstveno na programiranje a potom i na konfigursanje mašina alatki zasnovanih dvoosnom ravanskom rekonfigurabilnom mehanizmu sa paralelnom kinematikom.

ZAHVALNOST

U okviru ovog rada saopštavaju se rezultati istraživanja koja su realizovana u okviru projekta “Integrisana istraživanja u oblasti makro, mikro i nano mašinskog inženjerstva“ i podprojekta TR35022 „Razvoje nove generacije domaćih obradnih sistema“, koji finansijski podržava Ministarstvo prosvete, nauke i tehnološkog razvoja Vlade Republike Srbije po Ugovoru 451-03-68/2022-14/200105, od 4.02.2022. godine.

LITERATURA

[1] Tanev, T.K. (2000) Kinematics of a hybrid (parallel-serial) robot manipulator, Mechanism and Machine Theory, 35/9, p.p 1183–1196 DOI: 10.1016/S0094-114X(99)00073-7

[2] Wu, J., Wang, j., Li, T., Wang, L. (2007) Analysis and application of a 2-DOF planar parallel mechanism, ASME Journal of Mechanical Design, 129/4, p:p 434–437 DOI: 10.1115/1.2437800

[3] Wu, J., Wang, j., Wang, L. (2008) Optimal kinematic design and application of redudantly actuated 3DOF planar parallel manipulator, ASME Journal of Mechanical Design, 130/5, p.p.054503 DOI: 10.1115/1.2890118

[4] Sun, T., WU, H., Lian, B., et al.(2016) Stiffness modeling, analysis and evaluation of a 5 degree of freedom hybrid manipulator for friction stir welding, Proceedings of the Institution of Mechanical Engineers, Part C: Journal of Mechanical Engineering Science 331/13, p:p:4441–4456 DOI: 10.1177/09544062166689

[5] Huang, T., Li, Z., Li, M., Chetwynd, D.G., Gosselin, C.M. (2004) Conceptual design and dimensional syntesis of a novel 2-dof translational parallel robot for pick-and-place operations, ASME Journal of Mechanical Design, 126/3, p.p.449–455 DOI: 10.1115/1.1711822

[6] Romdhane, L. (1999): Design and analysis of a hybrid serial-parallel manipulator. Mechanism and Machine Theory, 34/7. pp.1037–1055 DOI: 10.1016/S0094-114X(98)00079-2

[7] Zheng, X.Z. , Bin, H.Z., Luo, Y.G. (2004). Kinematic analysis of a hybrid serial-parallel manipulator. The International Journal of Advanced Manufacturing Technology, Vol.23: pp.925–930 DOI: 10.1007/s00170-003-1782-z
[8] Lu, Y., Dai, Z. (2016). Dynamics model of redundant hybrid manipulators connected in series by three or more different parallel manipulators with linear active legs. Mechanism & Machine Theory, Vol.103, pp.222–235 DOI: 10.1016/j.mechmachtheory.2016.05.003
[9] Jovanovic, M., Rakovic, M., Tepavcevic, et al.(2017). Robotic fabrication of freeform foam structures with quadrilateral and puzzle shaped panels, Automation in Construction 74, p.p.28–38 DOI: 10.1016/j.autcon.2016.11.003
[10] Lee, S.H. , Ahn, D.G. , Yang, D.Y. (2003)Calculation and verification of rotation angle of a four-axis hotwire cutter for transfer-type variable lamination manufacturing using expandable polystyrene foam, The International Journal of Advanced Manufacturing Technology, Vol.22 p.p.175–183, DOI: 10.1007/s00170-002-1456-2
[11] Vasilić, G. (U postupku odbrane). *Koncepcijsko projektovanje jedne klase kompleksnih mašina alatki*, Doktorska disertacija, Univerzitet u Beogradu, Mašinski fakultet.
[12] Vasilić, G., Živanović, S., Kokotović, B., Dimić, Z. (2019). Configuring and analysis of a class of generalized reconfigurable 2-axis parallel kinematik machine, Journal of Mechanical Science and Technology, 33/7, p.p. 3407-3421 DOI: 10.1007/s12206-019-0636-z
[13] Vasilić, G., Živanović, S. (2016). Modeliranje i analiza rekonfigurabilnog dvoosnog paralelnog mehanizma MOMA sa osnaženim translatornim zglobovima, TEHNIKA Časopis saveza inženjera i tehničara Srbije, 71/1, p.p. 57-63 DOI: 10.5937/tehnika1601057V
[14] Živanović, S., Vasilić, G. (2014). Varijantnost konfigurisanja dvoosnog rekonfigurabilnog paralelnog mehanizma – MOMA. COMETa 2014, 2nd International Scientific Conference, University of East Sarajevo, Faculty of Mechanical Engineering
[15] Katz, R. (2007). Design principles of reconfigurable machines. The International Journal of Advanced Manufacturing Technology volume, Vol.34, p.p.430–439 DOI:10.1007/s00170-006-0615-2
[16] Moon, Y. (2006): Reconfigurable Machine Tool Design. Reconfigurable Manufacturing Systems and Transformable Factories. Springer, Berlin, Heidelberg. DOI: 10.1007/3-540-29397-3_7
[17] Koren, Y., Heisel, U., Jovane, F. Moriwaki, T., Pitschow, G., Ulsoy, G., Van Brussel, H. (1999). Reconfigurable manufacturing systems. CIRP Annals, 48/2, p.p.527–540, DOI:10.1016/S0007-8506(07)63232-6
[18] Huang, Z., Li, Q.C. (2002): General Methodology for Type Synthesis of Symmetrical Lower-Mobility Parallel Manipulators and Several Novel Manipulators, The International Journal of Robotics Research 21/2, p.p.131-146 DOI: 10.1177/027836402760475342
[19] Feng Gao, Weimin Li, Xianchao Zhao, Zhenlin Jin, Hui Zhaoc (2002): New kinematic structures for 2-, 3-, 4-, and 5-DOF parallel manipulator designs, Mechanism and Machine Theory, 37/11, p.p.1395-1411 DOI:10.1016/S0094-114X(02)00044-7
[20] Zheng, X. Z., Bin, H. Z., Luo , Y. G. (2004): Kinematic analysis of a hybrid serial-parallel manipulator, The International Journal of Advanced Manufacturing Technology Vol.23, p.p. DOI:10.1007/s00170-003-1782-z

[21] Romdhane, L. (1999): Design and analysis of a hybrid serial-parallel manipulator, Mechanism and Machine Theory Vol.34, Issue 7, p.p.1037-1055 DOI:10.1016/S0094-114X(98)00079-2

[22] ISO 6983-1:2009. Automation systems and integration - numerical control of machines-program format and definitions of address words. https://www.iso.org/standard/34608.html.

[23] Vasilić, G., Živanović, S. (2020). Configuring and analysis of complex multi-axis reconfigurable machine for wire cutting process, Mechanism and Machine Theory 149, p.p 103833. DOI: 10.1016/j.mechmachtheory.2020.103833

COMETa 2022
6th INTERNATIONAL SCIENTIFIC CONFERENCE
17th - 19th November 2022
Jahorina, B&H, Republic of Srpska
University of East Sarajevo
Faculty of Mechanical Engineering
Conference on Mechanical Engineering Technologies and Applications

INFLUENCE OF THE SLIDING VELOCITY ON THE INTENSITY OF GENERATION OF AIRBORNE WEAR PARTICLES OF POLYMERIC MATERIALS

Wojciech Tarasiuk[1], Aleksandar Kosarac[2], Tomasz Węgrzyn[3], Bożena Szczucka-Lasota[4], , Piotr Cybulko[5], Jan Piwnik[6]

Abstract: Modern materials used for plain bearings based on polymer materials are characterized by a low coefficient of friction and high abrasion resistance. They can work under heavy loads without lubrication. The wear particles released during their operation and getting into the air are usually small in size, ranging from several to several dozen nanometers. Such small particles in sufficiently high concentration can pose a threat to human health. The paper presents the results of experimental studies on the effect of the sliding velocity of polymer materials (iglidur X) used on slide bearings on the generation of wear particles. The counter-sample was a steel disc, and the unit pressure was in accordance with the recommendations of the plastics manufacturer.

Key words: polymer materials, tribology, wear, airborne particles

1 INTRODUCTION

Polymer materials are often used as plain bearing shells to form a friction pair with e.g. a steel shaft. They usually work with loads without lubrication. In dry friction conditions, as a result of wear of the friction elements, they generate airborne wear particles [1, 2]. Some of them settle a short distance from the friction knot, and some get into the air. Due to their small size, they can pose a threat to people in the vicinity

1 Dr inż. Wojciech Tarasiuk, Bialystok University of Technology, Bialystok, Poland, w.tarasiuk@pb.edu.pl
2 Prof. Aleksandar Kosarac, University of East Sarajevo, Sarajevo, BiH, Aleksandar Kosarac aleksandar.kosarac@ues.rs.ba
3 Prof. dr hab inż. Tomasz Węgrzyn, Silesian University of Technology, Katowice, Poland, tomasz.wegrzyn@polsl.pl
4 Dr hab inż. Bożena Szczucka Lasota, prof. PŚ, Silesian University of Technology, Katowice, Poland, bozena.szczucka-lasota@polsl.pl
5 Dr inż. Piotr Cybulko, Institute of Power Engineering in Białystok, Bialystok, Poland, p.cybulko@iezd.pl
6 Prof. dr hab. inż. Jan Piwnik, WSB Gdansk, Gdansk, Poland, j.piwnik@pb.edu.pl

of their generation. Their small amount is not dangerous, but in higher concentration they can pose a health risk [2, 3].

The separation of wear particles into the air from braking systems is already quite well known and widely researched [4-7]. However, in the case of polymer materials, there are no studies describing the generation processes of wear particles during dry friction. Polymer materials are characterized by a low coefficient of friction in combination with steel. However, their disadvantage is the limited temperature range in which they can operate. Plasticization of the surface can degrade friction conditions and lead to premature wear [8, 9].

Polymer materials such as PA6, PTFE, PET are used on various types of slides or shaft bushings operating in dry friction conditions. Often, however, their mechanical properties are insufficient for modern applications. This was the reason for the introduction of polymer composite materials to the market for plain bearings. These materials have all the advantages of base plastics, but they can work under higher loads and at higher temperatures [9, 10].

2 TESTED MATERIAL

Igus material was selected for testing with the designation iglidur X. According to the manufacturer, this material consists of three components [11]:

- base polymer,
- fibers and fillers,
- solid lubricants.

The appropriate proportion of these components and the even distribution of solid lubricant particles make the material self-lubricating and have increased resistance to abrasive wear. Table 1 shows its basic properties.

Table 1. *Properties of iglidur X* [11]

Material – properties	***Value***
Elasticity modulus	*8.100 MPa*
Shore D hardness	*85*
Compressive stress	*100 MPa*
Density	*1.44 g/cm^3*
Maximum recommended surface pressure	*150 MPa*
Maximum long-term working temperature	*250°C*
Maximum short-term working temperature	*315°C*

The counter-sample was a disc made of 42CrMo4 steel (Fig. 1).

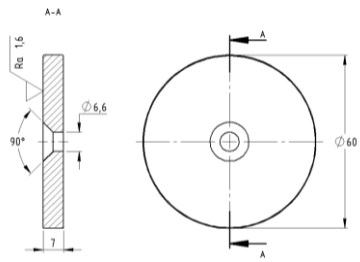

Figure 1. *Diagram of the disk used as a counter-sample – steel 42CrMo4*

3 RESEARCH METHODS

The test stand consisted of several devices. Its main element was the T-11 pin-on-disc tribometer, equipped with a special clean chamber that allows to separate the friction pair from the environment. A former PT50D compressor was attached to the tribometer, which forced air to the TSI 3074B filter system, from where the purified air was sent to the clean chamber. Here, the flowing air picked up wear particles and then went to TSI spectrometers. Nano SMPS 3910 spectrometer allowed the measurement of particle concentration in the size range from 10 nm to 420 nm divided into 13 fractions. The OPS 3330 spectrometer provided particle classification in the size range from 0.3 to 10 μm with division into 16 fractions. The diagram of the stand is shown in Fig. 2.

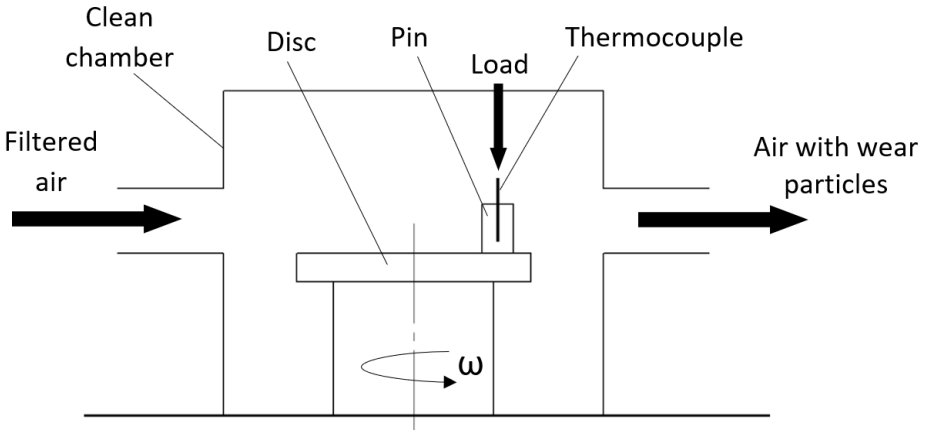

Figure 2. *The scheme of the test stand*

The temperature measurement was carried out using a K-type thermocouple placed in the center of the sample (pin) at a distance of 1 mm from the friction surface. The scheme of placing the thermocouple in the sample is shown in Fig. 2. Temperature values were recorded by the Graphtec GL-7000 recorder with a frequency of 1 Hz. Unit pressure of 0.6 MPa and three sliding velocity values were used in the tests: 1.2, 1.6 and 2.0 m/s. Three tests were performed for each value of the slip velocity, and the obtained results were averaged.

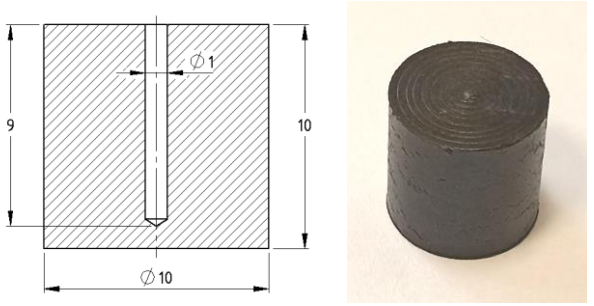

Fig. 2. *Schematic and photo of the iglidur X sample*

The friction radius was 20 mm. The friction distance for each of the tested samples was set at 1500 m. The friction time for a single sample was from 13 to 23 minutes, depending on the sliding speed.

4 RESULTS AND ANALISYS

During the tests, the friction force was recorded, which was used to determine the friction coefficient, the temperature in the pin near the contact surface, and the amount and size of airborne wear particles. Fig. 3 shows examples of the courses of the friction and temperature coefficients for the three tested values of the sliding velocity.

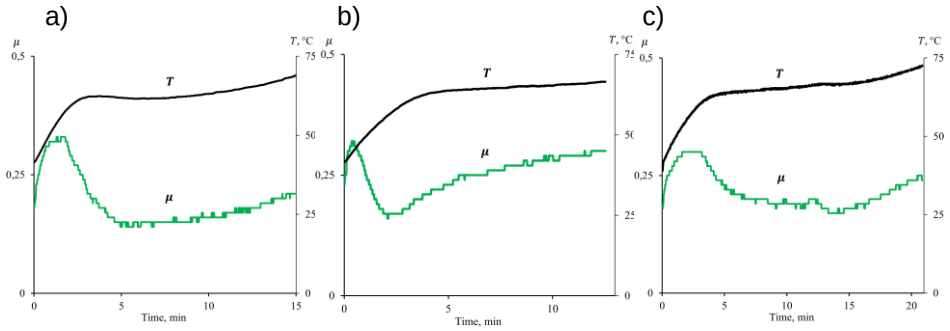

Figure 3. *Curves of the coefficient of friction and temperature during the test: a) v = 1.2 m/s, b) v = 1.6 m/s, c) v = 2 m/s*

We can see that the coefficient of friction increased at the beginning of the test, regardless of the sliding speed, then decreased after about 2 minutes, and then slowly increased again. The temperature rose rapidly in the initial phase of the test, to reduce the intensity of the rise after about 5 minutes. All tested cases were to be characterized by a similar course of the coefficient of friction and temperature. This was reflected in the separation of wear particles. The performed measurement included only particles that got into the air. Fig. 4 shows an example of the number of particles per cm^3 during the test for each of the tested sliding velocities.

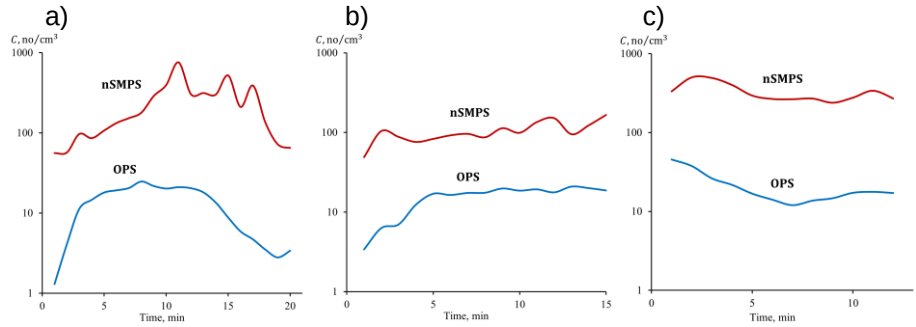

Figure 4. *The number of airborne wear particles per cm^3 during the test: a) v = 1.2 m/s, b) v = 1.6 m/s, c) v = 2 m/s*

The number of particles that was measured by the TSI OPS optical spectrometer was definitely smaller than the number of particles recorded by the electron spectrometer NanoSMPS. This means that, during the test, mainly small particles ranging from 10 to 420 nm were generated. Increasing the sliding speed stabilized the amount of released particles during the test. The reduction in velocity caused disturbances in the amount of particles generated during the test.

Fig. 5 shows the particle size distribution. We can observe here that, regardless of the sliding velocity, the largest amounts of wear particles have a size in the range 0.1 - 0.2 µm.

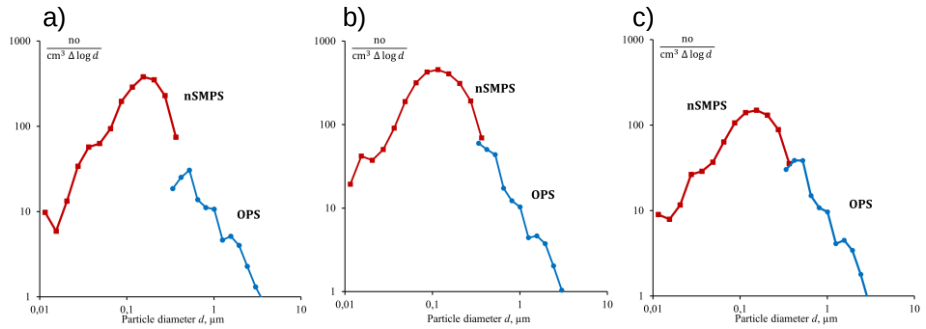

Figure 5. *Particle size distribution: a) v = 1.2 m/s, b) v = 1.6 m/s, c) v = 2 m/s*

Table 2 shows the collected values of the friction coefficients, temperature and the amount of released airborne wear particles during the test depending on the sliding speed.

Table 2. *Summary of the test results*

Sliding speed [m/s]	COF_{av}	COF_{max}	T_{av}	T_{max}	*NanoScan* C [no/cm^3]	*OPS* C *[no/cm^3]*
1.2	0.2	0.3	61.5	66.5	107,7	12.9
1.6	0.22	0.32	62	69.8	231	15.5
2.0	0.25	0.33	72.6	72.6	329.7	21.2

Analyzing the data in Table 2, we can see that the increase in the sliding velocity slightly increases the friction coefficient and temperature, while strongly influences the increase in airborne wear particles. Every 0.4 m/s increase in speed causes the doubling of the amount of released wear particles in the range from 10 to 420 nm.

5 CONCLUSIONS

The study of airborne wear particles is important from the point of view of ecology and human health. Plastics materials in this respect have been not enough researched. In the case of the tested material with the trade name iglidur X, we can say that:

- increasing the sliding velocity by 0.4 m/s doubles the amount of airborne wear particles with a size from 10 to 420 nm,
- the maximum size of airborne wear particles is about 4 μm,
- the dominant size of the released particles is in the range from 0.1 to 0.2 μm,
- the coefficient of friction and the temperature in the sliding contact slightly increase with the increase of the sliding speed.

ACKNOWLEDGMENT

The present work was supported by the National Science Centre, Poland [project number 2021/05/X/ST8/00885].

REFERENCES

[1] Tarasiuk, W., Nosko, A., Sharifullin, I., Nosko, O. Emission of airborne wear particles from a rubber material sliding on steel, *7th European Conference on Tribology: ECOTRIB 2019: 4th Austria-India-Symposium on Materials Engineering and Tribology : MaTri'19*: Book of abstracts, Wien, pp. 210.

[2] Olofsson, U., Olander, L., Jansson, A. Towards a model for the number of airborne particles generated from a sliding contact, *Wear* 267 (12) (2009) 2252–2256.

[3] Basu, Bikramjit & Kalin, Mitjan & Kumar B. V., Manoj. (2020). Mechanical Properties of Ceramics. 10.1002/9781119538790.ch4.

[4] Tarasiuk, W., Golak, K., Tsybrii, Y., Nosko, O. Correlations between the wear of car brake friction materials and airborne wear particle emissions, *Wear*, Volumes 456–457, 15 September 2020, 203361.

[5] Grigoratos, T., Martini, G. Brake wear particle emissions: a review, *Environ. Sci. Pollut. Control Ser*. 22 (4) (2015) 2491–2504.

[6] Wahlström, J., Lyu, Y., Matjeka, V., Söderberg, A.: A pin-on-disc tribometer study of disc brake contact pairs with respect to wear and airborne particle emissions. *Wear*, Vol. 384-385, 124-130, 2017.

[7] Nosko, O., Vanhanen, J., Olofsson, U. Emission of 1.3–10 nm airborne particles from brake materials, *Aerosol. Sci. Technol.* 51 (1) (2017) 91–96.

[8] Kosarac, A., Mladenovic, C., Zeljkovic, M., Tabaković, S., Knezev, M. (2022). Neural-Network-Based Approaches for Optimization of Machining Parameters Using Small Dataset. *Materials* 15 (3):700. DOI: 10.3390/ma15030700.

[9] Wieleba W., Capanidis D., Ziemiański K.: Własności tribologiczne wybranych kompozytów PTFE w warunkach tarcia mieszanego, Projektowanie, stosowanie i eksploatacja elementów maszyn i urządzeń z tworzyw sztucznych, pod red. J. Koszkula, Wydawnictwo Politechniki Częstochowskiej, 211–216 , Częstochowa 1996

[10] Wojciech Tarasiuk; Jan Piwnik; Bożena Szczucka-Lasota; Tomasz Węgrzyn; Piotr Cybulko, Emission of airborne wear particles from an intermetal Fe3Al and stellite 6 sliding on steel, 2022 *21st International Symposium INFOTEH-JAHORINA (INFOTEH)*, 21688640, 10.1109/INFOTEH53737.2022.9751258.

[11] Plastics for longer life. Igus, Inc., https://www.igus.pl/info/plain-bearings-iglidur-properties

COMETa 2022
6th INTERNATIONAL SCIENTIFIC CONFERENCE
17th - 19th November 2022
Jahorina, B&H, Republic of Srpska
University of East Sarajevo
Faculty of Mechanical Engineering
Conference on Mechanical Engineering Technologies and Applications

SHEET METAL FORMING USING VACUUM CAST POLYMER TOOL

Jovica Ilić[1], Mladomir Milutinović[2], Milija Kraišnik[3], Dejan Movrin[4]

Abstract: Sheet metal forming technology has a significant practical application and is applied in almost all branches of industry. Tool plays a crucial role in the forming process due to direct contact with the material. Since this is a deep drawing tool, special attention was paid to the fabrication of the drawing die, punch, and blank holder. The possibility of applying polymer deep drawing tool elements were analyzed. The main elements of the deep drawing tool were produced using vacuum casting technology..

Key words: Rapid Tooling, Deep Drawing, Sheet Metal Forming, Vacuum Casting

1 INTRODUCTION

The modern market constantly requires manufacturing companies to adapt to increasingly strict requirements regarding the degree of digitalization, product quality, reduction of product development time, and shortened product life cycle. A large percentage of sheet metal parts are produced using deep drawing technology. This technology allows for forming sheet metal, whereby we obtain spatial configurations such as containers, boxes, car body parts, etc., from a circular, rectangular or other shape sheet metal [1].

[1] MSc Jovica Ilić, senior teaching assistant, University of Banja Luka, Faculty of Mechanical Engineering, Banja Luka, Bosnia and Herzegovina, e-mail: jovica.ilic@mf.unibl.org
[2] PhD Mladomir Milutinović, associate professor, University of Novi Sad, Faculty of Technical Sciences, Novi Sad, Serbia, e-mail: mladomil@uns.ac.rs
[3] PhD Milija Kraišnik, associate professor, University of East Sarajevo, Faculty of Mechanical Engineering, East Sarajevo, Bosnia and Herzegovina, e-mail: milija.kraisnik@ues.rs.ba
[4] PhD Dejan Movrin, assistant professor, University of Novi Sad, Faculty of Technical Sciences, Novi Sad, Serbia, e-mail: movrin@uns.ac.rs

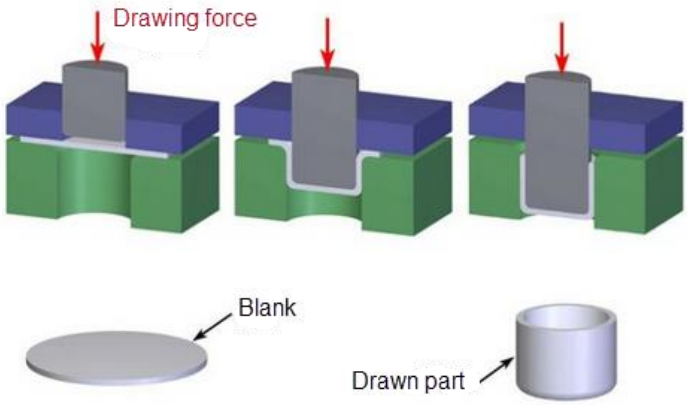

Figure 1. *Deep drawing process [2]*

The characteristic of deep drawing technology is the high cost of designing and producing deep drawing tools, but also the low production cost of parts produced using this technology in mass production. There is an increasing need for small batches of parts made with deep drawing technologies, which is often justified if the production of the tools is fast and cheap [3]. The production of classical conventional metal deep drawing tools generally does not meet these requirements. This paper analyzes the possibilities of using plastic elements of tools for deep drawing, i.e., using plastic to make the main elements of the tool, which are in contact with the material. The punch, die, and blank holder, which is in contact with the material, is made by vacuum casting technology using a two-component casting resin.

2 RAPID TOOLING USING VACUUM CASTING TECHNOLOGY

Vacuum casting technology is one of the adaptable techniques of rapid tooling due to the range of mechanical and physical properties that can be achieved using this technology, which is particularly important in the process of developing and manufacturing a new product. In addition, vacuum casting technology has a huge importance in the fabrication of a limited amount of precise parts in as short time as possible. The process of vacuum casting and making molds and tool parts consists of the following steps [4]:

1. Preparation of tool parts for the casting process. Setting the parting tape on the tool parts negatives that will facilitate the separation of silicone mold.
2. Bonding plastic gates on the tool parts negatives which has a role to form an inlet channel in the silicone mold and to facilitate the positioning and fixation of the negative in the silicone casting frame.
3. Calculation of the necessary quantity of silicone mixture to form a silicone mold to be used for molding the deep drawing tool parts. The silicone mixture is poured into the frame with fixed tool parts negatives and then the frame with the negative submerged in silicone is placed in a vacuum chamber in order to remove the residual air bubbles from silicon.
4. Positioning of the silicone mold in a vacuum chamber. After solidification of silicone, silicone mold is cut to parting line, during which we relieve the negative and get a silicone mold for casting a replica of a given negative

5. The molding halves are then combined and the next step is to calculate necessary quantities of resin for molding of the deep drawing tool parts. The amount of resin is commonly determined by weighing the individual master model which is increased by 20-30%, taking into account the loss of material in vessels and inlet channels. In this case, to cast the deep drawing tool parts, components made by Axson Technologies were used, thus by mixing them in the casting process the parts with physical characteristics according to Tab. 1 are obtained.
6. After a certain quantity of the material needed for molding and the proportion of the individual components of the material in a total amount are determined, then vacuum casting process follows. The casting process takes place in a vacuum chamber under conditions that are recommended for corresponding elements and components of the material.
7. After solidification of the molded material in a vacuum chamber, mold halves are separated and, if necessary, post-processing of the molded item follows.

Casting resins from the manufacturer Axson Technologies were used to produce the deep drawing tool elements. A casting resin combination of PX 223/HT was used, which consists of two components and their combination gives the mechanical and physical characteristics of the molded components according to Table 1 and Table 2.

Table 1. *Mechanical properties of vacuum casting resin PX 223/HT [5]*

Mechanical properties at 23°C for PX 223/HT			
Flexural modulus of elasticity	*ISO 178:2001*	*Mpa*	*2300*
Flexural strength	*ISO 178:2001*	*Mpa*	*80*
Tensile strength	*ISO 527:1993*	*MPa*	*60*
Elongation at break in tension	*ISO 527:1993*	*%*	*11*
Charpy impact resistance	*ISO 179/2D:1994*	*kJ/m^2*	*>60*
Hardnes at 23°C	*ISO 868:1985*	*Shore D1*	*80*
Hardnes at 23°C	*ISO 868:1985*	*Shore D1*	*> 65*

Table 2. *Physical properties of vacuum casting resin PX 223/HT [5]*

Physical properties for PX 223/HT				
		Part A	*Part B*	*Mixing*
Composition		*ISOCYANATE*	*POLYOL*	
Mixing ratio by wight at 25°C		*100*	*80*	
Aspect		*liquid*	*liquid*	*liquid*
Color		*colorless*	*black*	*black*
Viscosity at 25°C	*BROOKFIELD LVT*	*1.100*	*300*	*850*
Density of parts before mixing at 25°C	*ISO 1675:1975*	*1.17*	*1.12*	*-*
Density of cured mixing at 23°C	*ISO 2781:1988*	*-*	*-*	*1.14*

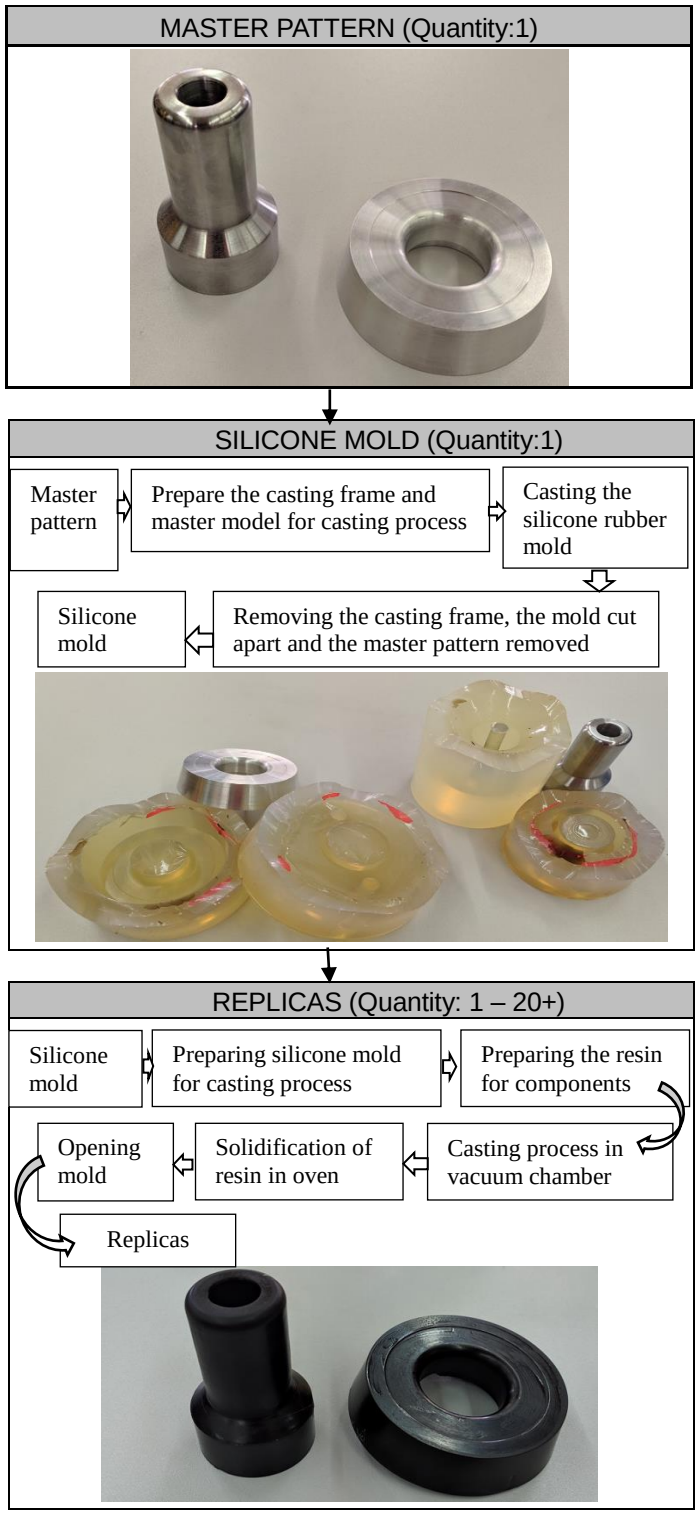

Figure 2. *Rapid tooling using vacuum casting technology*

3 PERFORMANCE OF DEEP DRAWING TOOL WITH POLYMER ELEMENTS

The polymer elements of the deep drawing tool, produced using vacuum casting technology, are into the existing construction of the deep drawing tool, shown in Figure 3.

Figure 3. *Deep drawing tool with polymer elements*

The basic process parameters and dimensions of the deep drawing tool are shown in Table 3.

Table 3. *Deep drawing process parameters*

Material:	DC01
Thickness:	0.8 mm
Blank diameter:	64 mm
Punch diameter:	33 mm
Die diameter:	34.65 mm
Lubricant	without lubricant

Under the mentioned conditions, a small batch of workpieces was made, from sheet metal material DC 01 with a thickness of 0.8 mm. A small batches of fabricated parts on a deep drawing tool located in Laboratory for technology of plasticity at Faculty of Mechanical Engineerig in Banja Luka is shown in Figure 4.

Figure 4. *Deep drawn parts*

4 CONCLUSION

In this paper is presented the possibility of using plastic tool elements in sheet metal forming using deep drawing. The advantages of vacuum casting technology, allows us to use a wide range of materials which is particularly significant here. By using different combinations of casting resins, we are able to obtain deep drawing tool elements with many different mechanical and physical characteristics and choose optimal resin components for individual tool elements. In this experiment, using the component PX 223/HT from the manufacturer Axson Technologies for a production of limited series of DC01 sheet metal parts with a thickness of 0.8 mm, satisfactory first results were obtained. On a series of about twenty drawn samples, there were no visible signs of wear or damage on the tool die, punch and blank holder, which were in direct contact with the sheet. The parts are dimensionally correct and in the tolerance. Although the production process was done dry, without lubricant, and there are no scratches or wrinkles on the samples since the polymer elements of deep drawing tool are less hard than the sheet material. This is particularly important from the point of view of ecology, since we do not use lubricant and therefore saves time and money because there is no need for subsequent degreasing of the workpieces. This experiment shows the possibility of applying this technology to make a small batch of samples. Further research is needed to determine the limit series of samples that can be made using polymer deep drawing tools produced using vacuum casting technology.

LITERATURE

[1] Schuh, G., Bergweiler, G., Bickendorf, P., Fiedler, F., Colag, C. (2020). Sheet Metal Forming Using Additively Manufactured Polymer Tools, *Procedia CIRP 93*, p.p. 20–25.

[2] IXmetal, Sheet Metal Fabrication, Deep drawing&Expanding https://www.ixmetal.com/processing-service/sheet-metal-fabrication/deep-drawing-expanding/, accessed 5. 10.2022.

[3] Durgun, I. (2015). Sheet metal forming using FDM rapid prototype tool, *Rapid Prototyping Journal*, vol. 21 iss 4, p.p. 412-422.

[4] Šljivić, M., Kraišnik, M., Ilić, J., Anić, J. (2018) Development of small batches of functional parts using integration of 3D printing and vacuum casting technology, A CTA TECHNICA CORVINIENSIS – Bulletin of Engineering, Tome XI, Fascicule 2, pp. 35-38

[5] RapidPrototyping.NL, Downloads, Datasheets material, VAC, https://www.rapidprototyping.nl/fileadmin/_migrated/content_uploads/VAC_PX_223HT_ABSlike_HighTemp_120_.pdf , accessed 21. 10.2022.

COMETa 2022
6th INTERNATIONAL SCIENTIFIC CONFERENCE
17th - 19th November 2022
Jahorina, B&H, Republic of Srpska
University of East Sarajevo
Faculty of Mechanical Engineering
Conference on Mechanical Engineering Technologies and Applications

AN INTELLIGENT ROBOTIC CELLS WITH TRANSPORT SYSTEM FOR FULLY AUTOMATED CUTTING TOOL ASSEMBLY

Uros Zuperl[1], Miha Kovačič[2]

Abstract: In the research, a system of three robot cells with three industrial robots and an intelligent conveyor system is designed and implemented for fully automated assembly and setting of cutting tool sets. Robotic cells with a transport system and a machine for setting cutting tools take care of the assembly, transport, setting and storage of cutting tool sets. With a touch screen and a visual SCADA system, the technologist communicates with the elements of the system and orders the correct set of cutting tool. The fully automated assembly, transport and tool setting system includes a smart transport system that works on chaos technology. This technology makes it possible, without programming, to deliver the right component of the cutting tool to the right technologist in the shortest possible time. The realized and tested system of automated cutting tool management demonstrated how effective the application of industrial robots and transport system without a centralized control system is.

Key words: Assembly, Cutting tool, Industrial robots, Transport system

1 INTRODUCTION

This chapter describes a fully automated assembly system of cutting tools for machining processes. The presented system consists of the main control system, four order terminals-touch screens, two robot cells and a transport system for the delivery of the components of the cutting tool set from the main tool warehouse through the assembly site, the cutting tool setting site and finally to the magazine in the machine tool [1]. machine. The entire structure of the cutting tool assembly system is shown schematically in Figure 1. The robot in the first robot cell transfers the components of the cutting tool from the drawers of the main cutting tool warehouse to an automated trolley. The automated trolley then brings the components of the tool's cutting set to the tool assembly unit. The robot in the second robot cell assembles the components into a

[1] Assoc. prof, Uros Zuperl, University of Maribor, Faculty of Mechanical Engineering, Smetanova 17, 2000 Maribor, Slovenia, uros.zuperl@um.si
[2] Assoc. prof, Miha Kovačič, ŠTORE STEEL, d.o.o., 3220 Štore, Slovenia, Faculty of mechanical engineering, University of Ljubljana, 1000 Ljubljana, Slovenia, miha.kovacic@store-steel.si

cutting tool assembly and returns the assembled cutting tool to the automated trolley. The trolley brings the assembled tool to the tool pre-setting machine. The robot in the third robot cell performs the manipulation of the assembled tool between the trolley and the Zoller Smile tool setting machine. The assembled and adjusted tool set is then brought to the machine tool magazine via an intelligent transport line. A smart transport system with Chaos technology ensures that the correct assembled tool is delivered to the appropriate machine tool. The operator of the machine tool submits a request for the appropriate set of the cutting tool via the ordering terminal. The order is sent via the Profibus connection to the control system, which ensures coordination and communication between all units of the assembly system [2].

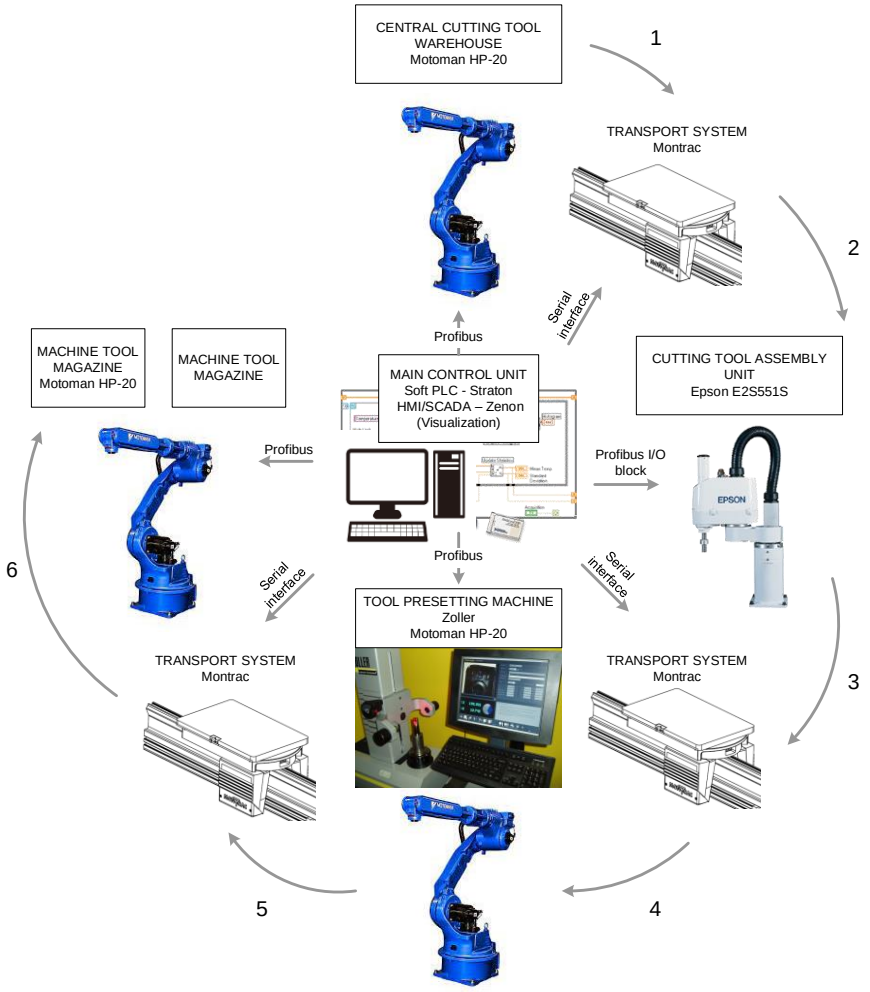

Figure 1. *Schematic representation of the structure of the system for automatic assembly of cutting tools.*

2 CUTTING TOOL ASSEMBLY UNIT

The cutting tool assembly unit consists of an Epson E2S551S scara-robot, a RC 420 robot controller, a GPL-40-1 gripper, a transport trolley with modular cutting tool

components, and a mounting station with a clamping device. The cutting tools are assembled by an Epson robot. The cutting tool components are taken directly from the automated trolley. As soon as the cutting tool component is in the robot gripper, it is placed on the fixture, where it is pneumatically positioned and clamped. In the following steps, the remaining components are individually transferred from the trolley and assembled into a tool assembly. When the tool is assembled, the robot informs the control system about the successful assembly operation. The control system calls the transport trolley. The robot waits for the trolley to pass and places the assembled cutting tool on the trolley. The trolley takes the assembled cutting tool to the Zoller tool setting machine. The unit for assembling the cutting tool set and the pneumatic cylinder is controlled by an embedded computer with the Windows operating system. The solenoid valves of the clamping cylinder, sensors and the robot are connected to the Profibus I/O block. The capacity of the assembly unit is 32 assembled cutting tools per hour.

3 TOOL PRE-SETTING UNIT

The unit for pre-setting the cutting tools consists of the tool pre-setting machine and of industrial robot Motoman HP-20 6 which is controlled by the Nx-100 controller. Communication with the main control unit is carried out via a Profibus connection. Based on the command of the control system, the robot picks up the assembled tool from the transport trolley and places it on the clamping device of the tool pre-setting machine. Inductive sensors check whether the assembled tool has been correctly inserted on the measuring machine. If the tool was not positioned correctly in the first attempt, the robot tries to position it again. As soon as the workpiece is properly inserted into the Zoller machine chuck, the machine measures the tool and transmits the tool dimensions to the machine tool. The measured tool is disengaged and placed back on the transport trolley. The transport traolley then delivers the tool to the tool magazine of the appropriate machine tool. The capacity of this unit is 42 measured tools per hour.

4 UNIT FOR DELIVERY OF TOOL COMPONENTS FROM THE CENTRAL WAREHOUSE

The unit consists of a Motoman HP-20 6 industrial robot controlled by an Nx-100 controller. Communication with the main control unit takes place via a Profibus connection. Based on the command of the control system, the robot transfers the individual components of the cutting tool from the drawers of the automated tool warehouse and places them on the automated trolley of the Montrac transport system. As soon as the tool components are correctly placed on the trolley, it takes the tool components to the tool assembly unit. The unit delivers components for the assembly of 19 cutting tools in one hour.

5 MONTRAC TRANSPORT LINE

The Montrac transport system transfers the assembled set of cutting tool to one of the two machine tools. The flexible system with modular construction is connected to the main control unit via a serial interface. The system consists of a track, which is a passive element and does not require maintenance [3]. Any number of self-propelled carts can be added to the track as needed. Compared to traditional systems, it uses up to 95% less energy [4]. Chaos Technology greatly reduces the need for programming and cabling [5].

6 CONTROL SYSTEM AND VISUALIZATION

The control system coordinates the operation of the system components and manages the technologists' orders. It converts the orders of the technologists into a set of requirements, and distributes them to the robot cells, the setting machine, the transport system [6], and the central tool storage. The control system is implemented on an embedded computer with the Windows operating system. Installed Straton software turns the computer into a powerful PLC controller. Zenon software is used to create a system monitoring panel and performs visualization of processes on order terminals. Zenon is used as a human-machine user interface. It is used to create a SCADA system. Requests for the assembly of four cutting tool sets can be made simultaneously on four KeTop T50 touch screens. The touch screens are used as order terminals. The order is then sent via Profibus on the onboard computer.

7 CONCLUSION

This paper presents a fully automated system for the management and assembly of cutting tools. The implemented system was manufactured and tested in a Slovenian tool shop. The results showed that industrial robots with intelligent transport system, tool setting machine and cutting tool storage can be effectively used in the process of automated cutting tool management. The robots assembled and transferred 35 different configurations of cutting tool sets to two machine tools. Extensive testing shows that the automated tool assembly system has a capacity of 17 assembled cutting tools per hour. The main goal of the project was to create an efficient and reliable communication between the three robot cells, the transport system, the presetting machine, the central tool warehouse, the machine tool and the order touch panels. Great attention was also paid to optimizing the transport logistics of the cutting tool components to the assembly unit.

REFERENCES

[1] Lazinica, A., Katalinic, B. (2005). Behavior of Transport Mobile Robot in Bionic Assembly System, Proceedings of IEEE International Conference on Mechatronics - ICM 2005, p.p. 220-225, 0-7803-8999-9, Taipei, Taiwan, October 2005, Taipei

[2] Lee, J., Bagheri, B., Kao, H. A. (2015). A cyber-physical systems architecture for industry 4.0-based manufacturing systems, Manufacturing Letters, 3, p.p. 18-23.

[3] Lucke, D., Constantinescu, C., Westkämper, E. (2008). Smart factory-a step towards the next generation of manufacturing, *In Manufacturing systems and technologies for the new frontier*, pp. 115-118. Springer, London.

[4] Molina, A., Rodriguez, C. A., Ahuett, H., Cortés, J. A., Ramírez, M., Jiménez, G., - Martinez, S. (2005). Next-generation manufacturing systems: key research issues in developing and integrating reconfigurable and intelligent machines, *International Journal of Computer Integrated Manufacturing*, 18(7), p.p. 525-536.

[5] Popa, D. O., Stephanou, H. E. (2004). Micro and mesoscale robotic assembly, *Journal of manufacturing processes*, 6(1), p.p 52-71.

[6] Chen, I. M. (2001). Rapid response manufacturing through a rapidly reconfigurable robotic workcell, *Robotics and Computer-Integrated Manufacturing*, 17(3), p.p 199-213.

COMETa 2022
6th INTERNATIONAL SCIENTIFIC CONFERENCE
17th - 19th November 2022
Jahorina, B&H, Republic of Srpska
University of East Sarajevo
Faculty of Mechanical Engineering
Conference on Mechanical Engineering Technologies and Applications

PLATFORM FOR TOOL WEAR MONITORING VIA CUTTING FORCE CONTROL

Uros Zuperl[1], Goran Munđar[2]

Abstract: This article presents a platform for tool wear monitoring in milling. Tool wear monitoring is performed indirectly through control of the cutting force. The adaptive neuro-fuzzy inference modeling (ANFIS) method was used to determine the relationships between the measured cutting forces and tool wear. The developed ANFIS model determines the flank wear of the cutting tool in real time according to the measured cutting forces at the corresponding cutting parameters. The developed monitoring platform based on the ANFIS model monitors tool wear in real time alerts the machine operator, adjusts the machining process, or stops it in case of excessive tool wear. The performance of the developed platform for tool condition monitoring (TCM) is investigated in several machining experiments.

Key words: Adaptive force control, ANFIS, Milling, TCM, Tool wear

1 INTRODUCTION

During the milling process, measuring tool wear and detecting damage of the cutting edge is difficult. Measuring tool wear and detecting tool damage is necessary for effective machining in the tool shops of the future. The topic is covered in many research, but there is no effective method or technique for monitoring tool wear during the cutting process. The hard-to-determine relationship between process characteristics and tool wear could be the reason for the absence of an effective monitoring method [1].

Researchers developed Tool condition monitoring systems (TCM) systems for milling processes with various sensors. Haber [2] used motor current and power for detecting tool wear. Achiche [3] used acoustic emission (AE) and cutting force signals for the detection of tool breakages. The dynamometer for measuring cutting forces in tool wear monitoring proved to be the most efficient.

In this research, a solution for monitoring tool wear in real time is given with the

[1] Assoc. prof, Uros Zuperl, University of Maribor, Faculty of Mechanical Engineering, Smetanova 17, 2000 Maribor, Slovenia, uros.zuperl@um.si

[2] Assist. Goran Munđar, University of Maribor, Faculty of Mechanical Engineering, Smetanova 17, 2000 Maribor, Slovenia, goran.mundjar@um.si

help of an on-line predictive model, which is made using an adaptive neuro inferential fuzzy (ANFIS) system. The ANFIS system predicts flank wear in real time based on measured cutting forces and relevant cutting parameters. The control application presented in this work includes the ANFIS predictive model, which is integrated into the existing cutting force control system.

The control application replaces the machine operator, who evaluates the current state of tool wear with his senses and related experiences. The role of the control application is to replace the machine operator. For the prediction of tool wear, a number of models based on classical statistical approaches, mechanical calculations and artificial intelligence systems have been employed.

The researches present regression models for predicting tool wear, fuzzy logic [4], and neural models. Many neural models [5, 6] of wear are presented, which is due to the excellence of neural networks to capture the non-linear relationships between the measured quantity and target quantity. The only drawback of neural networks is that it is not possible to mathematically calculate the connection between the inputs and the output of the model [7]. The link remains hidden from the user. This problem is solved in this research by using the ANFIS system, which also predicts the flank wear as a neural network and in addition ensures additional transparency of the model.

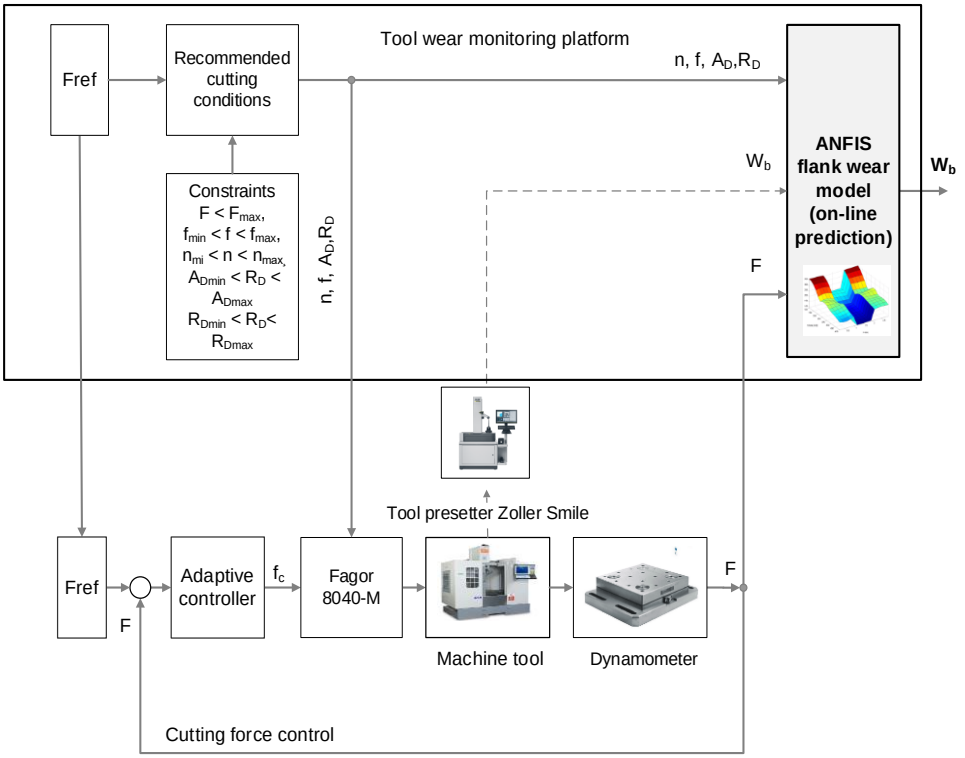

Figure 1. *Platform for tool wear monitoring via cutting force control*

2 ADAPTIVE CUTTING FORCE CONTROL SYSTEM

The scheme of adaptive regulation of cutting forces is shown in Figure 1. By adjusting the feedrate, the adaptive regulator regulates the cutting force on the cutting

tool and neutralizes disturbances such as inhomogeneity of the machined material and

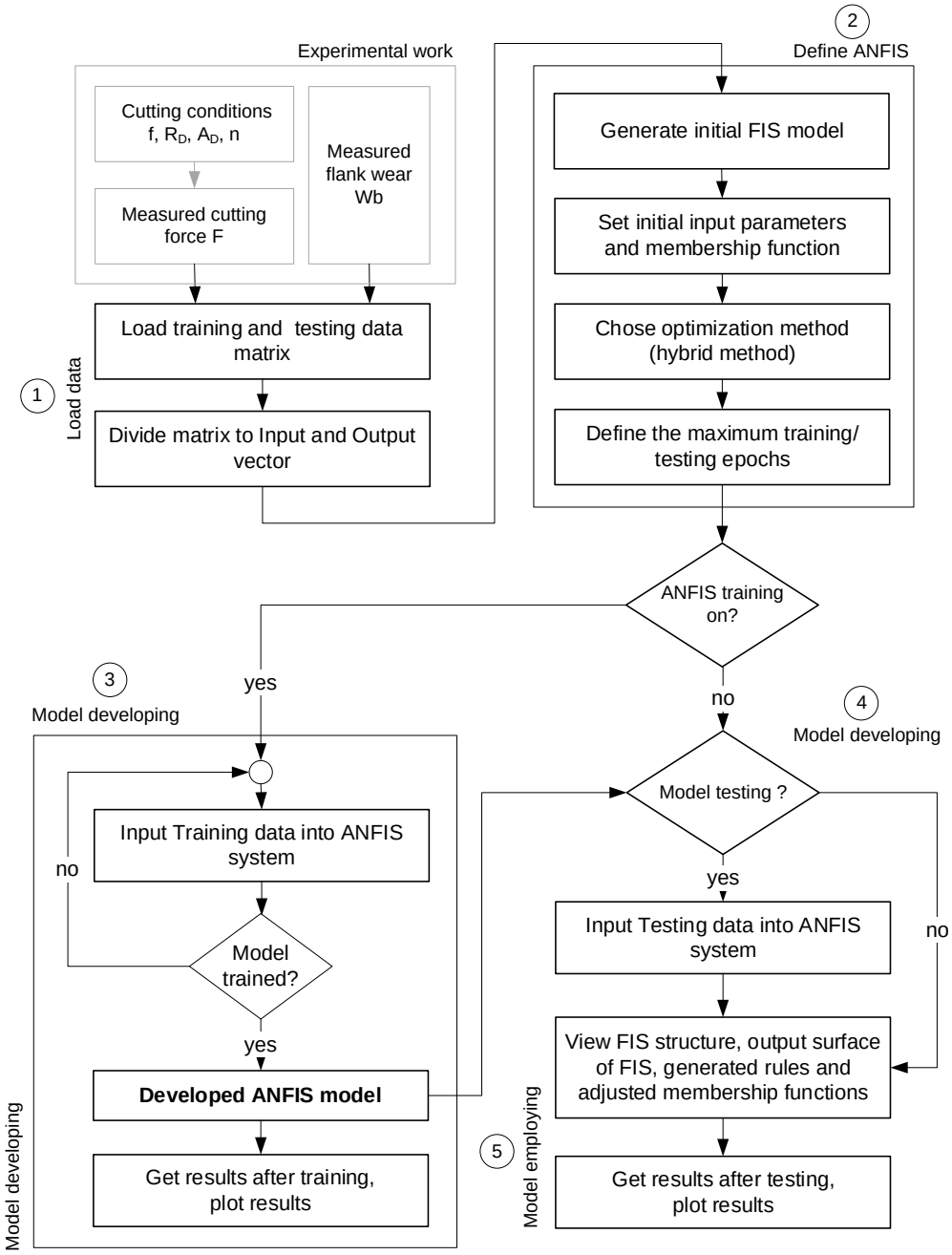

Figure 2. *Steps required to develop and use a tool wear model*

tool wear.

The controller is implemented in a Matlab script that is entered into Labview. In the feedback loop, the piezo dynamometer captures the maximum cutting force every

0.02 s.

The measured maximum force on the tool is compared to the reference cutting force Fref. Fref is the maximum force the tool can withstand without damaging the cutting edge or excessive tool wear. When a negative error is detected, the controller reduces feed rate and the cutting force.

The adaptive controller communicates with Fagor machine tool controls via DNC override functions.

The controller generates feedrate commands and sends them to the CNC controls and to the input of the ANFIS model to predict tool wear.

3 CUTTING TOOL WEAR MODEL FOR IN-PROCESS PREDICTIONS

In the research, a precise model was developed for on-line prediction of flank wear of cutting tool. The ANFIS method, which generates a fuzzy inference system (FIS), was used to create the prediction model.

A back-propagation algorithm is used to set the parameters of the membership functions. The effectiveness of the method lies in the fact that the FIS system learns (composes) based on the data that is being modeled.

FIS has a structure identical to an artificial neural network. This structure maps the input vector via input and output membership functions and associated parameters to outputs.

Figure 2 shows the algorithm for creating and using the tool wear model.

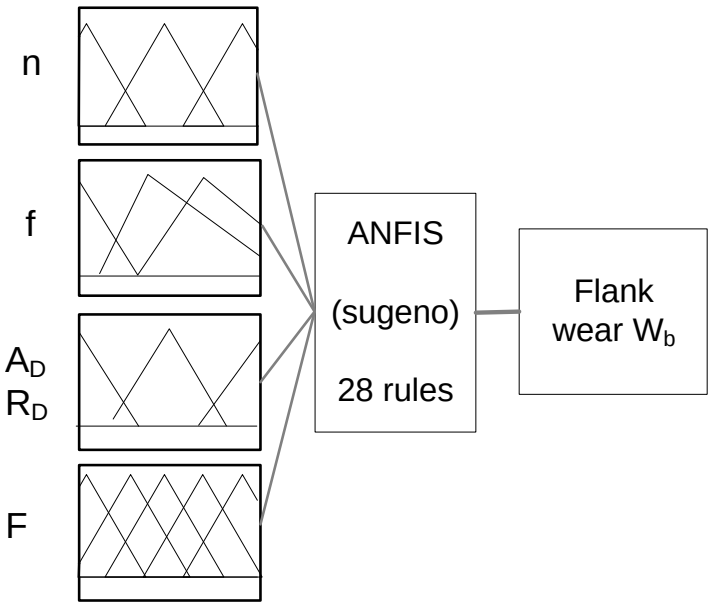

Figure 3. *FIS tool wear prediction system*

The tool wear prediction model is developed in five steps. Experimentally obtained data for model training and testing are loaded into the system in step 1.

The scaled data is arranged in a matrix consisting of input quantities and output quantity. The input quantities are the cutting parameters and the measured values of the cutting forces. The output quantity is the measured flank wear.

The data matrix is then split into a data set for training the model and a data set for testing the model. The data set for testing and learning consists of 400 data rows.

In the second step, the structure of the FIS model and parameters related to model training are defined. The structure used in the research is shown in Figure 3. The FIS has 5 inputs and one output connected with 28 if-then rules. In this step, the optimization method, the maximum number of training iterations, the maximum allowed error and the number and shape of membership functions are determined.

In the third step, model training takes place as ANFIS modifies its internal structure to correctly predict the tool wear. Model training was performed with 250 rows of the data matrix. Training is terminated when the prediction error becomes less than the defined maximum error or when 400 learning cycles are reached.

The fourth step involves using the model to predict tool wear. The learned model predicts tool wear based on the currently measured cutting forces with the corresponding cutting parameters.

After training, the inference system was able to estimate surface roughness from real-time measurements of cutting force and cutting conditions.

4 EXPERIMENTAL SET-UP

A Heller-type BEA02 CNC machine tool with a Fagor controller was chosen to perform the experiments. The workpieces were made of Ck 45 steel.

A solid carbide helical cutter with a diameter of 8.5 mm and two flutes was used in the experiment. The sintered tungsten carbide tool had a helix angle of 27.3° and a pitch angle of 4.28°. The blades had a PVD-TiAIN coating and a hardness of 1800 HV.

A Kistler 9255 piezoelectric dynamometer was installed on the machine table to measure the cutting forces.

Labview software took care of capturing and processing the measured signals. The voltage signals from the charge amplifier to the Labwave software were captured and transferred by a fast data acquisition card (National Instruments NI 9215 A).

Tool wear was measured using a pre-setting machine Zoller.

According to the experimental plan [8], measurements of cutting forces are carried out for the following combinations of cutting conditions: radial depth of cut: 0.75d, 0.5d, 0.25d; axial depth of cut: 1 mm, 2 mm, 4 mm; d- tool diameter (8.5 mm); feed speed: from 0.01 to 0.2 mm/tooth; rotation frequency: from 150 to 450 min^{-1}.The data is sorted into a data matrix.

5 RESULTS AND DISCUSSION

The results of the experiments confirmed the assumption that the predicted wear of the tool significantly depends on the thrust component of the cutting force.

From the data matrix with 400 rows, 250 rows of data were randomly selected to train the ANFIS model. The remaining rows were used to test the learned wear model. The model best-predicted tool wear at the FIS structure with triangular membership functions. The accuracy of the predictive model with triangular membership functions was 94 %. The average error of predicted and measured wear is 3.1 %. The most significant prediction error was observed at low rotational frequencies. The model training stopped after 51 iterations. The learning of the model was extremely fast, with the prediction error reaching a stationary state after 18 seconds.

The accuracy of the model on the training data set was 97%. Testing has shown that the ANFIS model predicts wear in real time without significant delays. With the help of a piezo dynamometer, we can predict very well the actual condition of the cutting tool.

The force sensor gives a reasonable estimate of the surface roughness.

6 CONCLUSION

Once the cutting force-tool wear relationships were established, the measured cutting force signals were used to predict tool wear in real time. A comparison was made between the actual measured tool wear and the predicted wear values with the ANFIS model. The comparison results showed good agreement.

The developed platform with the ANFIS method of predicting tool wear on-line has proven to be effective in monitoring the milling process, alerting the operator, and preventing tool breakage. The efficiency of the platform was reflected in the increased lifetime of the tool.

The developed ANFIS tool wear model predicts flank tool wear with 94% accuracy and displays it on the control panel.

NOMENCLATURE

A_D axial depth of cutting, mm

F_{ref} reference cutting force, N

F cutting force, N

f feed rate, mm/min

f_c feed rate command, mm/min

n spindle speed, N

R_D radial depth of cutting, mm

W_b flank wear, μm

REFERENCES

[1] Mulc, T., Udiljak, T., Cus, F., Milfelner, M., (2004). Monitoring cutting- tool wear using signals from the control system, *Strojniški vestnik – Journal of Mechanical Engineering*, 50, 12, pp. 568-579.

[2] Haber, R.E. (2013). Alique, Intelligent process supervision for predicting tool wear in machining processes, *Mechatronics*, p.p. 825-849.

[3] Achiche, S., Balazinski, M., Baron, L., Jemielniak, K. (2002). Tool wear monitoring using genetically-generated fuzzy knowledge bases, *Engineering Applications of Artificial Intelligence*, *15*(3-4), p.p. 303-314.

[4] Sokolowski, A. (2004). On some aspects of fuzzy logic application in machine monitoring, *Engineering Applications of Artificial Intelligence*, 17, p.p. 429-437.

[5] Kuo, R. J. (2000). Multi-sensor integration for on-line tool wear estimation through artificial neural networks and fuzzy neural network, *Engineering Applications of Artificial Intelligence*, 13(3), p.p. 249-261

[6] Sun, J., Hong, G. S., Wong, Y. S., Rahman, M., Wang, Z. G. (2006). Effective training data selection in tool condition monitoring system, *International Journal of Machine Tools and Manufacture*, 46(2), p.p 218-224.

[7] P. Fu, A.D. Hope, A.D, Intelligent Classification of Cutting Tool Wear States. Advances in Neural Networks, Vol. 39, 2008, pp. 1611-3349.

[8] Cus, F., Balic, J. (2000). Selection of Cutting Conditions and Tool Flow in Flexible Manufacturing System, *The International Journal for Manufacturing Science & Technology*, 2, p.p. 101-106.

COMETa 2022
6th INTERNATIONAL SCIENTIFIC CONFERENCE
17th - 19th November 2022
Jahorina, B&H, Republic of Srpska
University of East Sarajevo
Faculty of Mechanical Engineering
Conference on Mechanical Engineering Technologies and Applications

DEVELOPMENT AND CONTROL OF A VIRTUAL INDUSTRIAL SORTING PROCESS

Goran Munđar[1], Uroš Župerl[2]

Abstract: A virtual manufacturing method represents the emerging approach that allows companies to improve their processes in order to introduce new products more quickly to their markets in a cost-effective manner. This involves building a synthetic and integrated environment based on software tools and systems, such as Virtual Reality and Simulation, to facilitate such processes. This paper presents the development of virtual industrial environment, highlighting the development and control of virtual industrial process for sorting products by height using combination of two simulation software tools. Development of industrial process was performed using Factory I/O software tool, while the control program was developed using FluidSim software tool. This paper also highlights the usage of OPC communication protocol, that was used for communication between software tools during simulation.

Key words: Industry 4.0, Manufacturing, OPC communication protocol, Virtual Factory, Virtual industrial process

1 INTRODUCTION

The rapid advancement of technology in industry around the world is increasingly requiring knowledge and skills that are critical to the successful production of industrial applications. We encounter complex problems when planning and managing them, which require a wide range of skills from a variety of disciplines, such as mathematics, physics, computer science, electrical engineering, and logic programming. Industrial applications utilize a wide range of components, including sensors, actuators, electrical, mechanical, pneumatic, and hydraulic drives. In order to integrate these components into practical industrial applications, a great deal of time, money, and research is required [1]. The development of virtual systems in recent

[1] MSc Goran Munđar, University of Maribor, Faculty of Mechanical Engineering, Smetanova ulica 17, 2000 Maribor, Slovenia, goran.mundjar@um.si (CA)
[2] Assoc. prof. dr. Uroš Župerl, University of Maribor, Faculty of Mechanical Engineering, Smetanova ulica 17, 2000 Maribor, Slovenia, uros.zuperl@um.si

years has made industrial applications more efficient. Simulations of virtual systems use graphical computer simulations to simulate dynamic processes, which can be controlled by either simulated or real peripherals. It is primarily intended for engineers to use virtual systems as a means of inspecting and evaluating the performance of industrial applications developed using computers. The benefit of this method is that it is more cost-effective and does not pose any risk to persons or machines while developing and programming industrial applications [2].

The aim of this study is to develop a virtual industrial sorting process and to simulate its control using a computer simulation with the assistance of two software tools for simulating virtual systems. A first part of this paper will describe the creation of an electro-pneumatic industrial process utilizing the Factory I/O software tool. A virtual industrial environment can be created and simulated using Factory I/O by integrating components from a variety of major manufacturers [3]. Control of the virtual system may be achieved either through real PLC controllers or via virtual controllers.

In part two, we will present a sequential control chain for controlling the industrial process created in part one. This will be accomplished using the software tool FluidSim. FluidSim is a software environment for generating, simulating, and analysing electrical, hydraulic, digital, and electronic systems [4].

The third part of the paper will involve the simulation of a manufacturing process created in Factory I/O and controlled by a sequential controller created in FluidSim. The OPC Data Access communication protocol [5] will be used to communicate between Factory I/O and FluidSim through Festo Didactic EzOPC software tool [6].

2 INDUSTRIAL SORTING PROCESS

Our goal was to develop an industrial sorting process integrating electrical and pneumatic components. The aim of the work was to design a production system consisting of pneumatic and electric components. Boxes of three different sizes will enter the system, which the system will then sort according to their size.

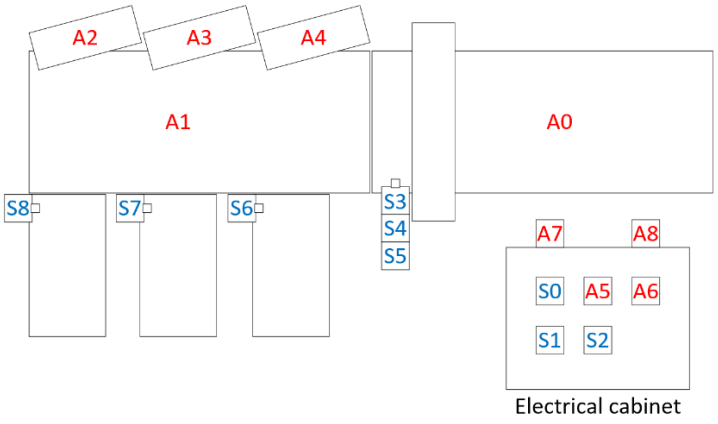

Figure 1. *Sketch of the industrial process*

As shown in figure 1, a sketch of the industrial process can be seen. Actuators are shown in red and sensors are shown in blue. In the following, we will describe all

components in more detail.

Several actuators will be required for the successful operation of an industrial process: 3 pivot arm sorters (A2, A3, A4), 2 belt conveyors (A1, A0), red light (A5), green light (A6), siren (A7) and emergency light (A8).

It was necessary to add sensors to the system in order to ensure the successful operation of the industrial process. The following sensors were used: 3 buttons (S0, S1,, S2), 3 diffuse photoelectric sensors to detect the size of the boxes at the beginning (S3, S4, S5) and 3 diffuse photoelectric sensors to detect the boxes after leaving the belt (S6, S7, S8).

2.1 Description of technological requirements

In this chapter, the technological requirements that must be implemented by the industrial process will be presented in detail.

At the beginning, all actuators are in their initial positions: the pivot arm sorters are in their initial position (A2, A3, A4), the siren (A7), emergency light (A8), green light (A6) and both conveyor belts (A0, A1) are turned off. At the beginning, only the red light (A5) is turned on. When S1 is pressed, the green light A6 turns on and the conveyor belt A0 turns on, after which boxes of three different sizes start entering the process. The size of the boxes is detected by sensors S3, S4 and S5. When a small box arrives in the process, only S3 turns on, when a medium-sized box arrives, S3 and S4 turn on, and when a large box arrives, all three sensors (S3, S4 and S5) turn on. When a small box is detected, the two actuators mounted on the A4 rotary arm (rotary arm pivot and rotary arm conveyor) are activated. Conveyor belt A1 is activated at the same time. When sensor S3 no longer detects the box, conveyor belt A0 is switched off. When the sensor S6 detects that the smaller box is leaving the conveyor belt, the conveyor belt A1 is switched off and the actuator A4 returns to the initial position. Conveyor belt A0 is also switched on at the same time. When a medium box is detected with sensors S3 and S4, both actuators mounted on the A3 rotary arm are activated. Conveyor belt A1 is activated at the same time. When sensor S3 no longer detects the box, conveyor belt A0 is switched off. When the sensor S7 detects that the box is leaving the conveyor belt, the conveyor belt A1 is switched off and A3 returns to the initial position. Conveyor belt A0 is also switched on at the same time. When a large box is detected with sensors S3, S4 and S5 both actuators mounted on the A2 rotary arm are activated. Conveyor belt A1 is activated at the same time. When sensor S3 no longer detects the box, conveyor belt A0 is switched off. When the sensor S8 detects that the box is leaving the conveyor belt, the conveyor belt A1 is switched off and A2 returns to the initial position. Conveyor belt A0 is also switched on at the same time.

When the S2 (Stop) button is pressed, the operation of the entire system stops until the S1 (Start) button is pressed. When the S0 (Emergency Stop) is switched on, the operation of the system stops immediately. Actuators A7 (siren) and A8 (emergency light) are switched on. After S0 is switched off, the actuators A7 and A8 are switched off.

3 VIRTUAL INDUSTRIAL PROCESS

We used the Factory I/O software tool to create a virtual industrial process. As part of the creation of the virtual industrial process in Factory I/O, four groups of components were used: actuators, sensors, structural components and generating components.

3.1 Sensors

The sensors we used in the creation of the virtual industrial process are 3 buttons and 6 diffuse photoelectric sensors.

The function of a button is to serve as an interface between an industrial process and the user. To operate the system, we used three buttons: the Start button for starting the system, the Stop button for stopping the system, and the Emergency Stop button for stopping it in an emergency. The other three sensors are used to detect boxes leaving the industrial process.

3.2 Actuators

In creating a virtual industrial process, we used 2 conveyor belts, 3 pivot arm sorters, 2 light indicators, siren and an emergency light.

Conveyor belts are used to transport products with a small mass. Their components include supporting elements, a belt on which the products are transported, and an electric motor that drives the belt. Digital control is used to control the electric motors on the conveyor belts. A conveyor belt can rotate at a maximum speed of 0.6 m/s.

The pivot arm sorter consists of a 45-degree front arm converter driven by a motor reductor. It is equipped with a smaller conveyor belt that helps divert transported items to adjacent components. The arm can rotate left or right depending on the selected configuration and allows for a 45-degree rotation.

3.3 Generating components

In a virtual industrial process, we need components that generate elements. In Factory I/O, this component is called EMITTER. A component can be specified the type of elements it can generate and the time difference between generation of individual elements. In the industrial process, we also used the element removal component called REMOVER. This component removes an element as soon as it arrives in its area. In our virtual industrial process we used 3 REMOVER components.

3.4 Entire process in Factory I/O

Figure 2 illustrates the entire virtual industrial process created in Factory I/O.

Figure 2. *Virtual industrial process created in Factory I/O*

4 CONTROL SYSTEM DEVELOPMENT

The purpose of this chapter is to describe the implementation of control using the FluidSim software tool. With the controller in FluidSim, we were able to control the industrial process developed in Chapter 3. A sequential control chain is used by the controller for controlling the system.

The controller was made from components found in the GRAFCET library within FluidSim. First, it was necessary to define the variables that we already used when creating the virtual process in the previous chapter. To define the variables, we used the GRAFCET I/O component, which can define 8 input and 8 output variables. Due to the larger number of inputs, we used two GRAFCET I/O components. For successful operation of the control, it is necessary to connect the variable values in FluidSim to the OPC server. By doing this, we will be able to send variable values from the control system in FluidSim to the virtual industrial process in Factory I/O, and vice versa. To connect the variables to the OPC server, we used the "FluidSim Input Port" and "FluidSim Output Port" components. Using the OPC communication protocol, the “FluidSim Input Port” component reads sensor values in an industrial process. Virtual industrial process receives actuator values via the OPC protocol through the “FluidSim Output Port component”. In our control system we used 2 "FluidSim Input Port" components and 2 "FluidSim Output Port" components. Input/Output components were connected to the GRAFCET I/O components as shown in Figure 3.

After defining the communication components, a sequential control chain can be constructed. Created virtual industrial process contains a large number of sensors and actuators, so we divided the entire system into 7 subsystems. System 1 takes care of the operation of the first conveyor belt. System 2 takes care of the operation of the second conveyor belt. System 3 takes care of the operation of the red and green lights on the electrical box. System 4 takes care of sorting the smallest boxes. System 5 takes care of sorting medium-sized boxes. System 6 takes care of sorting the largest boxes. System 7 takes care of the operation of the system in the event of an emergency shutdown. Each subsystem is made of one control chain. To create the control chains, we used the Transition, Step and Action components found in the GRAFCET library within FluidSim.

5 CONNECTION PART

This chapter describes the configuration settings of the Festo Didactic EzOPC OPC server and the communication configuration within the Factory I/O programs in FluidSim. In Festo Didactic EzOPC, an OPC server can be configured and defined. In this way, different OPC clients can be connected to each other.

Before setting up the server, it was necessary to select the appropriate type of process data and the type of controller. A Process Simulation in CIROS/COSIMIR was used as the data type for the process and a Controller in FluidSim was used as the controller type for the process. Figure 3 illustrates the definition of the OPC server.

Once the OPC server has been successfully configured, Factory I/O and FluidSim must be configured to communicate with the OPC server. The type of communication must first be configured in Factory I/O. We selected OPC Clident DA/UA. Afterwards, the OPC communication protocol must be configured in accordance with the requirements. The OPC server, the number of variables, and the filters for naming variables must be defined. To set the OPC communication protocol in FLuidSim, it is necessary to enable the OPC protocol. This can be done in Options - EasyPort/OPC/DDE Connection where OPC mode option should be selected. As a

next step, the FluidSim Input Port and FluidSim Output Port components must be assigned appropriate addresses for OPC communication. It is necessary to select the name of the OPC server (in our case, Festo Didactic EzOPC.1) and the corresponding address. We used the addresses VirtualPLC.AB1 and VirtualPLC.AB2 for the Input components, and the addresses VirtualPLC.EB1 and VirtualPLC.EB2 for the Output components.

After successful communication setup, simulation can be performed.

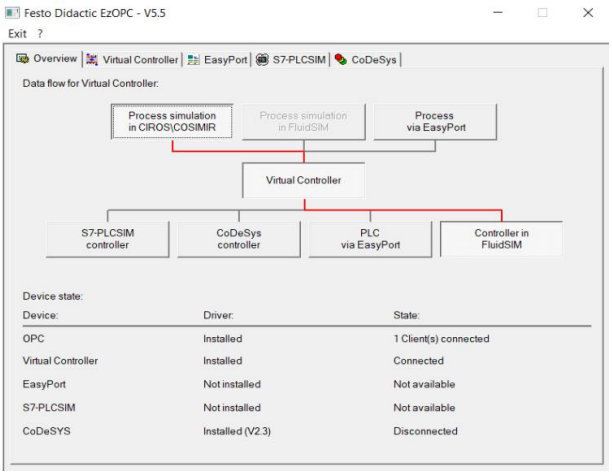

Figure 3. *Definition od the OPC server in Festo Didactic EzOPC*

6 RESULTS

We checked the operation of the OPC connection on the developed system for sorting boxes, which is presented in chapter 3. Due to complexity, we divided the entire system into 7 smaller subsystems. When starting the simulation in the Factory I/O and FluidSim programs, it is possible to check the operation of the virtual industrial process and its control.

The industrial process worked as follows: After pressing the START button, the industrial process started to run. The first conveyor belt that brings boxes into the process has turned on. When the box reached the three height sensors, the system determined what size the detected box was. The box was then sorted by size. The smallest boxes are sorted into the first chute, the medium-sized boxes into the second chute, and the largest boxes into the third chute. The sorting of the boxes is done with three rotating arms that allow the boxes to be sorted into their chute. When the box leaves the second conveyor belt, which is detected by the sensor, the first conveyor belt is switched on again, bringing a new box into the system. When the STOP button is pressed, the system stops working until the Start button is pressed again. When the emergency stop switch is activated, the system stops immediately. At the same time, the alarm light and siren are switched on.

Figure X shows a screenshot of the operation of a virtual industrial process. An industrial process created in Factory I/O is shown on the left side of the figure X. The developed control application in FluidSim is shown on the right side of figure X. Through the OPC communication protocol, the two parts can communicate in real time.

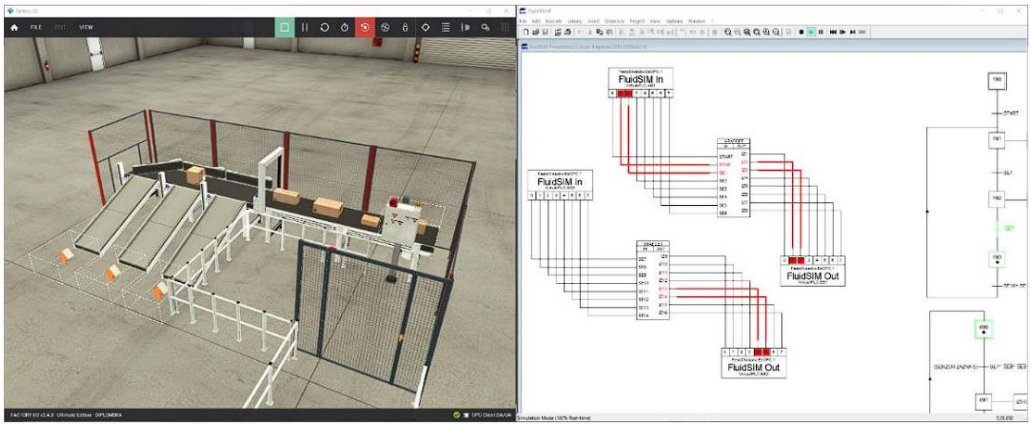

Figure 4. *Simulation of virtual industrial process in Factory I/O and FluidSim*

7 CONCLUSION

A growing number of software tools are being used to create, control, and simulate virtual industrial processes. This is done both in the development of new industrial applications as well as in the testing of controls on already developed industrial applications. As a result, industrial processes can be developed more rapidly, while planning costs are lower, since no real components have to be used. A virtual environment also provides a safer environment for developing new systems since injuries are very unlikely to occur.

In the first part, we described the operation of the industrial process for sorting boxes of three different sizes. There are nine actuators and nine sensors involved in the entire industrial process.

The second part of this article describes how to build a virtual industrial process with Factory I/O software. The industrial process was described in detail, including all the components and their installation. All actuators and sensors were also given names and addresses.

In the third part, we developed an industrial process controller in FluidSim. It consists of seven sequential control chains, each controlling an individual subsystem in the industrial process. We also defined components for OPC protocol communication in FluidSim.

The last part of the project involved testing and simulating the industrial process using an OPC connection. As a result, the industrial process operated smoothly. With all sensors and actuators in place, the controller managed the industrial process correctly.

The goals we set for ourselves were achieved in our work. Through Factory I/O, we have been able to successfully develop a more complex virtual industrial process. To control the sensors and actuators in FluidSim, a sequential control chain has been created. A virtual controller connected Factory I/O simulation to FluidSim simulation's sequential control chain. A developed industrial process has been successfully simulated. The virtual system created in this part can also be created in the real version, making this part a digital twin of the real version.

With OPC, virtual systems can be controlled in real time and errors in the control program can be found quickly. Because of this, it was easier to design a control program without injuring anyone or causing any damage to equipment.

REFERENCES

[1] Riera, B., Vigário, B. (2017). HOME I/O and FACTORY I/O: a virtual house and a virtual plant for control education. *IFAC-PapersOnLine*, *50*/1, p. p. 9144-9149.
[2] Poblacion Salvatierra, I. (2018). Simulation software for automation industry: Factory I/O and KUKASim software.
[3] Factory I/O User manual, https://docs.factoryio.com/manual/, access date: 20.10.2022
[4] Festo FluidSIM Pneumatics User's Guide, https://www.festodidactic.com/ov3/media/customers/1100/698528_fl_sim_p42_en_offset.pdf, access date: 15.10.2022
[5] Festo Manual EzOPC, https://www.festodidactic.com/ov3/media/customers/1100/04193590011200337 40.pdf, access date: 21.10.2022
[6] Mahnke, W., Leitner, S. H., & Damm, M. (2009). *OPC unified architecture*. Springer Science & Business Media.

COMETa 2022
6th INTERNATIONAL SCIENTIFIC CONFERENCE
17th - 19th December 2022
Jahorina, B&H, Republic of Srpska
University of East Sarajevo
Faculty of Mechanical Engineering
Conference on Mechanical Engineering Technologies and Applications

EVALUATION OF CHIP-TOOL INTERFACE TEMPERATURE BY ADAPTIVE NEURO FUZZY INFERENCE SYSTEM

Milos Milovancevic[1], Dalibor Petković[2]

Abstract: The main goal of the study is to make an optimization algorithm for evaluation of chip-tool interface temperature by adaptive neuro fuzzy inference system (ANFIS). ANFIS represent a heuristic optimization method with back propagation training in one direction and gradient descent algorithm in backwards. The experimental training data samples are acquired for published literature. There are operating parameters which have impact on the chip-tool interface temperature. Input attribute Environment has the smallest training error hence the highest influence on the temperature. Combination of cutting speed and environment has the smallest training error hence the highest influence on the temperature. Combination of cutting speed, feed rate and environment has the smallest training error hence the highest influence on the etch rate. The study considering different operating parameters simultaneously is believed to be the first on a small scale and to attract the interest of everyone.

Keywords: chip-tool interface; temperature; optimization; ANFIS

1 INTRODUCTION

Forms of the chip shapes could represent the quality of machining process. Although the chip can be considered as a waste material the chip forms can be very important since the forms can affect the machining process drastically and the quality of the machined product as well. The chip forms can be a critical feature which highly impacts the cutting process stability. One of the most important factors for the chip forms is temperature distributing in cutting zone due to contacts between cutting tool and working material [1]. Therefore, analyzing of the chip forms and temperature distribution in cutting zone has been of great interest for industrial research community [2]. It is very important to analyze the chip shapes formation and temperature

[1] University of Niš, Faculty for mechanical engineering, Serbia, milovancevic@masfak.ni.ac.rs
[2] University of Niš, Pedagogical Faculty in Vranje, Serbia

distribution in cutting zone since these factors could affect surface roughness, tool life, force components of the cutting process and product quality overall.

Chip formation and cutting zone area are important factors that have received limited attention. Cutting zone area grew weakly with increased cutting speed, levelling off at high cutting speed; however, it rose noticeably with increased feed [3]. Experimental investigation and finite element simulation were conducted in article [4] in order to acquire thorough understanding of the chip temperature and its effects on chip morphology, cutting forces, and surface roughness. There has existed a great deal of theory researches in term of chip production and chip breaking characteristics under conventional cutting and high speed cutting conditions, however, there isn't sufficient research on chip formation mechanism as well as its influence on cutting state regarding large workpieces under extreme load cutting [5]. High-speed cutting is widely employed in aerospace, automotive, die, and other industries. However, no comprehensive mechanism of high-speed cutting behavior was as yet comprehended completely. Models of thermal sources and fields of cutting temperature are proposed for analysis of thermal equilibrium between heat generation and energy consumption at high-speed dry cutting [6]. In article [7] was shown that the temperature in the shear zone decreases with a decrease in the chip thickness. This leads to lower thermal softening of the material and thus to higher specific cutting forces. Taking the formation of serrated chip into account, a theoretical method for prediction of tool temperatures in intermittent turning was proposed in article [8] to reveal the effects of cutting parameters on tool temperatures. Relatively large feed rate and relatively small depth of cut should be adopted to acquire the lowest tool temperature. Dramatic tool temperature variation in end milling can cause excessive tool wear and shorten its life, especially in machining of difficult-to-machine materials [9]. In study [10] was proposed an approach based on artificial neural network (ANN) to predict the experimental cutting temperatures generated in orthogonal turning of AISI 316L stainless steel and it was demonstrated that the established ANN model is a powerful one for predicting the experimental cutting temperatures.

Since many machining parameters could be changed in order to obtain optimal machining condition in this study the main aim was to determine the most important parameters of the process and especially focus is on the temperature distribution in cutting zone. Neuro-fuzzy approach was applied since it is highly suitable approach for the nonlinear system with many different parameters [11].

2 METHODOLOGY AND MATERIALS

2.1 Experimental setup

Experimental tests were performed during turning on the machine Model VDF-D480 10KW. Cutting zone temperature was measured during machining as can be seen in Figure 1a. Thermal camera was used for the temperature measurement in the cutting zone. The camera FLIR E50 which is thermal sensitive is shown in Figure 1b. The main features of the camera are:

- Class II laser product, 1mW power output.
- IR resolution - 43,200 (240x180) pixels,
- Measurement modes include 3 Spots, 3 Area Box, Isotherm, Auto Hot/Cold spots
- Bluetooth links camera to mobile devices,

- Picture-in-Picture,
- Auto Orientation.

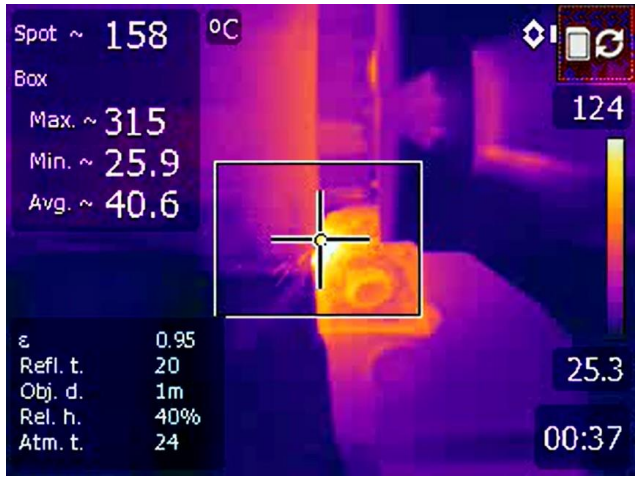

(a)

(b)

Figure 1: (a) *Temperature measurement in cutting zone and* (b) *thermal camera FLIR E50*

Surface roughness was measured by roughness meter, Perthometer M1 by Mahr Company. Roughness recordings were performed in Perthometer software. As the surface roughness measure, arithmetical average roughness Ra was used. The average values were evaluated for each of the specimens. The surface roughness was measured on the three specimen's sections – upper, lower and middle section and average values were determined. The roughness was measured 0.1 mm from the

upper and lower edges of the specimen. The experimental procedure of surface roughness measurement was performed on the Talysurf 6 (Taylor Hobson) system. This system could measure micro-geometric characteristics of the surface.

The cutting forces were measured experimentally. The experiment was composed of a dynamometer KISTLER type 9265A1, an amplifier KISTLER tip Ca5001, an AD converter Burb Brown type 2000 and a computer PC/AT 486 33MHz. For the signal acquisition software LT/CONTROL version 5.02 was used through a virtual instrument in order to track the cutting forces graphically.

After the experimental investigation for different cutting condition based on the experimental plan, the acquired signals of the cutting forces were analyzed. The name of the cutting tool was PTGNR 2525 M16 with TNMG 160404-CM 4C15 P15. Figure 2 shows the themral camera in action and the cutting process.

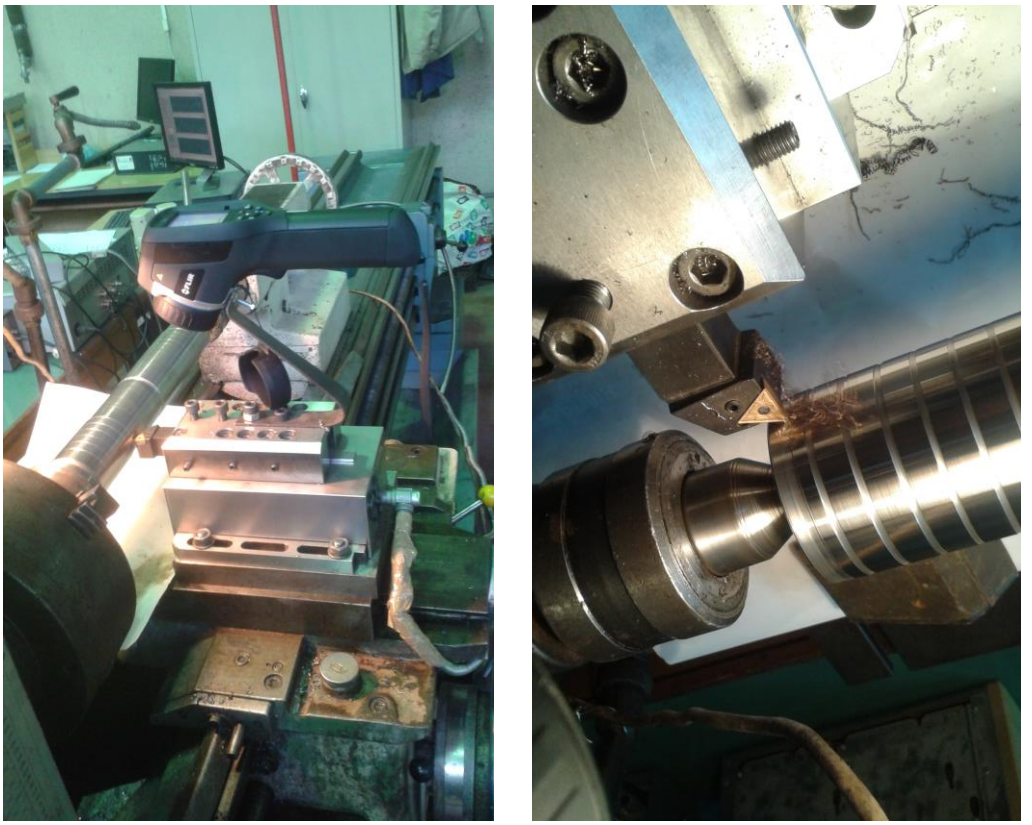

(a) (b)

Figure 2: (a) *Temperature measures in the cutting zone and* (b) *the cutting process*

In order to have the full control on the toll life and on the surface roughness as the main indicator of the machining process quality it is essential to measure the temperature in the cutting tool and in the chip as well. It is very important to know the temperature distribution in the cutting zone in order to understand and to control the machining process. Figure 3 shows the experimental setup scheme of the machining process and the temperature measurement in the cutting zone.

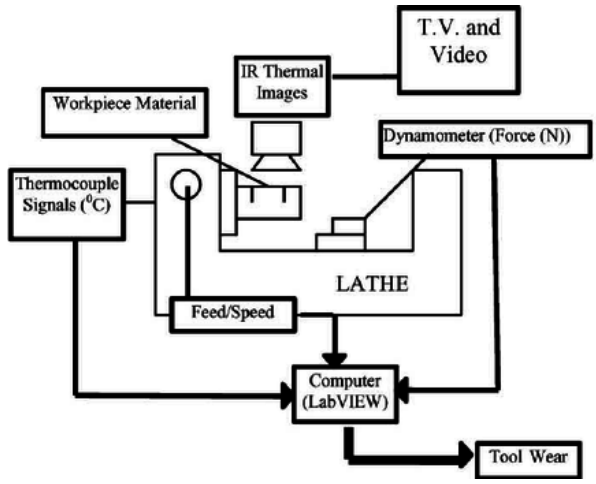

Figure 3: *Experimental setup scheme*

In the present study, the role of high-pressure coolant jet by water-insoluble mineral oil VG-68 on cutting temperature and tool life in turning C-60 steel, 17CrNiMo6 steel, and 42CrMo4 steel by uncoated SNMG and SNMM carbide inserts is experimentally investigated. To evaluate the effects of cutting speed, feed rate, environment (dry and HPC-assisted machining), materials, and cutting inserts on chip–tool interface temperature, mathematical models are formed based on response surface methodology and validity of the models are confirmed by employing various statistical evaluation techniques. Tables 1 and 2 shows the input or operating parameters which are varied in the design [12].

Table 1: *Numerical values of the input variables [12]*

Environment	Material	Cutting tool
Dry - 1	C-60 - 1	SNMG - 1
HPC - 2	17CrNiMo6 - 2	SNMM - 2
	42CrMo4 - 3	

Table 2: *Input and output variables [12]*

Input 1	Input 2	Input 3	Input 4	Input 5	Output
Cutting speed m/min	Feed rate mm/rev	Environment	Material	Cutting tool	Temperature
93	0.1	1	1	1	592
93	0.14	1	1	1	662
93	0.18	1	1	1	694

93	0.22	1	1	1	698
133	0.1	1	1	1	652
133	0.14	1	1	1	694
133	0.18	1	1	1	709
133	0.22	1	1	1	736
186	0.1	1	1	1	714
186	0.14	1	1	1	769
186	0.18	1	1	1	782
186	0.22	1	1	1	790
266	0.1	1	1	1	773
266	0.14	1	1	1	821
266	0.18	1	1	1	826
266	0.22	1	1	1	843
93	0.1	2	1	1	453
93	0.14	2	1	1	534
93	0.18	2	1	1	563
93	0.22	2	1	1	584
133	0.1	2	1	1	566
133	0.14	2	1	1	595
133	0.18	2	1	1	617
133	0.22	2	1	1	640
186	0.1	2	1	1	595
186	0.14	2	1	1	644
186	0.18	2	1	1	678
186	0.22	2	1	1	701
266	0.1	2	1	1	697
266	0.14	2	1	1	717
266	0.18	2	1	1	757
266	0.22	2	1	1	784
93	0.1	1	2	1	690
93	0.14	1	2	1	564
93	0.18	1	2	1	708
93	0.22	1	2	1	591
133	0.1	1	2	1	730
133	0.14	1	2	1	646
133	0.18	1	2	1	743
133	0.22	1	2	1	671
186	0.1	1	2	1	780
186	0.14	1	2	1	706

186	0.18	1	2	1	791
186	0.22	1	2	1	724
266	0.1	1	2	1	826
266	0.14	1	2	1	757
266	0.18	1	2	1	839
266	0.22	1	2	1	770
93	0.1	2	2	1	566
93	0.14	2	2	1	468
93	0.18	2	2	1	581
93	0.22	2	2	1	491
133	0.1	2	2	1	606
133	0.14	2	2	1	549
133	0.18	2	2	1	624
133	0.22	2	2	1	590
186	0.1	2	2	1	679
186	0.14	2	2	1	628
186	0.18	2	2	1	680
186	0.22	2	2	1	644
266	0.1	2	2	1	710
266	0.14	2	2	1	651
266	0.18	2	2	1	738
266	0.22	2	2	1	701
93	0.1	1	3	1	671
93	0.14	1	3	1	688
93	0.18	1	3	1	707
93	0.22	1	3	1	713
133	0.1	1	3	1	692
133	0.14	1	3	1	732
133	0.18	1	3	1	736
133	0.22	1	3	1	749
186	0.1	1	3	1	712
186	0.14	1	3	1	746
186	0.18	1	3	1	767
186	0.22	1	3	1	786
266	0.1	1	3	1	739
266	0.14	1	3	1	769
266	0.18	1	3	1	799
266	0.22	1	3	1	823
93	0.1	2	3	1	510

93	0.14	2	3	1	523
93	0.18	2	3	1	573
93	0.22	2	3	1	613
133	0.1	2	3	1	547
133	0.14	2	3	1	586
133	0.18	2	3	1	633
133	0.22	2	3	1	667
186	0.1	2	3	1	577
186	0.14	2	3	1	619
186	0.18	2	3	1	667
186	0.22	2	3	1	715
266	0.1	2	3	1	621
266	0.14	2	3	1	669
266	0.18	2	3	1	727
266	0.22	2	3	1	757
93	0.1	1	1	2	565
93	0.14	1	1	2	641
93	0.18	1	1	2	682
93	0.22	1	1	2	691
133	0.1	1	1	2	618
133	0.14	1	1	2	670
133	0.18	1	1	2	697
133	0.22	1	1	2	713
186	0.1	1	1	2	680
186	0.14	1	1	2	744
186	0.18	1	1	2	757
186	0.22	1	1	2	790
266	0.1	1	1	2	727
266	0.14	1	1	2	788
266	0.18	1	1	2	813
266	0.22	1	1	2	822
93	0.1	2	1	2	470
93	0.14	2	1	2	540
93	0.18	2	1	2	566
93	0.22	2	1	2	578
133	0.1	2	1	2	526
133	0.14	2	1	2	568
133	0.18	2	1	2	587
133	0.22	2	1	2	634

186	0.1	2	1	2	582
186	0.14	2	1	2	638
186	0.18	2	1	2	681
186	0.22	2	1	2	703
266	0.1	2	1	2	631
266	0.14	2	1	2	697
266	0.18	2	1	2	711
266	0.22	2	1	2	755
93	0.1	1	2	2	645
93	0.14	1	2	2	672
93	0.18	1	2	2	709
93	0.22	1	2	2	728
133	0.1	1	2	2	707
133	0.14	1	2	2	741
133	0.18	1	2	2	760
133	0.22	1	2	2	777
186	0.1	1	2	2	771
186	0.14	1	2	2	803
186	0.18	1	2	2	812
186	0.22	1	2	2	826
266	0.1	1	2	2	823
266	0.14	1	2	2	846
266	0.18	1	2	2	858
266	0.22	1	2	2	865
93	0.1	2	2	2	522
93	0.14	2	2	2	551
93	0.18	2	2	2	588
93	0.22	2	2	2	612
133	0.1	2	2	2	573
133	0.14	2	2	2	600
133	0.18	2	2	2	638
133	0.22	2	2	2	660
186	0.1	2	2	2	655
186	0.14	2	2	2	675
186	0.18	2	2	2	690
186	0.22	2	2	2	743
266	0.1	2	2	2	691
266	0.14	2	2	2	728
266	0.18	2	2	2	746

266	0.22	2	2	2	770
93	0.1	1	3	2	673
93	0.14	1	3	2	686
93	0.18	1	3	2	700
93	0.22	1	3	2	713
133	0.1	1	3	2	703
133	0.14	1	3	2	720
133	0.18	1	3	2	735
133	0.22	1	3	2	745
186	0.1	1	3	2	736
186	0.14	1	3	2	746
186	0.18	1	3	2	753
186	0.22	1	3	2	771
266	0.1	1	3	2	764
266	0.14	1	3	2	780
266	0.18	1	3	2	797
266	0.22	1	3	2	811
93	0.1	2	3	2	505
93	0.14	2	3	2	528
93	0.18	2	3	2	560
93	0.22	2	3	2	606
133	0.1	2	3	2	534
133	0.14	2	3	2	576
133	0.18	2	3	2	595
133	0.22	2	3	2	671
186	0.1	2	3	2	581
186	0.14	2	3	2	612
186	0.18	2	3	2	663
186	0.22	2	3	2	694
266	0.1	2	3	2	634
266	0.14	2	3	2	654
266	0.18	2	3	2	733
266	0.22	2	3	2	754

2.2 ANFIS METHODOLOGY

As shown in Figure 4, the ANFIS network contains five levels. The fuzzy inference system lies at the heart of the ANFIS network. Layer 1 accepts the inputs and uses membership functions to convert them to fuzzy values. The bell-shaped

membership function is employed in this study because it has the best capability for nonlinear data regression.

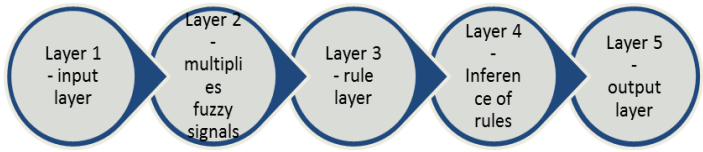

Figure 4: *ANFIS layers*

Bell-shaped membership functios is defined as follows:

$$\mu(x) = bell(x; a_i, b_i, c_i) = \frac{1}{1+\left[\left(\frac{x-c_i}{a_i}\right)^2\right]^{b_i}} \quad (1)$$

where $\{a_i, b_i, c_i\}$ is the parameters set and x is input.

The second layer multiplies the first layer's fuzzy signals and produces the rule's firing strength. The rule layers are the third layer, and they normalize all of the signals from the second layer. The fourht layer does rule inference and converts all signals to crisp values. The last layers summed all of the signals and provided a clean output value.

3 RESULTS

The best predictors for the different types of defects were chosen using the ANFIS approach. The selection is crucial, as is the preprocessing of the input parameters to eliminate irrelevant inputs. Following the command in MATLAB Software, the dataset is partitioned into a training set (odd-indexed samples) and a checking set (even-indexed samples):

```
>>[data] = temperature;
>>trn_data = data(1:2:end,:);
>>chk_data = data(2:2:end,:);
```

The function “exhsrch” conducts an exhaustive search of the available inputs to identify the set of inputs that have the greatest impact on the temperature. The function's first parameter defines the number of input combinations that will be tested during the selection process. In essence, "exhsrch" creates an ANFIS model for each combination, trains it for one epoch, and then publishes the results. The command line below is used to find the one and two most important attributes in forecasting outputs:

```
>> exhsrch(1,trn_data,chk_data);
```

```
>> exhsrch(2,trn_data,chk_data);
```

Figures 5-7 show the correlations of the influence of single, two and three input combinations on the temperature. The influence is determined based on RMSE training (trn) and checking (chk) errors. Input attribute **Environment** has the smallest training error hence the highest influence on the temperature. In other words, any small changes of the **Environment** would provide large oscillations of the temperature.

Figure 6 shows the optimal combination of two input attributes based on the temperature. Combination of **cutting speed** and **environment** has the smallest training error hence the highest influence on the temperature. In other words, if **cutting speed** and **environment** are changing in the same time it would produce the highest changing of the temperature.

Figure 7 shows the optimal combination of three input attributes based on the temperature. Combination of **cutting speed, feed rate** and **environment** has the smallest training error hence the highest influence on the etch rate. In other words, if **cutting speed, feed rate** and **environment** are changing in the same time it would produce the highest changing of the temperature.

Tables 3-5 shows numerical values of RMSE based on the prediction of temperature for one, two and three input attributes.

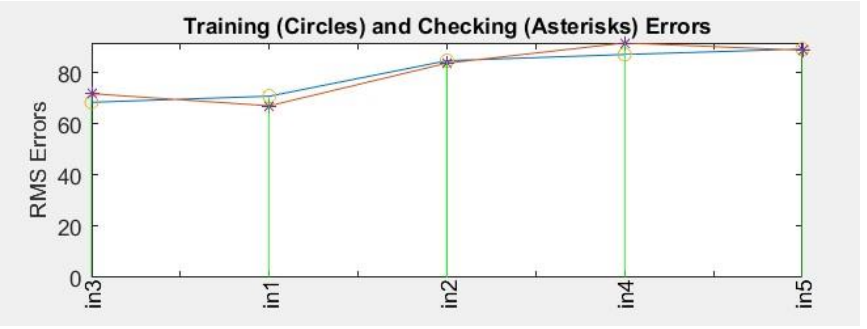

Figure 5: *Correlations of one input attribute with response*

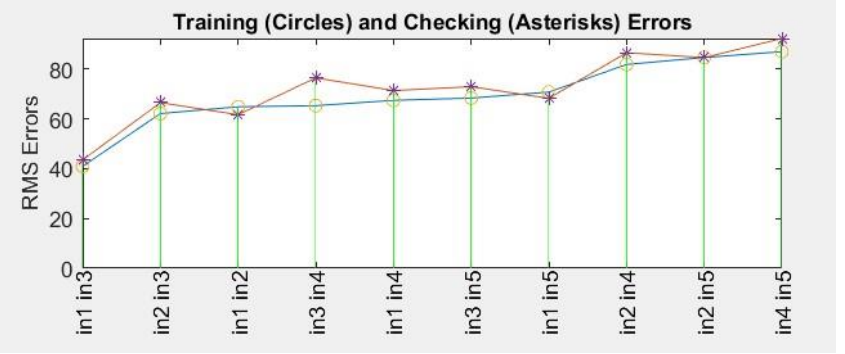

Figure 6: *Correlations of two inputs attribute with response*

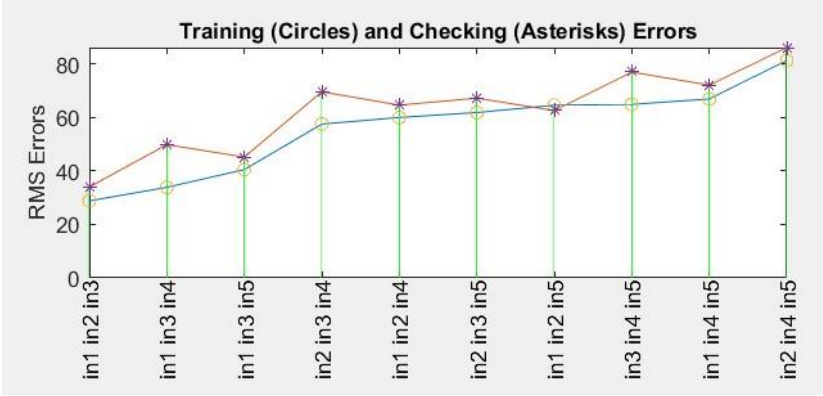

Figure 7: *Correlations of three inputs attribute with response*

Table 3: *Correlations of one attribute with response*

ANFIS model 1: in1 --> trn=70.9333, chk=67.1488
ANFIS model 2: in2 --> trn=84.7981, chk=83.8550
ANFIS model 3: in3 --> trn=68.5321, chk=71.9043
ANFIS model 4: in4 --> trn=87.2305, chk=91.7571
ANFIS model 5: in5 --> trn=89.3803, chk=88.8896

Table 4: *Correlations of two attributes with response*

ANFIS model 1: in1 in2 --> trn=64.8226, chk=61.6328
ANFIS model 2: in1 in3 --> trn=40.9577, chk=43.5176
ANFIS model 3: in1 in4 --> trn=67.4106, chk=71.3364
ANFIS model 4: in1 in5 --> trn=70.7269, chk=68.2225
ANFIS model 5: in2 in3 --> trn=62.1072, chk=66.4773
ANFIS model 6: in2 in4 --> trn=81.8142, chk=86.5173
ANFIS model 7: in2 in5 --> trn=84.5962, chk=84.5537
ANFIS model 8: in3 in4 --> trn=65.2682, chk=76.4268
ANFIS model 9: in3 in5 --> trn=68.3311, chk=72.8869
ANFIS model 10: in4 in5 --> trn=86.9476, chk=92.2298

Table 5: *Correlations of three attributes with response*

ANFIS model 1: in1 in2 in3 --> trn=28.8028, chk=34.0016
ANFIS model 2: in1 in2 in4 --> trn=59.9626, chk=64.5875
ANFIS model 3: in1 in2 in5 --> trn=64.5303, chk=62.5517
ANFIS model 4: in1 in3 in4 --> trn=33.8589, chk=49.8112
ANFIS model 5: in1 in3 in5 --> trn=40.4942, chk=45.1703
ANFIS model 6: in1 in4 in5 --> trn=66.8746, chk=72.0426
ANFIS model 7: in2 in3 in4 --> trn=57.5043, chk=69.5606
ANFIS model 8: in2 in3 in5 --> trn=61.8193, chk=67.1821
ANFIS model 9: in2 in4 in5 --> trn=81.2755, chk=86.0852
ANFIS model 10: in3 in4 in5 --> trn=64.8590, chk=76.9501

For further analyzing the optimal two-attributes is extracted and analyzed. There is always preferable to use models with small number of inputs. Figure 8 shows the ANFIS decision surface for the minimal checking error.

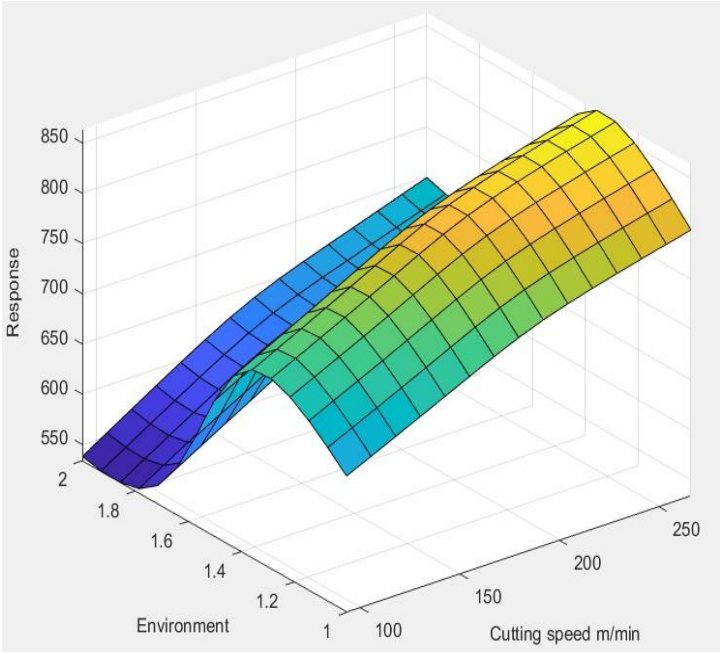

Figure 8: *Relationship between the optimal two-attributes and the temperature*

4 CONCLUSION

The paper illustrated a neuro-fuzzy-based method for monitoring the chip shapes and surface roughness based in temperature distribution in cutting zone for different machining parameters. Chip shapes and surface roughness are very important quality factors for machining process. Good chip shape means the best final products with the best surface roughness. In this research we analyzed temperature distribution influence in cutting zone on the chip shapes and surface roughness.

Neuro-fuzzy approach was applied since it is highly suitable approach for nonlinear systems with many different parameters. It is found that spot temperature is more influential than maximal temperature during the machining process.

REFERENCES

[1] Hwang, J., & Chandrasekar, S. (2011). Contact conditions at the chip-tool interface in machining. *International Journal of Precision Engineering and Manufacturing*, *12*(2), 183-193.

[2] Maruda, R. W., Krolczyk, G. M., Nieslony, P., Wojciechowski, S., Michalski, M., & Legutko, S. (2016). The influence of the cooling conditions on the cutting tool wear and the chip formation mechanism. *Journal of Manufacturing Processes*, *24*, 107-115.

[3] Ke, Q., Xu, D., & Xiong, D. (2017). Cutting zone area and chip morphology in high-speed cutting of titanium alloy Ti-6Al-4V. *Journal of Mechanical Science and Technology*, *31*(1), 309-316.

[4] Cui, X., Guo, J., Zhao, J., & Yan, Y. (2015). Chip temperature and its effects on chip morphology, cutting forces, and surface roughness in high-speed face milling of hardened steel. *The International Journal of Advanced Manufacturing Technology*, *77*(9-12), 2209-2219.

[5] Xianli, L. I. U., Genghuang, H. E., Fugang, Y. A. N., Yaonan, C. H. E. N. G., & Li, L. I. U. (2015). Large chip production mechanism under the extreme load cutting conditions. *Chinese Journal of Mechanical Engineering*, *28*(02), 1.

[6] An, H. P., Rui, Z. Y., Wang, R. F., & Zhang, Z. M. (2014). Research on cutting-temperature field and distribution of heat rates among a workpiece, cutter, and chip for high-speed cutting based on analytical and numerical methods. *Strength of Materials*, *46*(2), 289-295.

[7] Denkena, B., de Leon, L., & Köhler, J. (2010). Influence of scaled undeformed sections of cut on strain rate, cutting force and temperature. *Production Engineering*, *4*(5), 457-464.

[8] Cui, X., & Guo, J. (2017). Effects of cutting parameters on tool temperatures in intermittent turning with the formation of serrated chip considered. *Applied Thermal Engineering*, *110*, 1220-1229.

[9] Baohai, W., Di, C., Xiaodong, H., Dinghua, Z., & Kai, T. (2016). Cutting tool temperature prediction method using analytical model for end milling. *Chinese Journal of Aeronautics*, *29*(6), 1788-1794.

[10] Kara, F., Aslantaş, K., & Cicek, A. (2016). Prediction of cutting temperature in orthogonal machining of AISI 316L using artificial neural network. *Applied Soft Computing*, *38*, 64-74.

[11] Jang, J. S. (1993). ANFIS: adaptive-network-based fuzzy inference system. *IEEE transactions on systems, man, and cybernetics*, *23*(3), 665-685.

[12] Kamruzzaman, M., Rahman, S. S., Ashraf, M., Ibne, Z., & Dhar, N. R. (2017). Modeling of chip–tool interface temperature using response surface methodology and artificial neural network in HPC-assisted turning and tool life investigation. *The International Journal of Advanced Manufacturing Technology*, *90*(5), 1547-1568.

COMETa 2022
6th INTERNATIONAL SCIENTIFIC CONFERENCE
17th - 19th November 2022
Jahorina, B&H, Republic of Srpska
University of East Sarajevo
Faculty of Mechanical Engineering
Conference on Mechanical Engineering Technologies and Applications

FABRICATION OF ALUMINUM MATRIX COMPOSITES FOR AUTOMOTIVE INDUSTRY VIA FRICTION STIR PROCESSING TECHNIQUE – A REVIEW

Živana Jovanović Pešić [1], Dragan Džunić [2], Strahinja Milenković [3], Nikola Palić [4], Saša Nježić [5], Vukašin Slavković [6], Fatima Živić [7]

Abstract: Materials with strong corrosion resistance, superior wear resistance, and high strength-to-weight ratios are significant in the automobile sector. Aluminum, nickel, titanium, magnesium, and their alloys are the most commonly used materials in this branch of industry, depending on the desired qualities. Aluminum and its alloys have been significant during the production of MMCs. Aluminum matrix composite (AMC) has a wide range of applications in automobile industries, including mechanical parts such as pistons, engine cylinders, disc and drum brakes, engine connecting rods, and Cardan shafts. Friction Stir Processing (FSP) has become a popular method for creating surface composites on a variety of materials. Friction Stir Processing (FSP) is a unique approach evolved from the friction stir welding process, in which reinforcing particles are dispersed using a tool through a groove or hole in the matrix material. This paper attempts to review the current status of FSP position as a technology for surface modification and production of aluminum alloy surface composites in the automobile industry.

Key words: Friction Stir Processing (FSP), Aluminum matrix composite (AMC), automotive industry

[1] Živana Jovanović Pešić, Research Assistant, Faculty of Engineering University of Kragujevac, Kragujevac, Serbia, zixi90@gmail.com
[2] Dragan Džunić, Assistant Professor, Faculty of Engineering University of Kragujevac, Kragujevac, Serbia, dzuna@kg.ac.rs
[3] Strahinja Milenković, Research Assistant, Faculty of Engineering University of Kragujevac, Kragujevac, Serbia, strahinja.milenkovic@fink.rs
[4] Nikola Palić, Research Assistant, Faculty of Engineering University of Kragujevac, Kragujevac, Serbia, nikpa2112@gmail.com
[5] Saša Nježić, Assistant, Faculty of Medicine University of Banja Luka, Banja Luka, Bosnia and Herzegovina, sanjezic@yahoo.com
[6] Vukašin Slavković, Assistant Professor, Faculty of Engineering University of Kragujevac, Kragujevac, Serbia, vukasinsl@gmail.com
[7] Fatima Živić, Associate Professor, Faculty of Engineering University of Kragujevac, Kragujevac, Serbia, zivic@kg.ac.rs

1 INTRODUCTION

Friction stir processing is a novel solid-state surface modification method used in surface engineering to develop composite surface layers and modify the microstructure and properties of engineered materials. FSW (friction stir welding) technology, which was developed by The Welding Institute (TWI) [3], is the source of FSP, which was created by Mishra et al. [1,2], and is based on the same principles as FSW. In the FSP method, the material is plasticized as a result of the heat produced by the friction of a unique, non-consumable tool against the surface of the altered material. The tool heats up the sample, which causes the plasticized material to move. During the FSP process, the combined actions of heat and pressure lead to changes in the microstructure and morphology of the phases [4–6]. The resulting microstructural effects in FSP technology depend not only on the shape and size of the tool but also on the rotating speed, travel speed, and tool tilt angle [7–9].

The automobile industry has always struggled with two of the biggest problems: how to make cars lighter while also enhancing passenger safety. The first goal is crucial for enhancing vehicle performance, including acceleration, top speed, and fuel consumption. In case of a collision, the latter is essential to protect passengers. It is typically challenging to develop a product while simultaneously taking into account both of these factors. Aluminum is one of the materials that provide adequate strength while being lightweight.

2 FRICTION STIR PROCESSING (FSP) CONCEPT

FSP has two main sides in the workpiece: The Advancing Side and Retreating Side [7,8]. In FSP, the side of the workpiece that is moving forward is the side in which the tool's traverse and rotation directions are identical. The retreating side, on the other hand, has distinct traverse and rotation directions. In FSP Tool with a pin and Tool without a pin are used. Clamping is used to secure the workpiece to the backing plates. Previously defined rotating speed is then applied to the tool, which is then lowered into the workpiece until the shoulder makes contact with the surface. Heat is produced by friction, which is created when the tool's shoulder makes contact with the workpiece [7-9]. As a result of friction, heat is generated in FSP, which helps the material move more easily from the advancing side to the retreating side of the workpiece. FSP produced heat is below the melting temperature of the workpiece and this state is known as the solid-state process [10]. The previously defined traverse speed is provided to tool after plunging, enabling it to move in the transverse direction [11,12]. By combining the reinforcement and the workpiece, this rotating and traversing motion creates surface composites. However, because of the swirling motion of the polished surface, FSP also aids in grain refinement, recrystallized grain structure, and intense plasticity of the workpiece [13]. The FSP working principle is shown in Fig. 1.

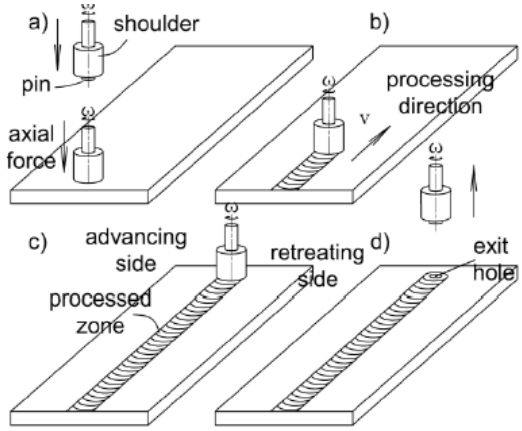

Figure 1. *FSP working principle [14]*

3 AUTOMOTIVE APPLICATIONS OF FSP

Materials with great corrosion resistance, good wear resistance, and high strength-to-weight ratios are crucial in the automobile industry. Aluminum, nickel, titanium, magnesium, and their alloys are primarily used in this industry based on the required qualities. Automotive parts built of Aluminum Matrix Composites (AMCs), which are produced by FSP, include engine cylinders, pistons, disc and drum brakes, engine connecting rods, and Cardan shafts.

3.1 Composites reinforced with Al_2O_3

Some proven applications of Al_2O_3 reinforced aluminium based composite in manufacturing industries are shown in Table 1. The impacts of friction stir processing (FSP) and friction stir vibration processing (FSVP) on the mechanical, wear, and corrosion parameters of the Al6061/SiO2 surface composite were studied by Barati, Abbasi, and Abedini (2019) [15]. SiO2 nanoparticles were used as the second phase particles in surface composites developed utilizing the FSP and FSVP procedures on the Al6061 alloy surface. The treated specimens' mechanical, wear, and corrosion characteristics were investigated. The experiments demonstrated that FSVP specimens had greater strength, ductility, and wear resistance than FSP specimens.

In a 2019 study, Titus Thankachan, Prakash, and Kavimani examined the effect of hybrid reinforcement particles on the microstructural, mechanical, and tribological characteristics of friction stir processed copper surface composites. According to the results, there was an increase in mechanical characteristics as particle dispersion increased. Due to the hardness and self-lubricating properties of the dispersed ceramic particles, an enormous increase in wear resistance was observed in regard to the increase in hybrid particle dispersion [16].

TiB_2 and B_4C ceramic reinforcement particles were added to the AA7005 alloy, which improved its ballistic resistance [17]. The surface composite was found to have a ballistic mass efficiency factor that was 1.6 times greater than the base alloy. Balakrishnan et al. produced cast aluminum matrix composites made of AA6061 and Al3Fe and then applied the friction stir technology. After FSP, the dislocation density significantly increased. Tensile strength and ductility were improved as a result of the microstructural modifications [18].

Table 1. *Some proven applications of Al_2O_3 reinforced aluminium based composite*

Manufacturer	**Components**
Toyota	Piston rings
Dupont	Connecting rods
Chrysler	Connecting rods
Honda	Engine blocks

3.2 Pistons

An explicit investigation is made into how FSP affects the microstructure, hardness, and mechanical characteristics of a piston alloy [19]. The as-cast eutectic LM13 aluminum alloy surface in the paper [20] was converted to a hypereutectic Al-Si alloy utilizing 5 μm Si particles via FSP, in an effort to better understand how tool geometry and process parameters affect particle distribution, microstructure, hardness, and strength. Adetunla and Akinlabi produced AMC's using multiple passes of friction stir processing (FSP) in order to enhance their corrosion performance and mechanical qualities. Ti-6Al-4V was chosen as the reinforcing particle while 7075 Al alloy was used as the matrix [21].

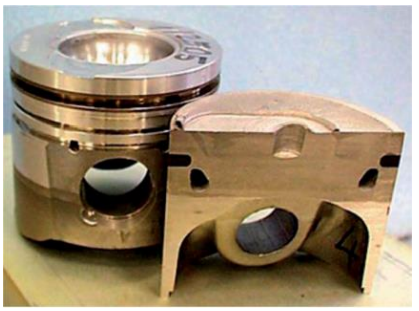

Fig.2 *Friction stir processed piston [22]*

4 CONCLUSIONS

A versatile method for creating matrix composites is FSP. The distinctive characteristics of this technique are the grain refinement attained by FSP and the solid state aspect of processing. The matrix composites have higher wear and corrosion resistance as well as high hardness. Ceramic particles and metallic particles are among the reinforcements that FSP has successfully introduced into metallic matrix. The manufacturing of matrix composites using FSP is a relatively new approach that provides easy particle dispersion. A literature review of aluminum matrix composites fabrication for automotive industry and the current state of understanding of FSP are discussed in this in this paper.

ACKNOWLEDGEMENT

This paper is funded through the EIT's HEI Initiative SMART-2M project, supported by EIT RawMaterials, funded by the European Union.

REFERENCES

[1] R.S. Mishra, Z.Y. Ma (2005) Friction Stir Welding and Processing. Materials Science and Engineering: R: Reports, 50, 1–78, doi: 10.1016/j.mser.2005.07.001.
[2] R. S. Mishra, M. W. Mahoney, (2007) 'Friction stir welding and processing', Materials Park, OH, ASM International.
[3] W.M. Thomas, E.D. Nicholas, J.C. Needham, M.G. Murch, P. Templesmith, and C.J. Dawes (1991), G.B. Patent Application No. 9125978.8.
[4] Richmire S, Haghshenas M. Friction stir welding of a hypoeutectic Al–Si alloy: microstructural, mechanical, and cyclic response. Int J Adv Manuf Technol. 2019;101: 3001–3019.
[5] Tutunchilar S, Givi MB, Haghpanahi M, et al. Eutectic Al–Si piston alloy surface transformed to modified hypereutectic alloy via FSP. Mater Sci Eng A. 2012; 534:557–567.
[6] Ma ZY, Mishra RS, Mahoney MW. Superplasticity in cast A356 induced via friction stir processing. Scr Mater. 2004; 50:931–935.
[7] Rathee, S.; Maheshwari, S.; Siddiquee, A. N. Issues and strategies in composite fabrication via friction stir processing: a review. Mater. Manuf. Process. 2018, 33(3), 239–261. DOI: 10.1080/10426914.2017.1303162.
[8] Heydarian, A.; Dehghani, K.; Slamkish, T. Optimizing powder distribution in production of surface nano-composite via friction stir processing. Metall. Mater. Trans. B Process. Metall. Mater. Process. Sci. 2014, 45(3), 821–826. DOI: 10.1007/s11663-014-0025-z.
[9] Nelaturu, P.; Jana, S.; Mishra, R. S.; Grant, G.; Carlson, B. E. Influence of friction stir processing on the room temperature fatigue cracking mechanisms of A356 aluminum alloy. Mater. Sci. Eng. A. 2018, 716(January), 165–178. DOI: 10.1016/j.msea.2018.01.044.
[10] Kurt, A.; Uygur, I.; Cete, E. Surface Modification of Aluminium by Friction Stir Processing. J. Mater. Process. Technol. 2011, 211(3), 313–317. DOI: 10.1016/j.jmatprotec.2010.09.020.
[11] Mishra, R. S.; Ma, Z. Y.; Charit, I. Friction stir processing: a novel technique for fabrication of surface composite. Mater. Sci. Eng. A. 2003, 341(1–2), 307–310. DOI: 10.1016/S0921-5093(02)00199-5.
[12] Bharti, S.; Dutta, V.; Sharma, S.; Ghetiya, N. D. Investigating the effect of tool speed on the mechanical properties of Al5052 Processed by friction stir processing. Mater. Today Proc. 2020. DOI: 10.1016/j.matpr.2020.05.547.
[13] Bharti, S.; Dutta, V.; Sharma, S.; Kumar, R. A. Study on the effect of friction stir processing on the hardness of Aluminum 6000 Series. Mater. Today Proc. 2019, 18(7), 5185–5188. DOI: 10.1016/j.matpr.2019.07.517.
[14] Milenkovic, S.; Zivic, F.; Jovanovic, Z.; Radovanovic, A.; Ljusic, P.; Grujovic, N. Review of Friction Stir Processing (FSP) Parameters and Materials for Surface Composites. Tribol. Ind. 2021, 43, 470–479, doi:10.24874/ti.1169.06.21.08.
[15] Barati, M., M. Abbasi, and M. Abedini. 2019. "The Effects of Friction Stir Processing and Friction Stir Vibration Processing on Mechanical, Wear and Corrosion Characteristics of Al6061/SiO2 Surface Composite." Journal of Manufacturing Processes 45: 491–497. doi: 10.1016/j.jmapro.2019.07.034.
[16] Titus Thankachan, K., S. Prakash, and V. Kavimani. 2019. "Investigating the Effects of Hybrid Reinforcement Particles on the Microstructural, Mechanical and Tribological Properties of Friction Stir Processed Copper Surface Composites." Composites Part B: Engineering 174: 107057.
doi: 10.1016/j.compositesb.2019.107057.

[17] Pol, N., G. Verma, R. P. Pandey, and T. Shanmugasundaram. 2019. “Fabrication of AA7005/TiB2-B4C Surface Composite by Friction Stir Processing: Evaluation of Ballistic Behaviour.” Defence Technology 15: 363–368. doi:10.1016/j.dt.2018.08.002.

[18] Balakrishnan, M., I. Dinaharan, R. Palanivel, and R. Sathiskumar. 2019. “Effect of Friction Stir Processing on Microstructure and Tensile Behavior of AA6061/Al3 Fe Cast Aluminum Matrix Composites.” Journal of Alloys and Compounds 785: 531–541. doi: 10.1016/j.jallcom.2019.01.211.

[19] Charandabi, F.K.; Jafarian, H.R.; Mahdavi, S.; Javaheri, V.; Heidarzadeh, A. Modification of Microstructure, Hardness, and Wear Characteristics of an Automotive-Grade Al-Si Alloy after Friction Stir Processing. Journal of Adhesion Science and Technology 2021, 35, 2696–2709, doi:10.1080/01694243.2021.1898858.

[20] Tutunchilar, S.; Besharati Givi, M.K.; Haghpanahi, M.; Asadi, P. Eutectic Al–Si Piston Alloy Surface Transformed to Modified Hypereutectic Alloy via FSP. Materials Science and Engineering: A 2012, 534, 557–567, doi: 10.1016/j.msea.2011.12.008.

[21] Adetunla, A.; Akinlabi, E. Fabrication of Aluminum Matrix Composites for Automotive Industry Via Multipass Friction Stir Processing Technique. Int.J Automot. Technol. 2019, 20, 1079–1088, doi:10.1007/s12239-019-0101-0.

[22] Amini A, Asadi P, Zolghadr P. Friction stir welding applications in industry. In: Givi MKB, Asadi P, editors. Advances in friction stir welding and processing. Cambridge (UK): Woodhead Publishing; 2014.

COMETa 2022
6th INTERNATIONAL SCIENTIFIC CONFERENCE
17th - 19th November 2022
Jahorina, B&H, Republic of Srpska
University of East Sarajevo
Faculty of Mechanical Engineering
Conference on Mechanical Engineering Technologies and Applications

KOMPARATIVNA ANALIZA SIMULACIONIH REZULTATA VREMENA 3+2-OSNE I 5-OSNE OBRADE OBLIKAČA

Strahinja Dašić[1], Suzana Petrović Savić[2], Bogdan Nedić[3]

Rezime: Virtuelni sistemi predstavljaju neizostavni deo projektovanja tehnologije za izrade delova složene geometrije, a sve sa ciljem unapređenja izrade realnog proizvoda i postizanja željenog kvaliteta i tačnosti gotovog dela. Veoma je važno da se brzo odrede i usvoje optimalni parametri obrade kako bi se skratilo vreme projektovanja. U radu je izvršena analiza simulacionih rezultata vremena 3+2-osne i 5-osne obrade oblikača i generisane su prostorne zavisnosti vremena obrade od brzine pomoćnog kretanja i dubine rezanja. Rezultati će biti iskorišćeni za uporednu analizu parametara virtuelne i realne obrade i na taj način oceniti pouzdanost podataka dobijenih korišćenjem CAM softvera.

Ključne reči: virtuelna obrada, petoosna obrada, vreme izrade, prostorne zavisnosti

COMPARATIVE ANALYSIS OF THE MACHINING TIME SIMULATION RESULTS FOR 3+2-AXIS AND 5-AXIS MILLING OF THE SHAPER

Abstract: Virtual systems represent an indispensable part of designing technology for the production of the parts of complex geometry, all with the aim of improving the production of a physical part and achieving the desired quality and accuracy of the finished part. It is very important to quickly determine and adopt the optimal machining parameters in order to shorten the design time. The paper analyzed the simulation results of the 3+2-axis and 5-axis processing time of the shaper and generated the spatial dependence of the processing time on the speed of the auxiliary movement and the cutting depth. The results will be used for a comparative analysis of the parameters of virtual and real machining and thus evaluate the reliability of the data obtained using the CAM software.

Key words: virtual processing, 5-axis machining, processing time, spatial dependence

[1]Strahinja Dašić, Univerzitet u Kragujevcu, Fakultet inženjerskih nauka, (strahinja@eastmold.rs), Srbija,
[2]doc. dr Suzana Petrović Savić, Univerzitet u Kragujevcu, Fakultet inženjerskih nauka, (petrovic.suzana@gmail.com), Srbija,
[3]prof. dr Bogdan Nedić, Univerzitet u Kragujevcu, Fakultet inženjerskih nauka, (nedic@kg.ac.rs), Srbija,

1 UVOD

Proizvodi komplikovane topologije zahtevaju preciznu i tačnu obradu kako bi ostvarili predviđenu funkciju. Poslednjih godina došlo je do unapređenja kako u računarstvu tako i u proizvodnim tehnologijama. Pri čemu je na taj način omogućeno inženjerima da značajno unaprede kvalitet, produktivnost i smanje troškove projektovanja i proizvodnje kroz automatizaciju niza faza tokom procesa razvoja proizvoda. Međutim, u realnosti može do doći do neslaganja između onoga što je projektovano i onoga što je proizvedeno, a uzročnici se mogu ogledati u neoptimizovanim ciklusima, raznim vrstama grešaka, potpuno neproizvodljivim dizajnom proizvoda, i sl. [1,2].

U cilju izbegavanja loših izlaza fizičkih proizvoda, veoma je važno definisati odgovarajuće i optimalne parametre tokom željene proizvodne operacije. Efikasan odabir parametara obrade pomaže u unapređenju proizvodnje i smanjenju troškova. Postoje različite kombinacije parametara kojima se može uticati na finalni proizvod, kao što je brzina rezanja, posmak, dubina rezanja, odabir alata, vreme izrade, i sl. [3].

Virtuelna obrada se pokazala korisnom u simulacijama i verifikacijama procesa obrade u virtuelnom okruženju. Inicijalni programi i parametri procesa se usvajaju kao ulazni parametri virtuelne obrade. Na osnovu njih moguće je izvršiti adekvatan odabir strategije obrade, a samim tim i pravovremeno otkriti moguće defekte kao što su urezivanje, kolizije, i sl. Simulacioni rezultati korisniku obezbeđuju mnoštvo informacija o uslovima obrade, npr. sile rezanja, opterećenje vretena, zone visokih temperatura, i sl. [4,5].

Kao što je već pomenuto, industrijski delovi zahtevaju visoku preciznost i kvalitet obrađenih površina što se postiže substraktivnim proizvodnim tehnologijama. Jedna od vodećih tehnologija (koje se izdvaja iz kompletnog dijapazona) je izrada delova korišćenjem višeosne obrade, a naročito pri izradi delova koji bi trebalo da imaju veliku krutost. Da bi se obezbedio potreban kvalitet i tačnost gotovog dela, teži se i razvoju hibridnih tehnologija, npr. simbioza aditivne proizvodnje i višeosne obrade ili implemntacija tehnologija veštačke inteligencije u aditivne tehnologije, odnosno proizvodne tehnologije [1,6]. Primenom tehnologija veštačke inteligencije se postiže brža i intuitivnija kastumizacija proizvoda, eknomičnost, izrada delove kompleksne geometrije sa predloženim parametrima obrade, preciznost i kvalitet površina sa ciljem obezbeđenja kompletne funkcionalnosti proizvoda.

Cilj ovog rada je da se izvrši uporedna analiza vremena izrade obrade oblikača ravnih ivica obradom 3+2-osna i simultanom 5-osnom obradom i da se generišu prostorne zavisnosti vremena od brzine pomoćnog kretanja i dubine rezanja, a sve sa ciljem što ekonomičnog i optimalnog korišćenja obradnog centra nakon virtuelne simulacije izrade gotovog proizvoda. Istraživanje je urađeno za potrebe kompanije East Mold iz Kragujevca.

2 MATERIJALI I METODI

2.1 Tehnološki postupak i simulaciona obrada

Petoosna (3+2) obrada može se posmatrati kao klasična 3-osna obrada sa mogućnošću rotacije stola oko adekvatnih osa. Pozicioniranje predmeta obrade u radni položaj podrazumeva transformaciju koordinatnog sistema tako da osa alata uvek bude Z-osa i da se obrada izvrši u XY ravni. Simultana 5-osna obrada podrazumeva kretanje, odnosno rotaciju alata duž/oko adekvatnih pet osa obrade. Ovaj način obrade

podrazumeva stalnu transformaciju koordinatnog sistema [7,8].

U eksperimentu je korišćen zapreminski model oblikača. Obrada oblikača je izvedena 3+2-osnom i simultanom 5-osnom obradom sa identičnim parametrima obrade za različite vrste alata. Materijal predmeta obrade je alatni čelik 1.2379 (Č4850).

Algoritam kreiranja virtuelne obrade je prikazan na slici 1. Za projektovanje tehnološkog postupka, generisanje putanje alata, predviđanja vremena obrade i simulacije je korišćen softver NCG CAM (https://www.ncgcam.com/). Ovaj softver je pogodan za obradu svih vrsta oblika, za obradu kalupa, prototipova i preciznu površinsku obradu.

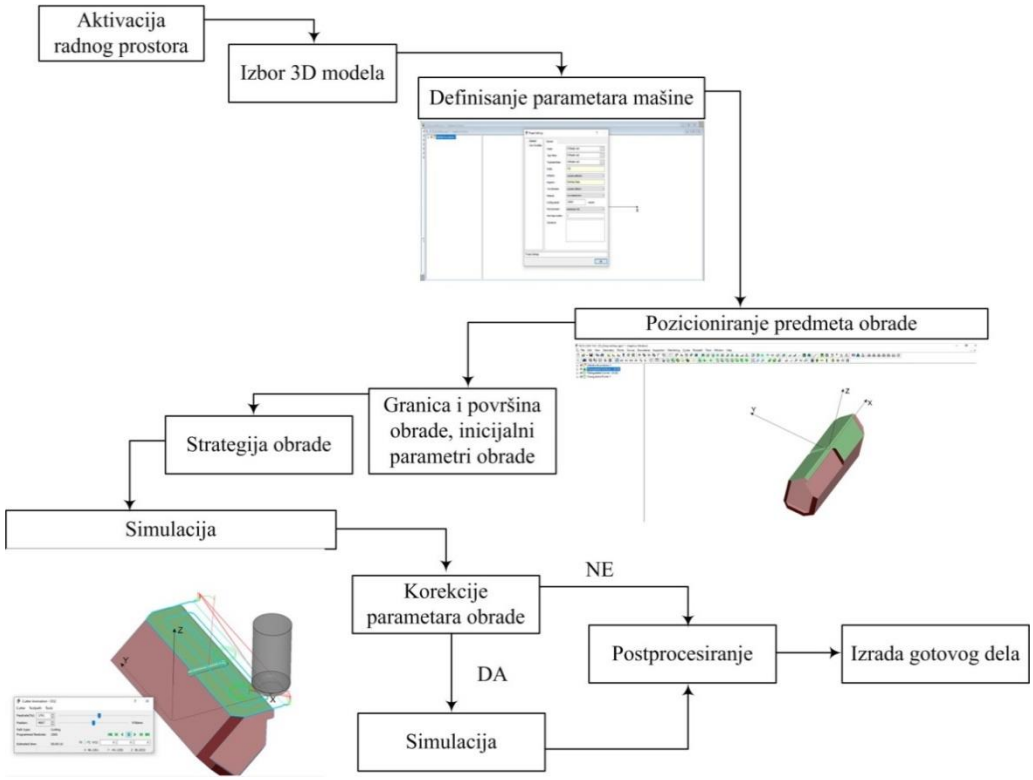

Slika 1. *Algoritam kreiranja virtuelne obrade u okviru softvera NCG CAM*

2.2 Vizuelizacija simuliranog vremena obrade od dubine rezanja i brzine pomoćnog kretanja

Vizuelizacija zavisnosti simuliranog vremena obrade od dubine rezanja i brzine pomoćnog kretanja je izvršena u programabilnom okruženju MATLAB (www.mathworks.com). Kreiranje prostornih zavisnosti podrazumeva definisanje funkcije oblika:

$$z = f(x, y) \tag{1}$$

gde su *x* i *y* nezavisne promenljive a *z* je zavisna promenljiva. Ovo podrazumeva da se vrednost *z* može izračunati za bilo koju kombinaciju *x* i *y*.

Da bi se prikazala prostorna zavisnost gore pomenutih parametara potrebno je da se kreira mreža u *xy* ravni i da se izvrši proračun vrednosti *z* u svakoj tački mreže. Nakon toga je moguće izvršiti štampanje prostornog grafika. Kako bi se dobili kontinualni glatki grafici korišćena je Hermitova interpolacija.

3 REZULTATI

Rezultati su prikazani tabelarno (tabela 1 i tabela 2) i kroz prostorne grafike (Sl.2 i Sl.3) na kojima je prikazana zavisnost simuliranog vremena obrade od dubine rezanja i brzine pomoćnog kretanja nakon izvršena tri simulaciona testiranja.

U rezultatima se jasno uočava da sa povećavanjem brzine pomoćnog kretanja i dubine rezanja dolazi i do smanjenja vremena obrade. Vrednosti za simulirano vreme 3+2-ose obradu su manje u odnosu na vrednosti za simulirana vremena 5-osne obrade. Ta razlika se kreće u rasponu od 3% do 12%, kako za grubu tako i za finu obradu [9].

Tabela 1. *Vrsta alata, parametri obrade rezanjem i vreme obrade za grubu obradu*

	Broj obrtaja, o/min	Brzina pomoćnog kretanja, mm/min	Dubina rezanja, mm	Vreme, s		Alat
				5 osa	3+2 ose	
I	2100	2000	0,2	106	95	Vretenasto glodalo 12r05
II	2100	1200		155	137	
III	2100	800		203	180	
I	2100	2000	0,15	138	121	
II	2100	1200		202	195	
III	2100	800		266	245	
I	2100	2000	0,1	397	377	
II	2100	1200		582	555	
III	2100	800		766	628	
I	7500	2000	0,2	83	75	Loptasto glodalo 8r4
II	7500	1200		137	120	
III	7500	800		206	187	
I	7500	2000	0,15	125	104	
II	7500	1200		207	182	
III	7500	800		310	270	
I	7500	2000	0,1	240	212	
II	7500	1200		400	368	
III	7500	800		695	612	
I	8500	2000	0,2	10	8	Loptasto glodalo 4r2
II	8500	1200		17	15	
III	8500	800		29	27	
I	8500	2000	0,15	14	12	
II	8500	1200		24	22	
III	8500	800		42	37	
I	8500	2000	0,1	43	40	
II	8500	1200		72	66	
III	8500	800		126	111	

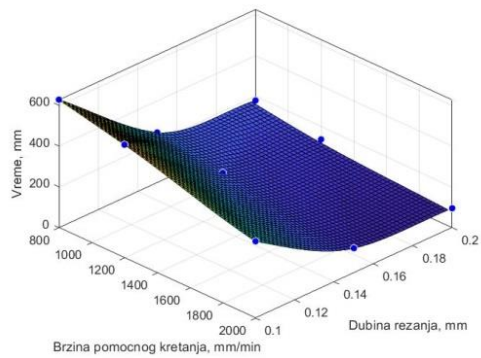

a)

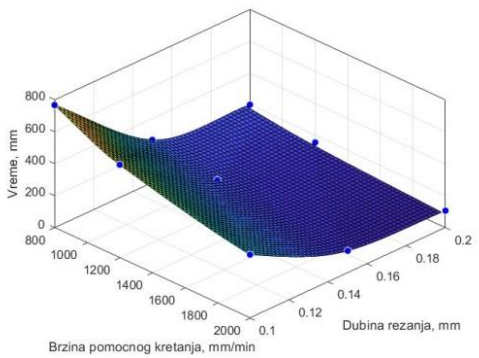

b)

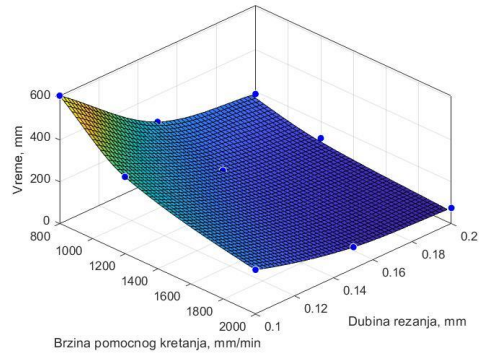

c)

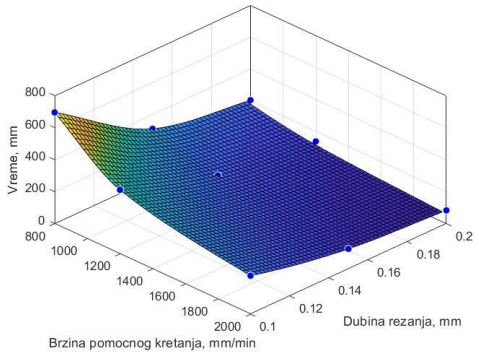

d)

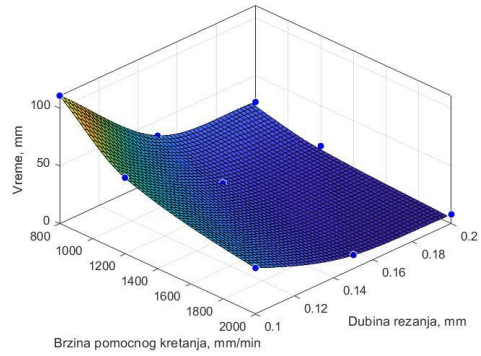

e)

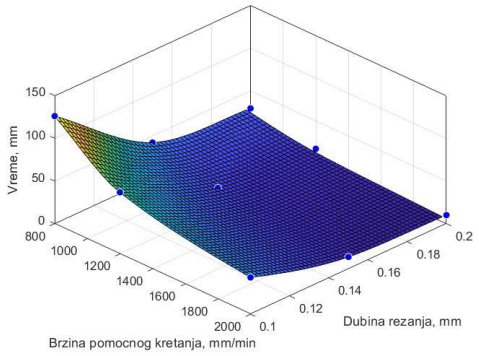

f)

Slika 2. *Zavisnost vremena izrade od brzine pomoćnog kretanja i dubine rezanja za:*
a) grubu 3+2-osnu obradu korišćenjem vretenastog glodala 12r0,5,
b) grubu 5-osnu obradu korišćenjem vretenastog glodala 12r0,5,
c) grubu 3+2-osnu obradu korišćenjem loptastog glodala 8r4,
d) grubu 5-osnu obradu korišćenjem loptastog glodala 8r4,
e) grubu 3+2-osnu obradu korišćenjem loptastog glodala 4r2,
f) grubu 5-osnu obradu korišćenjem loptastog glodala 4r2 (nastavak)

Tabela 2. Vrsta alata, parametari obrade rezanjem i vremena obrade za finu obradu

	Broj obrtaja, o/min	Brzina pomoćnog kretanja, mm/min	Dubina rezanja, mm	Vreme, s		Alat
				5 osa	3+2 ose	
I	6000	2500	0,1	777	369	Loptasto glodalo 12r6
II	6000	2000		971	462	
III	6000	1500		1294	615	
I	6000	2500	0,05	1034	490	
II	6000	2000		1292	612	
III	6000	1500		1722	816	
I	6000	2500	0,02	1547	733	
II	6000	2000		1933	916	
III	6000	1500		2577	1222	
I	7500	2500	0,1	71	69	Loptasto glodalo 8r4
II	7500	2000		121	116	
III	7500	1500		211	192	
I	7500	2500	0,05	143	128	
II	7500	2000		245	222	
III	7500	1500		429	400	
I	7500	2500	0,02	362	345	
II	7500	2000		620	599	
III	7500	1500		1085	1004	
I	8500	2500	0,1	46	38	Loptasto glodalo 4r2
II	8500	2000		69	64	
III	8500	1500		95	91	
I	8500	2500	0,05	89	57	
II	8500	2000		133	95	
III	8500	1500		177	143	
I	8500	2500	0,02	100	95	
II	8500	2000		182	171	
III	8500	1500		279	268	

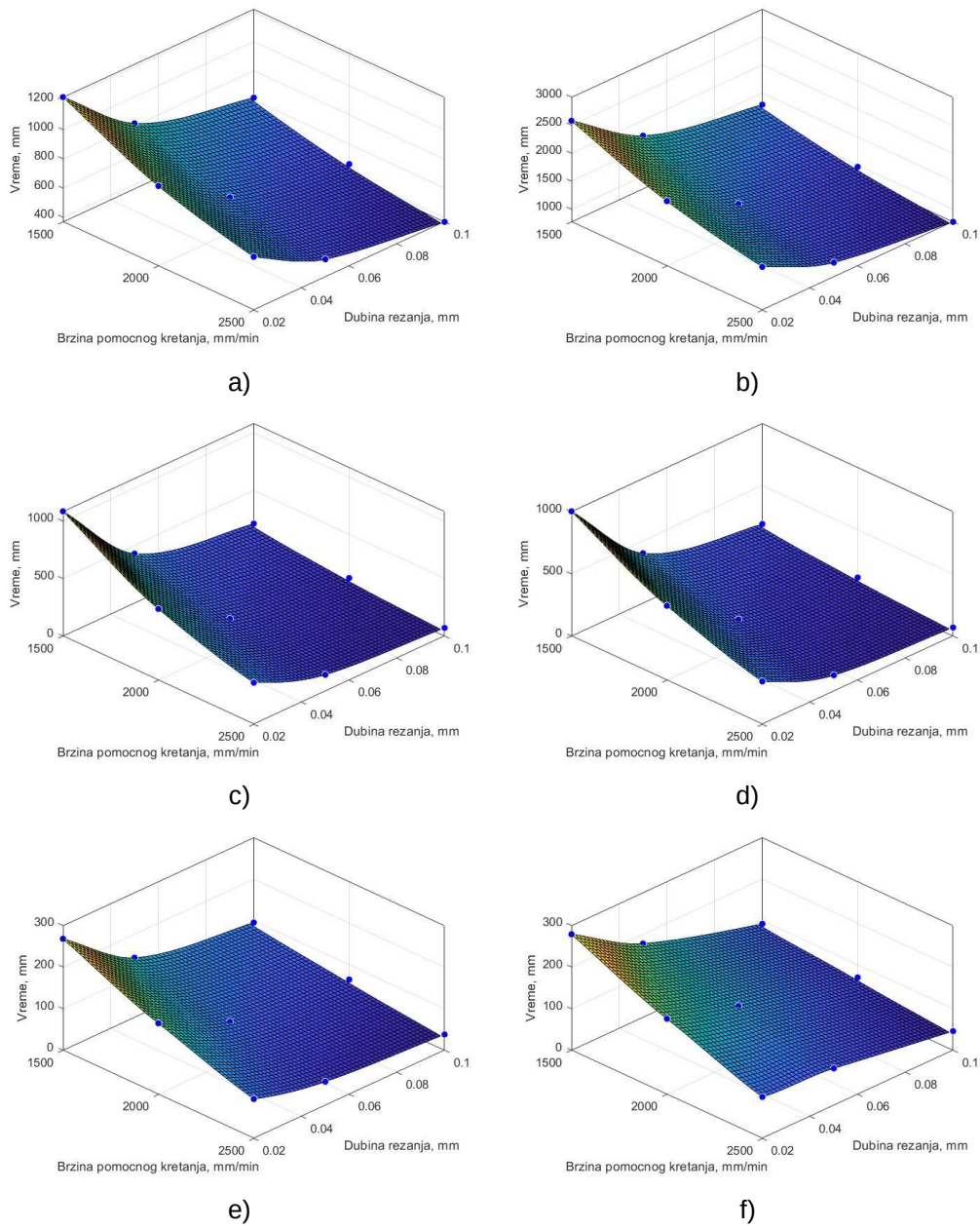

Slika 3. *Zavisnost vremena izrade od brzine pomoćnog kretanja i dubine rezanja za:*
a) Finu 3+2-osnu obradu korišćenjem vretenastog glodala 12r0,5,
b) Finu 5-osnu obradu korišćenjem vretenastog glodala 12r0,5,
c) Finu 3+2-osnu obradu korišćenjem loptastog glodala 8r4,
d) Finu 5-osnu obradu korišćenjem loptastog glodala 8r4,
e) Finu 3+2-osnu obradu korišćenjem loptastog glodala 4r2,
f) Finu 5-osnu obradu korišćenjem loptastog glodala 4r2

4 ZAKLJUČAK

U dinamičnom tržišnom okruženju od velikog je značaja postojanje mogućnosti predviđanja preciznog vremena obrade. U prikazanom istraživanju posmatrana je zavisnost vremena od brzine pomoćnog kretanja i dubine rezanja. Konkretan model će se brže izraditi korišćenjem 3+2-osne obrade. Generisani grafici mogu poslužiti za predviđanje vremena netestiranih slučajeva (drugačija dubina rezanja ili brzina pomoćnog kretanja). Rezultati će biti iskorišćeni za uporednu analizu parametara virtuelne i realne obrade i na taj način oceniti pouzdanost podataka dobijenih korišćenjem NCG CAM softvera.

LITERATURA

[1] Mirzendehdel, A.M., Behandish, M., Nelaturi, S.: *Topology optimization with accessibility constraints for multi-axis machining*, Computer-Aided Design, Vol. 122, pp. 102825, 2020.

[2] Grešova, Z., Ižol, P.: *Comparasion of simulated and real production times for 3-axis and 5-axis milling of sharped surfaces*, Transfer inovácii, Vol. 44/2021, pp. 9-12, 2021.

[3] Hassan, M.S., Amin, A.M.: *Optimisation of surface roughness in the CNC milling process*, Research progress in mechanical and manufacturing engineering, Vol. 3, pp. 267-277, 2022.

[4] Jarosz, K., Nieslony, P., Löschnner, P.: *The effect of changes in depth of cut and cutting speed of CNC toolpaths on turning process performance*, Archieves of mechanical technology and materials, Vol. 38, pp. 40-44, 2018.

[5] Nie, Z.: *Efficient cutter-workpiece engagement determination in multi-axis milling by voxel modeling*, PhD dissertation, The University of British Columbia, 2022.

[6] Bo, P., González, H., Calleja, A., de Lacalle, L.N.L., Barton, M.: *5-axis double-flank CNC machining of spiral bevel gears via custum-shaped tools - Part I: modeling and simulation*, Precision Engineering, Vol. 62, pp. 204-212, 2020.

[7] Tabaković, S., Kerepeši, M.: *Automatizovano programiranje numeričkih upravljanih mašina alatki za obradu glodanjem sa 4 i 5*, Zbornik radova Fakulteta tehničkih nauka, Novi Sad, Vol. 6, pp. 1015-1018, 2021.

[8] Živković, S.: *Razvoj postprocesora za petoosne glodalice sa dvostruko rotirajućom glavom*, Tehnika, Vol. 69, pp. 781-788, 2014.

[9] Ižol, P., Varga, J., Vrabel', M., Demko, M., Greš, M.: *Evaluation of 3-axis and 5-axis milling strategies when machining freeform surface features*, Journal of Production Engineering, Vol. 25, pp. 1-4, 2022.

COMETa 2022
6th INTERNATIONAL SCIENTIFIC CONFERENCE
17th - 19th November 2022
Jahorina, B&H, Republic of Srpska
University of East Sarajevo
Faculty of Mechanical Engineering
Conference on Mechanical Engineering Technologies and Applications

FEM ANALYSIS OF THE STRESS STRAIN RATE DURING HOT FORGING OF STEEL NONROTATIONAL FORM

Nikola Kostić[1], Saša Ranđelović[2], Sandra Stanković[3]

Abstract: The simulation of the clutch lever forging process was carried out using Qform software, which is based on numerical and finite element methods, while the tool itself was modeled in SolidWorks CAD software. The stress-deformation state of the workpiece in the process of hot forging in an asymmetric dies for forging with excess material, which represents one of the most common technologies in modern industrial processes of the metalworking industry was analyzed and monitored in this paper.
Key words: Hot forging, FEM, stress, strain, die.

1 INTRODUCTION

The process of forging involves changing the initial dimensions of the heated metal into desired shape with the help of dies. The resulting finished piece is transformed into the final product with minimal additional processing, and in some cases it is the final product [1].

Today, from the total number of parts produced by forging, 50% to 80% of them are produced by forging in tool, which allows as to obtain parts of complex geometry that, with little or no additional processing, give the finished product [2].

The technology of forging in molds is justified in cases of serial or mass production due to the need to make robust and expensive tools that can withstand the large deformation forces that occur in the production process, as well as the need for machines that need to have high power [2, 3].

In order to achieve the desired mechanical characteristics of the product, phenomena that occur during the deformation process that affect and leads to inhomogeneity must be taken into account. Inhomogeneity originates from shear stress in the material of workpiece that cause heat generation which results in stress and

[1]MSc, Nikola Kostić, Akademija tehničko-vaspitačkih strukovnih studija odsek Niš, Niš, Srbija, nikola.kostic@akademijanis.edu.rs
[2]Prof. dr Saša Ranđelović, Mašinski fakultet Univerziteta u Nišu, Srbija, sasa.randjelovic@masfak.ni.ac.rs
[3] MSc, Sandra Stanković, Akademija tehničko-vaspitačkih strukovnih studija odsek Niš, Niš, Srbija, sandra.stankovic@akademijanis.edu.rs

deformation inhomogeneity during forging that can lead to a reduction of mechanical characteristics of the product [4].

Software tools that are used in the process of simulating the forging process use numerical methods that are based on the finite element method. By applying numerical methods in the process of simulating the forging process, it is possible to monitor material flow processes, analyze loads during forging, detect defects and monitor them, as well as monitoring and analyze the stress and strain [4]. Software solutions allow us to optimize the forging process by monitoring key parameters and simulating the process to identify the defects during forging process, and the results obtained within the simulation are almost identical to those that would be obtained experimentally with a significantly lower time and money spent [5].

Numerical simulation methods can in principle answer questions such as "how many machining steps are required for a given product", "can the finished product be obtained only by forging, and can be avoid the post-machining process", " will the tools withstand cyclic load stress that is unavoidable in high-volume hot forging', whether the final product will have the required grain structure and mechanical properties' and so on [6]. In the work of M.R.Rahul and others [7], a finite element simulation was performed, which was used to examine the deformation distribution and material flow during hot deformation, which helps in predicting the actual material flow in the forging process. In the work of J. O. Obiko et al. [8] three-dimensional finite element analysis in Deform 3D software was used to investigate the behavior of plastic deformation during forging of Ks20CrMoV121 steel. The focus of the work was on examining the influence of forging temperature on the distribution of deformation, stress and particle flow rate during the forging process.

2 FEM PREPROCESING SIMULATION

The dimensions and geometry of the forged part at the end of the forging process are defined by the tool geometry, which plays a decisive role in the process of plastic deformation [1, 9].

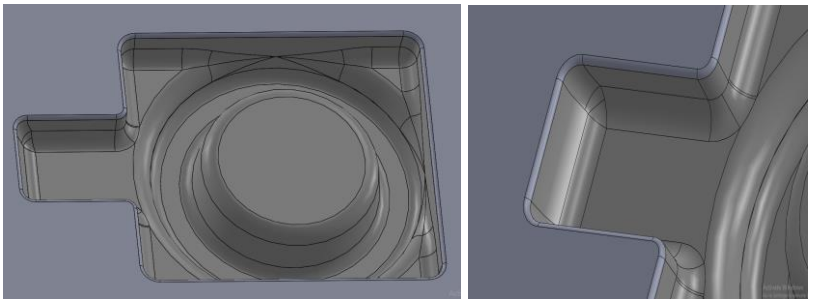

Figure 1. *Geometry of forging tool with detail*

The pre form in the process of hot forging is dimensioned so that it has an aditional volume, in order to ensure filling of the engraving of the tool and the excess of material into the flash gutter. This ensures that even the outermost parts of the tool volume are filled in the forging process. The workpiece in the simulation is cylindrical in shape with a diameter of 65 mm and a length of 75 mm made of steel S355J2.

The simulation process of the hot forging process of the crankcase is simulated in the software QForm v10.1.0. which is based on the finite element method. The input data used in the crank case forging simulation process are:

- Workpiece temperature 1100 °C,
- Dies temperature 200 °C,
- Workpiece material S355J2,
- Dies material H13 6408,
- Forging machine - hammer with available energy of 69 kJ,
- The lubricant used is a salt solution, which has the following characteristics: friction law according to Levanov, which is 1.25, heat transfer coefficient 45000 W/(m^{2}K), pause coefficient 0.05,
- Ambient temperature 20 °C.

The characteristics of the material in the simulation are determined as follows. The flow stress of the material is given by the diagram in figure 2, while the Passon coefficient is given as a constant value of 0.3. The material characteristics data are taken from the QForm v10.1.0 software database. which can be modified according to the needs of the user.

The yield stress of the material, or the stress-strain curve, is the area in which the forging process itself takes place and as such it is important for understanding and implementing the forging process of bulk forging. Based on a given diagrame, we can understand how the metal behaves when it is deformed and how it hardens under those deformations and from this we can predict what force is necessary to applay so the material continues with plastic flow [10]. The flow stress (napon tecenja) of the material and its behavior at the processing temperature of 1100 °C is given in Figure 2, on the basis of which the simulation was performed.

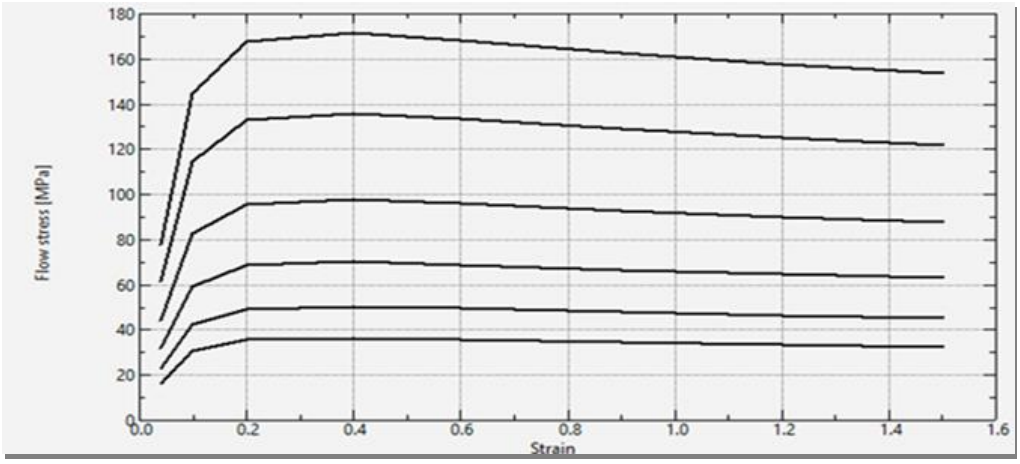

Fig. 2. Flow stress for material S355J2 on temperature 1100 °C

In the simulation, the workpiece is defined as a deformable body, while the tool is defined as a non-deformable rigid body. By using this approach, where the dies is taken for a non-deformable body, the processing time is greatly reduced, while having little or no significant impact on the quality of the obtained results. During discretization, the real continuous object is replaced by a set of a finite number of smaller domains (finite elements), and in each of them the required function is approximated by a collection of polynomials of a lower degree [11].

3 FEM SIMULATION RESUALTS

The dies load itself starts from 0 N, which represents the state before the dies comes into contact with the workpiece, and then increases until the end of the process when reaches its maximum value of 11.72 MN at the end of the forging process. The dies load increases evenly and slightly up to 6 $\times 10^{-3}$ s of the forming process at the amounts to 0.66 MN, after which it increases rapidly until the end of the forming process.

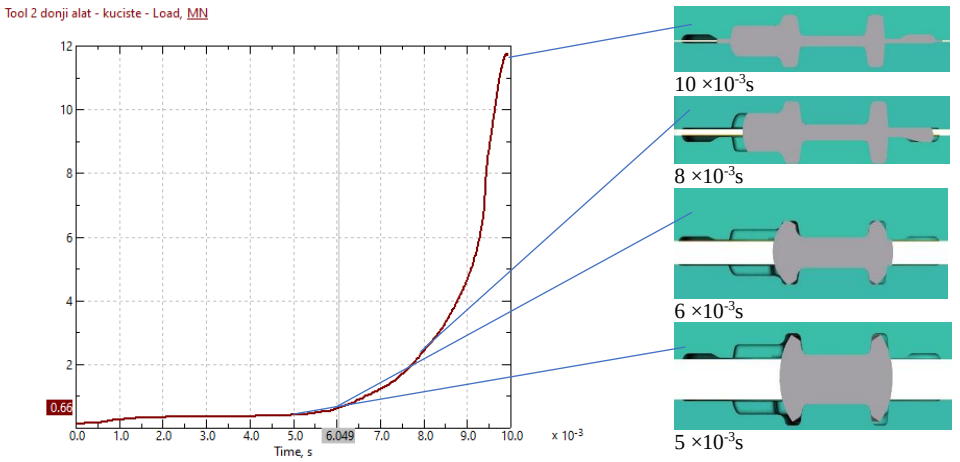

Figure 3. *Dies load chart*

Based on the obtained results, it can be concluded that the highest concentration of critical stresses occurs in the areas of the formation of the flash as well as in the places of sudden changes in the geometry of the dies. Based on the obtained results, the maximum stress appears at the place where the flash is formed and it is 181.537 MPa while the minimum effective stress is 46.3731 MPa.

At the place of formation of the flash a sudden change in the geometry of the die chases the intensive flow of material in those areas witch is observed [11,12]. At the obsrved yield area, five points were monitored where can be sean a jump in the effective stress of the material, point number 1 has a efective stress value of 154,475 MPa at the beginning of material flow and reaches a value of 173,756 MPa at point number 3 and at the very exit point number 5 the stress drops to value of 141,326 MPa.

The highest effective stresses are found in the zones of formation of the flash of the material witch is in contact with the tool, where there is a high concentration of load forces on the forging part, as well as due to sudden changes in the geometry of the tool. The shape of the tool in those areas is designed to prevent excess material from flowing into the flash gutter until the die cavity is completely filled so it can be achieved the desired quality of forged part.

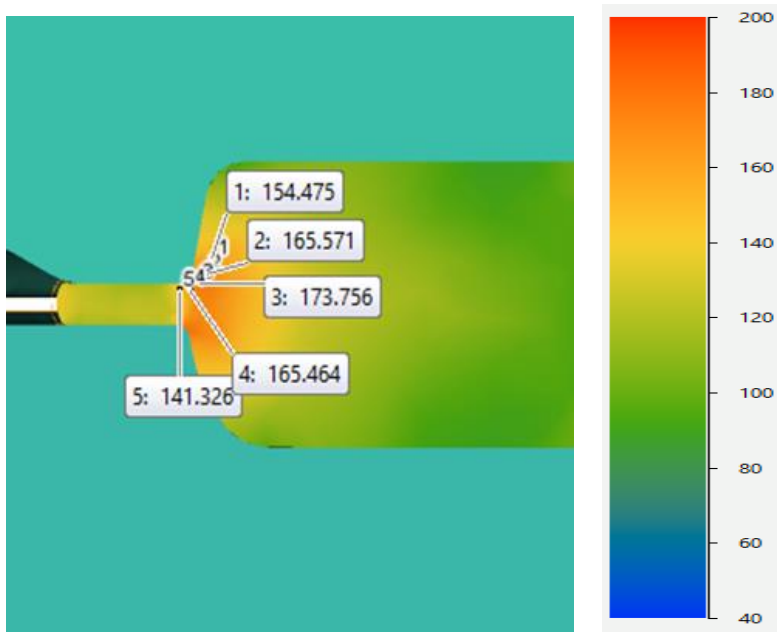

Figure 4. *Field of effective strees at cross section near transfer radius of forging part*

The highest concentration of stress occurs in the central part of the forging part due to the reduction of the amount of volume of material in forged part, while in the parts where a larger amount of material is present, lower stress of the material occur. The die geometry engraved cavity of the tool based on the simulation indicates that it is fully filled and that the forging part has excess material that has enterd in the flash.

The plastic strain that occur during hot forging proceses can be seen at Figure 5, where the highest degree of plastic strain can be seen in the areas of the formation of the flash of the forged part and its valy is 13.4518. While in the areas where the material has filled the cavity of the dies the material is not in a plastic state.

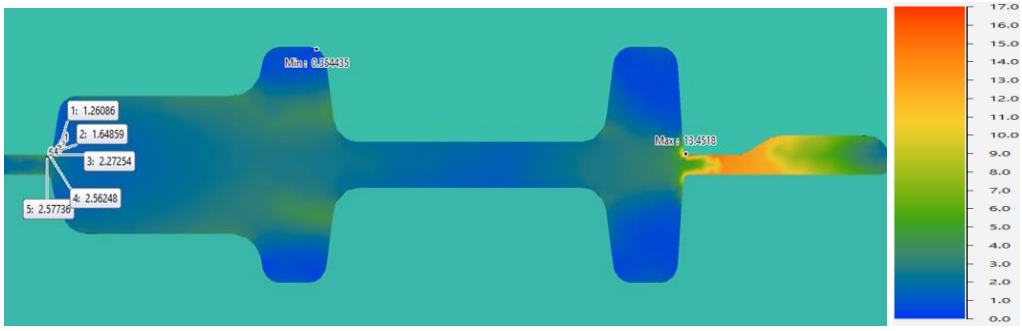

Fig. 5. Plastic strain in cross section of the workpiece

Figure 6 shows the rate of deformation. which is most intensed in the areas where the material continues to flow, in the areas where the flash is formed in contact

with the tool [11,12]. The rate of deformation in the monitored area ranges from 651.767 1/s at the beginning of the radius of the curve of toll, while in the middle of the radius of the curve its most intense effective stresses are located witch valy is 2924.23 1/s, and at the exit of the radius value drops to 1156.79 1/s.

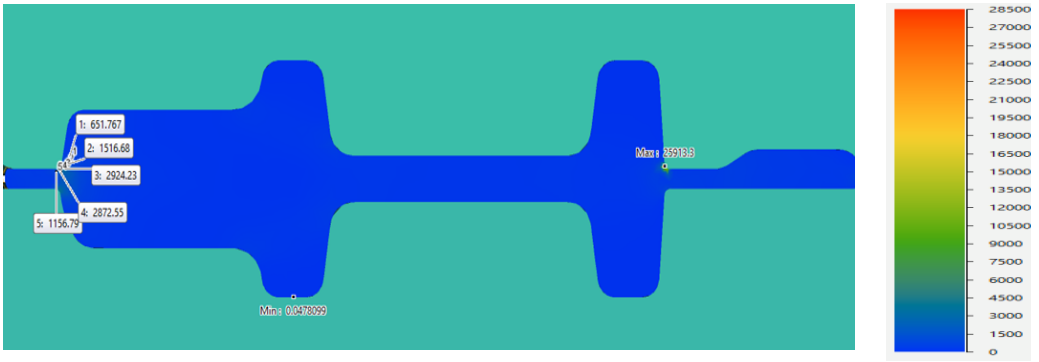

Figure 6. *Strain rate in cross section of the workpiece*

The simulation results and obteintd finished piace in simulation matches the real finished piace obteand in real industral conditions . The real finished can be seen in Figure 7.

Figure 7. *Finished part obtained in industry*

4 CONCLUSION

In the paper, the stress-strain state during forgings of part made of S355J2 material were monitored by FEM simulation based on numerical methods. The monitored die indicates that there is a sudden increase in the tool load in the forging proces which can be seen in Fig. 2, which occurs due to the occurrence of large degrees of deformation and hardening of materials, which is accompanied by a greater resistance of the material to further deformation during forging proces.

Based on the obtained results, it is possible to conclude that the forging process itself can be improved in terms of reducing the input material by making the flow of material harder in the field of occurrence of maximum stress, i.e., the lowering flow of material into the right part of the excess material flash according to Fig. 5, by making the opening of the excess material further reduced and to direct the flow of excess material to the left part of the tool. During the analysis of the parameters of the results of the stress-deformation state, it was determined that there are no breaks in the material during flow and that there is no occurence of material laps during forging process.

ACKNOWLEDGEMENT

This paper presents the results of the research conducted within the project “Research and development of new generation machine systems in the function of technological development of Serbia” funded by the Faculty of Mechanical Engineering, University of Niš, Serbia

REFERENCES

[1] Beddoes J, Bibby MJ (1999) Principles of metal manufacturing processes. Butterworth-Heinemann, Oxford. ISBN 0 340 73162 1

[2] Gronostajski, Z., Hawryluk, M., Jakubik, J., Kaszuba, M., Misiun, G., & Sadowski, P. (2015). Solution Examples of Selected Issues Related to Die Forging. Archives of Metallurgy and Materials, 60(4), 2773–2782. doi:10.1515/amm-2015-0446

[3] Rajiev, R., & sadagopan, P. (2018). Simulation and Analysis of hot forging dies for Pan Head bolt and insert component. Materials Today: Proceedings, 5(2), 7320–7328. doi:10.1016/j.matpr.2017.11.401

[4] Obiko, J., Mwema, F., & Akinlabi, E. T. (2020). Strain rate-strain/stress relationship during isothermal forging: A Deform-3D FEM. Engineering Solid Mechanics, 1–6. doi:10.5267/j.esm.2019.9.003

[5] Wangchaichune, S., & Suranuntchai, S. (2018). Finite Element Simulation of Hot Forging Process for KVBM Gear. Applied Mechanics and Materials, 875, 30–35. https://doi.org/10.4028/www.scientific.net/AMM.875.30

[6] Hartley, P., & Pillinger, I. (2006). Numerical simulation of the forging process. Computer Methods in Applied Mechanics and Engineering, 195(48-49), 6676–6690. doi:10.1016/j.cma.2005.03.013

[7] Rahul, M. R., Samal, S., Venugopal, S., & Phanikumar, G. (2018). Experimental and finite element simulation studies on hot deformation behaviour of AlCoCrFeNi 2.1 eutectic high entropy alloy. Journal of Alloys and Compounds, 749, 1115–1127. doi:10.1016/j.jallcom.2018.03.262

[8] Obiko, J. O., Mwema, F. M., & Bodunrin, M. O. (2019). Finite element simulation of X20CrMoV121 steel billet forging process using the Deform 3D software. SN Applied Sciences, 1(9). doi:10.1007/s42452-019-1087-y

[9] S. Ranđelović, V. Marinković," Proizvodne tehnologije obrada plastičnim deformisanjem" Niš 2017, ISBN 978-866055-096-7.
[10] SHI, R., & LIU, Z. (2011). Hot Deformation Behavior of P92 Steel Used for Ultra-Super-Critical Power Plants. Journal of Iron and Steel Research, International, 18(7), 53–58. doi:10.1016/s1006-706x(11)60090-3
[11] QForm, User guide, VX 8.2.4, 2018.
[12] QForm, Manual refrence, VX 8.2.4, 2018.

COMETa 2022
6th INTERNATIONAL SCIENTIFIC CONFERENCE
17th - 19th November 2022
Jahorina, B&H, Republic of Srpska
University of East Sarajevo
Faculty of Mechanical Engineering
Conference on Mechanical Engineering Technologies and Applications

EKSPERIMENTALNO I NUMERIČKO ODREĐIVANJE INTENZITETA DISTORZIJE KOD KUTIJE ELEKTRIČNOG ORMARA IZRAĐENOG OD UV STABILIZOVANOG ABS-a

Edin Šunje[1], Edin Džiho[2]

Rezime: Procesom brizganja plastike izrađuju se dijelovi složene geometrije i veoma uskih tolerancija. Kako bi zadovoljili dimenzionalne zahtjeve, potrebno je predvidjeti na koji način će se dio deformisati, a intenzitet deformacije svesti na minimum. Jedan od najčešćih faktora koji utječu na dimenzionalnu stabilnost brizganih komada jesu geometrija, materijal, debljina stijenke komada, skupljanje, procesni parametri. Pojava skupljanja je osobina polimernih materijala i nije je moguće u potpunosti eliminisati. Procesnim parametrima je moguće koompenzirati deformacije komada do određenog nivoa. Kod uniformnog skupljanja komad se neće deformisati samo će postati manji, što je jednostavno kompenzirati skaliranjem. Diferencijalno skupljanje najčešće dovodi do distorzije komada, koja će biti predmet istraživanja u ovom radu.

Ključne riječi: ABS, skupljanje, distorzija, brizganje plastike

EXPERIMENTAL AND NUMERICAL DETERMINATION OF WARPAGE INTENSITY IN ELECTRIC BRAKER PANEL BOX MADE OF UV STABILISED ABS

Abstract: Injection molding technology is generally used for production of tight tolerances complex geometry parts. In order to meet dimensional requirements, it is necessary to estimate intensity and the shape of warpage, whereas the intensity should be minimized or compensated during mold tooling. The most influential parameters on dimensional stability are part geometry, type of material, wall thickness, shrinkage, and process parameters. Shrinkage is the property of polymeric materials which is not possible to avoid but is possible to reduce by varying process parameters. If the shrinkage is uniform the part won't be deformed just becomes smaller, it can be simply compensated by part scaling. Differential shrinkage leads to part warpage, this phenomenon has been investigated in this paper.

Key words: ABS, shrinkage, warpage, injection molding

[1] Doc.dr. Edin Šunje, Univerzitet Džemal Bijedić, Mašinski fakultet, Mostar, BiH, edin.sunje@unmo.ba
[2] Doc.dr. Edin Džiho, Univerzitet Džemal Bijedić, Mašinski fakultet, Mostar, BiH, edin.sunje@unmo.ba

1 RAZUMJEVANJE FENOMENA SKUPLJANJA I DISTORZIJE OTPRESAKA

Dimenzije otpresaka se primarno određuju dimenzijama kalupne šupljine, a sekundarno prema svim varijablama koje utječu na proces injekcionog presovanja plastomera (temperature, pritici, vremena). Iskustvo je pokazalo da su dimenzionalna odstupanja otpresaka često korigovana promjenom režima procesa brizganja. Izotropni dimenzionalni problemi se mogu korigovati procesnim parametrima, ukoliko je u pitanju više dimenzija onda je teško izvršiti korekcije kroz parametre brizganja. Skupljanje i naknadno skupljanje su prirodna posljedica procesa brizganja. Ova pojava utječe na tolerancije koje se mogu postići procesom injekcionog presovanja plastomera. Dalje, promjene na otprescima mogu nastati kao posljedica promjene temperature ili uvjeta okoline. Promjene se manifestuju kao toplinska ekspanzija ili kontrakcija, kroz apsorpciju vlage ili drugih otapala.

Skupljanje u kalupu je ono skupljanje koje se javlja u periodu od 24 sata nakon brizganja. Definiše se kao razlika u dimenzijama kalupne šupljine i otpreska, gdje se mjerenje vrši na sobnoj temperaturi. Obično se skupljanje kreće u granicama između 1.7% ÷ 2.2%, osim kod materijela koji sadrže superčvrsta vlakna gdje je procenat skupljanja znatno niži. Postoji dosta podataka o intenzitetu skupljanja različitih materijala od različitih proizvođača, međutim, ovi podaci se mogu koristiti samo orijentaciono jer je poznato da skupljanje zavisi od geometrije i parametara procesa brizganja. Na skupljanje plastomera utječe niz faktora, a neki od njih su oblik otpreska i debljina stijenke, putevi tečenja, tip ulivnog sistema, sposobnost tečenja izabranog plastomera, naknadni pritisak, vrijeme djelovanja naknadnog pritiska, temperatura kalupa.

Veliki broj plastomera koji se upotrebljavaju za različite primjene zahtijeva od konstruktora kalupa i otpreska veliko poznavanje mnoštva podataka za tu vrstu plastomera. Može se reći da različite vrste plastomera imaju različite vrijednosti skupljanja, kako u kalupu tako i naknadno skupljanje van kalupa. Naknadno skupljanje je ono skupljanje koje se desi nakon 24 sata po završetku procesa brizganja. Posljedica je kontinuirane kristalizacije i relaksacije zaostalih napona i kretanja ka stabilnom stanju. Otpresci koji se dobiju u kalupima s preporučenom temperaturom od 90 °C ili više imaju nizak procenat naknadnog skupljanja što osigurava dobru dimenzionalnu stabilnost otpresaka. Međutim, pri dobijanju otpresaka iz hladnih kalupa <80 °C, izraženije je naknadno skupljanje. Pojavu je relativno jednostavno objasniti. Kao posljedica niske temperature kalupa, značajno je odvođenje toplote, a time i brže hlađenje što ostavlja polimer u nestabilnom stanju. Kao poslijedica se javlja značajna rekristalizacija. Ukoliko se takvi otpresci izlože visokoj temperaturi, rekristalizacija uzrokuje značajno naknadno skupljanje otpreska.

Ukoliko je skupljanje po čitavom otpresku uniformno otpresak se neće niti deformisati niti iskriviti, već se skupiti i postati manji. Distorzija se može posmatrati kao deformacija gdje površine otpreska ne prate zadati oblik [1-2]. Distorzija otpreska je poslijedica zaostalih napona koji se javljaju uslijed nejednakog skupljanja plastomera. Različito skupljanje se javlja kao poslijedica orjentacije molekula ili vlakana, razlike temperatura u samom otpresku, ispunjenosti kalupne šupljine, odstupanja u pritisku unutar kalupne šupljine. Najveći utjecaj na pojavu distorzije imaju materijal, geometrija komada, alat i procesni parametri [3]. Neuniformno i asimetrično hlađenje otpreska može uzrokovati nejednako skupljanje. Materijal se hladi i skuplja nekonzistentno od zidova ka centru uzrokujući distorziju nakon izbacivanja otpreska. Na slici 1. je prikazan rezultat djelovanja izraženog skupljanja u kombinaciji sa slabim hlađenjem na distorziju otpreska.

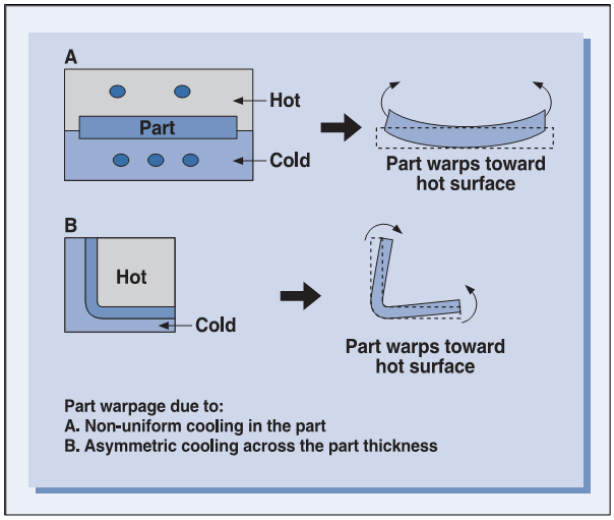

Slika 1. *Distorzija otpresaka kao posljedica neuniformnog (a) i asimetričnog hlađenja (b)*

Poznato je da skupljanje raste s porastom debljine stijenke. Najčešći uzrok pojave distorzije kod vlaknima neojačanih termoplasta je skupljanje koje se javlja kao posljedica različite debljine stijenke otpreska. Očigledno je da razlika u stepenu hlađenja i stepenu kristalizacije raste kod otpresaka promjenjive geometrije (debljine stijenke). Izraženije volumetrijsko skupljanje, kao poslijedica visokog stepena kristalizacije, u područjima gdje je hlađenje lagano vodi ka nejednakom skupljanju a time i distorziji otpresaka.

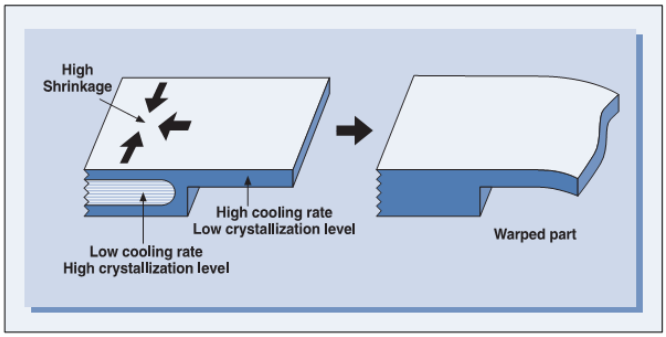

Slika 2. *Utjecaj skupljanja i neuniformnog hlađenja na distorziju otpreska*

Loš dizajn može bitno utjecati na neuniformnono hlađenje, a tim indirektno preko skupljanja na distorziju otpreska. Loše hlađenje stijenke na strani gdje se nalaze rebra uzrokuje lagano hlađenje materijala na toj strani, što može uzrokovati distorziju otpreska. Na slici 3. je prikazan primjer utjecaja lošeg dizajna na pojavu distorzije otpreska. Na ovu pojavu mogu utjecati i ojačanja u obliku vlakna (stakla ili karbona).

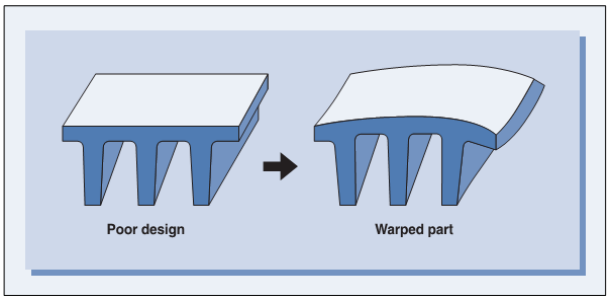

Slika 3. *Utjecaj lošeg projektovanja na distorziju otpreska*

Procesom brizganja plastike se proizvode dijelovi veoma kompleksne geometrije i uskih tolerancija. Uzimajući u obzir gore navedeno, možemo zaključiti da je postizanje dimenzionalne stabilnosti proizvoda kompleksan i izazovan zadatak. Pored poznavanja procenta skupljanja materijala, neophodno je predvidjeti oblik i intenzitet deformacije radnog komada još u fazi razvoja alata. Primjena numeričkih metoda simulacije procesa je nezaobilazan alat kod proces brizganja plastike.

2 NUMERIČKA ANALIZA PROCESA BRIZGANJA PLASTIKE – STUDIJA SLUČAJA

U ovom radu je analziran proces brizganja kućišta elektro-razvodng ormara korištenjem numeričkih metoda. Materijal od kojeg je ormar izrađen je ABS, UV i temperaturno stabilizovan.

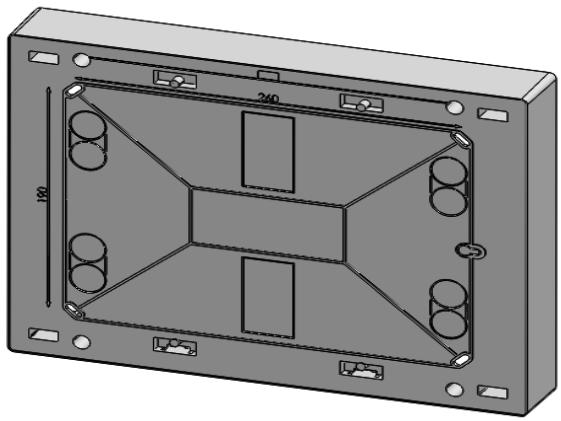

Slika 4. *Izgled radnog komada*

Prije uspostavljanja numeričkog modela neophodno je izvršiti detaljnu inspekciju geometrije, kako bi se izbjeglo generisanje neorijentisanih konačnih elemenata ili elemenata sa slobodnim ivicama, što je neprihvatljivo u ocjeni kvaliteta numerikog modela. Također, elemente kao što su brojevi, kote, mikro izdanci i radijusi je potrebno eliminisati, jer njihov untjecaj na konačan rezultat je zanemarljiv, a mogu značajno negativno utjecati na kvalitet mreže konačnih elemenata. Kod uspostavljanja numeričkog modela korišteni su dual-doman povrinški elementi koji su preporučeni za analizu tankostijenih elemenata.

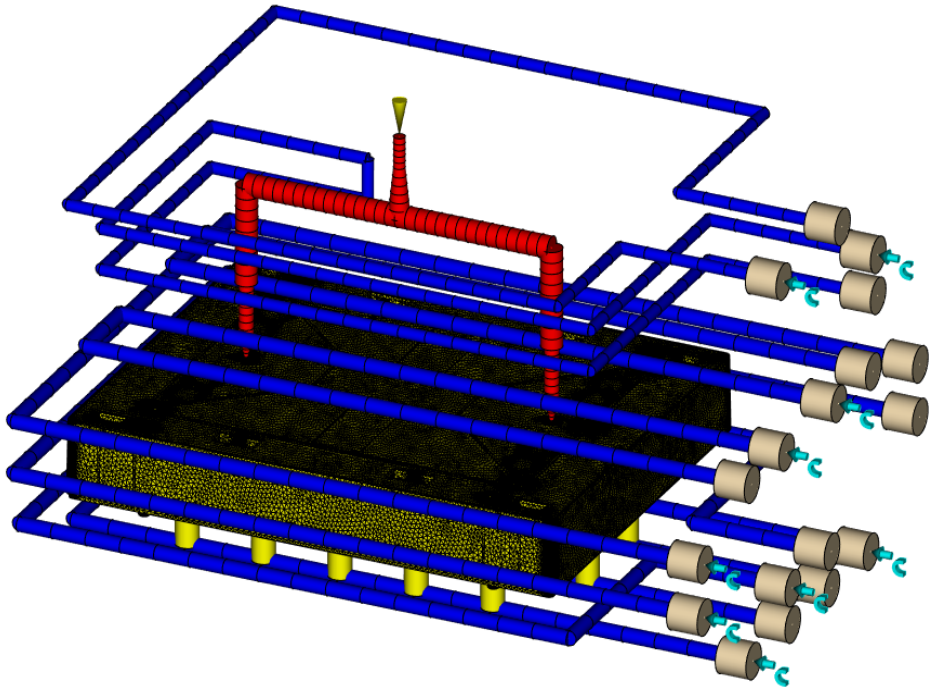

Slika 5. *Izgled numeričkog modela*

Analizirani komad se brizga u dvije tačke korištenjem toplog ulivnog sistema, što je bilo nepophodno imajući u vidu dug put tečenja rastopa kao i relativno tanak poprečni presjek komada. Ulivni i rashladni sistemi su predstavljeni grednim konačnim elementima gdje su svakom sistemu dodjeljeni odgovarajući atributi. Projektovanje sistema hlađenja kod kutijastih radnih komada predstavlja svojevrstan izazov jer je neophodno obezbjediti uniformno hlađenje komada sa obje strane. U analiziranom komadu je korišten sistem blendi kako bi se adekvatno odvela toplota iz unutrašnjosti kutije. Blende su također predstavljene grednim elementima, prečnika 16 mm i koeficijentom efikasnosti prenosa toplote 0.5.(0-0.5) Koeficijent efikasnosti prenosa toplote kod konvencionalnih kanala za hlađenje iznosi 1 (0-1). Za procejnu kvaliteta numeričkog modela korišteni su odgovarajući alati unutar software-a Moldflow Synergy. Uspostavljen je balans između kvaliteta mreže i potrebnih resursa, kako bi simulacija završila u razumnom vremenskom periodu, što je bio predmet ranijih istraživanja [4].

Nakon pripreme i ocjene numeričkog modela urađena je simulacija procesa brizganja sa identičnim proizvonim parametrima. Neki od parametara su prikazani u tabeli 1. Iz prikazanog se može zaključiti diferencirano temperiranje dizna i izbacivačke strane alata, kao jednog od načina kontrole distorzije komada.

Tabela 1. *Procesni parametri*

Parametar	Vrijednost	Jedinica
Pritisak brizganja	1200	[bar]
Vrijeme brizganja	5.9	[s]
Kontrola (V/P)	Automatski	

Parametar	Vrijednost	Jedinica
Naknadni pritisak	300/250	[bar]
Vrijeme djelovanja naknadnog pritiska	2.2	[s]
Temperatura rastopa	248	[°C]
Temperatura medija za temperiranje	30/40	[°C]

3 KOMPARACIJA REZULTATA I DISKUSIJA

Nakon provedenih analiza, koje su često iterativan proces, pristupilo se analizi rezutata simulacije i njihovoj komparaciji sa izmjerenim vrijednostima na fizičkom modelu.

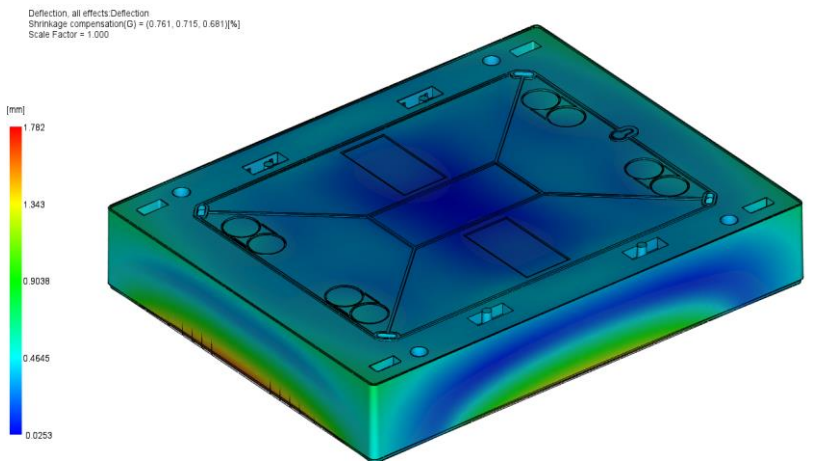

Slika 6. *Vrijednosti distorzije razvodnog ormara*

Na slici 6. su prikazane vrijednosti distorzije kutije razvodnog ormara. Na osnovu rezultata analize je vidljivo da su vrijednosti skupljanja po osama x,y,z respektivno 0.761, 0.715. 0.681%. Skupljanje mora biti uzeto u obzir pri izradi komada. Raspon rezultata se kreće na skali od 0.025 do 1.782 mm. Efekat globalnog skupljanja je izuzet iz rezultata, jer je komad predhodno skaliran. U rezultatima je prikazan zbir utjecaja efekata diferencijalnog hlađenja i efekat orjentacije molekula. Na slici 7. su prikazani pomaci čvorova gornjeg brida kutije ormara počevši od krajnje lijeve tačke. Iz prikazanog je vidljivo da je radni komad deformisan na takav način da se maksimalna odstupanja u odnosu na CAD geometriju javljaju na početku i krajevima kontrolisanih bridova, čije se vrijednosti smanjuju prema sredini. U tabeli 2. su prikazane vrijednosti odstupanja kontrolnih tačaka. Kontolne tačke su izabrane na početku, sredini i kraju svakog brida.

Tabela 2. *Vrijednosti pomaka čvorova kontrolisanoih bridova u kontrolnim tačkama*

Lokacija očitanja vrijednosti	U_1 [mm]	U_2 [mm]	U_3 [mm]	U_1 - U_2 [mm]	U_1- U_3 [mm]
E1	1.324	0.6802	1.317	0.6438	0.007
E2	1.326	0.958	1.313	0.368	0.013
E3	1.314	0.678	1.301	0.636	0.013
E4	1.319	0.979	1.336	0.34	-0.017

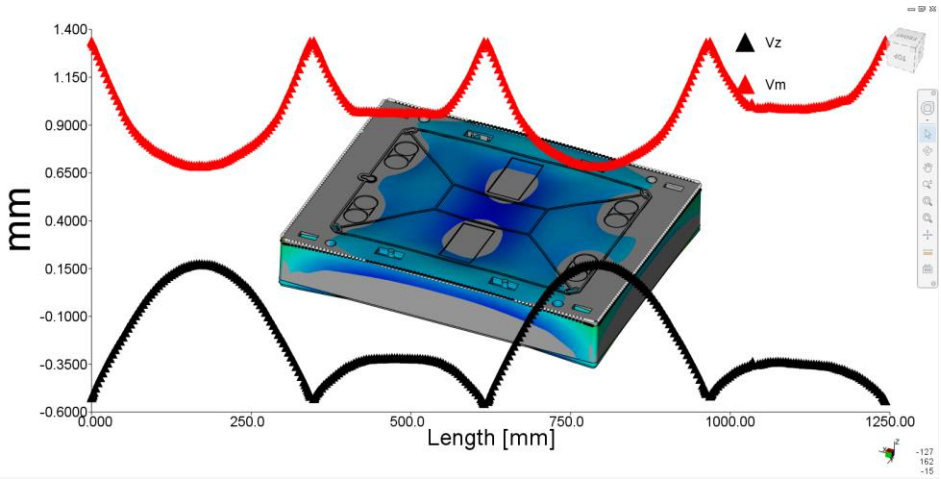

Slika 7. *Pomaci čvorova gornjeg brida kutije ormara po z-osi*

Iz tabele 2. je uočljivo da odstupanja sredine dužih bridova u odnosu na krajeve iznose približno 0.64 mm i gotovo su dvostruko veća od ostupanja sredine u odnosu na krajeve kod kraćih bridova, čija vrijednost iznosi 0.34-0.36 mm. Kontrolno mjerenje na stvarnom komadu je izvršeno korištenjem mjernog sata sa ticalom prečnika 4 mm i očitanjem od 0.01 mm. U tabeli 3. su prikazane relativne vrijednosti odstupanja sredine od krajeva bridova.

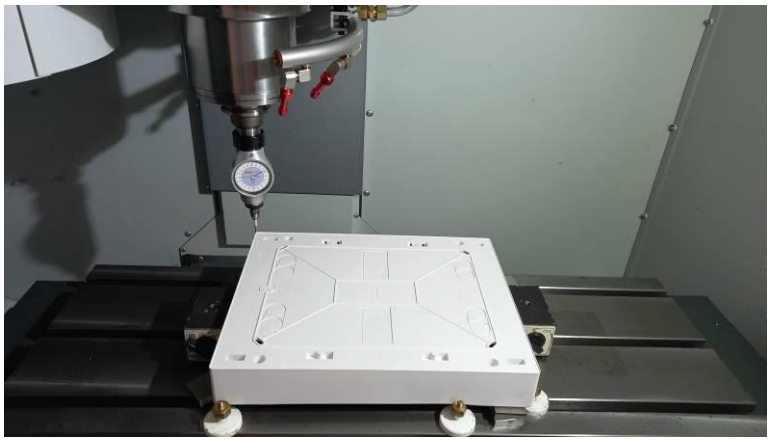

Slika 8. *Verifikacija rezultata korištenjem mjernog sata*

Tabela 3. *Izmjerene vrijednosti relativnog odstupanja u kontrolnim tačkama*

Lokacija očitanja vrijednosti	U_1 [mm]	U_2 [mm]	U_3 [mm]	$U_1 - U_2$ [mm]	$U_1 - U_3$ [mm]
E1	0	0.68	0.07	0.68	0.07
E2	0	0.14	0.11	0.14	0.11
E3	0	0.62	0	0.62	0
E4	0	0.14	0.04	0.14	0.04

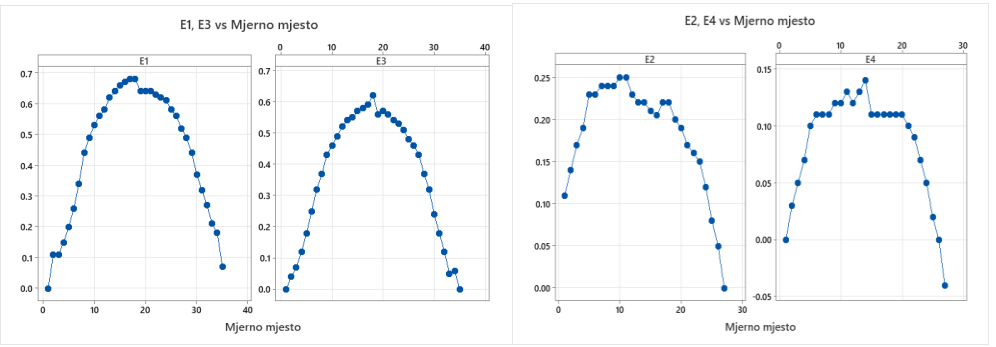

Slika 9. *Izmjerene vrijednosti relativnog odstupanja ivice kutije ormara*

Poređenjem rezultata fizičkog mjerenja i simulacionog eksperimenta je vidljivo da rezultati simulacionog eksperimenta prate trendom i intenzitetom rezultate fizičkog eksperimenta. Odstupanja rezultata simulacionog ekperimenta u odnosu na fizičko mjerenje iznosi svega 0.04 mm na dužim ivicama dok su odstupanja na kraćim ivicama E2 i E4 nešto veća i iznose 0.2 mm.

4 ZAKLJUČAK

U radu je provedena eksperimentalna verifikacija rezultata simulacije procesa brizganja kutije razvodnog ormara izrađenog od stabilizovanog ABS-a. Istraživanje je pokazalo visok stepen pouzdanosti rezultata simulacije. Pouzdanost rezultata simulacije zavisi prije svega od kvalitetne pripreme numeričkog modela kao i od raspoloživosti adekvatnog materijala u software-skoj bazi materijala. Neophodno je da za materijal budu definisane pVT vrijednosti, reološke, termičke i mehaničke osobine. Ukoliko su ispoštovani gore navedeni uslovi, može se zaključiti da se rezultati simulacije procesa brizganja mogu koristiti sa dovoljnim stepenom pouzdanosti, što skraćuje vrijeme tehnološkog postupka bez primjene skupih i dugotrajnih proba. Moguće je predvidjeti rezultate simulacije samo za skupljanje, dok naknadno skupljanje nije moguće predvidjeti jer zavisi od atmosferskih uslova, načina skladištenja, površinske zaštite i drugih uslova.

LITERATURA

[1] Robert A. Malloy, Plastic Part Design for Injection Molding, Drugo izdanje, Carl Hanser Verlag, Munich 2010, ISBN-13: 978-1-56990-436-7,
[2] Maw-Ling Wang, Rong-Yeu Chang, Chia-Hsiang (David) Hsu, Molding Simulation: Theory and Practice, ISBN: 978-1-56990-619-4, 2018
[3] Design guide, Performance and Value With Engineering Plastics, Design Brochure.qxd (hankyan.com), pristupljeno 01.11.2022
[4] Edin Šunje, Influence of Mesh Type on Injection Molding Process Simulation Results Reliability, International Journal of Engineering & Technology IJET-IJENS Vol:17 No:01

COMETa 2022
6th INTERNATIONAL SCIENTIFIC CONFERENCE
17th - 19th November 2022
Jahorina, B&H, Republic of Srpska
University of East Sarajevo
Faculty of Mechanical Engineering
Conference on Mechanical Engineering Technologies and Applications

AN OVERVIEW OF ADVANCED JOINING TECHNIQUES FOR POLYMER AND COMPOSITE MATERIALS

Elisaveta Doncheva[1], Aleksandra Krstevska[2]

Abstract: Products and structures made of polymers and composites require efficient and advanced material joining processes in modern structural engineering to achieve high quality and performance. Designers or engineers must think about and understand the various joining solutions available and how they can be improved with advanced technological processes. Understanding the advantages and disadvantages of each potential technique from the beginning of the project is critical. While this paper summarizes all joining methods, it focuses on the most recent advancements and recommendations on various welding techniques. The goal of this work is to provide up-to-date information as well as to describe promising solutions and techniques that have been developed and proposed for future work.

Key words: Adhesive bonding, Composites, Joining, Polymers, Processing techniques, Welding

1 INTRODUCTION

Polymer and polymer composite materials are well-known engineering materials that, due to their excellent combination of properties, are used in a wide range of important applications such as packaging, construction, equipment, electronic parts, automotive parts, mechatronics, bioengineering, energy, oil and gas, sports and leisure and aerospace. Their application far outnumbers that of any other material available due to the numerous benefits they provide, such as good toughness, high strength-to-weight ratio, non-corrosiveness, good chemical resistance, improved design flexibility, moisture resistance, low thermal and electrical conductivity, ease of fabrication into complex shapes [1]. Engineering polymers have excellent mechanical, thermal, optical, and chemical properties and improved workability [2]. Furthermore, the properties can be altered by incorporating various compounds, reinforcing agents, colorants, plasticizers,

[1]Ph.D.Elisaveta Doncheva, Faculty of mechanical engineering, Skopje, North Macedonia, elisaveta.doncheva@mf.edu.mk
[2]M.Sc Aleksandra Krstevska, Faculty of mechanical engineering, Skopje, North Macedonia, aleksandra.krstevska@mf.edu.mk

stabilizers, flame retardants, and other substances [1]. In general, composite materials are made up of at least two materials that do not dissolve or blend together but work together to provide properties that outperform the individual materials [3]. There are three distinct regions in composites: the matrix, the reinforcement, and the interface. Properties can be tailored to a specific need by selecting the right combination and the manufacturing process that brings these regions together. The matrix material can be any material, but the most common ones are ceramic, metal, or polymer. There are numerous polymer matrices encountered on the market, with thermosets and thermoplastic composites being the most common [4]. Table 1 lists some of the polymers and polymer composites used and their characteristics.

Table 1. *Engineering polymers and polymer-based composites*

Polymers and polymeric composites		**Characteristics and application**	**References**
Thermoset polymer	Epoxy (EP)	Resin as cohesive material in adhesive, great impact resistance, stiffness, durability	[2],[4]
Polymer composite	Carbon fiber-reinforced epoxy (CE)	Cohesion of fiber-reinforced composite, high inherent specific strength, excellent design flexibility, CE composites incorporate nanofillers	[2],[4],[5]
Polyurethane (PU)	Thermoplastic PU Flexible PU Rigid PU PUI Water-borne PU	Thermal insulator, flexible sealant rigid, flexible, thermoplastic, waterborne, binders, coating, adhesives, and elastomers. Used in industrial equipment, paints, liquid coatings, elastomers, rigid insulations, elastic fibers, flexible foams, integral skins.	[2],[4],[6]
Polyolefin plastic	Polyethylene (PE)	Excellent mechanical, processing properties, chemical stability, high ductility and impact strength, low friction, strong creep under persistent force, water repellent, good electrical insulator, good pressure and radiation resistance, non-toxic. Used in packaging, biomedical applications, production of film, pipes, anti-corrosive agents, electrical insulation.	[2],[4],[7]
Acrylic polymer	Acrylic	Strong, stiff, transparent, excellent fatigue endurance, impact resistance, good toughness. Used for lighting, electronics screen, automotive components, outdoor glazing in architecture, construction.	[2],[4],[8]
Thermoplastic	Naylon 6 (PA6) or Polyamide 6	Used in the automotive sector for moulded components, with a tensile strength of 81.4MPa, young's modulus 2.8 GPa	[2],[4]
Thermolastic polyamide	Naylon 66 (PA66)	Harder and stronger than nylon 6, high-quality general-purpose wear-resistant. Used in mechanical engineering, automotive and general machinery construction - plain bearings, coil bodies, guide and clutch parts, gears, cams, rollers, slide bearings, seal rings and guide rails	[2],[4],[9]

Composite PA6 + glass fiber	Polyamide 6 glass reinforced PA6 GF	Used in the automotive sector for high-strength and durable moulded components,	[2],[4]

Understanding the performance differences and joining capabilities of polymer and polymer composite materials can assist in product and sourcing decisions. Joining is an essential manufacturing technique that is constantly improving, especially in structural applications for the production of modern engineering products and structures. Many factors, including desired output, project budget, availability of machinery and equipment, and required joint quality, influence the decision to select the best joining solution for a specific application [3]. Joint performance is critical for ensuring compliance with the purpose as well as all applicable design codes and specifications. When selecting materials and overall design, it is important to consider the joining technique in order to facilitate the joining mechanism while maintaining structural performance and other design criteria [3]. Mechanical fastening, adhesive and solvent bonding, and welding are the three major methods for joining plastics and composites [5]. Furthermore, hybrid joining methods that combine these various techniques in a single joint are viable options [2]**.** A decision on joining process options is influenced by several factors, including material, joint configuration, connection strength, process cost, speed, and production quantity. Welding is an appropriate process for thermoplastic polymers and composites because heat can melt the connecting interface, resulting in a weld after cooling. On the other hand, thermoset systems can be joined using adhesive bonding or mechanical fastening. Some methodologies are inapplicable due to the specifics of joint configurations and geometry, and alternative solutions, such as the use of hybrid processes, where multiple joining processes are used to achieve higher-performing joints and design, are required [2]. Plastic welding techniques are classified according to the nature of the heating source: techniques that use an external heat source, techniques that generate heat through mechanical movement, and techniques that use electromagnetism directly. Some of these techniques can be used for polymer composites but knowing that composites have their advanced properties from the reinforcement the weld will be the weak point.

This article describes good-joining practices for polymers and composites and the factors that influence the selection of the joining process. Adhesive bonding, mechanical joining, and some welding techniques are covered in detail, with an emphasis on the most recent advances in the field. Following the extensive literature review, future research and recommendations are proposed.

2 JOINING POSSIBILITIES OF POLYMERS AND COMPOSITES - METHODS OF MECHANICAL JOINING, ADHESIVE BONDING AND WELDING

The structural integrity is heavily reliant on the quality and durability of joints, which can be a weak point in the assembly. As a result, selecting an effective method of joining is critical for meeting functional requirements and ensuring structural stability. The forces that affect joints can be mechanical, physical and chemical and the joining processes can be classified as mechanical fastening, adhesive bonding and welding [1-3],[10]. There are numerous possibilities within each category and combinations of different joining processes that can be used concurrently, referred to as a hybrid joining process, which has demonstrated credibility in many cases. However, deciding on a joining solution for a specific application remains difficult. It entails making trade-off

decisions between properties and priorities such as performance, cost, time, weight, and overall quality [3].

2.1 Mechanical fastening

Mechanical fastening of polymers and composites is a simple and low-cost technique that generates connection forces between two or more materials by using mechanical loads or auxiliary mechanical components. Mechanical joining employs fasteners such as screws, nuts, bolts, washers, rivets, and pins or with integrated design elements of snap-fit or press-fit joints [3][10]. When high-performance joints are required, mechanical fasteners can be difficult to use, but in most cases, they are the simplest and cheapest solution, especially when different types of materials are to be joined. The disadvantage of using this technique is that highly localized stresses can form around the fasteners, which can cause subsequent in-service corrosion and also it is not a leakproof technique. When used on soft and low-strength materials such as polymers and some polymer composites, damage is unavoidable. The holes required for fasteners cause micro and macro damage to the polymer and composites, making strength degradation difficult to avoid [3]. They can also increase the weight of the structure, which can be a disadvantage in some applications, such as aircraft. Fasteners can be metallic or nonmetallic, permanent or removable, depending on the structure's life expectancy and load capacity. The selection of joining fastener, joint configuration, geometric parameters, lay-up stacking sequence, clearance between fastener and hole, preload or initial clamping force all influence mechanical joint design [3]. This method of joining is widely used in electronics, aerospace, automotive, civil engineering, and mechanical construction. With proper designing and numerical modeling of mechanical fasteners, stress concentrations at joints can be determined [2]. Mechanical joining through attachment with no third body fastener is possible if the joined parts are designed to provide an interlocking connection that resists load through the joint [3]. However, in the case of composites, the complexity of moulding in the interlocking features can be difficult. Other mechanical attachment methods, such as cinching and clinching, are not generally applicable to composites [3].

2.2 Adhesive bonding

Adhesive bonding has proven to be an excellent joining strategy in structures with complex designs that also necessitate high-performance joints. The field's development has been very rapid in recent years, particularly with numerical methods that researchers have investigated in order to predict the stress fields' dependency on geometry and analyze the performance of joints [2]. It can be used to join various materials, but in many cases, one of the materials that must be bonded is polymer or polymer composite. In this joining process, the adhesive is applied to the interface that is intended to be connected, and depending on the type of adhesive, a solid connection is obtained after melting or polymerizing. In order to attain high quality, the joint is pressed together. Although the established adhesive joint is completely leak-proof and can be done with various materials and shapes, it is not suitable for high-volume production due to the high material cost and long curing time [1]. Adhesives can be polymers with low surface energy, resulting in weak adhesion; this is why surface treatments are required. The passive surface treatment changes the surface properties, whereas the active surface treatment changes the chemistry, but both increase the surface energy [2].

With adhesive bonding, composites can be produced by adhering a resin (thermoplastic or thermoset) to structural fibers, but by definition, adhesive bonding

should be considered a surface-driven process in which stresses and strains are transferred across an interface that connects two planes: the substrate and the adhesive. If the adhesive bond is less than 100μm thick, it is considered to be a single interphase between the surfaces, however, if it is thicker, it is treated as a separate component, with the joint described as a sandwich of two substrates, two interphases, and a layer of adhesive [3]. Load transfer in composites can cause failure outside of the adhesive/interface region due to z-direction adhesion between fiber layers, making the resin the weakest point [3]. The adhesive joints are sensitive to cleavage forces and small peel loads, therefore it is recommended that the joint design should be in such a manner that the adhesives are loaded in compression and shear. When connecting sheet materials, the load-carrying capacity of a joint does not increase gradually with the joint area because maximum stress at the leading and trailing edges of the joint limits the load-carrying ability. Examples of adhesive joint configurations are shown in figure1.

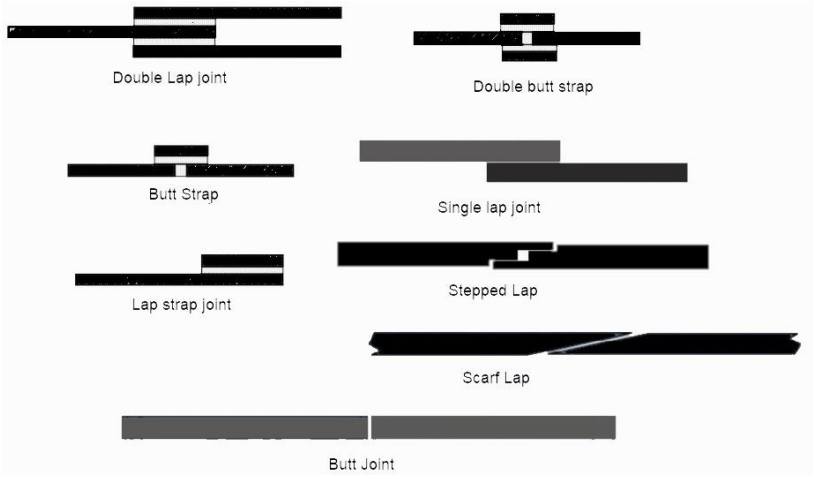

Figure 1. *Various simple adhesive joint configurations*

Today, numerical methods in the design process can be used to determine the best geometry and materials that can withstand loading and working conditions. Any potential fractures or damages in the adhesive joint can be revealed by the analysis. The numerical modeling techniques are appropriate for determining the influence of geometrical parameters because they have been validated through experimental work. The interaction between the mechanical behavior of the substrate and the adhesive is the most important factor influencing joint performance when polymeric or composite substrates are used [2]. Even though adhesive bonding performs better under fatigue load, there are still dangers of fatigue failure that need to be investigated experimentally and numerically. It can be concluded that it is a useful technique for a wide range of applications, particularly when joining polymers or composites. To achieve good joint quality, special attention should be paid to surface treatments of polymer materials, as well as proper joint design and numerical analysis. In addition, when designing joints with adhesive bonding, one should consider the joint's working conditions, such as high humidity environments and fatigue loads[2]. When additional support is required, hybrid joints are an excellent choice, especially if peel or cleavage forces are present. Although the adhesive is a secondary joining component, it contributes to the connection's overall stability. Adhesive bonding may appear to be a great solution for joining polymers and composites, but some considerations must be made before making a final decision. The

joints cannot be easily disassembled with additive joining, and elevated temperatures and specialized fixtures may be required. High-strength adhesives have poor properties, are brittle, and are sensitive to oil and moisture. Surface preparation and cleanliness are also important for consistent results, and thermal residual stresses can be induced [10][14].

2.3 Welding

Polymers and composites can be joined using a variety of welding techniques. Polymer welding, also known as fusion bonding, involves the application of heat to the contacting interfaces in order to melt the polymer, and after cooling, a solid joint is formed through intermolecular diffusion and polymeric chain entanglement processes. Thermoplastic composites can be melted and reshaped, so they can be welded. Thermoset matrix composites, on the other hand, can be joined with welding but only if the interface is a thermoplastic layer that can be melted, forming the joint that will hold the two parts together. Welding processes are classified into three types based on the energy source used to generate heat: electromagnetic heating, mechanical heating, and externally heated techniques[3][8]. The welding processes can also be categorized according to frictional heating, electromagnetic heating, bulk heating, and heating with thermal techniques [14]. There are various welding technologies that can be used in various situations, each with advantages and disadvantages that make them more or less suitable for a specific application.

Friction stir welding (FSW) is a joining process that is in a solid state, with minimum energy applied on the joining surface that is generated by the vibration or friction of a metallic pin. The generated heat melts the components that are aligned and pressured towards each other and after cooling they form a joint. A solid connection is achieved because the energy released by friction in combination with the pressure applied softens the base material without melting. This increases the activation energy between the surfaces causing plastic deformation and the joint is formed through the forging process. FSW of thermoset polymer is impossible because the materials will degrade, but thermoplastics can be welded with FSW with vibration, rotary friction, ultrasonic and orbital welding. In general, all of the challenges that come during welding are mostly the parameters and other manufacturing characteristics. The rotation of the pin will influence the area of heat affected zone (HAZ), and the faster rotation will result in a wider zone [10][12]. Other design parameters like feed speed and tooth depth will influence the mechanical properties of the joint [2]. This joining process is used in the automotive industry because the trend is toward lighter, safer, less expensive, and more environmentally friendly vehicles and reinforced polymer composites are a promising material that can be a good substitute for the formerly used steel and cast iron. Polymers such as polyethylene (PE), polypropylene (PP), polycarbonate (PC), polystyrene (PS), polyamide (PA), polymethyl methacrylate (PMMA), and other thermoplastics, as well as nanocomposites, can be successfully welded using the FSW process [12]. FSW is a quick and simple method of joining thermoplastic polymers and composites. Nevertheless, the effectiveness of this method is heavily dependent on the welding parameters. By analyzing the stresses and thermal gradients generated, finite element analysis can be used to optimize parameters.

Resistance welding involves the heating of an electrically conductive implant that is placed between two parts to be joined. The heat in the implant is generated thanks to the electrical resistance while passing a high electric current through the piece. With this generated heat, the surrounding thermoplastic softens and melts, and the welded joint forms after it cools down under adequate pressure. The contact between the

surfaces and molecular diffusion is ensured with pressure [14]. The implants are electrically conductive materials (metallic) in different forms and shapes (wire or mesh form) or they can be unidirectional carbon fiber strips [3]. In general, the electric current used is DC or low-frequency AC, but there is a new variation of the technique that uses electrical current in the form of intense pulses (high energy impulses with pauses), called impulsive resistance welding (IRW). It uses less energy to melt the matrix and removes the overheating and delamination problems of the welded surfaces. The weld quality can be enhanced if the correct amount of energy and thermal insulation are used [3]. This technique is considered to be fast, simple, and applicable to large structures, for joining of carbon-fiber reinforced composites and thermoplastics except for the parts where there is heavy carbon loading or non-insulated components are used. There are also some common problems with this joining process, like uneven heating and the possibility of fiber movements [14]. There are other welding processes that fall under the electromagnetic heat group, like induction, microwave welding, and dielectric welding that are also suitable for the welding of polymers and thermoplastic composites.

The third category is thermal welding, which involves heating the two parts at the contacting surfaces to cause a decrease in viscosity, then pressing the parts together and slowly cooling down below the glass temperature to form a solid connection between the parts [14]. Under this category fall hot plate, hot gas, radiant, infrared, and laser welding. For a variety of reasons, *laser welding* stands out. For starters, it is capable of producing highly accurate and strong joints with tighter tolerances [1]. This is also possible with electron beam welding, but it would be more expensive due to the complexities of the equipment and setup [1]. The procedure involves bringing the two parts into contact, after which the laser beam heats up the absorbing material, which then heats up the translucent material via conduction. It is critical that one of the two materials is transparent enough to allow laser radiation to pass through while the other is absorbent enough. Weld quality is determined by laser characteristics, welding time, and material type [14].

3 CONCLUSIONS

This article examines several joining strategies for producing higher-quality joints when polymers or composites are used as basic materials in production. However, joint quality is a subjective term, and in order to accurately analyze it, specific analysis for the specific applications must be performed. According to the findings of this review, adhesive bonding, mechanical joining, and welding processes such as FSW and laser welding are already in use in a variety of advanced technological applications. The joints are strong and free of defects, but their potential can be increased by further optimizing the process parameters. Future research and development should focus on a broader range of materials in order to investigate the capabilities of joining various materials. Hybrid joints are a promising solution for improving the properties of specific joint designs. Combining techniques like FSW and laser welding, or laser welding and mechanical joining has the potential to reduce energy consumption. Other advantages may also emerge, such as the ability to obtain stronger joints for various materials and complex designs.

REFERENCES

[1] Kumar, N., Kumar, N., Bandyopadhyay, A. (2021). A State-of-the-Art Review of Laser Welding of Polymers - Part I: Welding Parameters. *Welding Journal*.

[2] Silva, L.R., Marques, E.A., & Da Silva, L.F. (2021). Polymer joining techniques state of the art review.*Welding in the World, 65*, pp.2023 - 2045.
[3] Worrall, C., Kellar, E., Vacogne, Ch. (2020). *Joining of Fibre-reinforced Polymer Composites - A Good Practice Guide*, Composites UK Ltd.
[4] Ngo, T. (2020). Introduction to Composite Materials. *Composite and Nanocomposite Materials - From Knowledge to Industrial Applications*.
[5] De, S., Fulmali, A.O., Shivangi, P.N., Choudhury, S., Prusty, R.K., Ray, B.C. (2020). Interface modification of carbon fiber reinforced epoxy composite by hydroxyl/carboxyl functionalized carbon nanotube. *Materials Today: Proceedings, 27*, 1473-1478.
[6] Akindoyo, J.O., Beg, M.D., Ghazali, S., Islam, M.R., Jeyaratnam, N., Yuvaraj, A.R. (2016). Polyurethane types, synthesis, and applications – a review.*RSC Advances, 6*, 114453-114482.
[7] Zhong, X., Zhao, X., Qian, Y., & Zou, Y. (2018). Polyethylene plastic production process. *Insight - Material Science*.
[8] Chan, J.X., Hassan, A., Wong, J.F., Majeed, K. (2020). Plastics in Outdoor Applications.
[9] Parth, K. V., (2016). Nylon (Chemistry, Properties, and Uses), *International Journal of Scientific Research*, Vol.5., Issue 9, pp. 349 -351.
[10] Šercer, M., & Raos, P. (2010). *Joining of Plastics and Composites*.
[11] Lambiase, F., Scipioni, S.I., Lee, C., Ko, D., Liu, F. (2021). A State-of-the-Art Review on Advanced Joining Processes for Metal-Composite and Metal-Polymer Hybrid Structures.*Materials, 14*.
[12] Kumar, H. (2020). Studies on Friction Stir Welding of Polymers- A Review.*International Journal of Engineering Research and, 9*.
[13] Wahab, M.A. (2015). Joining composites with adhesives: theory and applications.
[14] . Roos, L. W. M., & Kalas, V. Welding of thermoplastic composites;

COMETa 2022
6th INTERNATIONAL SCIENTIFIC CONFERENCE
17th - 19th December 2022
Jahorina, B&H, Republic of Srpska
University of East Sarajevo
Faculty of Mechanical Engineering
Conference on Mechanical Engineering Technologies and Applications

INFLUENCES OF THE MILLING DIRECTION ON SURFACE QUALITY ON MILLING X155CrVMo12-1 STEEL

Igor Babić[1], Aleksandar Košarac[2]

Abstract: Surface quality is one of the main characteristics of a product and manufacturing process. In milling, there are two possible ways a tool moves relative to the movement of the workpiece – up and down milling. This paper investigates the effect of milling direction on surface quality and shows that the effect is independent of quality in terms of the arithmetic average of the roughness profile – Ra.

Keywords: tool, quality, machining, metal cutting, direction

1 INTRODUCTION

This paper investigates the influence of the tool movement direction on surface quality when milling steel using a carbide endmill, high-speed steel (HSS) endmill, and carbide insert endmill. The surface roughness is measured and displayed using the arithmetic average of the roughness profile – Ra as a surface quality indicator. The obtained results show that using the same parameters on climb milling gives significantly better surface quality than conventional milling.

2 RESEARCH OVERVIEW

For the past 20 years, there is a growing tendency to increase machining productivity and surface quality driven by the growing market competition which transformed machining steel towards more productive methods like High-speed machining (HSM), High-efficiency milling (HEM), dry cutting[1], hard milling and similar. These methods are grounded on high cutting speeds, fast feeds, using the whole flute length, and machining without coolant. These trends demand tools of greater quality that will stay stable even in high-stress conditions and will degrade in such a way as to have the least effect on surface quality, [1-4]. Jozić [5] researches the effect of milling direction on flank wear while milling hardened steel. Samsudeen et. al. 6] research

[1] Dipl. Inž. Maš., Igor Babić, Višegrad, Republika Srpska, BiH, igor.babic2@gmail.com
2 Dr. Aleksandar Košarac, associate professor, University of East Sarajevo, Faculty of Mechanical Engineering, aleksandar.kosarac@ues.rs.ba

cutting forces and tool wear when milling Ti-6A-4V titanium and give us the optimal cutting feeds and speeds for finish passes. Odedey et. al. [7] research tool wear when dry machining AISI 316 steel using carbide inserts with Physical vapor deposition (PVD) coatings, and establish the connection between cutting feeds and speeds and tool wear. Wojciechowskia et. al. [8] research the milling of X155CrVMo-12 steel using ball mill. They state that carbide tools have greater tool life when cutting with speeds up to 300 m/min compared with CBN tools. Bouzakis et. al. [9] analyze the effect of milling direction on tool life when using endmills with PVD coatings on AISI 304 steel. Hosni et. al. [10] research tool wear of carbide endmills with PVD coatings while milling hardened AISI D2 steel without using coolant. N.F. Kundor et. al. [11] also research tool wear and surface finish quality when dry milling hardened AISI D2 steel. J. A. Arsecularante et. al. [12] research the effect of different cutting parameters when turning hardened AISI D2 steel with PCBN tools. Vinayak et. al. [13] research the workability of hardened AISI D2 steel while dry cutting and establish a connection between different milling parameters and tool life and surface finish quality. For better transparency, the research overview and used parameters are grouped in table 1.

Table 1. *Research overview:*

Author, year	***Work material***	***Hardened***	***Process, Milling parameters***
Jozić (2015)	42CrMo4	Yes	Dry milling Cutting speed: 45-145 m/min Axial depth of cut (ADOC): – 5mm Radial depth of cut (RDOC): 0.5 – 2 mm Feed: 0.005-0.095 mm/tooth Tool coating: TiAlN
Samsudeen (2015)	Ti6Al4V	No	Titanium alloy milling. Cutting speed: 20-50 m/min ADOC: 1mm (slot milling) Feed: 0.02-0.08 mm/tooth
Odedey (2017)	AISI 316	No	Dry milling Cutting speed: 145 – 260 m/min ADOC: 1-2mm Feed: 58 – 520 mm/min Tool coating: TiAlN-PVD
Wojciechowskia (2012)	X155CrVMo12-1	No	Ball milling with WC i CBN tools. Cutting speed: 100 - 140 m/min Feed: 0.1 - 0.2 mm/tooth RDOC: 0.2 - 1.8 mm
Bouzakis *(2014)*	AISI 304L	No	Face milling with cemented carbide inserts. Cutting speed: 300 m/min ADOC: 0.12 mm Tool coating: TiAlN.
N A J Hosni (2014)	AISI D2	Yes	Dry milling Cutting speed: 80-120 m/min Feed: 0.05 mm/tooth ADOC: 0.5 mm RDOC: 3, 4, 5 mm Tool coating: TiAlN-PVD

Hik Faizu Kundor (2016)	AISI D2	Yes	Dry milling Cutting speed: 50-90 m/min Feed: 0.02-0.04 mm/tooth ADOC: 1mm RDOC: 20 mm Carbide inserts with CVD coating.
J.A. Arsecularatne (2005)	AISI D2	Yes	Turning Cutting speed: 70-120 m/min Feed: 0.08-0.2 mm/revolution Depth of cut: 0.5 mm
Vinayak H.G. (2016)	AISI D2	Yes	Dry milling Cutting speed: 90-180 m/min Feed: 0.1-0.4 mm/revolution Tungsten carbide tool.

3 EXPERIMENTAL SETUP

The experimental part of the research is conducted in the laboratory for CNC machine tools on the Faculty of Mechanical Engineering, the University of Eastern Sarajevo., For those purposes, an EMCO Concept Mill 250 milling center was used. The arithmetic mean roughness Ra was measured using a Mitutoyo SURFTEST SJ-210 portable surface roughness measuring device. The following setting parameters have been used: λf = 2.5 μm, λc = 0.08mm, ln = 4 mm. Workpiece hardness was measured on a Mitutoyo HR-110MR Rockwell hardness testing machine in 3 layers and gave a mean hardness of 20HRC.

The workpiece material is X155CrVMo12-1 tool steel, also known as D2, in a normalized state.

In this experiment 3 different endmills were used:

1. SUMITOMO Insert mill – WEZ 11016E Φ16x46 mm with carbide inserts AOM T11 T3 08 PEER-G.
2. Carbide endmill – EMCA ICE MILL 0300M 1000 Φ16x46 mm with AlCrN coating.
3. HSS endmill Φ10 manufactured by Jugoalat Trebinje.

Cutting parameters used for the given combination of the tool-workpiece-milling center are chosen as optimally recommended by the literature [14-20] and the tool manufacturer [20-22]. Milling with carbide inserts and carbide endmills has been performed with no coolant (dry cutting), while for milling with HSS endmills synthetic cutting fluid was used.

The experiments were grouped into 3 groups based on the tool and milling parameters., Experiment results are shown in Table 2.

Table 2. *Experimental setup and results.*

No:	Parameters	Surface quality, results
E.1	Vs = 120 m/min fz = 0.125 mm/tooth a_a = 5 mm a_r = 2.5 mm Dry cutting Carbide insert Climb milling	Ra roughness is inside the 0.250 – 0.650 micrometers range. After 85.5 minutes of cutting the measured Ra roughness is 0.290 micrometers. The measured roughness decreases even as the tool wear is increasing.

E.2	Vs = 120 m/min fz = 0.125 mm/tooth a_a = 5 mm a_r = 2.5 mm Dry cutting Carbide insert Conventional milling.	It was impossible to measure surface roughness because of bad surface quality and the danger of damaging measuring equipment.
E.3	Vs = 105 m/min fz = 0.03 mm/tooth a_a = 10 mm a_r = 1 mm Dry cutting Carbide endmill Climb milling	The mean measured Ra roughness is 0,248 micrometers.
E.4	Vs = 105 m/min fz = 0.03 mm/tooth a_a = 10 mm a_r = 1 mm Dry cutting Carbide endmill Conventional milling	The mean measured Ra roughness is 0,709 micrometers. A significant visual difference in surface quality is visible between climb and conventional milling.
E.5	Vs = 20 m/min fz = 0.05 mm/tooth a_a = 10 mm a_r = 1 mm Synthetic cooling fluid HSS endmill Climb milling	The mean measured Ra roughness is 0,843 micrometers.
E.6	Vs = 20 m/min fz = 0.05 mm/tooth a_a = 10 mm a_r = 1 mm Synthetic cooling fluid HSS endmill Conventional milling.	It was impossible to measure surface roughness because of bad surface quality and the danger of damaging measuring equipment. A significant visual difference in surface quality is visible between climb and conventional milling.

Legend:
a_a – axial depth of cut - ADOC
a_r – radial depth of cut - RDOC
V_s – cutting speed
fz – feed.

4 EXPERIMENT RESULTS

4.1 Experiments 1 and 2

Experiments 1 and 2 were done using a carbide insert endmill with a single insert. Experiment 1 uses climb milling and the surface roughness is inside the 0.270-0.610 Ra-micrometers range as shown in figure 1. Experiment 2 uses conventional milling with all the other parameters same as in experiment 1, and the surface quality is

visually so bad that the surface roughness can not be safely measured because it would result in damage to the measuring equipment. The magnified surface after the second experiment is shown in Figure 2.

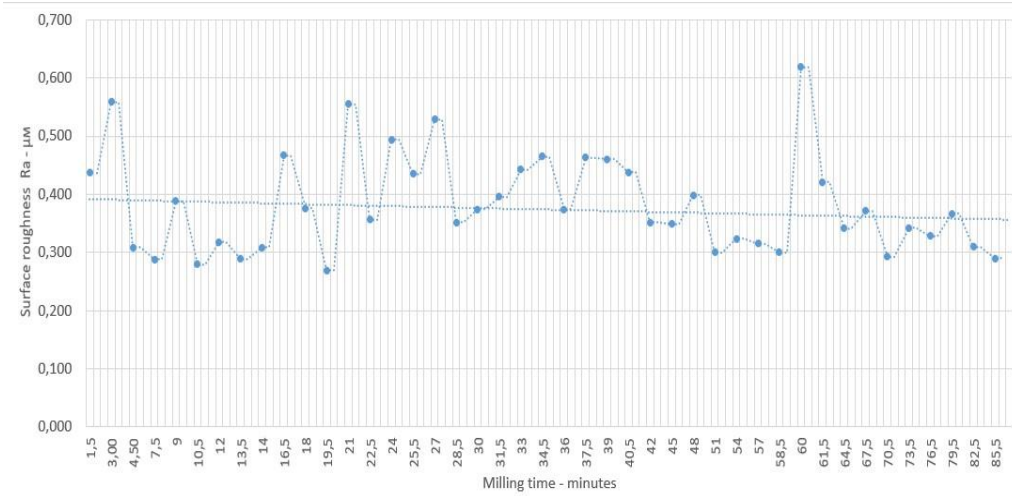

Figure 1. *Surface roughness-milling time graph.*

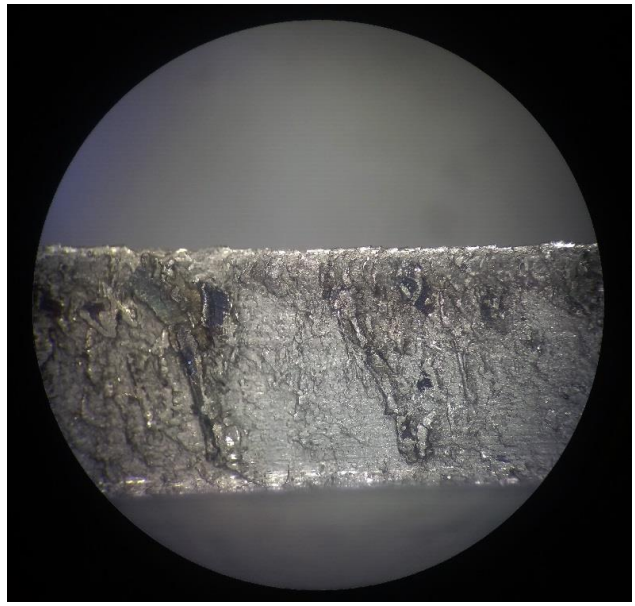

Figure 2. *Magnified image of the surface after a conventional milling pass.*

4.2 Experiments 3 and 4

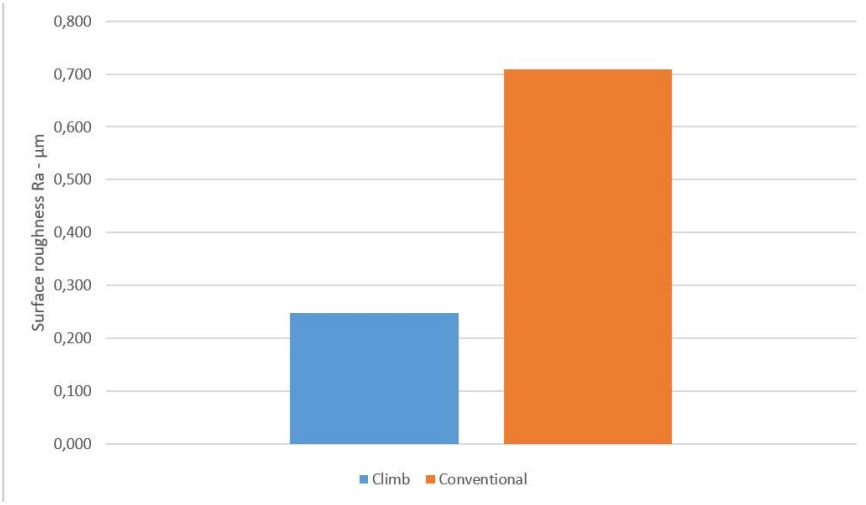

Figure 3. *Mean surface roughness for Experiment 3 (Climb) and Experiment 4 (Conventional).*

Experiments 3 and 4 were done using a carbide endmill with identical parameters, only the milling direction was varied. Experiment 3 uses climb milling and the mean surface roughness measure 0.248 Ra-micrometers, while experiment 4 uses conventional milling, and the mean surface roughness measures 0.709 Ra-micrometers.

5 EXPERIMENTS 5 AND 6

Experiments 5 and 6 were done with an HSS endmill, the only difference being that experiment 5 was done using climb milling and experiment 6 was done using conventional. The mean surface roughness measures 0.843 Ra-micrometers for experiment 5, while the surface roughness could not be measured for experiment 6 because it would result in damage to the measuring equipment. The magnified milled surface is shown side by side in figure 5.

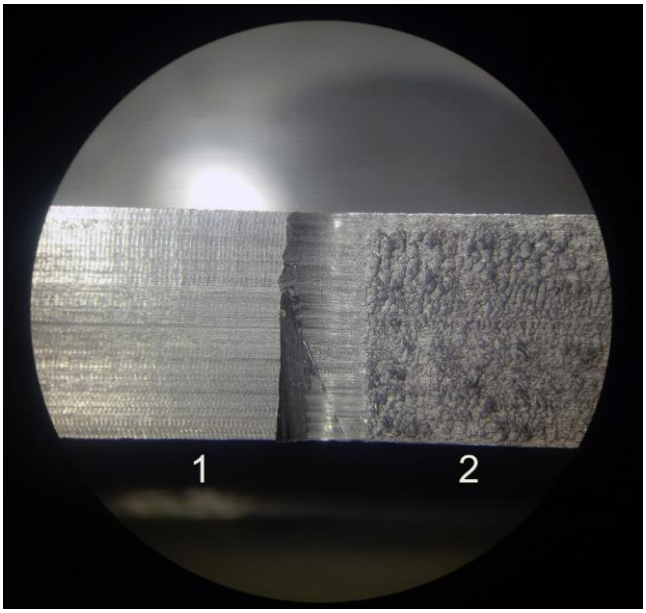

Figure 5. *Visual comparison of the milled surfaces for 1) Climb milling (Experiment 5), 2) Conventional milling (Experiment6.)*

6 CONCLUSIONS

1. Surface roughness can be viewed as a function of the milling direction.
2. Regardless of endmill type and material used climb milling gives visually better surface quality compared to conventional milling, also the measured surface roughness is smaller for climb milling.
3. It can be seen that a bigger influence on surface roughness has the milling direction compared to cutting speed and feeds.
4. Surface quality after conventional milling can be so bad that it can not be safely measured using contact methods.
5. There is no justification for using conventional milling over climb milling in modern machining from the standpoint of surface quality.

REFERENCES:

[1] Košarac A., Šikuljak L., Obradović Č., Mlađenović C., Zeljković M.: "Cutting parameters influence on surface roughness in AL 7075 milling" 2020 19th .international Symposium INFOTEH-JAHORINA (INFOTEH), 2020, pp. 1-6, doi: 10.1109/INFOTEH48170.2020.9066273.

[2] Košarac A., Šikuljak L., Šalipurević M., Mlađenović C., Zeljković M.: "Prediction of self-excited vibrations occurrence during aluminum alloy AL 7075 milling." 2019 18th International Symposium INFOTEH-JAHORINA (INFOTEH), 2019, pp. 1-6 doi: 10.1109/INFOTEH.2019.8717781.

[3] .Gordana Globočki – Lakić, Obrada metala rezanjem, teorija, modeliranje, simulacija, Banja Luka 2010

[4] Gordana Globočki – Lakić, Branislav Sredanović, Alati i pribori u obradi rezanjem, Banja Luka 2016.

[5] Jozić S., Bajić D.: „Flank wear and surface roughness in the milling of hardened steel“, Metalurgija Sisak – Zagreb, 2015.
[6] Samsudeen S. S., Rakesh N., Nisaantha K. N., Krishnaraj V.: Study on cutting forces and tool wear during end milling of Ti-6Al-4V, International journal of mechanical and production engineering, 2015.
[7] Odedeyi P. B., Abou-El-Hossein K., Oyekunle F., Adeleke A. K.: Effects of machining parameters on tool wear progression in end milling of AISI 316, Proceedings of the Canadian society for mechanical engineering international congress, 2020.
[8] Wojchiechowskia S., Twardowskia P.: Tool life and process dynamics in high-speed ball end milling of hardened steel, 5th CIRP conference on high-performance cutting, 2012.
[9] Bouzakis, K.-D. et al: Coated tools' performance in up and down milling stainless steel, explained by film mechanical and fatigue properties, WEAR, *2013*
[10] N. A. J. Hosni., M. Lajis., N. H. Rafail.: Tool Life and Flank Wear of Physical Vapour Deposited TiAlN Multilayer Coated Carbide End Mill Inserts when Machining AISI D2 Hardened Steel under Dry Cutting Condition, Advanced materials research, 2014.
[11] N. F. Kundor, N. W. Awang., N. Berahim.: Tool wear and surface roughness in machining AISI D2 tool steel, Indian journal of science and technology, 2016.
[12] J. A. Arsecularante, L. C. Zhang., C. Montross., P. Mathew.: On machining of hardened AISI D2 steel with PCBN tools, Journal of materials processing technology, 2005.
[13] V. N. Gaitonde, S. R. Karnik., C. H. A. Maciel., J. C. C. Rubio., A. M. Abrao.: Machinability Evaluation in Hard Milling of AISI D2 Steel, Materials research, 2016.
[14] ISO 8688 – 1:1989, Tool life testing in milling-Part 1: Face milling.
[15] ISO 8688 – 2:1989, Tool life testing in milling-Part 2: End milling.
[16] ISO 3685 – 1993, Tool life testing with single-point turning tools.
[17] Kalajdžić, M., Tanović, Lj., Babić, B., Glavonjić, M., Miljković, Z.,Puzović, R., Kokotović, B., Popović, M., Živanović, S., Tošić, D.,Vasić, I.: Tehnologija obrade rezanjem, Priručnik, Univerzitet u Beogradu, Mašinski fakultet, Beograd, 1999.
[18] Kalajdžić M.: Tehnologija mašinogradnje, Univerzitet u Beogradu, Mašinski fakultet, Beograd, 2001
[19] Milikić, D., Gostimirović, M., Sekulić, M.: Osnove tehnologije obrade rezanjem, Univerzitet u Novom Sadu, Fakultet tehničkih nauka, 2015.
[20] Sumitomo – New milling tools 20/21 – Katalog za 2020/21.
[21] http://www.korloy.com/ - Pristupljeno 18.03.2022.
[22] https://fswizard.com - Pristupljeno 18.03.2022.

COMETa 2022
6th INTERNATIONAL SCIENTIFIC CONFERENCE
17th - 19th December 2022
Jahorina, B&H, Republic of Srpska
University of East Sarajevo
Faculty of Mechanical Engineering
Conference on Mechanical Engineering Technologies and Applications

DIGITALIZATION OF CULTURAL AND HISTORICAL HERITAGE LEADS TO ITS PRESERVATION USING 3D TECHNOLOGIES

Mina Šibalić[1], Marko Mumović[2], Aleksandar Vujović[3], Nikola Šibalić[4], Jelena Jovanović-Šaković[5]

Abstract: The protection and preservation of cultural and historical heritage play an important role in preserving a country's cultural identity. Cultural heritage includes tangible and intangible cultural assets. The importance of three-dimensional (3D) technology in various fields of science is growing exponentially, and is used in studies related to cultural heritage and includes 3D scanning, 3D modeling, as well as virtual reality (VR) and augmented reality (AR) used to preform virtual presentations of monuments and ancient artifacts. The application of digitalization of cultural heritage has many advantages, among other things, they participate in the overall development of the information community, while modern information technologies enable efficient organization and storage of data. The 3D scanner collects information about the object, and converts its analog form into a digital form very quickly. The concept of digitalization has made it possible for unknown 3D shapes to be replicated in a much faster and easier way.This paper aims at showing the advantages of applying 3D technology in the function of protecting cultural and historical heritage. This type of storage of data on cultural, historical and artistic assets is very important, given that there is a danger of their partial or complete destruction over time, due to natural disasters or other adverse events. Archived data would make it possible to make replicas of original goods through 3D printing (3DP), which would have to follow certain quality standards.

Keywords: Cultural and historic heritage, digitalization, 3D technologies

[1] Spec. sci Mina Šibalić, University of Montenegro, Faculty of Mechanical Engineering, Podgorica, Montenegro, minasibalic@edu.ucg.ac.me
[2] Mr Marko Mumović, Univeristy of Montenegro, Faculty of Mechanical Engineering, Podgorica, Montenegro, markomumovic@gmail.com
[3] Dr Aleksandar Vujović, Univeristy of Montenegro, Faculty of Mechanical Engineering, Podgorica, Montenegro, aleksv@ucg.ac.me
[4] Dr Nikola Šibalić, Univeristy of Montenegro, Faculty of Mechanical Engineering, Podgorica, Montenegro, nikola@ucg.ac.me
[5] Dr Jelena Jovanović-Šaković, Univeristy of Montenegro, Faculty of Mechanical Engineering, Podgorica, Montenegro, jelenajov@ucg.ac.me

1 INTRODUCTION

Cultural heritage means goods that are inherited from previous generations or that are created in the present, and have cultural and artistic value and should be preserved for future generations. These goods are most often under different protection regimes and with their symbolism they represent elements of touristic development, and thus of economic potential.

The protection and preservation of cultural and historical heritage plays an important role in preserving a country's cultural identity. Cultural monuments that have been exposed to certain forms of destruction for centuries need to be protected. Devastation can be intentional – exposure to illegal actions, or caused by time. The heritage that is in the external environment is very susceptible to changes and damage due to weather. These damages change the character and shape of buildings and monuments. Such influence has its continuity and in the following years it will certainly lead to the collapse of the initial form and appearance of a significant number of exhibits located in the external environment. It should be mentioned that there are also cases of desecration, i.e. deliberate destruction of cultural monuments.

In recent years, 3D scanning has become part of a coherent and non-contact approach to cultural heritage documentation and its long-term preservation. Unlike silver-based photographic film, digital recording does not require a long and expansive process of chemical development. Digital files are stored compactly and this information is accessed via a computer. If necessary, they are freely manipulated in terms of further processing or sending to another address within a few seconds of creation [1].

The 3D scanner collects information about the object and converts its analog form into a digital form very quickly. Unknown 3D shapes can be replicated in a much faster and easier way by the process of reversible engineering, with the help of the concept of digitalization. The digitalization of cultural heritage was included in the list of priorities in the field of culture during the French Presidency of the Council of the European Union in 2008 [2].

Preserving of cultural and historical assets, recording surfaces and shapes of the highest possible resolutions, their classification and archiving in the primary format, so that the obtained data with further technological progress can be further processed is very important for the process of improving cultural heritage using 3D technology. Archived data would allow replicas of original goods to be made through 3DP.

3D technologies are increasingly present in all areas, including the function of protection of cultural and historical heritage. Due to the great application of these technologies, they are developing at a high speed and new knowledge is being gained. The application of modern technologies – 3D scanners – has been used for many years in the field of studying and preserving cultural and historical heritage. Digitalization provides an opportunity to preserve the digital content of archaeological, artistic and historically important objects [3].

2 SIGNIFICANCE OF CULTURAL HERITAGE

Cultural heritage is recognized as an important factor of a country's identity and a long-term resource for sustainable development. It is necessary to continuously carry out activities related to its protection and preservation, improvement, raising citizens' awareness of the importance and significance of cultural heritage, and creating and environment for understanding cultural heritage and its role in society, especially for

cultural, tourist and economic development. Cultural heritage is transmitted through education and conservation.

It is very important to preserve cultural diversity through the improvement of the condition and values of all types of cultural goods, fostering creativity and understanding between different cultures, and promoting dialogue between cultures and religions. Also, through that, knowledge about the values and significance of cultural goods is further spread. The goal of protection of cultural goods is the preservation and improvement of cultural goods and their transmission to future generations in an authentic form, as well as providing conditions for the survival of cultural goods and for preserving their integrity. 3D technologies can ensure the sustainable use of cultural goods, according to their traditional or new appropriate purposes, for a better quality of life and human development itself.

Cultural heritage represents the historical connection of the past, present and future and determines the identity of a nation. In the era of globalization, cultural heritage ensures that a culture is remembered, as well as that mutual respect between different cultures is developed [4].

The study of human history is often done through found objects, because they provide a concrete basis. Tangible heritage includes movable and immovable heritage.

Intangible cultural heritage is usually defined as the absence of physical presence. Includes traditions or living expressions inherited from our ancestors and passed on to our descendants, such as performing arts, rituals, knowledge and practices related to nature, religious ceremonies, traditional craft skills, music, dance, literature, theater, languages, food. Intangible heritage is especially difficult to protect because it is only experienced and cannot be stored in a protected place to be preserved. Due to the rapid development of civilization and the migration of people, this type of culture is often forgotten. That is why the preservation of intangible cultural property is an important element of today's world. Intangible cultural heritage gives a sense of identity and it can be protected by various methods such as VR and use of 3D technologies [1]. 3D, four-dimensional (4D) motion recording systems enable recording of the way activities are preformed, their consolidation and presentation for the next generations. Often digital technologies, e.g. audiovisuals are combined with 3D techniques for better presentation of cultural elements.

Even though the best way to preserve intangible heritage is to use it as often as possible, while the use of 3D technologies is revolutionary to preserve tangible cultural heritage. This type of storage of data on cultural, historical and artistic assets is very important since there is a danger of their partial or complete destruction over time, due to natural disasters or some other adverse event.

Technology has begun to shape individual experiences in unusual ways. Modern technology has begun to show changes in the museum experience. The concept of the museum is changing along with the new trend of digitalization. A large number of museums have started projects to digitize entire collections.

The main foundation of every country and every society is its culture. Culture is not something that is created in a day, a week or a month. The development of culture in society is a long process.

The objectives of the protection of cultural property are [4]:

- preservation and promotion of cultural assets and their transmission to future generations in authentic form;
- ensuring the sustainable use of cultural property, in accordance with their traditional or new appropriate purpose, for human development and quality

of life;
- disseminating knowledge about the advantages and importance of cultural assets;
- preserving cultural diversity by improving the condition and values of all types of cultural goods, fostering creativity and understanding of different cultures and promoting dialogue between cultures and religions;
- providing conditions for cultural goods, in accordance with their purpose, to meet the cultural, scientific and educational needs of individuals and society;
- prevention of actions and activities that may change the appearance, properties, peculiarities, meaning or significance of the cultural property;
- prevention of illegal trade and relocation of cultural property.

Also, investing in cultural heritage is beneficial for the local economy both in terms of consumption, but also in terms of increasing employment and income. In economic terms, most cultural assets are used for economic exploitation mainly through tourism [5]. A study for the city of Rosor in Norway found that cultural heritage tourism in the region contributes about 7% to total employment and income [6]. With the technology of digitalization, archeological sites, that date back centuries, can be presented to the world public. One such example is shown in fig 1.

Figure 1. *Example of digitalization of destroyed cultural property [8]*

3 ASPECTS OF APPLICATION OF 3D TECHNOLOGY IN THE FUNCTION OF CULTURAL HERITAGE PROTECTION

“New technologies” such as 3D scanning and 3D printing are increasingly used in the world as one of the leading methods in the process of preserving elements of the native culture [8]. Fig 2 and fig 3 show the interface of VXelements software, supported by Creaform Go! Scan 50 (hand held 3D scanner), that was used to scan the Bust of Njegos, as an example for this paper. The bust is 30 *cm* tall and 15 *cm* wide. Fig 2 shows two different scans being merged, because the scanning couldn’t be completed in only one position. Fig 3 shows completed 3D scan which is later trsnsformed to .stl file and can be printed or further worked on in another software.

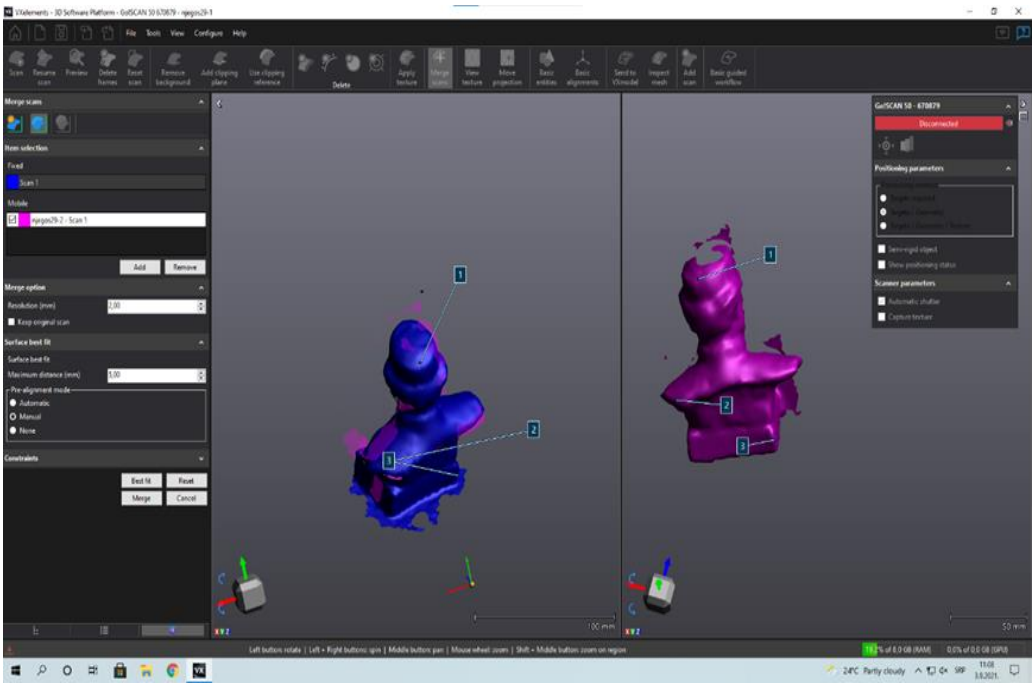

Figure 2. *Merging two separate 3D scans*

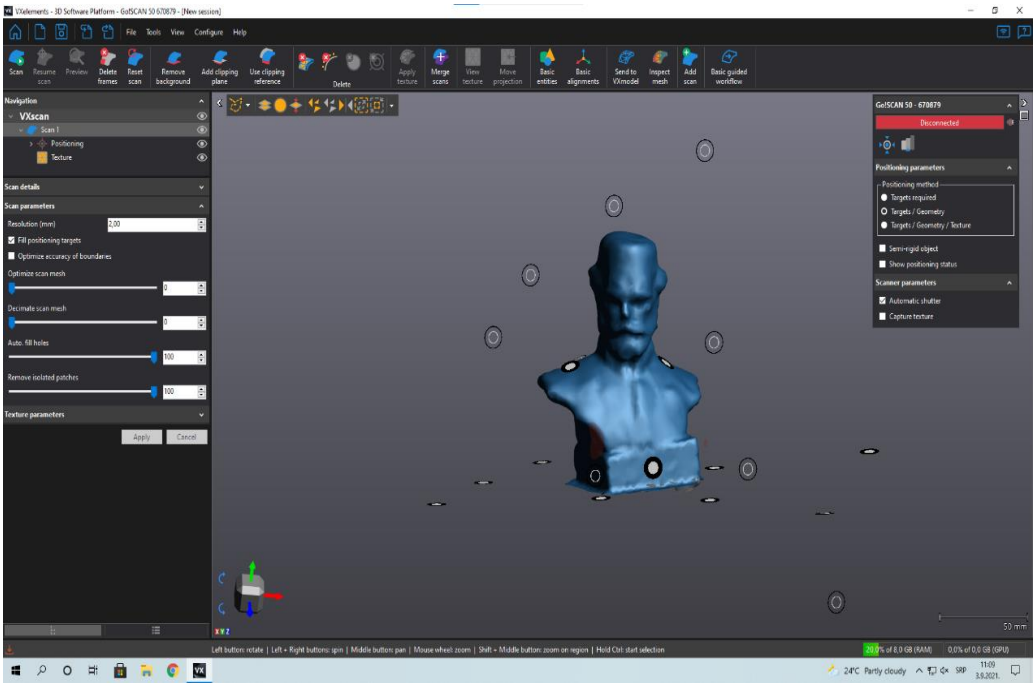

Figure 3. *Completed 3D scan of the Bust of Njegos*

Digital copies of certain items, which are classified as museum treasures, can be easily presented online, which would avoid storing items in the museum's archives due to the lack of exhibition space. This type of copy is suitable for exchange with researchers, other institutions, or to be used for 3DP true copies in appropriate material.

The time in which we live is the period of digitalization and the practice of modern IT achievements. It is necessary to constantly monitor trends in the world and to implement them both in fashion and in the field of protection of cultural heritage. By applying modern information technologies and achievements, through the digitalization of cultural heritage, the way of activities in communication, presentation, exhibition, transport of cultural heritage and implementation of these activities in an adequate way has been improved.

Conservation refers to the following areas of study [9]:

- Documentation – documentation is related to the storage of different types of information.
- Protection – protection is defined as actions against damage, destruction or other loss of cultural property.
- Reconstruction – reconstruction is the process of visualizing the cultural property of buildings in order to better understand them.
- Restoration – restoration is a set of actions that include the following tasks: integration and replacement of non-original elements, reconstruction, retouching and filling.
- Conservation – conservation refers to extending the life of cultural heritage while strengthening the transmission of its important messages and heritage values.

In addition to 3D printers, 3D scanners are also very common, which in a few minutes can collect information about a particular object, which would otherwise take much more time to be generated in CAD software. 3D scanners are three-dimensional measuring devices used to capture objects from the real world or environment so that they can be analyzed in the digital world. The latest generations of 3D scanners do not require contact with the physical object being captured, which makes them very suitable for capturing artifacts. One of the roles of a 3D scanner is to obtain complete or partial 3D measurements of any physical object. Most of these devices generate points or measures of extremely high density.

The aim of the application of 3D technologies in the function of protection of cultural and historical heritage is to provide activities that lead to:

- adequate protection of cultural heritage from the influence of time and development of the best basis in case of need for restoration;
- adequate protection against malicious and illegal acts of devastation or unauthorized alienation of cultural heritage;
- an authentic presentation of cultural heritage for future generations and unequivocally clearly presents cultural heritage that will avoid possible disputes in the future;
- the development of an adequate basis for communication with all stakeholders in terms of display, exhibition, transport of cultural property and more.
- This goal can be achieved by applying modern 3D technologies in the function of:
- the development of a digital register of the cultural heritage of a certain

country, for the needs of adequate, efficient and effective records, management and protection;

- creation of a 3D digital database of cultural heritage for the needs of restoration according to a model that fully corresponds to the original;
- creation of a 3D database for the needs of reversible engineering, ie repair due to damage, according to a computer model that fully corresponds to the original;
- making 3D models for the purpose of simple reproduction of certain exhibits using 3D printers, and for the purpose of exhibiting replicas or simpler production of promotional souvenirs that fully correspond to the original, or for the purpose of making adequate packaging for transporting sensitive exhibits and others;
- creation of 3D models for the needs of online presentation in remote destinations;
- the development of a 3D model database as a basis for an integrated and centralized information system for the managements and protection of cultural property in Montenegro.

4 CONCLUSION

"Photography is a time capsule that stretches from the past to the future." (Henry Jesionka)

The application of 3D scanners and 3D printers is becoming part of everyday life. The protection of cultural and historical assets with the help of 3D technologies is currently the leading science in the world of museums. 3D scanners play a major role in the process of digitizing cultural property. They allow a specific part for which there is no drawing or 3D model to be easily reproduced or enhanced.

"Our world has developed a great appetite for information in visual form, and digital imaging has such vast technical and economic benefits as a way to meet this requirement, which it seems certain will succeed in photography as our primary medium of visual recording." (William Mitchell, 2001)

Cultural property includes places, things and practices that society considers important and worth preserving. Currently, this topic of improving the protection of cultural property is occupying world attention and is becoming increasingly popular. Social scientists emphasize the importance of cultural heritage in supporting ethnic and national recognition. Digitization of cultural heritage collections has become an essential task in fulfilling the function of protection of cultural and historical property. It is necessary to use all technologies in the practice of digitalization, in order to preserve and spread the culture visually for posterity.

ACKNOWLEDGEMENT

This study has been supported by the Central European Initiative (CEI) as an action of technology transfer in the territories of Central Europe, within the context of the project "Composites for All".

REFERENCES

[1] Brumann, C. International Encyclopedia of the Social & Behavioral Sciences. ScienceDirect. https://www.sciencedirect.com/referencework/9780080970875/international-encyclopedia-of-the-social-and-behavioral-sciences. Accessed 23 Nov 2021.

[2] Stamenović, G., & Rančić, D. Application of modern information technologies in order to promote tourism and preserve cultural heritage.

[3] Application of 3D printing and 3d scanning in archeology, culture and protection of monuments. Solfins doo. (n.d.). https://solfins.com/blog/3d-print-scan-6/post/primena-3d-stampe-i-3d-skeniranja-u-arheologiji-oblasti-kulture-i-zastite - monument-340. Accessed 23 Nov 2021.

[4] Administrator. (2019, October 2). The significance of Cultural Heritage. Eritrea Ministry Of Information. https://shabait.com/2019/10/02/the-significance-of-cultural-heritage/. Accessed 23 Nov 2021.

[5] Manasakis, C., Alexandrakis, G., & Kampanis, N. (2019). Economic and Societal Impacts on Cultural Heritage Sites, Resulting from Natural Effects and Climate Change. Heritage. Accessed 23 Nov 2021.

[6] *Economic impacts of cultural heritage* https://www.researchgate.net/publication/248546198_Economic_impacts_of_cultural_heritage_-_Research_and_perspectives. Accessed 23 Nov 2021.

[7] https://arheopress.hr/wp-content/uploads/2020/03/3D-izlo%C5%BEba-Sirija.jpg

[8] Šibalić, M., 2021. Specialist paper, Application of 3D technologies in the function of protection of cultural and historical assets.

[9] Conservation of cultural heritage. http://uis.unesco.org/en/glossary-term/conservation-cultural-heritage. Accessed 20 Feb 2022.

COMETa 2022
6th INTERNATIONAL SCIENTIFIC CONFERENCE
17th - 19th December 2022
Jahorina, B&H, Republic of Srpska
University of East Sarajevo
Faculty of Mechanical Engineering
Conference on Mechanical Engineering Technologies and Applications

EXPERIMENTAL EXAMINATION OF THE APPLICABILITY OF ADDITIVE TECHNOLOGIES IN THE FIELD OF RAPID TOOLING - INJECTION MOLDING

Miloš Pjević[1], Mihajlo Popović[2], Mladomir Milutinović[3], Dejan Movrin[4], Ljiljana Stefanović[5]

Abstract: In this paper, an experimental examination/analyzing applicability and machinability of the polymer material's core and cavity formed using additive technology (rapid tooling) was conducted. Achieving the price reduction of the final product, as well as the price of the mold for plastic injection through the introduction of rapid tooling injection molding can be applied, not only to mass production, but also to small series production. This research is limited to obtaining plane parts of simpler geometry from polypropylene polymer material. Obtained results showed that, at this point, it is not directly possible to completely produce a core and cavity only through additive technologies. In order to achieve some tolerances at specific places, it is still necessary that the core and cavities are machined with conventional methods. On the other hand, it turned out that by using a polymer core and cavity, it is possible to produce a smaller series of the parts.

Key words: Rapid Tooling, Additive Technologies, Injection Molding, 3D Printing.

1 INTRODUCTION

Injection molding as the mass production method was introduced in late 19th century, by two American inventors J. S. Hyatt and J. W. Hyatt [1]. Up to this date, do

[1] dr Miloš Pjević, Assistant Professor, Faculty of Mechanical Engineering, University of Belgrade, Belgrade, Serbia, mpjevic@mas.bg.ac.rs
[2] dr Mihajlo Popović, Associate Professor, Faculty of Mechanical Engineering, University of Belgrade, Belgrade, Serbia, mpopovic@mas.bg.ac.rs
[3] dr Mladomir Milutinović, Associate Professor, Faculty of Technical Sciences, University of Novi Sad, Novi Sad, Serbia, mladomil@uns.ac.rs
[4] dr Dejan Movrin, Assistant Professor, Faculty of Technical Sciences, University of Novi Sad, Novi Sad, Serbia, movrin@uns.ac.rs
[5] Ljiljana Stefanović, Teaching Assistant, Faculty of Technical Sciences, University of Novi Sad, Novi Sad, Serbia, ljiljanastefanovic@uns.ac.rs

to cost effectiveness, injection molding is applicable only in the mass production. The main reason is production cost of the molding tool itself.

With introduction of the additive technologies, it is possible to completely review the application of certain methods of manufacturing parts. Some parts that require complex milling operations or casting operations can be produced in a simple and easy way using additive technologies [2-5]. In recent years, a large percentage of the research has been focused on examining the application of additive technologies in the field of rapid tooling for the needs of injection molding [6-13].

2 RAPID TOOLING

Rapid tooling as the as an area of application of additive technologies, is not only used for various auxiliary tools such as jigs and fixtures, but also has a huge application in the field of injection molding of polymer materials.

For the purposes of the experiments of this paper, a ČAD model of the mold (Fig. 1a) for a planar part representing a face mask carrier was created. Formed CAD model, in addition to the mold cavities, it contains channels for the flow of the coolant in order to temper the tool properly. The CAD mold model is formed in such a way that two face mask carriers should be formed during one injection molding process. The part is oriented in such a way that the part where the mold cavity is located has a better quality of surface, that is, that part of the mold is not in contact with the supports (Fig. 1b).

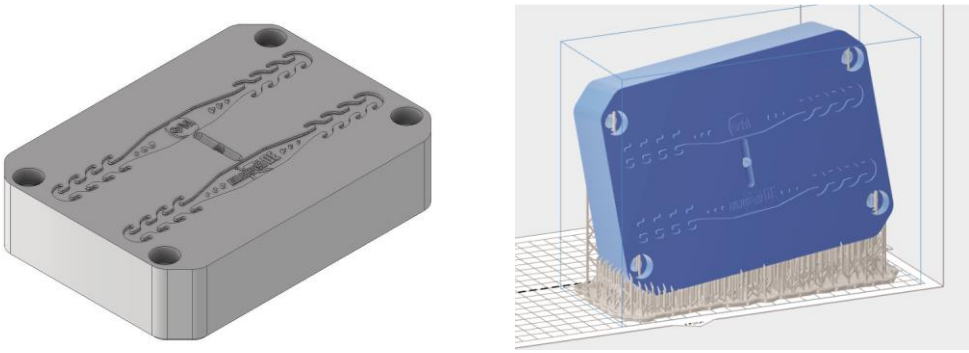

a) b)

Figure 1. *a) CAD model of the mold and b) production preparation*

The mold is produced on the Formlabs printer, on the model The Form 3L (Fig. 2a), using layer height 0.1mm. Photopolymer material that is used is Rigid 4000 V1. Printing time was estimated in approximately 25 hours.

In order to obtain optimal physical-mechanical properties of the printed part, in addition to cleaning rest of the photopolymer, the part was additionally postprocessed by additional irradiation under the UV light (curing).

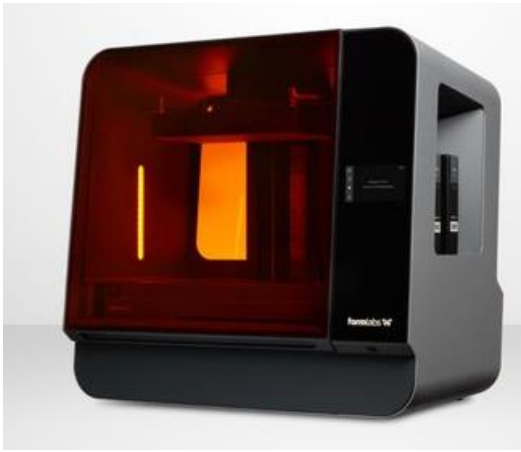

a)

b)

Figure 2. *a) 3D printer Form 3L and b) printed part*

3 EXPERIMENTAL SETUP

As the tool for injection molding must satisfy certain criteria in the direction of production quality, that is, the quality of the processed surface, as well as dimensional accuracy, it is necessary to additionally post-process the printed part. This implies the subsequent treatment of the surfaces that were in contact with the supports, usually by the grinding method (Fig. 3a). It is also necessary to make technological threads for the later removal of the mold from the tool housing (Fig. 3b).

a)

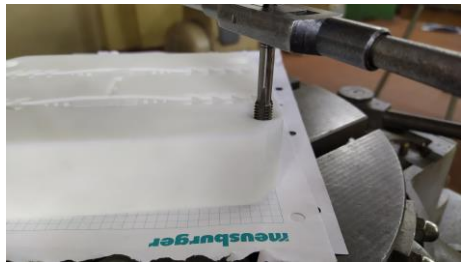

b)

Figure 3. *a) Tapping technological threads and b) grinding of the support surfaces*

As for the tool housing, standard modular tool was used from the manufacturer Meusburger. In order to achieve greater flexibility and reduce the cost of the tool, a plate used for positioning the ejector was also made using additive technologies (Fig. 4). The used standard modular housing is designed so that the complete sub-assembly consisting of the mold and ejector system can be replaced with great ease. In this way, if the mold is damaged, it can be replaced very efficiently.

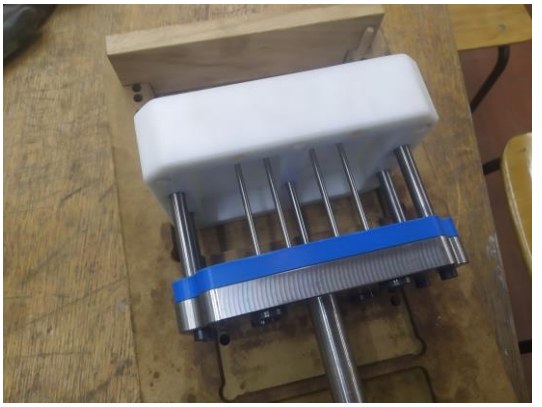

Figure 4. *Assembling the ejector with the mold*

The mold in the sub-assembly with the ejector system is attached to the core side of the tool (Fig. 5a). In the cavity side of the tool, a flat insert (mold) made of aluminum is formed, in the center of which there is a sprue bush (Fig. 5b). Tool tempering was performed only on the side of the mold produced by additive technologies. The cooling system is formed so that the coolant passes through both - the modular housing and the mold.

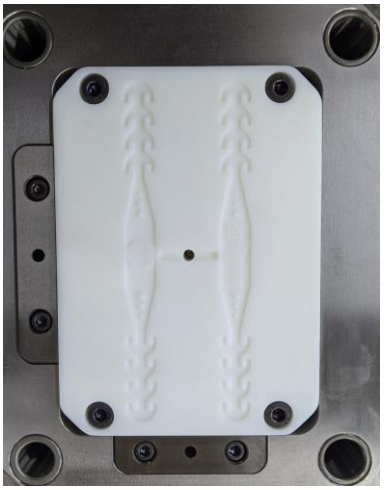

a)

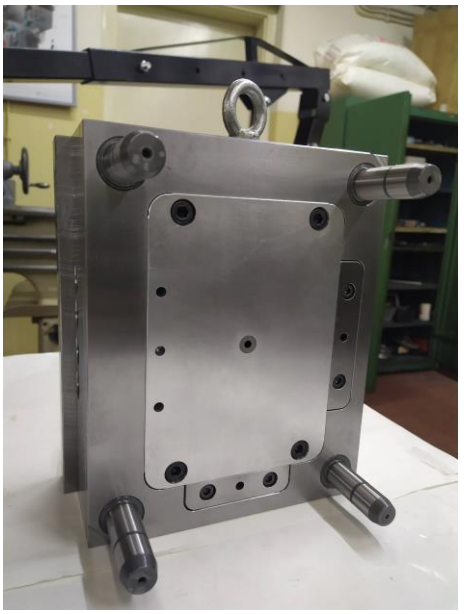

b)

Figure 5. *a) Core and b) cavity side of the molding tool*

The injection molding experiments were formed so that polypropylene was chosen as the desired material for the face mask carrier.

4 RESULTS

Since working with polymer molds is still an unknown, the correct selection of injection pressure can be challenging. In the experiment.

After reaching the desired melting temperature (205 °C), as well as tempering the tool, the experiments were started with lower values of pressures, to establish the lower limit. This led to incomplete mold cavity filling (Fig. 6a). After the upper pressure limit was established, the injected melt volume was exceeded. As a result, there was flashing on the parting surface on a large scale (Fig. 6b).

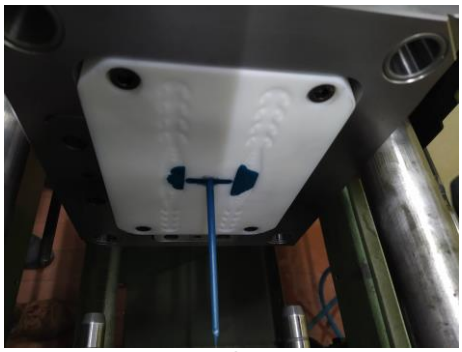

a)

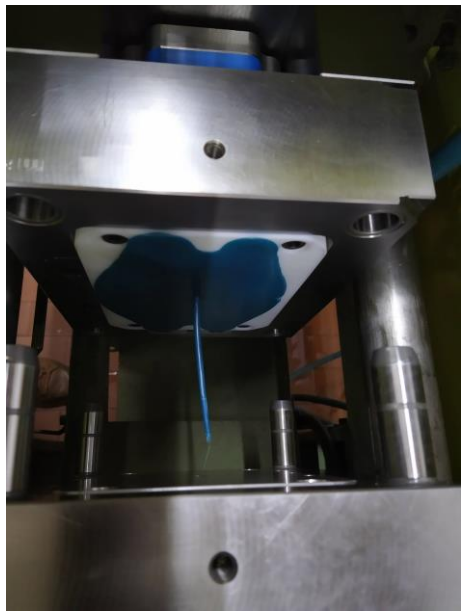

b)

Figure 6. *a) Insufficient filling of the mold cavity and b) flashing on the parting surface*

After gradually adjusting the injection pressure (Fig. 7)., a part was obtained that fully meets the set criteria. After 100 injection cycles, where two parts are obtained in one cycle, there was no damage to the mold cavities.

When comparing the time necessary for the correct selection of the injection parameters in which the desired part is obtained (Fig. 8) and the cost of making the mold itself using additive technologies with the conventional way of making tools for injection molding, the conclusion is reached that the application of injection molding can be reduced to individual or small batch production.

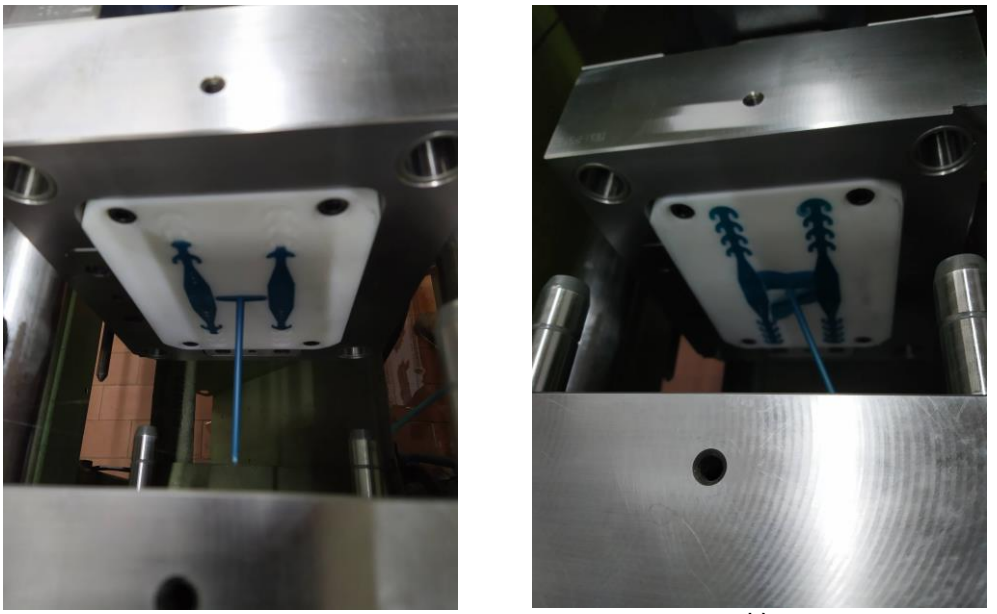

a) b)

Figure 7. *a) Insufficient filling of the mold cavity and b) flashing on the parting surface*

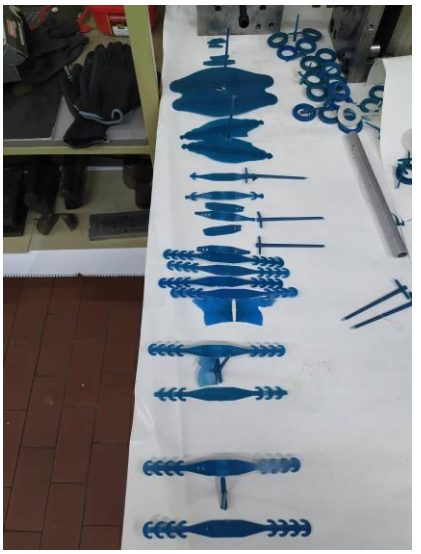

Figure 8. *Iterative reporting of obtained parts during the experiment*

5 CONCLUSION

The application of additive technologies with the appearance of newer materials, which have better and better physical and mechanical properties, plays an increasingly important role in production engineering as a whole.

When talking about the application of additive technologies in the field of

injection molding, experiments have established that parts of the desired shape and dimensional accuracy can be obtained with great certainty.

The conclusion is that in the coming period, injection molding can not only be used in mass production, but will slowly take its place in individual and small-batch production, especially when a small mass of product is required.

REFERENCES

[1] J. S. Hyatt & J. W. Hyatt. (1872). U.S. Patent No. 133229. United States Patent Office.

[2] Williams, C. B., Mistree, F., & Rosen, D. W. (2011). A functional classification framework for the conceptual design of additive manufacturing technologies. Journal of Mechanical Design, 133(12).

[3] Rakov, D. L., & Sukhorukov, R. Y. (2021). Classification and analysis of additive technologies based on the morphological approach. *Journal of Machinery Manufacture and Reliability*, *50*(7), 616-621.

[4] Frandsen, C. S., Nielsen, M. M., Chaudhuri, A., Jayaram, J., & Govindan, K. (2020). In search for classification and selection of spare parts suitable for additive manufacturing: a literature review. *International Journal of Production Research*, *58*(4), 970-996.

[5] Kadir, A. Z. A., Yusof, Y., & Wahab, M. S. (2020). Additive manufacturing cost estimation models—a classification review. *The International Journal of Advanced Manufacturing Technology*, *107*(9), 4033-4053.

[6] Korotchenko, A., Khilkov, D., Tverskoy, M., & Khilkova, A. (2020). Use of additive technologies for metal injection molding. *Engineering Solid Mechanics*, *8*(2), 143-150.

[7] Lozano, A. B., Álvarez, S. H., Isaza, C. V., & Montealegre-Rubio, W. (2022). Analysis and Advances in Additive Manufacturing as a New Technology to Make Polymer Injection Molds for World-Class Production Systems. *Polymers*, *14*(9), 1646.

[8] Huang, R., Riddle, M. E., Graziano, D., Das, S., Nimbalkar, S., Cresko, J., & Masanet, E. (2017). Environmental and economic implications of distributed additive manufacturing: the case of injection mold tooling. *Journal of Industrial Ecology*, *21*(S1), S130-S143.

[9] Schuh, G., Bergweiler, G., Lukas, G., & Oly, M. (2020). Towards Temperature Control Measures for Polymer Additive Injection Molds. *Procedia CIRP*, *93*, 90-95.

[10] Garcia, J. L., Koelling, K. W., Xu, G., & Summers, J. W. (2004). PVC degradation during injection molding: Experimental evaluation. *Journal of Vinyl and Additive Technology*, *10*(1), 17-40.

[11] Rajamani, P. K., Ageyeva, T., & Kovács, J. G. (2021). Personalized mass production by hybridization of additive manufacturing and injection molding. *Polymers*, *13*(2), 309.

[12] Paganin, L. C., & Barbosa, G. F. (2020). A comparative experimental study of additive manufacturing feasibility faced to injection molding process for polymeric parts. *The International Journal of Advanced Manufacturing Technology*, *109*(9), 2663-2677.

[13] Dinu, E., Besnea, D., Ping, A. S., Spanu, A., Moraru, E., & Panait, I. (2020, September). Device for Injection Molding Realized by Additive Technologies. In *International Conference of Mechatronics and Cyber-Mixmechatronics* (pp. 139-148). Springer, Cham.

COMETa 2022
6th INTERNATIONAL SCIENTIFIC CONFERENCE
17th - 19th December 2022
Jahorina, B&H, Republic of Srpska
University of East Sarajevo
Faculty of Mechanical Engineering
Conference on Mechanical Engineering Technologies and Applications

CORRELATION BETWEEN MICRO-CUTTING AND STATIC INDENTATION

Miloš Pjević[1], Mihajlo Popović[2], Radovan Puzović[3]

Abstract: Micro-cutting as a material processing process is completely different from classic macro cutting. Defining the mechanism of micro-cutting is one of the goals followed by the world's researchers. One of the most common approaches so far is the identification of micro-cutting with the static indentation of an indenter, which is the subject of this paper. In the case of micro-cutting of brittle materials, where the presence of its destruction during processing is pronounced, by static indentation it is possible to establish which types of cracks occur inside the material. Another important thing is that with this method it is also possible to define the critical penetration depth below which brittle materials can be processed by the mechanism of plastic deformation.

Key words: Critical penetration depth, Micro-cutting, Brittle materials, Static indentation.

1 INTRODUCTION

With the history of over 100 years old, cutting technology represent one of the most common used technics in the processing industries. Accumulated knowledge during this period, provided the possibility to interduce such algorithms for cutting parameters. Outputs are cutting parameters in the form of cutting depth, speeds and feeds, and also adaptive tool path which maintains constant angle of cutting. The result is more stable cutting with less vibration of the tool and part setup, and also higher tool life. All of this cannot be possible without detailed knowledge of the mechanism of the macro-cutting.

With exponential increase of the demand defined by the market, more often micro-cutting must be applied during the processing process. With dimensional

[1] dr Miloš Pjević, Assistant Professor, Faculty of Mechanical Engineering, University of Belgrade, Belgrade, Serbia, mpjevic@mas.bg.ac.rs
[2] dr Mihajlo Popović, Associate Professor, Faculty of Mechanical Engineering, University of Belgrade, Belgrade, Serbia, mpopovic@mas.bg.ac.rs
[3] dr Radovan Puzović, Full Time Professor, Faculty of Mechanical Engineering, University of Belgrade, Belgrade, Serbia, rpuzovic@mas.bg.ac.rs

reduction, it is established that well known mechanisms of the macro-cutting cannot be applied on the micro-cutting. In addition, machining the parts with brittle properties, new cutting mechanism must be defined.

Although research on this topic has been going on since the mid-seventies of the last century [1-4], in the last years, big breakthrough is achieved in the field of micro cutting of the brittle materials [5-12]. One of the proposed mechanisms that describes phenomenon that occurs in the micro cutting process is based on the static indentation.

2 MICRO CUTTING MECHANISM BASED ON THE STATIC INDENTATION

The static indentation is one of the used methods that can be used for possible identification of the phenomenon that occurs during micro-cutting.

The method consists of two phases. The first phase represents the indentation of the diamond tool (indenter) into the workpiece, while the second phase refers to the microscopic observation of the footprint formed on the surface of the workpiece (Fig. 1).

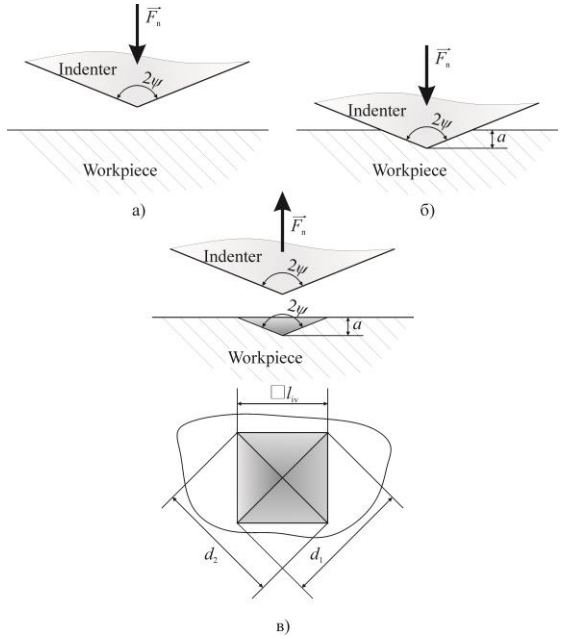

Figure 1. *Static indentation process*

In this method, only the normal force exerted by the indenter on the workpiece is present. Appropriate results can be obtained with this method, however, not including the tangential component of the cutting force leads to the fact that it is not possible to precisely define the micro-cutting mechanism of brittle materials with certainty. On the other hand, with this method, it is possible to roughly determine the range in which cracks can appear under the action of the appropriate pressing force, and it is known that cracks are an inevitable phenomenon in the process of the formation of chips due to the processing of brittle materials.

Depending on the value of the indentation force, i.e. the depth of penetration of the indenter, three phenomena are possible on the surface of the material (Fig. 2).

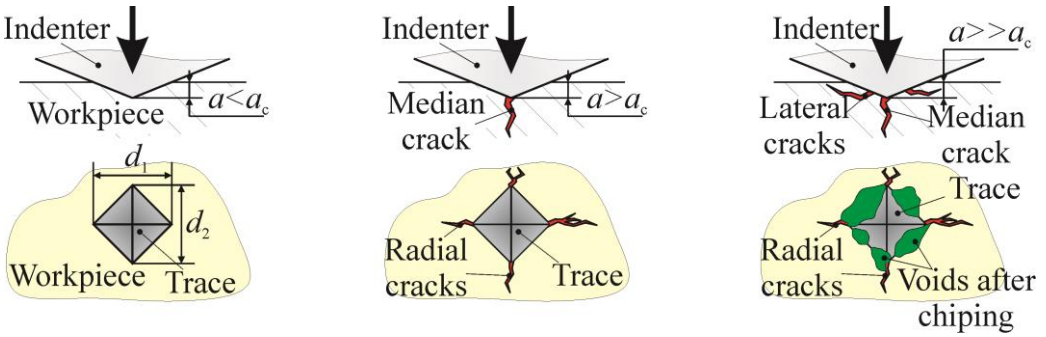

Figure 2. *Static indentation process*

The first case represents a trace that was created without the presence of material destruction. In the next case, with an increase of the penetration depth, the formation of cracks inside the material can be observed, while in the last case, separation of the material was also observed.

3 EXPERIMENTAL SETUP

In order to evaluate proposed mechanism that is based on the static indentation, experiments were conducted on the micro hardness tester presented in Fig. 3.

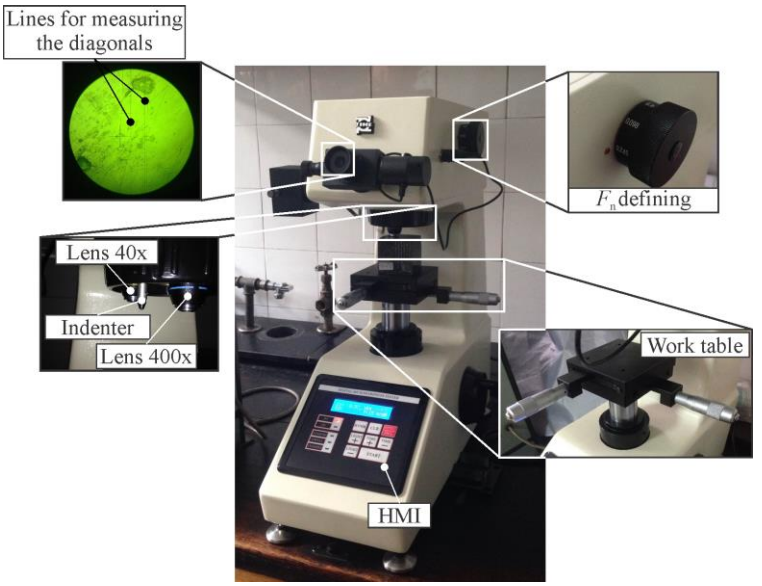

Figure 3. *Experimental setup.*

Material that is tested is marble Plavi tok. To determine critical penetration depth, below which there is no presence of the cracks in the material, indentation force was varied in the range from 0.098 [N] up to 9.807 [N]. Every test is repeated four times for dwell time T=0 and T=15 [s].

4 RESULTS

In the Fig. 4, there are some of the traces made by the indenter. At lower penetration depth there is a clear sign that there no evidence of the crack formation within the workpiece. This shows that brittle material can be machined without its destruction in the so-called ductile mode. When transition from ductile to brittle fracturing mode occurs, within material, formation of the median, radial and lateral cracks is present.

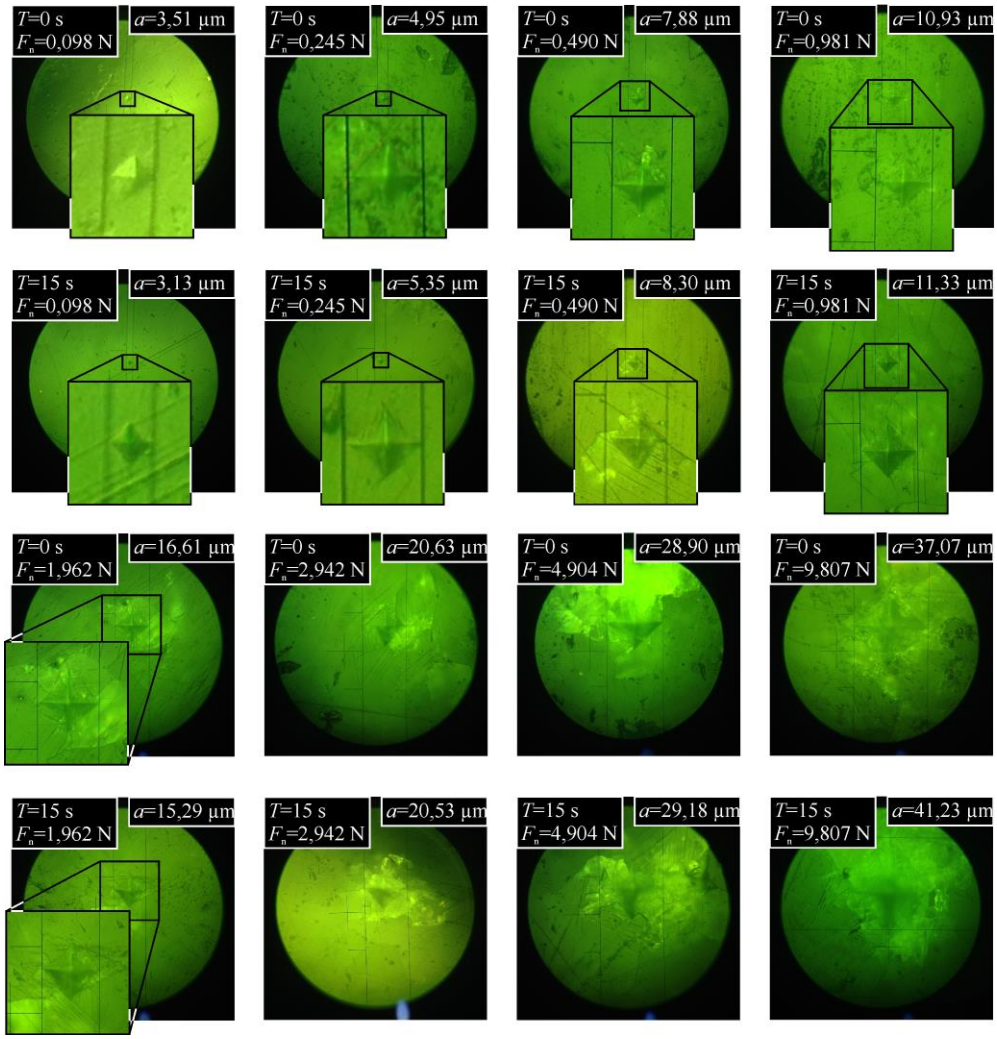

Figure 4. *Formed traces by the indenter.*

In Figure 4, it is clear that case 1 can be seen at lower penetration depths (5.73 µm). At this stage, there are no signs of cracking within the material. In case 1, the material is purely plastically deformed, i.e., the depth of penetration has not exceeded its critical value. Exceeding the critical penetration depth, case 2 occurs, in which the process of formation of cracks (median and radial) is noticeable. Case 2 is within the limits of the penetration depth of 11.33 µm. Beyond this depth, case 3 occurs, in which

the previously mentioned cracks are joined by lateral cracks that lead to the separation and destruction of the material.

When compared with single grit micro-cutting, presented in the Fig. 5, it can be told that the same cracks appear during static indentation, as well as possibility to obtain ductile mode.

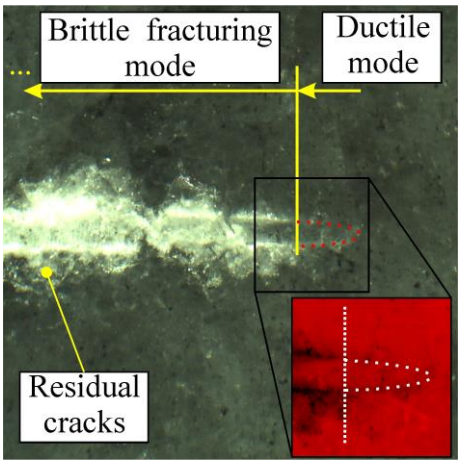

Figure 4. *Formed traces by the indenter.*

5 CONCLUSION

Conducting static indentation experiment on the brittle material, can be used in order to evaluate the types of the cracks that occur within the material itself during micro-cutting in the brittle fracturing mode. In addition, critical penetration depth that separate brittle fracturing mode and ductile mode can be established. On the other hand, static indentation can be also used to determine, is there presence of the ductile mode when machining brittle materials.

One of the downsides of this kind of mechanism proposal, is that there is no presence of the tangential components of the cutting force that can further induce crack growth within the material, and also orientate their growth direction.

REFERENCES

[1] Lawn, B., & Wilshaw, R. (1975). Indentation fracture: principles and applications. *Journal of materials science*, *10*(6), 1049-1081.

[2] Evans, A. G., & Wilshaw, T. R. (1976). Quasi-static solid particle damage in brittle solids—I. Observations analysis and implications. *Acta Metallurgica*, *24*(10), 939-956.

[3] Lawn, B. R., & Evans, A. G. (1977). A model for crack initiation in elastic/plastic indentation fields. *Journal of Materials Science*, *12*(11), 2195-2199.

[4] Marshall, D. B., & Lawn, B. R. (1979). Residual stress effects in sharp contact cracking. *Journal of Materials Science*, *14*(8), 2001-2012.

[5] Malkin, S., & Hwang, T. W. (1996). Grinding mechanisms for ceramics. *CIRP annals*, *45*(2), 569-580.

[6] Subhash, G., Loukus, J. E., & Pandit, S. M. (2002). Application of data dependent systems approach for evaluation of fracture modes during a single-grit scratching. *Mechanics of materials*, *34*(1), 25-42.
[7] Ghosh, D., Subhash, G., Radhakrishnan, R., & Sudarshan, T. S. (2008). Scratch-induced microplasticity and microcracking in zirconium diboride–silicon carbide composite. *Acta Materialia*, *56*(13), 3011-3022.
[8] Anton, R. J., & Subhash, G. (2000). Dynamic Vickers indentation of brittle materials. *Wear*, *239*(1), 27-35.
[9] Ghosh, D., Subhash, G., Sudarshan, T. S., Radhakrishnan, R., & Gao, X. L. (2007). Dynamic indentation response of fine-grained boron carbide. *Journal of the American Ceramic Society*, *90*(6), 1850-1857.
[10] Subbiah, S., & Melkote, S. N. (2007). Evidence of ductile tearing ahead of the cutting tool and modeling the energy consumed in material separation in micro-cutting.
[11] Chiaia, B. (2001). Fracture mechanisms induced in a brittle material by a hard cutting indenter. *International Journal of Solids and structures*, *38*(44-45), 7747-7768.
[12] Yuanqiang, T., Dongmin, Y., & Yong, S. (2008). Study of polycrystalline Al2O3 machining cracks using discrete element method [J]. *International Journal of Machine tool & Manufacture*, *48*(9), 975-982.
[13] Pjević M. (2019). Investigation of the tool tip radius and the cutting speed influence on the quality indicators in the micro cutting materials based on marble and granite – Doctoral Dissertation. *University of Belgrade, Faculty of Mechanical Engineering, Belgrade, Serbia*, *in Serbian*.

COMETa 2022
6th INTERNATIONAL SCIENTIFIC CONFERENCE
17th - 19th November 2022
Jahorina, B&H, Republic of Srpska
University of East Sarajevo
Faculty of Mechanical Engineering
Conference on Mechanical Engineering Technologies and Applications

TOOL GEOMETRY EFFECT ON MATERIAL FLOW AND MIXTURE IN FSW

Nada Ratković[1], Živana Jovanović Pešić [2], Dušan Arsić [3], Miloš Pešić [4], Dragan Džunić [5]

Abstract: FSW is a solid-state joining process. It is widely used for joining hard alloys like steel, titanium, and aluminum which are very difficult to join by fusion welding. FSW joint quality is mainly influenced by shoulder and pin geometry, its diameter, tool material, tool rotation speed, and linear traveling speed. The paper presents a brief overview of the tools used during the FSW procedure. The influence of the tool pin on the material flow and mixture was analyzed in detail. In addition, the primary and secondary material flow and how it is affected by the shape and dimensions of the tool pin are also discussed.

Key words: FSW, FSW tool, material flow

1 INTRODUCTION

Friction Stir Welding (FSW) also called "friction welding with a tool" is one of the advanced types of welding technology. Since it was patented (in 1991 at the TWI Institute, Cambridge) until today, this procedure has been developed and has reached a dynamic and wide field of application [1,2]. It is represented in the production processes of various industries: aviation, railway, military, automobile, etc. [3,4].

FSW process enables plate materials welding in all possible positions. It is also possible to join different materials [5]. It is particularly important that hard-to-weld materials, such as aluminum alloys, can be welded with high quality. It is possible to

[1] Nada Ratković, Associate Professor, Faculty of Engineering University of Kragujevac, Kragujevac, Serbia, nratkovic@ kg.ac.rs
[2] Živana Jovanović Pešić, Research Assistant, Faculty of Engineering University of Kragujevac, Kragujevac, Serbia, zixi90@gmail.com
[3] Dušan Arsić, Assistant Professor, Faculty of Engineering University of Kragujevac, Kragujevac, Serbia, dusan.arsic@fink.rs
[4] Miloš Pešić, Junior Research Assistant, Institute for Information Technologies University of Kragujevac, Kragujevac, Serbia, milospesic@uni.kg.ac.rs
[5] Dragan Džunić, Assistant Professor, Faculty of Engineering University of Kragujevac, Kragujevac, Serbia, dzuna@kg.ac.rs

obtain a welded joint with excellent mechanical characteristics, which exceeds the strength of the base material (BM). At the beginning of the application of this procedure, only straight line connections were made, and later curvilinear ones, including circular ones.

The physical essence of the joint formation process itself is the same as in ordinary (conventional) friction welding. However, heat is not released by friction directly between the contact surfaces of the parts to be joined, but indirectly, using a special tool.

2 TOOL GEOMETRY

Tool geometry represents a very important and most influential parameter of the FSW process. The tool consists of two concentric parts: the supporting part and the working part. The tool is cylindrical in shape (Fig. 1). The supporting part is the body, and the working part is the pin of the tool. The pin has a smaller diameter and is usually conical in shape, and it can be threaded, grooved, and similar.

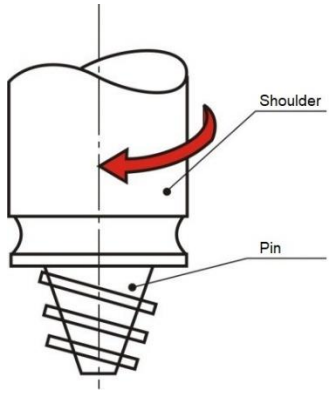

Fig.1 *FSW tool [6]*

The pin of the tool first comes into contact with the elements that need to be joined (plates). After that in welding plates keyhole is formed. The formation of the keyhole is achieved by penetrating through both welded elements until the tool shoulder achieves contact with the upper surface of the plates.

The shoulder of the tool needs to keep the material inside the welding zone. This can be enabled with a sufficiently large pressure from the tool shoulder on the front surfaces of welding plates. The tool shoulder can be with a flat or profiled surface of different configurations. The shape of the shoulder profile can be with scrolled, knurled, ridged, grooved, or a concentric circles (Fig. 2).

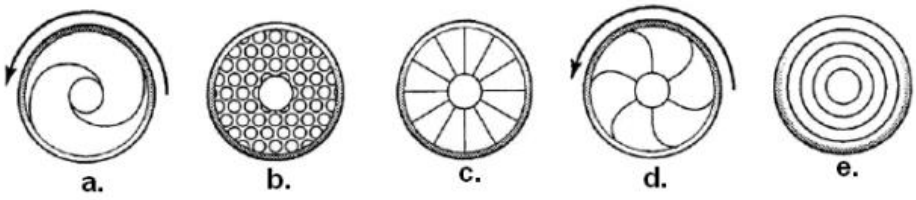

Fig. 2 *Shapes of the tool shoulder profile for the FSW process can be: a. scrolled, b. knurled, c. ridged, d. grooved, e. concentric circles [7]*

A featured shoulder advantage is due to better friction, which contributes to better generation and conduction of heat, as well as a better mixture of materials. The concave profile of the tool shoulder is designed to provide a "reservoir" of the material above the surface of the weld face, facilitate material flow around the tool and reduce plate thickness in the weld zone. In this way, a smooth and flat weld face is achieved thanks to the featured shoulder.

The shape of the tool pin and its dimensions, the length of the pin, the diameter, the tilt angle of the tool, the depth of immersion of the tool, the vertical force of the tool, the thickness of the weld plates, and a number of other factors affect the properties of the welded joint.

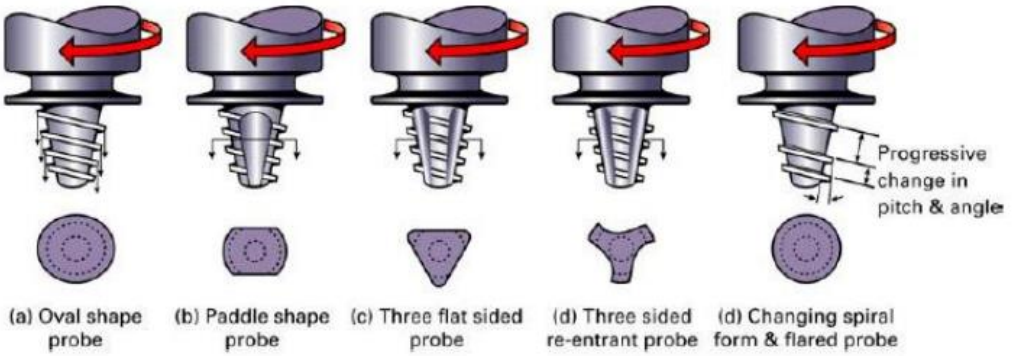

Fig. 3 *Profiled tool pin shapes for FSW process [7]*

The spirally profiled tool pin (Fig. 3) ensures good friction and material mixture, pushing it down so that a high-quality weld face is obtained, especially if the tool with three spiral flutes is used (Fig. 4).

Fig. 4 *Tool for FSW process with three spiral flutes [6]*

The pin profile of this tool is designed to reduce the weight of the tool and allow better material mixture. There are also tools with different geometrical pin shapes such as triangular, square, polygonal, and similar (Fig. 5).

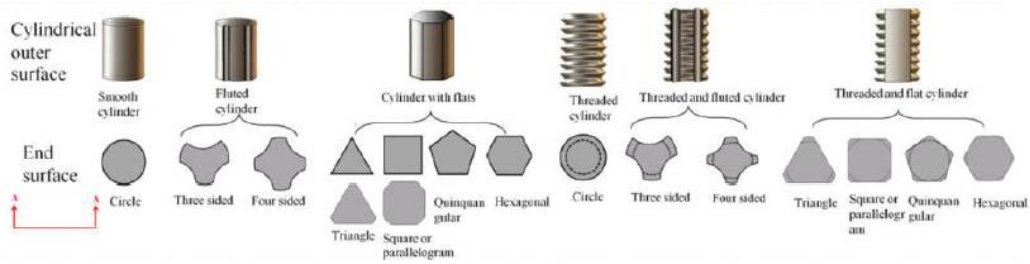

Fig. 5 *Tools with different pin shapes [8]*

For lap welding of aluminum alloy sheets, a multi-stage tool has been developed, the pin of which is a pentagonal profile (Figure 6) with reduced diameter, so that it achieves a good material mixture and does not reduce the thickness of the joint thanks to the concave profile of the tool shoulder.

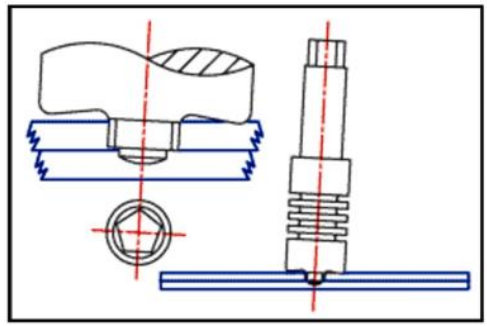

Fig. 6 *Schematic of the multi-stage tool for the FSW process [6]*

Geometric adjustments are necessary for the FSW tool in order to make the welding process more efficient. The tool should be set to a small leading angle in relation to the workpiece normal (1° - 3°), thus the axis is slightly inclined in relation to the axis of the machine spindle (Fig. 7). Asymmetric position of the tool pin enables a better flow and mixture of the material.

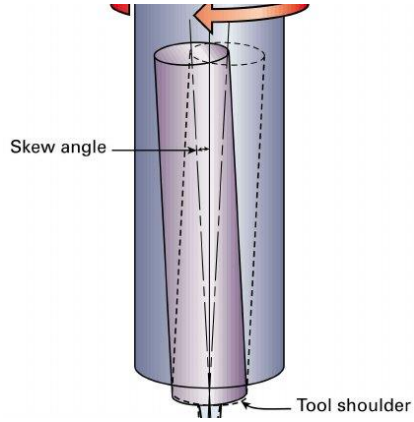

Fig. 7 *Schematic of the asymmetric tool for the FSW process [8]*

3 MATERIAL FLOW AND MIXTURE DURING THE FSW PROCESS

The FSW process is characterized by three-dimensional material flow (translational, rotational, and vertical). By researching the process itself, it was determined that the material flow can be described by two components: primary and secondary.

Primary flow refers to the material flow around the tool pin. This flow is analogous to the laminar flow of liquid around a rotating cylinder (Fig. 8). The shape of the tool pin determines the stream flow, both in the longitudinal and the vertical direction. Fig. 9 shows a simplified schematic of the two-dimensional material flow around the tool pin during the FSW process.

The tool pin thread is designed to push the material vertically down toward the root of the weld, thereby causing a vertical component of material flow.

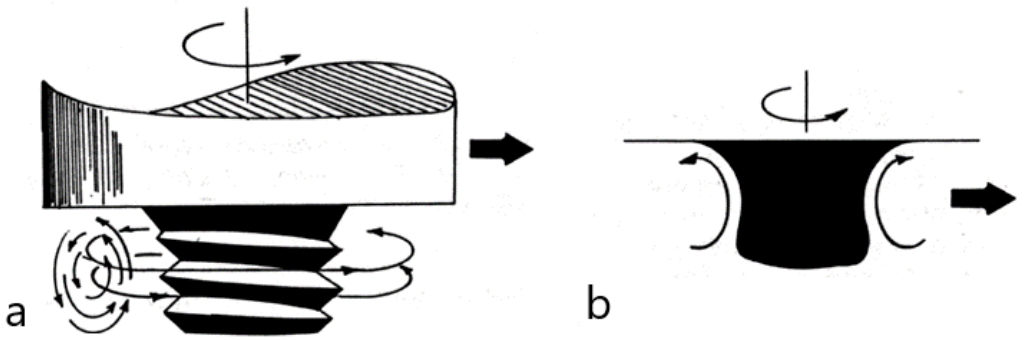

Fig.8 *Scheme of material flow around the tool pin during the FSW process a - turbulent flow, b - laminar flow [6]*

Additional vertical material flow occurs through the rotation of the tool shoulder. A part of the material immediately below the tool rotates around the top of the tool multiple times.

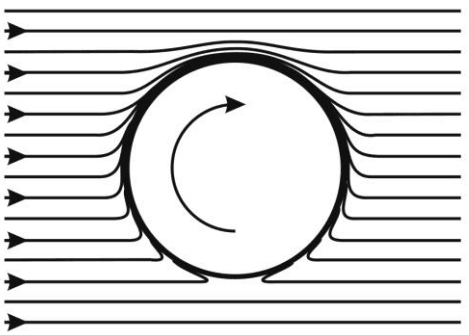

Fig.9 *Schematic of the two-dimensional material flow around the tool pin during the FSW process [6]*

Secondary material flow occurs when material that was previously located on the retreating side of the weld near the weld face flows and remains on the advancing side of the weld face. Secondary material flow is characteristic of thinner plates.

4 CONCLUSIONS

Given that FSW is a completely non-linear process, it is difficult to give a comprehensive, clear definition of material flow, because FSW does not allow geometric simplification due to its configuration. Geometric simplification is not possible because there is a complex three-dimensional flow and material mixture around the tip of the tool that is different on the advancing and retreating sides as well as in relation to the body of the tool. This points to the fact that there is neither a line nor a plane of symmetry to consider.

It is important to note that this represents a viscous-plastic material flow, created by the interaction of a solid body (tool) and a rigid base that supports the joint, and on the other side of the base material, which has basically elastic behavior. This means that there is a need for the so-called "hybrid" formulation that takes into account both phenomena, and is based on rigid body mechanics and fluid mechanics.

ACKNOWLEDGEMENT

This research is partly supported by the Ministry of Education and Science, Republic of Serbia, Grant 451-03-68/2022-14/ 200378, Grant III41007, and TR 35021.

REFERENCES

[1] Thomas, W.M., Nicholas, E.D., Needham, J.C., Murch, M.G., Templesmith, P., Dawes, C.J. (1991), G.B. Patent Application No.9125978.8.
[2] Dawes, C., Thomas W., (1995), TWI Bulletin 6, November/December, p. 124.
[3] Thomas, W.M., Nicholas, E.D. (1997) Friction stir welding for the transportation industries. *Mater Des*,18:269–73.
[4] Heidarzadeh, A., Mironov, S., Kaibyshev, R., Çam, G., Simar, A., Gerlich, A., Khodabakhshi, F., Mostafaei, A., Field, D.P., Robson, J.D., et al. (2021) Friction Stir Welding/Processing of Metals and Alloys: A Comprehensive Review on Microstructural Evolution., *Progress in Materials Science*, 117, 100752, doi:10.1016/j.pmatsci.2020.100752.
[5] Mishra, R.S., Ma Z.Y., (2005) Friction Stir Welding and Processing. *Materials Science and Engineering: R: Reports*, 50, 1–78, doi:10.1016/j.mser.2005.07.001.
[6] Ratković, N. (2009), *Friction welding process of machine parts of different shapes and materials* (in Serbian), PhD thesis, Faculty of Engineering, University of Kragujevac, Kragujevac.
[7] Meilinger, Á., Török I., (2013), The importance of Friction Stir Welding,Tool, *Production Processes and Systems*, vol. 6. No. 1., pp. 25-34.
[8] Zhang, Y.N., Cao, X., Larose, S., Wanjara, P. (2012) Review of Tools for Friction Stir Welding and Processing, *Canadian Metallurgical Quarterly*, 51, 250–261, doi:10.1179/1879139512Y.0000000015.

COMETa 2022
6th INTERNATIONAL SCIENTIFIC CONFERENCE
17th - 19th November 2022
Jahorina, B&H, Republic of Srpska
University of East Sarajevo
Faculty of Mechanical Engineering
Conference on Mechanical Engineering Technologies and Applications

TOOL GEOMETRY EFFECT ON MATERIAL FLOW AND MIXTURE IN FSW

Nada Ratković[1], Živana Jovanović Pešić [2], Dušan Arsić [3], Miloš Pešić [4], Dragan Džunić [5]

Abstract: FSW is a solid-state joining process. It is widely used for joining hard alloys like steel, titanium, and aluminum which are very difficult to join by fusion welding. FSW joint quality is mainly influenced by shoulder and pin geometry, its diameter, tool material, tool rotation speed, and linear traveling speed. The paper presents a brief overview of the tools used during the FSW procedure. The influence of the tool pin on the material flow and mixture was analyzed in detail. In addition, the primary and secondary material flow and how it is affected by the shape and dimensions of the tool pin are also discussed.

Key words: FSW, FSW tool, material flow

1 INTRODUCTION

Friction Stir Welding (FSW) also called "friction welding with a tool" is one of the advanced types of welding technology. Since it was patented (in 1991 at the TWI Institute, Cambridge) until today, this procedure has been developed and has reached a dynamic and wide field of application [1,2]. It is represented in the production processes of various industries: aviation, railway, military, automobile, etc. [3,4].

FSW process enables plate materials welding in all possible positions. It is also possible to join different materials [5]. It is particularly important that hard-to-weld materials, such as aluminum alloys, can be welded with high quality. It is possible to

[1] Nada Ratković, Associate Professor, Faculty of Engineering University of Kragujevac, Kragujevac, Serbia, nratkovic@ kg.ac.rs
[2] Živana Jovanović Pešić, Research Assistant, Faculty of Engineering University of Kragujevac, Kragujevac, Serbia, zixi90@gmail.com
[3] Dušan Arsić, Assistant Professor, Faculty of Engineering University of Kragujevac, Kragujevac, Serbia, dusan.arsic@fink.rs
[4] Miloš Pešić, Junior Research Assistant, Institute for Information Technologies University of Kragujevac, Kragujevac, Serbia, milospesic@uni.kg.ac.rs
[5] Dragan Džunić, Assistant Professor, Faculty of Engineering University of Kragujevac, Kragujevac, Serbia, dzuna@kg.ac.rs

obtain a welded joint with excellent mechanical characteristics, which exceeds the strength of the base material (BM). At the beginning of the application of this procedure, only straight line connections were made, and later curvilinear ones, including circular ones.

The physical essence of the joint formation process itself is the same as in ordinary (conventional) friction welding. However, heat is not released by friction directly between the contact surfaces of the parts to be joined, but indirectly, using a special tool.

2 TOOL GEOMETRY

Tool geometry represents a very important and most influential parameter of the FSW process. The tool consists of two concentric parts: the supporting part and the working part. The tool is cylindrical in shape (Fig. 1). The supporting part is the body, and the working part is the pin of the tool. The pin has a smaller diameter and is usually conical in shape, and it can be threaded, grooved, and similar.

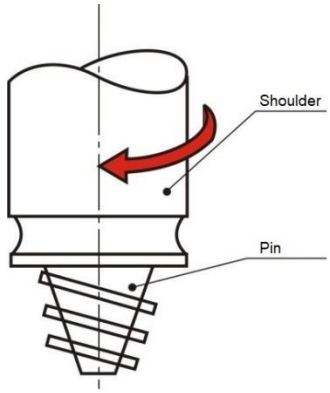

Fig.1 *FSW tool [6]*

The pin of the tool first comes into contact with the elements that need to be joined (plates). After that in welding plates keyhole is formed. The formation of the keyhole is achieved by penetrating through both welded elements until the tool shoulder achieves contact with the upper surface of the plates.

The shoulder of the tool needs to keep the material inside the welding zone. This can be enabled with a sufficiently large pressure from the tool shoulder on the front surfaces of welding plates. The tool shoulder can be with a flat or profiled surface of different configurations. The shape of the shoulder profile can be with scrolled, knurled, ridged, grooved, or a concentric circles (Fig. 2).

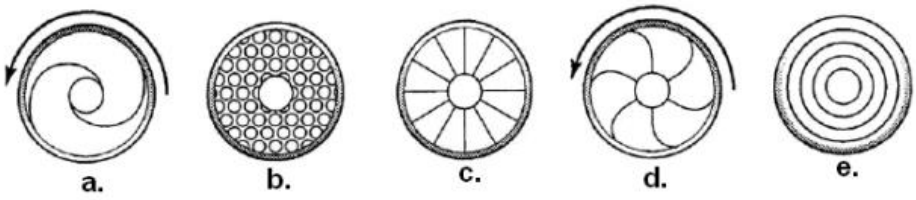

Fig. 2 *Shapes of the tool shoulder profile for the FSW process can be: a. scrolled, b. knurled, c. ridged, d. grooved, e. concentric circles [7]*

A featured shoulder advantage is due to better friction, which contributes to better generation and conduction of heat, as well as a better mixture of materials. The concave profile of the tool shoulder is designed to provide a "reservoir" of the material above the surface of the weld face, facilitate material flow around the tool and reduce plate thickness in the weld zone. In this way, a smooth and flat weld face is achieved thanks to the featured shoulder.

The shape of the tool pin and its dimensions, the length of the pin, the diameter, the tilt angle of the tool, the depth of immersion of the tool, the vertical force of the tool, the thickness of the weld plates, and a number of other factors affect the properties of the welded joint.

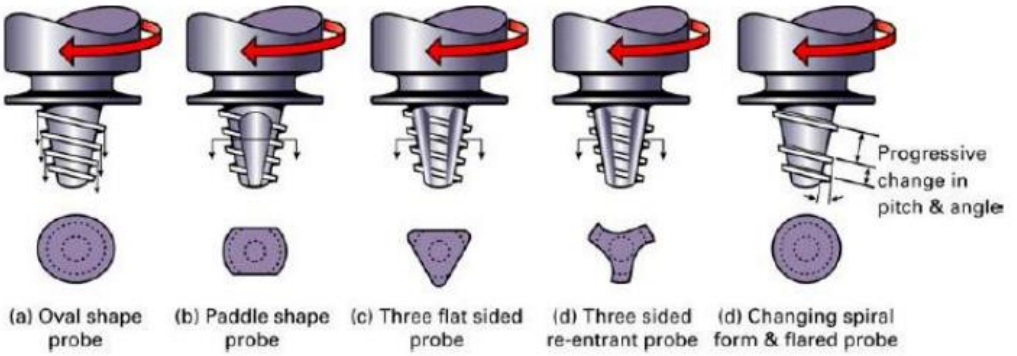

Fig. 3 *Profiled tool pin shapes for FSW process [7]*

The spirally profiled tool pin (Fig. 3) ensures good friction and material mixture, pushing it down so that a high-quality weld face is obtained, especially if the tool with three spiral flutes is used (Fig. 4).

Fig. 4 *Tool for FSW process with three spiral flutes [6]*

The pin profile of this tool is designed to reduce the weight of the tool and allow better material mixture. There are also tools with different geometrical pin shapes such as triangular, square, polygonal, and similar (Fig. 5).

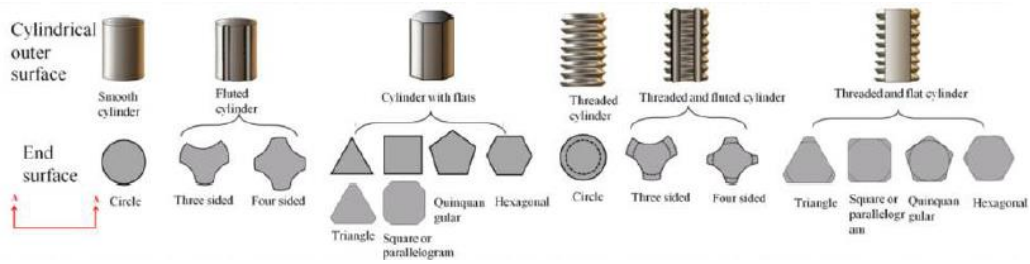

Fig. 5 *Tools with different pin shapes [8]*

For lap welding of aluminum alloy sheets, a multi-stage tool has been developed, the pin of which is a pentagonal profile (Figure 6) with reduced diameter, so that it achieves a good material mixture and does not reduce the thickness of the joint thanks to the concave profile of the tool shoulder.

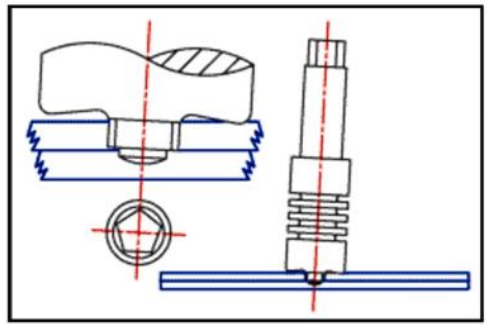

Fig. 6 *Schematic of the multi-stage tool for the FSW process [6]*

Geometric adjustments are necessary for the FSW tool in order to make the welding process more efficient. The tool should be set to a small leading angle in relation to the workpiece normal (1° - 3°), thus the axis is slightly inclined in relation to the axis of the machine spindle (Fig. 7). Asymmetric position of the tool pin enables a better flow and mixture of the material.

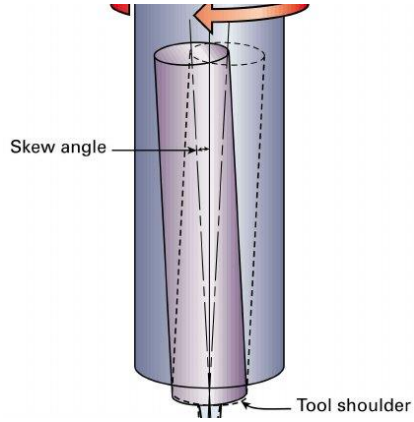

Fig. 7 *Schematic of the asymmetric tool for the FSW process [8]*

3 MATERIAL FLOW AND MIXTURE DURING THE FSW PROCESS

The FSW process is characterized by three-dimensional material flow (translational, rotational, and vertical). By researching the process itself, it was determined that the material flow can be described by two components: primary and secondary.

Primary flow refers to the material flow around the tool pin. This flow is analogous to the laminar flow of liquid around a rotating cylinder (Fig. 8). The shape of the tool pin determines the stream flow, both in the longitudinal and the vertical direction. Fig. 9 shows a simplified schematic of the two-dimensional material flow around the tool pin during the FSW process.

The tool pin thread is designed to push the material vertically down toward the root of the weld, thereby causing a vertical component of material flow.

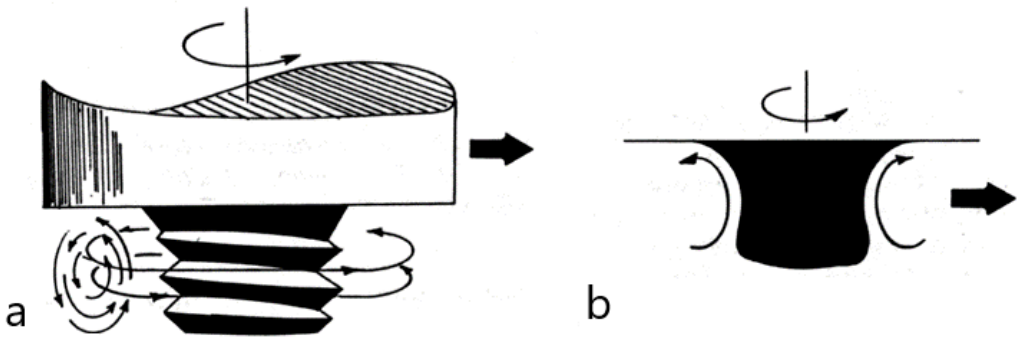

Fig.8 *Scheme of material flow around the tool pin during the FSW process a - turbulent flow, b - laminar flow [6]*

Additional vertical material flow occurs through the rotation of the tool shoulder. A part of the material immediately below the tool rotates around the top of the tool multiple times.

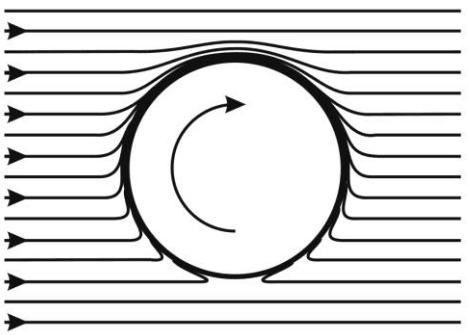

Fig.9 *Schematic of the two-dimensional material flow around the tool pin during the FSW process [6]*

Secondary material flow occurs when material that was previously located on the retreating side of the weld near the weld face flows and remains on the advancing side of the weld face. Secondary material flow is characteristic of thinner plates.

4 CONCLUSIONS

Given that FSW is a completely non-linear process, it is difficult to give a comprehensive, clear definition of material flow, because FSW does not allow geometric simplification due to its configuration. Geometric simplification is not possible because there is a complex three-dimensional flow and material mixture around the tip of the tool that is different on the advancing and retreating sides as well as in relation to the body of the tool. This points to the fact that there is neither a line nor a plane of symmetry to consider.

It is important to note that this represents a viscous-plastic material flow, created by the interaction of a solid body (tool) and a rigid base that supports the joint, and on the other side of the base material, which has basically elastic behavior. This means that there is a need for the so-called "hybrid" formulation that takes into account both phenomena, and is based on rigid body mechanics and fluid mechanics.

ACKNOWLEDGEMENT

This research is partly supported by the Ministry of Education and Science, Republic of Serbia, Grant 451-03-68/2022-14/ 200378, Grant III41007, and TR 35021.

REFERENCES

[1] Thomas, W.M., Nicholas, E.D., Needham, J.C., Murch, M.G., Templesmith, P., Dawes, C.J. (1991), G.B. Patent Application No.9125978.8.
[2] Dawes, C., Thomas W., (1995), TWI Bulletin 6, November/December, p. 124.
[3] Thomas, W.M., Nicholas, E.D. (1997) Friction stir welding for the transportation industries. *Mater Des*,18:269–73.
[4] Heidarzadeh, A., Mironov, S., Kaibyshev, R., Çam, G., Simar, A., Gerlich, A., Khodabakhshi, F., Mostafaei, A., Field, D.P., Robson, J.D., et al. (2021) Friction Stir Welding/Processing of Metals and Alloys: A Comprehensive Review on Microstructural Evolution., *Progress in Materials Science*, 117, 100752, doi:10.1016/j.pmatsci.2020.100752.
[5] Mishra, R.S., Ma Z.Y., (2005) Friction Stir Welding and Processing. *Materials Science and Engineering: R: Reports*, 50, 1–78, doi:10.1016/j.mser.2005.07.001.
[6] Ratković, N. (2009), *Friction welding process of machine parts of different shapes and materials* (in Serbian), PhD thesis, Faculty of Engineering, University of Kragujevac, Kragujevac.
[7] Meilinger, Á., Török I., (2013), The importance of Friction Stir Welding,Tool, *Production Processes and Systems*, vol. 6. No. 1., pp. 25-34.
[8] Zhang, Y.N., Cao, X., Larose, S., Wanjara, P. (2012) Review of Tools for Friction Stir Welding and Processing, *Canadian Metallurgical Quarterly*, 51, 250–261, doi:10.1179/1879139512Y.0000000015.

APPLIED MECHANICS AND MECHATRONICS

COMETa 2022
6th INTERNATIONAL SCIENTIFIC CONFERENCE
17th - 19th November 2022
Jahorina, B&H, Republic of Srpska
University of East Sarajevo
Faculty of Mechanical Engineering
Conference on Mechanical Engineering Technologies and Applications

STRUKTURNA ANALIZA I OPTIMIZACIJA IMPLANTATA KOJI SE KORISTE U SANIRANJU PRELOMA DUGIH KOSTIJU

Nikola Korunović[1], Jovan Aranđelović[2]

Rezime: Prelomi dugih kostiju, a naročito proksimalni prelomi butne kosti, često se saniraju upotrebom unutrašnje fiksacije. Ako su prelomi jednostavni i hirurzi iskusni, ovo je uglavnom rutinski proces. Međutim, ako su prelomi složeni i/ili hirurzi manje iskusni, postoji mnogo prostora za greške u izboru i pozicioniranju fiksatora. To može dovesti do otkaza fiksatora i potrebe za ponovljenim hirurškim zahvatom, što predstavlja dodatnu traumu za pacijenta. Na Mašinskom fakultetu Univerziteta u Nišu sprovedena su istraživanja iz kojih su proistekli metodi za strukturnu analizu i optimizaciju implantata namenjeni rešavanju navedenih problema. Pri tome su kreirani fleksibilni i robusni CAD modeli i modeli konačnih elemenata sklopa kosti i implantata, koji su dvosmerno asocijativni i mogu se koristiti u studijama osetljivosti i strukturnoj optimizaciji.

Ključne riječi: fiksator, metod konačnih elemenata, optimizacija structure, ortopedski, parametarski CAD model

STRUCTURAL ANALYSIS AND OPTIMIZATION OF IMPLANTS USED IN TREATMENT OF LONG BONES FRACTURES

Abstract: Long bone fractures, especially proximal femoral fractures, are often treated using internal fixation. If the fractures are simple and surgeons experienced, this is mostly a routine process. Nevertheless, if the fractures are complex and/or the surgeons are less experienced, there is a lot of space for error in fixator selection and positioning. This may lead to fixator failure and the need for an extra surgery, which represents an additional trauma for the patient. Research has been performed at University of Nis, Faculty of mechanical engineering, which yielded methods for structural analysis and optimization of implants that are intended for solving the aformentioned problems. Thereby, flexible and robust CAD and finite element models of bone-implant assemblies were created, which are bidirectinaly associative and may be used in sensitivity studies and structural optimization.

[1] Dr Nikola Korunovic, Faculty of Mechanical Engineering in Nis, Serbia, nikola.korunovic@masfak.ni.ac.rs

[2] Jovan Aranđelović, Faculty of Mechanical Engineering in Nis, Serbia, jovan.arandjelovic@masfak.ni.ac.rs

Key words: FEM, Fixator, Orthopedic, Parametric CAD model, Structural optimization

1 INTRODUCTION

Internal fixation is a well-established method for treatment of long bone fractures, especially those of the proximal femur. One of the devices used for this purpose is the Selfdynamisable internal fixator (SIF), patented by late prof. Mitkovic [1,2]. It is a medical device of a modular structure, extensively used in clinical practice. Although SIF failures are very rare, clinical studies showed that screw breaking occurred in 2.6% of the fixations and that the bar broke at the connection to the trochanteric unit in 0.3% cases [1]. These results showed that there was room for improvement in SIF durability [3]. In this context, for a known SIF configuration and position on the bone (Fig. 1), structural analysis was used to assess bone and fixator stresses and strains, which can be related to the fixator durability and the success of bone healing.

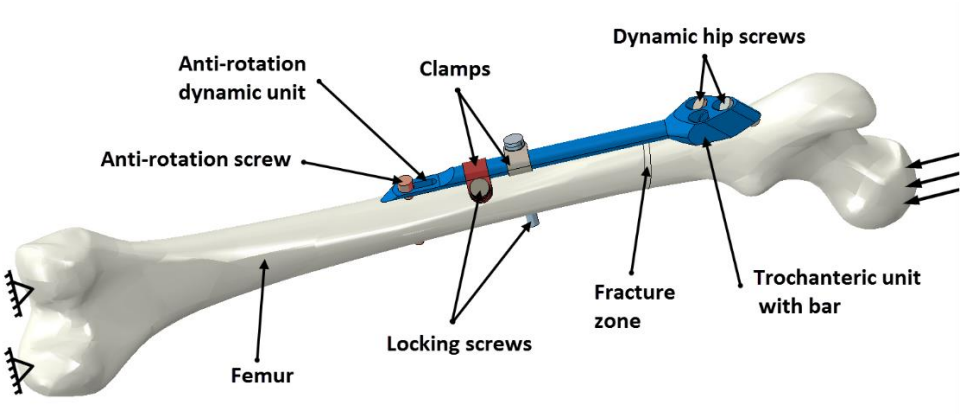

Figure 1. *SIF configuration and position on the bone when used in treatment of proximal femoral fractures*

CAD and FE models of femur used during the analysis were based on a subject-specific CT image set of lower extremities [4]. A number of anatomical landmarks (planes, axes, curves, points) [5] were created on the CAD model of the femur to serve as geometrical references for positioning of the fixator and for definition of boundary conditions and loads for finite element analysis (FEA). Thereby, assembly constraints were defined in such a way that flexibilility and robustness of femur-SIF assembly were achieved [3,6].

After the FE model (that was bidirectionally associated with CAD model) was built (Fig. 2), it was used in structural analysis, sensitivity analysis and structural optimization. Assembly constraints that were alowed to be changed during the surgery, were chosen as design variables [3,6]. Structural analysis results were interpreted to find the typical locations of maximum fixator stress (Fig. 3), which may be related to its durability. Response surface analysis results were used to assess the sensitivity of fixator stress to the change of design variables (Fig. 4) and come to general conclusions and recommendations considering fixator configuration. Structural optimization was used to find the optimal values of fixator dimensions, while simultaneously minimizing its maximum stress and mass [6].

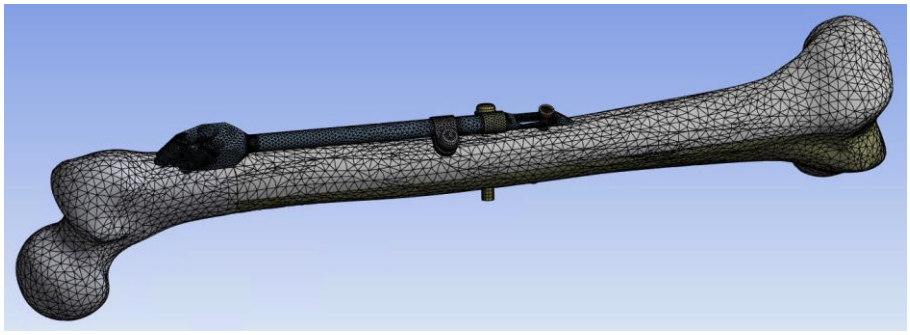

Figure 2. *FE model of femur-SIF assembly*

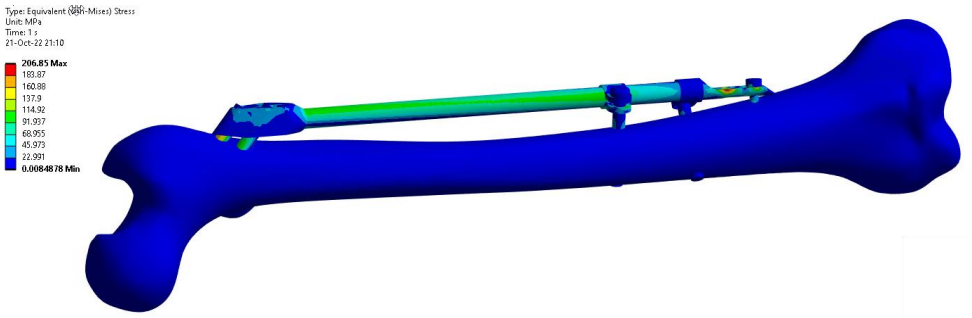

Figure 3. *Stresses of femur-SIF assembly for a given set of input parameters*

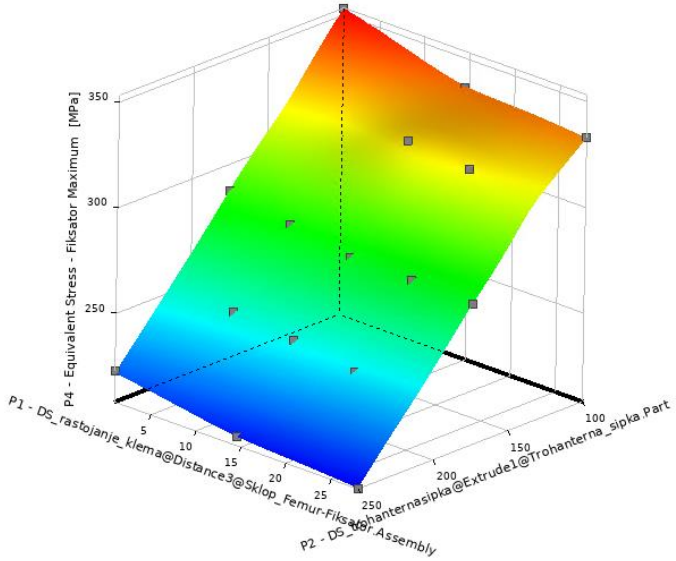

Figure 4. *Typical sensitivity of fixator stress to the change of input parameters*

Detailed description of CAD and FE models of femur-SIF assembly as well as the results of the aforementioned analyses are given in papers [3, 6-12].

ACKNOWLEDGEMENT

This research was financially supported by the Ministry of Education, Science and Technological Development of the Republic of Serbia (Contract No. 451-03-68/2022-14/ 200109).

LITERATURA

[1] Mitkovic M, Milenkovic S, Micic I, Mladenovic D, Mitkovic M (2012) Results of the femur fractures treated with the new selfdynamisable internal fixator (SIF). European journal of trauma and emergency surgery 38 (2):191-200
[2] Micic I, Mitkovic M, Park I-H, Mladenovic D, Stojiljkovic P, Golubovic Z, Jeon I-H (2010) Treatment of subtrochanteric femoral fractures using Selfdynamisable internal fixator. Clinics in orthopedic surgery 2 (4):227-231
[3] Korunovic N, Marinkovic D, Trajanovic M, Zehn M, Mitkovic M, Affatato S (2019) In silico optimization of femoral fixator position and configuration by parametric CAD model. Materials 12 (14):2326
[4] Petrovic S, Korunovic N (2018) Imaging in Clinical and Preclinical Practice. In: Biomaterials in Clinical Practice. Springer, pp 539-572
[5] Vitkovic N, Milovanovic J, Korunovic N, Trajanovic M, Stojkovic M, Mišic D, Arsic S (2013) Software system for creation of human femur customized polygonal models. Computer Science and Information Systems 10 (3):1473-1497
[6] Korunovic, N., & Arandjelovic, J. (2022). Structural Analysis and Optimization of Fixation Devices Used in Treatment of Proximal Femoral Fractures. In Personalized Orthopedics (pp. 503-533). Springer, Cham.
[7] Korunović, N., Stojković, M., Milovanović, J., Vitković, N., Trifunović, M., Manić, M., & Trajanović, M. (2016). Bioengineering and tire design related research at LIPS laboratory: A summary of results. Journal of Serbian Society for Computational Mechanics, 10(1), 71-101.
[8] Korunovic N, Trajanovic M, Mitkovic M, Vitkovic N, Stevanovic D (2015) A parametric study of selfdynamisable internal fixator used in femoral fracture treatment. Paper presented at the NAFEMS World Congress 2015 inc. the 2nd International SPDM Conference, San Diego, 21. - 24. June
[9] S.Vulovic, N.Korunovic, M.Trajanovic, N.Grujovic, N. Vitkovic , "Finite element analysis of CT based femur model using finite element program PAK" Journal of the Serbian Society for Computational Mechanics / Vol. 5 / No. 2, 2012 / pp. 160-166
[10] Korunovic N, Trajanovic M, Stevanovic D, Vitkovic N, Stojkovic M, Milovanovic J, Ilic D Material characterization issues in FEA of long bones. In: SEECCM III 3rd South-East European conference on computational mechanics—an ECCOMAS and IACM special interest conference, Kos Island, Greece, 2013. pp 12-14
[11] Korunovic N, Trajanovic M, Mitkovic M, Vulovic S (2010) From CT scan to FEA model of human femur. IMK-14-Istrazivanje i razvoj 16 (2):45-48 (In Serbian)
[12] Trajanović, M., Korunović, N., Milovanović, J., Vitković, N., Mitković, M. (2010). Application of computer models of mitković selfdynabizable internal fixator in rehabilitation of femur traumas. Facta universitatis, Series: Mechanical Engineering, 8(1), 27-38.

COMETa 2022
6th INTERNATIONAL SCIENTIFIC CONFERENCE
17th - 19th November 2022
Jahorina, B&H, Republic of Srpska
University of East Sarajevo
Faculty of Mechanical Engineering
Conference on Mechanical Engineering Technologies and Applications

DESIGN OF THE MECHATRONIC SYSTEM FOR ACCESS CONTROL TO PROTECTED AREAS OF PRODUCTION LINES

Goran Šiniković[1], Nenad Gubeljak[2], Emil Veg[3], Ivan Milanković[4], Mladen Regodić[5]

Abstract: One of the critical characteristics of machine plants is safety at work. Safety barriers are one of the measures to reduce risk at work. Barriers are often used when controlling access to zones of increased danger is necessary. The type of protection depends on the type of industrial plant, risk assessment, and applicable regulations. To achieve the desired functionality, proper application and complete integration of the protection system into an existing management system are necessary. The paper shows the structural solution of the protection system in the printing plant of the "Tetra Pak" company from Gornji Milanovac. The main requirement is to provide entry to the protected zone only after the entry request has been sent and processed. Another requirement is to stop the plant in a predefined position. To meet the requirements, it is necessary to determine the required SIL (System Integrity Level) from the reference standard and determine the electronic components properly. In addition, complete knowledge of all processes and cycles of the production line is necessary. Safety electrical components were used to implement the project: Safety PLC, Electromagnetic Safety Locks with Call buttons, Emergency-Stop buttons, and optoelectronic and inductive sensors.

Keywords: Safety el. components, Safety PLC, SIL (Sistem Integrity Level)

1 INTRODUCTION

Protective barriers are one of the measures that reduce the risk in plant operation. Their primary function is to provide working space, reduce the risk of injury to operators and workers who maintain the equipment, and increase safety at work. Protective barriers should prevent access to dangerous plant areas until the necessary conditions are met. Such protection is used in all branches of industry, especially in sectors with a high automation degree.

[1] Dr Goran Šiniković, UNI of Belgrade, Faculty of Mech. Engineering (CA), Serbia, gsinikovic@mas.bg.ac.rs
[2] Dr Nenad Gubeljak, UNI of Maribor, Faculty of Mechanical Engineering, Slovenia, nenad.gubeljak@um.si
[3] Dr Emil Veg, UNI of Belgrade, Faculty of Mechanical Engineering, Serbia, eveg@mas.bg.ac.rs
[4] Ivan Milanković, ivanmilankovic032@gmail.com
[5] Mladen Regodić, UNI of Belgrade, Faculty of Mechanical Engineering, Serbia, mregodic@mas.bg.ac.rs

This type of protection method depends on the needs of industrial plants, risk assessment and respective occupational safety regulations in place.

Such protection also has significant financial justification. Reducing workplace injuries affects a company's reputation and the costs associated with workers' injuries and insurance. By providing physical barriers around machines, production lines, and robots, companies protect their employees – an essential resource.

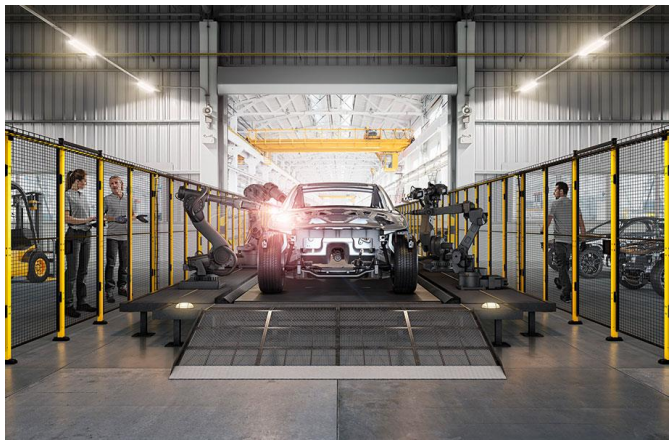

Figure 1. *Use of Protective barriers on robotic production lines in the automotive industry*

This paper communicates the implementation of this type of protection in the specific case of the press line in the company "Tetra Pak" from Gornji Milanovac. During the execution of this project, a safety programmable logic controller (Safety PLC), protective panels, electromagnetic safety locks with call buttons, and optoelectronic and inductive sensors were used.

2 STANDARDS AND SAFETY MEASURES APPLIED TO PROTECT ACCESS TO MACHINERY

One of the critical operating parameters of any machine is operational safety. Aiming to regulate this area, different standards and legal regulations were introduced. The most important standard in this field is ISO13849-1 [4]. Among other things, the standard covers the area of designing complex electrical, electronic and programmable systems with a safety function. The implementation of standards means that the system needs to be validated when designing a system and configuring its structure. In other words, the probability of system failure has to be calculated.

The very notion of the standard is related to machine security. Still, it is directly related to safety measures implemented to protect access to machines. The standard is based on a probabilistic approach for assessing the safety of control systems. The standard is mainly applied to electrical, electronic and programmable components.

Within the EN ISO 13849-1 standard, there are two protection structures, **PL** (Performance Level) and **SIL** (Safety Integrity Level). The requirements for choosing one of the listed structures depend on the user's needs and the industry branch where the standard is applied.

PL (Performance Level) is a technologically neutral concept that can be used

for electrical, mechanical, pneumatic, and hydraulic safety solutions. PL is a measure of the reliability of the safety function. It is divided into five levels, from **a** to **e**. The five PL levels (a-e) correspond to specific ranges of PFHD-values (probability of dangerous failure per hour). This parameter indicates how likely a dangerous failure will occur in one hour.

SIL (Safety Integrity Level) refers to the functional safety of electrical, electronic and programmable electronic control systems. SIL sets requirements for machine safety control. The reliability level of such a system is classified according to the safety integrity level (SIL) from **1** to **3**. If a safety circuit must comply with a specific SIL, the designer must calculate the probability of system failure in addition to constructing the system structure.

Table 1. *Relationship between performance level (PL) and Safety Integrity Level (SIL)*

PL	SIL
a	No correspondence
b	1
c	1
d	2
e	3

The PL of the system shall be determined by the estimation of the following aspects: Category (structural requirement), Mean time to dangerous failure (MTTFd), Diagnostic coverage (DC) and Common cause failure (CCF).

The design of safety-related parts of control systems is an iterative process completed in several steps.

2.1 Define the requirements of the safety functions

This is the most important step. First of all, the required properties must be defined for the safety functions. For safety gate guarding on a machine, for example, hazardous movements must be shut down when the safety gate is opened. It must not be possible for the machine to restart while the safety gate is open.

2.2 Determination of required performance level PLr

The greater the risk, the higher the requirements of the control system. The contribution of reliability and structure can vary depending on the technology used. The level of each hazardous situation is classified into five stages from **a** to e. With **a**, the **control function's contribution to risk reduction** is low, and with PL **e,** it is high. The risk graph can be used to determine the required Performance Level (PLr) for the described safety function.

According to EN ISO 13849-1, PLr is evaluated using three factors: severity of injury (S), frequency and/or exposure to hazard (F) and the possibility of avoiding hazard or limiting harm (P). Each of the factors has two possible values, 1 and 2. Once the factors S, F and P have been determined, PLr can also be determined

Figure 2 shows the graph based on which PLr (Performance Level Required) is determined for different levels of risk from low to high.

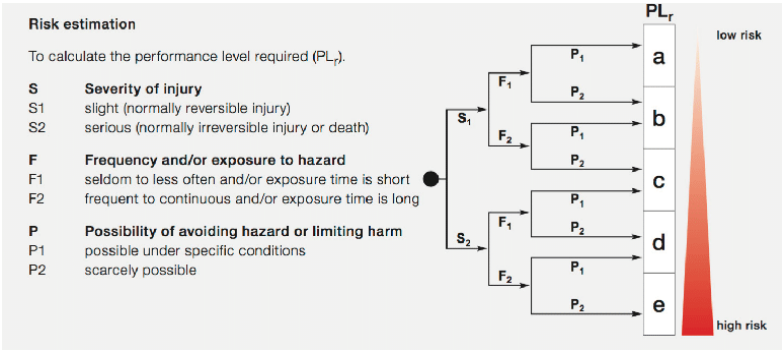

Figure 2. *Performance Level Required (PLr)*

2.3 Design and technical implementation of the safety functions

The safety function is separated into sensor, logic and actuator to determine the achieved Performance Level. Each of these subsystems contributes to the safety function. All the necessary performance data is available from the component producer. Producers provide a user-friendly calculation tool for this purpose.

2.4 Verification

This step determines how the achieved Performance Level matches the required Performance Level. The achieved PL must be greater than or equal to the PLr required from the risk assessment. This means a “green light” for the machine design.

2.5 Validation

Alongside the purely qualitative requirements for the design of safety systems, it is also important to avoid systematic failures. This happens during validation.

3 PROBLEM AND TECHNICAL REQUIREMENTS DEFINING

One of the basic technical requirements that the system should meet is to enable operators to access the plant only after the request has been sent and processed by the management system and the plant has been halted. Access permission cannot be obtained at an arbitrary production line time and position. It is necessary to bring the machines to the ‘‘best position’’ to stop the plants. By the most favourable position, we mean the position where the production line, after stopping and intervention, can be put into regular operation with minimal losses in time and material.

To meet the request, it is impossible to stop the plant immediately using the Emergency Stop button. It requires the use of complex electronic components. In the control program of the PLC, it is necessary to define the appropriate conditions for stopping the plant, i.e., a combination of input signals on the PLC.

In the first step, it is necessary to determine the Performance level required (PLr) to select system components properly. In the specific case, by entering parameters S, F and P into ABB Software Tool ***SISTEMA*** [6], we conclude that the required Performance level is **PLr-d/SIL-2**. Considering the high level of required PLr, it is necessary to use electronic components with a safety function – Safety PLC. In addition to standard control functions, the Safety PLC must carry out additional monitoring functions and ensure redundancy should there be any errors and failures,

both with peripherals and communication as well as with the central control unit. Safety PLCs usually contain a redundant microprocessor that takes over the function of the primary microprocessor in the event of failure.

The operation of the Safety PLC is based on the “protection layers” concept, which enables reaching the required level of protection. In industrial practice, it is most often PL-e/SIL-3. The protection layers include four parts: safety input modules, safety communication (data exchange network), safety (redundant) microprocessor, and safety output modules.

After selecting components, we must determine the realized PL for which we use software tools delivered by safety equipment manufacturers. Within those tools, there are libraries with parameter values for individual electronic components.

In this case, we used the Siemens ***Safety Evalution Tool*** to determine PL, i.e., SIL. By entering the parameters for the selected components, we determined that the achieved performance level was **PL-e/SIL-3**, which was above the required level.

4 DESIGN SOLUTION

The protective barrier system consists of a 40 m protective fence, 11 doors and 11 electromagnetic locks with buttons. It was designed to have manual buttons, microswitches and electromagnetic locks on the door. By pressing the manual button, the operator sends a request to the PLC to enter the protected area. The signals from the buttons go to the safety input modules. Through safety communication, they are forwarded to the CPU to be processed. Based on their states and the control program loaded into the working memory of the PLC, the output states in the safety output modules are set. The output modules are connected to the electromagnetic locks on the protective fences. When the conditions for safe entry and stay in the protected zone (defined in the PLC control program) are met, a signal is sent via the safety output module to the solenoid of the electromagnetic lock, which is then unlocked. After the intervention, the operator leaves the protected zone. Closing the door initiates contact with the microswitch of the lock. It sends a signal to the security input module as confirmation that the fence has closed. This confirmation is necessary to restart the plant. By starting the plant, all electromagnetic locks are locked, thus preventing any attempt to enter the secured area while the plant is in its operating mode.

4.1 System components description

After setting up the protection system concept, it is necessary to choose adequate components and equipment. These include a suitable safety programmable logic controller (Safety PLC), electromagnetic safety locks with call buttons, emergency-stop buttons, and optoelectronic and inductive sensors for determining the position of the rolls and protective panels.

The main criteria when choosing components are that they satisfy the safety function and the acceptable price.

4.1.1 Protective panels

The first step in the selection of components is the selection of protective fences - barriers. The company “AXELENTE” was chosen as the leader in producing this type of equipment [5]. One of the main reasons for choosing this type of fence is its high quality, easy assembly and disassembly, and high flexibility. The panels used have the catalogue number W321-220100.

4.1.2 Safety electromagnetic locks

Figure 3 shows an electromagnetic lock with call buttons and LED indication.

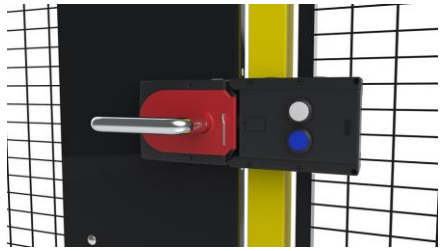

Figure 3. *Electromagnetic lock with a call button*

Figure 3 shows the blue button used for calling, i.e., approval of the control element to enter the safe zone. The white LED indicator shows the state when the lock is locked.

The lock has an intelligent system whose position is detected by RFID transponders. Such a device detects a signal in the lock mechanism that has a unique code. This prevents misuse of the system and enables the achievement of the highest safety category 4/PL-e according to EN ISO 13849-1, i.e., SIL 3 according to EN 62061.

There is a mechanical unlocking system under the lock itself, enabling it to be opened in the event of a power failure. The handle is made of a robust and easy-to-grip material that can be rotated 90 degrees.

4.1.3 PLC controler (SIEMENS ET 200 SP)

The main electronic component of the system is the PLC. For this project, we chose *Siemens ET 200 SP* [7]. The selected controller belongs to the class of the new generation of Siemens controllers, which offers several advantages. Firstly, there is a possibility of expansion of input and output modules and the integrated Safety card. Figures 4a and 4b show the selected Siemens controller model.

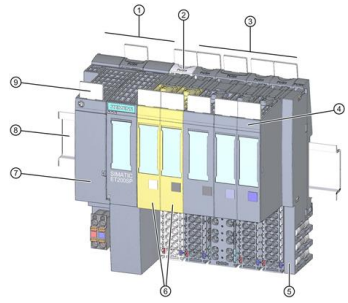

(a) (b)

Figure 4. *Siemens contoler ET 200 SP*

The PLC consists of the following components: 1. Interface module, 2. Network connection panel, 3. Voltage distribution by modules, 4. Input/output module, 5. Server module, 6. Safety input/output module, 7. Bus adapter, 8. DIN rail for PLC installation.

4.2 Security system structure

The entire Safety system works by opening any of the eleven doors, interrupting the closed door signal. This is achieved using two pairs of contacts located in the lock itself. The light indication on the lock is turned on by sending the signal that the door is open. Emergency Stop buttons are also part of the Safety system. Emergency Stop buttons and locks are connected via two channels to the PLC for safety reasons.

The built-in PLC has five Safety modules - three modules for input and two for output signals. Both types of modules can receive up to 16 signals. The 7U2 digital input card is connected to the lock status signals, starting from address I0.0 to address I1.2. Signals from the call button for entering the safe zone, from address I1.3 to I1.7, are also connected to the same card and Emergency Stop buttons. The second card has the same set-up with addresses I3.2 to I3.7.

The following essential system components are optoelectronic and inductive sensors. Thanks to these sensors, we have information about the position of the roll at all times. After meeting the required conditions, a signal is sent to the output modules to stop the line.

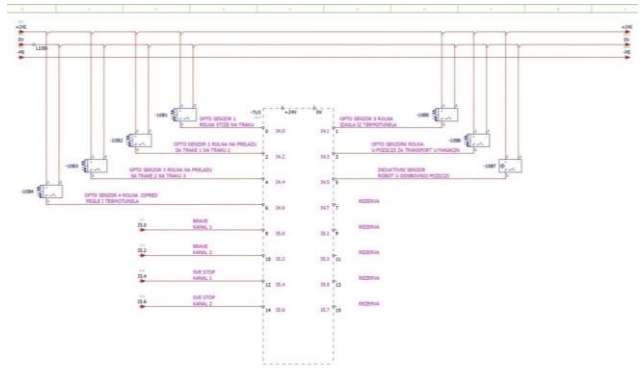

Figure 5. *Digital input card with roll position sensors*

4.3 Ladder diagram [1]

The Ladder diagram, according to which the machine performs certain functions, is developed in Siemens Simatic software, version S7. In the first step, the conditions for starting the machine are defined. The first condition is that all locks and all Emergency Stop buttons are closed. When all conditions are met, the plant can start. It is one of the main requirements of Safety protection.

The part of the program which sends an invitation to enter the safe zone is made in the second step.

Step three is the most important and complex because the position where the line will stop depends on it. All the conditions found in that line of code must be met to stop a line at the required position. The first condition is that the optoelectronic sensor, whose address is I4.0, detects the position of the roll on conveyor no. 1. The optoelectronic sensor, whose address is I4.2, has the task of sending information that the roll has moved from the conveyor 1 to conveyor 2. The optoelectronic sensor with address I4.3 has the function of sending information that the roll has moved from conveyor 2 to conveyor 3. That information is essential for restarting the line. The roll must not remain in position between the two conveyors.

The transfer of the roll from the conveyor to the pallet with finished products is carried out by a robot. An essential condition is that the position of the robot arm must be in its initial position.

The next critical point in the entire system is the thermal tunnel. The line must not be stopped while the roll is in the thermal tunnel because it could overheat and catch fire. Because of all the above, the signal about the roll exit from the thermal tunnel is of great importance.

Due to the magnitude of the drive, many locks, and the Emergency Stop buttons, it is necessary to have light signalling on the control panel about the status of all locks and buttons. The last step of the program provides a light indication of an open door and activated Emergency Stop buttons.

5 CONCLUSION

The paper presents the structural solution of the mechatronic protection system on the press line in the “Tetra Pak” plant from Gornji Milanovac. The solution offers a description of the system and all its components. The protection system includes Safety PLC, protective panels, safety locks with call buttons, Emergency Stop buttons, and optoelectronic and inductive sensors. The set requirements were met by implementing a system of protective barriers and equipment to control access to the protected zone. First, following SIL, protection level 3 was achieved, which was above the required value (SIL 2). In this way, the requirement of the standard was met, and the future upgrade of the system without replacing the main parts was also made possible. In addition, it was possible for the machine to take the most favourable position when stopping, which was one of the company’s main requirements.

The most common cause of work-related injuries is human negligence and non-compliance with prescribed procedures. This type of protection does not allow workers to disobey prescribed steps and defined procedures.

No technical system is absolutely safe, and work-related injuries occur despite the application of the protection system. However, by applying the concept of “protection layers” and with the use of safety PLCs, the protection level degree 3 (according to SIL) can be achieved, which significantly reduces the risk of injuries and reduces it to an acceptable level.

LITERATURE

[1] Dragan M. Marinković, *Programabilni logički kontroleri: Uvod u programiranje i primenu, 2. dopunjeno izdanje,* Mikro knjiga, Beograd, 2018.
[2] Darko Marčetić, Marko Gecić, Boris Marčetić, *Programabilni logički kontroleri i komunikacioni protokoli u elektrotehnici,* FTN Novi Sad Izdavaštvo, Novi Sad, 2013.
[3] Frank D. Petruzella, *Programabilni logički kontroleri,* Mikro knjiga, Beograd, 2011.
[4] EN ISO 13849-1:2015 Safety of machinery -- Safety-related parts of control systems -- Part 1: General principles for design
[5] https://www.axelent.com/rs/products/machine-guarding/x-guard-machine-guarding/
[6] https://search.abb.com/library/Download.aspx?DocumentID=2TLC172003B02002&LanguageCode=en&DocumentPartId=&Action=Launch
[7] https://cache.industry.siemens.com/dl/files/293/58649293/att_863460/v1/et200sp_system_manual_en-US_en-US.pdf

COMETa 2022
6th INTERNATIONAL SCIENTIFIC CONFERENCE
17th - 19th November 2022
Jahorina, B&H, Republic of Srpska
University of East Sarajevo
Faculty of Mechanical Engineering
Conference on Mechanical Engineering Technologies and Applications

ANALIZA TRENDA PATENATA IZ INDUSTRIJE 4.0 I IMPLEMENTACIJE ROBOTSKE TEHNOLOGIJE U ZEMALJAMA KINA, USA, JAPAN, REPUBLIKA KOREJA I NJEMAČKA

Isak Karabegović[1], Raul Turmanidže[2] , Predrag Dašić[3]

Rezime: Istraživanja i razvoj u novim tehnologijama, kao i brzi tempo implementacije inovacija novih tehnologija, a posebno digitalizacija i automatizacija, imaju glavnu ulogu u oblikovanju budućeg svijeta. Osnovne karakteristike vremena u kojem živimo i radimo jesu nevjerovatna brzina promjena u svim oblastima ljudskog djelovanja, koja je rezultat nevjerovatnog napretka u nauci i tehnologiji. Prije svega, to se odnosi na informaciono-komunikacione tehnologije, biomedicinske tehnologije, kognitivnu psihologiju, vještačku inteligenciju i robotizaciju. Tehnološke inovacije obećavaju transformaciju svijeta u kojem živimo u svim njegovim dimenzijama. Ipak, da bi se dobrobiti inovacija mogle adekvatno iskoristiti nužno je da se kao društvo prilagodimo dolazećim promjenama. Također, moramo imati u vidu da ove promjene dolaze u vremenu koje je od ranije obilježeno neizvjesnošću, turbulentnim promjenama i hiperkonkurencijom. Razvoj i implementacija novih tehnologija u poslovanju motivirana je brojnim tehničkim i ekonomskim razlozima: poboljšanje kvalitete gotovih proizvoda (strojna obrada, itd.), povećanje produktivnosti i smanjenje udjela rada (u procesu montaže), povećanje stope homogenosti kvalitete proizvoda u svim proizvodnim procesima vezanim za primjenu robotske tehnologije, povećanje razine sigurnosti radnika smanjenje angažovanosti radne snage kod rutinskih i reproducibilnih procesa, minimiziranje ukupnih troškova proizvodnje i troškova održavanja uređaja u proizvodnom procesu, a sve sa svrhom adekvatnih odgovora na izazove konkurencije i sve strožije zahtjeve kupaca.U radu je analiziran trend globalnih inovacija iz Industrije 4.0 općenito, kao i trend inovacija iz Industrije 4.0 u različitim industrijskih područjima, kao i u najrazvijenijim zemljama kao što su Japan USA, Kina, Republika Koreja i Njemačka. Isto tako data je analiza implementacije osnovne tehnologije Indsutije 4.0 robotske tehnologije u ovim zemljama, kao i uporedna analiza patenata iz robotike u navedenim zemljama sa konkretnim zaključcima.

[1] Prof.dr.Isak Karabegović, Akademija nauka I umjetnosti Bosne i Hercegovine (ANUBiH), Sarajevo, Bosna i Hercegovina, E-mail: isak1910@hotmail.com
[2] Prof.dr.Raul Turmanidze, Georgian Technical University (GTU), Tbilisi, Georgia
[3] Prof. Predrag Dašić, Akademija strukovnih studija Šumadija (ASSŠ) Odsek Trstenik, Trstenik, Srbija,

Ključne riječi: Industrija 4.0, patenti u Industriji 4.0, inovacije, industrijski roboti.

ANALYSIS OF PATENT TRENDS FROM INDUSTRY 4.0 AND THE IMPLEMENTATION OF ROBOT TECHNOLOGY IN THE COUNTRIES OF CHINA, USA, JAPAN, REPUBLIC OF KOREA AND GERMANY

Abstract: Research and development in new technologies, as well as the fast pace of implementation of new technology innovations, especially digitization and automation, play a major role in shaping the future world. The basic characteristics of the time in which we live and work are the incredible speed of changes in all areas of human activity, which is the result of incredible progress in science and technology. First of all, it refers to information and communication technologies, biomedical technologies, cognitive psychology, artificial intelligence and robotization. Technological innovations promise to transform the world we live in in all its dimensions. However, in order to adequately utilize the benefits of innovation, it is necessary for us as a society to adapt to the coming changes. Also, we must keep in mind that these changes come in a time that has been marked by uncertainty, turbulent changes and hyper-competition. The development and implementation of new technologies in business is motivated by a number of technical and economic reasons: improving the quality of finished products (machine processing, etc.), increasing productivity and reducing the share of labor (in the assembly process), increasing the rate of homogeneity of product quality in all production processes related to the application of robotic technology, increasing the level of worker safety, reducing the involvement of the workforce in routine and reproducible processes, minimizing total production costs and device maintenance costs in the production process, all with the purpose of adequate responses to competition challenges and increasingly strict customer requirements. The paper analyzes the trend of global innovation from Industry 4.0 in general, as well as the trend of innovation from Industry 4.0 in different industrial areas, as well as in the most developed countries such as Japan USA, China, Republic of Korea and Germany. An analysis of the implementation of the basic technology of Industry 4.0 robotic technology in these countries is also given, as well as a comparative analysis of robotics patents in the mentioned countries with concrete conclusions.

Key words: Industry 4.0, patents in Industry 4.0, innovations, industrial robots.

1 UVOD

Trenutno u svijetu se implementacija četvrte industrijske revolucije (Industry 4.0 ili 4IR) koja se oslanja na digitalizaciju i umrežavanje, drugim rječima Industrija 4.0 predstavlja okvir nove industrijske revolucije koja pokreće velike promjene kako u procesima proizvodnje tako u vrijednostima stvaranja i ponašanju potrošača. Industrija 4.0 transformiše dosadašnje proizvodne procese u nove generacije proizvodnih procesa koji su digatalizovani, a zasnovani su na kombinaciji sajber-fizičkih sistema (CPS) i digitalnih tehnologija. Industrija 4.0 obezbjeđuje inteligentne proizvodne procese koji su integralni u kojima se povezuju fizički svijet sa digitalnim i virtualnim svijetom [1-4]. Koncept Industrije 4.0 se bazira na inteligentnom povezivanju mašinstva, elektronike i softvera, što doprinosi razvoju novih tehnologija i poslovnih modela, kao i novih prilaza u radu i razmišljanju. Svjedoci smo svakodevnom razvoju i implementaciji novih tehnologija koje se uključuju u koncept Industrije 4.0. Nabrojimo bazne tehnologije na kojima se zasniva koncept Industrije 4.0: Cyber-Physical

Systems (CPS), Digital Product Memory (DPM), Radio Frequency Identification (RFID), Near Field Communication (NFC), Smart Machining (SM), Machine-to Machine (M2M), Man-Machine Interaction (MMI), Assisted Operator, Robotics, Smart Sensors (SS), Energy Efficiency Monitoring (EEM), Renewable Energy Integration (REI), Smart/Mobile Maintenance, Codition Monitoring (CM), Augmented Reality (AR), Virtual Reality (VR), Quick Response (QR) Code, Digital Twin (DT), Digital Shadow (DS), Reconfigurable Factory (RF), Plug & Procude, Shop Food Menagment I4.0, Lean Management (LM), Batch Size 1, Pick by Light (PbL), Smart Devices (SD), Horizontal & Vertical Integration, Industrial Cyber Security, Real-Time Communication (RTC), Manufacturing Execution Systems (MES), Enterprise Resource Planning (ERP), Intelligent Logistics, Supplier Relationship, Customer Relationship, Additive Manufacturing (AM), Internet of Thing (IoT), Industrial Internet of Thing (IIoT), Cloud Computing (CC), Artificial Intelligence (AI), Big Date and analytics, Smart Factory (SF) i sl. Od nabrojanih baznih tehnologija Industrije 4.0 izdvojit ćemo najvažnije tehnologije koje transforiraju proizvodne procese odnosno industrijsku proizvodnju, a to su: Robotics, Smart Sensors (SS), Internet of Thing (IoT), Industrial Internet of Thing (IIoT), Horizontal & Vertical Integration, Cloud Computing (CC), Cyber Security, Additive Manufacturing (AM), Augmented Reality (AR), Big Date and analytics, Artificial Intelligence (AI) i dr.

Jedna od bitnih karakteristika Industrije 4.0 jeste multi-disciplinarno inženjerstvo kroz cijeli proizvodni proces, ali ne samo to već i cijeli životni ciklus proizvoda [5-9]. Da bi se ovo ostvarilo potrebno je imati inženjerski pristup u svim fazama razvoja proizvoda od dizajna, razvoja, izrade i kao takve pružaju izvrsnu potporu proizvodnom procesu i proizvodnom okruženju, isto tako sve informacije dostupne tokom cijelog životnog ciklusa proizvoda te tako omogućuju fleksibilniji proizvodni proces, lake modifikacije i prototipe u samom procesu izrade proizvoda. Razvoj navedenih tehnologija omogućuje razvoj koji se temelji na tehnologijama, automatizaciji i autonomnosti istog.

Sve više se koristi umjetna inteligencija (Artificial Intelligence (AI)) u automatizaciji proizvodnih procesa, a najveći udio daje robotika, autonomna vozila, autonomni servisni roboti, pametni senzori, roboti koji rade rame uz rame sa ljudima na poslovima koji su opasni za zdravlje ljudi, a roboti ih mogu obavljati i puno brže [10-14]. Razvoj navedenih tehnologija i njihova implementacija može se pratiti preko broja globalnih inovacija odnosno odobrenih patenata u svijetu, koje dramatično ubzano rastu. Da bismo dobili stvarnu sliku napravili smo analizu globalnog trenda inovacija iz Industrije 4.0.

2 TREND GLOBALNIH INOVACIJA IZ INDUSTRIJE 4.0

Trend globalnih inovacija u nabrojanim tehnologijama u Industriji 4.0 tokom posljednje decenije ubrzano raste što nam najbolje pokazuje slika 1. Na slici 1 prikazan je trend procentualnog globalnog rasta međunarodnih porodica papenata (International patent families – IPF) u tehnologijama Industrije 4.0 u odnosu na sve druge tehnološke oblasti za period 2003-2018 godina. Ovdje moramo napomenuti da svaki IPF pokriva jedan izum i uključuje prijave za patente koje su podnesene i objavljene u nekoliko patentnih ureda.

Globalni trend rasta IPF-ova u tehnolgijama Industrije 4.0 od 2010 godine ima ekstemni rast tako da je od 2010. godine do 2018. godine prosječna godišnja stopa rasta iznosila oko 20%. Ako uzmemo prosječni trend rasta za petnaest godina od

2003. godine do 2018.iznodi oko 14,8%. Upoređujući godišnji porast IPF-ova za tehnologije industrije 4.0 sa IPF-ova u svim oblastima vidimo da je u 2018. godini skoro pet puta veći.

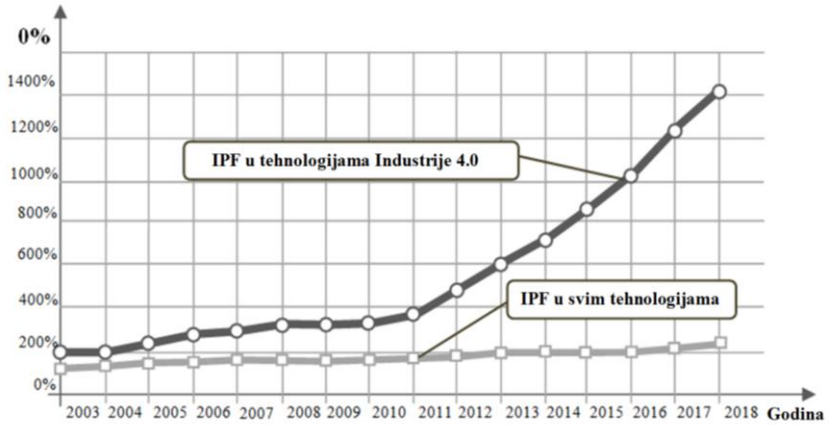

Slika 1. *Trend procentualnog globalnog rasta međunarodnih porodica papenata (IPF) u tehnologijama Industrije 4.0 u odnosu na sve druge tehnološke oblasti za priod 2003-2018 godina [5]*

Izvor: Evropski zavod za patente (European Patent Office – EPO)

U 2018. godini broj IPF-ova u tehnologijama Industrije 4.0 je iznosio oko 36.700 prijava. Ovdje je interesantno vidjeti kakav je trend prijava PIF-ova iz tehnologija Industrije 4.0 u tehnološkim poljima. Na slici 2 prikazan je globalni trend rasta IPF-ova u tehnologijama Industrije 4.0 u tehnološkim oblastima: industriji, vozilima, servisu i infrastrukturi, za deset godina za period 2008-2018. godine.

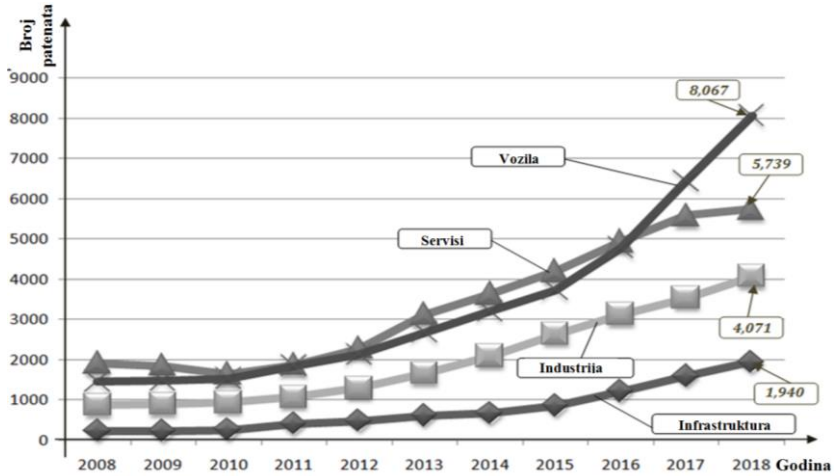

Slika 2. *Globalni trend rasta međunarodnih porodica papenata (IPF) u oblastima industrije, vozila, servisa i infrastrukture u svijetu za period 2008-2018 godine [1,5]*

Na osnovu slike 2 može se doći do zaključka da od 2010. godine globalni trend prijava PIF-ova iz tehnologija Industrije 4.0 u svim navedenim tehnološkim poljima ima intenzivan rast. Na prvom mjestu je oblast vozila gdje je 2018. godini prijavljeno 8.065 PIF-ova prijava, dok je na drugom mjestu oblast servisa sa 5.739 prijavljenih PIF patenata. Isto tako zabilježen je trend rasta prijave PIF patenata iz godine u godinu tako da je u 2018. godini iz industrije bilo 4.071 prijava, a iz infrastrukture 1.904 prijave patenata. Ovakav tren je očekivan iz razloga što je automobilska industrija na globlanom tržištu i kompanije da bi bile vodeće u svijetu ulazu u implementaciju Industije 4.0, da bi u potpunosti svoje proizvodne procese učinili fleksibilnim i inteligentnim.

Na slici 3 prikazan je napravljena je analiza globalnog trenda rasta IPF-ova u tehnologijama Industrije 4.0 u razvijenim zemljama u svijetu i Evropskoj Uniji (EU).

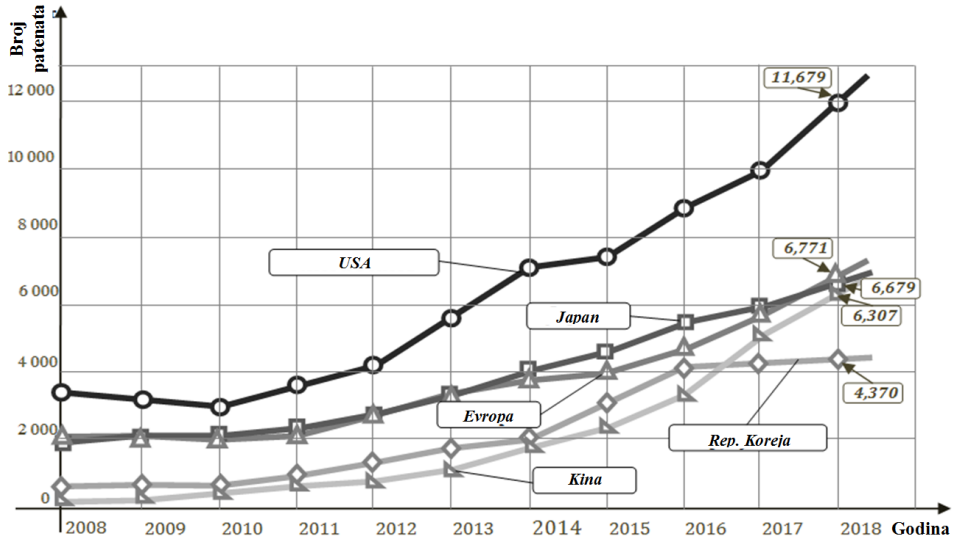

Slika 3. *Globalni trend rasta međunarodnih porodica papenata (IPF) u tehnologijama Industrije 4.0 u Evropskoj Uniji (EU), USA, Japanu, Republici Koreji i Kini u periodu 2008-2018. godini [1-2, 5]*

Globalni trend rasta IPF-ova u tehnologijama Industrije 4.0 u Evropskoj Uniji (EU), USA, Japanu, Republici Koreji i Kini od 2008. godine kontinuirano iz godine u godinu raste i sve više se povećava. Moramo izdvojiti USA koja je na prvom mjestu i odskače od ostalih praćenih zemalja, tako da je u 2018. godini imala 11.679 prijavljenih IPF patenata, a na drugom mjestu izmjenjuje se Japan i Evropska Unija (Švedska, Švicarska, Velika Britanija, Finska, Njemačka, Španija, Italija, Francuska, Holandija - razvijene zemlje EU) skoro sa istom prijavom IPF patenata u 2018. godine (u EU je prijavljeno 6.771, a u Japanu 6.679 prijavljenih IPF patenata). Na trećem mjestu je Kina u kojoj je u 2018. godini prijavljeno 6.307 IPF patenata, poslije nje je Republika Koreja sa 4.370 prijavljenjih IPF patenata. Ovakav trend rasta je nastavljen sve do danas, a za očekivati je da sličan trend rasta bude i u narednim godinama. Na osnovu slike 2 vidimo da je vodeća automobilska industrije po prijavi IPF-ovih patenata, a u ovoj industriji se najviše koriste osnovne tehnologije Industrije 4.0, kao što su: robotika, claud računarstvo (CC), senzori, radio frekventna identifikacija (RFID)

itd. U radu je napraviljena uporedna analizu implementacije industrijskih robota u proizvodnim procesima u USA, Japanu, Republici Koreji, Njemačkoj sa Kinom jer su ovo top zemlje po prijavi inovacija iz Industrije 4.0.

3 UPORENA ANALIZA TRENDA PATENATA I IMPLEMENTACIJE ROBOTSKE TEHNOLOGIJE U PROIZVODNE PROCESE U ZEMALJAMA USA, JAPANU, REPUBLICI KOREJI I NJEMAČKOJ SA KINOM

Da bismo obrazložili uporednu analizu implementacije robotske tehnologije napravljena je analiza implementacije industrijskih robota u svijetu. Statističke podatke za broj industrijskih robota preuzeti su od Međunarodne federacije za robotiku (International Federation of Robotics – IFR), Ekonomske komisije pri UN za Evropu (UNECE) i Organizacije za ekonomsku kooperaciju i razvoj (OECD) [17-20], koji su grafički prikazani na slijedećim slikama.

U svijetu od 2010. godine trend implementacije industrijskih robota imao rastući karakter sve do 2018. godine (slika 4). Rast trenda je bio sa 118.000 jedinica industrijskih robota u 2010. godini do 422.000 jedinica industrijskih robota u 2018. godini, drugim rječima za samo osam godina implementacija se povećala oko 3,5 puta (CGI indeks je 357,63 % za 2018. godinu u odnosu na 2010. godinu). U 2019 i 2020. godini trend implementacije industrijskih robota je smanjen tako da je u 2020. godini iznosio oko 384.000 jedinica robota, tako da je u tom periodu AGR indeks bio -11,61 % za 2019. godinu i 2,95 % za 2020. godinu (slika 4). Najveći AGR indeks bio je 2011. godini (AGR=40,68 %), pa zatim u 2014. godini (AGR=28,65 %) itd. (slika 4). Srednja vrednost AGR indeksa za ovaj period bila je AAGR=13,48 %. Razlog što je trend implementacije industrijskih robota smanjen je jer svijet zahvatila pandemija virusa COVID-19. Očekivanja su da će nakon prestanka pandemije u svijetu doći do porasta trenda implementacije industrijskih robora u svijetu.

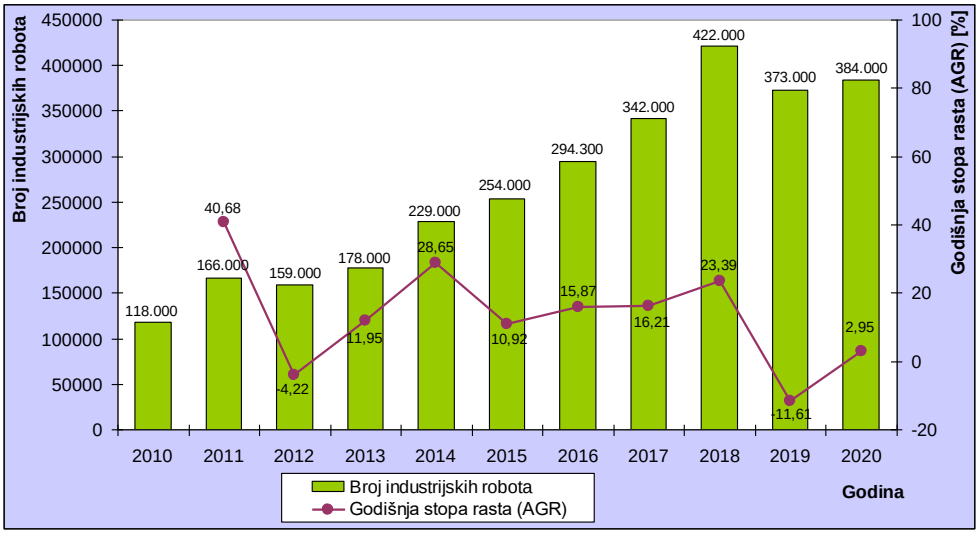

Slika 4. *Trend implementacija industrijskih robota u svijetu na godišnjem nivou u periodu 2010-2020. godine [25-34]*

Na slici 5 prikazan je trend implementacije industrijskih robota u svijetu na godišnjem nivou u periodu 2010-2020. godinu.

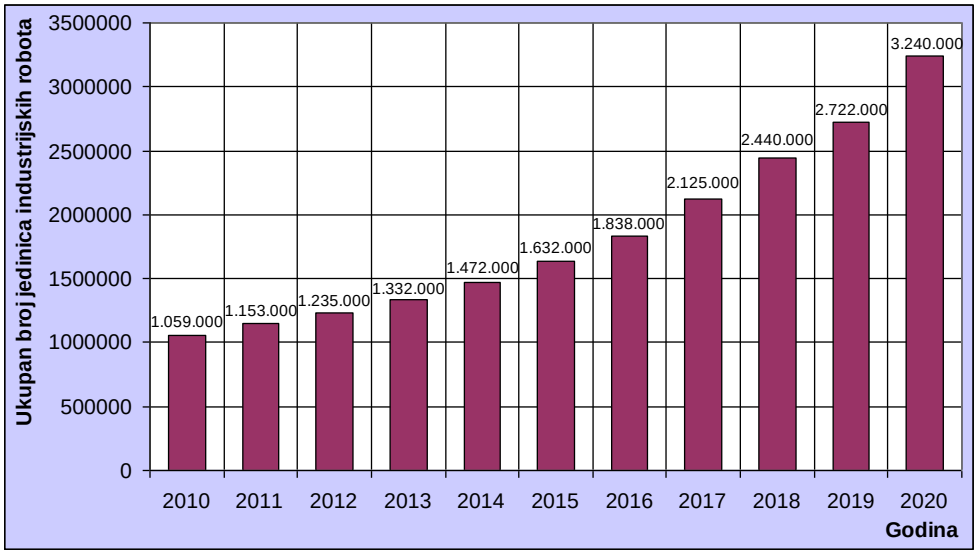

Slika 5. *Ukupna implementacija industrijskih robota u svijetu u periodu 2010-2020. godine [24-33]*

Analizom ukupnog trenda implementacije industrijskih robota u svijetu vidimo da ima rastući karakter (slika 5), i može se kazati da se implementacija odvija po skoro eksponencijalnoj funkciji. Za samo deset godina ukupna implementacija industrijskih robota se povećala za 3 puta (sa 1.059.000 jedinica industrijskih robota povećala se na 3.240.000). Razlog za rastući trend implementacije industrijskih robota je upravo implementacija Industrije 4.0 u kompanijama koje moraju da zadrže svoje pozicije na globalnom tržištu.

Sama implementacija industrijskih robota po kontinentima za period 2010-2020.godine data je na slici 6.

Na osnovu trenda implementacije industrijskih robota po kontinentima za period 2010-2020. godine koji je prikazan na slici 6 može se zaključuti da je Azija/Australija na prvom mjestu i daleko je veća implementacija robota u odnosu na Evropu i Ameriku. Trend na ovom kontinentu ima rastući karakter sve do 2018.godine, a onda zbog pandemije virusa Covid-19 dolazi do blagog pada u implementaciji, ali u 2020. godini je više implementirano nego u 2019. godini. Implementacija industrijskih robota u Aziji/Australiji je 2020. godini iznosila oko 226.000 jedinica robota.

Na drugom mjestu po implementaciji industrijskih robota je kontinent Evropa kod koje je u odnosu na Aziju/Australiju implementacija industrijskih robota oko 3x niža. Na trećem mjestu je Amerika koja nesto manje implementira industrijskih robota na godišnjem nivou u odnosu na Evropu. Trend i u Evropi i Americi za vrijeme pandemije virusa je opao kao kod Azije/Australije i ako je imao blagi trend povećanja. U narednom periodu je za očekivati trend povećanja implemntacije industrijskih robota na sva tri kontinenta. Intresantno je vidjeti trend implementacije industrijskih robota po industrijama i gdje se najviše industrijskih roboti implementiraju.

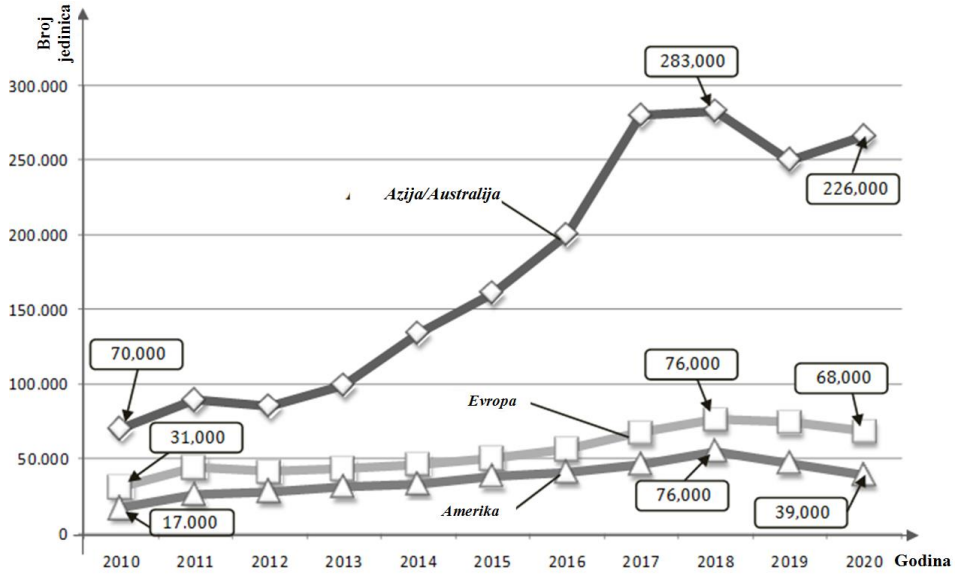

Slika 6. *Trend implementacija industrijskih robota u svijetu na godišnjem nivou u periodu 2010-2020 godine na kontinetima Azija/Australija, Evropa i Amerika [11,24,25-34]*

Na slici 7 prikazana je implementacija industrijskih robota u procentinualnom iznosu u svijetu po industrijskim granama u godinama 2018, 2019 i 2020. godini. Na osnovu analize grafika prikazanih na slici 7 može se zaključiti da se izdvajaju dvije industrije i to automobilska industrija i elektro/elektonička industrija u koje je implementirano oko 50% ukupno instaliranih industrijski robota u svijeti svake godine.

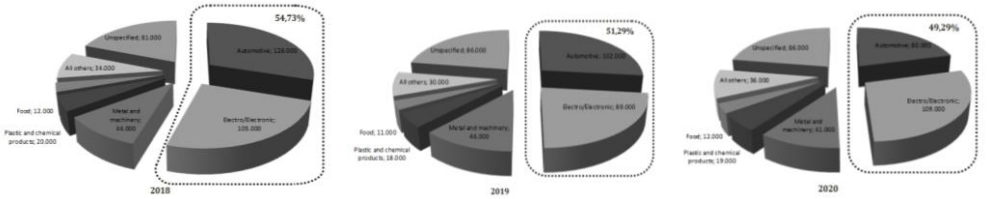

Slika 7. *Implementacija industrijskih robota procentualna po industrijskim granama u svijetu u 2018, 2019 i 2020.godini [25-27]*

Poslije ove dvije industrije na trećem mjestu je metalna industrija, a zatim je industrija plastike i gume i posljednja je industrija hrane. Iz godine u godinu vidimo da procenti implementacije industrijskih robota po navedenim industrijama malo odudaraju zavisno od trenutnog stanja u svijetu, jer u vrijeme pandemije virusa Covid-19 nešto se povećao procenat implementacije industrijskih robota u elektro/elektroničkoj industriji u odnosu na automobilsku industriju. Ovakav trend je očekivan iz razloga što kompanije u automobilskoj industriji automatiziraju svoje proizvodne procese, a dugogodišnjim razvojem informaciono komunikacionih tehnologija i razvojem i napredkom novih tehnologija došlo je do povećanja proizvodnje u elekto/elektoničkoj industriji i kompanije automatiziraju proizvodne procese da bi oskrbili tržište (primjer je upotreba najnovijih telefona).

U narednim godinama trend implementacije industrijskih robota u ove dvije industrije će se naglo povećavati ako se zna da je u toku implemetacije Industrije 4.0 koju implementiraju sve kompanije koje su u vrhu na globalnom tržištu [11, 15,16,21-23]. Za dobijanje prave slike treba vidjeti koje su zemlje u svijetu u kojima se implementira najviše industrijskih robota, a odgovor nam pruža slika 8.

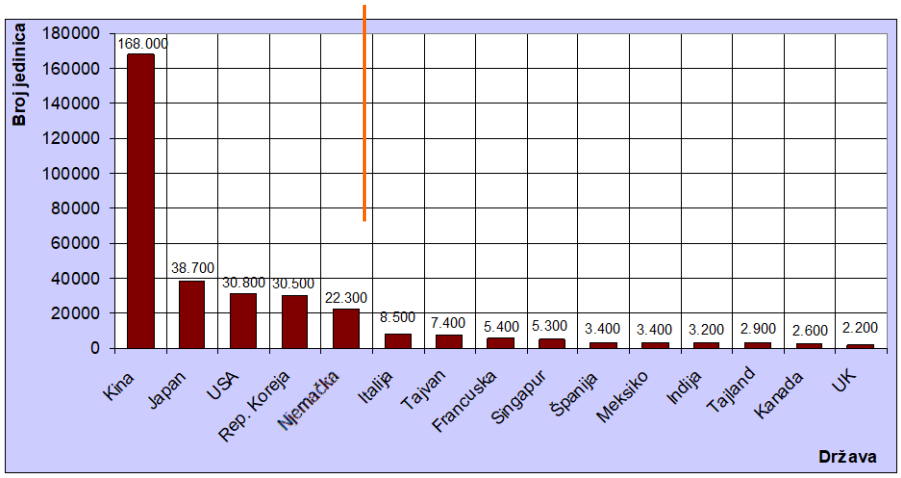

Slika 8. *Implementacija industrijskih robota u 2020. godini u petnaest top zemalja u svijetu [25]*

Analizom implementacije industrijskih robota u 2020. godini koja je prikazana na slici 8 [6], može se zaključuti da je prvi pet top zemalja: Kina, Japan, USA, Republika Koreja i Njemačka. Na prvom mjestu je Kina sa oko 168.000 jedinica implementiranih robota, na drugom mjestu Japan sa oko 38.700 jedinica robora, na trećem mjestu USA sa oko 30.800 jedinica implementiranih robota, četvrta je Republika Koreja sa oko 30.500 jedinica robota i na petom mjestu je Njemačka sa oko 22.300 jedinica implementiranih robota. Ostali deset top zemalja u svijetu su: Italija, Tajvan, Singapur, Španija, Meksiko, Indija, Tajland, Kanada i Ujedinjeno Kraljevstvo (UK) gdje se implementacija industrijskih robota kreće od oko 8.500 do 2.200 jedinica robota zavisno od zemlje što se može vidjeti na slici 8 koliko je robota u kojoj zemlji implementirano.

Ovakav tren je za očekivati iz razloga što se održava u posljednjih nekoliko godina, a znajući da prvih pet zemalja imaju razvijenu automobilski i elektro/elektroničku industriju gdje smo zaključili da se u ove dvije industrije implementira oko 50% svih industrijskih robota u svijetu na godišnjem nivou. Drugi razlog za ovakav trend je što ove zemlje implementiraju Industriju 4.0 koju je nemoguće implementirati bez industrijskih robota, jer je robotska tehnologija jedna od osnovnih tehnologija Industrije 4.0. Treći razlog za ovakav trend je što ove zemlje ulažu u istraživanje i razvoj u inovacije u robotskoj tehnologiji te implementaciju u proizvodne procese što pokazuje trend odobrenih patenata iz robotike u zemljama Kina, Japan, Republika Koreja, USA i Njemačka u periodu 2005-2019. godine (slika 9). Dolazimo do zaključka da je u ovih 14. godina u Kini odobreno 25.154 patenata iz robotike koja je na prvom mjestu u svijetu, na drugom mjestu je Japan sa odobrenih 15.130 patenata iz robotike, treća je Republika Koreja sa 11.144 odobrena patenata iz

robotike, četvrte su USA sa 9.554 odobrena patenta iz robotike i na petom mjestu je Njemačka sa 3.439 odobrenih patenata iz robotike. Takođe, pošto je robotska tehnologija osnovna tehnologija za implementaciju Industrije 4.0 u ovim zemljama je došlo do povećanja istraživanja, razvoja i implementacije robotske tehnologije (slika 9).

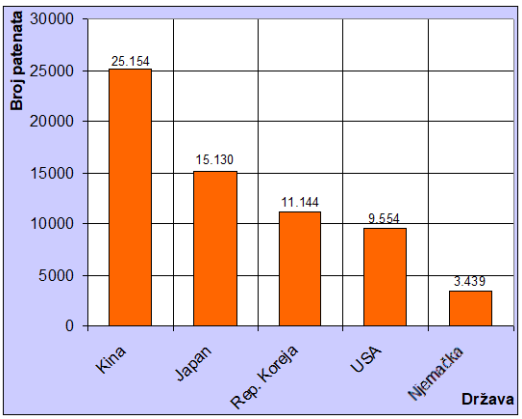

Slika 9. *Trend odobrenih patenata iz robotike u zemljama Kina, Japan, Republika Koreja, USA i Njemačka u periodu 2005-2019*

Na slici 10 prikazan je trend odobrenih patenata iz robotike u zemljama Kina, Japan, Republika Koreja, USA, Njemačka u 2019. godini. Na prvom mjestu je Kina sa 5.430 odobrenih patenata iz robotike u 2019. godini, druge su USA sa 2.155 odobrenih patenata, na trećem mjestu je Japan sa 1.906 odobrenih patenata iz robotike, zatim Republika Koreja sa 1.215 odobrenih patenata i Njemačka sa 566 odobrena patenta iz robotike. Ovim dokazujemo činjenicu da ovih pet zemalja sa pravom predstavljaju top zemlje u svijetu po implementaciji industrijskih robota, jer ulažu u razvoj i istraživanje u robotskoj tehnologiji. Isto tako, vrše implementaciju Industrije 4.0 da bi njihove kompanije bile konkurentne na globalnom tržištu u svijetu [35-37]. Nakon analize odobrenih patenata iz robotske tehnologije interesantno je vidjeti trend implementacije industrijskih robota u svakoj od ovih pet top zemalja u svijetu.

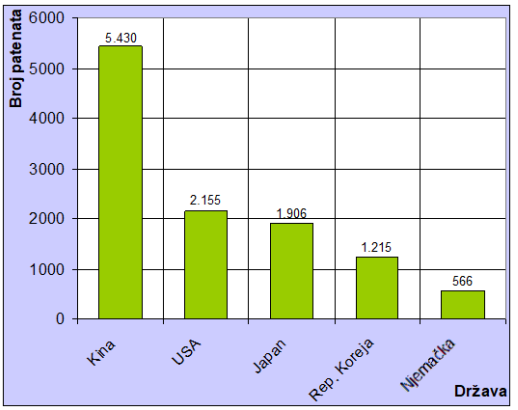

Slika 10. *Trend odobrenih patenata iz robotike u zemljama Kina, Japan, Republika Koreja, USA, Njemačka u 2019. godini*

4 ZAKLJUČAK

Implementacijom Industrije 4.0 moramo ostvariti da savremeni proizvodni sistemi moraju biti fleksibilni/agilni, integrisani, reaktivni, i isplativi istovremeno kako bi industrijskim kompanijama omogućili da ostanu globalno konkurentne. Globalni trend rasta IPF-ova u tehnolgijama Industrije 4.0 od 2010. godine ima ekstemni rast tako da je od 2010. godine do 2018. godine prosječna godišnja stopa rasta (AAGR) iznosila 13,48 %. Upoređujući godišnji porast IPF-ova za tehnologije industrije 4.0 sa IPF-ova u svim oblastima vidimo da je u 2018. godini skoro pet puta veći. U 2018. godini broj IPF-ova u tehnologijama Industrije 4.0 je iznosio oko 36.700 prijava.

Na osnovu analize dolazimo do zaključka da, globalni trend prijava IPF-ova u tehnologijama Industrije 4.0 u tehnološkim oblastima: industrija, vozila, servisi i infrastruktura, od 2010. godine u svim navedinm tehnološkim poljima ima intenzivan rast. Na prvom mjestu je oblast vozila gdje je 2018. godini prijavljeno 8.065 PIF-ova prijava. Takođe, globalni trend rasta IPF-ova u tehnologijama Industrije 4.0 u Evropskoj Uniji (EU), USA, Japanu, Republici Koreji i Kini od 2008. godine kontinuirano iz godine u godinu raste i sve više se povećava.

Od velikog broja baznih tehnologija (preko 40 po nekim autorima) Industrije 4.0 robotika je među prvim baznim tehnologijama Industrije 4.0. Trend rasta prijave i implementacije inovacija i patenata iz novih tehnologija koje su osnova industrije 4.0 svake godine se povećava, a vidjeli smo da je Kina na prvom mjestu po prijavi patenata ali oni nisu inovativni, jer postoji ogroman broj niskokvalitetnih inovacija iz Industrije 4.0 u Kini. Trend implementacije industrijskih robota u svijetu u posljednjih deset godina je u porastu, a nastavit će sa povećanjem primjene robota u idućim godinama upravo zahvaljujući implementaciji Industrije 4.0. Dvije industrije su u svijetu vodeće po primjeni industrijskih robota i to elektro/elektronička industrija i automobilska industrija koje su u 2020. godini primjenili 50% industrijskih robota. Na prvom mjestu po primjeni je zemlja Kina sa oko 168.400 jedinica robota. Kina je u posljednim godinama uvjek prva u svijetu po implementaciji robota, a razlog za to je što je cijena radnika u Kini u posljednjim godinama u porastu, te se mnoge komapanije odlučuju za automatizaciju, drugi razlog je što se u Kini implementira strategija pod nazivom „Made in China 2025“ gdje želi da postane do 2025. godine tehnološki najrazvijenija zemlja u svijetu, i treći razlog je što je Kina prva u svijetu po proizvodnji automobila gdje se industrijski roboti implementiraju, kao što je veliki izvornik proizvoda iz elekto/elektoničke industrije gdje se najviše implementiraju industrijski roboti. Robotska tehnologija ima svijetlu budućnost u narednim godinama.

ZAHVALNOST

Rad je nastao u okviru projekta "Implementation of Industry 4.0 in Companies of Bosnia and Herzegovina: Education for the Implementation of Industry 4.0 Technology" koji finansira Federalno ministarstvo obrazovanja i nauke Federacije Bosne i Hercegovine.

LITERATURA

[1] Karabegović, I.; Kovačević, A.; Banjanović-Mehmedović, L. & Dašić, P. (editors): *Handbook of research on integrating Industry 4.0 in business and manufacturing*.

Hershey (Pennsylvania – USA): IGI Global, 2020. – 661 pp. ISBN 978-1-7998-2725-2. doi: 10.4018/978-1-7998-2725-2.
[2] Schwab, K.: *The Fourth Industrial Revolution*. Geneva (Switzerland): Word Economic Forum (WEF), 2016. – 171 pp. ISBN 978-1-944835-01-9.
[3] Dašić, P.: *Naučno-tehnološki trendovi*: *Odabrani naučno-stručni radovi*. Vrnjačka Banja: SaTCIP Publesher Ltd., 2020. – 305 str. ISBN 978-86-6075-072-5.
[4] Dašić, P. & Turmanidze, R.: Industrija 4.0: Stvarnost ili predviđanje. *Zbornik radova Internacionalnog univerziteta Travnik / Proceedings of the International University of Travnik*, God. 6, br. 16 (2017), pp. 80–89. ISSN 2232-8807.
[5] Meniere, Y.; Philott, J.; Rodriguez, J.P.; Rudyk, I. & Wienold, N.: *Patents and the Fourth Industrial Revolution*. Munich (Germany) European Patent Office (EPO), 2020, pp:7–18.
[6] Konaev, M. & Abdulla, S.M.: *Trend in Robotics Patents*. Center for Security and Emerging Technology, 2021, pp. 1–34.
[7] Karabegović, I.; Karabegović, E.; Mahmić, M. & Husak, E.: The Implementation of Industry 4.0 in the function of application of industrial and service robots in production processes. In: *Proceedings of the International Scientific Conference "Application of Industriy 4.0 on Opportunity for a New Step Forward in All Industrial Branches"*; Special Editon, Vol. 20; Sarajevo, Bosnia and Herzegovina; 14 April 2022. Sarajevo (Bosnia and Herzegovina): Academy of Sciences and Arts of Bosnia and Herzegovina (ANUBiH), 2022, pp. 103–117. ISBN 978-9926-410-75-9. doi: 10.5644/PI2022.202.24.
[8] Karabegović, I.; Karabegović, E.; Mahmić, M. & Husak, E.: Chapter 1: The implementation of Industry 4.0 by using industrial and service robots in the production processes. In: *Handbook of Research on Integrating Industry 4.0 in Business and Manufacturing*. Hershey (Pennsylvania – USA): IGI Global, 2020, pp. 1–30. ISBN 978-1-7998-2725-2. doi: 10.4018/978-1-7998-2725-2.ch001.
[9] Chryssolouris, G.; Mavrikios, D.; Papakostas, N.; Mourtzis, D.; Michalos, G. & Georgoulias, K.: Digital manufacturing: History, perspectives and outlook. *Proceedings of the Institution of Mechanical Engineers*, Part B: Journal of Engineering Manufacture, Vol. 223, Issue 5 (May 2009), pp. 451–462. ISSN 0954-4054. doi: 10.1243/09544054JEM1241.
[10] Karabegović, I. & Karabegović, E.: The role of collaborative service robots in the implementation of Industry 4.0**.** *International Journal of Robotics and Automation Technology*, Vol. 6 (2019), pp. 40–46. eISSN 2409-9694. doi: 10.31875/2409-9694.2019.06.5.
[11] Wang, K.: Intelligent predictive maintenance (IPdM) system – Industry 4.0 scenario. *WIT Transactions on Engineering Sciences*, Vol. 113 (2016), pp. 259–268, eISSN 1743-3533. doi: 10.2495/IWAMA150301.
[12] Müller, J.M.; Buliga, O. & Voigt, K.I.: Fortune favors the prepared: How SMEs approach business model innovations in Industry 4.0. *Technological Forecasting and Social Change*, Vol. 132 (July 2018), pp. 2–17. ISSN 0040-1625. doi: 10.1016/j.techfore.2017.12.019.
[13] Karabegović, I.: The role of industrial and service robots in fourth industrial revolution with focus on China. *Journal of Engineering and Architecture*, Vol. 5, Issue2 (December 2017), pp. 110–117. ISSN 2334-2986. doi: 10.15640/jea.v5n2a9.
[14] Karabegovic, E.; Karabegovic, I. & Hadzalic, E.: Industrial robot application trend in World's metal industry. *Inžinerinė Ekonomika – Engineering Economics,* Vol. 23, Issue 4 (2012), pp. 368–378. ISSN 1392-2785. doi: 10.5755/j01.ee.23.4.2567.

[15] Hermann, M.; Pentek, T. & Otto, B.: Design principles for Industrie 4.0 scenarios. In: *Proceedings of the 49th Hawaii International Conference on System Sciences (HICSS-2016)*; Koloa, Hawaii, USA; 5-8 January 2016. Piscataway (New Jersey – USA): Institute of Electrical and Electronics Engineers (IEEE), 2016, pp. 3928–3937. ISSN 1530-1605 and eISBN 978-0-7695-5670-3. doi: 10.1109/HICSS.2016.488.

[16] Thoben, K.D.; Wiesner, S. & Wuest, T.: "Industrie 4.0" and smart manufacturing - A review of research issues and application examples. *International Journal Automation Technology (IJAT)*, Vol. 11, Issue 1 (2017), pp. 4–16. ISSN 1881-7629. doi: 10.20965/ijat.2017.p0004.

[17] Karabegović, I.: The role of industrial and service robots in the fourt industrial revolution. *Acta Technica Corviniensis – Bulletin of Engineering*, Vol. 11, Issue 2 (April-June 2018), pp. 11–16. eISSN 2067-3809.

[18] Karabegović, I.; Karabegović, E.; Mahmić, M. & Husak, E.: The application of service robots for logistics in manufacturing processes. *Advances in Production Engineering & Management (APEM)*, Vol. 10, Issue 4 (December 2015), pp. 185–194. ISSN 1854-6250. doi: 10.14743/apem2015.4.201.

[19] Karabegović, I.; Karabegović, E.; Mahmić, M. & Husak, E.: Implementation of Industry 4.0 and industrial robots in the manufacturing processes. *Lecture Notes in Networks and Systems (LNNS)*, Vol. 76 (2019), pp. 3–14. ISSN 2367-3370 and ISBN 978-3-030-18071-3. doi: 10.1007/978-3-030-18072-0_1.

[20] Karabegović, I. & Husak, E.: Industry 4.0 based on industrial and service robots with application in China. *Journal Mobility and Vehicle*, Vol. 44, Issue 4 (2018), pp. 59–71. ISSN 1450-5304. doi: 10.24874/mvm.2018.44.04.04.

[21] Mićić, V.: Industry 4.0 development conditions in the Republic of Serbia. *Facta Universitatis*, Series: *Economcs and Organization*, Vol. 17, Issue 2 (2020), pp. 97–112. ISSN 0354-4699. doi: 10.22190/FUEO191112008M.

[22] Oesterreich, T.D. & Teuteberg, F.: Understanding the implications of digitisation and automation in the context of Industry 4.0: A triangulation approach and elements of a research agenda for the construction industry. *Computers in Industry*, Vol. 83 (December 2016), pp. 121–139. ISSN 0166-3615. doi: 10.1016/j.compind.2016.09.006.

[23] Sinay, J. & Kotianová, Z.: Automotive industry in the context of industry 4.0 strategy. *Transactions of the VSB – Technical University of Ostrava*: *Safety Engineering Series*, Vol. 8, Issue 2 (2018), pp. 61–65. ISSN 1805-3238. doi 10.2478/tvsbses-2018-0014.

[24] Karabegović, I.; Husak, E. & Dašić, P.: The role of service robots in Industry 4.0 – Smart automation of transport. *International Scientific Journal "Industry 4.0"*, Vol. 4, Issue 6 (2019), pp. 290–292. ISSN 2534-8582.

[25] *World Robotics 2020 Report*: *Industrial Robots, Service Robots*. Frankfurt am Main (Germany): International Federation of Robotics (IFR), Statistical Department, 2020. (URL: https://ifr.org/).

[26] *World Robotics 2019 Report*: *Industrial Robots, Service Robots*. Frankfurt am Main (Germany): International Federation of Robotics (IFR), Statistical Department, 2019. (URL: https://ifr.org/).

[27] *World Robotics 2018 Report*: *Industrial Robots, Service Robots*. Frankfurt am Main (Germany): International Federation of Robotics (IFR), Statistical Department, 2018. (URL: https://ifr.org/).

[28] *World Robotics 2017 Report*: *Industrial Robots, Service Robots*. Frankfurt am Main (Germany): International Federation of Robotics (IFR), Statistical Department, 2017. (URL: https://ifr.org/).
[29] *World Robotics 2016 Report*: *Industrial Robots, Service Robots*. Frankfurt am Main (Germany): International Federation of Robotics (IFR), Statistical Department, 2016. (URL: https://ifr.org/).
[30] *World Robotics 2015 Report*: *Industrial Robots, Service Robots*. Frankfurt am Main (Germany): International Federation of Robotics (IFR), Statistical Department, 2015. (URL: https://ifr.org/).
[31] *World Robotics 2014 Report*: *Industrial Robots, Service Robots*. Frankfurt am Main (Germany): International Federation of Robotics (IFR), Statistical Department, 2014. (URL: https://ifr.org/).
[32] *World Robotics 2012 Report*: *Industrial Robots, Service Robots*. Frankfurt am Main (Germany): International Federation of Robotics (IFR), Statistical Department, 2012. (URL: https://ifr.org/).
[33] *World Robotics 2011 Report*: *Industrial Robots, Service Robots*. Frankfurt am Main (Germany): International Federation of Robotics (IFR), Statistical Department, 2011. (URL: https://ifr.org/).
[34] *World Robotics 2010 Report*: *Industrial Robots, Service Robots*. Frankfurt am Main (Germany): International Federation of Robotics (IFR), Statistical Department, 2010. (URL: https://ifr.org/).
[35] Around the physical-digital-physical loop: A look at current Industry 4.0 capabilities. Dosputno na Web strani: https://www2.deloitte.com/us/en/ insights/focus/industry-4-0/challenges-on-path-to-digital-transformation/physical-digital-physical-loop.html [Pristupljeno: 15.10.2022].
[36] *Technology and Innovation Report 2021*: *Catching technological waves – Innovation with equity*. UNCTAD/TIR/2020. New York (New York – SA): United Nations Conference on Trade and Development (UNCTAD), 2021. – 170 pp. ISSN 2076-2917 and ISBN 978-92-1-113012-6. Dosputno na Web strani: https://unctad.org/system/files/official-document/tir2020_en.pdf [Pristupljeno: 15.10.2022].
[37] Karabegović, I.; Ćar, M.B.; Šestić, M.; Stupar, S.; Karabegović, E.; Husak, E.; Mahmić, M.; Isić, S.; Vojić, S.; Banjanović-Mehmedović, L.; Buljan, S.; Lemeš, S. & Uzunović-Zaimović, N.: Industry of Bosnia and Herzegovina within Industry 4.0. In: *Proceedings of the International Scientific Conference "Application of Industriy 4.0 on Opportunity for a New Step Forward in All Industrial Branches"*; Special Editon, Vol. 20; Sarajevo, Bosnia and Herzegovina; 14 April 2022. Sarajevo (Bosnia and Herzegovina): Academy of Sciences and Arts of Bosnia and Herzegovina (ANUBiH), 2022, pp. 49–68. ISBN 978-9926-410-75-9. doi: 10.5644/PI2022.202.20.

COMETa 2022
6th INTERNATIONAL SCIENTIFIC CONFERENCE
17th - 19th November 2022
Jahorina, B&H, Republic of Srpska
University of East Sarajevo
Faculty of Mechanical Engineering
Conference on Mechanical Engineering Technologies and Applications

FINITE ELEMENT ANALYSIS OF HELICOPTER AEROSPATIALE GAZELLE SA 341H SKID LANDING GEAR DURING NORMAL LANDING USING STATIC LOAD APPROXIMATION

Branimir Krstić [1], Lamine Rebhi [2], Younes Djemaoune [3], Mirko Dinulović [4]

Abstract: This paper deals with numerical investigation of stress and displacement state of the helicopter Aerospatiale Gazelle SA 341H skid landing gear during normal landing in no-wind condition using static load approximation. The skid landing gear consists of two skid tubes and two cross tubes connected by four vertical spring tubes. The most common failure of this type of landing gear occurs due to the fracture of the rear cross tube. In order to identify areas of high stress concentration, a structural FE model, in Dassault Systemes Catia V5-6R2018 Generative Structural Analysis Workbench, was implemented. The stress field of the helicopter skid landing gear rear cross tube was obtained according to the Von Mises criterion. Finite element analysis confirmed that the maximum value of Von Mises stress is sufficiently below the yield strength of the AISI 4135 alloy steel.

Key words: Aerospatiale Gazelle SA 341H, Finite element analysis, Helicopter landing gear, Hovering, Landing

1 INTRODUCTION

Landing gears provide aircraft support when on the ground and absorb the loads during landing and take-off. They represent an extremely important aircraft system and have to be designed, manufactured and maintained in a proper way to secure a high reliability in service. To successfully perform their functions with minimum weight, they are made of materials with high specific strengths [1]. Failure of any structural component of landing gear assembly can lead to serious accident [2-8].

[1] PhD, Branimir Krstić, Military Academy University of Defence in Belgrade (CA), Belgrade, Republic of Serbia, branimir.krstic@va.mod.gov.rs
[2] PhD, Lamine Rebhi, Ecole Militaire Polytechnique, BP 17 Bordj El-Bahri Alger, Algeria, rebhi.lamine@gmail.com
[3] PhD, Younes Djemaoune, Ecole Militaire Polytechnique, BP 17 Bordj El-Bahri Alger, Algeria, younes.djemaoune@gmail.com
[4] PhD, Mirko Dinulović, Faculty of Mechanical Engineering University of Belgrade, Belgrade, Republic of Serbia, mdinulovic@mas.bg.ac.rs

Skid gear is a most common type of landing gear applied to lightweight helicopters. Its major advantages over conventional oleo gear are simplicity, lightweight, low cost and reduced maintenance. In case of normal landings, the landing energy is stored in tubular spring members. On the other side, for harder landings, this energy is absorbed by permanent deformation of the spring members. The static deflections of the skid gear are usually less than those of oleo gear. The efficiency of skid gear is approximately 50% until the load in the spring member exceeds the elastic limit. If the load is above the yield strength of the member, the efficiency of the skid gear is comparable to that of the conventional gear [9].

To identify type and value of relevant loads that helicopter skid gear is subjected to, it is necessary to analyze all possible landing procedures. Helicopters with skid gear use both symmetrical and asymmetrical landings depending on helicopter's size, weight, operational factors, terrain, etc. Except the ideal symmetrical landing (so called level landing), simultaneously with whole both skids, helicopters can make first contact with ground using one or both skids by their forward or backward ends.

Figure 1. *Helicopter Aerospatiale Gazelle SA 341H*

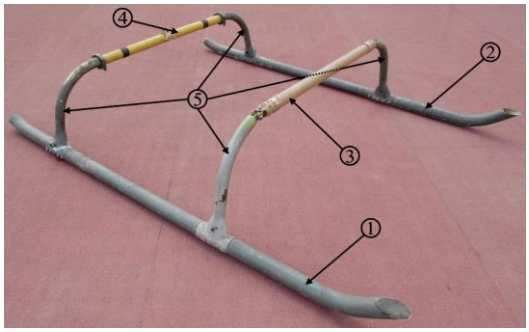

Figure 2. *Landing gear assembly of helicopter Aerospatiale Gazelle SA 341H: 1 - right skid tube, 2 - left skid tube, 3 - forward cross tube, 4 - rear cross tube, 5 - spring tubes*

This paper highlights the finite element analysis of the military multi-role, lightweight, single-engine, helicopter Aerospatiale Gazelle SA 341H (Figure 1.) skid landing gear. The helicopter skid landing gear (HSLG) consists of two skid tubes and two cross tubes as is shown in Figure 2. Skid and cross tubes are connected by four vertical spring tubes. Both skid tubes and the forward cross tube are made of

aluminum alloy while the rear cross tube and all four spring tubes are made of AISI 4135 alloy steel. The most common failure of this type of landing gear occurs due to the fracture of the rear cross tube [2,3]. Therefore, the numerical investigation of stress and displacement state of the HSLG rear cross tube was carried out by means of finite element analysis within Dassault Systemes Catia V5-6R2018 Generative Structural Analysis Workbench.

2 HOVERING FLIGHT AND NORMAL LANDING OF HELICOPTER AEROSPATIALE GAZELLE SA 341H

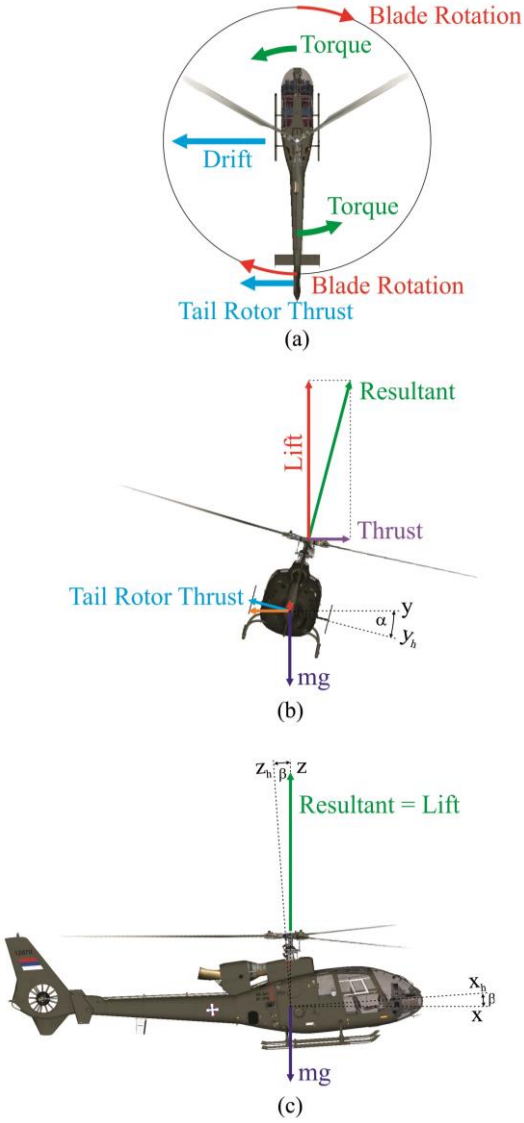

Figure 3. *Forces acting on a helicopter Aerospatiale Gazelle SA 341H during hover in no-wind condition*

A normal landing of helicopter Aerospatiale Gazelle SA 341H is initiated from stable hover with the skids 1 to 1,5 meters above reference point on the ground. This height ensures that the skids are well clear of the ground and any low obstacles, and also allows to land safely, even in case of sudden engine failure [10]. To maintain a nearby motionless flight, it is necessary to eliminate drift in the horizontal plane by cyclic and keep desired altitude by collective.

As the main rotor of helicopter Gazelle rotates in clockwise direction, the fuselage tends to rotate counter clockwise. In order to prevent uncontrolled rotation of fuselage about rotor shaft axis and control the helicopter's nose direction (heading), the tail rotor produces thrust in a direction opposite to the torque, Figure 3a. Simultaneously, tail rotor thrust moves helicopter laterally to the left (this motion is known as a "translating tendency" or "drift"), Figure 3a. Pushing the cyclic to the right, the tip-path plane is tilted opposite to tail rotor thrust generating force that counteracts this drift, Figure 3b. Counteracting translating tendency in a helicopter with a clockwise main rotor system causes the right skid to hang lower while hovering, Figure 3b. On the other side, due to the rotor mast built-in tilt angle, helicopter also tends to move forward. Therefore it is necessary to place the rotor mast in vertical position i.e. to place the tip-path plane in horizontal by slightly pushing the cyclic to the backward. As a result of this correction, helicopter's fuselage tilts nose up, Figure 3c. Based on the all abovementioned, it is clear that in the case of normal landing of helicopter Aerospatiale Gazelle SA 341H, helicopter realizes the first contact with the ground through the backward end of the right skid tube of landing gear, Figure 4.

Figure 4. *Landing of helicopter Aerospatiale Gazelle SA 341H at the moment of initial touchdown of backward end of right skid tube of landing gear.*

Also, according to the operational manual as well as the pilot's statement, the normal landing of the helicopter Gazelle consists of the next four steps (Figure 5.):

1. backward right skid first;
2. whole right skid second;
3. backward left skid third and;
4. whole left skid.

To perform this specific landing, skid gear must be very flexible allowing significant bending and torsional deformations of cross and spring tubes. It is important to point out that emergency landing, so called "bump" and "drop", with extremely high dynamic loads is obligatory considered for stress analysis during the phase of helicopter design. Also, according to service documentation Gazelle helicopter had never performed such landing prior to failure. Therefore, stress state of each part of landing gear assembly was identified in a case of normal landing.

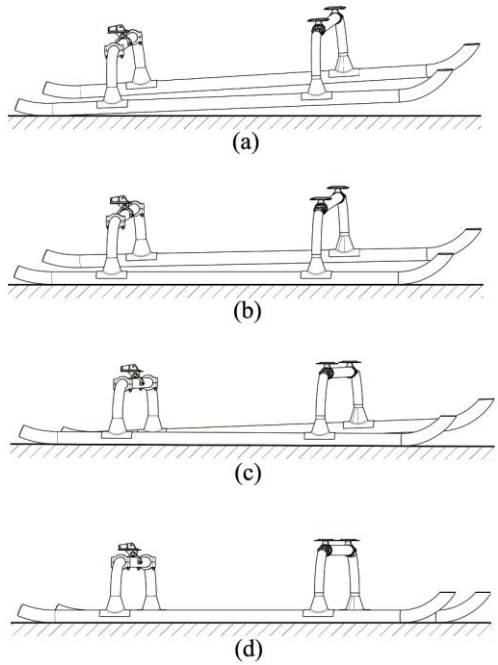

Figure 5. *Landing of helicopter Aerospatiale Gazelle SA 341H at the moment of initial touchdown of backward end of right skid tube of landing gear.*

3 FINITE ELEMENT ANALYSIS

The 3D solid assembly of complete HSLG, identical to the real physical model of Gazelle, was developed in Dassault Systemes Catia V5-6R2018 Generative Structural Analysis Workbench, Figure 6. Continuum of the previously modeled 3D geometry of the HSLG was meshed by a 4-nodes linear tetrahedral solid elements generating FE model of 2,741,747 nodes and 12,615,979 elements. The contact definitions between all elements of the assembly were defined as rigid connection. In addition, the appropriate geometry entities of fuselage attachment solid elements were restrained.

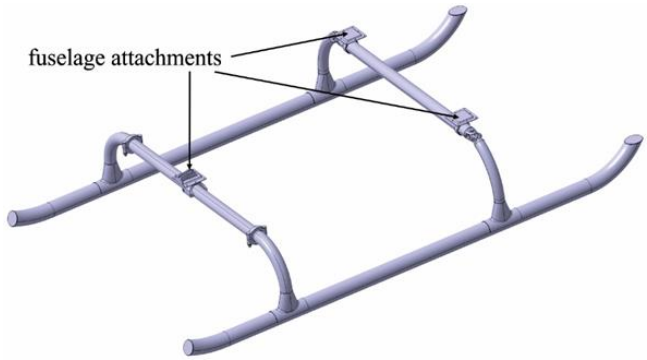

Figure 6. *3D solid model of skid landing gear assembly of helicopter Aerospatiale Gazelle SA 341H.*

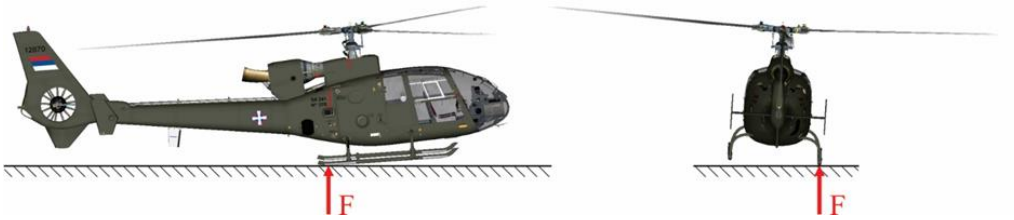

Figure 7. *Schematic representation of static force F acting on the backward end of the right skid tube of landing gear during initial contact with the ground (view from the right and rear side).*

The development of numerical model of skid landing gear was based on the assumption that a pilot performs a vertical landing from stable hover with softly and smoothly touchdown on flat, hard surface in no-wind condition. When landing performs in these conditions, there are no impact loads and it can be considered that the helicopter skid landing gear is exposed to static load due to ground reaction at initial touchdown. The value of static force F acting on the backward end of the right skid tube of landing gear during initial contact with the ground (Figure 7.) was determined applying the following equation [1]:

$$F = W_g \left(1 - L\right) \tag{1}$$

where W_g is the gross weight of helicopter (daN) and L is the ratio of rotor lift to gross weight (throughout touchdown L~2/3). Inserting the value for the gross weight of the helicopter Aerospatiale Gazelle SA 341H into the above equation, the load of landing gear during initial contact with the ground was calculated as follows:

$$F = 18000\left(1 - \frac{2}{3}\right) = 6000 \text{ daN} \tag{2}$$

The obtained force was applied to the backward end of the right skid tube.

To calculate stress and displacement, linear finite element method was applied using a structural FE model, in Catia V5-6R2018 Generative Structural Analysis Workbench. Finite element analysis results showed that the crack [2] was not initiated in the most stress region of the HSLG rear cross tube (Figure 8.), but in the region with significant stress concentration effects due to sudden change in the geometric shape of right end of the rear cross tube (Figure 9.). Also, the maximum displacement occurs in this zone, Figure 10. However, the maximum value of Von Mises stress (601 MPa) is sufficiently below the yield strength (800 MPa) of the AISI 4135 alloy steel.

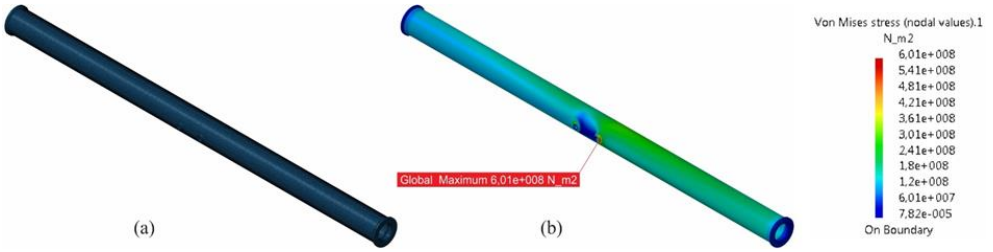

Figure 8. *(a) FE model of the rear cross tube and (b) FE model of the rear cross tube showing the node with maximum stress value.*

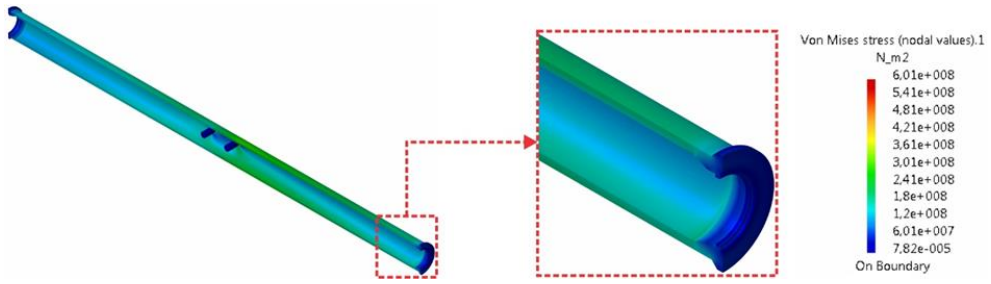

Figure 9. *Von Mises stress field of the structure of the rear cross tube of skid landing gear.*

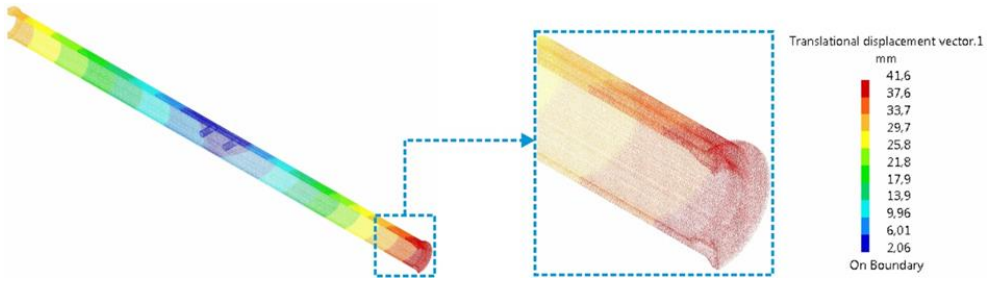

Figure 10. *Displacement field of the structure of the rear cross tube of skid landing gear.*

4 CONCLUSIONS

The the numerical investigation of stress and displacement state of the rear cross tube of the Aerospatiale Gazelle SA 341H skid landing gear during normal landing in no-wind condition confirmed that the maximum values of stress and displacement are in the safe zone and sufficiently below the critical values.

REFERENCES

[1] M. Roth, M.Yanishevsky, P. Beaudet, Failure analysis of aircraft landing gear components, First International Conference on Failure Analysis. , ASMInternational, 1992.
[2] B. Krstic, L. Rebhi, D. Trifkovic, N. Khettou, M. Dodic, S. Peric, M. Milovancevic, Investigation into recurring military helicopter landing gear failure, Engineering Failure Analysis 63 (2016) 121–130.
[3] D. Rakovic, A. Simonovic, A. Grbovic, LJ. Radovic, M. Vorkapic, B. Krstic, Fatigue fracture analysis of helicopter landing gear cross tube, Engineering Failure Analysis 129 (2021) 105672.
[4] C.R.F. Azevedo, E. Hippert Jr., G. Spera, P. Gerardi, Aircraft landing gear failure: fracture of the outer cylinder lug, Engineering Failure Analysis 9 (2002) 1–15.
[5] C.R.F. Azevedo, E. Hippert Jr., Fracture of an aircraft's landing gear, Engineering Failure Analysis 9 (2002) 265–275.
[6] F. Bagnoli, M. Bernabei, Fatigue analysis of a P180 aircraft main landing gear wheel flange, Engineering Failure Analysis 15 (2008) 654–665.

[7] F. Bagnoli, F. Dolce, M. Colavita, M. Bernabei, Fatigue fracture of a main landing gear swinging lever in a civil aircraft, Engineering Failure Analysis 15 (2008) 755–765.
[8] L.A.L. Franco, N.J. Lourenc, M.L.A. Grac, O.M.M. Silva, P.P. Campos, C.F.A. von Dollinger, Fatigue fracture of a nose landing gear in a military transport aircraft, Engineering Failure Analysis 13 (2006) 474–479.
[9] Engineering design handbook, Helicopter engineering, Part one, Preliminary design, National technical information service, US department of commerce Springfield, 1974.
[10] Helicopter Flight Training Manual, TP 9982E (06/2006), second edition, Department of Transport Canada, Canada, 2006.

COMETa 2022
6th INTERNATIONAL SCIENTIFIC CONFERENCE
17th - 19th November 2022
Jahorina, B&H, Republic of Srpska
University of East Sarajevo
Faculty of Mechanical Engineering
Conference on Mechanical Engineering Technologies and Applications

ZNAČAJ INDUSTRIJSKE INFORMACIONE BEZBEDNOSTI U UPRAVLJAČKIM SISTEMIMA

Stevan Stankovski[1], Gordana Ostojić [2]

Rezime: U okviru industrijskih upravljačkih sistema sve je veći broj sistema koji su zasnovani na arhitekture kao što su računarstvo u oblaku ili računarstvo na ivici. Ove arhitekture imaju mnoge prednosti, ali u industrijskoj praksi usvajanje ovih arhitektura ide sporo. Jedan od razloga je kako prevazići povezane rizike, posebno vezane za industrijsku informacionu bezbednosti. U tradicionalnim arhitekturama upravljačkih sistema, operativna tehnologija (OT) je često bila izolovana od Interneta. Uvođenje računarstva u oblaku u upravljačke sisteme i premeštanje podataka sa OT preko Interneta u oblak može imati veliki uticaj na bezbednost i pouzdanost upravljačkih sistema. Ovaj uticaj može dovesti do smanjenja performansi upravljačkih sistema. U ovom radu se razmatraju neki aspekti i značaj industrijske informacione bezbednosti.

Ključne riječi: industrijska informaciona bezbednost, računarstvo u oblaku, računarstvo na ivici

IMPORTANCE OF INDUSTRIAL CYBER SECURITY IN CONTROL SYSTEMS

Abstract: In industrial control systems, there is a growing number of systems with architectures such as cloud computing or edge computing. These architectures have many advantages, but in industrial practice, we can see that the adoption of these architectures is slow. One of the reasons is how to overcome the associated risks, especially related to industrial cyber security. In traditional management system architectures, operational technology (OT) was often isolated from the Internet. Introducing cloud computing into control systems and moving data from OT over the Internet to the cloud can have a major impact on the security and reliability of control systems. This influence can lead to a reduction in the performance of control systems. This paper discusses some aspects and the importance of industrial cyber security.

Key words: industrial cyber security, cloud computing, edge computing

[1] Prof. dr Stevan Stankovski, Fakultet tehničkih nauka, Centar za identifikacione tehnologije, Univerzitet u Novom Sadu, Srbiija, stevan@uns.ac.rs
[2] Prof. dr Gordana Ostojić, Fakultet tehničkih nauka, Centar za identifikacione tehnologije Univerzitet u Novom Sadu, Srbiija, goca@uns.ac.rs

1 UVOD

Procesi automatizacije u industrijskim okruženjima, zasnovani na programabilnim logičkim kontrolerima (PLK), svoju masovnost su počeli osamdesetih godina prošlog veka [1,2]. Zbog svoje arhitekture, za PLK se koristi i drugi termin: industrijski računar. Termin industrijski računar može da bude od pomoći, u cilju boljih razumevanja njegovih mogućnosti i okruženja u kojem se nalazi. Takođe, ako se pogleda razvoj industrijskih računara i računara u poslovnom (sobnom) okruženju, mogu se videti ogromne sličnosti [3,4]. Zbog svoje specifičnosti koje nosi industrijsko okruženje, promene koje se dešavaju u računarima koje se koriste u ne industrijskom okruženju, se sporije usvajaju i primenjuju.

Period u kojem se primenjivao koncept da se PLK koristi samo za svoju glavnu funkciju, a to je da na osnovu ulaznih signala (digitalnih/analognih) donose odluke koje se prenose na izlazne signale (digitalne/analogne) je davno prošao. Počevši od trenutka kada su PLK počeli međusobno da se povezuju (umrežavanju), prestao je period u kojem se obrađuju podaci dobijeni memorisanjem stanja na osnovu ulaznih i izlaznih signala, i nastaje vreme koji podrazumeva i obradu podataka koji se prikupljaju i na osnovu podataka dobijenim povezivanjem (umrežavanjem) PLK, računara, senzora, motora, i drugih industrijskih uređaja koji u sebi sadrže procesorske i komunikacione mogućnosti. Ovo vreme se može podeliti u nekoliko perioda, kao što su periodi koji podrazumevaju arhitekturu klijent/server, arhitekturu u oblaku ili arhitekturu računarstva na ivici [5-8].

Ove arhitekture su donele akcenat na prikupljanju, obradi i prenosu podataka, a ne na samoj obradi ulaznih/izlaznih signala. Ujedno su donele sa sobom i rizik od ne ovlašćenog korišćenje podataka, pre svega zbog toga operativna tehnologija (OT) postoje vidljiva preko računara na oblaku izvan samog računarskog/upravljačkog kruga u koje se ona nalazi. (Pod OT podrazumeva se celokupan hardver i softver koji se koristi za rad i upravljanjem industrijske opreme, procesima i stanjim u jednom industrijskom okruženju.) U cilju sprečavanja ne ovlašćenog korišćenja podataka iz OT, kao i njihove zloupotrebe, u projektovanju upravljačkih sistema se sve više mora voditi računa o industrijskoj informacionoj bezbednosti podataka. Industrijska informaciona bezbednost ima dosta sličnosti sa poslovnom informacionom bezbednošću, ali i značajne razlike [9-10]. U tekstu koji sledi biće dat akcenat na onim aspektima koji potvrđuju koji značaj industrijska informaciona bezbednost ima u upravljačkim sistemima.

2 INDUSTRIJSKA INFORMACIONA BEZBEDNOST

Zbog svoje povezanosti (umreženosti) od PLK, kao najvažnijeg upravljačkog procesorskog elementa, se očekuje da bude otporan na sve vrste pretnji/napada, bilo da su napadi eksterni ili interni, koji mogu da kompromituju njegov rad. Nedostatak ili slaba bezbednost podatka kojim raspolaže PLK, može dovesti do katastrofalnih posledica u zavisnosti od oblasti primene. Na primer, ako bi postojao problem u bezbednosti PLK koji se koristi u termo-energetskim sistemima, to bi predstavljalo veliku pretnju kako za šire tako i za uže okruženje. Upravo zbog toga, kao što je već napomenuto, PLK ne mora da povezan na Internet [11]. U cilju boljeg razumevanja Sistema zasnovanih na PLK i stvaranja bolje zaštite, moguće je ceo sistem podeliti na tri dela: 1) sajber, 2) sajber-fizički i 3) fizički (engleski termini su: cyber, cyber-physical i physical) [12-13]. Fizički deo sistema predstavlja sve komponente koje su u direktnom kontaktu sa stvarnim svetom, kao što su senzori i aktuatori. Sajber i sajber-fizički delovi sistema nemaju direktne veze sa stvarnim svetom i predstavljaju hardver, softver,

komunikacione kanale, sistema za nadzor i upravljanje, … Ova dva pomenuta dela sistema dele neke zajedničke funkcionalnosti, ali je ključna razlika između njih način interakcije sa fizičkim delom sistema. Sajber-fizički deo komunicira direktno sa fizičkim delom, dok sajber deo ne komunicira direktno. Sajber-fizički deo je posrednik između sajber i fizičkog dela. Sajber, sajber-fizički i fizički delovi upravljačkog sistema mogu se predstaviti kao na slici 1 [12].

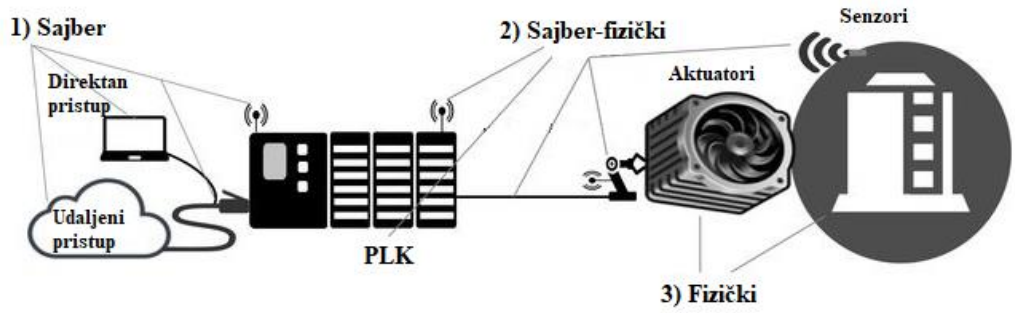

Slika 1. *Delovi upravljačkog sistema (zasnovano na [12])*

Komunikacioni kanali koji se koriste u upravljačkim sistemima mogu biti žičani i bežični. Podela na delove koje je navedene na slici 1, kako i veze koje su predstavljene, ne označavaju jedini moguću scenariji koji može da se pojavi u stvarnim realizacijama. Kao jedan od dobar primera je i korišćenje koncepta industrijskog interneta stvari (IIoT - od engleskog termina Industrial Internet of Things), koji se po sebi predstavlja veliki izazov sa stanovišta informacione bezbednosti [14-15].

Kada se govori o informacionoj bezbednosti upravljačkih sistema, zapravo treba krenuti od pretnji koje mogu da se upute posmatranom upravljačkom sistemu. U suštini, najgrublja podela na pretnje (zapravo njihov nastanak) je da da mogu biti unutrašnje i spoljne. Jedna od mogućih definicija pretnje je da je pretnja „skup okolnosti koje imaju potencijal da izazovu gubitak ili štetu“ [16]. Sve pretnje se usmerene da naruše poverljivost, integritet i dostupnost podataka koje se nalaze u napadnutom sistemu.

Pretnja, kao njen nastanak se može posmatrati kroz različite faktore [17-18]. U većini pretnji se mogu prepoznati pet faktora. Prvi faktor je izvor pretnje, on predstavlja napadača. Napadi mogu biti namerno izvedeni od strane pojedinca ili grupe ljudi. Napadi mogu biti i slučajni, na primer u slučaju otkaza komponenti upravljačkog sistema, prirodnih katastrofa (poplava, zemljotresa, klizanja tla, ...), katastrofa izazvanih ljudima (požari, eksplozije) ili kvarovi na infrastrukturi (kvar struje ili telekomunikacija). Drugi faktor je cilj koji se postiže izvođenjem napada. Ciljevi mogu biti aplikacije unutar upravljačkog sistema, njegove komponente ili njegovi korisnici. Treći faktor je motiv. Napadači obično imaju niz različitih motiva kao što su špijunaža, kriminal, terorizam, politički, osveta, ... Četvrti faktor je metod napada. Napad može biti zasnovan na jednom ili više od sledeća četiri mehanizma: presretanje, prekid, modifikacija ili izmišljanje. Peti faktor predstavlja posledice mogućeg napada. Posledice mogu biti poverljivost, integritet, dostupnost, privatnost ili bezbednost.

Gore navedeni faktori su najvažniji o kojima treba voditi računa o mogućim pretnjama. Pored njih, u poslednje vreme se mora voditi i drugim faktorima koji mogu posredno/indirektno ostvariti pretnje. U upravljačkim sistemima, sve više se odluke donose ne samo na trenutnim stanjima, nego i na osnovu ponašanja sistema u prethodnom vremenskom periodu. U ovim slučajevima se često koriste i različite

metode veštačke inteligencije (VI) koje svoje odluke donose na osnovu skupa (skupova) koji opisuju ponašanje upravljačkih sistema u određenim vremenskim periodima. Ovi skupovi, su zapravo obučavajući skupovi, na osnovu kojih se primenom metoda VI donose odluke. Kompromitovanje obučavajućeg skupa, takođe može dovesti do realizacije pretnji i katastrofalnih posledica na sam upravljački sistem i njegovu okolinu [17,19, 20].

Statistika sajber napada, pokazuje da su najveći broj napada izveli pojedinci/grupe koji su sada, ili su bili deo ljudskih resursa, koji su bili povezani sa napadnutim upravljačkim sistemom. Na žalost broj napada koji se ostvaruje u sajber (digitalnim) sistemima se ne smanjuje, i upravo zbog toga se mora sve više mora pažnja usmeravati i na informacionu bezbednost [5, 21-23]. Pretnje upravljačkom sistemu se mogu podeliti i prema onim delovima na koje su usmerene, i prema tome se mogu grupisati u tri tipa pretnji: sajber, sajber-fizičke i fizičke pretnje.

Najveći broj pretnji/napada se u ostvaruje u komunikacionim procesima i na komunikacionim kanalima. Najveću ranjivost jednog upravljačkog sistema nastaje u onom slučaju kada se povezuje na najveću računarsku mrežu na svetu – Internet. Tog trenutka, postoje izložen svi mogućim sajber napadima. Za napadače je ovaj deo i najjednostavniji, a pre svega što je na Internetu u opticaju samo jedan, dobro poznat, komunikacioni protokol TCP/IP, koji se ujedno koristi u unutar sajber i sajber fizičkih delova upravljačkog sistema [11, 24-25]. U sajber-fizičkom delu, je prisutan veći broj komunikacionih protokola, što u jednu ruku usložnjava realizaciju upravljački sistema, ali istovremeno i sužava broj onih koji su u mogućnosti da ostvare pretnje/napade. U fizičkom delu upravljačkog sistema jer prisutan najmanji broj pretnji/napada. Senzori i aktuatori su i dalje u najvećem broju upravljačkih sistema sa PLK povezani preko digitalnih i analognih ulazno/izlaznih signala, što onemogućava bilo koji sajber napad. Ipak, pojavom IIoT, kao i određenih industrijskih komunikacionih protokola kojima se povezuju senzori i aktuatori sa PLK, značajno se povećava mogućnost pojave pretnji/napada koji ugrožavaju celokupnu informacioni bezbednost upravljačkih sistema.

3 ZAKLJUČCI

Period u kojem su projektanti industrijskih upravljačkih sistema, samo brinuli o tome kako će da realizuju upravljački algoritam i izboru OT, je davno prošao. Koncepti koji se sve više primenjuju u savremenoj industrijskoj proizvodnji, se mogu svesti na jednu konstataciju: da sve mora da bude on-line vidljivo. Ovi koncepti donose niz prednosti, ali za njihovu realizaciju se u delu upravljačkih sistema, sada mora pažnja posvećivati i tome kako se podaci, kao resurs, izloženi raznim pretnjama/napadima, kojim se ugrožava celokupna bezbednost posmatranog sistema.

Industrijska informaciona bezbednost je segment koji će u narednom periodu imati podjednak značaj kao što i upravljački algoritmi imaju u jednom upravljačkom sistemu. U okviru ovog rada, izneta su kratka, osnovna, razmatranje u vezi ove oblasti, sa osnovim ciljem, da se ukaže da bez dobrog rešenja informacione bezbednosti, nema i dobro rešenog upravljačkog sistema.

LITERATURA

[1] Bennett, S. (1993). *A History of Control Engineering 1930-1955*. London: Peter Peregrinus Ltd. On behalf of the Institution of Electrical Engineers. ISBN 978-0-86341-280-6.

[2] Stankovski, S., Ostojić, G., Šaponjić, M., Stanojević, M., Babić, M., (2020). Using micro/mini PLC/PAC in the Edge Computing Architecture, 19th International Symposium INFOTEH-JAHORINA (INFOTEH), East Sarajevo, Bosnia and Herzegovina, 2020, pp. 1-4.
[3] Ceruzzi, P. E. (2012). *Computing: A Concise History*, MIT press, 2012.
[4] Stankovski, S., Ostojić, G., Baranovski, I., Babić, M., Stanojević, M. (2020). The Impact of Edge Computing on Industrial Automation, 2020 19th International Symposium INFOTEH-JAHORINA (INFOTEH), East Sarajevo, Bosnia and Herzegovina, 2020, pp. 1-4.
[5] Stankovski, S., Ostojić, G., Baranovski, I., Babić, M., Stanojević, M. (2020). The Impact of Edge Computing on Industrial Automation, 2020 19th International Symposium INFOTEH-JAHORINA (INFOTEH), East Sarajevo, Bosnia and Herzegovina, 2020, pp. 1-4.
[6] Miller, L., (2020). Edge Computing For Dummies, John Wiley & Sons, Inc., Hoboken, New Jersey.
[7] Stankovski, S., Ostojic, G., Baranovski, I., Tegeltija, S., Smirnov, V. (2022). Robust automation with PLC/PAC and edge controllers, IFAC-PapersOnLine, 55 (4), pp. 316-321.
[8] Stankovski, S., Ostojić, G., Nićin, M., Baranovski, I., Tarjan, L. (2020). Edge Computing for Fault Detection in Smart Systems, In: Zdravković, M., Konjović, Z., Trajanović, M. (Eds.) ICIST 2020 Proceedings Vol.1, pp.22-26.
[9] Creery, A., Byres, E.J., (2005). Industrial cybersecurity for power system and SCADA networks, *Record of Conference Papers Industry Applications Society 52nd Annual Petroleum and Chemical Industry Conference*, pp. 303-309.
[10] Hypponen, M. (2022). If It's Smart, It's Vulnerable, Wiley, Hoboken, New Jersey
[11] Francia III, G. A., Thornton, D., Dawson, J., (2012). Security best practices and risk assessment of SCADA and industrial control systems. In Proceedings of the international conference on security and management (SAM), (p. 1).
[12] Humayed, A.; Lin, J., Li, F.Luo, B., (2017). Cyber-physical systems security-A survey. IEEE Internet of Things Journal, 4(6), pp. 1802-1831.
[13] Babić, M.; Stanojević, M.; Ostojić, G., Tegeltija, S. Stankovski, S. (2022). One Approach to the Detection of Illegal Occupation of Parking Spaces Reserved for Persons with Disabilities, Proceedings of the 33rd DAAAM International Symposium.
[14] Stankovski, S., Ostojić,G., Zhang, X., (2016) Influence of Industrial Internet of Things on Mechatronics, *Journal of Mechatronics, Automation and Identification Technology*, vol. 1, no.1. pp. 1-6, March, 2016.
[15] Tarjan, T., Šenk, I., Obućina, J. E., Stankovski, S., Ostojić, G., (2020). Extending Legacy Industrial Machines by a Low-Cost Easy-to-Use IoT Module for Data Acquisition, *Symmetry* 12(9), 1486; https://doi.org/10.3390/sym12091486
[16] Ankaralı, Z. E.; Demir, A. F.; Qaraqe, M.; Abbasi, Q. H.; Serpedin, E.; Arslan, H. & Gitlin, R. D. (2015, September). Physical layer security for wireless implantable medical devices. In 2015 IEEE 20th International Workshop on Computer Aided Modelling and Design of Communication Links and Networks (CAMAD) (pp. 144-147). IEEE.
[17] Stankovski, S., Ostojić, G., Nićin, M., Baranovski, I., Tarjan, L. (2020) Edge Computing for Fault Detection in Smart Systems, In: Zdravković, M., Konjović, Z., Trajanović, M. (Eds.) ICIST 2020 Proceedings Vol.1, pp.22-26.
[18] Cárdenas, A.A., Amin, S., Sinopoli, B., Giani, A., Perrig, A., Sastry, S., (2009). Challenges for Securing Cyber Physical Systems, In Workshop on future directions in cyber-physical systems security (Vol. 5, No. 1).

[19] Nemet, N., Ostojić, G., Kukolj, D., Stankovski, S., Jovanovic, D., (2019) Feature Selection Using Combined Particle Swarm Optimization and Artificial Neural Network Approach," *Journal of Mechatronics, Automation and Identification Technology*, vol. 4, no. 1, pp. 7–11.
[20] Stankovski, S., Kukolj, D., Ostojić, G., Baranovski, I., Nemet, S., (2021) Trends in Artificial Intelligence for Automated Industrial Systems, *Journal of Mechatronics, Automation and Identification Technology*, vol. 6, no.1. pp. 9-13.
[21] The Latest 2022 Cyber Crime Statistics,https://aag-it.com/the-latest-2022-cyber-crime-statistics/, pristupljeno 24.10.2022.
[22] Leverett, É., Wightman, R., (2013). Vulnerability inheritance programmable logic controllers. In Proceedings of the Second International Symposium on Research in Grey-Hat Hacking.
[23] Slay, J., Miller, M. (2007). Lessons learned from the Maroochy water breach. In International conference on critical infrastructure protection, Springer, Boston, MA, pp. 73-82.
[24] Harris, B., Hunt, R., (1999). TCP/IP security threats and attack methods, Computer communications, 22(10), pp. 885-897.
[25] Francia III, G. Thornton, D. Brookshire, T., (2012). Cyberattacks on SCADA systems, In Proc. 16th Colloquium Inf. Syst. Security Educ, pp. 9-14.

COMETa 2022
6th INTERNATIONAL SCIENTIFIC CONFERENCE
17th - 19th November 2022
Jahorina, B&H, Republic of Srpska
University of East Sarajevo
Faculty of Mechanical Engineering
Conference on Mechanical Engineering Technologies and Applications

STABILITY ANALYSIS OF CONCRETE ARCH DAM USING FINITE ELEMENT METHOD

Dragan Rakić[1], Miroslav Živković[2], Milan Bojović[3], Slobodan Radovanović[4], Aleksandar Bodić[5], Nikola Milivojević[6], Dejan Divac[7]

Abstract: This paper presents the procedure of numerical stability analysis of a concrete arch dam using the finite element method. Based on the geometry of the dam and the associated rock mass, an optimal finite element mesh of the model was created. Boundary conditions and loads were set so that they correspond to the real conditions of exploitation of the dam. The rock mass is divided into five quasi-homogeneous zones in accordance with the geological maps obtained from the field survey. The mechanical behavior of the dam model and the surrounding rock mass is described using the Hoek-Brown material model. The parameters of the material model were obtained through the identification process using experimental tests of soil samples at the site and in the vicinity of the structure. Numerical simulations of filtration, thermal and stress-deformation processes at the dam are performed using PAK software. In the presented analysis, the control of the permissible compressive and tensile stresses is performed according to the USBR recommendations, where the distance between the actual stress and the permissible stress in the concrete is shown. The global safety factor of the dam is determined using the shear strength reduction method.

Key words: Concrete arch dam, Finite element method, Hoek-Brown material model, PAK, Stability analysis

[1] PhD Dragan Rakić, Faculty of Engineering University of Kragujevac, Kragujevac, Serbia, drakic@kg.ac.rs
[2] PhD Miroslav Živković, Faculty of Engineering University of Kragujevac, Kragujevac, Serbia, zile@kg.ac.rs
[3] Milan Bojović, Faculty of Engineering University of Kragujevac, Kragujevac, Serbia, mbojovic@outlook.com
[4] PhD Slobodan Radovanović, Jaroslav Černi Water Institute, Belgrade, Serbia, slobodan.radovanovic@jcerni.rs
[5] Aleksandar Bodić, Faculty of Engineering University of Kragujevac, Kragujevac, Serbia, abodic@uni.kg.ac.rs
[6] PhD Nikola Milivojević, Jaroslav Černi Water Institute, Belgrade, Serbia, nikola.milivojevic@jcerni.rs
[7] PhD Dejan Divac, Jaroslav Černi Water Institute, Belgrade, Serbia, dejan.divac@jcerni.rs

1 INTRODUCTION

This paper presents the procedure for the stability analysis of the concrete arch dam using the finite element method [1, 2]. The analysis procedure is shown on the „Komarnica“ dam model. Komarnica is a river located in Montenegro on which the construction of a concrete arch dam is planned. Based on the geometry of the dam and the associated rock mass, a three-dimensional finite element model was created. Based on the conducted experimental tests, geological maps of the terrain were obtained. Within the FE model, the associated rock mass is divided into 5 quasi-homogeneous environments using obtained geological maps of the terrain. The Hoek-Brown material model [3, 4, 5] is used to describe the mechanical behaviour of the dam and the surrounding rock mass. The material model parameters are obtained by the identification procedure. For the purpose of parameter identification experimental tests of soil samples at dam site and surrounding area are used. Boundary conditions and loads are specified on the FE model so that they correspond to the real conditions of dam exploitation. Numerical analysis is performed using PAK software [6, 7], while FEMAP [8] software is used for pre and post-processing of the model. The results of the stability analysis of the dam are given in the paper. The global factor of safety of the dam is calculated using the shear strength reduction method. The value of the factor of safety for the specified load case is given in the paper. Permissible compressive and tensile stress according to USBR recomendations is used as strength criterion. Results of the permissible compressive and tensile stresses control according to the USBR recommendations is given [9].

In the second chapter, the theoretical basis of the Hoek-Brown material model, shear strength reduction method and control of permissible compressive and tensile stresses are given.

In the third chapter, the 3D FE model of the dam is described. In this chapter boundary conditions and loads assigned to the model, as well as the material parameters of the Hoek-Brown model are given.

In the fourth chapter, the results of stability analysis, control of permissible compressive and tensile stresses, as well as the obtained factor of safety are given.

2 THEORETICAL BASIS

2.1 Hoek-Brown material model

The mechanical behaviour of the rock mass is most often described using Hoek-Brown material model. This material model combines the results of research into the brittle failure of intact rock by Hoek [10] and on model studies of jointed rock mass behaviour by Brown [11]. Initially, this model started from the properties of intact rock and then added factors to reduce these properties based on the characteristics of joints within a rock mass [5].

The failure surface of Hoek-Brown material model is function of stress state and can be defined by applying the stress invariants in following form [13]:

$$f = \frac{I_1}{3} m_b \sigma_{ci} + m_b \sigma_{ci} \sqrt{J_{2D}} \left(\cos\theta - \frac{1}{\sqrt{3}} \sin\theta \right) - s\sigma_{ci}^{\ 2} + 4J_{2D} \cos^2\theta = 0 \qquad (2)$$

where σ_{ci}, m_b, s, α represent material model parameters, while I_1, J_{2D} and θ are stress invariants.

The failure surface of this material model represents an irregular six-sided pyramid of hyperboloid sides whose axis, in main stresses space, coincides with the hydrostatic axis, as shown in Fig. 1.

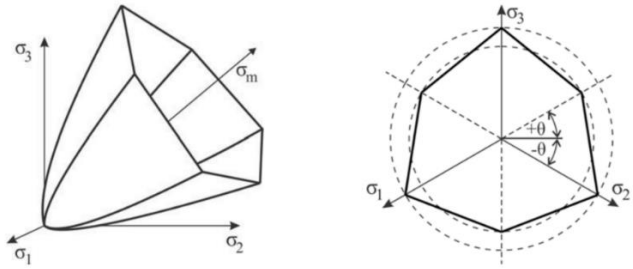

Figure 1. *Failure surface of Hoek-Brown material model*

2.2 Global factor of safety

The global factor of safety of the dam is determined using the shear strength reduction method. It represents the ratio of the material shear strength and the shear stresses in the material. This means that the global stability loss of the structure will occur in case when shear stress value in the material τ becomes equal to the value of the shear strength of the material τ_f [14]. The shear strength reduction can be described by the equation:

$$\tau^{red} = \frac{\tau_f}{F} \tag{3}$$

When it comes to the numerical stability analysis of dam, the initial stress state is first determined, where the reduction factor has a value of 1. Then the reduction factor is gradually increased, which reduces the material shear strength. The reduction factor is increased until there is a loss of dam stability i.e. until it is impossible to achieve the convergence or a increase the displacement increment. The maximum value of the shear strength reduction factor for which the dam is stable is the value of the global factor of safety *F* [15].

2.3 Strength criteria

Permissible compressive and tensile stress in accordance with the recommendations is used as strength criterion. Control of permissible compressive and tensile stresses, according to USBR (United States Bureau of Reclamation) recommendations, implies that the permissible compressive stress value, for the defined load case, is 10.3 MPa and the value of the permissible tensile stress is 1.03 MPa. Due to the triaxial stress state, an envelope of permissible stress values is formed, which is obtained by taking in to account the permissible compressive stress and the permissible tensile stress. For each integration point in the FEM model, the triaxial stress components are calculated, which is compared with the allowable stress value obtained on the basis of the allowable compressive and tensile stress values.

From the failure function of Hoek-Brown material model (2) material constants m_b and s are determined, while σ_{ci} is adopted to be the same value as permissible compressive stress. By solving the system of equations, the values of the material parameters s and m_b are obtained. By substituting the calculated values of the

parameters m_b and s into the failure function of the Hoek Brown material model, the maximum value of the second stress invariant deviator for the envelope of permissible stresses $q^* = \sqrt{J_{2D}}$ can be determined. On the other hand, using the obtained values for the principal stresses σ_1, σ_2 and σ_3, stress deviator q can be determined. Finally, the distance from the surface representing the permissible stress envelope calculated by:

$$u = \left(1 - \frac{q}{q^*}\right) \cdot 100 \tag{5}$$

In this way, field of distance between the actual and permissible stress is formed, where, based on graphical display, more can be concluded about the load of structure.

3 3D MODEL OF CONCRETE ARCH DAM

3.1 Model geometry

The model geometry includes the dam, associated rock mass with geotechnical environments and injection curtain (Fig. 4). The model dimensions are 800x480 m. The lowest elevation of the model is 300 m asl, while the highest is 1000 m asl.

Figure 4. *Model geometry*

The concrete part of the model represents dam. The rock mass is modelled to include geological structures (faults and other characteristic zones) relevant to the model. In order to more realistically model the complex rock structure in the dam area, the rock mass is divided into 5 rock environments. The injection curtain, is also included in the model. Depth of the injection hols is 106 m at the lowest part of the dam, while the curtain thickness in the model is 5 m.

3.2 Finite element model

The finite element mesh of the arch dam was created using parabolic tetrahedral finite elements. The model consists of 1.3 million nodes and about 1.0 milion elements.

In order to achieve the optimal number of finite elements, different element sizes per volume were defined in different model zones. Elements with an average size of 3.5 m are generated in the concrete dam.

The terrain geometry is divided into five quasi-homogeneous zones based on experimental research. Zones are labelled A to B, where A and B represent fault structures. In order to preserve mesh elements quality, minimum size of the elements in the rock mass is dictated by the dimensions of the quasi-homogeneous zones. In the

zones of narrow faults (width 1.5 m), the average size of the elements is 5 m with a gradual transition to a size of 10 m in faults of a larger width. The elements gradually increase in size up to the model boundary, where the average size of the elements is 40 m. By controlling the element sizes in different zones, the number of elements is minimized while preserving the optimal mesh quality. Fig. 5 shows finite element mesh of model in isometric view.

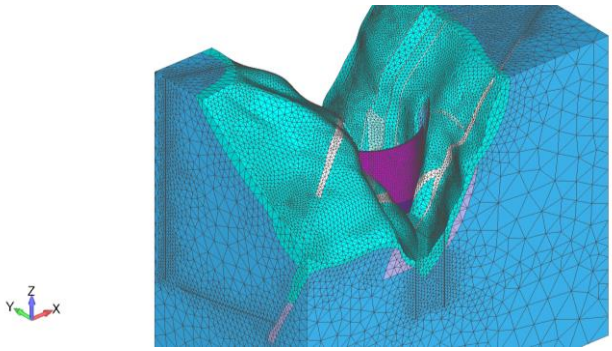

Figure 5. *Finite element mesh of model – 3D view*

3.3 Loads and boundary conditions of the model

Boundary conditions and loads are set so that they correspond to the real conditions of exploitation of the dam. The model dimensions are defined in such a way as to eliminate the influence of boundary conditions on the analysis.

The boundary conditions that were applied on the model are: fixed bottom of the model and constrained horizontal displacement of nodes in the direction perpendicular to the vertical sides that represent the model boundaries.

The loads used in the stability analysis of the dam are dead (self) weight, hydrostatic pressure, thermal loads and filtration forces.

In the model, the thermal effect is applied as follows: on the upstream and downstream surfaces below water level, the water temperature is set (temperature of reservoir water and downstream water). The water temperature is set as a boundary condition on the wetted surfaces of the model according to Bofang's distribution by accumulation depth [16]. The air temperature is set on all other surfaces of the terrain and the dam. At the bottom of the model, the rock temperature is applied, which can be considered constant after certain depth. Based on these boundary conditions, a steady state thermal analysis is performed. The temperature field obtained by the thermal analysis is then used in the structural analysis in order to take into account the influence of temperature on the stress-strain state of the dam.

The hydrostatic pressure is set on all model surfaces below water level. Therefore, there are pressures on the dam and terrain from the reservoir water, as well as pressures from the downstream water.

The filtration forces are determined in the analysis of filtration and are used as loads in the stability analysis. On the upstream surfaces of the dam and the terrain, a hydraulic potential corresponding to the water level in the reservoir is set. On the downstream surfaces of the dam and the terrain, a hydraulic potential corresponding to the water level on the downstream side is applied.

The model is loaded with 4 independent loads, which ultimately act simultaneously. In the first phase, only self-weight acts on model. After the self-weight reaches a maximum constant value, the displacements are reset, and obtained stress

values represent the initial stress state for the next phase. In the second phase, hydrostatic pressure is applied on the model. After that, the third phase defines the effect of filtration forces. In the fourth, final phase, temperature is applied to the model.

The load case considered in this paper includes the following load combinations:

- water level in the reservoir at an altitude of 811.0 m asl and
- winter temperature conditions

3.4 Material parameters

The material model used for the numerical stability analysis of the dam is the Hoek-Brown material model. The material parameters for different zones in the model are given in Table 1.

Table 1. *Material parameters*

Model zones	σ_{ci} [MPa]	m_b [-]	s [-]	a [-]	Elasticity modulus (MPa)
Concrete	40.00	9.4860	0.4475	0.5000	34000
GT env. - A	61.48	0.8794	0.0008	0.5000	3400
GT env. - B	62.59	1.0746	0.0014	0.5001	5100
GT env. - C	49.25	1.7820	0.0065	0.5040	15250
GT env. - D	71.75	2.1300	0.0113	0.5030	24629
GT env. - E	92.50	2.5790	0.0205	0.5020	36051

Experimental tests were performed on the samples collected from the dam construction site. Based on the results of the experimental tests, using identification procedure, parameter values for different model zones are obtained.

4 ANALYSIS RESULTS

4.1 Stress-strain analysis

The analysis results are shown in 3D view and a vertical section along the dam axis. Fig. 7 shows the calculation results in form of the failure distance:

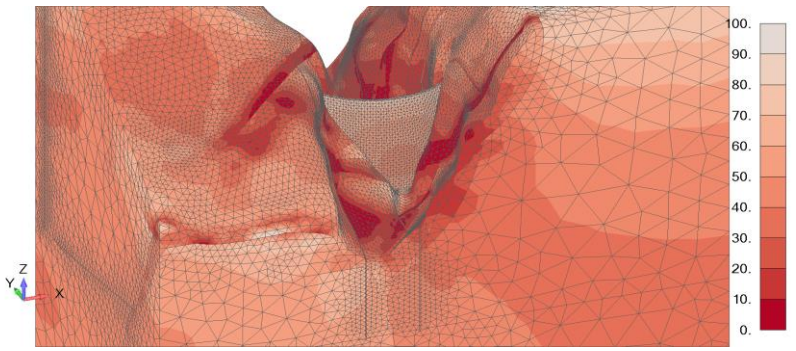

Figure 7. *Failure distance – 3D view*

Based on the Fig. 7, it can be concluded that the rock mass zones around the dam have lower values of failure distance. Therefore, those zones are more critical and

eventual failure of the structure may occur within them. Zones further away from the structure have higher values of failure distance.

4.2 Strength criteria

Permissible compressive and tensile stress in accordance with the recomendations is used as strength criterion. The control of permissible compressive and tensile stress is performed for arch dam according to the USBR recommendations, as described in chapter 2.3. Fig. 9 shows the fields in which the permissible stresses for defined load case are exceeded (red colour) or satisfied (blue colour). Results are shown in upstream and downstream dam face.

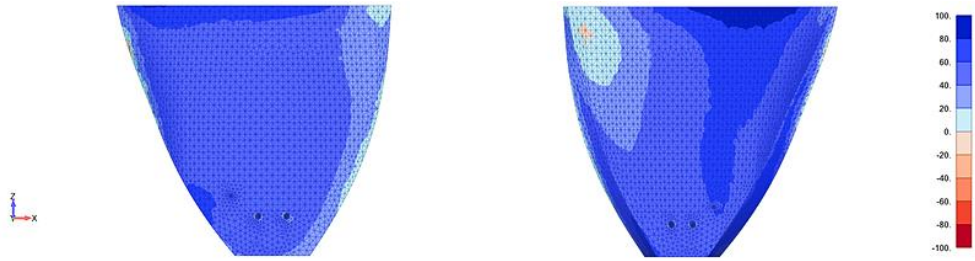

Figure 9. *Permissible compressive and tensile stress distance – upstream view*

Based on the Fig. 9 it can be concluded that strength criteria is satisfied in the greater part of the dam. In the dam flanks, smaller zones in which permissible stresses are exceeded can be observed.

4.3 Dam factor of safety

After the numerical analysis of the model for the defined load case is performed, the dam factor of safety is determined. The factor of safety is determined by the shear strength reduction method, as described in chapter 2.2. The obtained value of dam safety factor is 2.79.

5 CONCLUSIONS

In this paper, a numerical stability analysis of concrete arch dam is performed using the finite element method. An optimal finite element mesh is created based on the geometry of the dam and the surrounding rock mass. Boundary conditions and loads corresponding to real dam exploitation conditions are set on the model. The Hoek-Brown material model is used to describe the mechanical behaviour of the model. The calculation was performed using PAK software. The global factor of safety is determined using the shear strength reduction method. In addition to the calculation results and the global factor of safety, control of permissible compressive and tensile stresses according to USBR recommendations is given. The results obtained by FEM analysis show that this procedure can be used for effective stability analysis of concrete arch dams. It can be concluded that the finite element method has become almost indispensable in the stability analysis of geotechnical structures because it takes into account all the specificities of the structure with much greater reliability, unlike classical, analytical methods.

ACKNOWLEDGEMENT

This research is partly supported by the Ministry of Education and Science, Republic of Serbia, Grant TR32036 and Grant TR37013.

REFERENCES

[1] M. Kojić, R. Slavković, M. Živković and N. Grujović (2010), *Finite element method 1*, Faculty of Mechanical Engineering, University of Kragujevac, Kragujevac
[2] K. J. Bathe (1996), *Finite Element Procedures*, Massachusetts Institute of Technoogy: Prentice Hall, Inc., Massachusetts
[3] E. Hoek and E. Brown (1980), *Underground Excavations in Rock*, Institution of Mining and Metallurgy, London
[4] E. Hoek (1983), "Strength of jointed rock masses", *Geotechnique*, vol. 33, no. 3, pp. 187-223
[5] E. Hoek, C. Carranza-Torres and B. Corkum (2002), *Hoek-Brown failure criterion – 2002 Edition*, in Proc. NARMS-TAC Conference, Toronto
[6] M. Kojić, R. Slavković, M. Živković and N. Grujović (2016), *PAKS - Program for structural analysis using FEM – User manual*, Faculty of Engineering, University of Kragujevac, Kragujevac
[7] M. Kojić, N. Filipović, R. Slavković, M. Živković and N. Grujović (1999), *PAK-P, Program for FE Analysis of FlowThrough Porous Media*, Faculty of Mechanical Engineering, University of Kragujevac, Kragujevac
[8] Siemens (2015), *FEMAP User Guide Version 11.2*, Siemens PLM Software Inc.
[9] B. o. R. United States Department of the Interior (1977), *Design Criteria for Concrete Arch and Gravity Dams*, US
[10] E. Hoek (1968), "Brittle failure of rock," *Rock Mechanics in Engineering Practice*, pp. 99-124
[11] E. Brown (1970), "Strength of models of rock with intermittent joints," *Journal of the Soil Mechanics and Foundations Division*, vol. 96, no. 6
[12] E. Hoek, P. Kaiser and W. Bawden (1995), *Support of Underground Excavation in Hard Rock*, A.A. Balkema, Roterdam
[13] D. Rakić (2014), *Development and application of porous media material models in static and dynamic analysis of embanked dams*, PhD thesis, Faculty of Engineering, University of Kragujevac, Kragujevac
[14] Z. Berisavljević, D. Berisavljević, V. Čebašek and D. Rakić (2015), "Slope stability analyses using limit equilibrium and soil strength reduction methods," *Građevinar*, vol. 67, no. 10, pp. 975-983
[15] M. Bojović, D. Rakić, S. Vulović, M. Živković, D. Divac, N. MIlivojević, S. Radovanović and V. Milivojević (2016), *Stability analysis of concrete gravity dam using finite element method*, YU INFO 2016 – 21th Conference and Exhibition, Kopaonik
[16] B. Zhu (1997), "Prediction of water temperature in deep reservoirs," *Dam Engineering*, vol. 8, no. 1, pp. 13-25

COMETa 2022
6th INTERNATIONAL SCIENTIFIC CONFERENCE
17th - 19th November 2022
Jahorina, B&H, Republic of Srpska
University of East Sarajevo
Faculty of Mechanical Engineering
Conference on Mechanical Engineering Technologies and Applications

SPEED CONTROL OF AC MOTOR IN HYDRAULIC SYSTEM BY USING U/f CONTROL METHOD IN MATLAB SIMULINK

Jelena Erić Obućina[1], Stevan Stankovski[2], Gordana Ostojić[3]

Abstract: In an effort to adapt the capacity of the pump in the hydraulic system to the requirements of the machine it drives, a large number of regulators, hydraulic-mechanical devices, often with electronic control, have been developed. Hydraulics and electronics have been intensively complementing each other in recent years, so that in a certain area of application, pumps with hydraulic-electronic regulators are being replaced with pumps of constant specific volume with variable speed (frequency regulator control). The paper presents research into the way electric motors are controlled, as well as the efficiency itself, which is reflected in energy savings and is dominant in application in hydraulic systems. This is seen through modeling and simulation, as well as experimental results.

Key words: energy saving, frequency regulator, hydraulic system, regulation

1 INTRODUCTION

Within the basic functions of the hydraulic system, energy transformation, the construction of the hydraulic system must fulfill another important requirement. This requirement is that energy losses in the energy transformation path must be minimal. The total loss of energy in the hydraulic system arises as a result of: a) pressure drop, b) volume losses within the components, c) uncoordinated pump characteristics with the maximum and necessary [1, 2, 8].

Losses due to pressure drop can be reduced by the construction of hydraulic components that provide the necessary pressure in the system. In reducing the volume losses in the hydraulic system, in fact, the characteristics of the pump are adjusted with the requirements that occur in the system. This means that the operation of the

[1] mr Jelena Eric Obucina, Shumadia Academy of Professional Studies, Department in Trstenik, Radoja Krstica 19, 37240 Trstenik, Serbia, jobucina@asss.edu.rs (CA),
[2] dr Stevan Stankovski, University of Novi Sad, Faculty of Technical Sciences, Trg Dositeja Obradovica 6, 21000 Novi Sad, Serbia, stevan@uns.ac.rs
[3] dr Gordana Ostojic, University of Novi Sad, Faculty of Technical Sciences, Trg Dositeja Obradovica 6, 21000 Novi Sad, Serbia, goca@uns.ac.rs

hydraulic system must be monitored at all times and meet the requirements that are required at that moment. [1, 2, 7, 8].

The development of electronics creates new spaces for the development of hydraulics, not only in the field of component design, but also in control systems. [2] Today electric motors are an important standard industrial product. These motors are designed to run at a fixed speed and work has been going on for many years to optimise the control of their running speed. Because of the ever-increasing degree of automation in industry, there is a constant need for more automatic controls, and a steady increase in production speeds and better methods to further improve the efficiency of production plants are being developed all the time.

A static frequency converter is an electronic unit which provides infinitely variable control of the speed of three-phase AC motors by converting fixed mains voltage and frequency into variable quantities. Whilst the principle has always remained the same, there have been many changes from the first frequency converters, which featured thyristors, to today's microprocessorcontrolled, digital units.

It was not until the static frequency converter was introduced that three-phase AC motors with infinitely variable speed could be used effectively. [8].

The vast majority of the static frequency converters used by industry today to control or regulate the speed of three-phase AC motors are designed according to two different principles:

• frequency converters without an intermediate circuit (also known as direct converters), and

• frequency converters with a variable or constant intermediate circuit.

Today, the frequency converter controlled, three-phase AC motor is a standard element in all automated process plants as well as in hydraulic systems. Apart from its ability to use the good properties of three-phase AC motors, infinitely variable speed regulation is often a basic requirement because of the design of the plant. [7, 8]

Energy can be saved if the motor speed matches requirements at any given moment in time. This applies in particular to centrifugal pumps and fan drives where the energy consumed is reduced by the cube of the speed. A drive running at half speed thus only takes 12.5% of the rated power.

2 APPLICATION OF FREQUENCY REGULATOR IN HYDRAULIC SYSTEM FOR REGULATING CAPACITY GEAR PUMPS

Controling of capacity of constant-volume capacities pumps rarely in hydraulic drive designs. In the last twenty years, in parallel with the development of the structure, the improvement of technical characteristics and the fall in the price per kW of power, the frequency regulators are modest, but all the glasses are used in the construction of hydraulic systems. For such a trend, the development of the construction of gear pumps was necessary, in fact, their penetration into the area of higher operating pressures (250 to 300 bar) and larger capacities. The following figure shows a hydraulic system with a gear pump, as a source of hydraulic energy and a frequency regulator, as an electronic component that regulates pump capacity. [4, 6, 7].

The system works by including, at the start, an electric motor, as an energy source, and a frequency regulator on which the reference value of the pressure to be maintained in the system is assigned. The frequency controller serving as a controller has an integrated PID controller that maintains a reference pressure value. Frequency

regulator, slightly clogged pump, and then changes the rotation to keep the pressure at the set value. By activating the command to put the system into operation, the hydraulic pump is running in the order of the desired output, i.e. the reference value to be achieved on the executive body, i.e. hydraulic cylinder, maintains the set value. [7, 8]

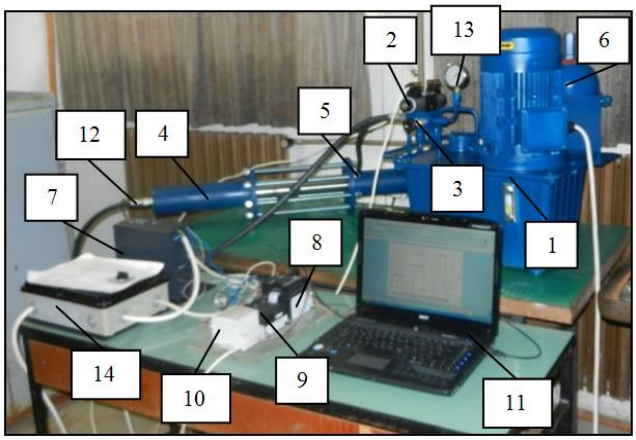

Figure 1. The hydraulic system of regulation capacity gear pump frequency converter [4, 6, 7, 8]

Components of the hydraulic system are:

1 - hydraulic power pack, 2 - hydraulic valve, 3 - safety valve, 4 - hydraulic cylinder, 5 - hydraulic cylinder for load, 6 - hydraulic accumulator, 7 - frequency converter, 8 - PLC CP1L, 9 - a module for acquisition CP1W - MAD11, 10 - DC module 24V, 11 - computer, 12 - pressure transmitter, 13 - manometer, 14 - clutch.

The actual pressure value is obtained from a pressure transmitter mounted on a hydraulic cylinder, more precisely at a pressure measurement point in the hydraulic cylinder, and directly connected to the frequency regulator. In the event of a larger force required, the frequency regulator will refer to the speed of the electric motor, thereby pumping up the flow, as it will require a higher pressure value that is directly related to the force on the hydraulic cylinder. [6, 7, 8]

Also, in case of necessary less force ie. pressure on the hydraulic actuator, this will, via the return connection, react to the frequency regulator which will reduce the speed of the drive shaft of the hydraulic pump and it will give a lower flow.

The results obtained during the experimental work are shown in Figure 2 and determine the dependence of the speed of the electric motor and pressure in the hydraulic system [4, 6, 7, 8].

Figure 2 shows that the different speeds of the three-phase AC motor correspond to the pressure in the hydraulic system. This will confirm a theoretical consideration that the frequency regulator in the hydraulic system saves energy because the system does not always work at high pressure, but will also have the appropriate pressure, which is provided by the speeds of the three-phase AC motor, depending on the required force.

The second variant of this experimental part is that the frequency controller is operated via a PLC, which then receives the pressure value from the transmitter and sends the command to the frequency regulator. [8]

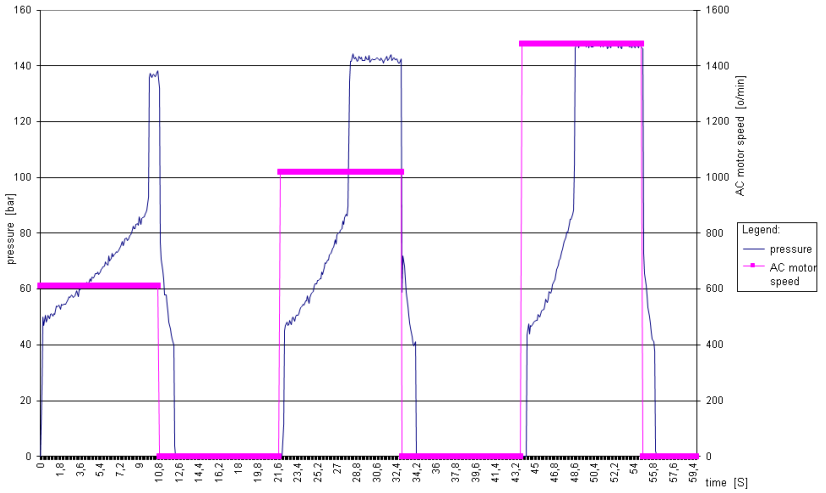

Figure 2. Diagram depending on the pressure in the hydraulic system and the number of revolutions of electric motors [4, 6, 7, 8]

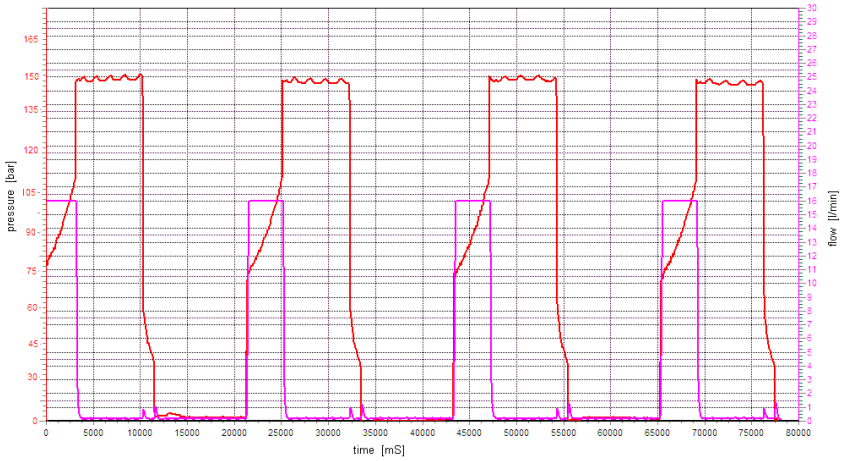

Figure 3. Diagram of change of pressure and flow in time [6]

2.1 Simulation model of V/f control method

Modeling and simulation are two inseparable processes that contain a complex of activities related to building models and experimenting with models in the sense of obtaining information about the behavior of the modeled process [2, 10, 11]. There, modeling primarily refers to the relationship between the actual process and that model, while simulation deals with the connection between the mathematical and simulation models. A simulation model is a model of a process or system that is created using a computer program and can be flexible for experimentation. [10, 11, 12] Due to the increasing participation of automation in the industry, there is a constant

need for automatic control, a continuous increase in the production rate and better methods for improving the level of utility plants are constantly evolving and improving. Electric motors are still important standard industrial product. Until they emerged drives it was not possible to fully control the speed of three-phase AC motor.

In addition to full-speed control AC motors, the use of the frequency converter offers many other ad-vantages:

1. Energy savings are especially nowadays one of the priority claim. This primarily applies to plants with pumps and fans, where power consumption is proportional to the speed cubed. For example, a drive that runs at half speed consumes only 12.5% of the nominal power.

2. Adjust the speed of the manufacturing process offers many advantages in terms of increased productivity, reduced maintenance costs, etc..

3. Starts and stops the machine can be fully con-trolled speed drastically reduced. Using gentle acceleration and deceleration, avoiding the stress and sudden strikes in mechanical assemblies.

4. In addition to reducing maintenance costs, im-proving the working environment.

As stated, drives control the speed of the motor by changing the frequency of the motor voltage.

A mathematical model for a system shows the de-pendencies between output and input quantities of the system or parts of the system and is expressed by ap-propriate differential or integral-differential equations. Basic laws of physics are applied to establish a suitable mathematical model for a dynamic component of the system. In the case of hydraulic systems it is the law of conservation of energy.

The purpose of setting up a mathematical model is to better describe the dynamic behavior of a system com-ponent. In order for the mathematical model to be used in the synthesis of system management algorithms, it is not necessary to describe all the physical phenomena that can take place in the component, because such a system would become too complex. By analyzing the behavior of the system as a whole, we came to the con-clusion that a large number, by the physical nature of different processes, are described by a mathematical model of the same type.

Theoretical analysis is the most basic and cheapest method of system analysis. Simulation results and re-search are based on theoretical research and are a con-firmation of that part of the research. While, the third part of the comprehensive system overview represents the most complex and credible way of system overview. Experimental analysis of the system enables the design of a regulator that will enable a better solution of the system itself, ie. more successful system design, be-cause it will point to problems that may arise in system regulation.

In order to analyze the system using linear analysis methods, it must not contain nonlinearities. Therefore, it is necessary to analyze the system additionally, and all those parameters that do not have a major impact on the dynamic behavior of the system are ignored.

3 CONCLUSION

In this paper, data analysis and experimental data show that the use of the frequency converter in the hydraulic system useful. The diagram on figure 4. below, it is concluded that from the standpoint of economy, in the area of lower pressure, a

combination of the gear pump and the frequency converter is more favorable than the piston-axial pump with hydraulic regulator.

Designed hydraulic system in which the pump is replaced by a variable capacity pump whose capacity is altered by changing the number of revolutions, removes all doubt about a possible replacement of conventional hydraulic controllers with frequency converters. When the hydraulic system in which it is possible to substitute the variable capacity pump with a constant pump capacity and frequency converter, a dominant influence on the application of the system of regulation of pump capacity has a price-performance ratio and energy conservation. Area viability of the application of frequency regulator in relation to hydraulic, with the same capacity of the pump depends on the pressure and everything is on the higher range of applications of frequency converters is narrow and vice versa. There is no universal rule, so every hydraulic system and the pump must be the subject of a specific analysis or an exceptional profit for hydraulic systems where the pump can be replaced by a variable capacity pump capacity constant with frequency converter [4, 7, 9].

Figure 3 shows a diagram of the experimentally obtained pressure dependence of the flow pressure for the hydraulic system in which the frequency regulator is installed in order to provide different speeds for different forces. This all results in energy savings in the hydraulic system.

LITERATURA

[1] Savic V. (2014). *Uljna hidraulika 4*, deo 1, IKOS Novi Sad.
[2] Savic V. (2014). *Uljna hidraulika 4*, deo 2, IKOS Novi Sad.
[3] Merritt, H. E. (1967). *Hydraulic control systems*, John Wiley & Sons Inc., New York.
[4] Savic V., Eric Obucina J., Knezevic D., Ivanisevic A., Balovic B., Kizic S., (2015). Technical-economic view of the replacement of pumps with variable volume pumps a constant volume of the fre-quency converter, *12. International Conference DEMI*, Banja Luka
[5] Exner H., Freitag R. (2011). Hidraulics Basic Princips, Bosch Rexroth.
[6] Eric Obucina J., Cajetinac S., Stankovski S., Ostojic G. (2016). Modern Solutions Management Capacity Hydraulic Pumps Using Frequency Regulation, *XIII International SAUM Conference Niš*, Serbia, November 09th-11th.
[7] Eric Obucina J., Stankovski S., Savić V., Ostojic G., Cajetinac S. (2017). Energy savings using frequency regulation in the hydraulic system with a pump of constant displacement, *13. International Conference DEMI*, Banja Luka
[8] Eric Obucina J., Stankovski S., Ostojic G. S. Cajetinac, S. Aleksandrov (2018).: U/f CONTROL FOR VARIABLE SPEED THREE-PHASE AC MOTOR IN HYDRAULIC SYSTEM, Conference of Mechanical Engineering Technologies and Application COMETa 2018, 27.-30.11.2018., Jahorina, Republic of Srpska, B&H
[9] Bose B. K.(1996).Power Electronics and Variable Frequencies Drives, IEEE Press.
[10] E. Gnesi, J-C. Maré, J. L. Bordet, Modeling of EHA Module Equipped with Fixed-Displacement Vane Pump, The 13th Scan-dinavian International Conference on Fluid Power, SICFP2013, June 3-5, 2013, Linköping, Sweden
[11] M. Wang and P. Y. Li, Passivity based adaptive control of a two chamber single rod hydraulic actuator. In Proc. of The 2012 ACC, Montreal, Canada, 2012.
[12] Lovrec D., Ulaga S. (2007). Pressure control in hydraulic systems with variable or constant pumps, *Experimental Techniques*, Vol. 31, No. 2, 33-41.

COMETa 2022
6th INTERNATIONAL SCIENTIFIC CONFERENCE
17th - 19th November 2022
Jahorina, B&H, Republic of Srpska
University of East Sarajevo
Faculty of Mechanical Engineering
Conference on Mechanical Engineering Technologies and Applications

DALJINSKI UPRAVLJAN PRIGUŠNO-NEPOVRATNI VENTIL – FINALNA VERZIJA PROTOTIPA

Vule Reljić[1], Đorđe Dostanić[2], Slobodan Dudić[3], Jovan Šulc[4], Ivana Milenković[5], Vladimir Jurošević[6]

Rezime: U skladu sa potrebom za daljinskim upravljanjem protokom vazduha pod pritiskom, kako bi aktuator u svakom trenutku radio optimalnom brzinom, na Fakultetu tehničkih nauka u Novom Sadu je, kroz nekoliko iteracija, razvijan daljinski upravljan prigušno-nepovratni ventil. Ovaj rad prikazuje finalnu verziju prototipa pomenutog uređaja, pri čemu je, u poređenju sa prethodnom verzijom, akcenat stavljen na smanjenje gabaritnih dimenzija, omogućavanje upravljanja uređajem putem WiFi komunikacije odnosno unapređenje u vidu mobilnosti uređaja.

Ključne riječi: daljinsko upravljanje, vazduh pod pritiskom, prigušno-nepovratni ventil

REMOTELY-CONTROLLED ONE-WAY FLOW CONTROL VALVE – THE FINAL VERSION OF THE PROTOTYPE

Abstract: In accordance with the need for remote control of the compressed air flow, so that the actuator works at the optimal speed during time, a remotely controlled one-way flow control valve was developed at the Faculty of Technical Sciences in Novi Sad, through several iterations. This paper shows the final version of the prototype of the mentioned device, where the emphasis is placed on the reduction of overall dimensions, enabling device control via WiFi communication, i.e. improvement in the form of device mobility, compared to the previous version.

[1] Doc. dr Vule Reljić, Fakultet tehničkih nauka Univerziteta u Novom Sadu, Novi Sad, Republika Srbija, vuketa90@uns.ac.rs (CA)
[2] Dipl. inž. mehatron. Đorđe Dostanić, ICM Electronics d.o.o, Novi Sad, Republika Srbija, djordjedu96@gmail.com
[3] Prof. dr Slobodan Dudić, Fakultet tehničkih nauka Univerziteta u Novom Sadu, Novi Sad, Republika Srbija, dudic@uns.ac.rs
[4] Prof. dr Jovan Šulc, Fakultet tehničkih nauka Univerziteta u Novom Sadu, Novi Sad, Republika Srbija, sulc@uns.ac.rs
[5] Prof. dr Ivana Milenković, Fakultet tehničkih nauka Univerziteta u Novom Sadu, Novi Sad, Republika Srbija, ivanai@uns.ac.rs
[6] Master inž. mehatron. Vladimir Jurošević, Fakultet tehničkih nauka Univerziteta u Novom Sadu, Novi Sad, Republika Srbija, vladimirjurosevicvl@uns.ac.rs

Key words: Remote control, compressed air, one-way flow control valve

1 UVOD

U zavisnosti od toga koji tip upravljačkog problema se rješava, često je potrebno smanjiti brzinu pneumatskog aktuatora kako bi isti uvijek radio optimalnom a ne maksimalnom brzinom. Naime, maksimalne brzine rezultuju većim habanjem što dovodi do skraćenja radnog vijeka komponenti i sistema pa pneumatski aktuatori treba da se kreću brzinama koje su najekonomičnije za upravljački sistem i samu mašinu [1]. Smanjenje brzine kretanja vazduha pod pritiskom moguće je izvesti na dva načina [2]:

- korišćenjem prigušnice, pri čemu se pomenuta prigušnica postavlja na odrzrakama komandnog razvodnika;
- korišćenjem prigušno-nepovratnog ventila, pri čemu se pomenuti ventil postavlja između komandnog razvodnika i pneumatskog cilindra, kako bi se omogućilo nesmetano punjenje komore cilindra vazduhom pod pritiskom u jednom smjeru a prigušenje u drugom smjeru.

Prednost prvog načina postavljanja prigušenja je što se komandni razvodnici sa prigušnicama najčešće nalaze u komandnim ormanima pa su im pristup i podešavanje olakšani. Pored toga, prigušnica je jeftinija od prigušno-nepovratnog ventila. Sa druge strane, nedostatak ovog načina postavljanja prigušenja je to što se, zbog udaljenosti prigušnice od cilindra, uticaj prigušenja ne osjeti odmah odnosno prvi dio hoda je bez prigušenja brzine. Pri tome, ako je hod cilindra kratak a vod do prigušnice dugačak, može da se desi da se uopšte ne osjeti dejstvo prigušenja.

Prednost drugog načina postavljanja prigušenja je da se prigušenje osjeti odmah pri početku kretanja i da traje tokom cijelog hoda. Sa druge strane, nedostatak ovog načina postavljanja prigušenja, uz već pomenutu cijenu, je to što se prigušno-nepovratni ventili, bilo da su direktno postavljeni na tijelo cilindra, bilo da su postavljeni na vodu između komandnog razvodnika i cilindra, često na nepristupačnim mjestima i njihovo podešavanje je otežano. To posebno dolazi do izražaja kod fleksibilnih proizvodnih sistema u kojima se rukuje različitim predmetima rada pa je često potrebno mijenjati podešavanje prigušenja kako bi se tekuća operacija rada sinhronizovala sa drugom, koja iz nekog razloga duže traje. U tim slučajevima je, dakle, moguće smanjiti brzinu, a samim tim povećati pouzdanost, odnosno produžiti životni vijek komponente [3]. U tu svrhu moguće je primijeniti daljinsko upravljanje prigušno-nepovratnim ventilom, što je i urađeno na Fakultetu tehničkih nauka pa je, kroz nekoliko iteracija [4-6], razvijan prototip daljinski upravljanog prigušno-nepovratnog ventila.

U skladu sa tim, ovaj rad prikazuje finalnu verziju prototipa pri čemu je, u poređenju sa prethodnim verzijama [4-6], akcenat stavljen na smanjenje gabaritnih dimenzija te omogućavanje upravljanja uređajem putem WiFi komunikacije, odnosno unapređenje u vidu mobilnosti uređaja. Sam rad je organizovan na način da se u odjeljku 2 prikazuje finalna verzija mehaničke konstrukcije uređaja a u odjeljku 3 novi način upravljanja uređajem. Na samom kraju, u odjeljku 4 izvedeni su najvažniji zaključci i dati pravci daljih istraživanja.

2 MEHANIČKA KONSTRUKCIJA PROTOTIPA UREĐAJA

Osnovni zadatak je podrazumijevao smanjenje gabaritnih dimenzija posljednje razvijene verzije daljinski upravljanog prigušno-nepovratnog ventila [6] a to je postignutno zamjenom nekih komponenti drugim odgovarajućim, ali manjih dimenzija, kao i modelovanjem novog kućišta uređaja. Modelovanje kućišta uređaja je izvršeno u

softverskom okruženju Inventor 2021, pri čemu se vodilo računa o tome da kućište prati liniju komponenti u svom unutrašnjem dijelu. Samo kućište se sastoji iz dva dijela, osnovne konstrukcije i poklopca, koji su povezani pomoću žljebova koji se nalaze na ivicama poklopca [7]. Osnovna konstrukcija (slika 1, pozicija 1) je u cjelini napravljena sa nosačima za koračni elektromotor i prigušno-nepovratni ventil.

U središnjem dijelu uređaja postavljeni su standardni prigušno-nepovratni ventil, proizvođača Festo, oznake GRA-1/4-B (slika 1, pozicija 2) i koračni elektromotor, oznake NEMA 14 (slika 1, pozicija 4), povezani pomoću namjenski razvijene spojnice (slika 1, pozicija 3). Sa desne bočne strane kućišta postavljeni su mikrokontroler, oznake ESP8266 NodeMCU (slika 1, pozicija 5), koji se koristi za upravljanje uređajem, kao i stabilizator napona, oznake LM7805 (slika 1, pozicija 7), koji je korišćen za napajanje mikrokontrolera, te drajver za koračni elektromotor, oznake A4988 (slika 1, pozicija 6). Sa lijeve bočne strane kućišta, kao izvor napajanja električnom energijom, postavljena je LiPo baterija kapaciteta 500 mAh (slika 1, pozicija 8), kao i komponenta za kontrolu napona iste (slika 1, pozicija 9).

Na samom kućištu, ostavljeni su otvori za:

- prekidač za pokretanje cijelog uređaja (slika 1, pozicija 10) i prekidač za pokretanje komponente za kontrolu napona baterije (slika 1, pozicija 11);
- priključke za punjenje baterije ili eksterno napajanje uređaja (slika 1, pozicija 12);
- vizuelnu kontrolu napona baterije (slika 1, pozicija 14);
- priključke prigušno-nepovratnog ventila za protok vazduh pod pritiskom (slika 1, pozicija 13);
- priključak za serijsku komunikaciju mikrokontrolera (sa zadnje strane kućišta).

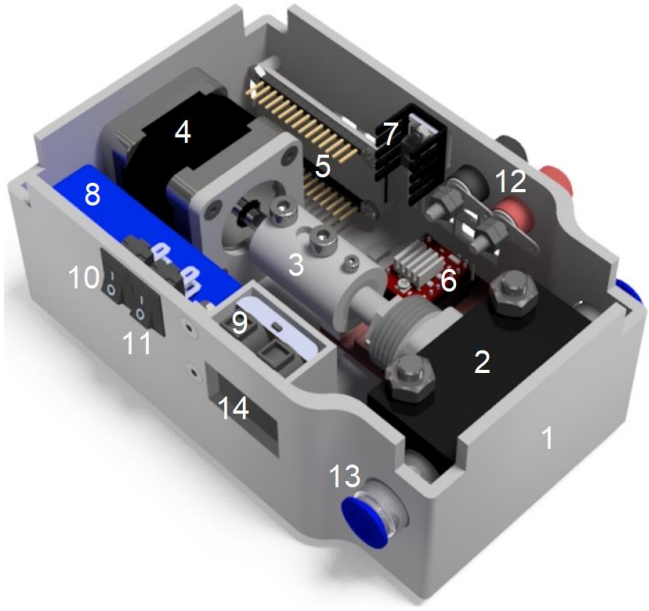

Slika 1. *3D model finalne verzije prototipa uređaja [7]*

Nakon modelovanja, izrađeno je samo kućište kao i svi neophodni nosači pomoću 3D štampača, pri čemu je kao materijal korišćen PLA filament, te je izvršena

integracija svih definisanih elemenata uređaja u jedinstvenu cjelinu. Konačan izgled dobijenog prototipa uređaja prikazan je na slici 2.

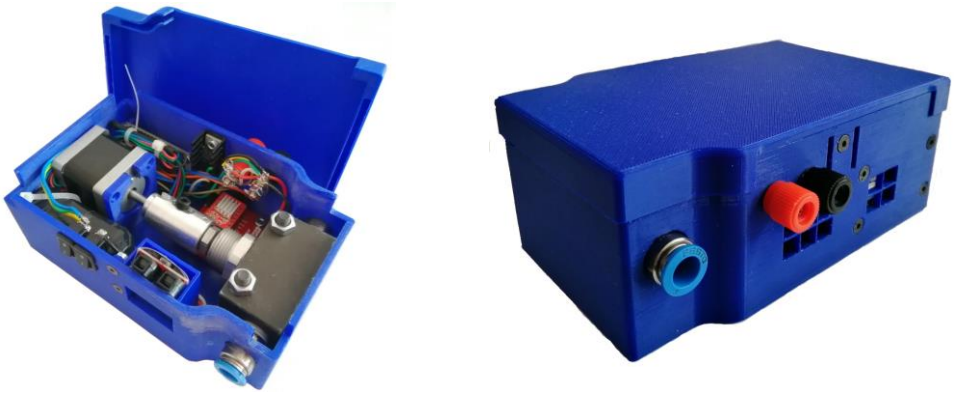

(a) *(b)*

Slika 2. *Konačan izgled prototipa daljinski upravljanog prigušno-nepovratng ventila [7]: a) unutrašnjost kućišta sa postavljenim komponentama; b) poklopac postavljen na kućište*

3 DALJINSKO UPRAVLJANJE UREĐAJEM

Pored smanjenja gabaritnih dimenzija daljinski upravljanog prigušno-nepovratnog ventila, u poređenju sa posljednje razvijenom verzijom [6], bilo je potrebno omogućiti i daljinsko upravljanje uređajem bežičnim putem. U tu svrhu je, prije svega, obezbijeđeno interno napajanje uređaja putem baterije, a zatim i realizovana nova korisnička aplikacija koja omogućava daljinsko upravljanje uređajem pomoću mobilnog telefona ili tableta. Naime, za povezivanje sa uređajem neophodna je korisnička Blynk aplikacija (slika 3) namjenski razvijena za uređaj, kao i stabilna internet konekcija. Bitno je napomenuti i to da je za uređaj neophodno obezbijediti lokalnu WiFi mrežu, čiji se parametri unose u sam programski kod [7].

Slika 3. *Korisnička aplikacija [7]*

Upravljački algoritam je implementiran u programskom jeziku C i izvršava se na NodeMCU razvojnom okruženju [7]. Algoritam je organizovan na taj način da su definisana dva bitna ulazna parametra:

- radni pritisak sistema (u konkretnom slučaju moguće je definisati vrijednost radnog pritiska od 2 bara, 5 bara ili 6 bara [6]);
- procenat otvorenosti prigušno-nepovratnog ventila (u konkretnom slučaju moguće je definisati procenat od 0% do 100%).

Sa druge strane, kao izlazni parametar je definisan broj koraka elektromotora. Vrijednost ulaznih parametara se preko aplikacije proslijeđuje na server, te se u međusobnoj komunikaciji mikrokontrolera i servera preuzimaju ulazni parametri. Nakon očitavanja vrijednosti sa servera, NodeMCU preduzima sve potrebne akcije kako bi se dobio željeni izlaz. U slučaju korektno zadatih ulaznih vrijednosti, prvo se određuje smjer obrtanja koračnog elektromotora. Naime, ukoliko je nova željena vrijednost otvorenosti prigušno-nepovratnog ventila veća od prethodno definisane, bira se smjer obrtanja u smjeru kazaljke na satu, čime dolazi do povećanja protoka vazduha pod pritiskom. U suprotnom, bira se smjer suprotan smjeru kazaljke na satu, na osnovu čega dolazi do smanjenja protoka vazduha pod pritiskom.

Interpolacioni polinom daje apsolutni broj koraka za zadati procenat otvorenosti, tj. broj koraka u odnosu na potpuno zatvoren prigušno-nepovratni ventil. Nakon podešenog smjera obrtanja, potrebno je izračunati broj koraka za podešavanje prethodne i nove vrijednosti otvorenosti prigušno-nepovratnog ventila. Relativni broj koraka između ove dvije vrijednosti predstavlja apsolutnu vrijednost njihove razlike. Nakon izračunavanja potrebnog broja koraka poziva se funkcija koja šalje upravljačke impulse ka drajveru čime se vratilo koračnog elektromotora okreće za izračunati broj koraka. Kada se na izlazu prigušno-nepovratnog ventila dostigne zadati procenat otvorenosti, ažurira se prethodna vrijednost istog.

Pokretanje same aplikacije se vrši pritiskom dugmeta „*Play*“ (slika 4a). Dok je aplikacija u pomenutom režimu, nije moguće vršiti podešavanje vidžeta, njihovo pomjeranje, kao ni dodavanje novih. Za pomenute radnje, potrebno je preći u režim „*Edit*“ pritiskom na dugme „*Stop*“ (slika 4b).

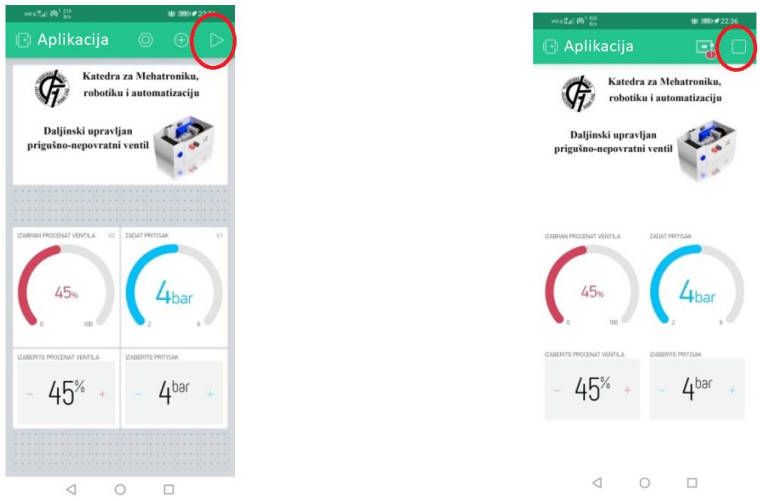

(a) *(b)*

Slika 4. *Pokretanje aplikacije [7]: a) prelazak iz režima „Edit“ u režim „Play“; b) obrnut proces*

Informaciju o tome da li je mikrokontroler trenutno povezan na definisanu WiFi mrežu, kao i tačno vrijeme prelaska u status „*Online*“ ili „*Offline*“, moguće je vidjeti pritiskom na zaokruženo dugme (slika 5). Kada je mikrokontoler u statusu „*Online*“, crveni kružić ne postoji.

Slika 5. *Provjera statusa mikrokontrolera [7]*

4 ZAKLJUČAK

U ovom radu je prikazana realizacija finalne verzije prototipa daljinski upravljanog prigušno-nepovratnog ventila. Pomenuti prototip uređaja omogućava daljinsku regulaciju protoka vazduha pod pritiskom, korišćenjem korisničke aplikacije instalirane na mobilnom telefonu i tabletu. Time se rješava problem otežanog podešavanja prigušenja u slučajevima kada su prigušno-nepovratni ventili na nepristupačnim mjestima. To posebno dolazi do izražaja u slučaju fleksibilnih proizvodnih sistema kod kojih je prilično često potrebno mijenjati brzinu kretanja, u zavisnosti od predmeta rada kojima se trenutno manipuliše pri čemu svaki sljedeći predmet rada može biti drugačiji od prethodnog, odnosno faktor serijnosti može biti čak i jednak jedan.

U poređenju sa prethodnom verzijom daljinski upravljanog prigušno-nepovratnog ventila, smanjene su gabaritne dimenzije a omogućeno je i daljinsko upravljanje putem WiFi komunikacije, čime je izbjegnuta potreba za upotrebom žičanih provodnika. Time je dobijena finalna verzija prototipa uređaja u pogledu mehaničke konstrukcije uređaja. Pravci daljih istraživanja biće usmjereni na dopunu programskog koda kako bi se omogućilo pravilno upravljanje protokom vazduha pod pritiskom za bilo koju vrijednost radnog pritiska (bez ograničenja na vrijednosti radnog pritiska od 2 bara, 5 bara ili 6 bara), te realizaciju konačne verzije korisničke aplikacije kako bi se dobio finalni proizvod.

ZAHVALNOST

Ova rad predstavlja rezultat aktivnosti koje je jednim delom podržalo Ministarstvo prosvete, nauke i tehnološkog razvoja Republike Srbije kroz projekat „Unapređenje nastavnih procesa na DIIM kroz implementaciju rezultata naučno-istraživačkog rada u oblasti Industrijskog inženjerstva i menadžmenta“.

LITERATURA

[1] Campbell, S., (2011) Guidelines for Selecting Pneumatic Cylinders. https://www.machinedesign.com/pneumatics/guidelines-selecting-pneumatic-cylinders, pristupljeno 17. 10. 2022

[2] Šešlija, D., (2020). *Implementacija automatskih sistema: pneumatski sistemi,* Fakultet tehničkih nauka Univerziteta u Novom Sadu, Novi Sad.

[3] Reljić, V., (2020). *Daljinsko upravljanje digitalnom pneumatikom u konceptu Industrije 4.0*, Doktorska disertacija, Fakultet tehničkih nauka Univerziteta u Novom Sadu, Novi Sad.

[4] Šulc, J., Reljić, V., Bajči, B., Šešlija, D., Buač, T. (2017). Development of pneumatic valve remote control. *Proceedings of the 8th PSU-UNS International Conference on Engineering and Technology (ICET-2017)*, Novi Sad, Serbia, June 8-10, 2017, University of Novi Sad, Faculty of Technical Sciences, Paper No. T10-1.2, pp. 1-4

[5] Bajči, B., Dudić, S., Šulc, J., Reljić, V., Šešlija, D., Milenković, I. (2019). Demonstration: Using Remotely Controlled One-Way Flow Control Valve for Speed Regulation of Pneumatic Cylinder. *In: Auer, M., Langmann, R. (eds) Smart Industry & Smart Education. REV 2018. Lecture Notes in Networks and Systems*, vol 47. Springer, Cham. https://doi.org/10.1007/978-3-319-95678-7_16

[6] Reljić, V., Trišić, Ž., Šešlija, D., Milenković, I. (2022). Improving the Reliability of Pneumatic Control Systems by Using Remotely-Controlled One-Way Flow Control Valve. *In: Lalic, B., Gracanin, D., Tasic, N., Simeunović, N. (eds) Proceedings on 18th International Conference on Industrial Systems – IS'20. IS 2020.* Lecture Notes on Multidisciplinary Industrial Engineering. Springer, Cham. https://doi.org/10.1007/978-3-030-97947-8_9

[7] Dostanić, Đ. (2020). *Unapređenje postojećeg prototipa daljinski upravljanog prigušno-nepovratnog ventila*, Diplomski rad, Fakultet tehničkih nauka Univerziteta u Novom Sadu, Novi Sad.

COMETa 2022
6th INTERNATIONAL SCIENTIFIC CONFERENCE
17th - 19th November 2022
Jahorina, B&H, Republic of Srpska
University of East Sarajevo
Faculty of Mechanical Engineering
Conference on Mechanical Engineering Technologies and Applications

DESIGN OF FRACTIONAL - ORDER PI CONTROLLER FOR MULTIVARIABLE PROCESS

Janani Rajaraman[1], Saša Prodanović[2], Ljubiša Dubonjić[3]

Abstract: This article presents design and analysis of fractional order PI controller for a pilot plant binary distillation column. Design of controller for a multivariable (multi-input multi-output – MIMO) process is a challenging task due to loop interaction and system with dead time. The first order model with dead time (FOPDT) model is obtained for the overall open loop transfer function of the system. This work aims on the comparative study of one conventional controller along with fractional order controller based on the performance measures for a pilot plant binary distillation column.

Key words: Decentralized controller, MIMO process, Fractional - order PI controller

1 INTRODUCTION

In most of the chemical industries the process are multiple input and multiple output process. The most important feature of the multivariable systems is the interactions between its variables or cross couplings. Therefore, systems with multiple actuating control inputs and process outputs are defined as multi-input multi-output (MIMO) systems. Due to the presence of the loop interactions in the multivariable system, the closed loop control system designed should be strong and efficient. The interactions that are due to the change in one input affect many output variables. The appropriate pairing of input and output using suitable loop pairing techniques could minimize the adverse interactions. There are a lot of methods for controller design. Fractional - order PID controllers are very useful one, because it gives more possible sets of controller parameters between an integer degrees of controller terms [1-5]. Various tuning rules are given in [6,7]. Many researchers deal with already known methods for PID controller design in combination with fractional-order ones [8-10].

[1] PhD Janani Rajaraman, assistant professor, Department of Electronics and Instrumentation Engineering Sri Chandrasekharendra Saraswathi Viswa Mahavidyalaya, Enathur, Kanchipuram 631561, India, janani.rajaraman@kanchiuniv.ac.in

[2] PhD Saša Prodanović, associate professor, University of East Sarajevo, Faculty of Mechanical Engineering, East Sarajevo, B&H, sasa.prodanovic@ues.rs.ba (CA)

[3] PhD Ljubiša Dubonjić, assistant professor, University of Kragujevac, Faculty of Mechanical and Civil Engineering in Kraljevo, Kraljevo, Serbia, dubonjic.lj@mfkv.kg.ac.rs

Distillation is a process in which a liquid or vapor mixture of two or more substances is separated into its component fractions with desired purity. In multi loop control, the MIMO processes are treated as a collection of multi single loops and a controller is designed and implementd on each loop by taking loop interaction into account. For the MIMO processes with severe loop interactions, the decoupling control schemes are often preferred. Due to that, in recent years numerous investigations aim to develop fractional order PID controller for MIMO process [11-17].

The paper is organized as follows. After Introduction in this section, Section 2 gives design methodology for fractional order PID controller and Gain margin-phase margin controller design methodology. Section 3 represents the design and simulation of PID controller, i.e. its shorter variant PI controller, for lab scale interacting distillation process followed by the simulation and comparative analysis and Conclusion in Section 4.

2 DESIGN METHODOLOGY

2.1 Fractional - Order PID Controller Design

The work of fractional order proportional integral derivative (FOPID) controller is same as that of the PID controller however it gives better response than the PID controller as it have five tuning parameters such as K_P, K_i, K_d, λ and μ, where K_P is the proportional gain, K_i is the Integral gain and K_d is the derivative gain, λ is integration fractional-order and μ is differential fractional-order for the FOPID controller.The fractional order differentiator can be denoted by a general fundamental operator $a^{D_t^q}$ as a generalization of the differential and integral operators, which is defined in (1).

$$a^{D_t^q} = \begin{cases} \dfrac{d^q}{dt^q} & ,R(q) > 0 \\ 1 & ,R(q) = 0 \\ \displaystyle\int_a^t (d\tau)^{-q} & ,R(q) < 0 \end{cases} \tag{1}$$

Where q is the fractional order which can be complex number, the constant a is related to the initial conditions. Minimization technique is used to determine the optimum settings of the fractional integration order λ and the fractional differentiation order μ of the $PI^{\lambda}D^{\mu}$ controller. The Integral of Square Error (ISE) is given ba (2).

$$J = \int_0^{\infty} [e(t)]^2 dt = \int_0^{\infty} [r(t) - Y(t)]^2 dt \tag{2}$$

Where $e(t)$ is the error signal, $r(t)$ is reference value and $Y(t)$ is process output.

The equation of the FOPID in Laplace domain is given by (3).

$$G_c(s) = K_P + \frac{K_i}{s^{\lambda}} + K_d s^{\mu} \tag{3}$$

A usually specified control requirement is also to minimise the Integral of Absolute Error (IAE). The Approximate M-constrained Integral Gain Optimisation (AMIGO) method [18] is used to determine the controller parameters because it is suitable for first order plus dead time (FOPDT) models, which very well describe most of processes in industry.

Proportional and integral parametres are given with (4) and (5), where K is process gain, T is process time constant, L is process dead time and T_i is integral time constant.

$$K_P = \frac{1}{K}\left(0.2 + 0.45\,\frac{T}{L}\right) \tag{4}$$

$$T_i = \left(\frac{0.4L + 0.8T}{L + 0.1T}\right)L \tag{5}$$

2.2 Gain Margin - Phase Margin Controller Design

The gain and phase margins are important measures of robustness, associated with frequency response. It is also know from classical control that phase margin is related to the damping of the system, and can therefore also serve as a performance measure. Accurate and simple analytical formulae are derived to tune/design the proportional integral controller for the commonly used first-order plus dead time plant model to meet gain margin and phase margin specifications. Let $G_p(s)$and $G_c(s)$ denote the process and controller transfer function respectively. From the basic definitions of gain margin and phase margin, following are the set of equations obtained (6-9).

$$arg\left[G_{pii}(j\omega_{pii})G_{cii}(j\omega_{pii})\right] = -\pi \tag{6}$$

$$A_{mii} = \frac{1}{\left|G_{pii}(j\omega_{pii})G_{cii}(j\omega_{pii})\right|} \tag{7}$$

$$\left|G_{pii}(j\omega_{gii})G_{cii}(j\omega_{gii})\right| = 1 \tag{8}$$

$$\varphi_{gii} = arg\left[G_{pii}(j\omega_{gii})G_{cii}(j\omega_{gii})\right] + \pi \tag{9}$$

Where A_{mii} and φ_{gii} are desired gain and phase margin, ω_{gii} and ω_{pii} $(i = 1, 2)$ are gain and phase cross over frequencies, respectively. The PI controller is given by (10).

$$G_c(s) = K_c\left(1 + \frac{1}{sT_i}\right) \tag{10}$$

The PI tuning parameters are given by (11), (12) and (13).

$$K_c = \frac{\omega_p \tau}{A_m k_p} \tag{11}$$

$$T_i = \left(2\omega_p - \frac{4{\omega_p}^2\theta}{\pi} + \frac{1}{\tau}\right)^{-1} \tag{12}$$

$$\omega_p = \frac{A_m\varphi_m + \frac{1}{2}\pi(A_m - 1)}{\left({A_m}^2 - 1\right)\theta} \tag{13}$$

3 SIMULATION RESULTS

3.1 WB Model

Wood and Berry (WB) model of distillation column [19] is considered for the simulation and comparison purposes. The process transfer function model is given by (14), and decentralized controller has been designed for it.

$$\begin{bmatrix} X_D(s) \\ X_B(s) \end{bmatrix} = \begin{bmatrix} \dfrac{12.8e^{-s}}{16.7s+1} & \dfrac{-18.9e^{-3s}}{21s+1} \\ \dfrac{6.6e^{-7s}}{10.9s+1} & \dfrac{-19.4e^{-3s}}{14.4s+1} \end{bmatrix} \begin{bmatrix} R(s) \\ S(s) \end{bmatrix} \tag{14}$$

Where $X_D(s)$ it the distillate and $X_B(s)$ is water. The inputs *R*(*s*) and *S*(*s*) are the reflux flow rate and steam flow rate, respectively. The process has the off-diagonal elements has no right half plane (RHP) poles and diagonal elements has no RHP zeros then the decoupler matrix is obtained as (15).

$$D(s) = \begin{bmatrix} 1 & \dfrac{315.63s+18.9}{268.8s+12.8}e^{-2s} \\ \dfrac{95.04s+6.6}{211.46s+19.4}e^{-4s} & 1 \end{bmatrix} \tag{15}$$

Considering the loop interactions the open loop transfer function of WB model is obtained in the form of FOPDT model (16) and (17).

$$\mathrm{q}_1 = \frac{6.37\mathrm{e}^{-1.36s}}{5.19s+1} \tag{16}$$

$$q_2 = \frac{-9.65e^{-3.49s}}{4.25s+1} \tag{17}$$

3.2 Simulation results

Having in mind that in the most cases FOPDT processes are very good controlled with PI controller, in this research this shorter kind of controller has been designed. It is important to say that AMIGO based FOPID controller is designed with integration order λ=1.2, that has been determined using simulations. Table 1. shows tuning parameters for PI controllers for both loops of WB distilation collumn from two different methods.

Table 1. *PI Tuning parameters for two controller design methods*

Process model	Controller design method	Values of controller parameters	
		$\boldsymbol{K_P}$	$\boldsymbol{K_i}$
Wood – Berry model	AMIGO based FOPID controller	Loop 1: 0.30 Loop 2: -0.0775	Loop 1: 0.088 Loop 2: -0.0181
	Gain Margin – Phase Margin method	Loop 1: 0.0784 Loop 2: -0.0380	Loop 1: 0.0554 Loop 2: -0.0174

Fig. 1. shows the simulation stuides for the obtained controller with good tracking of servo response.

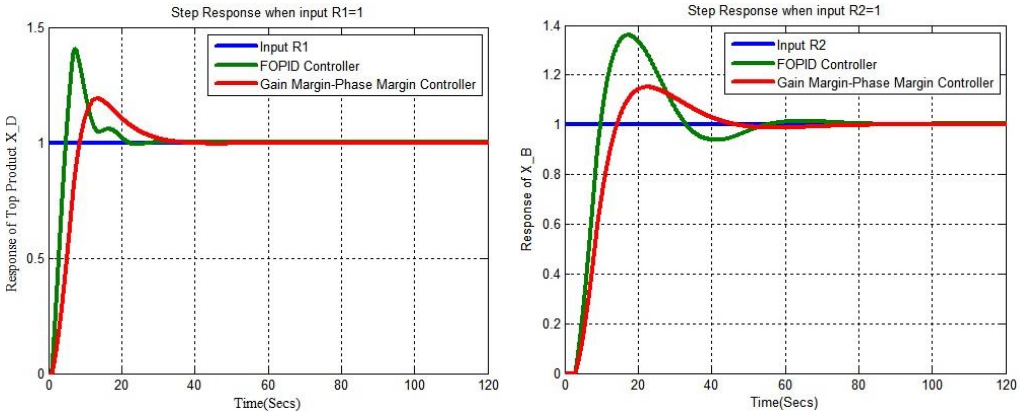

a) b)

Figure 1. Servo responses a) Output XD, b) Output XB

After performing of simulations, analysis of performance indices such as IAE, ISE, ITAE (Integral of Time Absolute Error), ITSE (Integral of Time Squared Error) has been carried out and presented in Table 2. for both methods of controller design. It is noticable that calculated errors are smaller in the case of AMIGO Based FOPID Controller. As it can been seen the focus in the controller design has been put to the stationary state.

Table 2*. Comparison of performance index for servo responses*

Method	IAE	ISE	ITAE	ITSE
AMIGO Based FOPID Controller	18.55	9.846	153.814	33.134
Gain Margin – Phase Margin Controller	19.69	11.18	187.23	46.38

4 CONCLUSION

Performed research leads to the conclusion that fractional - order PI controller designed based on AMIGO method can be used for MIMO processes with dead time. Controller design has been carried out with emphasis to the stationary state more than transition process, taking care about system stability. The effectiveness of suggested approach over conventional (integer degree) Gain Margin - Phase Margin controller design is proven by performance indices IAE, ISE, ITAE, ITSE.

REFERENCES

[1] Podlubny, I. (1999). Fractional-Order Systems and $PI^{\lambda} D^{\mu}$ - Controllers, *IEEE Transactions on automatic control, 44/1,* p.p. 208–214.

[2] Petraš, I. (2011). Practical aspects of tuning and implementation of fractional-order controllers, *Proceedings of the ASME 2011 International Design Engineering*

Technical Conferences & Computers and Information in Engineering Conference IDETC/CIE 2011, Washington, DC, USA.

[3] Edet, E., Katebi, R. (2018). On Fractional-order PID Controllers, *IFAC PapersOnLine* 51/4, p.p. 739–744.

[4] Shah, P., Agashe, S. (2016). Review of fractional PID controller, *Mechatronics*, 38, p.p. 29–41.

[5] Tejado, I., Vinagre, B.M., Traver, J.M., Prieto-Arranz, J., Nuevo-Gallardo, C. (2019). Back to Basics: Meaning of the Parameters of Fractional Order PID Controllers, *Mathematics*, 7, 530.

[6] Valerio, D., Sa da Costa, J. (2006). Tuning-rules for fractional PID Controllers, *Proceedings of the 2nd IFAC Workshop on Fractional Differentiation and its Applications*, Porto, Portugal.

[7] Padula, F., Visioli, A. (2011). Tuning rules for optimal PID and fractional-order PID controllers, *Journal of Process Control*, 21, p.p. 69–81.

[8] CAO, J-Y,. LIANG, J., CAO, B-G. (2005). Optimization of fractional order PID controllers based on genetic algorithms, *Proceedings of the Fourth International Conference on Machine Learning and Cybernetics*, Guangzhou, p.p. 5686-5689.

[9] Yeroglu, C., Tan, N. (2011). Note on fractional-order proportional-integral-differential controller design, *IET Control Theory Appl.* 5/17, p.p. 1978–1989.

[10] Mandić, P.D., Šekara, T.B., Lazarević, M.P., Bošković, M. (2017). *ISA Trans*. 67, p.p. 76-86.

[11] Sivananaithaperumal, S., Baskar, S. (2014). Design of multivariable fractional order PID controller using covariance matrix adaptation evolution strategy, *Archives of Control Sciences*, 24(LX)/2, p.p. 235–251.

[12] Sabura, B.U., Lakshmanaprabu, S.K. (2015). Multivariable Centralized Fractional Order PID Controller tuned using Harmony search Algorithm for Two Interacting Conical Tank Process, *SAI Intelligent Systems Conference*, London, UK, p.p. 320–327.

[13] Song, X., Chen, Y.Q., Tejado, I., Vinagre, B.M. (2011). Multivariable fractional order PID controller design via LMI approach, *18th IFAC World Congress (IFAC'11)*, Milano, Italy, p.p. 13960–13965.

[14] Sruthi, V.J., Binu, L.S. (2016). Fractional Order PID Controller for Level Control in a Spherical Tank. *International Journal of Engineering Research & Technology (IJERT): NCETET - 2016 Conference Proceedings,* 4/17, p.p. 1–5.

[15] Haji Haji, V., Monje, C.A. (2018). Fractional Order PID Control of a MIMO Distillation Column Process Using Improved Bat Algorithm, *Soft Computing*, 23/18, p.p. 8887-8906.

[16] Bhookya, J., Jatoth, R.K. (2019). Fractional Order PID Controller Design for Multivariable Systems using TLBO, *Chemical Product and Process Modeling*, p.p. 1-12.

[17] Nourelhouda, F., Abdelmadjid, K. (2022). The impact of fractional order control on multivariable systems, *Algerian journal of signals and systems (AJSS)*, 7/1, p.p. 7-12.

[18] Romero Perez, J.A., Balaguer Herrero, P. (2012). Extending the AMIGO PID tuning method to MIMO systems, *IFAC Conference on Advances in PID Control PID'12*, Brescia, Italy.

[19] Wood, R.K., Berry, M.W. (1973). Terminal composition control of binary distillation column, *Chem. Eng. Sci,* 28, p.p. 1707-1717.

COMETα 2022
6th INTERNATIONAL SCIENTIFIC CONFERENCE
17th - 19th November 2022
Jahorina, B&H, Republic of Srpska
University of East Sarajevo
Faculty of Mechanical Engineering
Conference on Mechanical Engineering Technologies and Applications

ISPITIVANJE ZAMORNIH KARAKTERISTIKA LEGURE ALUMINIJUMA 242.0 S CILJEM PROCJENE INTEGRITETA AVIONSKOG CILIDARSKOG SKLOPA SA PRSLINOM

Nikola Vučetić[1], Gordana Jovičić[2], Ranko Antunović[1], Vladimir Milovanović[2], Branimir Krstić[3], Dejan Jeremić[1]

Rezime: U cilju procjene integriteta cilindarskog sklopa avionskog motora Lycoming IO-360-B1F usljed pojave prsline na glavi cilindra potrebno je izvršiti niz eksperimentalnih ispitivanja legure aluminijuma 242.0 kao sastavnog materijala glave cilindra, među kojima je ispitivanje zamornih karakteristika na sobnoj i na povišenoj temperaturi. Dobijeni rezultati korišćeni su kao ulazni podaci u numeričkoj strukturnoj analizi razmatranog cilindarskog sklopa. Cilj ispitivanja materijala na zamor jeste odrediti dinamičku čvrstoću, odnosno najveći dinamički napon koji materijal pri određenom broju promjena opterećenja može da izdrži, a da pri tome ne dođe do loma.

Ključne riječi: avionski cilindarski sklop, numerička analiza, prslina, zamor materijala.

TESTING OF THE FATIGUE PROPERTIES OF ALUMINUM ALLOY 242.0 WITH THE PURPOSE OF THE INTEGRITY ASSESSMENT OF AN AIRCRAFT CYLINDER ASSEMBLY WITH A CRACK

Abstract: In order to assess the integrity of the cylinder assembly of the Lycoming IO-360-B1F aircraft engine due to the appearance of the crack on the cylinder head it is necessary to perform a series of experimental tests of aluminum alloy 242.0 as a

[1] Dr Nikola Vučetić, docent, Univerzitet u Istočnom Sarajevu, Mašinski fakultet, Istočno Sarajevo, BiH, nikola.vucetic@ues.rs.ba (CA)
[2] Dr Gordana Jovičić, redovni profesor, Univerzitet u Kragujevcu, Fakultet inženjerskih nauka, Kragujevac, Srbija, gjovicic.kg.ac.rs@gmail.com
[1] Dr Ranko Antunović, redovni profesor, Univerzitet u Istočnom Sarajevu, Mašinski fakultet, Istočno Sarajevo, BiH, ranko.antunovic@ues.rs.ba
[2] Dr Vladimir Milovanović, docent, Univerzitet u Kragujevcu, Fakultet inženjerskih nauka, Kragujevac, Srbija, vladicka@kg.ac.rs
[3] Dr Branimir Krstić, vanredni profesor, Univerzitet odbrane u Beogradu, Vojna akademija, Beograd, Srbija, branimir.krstic@va.mod.gov.rs
[1] Dr Dejan Jeremić, docent, Univerzitet u Istočnom Sarajevu, Mašinski fakultet, Istočno Sarajevo, BiH, dejan.jeremic@ues.rs.ba

constituent material of the cylinder head, among which is the testing of fatigue properties at room and elevated temperature. The obtained results were used as input data in the numerical structural analysis of the considered cylinder assembly. The main aim of material fatigue testing is to determine the dynamic strength, that is the maximum dynamic stress that the material can withstand with a certain number of load changes without breaking.

Key words: aircraft cylinder assembly, numerical analysis, crack, material fatigue.

1 UVOD

Odlučujući faktor za pojavu loma nije samo amplituda opterećenja, već i učestalost ponavljanja opterećenja. Usljed dugotrajnog djelovanja periodično promjenljivih opterećenja može da se javi postepeno razaranje materijala izazvano pojavom koja se naziva zamor materijala.

Pored visine opterećenja i njegove frekvencije postoji i niz drugih parametara koji utiču na dinamičku čvrstoću materijala, među kojima su kvalitet i stanje površine, koroziona oštećenja, temperatura i slično [1-4].

2 UZORCI ZA ISPITIVANJE ZAMORA MATERIJALA

Oblik i dimenzije epruveta propisani su odgovarajućim standardima, u zavisnosti od svrhe i načina ispitivanja na zamor. Broj potrebnih epruveta za određeno ispitivanje može biti različit, što zavisi od vrste i broja podataka koji se traže [5].

Ispitivanje zamornih karakteristika legure aluminijuma 242.0 vršeno je na sobnoj ($23 \pm 5\,°C$) i na povišenoj ($200 \pm 5\,°C$) temperaturi. Zamorne karakteristike legure aluminijuma 242.0, usljed visokocikličnog opterećenja, dobijene su na osnovu rezultata pri ispitivanju epruveta (slika 1 i slika 2) opterećenih na čisto naizmjenično promjenljivo opterećenje. Epruvete su izložene visokocikličnom zamoru u uslovima kontrolisanog napona u skladu sa standardima ASTM E468-90 [6] i ASTM E466-96 [7].

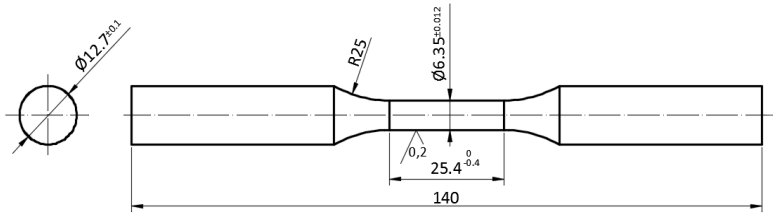

Slika 1. *Oblik i dimenzije epruvete za ispitivanje zamornih karakteristika na sobnoj temperaturi*

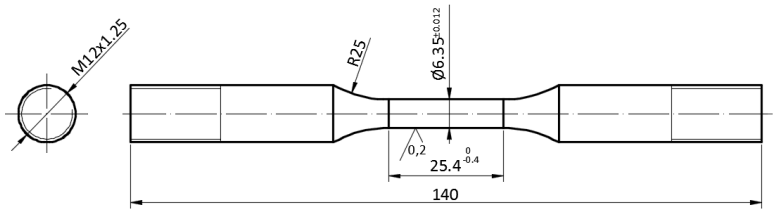

Slika 2. *Oblik i dimenzije epruvete za ispitivanje zamornih karakteristika na povišenoj temperaturi*

Prilikom izrade epruveta neophodno je obratiti pažnju na hrapavost, odnosno kvalitet obrađene površine u cilju eliminisanja mogućih zareza, odnosno koncentracije napona, koji mogu biti potencijalna mjesta nastanka prslina. Sve epruvete za ispitivanje zamornih karakteristika materijala izrađene su u Laboratoriji za CNC mašine alatke i CIM sisteme na Mašinskom fakultetu u Istočnom Sarajevu.

3 EKSPERIMENTALNA POSTAVKA

Eksperimentalna ispitivanja zamornih karakteristika legure aluminijuma 242.0 na sobnoj temperaturi vršena su na Fakultetu inženjerskih nauka Univerziteta u Kragujevcu u Centru za inženjerski softver i dinamička ispitivanja. Određivanje zamornih karakteristika pomenutog materijala na povišenoj temperaturi izvršeno je na Institutu „Kemal Kapetanović“ u Zenici.

3.1 Postupak ispitivanja na sobnoj temperaturi

Ispitivanje zamornih karakteristika materijala čisto naizmjenično promjenljivim opterećenjem na sobnoj ($23 \pm 5\,^{\circ}\mathrm{C}$) temperaturi (slika 3) izvedeno je na servohidrauličnom pulzatoru SHIMADZU, tip EHF-EV101K3-070-0A.

Slika 3. *Postupak ispitivanja zamornih karakteristika materijala na sobnoj ($23 \pm 5\,^{\circ}\mathrm{C}$) temperaturi*

U toku ispitivanja zamornih karakteristika materijala frekvencija je iznosila 10-20 Hz, pri čemu je kao kriterijum otkaza, odnosno inicijalizacije prsline, uzet brzi gubitak krutosti, to jeste pad amplitude napona za 10%. Pripremljene epruvete za ispitivanje zamornih karakteristika na sobnoj temperaturi prikazane su na slici 4.

Slika 4. *Epruvete za ispitivanje zamornih karakteristika na sobnoj temperaturi - izgled prije ispitivanja*

3.2 Postupak ispitivanja na povišenoj temperaturi

Ispitivanje zamornih karakteristika materijala jednoosnim, aksijalnim, čisto naizmjeničnim opterećenjem na povišenoj temperaturi (slika 5) izvedeno je na visokofrekventnom pulzatoru za dinamička ispitivanja tip 10 HFP 422 proizvođača Amsler.

Slika 5. *Postupak ispitivanja zamornih karakteristika materijala na povišenoj temperaturi*

Neposredno prije testa epruveta je zajedno sa alatom postavljena u komoru za zagrijavanje, slika 6. Sa slike 6 može se vidjeti da je ostvaren direktan kontakt termoelemenata sa alatom, odnosno sa ispitivanom epruvetom.

Slika 6. *Postavljanje epruvete u komoru za zagrijavanje*

Nakon toga podešena je temperatura zagrijavanja komore pulzatora na 200 °C. Epruvete su podvrgnute jednoosnom, aksijalnom, čisto naizmjenično promjenljivom cikličnom opterećenju sa stepenom promjenljivosti napona R=-1. U toku ispitivanja zamornih karakteristika materijala frekvencija je iznosila 10-20Hz.

Pripremljene epruvete za ispitivanje zamornih karakteristika na povišenoj temperaturi prikazane su na slici 7.

Slika 7. *Epruvete za ispitivanje zamornih karakteristika na povišenoj temperaturi - izgled prije ispitivanja*

Lom jedne od ispitivanih epruveta nakon završenog testa prikazan je na slici 8.

Slika 8. *Lom ispitivane epruvete nakon testa*

4 REZULTATI I DISKUSIJA

U tabeli 1 prikazani su eksperimentalni rezultati ispitivanja navedenih epruveta legure aluminijuma 242.0 izloženih čisto naizmjenično promjenljivom opterećenju u uslovima kontrolisanog napona.

Tabela 1. *Rezultati jednoosnog, aksijalnog ispitivanja epruveta legure aluminijuma 242.0 izloženih čisto naizmjenično promjenljivom opterećenju [8]*

Oznaka uzorka	σ_a **[MPa]**	**Frekvencija [Hz]**	**Broj ciklusa -** N_f
1-S	100	10	1764
2-S	90	10	4237
3-S	80	10	16878
4-S	70	10	64844
5-S	60	20	201590
6-S	55	20	392380
7-S	50	20	797690
8-S	45	20	1430640

Na osnovu eksperimentalnih rezultata iz tabele 1 i na osnovu statističkih analiza, u skladu sa standardom ASTM E739-91 [9] određene su zamorne karakteristike legure aluminijuma 242.0.

U tabeli 2 prikazani su parametri zamora jednoosnog ispitivanja epruveta legure aluminijuma 242.0 izloženih čisto naizmjenično promjenljivom opterećenju u uslovima kontrolisanog napona.

Tabela 2. *Zamorne karakteristike legure aluminijuma 242.0 pri jednoosnom ispitivanju epruveta izloženih čisto naizmjenično promjenljivom opterećenju [8]*

Veličina	**Vrijednost**
Faktor zamorne čvrstoće $\sigma_f^{'}$	224.5
Eksponent zamorne čvrstoće b	-0.100

S-N kriva u polu-logaritamskoj skali, prikazana na slici 9, određena je na osnovu eksperimentalno dobijenih zamornih karakteristika pri jednoosnom ispitivanju epruveta legure aluminijuma 242.0 izloženih čisto naizmjenično promjenljivom opterećenju u uslovima kontrolisanog napona.

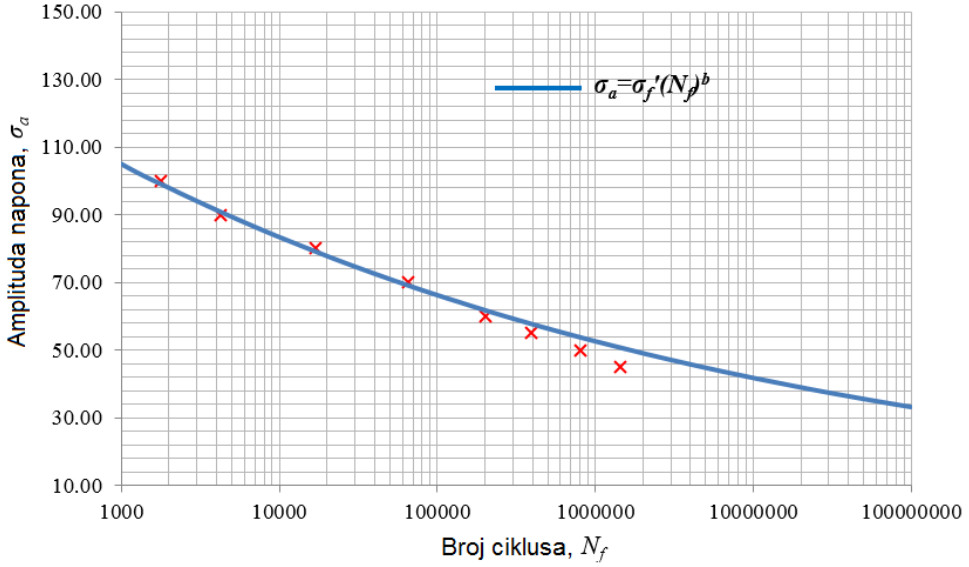

Slika 9. *S-N kriva legure aluminijuma 242.0 dobijena ispitivanjem pri čisto naizmjenično promjenljivom opterećenju na sobnoj temperaturi [8]*

Može se uočiti da nema velikog rasipanja dobijenih rezultata na S-N krivoj sa slike 9. Ispitivanom materijalu, odnosno leguri aluminijuma 242.0 odgovara zamorna čvrstoća od 35 MPa. Može se smatrati da je to vrijednost napona pri kome bi materijal imao „beskonačan“ životni vijek.

U tabeli 3 prikazani su eksperimentalni rezultati jednoosnog, aksijalnog ispitivanja navedenih epruveta legure aluminijuma 242.0 na povišenoj temperaturi izloženih čisto naizmjenično promjenljivom opterećenju u uslovima kontrolisanog napona.

Tabela 3. *Rezultati jednoosnog, aksijalnog ispitivanja epruveta legure aluminijuma 242.0 na povišenoj temperaturi izloženih čisto naizmjenično promjenljivom opterećenju*

Oznaka uzorka	σ_a **[MPa]**	**Frekvencija [Hz]**	**Broj ciklusa - N_f**
1-P	100	10	1352
2-P	90	10	3870
3-P	80	10	15219
4-P	70	10	57350
5-P	65	10	87660
6-P	60	20	178970
7-P	55	20	330800
8-P	50	20	724310
9-P	45	20	1270920

Na osnovu eksperimentalnih rezultata iz tabele 3 i na osnovu statističkih analiza, u skladu sa standardom ASTM E739-91 [9] određene su zamorne karakteristike legure aluminijuma 242.0 na povišenoj temperaturi.

U tabeli 4 prikazani su parametri zamora jednoosnog ispitivanja epruveta legure aluminijuma 242.0 na povišenoj temperaturi izloženih čisto naizmjenično promjenljivom opterećenju u uslovima kontrolisanog napona.

Tabela 4. *Zamorne karakteristike legure aluminijuma 242.0 na povišenoj temperaturi pri jednoosnom ispitivanju epruveta izloženih čisto naizmjenično promjenljivom opterećenju*

Veličina	Vrijednost
Faktor zamorne čvrstoće $\sigma_f^{'}$	219.7
Eksponent zamorne čvrstoće b	-0.102

S-N kriva u polu-logaritamskoj skali, prikazana dijagramom na slici 10, određena je na osnovu eksperimentalno dobijenih zamornih karakteristika pri jednoosnom ispitivanju epruveta legure aluminijuma 242.0 na povišenoj temperaturi izloženih čisto naizmjenično promjenljivom opterećenju u uslovima kontrolisanog napona.

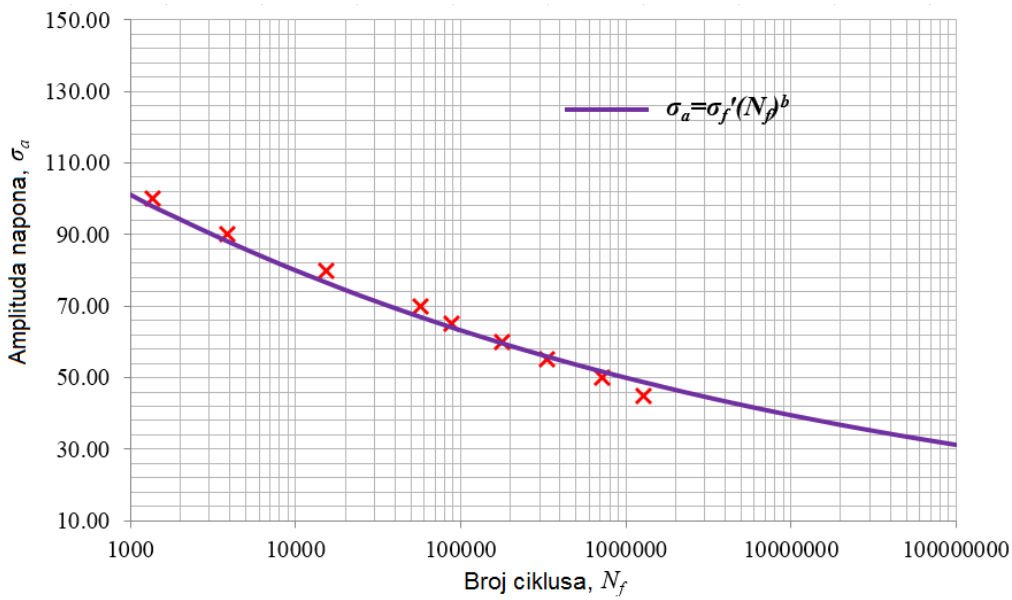

Slika 10. *S-N kriva legure aluminijuma 242.0 dobijena ispitivanjem pri čisto naizmjenično promjenljivom opterećenju na povišenoj temperaturi*

Povećavanjem temperature dolazi do opadanja zamorne čvrstoće legure aluminijuma 242.0. Na osnovu dobijenih rezultata uočava se da na temperaturi od broj ciklusa za isti nivo opterećenja opada poredeći sa rezultatima dobijenim ispitivanjem materijala na sobnoj temperaturi.

U tabeli 5 dato je poređenje rezultata ispitivanja zamora legure aluminijuma 242.0 dobijenih pri istoj amplitudi napona na sobnoj i na povišenoj temperaturi.

Tabela 5. *Poređenje rezultata ispitivanja zamora legure aluminijuma 242.0 dobijenih na sobnoj i na povišenoj temperaturi*

Oznaka epruvete	Amplituda napona	Broj ciklusa do otkaza - N_f	Oznaka epruvete	Amplituda napona	Broj ciklusa do otkaza - N_f	Smanjenje broja ciklusa do otkaza [%]
1-S	100	1764	**1-P**	100	1352	**23.4**
2-S	90	4237	**2-P**	90	3870	**8.7**
3-S	80	16878	**3-P**	80	15219	**9.8**
4-S	70	64844	**4-P**	70	57350	**11.6**
5-S	60	201590	**6-P**	60	178970	**11.2**
6-S	55	392380	**7-P**	55	330800	**15.7**
7-S	50	797690	**8-P**	50	724310	**9.2**
8-S	45	1430640	**9-P**	45	1270920	**11.2**

Rezultati iz prethodne tabele pokazuju da pri temperaturi od $200°C$, pri istoj amplitudi napona, dolazi do smanjenja broja ciklusa do otkaza legure aluminijuma 242.0 od 8.7% do 23.4%. Povećanjem temperature dolazi do opadanja otpornosti materijala na plastične deformacije [10].

Na slici 11 predstavljen je uporedni prikaz S-N krivih legure aluminijuma 242.0 dobijenih ispitivanjem epruveta na sobnoj i na povišenoj temperaturi od $200°C$.

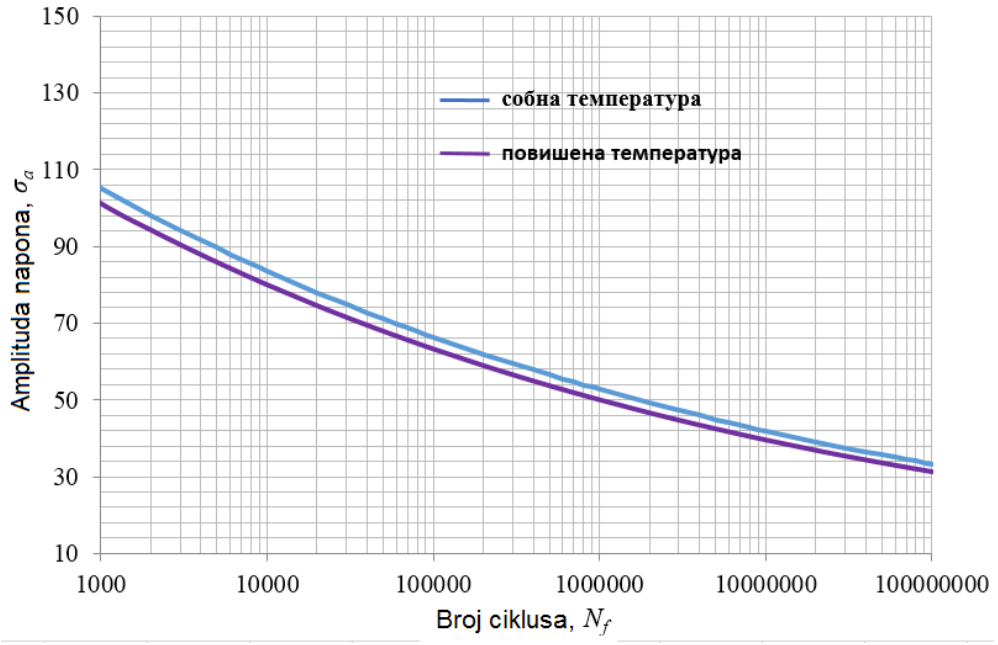

Slika 11. *Uporedni prikaz S-N krivih legure aluminijuma 242.0 dobijenih ispitivanjem epruveta na sobnoj i na povišenoj temperaturi*

5 ZAKLJUČAK

Legura aluminijuma 242.0 se koristi za izradu glava cilindara avionskih motora, što predstavlja izuzetno odgovornu funkciju za ovaj materijal. Stoga, veoma je važno poznavati osobine ovoga materijala, kako hemijske, tako i mehaničke i to na sobnim i na povišenim temperaturama. Činjenica je da se u dostupnoj literaturi nalazi veoma mali broj podataka vezanih za mehaničke karakteristike navedenog materijala. Iz tog razloga potrebno je naglasiti i istaći značaj prikazanih eksperimentalnih istraživanja legure aluminijuma 242.0 prikazanih u okviru ovog poglavlja disertacije. Svaki novi podatak i određena mehanička karakteristika materijala predstavlja veliki doprinos u oblasti ispitivanja konstruktivnih elemenata izrađenih od ovoga materijala. Posebno je važno istaći značaj ispitivanja zamornih karakteristika legure aluminijuma 242.0 na povišenoj temperaturi. Dobijeni rezultati biće direktno korišćeni za procjenu integriteta razmatranog cilindarskog sklopa kao ulazni materijalni podaci neophodni za numeričke proračune.

LITERATURA

[1] Kuwazuru, O., Murata, Y., Hangai, Y., Utsunomiya, T., Kitahara, S., Yoshikawa, N. (2008). X-ray CT inspection for porosities and its effect on fatigue of die cast aluminium alloy. *Journal of Solid Mechanics and Materials Engineering*, Vol. 2, No. 9, pp.1 220-1231.

[2] Akula, G., Satyanarayana, V.V., Kumar, A.G., Kadali, V. (2018). Effect of Surface Roughness on Fatigue Life of Al 6160 Alloy. *International Journal of Innovative Research in Science, Engineering and Technology*, Vol. 7. pp. 9599-9603.

[3] Wang, M., Pang, J.C., Li, S.X., Zhang, Z.F. (2017). Low-cycle fatigue properties and life prediction of Al-Si piston alloy at elevated temperature. *Materials Science and Engineering*, Vol. 704, pp. 480-492.

[4] Fan, K.L., Liu, X.S., He, G.Q., Chen, H. (2015). Elevated temperature low cycle fatigue of a gravity casting Al-Si-Cu alloy used for engine cylinder heads. *Materials Science and Engineering*, Vol. 632, pp. 127-136.

[5] Stephens, R., Fatemi, A., Stephens, R, Fuchs, H. (2001). *Metal Fatigue in Engineering*. New York: John Wiley & Sons Inc.

[6] ASTM: E468-90 (2004). Standard Practice for Presentation of Constant Amplitude Fatigue Test Results for Metallic Materials.

[7] ASTM: E466-96 (2002). Standard Practice for Conducting Force Controlled Constant Amplitude Axial Fatigue Tests of Metallic Materials.

[8] Nikola VUČETIĆ, Gordana JOVIČIĆ, Branimir KRSTIĆ, Miroslav ŽIVKOVIĆ, Vladimir MILOVANOVIĆ, Josip KAČMARČIK, Ranko ANTUNOVIĆ (2020). Further investigation of the repetitive failure in an aircraft engine cylinder head - Mechanical properties of Aluminum alloy 242.0. MECHANIKA, Vol. 26, No. 4, ISSN 1392-1207

[9] ASTM: E739-91 (2004). Standard Practice for Statistical Analysis of Linear or Linearized Stress-Life (S-N) and Strain-Life (ε-N) Fatigue Data

[10] Kahl, S., Ekström, H.E., Mendoza, J. (2014). Tensile, Fatigue and Creep Properties of Aluminum Heat Exhanger Tube Alloys for Temperatures from 293 K to 573 K (20°C to 300°C). *Metallurgical and Materials Transactions A*, Vol. 45A, No. 2, pp. 663-681.

COMETa 2022
6th INTERNATIONAL SCIENTIFIC CONFERENCE
17th - 19th November 2022
Jahorina, B&H, Republic of Srpska
University of East Sarajevo
Faculty of Mechanical Engineering
Conference on Mechanical Engineering Technologies and Applications

PHASE-FIELD MODELING OF DAMAGE IN ALUMINUM ALLOY

Jelena Živković[1], Vladimir Dunić[2], Vladimir Milovanović[3], Miroslav Živković[4]

Abstract: Phase-Field Damage Model (PFDM) is a cutting-edge simulation tool for prediction of damage and crack evolution in materials. This paper shows simulation of AA5083-H321 ductile behavior using the modified PFDM coupled with a von Mises metal plasticity model. Uniaxial tensile tests at room temperature were performed on AA5083-H321 flat specimens in order to identify material parameters for numerical simulation and to verify the modified PFDM implemented into in-house software PAK. Comparison of the obtained results showed good agreement between experimental and simulation force-displacement responses.

Key words: Phase-field damage modeling, aluminum alloy, ductile fracture

1 INTRODUCTION

Phase-Field Damage Model (PFDM) coupled with von Mises metal plasticity was successfully used for simulation of S355 behavior in [1,2] by modifying the hardening function and the coupling variable. Two-intervals hardening function used in that research is then modified in [3], in order to simulate the aluminum alloy (AA) behavior. The improvements of coupled PFDM with plasticity are implemented into the in-house software PAK, developed at Faculty of Engineering, University of Kragujevac, Serbia. This paper shows the verification of implemented model by comparing the force-displacement diagrams obtained by numerical simulations and experimental tests. Sensitivity of the implemented model to the applied displacement increment size was also studied. Three AA5083-H321 flat specimens were investigated by static uniaxial tension tests at room temperature in order to use the representative specimen's recorded results to identify material parameters for numerical simulation. Comparison of results obtained by experiment and numerical simulations showed a

[1] PhD, Jelena Živković, Faculty of Engineering, University of Kragujevac (CA), Kragujevac, Serbia, jelena.zivkovic@kg.ac.rs
[2] PhD, Vladimir Dunić, Faculty of Engineering, University of Kragujevac, Kragujevac, Serbia, dunic@kg.ac.rs
[3] PhD, Vladimir Milovanović, Faculty of Engineering, University of Kragujevac, Kragujevac, Serbia, vladicka@kg.ac.rs
[4] PhD, Miroslav Živković, Faculty of Engineering, University of Kragujevac, Kragujevac, Serbia, miroslav.zivkovic@kg.ac.rs

good match and implemented model was successfully verified.

2 PHASE-FIELD DAMAGE MODEL COUPLED WITH PLASTICITY

Degradation function $g(d)$ for PFDM is proposed by Ambati et al. [4,5] as

$$g(d) = (1-d)^{2p}, \tag{1}$$

where p represents a variable that couples PFDM and von Mises metal plasticity model. Authors of this paper modified the coupling variable in a way that its value is $p = 0$ until the equivalent plastic strain reaches the critical value, i.e. $\frac{\bar{\varepsilon}_p}{\bar{\varepsilon}_p^{crit}} < 1$, because the material is considered to be undamaged in that case, and the value of coupling variable is $p = \frac{\bar{\varepsilon}_p}{\bar{\varepsilon}_p^{crit}} - 1$ in case that $\frac{\bar{\varepsilon}_p}{\bar{\varepsilon}_p^{crit}} \geq 1$. Dependence of modified coupling variable on equivalent plastic strain is shown as continuous line in Figure 1, and the dashed line represents the value of coupling variable defined by Ambati et al. in [4].

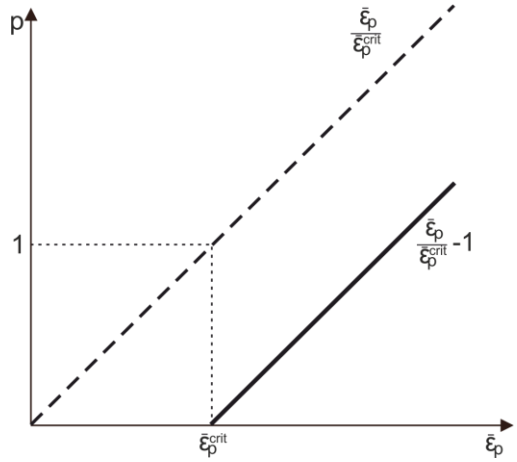

Figure 1. *Dependence of coupling variable on equivalent plastic strain*

In order to simulate behavior of aluminum alloy, that exhibits linear hardening after yielding occurs, it was necessary to modify the two-intervals hardening function used in [2] to describe the idealized response as continuous line in Figure 2. In the first interval, when $\bar{\varepsilon}_p < \bar{\varepsilon}_{p0}$, the yield stress can be defined by the linear hardening function parameter H_0 as

$$\sigma_y = \sigma_{yv} + H_0 \bar{\varepsilon}_p . \tag{2}$$

The second interval starts when $\bar{\varepsilon}_p \geq \bar{\varepsilon}_{p0}$ and the nonlinear increase of the stress can be defined by Simo hardening function as

$$\sigma_y = \sigma_{y0} + \left(\sigma_{y0,\infty} - \sigma_{y0}\right)\left(1 - e^{-n\left(\bar{\varepsilon}_p - \bar{\varepsilon}_{p0}\right)}\right) + H\left(\bar{\varepsilon}_p - \bar{\varepsilon}_{p0}\right), \tag{3}$$

where $\sigma_{y0} = \sigma_{yv} + H_0 \bar{\varepsilon}_{p0}$. The dashed line in Figure 2 represents the theoretical influence of modified PFDM coupled with von Mises metal plasticity model. More details and stress integration algorithm for von Mises large strain plasticity are given in [1-3].

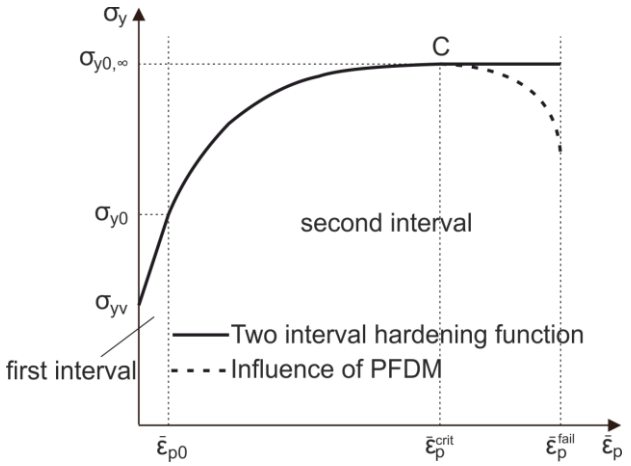

Figure 2. *Idealized stress-strain response of AA5083*

3 VERIFICATION OF MODIFIED PFDM

Three AA5083-H321 flat specimens, shown in Figure 3(a), were investigated at the Centre for Software Engineering and Dynamical Testing, Faculty of Engineering, University of Kragujevac, Serbia. Static uniaxial tensile tests were carried out at room temperature with a stroke control rate of 3 mm/min. Gauge length of the used extensometer MFA25 is 50 mm. Recorded force-displacement responses are shown in Figure 3(b). Fracture occurred within the gauge length only in case of a specimen wirh label 26, so those results are chosen as representative for verification of modified PFDM.

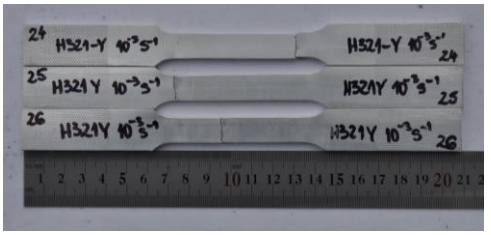

(a)

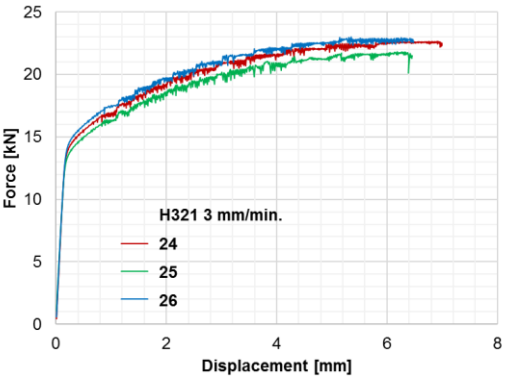

(b)

Figure 3. (a) AA5083-H321 specimens after uniaxial tensile tests; (b) recorded force-displacement response for AA5083-H321 specimens

Material parameters for PFDM simulation are obtained from real stress-real

strain curve of the specimen 26 and by calibration using the least squares method. Obtained values are given in Table 1, where E is Young's modulus, v is Poisson's ratio, H is hardening modulus, G_V is critical fracture release rate per unit volume, n is hardening exponent and l_c is characteristic length-scale parameter.

Table 1. *Material parameters used for PFDM simulation*

E [MPa]	v [-]	σ_{yv} [MPa]	$\sigma_{y0,\infty}$ [MPa]	H [MPa]	H_0 [MPa]	G_V [MPa]	n [-]	l_c [mm]	$\bar{\varepsilon}_P^{crit}$ [-]	$\bar{\varepsilon}_{P0}$ [-]
70150	0.33	200.6	412.89	146.17	19817	2.55	20.3	0.01	0.11	0.0033

Model used for FEM simulation was 1/8 of the gauge section of tested specimen because of the three symmetry planes. Geometrical imperfection was prescribed as a 0.01% linear decrease of width and thickness where occurrence of necking is expected [3]. Four different displacement increments were applied to the top surface nodes of the FE model in order to investigate the sensitivity of the implemented method to the size of the displacement increment and results are shown in Figure 4.

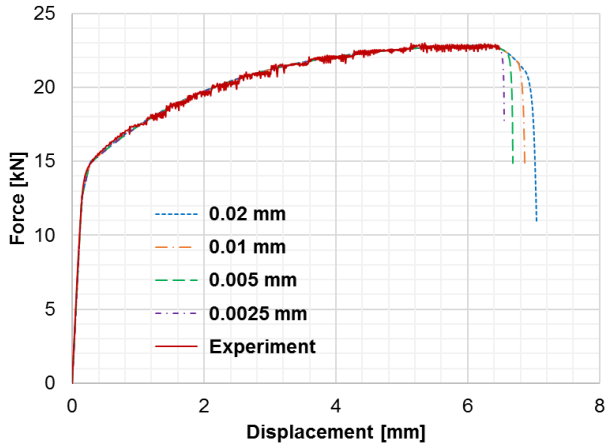

Figure 4. *Force-displacement diagrams obtained for different displacement increments*

The force-displacement response in softening zone is different for various displacement increments, so the part after the fracture point shouldn't be analyzed using this approach. Comparison of force-displacement diagrams obtained experimentally and by numerical simulations is shown in Figure 5. Two different FEM simulations with displacement increment of 0.0025mm were performed – by von Mises plasticity model ("Plasticity") and by PFDM coupled with plasticity ("PFDM + plasticity"), and the latter successfully reproduced the experimentally recorded response.

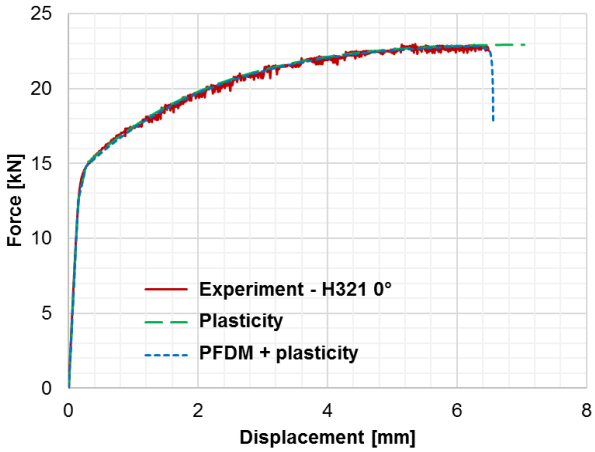

Figure 5. *Force-displacement response of the numerical simulations and experiment*

Figure 6(a) shows simulation results for the equivalent plastic strain field obtained by "pure" plasticity model and results obtained by PFDM coupled with plasticity are shown in Figure 6(b). It can be noticed that damage field, shown in Figure 6(c), has a big influence on localization of plastic strains and it can be concluded that the fracture process in material is caused by the occurrence of damage. Both equivalent plastic strain field and damage field, obtained by PFDM + plasticity simulation, are localized in the fracture zone of the experimentally tested specimen.

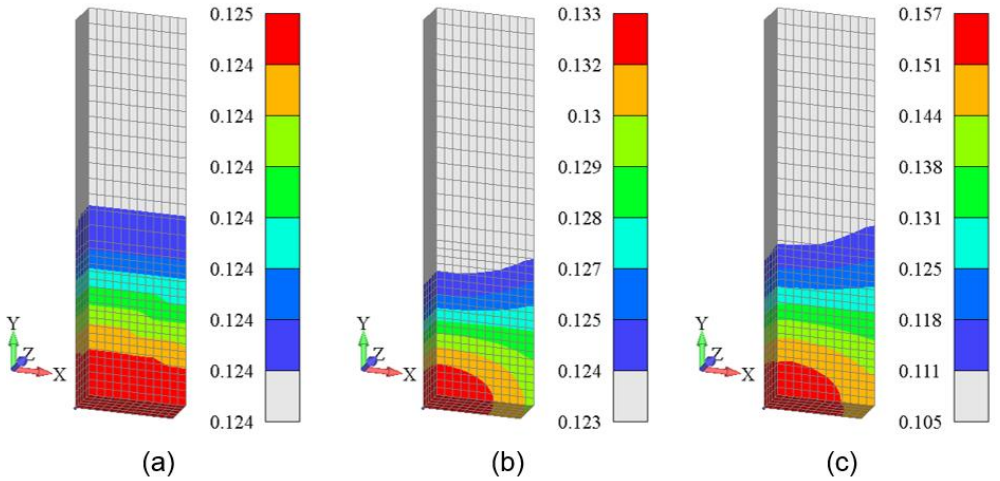

Figure 6. *Simulation results: (a) effective plastic strain field – Plasticity; (b) effective plastic strain field – PFDM + plasticity; (c) Damage field – PFDM + plasticity*

4 CONCLUSIONS

Authors previously verified [1,2] that PFDM coupled with von Mises metal plasticity, implemented into in-house software PAK, can successfully simulate behavior of steel structures. This paper shows three AA5083-H321 flat specimens that were investigated by static uniaxial tension tests at room temperature and the two-intervals hardening function that was modified in order to simulate the recorded response of

AA5083-H321 by using PFDM coupled with plasticity. Experimentally obtained force-displacement diagram is compared to diagrams obtained by two different FEM simulations - von Mises plasticity model and by PFDM coupled with plasticity and a good match between force-displacement diagrams is observed. Comparison of the damage field and the equivalent plastic strain field obtained by PFDM coupled with plasticity showed that the cause of the fracture of the specimen is the occurrence of damage. This and previous papers [1-3] show that implemented modified PFDM coupled with von Mises plasticity can be used to simulate the experimental response of various types of metallic materials with minimal modifications of the hardening function.

ACKNOWLEDGEMENTS

This research was funded by Ministry of Education, Science and Technological Development, Republic of Serbia, Grant TR32036.

REFERENCES

[1] Živković, J. (2022). Unapređenje, implementacija i eksperimentalna verifikacija numeričkog modeliranja oštećenja i loma metala primenom faznog modeliranja. *Doktorska disertacija*, Fakultet inženjerskih nauka Univerziteta u Kragujevcu, Kragujevac, Srbija.

[2] Živković, J., Dunić, V., Milovanović, V., Pavlović, A., Živković, M. (2021). A modified phase-field damage model for metal plasticity at finite strains: numerical development and experimental validation. *Metals***,** vol. 11, no. 1, p.p. 47.

[3] Dunić, V., Živković, J., Milovanović, V., Pavlović, A., Radovanović, A., Živković, M. (2021). Two-intervals hardening function in a phase-field damage model for the simulation of aluminum alloy ductile behavior. *Metals***,** vol. 11, no. 11, p.p. 1685.

[4] Ambati, M., Gerasimov, T., De Lorenzis, L. (2015). Phase-field modeling of ductile fracture. *Computational Mechanics***,** vol. 55, p.p. 1017-1040.

[5] Ambati, M., Kruse, R., De Lorenzis, L. (2016). A phase-field model for ductile fracture at finite strains and its experimental verification. *Computational Mechanics***,** vol. 57, p.p. 149-167.

COMETa 2022
6th INTERNATIONAL SCIENTIFIC CONFERENCE
17th - 19th November 2022
Jahorina, B&H, Republic of Srpska
University of East Sarajevo
Faculty of Mechanical Engineering
Conference on Mechanical Engineering Technologies and Applications

SLOPE ANGLE INFLUENCE ON THE QUALITY OF SURFACEOVERHANGS ON LOW-COST 3D PRINTERS

Strahinja Djurović[1], Dragan Lazarević[2], Slobodan Malbašić[3], Živče Šarkoćević[4], Milan Blagojević[5]

Abstract: Fused deposition modelling (FDM) is a material extrusion method of additive manufacturing where materials are extruded through a nozzle and joined together to create 3D printed objects. Most FDM systems allow you to adjust several process parameters. These include various travel speeds, layer height, cooling fan intensity and nozzle and build platform temperatures. In addition, in order to achieve better print quiality, there are many software settings that can be used/modified and one of them are overhangs. Overhangs are specific geometrical parts of a 3D printed specimen. They are the shapes that extend outward, so they don't have direct support from the previously printed layer hence why they are challenging to print. This paper present the influence of the slope angle on overhang surface quality using a low-cost 3D printer, the Creality 10-S. 5 specimens were printed and the printed surface quality was measured with a EHEV1-200USB DIGITAL PEN camera.

Keywords: Fused Deposition Modeling, Overhangs, Surface quality, 3D printing

1 INTRODUCTION

3D printing technology, known as additive manufacturing or rapid prototyping, is a technology based on three-dimensional models that uses materials such as plastics, adhesive materials and metal powders to build materials layer by layer [1]. This technology allows a creation of a three dimensional object by laying down layers

[1] Asistent, Strahinja Djurović, Akademija Strukovnih Studija Kosovsko Metohijska, Leposavić, Republika Srbija, vstrahinja.djurovic@akademijakm.edu.rs
[2] Docent, dr Dragan Lazarević, Fakultet Tehničkih Nauka, Kosovska Mitrovica, Republika Srbija, dragan.lazarevic@pr.ac.rs
[3] mr Slobodan Malbašić, Uprava za odbrambene tehnologije, Beograd, Republika Srbija, slobodan.malbasic@mod.gov.rs
[4] Vanredni profesor, dr Živče Šarkoćević, Fakultet Tehničkih Nauka, Kosovska Mitrovica, Republika Srbija, zivce.sarkocevic@pr.ac.rs
[5] Asistent, Milan Blagojevic, Fakultet Tehničkih Nauka, Kosovska Mitrovica, Republika Srbija, milan.blagojevic@pr.ac.rs

of materials from a digital computer model and printers then put the desired material in consecutive layers to create a physical object from a digital file [2]. The printer reads the cross-sectional information in the file and uses liquid, powder or sheet materials to combine them. The cross-sections are printed layer by layer, and then the cross-sections of each layer are glued together in various ways to create a solid body. It can process and manufacture samples of more complicated original embryos, while greatly improving the speed and efficiency of processing and manufacturing [3]. A large number of Additive manufacturing processes are now available. Some of the methods melt or soften material to produce the layers, e.g. selective laser melting(SLM), selective laser sintering (SLS), while others cure liquid materials using different other technologies, e.g. stereolithography (SLA) and With laminated object manufacturing (LOM) [4], and one of the most popular and used is fused deposition modeling (FDM). In order to build complex shaped parts, FDM uses support material apart from the build material which supports the overhanging structures during the process and helps in maintaining structural integrity of part until it is strengthened before the support material is removed by breaking or by dissolving using appropriate solvents[5]. This paper present the influence of the slope angle on overhang surface quality, without using support.

2 FUSED DEPOSITION MODELING

Fused deposition modeling (FDM) method was developed by S. Scott Crump in the late 1980s and was designed in 1990 by Stratasys. Fused deposition modeling (FDM) is the first example of a material extrusion system [6]. FDM works on an “additive” principle by laying down material in layers; a plastic filament or metal wire is unwound from a coil and supplies material to produce a part. The process is simple: (1) Pre-processing: Buildpreparation software slices and positions a 3D CAD file and calculates a path to extrude thermoplastic and any necessary support material. (2) Production: The 3D printer heats the thermoplastic to a semi-liquid state and deposits it in ultra-fine beads along the extrusion path [7]. Usually 1.75 - 3 mm wire thickness is used. During 3D printing, the material in the form of wire is melted by passing a 0.4 mm diameter mold and the production is carried out by axial movement [8]. One of the key advantages of FDM (both desktop and industrial) is the technology’s wide range of materials. This includes commodity thermoplastics such as PLA (polylactic acid) and ABS (acrylonitrile butadiene styrene), engineering materials like TPU (thermoplastic polyurethane) and PETG and high-performance thermoplastics, including PEEK, PEI and ULTEM [9]. Many different industries choose to use FDM 3D printing. Industries including automotive and a wide range of consumer goods manufacturers. They use FDM because it helps to aid their product development, their prototyping and their manufacturing process. FDM printing has the ability to create extremely detailed objects, it makes it the ideal choice for those industries that use need to create parts that need to be tested for fit and form [10].

2.1 OVERHANGS IN FUSED DEPOSITION MODELING

3D print overhangs (Fig.1) are geometric shapes in a 3D model that extends outwards and beyond the previous layer. Overhangs have no direct support on it so it is difficult to be printed.Overhangs arise from the common layer-by-layer approach in 3D printing. When you get to the underside of a slope, each subsequent layer must protrude slightly beyond the layer before it. This can presenting a problem in printing. Some of the plastic extends into thin air, and gravity will start to pull it down.

Depending on the angle of the slope being printed, we can characterize the overhang as being printable or extreme.There is a general rule when it comes to 3D printing overhangs. The angle of the overhang should not exceed 45°. This is to make sure that each successive layer has enough support on it. This also means that at 45°, the 3D model is printed well because every layer is in about 50% contact with the layer below it [11, 12]. With a 75° angle, each successive layer is offset by nearly 80%, In other words, less than 20% of each new layer remains in contact with the layer below [13]. There are several ways to improve overhangs: increasing fan cooling of parts, decreasing layer height, changing the orientation of model, reducing printing speed etc [14].

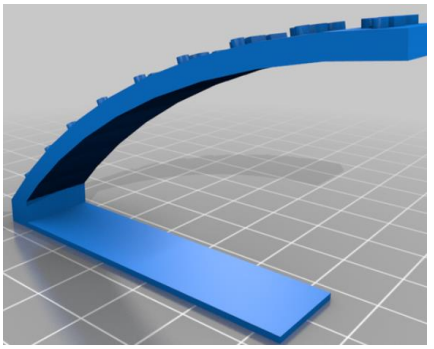

Figure 1. *Overhang slope angle test 45-85 deg [15]*

3 MATHERIALS AND METHODS

Overhang slope angle specimens (Figure. 2) were printed on low-cost Creality 10-s printer, which is located at Faculty of Tehnical Science in Kosovska Mitrovica. Characteristics of printer are: Large build area of 300x300x400mm, print speed normal 60mm/s - max 100mm/s, nozzle diameter 0.4, materials: ABS. PLA, TPU.

Figure 2. *Creality 10-s printer [16]*

STL file (Figure 3) was obtained trough the Ultimaker Cura softwer for slicing 3D CAD file. Printing settings was: standard quality 0.2 mm, infill density 100%, cooling was enabled and support structure disabled, printing temperature 200°c, printing speed 50mm/s, matherial PLA, overhang slope angle from 45-85°c. Dimension of model are: 85x49.1x15mm, printing time 2h 51min. The topography of the characteristic surfaces

was photographed with a magnifying digital camera EHEV1-200USB DIGITAL PEN (Figure 4). The features of this camera are: high-quality CMOS sensor with 2 MP, resolution 1600x1200, USB2.0 port, number of frames per second 20, magnification of 1-400h and focus 10mm - ∞.

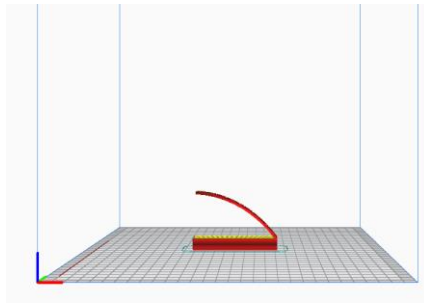

Figure 3. *Overhang model in Cura*

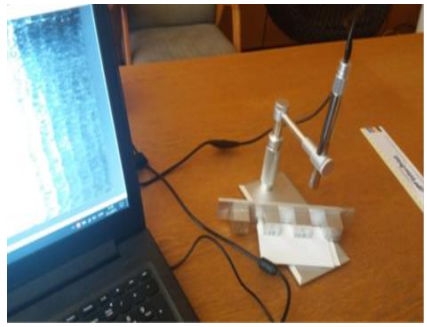

Figure 4. *EHEV1-200USB DIGITAL PEN camera*

4 RESULTS AND ANALYSIS OF RESULTS

In this chapter, the printed surface with different slope angles is shown and analyzed. Figures 5 and 6 (angles of 45 and 50 degrees) show that these angles still give a good surface quality without support. Figures 7 and 8 show that at angles of 55 and 60 degrees, minimal surface changes occur. Figures 9, 10 and 11 show the deviation of the layers because the previous layers are not in good contact with the surface. Figures 12 and 13 indicate a significantly poor quality of the surface and connection of the layers, because the previous layers are in the air and have no support and gravity started to pull it down.

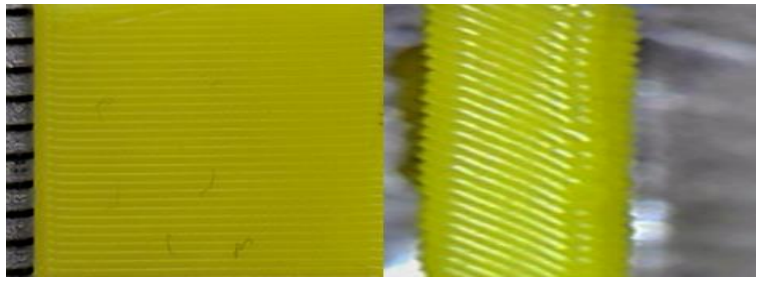

Figure 5. *45º slope angle*

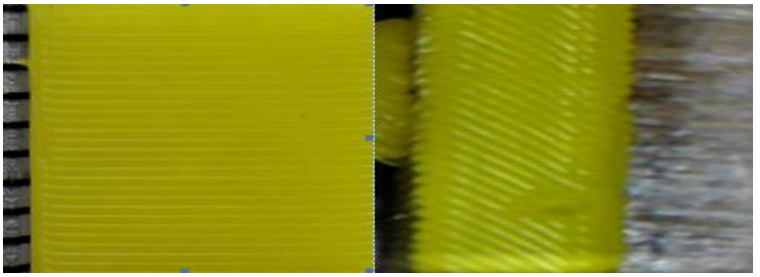

Figure 6. *50º slope angle*

Figure 7. *55º slope angle*

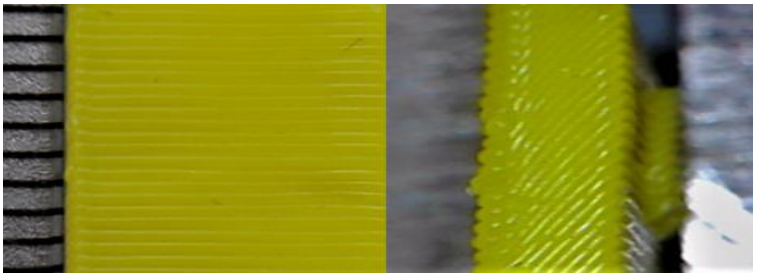

Figure 8. *60º slope angle*

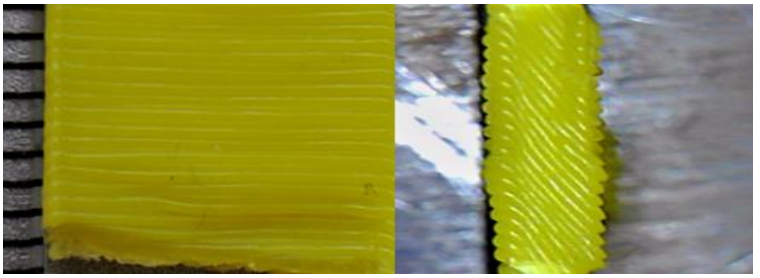

Figure 9. *65º slope angle*

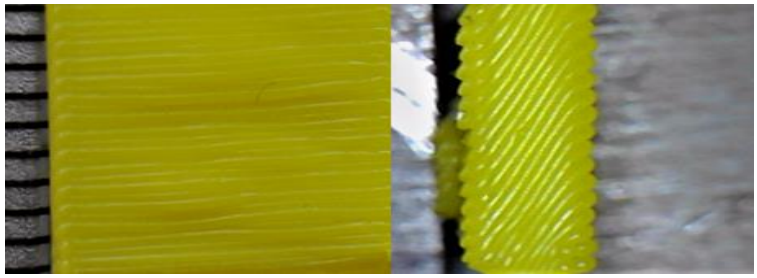

Figure 10. *70º slope angle*

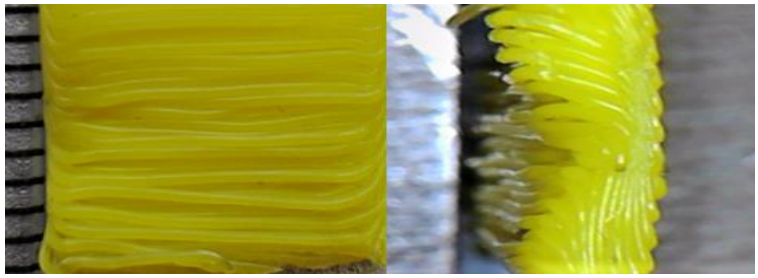

Figure 11. *75º slope angle*

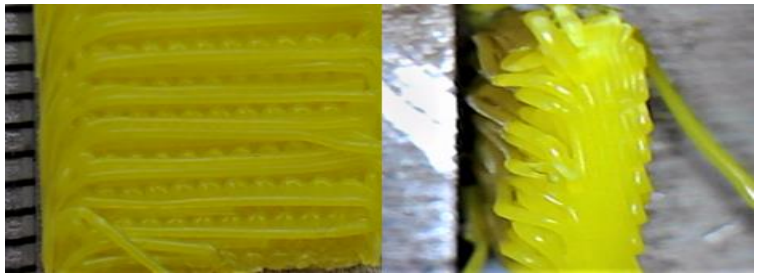

Figure 12. *80º slope angle*

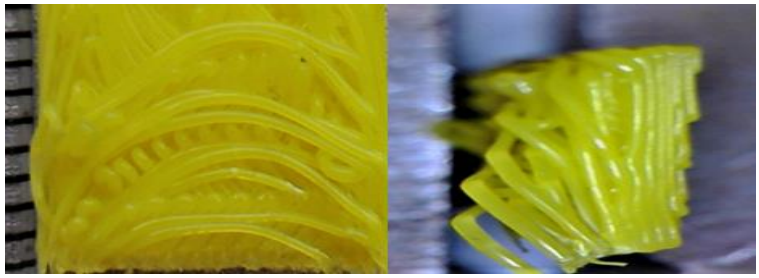

Figure 13. *85º slope angle*

5 CONCLUSION

The influence of the slope angle overhang on 3D printed surface quality was investigated in this paper. There are different types of software settings that can be used to get a better surface quality with this printing method. It is possible to print parts at different slope angles without support, but as the slope increases, the quality of the surface decreases, because the layers are not able to connect with the previous layer, because they hang in the air and gravity pulls them down.

LITERATURE

[1] Botao, H., Guomin, L. (2020). "3D Printing Technology and Its Application in Industrial Manufacturing", *Materials Science and Engineering*, doi:10.1088/1757-899X/782/2/022065

[2] Avinc, O., Yildirim, F., Yavas, A., Kalayci, E. (2017). "3D printing technology and its influences on the textile industry*", International Journal of Industrial Electronics and Electrical Engineering,* Volume-5, Issue-7.

[3] Haocheng ,D., Shaoqian, C. (2020)"Development and Application of 3D Printing and Its Materials", *Insight - Material Science* p.p. 28-31.

[4] Gokhare,V.G.,Jijabai,J.,Dr.Raut,D.N. A Review paper on 3D-Printing Aspects and Various Processes Used in the 3D-Printing *International Journal of Engineering Research & Technology* (IJERT) Vol. 6 Issue 06, June – 2017. ISSN: 2278-0181 IJERTV6IS060409

[5] Chennakesava, P., Shivraj Narayan,Y. (2014). "Fused Deposition Modeling – Insights", *International Conference on Advances in Design and Manufacturing (ICAD&M'14).*

[6] Stansbury, W.J., Idacavage, M.J. (2016). "3D Printing with polymers: Challenges among expanding options and opportunities," Dental Materials, Volume 32, p.p. 54-64

[7] Golub, M., Guo, X., Jung, M., Zhang, J.: (2016). ***3D*** printed abs and carbon fiber reinforced polymer specimens for engineering education, 145th *TMS Annual Meeting & Exhibition, REWAS*

[8] Çabuk, N., Çabuk, S. (2018). "3D Printers And Application Fields", *1. International technological sciences and design symposium,* p.p*. 349-356.*

[9] Hubs: (https://www.hubs.com/knowledge-base/what-is-fdm-3d-printing/, accessed 03.04.2022.

[10] https://tractus3d.com/knowledge/learn-3d-printing/fdm-3d-printing/, accessed 24.10.2022.

[11] https://www.cmac.com.au/blog/improving-3d-print-overhangs-bridges, accessed 24.10.2022.

[12] https://all3dp.com/2/3d-printing-overhang-how-to-master-overhangs-exceeding45/, accessed 24.10.2022.

[13] https://www.3dsourced.com/rigid-ink/how-to-print-overhangs-bridges-exeeding-the-45-degree-rule/, accessed 24.10.2022.

[14] https://3dprinterly.com/how-to-improve-overhangs-in-your-3d-printing/, accessed 24.10.2022.

[15] https://www.thingiverse.com/thing:4557977 , accessed 24.10.2022.

[16] https://www.creality3dofficial.com/products/official-creality-cr-10s-3d-printer accessed 24.10.2022.

COMETa 2022
6th INTERNATIONAL SCIENTIFIC CONFERENCE
17th - 19th November 2022
Jahorina, B&H, Republic of Srpska
University of East Sarajevo
Faculty of Mechanical Engineering
Conference on Mechanical Engineering Technologies and Applications

IMPROVED PROCEDURE FOR NUMERICAL ANALYSIS OF VEHICLE TRANSPORT PLATFORM

Milan Bojović[1], Miloš Pešić[2], Nikola Jović[3], Aleksandar Bodić[4], Vladimir Milovanović[5]

Abstract: The procedure for numerical analysis of platform for vehicles transport is presented in this paper. The structural analysis is performed using a finite element method. Model is prepared in software Femap and calculation performed in NX Nastran. Platform structural analysis requires consideration of various loading cases for different vehicles. As a result, it is necessary to assign a large number of loads manually, which takes a lot of engineering time. An API (Application Programming Interface) script has been created to automatize load assignment. Based on the starting position on the platform, vehicle wheelbase and wheels tread surface the API calculates pressure values and creates load sets. In this way, multiple load sets that simulate different vehicle positions on the platform are created automatically. Based on the presented procedure, it can be concluded that significant saving of engineering time is achieved.

Key words: API, FEM Analysis, Vehicle Transport Platform

1 INTRODUCTION

The needs of the human community for the transportation of people and goods with an increasing number of motor vehicles in the world require an increase in the safety of the vehicles themselves, as well as a reduction in the toxic emission of exhaust gases. For this reason, there is a trend toward greater use of vehicles with electric drive. In order to satisfy the market demand for these vehicles, it is necessary to transport them. The aim of this paper is to examine whether the existing platforms for transporting vehicles with conventional drive can transport significantly heavier vehicles with electric

[1] Milan Bojović, Faculty of Engineering University of Kragujevac, Kragujevac, Serbia, milan.bojovic@uni.kg.ac.rs
[2] Miloš Pešić, Institute for Information Technologies University of Kragujevac, Kragujevac, Serbia, milospesic@uni.kg.ac.rs
[3] Nikola Jović, Faculty of Engineering University of Kragujevac, Kragujevac, Serbia, njovic1995@gmail.com
[4] Aleksandar Bodić, Faculty of Engineering University of Kragujevac, Kragujevac, Serbia, abodic@uni.kg.ac.rs
[5] PhD Vladimir Milovanović, Faculty of Engineering University of Kragujevac, Kragujevac, Serbia, vladicka@kg.ac.rs

drive.

Numerical analysis of a vehicle transport platform requires consideration of different load cases for different transporting vehicles. For this reason, it is necessary to set manually a large number of loads. This way of assigning loads requires a lot of engineering time, so it is essential to automatize the load assignment process. For this reason, an API script is created. API has a wide application in numerical analysis. Some of the application examples are: for setting the load caused by the wind [1], the API program has been written for the calculation of the load from bulk materials onto the sides and the bottom of the wagon [2]. In paper [3], API was used for connecting FEMAP with MS Word, and generating images for the analysis report. In this paper, API was used for assigning loads. API takes into account the vehicle's initial position on the platform, the wheelbase, and the wheel tread as input parameters. Based on these input parameters, API assigns loads on the platform and creates multiple load sets.

In this paper, the procedure of numerical analysis of the vehicle transport platform using the finite element method is presented. The model is created in the pre- and post-processing software Femap [4]. Using the created API script, different load cases corresponding to vehicle positions on the platform were specified. The calculation is performed in NX Nastran software.

In the second chapter, the basics of the API and its application within the Femap software, are briefly explained.

In the third chapter, the FEM model, loads, and boundary conditions are presented. Also, a detailed description of the API script for assigning loads is given.

At the end of the paper, a presentation and discussion of the obtained results are given.

2 APPLICATION PROGRAMMING INTERFACE (API)

An Application Programming Interface (API) represents user interface to implemented functionality that programmers can use to perform various operations. Using an API, the data or services of a software application can be exposed as a set of predefined resources, such as methods, objects, or URIs. In this way, data or services can be accessed by other applications without the need to implement basic objects and procedures. Today, APIs are at the center of many modern software architectures [5, 6].

The FEMAP API is an object-oriented system. This means that all data is represented as discrete objects that the user and other objects can interact with. There are two levels of objects in the API: the application object, and other objects. The first level includes one object, which is the Femap application object. For each application that is written, it is necessary to define and reference a Femap application object that defines the connection between the application and the Femap software. The application object includes data and functionality of a global nature. Application object properties include all global settings of the Femap session, while almost all functions provided by the Femap software menus are available as methods within application object [7].

Detailed description about the API script for load assignment on the vehicle transport platform is given in chapter 3.2.

3 NUMERICAL ANALYSIS OF VEHICLE TRANSPORT PLATFORM

3.1 Finite element model

FE model of vehicle transport platform (Figure 1) is created in Femap software using 2D plate 4-noded elements and 3D hexahedral 8-noded elements. Due to the

symmetry of the vehicle transport platform model, only one half is created. FE model consists of 81633 finite elements and 94943 nodes.

Since only half of the platform is modelled, symmetry boundary conditions are set in the model symmetry plane. Loads that are set on model are self-weight and the load from the vehicles. Loads of transported vehicle are assigned using an API script. This script is created so that the pressures are set on the platform based on the vehicle wheelbase, wheel tread area and the initial position of the vehicle on the platform. In this way, it is possible to simulate the transport of different types of vehicles (different wheelbase), as well as different vehicle positions on the platform.

Figure 1. *FE model of vehicle transport platform*

3.2 API

To automatize load assignment, an API (Application Programming Interface) script has been created. The algorithm based on which the API was developed is shown in Figure 2.

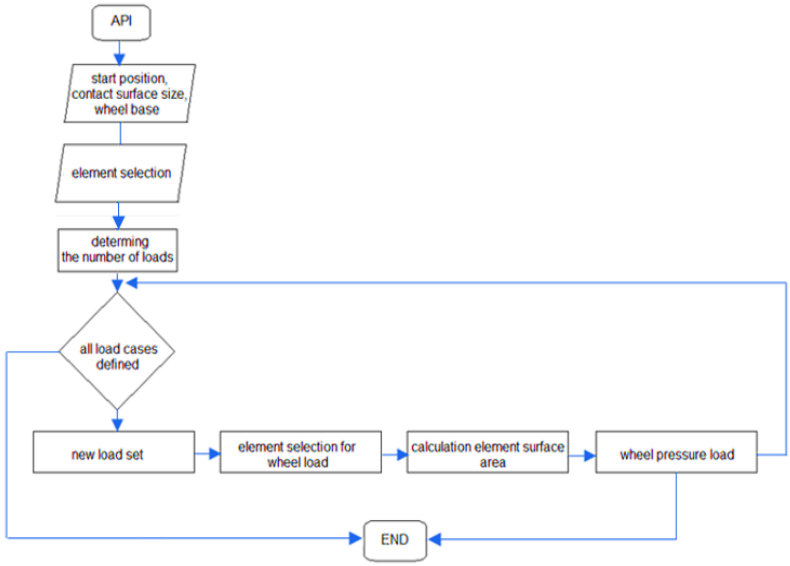

Figure 2. *API algoritam for load definition*

Defining input data is the first step (dimensions of tread surface, initial position, wheelbase, load). Second step is the selection of all tread elements which is done through face element selection. In the first two steps, initial data is entered manually by

the user. Based on the entered initial data by user, the API determines the center of mass of all selected elements. After that, API determines the number of possible vehicle positions on the platform based on wheel tread surface and selected elements (step 2). Next step is creation of new load sets, and setting the self-weight of the platform in all load sets. After that, based on the center of mass of the elements (step 3) and the wheel tread surface dimensions, the elements included in the tread surface for each load case are defined. The area of the elements that define the tread surface is calculated in the next step. Finally, based on the calculated element area and the force exerted by the wheel on the platform, the pressure value is calculated and set in the appropriate load set.

3.3 Load position description of the platform

Vertical loads on the platform come from the wheels (weight of 0.50 t per wheel is multiplied by a dynamic factor of 1.30 and equals 0.65 t per wheel) and the load from each wheel is given as the pressure on the load-carrying surface (cca140 x 160 mm). The initial distance between wheel axles is determined in order to define load cases. The scheme of the position of the car with the distance between wheel axles is shown in Fig. 3.

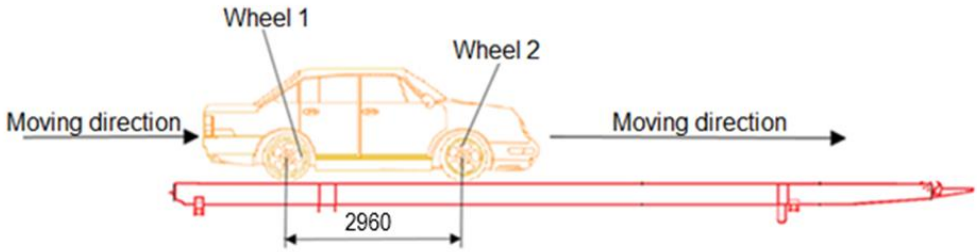

Figure 3. *Scheme of position of the cars*

Wheels tread surface dimensions are 420x15040 mm and it is divided into three strips: A (red color), B (blue color), and C (green color) with dimensions cca140x15040 mm each. Strips A, B, and C are divided into 76 positions in the direction of the longitudinal axis. For each strip (A, B, and C), 76 load cases are defined. The total number of load cases is 228. Fig. 4 shows the load sets created using API for different vehicle positions for all three strips.

Figure 4. *Load assignment using API*

With this procedure, it is possible to significantly save engineering time. Otherwise, a large number of load sets would be assigned manually by the user.

3.4 Results

MultiSet linear analysis is performed in NX Nastran software. Each calculation set corresponds to a different vehicle position on the platform. **Error! Reference source not found.** show maximal vertical displacements of the central node on the platform for all load sets.

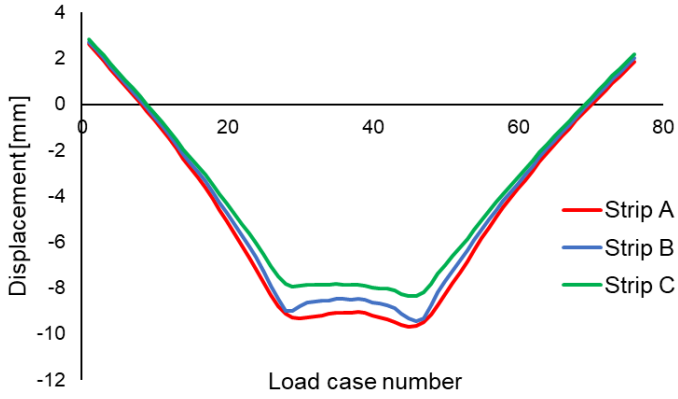

Figure 5. *Vertical displacement of the central node*

Based on the results from the Fig. 5, it can be concluded that the maximal vertical displacement of the central node on the platform is dependent on the wheel position. When the vehicle arrives at the platform, the vertical displacement of the central node of the platform is the smallest. As the vehicle position moves toward the center of the platform, the vertical displacement of the center node increases. The highest value of vertical displacement is when the vehicle is in the middle of the platform, which corresponds to load case 45 in strip A. The value of maximal vertical displacement for load case 45 in strip A is 9.68 mm.

The most unfavourable load case for the entire platform is load case 71 in strip A. The maximum value of von Mises equivalent stress for presented load case is 168.48 MPa.

Figure 6. *Von Mises equivalent stress field*

4 CONCLUSION

The procedure for the numerical analysis of the vehicle transport platform using the finite element method is given in this paper. The presented analysis of the platform was carried out in order to examine the possibility of transporting vehicles with electric drive. The original purpose of the platform was to transport vehicles with a conventional drive.

In order to avoid manually defining a large number of load cases, an API script was created for assigning loads. Based on the vehicle's initial position, the wheelbase and the wheel tread API assign loads on the platform and create multiple load sets.

The finite element model of the vehicle transport platform is created in Femap software. MultiStep linear analysis is performed in NX Nastran software. Each calculation step corresponds to a different position of the vehicle on the platform. Results are shown in form of vertical displacement for all load cases of the platform and the maximum value of von Mises equivalent stress for the most unfavourable load case. The presented results show that significantly loaded zones on the platform correspond to vehicle position for the considered load case. Based on the obtained results, it can be concluded that the procedure given in this paper for the numerical analysis of the vehicle transport platform is effective.

ACKNOWLEDGEMENT

This research is partly supported by the Ministry of Education and Science, Republic of Serbia, Grant 451-03-68/2022-14/ 200378, and Grant TR32036.

REFERENCES

[1] S. Vulović, R. Vujanac, M. Živković, M. Topalović and A. Dišić (2020), *FEM modelling of wind load on industrial filter;* 5th International Scientific Conference, Cometa 2020 "Conference on Mechanical Engineering Technologies and Applications", East Sarajevo, RS, B&H, pp. 138-145, ISBN 978-99976-719-8-1.
[2] S. Vulovć, D. Pavlović, M. Živković, R. Vujanac and M. Topalović (2021), *Analysis of freight wagons for transporting of bulk materials;* 5th Serbian-Greek Symposium on Advanced Mechanics, Kragujevac, Serbia.
[3] S. Vulović, M. Bojović and M. Topalović (2020), *Automation of FEM Analysis Report Generation using Visual Basic FEMAP API*. In: Zdravković, M., Konjović, Z., Trajanović, M. (Eds.) ICIST 2020 Proceedings, pp.10-15.
[4] Siemens (2015), FEMAP User Guide Version 11.2, Siemens PLM Software Inc.
[5] M. P. Robillard (2009), “What Makes APIs Hard to Learn? Answers from Developers,” IEEE Software, 26/6, p.p. 27-34
[6] M. Meng, S. Steinhardt and A. Schubert (2017), "Application Programming Interface Documentation: What Do Software Developers Want?" Journal of Technical Writing and Communication, 48/3, p.p. 1-36
[7] Siemens (2021), FEMAP API Reference, Siemens Digital Industries Software Inc

COMETa 2022
6th INTERNATIONAL SCIENTIFIC CONFERENCE
17th - 19th November 2022
Jahorina, B&H, Republic of Srpska
University of East Sarajevo
Faculty of Mechanical Engineering
Conference on Mechanical Engineering Technologies and Applications

MODULARNI MEHATRONIČKI SISTEMI SA INDUSTRIJSKI ORIJENTISANIM PRISTUPOM

Zorana Mandić[1], Slobodan Lubura[2], Nikola Kukrić[3]

Rezime: Sa današnjim fenomenima u nauci i tehnologiji koji unose nove izazove, sve više se napušta kovnecionalna podijela inženjerskih nauka te rastu zahtjevi za zapažajuće znanje i vještine iz više komplementarnih nauka. Kao jedna od oblasti inženjerstva, koju karakteriše visok nivo sprege između elektrotehnike, mašinstva, automatskog upravljanja i računarstva jeste oblast mehatronike koja predstavlja sinergiju svih gore pomenutih inženjerskih nauka. Od kraja šezdesetih godina prošlog vijeka kada je potekla kovanica riječi mehatronika do danas, samog vrhunca četvrte industrijske revolucije, značaj i prisutnost mehatroničkih sistema su sve više izraženi. O značaju i poziciji mehatroničkih sistema te njihovom uključivanju u obrazovni proces inženjera elektrotehnike biće riječi u nastavku. Način organizovanja jednog ovako izazovnog silabusa korišćenjem modernih mehatroničkih stanica kompanije Festo na visokoobrazovnoj ustanovi Elektrotehničkog fakulteta biće predstavljen kao primjer.

Ključne riječi: mehatronika, didaktičke stanice, obrazovni proces.

MODULAR MECHATRONIC SYSTEMS WITH AN INDUSTRIAL-ORIENTED APPROACH

Abstract: With today's challenging phenomena in science and technology the conventional division of engineering sciences is increasingly being abandoned and the demands for observational knowledge and skills from more complementary sciences are growing. As one of the fields of engineering, which is characterized by a high level of coupling between electrical engineering, mechanical engineering, automatic control, and computing is the field of mechatronics, which represents the synergy of all the above-mentioned engineering sciences. From the end of the sixties of the last century,

[1] Dipl. inž. Zorana Mandić, Univerzitet u Istočnom Sarajevu, Elektrotehnički fakultet, Istočno Sarajevo, Bosna i Hercegovina, zorana.mandic@etf.ues.rs.ba
[2] Prof. dr Slobodan Lubura, Univerzitet u Istočnom Sarajevu, Elektrotehnički fakultet, Istočno Sarajevo, Bosna i Hercegovina, slobodan.lubura@etf.ues.rs.ba
[3] Dipl. inž. Nikola Kukrić, Univerzitet u Istočnom Sarajevu, Elektrotehnički fakultet, Istočno Sarajevo, Bosna i Hercegovina, nikola.kukric@etf.ues.rs.ba

when the word mechatronics was coined, to today, the peak of the fourth industrial revolution, the importance and presence of mechatronic systems have been increasingly pronounced. The importance and position of mechatronic systems and their inclusion in the educational process of electrical engineers will be discussed below. The method of organizing such a challenging syllabus using modern mechatronic stations of the Festo company at the higher education institution of the Faculty of Electrical Engineering will be presented as well.

Key words: mehatronics, didactics stations, education

1 UVOD

Oblast mehatronike smatra se jednom od mlađih oblasti inženjerska, a počeci razvoja vezuju se za sredinu prošlog vijeka. U tom periodu novo razvijene mehaničke komponente posjedovale su i određene elektronske karakteristike. Upravo na semantičkoj simbiozi *mehanike* i *elektronike* leži i kovanica riječi *mehatronika*, koja je po prvi put iskorišćena u 1959. godine Japanu kako bi se opisao mehanički uređaj sa elektronskim karakteristika. Upravo od semantičke osnove riječi mehatronika može se formirati definicija ove oblasti. U literaturi se mogu susresti definicije mehatornike kao integracije mašinstva sa elektronikom, računarstvom i sistemima upravljana u cilju dizajniranja i razvijanja novih uređaja i procesa [1]. Neki autori pri definisanju mehatronike koriste širi pojam elektrotehnike umjesto elektronike [2], a neki autori navode i oblast mjerenja kao zasebnu oblast u sinergije same mehatronike. Jasno je da ono po čemu se ove definicije razlikuju jeste koja to oblast elektrotehnike predstavlja pilar mehatronike, dok su mašinstvo, automatsko upravljanje i računarstvo jasno izdvojeni kao preostala tri pilara. Često se u literaturi može pronaći slikovita definicija mehatornike, predstavljena na slici 1.

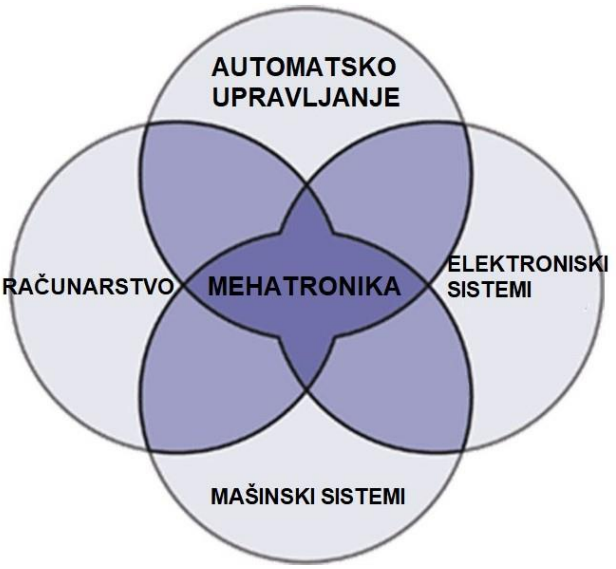

Slika 1. *Grafički prikaz discipline koje obuhvata oblast mehatronike*

Jasno je da, iako, definisane kao četiri zasebne nauke i tehnologije one nisu izolovane, već se razvijaju i podsistemi kao što su kontrolna elektronika, ali i digitalni sistemi upravljanja, elektomehanika i druge.

2 MEHATRONIČKI SISTEMI U INDUSTRIJI I OBRAZOVANJU

Kvalitetna veza između industrije i obrazovnih ustanova bazira se na spregnutoj korelaciji. Sa jedne strane industrija zahtjeva visokoobrazovane i učene inženjere od obrazovnih institucija, dok sa druge strane obrazovne ustanove zahtijevaju kvalitetna radna mjesta za buduće inženjere i finansijsku i tehničku podršku institucija kad god je to moguće. Kao svjedoci četvrte industrijske revolucije ili *Industry 4.0* suočeni smo sa brojim mogućnostima u raznim poljima istraživanja: Interneta stvari, Vještačke inteligencije, Mašinskog učenja i drugih, ali sa brojnim mogućnostima dolaze i izazovi. Kao što su kako se prilagoditi revolucionarnim promjenama u industriji i kako implementirati nove tehnološke napretke u već postojeći sistem obrazovanja. Oblast mehatronike je snažno zastupljena u današnjoj industriji i jedan je od pokretača revolucije 4.0 [3] te je neophodno osnaživanje mehatroničkih kurikuluma i razvijanje inženjerskih vještina tokom osnovnog obrazovanja. Prema statističkim podacima kompanije *Recruiter* koja je vršila predikciju trenda zaposlenja inženjera mehatronike, očekuje se godišnji porast broja zaposlenih inženjera od 1.45% u toku narednih sedam godina. Sa druge strane, analiza dosadašnjih trendova ukazuje na pad broja radnih mjesta od 4.60% sve do 2017. godine kada se bilježi novi rast [5].

Imajući u vidu industrijske trendove i statističke pokazatelje, Elektrotehnički fakultet Univerziteta u Istočnom Sarajevu je prepoznao značaj te uvrstio mehatorničke sisteme u osnovni studije inženjera elektrotehnike na studijskom odsjeku automatika i elektronika. Kurs je baziran laboratorijskom radu sa didaktičkim MPS stanicama kompanije *Festo*, koje predstavljaju skalirane mehatorničke sisteme za obrazovne potrebe, a o kojima će biti riječi u nastavku.

3 DIDAKTIČKE STANICE U OBRAZOVNOM PROCESU

Ishodi učenja realizovanog kursa Moderni mehatronički sistemi na Elektrotehničkom fakultetu definisani su kroz par tačaka. Po uspješnom savladavanju gradiva od studenata se očekuje visok nivo razumijevanja rada mehatroničkih sistema kao i mogućnost odabira ulaznih i izlaznih komponenti jednog takvog sistema. Sem izraženog znanja pojedinačnih proizvodnih procesa, očekuje se i mogućnost integracije pojedinačnih jednostavnih procesa u jednu složenu proizvoljnu liniju. Uspješno savladavanje kursa donijeće dublje razumijevanje softverskih tehnika za programiranje i umrežavanje programabilnih logičkih kontrolera kao upravljačkih jedinica. Neizostavan dio mehatroničkih sistema predstavljaju industrijski roboti te je jedan od ishoda simulacija rada ovakvog robota u proizvodnoj ćeliji. Na osnovu očekivanih rezultata učenja formirane su laboratorijske vježbe koje se izvode na didaktičkim *Festo* stanicama.

Mehatroničke MPS stanice su funkcionalne, upravljive makete osmišljene za trening i učenje osnova automatskog upravljanja u industriji, za upoznavanje sa najzastupljenijim senzorima u proizvodnim procesima kao i za trening i učenje osnovnih programskih jezika za rad sa programabilnim logičkim kontrolerima. Kao takve ove stanice predstavljaju osnovu laboratorijskih vježbi na Elektrotehničkom fakultetu predmeta koji se tiču oblasti mehatronike. Na raspolaganju je ukupno pet mehatroničkih stanica, prikazanih na slici 2, od kojih svaka vrši jedinstven industrijski zadatak.

Slika 2. *Mehatroničke didaktičke stanice u laboratoriji za Industrijsku automatiku*

Kratak opis svake od ovih stanica zajedno sa funkcijom koju obavljaju biće predstavljeno u nastavku.

3.1 Opis rada didaktičnih stanica

Stanica za distribuciju predmeta se sastoji od dva modula: modula magacina u kojem su smješteni predmeti, maksimalno njih osam te modula rotacione ruke. Predmeti smješteni u magacin se pomoću rotacione ruke, koja na svom kraju ima vakuum čašu za pričvršćivanje, distribuiraju ka narednim stanicama.

Obrada predmeta se vrši na stanici koja obavlja više funkcija. Vrši se provjera orjentacije predmeta, proces obrade tj. bušenja predmeta te odlaganje predmeta u narednu stanicu. Ove tri funkcije se vrše simultano kroz više paralelnih grana.

Na osnovu karakteristika predmeta: boje i materijala, stanica za sortiranje vrši razvrstavanje predmeta po kanalima. Ove funkcije obavlja kroz tri modula, a to su modul za detekciju predmeta I određivanje njegovih karakteristika, modula pokretne trake I modula sa kanalima.

Funkcija stanice za testiranje je da odredi karakteristike materijala predmeta, da provjeri visinu te da na osnovu tih podataka predmet proslijedi narednoj stanici ili ga odbaci kao neispravan. Testiranje ispravnosti predmeta je bitan segment u proizvodnom procesu jer se na taj način neispravni predmeti odbacuju smanjujući šansu da dođe do zastoja proizvodnje zbog jednog takvog predmeta. Ova stanica takođe ima nezavisne module: za podizanje predmeta na prvi nivo, modula za mjerenje te modula sa kanalima za odlaganje.

Kroz stanicu za rukovanje predmetima se manipuliše pomoću fleksibilnog *PicAlfa* modula sa dvije ose i hvataljke koji na osnovu vrste predmeta premješta ga ka narednoj stanici ili odlaže na namijenjenim nosačima.

Pomenute mehatroničke stanice mogu se koristiti odvojeno za rješavanje pojedinačnih zadataka, ali postoji i mogućnost njihovog povezivanja kako bi se mogao simulirati komplikovaniji industrijski proces, što je prikazano u narednoj tabeli.

Tabela 1. *Međusobno povezivanje mehatroničkih stanica*

	Naredna MPS stanica				
MPS stanica	Za distribuciju	Za testiranje	Za obradu	Za rukovanje predmetima	Za sortiranje
Za distribuciju		Povezivanje moguće	Povezivanje nije moguće	Povezivanje nije moguće	Povezivanje moguće
Za testiranje	Povezivanje nije moguće		Povezivanje moguće	Povezivanje moguće	Povezivanje moguće
Za obradu	Povezivanje nije moguće	Povezivanje nije moguće		Povezivanje moguće	Povezivanje moguće
Za rukovanje predmetima	Povezivanje nije moguće	Povezivanje nije moguće	Povezivanje moguće	Povezivanje nije moguće	Povezivanje moguće
Za sortiranje	Povezivanje nije moguće	Povezivanje nije moguće	Povezivanje nije moguće	Povezivanje nije moguće	

3.2 Programabilni logički kontroleri

U svakoj od pomenutih stanica postavljen je programabilni logički kontroler - PLK kompanije *Siemens* koji predstavlja upravljačku jedinicu na kojoj se izvršava algoritam upravljanja. Radi se o SIMATIC 300 [6] stanici sa CPU314C-2 PN/DP modulom. Ova centralna procesorska jedinica sadrži 192 kB radne memorije, 24/16 digitalnih ulaza/izlaza, četiri analogna ulaza te dva analogna izlaza. Sem toga, sadrži 1 PT100 mjerni pretvarač temperature, a podržava MPI/DP komunikaciju do 12 Mbit/s. Vrijeme obrade se kreće od 0,06 µs u slučaju operacija na bitovima do 0,59 µs u slučaju izvršavanja aritmetičkih operacija sa pokretnim zarezom. Ukupan broj blokova (organizacionih blokova, blokova podataka, funkcija i funkcijskih blokova) je 1024. Maksimalan broj brojača i tajmera je 256, gdje je maksimalna vrijednost brojača do 255, a rezolucija tajmera se kreće od 10 ms do 9 990 s. Za napajanje se koristi modul PS 307 5A, izlaznog napona 24 VDC i izlazne struje 5 A. Za komunikaciju stanice za programiranje (personalni računar) sa PLK korišćen je MPI protokol.

Kako su zadaci sa kojima se suočavaju studenti sekvencijalnog tipa za realizaciju algoritama upravljanja iskorišćen je programski jezik S7-GRAPH, sadržan u softveru SIMATIC Manager kompanije *Siemens.* Ovaj programski jezik je grafički jezik baziran na GRAFCET (jezik za specifikaciju sekvencijalnih upravljačkih algoritama) u skladu sa standardom DIN EN 60848 (skraćeno IEC 60848).

3.3 Ulazne i izlazne komponente didaktičkih stanica

Svaka od opisanih stanica opremljena je sa velikim brojem ulaznih diskretnih komponenata od kojih su najzastupljeniji prekidači. Radi se o mehaničkim prekidačima koji stanje svojih kontakata mijenjaju pod uticajem operatera ili pri dostizanju određenih vrijednosti procesnih veličina (*). Kao jedna od klasa procesnih prekidača koja se izdvaja po svojoj primjeni su elektronski procesni prekidači. Od analognih ulaznih komponenti stanica za testiranje posjeduje linearni senzor pozicije – potenciometar. Klasifikacija i popis ulaznih komponenti kojima su opremljene date stanice prikazane su u tabeli 2..

Preko izlaznih komponenti vrši se upravljanje nekim tehnološkim procesom ili nekom od procesnih veličina, a opisane didaktičke stanice su opskrbljene sa elektromotorima i pneumatskim cilindrima kao većinskim izvršnim organima Većina stanica kao izvršne organe posjeduje pneumatske translacijske cilindre dok se mogu susresti i rotacijski cilindri. Kao upravljački elementi cilindara korišćeni su pneumatski ventili od kojih najčešće razvodnici zajedno sa drugim vrstama ventila. Korišćeni

razvodnici su usmjeravaju tok radnog medijuma – u ovom slučaju vazduha, a aktivirani su električno. Lista izlaznih komponenti stanica prikazana je u tabeli 3.

Tabela 2: *Lista ulaznih komponenti didaktičkih stanica*

	ULAZNE KOMPONENTE					
	Diskretne					**Analogne**
	Ručni prekidači		**Elektronski procesni prekidači**			**Senzor pozicije**
MPS stanica	Granični prekidači	Tasteri	Induktivni senzor	Kapacitivni senzor	Optički senzor	
Za distribuciju	2	3	1	0	1	0
Za testiranje	0	3	1	1	1	1*
Za obradu	2	3	4	0	0	0
Za rukovanje predmetima	2	3	0		2	0
Za sortiranje	2	3		1	3	0

* digitalizacija signala izvršena preko komparatora i praga okidanja

Tabela 3: *Lista izlaznih komponenti didaktičkih stanica*

	IZLAZNE KOMPONENTE		
	Elektromotori	**Pneumatski cilindri**	
		translacijski	rotacijski
MPS Stanice			
Za distribuciju	0	1	1
Za testiranje	0	2	0
Za obradu	3	0	0
Za rukovanje predmetima	0	2	0
Za sortiranje	1	2	0

Imajući u vidu gradivne dijelove MPS stanica moguće je formirati vizuelnu predstavu zastupljenosti različitih elemenata svake od četiri inženjerske grane koje ulaze su definisanu oblast mehatronike. Takva klasifikacija prikazana je na slici 3.

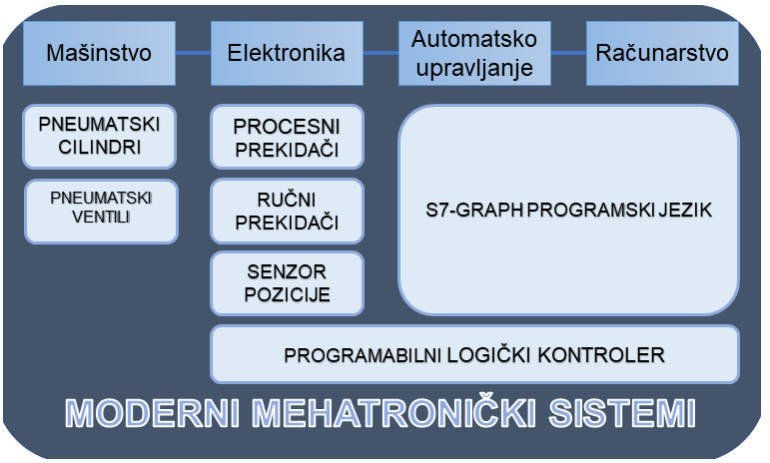

Slika 3. *Pozicija pojedinačnih komponenti korišćenih MPS stanica u jednom mehatroničkom sistemu*

Na osnovu slike X može se zaključiti da studenti dobijaju sveobuhvatno znanje koje je rasprostranjeno duž sve četiri oblasti te kao produkt ovakvo organizovanog predmeta dobija se realizovan industrijski proces u individualnoj formi, ali i kao složena proizvoljna linija. Svakoj od gradivnih jedinica sa slike pristupa se pojedinačno, a zatim

4 ZAKLJUČCI

Imajući u vidu nagli i užurbani razvoj tehnologije tokom trenutne četvrte industrijske revolucije, te smjer u kojem industrija napreduje nesumnjivo je da položaj mehatorničkih sistema zauzima bitno mjesto. Karakterističan položaj mehatroničkih sistema čini sinergija više inženjerskih grana koje na jedinstven način dovode do razvoja i unapređenja industrijskih i proizvoljnih procesa. S obzirom na položaj, značaj ali i buduće predikcije od velike je važnosti ponuditi i realizovati kurs koji će se ticati mehatroničkih sistema tokom osnovnog obrazovanja budućih inženjera elektrotehnike. Kao centar organizacije jednog ovako izazovnog silabusa iskorišćene su didaktičke MPS stanice kompanije *Siemens,* a čije gradivne jedinice su predstavljene u ovom radu.

LITERATURA

[1] Peter Kopacek, A Mechatronics Management Laboratory, Improving Stability in Developing Nations through Automation 2006,Elsevier, 2006
[2] David Hodgson, Mechatronics and Physical Computing, Exploring Engineering, Academic Press, 2021
[3] Stankovski, S., Ostojić, G., Zhang, X., Baranovski, I., Tegeltija, S., & Horvat, S, Mechatronics, identification tehnology, industry 4.0 and education, Infoteh-Jahorina, 2019
[4] *Recruiter,* dostupno na: https://www.recruiter.com/careers/mechatronics-engineers/outlook/
[5] SIMATIC S7-300 datasheet, dostupno na: https://support.industry.siemens.com

COMETa 2022
6th INTERNATIONAL SCIENTIFIC CONFERENCE
17th - 19th November 2022
Jahorina, B&H, Republic of Srpska
University of East Sarajevo
Faculty of Mechanical Engineering
Conference on Mechanical Engineering Technologies and Applications

UPRAVLJANJE I AUTOMATIZACIJA LIFTOVA: BAZIČNA TEHNOLOGIJA I NOVA DOSTIGNUĆA

Rade Vasiljević[1]

Rezime: U ovom radu je razmatrano upravljanje i automatizacija kod liftova. U prvom delu rada opisana je u kratkoj formi bazična tehnologija. U drugom delu rada istaknuta su nova dostignuća.

Ključne riječi: liftovi, upravljanje, automatizacija, bazična tehnologija, nova dostignuća

CONTROL AND AUTOMATION OF THE LIFTS: BASIC TECHNOLOGY AND NEW ACHIEVEMENTS

Abstract: In this paper, the control and automation of lifts is considered. In the first part of the paper, the basic technology is described in a short form. In the second part of the paper, new achievements are highlighted.

Key words: Lifts, Control, Automation, Basic technology, New achievements

1 UVOD

Kod tehničkih sistema, upravljanje je uglavnom automatsko, koje podrazumeva poboljšanje ili održavanje funkcionisanja objekta upravljanja bez učešća čoveka saglasno unapred zadatom cilju. Ostvarivanje automatskog upravljanja dizalično-transportnih mašina zadire u sve grane privrede.

Od dizaličnih mašina najveća mogućnost povećanja kapaciteta se ostvaruje automatizacijom rada putničkih liftova [1]. Lift je dizalična mašina koja se koristi za vertikalni prevoz putnika i robe. Automatizacija liftova je od velikog značaja jer od nje zavisi kapacitet i vek lifta. Liftovi imaju poseban značaj u gradovima sa velikim brojem višespratnica sa desetine spratova iznad zemlje (npr. Njujork) i velikih oblakodera sa visinom od stotinak metara. Ali liftovi imaju i značajnu ulogu i u malim javnim zgradama, hotelima i tržnim centrima. Poboljšanje karakteristika organa upravljanja dovode do efikasnosti lifta. Efikasnost lifta je razmatrana u [2].

[1] Dr-Inž, Rade Vasiljević, VTŠAS, Beograd, Srbija, r.r.vasiljevic (CA)

2 BAZIČNA TEHNOLOGIJA UPRAVLJANJA I AUTOMATIZACIJA LIFTOVA

Organi bazičnog nivoa upravljanja liftova su elektromehanički releji i grupni upravljač [3]. Uspostavljanje režima rada i realizacija zadane tehnologije rada lifta postiže se dejstvom na aparaturu upravljanja. Pri *tasterskom upravljanju* kola kalema relejno-kontaktne aparature se spajaju ili razdvajaju pomoću tastera upravljanja. Komandna tabla sa tasterima može se postaviti u kabini (unutrašnje upravljanje) ili u prostoru liftovskog šahta osnovnog sprata (spoljašnje upravljanje). Startovanje kabine lifta se vrši pritiskom na taster, a zaustavljanje se realizuje automatski. Kod *polužnog upravljanja* (stariji liftovi) u kabini je integrisan polužni aparat, koji spaja ili razdvaja kola kalema relejno-kontaktne aparature, kojom se upravlja elektromotorom. Startovanje i zaustavljanje kabine lifta se vrši ručnim obrtanjem poluge komandnog aparata.

2.1 Vrste upravljanja liftova

U zavisnosti od primenjenog stepena automatizacije u liftove se ugrađuje *podeljeno upravljanje* ili *sabirno upravljanje*.

2.1.1 Podeljeno upravljanje

Kod teretnih liftova i neautomatizovanih liftova stanbenih kuća sistem upravljanja konstruiše se sa pretpostavkom da je dežurstvo pratioca lifta konstantno. Pratioc lifta može se nalaziti u kabini lifta (*unutrašnje upravljanje*) ili u prostoru onog sprata gde se proizvodi opterećenje kabine (*spoljašnje upravljanje*). U oba slučaja na mestu pratioca lifta se koncentrišu svi signali kojima se poziva kabina lifta. U aparatima za signalizaciju koristi se brojač ili svetlosna signalna ploča, na koje se deluje pomoću spratnog pozivnog tastera. Redosled izvršavanja pristiglih poziva uspostavlja pratilac lifta, koji pritiska taster naredbe, upućujući kabinu na neki od naručenih spratova. Za vreme kretanja kabine pozivi tom broju i usputnim se ne izvršavaju. Za zaustavljanje kabine pritisak na dugme upravljanja, osim dugmeta “stop”, ne mora dovesti do promene kretanja kabine (pravila Gosgortehnadzora [3]). Svaka naredba ili poziv izvršava se podeljeno. Podeljeno upravljanje odgovara radu teretnih, bolničkih i putničkih (male stanbene zgrade) liftova. U putničkim liftovima višespratnih stanbenih zgrada, poboljšanje rada opsluživanja (prijem i izvršavanje usputnih poziva na dole) ostvaruje se bitnom izmenom i dopunom opreme jednoobrazno podeljenog upravljanja. To povećava produktivnost lifta u jutarnjim časovima, kada je svaki putnik lifta usmeren na dole. Smanjuje se prazan hod kabine po pozivima tj. potrošnja električne energije.

2.1.2 Sabirno upravljanje

Kod sabirnog upravljanja, kabina pri kretanju po naredbi, automatki se odaziva na sve usputne pozive. Karakter najvećeg opterećenja lifta (špic) nije isti u administrativnim višespratnim zgradama i u stanbenim zgradama. U prvim zgradama, u dnevnim satima su izražena međuspratna premeštanja. Već nedostaje ispunjavanje usputnih poziva u jednu stranu, a potrebno je ispunjavanje istih u obe strane kretanja pri uslovima maksimalnog smanjenja vremena čekanja kabine. Ove zahteve ne može da ispuni podeljeno upravljanje, nego savršenije upravljanje (sabirno).

Pri kretanju nagore kabina se automatski zaustavlja na spratovima (na kojima ima putnika) i fiksira poziv ka vrhu. Pri ulasku u kabinu lifta putnici pomoću dugmadi na konrolnoj tabli registruju spratove na kojima žele da se kabina zaustavi. Kabina se zaustavlja na međuspratovima i po redu ih prolazi. Posle ispunjenja poslednje registovane naredbe kabina produžava kretanje ka vrhu ili ka dnu. Kabina se odaziva

na sve usputne pozive ka vrhu. Kada se izvrše sve naredbe, kabina se javlja na sledeći poziv ka vrhu (najvišem spratu). Pri kretanju ka vrhu (za najvišim pozivom ka dnu) kabina ne prima pozive za dole, jer nisu usputni. Samo na povratnom putu (dole), saglasno naredbi ispunjenja najvišeg poziva odozdo, kabina se odaziva na sve usputne pozive na međuspratovima ka dole. Posle ispunjenja svih naredbi za pozive odozdo, kabina se vraća na osnovni sprat (ciklus je završen).

Pri sabirnom upravljanju srednje vreme čekanja opsluživanja je manje nego pri podeljenom upravljanju. Široko se primenjuje kod putničkih liftova u administrativnim zgradama. Signalizacija o pozivu nije potrebna. Može se koristiti za jedan lift i grupu liftova (koncentrisani u objektu). Naredbe od pozivnih dugmadi registruju se po sistemu komandi (npr. simplex, duplex, triplex, kvadrplex i sl.). Sabirne komande zavise od potreba kupca i kapaciteta. Pri pozivima sa svih liftova, SAU izvršava najoptimalniji redosled komandi, a zatim se kabine liftova automatski vraćaju na svoje početne stanice. To dva puta skraćuje vreme u odnosu na običan sistem pojedinačnih poziva svakog lifta. U periodu špica može se obezbediti automatski rad liftova prema zadatom programu. Programom se zadaje da određeni liftovi opslužuju unapred definisanu zonu (ne zaustavljaju se na svakoj stanici). SAU se može ograničiti veličina opterećenja, tako što se u slučaju preopterećenja uključuje indikator opterećenja, koji je povezan sa površinom poda kabine koju putnici pri ulazu opterećuju. Kabina započinje kretanje samo ako je opterećena sa najmanje 80% nominalne nosivosti. Ako je opterećenje manje od 80% nosivosti, lift se uključuje samo nakon unapred zadatog vremena.

2.2 Sistemi upravljanja elektropogonom i automatizacija rada liftova

Kod liftova, bezbednost putnika je najbitniija. Funkcionisanje liftova mora da bude takvo da sistem upravljanja (SU) onemogućava opterećenje kabine preko njene nosivosti. Da bi se ispunili ovi zahtevi, ploča kabine mora biti izabrana po principu slobodnog punjenja. U šemu se uvodi uređaj koji ukazuje na preopterećenje. Ako se kabina preoptereti, onda se blokira aparatura upravljanja i kretanje kabine nije moguće. U višespratnim javnim i administrativnim zgradama, kabine liftova su proračunate po slobodnom punjenju i imaju sabirno upravljanje. To obezbeđuje automatizaciju rada liftova po pozivu. U slučaju špica, ako jedan lift ne može da obezbedi nužnu produktivnost, onda se montiraju dva parna lifta ili grupa liftova (npr. tri, četiri). Automatizacija rada parnih liftova sa opštim dugmadima poziva, realizuje se tako što kada se jedna kabina kreće ka gore drugoj je dozvljeno kretanje samo nadole. Za grupu liftova sa opštim dugmadima poziva, predviđaju se režimi rada (jutarnji, dnevni i večernji). SU elektropogonom liftova mogu se podeliti prema više kriterijuma [1,3].

2.2.1 SU prema načinu delovaja na aparate upravljanja

Razlikuju se SU sa polugom i SU sa dugmadima. Kod upravljanja pomoću poluge, pogon i zaustavljanje kabine lifta ostvaruje ručnim dejstvom na polugu komandnog aparata kabine. Tačnost zaustavljanja zavisi od kvalifikacije i iskustva vodiča. Kod upravljanja pomoću dugmadi, pogon kabine ostvaruje pritiskom na dugmad. Zaustavljanje je automatizovano. Upravljanje pomoću dugmadi može biti obično i usavršeno. Obično upravljanje koristi običnu dugmad, čije glave se posle pritiska vraćaju u prethodni položaj. Usavršeno upravljanje koristi dugmad sa zadržavajućim eletromagnetom, čije glave posle pritiska ostaju u uvučenom položaju. Kod običnog upravljanja moguće je samo podeljeno izvršavanje naredbi i poziva. Usavršeno upravljanje omogućava podeljeno izvršvanje naredbi i registraciju nekoliko naredbi sa sledećim javljanjem tih naredbi za vreme kretanja kabine ka registrovanim

spratovima. Ispunjava jednostrane usputne pozive. Ostvarivo je i sabirno upravljanje.

2.2.2 SU prema rasporedu dugmadi naredbe odnosno kabine

Prema rasporedu dugmadi naredbe upravljanje može biti *spoljašnje* i *unutrašnje*. Kod spoljašnjeg upravljanja aparatura pogona je van kabine (na spratnoj ploči). Kod unutrašnjeg upravljanja aparatura pogona je smeštena u kabini lifta. Za trgovinske i male teretne liftove moguće je samo spoljašnje upravljanje. Za teretne liftove moguće je spoljašnje upravljanje (bez vodiča) i unutrašnje upravljanje (sa vodičem). Prednost spoljašnjeg upravljanja je bolje iskorišćenje kabine, a nedostatak kod teretnih liftova je potreba dežurstva lica za ukrcavanje na svakoj spratnoj ploči.

2.2.3 SU prema načinu vraćanja oslobođene kabine na osnovni (ukrcni) sprat

Prema ovom kriterijumu SU mogu biti:

- *Posredstvom pozivnih dugmadi na prvom spratu ili pultu dispečera*. Vraćanje kabine je sa otvorenim vratima i bez vodiča. Primenjuje za putničke liftove;
- *Posredstvom dugmadi ili poluge aparata u kabini*. Vraćanje kabine je sa zatvorenim vratima i sa vodičem. Primenjuje se za teretne i putničke liftove.
- *Posredstvom releja sa zaustavnim vremenom*. Vraćanje kabine je automatsko sa otvorenim vratima po isteku nekoliko zaustavnih vremena. Primenjuje se u višespratnim i visokim zgradama za punu automatizaciju pojedinačnih liftova.

2.2.4 SU prema tipu pogona vrata kabine i okna lifta

Vrata kabine i okno liftova izrađuju se sa *ručnim* i *električnim pogonom*. Ručni pogon se primenjuje kod malih teretnih, bolničkih i putničkih (stanbene zgrade) liftova. Električni pogon, sa obezbeđenim automatskim otvaranjem i zatvaranjem vrata, primenjuje se kod liftova javnih zgrada.

2.2.5 SU prema prisustvu ili odsustvu pozivnih dugmadi na spratnim pločama

Na međuspratovima, *pozivna dugmad nisu potrebna* u slučajevima: 1) mali i teretni liftovi bez vodiča (teret se naručuje telefonom, povratni “špicevi” tereta nisu veliki i mogu biti opsluženi kabinom koja se vraća) i 2) lift se ne koristi pri kretanju ka dole (u malim stanbenim domovima). U svim ostalim slučajevima, na međuspratovima, *pozivna dugmad moraju da postoje* za putničke liftove (stanbene i javne zgrade).

2.2.6 SU prema tipu primenjenih pozivnih dugmadi

Kod ovih SU liftova primenjuju se dva tipa pozivnih dugmadi, i to:

- *Jednostruka dugmad*. Primnjuju se kod teretnih liftova, kada nije potrebno pokazivati smer poziva i putničkih liftova u stanbenim zgradama bez međuspratnog kretanja, gde svi pozivi sa viših spratova imaju smer ka dole;
- *Dvostruka dugmad*. Primenjuju se kod putničkih liftova u javnim zgradama sa napornim međuspratnim kretanjem. Omogućavaju podeljeno zvanje kabine za kretanje ka dole i sledeće kretanje ka vrhu. Imaju strelicu za smer poziva.

2.2.7 SU prema načinu delovanja pozivnih dugmadi

Način delovanja pozivnih dugmadi može biti dvojak, i to:

- *Signalni poziv*. Pozvano dugme dejstvuje samo na signalizaciju. Izbor pravca kretanja, fiksiranje sprata i puštanje kabine u pogon vrši vodič lifta;
- *Automatski poziv*. Pozvano dugme deluje na signal i na električnu šemu, ostvarujući izbor pravca kretanja, fiksiranje sprata i pripremu šeme za pogon. Impuls za početak kretanja kabina dobija od vodiča lifta.

2.2.8 SU prema redosledu ispunjenih poziva

SU, prema redosledu ispunjenih poziva, se dele na:

- *SU bez izvršavanja usputnih poziva*. Izvršavanje usputnih poziva nije predviđeno za teretne i bolničke liftove;
- *SU sa izvršavanjem usputnih poziva*. Za putničke liftove javnih zgrada predviđena je ugradnja dvostranih usputnih poziva (ka dole/ka gore). U putničkim liftovima (stanbene i javne zgrade) u prvom redu se izvršavaju naredbe. Pozivi se ispunjavaju kao usputni, i to prvo najviši. Za putničke liftove stanbenih zgrada svrsishodno je predvideti i ispunjavanje usputnih poziva ka dole. To poboljšava opsluživanje u špicu, kroz smanjenje praznih hodova lifta.

2.2.9 SU prema odsustvu ili prisustvu saglasnosti rada lifta

Saglasnost se ne predviđa ako je lift isključivo putnički ili teretni. U slučaju da je broj spratova veći od 10, mora se montirati rezervni putnički lift. To važi i kada je jedan lift dovoljan za opsluživanje zgrade. Oba lifta se opremaju istim sistemom pozivnih dugmadi. Rad parnih liftova je usklađen tako da se druga kabina odaziva na pozive koji se javljaju sa spratova koji su iznad sprata na kome se nalazi prva kabina (ide dole). Ova organizacija rada parnih liftova smanjuje vreme čekanja opsluživanja i prazne hodove kabine i obezbeđuje najbolju produktivnost dve kabine (istovremeni rad). Kod putničkih liftova, u slučaju mnoštva putnika i kada par liftova nije dovoljan, u javnim zgradama se montira jedna ili više grupa liftova. Broj liftova u jednoj grupi je 3...6. Rad liftova treba da bude takav da se gužva ravnomerno raspodeli na sve liftove.

2.2.10 SU prema obimu signalizacije o radu lifta

SU lifta može da uključuje sve ili neki od sledećih vidova signalizacije:

- signalizacija na ploči o primanju naredbi za ispunjavanje i o pravcu u kom će krenuti kabina posle pritiska pogonskog dugmeta,
- signalizacija u kabini o broju spratova koje prolazi kabina,
- signalizacija na osnovnom (ukrcnom) spratu da je kabina slobodna,
- signalizacija na spratnim pločama o prijemu poziva i ispunjavanju,
- signalizacija na spratnim pločama o položaju kabine ili o približavanju kabine ka spratu i o njenom poslednjem kretanju koje je izvršila,
- signalizacija na osnovnom spratu o opterećenju kabine i spremnosti da krene, i
- signalizacija na ploči dežurnog u predvorju.

Za mnoge liftove, signalizacija se može ograničiti samo na tablu. Kompletna signalizacija je neophodna samo za brzohodne i brze putničke liftove, koji se montiraju po grupama u javnim i administrativnim zgradama (velika gužva putnika).

2.3 Tipovi sistema elektropogona (EP) i upravljanja liftovima

Tipovi sistema EP i upravljanja liftovima sa njihovom primenom [1,3]:

- *EP*: Sa naizmeničnom strujom (AC) i jenobrzinskim kratko-spojenim elektromotorom (EM). *SU*: Upravljanje je spoljašnje pomoću dugmadi, iz 1 ili 2 centra (ka vrhu sa dna / ka dnu sa vrha). Zaustavljanje je automatsko sa mehaničkom aparaturom. Pri upravljanju sa jednog mesta signalizacija je zvučna. *Primena*: Trgovački i mali teretni liftovi sa opsluživanjem iz 2 mesta.
- *EP*: Sa AC i jenobrzinskim kratko-spojenim EM. *SU*: Upravljanje je spoljašnje pomoću dugmadi, sa spratne ploče ukrcnog sprata. Zaustavljanje je automatsko posredstvom mehaničkih spratnih uređaja. Pozivi su signalni. *Primena*: Mali teretni liftovi sa 3...14 stanica.
- *EP*: Sa AC i dvobrzinskim kratko spojenim EM. *SU*: Upravljanje je spoljašnje pomoću dugmadi, sa jednog ili dva mesta (ka vrhu sa donjeg sprata, a ka dole sa gornjeg sprata). Zaustavljanje je automatsko posredstvom mehaničkih uređaja. Pri upravljanju sa jednog mesta signalizacija je zvučna. *Primena*: Teretni liftovi sa 2 stanice i bez vodiča.
- *EP*: Sa AC i dvobrzinskim kratko-spojenim EM. *SU*: Upravljanje je spoljašnje pomoću dugmadi, sa spratne ploče ukrcnog sprata. Zaustavljanje je automatsko posredstvom mehaničkih i induktivnih spratnih uređaja. Pozivi su signalni. *Primena*: Teretni liftovi sa 3...14 stanica i bez vodiča.
- *EP*: Sa AC i jenobrzinskim kratko-spojenim EM. *SU*: Upravljanje je sa polugom. Zaustavljanje nije automatizovano. Impuls za zaustavljanje daje vodič. Pozivi su signalni. *Primena*: Privremeni liftovi (građevinski i teretni) sa 3...14 stanica.
- *EP*: Sa AC i jednobrziskim EM sa kontaktnim prstenovima. *SU*: Upravljanje je pomoću poluge. Zaustavljanje nije automatizovano. Impuls za zaustavljanje daje vodič. Pozivi su signalni. *Primena*: Privremeni građevinski i teretni liftovi sa 3...14 stanica, vodičem i napajanjem sa mreže ograničene mogućnosti.
- *EP*: Sa AC i dvobrzinskim kratko-spojenim EM. *SU*: Upravljanje je unutrašnje sa dugmadima. Zaustavljanje automatsko pomoću mehaničkih uređaja. Pozivi su signalni. *Primena*: Teretni liftovi sa vodičem i opsluživanjem sa 2 mesta.
- *EP*: Sa AC i dvobrzinskim kratko-spojenim EM. *SU*: Upravljanje je unutrašnje pomoću dugmadi. Zaustavljanje je automatsko posredstvom mehaničkih i induktivnih spratnih uređaja. Pozivi su signalni. *Primena*: Bolnički i teretni liftovi sa 3...14 stanica i vodičem.
- *EP*: Sa AC i jenobrzinskim kratko-spojenim EM. *SU*: Upravljanje je unutrašnje pomoću dugmadi. Zaustavljanje je automatsko posredstvom mehaničkih ili induktivnih spratnih aparata. Pozivi su automatski samo pri kretanju na dole. Prvo se izvršava najviši poziv. *Primena*: Putnički liftovi za malospratne stambene zgrade sa brzinom kretanja od 0.65 m/s.
- *EP*: Sa AC i jednobrzinskim kratko-spojenim EM *SU*: Upravljanje je unutrašnje pomoću dugmadi. Zaustavljanje je automatsko pomoću induktivnih uređaja. Pozivi su automatski samo za kretanje ka dole. Prvo se izvršava najviši poziv, a zazim ostali pozivi kao usputni pri kretanju kabine ka dole. *Primena*: Putnički liftovi stanbenih zgrada sa do 14 stanica i brzinom od 1.0 m/s.
- *EP*: Sa AC i dvobrzinskim kratko-spojenim EM ($v \geq 1.0$ m/s) ili jednosmernom strujom - DC ($v \geq 1.5$ m/s). *SU*: Upravljanje je unutrašnje pomoću dugmadi.

Vrata okna i kabine su automatska. Pozivi su automatski za kretanje u oba smera. Pri pozivu za kretanje kabine na dole prvo se izvršava najviši poziv, a pozivi za kretanje ka gore i ostali pozivi za kretanje ka dole se izvršavaju kao usputni. *Primena*: Pojedinačni putnički liftovi javnih i administrativnih zgrada.

- *EP*: Sa AC i dvobrzinskim kratko-spojenim EM ($v \geq 1.0$ m/s) ili DC ($v \geq 1.5$ m/s). *SU*: Upravljanje je slično kao kod prethodnog tipa SU. Pozivni aparati su opšti za par liftova. Rad para liftova organizovan tako da su isključene mogućnosti zaustavljanja oba lifta po jednom pozivu na istom spratu i praznih hodova kabine. *Primena*: Parni putnički liftovi javnih i administrativnih zgrada.
- *EP*: Sa AC i dvobrzinskim kratko-spojenim EM ($v \geq 1.0$ m/s) ili DC ($v \geq 1.5$ m/s). *SU*: Upravljanje je slično kao kod prethodna dva tipa SU. Pozivni aparati su opšti za grupe 3...6 liftova. Odlazak liftova sa osnovnog sprata izvodi se automatski po propisanom režimu. Predviđeni su jutarnji, dnevni i večernji režim rada. *Primena*: Grupni putnički liftovi javnih i administrativnih zgrada.

3 NOVA DOSTIGNUĆA TEHNOLOGIJE UPRAVLJANJA LIFTOVIMA

SU novih liftova su mnogo pametniji. U odnosu na bazičnu tehnologiju, organi srednjeg nivoa upravljanja liftovima zasnovani su mikroprocesorima. Napredni nivo upravljanja liftovima je softverski određen (npr. cilj otpremanja). U narednom tekstu u kratkoj formi će biti predstavljena nova dostignuća u tehnologiji upravljanja liftovima.

Energetski efikasan softver. U poslednje dve i po decenije se nametnula posebna tehnička disciplina pod nazivom ″Upravljanje zgradama (Building Automation - BAU)″ [4], čiji rezultat su pametne zgrade. Ove zgrade se projektuju i grade za dugoročnu održivost i minimalan uticaj na čovekovu okolinu. One omogućavaju komfor i bezbednost korisnicima. SU minimizira energetske i eksploatacione troškove. Za njihovo funkcionisanje nephodni su mnogobrojni podsistemi, a jedan od njih je podsistem za kontrolu liftova. Napredni softver olakšava sledeće funkcije: otpremanje ka cilju, regulaciju realnog vremena čekanja, regulaciju vremena stendbaja i odziv mreže. Sve to smanjuje potrošnju energije za oko 50% u poređenju sa osnovnim uslovima [2]. Novi softver (energetski efikasan softver) za kontrolu liftova omogućava sprovođenje studija saobraćaja liftova, koje informišu kako ciklus lifta utiče na njegovu potrošnju energije. Analizirajući nepravilnu prirodu rada lifta, broj pređenih spratova, periode najvećeg opterećenja, kretanja sa malim opterećenjem i praznim hodom, истраживачи i projektanti mogu kreirati modele potrošnje energije. Ovi modeli pomažu da se razviju efikasne strategije kontrole i daju preporuke za optimalno upravljanje.

Sistemi za otpremu odredišta. Za rešenje problema ″špica″ inženjeri-projektanti su izmislili sistem za otpremu odredišta (Destination Dispatching Systems-DDS). To je tehnika optimizacije, koja kod instalacija sa više liftova grupiše putnike za iste destinacije u iste liftove. U realnom vremenu, sistem analizira ulazne podatke od putnika i efikasno grupiše njihova odredišta. Rezultat ove optimizacije je smanjenje broja zaustavljanja u svakom putovanju liftom. Nakon ulaska u odredište korišćenjem tastatura ili ekrana osetljivih na dodir na odredišnom operacionom ekranu (u predvorju), sistem brzo signalizira i usmerava svakog putnika do dodeljenog lifta da se ukrca. Više detalja o DDS, vidi u [5].

Softveri za protok ljudi. Slično DDS, za protok ljudi je implementirana su rešenja da ublaže protok ljudi i upravljaju potražnjom za liftovima (uglavnom u ekstremnim slučajevima). KONE je implementirao poseban softver za grupnu kontrolu. Ovaj softver uključuje i mogućnosti veštačke inteligencije za učenje i praćenje obrazaca saobraćaja putnika u cilju optimizacije rešenja za protok ljudi.

Rešenja za mirovanje. Ova rešenja isključuju opremu lifta kada se ne koristi, obezbeđujući značajne uštede energije. Ušteda energije je posebno značajna u zgradama sa periodima niske upotrebe lifta. Senzori i softver u kabini automatski prelaze u ″režim spavanja″. Drugim rečima, senzori i softver isključujuju svetla, ventilatore, muziku i video ekrane (kada nisu zauzeti). Na ovaj način može se uštedeti u granicama 25%...80% ukupne potrošnje lifta,

Kompjuterizovani sistemi za otpremu odredišta. Ovi sistemi su implementirani sa ciljem brže realizacije usluge. U njima su svi liftovi u zgradi (npr. 50) povezani preko interneta. Putnici koji se kreću ka istoj destinaciji grupišu se i dele lift. U cilju poboljšanja bezbednosti, koriste se obavezne građevinske propusnice (podaci o vlasnicima i mestu rada). Kada posetioci očitaju karticu na okretnici, podaci sa kartice se prenose u lift. Digitalni ekran svetli sa brojem lifta, koji čeka u vremenu bliskom realnom. Zaposleni i posetioci, koji imaju ovlašćenje da pristupe na nekoliko spratova, mogu da zaobiđu sistem i promene svoje odredište na ekranu na dodir (van lifta).

Kompjuterizovane valjkaste vođice. Liftovi da bi savladali velike daljine sa velikim brzinama, osim snažnih motora i jake struje, neophodne su izuzetno glatke šine i šinski spojevi. Na postizanje savršeno ravnog kretanja kabine u visokim zgradama utiče više faktora (npr. ograničena dužina šinskih elemenata (oko 4.9 m), promena temperature, sila vetra i dr.). Ovaj problem kompanija ThyssenKrupp je rešila pomoću kompjuterizovanih valjkastih vođica, koji ublažavaju neravnine na šinama delovanjem sila u suprotnom smeru. Ove vođice drže točkove lifta u kontaktu sa šinama dok se kabina diže ili spušta.

Senzori preopterećenja. Povezan je sa podom kabine tako da se opterećuje se težinom putnika pri ulazu, uključuje se ako je lift preopterećen i kabina neće započeti kretanje.

Senzori požara. U slučaju požara, uključuje se senzor požara, kabina se spušta na početnu (donju) stanicu, otvaraju se vrata, putnici izlaze i lift više ne reaguje

Senzori ljuljanja. Izgradnja sve viših nebodera uporedno je uticala da užad i kaiševi kod liftova budu vrlo dugački. Zbog velike dužine užadi ili kablova, usled jakih vetrova, njihovo kretanje može postati opasno i oštetiti šahtove liftova. U tom cilju su implementirani kompjuterizovani sistemi za otpremu odredišta. Na vrhu liftova se ugrađujui senzori ljuljanja, koji daju informacije ako pokreti i vibracije lifta postanu prejaki. Ako dođe do ovakvog slučaja, lift se privremeno isključuje.

Sistem za održavanje liftova. On u jednom WTC-u koristi Microsoft's Azure Intelligent Systems Service. Na probleme reaguje proaktivno tj. kontinuirano u realnom vremenu šalje podatke serviserima, koji preduzimaju korake za sprečavanje otkaza.

Budući razvoj liftova ide u pravcu revulucionarnog sistema multi lifta (tehnologija elektromagnetnog lebdenja), vertikalnog metroa i svemirskog lifta.

4 ZAKLJUČCI

Ovaj rad je prvo prikazao bazičnu tehnologiju upravljanja liftovma, a zatim istakao neka nova dostignuća. Ukazano je na budući razvoj liftova.

Intezivno takmičenje u naučnom istraživanju i proizvodnji liftova, čini verovatnim dalji razvoj liftova a samim tim i sistema upravljanja. Očekuje se da će budući liftovi sa aspekta upravljanja i automatizacije biti efikasniji. Tehnologija upravljanja liftovima će nastaviti da igra bitnu ulogu u razvoju liftova.

LITERATURA

[1] Vasiljević, R. (2001). Električni pogon, upravljanje i automatizacija liftova, Seminarski rad, Mašinski fakultet, Beograd
[2] Harvey, S., Harry, M., Sameer, K. (2015). Function and Functionality in the Conceptual Design Process. KGH - klimatizacija, grejanje, hlađenje, vol. 44, no. 3, p.p. 51-56.
[3] Корнеев, К., Коротов, Г., Моцохейн, С., Жданов, В. (1958). Лифты – пассажирские и грузовые, Машиногиз, Москва.
[4] Arsić, S., Stankov, S., Danilović, N. Upravljanje inteligentnim zgradama. KGH – klimatizacija, grejanje, hlađenje, Zbornik Međunarodnog kongresa o procesnoj industriji – Procesing, [S.l.], vol. 26, n1, may 2017.
[5] Al-Kodmany, K. (2015). Tall Buildings and Elevators: A Review of Recent Technological Advances. Buildings, vol. 5, p.p. 1070-1104.

COMETa 2022
6th INTERNATIONAL SCIENTIFIC CONFERENCE
17th - 19th November 2022
Jahorina, B&H, Republic of Srpska
University of East Sarajevo
Faculty of Mechanical Engineering
Conference on Mechanical Engineering Technologies and Applications

PROGRAMIRANJE OPERATORSKOG PANELA ZA NADZOR RADA PUMPNE STANICE SA WINCC (TIA PORTAL) PROGRAMSKIM PAKETOM

Milan Simović[1], Slobodan Lubura[2]

Sažetak: U radu je opisan sistem automatskog upravljanja i nadzora pumpnom stanicom Matura koja se nalazi na rijeci Savi na području grada Srbca. Sistemom se upravlja pomoću uređaja PLC (Programable Logic Controler) iz serije Siemens SIMATIC S7-1200, vizuelizacija i upravljanje realizovano je preko operatorskog panela (HMI) iz serije Siemens SIMATIC KTP700. Navedeni sistem obuhvata upravljanje svim izvršnim elementima procesa (motorima pumpi, rešetki, grabuljama, ustavama, itd.) i nadzor putem povratnih signala sa senzora (davača signala, ultrazvučni senzori nivoa, transmiteri pritiska, itd.)

Ključne riječi –;HMI; PLC,PC, SCL,SCADA,TIA

PROGRAMMING THE OPERATOR PANEL FOR CONTROL AND MONITORING THE OPERATION OF PUMPING STATIONS USING THE WINCC (TIA PORTAL) SOFTWARE PACKAGE

Abstract: The paper presents a system of automatic monitoring and control of a pumping station Matura along the embankment of the Sava River in the area of the city of Srbac. The system is controlled by a PLC (Programmable Logic Controller) from the Siemens SIMATIC S7-1200 series, visualization and control is realized through an operator panel (HMI). from the SIMATIC KTP700 series. The mentioned system includes management of all executive elements of the process (pump motors, grates, rakes, foundations, etc.) and monitoring through feedback signals from sensors (signal generators, ultrasonic level sensors, pressure transmitters, etc.)

Key words: HMI; PLC,PC, SCL,SCADA,TIA

[1] Milan Simović, Elektrotehnički fakultet , I.Sarajevo,BiH, milan.simke@yahoo.com
[2] Prof. dr. Slobodan Lubura, Elektrotehnički fakultet , I.Sarajevo,BiH, slobodan.lubura@etf.ues.rs.ba

1 UVOD

Automatizacija je pokretačka snaga savremenog tehnološkog napretka. Ljudi uvjek teže za lakšim i efikasnijim načinom rukovanja odgovarajućom opremom i procesom. Tehnologija brzo raste kao i izazovi za efikasno korišćenje iste. Mnogo savremene opreme zahtjeva veoma vješte, dobro upućene operatere da bi pravilno rukovali njom. Pošto se želi da mašine, procesi i njihova kontrola budu laki za korišćenje, laki za čitanje, razumjevanje, računanje i manipulisanje. Operatorski paneli kao dio procesa obezbjeđuju međusobnu interakciju ljudi i mašina HMI (eng. Human Machine Interfejs). Igraju važnu ulogu u oblasti industrijske automatizacije. Pored industrijske automatizacije, operatorski paneli se mogu naći i u drugim industrijskim oblastima i sektorima, obično se instaliraju blizu samog automatizacijskog procesa u radnoj oblasti i imaju za cilj da prevedu signale koji dolaze iz PLC-a u grafičke signale koje je lakše razumjeti.

U ovom radu je detaljno opisan jedan proces automtizacije koji obuhvata upravljanje i nadzor sistemom pumpi raspoređenih duž sliva rijeke Save na području grada Srbca. Tokom visokih vodostaja 2009, 2010. i maja 2014. godine. Republika Srpska je pretrpila velike štete zbog ne razvijenog sistema prevencije od poplava. Ministarstvo poljoprivrede, šumarstva i vodoprivrede u koordinaciji sa Ministarstvom finansija, Ministarstvom javne uprave i lokalne samouprave u Republici Srpskoj uz pomoć konsultanta Evropske investicione banke (EIB) identifikovali su 134 hitne i kratkoročne sanacijske mjere [11]. Jedna od definisanih mjera je izrada sistema automatskog nadzora i upravljanja pumpnim stanicama duž nasipa rijeke koji je detaljno opisan u ovom radu.

2 PROGRAMABILNI LOGIČKI KONTROLERI PLC

Programabilni logički kontroleri PLC (eng. Programable Logic Controler) su mali digitalni računari koji se koriste u savremenim kontrolnim aplikacijama. PLC je jedna od najvažnijih komponenti današnjeg naprednog sistema kontrole i automatizacije Oni su fleksibilni za programiranje prema potrebama korisnika i sposobni su da generišu signale koji mogu da kontrolišu mašine i procese u industriji. Međunarodna elektrotehnička komisija IEC (International Electrotechnical Commission) defineše PLC kao:

“Programabilni logički kontroler (PLC), je digitalni elektronski aparat sa programabilnom memorijom za skladištenje instrukcija za implementaciju specifičnih funkcija kao što su logika, sekvenciranje, tajming, brojanje i aritmetika, za kontrolu mašina i procesa.” [3]

2.1 Hardverska organizacija PLC_a

Programabilni logički kontroleri PLC sadrže sve elemente standardne arhitekture digitalnog računara, Slika 1 u nastavku. Glavne hardverske komponente programabilnog logičkog kontrolera (PLC_a) su sledeće:

- **Napajanje** – može biti eksterna jedinica ili interna za PLC.
- **Ulazni moduli** – mogu biti analogni ili digitalni.
- **Izlazni moduli** – mogu biti analogni ili digitalni.
- **CPU** – Centralna procesorska jedinica može biti jednoprocesorska ili višeprocesorska.
- **Memorija** – mogu biti fiksna ili promenljiva.
- **mikroprocesor** – izvršava funkcije operativnog sistema i korisničkog

programa.

- **komunikacije** – povezivanje i komunikacija sa nadređenom stanicom za programiranje
- **Kućište (Rack)** - Garantuje i mehaničko i električno povezivanje različitih internih modula i zaštitu od spoljašnje sredine.

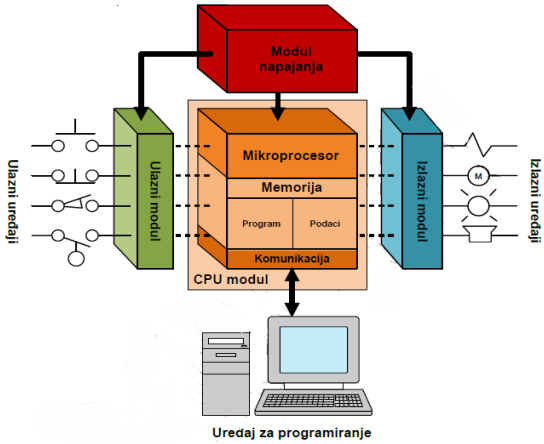

Slika 1. *Uopštena struktura PLC_a [8]*

2.2 SIMATIC S7 1200 PLC

SIMATIC S7-1200 je PLC najnovije generacije kompanije Simens. Može se reći da je nasljednik prethodnih serija PLC-ova, S7-300 i S7-400, za koje se i dalje predviđa da će biti sastavni dio industrije u narednim godinama. S7-1200 je trenutno jedan od bržih PLC-ova dostupnih na tržištu. Ima najnovije tehnološke karakteristike kao što su Profinet port kao standard, integrisana bezbjednost, integrisana dijagnostika sistema. Dizajniran je za maksimalnu inženjersku efikasnost i jednostavnost za korisnika.

Za realizaciju projekta u ovom radu korišćen je kontroler SIMATIC S7 1200 tip: 1214C DC/DC/RLY [10].

3 TIA PORTAL PROGRAMSKI PAKET

TIA Portal (eng. Totalli Integrated Automation Portal) je najnoviji softver za automatizaciju kompanije Simens. To je softver sa jednim inženjerskim i softverskim okruženjem za sve potrebne zadatke kompletnog automatizacijskog procesa. Prethodna generacija softvera (Step7, WinCC Flexible, WinCC explorer itd.) koji su morali da se koriste zasebno za različite zadatke integrisana je u jedan softver. Softverski paket je dizajniran na takav način da obezbjeđuje maksimalnu lakoću korišćenja i maksimalnu inženjersku efikasnost. Softverski paket omogućava kompletan tok programiranja od izbora hardverske konfiguracije, programiranje do vizuelizacije i simulacije.

3.1 PLC programiranje TIA Portal

Simens okruženje je unaprjed definisano za simboličko programiranje, programski jezici za programiranje PLC uređaja u TIA random okruženju a definisani

po standardu IEC 61131-3 su [13]:

- Instrukcione Liste AWL/STL (prema standardu IEC 61131-3 “AWL/IL")
- Lederer dijagram KOP/LAD (prema standardu IEC 61131-3 "KOP/LD")
- Funkcijski blok dijagram FUP/FBD (prema standardu IEC 61131-3 "FUP/FBD")
- Structured Control Language ST/SCL (prema standardu IEC 61131-3 "ST")
- S7-GRAPH (prema standardu IEC 61131-3 “AS/SFC")

U Simens aplikacijama, “Structured Text” (ST) se naziva „Structured Control Language “(SCL). SCL je tekstualni jezik visokog nivoa koji je lak za razumjevanje, i pruža mnoge prednosti u odnosu na tradicionalno programiranje upotrebom Leder dijagrama. SCL pruža inženjeru okruženje koje je više slično računarskom jeziku. TIA Portal obezbjeđuje SCL editor koji se koristi za konstruisanje logike i uokvirivanje naredbi programa. U projektu predstavljenom u ovom radu korišćen je SCL kao jezik za programiranje PLC uređaja.

4 WINCC (TIA PORTAL)

WinCC (TIA Portal) je dio novog integrisanog inženjerskog paketa koji nudi konzistentno okruženje za programiranje i konfiguraciju aplikacija i opreme na polju interakcije čovjek-mašina (HMI). Sa WinCC-om, programer može da stvori vezu između operatera i opreme procesa, uključujući vizuelizaciju, kontrolu procesa, prikaz alarma, arhiviranje vrijednosti procesa i istorije alarma, i upravljanje varijablama procesa ili mašina. WinCC (TIA Portal) je softver za sve HMI aplikacije, u rasponu od najjednostavnijih operativnih rešenja sa osnovnim panelima do SCADA aplikacija na višekorisničkim sistemima baziranim na PC-u. SIMATIC WinCC (TIA Portal) inženjerski softver je dostupan u verzijama WinCC Basic, WinCC Comfort, WinCC Advanced i WinCC Professional.WinCC Advanced i WinCC Professional su takođe dostupni kao odvojeni softverski paketi.

4.1 Radno okruženje WINCC TIA Portal

Radno okruženje u programskom paketu WinCC se sastoji iz više dijelova. Neki dijelovi radne površine nisu vidljivi dok se ne aktivira odgovarajuća funkcionalnost. Osnovni elementi radnog prostora WinCC Flexible TIA Portal su:

1. Radno područje (Work area)
2. Pregled projekata (Project tree)
3. Pregled osobina (Property view)
4. Alatni okvir (Troolbox)
5. Biblioteka (Library)

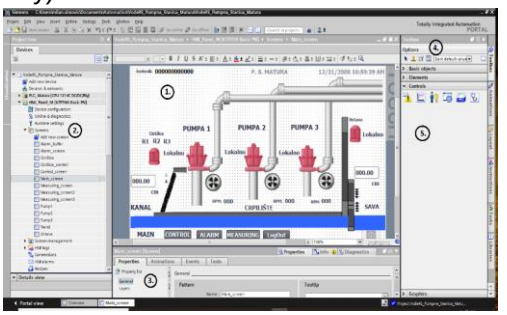

Slika 2. *WinCC TIA portal radno okruženje*

5 SISTEM AUTOMATSKOG UPRAVLJANJA PUMPNOM STANICOM MATURA NA RIJECI SAVI

U ovom radu je detaljno opisan projekat automatskog upravljanja i nadzora pumpnom stanicom Matura na rijeci Savi na području grada Srbca.

5.1 Opis sistema

Upravljanje sistemom je realizovano pomoću lokalne SCADA_e, koja se sastoji od PC stanice, PLC_a i HMI uređaja. Sistem obuhvata upravljanje svim izvršnim elementima sistema (motorima pumpi, rešetki, grabuljama, ustavama, itd.) i nadzor putem povratnih signala. Lokalni sistem omogućava sledeće funkcionalnosti:

- Omogućava nesmetano prebacivanje između ručnog i automatskog režima upravljanja. U automatskom režimu pumpa će biti upravljana u skladu sa nivoom vode. Na rad pumpi mogu uticati softverski generisani uslovi (prevencija praznog hoda ili neka druga zaštitna funkcija). U ručnom režimu je moguće uključiti/isključiti bilo koju od pumpi upravljanjem preko panela (HMI).
- Omogućava softversko prebacivanje izmedju manuelnog i automatskom režima upravljanja za čišćenje rešetki pumpi. U automatskom režimu čišćenjem rešetki se upravlja u skladu sa razlikom nivoa vode u kanalu i crpilištu . U manuelnom režimu moguće je pokrenuti ili stopirati čišćenje rešetke upravljanjem sa panela (HMI).
- Omogućava prikazivanje statusa definisanih alarma i događaja (statusa aparata) vezanih za stanje opreme na terenu
- Omogućava dinamičko prikazivanje uključenosti pojedinačnih aparata na HMI panelu.

Blok šema komunikacije na nivou sistema između različitih uređaja prikazana je na slici 3 u nastavku.

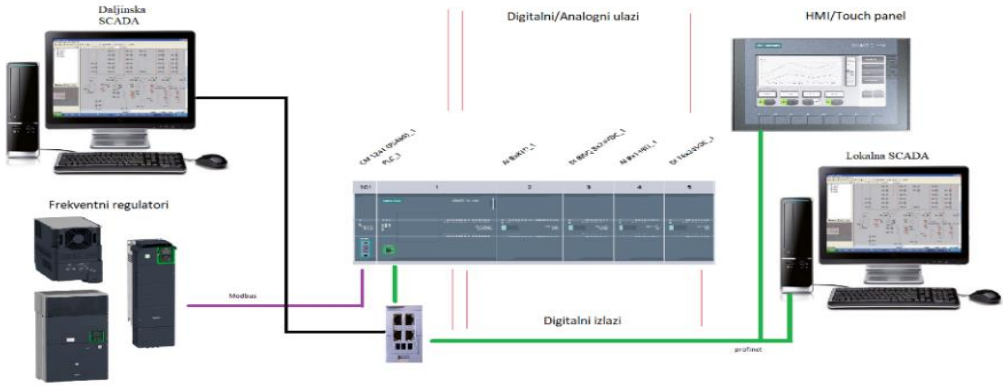

Slika 3. *Blok šema komunikacije sistema*

5.2 Vizuelizacija i prikaz

Na osnovu usvojenog projekta i usaglašene liste signala definisani su procesni tagovi u PLC_u. Na osnovu procesnih tagova i logičkih promjenjivih za nadzor i upravljanje u memoriji PLC_a (data blokovi u PLC_u) definišu se tagovi u HMI uređaju

(spoljašnji tagovi) koji se koriste za grafički prikaz i kontrolu sistema. Grafički prikaz je podijeljen na nekoliko ekrana preko kojih se vrši vizualizacija, nadzor i kontrola procesa. Pritiskom na određeni dio ekrana otvara se odgovarajući prozor za zadavanje komandi, promjene parametara ili čitanje informacija iz dijela procesa koji su tim dijelom ekrana prikazani. Vizualizacija procesa upravljanja prikazana je na operatorskom panelu proizvođača Simens model SIMATIC KTP700 Basic PN.

Na glavnom prozoru "MAIN", Slika 4 prikazani su osnovni elemeni i osnovni parametri sistema. Moguće je pratiti prirast vode u kanalu i prirast vode sa strane rijeke Save. Moguće je grafički pratiti i statuse pumpi koje mogu biti u režimu lokalnog ili daljinskog upravljanja, režimu dostupne/nedostupne i u režimu stratovane/stopirane.

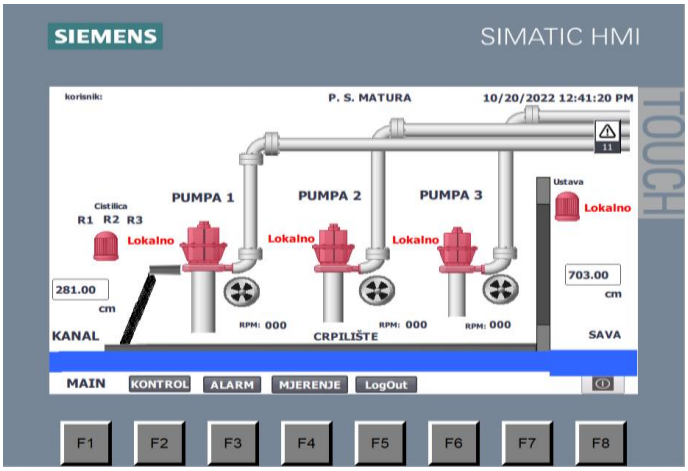

Slika 4. *HM glavni prozor sistema*

Ekranima za prikaz mjerenja pristupa se iz glavnog prozora pritiskom na taster "Mjerenje" koji se nalazi u navigacionom dijelu menija. Prozor mjerenja Slika 5 se satoji iz četiri dodatna prozora gdje su prikazana sva mjerenja u sistemu, od prirasta vode na pumpnoj stanici do mjernih parametra motora pumpi i frekventnih regulatora.

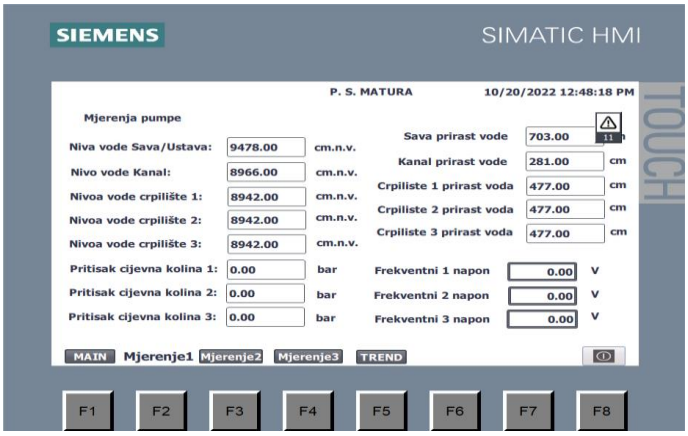

Slika 5. *HMI Prozor mjernja*

Prozor za upravljanje „Kontrol“ je glavni prozor za upravljanje pumpnom stanicom. Za pristup navedenom prozoru potrebna je autorizacija, tj logovanje korisnika koji ima prava za upravljanje sistemom. Kredencijali korisnika koji je ulogovan ispisani su u gornjem lijevom dijelu prozora. U gornjem lijevom uglu prozora nalaze se i tasteri za izbor režima upravljanja Ručno/Automatski. U ručnom režimu upravljanja moguće je startovati pumpe pojedinačno, podešavati brzinu i setovati vrijednosti parametara. Dok u automatskom režimu sistem radi samostalno, slika 6.

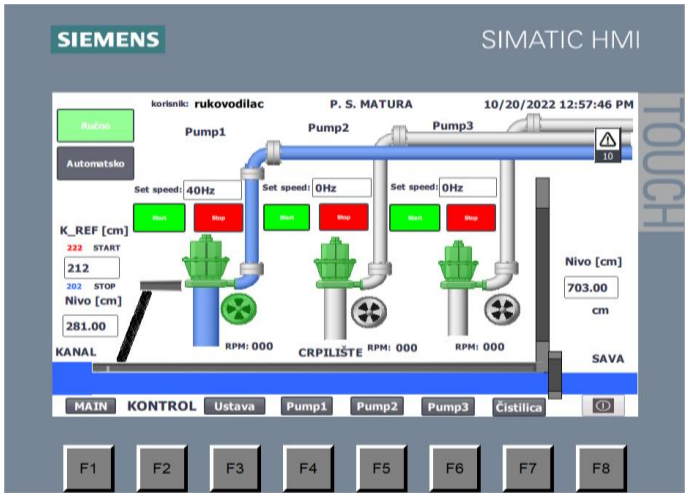

Slika 6. *HMI prozor za upravljanje sistemom*

Možda najvažniji prozor za praćenje parametara sistema pumpnih stanica je prozor alarma. Prozoru alarma pristupa se iz glavnog prozora “Main” pritiskom na taster “Alarm” u navigacionom dijelu menija.

Prozor alarma sastoji se iz dva prozora, i to prozor korisničkih alarma koji su bili ili su trenutno aktivni, prozor “Alarmi” i prozor svih alarma i korisničkih i sistemskih, koji su bili aktivni od startovanja PLC_A, arhiva svih alarma “Alarm bafer”, Slika 7.

Slika 7. *HMI prozor alarma*

6 ZAKLJUČAK

U ovom radu je prezentovan sistem automatskog nadzora i upravljanja pumpama duž nasipa rijeke Save za zaštitu od poplava u periodima velikih vodostaja na lokaciji grada Srbca. Sistem je dizajniran i implementiran upotrebom PLC uređaja za automatizaciju procesa i HMI uređaja za vizualizaciju i upravljanje procesom u realnom vremenu. Modelovanje kompletnog sistema izvršeno je upotrebom TIA Portal softverskog alata. Primjenom WinCC programskog okruženja kao dio TIA Portal okruženja ostvareno je upravljanje i vizualizacija pomoću HMI panel koji se nalazi fizički pored PLC uređaja i omogućava intuitivno upravljanje sistemom. Sistem ostavlja mogućnost za dalju nadogradnju upravljanja i nadzora. Ostavljena je mogućnost ostvarivanja komunikacije sa daljinskim centrom upravljanja koji bi trebao da se nalazi u Bijeljini gdje je glavno sjedište ustanove „Vode Srpske“.

LITERATURA

[1] F.Bakri Farah, "Use of SCADA system for remote monitoring of Khartoum state water corporation",*Master teza, Sudan University of Science and Technology, 2017*

[2] M.Mecca. "Design and implementation of two comprehensive automated systems with siemens PLCs", *Master teza, Politecnico di Torino, April 2020.*

[3] D.Serna Lara. "Conroling of pneumatic positioning system by means of a PLC", *Master teza, Politecnico di Torino, April 2018.*

[4] B.Pramanik, Optimization and development of Mould Level Control with MATLAB/Simulink and Comparison of energy consumption between the electric and hydraulic drive unit", *Master teza, TH Koln (University of applied sciences), 2018.*

[5] S. Adhikari, "Operator Machine Control using Siemens PLC an HMI", *Master teza, University of Toledo Decembar 2018.*

[6] Siemens AG, "SIMATIC WinCC(TIA Portal) GMP Engineering Manual", *Nurnberg, Germany, Mart 2019.*

[7] M. Gaco, "Održavanje nivoa tečnosti u rezervoaru korištenjem S7 300 PLK i WINCC programskog paketa", *Diplomski rad, Univerzitet u I. Sarajevu, februar 2021*.

[8] E. Gegić, *"*Programiranje touch ekrana sa WINCC flexible paketom*"*, *Diplomski rad, Univerzitet u I. Sarajevu, Januar 2021*

[9] PLC 247, https://plc247.com/difference-between-wincc-flexible-wincc-7-x-and-wincc-tia-portal/ , Avgust 2022

[10] Automation 24, https://www.automation24.com/siemens-tia-portal , Avgust 2022.

[11] Kaldera Company, " Idejni projekat pumpi Matura ", *Idejni mašinski projekat, Banja Luka, Decembar 2020.*

[12] Siemens global, https://new.siemens.com/global/en/products/automation/systems/industrial/plc/s7-1200.html , Septembar 2022,

[13] Implementation Aspects of the PLC Standard IEC 1131-3 , https://www.sciencedirect.com/science/article/pii/S147466701743607X , Septembar 2022.

MACHINE DESIGN, SIMULATION AND MODELING

COMETα 2022
6th INTERNATIONAL SCIENTIFIC CONFERENCE
17th - 19th December 2022
Jahorina, B&H, Republic of Srpska
University of East Sarajevo
Faculty of Mechanical Engineering
Conference on Mechanical Engineering Technologies and Applications

ANALIZA I OPTIMIZACIJA GEOMETRIJSKIH KARAKTERISTIKA ČEONOG NOSAČA DVOGREDNE MOSNE DIZALICE

Goran Pavlović[1], Mile Savković[2], Nebojša B. Zdravković[3], Goran Marković[4]

Rezime: U ovom istraživanju prikazan je postupak optimalnog projektovanja čeonog nosača dvogredne mosne dizalice, za varijantu kada su glavni nosači mosne dizalice iznad čeonih nosača. Pored velike pažnje koja se posvećuje dizajnu glavnih nosača, veoma važnu ulogu i odgovornost imaju i čeoni nosači, koji obezbeđuju stabilno kretanje celokupne strukture mosne dizalice duž dizalične staze. Iz tog razloga imaju i veću odgovornost u celoj strukturi mosne dizalice, tako da je izbor geometrijskih karakteristika poprečnog preseka čeonih nosača od velikog značaja koji se ogleda kako u pogledu krutosti, tako i vezi ovih nosača sa glavnim nosačem mosne dizalice. U ovom istraživanju izvršene su analiza i optimizacija kutijastog poprečnog preseka zavarenog čeonog nosača u dve varijante i pokazana je opravdanost ovakvog pristupa projektovanja, u pogledu uštede materijala. Kao primer korišćena je jedna dvogredna mosna dizalice koje se nalaze u eksploataciji. Kao metodologija za postupak optimizacije primenjen je jedan metaheuristički algoritam, s obzirom da ovakve metode u poslednje vreme imaju sve veću primenu za najrazličitije inženjerske probleme.

Ključne riječi: Metaheuristika, Noseća struktura, Optimalni dizajn, Stabilnost limova

ANALYSIS AND OPTIMIZATION OF GEOMETRIC PROPERTIES OF A CRANE END TRUCK OF A TOP RUNNING DOUBLE-GIRDER OVERHEAD CRANE

Abstract: In this research, the procedure of optimal design of an end truck of a double-girder overhead crane is presented for the variant when the main girders of an overhead crane are above end trucks. In addition to the great attention paid to the design of the main girders, end trucks also have a very important role and

[1] Naučni saradnik dr Goran Pavlović, Univerzitet u Nišu, Elektronski fakultet u Nišu, Niš, Srbija, goran.pavlovic@elfak.ni.ac.rs
[2] Redovni profesor dr Mile Savković, Univerzitet u Kragujevcu, Fakultet za mašinstvo i građevinarstvo u Kraljevu, Kraljevo, Srbija, savkovic.m@mfkv.kg.ac.rs
[3] Vanredni profesor dr Nebojša B. Zdravković, Univerzitet u Kragujevcu, Fakultet za mašinstvo i građevinarstvo u Kraljevu, Kraljevo, Srbija, zdravkovic.n@mfkv.kg.ac.rs
[4] Vanredni profesor dr Goran Marković, Univerzitet u Kragujevcu, Fakultet za mašinstvo i građevinarstvo u Kraljevu, Kraljevo, Srbija, markovic.g@mfkv.kg.ac.rs

responsibility, ensuring the stable movement of the entire structure of an overhead crane along the crane runways. For that reason, they have a greater responsibility in the entire structure of the bridge crane, so the choice of geometric characteristics of the cross-section of end trucks is of great importance, which is reflected in terms of rigidity and connection of these girders with the main girders of the bridge crane. In this research, the analysis and optimization of the box cross-section of the welded end trucks in two variants were performed. The justification of this design approach was shown in terms of material savings. For example, one double-girder overhead crane was used, which is in operation. One metaheuristic algorithm has been applied as a methodology for the optimization procedure, considering that such methods have recently been increasingly used for various engineering problems.

Key words: Carrying structure, Metaheuristics, Optimal design, Plate stability

1 UVOD

Čeoni nosači su sastavni delovi noseće strukture mosne dizalice i predstavljaju njene vrlo odgovorne segmente. Pored obezbeđivanja kretanja cele konstrukcije mosne dizalice duž dizalične staze, neophodno je da zadovoljavaju i uslove čvrstoće, krutosti i stabilnosti. Iz ovih razloga, čeoni nosači imaju veliku odgovornost, pa je izbor geometrijskih karakteristika poprečnog preseka ovih nosača od velikog značaja. Za strukturu čeonih nosača najčešće se koristi kutijasti oblik poprečnog preseka (standardni ili zavareni profili, u zavisnosti od nosivosti).

Zvog svog značaja, ovi segmenti mosne dizalice su predmet istraživanja u brojnim publikacijama. Metod konačnih elemenata (MKE) ima veliki značaj kod analize struktura dizalica. Istraživanje [1] se bavi primenom metode podmodela, koja je visoke efikasnosti i preciznosti u rešavanju složenih problema napona i deformacija, na nosećoj strukturi mosne dizalice. Dobijeni rezultati su bili od velikog značaja za konačni dizajn proizvoda. U radu [2] analizirana je promena naponskih stanja, kako na glavnom nosaču, tako i na čeonim nosačima jednogredne mosne dizalice, u zavisnosti od promene nosivosti dizalice. MKE analiza celokupne noseće strukture dvogredne mosne dizalice izvršena je u radu [3], kako bi se utvdila najkritičnija mesta na čeonim i glavnim nosačima mosne dizalice. Uticaj iskošenja, kao i uticaj uzdužnih sila koje nastaju pri kretanju mosnih dizalica duž dizalične staze, i njihovo dejstvo na točkove čeonih nosača, takođe je predmet istraživanja, što je prikazano u [4].

Pored MKE, često se kod nosećih struktura primenjuje i anlitički pristup. U radu [5] su izvršene analiza i optimizacija čeonog nosača dvogredne mosne dozalice, primenom Matlab softverskog paketa, dok je u [6] primenjen jedan metaheuristički algoritam optimizacije na čeonom nosaču jednogredne mosne dizalice.

Metaheuristički algoritmi optimizacije zadnjih godina imaju sve veću primenu kod najrazličitijih inženjerskih problema, što se može videti i u istraživanjima [7,8].

Cilj ovog istraživanja je da se izvrše analiza i optimizacija mase zavarene strukture čeonog nosača sa kutijastim poprečnim presekom, za dve varijante izvođenja, i dva tipa materijala, kako bi se pokazala ostvarena ušteda u materijalu i opravdanost takvog pristupa analizi i optimizaciji.

2 MATEMATIČKI MODEL OPTIMIZACIONOG PROBLEMA

Optimizacija mase čeonog nosača dvogredne mosne dizalice i geometrijskih parametara kutijastog poprečnog preseka jesu tema ovog istraživanja.

Struktura noseće čelične konstrukcije dvogredne mosne dizalice, kao i statički

model čeonog nosača prikazani su u radu [5]. Takođe, svi izrazi neophodni za izračunavanje potrebnih statičkih veličina prikazani su u pomenutom istraživanju.

Matematička formulacija za ovaj jednociljni višekriterijumski problem optimizacije definiše se na sledeći način:

$$\min\left\lfloor f_{obj}(X)\right\rfloor, \tag{1}$$

prema

$$g_i\left(X\right)\le 0,\ d_j \le x_j \le u_j, \tag{2}$$

gde su: $f_{ob}(X)$ funkcija cilja, $g_i(X)$ funkcije ograničenja, i=1,..,m broj funkcija ograničenja, j=1,..,n broj varijabli, X vektor od n varijabli, d_j donja granica j-te varijable i u_j gornja granica j-te varijable.

Ulazni podaci za ovaj optimizacioni problem su sledeći:

$$\begin{aligned} &Q,\ L,\ l_c,\ l,\ m_G,\ m_k,\ b_k,\ A_p,\ D_t,\ b_t,\ b_{t\check{s}},\ b_{\check{s}},\\ &R_e,\ \nu_1,\ \gamma,\ \psi,\ k_a,\ x_2,\ y_2,\ a_1,\ a_2,\ h_2,\ h_3\ \ K, \end{aligned} \tag{3}$$

gde su: Q=20 t nosivost dizalice, L=18,75 m raspon mosta dizalice; l_c=4 m dužina čeonog nosača, l=2 m rastojanje između glavnih nosača mosne dizalice, m_G=5,28 t masa glavnog nosača, m_k=0,85 t masa kolica sa vitlom, b_k=100 cm rastojanje između točkova kolica, A_p=134,36 cm^2 površina poprečnog preseka standardnog čeonog nosača, D_t=25 cm prečnik točka čeonog nosača, b_t=11,5 cm širina točka čeonog nosača, $b_{t\check{s}}$=7,9 cm unutrašnja širina točka čeonog nosača, $b_{\check{s}}$=6 cm širina šine dizalične staze, R_e=23,5 kN/cm^2 za S235 i R_e=35,5 kN/cm^2 za S355 naponi na granici tečenja materijala čeonog nosača, v_1=1,5 faktor sigurnosti, γ=1,05, ψ=1,15, k_a=0,1 koeficijenti dizalice, [9], x_2=15,3 cm, y_2=48,5 cm geometrijski parametri glavnog nosača dizalice, a_1=5 cm, a_2=5 cm, h_2=1,5 cm, h_3=1,5 cm geometrijske vrednosti čeonog nosača (Slika 1) i K=1/1000 koeficijent krutosti čeonog nosača. Ovi se podaci odnose na primer čeonog nosača jedne dvogredne mosne dizalice.

2.1 Funkcija cilja i varijable optimizacije

Smanjenje mase čeonog nosača podrazumeva smanjenje površine kutijastog poprečnog preseka čeonog nosača (Slika 1), koja predstavlja funkciju cilja f_{obj}.

Matematička formulacija funkcije cilja je sledeća:

$$f_{obj}(X) = A_c(x_1, \dots, x_n) = A_c(b_1,\ h,\ t_1,\ t_2,\ s), \tag{4}$$

gde su: A_c površina kutijastog poprečnog preseka, b_1, h, t_1, t_2, s varijable optimizacije (Slika 1).

Površina poprečnog preseka A_c (Varijanta 1) čeonog nosača se računa prema:

$$A_c = b\cdot\left(t_1+t_2\right)+2\cdot h\cdot s. \tag{5}$$

Širina pojasnog lima b se određuje prema (Slika 1):

$$b = b_1 + 6\cdot s, \tag{6}$$

dok se za specijalni slučaj (Varijanta 2), kada se širina gornjeg pojasa poklapa sa vertikalnim limom (b'), računa prema:

$$b' = b_1 + 2\cdot s, \tag{7}$$

a površina A'_c se u tom slučaju određuje na sledeći način:

$$A'_c = b' \cdot (t_1 + t_2) + 2 \cdot h \cdot s. \tag{8}$$

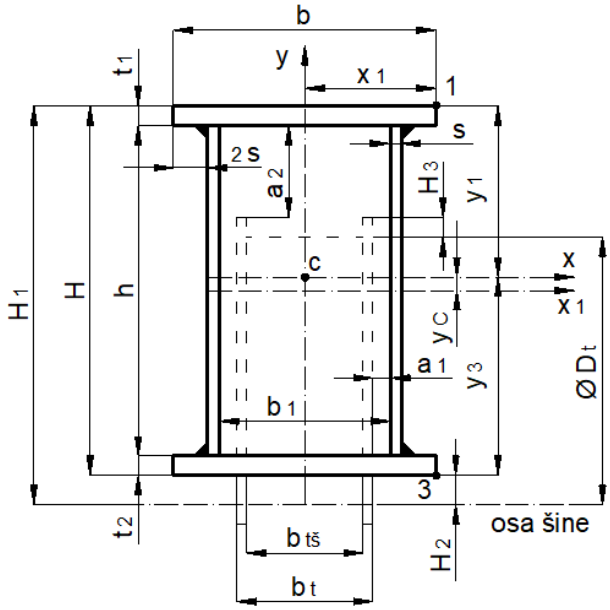

Slika 1. *Kutijasti poprečni presek čeonog nosača*

Neophodne geometrijske karakteristike kutijastog poprečnog preseka se računaju po sledećim izrazima:

$$y_c = \left\lfloor b \cdot t_1 \cdot (h + t_1) - b \cdot t_2 \cdot (h + t_2) \right\rfloor / (2 \cdot A_c), \tag{9}$$

$$I_{x1} = s \cdot h^3 / 6 + b \cdot \left(t_1^3 + t_2^3\right) / 12 + b \cdot \left\lfloor t_1 \cdot (h + t_1)^2 + t_2 \cdot (h + t_2)^2 \right\rfloor / 4, \tag{10}$$

$$I_x = I_{x1} - A_c \cdot y_c^2, \tag{11}$$

$$I_y = h \cdot s^3 / 6 + b^3 \cdot (t_1 + t_2) / 12 + h \cdot s \cdot (b_1 + s)^2 / 2, \tag{12}$$

gde su: y_c položaj glavne težišne ose poprečnog preseka (Slika 1), I_{x1} moment inercije za pomoćnu težišnu osu x_1, I_x i I_y glavni momenti inercije.

2.2 Funkcije ograničenja

Kod ove vrste noseće strukture potrebno je da budu zadovoljeni uslovi čvrstoće, lokalne stabilnosti limova (gornji pojasni lim i vertikalni limovi), kao i određene geometrijske preporuke (Slika 1).

Kriterijumi čvrstoće u tačkama 1 i 3 kutijastog profila (Slika 1) se proveravaju na sledeći način:

$$\sigma_{u1} = M_V / W_{x1} + M_H / W_y \le \sigma_{dop} = R_e / \nu_1, \tag{13}$$

$$\sigma_{u3} = M_V / W_{x3} + M_H / W_y \le \sigma_{dop}, \tag{14}$$

$$W_{x1} = I_x / y_1,\ W_{x3} = I_x / y_3,\ W_y = I_y / x_1, \tag{15}$$

$$y_1 = H/2 - y_c,\ y_3 = H/2 + y_c,\ x_1 = b/2, \tag{16}$$

$$H = h + t_1 + t_2, \tag{17}$$

gde su: σ_{u1}, σ_{u3} maksimalni naponi u tačakam 1 i 3, respektivno, σ_{dop} dopušteni napon, M_V, M_H momenti savijanja u obe ravni, prema [5], W_{x1}, W_{x3}, W_y otporni momenti inercije, y_1, y_3, x_1 i H geometrijski parametri (Slika 1).

Provera lokalne stabilnosti gornjeg pojasnog lima se vrši prema standardu [10]:

$$\sigma_f = \nu_1 \cdot \left(M_V / W_{x1} + M_{H,f} / W_y \right) \le \min\left(\sigma_{dop,f},\ R_e \right), \tag{18}$$

$$M_{H,f} = M_H \cdot \left(b_1 + s \right) / b, \tag{19}$$

$$\sigma_{dop,f} = \nu_1 \cdot \chi_f \cdot C_f \cdot R_e, \tag{20}$$

gde su: σ_f maksimalna vrednost napona za gornji pojasni lim, $\sigma_{dop,f}$ dopušteni napon gornjeg pojasnog lima, i χ_f, C_f, koeficijenti, prema [10].

Provera lokalne stabilnosti vertikalnih limova se vrši prema standardu [10]:

$$\sigma_w = \nu_1 \cdot \left(M_{V,w} / W_{x1} + M_{H,f} / W_y \right) \le \min\left(\sigma_{dop,w},\ R_e \right), \tag{21}$$

$$M_{V,w} = M_V \cdot \left(h - 2 \cdot y_c \right) / \left(H - 2 \cdot y_c \right), \tag{22}$$

$$\sigma_{dop,w} = \nu_1 \cdot \chi_w \cdot C_w \cdot R_e, \tag{23}$$

gde su: σ_w maksimalna vrednost napona za vertikalni lim, $\sigma_{dop,w}$ dopušteni napon vertikalnog lima, i χ_w, C_w koeficijenti, prema [10].

Provera krutosti čeonog nosača se određuje na sledeći način:

$$f_{\max} = f_1 + f_2 + f_3 + f_4 + f_q \le f_{dop} = K \cdot l_c, \tag{24}$$

$$f_1 = F_A \cdot l_c^{\,3} \cdot \left[b_A / \left(2 \cdot l_c \right) \right] \cdot \left\{ 0,75 - \left(b_A / l_c \right)^2 + \left[\left(l_c / 2 - a_A \right) / l_c \right]^3 \right\} / \left(6 \cdot B_x \right), \tag{25}$$

$$f_2 = F_C \cdot l_c^{\,3} \cdot \left[b_C / \left(2 \cdot l_c \right) \right] \cdot \left\lfloor 0,75 - \left(b_C / l_c \right)^2 \right\rfloor / \left(6 \cdot B_x \right), \tag{26}$$

$$f_3 = -M_A \cdot l_c^{\,2} \cdot \left\{ 0,5 \cdot \left[0,75 - 3 \cdot \left(b_A / l_c \right)^2 \right] + 3 \cdot \left[\left(l_c / 2 - a_A \right) / l_c \right]^2 \right\} / \left(6 \cdot B_x \right), \tag{27}$$

$$f_4 = M_C \cdot l_c^{\,2} \cdot \left\lfloor 0,75 - 3 \cdot \left(b_C / l_c \right)^2 \right\rfloor / \left(12 \cdot B_x \right), \tag{28}$$

$$f_q = 5 \cdot \gamma \cdot q_c \cdot l_c^{\,4} / \left(384 \cdot B_x \right), \tag{29}$$

gde su: f_{max} maksimalni ugib na sredini čeonog nosača, f_1 ugib od opterećenja F_A, [5], f_2 ugib od opterećenja F_C, [5], f_3 ugib od opterećenja M_A, [5], f_4 ugib od opterećenja M_C, [5], f_5 ugib od sopstvene težine čeonog nosača q_c, [5], f_{dop} dozvoljeni ugib čeonog nosača, B_x savojna krutost čeonog nosača i b_A, a_A, b_C rastojanja, [5].

Takođe, neophodno je da budu zadovoljeni i sledeći uslovi (Slika 1):

$$b_1 \ge b_t + 2 \cdot a_1, \tag{30}$$

$$H + H_2 \geq D_t + H_3 + a_2 + t_1. \tag{31}$$

3 REZULTATI OPTIMIZACIJE

U ovom istraživanju problema optimizacije kutijastog poprečnog preseka čeonog nosača dvogredne mosne dizalice primenjen je algoritam vilinog konjica, Dragonfly Algorithm (DA), [11]. Detaljan opis ovog algoritma prikazan je u pomenutoj literaturi. Varijable postupka optimizacije su: b_1, h, t_1, t_2, s (Slika 1). Optimizacija je izvršena u Matlab softverskom paketu, primenom DA koda.

Na primeru čeonog nosača jedne postojeće dvogredne mosne dizalice posmatraće se predloženi optimizacioni model.

Funkcija cilja optimizacijonog problema je predstavljena u relaciji (4), dok funkcije ograničenja čine izrazi: (13), (14), (18), (21), (24), (30) i (31).

Kontrolni parametri postupka optimizacije: N_{pop}=100 – veličina populacije, *Max_It*=500 – maksimalni broj iteracija.

Donje i gornje granične vrednosti varijabli su: $b_t \leq b \leq 30$, $D_t \leq h \leq 70$,

$0{,}6 \leq t_1 \leq 3$, $0{,}6 \leq t_2 \leq 3$, $0{,}5 \leq s \leq 2$.

Izvršeno je ukupno po deset simulacija za svaku varijantu i materijal, pri čemu su odabrana najbolja rešenja (Tabele 1-4). Takođe, posmatrano je i ograničenje visine nosača, pri čemu je usvojeno da visina nosača H mora biti manja od maksimalne dozvoljene visine H_{max}=50 cm. Tabele 1-4 prikazuju optimalne vrednosti geometrijskih parametara čeonog nosača, optimalne površine poprečnog preseka čeonog nosača, kao i uštedu u materijalu. Sve optimalne vrednosti su zaokružene na četiri decimale.

Table 1. Rezultati optimizacije za Vatijantu 1

Materijal	b_1 (cm)	h (cm)	t_1 (cm)	t_2 (cm)	s (cm)	A_{co} (cm^2)	Ušteda (%)
S235	21,6763	53,5444	0,6596	0,6000	0,5000	84,6260	37,02
S355	21,5000	54,3530	0,6000	0,6000	0,5000	83,7530	37,67

Table 2. Rezultati optimizacije za Vatijantu 1 (sa ograničenjem visine nosača)

Materijal	b_1 (cm)	h (cm)	t_1 (cm)	t_2 (cm)	s (cm)	A_{co} (cm^2)	Ušteda (%)
S235	30,0000	48,7041	0,6959	0,6000	0,5000	91,4681	31,92
S355	30,0000	48,7041	0,6959	0,6000	0,5000	91,4681	31,92

Table 3. Rezultati optimizacije za Vatijantu 2

Materijal	b_1 (cm)	h (cm)	t_1 (cm)	t_2 (cm)	s (cm)	A'_{co} (cm^2)	Ušteda (%)
S235	21,8329	54,1371	0,7076	0,6000	0,5000	83,9925	37,49
S355	21,5000	55,5543	0,6000	0,6000	0,5000	82,5543	38,56

Table 4. Rezultati optimizacije za Vatijantu 2 (sa ograničenjem visine nosača)

Materijal	b_1 (cm)	h (cm)	t_1 (cm)	t_2 (cm)	s (cm)	A'_{co} (cm^2)	Ušteda (%)
S235	27,0327	48,4300	0,7917	0,7494	0,5000	91,6327	31,80
S355	30,0000	48,6143	0,7448	0,6402	0,5000	91,5492	31,86

gde su A_{co} i A'_{co} optimalne površine za Varijantu 1 i Varijantu 2, respektivno.

4 ZAKLJUČCI

U ovom istraživanju problema optimizacije kutijastog poprečnog preseka čeonog nosača dvogredne mosne dizalice primenjen je algoritam vilinog konjica (DA).

Cilj istraživanja je bilo smanjiti masu, odnosno površinu poprečnog preseka čeonog nosača. Kao kriterijumi optimizacije posmatrani su čvrstoća nosača, lokalna stabilnost limova nosača, ugib nosača, kao i određena geometrijska ograničenja.

Na osnovu Tabela 1-4 se vidi da je ostvarena velika ušteda u materijalu, naročito za slučaj kada nema ograničenja visine nosača (Tabela 1 i Tabela 3). Takođe, primećuje se da izbor materijala ima mali uticaj na rešenja, pri čemu S355 postiže bolje rezultate u odnosu na S235, osim za slučaj prikazan u Tabeli 2. Za posmatrane zadate uslove može se primetiti da Varijanta 2 daje bolju uštedu u odnosu na Varijantu 1, kada nema ograničenja visine nosača (Tabela 1 i Tabela 3), dok u slučaju ograničenja visine nosača Varijanta 1 ostvaruje bolje rezultate (Tabela 2 i Tabela 4).

Na osnovu ovoga se dokazala opravdanost primene predstavljenog pristupa analizi i optimizaciji mase čeonog nosača, kao i primenjenog metoda optimizacije.

Za dalja istraživanja je neophodno primenjivati slične metaheurističke algoritme optimizacije, kako bi se izvršila njihova komparacija i dale preporuke u izboru algoritama koje se odnose na ove vrste nosećih struktura. Neophodno je u optimizacioni proces uvesti i dodatne funkcije ograničenja, koje se odnose na vrstu materijala, zamor, čvrstoću zavarenih veza, tehnologičnost, i sl. Takođe, od značaja su i ekonomski i zeleni aspekt projektovanja i proizvodnje.

ZAHVALNOST

Ovaj rad je podržan od strane Ministarstva prosvete, nauke i tehnološkog razvoja Republike Srbije kroz Ugovor o realizaciji i finansiranju naučno-istraživačkog rada u 2022. godini, čiji je evidencioni brojevi 451-03-68/2022-14/200102 i 451-03-68/2022-14/200108.

NOMENKLATURA

A površina poprečnog preseka, cm^2
a rastojanje, cm
B savojna krutost, kNcm^2
b širina, cm
C koeficijent, prema [10]
f ugib, cm
g_i funkcija ograničenja
H, h visina nosača, visina, respektivno, cm
I_x, I_y glavni moment inercije, cm^4
K koeficijent krutosti koji zavisi od načina upravljanja dizalicom i pogonske klase
k_a dinamički koeficijent opterećenja dizalice u horizontalnoj ravni, [9]
L raspon dizalice, m
l, l_c rastojanje između glavnih nosača, dužina čeonog nosača, respektivno, m
l_j, u_j donja, odnosno gornja vrednost promenjive x_j, cm
M_V, M_H momenti savijanja u vertikalnoj i horizontalnoj ravni, kNcm
m masa, t
Q nosivost dizalice, t
q specifična težina, kN/cm
R_e, napon na granici tečenja za materijal čeonog nosača, kN/cm^2

s, t debljine limova, cm
W otporni moment inercije, cm^3
X, x_j vektor od n varijabli,varijable (promenjive), cm
γ koeficijent koji zavisi od pogonske klase dizalice, prema [9]
χ koeficijent izvijanja, prema [10]
ν_1 koeficijent sigurnosti za 1. slučaj opterećenja
σ napon, kN/cm^2
ψ dinamički koeficijent oscilovanja, prema [9]
dop dozvoljena vrednost
f gornji pojasni lim
G glavni nosač
k kolica
š šina
t točak čeonog nosača
u ukupna vrednost
w vertikalni lim

LITERATURA

[1] Yixiao, Q., Ji, J., Haiming, Y. (2016). High Precision Analysis of Stress Concentration in Girder High Precision Analysis of Stress Concentration in Girder Structure of Casting Crane, *International Journal of Science and Qualitative Analysis*, 2/2, p.p. 14-18.
[2] Ling, Z., Wang, M., Xia, J., Wang, S., Guo, X. (2018). Stress Analysis for the Critical Metal Structure of Bridge Crane, *IOP Conference Series: Earth and Environmental Science*, 108, 022056.
[3] Li, H., Wu, H. (2015). Study on bridge structure of bridge crane, *5th International Conference on Civil Engineering and Transportation (ICCET 2015)*, Guangzhou, China, p.p. 1776-1779.
[4] Hrabovsky, L. (2016). Action on Crane Runway Caused by Horizontal Forces due to Crane Skewing, *Key Engineering Materials*, 669, p.p. 391-399.
[5] Pavlović, G., Savković M., Zdravković, B.N., Marković, G. (2021). Optimal design of end carriage structures, *XXV International Scientific Conference (TRANSPORT 2021)*, Sofia, Bulgaria, Vol. 19/3, 2114.
[6] Pavlović, G., Savković, M., Zdravković, N., Marković, G. (2020). Optimization design of end carriage of the single-girder bridge crane structure, *MTC AJ*, 18/3, 1939.
[7] Pavlović, G., Jerman, B., Savković, M., Zdravković, N., Marković, G. (2022). Metaheuristic applications in mechanical and structural design, *Enginering TODAY*, 1/1, p.p. 19-26.
[8] Pavlović, G., Savković, M., Marković, G., Zdravković, N., Stanojković, J. (2018). Optimal design of welded I-beam of slewing pillar jib crane, *IMK – 14, Research&Development in Heavy Machinery*, 24/3, p.p. 77-84.
[9] Ostrić, D., Tošić S. (2005). *Dizalice*, Institut za mehanizaciju Mašinskog Fakulteta Univerziteta u Beogradu, Beograd.
[10] Jugoslovenski zavod za standardizaciju (1986). SRPS U.E7.121*, Proračun izbočavanja limova*, Beograd.
[11] Mirjalili, S. (2016). Dragonfly algorithm: a new meta-heuristic optimization technique for solving single-objective, discrete, and multi-objective problems, *Neural Comput & Applic*, 27, p.p. 1053–1073.

COMETa 2022
6th INTERNATIONAL SCIENTIFIC CONFERENCE
17th - 19th November 2022
Jahorina, B&H, Republic of Srpska
University of East Sarajevo
Faculty of Mechanical Engineering
Conference on Mechanical Engineering Technologies and Applications

BAUKASTEN SISTEM GRADNJE PLANETARNIH PRENOSNIKA

Vojislav Miltenović[1], Biljana Marković[2], Milan Tica[3]

Rezime: U odnosu na klasične prenosnike, planetarni prenosnici imaju niz prednosti. Najznačajnija prednost je kompaktna konstrukcija, koja se postiže grananjem i ponovnim sumiranjem energije. Na taj način dobijaju se male gabaritne dimenzije planetarnih prenosnika. Pored toga imaju i visoku tačnost pozicioniranja i visok stepen iskorišćenja, što im omogućuje široku primenu u industriji. Njihove prednosti se mogu uvećati primenom baukasten sistema gradnje. Na taj način dobija se familija planetarnih prenosnika čiji prenosni odnos obuhvata široko područje, što se postiže izmenom pojedinih modula prenosnika. U radu je prikazan baukasten princip gradnje planetarnih prenosnika na konkretnom primeru, sa detaljnom razradom kompletne konstrukcije prenosnika.

Ključne riječi: planetarni prenosnik, baukasten, familija, proračun

BAUKASTEN PLANETARY TRANSMISSION CONSTRUCTION SYSTEM

Abstract: Compared to classic transmissions, planetary transmissions have a number of advantages. The most significant advantage is the compact construction, which is achieved by branching and resumming the energy. In this way, the overall dimensions of the planetary gears are small. In addition, they have high positioning accuracy and a high degree of utilization, which enables them to be widely used in industry. Their advantages can be increased by applying the Baukasten construction system. In this way, a family of planetary transmissions is obtained whose transmission ratio covers a wide area, which is achieved by changing individual transmission modules. The paper presents the Baukasten principle of building planetary transmissions on a concrete example, with a detailed elaboration of the complete structure of the transmission.

Key words:, baukasten, calculation, family, planetary transmission

[1]Prof. dr Vojislav Miltenović, Inovacioni centar ICUN, Niš, Republika Srbija, vojamiltenovic@yahoo.com
[2]Prof. dr Biljana Marković, Mašinski fakultet Istočno Sarajevo, Istočno Sarajevo, Republika Srpska, BiH, biljana.markovic@ues.rs.ba
[3]Prof. dr Milan Tica, Mašinski fakultet Banja Luka, Banja Luka, Republika Srpska, BiH, mila.tica2012@gmail.com

1 UVOD

Planetni prenosnici su zupčasti ili frikcioni prenosnici koji pored fiksnih vratila imaju i osovinu, koja se preko odgovarajućeg nosača kreće po kružnoj putanji. Na fiksnim vratilima uležišteni su centralni zupčanici, koji mogu da se okreću oko centralne ose. Na pokretnoj osovini uležišten je zupčanik koji se pored rotacije oko sopstvene ose, zajedno sa osovinom okreće i oko centralne ose. Po uzoru na kretanje planeta oko sunca centralni zupčanik naziva se i sunčani zupčanik, dok se zupčanik koji kruži oko centralne ose naziva planetarni zupčanik. U praksi se koriste veći broj planetarnih zupčanika, postavljenih u odgovarajuću konstrukciju, odnosno nosač planetarnih zupčanika.

U odnosu na obične prenosnike, planetarni presnosnici imaju niz prednosti:

- Kompaktna konstrukcija, koja se postiže primjenom ozubljenog vijenca u kome su postavljena koaksijalna vratila;
- Prenos većih obrtnih momenata, koja je omogućena grananjem i ponovnim sumiranjem snage preko većeg broja planetarnih zupčanika;
- Simetričnim postavljanjem planetarnih zupčanika postiže se dobra uravnoteženost;
- Mogućnost ostvarivanja velikih prenosnih odnosa, kao i različitih prenosnih odnosa;
- Izvođenje prenosa snage sa više stepeni slobode (diferencijalni prenosnici).
- Mogućnost jednostavne konstrukcije višestepenih mjenjača primjenom spojnica i kočnica.

Nedostaci planetarnih prenosnika:

- Komplikovana kompaktna konstrukcija, koja traži ispunjenje većeg broja graničnih uslova;
- Kod visokih brojeva obrtaja, dodatno opterećenje ležajeva zbog centrifugalne sile;
- Zahtjevi za visokim kvalitetom izrade, što uvećava cijenu prenosnika;
- Prenosni odnos ispod 3.5 teško ostvariv;

Jednostavni obični prenosnik ima minimum 2 vratila na kome je uležišten jedan zupčasti par (jednostepeni prenosnik). Planetarni prenosnik sa minimum 2 vratila i jednom pokretnom osovinom predstavlja dvostepeni prenosnik. Kružno kretanje planetarnog zupčanika (Slika1) mora biti koaksijalno u odnosu na oba centralna zupčanika sa kojima se nalazi u sprezi. Koaksijalno kretanje planetarnih zupčanika omogućuje konstrukcija – nosač koji takođe ima funkciju ulaznog ili izlaznog vratila prenosnika. Prema tome, ose obrtanja centralnih zupčanika i osa nosača planetarnih zupčanika moraju da se poklope.

Na Slici 1. prikazana je jednostavna konstrukcija planetarnog prenosnika koja se najčešće primjenjuje za industrijske prenosnike. Može da se koristi i kao reduktor i kao multiplikator. Ako se koristi kao reduktor, onda se snaga dovodi na vratilo sunčanog zupčanika, a sunčani zupčanik preko planetarnih zupčanika dovodi u obrtno kretanje nosač planetarnih zupčanika, te snagu vodi do izlaznog vratila. Za slučaj da se koristi kao multiplikator, dovod snage je preko vratila nosača planetarnih zupčanika, a odvod preko vratila sunčanog zupčanika. Ozubljeni vijenac je u oba slučaja nepokretan.

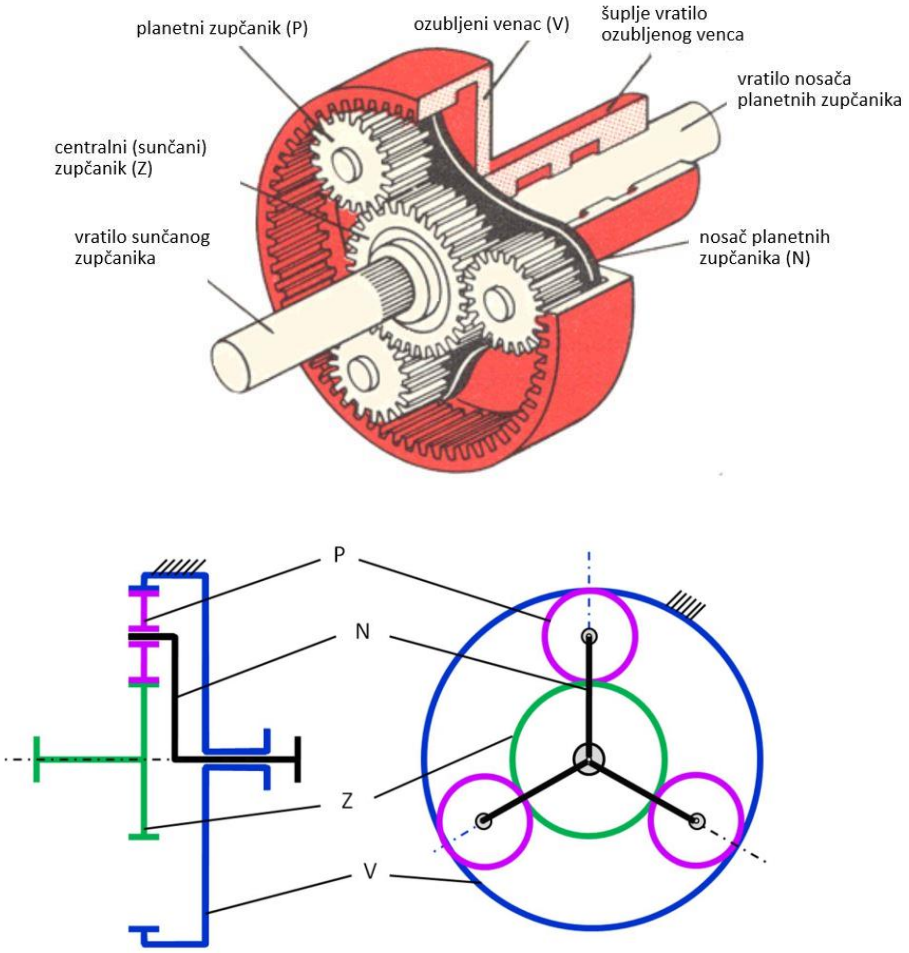

Slika 1. *3D model i šematski prikaz planetarnog prenosnika [1]*

U Tabeli 1. dat je šematski prikaz varijanti jednostavnih planetarnih prenosnika sa izrazima za određivanje i graničnim vrijednostima prenosnih odnosa i stepena iskorišćenja.

Tabela 1. *Prenosni odnosi i stepeni iskorištenja planetarnih prenosnika*

Tip			AI	A+I	A+A	I+I
Funkcija elementa Ulaz snage	Izlaz snage	Fiksiran	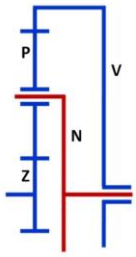	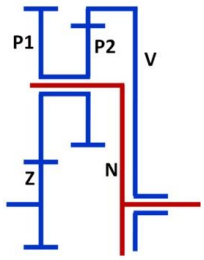	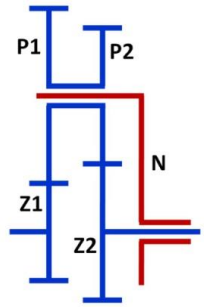	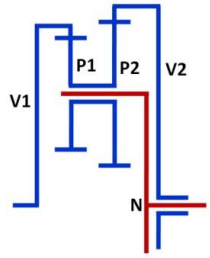
Z (V1)	V	N	$i_{OZ}=\frac{z_V}{z_Z}$ $\eta_0=\eta_{0ZP}\cdot\eta_{0PV}$	$i_{OZ}=\frac{z_{P1}}{z_Z}\cdot\frac{z_V}{z_{P2}}$ $\eta_0=\eta_{0ZP1}\cdot\eta_{0P2V}$	$i_{OZ}=\frac{z_{P1}}{z_{Z1}}\cdot\frac{z_{Z2}}{z_{P2}}>1$ $\eta_0=\eta_{0Z1P1}\cdot\eta_{0P2Z2}$	$i_{OZ}=\frac{z_{P1}}{z_{V1}}\cdot\frac{z_{V2}}{z_{P2}}>1$ $\eta_0=\eta_{0V1P1}\cdot\eta_{0P2V2}$
Z (V1)	N	V	$i_{ZN}=1-i_{OZ}$ $\eta=\frac{1-i_{OZ}\cdot\eta_0}{1-i_{OZ}}$	$i_{ZN}=1-\frac{z_{P1}}{z_Z}\cdot\frac{z_V}{z_{P2}}$ $\eta=\frac{1-i_{OZ}\cdot\eta_0}{1-i_{OZ}}$	$i_{ZN}=1-\frac{z_{P1}}{z_{Z1}}\cdot\frac{z_{Z2}}{z_{P2}}$ $\eta=\frac{i_{OZ}\cdot\eta_0-1}{i_{OZ}-1}$	$i_{V1N}=1-\frac{z_{P1}}{z_{V1}}\cdot\frac{z_{V2}}{z_{P2}}$ $\eta=\frac{i_{OZ}\cdot\eta_0-1}{i_{OZ}-1}$
N	Z (V1)	V	$i_{NZ}=\frac{1}{1-i_{OZ}}$ $\eta=\frac{1-i_{OZ}}{1-\frac{i_{OZ}}{\eta_0}}$	$i_{NZ}=\frac{1}{1-\frac{z_{P1}}{z_Z}\cdot\frac{z_V}{z_{P2}}}$ $\eta=\frac{1-i_{OZ}}{1-\frac{i_{OZ}}{\eta_0}}$	$i_{NZ}=\frac{1}{1-\frac{z_{P1}}{z_{Z1}}\cdot\frac{z_{Z2}}{z_{P2}}}$ $\eta=\frac{i_{OZ}-1}{\frac{i_{OZ}}{\eta_0}-1}$	$i_{NV1}=\frac{1}{1-\frac{z_{P1}}{z_{V1}}\cdot\frac{z_{V2}}{z_{P2}}}$ $\eta=\frac{i_{OZ}-1}{\frac{i_{OZ}}{\eta_0}-1}$
V	N	Z (V1)	$i_{VN}=\frac{1}{1-i_{OZ}}$ $\eta=\frac{\eta_0-i_{OZ}}{1-i_{OZ}}$	$i_{VN}=1-\frac{1}{\frac{z_{P1}}{z_Z}\cdot\frac{z_V}{z_{P2}}}$ $\eta=\frac{\eta_0-i_{OZ}}{1-i_{OZ}}$	$i_{Z2N}=1-\frac{1}{\frac{z_{P1}}{z_{Z1}}\cdot\frac{z_{Z2}}{z_{P2}}}$ $\eta=\frac{i_{OZ}\cdot\eta_0-1}{\eta_0\cdot(i_{OZ}-1)}$	$i_{V2N}=1-\frac{1}{\frac{z_{P1}}{z_{V1}}\cdot\frac{z_{V2}}{z_{P2}}}$ $\eta=\frac{i_{OZ}\cdot\eta_0-1}{\eta_0\cdot(i_{OZ}-1)}$

Tabela 1. *Prenosni odnosi i stepeni iskorištenja planetarnih prenosnika - nastavak*

Tip			AI	A+I	A+A	I+I
Funkcija elementa			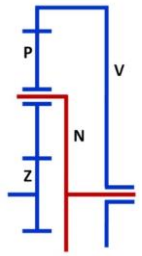	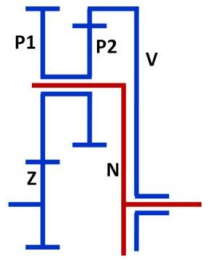	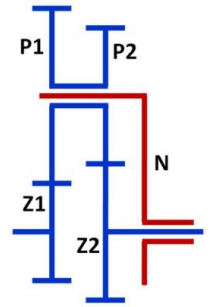	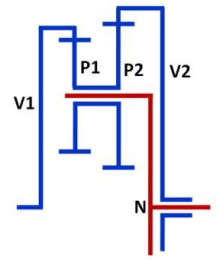
Ulaz snage	Izlaz snage	Fiksiran				
N	V	Z (V1)	$i_{NV}=\frac{1}{1-\frac{1}{i_{OZ}}}$ $\eta=\frac{1-i_{OZ}}{\frac{1}{\eta_0}-i_{OZ}}$	$i_{NV}=\frac{1}{1-\frac{z_Z}{z_{P1}}\cdot\frac{z_{P2}}{z_V}}$ $\eta=\frac{1-i_{OZ}}{\frac{1}{\eta_0}-i_{OZ}}$	$i_{NZ2}=1-\frac{1}{\frac{z_{Z1}}{z_{P1}}\cdot\frac{z_{P2}}{z_{Z2}}}$ $\eta=\frac{i_{OZ}-1}{i_{OZ}-\eta_0}$	$i_{NV2}=1-\frac{1}{\frac{z_{V1}}{z_{P1}}\cdot\frac{z_{P2}}{z_{V2}}}$ $\eta=\frac{i_{OZ}-1}{i_{OZ}-\eta_0}$

Oznake: i_{OZ} – prenosni odnos za fiksirani nosač planetarnih zupčanika i ulaz snage na sunčani zup.
η_0 – stepen iskorištenja za fiksirani nosač planetarnih zupčanika, običan prenosnik
z_V – broj zubaca ozubljenog vijenca (neg.predznak)

2 DEFINISANJE FAMILIJE PLANETARNIH PRENOSNIKA

2.1 Konstrukcioni aspekti kod izvođenja planetarnih prenosnika

Prenosni odnos: Prečnici zupčanika planetarnih prenosnika zavise od izabranih prenosnih odnosa. Sa druge strane postoje geometrijska ograničenja vezana za međusobni položaj i uležištenje sunčanog i planetarnih zupčanika. Zbog toga je maksimalni prenosni odnos jednostepenog planetarnog prenosnika sa 3 planetarna zupčanika ograničena na 12. Minimalna vrijednost prenosnog odnosa ograničena je na 4 (izuzetno 3.5).

Uslov saosnosti: Kod planetarnog prenosnika (Slika 1.) poklapaju se ose sunčanog zupčanika i ozubljenog vijenca sa osom vratila nosača planetarnih zupčanika. Zbog toga mora biti ispunjen uslov saosnosti, odnosno osna rastojanja sunčanog zupčanika i planetarnih zupčanika jednaka su osnom rastojanju planetarnih zupčanika i ozubljenog vijenca.

$$a = a_{ZP} = \left|a_{PV}\right| = r_Z + r_P = \left|r_P + r_V\right| \tag{1}$$

Broj planetarnih zupčanika: Najčešće se uzima da broj planetarnih zupčanika bude 3. Na taj način se prenos snage i opterećenja ravnomjerno raspoređuje na planetarne zupčanike, odnosno postiže de dinamička ravnoteža. Pri izboru broja planetarnih zupčanika treba biti ispunjen uslov da ne dođe do preklapanja tjemenih dijelova susjednih zupčanika (uslov susjedstva). Preporučuje se da minimalno rastojanje između tjemenih prečnika planetarnih zupčanika bude ≥1mn, gde je mn mudul. Ovaj uslov ispunjen je ukoliko je broj planetarnih zupčanika p:

$$p \le \frac{\pi}{arc\,sin\dfrac{d_{aP}+m_n}{d_{wZ}+d_{wP}}} \tag{2}$$

Uslov montaže: Osnovni uslov koji se ovde postavlja je da planetarni zupčanici budu ravnomjerno i simetrično raspoređeni po obimu, jer su tada radijalne sile spregnutih parova uravnotežene, a uravnotežen je i nosač planetarnog zupčanika. To će biti ispunjeno ukoliko za broj planetarnih zupčanika *p* izabrani brojevi zubaca sunčanog zupčanika z_Z i ozubljenog vijenca z_V zadovoljavaju uslov:

$$\frac{z_Z - z_V}{p} = ceo\ broj \tag{3}$$

U izrazu (3) broj zubaca ozubljenog vijenca z_V uzima se sa negativnim predznakom.

2.2 Definisanje familije

Za dalje razmatranje usvojeni su sledeći radni parametri prenosnika:

- ulazni brojevi obrtaja n_{PPul} = 750 min^{-1}
- radni prenosni odnos i_{PP} = 3 ... 8
- maksimalna snaga P = 100 kW
- radni vijek L_h = 100.000 sati.

S obzirom da se radni prenosni odnos kreće u dosta širokim granicama (i_{PP}=3-8), potrebno je projektovati familiju prenosnika, jer standardom nije pokriveno kompletno područje prenosnog odnosa. Najbolje mogućnosti u tom pogledu pružaju planetarni prenosnici tipa **AI** (Tabela 1.). Sa jednom kompletnom konstrukcijom kućišta i istim ozubljenim vijencem, moguće je zamjenom centralnog zupčanika i seta planetarnih zupčanika sa nosačem (Slika 1.) po baukasten principu dobiti familiju planetarnih prenosnika sa različitim prenosnim odnosom.

Saglasno teorijskim osnovama o planetarnim prenosnicima [2] iterativnim putem se dolazi do familije planetarnih prenosnika (Tabela 2.).

Tabela 2. *Geometrijski podaci o familiji planetarnih prenosnika*

Var.	z_Z	z_P	z_V	m_n	d_Z	d_P	d_V	b	a_{ZP}	a_{PV}	a_{usv}	i_{OZ}	i_{ZNR}	i_{ZNM}	p = 3
				mm	mm	mm	mm	mm	mm	mm	mm				usl. mont.
1	18	51	-120	3.5	63	178.5	-420	56 ,50, 56	120.75	-120.75	121	-6.67	7.67	0.130	**46**
2	21	49	-120	3.5	73.5	171.5	-420	56 ,50, 56	122.5	-124.25	124	-5.71	6.71	0.149	**47**
3	24	48	-120	3.5	84	168	-420	56 ,50, 56	126	-126	126	-5.00	6.00	0.167	**48**
4	30	45	-120	3.5	105	157.5	-420	56 ,50, 56	131.25	-131.25	130	-4.00	5.00	0.200	**50**
5	36	42	-120	3.5	126	147	-420	56 ,50, 56	136.5	-136.5	136	-3.33	4.33	0.231	**52**
6	39	40	-120	3.5	136.5	140	-420	56 ,50, 56	138.25	-140	140	-3.08	4.08	0.245	**53**
7	48	36	-120	3.5	168	126	-420	56 ,50, 56	147	-147	147	-2.50	3.50	0.286	**56**

Kao što može da se vidjeti iz Tabele 2., modul svih zupčanika kod svih varijanti je isti i iznosi m_n=3.5mm. Kako je i broj zubaca ozubljenog vijenca kod svih varijanti isti (z_V=120), to je uz odgovarajuća pomjeranja profila alata, kinematski prečnik ozubljenog vijenca kod svih varijanti isti. Ovaj uslov omogućuje da se po baukasten principu razvije 7-člana familija planetarnih reduktora za radnim prenosnim odnosom u_{PP} = 3.5 do 8. Kod svih varijanti prenosnika ispunjen je uslov saosnosti (1), susjednosti (2) i uslov montaže (3). Na slici 2 dat je 3D prikaz planetarnih zupčanika varijante 1 i 7.

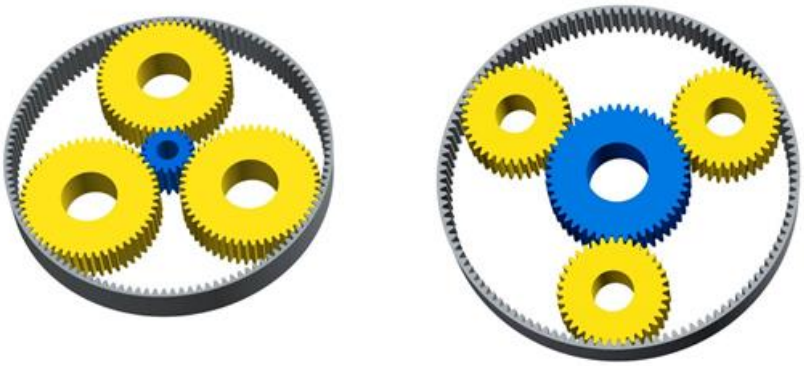

(a) *(b)*

Slika 2. *3D prikaz planetarnih zupčanika varijante 1 (i_{ZNR}=7,67) i varijante 7 (i_{ZNR}=3,5)*

3 NOSIVOST REPREZENTATIVNOG PRENOSNIKA

Kao reprezentativni planetarni prenosnik izabrana je varijanta 1 (Tabela 2.). Ova varijanta ima najveći prenosni odnos, tako da u eksploatacionim uslovima prenosi najveće opterećenje, a zahtjevna je i u pogledu ispunjenja uslova kompaktnosti konstrukcije i baukasten uslova montaže. Ostale varijante su manje opterećene, imaju manji prenosni odnos, pa predstavljaju i lakše konstrukciono rešenje sa aspekta izrade i montaže.

Proračun nosivosti planetarnog prenosnika varijante 1 izveden saglasno teorijskim osnovama [2], odnosno prema ISO 6336-3:2007 Metoda B, za sledeće podatke:

- ulazni broj obrtaja: n_{PPul} = 750 min^{-1}
- kinematski prenosni odnos: u_{PPR} = 7,67
- nominalna snaga: P = 100 kW
- radni vijek; L_h = 100.000 h
- faktor radnih uslova: K_A=1,25.

Prema teorijskim osnovama [2] izvršen je proračun geometrije planetarnog prenosnika tipa **AI** varijante 1. Rezultati proračuna prikazani u Tabeli 3. pokazuju da geometrija zadovoljava granične uslove i da ne postoje nikakve smetnje pri sprezanju zupčanika. Ispunjeni su i uslovi koaksijalnosti, montaže i broja planetarnih zupčanika u cilju izbjegavanja preklapanja tjemenih dijelova planetarnih zupčanika - uslov susjednosti.

Tabela 3. *Geometrijske mjere zupčanika planetarnog prenosnika*

No	Veličina	Ozna.	Dim.	Vrijednost		
				Sunč.zup.	Plan.zup.	Ozub.vijen.
1	Standardni profil			1.25/0.30/1.0	1.25/0.25/1.0	1.25/0.38/1.0
2	Broj zubaca	z		18	51	-120
3	Normalni modul	m_n	mm	3,5		
4	Ugao nagiba profila alata	α_n	°	20		
5	Ugao dodirnice	α_w	°	20.323		20.323
6	Nulto osno rastojanje	a_d	mm	120.750		-120.750
7	Koef. pomjeranja profila	x	-	0.3456	-0.2736	0.2016
8	Prečnici podionih kružnica	d	mm	63.000	178.500	-420.000
9	Prečnici osnovnih kružnica	d_b	mm	59.201	167.735	-394.671
10	Prečnici kinem.kružnica	d_w	mm	63.130	178.870	-420.870
11	Prečnici tjemenih kružnica	d_a	mm	72.415	183.581	-411.589
12	Prečnici podnožnih kružnica	d_f	mm	56.669	167.835	-427.339
13	Visina zupca	h	mm	7.873	7.873	7.875
14	Debljina zupca na tjem. kružnici	s_{an}	mm	1.840	2.849	3.136
15	Podioni korak	p_t	mm	10.996		
16	Osnovni korak	p_{bt}	mm	10.332		
17	Aktivna dužina dodirnice	g_a	mm	16.133		20.934
18	Stepen sprezanja	ε_α	-	1.561		2.026

Tabela 4. *Nosivost zupčanika planetarnog prenosnika – faktori opterećenja*

No	Veličina	Ozn.	Dim.	Vrijednost		
				Sun.zup.	Plan.zup.	Ozub.vijen.
1	Snaga	P	kW	100		
2	Ulazni br.obrtaja nosača pl.zup.	n_{ul}	min^{-1}	**97,8**		
3	Izlazni br.obrtaja sun.zup	n_{izl}	min^{-1}	**750**	230,2	0
4	Broj zubaca	z		18	51	-120
5	Radni prenosni odnos	i_{uk}		0,13		
6	Parc. kinematski prenosni odnos	u		2,833		-2,353
7	Radni vijek	L_h	h	200000		
8	Obrtni moment	T	Nm	1273	-	8488
9	Obrtni moment na nosaču plan.zup.	T_N	Nm	9761,5		
10	Faktor raspodjele opet.između plan.zup.	K_γ			1,12	
11	Materijali			17NiCrMo6-4	18CrNiMo7-6	42 CrMo 4
12	Termohemijska obrada			cementacija	cementacija	nitriranje
13	Površinska tvrdoća			HRC 60	HRC 61	HV 550
14	Kvalitet izrade			6	6	7
15	Srednja visina neravnina bokova	R_{zH}	μm	4.80	4.80	20
16	Srednja visina neravnina podnožja	R_{zF}	μm	20	20	20
17	Trajna dinam.izdržljivost podnožja	σ_{Flim}	N/mm^2	430	500	370
18	Trajna dinam.izdržljivost bokova	σ_{Hlim}	N/mm^2	1500	1500	1000
19	Zatezna čvrstoća	R_m	N/mm^2	1200	1200	1100
20	Granica tečenja	R_e	N/mm^2	850	850	900
21	Faktor radnih uslova	K_A		1,25		
22	Obimna sila na pod. cilindru	F_t	N	13473		13473
23	Radijalna sila	F_r	N	4904		4904
24	Jedinična obimna sila	w	N/mm	259		259
25	Obimna brzina	v_t	m/s		2.15	
26	Faktor unut.dinam. sila	K_v		1.01		1.04

27	Teorijska jedin.krutost	c'_{th}	N/mm/μm	13.882		21.830
28	Srednja jedin.krutost	c'	N/mm/μm	11.492		14.513
29	Srednja krutost parova zubaca	c_γ	N/mm/μm	16.331		25.682
30	Odstupanje mjera pri izradi	f_{ma}	μm	14.14		14.87
31	Odstupanje zbog el.deformacija	f_{sh}	μm	14.56		0.06
32	Početno odstupanje pravca boč.linije	$F_{\beta x}$	μm	11.87		7.92
33	Smanjenje odstupanja usled razrade	y_β	μm	1.78		1.19
34	Stvarno odstup.pravca bočne linije	$F_{\beta y}$	μm	10.09		6.74
35	Faktor rasp.opterećenja duž bočne linije	$K_{H\beta}$		1.21		1.22
36	Faktor rasp.opterećenja duž bočne linije	$K_{F\beta}$		1.17		1.18
37	Faktor rasp.opterećenja. na parove zubaca	$K_{H\alpha}$		1.00		1.16
38	Faktor rasp.opterećenja. na parove zubaca	$K_{F\alpha}$		1.00		1.16
39	Broj obrtaja u radnom vijeku	N_L	$\times 10^6$	23478	2762	3521
40	Podmazivanje potapanjem ulje	Klübersynth GH 6-1500: sintetičko ulje na bazi poliglikola				
41	Kinematska viskoznost na 40°C	ν_{40}	mm²/s	1500		
42	Kinematska viskoznost na 100°C	ν_{100}	mm²/s	232		
43	FZG-Test A/8.3/90 (ISO 14635-1:2006)			14		
44	Specifična gustina na 15°C	ρ_{oil}	kg/dm³	1,080		
45	Radna temperatura ulja	T_S	°C	70		

Tabela 5. *Nosivost zupčanika planetarnog prenosnika – izdržljivost podnožja*

No	Veličina	Ozn.	Dim.	Vrijednost		
				Sun.zup.	Planet.zup.	Ozublj.vijen.
1	Proračun *ISO 6336-3:2007 Methode: B*					
2	Efektivna širina zupca	b_{eff}	mm	56	52	56
3	Krak sile	h_F	mm	3.55	4.46/2.87	3.60
4	Napadni ugao	α_{Fen}	°	22.54	19.16/15.88	19.98
5	Debljina zupca u kritičnom presjeku	s_{Fn}	mm	7.30	7.30/7.30	9.45
6	Radijus zaobljenja u kritičnom presjeku	ρ_F	mm	1.47	1.82/1.82	1.58
7	Faktor oblika zupca	Y_F		1.38	1.77/1.16	0.85
8	Faktor koncentracije napona	Y_S		2.17	1.84/2.13	2.60
9	Faktor kosih zuba	Y_β		1,00		1,00
10	Radni napon	σ_F	N/mm²	312.6	367.2/324.3	269.4
11	Rel. faktor osetljivosti na konc.napona	$Y_{\delta reT}$		1.000	0.995/0.995	1.020
12	Relativni faktor hrapavosti	Y_{RrT}		0.957	0.957	0.982
13	Faktor veličine presjeka	Y_X		1.000	1.000	1.000
14	Faktor radnog vijeka	Y_{NT}		0.850	0.872	0.868
15	Faktor promjenjivosti opterećenja	Y_M		1.000	0.700	1.000
16	Faktor koncen. napona opitnog zup.	Y_{ST}		2,00		
17	Kritični napon	σ_{Fkr}	N/mm²	699.3	581.3/581.3	643.3
18	Stepen sigurnosti	S_F		2.24	1.58/1.79	2.39
19	Minimalni stepen sigurnosti	S_{Fmn}		1.40	1.40	1.40
20	Maksimalna snaga	P_{max}	kW	160	113/128	170

U Tabeli 4. dati su opšti podaci o prenosniku kao proračun faktora opterećenja. Faktori opterećenja određeni su prema teorijskom osnovama [2], [4].

U tabelama 5. i 6. prikazani su rezultati proračuna nosivosti zupčanika po kriterijumu izdržljivosti podnožja i bokova zubaca. Proračun je izveden prema ISO 6336-3:2007 Methode B. Nosivost zupčanika u potpunosti zadovoljava, jer su svi stepeni sigurnosti veći od minimalno dozvoljenih vrednosti.

Tabela 6. *Nosivost zupčanika planetarnog prenosnika – izdržljivost bokova*

No	Veličina	Ozn.	Dim.	Vrijednost		
				Sun.zup.	Plan.zup.	Ozub.vijen.
1	Proračun *ISO 6336-3:2007 Methode: B*					
2	Faktor oblika boka zupca	Z_H		2.47		2.47
3	Faktor elastičnosti materijala	Z_E		189.81		189.81
4	Faktor stepena sprezanja	Z_ε		0.902		0.811
5	Faktor kosih zubaca	Z_β		1.000		1.000
6	Efektivna širina zupca	b_{eff}	mm	52		52
7	Faktor jednostruke sprege	Z_B, Z_D		1.01	1.00/1.00	1.00
8	Radni napon	σ_H	N/mm^2	1267	1250/471	471
9	Faktor radnog vijeka	Z_{NT}		0.850	0.884	0.867
10	Faktor podmazivanja			1.127	1.127/1.191	1.191
11	Faktor obimne brzine			0.965	0.965/0.943	0.943
12	Faktor hrapavosti			0.958	0.958/0.902	0.902
13	Faktor razlike tvrdoće spreg.zubaca			1.0	1.0/1.0	1.0
14	Faktor veličine presjeka			1.0	1.0	1.0
15	Kritični napon	σ_{Hkr}	N/mm^2	1328	1381/1344	878
16	Stepen sigurnosti	S_H		1.06	1.11/2.85	1.87
17	Minimalni stepen sigurnosti	S_{Hmn}		1.00	1.00	1.00
18	Maksimalna snaga	P_{max}	kW	110	122/814	348

4 KONSTRUKCIONO RJEŠENJE PRENOSNIKA

Na osnovu podataka dobijenih u okviru proračuna geometrije i nosivosti (tabele 3…6) u softverskom paketu SOLID WORKS urađeno je kompletno konstrukciono rešenje planetarnog prenosnika [3]. Na Slici 3. dat je presjek prenosnika.

Radi detaljnog objašnjenja konstrukcionog rješenja, njegovih sklopova i načina fukcionisanja, na slikama 3. do 5. prikazan je prenosnik u presjeku, sa pregledom vitalnih sklopova.

Kompletna konstrukcija prenosnika smještena je u kućištu koje se za osnovu pričvršćuje sa 4 zavrtnja. Sklopovi ulaznog i izlaznog dijela kućišta povezani su zavrtnjevima, tako da čine kompaktnu konstrukciju jednostavnu za montažu i održavanje. Između ova dva sklopa postavljen je sklop ozubljenog vijenca i sa njima povezan zavrtnjevima. Navedeni sklopovi su tako konstrukciono izvedeni da su isti za kompletnu familiju planetarnih prenosnika datih u Tabeli 2.

Ostali sklopovi prenosnika menjaju se za svaki član familije iz Tabele 2. Njih čine izlazno vratilo, sklop nosača planetarnih zupčanika, set planetarnih zupčanika sa kompletnim uležištenjem i ulazno vratilo koje je izrađeno izjedna sa sunčanim zupčanikom (Slika 4.). Pošto se radi o uravnoteženju sila zupčastih parova, a u cilju adekvatne kompaktnosti konstrukcije, izlazno i ulazno vratilo prenosnika uležištena su na zajedničkom ležaju. To je kruti ležaj, prsteni kuglični dvoredi ležaj sa kosim dodirom.

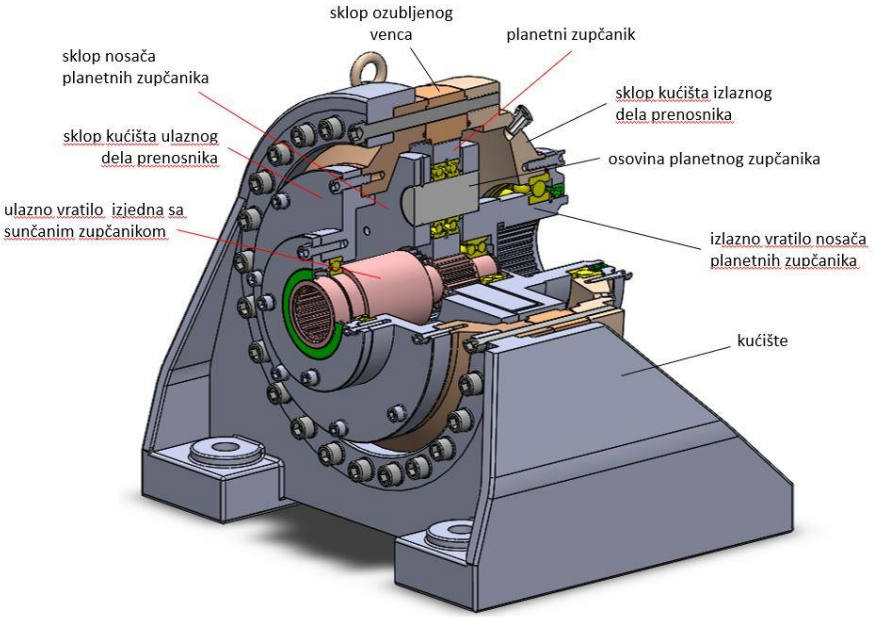

Slika 3. *Konstrukciono rješenje planetarnog prenosnika, presjek*

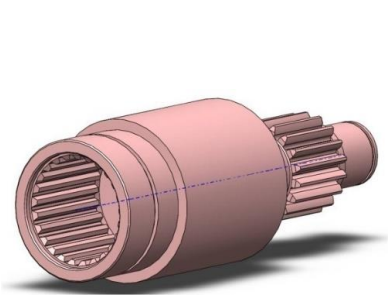

Ulazno vratilo izrađeno izjedna sa sunčanim zupčanikom

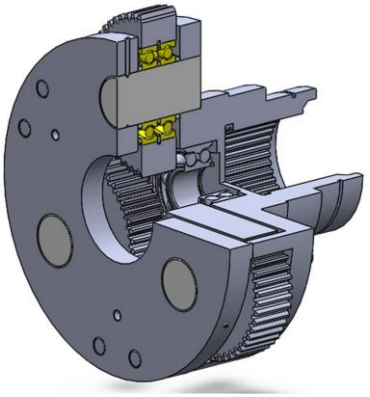

Izlazno vratilo, sklop nosača planetarnih zupčanika i set planetarnih zupčanika sa kompletnim uležištenjem

Slika 4. *Izmenljivi sklopovi planetarnog prenosnika*

Izlazno vratilo nosača planetarnih zupčanika vezuje se sa radnom mašinom preko ozubljenog spoja DIN 5480. Ulazno vratilo prenosnika ima veći broj obrtaja a manje opterećenje, pa je i manjih dimenzija od izlaznog vatila. Povezuje se sa pogonskom mašinom direktno preko ozubljenog spoja sa evolentnim bokovima.

Sklopovi planetarnog zupčanika i nosača planetarnog prenosnika sa izlaznim vratilom prikazani su na Slici 5.

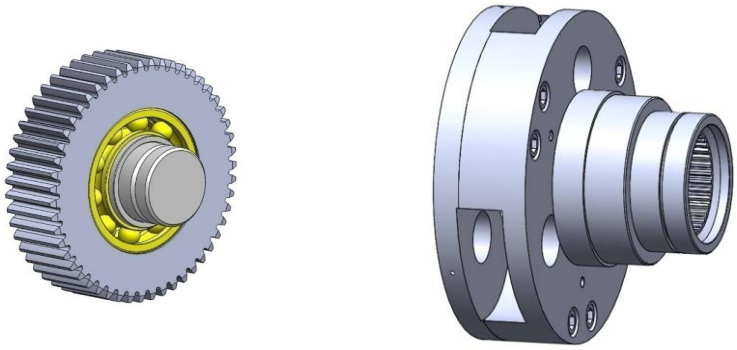

Slika 5. *Sklop planetarnog zupčanika i sklop nosača planetarnog zupčanika*

Naprijed izloženo objašnjenje konstrukcionog rješenja odnosi se za slučaj da se planetarni prenosnik koristi kao reduktor (prenosni odnos i_{ZNR} u Tabeli 2.). Isti planetarni prenosnik može se primjeniti i kao multiplikator. U Tabeli 2. za kompletnu familiju dat je i prenosni odnos planetarnog multiplikatora i_{ZNM}.

5 ZAKLJUČAK

U okviru ovog rada prikazan je baukasten princip gradnje planetarnih prenosnika. Definisana je familija planetarnih prenosnika, a za reprezentativni član familije razvijeno je kompletno konstrukciono rješenje. Definisana familija planetarnih prenosnika nominalne snage P=100 kW, pokriva prenosne odnose i_{ZNR}=3.5...8 za slučaj da se prenosnik primjenjuje kao reduktor, odnosno i_{ZNM}=0,130...0,286 ako se prenosnik primjenjuje kao multiplikator. Sprovedeni proračun pokazuje da prenosnik ima zadovoljavajuću geometriju i nosivost. Prenosnik je kompaktne konstrukcije sa priključkom pogonske i radne mašine preko ozubljenih spojeva. Konstrukcija je urađena na modularnom principu, tako da se za kompletnu familiju sklopovi kućišta prenosnika i ozubljenog venca ne mijenjaju, već se kod odgovarajuće varijante mijenja samo ulazno vratilo sa nosačem i setom planetarnih zupčanika i izlazno vratilo sa sunčanim zupčanikom. Na taj način smanjeni su troškovi izrade prenosnika, skraćeno vrijeme izrade i isporuke i obezbjeđeno pouzdano izvršenje radne funkcije.

LITERATURA

[1] https://wiki.induux.de/Planetengetriebe
[2] Miltenović, V., Tica, M., Marković, B., (2020) *Konstrukcioni elementi u mašinogradnji 2,* Univerzitet u Istočnom Sarajevu, Mašinski fakultet, ISBN 978-99976-719-5-0
[3] *Razvoj i projektovanje planetnih multiplikatora specijalne namene za mikro hidroelektane*- Projekat Fonda za inovacionu delatnost – Program Inovacioni vaučer. ID 209. Realizator: Inovacioni centar Univerziteta u Nišu. Korisnik: TEHNOS PROFI D.O.O SUVI DO, Niš. 2020.
[4] http://www.icun.ni.ac.rs/index.php/sr/delatnost/projekti/12-projekti/inovacioni/
[5] DIN3990. *Tragfähigkeitsberechnung von Stirnrädern*. Teil 1..6. 2012.

COMETa 2022
6th INTERNATIONAL SCIENTIFIC CONFERENCE
17th - 19th December 2022
Jahorina, B&H, Republic of Srpska
University of East Sarajevo
Faculty of Mechanical Engineering
Conference on Mechanical Engineering Technologies and Applications

INFLUENCE OF MATERIALS ON THE EFFICIENCY OF WORM GEAR TRANSMISSION

Blaža Stojanović[1], Aleksandar Vencl[2], Aleksandar Skulić[3], Slavica Miladinović[4], Sandra Gajević[5]

Abstract: This paper presents the results of experimental research of efficiency of a worm gearbox which was designed for that purpose. The gearbox housing is of a welded construction with side openings, which enables simple assembly and disassembly of worm pairs, bearings and other elements. Two worm pairs with the same geometric characteristics were used for testing, where the worms are made of improved steel 42CrMo4 and the worm gears are made of zinc-aluminum alloy ZA12 and aluminum alloy A356. The values of the efficiency were determined at different operating modes of the gearbox (loads and rotational speeds), where mineral oil with a viscosity of 460 mm2/s was used as a lubricant. According to the previously defined working conditions, the power losses and friction coefficient of the worm gear pairs were calculated. Based on the test results, it is concluded that the values of the efficiency of the worm gear pair 42CrMo4/ZA12 are significantly higher compared to the worm gear pair 42CrMo4/A356, which is the result of lower power losses and lower values of the coefficient of friction.

Key words: degree of efficiency, worm gears, material, power losses.

1 INTRODUCTION

Worm gearboxes have a number of advantages compared to other types of transmissions, which are reflected in compact construction, high transmission ratio,

[1] PhD, Blaža Stojanović, University of Kragujevac, Faculty of Engineering, Kragujevac, Serbia; blaza@kg.ac.rs
[2] PhD, Aleksandar Vencl, University of Belgrade, Faculty of Mechanical Engineering, Belgrade, Serbia; avencl@mas.bg.ac.rs
[3] MSc, Aleksandar Skulić, University of Kragujevac, Faculty of Engineering, Kragujevac, Serbia; aleksandarskulic@gmail.com
[4] MSc, Slavica Miladinović, University of Kragujevac, Faculty of Engineering, Kragujevac, Serbia; slavicam@kg.ac.rs
[5] PhD, Sandra Gajević, University of Kragujevac, Faculty of Engineering, Kragujevac, Serbia; sandrav@kg.ac.rs

high load capacity, reliable and quiet operation, etc., and because of this, they are widely used for both power transmission and motion transmission [1]. The main disadvantage of the worm gearbox is a relatively low efficiency, which is a consequence of the high sliding friction between the tooth flanks of meshed gears, which leads to significant power losses and heating of the worm gearbox. In addition to sliding friction between gear teeth, friction also occurs in bearings, between lubricant and gears, in shaft seals, etc. [2].

Power losses in a worm gearbox can vary within wide limits depending on a large number of influencing factors [3, 4]. One of the most important is the type of material of meshed gears [5]. A high value of dynamic durability, high resistance to wear and pitting, good sliding conditions and a high efficiency of the worm pair are required from the material for the production of worm gear pair. A combination of materials for meshed gears that will meet the complex requirements of meshing should be selected.

A worm gear pair is a sliding joint characterized by a linear contact between the meshed elements. Since the worm has a much higher rotational speed than the worm gear, a material of higher hardness is chosen for its production in order to prevent rapid wear. The choice of material for making the worm largely depends on the operating mode of the transmission. Thus, in the case for low speeds and loads, worms of improved steel are chosen, while for transmissions of higher power, cemented or flame-hardened worms are used, which are ground and polished with a hardness ranging between 59 and 65 HRC. Tin and aluminum bronze and brass are mainly used for the production of worm gears. In the case of lower speeds and loads, pearlitic gray cast iron and nodular cast iron are used. In addition, zinc alloys, magnesium alloys and plastics are also used for production of worm gears [6-10]. The best tribological characteristics are achieved when the worm is made of hardened and ground steel and the worm gear is made of centrifugally cast tin bronze.

The main goal of this research is the application of new materials for the production of worm gears and the investigation of their influence on power losses and the efficiency of the transmission. These are materials with zinc-aluminum (alloy ZA12) and aluminum base (alloy A356). The use of these materials aims to reduce the weight of the worm gearbox and the power losses, provide better friction and wear conditions, as well as longer service life, etc.

2 GEARBOX POWER LOSS MODEL

During the meshing of gear teeth, high contact pressures, friction, flank wear, and heating occur, which limit the amount of power that can be transmitted by the worm gearbox. The power on the output shaft of the transmission is less than the input power by the amount of losses that occur during operation due to various resistances. The total power losses P_G of worm gearbox consist of power losses due to friction in the meshing of gear teeth, power losses in bearings, power losses at idle speed, power losses in shaft seals and other losses, respectively [11]:

$$P_G = P_{GZ} + P_{GL} + P_{G0} + P_{GD} + P_{GX} \tag{1}$$

Total power losses can basically be divided into load-dependent and load-independent power losses. For both cases, power losses due to friction in the gear meshing (P_{GZ} and P_{GZ0}) and power losses in the bearings (P_{GL} and PG_{L0}) have their share. Power losses in seals P_{GD} and other losses P_{GX} in gear transmission are losses that do not depend on the load (Figure 1) [12].

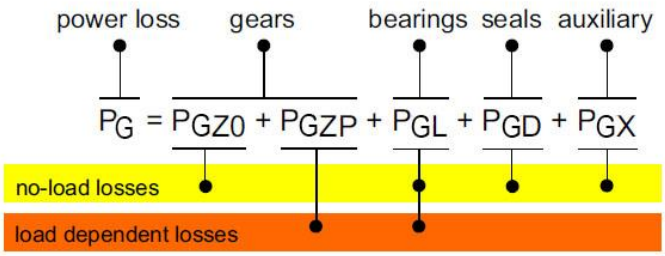

Figure 1. *Power losses in gearbox* [12]

Most gearboxes work in variable operating conditions where speed and load change frequently, so it is very difficult to develop a simple and general approach for calculating power losses. In the available literature, calculations are mostly based on existing analytical methods that are quite complex and generally require appropriate experimental data for a realistic assessment of power losses [13-16].

3. EXPERIMENTAL SETUP AND MEASUREMENTS

3.1 Gearbox test rig

Experimental tests of the efficiency of the single-stage worm gearbox were carried out on the AT200 device shown on figure 2. The device consists of an electromotor (1) with a nominal power of 0.2 kW, which is supported by two bearings on the upper part of the base so that it can rotate around its longitudinal axis. The input torque of the electromotor is determined by means of a dynamometer with a lever (2) located on the front side of the stand. Changing the load on the output shaft of the transmission is achieved by means of an electromagnetic brake (3), which can take over a torque of up to 10 Nm. The magnitude of the output torque is determined by means of a dynamometer (4) which is connected to the lever located on the brake. Changing the operating mode of the transmission (rotational speed and load) is done using the potentiometer located on the control unit (5). The working temperature of the oil is measured using a thermometer (6).

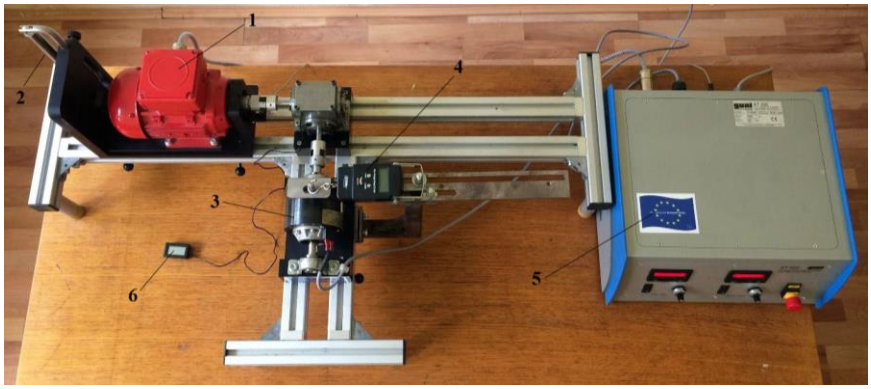

Figure 2. *AT200 device*

Two worm gear pairs with a transmission ratio of 18 and an axial distance of 31 mm were used for the test. The worm is the driving element and is made of 42CrMo4 tempered steel, while the worm gears are made of zinc-aluminum ZA12 and aluminum alloy A356 (Figure 3).

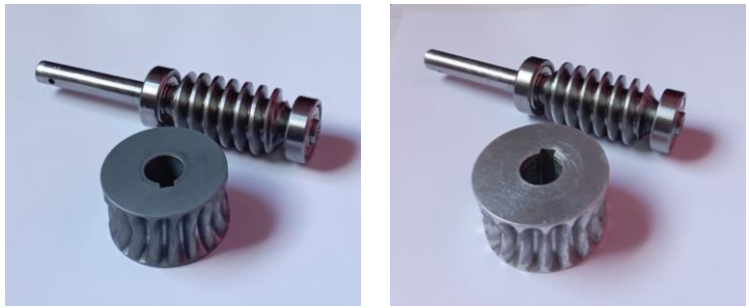

a) *b)*

Figure 3. *Tested worm gear pairs: a) 42CrMo4/ZA12; b) 42CrMo4/A356*

The worm gear shaft is supported by two single-row deep groove ball bearings with radial contact type 6000 RZ, while the worm gear shaft is supported by two single-row deep groove ball bearings type 6001Rs.

3.2 Results and discussion

3.2.1 Gearbox efficiency

The test for the efficiency is based on varying two different values of the rotational speed of 1500 min^{-1} and 2500 min^{-1}, five levels of load (output torques), while mineral oil with a viscosity of 460 mm^2/s is used as a means of lubrication. The output torque is changed by changing the current on the control unit in the interval 0.1 A to 0.2 A with a change step of 0.025 A. Considering both worm pairs, the average values of the output torque T_2 ranged between 2.11-5.32 Nm. Based on the experimentally measured values of the input and output torques, the values of the efficiency of the transmission were determined according to the following expression:

$$\eta = \frac{P_2}{P_1} = \frac{T_2}{T_1 \cdot i} \tag{2}$$

Graphical representation of of the measurement results for different test conditions is given in Figure 4. At the same time, a dependence was established between the efficiency of the transmission and the output torque.

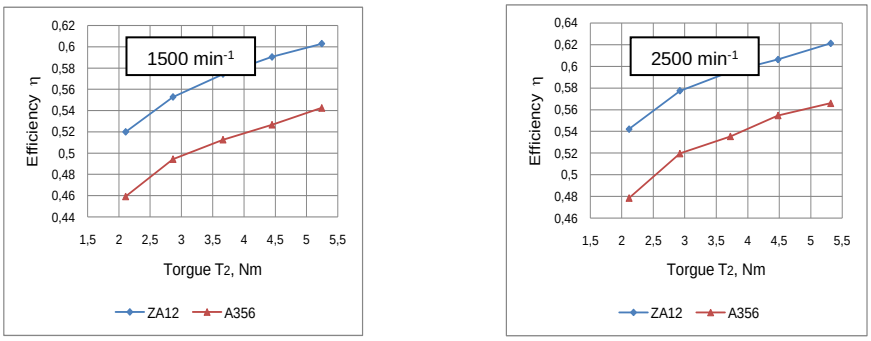

Figure 4. *Values of gear efficiency for different worm gear materials*

From the diagram, it can be observed that the values of the efficiency of the worm gearbox increase with the increase of the output torque as well as at higher rotational speed (circumferential speeds of the gears). Namely, at low circumferential speeds and relatively high specific pressures on the flanks of the teeth, borderline to mixed lubrication is achieved. However, with an increase in circumferential speed, an oil film forms more easily between the meshing gear teeth, which creates the conditions for hydrodynamic lubrication, which results in higher values of efficiency. This course of change in the efficiency is noticeable in both worm gear pairs. By comparing the measured results, it can be observed that the values of efficiency of the worm gearbox with gear pair 42CrMo4/ZA12 range between 0.51-0.62. Depending on the working conditions, these values are higher between 9% and 13% compared to the gear pair 42CrMo4/A356 where the efficiency ranges from 0.45-0.57.

3.2.2 Power losses

The calculation of power losses in the worm gear was performed according to the defined test conditions for both experimental worm gear pairs. First, power losses *in* bearings P_{GL} and shaft seals P_{GD} were determined according to the mathematical calculation of the bearing manufacturer SKF [17]. The calculation of these losses was made depending on the load of the worm gear pair, the input rotational speed and the viscosity of the oil at operating temperatures.

The power losses in the gear mesh are determined based on the experimentally obtained values of the efficiency of the worm gearbox and the power losses in the bearings and shaft seals according to the following expression:

$$P_{GZ} = P_1 \cdot (1-\eta) - P_{GL} - P_{GD} \tag{3}$$

The results of the calculation of power losses in gear mesh for different materials of worm gear pairs and different working conditions are shown in Figure 5.

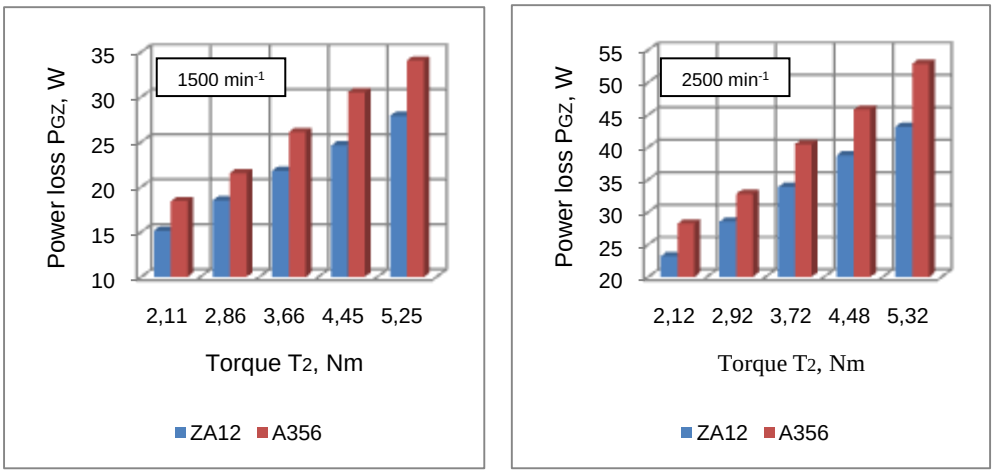

Figure 5. *Effect of materials on power losses in gear mesh for different operating conditions*

Based on the diagram, it can be concluded that the power losses in the gear mesh increase with the increase in load and rotational speed. At higher loads, the operating temperature rises, which leads to a reduction in the oil film and greater power losses. On the other hand, with the increase in circumferential speed, the total transmitted power of the worm gearbox also increases, with a reduction in the load on the worm gear pair and easier formation of an oil film. The lowest power losses occur in the 42CrMo4/ZA12 worm gear mesh and range from 15-43 W. Looking at different load levels and gear circumferential speeds, these losses are lower between 16% and 24% compared to the 42CrMo4/ZA12 worm pair. A356. A greater difference in power losses is noticeable at higher torque outputs and higher rotational speed.

Based on the calculated values of power losses, the efficiency of the worm gear pair η_z can be determined, which represents the ratio of the output P_{2Z} and the input power P_{1Z} of the worm gearbox, that is:

$$\eta_z = \frac{P_{2Z}}{P_{1Z}} \tag{4}$$

The input power of the worm gear pair P_{1Z} is obtained when the power of the electric motor P_1 is reduced by the power losses in the bearings P_{GLA} and P_{GLB} and the shaft seals P_{GDI} [18]:

$$P_{1Z} = P_1 - P_{GLA} - P_{GLB} - P_{GDI} \tag{5}$$

The output power of the worm gear pair P_{2Z} is the power transmitted to the worm gear shaft. It is obtained when the useful power on the output shaft P_2 is increased by the losses in the bearings P_{GLC} and P_{GLD} and the seals of the worm gear shaft P_{GDII} [18]:

$$P_{2Z} = P_1 - P_{GLC} + P_{GLD} + P_{GDII} \tag{6}$$

The values of the worm gear pair efficiency are determined according to expression 4 for experimental operating conditions. These values ranged from 0.55-0.65 for a worm gear pair with a worm gear made of ZA12 alloy and within 0.49-0.58 for a worm gear pair with a worm gear made of A356 alloy.

4 CONCLUSIONS

Through a comprehensive analysis of the experimental results, it can be concluded that the values of the efficiency increase with the increase of the load and the circumferential speed of the gears. The material of the meshed gears, operating temperature, power losses and the amount of friction in the contact zone of the gear teeth, as well as power losses in the bearings and shaft seals, have a significant influence on this course of change.

The type of material of the meshed gears has the greatest influence on the efficiency. Taking into account different operating conditions, the worm gearbox efficiency ranged between 0.51-0.62 for the worm gear pair 42CrMo4/ZA12 and between 0.45-0.57 for the worm gear pair 42CrMo4/A356. Depending on the load level and circumferential speeds of the gears, the values of the efficiency of the worm gearbox with the worm gear pair 42CrMo4/ZA12 are higher between 9% and 13% compared to the previous worm gear pair. As a result of the higher efficiency, power losses in the gear mesh of the 42CrMo4/ZA12 worm gear pair are lower between 16% and 24%, while the friction coefficient values are lower between 25% and 34% compared to the 42CrMo4/A356 worm gear pair.

Therefore, it is evident that a worm gear pair with a worm gear made of ZA12 alloy has better tribological characteristics and a better ability to maintain an oil film between the meshed gear teeth compared to a worm gear pair with a worm gear made of A356 alloy, which gives a recommendation for the use of this alloy for the manufacture of worm gears.

REFERENCES

[1] Dudás, I. (2005). *The theory and practice of worm gear drives*. Penton Press, London.
[2] Magyar B, Sauer B. (2014). Calculation of the efficiency of worm gear drives. International Gear Conference, 26th–28th August, Lyon, p.p.15–23.
[3] Michaelis, K., Höhn, B. R., & Hinterstoißer, M. (2011). Influence factors on gearbox power loss. *Industrial lubrication and tribology*. 63/1, p.p. 46–55.
[4] Skulić, A., Krsmanović, D., Radosavljević, S., Ivanović, L., Stojanović, B. (2017). Power losses of worm gear pairs. *Acta Technica Corvininesis-Bulletin of Engineering*, 10/3, p.p. 39-45.
[5] Sabiniak, H. G. (2017). Testing worm gears with cooperating elements made of different materials. *Proceedings of the Institution of Mechanical Engineers, Part J: Journal of Engineering Tribology*, 231/3, p.p. 341-346.
[6] Nikolić V. (2004). *Mašinski elementi*, Mašinski fakultet u Kragujevcu, Kragujevac.
[7] Radzevich, S. P. (2016). *Dudley's handbook of practical gear design and manufacture*. CRC press.
[8] Kim, S. H., Shin, M. C., Byun, J. W., & Chu, C. N. (2012). Efficiency prediction of worm gear with plastic worm wheel. *International Journal of Precision Engineering and Manufacturing*, 13/2, p.p. 167-174.

[9] Fontanari, V., Benedetti, M., Straffelini, G., Girardi, C., & Giordanino, L. (2013). Tribological behavior of the bronze–steel pair for worm gearing. *Wear*, 302/1, p.p. 1520-1527.
[10] Fontanari, V., Benedetti, M., Girardi, C., & Giordanino, L. (2016). Investigation of the lubricated wear behavior of ductile cast iron and quenched and tempered alloy steel for possible use in worm gearing, *Wear*, 350, p.p. 68-73.
[11] DIN 3996: Tragfähigkeitsberechnung von ZylinderSchneckengetrieben mit sich rechtwinklig kreuzenden Achsen, September, 9/2012.
[12] Höhn, B. R., Michaelis, K., & Hinterstoißer, M. (2009). Optimization of gearbox efficiency. *Goriva i maziva*, 48/4, p.p. 462.
[13] Paschold, C., Sedlmair, M., Lohner, T., & Stahl, K. (2020). Efficiency and heat balance calculation of worm gears. *Forschung im Ingenieurwesen*, 84/2, p.p.115-125.
[14] Fernandes, C. M., Marques, P. M., Martins, R. C., & Seabra, J. H. (2015). Gearbox power loss. Part I: Losses in rolling bearings. *Tribology International*, 88, p.p. 298-308.
[15] Fernandes, C. M., Marques, P. M., Martins, R. C., & Seabra, J. H. (2015). Gearbox power loss. Part II: Friction losses in gears. *Tribology International*, 88, p.p. 309-316.
[16] Monz, A. (2012). *Tragfähigkeit und Wirkungsgrad von Schneckengetrieben bei Schmierung mit konsistenten Getriebefetten*, Doctoral dissertation, Technische Universität München.
[17] SKF. (2014). Hauptkatalog, Das Wälzlager-Handbuch für Studenten Neuwertig, Januar
[18] Miltenović, Đ. (2017). *Istraživanje termičke stabilnosti i habanja pužnih prenosnika*. Doktorska disertacija. Univerzitet u Banjoj Luci, Mašinski fakultet.

COMETa 2022
6th INTERNATIONAL SCIENTIFIC CONFERENCE
17th - 19th November 2022
Jahorina, B&H, Republic of Srpska
University of East Sarajevo
Faculty of Mechanical Engineering
Conference on Mechanical Engineering Technologies and Applications

ANALYSIS OF GEAR RATIOS OF TWO DIFFERENT TYPES OF CYCLOID DRIVE TRAIN

Milan Tica[1], Tihomir Mačkić[2], Nenad Marjanović[3], Sanjin Troha[4], Miroslav Milutinovic[5],

Abstract: The cyclo drive train is a special variant of the planetary drive train, where the planets are gears with a cycloid profile, while rollers are placed on the central gears (wheels). An analysis of the gear ratios of two types of cycloid drive train was performed. The first type is a classic cycloid drive train, while the second is a special variant with stepped planets. The cycloid drive with stepped planets can achieve very large gear ratios, while using central gears with a relatively small number of rollers.

Key words: Cycloid drive train, Gear ratio, Stepped planets

1 INTRODUCTION

The cycloid drive trains or drive train with cycloid profile gears can achieve high gear ratio in single stage and have many advantages, as compactness and simplicity of production. They are mainly planetary drive trains, which are used today as speed reducers with classic cycloid gear (figure 1a). Also, it is possible to use the special cycloid stepped gears (figure 1b), which enables a reduction in the volume of the drive train and a smaller number of rollers.

Due to the complicated and costly construction, the use of drive train with cycloid gears was avoided in the past. With the development of the modern CNC machining centers, it is possible to make the production process of these gears cheaper and simpler. Because of very wide area of application, production of cycloid drives has growing character and wide area of application: processing equipment, conveyors, presses, mixers, food industry, robots, automotive plants, spinning

[1] Phd, Milan Tica, Faculty of Mechanical Engineering, University of Banja Luka, Banja Luka, Bosnia and Herzegovina, milan.tica@mf.unibl.org (CA)
[2] MSc, Tihomir Mačkić, Faculty of Mechanical Engineering, University of Banja Luka, Banja Luka, Bosnia and Herzegovina, tihomir.mackic@mf.unibl.org
[3] Phd, Nenad Marjanović, Faculty of Engineering, Kragujevac, Serbia, nesam@kg.ac.rs
[4] Phd, Sanjin Troha, Faculty of Engineering, University of Rijeka, Rijeka, Croatia, sanjin.troha@riteh.hr
[5] Phd, Miroslav Milutinović, Faculty of Mechanical Engineering, University of East Sarajevo, East Sarajevo, Bosnia and Herzegovina, miroslav.milutinovic@ues.rs.ba

machines, cranes, etc.

(a) (b)

Figure 1. *Classic cycloid gear (a), Stepped cycloid gear (b)*

2 CYCLOID DRIVE TRAIN WITH TWO DEGREES OF FREEDOM (DOF)

In the analysis of a simple cycloid drive, it can be started from an elementary planetary mechanism with internal coupling, replacing, for example, classic involute gears with cycloid gears (figure 2a). Members of the planetary mechanism whose axis coincides with the central axis and receive the external torques are called the basic members [1].

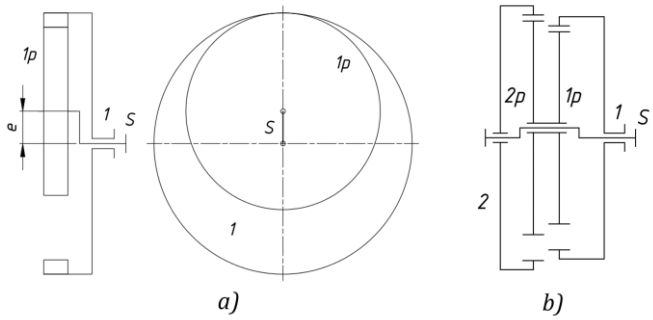

Figure 2. *Transformation of elementary mechanism to simple cycloid drive train*

The members of the elementary mechanism, the central gear (1) and the carrier (S), whose axes of rotation coincide with the base axis, can't be used in this case for the transfer of energy. This can be accomplished by adding another central gear or wheel (2) with the pins placed on the periphery, which meshes with the second cycloid gear (2p) (figure 1.b). The cycloid gears (1p) and (2p) are tightly connected in this case. This gives a simple cycloid drive or three-shaft cycloid drive with two DOF or *three-shaft cycloid drive train*. In literature, such coupled planetary gears (figure 2b) are called *stepped planets* [2, 3].

2.1 Gear ratio of three-shaft cycloid drive train

When denoting the gear ratios, it is necessary to make a difference when

denoting the gear ratios of three-shaft cycloid drive with two DOF from two-shaft cycloid drive with one DOF. Therefore, in this study, will be used proposal [4], that the symbol "*i*" means only a constant, design dependent gear ratios (with one DOF).

The orders of two subscripts denote the order of input and output members. For the gear ratios of simple cycloid drive train with two DOF, will be used the symbol "*k*", so that, for example,

$$k_o = k_{12} = \frac{n_1}{n_2} = \frac{1}{k_{21}}, \tag{1}$$

represents the gear ratio between shafts 1 and 2.

It is possible to derive the equations for all gear ratios of simple cycloid drive with stepped gear (Table 1).

Table 1. *Equations of gear ratios of three-shaft cycloid drive train*

Reduced notation	Gear ratio $f(k_o)$
$k_{12} = i_o + (1 - i_o) k_{s2}$	$k_{12} = k_o$
$k_{21} = \frac{1}{i_o} + \left(1 - \frac{1}{i_o}\right) k_{s1}$	$k_{21} = \frac{1}{k_o}$
$k_{1S} = (1 - i_o) + i_o k_{2S}$	$k_{1S} = \frac{1 - i_o}{1 - \frac{i_o}{k_o}}$
$k_{S1} = \frac{1 - i_o k_{21}}{1 - i_o}$	$k_{S1} = \frac{1 - \frac{i_o}{k_o}}{1 - i_o}$
$k_{2S} = \frac{k_{1S} - (1 - i_o)}{i_o}$	$k_{2S} = \frac{1 - i_o}{k_o - i_o}$
$k_{S2} = \frac{k_{12} - i_o}{1 - i_o}$	$k_{S2} = \frac{k_o - i_o}{1 - i_o}$

3 GEAR RATIO OF TWO-SHAFT CYCLOID DRIVE TRAIN

It will be analyzed only drives with the numbers of pins of ring gear by one greater than the numbers of teeth of cycloid planet gear. The gear drives shown in figure 2b have two degrees of freedom (DOF). By blocking one of the basic members, a *two-shaft cycloid drive* is provided, which has only one DOF.

The cycloid drive works as classical gearbox (with a fixed and not rotating shafts) when the eccentric shaft is stopped. This simple working mode can be termed as the basic mode whereby the *basic gear ratio* is realized:

$$i_o = \left(\frac{n_1}{n_2}\right)_{n_S = 0}, \tag{2}$$

where is: n_1- speed of ring gear shaft *1*,
n_2- speed of ring gear shaft *2*,
n_S- speed of eccentric shaft *S*.

The complex general state of motion of a simple cycloid drive can be explained as the superposition of two partial motions. The first partial motion is the rotation of central ring rear (turning and meshing with planets), relative to the carrier. The second partial motion is an equal rotation of all shafts of basic members and it is same as rotation of carrier (eccentric shaft S).

If the two partial motions are superimposed, the total speed of each shaft is obtained as the sum of its partial speed and the basic gear ratio become [5]:

$$i_{12} = i_o = \frac{n_1'}{n_2'} = \frac{n_1 - n_S}{n_2 - n_S}, \qquad \text{so that}$$

$$n_1 - i_o n_2 + (i_o - 1) n_S = 0. \tag{3}$$

From the equation (3), the shaft speed of a simple cycloid drive is obtained as follows:

$$\begin{aligned} n_1 &= i_o n_2 + (1 - i_o) n_S, \\ n_2 &= \frac{n_1 - n_S(1 - i_o)}{i_o}, \\ n_S &= \frac{n_1 - i_o n_S}{(1 - i_o)}. \end{aligned} \tag{4}$$

If the numbers of rollers of central gear by one greater than the numbers of teeth of cycloid planet gear, then the basic gear ratio of stepped gear cycloid drive is [6]:

$$i_o = i_{11p} i_{2p2} = \frac{n_1}{n_{1p}} \frac{n_{2p}}{n_2} = \frac{n_1}{n_2} = \frac{z_{1p}}{z_1} \frac{z_2}{z_{2p}} = \frac{z_2(z_1 - 1)}{z_1(z_2 - 1)}, \tag{5}$$

where is: $n_{1p} = n_{2p}$ – speed of stepped planets,
z_{1p} - the number of teeth on a cycloid gear *1*,
z_{2p} - the number of teeth on a cycloid gear *2*,
z_1 - the number of rollers on a wheel *1*,
z_2 - the number of rollers on a wheel *2*,
i_{11p} - gear ratio between wheel *1* and cycloid gear *1*,
i_{2p2} - gear ratio between cycloid gear *2* and wheel *2*.

Similar to previous, basic gear ratio of classic cycloid drive is:

$$i_o = i_{1p} i_{p2} = \frac{n_1}{n_2} = \frac{z_1 - 1}{z_1}, \tag{6}$$

where is: z_1 - the number of rollers on a wheel *1*,
i_{1p} - gear ratio between wheel *1* and cycloid gear,
$i_{p2} = 1$ - gear ratio between cycloid gear and wheel (disc) *2*.

The gear ratios of the tree possible options of two-shaft cycloid drive can be obtained using equations from Table 1, by setting appropriate gear ratio equal to zero if shaft was stopped (Table 2).

Table 2. *Gear ratios of two variants of cycloid drive*

Working mode	Gear ratio of stepped cycloid drive train *f*(z_1, z_2)	Gear ratio of classic cycloid drive train *f*(z_1)
Minimum increase	$i_{12} = \frac{z_2(z_1 - 1)}{z_1(z_2 - 1)}$	$i_{12} = \frac{z_1 - 1}{z_1}$
Minimum reduction	$i_{21} = \frac{z_1(z_2 - 1)}{z_2(z_1 - 1)}$	$i_{21} = \frac{z_1}{z_1 - 1}$
Maximum increase	$i_{1S} = \frac{z_2 - z_1}{z_1(z_2 - 1)}$	$i_{1S} = \frac{1}{z_1}$
Maximum reduction	$i_{S1} = \frac{z_1(z_2 - 1)}{z_2 - z_1}$	$i_{S1} = z_1$
Reversible increase	$i_{2S} = \frac{z_1 - z_2}{z_2(z_1 - 1)}$	$i_{2S} = \frac{1}{1 - z_1}$
Reversible reduction	$i_{S2} = \frac{z_2(z_1 - 1)}{z_1 - z_2}$	$i_{S2} = 1 - z_1$

Cycloid drive train is mainly used as speed reducers. In order to understand the nature of the change in gear ratios, the theoretical models of a classical cycloid drive and cycloid drive with stepped planets will be considered. It is obvious, from table 2, that if the number of rollers $z_1 = z_2$, there is a self-locking of the cycloid drive train with stepped planets. The variant with stepped planets is not used in practice for now, so it is very interesting to examine its possibilities.

Figure 3 shows the changing in gear ratios for maximum reduction (i_{S1}) and reversible reduction mode (i_{S2}). Number of rollers of wheel *1* is one less than the number of rollers wheel *2* are changing. This ratio of the number of rollers is mostly used with classic ones, while it can be different on cycloid drive with stepped planets. It is obvious that the classic cycloid drive can achieve a much smaller gear ratio compared to the cycloid drive with stepped planets, with the same number of rollers on wheel *1*. This enables the production of gear drive with smaller dimensions and a large gear ratio.

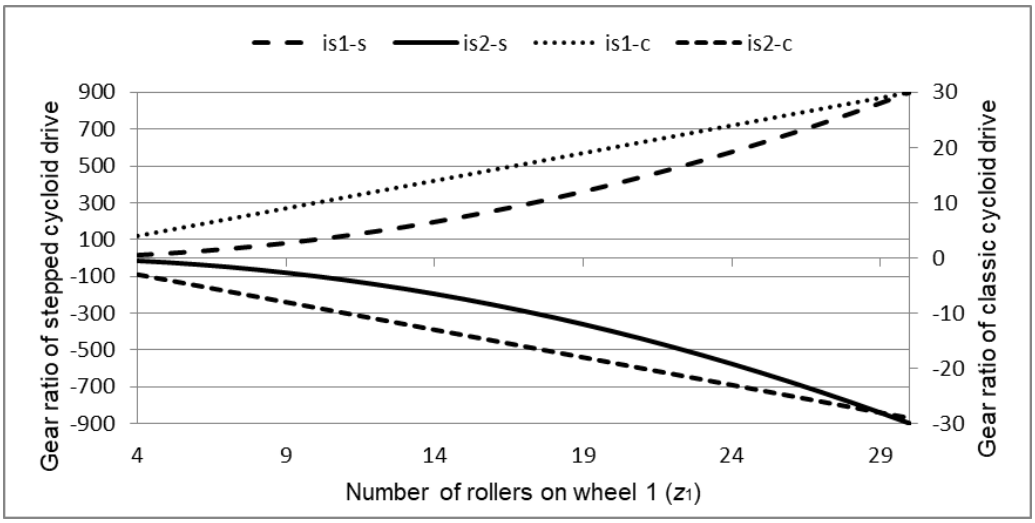

Figure 3. *Gear ratios of reduction working modes*

4 CONCLUSION

The cycloid drive with stepped planets can achieve very large gear ratios, while using ring gears (wheels) with a relatively small number of rollers. This makes it possible to design high gear ratio drive trains with small dimension.

In future research, it is necessary to analyze the efficiency of these drive trains and find the conditions under which self-locking occurs.

LITERATURA

[1] Tanasijević, S., Vulić, A., „Mehanički prenosnici“, Jugoslovensko društvo za tribologiju, Kragujevac,1994.
[2] Looman, J., Zahnradgetriebe: Grundlagen, Konstruktion, Anwendung in Fahrzeugen; Berlin: Springer-Verlag (1996).
[3] Müller, H. W, Die Umlaufgetriebe; Berlin: Spinger-Verlag (2001).
[4] Wolf, A.: Die Umlaufgetriebe und ihre Berechnung; VDI-Z. (91/22); pp. 597–603 (1949).
[5] Willis, R, Principles of Mechanism. London: Parker 1841.
[6] Mačkić, T., Tica, M., Šuba, R.,: Transmission characteristics of simple cycloid drive with stepped planets. IOP Conference Series Materials Science and Engineering 659 (2019) 012071.

COMETa 2022
6th INTERNATIONAL SCIENTIFIC CONFERENCE
17th - 19th November 2022
Jahorina, B&H, Republic of Srpska
University of East Sarajevo
Faculty of Mechanical Engineering
Conference on Mechanical Engineering Technologies and Applications

STRUCTURAL INTEGRITY ASSESSMENT OF THICK-WALLED PRESSURE VESSEL

Nedeljko Vukojević[1], Amna Bajtarević-Jeleč[2]

Abstract: In this paper the condition and structural behavior of a vertical thick-walled pressure vessel (high-pressure vessel) is analyzed. The construction of the vessel includes four cantilevered support legs that support the vessel. The support legs were welded to the outer panels. In order to determine defects in welds, non-destructive tests were carried out. High values of residual stresses in the welded zone were measured using hole-drilling method. Structural behaviour of structure with fractures was analyzed using the finite element analysis. ANSYS Mechanical software was used for numerical analysis. The structural integrity assessment for different positions and dimensions of the fracture was carried out using analytical methods.

Key words: pressure vessels, fracture, residual stresses, fracture mechanics, structural integrity

1 INTRODUCTION

The structures used very often in industry, should be completely defined especially in the aspect of safety. One of the most responsible mechanical structures are pressure vessels, which are used as accumulation stations, reactors, hydraulic and pneumatic cylinders as defined by the standard [1]. On the other hand, safety assessment of pressure vessels could not be completely based on strictly standard defined requirements and technical regulations. For integrity assessment of such structures, it is necessary to apply a more detailed procedure that includes a global and local approach. The global approach refers to material strength, so safety of structure is analyzed based on permissible stresses. On the other hand, in order to achieve better picture of condition and operational safety of pressure vessel, it is necessary to take into account the manufacturing technology, operational conditions, as well as the presence of fractures in the structure [2].

[1]Full professor, Nedeljko Vukojević, Faculty of Mechanical engineering, Zenica, B&H, nedeljko.vukojevic@unze.ba
[2] MA, Amna Bajtarević-Jeleč, Faculty of Mechanical engineering, Zenica, B&H, amna.bajtarevic@unze.ba

The structure integrity assessment of structures with fractures can be carried out using two-parameter methods in which two possible limiting cases are taken into account during the calculation, i.e. plastic collapse and completely brittle fracture. In paper [3], two-parameter methodology - SINTAP was applied for integrity assessment of seamless steel pipe with fractures.

In this paper, a structural integrity analysis of a thick-walled pressure vessel that used in exploitation, in presence of known fractures was performed. Structural integrity was carried out using the SINTAP method from the aspect of operating stresses.

2 TECHNICAL DESCRIPTION OF THE CONDUCTED RESEARCH

2.1 Description of pressure vessel

The subject of this paper is structural integrity analysis of thick-walled pressure vessel used in exploitation. The model of vessel is shown in Figure 1. The vessel is thick-walled, vertical and supported by four cantilever legs welded to the structure. In the HAZ of welded joints on the external vessel surface, fractures were detected. Non-destructive methods were used to determine the real dimensions and orientation of the fractures. Also, residual stresses were measured with strain gauges. High values of residual stresses were determined, arising as a result of welding [4]. The material of vessel is isotropic, austenitic steel 40Mn6 whose mechanical characteristics were determined by experimental tests and defined in Table 1. The working pressure of the vessel during exploitation is 350 bar.

Table 1. *Mechanical characteristics of material 40Mn6*

Yield strength R_{eH} [MPa]	*319*
Tensile strength R_m [MPa]	*591*
Modulus of elasticity E [GPa]	*205*
Fracture toughness K_{IC} [MPa$\sqrt{m}$]	*80*

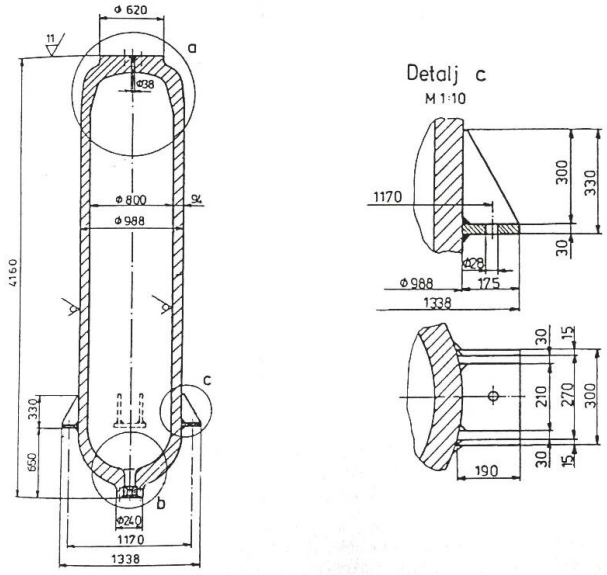

Figure 1. *Technical drawing of the observed pressure vessel*

2.2 Characteristics of detected fractures

In order to determine dimensions and orientation of fractures at external surface of vessel, non-destructive methods are used. The fractures were caused by residual stresses in the heat affected zone of weldments. Figure 2a shows the positions of detected fractures, and figure 2b shows their dimensions.

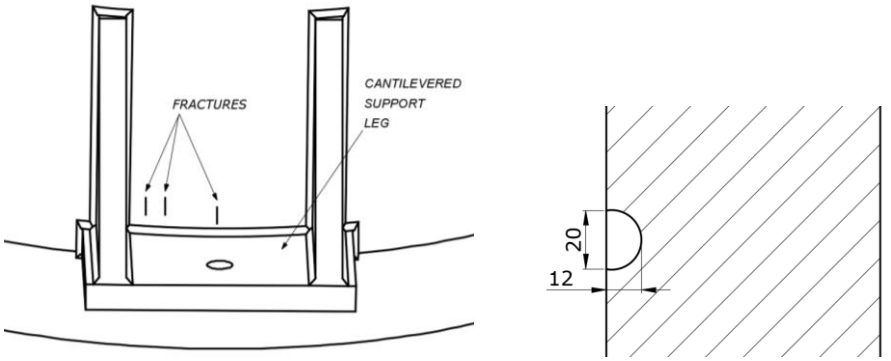

Figure 2. *Locations of fractures on the vessel (a), Dimensions of fractures (b)*

All detected fractures are semi-elliptical shape, same dimensions, longitudinally oriented, on the external surface of pressure vessel.

3 NUMERICAL ANALYSIS

3.1 Numerical stress calculation

In order to determine intensity and distribution of stress and as well as stress concentration locations inside the observed pressure vessel, a numerical calculation was carried using element method in the software ANSYS Mechanical. Considering that vessel is supported on cantilever supports, boundary conditions were introduced in form of displacements in vertical direction. According to stress analytical calculation inside thick-walled pressure vessel [1], the value of the main circumferential stress on cylindrical part of the vessel is 133.27 MPa. Figure 3 shows the result of numerical calculated circumferential stress in presence of working pressure. Considering numerical and analytical values of stress are the same, defined boundary conditions for numerical analysis are verified.

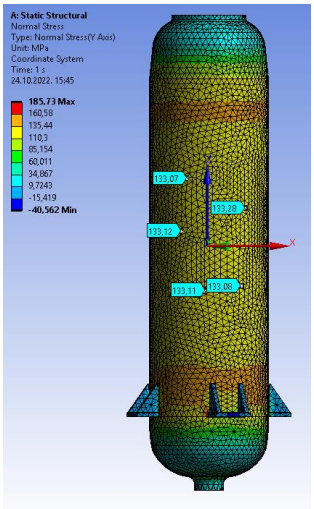

Figure 3. *Distribution of circumferential stresses inside the vessel*

Considering that stress distribution in the area of weldments is important for further analysis, a numerical analysis was performed on the submodel, where denser FE mesh was applied. Figure 4 shows numerical calculation result of circumferential stresses around the welded feet. In this way, the areas with the highest stress concentration are defined, which represent critical places from the aspect of structural integrity.

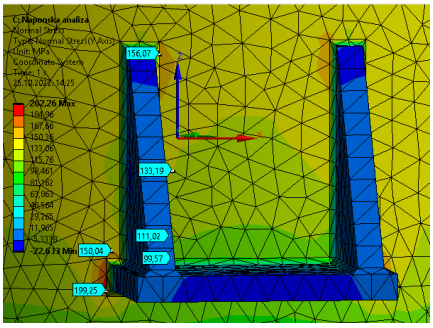

Figure 4. *Distribution of circumferential stresses in the weld area of cantilever feet*

3.2 Definition of fractures

In order to check the integrity of vessel, a numerical calculation of the stress intensity factor was carried out. Fractures were observed in different positions near the welds of cantilever feet, on the external surface of the vessel. Fractures are simulated based on real detected fractures. Also, additional fractures are simulated at locations of stress concentration. Geometric parameters of the fractures as well as their arrangement inside the vessel are shown in figure 5a and 5b, respectively.

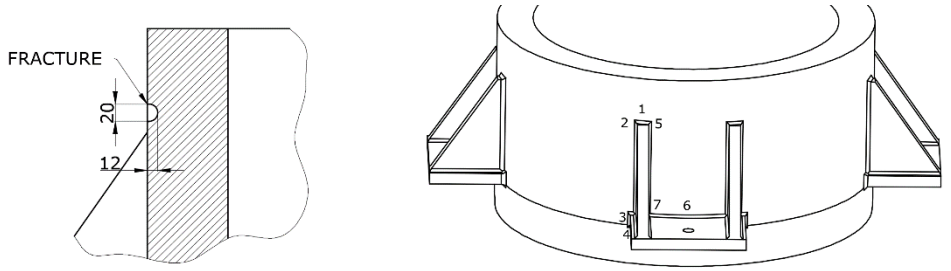

(a) (b)

Figure 5. *Geometric parameters of the fracture (a), Locations of the fractures on the observed part of the vessel (b)*

3.3 Numerical calculation of stress intensity factor

Calculation of the required values of stress intensity factor of fracture for first fracture mode (K_I) was carried out numerically using commercial software Ansys Mechanical 2021. Table 1 presents the values of calculated circumferential stress and intensity factor for the observed positions of fractures shown in Figure 3b.

Table 1. *Results of the numerical calculation of the fracture stress intensity factor (K_I)*

Fracture position	*1*	*2*	*3*	*4*	*5*	*6*	*7*
Circumferential stress intensity [MPa]	*132.36*	*143.83*	*180.0*	*107.62*	*139.9*	*106.35*	*111.02*
K_I [MPa√m]	*19.8*	*21.6*	*24.5*	*17.8*	*21.3*	*16.1*	*17*

4 STRUCTURAL INTEGRITY ASSESSMENT

In order to assess the structural integrity of pressure vessel, the SINTAP methodology was applied [5].

4.1 Defining of yield parameter, L_r

The yield parameter L_r, according to the SINTAP procedure, is defined as the ratio between the applied pressure and the limit value. As part of the calculation, working pressure of the vessel in exploitation in amount of 350 bar was applied. Limiting pressure values are determined according to the expression [6]:

$$p_y = \sigma_y \cdot \frac{t}{r_i} \cdot \frac{1 - \frac{t}{a}}{1 - \frac{a}{M \cdot t}} \tag{1}$$

Where:

- c –semi-axis of the fracture
- t – vessel wall thickness
- r_i – inner radius of the vessel
- r_e – external radius of the vessel

- M – an auxiliary quantity determined by the expression:

$$M = \sqrt{1 + 1.61 \cdot \frac{c^2}{r_e \cdot t} - 0.0135 \cdot \frac{c^4}{{r_e}^2 \cdot t^2}} \tag{2}$$

The limit value of pressure according to expressions (1) and (2) is p_y=74.71 MPa for a fracture with dimensions according to Figure 3a, at external surface of vessel. Therefore, the value of the yield parameter is:

$$L_r = \frac{p}{p_y} = \frac{35}{74.74} = 0.468 \tag{3}$$

4.2 Defining the failure line f(Lr)

To define the fracture line, the basic level was used in this paper. Tensile strength, yield strength and fracture toughness were adopted from [4]. Expressions were used to define the fracture line according to [5]:

$$f(L_r) = \left[1 + \frac{1}{2} \cdot L_r^2\right]^{-\frac{1}{2}} \cdot \left[0{,}3 + 0{,}7 \cdot e^{-\mu L_r^6}\right] \quad za\ 0 \le L_r \le 1 \tag{4}$$

Where:

$$\mu = min \begin{cases} 0{,}001 \cdot \dfrac{E}{R_{p0,2}} \\ 0{,}6 \end{cases} \tag{5}$$

$$f(L_r) = f(1) \cdot L_r^{\frac{N-1}{2N}} \qquad za\ 1 \le L_r \le L_r^{max} \tag{6}$$

Where:

$$N = 0{,}3 \cdot \left[1 - \frac{R_{p0,2}}{R_m}\right] \tag{7}$$

$$L_r^{max} = \frac{1}{2} \cdot \left[\frac{R_{p0,2} + R_m}{R_{p0,2}}\right] \tag{8}$$

4.3 Defining the parameter K_r

The K_r parameter according to [5] represents the ratio of fracture stress intensity factor and fracture toughness of the material. Table 2 presents the values of parameter K_r for the observed positions of the fractures according to Figure 3b.

Table 2. *Values of the K_r parameter for the observed fracture positions*

Fracture position	*1*	*2*	*3*	*4*	*5*	*6*	*7*
K_r	*0.23294*	*0.25412*	*0.28824*	*0.20941*	*0.25059*	*0.18941*	*0.2000*

4.4 Failure Assessment Diagram

Based on all determined values, a Failure Assessment Diagram (FAD) was created. Figure 4 shows the FAD diagram for the observed fracture positions.

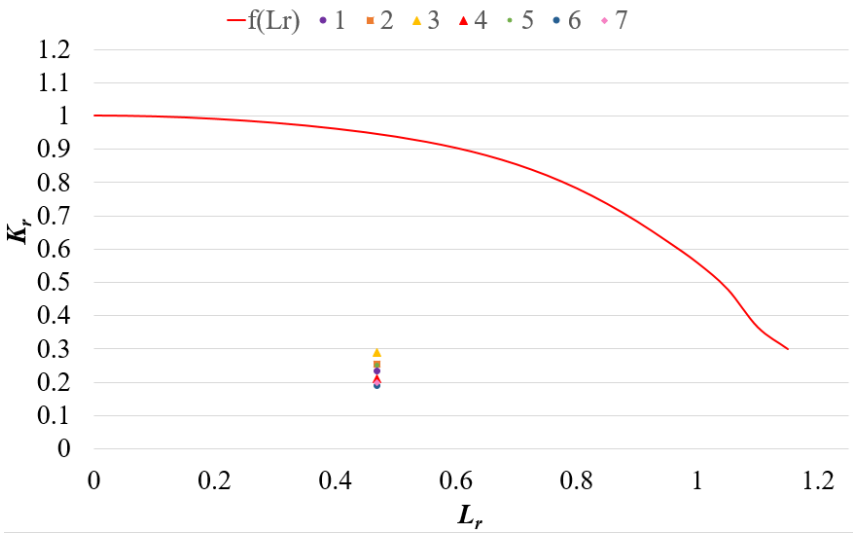

Figure 6. *FAD diagram for observed fracture positions*

As shown in Figure 6, all observed points are located below the FAD curve. Therefore, it can be concluded that no fracture position is potentially unsafe for the construction, from the aspect of working stresses. The position of the fracture that is closest to the FAD curve is position 3. This position of the observed point on the FAD curve is expected considering that highest stress concentration determined in this area.

5 CONCLUSIONS

The structural integrity analysis of the thick-walled pressure vessel in presence of fractures was performed using numerical and analytical methods. The stress intensity factors of the fracture were determined by numerical calculation, using the finite element method by ANSYS Mechanical. Analytical calculation, in accordance with the SINTAP methodology, was used to calculate the limit pressure value, and then create a FAD diagram in order to check whether the fractures at the observed positions are potentially unsafe for the structure. A total of three fractures in the longitudinal direction with the same dimensional characteristics were detected by non-destructive methods (Figure 2a). Structural integrity was observed through a total of seven fractures, whereby, for the purpose of analysis, all potentially critical positions of the fracture were observed, i.e. locations of stress concentration (Figure 5b).

Considering that the depth of the fracture compared to the thickness of the vessel wall is significantly smaller, i.e. a/t=0.127, it is expected that a fracture of this dimension will not significantly threaten the integrity of the structure in any position, which is proven by the FAD diagram (Figure 6). It is important to know that the complete analysis was carried out from the aspect of working stress, while residual stresses that arise as a result of welding were not considered. The subject of further research can be a SINTAP analysis of the observed structure from the aspect of operating and secondary stresses, whereby the secondary stresses represent the measured residual stresses.

REFERENCES

[1] BS EN 13445-3:2021 - Specifying requirements for the design, construction, inspection and testing of unfired pressure vessels made from steels and steel castings as well as additional materials such as cast iron, aluminium and nickel, 2021.

[2] B. Rose, S. Anil. (2020) Design of Metallic Pressure Vessels - A Fracture Mechanics based Approach, International Research Journal of Engineering and Technology (IRJET), vol 07.

[3] A. Bajtarević-Jeleč, M. Manjgo, N. Vukojević, F. Hadžikadunić, J. Kačmarčik. (2022) Seamless steel pipe integrity assessment based on SINTAP procedure and numerical analysis, *10th International scientific and expert conference*, Slavonski Brod.

[4] Vukojević, N. (2006). *Prilog procjeni integriteta i ponašanja debelostjenih posuda velikih dimenzija pod pritiskom*, Doktorska disertacija, Mašinski fakultet, Zenica.

[5] U. Zerbst, M. Schodel, S. Webster, R. Ainsworth: Fitness for Service Fracture Assessment of Structures Containing Fractures, A Workbook based on the European SINTAP/FITNET Procedure, Elsevier, 2007.

[6] W. Brocks, H. Krafka, G. Kunecke and K. Wobst (1992). Stable fracture growth of axial flaws in pressure vessels, *Nuclear Engineering and Design 135*, p.p. 151-160.

COMETa 2022
6th INTERNATIONAL SCIENTIFIC CONFERENCE
17th - 19th November 2022
Jahorina, B&H, Republic of Srpska
University of East Sarajevo
Faculty of Mechanical Engineering
Conference on Mechanical Engineering Technologies and Applications

COMPARATIVE ANALYSIS OF LOAD CARRYING CAPACITY OF SHEAR-LOADED BOLTED JOINTS

Pavle Ljubojević[1], Ivan Simonović[2], Tatjana Lazović[3]

Abstract: The function of shear-loaded bolted joints is the prevention of joint members' slip. This can be achieved in two ways, depending on the construction, i.e. relative dimensions of bolts and holes in connected parts. There are two types of shear-loaded bolted joints, clamped (friction) and fitted bolted joints. In both cases, a connection between joint members is shear-loaded, but the bolts have different stress and strain states. In clamped bolted joints the actual load is tensile stress, while fitted bolts are loaded with shear and contact pressure. In this paper, a comparative analysis of the load capacity (safety factors) of clamped and fitted bolts, under the same geometrical and operational conditions was performed. The analysis showed multiple higher load-carrying capacity of fitted bolts that go up to 60 times(!).

Key words: clamped bolted joints, fitted bolted joints

1 INTRODUCTION

A machine system may consist of a greater or lesser number of components with different complexity and composition. The load carrying capacity of parts of different joint types is a crucial aspect of the evolution of machine construction. Bolted joints are one of the most commonly used joints. Due to a number of advantages, such as low manufacturing costs and simple assembly and disassembly, they are widely used in all industries, including the automotive, aerospace, civil, and boating sectors, among others [1]. As evidence of the significance of screw threads, the key element of bolted joints, the very first ISO technical committee was devoted to them. The fundamental classification of bolted joints is determined by the direction of the external load. Bolted joints are, based on that, divided into tensile joints and shear joints. For tensile joints, the load acts in the direction of the bolt's axes, opposite to shear joints,

[1] Assist. Pavle Ljubojević, University of Belgrade, Faculty of Mechanical Engineering, Belgrade, Serbia, pljubojevic@mas.bg.ac.rs
[2] Assist. Ivan Simonović, University of Belgrade, Faculty of Mechanical Engineering, Belgrade, Serbia, isimonovic@mas.bg.ac.rs
[3] Prof. dr Tatjana Lazović, University of Belgrade, Faculty of Mechanical Engineering, Belgrade, Serbia, tlazovic@mas.bg.ac.rs

where the load is perpendicular to the bolt's axis. The distinction between these two groups is substantial and not insignificant. The joint spot, as a discontinuity presents a place for creating high stress that can initiate failure [2]. They differ in how they respond to load, how they fail, how they are assembled and disassembled, as well as how they are calculated and manufactured. Some joints endure both shear and tensile loads, but they are referred to by the name of the prevailing load [3]. Even though bolted joints are simple in design, they must be extremely reliable when they are used. Their failure might result in the breakdown of the entire assembly or machine and result in significant harm. Failure can be caused by volumetric destruction of the threaded part of the screw thread, or by the nut or screw self-loosening. The calculation of bolted joints focuses on the selection of shape, material, dimensions, number of bolts, and their arrangement, which will be operationally reliable [4-6]. The load carrying capacity of shear-loaded bolted joints, as very important elements of complex machine assemblies and systems.

2 SHEAR-LOADED BOLTED JOINTS

The operating load of the shear-loaded bolted joints is perpendicular to the axis of the bolt. The primary objective of shear-loaded bolted joints is to avoid relative movement (sliding) and separation of joint members. The load of group shear loaded bolted joint can be force or torque (Figure1).

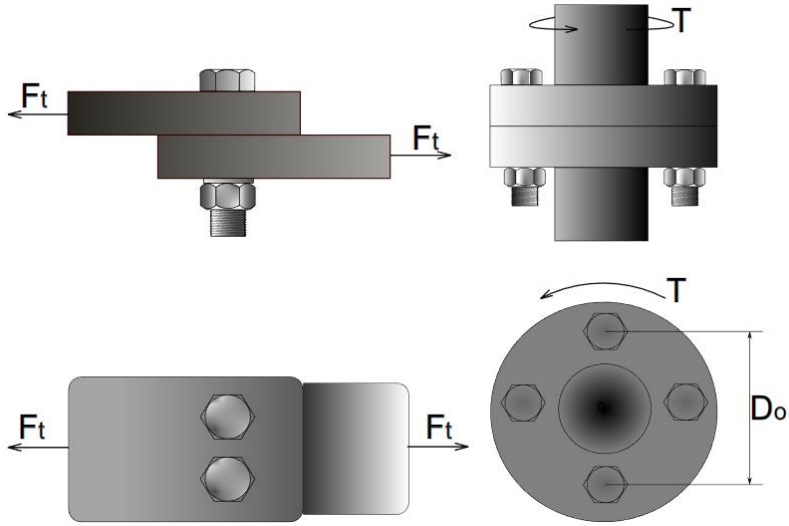

Figure 1. *Shear loaded bolted joints*

Two types of shear-loaded bolted joints exist. The first is a fitted (bearing type) bolted joint, whereas the second is a clamped (friction) bolted joint. With fitted bolted joints, the load is transferred from one area of the connection to another through the unthreaded part of the bolt body [4-6]. This kind of bolt behaves like a pin. In the case of clamped bolted joints, the relative movement of the joined components is prevented by the acting of frictional force of appropriate intensity, which is dependent on the tightening torque.

2.1 Fitted bolted joints

In a fitted bolt, the load, in the form of shear force and contact pressure, is transmitted through the unthreaded part of the bolt body (Figure 2a). To transfer the load straight over the bolt body, a transition fit must be formed. The suggested fits are H7/k6 and H7/n6 [5, 6]. A minor clearance may form between the member joint and the bolt, but the likelihood of this occurring is extremely low. If there is a clearance, the load distribution becomes inequal. This issue can be prevented by incorporating a 0.1 mm tolerance into the non-threaded part of the bolt body. The threaded part of bolt is non-load-carrying and with nut helps to prevent the separation of joint elements.

2.2 Clamped bolt joints

Unlike fitted bolted joints, where preload is not required, clamped bolted joints are provided with strictly calculated tightening torque values. This type of joint is realized with bolts whose nominal (major) thread diameter is smaller than the hole in the joint members (Figure 2b). The reduced accuracy of manufactured hole and bolt reduces the costs of making and assembling and makes this type of joint more economical. By tightening the bolt with precise tightening torque, the slipping resistance of joint members is created. Frictional force occurs between joint members due to clamping force caused by tightening torque. For clamped bolted joints to perform their function successfully, self-loosing must be prevented. In addition, the bolt must have the necessary volumetric strength.

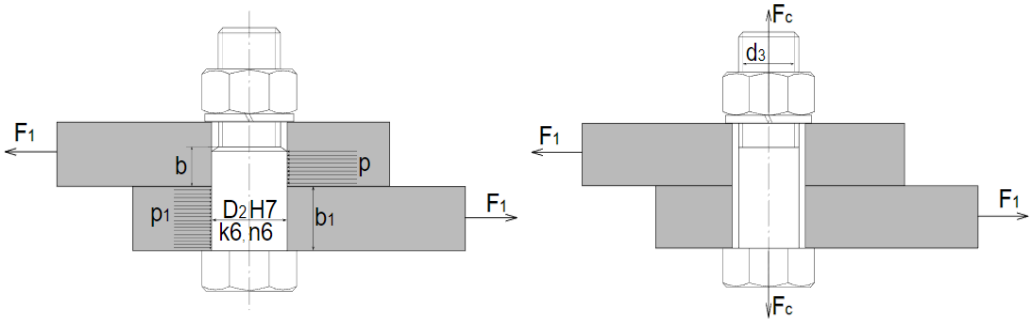

Figure 2. *a) Fitted bolted joint; b) Clamped bolted joint*

3 BOLTED JOINT LOAD CARRYING CAPACITY

Load carrying capacity of fitted bolted joints is limited by resistance to shear and contact pressure. Shear and contact pressure safety factors are given by expressions:

$$S_\tau = \frac{[\tau]}{\tau_s} = \frac{0.7R_e}{\frac{F_s}{A_s}} = \frac{0.7R_e D_2^2 \pi}{4\frac{F_t}{n}\xi_{ie}} = \frac{0.7R_e D_2^2 \pi n}{\frac{T}{D_o/2}\xi_{ie}} = \frac{0.7R_e D_2^2 \pi n D_o}{8T\xi_{ie}}, \quad (1)$$

$$S_p = \frac{[p]}{p} = \frac{1.2R_e}{\frac{F_p}{A_p}} = \frac{1.2R_e bD_2}{\frac{F_t}{n}\xi_{ie}} = \frac{1.2R_e bD_2 n}{\frac{T}{D_o/2}\xi_{ie}} = \frac{1.2R_e bD_2 nD_o}{2T\xi_{ie}}. \quad (2)$$

Since the number of bolts n, pitch diameter D_o, and torque T are constant, the ratio of equations (1) and (2) is:

$$\frac{S_p}{S_\tau} = \frac{4.8b}{0.7D_2\pi} = 2.1827\frac{b}{D_2}. \quad (3)$$

From the condition of equal volumetric and contact load carrying capacity of fitted bolts ($S_\tau = S_p$), based on equation (3), the length of contact between the bolt and joint member is $b = 0.4581D_2$. Hence, based on equation (3) it can be written as:

$$S_\tau = S_p = \frac{0.2749R_e D_2^2 nD_o}{T\xi_{ie}}. \quad (4)$$

Clamped bolted joints are loaded in the axial direction by the clamping force needed for the prevention of joint members' slip. Appropriate safety factor:

$$S_\sigma = \frac{[\sigma]}{\sigma} = \frac{R_e}{\frac{F_c}{A_{min}}} = \frac{R_e d_3^2\pi}{4\frac{F_1 S_\mu \xi_c}{\mu}} = \frac{R_e d_3^2\pi\mu}{4\frac{F_t S_\mu \xi_c}{n}\xi_{ie}} = \frac{R_e d_3^2\pi\mu n}{4\frac{TS_\mu\xi_c}{D_o/2}\xi_{ie}} = \frac{R_e d_3^2\pi\mu nD_o}{8TS_\mu\xi_c\xi_{ie}}. \quad (5)$$

The ratio of the load carrying capacity of fitted and clamped bolted joints for the same operating conditions can be represented as a ratio of safety factors given by equations (4) and (5):

$$\frac{S_f}{S_c} = \frac{S_\tau}{S_\sigma} = 0.7\frac{S_\mu\xi_c}{\mu}\left(\frac{D_2}{d_3}\right)^2 = C\left(\frac{D_2}{d_3}\right)^2. \quad (6)$$

The recommended value ranges of the slip safety factor of the clamped bolted joints, the friction coefficient between joint members, and the joint clamping factor are S_μ = 1.2 - 1.8; μ = 0.1 - 0.3; ξ_c = 1.5 - 2.0. According to these values, constant C in equation (6) has values in the range: C = 6 ... 36. Hence, equation (6) obtains the following form:

$$\frac{S_f}{S_c} = 0.7(6...36)\left(\frac{D_2}{d_3}\right)^2 = (4.2...25.2)\left(\frac{D_2}{d_3}\right)^2. \quad (7)$$

Based on this ratio, it can be concluded that the load carrying capacity ratio of fitted and clamped bolted joints depends on the geometrical parameters of threads and bolts, under the same operating conditions. The data of the analyzed bolts (M6 – M24) and obtained extreme safety factor ratios are given in Table 1. Dependencies from Table 1. are shown in Figure 3.

Table 1. *Extreme safety factor ratios of fitted and clamped bolted joints*

Thread diameter d (mm)	Fitted bolt diameter D_2 (mm)	Minor thread diameter d_3 (mm)	D_2/d_3	$(S_f/S_c)_{min}$	$(S_f/S_c)_{max}$
6	7.2	4.773	1.50849	9.557	57.343
8	9.2	6.466	1.42283	8.503	51.016
10	11.2	8.160	1.37255	7.912	47.474
12	13.2	9.853	1.33969	7.538	45.228
14	15.2	11.546	1.31647	7.279	43.674
16	17.2	13.546	1.26975	6.771	40.629
18	19.2	14.933	1.28574	6.943	41.659
20	21.3	16.933	1.25790	6.646	39.874
22	23.3	18.933	1.23066	6.361	38.166
24	25.3	20.319	1.24514	6.512	39.069

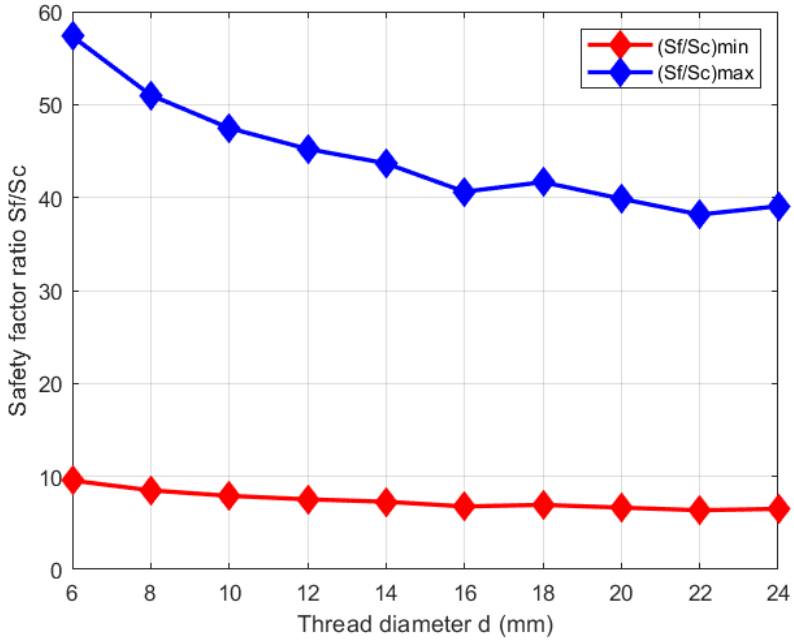

Figure 3. *Safety factor ratio vs. thread diameter*

4 CONCLUSIONS

Carried out analysis showed that the condition of equality of the surface and volumetric safety factor of the fitted bolted joints is that the length of contact between the bolt and joint member should be approximately 0.5 of the bolt diameter. The safety factor ratio of fitted and clamped group bolted joints S_f/S_c (for the same number of bolts on the same pitch diameter) varies in the interval from 6 to 60, depending on the value of the varied parameters (slip safety factor of the clamped bolted joints, the friction coefficient between joint members and the joint clamping factor) and the nominal thread diameter. Safety factor ratio S_f/S_c decreases with increasing bolt nominal thread diameter. The maximal safety factor ratio is more sensitive to changes in the nominal thread diameter.

ACKNOWLEDGEMENT

This work was supported by Ministry of Education, Science and Technological Development of the Republic of Serbia (Contract No. 451-03-68/2022-14/200135, dated 4 February 2022).

NOMENCLATURE

A_s shear area, mm^2
b length of contact between fitted bolt and joint member, mm
D_2 fitted bolt diameter, mm
d_3 minor thread diameter, mm
D_o group bolted joint pitch diameter, mm
F_1 load of single clamped bolted joint, N
F_c clamping load, N
F_s shear load, N
F_t group bolted joint load, N
n number of bolts in group bolted joint
p contact pressure between fitted bolt and joint member, N/mm^2
[p] critical contact pressure, mm
R_e yield stress, N/mm^2
T torque transferred by group bolted joint, Nmm
[τ] critical shear stress, N/mm^2
ξ_{ue} factor of load distribution inequality
max maximum
min minimum

LITERATURA

[1] Omar, R., Rani, M. A., Yunus, M. A. (2020). Representation of bolted joints in a structure using finite element modelling and model updating. *Journal of Mechanical Engineering and Sciences*, vol. 14, no. 3, p.p. 7141–7151.
[2] Frocht, M. M., Hill, H. N. (1940). Stress-concentration factors around a central circular hole in a plate loaded through pin in the hole.
[3] Bickford, J. H. (2007). *Introduction to the design and behavior of bolted joints: non-gasketed joints*, CRC press, Boca Raton, Florida.
[4] Budynas, R. G., Nisbett, J. K. (2011). *Shigley's mechanical engineering design*, McGraw-hill, New York.
[5] Mitrović, R., Ristivojević, M., Rosić, B. (2021). *Machine elements 1* (in Serbian), Faculty of Mechanical Engineering, University of Belgrade.
[6] Ognjanović, M. (2016). *Machine elements* (in Serbian), Faculty of Mechanical Engineering, University of Belgrade.

COMETa 2022
6th INTERNATIONAL SCIENTIFIC CONFERENCE
17th - 19th November 2022
Jahorina, B&H, Republic of Srpska
University of East Sarajevo
Faculty of Mechanical Engineering
Conference on Mechanical Engineering Technologies and Applications

EFFICIENCY OF NON-PIN WHEEL CYCLOID REDUCER CONCEPT

Milan Vasić[1], Mirko Blagojević[2], Miloš Matejić[3]

Abstract: Defining new concepts is of vital importance for the further development of cycloid reducers, which are increasingly used in industry. In order to reduce shock loads, backslash, noise, vibrations, and production costs, a new, non-pin wheel concept was developed. However, the use of stationary circular segments instead of rotating ring gear rollers significantly affects the amount of friction. Therefore, this paper aims to analyze the power losses in the contacts of elements of the non-pin wheel cycloid reducer concept. The test was made for different sizes of cycloid reducers, and one of the most acceptable models proposed by Malhotra was used to determine the non-pin wheel concept efficiency. For the calculation of the forces occurring on the basic components, the assumption that it is an ideal meshing case was used. The simulation results show that the greatest power losses occur precisely in the contact between the teeth of the cycloid disc and the stationary circular segments, where sliding friction is dominant.

Key words: cycloid reducers, non-pin wheel concept, efficiency

1 INTRODUCTION

Cycloidal power transmissions are mechanical transmissions that are widely used in robotics, aviation, CNC machines and other branches of industry, and increasingly in electric cars [1,2]. They have compact design, low weight, high transmission ratio, high efficiency, long and reliable work life.

Recent research [3,4] shows that due to the rotation of cycloid discs at high speed, vibrations occur on the rollers of the ring gear due to the impact of the cycloid disc on them (Figure 1). Also, due to the sliding contact between the rollers and the pins of the ring gear, as well as the inability to form an adequate oil film, greater losses occur.

[1] MSc, Milan Vasić, The Academy of Applied Technical Studies Belgrade, The College of Applied Engineering Sciences in Pozarevac, Belgrade, Serbia, mvasic@atssb.edu.rs (CA)

[2] PhD, Mirko Blagojević, University of Kragujevac Faculty of Engineering, Kragujevac, Serbia, mirkob@kg.ac.rs

[3] PhD, Miloš Matejić, University of Kragujevac Faculty of Engineering, Kragujevac, Serbia, mmatejic@kg.ac.rs

Therefore, *Hwang* and *Hsieh* [4] proposed a new cycloid reducer concept where, instead of rotating rollers of the ring gear, stationary circular segments are used that are made flush with the housing, a non-pin wheel concept (Figure 1). In this way, the rolling friction in the contact between the teeth of the cycloid disc and the now stationary circular segments is replaced by the sliding friction. The disadvantage of this concept is that the contact stresses on the sides of the cycloid disc teeth are higher than in the case of the classic concept, and the most significant advantages are: lower shock loads, lower idle speed, lower noise and vibrations [5,6,7]. In the professional literature, there are many papers dealing with the efficiency of cycloid reducers [8,9,10]. *Kudryavtsev* [11] described cycloid reducers in detail and presented a procedure for calculating forces and power losses. In his doctoral dissertation, *Lehmann* [12] built on *Kudryavtsev's* research and modified his method for forces calculation. *Malhotra* [13] derived analytical expressions for calculating the total friction force work on the basis of which the efficiency of the cycloid reducer is determined.

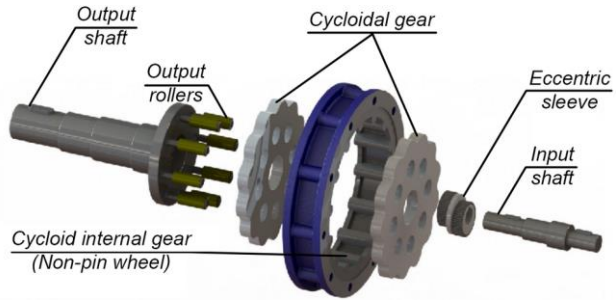

Figure 1. *Disassembled single-stage cycloid reducer of non-pin wheel concept*

Davoli, *Gorla* and others [14] presented the results of the theoretical and experimental analysis of the efficiency of the new cycloid reducer concept. *Pham*, *Bednarczyk* and others [15,16,17] analyzed the dependence of the efficiency on production tolerances as well as inevitable errors during production, which also occur during thermal expansions. *Blagojević* et al. [18] analyzed the dependence of the efficiency on the friction coefficient in the contact between the cycloid disc and the rollers of the ring gear. *Mihailidis* [19] presented a new approach for determining the efficiency, by calculating the friction at each contact point. *Mačkić* [20] investigated the influence of geometrical parameters cycloid reducers efficiency. *Matejić* et al. [21] presented a procedure for determining the efficiency of a two-stage cycloid reducer using *Autodesk INVENTOR* software. *Sensinger* [22] used optimization to increase the efficiency of cycloid reducers. *Olejarczyk* [23] analyzed the impact of installing a sliding and needle bearing on the efficiency, as well as the application of mineral and synthetic oil [24]. Based on the literature review, it can be concluded that researchers are dealing with various aspects to increase efficiency of cycloid reducers. Therefore, the goal of this paper is to determine the value of efficiency of the non-pin wheel concept. The analysis was performed in the MATLAB software package, in which the existing comprehensive expressions for calculating the total friction force work are implemented [13].

2 CYCLOID REDUCER LOADS

During the operation of the cycloid reducer, a torque (T_1) is generated on the cycloid disc as a result of the action of the driving torque (T_{in}), which is shown in Figure

2. The relationship between the torques is as follows [25,26,27]:

$$T_1 - T_2 + T_{\text{in}} = 0 \tag{1}$$

where are: T_2 torque on the ring gear (*Nm*).

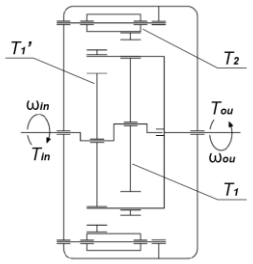

Figure 2. *Kinematic diagram of cycloid reducer, [27]*

In single-stage cycloid reducers where only one cycloid disc is used, if losses are neglected, the torque on the cycloid disc (T_1) is equal to the output torque (T_{ou}), that is, $T_1=T_{\text{ou}}$.

When two cycloid discs are used in a single-stage cycloid reducer, which is the most common case, according to the recommendation from the literature [11,27], the torque on one cycloid disc (T_1) is equal to $T_1=0{,}55\cdot T_{\text{ou}}$. In this way, the influence of uneven load distribution is taken into account.

The output torque can be determined based on the input torque (T_{in}) and the transmission ratio (u_{CR}):

$$T_{\text{ou}} = T_{\text{in}} \cdot \left| u_{\text{CR}} \right| \cdot \eta_{\text{CR}} \tag{2}$$

where: η_{CR} – cycloid reducer efficiency.

The torques T_1, T_2 and T_{in} acting on the elements of the cycloid reducer produce three reactions, namely [11-12,25-32]:

- eccentric force - F_{E};
- the normal force at the current point of contact between the tooth of the cycloid disc and the roller of the ring gear (normal force) - F_{N};
- normal force at the current point of contact between the output rollers and hole in the cycloid disc (output force) - F_{K}.

The distribution of forces on one cycloid disc is shown in Figure 3 and applies both to the classic and to the non-pin wheel conception of the cycloid reducer. On the second cycloid disc, which is not shown, and is rotated by 180° in relation to the first cycloid disc, exactly the same forces act, and for this reason only one cycloid disc will be considered in the further discussions.

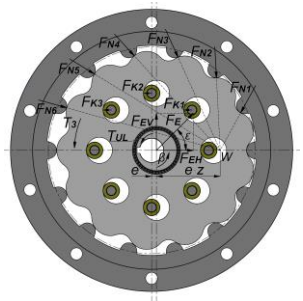

Figure 3. *Distribution of forces and torques acting on cyclid discs in the initial position*

Theoretical models from the literature are used to calculate the normal (F_N) and output force (F_K) [11,12,27]. However, these models do not take into account the modifications of the cycloid disc tooth profile as well as the elastic deformations of the elements participating in the load transfer process [25].

In the theoretical case, when there are no clearances in the cycloid reducer, both cycloid discs are in contact with half of the rollers of the ring gear and the output rollers that participate in the load transfer process. However, in practice this is not the case because there are gaps: due to production, easier assembly and disassembly, better lubrication [33]. The size of the gap directly affects the number of rollers that are in contact with the cycloid disc, so that with an increase in the gap, the number of loaded rollers decreases [34]. Therefore, the calculated force values should be considered approximate.

The normal force on the i-th roller of the ring gear is determined according to expression (3) [12,27]:

$$F_{Ni} = \left(c \cdot \Delta\beta\right) \cdot r_1 \cdot \sin\psi_i \tag{3}$$

where: c – stiffness of the roller of the ring gear (N/mm); $\Delta\beta$ – angular rotation of cycloid disc (°); r_i – distance between the point of contact of the i-th roller of the ring gear and cycloid disc measured from the center of the cycloid disc (mm); ψ_i – the angle of direction of the normal force (F_{Ni}) [27].

The output force on the j-th roller is determined according to the equation [12,27]:

$$F_{Ki} = \left(c_K \cdot \Delta\varphi\right) \cdot r_{Ki} \cdot \sin\psi_{Ki} \tag{4}$$

where: c_K – stiffness of the output roller (N/mm); $\Delta\varphi$ – small angular displacement of cycloid disc (°); r_{Kj} – the distance between the point of contact of the j-th output roller and the cycloid disc measured from the center of the cycloid disc (mm); ψ_{Kj} – the angle between the output force (F_{Kj}) on the j-th output roller and the direction connecting the point of contact of that same roller and cycloid disc with the center of the cycloid disc (°).

The eccentric force is determined as the resultant of the horizontal (F_{EH}) and vertical (F_{EV}) components [12,27,35]:

$$F_E = \sqrt{F_{EH}^2 + F_{EV}^2} \tag{5}$$

The horizontal component of the eccentric force is determined based on the equation:

$$F_{EH} = \sum_i{}' F_{Ni} \cdot \sin x_i + \sum_j{}' F_{Kj} \tag{6}$$

where: x_i – angle between the meshing force of the i-th roller of the ring gear and the vertical direction (°).

The vertical component of the eccentric force is determined according to the equation:

$$F_{EV} = \frac{T_{in}}{e} \tag{7}$$

where: e - eccentricity size (mm).

3 NON-PIN WHEEL CYCLOID REDUCER POWER LOSES

The procedure for determining the efficiency of the cycloid reducer is based on the calculation of the total power losses that occur due to overcoming the resistance to the movement of rotating elements in mutual contact.

Table 1. *Presentation of identified contacts that cause resistance to movement*

Contact of a needle bearing with an eccentric cam and a cycloid disc – (a) (rolling friction)
Contact of output rollers with cycloid disc – (b) (rolling friction)
Contact of the stationary circular segments of the ring gear with the cycloid disc - (c) (sliding friction)
Contact between output rollers and pins – (d) (sliding friction)

Identified contacts in cycloid reducers of the non-pin wheel concept that cause movement resistance are shown in Table 1, while their locations are shown in Figure 4. At the same time, the power losses in the sealing elements and bearings were neglected, except for the cycloid disc bearing.

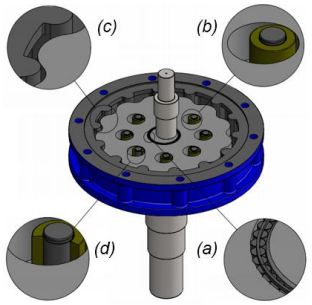

Figure 4. *Locations of contacts that cause resistance to movement in the non-pin wheel design of cycloid reducers*

It should be emphasized that with the non-pin wheel concept, the rolling friction between the rollers of the ring gear and the cycloid disc teeth is replaced by the sliding friction between the stationary circular segments of the ring gear and the cycloid disc teeth. Also, with the non-pin wheel concept, the contacts between the rollers and the pins of the ring gear are lost, thus reducing the corresponding power losses compared to the classic concept.

4 MATHEMATICAL MODEL FOR CALCULATING THE EFFICIENCY OF NON-PIN WHEEL CYCLOID REDUCER CONCEPT

Determining the efficiency of the cycloid reducer [13] is based on the calculation of the total work of the friction force (W_M) and its implementation in the equation:

$$\eta_{CR} = \frac{T_{in} \cdot 2\pi - W_M}{T_{in} \cdot 2\pi} \tag{8}$$

The total work of the friction force represents the integral of the total elementary work dW for a period of one revolution of the input shaft, i.e. $1/z_1$ revolution of the cycloid disc:

$$W_M = \int_0^{\frac{2\pi}{z}} dW \tag{9}$$

where: z_1 – number of cycloid disc teeth.

The total elemental work dW for the non-pin wheel concept includes: elemental work of friction in the cycloid disc bearing (dW_1), elemental work of rolling friction

between the output rollers and holes in the cycloid disc (dW_2), elemental work of sliding friction between the cycloid disc and of stationary circular segments of the ring gear (dW_3) and elementary work of sliding friction between output rollers and pins (dW_4).

$$\mathrm{d}W = \mathrm{d}W_1 + \mathrm{d}W_2 + \mathrm{d}W_3 + \mathrm{d}W_4 \tag{10}$$

The elementary work due to friction in the cycloid disc bearing (dW_1) can be determined based on the equation:

$$\mathrm{d}W_1 = f_{\mathrm{r1}} \cdot F_{\mathrm{E}}(\beta) \cdot \frac{D_{\mathrm{SR}}}{d_{\mathrm{kt}}} \cdot z_1 \cdot \mathrm{d}\beta \tag{11}$$

where: $f_{r1}=\mu_{r1} \cdot d_{kt}/2$ – rolling resistance arm of cycloid disc bearing (mm); μ_{r1} – coefficient of rolling friction in cycloid disc bearing; $F_E(\beta)$ - current value of eccentric force (N); $D_{SR}=(D_{CZ}+d_{CZ})/2$ – mean diameter of cycloid disc bearing (mm); D_{CZ} – outer diameter of cycloid disc bearing (mm); d_{CZ} – internal diameter of cycloid disc bearing (mm); d_{kt} – diameter of the rolling body (pin, roller, ball) in the cycloid disc bearing (mm); β – driving angle (°).

The elementary work of the rolling friction between the output rollers and the opening in the cycloid disc (dW_2) can be determined based on the equation:

$$\mathrm{d}W_2 = f_{\mathrm{r2}} \cdot \sum_{j=1}^{q} F_{\mathrm{Kj}}(\beta) \cdot z_1 \cdot \mathrm{d}\beta \tag{12}$$

where: $f_{r2}=\mu_{r2} \cdot D_{VK}/2$ – rolling resistance arm of the output roller (mm); μ_{r2} – coefficient of rolling friction between the output rollers and the opening in the cycloid DISC; D_{VK} – diameter of output roller (mm); $F_{Kj}(\beta)$ - current value of the output force on the *j*-th output roller (N); q – the current number of output rollers participating in meshing with the cycloid disc. If the total number of output rollers is an even number, then $q=u/2$, and if it is odd, then $q=(u-1)/2$.

The elementary work of the sliding friction between the cycloid disc and the stationary circular segments of the ring gear (dW_3) can be determined based on the equation:

$$\mathrm{d}W_3 = \mu_{\mathrm{s3}} \cdot \sum_{i=1}^{p} F_{\mathrm{Ni}}(\beta) \cdot \frac{D_0}{2} \cdot (z_1 + 1) \cdot \mathrm{d}\beta \tag{13}$$

where: μ_{s3} – the sliding friction coefficient between the fixed circular segments and the cycloid disc, $F_{Ni}(\beta)$ – the current value of the normal force on the *i*-th segment of the ring gear (N); D_0 – diameter of the circular segment (mm); *p* – the current number of circular segments participating in the load transfer process. If the total number of circular segments *p* is an even number, then $p=z_2/2$, and if it is odd, then $p=(z_2+1)/2$.

The elementary work of sliding friction between output rollers and pins (dW_4) can be determined based on the equation:

$$\mathrm{d}W_4 = \mu_{\mathrm{s1}} \cdot \sum_{j=1}^{q} F_{\mathrm{Kj}}(\beta) \cdot \frac{d_{\mathrm{VK}}}{2} \cdot z_1 \cdot \mathrm{d}\beta \tag{14}$$

where: μ_{s1} – sliding friction coefficient between output rollers and pins; d_{VK} – diameter of output rollers (mm). The total work of the friction force *W* of the non-pin wheel design is calculated based on the comprehensive equation:

$$W = \frac{f_{\mathrm{r1}} \cdot D_{\mathrm{SR}} \cdot z_1}{d_{\mathrm{kt}}} \int_0^{\frac{2\pi}{z_1}} F_{\mathrm{E}}(\beta) \cdot \mathrm{d}\beta + z_1 \cdot \left(f_{\mathrm{r2}} + \frac{\mu_{\mathrm{s1}} \cdot d_{\mathrm{VK}}}{2} \right) \int_0^{\frac{2\pi}{z_1}} \sum_{j=1}^{q} F_{\mathrm{Kj}}(\beta) \cdot \mathrm{d}\beta + (z_1 + 1) \cdot \left(\frac{\mu_{\mathrm{s3}} \cdot D_0}{2} \right) \int_0^{\frac{2\pi}{z_1}} \sum_{i=1}^{p} F_{\mathrm{Ni}}(\beta) \cdot \mathrm{d}\beta \tag{15}$$

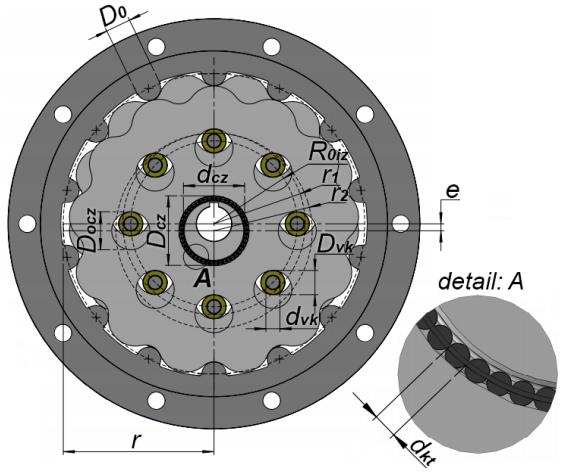

Figure 5. *Dimensions of the cycloid reducer vital elements*

5 EFFICIENCY ANALYSES OF NON-PIN WHEEL CONCEPT

The analysis of the cycloid reducer efficiency of the non-pin wheel concept is based on the testing of cycloid reducers of different sizes.

Therefore, for the purposes of this research, the values of certain parameters [36] were taken from the Sumitomo company catalog, namely input power P_{ul}=(2.2; 3; 4; 5.5; 7.5; 11) kW and transmission ratios u_{CR}=(11; 13; 15; 17; 21; 25). The data for the standard RPM's of the electric motor were taken from the catalog of the company ATB Sever [37] and it is n_{in} =(600; 750; 1000; 1500; 3000) min^{-1}.

The theoretical value of the efficiency largely depends on the adopted values of the friction coefficients of sliding (μ_s) and rolling (μ_r). At the same time, these values are not constant during the reducer operation, and depend on the lubrication regime, working temperatures, the quality of the processed surfaces, the load on the rollers and other factors.

Therefore, the impact of different values of friction coefficients on the efficiency was primarily tested. The test was performed with the assumption that all the individual friction coefficients of sliding (μ_s) and rolling (μ_r) have the same values. Specific sizes of vital elements were used for research: D_{CZ}=40 mm; d_{CZ}=35 mm; d_{kt}=5 mm; z_1=13; z_2=14; D_{VK}=10,4 mm; d_{VK}=5,2 mm; D_0=14 mm; u=8; P_{in}=4 kW.

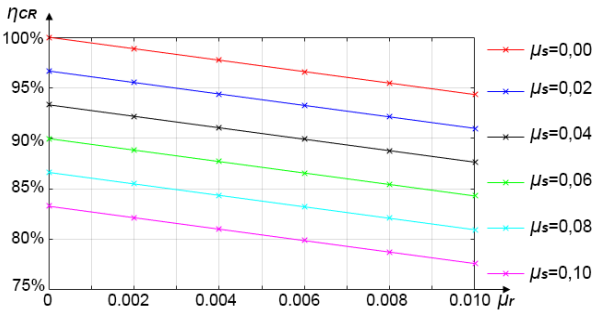

Figure 6. *Dependence of the efficiency on different values of friction coefficients*

Table 2 shows the recommended values of sliding and rolling friction coefficients taken from the literature, while Table 3 shows their adopted values. From Figure 6, it is obvious that with the increase in friction coefficients, the efficiency has a decreasing trend.

Table 2. *Recommended values of sliding and rolling friction coefficients*

	μ_{r1}	μ_{r2}	$\mu_{s1}=\mu_{s2}$	μ_{s3}
[11]			0,07	
[13]			0,01÷0,08	
[38]	0,005			
[39]		0,006		
[40]		0,003	0,03	
[41]				0,03÷0,05

Table 3. *Adopted values of sliding and rolling friction coefficients*

μ_{r1}	μ_{r2}	$\mu_{s1}=\mu_{s2}$	μ_{s3}
0,005	0,0045	0,05	0,004

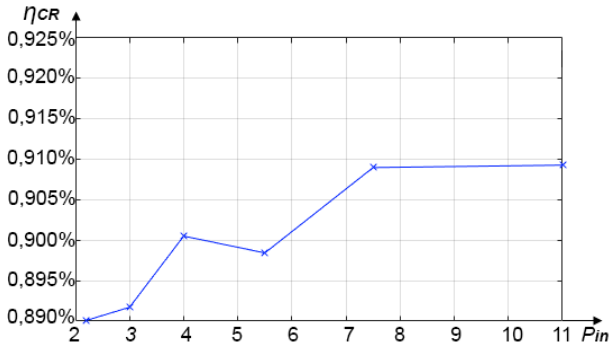

Figure 7. *Dependence of the efficiency on the input power*

The dependence of the efficiency (η_{CR}) on the input power (P_{in}) at a constant transmission ratio u_{CR}=13 and the input speed n_{in}=1500 min^{-1} is shown in Figure 7. The input power varies in an interval of 2,2 kW to 11 kW. With an increase in input power, the efficiency of the cycloid reducer also increases.

The dependence of the efficiency (η_{CR}) on the transmission ratio (u_{CR}) at constant power P_{in}=4 kW and input speed n_{in}=1500 min^{-1} is shown in Figure 8. The transmission ratio varies in the range from 11 to 25. With an increase in the transmission ratio, the efficiency of the cycloid reducer decreases because the number of contacts of the circular segments with the cycloid disc increases.

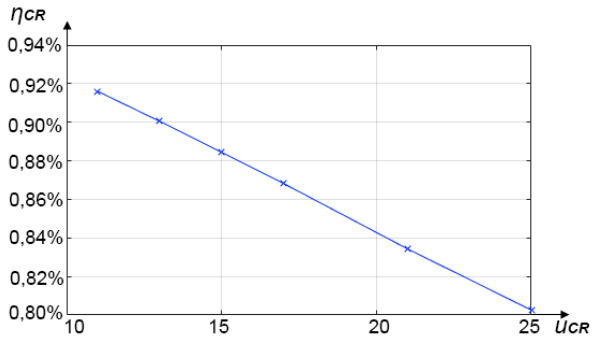

Figure 8. *Dependence of the efficency on the transmission ratio*

Partial losses in the identified contacts have a different distribution in the calculated efficiency, so it is necessary to know their distribution.

The dependence of the partial power losses (W_1,W_2,W_3,W_4) on the input power (P_{in}) at a constant transmission ratio u_{CR}=13 and the input speed n_{in}=1500 min^{-1} are shown in Figure 9.

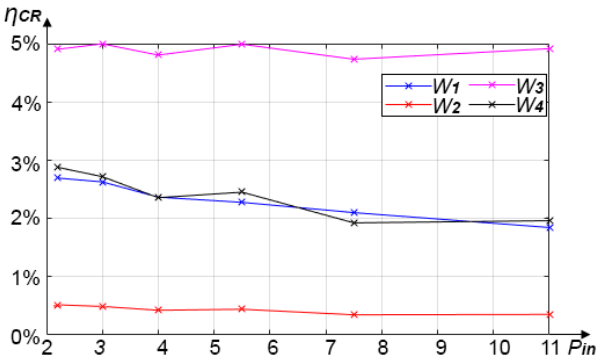

Figure 9. *Dependence of partial power losses on input power*

The biggest power losses occur in the contact of the stationary circular segments with the cycloid disc (W_3=4.73% ÷ 4.99%), which causes a lower efficency of the non-pin wheel concept. Also, significant power losses occur in the contacts of the output rollers and pins (W_4=1.92% ÷ 2.88%), as well as in the cycloid disc bearing (W_1=1.84% ÷ 2.66%). The losses in the contact of the output rollers with the openings in the cycloid disc are significantly lower compared to the previously mentioned ones.

Dependence of partial power losses (W_1,W_2,W_3,W_4) on transmission ratio (u_{CR}) at constant power P_{in}=4 kW and input speed n_{in}=1500 min^{-1} are shown in Figure 10.

The greatest power losses occur in the contact of stationary circular segments with cycloid disc (W_3=4.12% ÷ 8.44%). Also, significant power losses occur in the contacts of the output rollers and pins (W_4=1.83% ÷ 6.14%), as well as in the cycloid disc bearing (W_1=2.12% ÷ 4.06%).

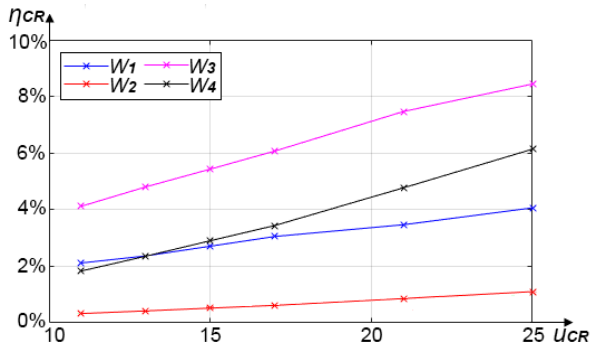

Figure 10. *Dependence of partial power losses on transmission ratio*

6 CONSCLUSION

This paper presents an analysis of the value of the efficiency of the relatively new, non-pin wheel concept of the cycloid reducer. The test was made for different sizes of catalog cycloid reducers.

The detailed analysis provides a good theoretical basis and help for further improvements of the cycloid reducer of the non-pin whel concept, as it indicates the locations of the contacts with the highest power losses.

In the analysis, the Malhotra model was used, which takes into account the losses in the cycloid disc bearing, on the output rollers, pins and on stationary circular segments. The input power of the cycloid reducer, the transmission ratio and the input speed were varied.

Research has shown that with an increase in the transmission ratio, the efficiency of the cycloid reducer decreases because the number of contacts of the circular segments with the cycloid disc increases. Increasing the input power has a positive effect on the efficency.

The largest individual loss occurs in the contact of the stationary circular segments of the ring gear with the cycloid disc (4.12÷8.44%) for the tested cycloid reducer sizes). It is precisely this loss that causes the lower value of the efficiency of the non-pin wheel concept.

In future research, it would be very useful to investigate the possibilities of reducing these losses by using new materials and more efficient types of lubrication.

REFERENCES

[1] Pham A.D., Ahn H.J. (2018). High Precision Reducers for Industrial Robots Driving 4th Industrial Revolution: State of Arts, Analysis, Design, Performance Evaluation and Perpective, International Journal of Precision Engineering and Manufacturing-Green Technology, Vol. 5, No. 4, pp. 519-533.

[2] Li X., Chen B., Wang Y., Sun G., Lim C. T. (2015). Geometry Design of a Non-Pin Cycloid Drive for In-Wheel Motor, SAE Technical Papers 2015.

[3] Chiu-Fan Hsieh (2014). Dynamics Analysis of Cycloidal Speed Reducers With Pinwheel and Nonpinwheel Designs, Journal of Mechanical Design, Volume 136, No. 9, pp. 11.

[4] Hwang Y. W., Hsieh C. F. (2007). Geometric Design Using Hypotrochoid and Nonundercutting Conditions for an Internal Cycloidal Gear, Journal of mechanical design, Vol. 129, No. 4, pp. 369-463.

[5] Wang Y. Liu G., Yu H., Mao H., He K. (2017). Analysis of Meshing Characteristics of Pin sand Pin Housing Integral Structure in Cycloidal Planetary Drive, Conference: ASME 2017 International Mechanical Engineering Congressand Exposition, Vol. 2, pp. 8.
[6] Chen Z., Ou Y., Long S., Peng W., Yang Z. (2018). Vibration Characteristics Analysis of the New Pin-Cycloid Reducer, Journal of the Braziian Society of Mechanical Sciences and Engineering, Vol. 40, pp. 1-17.
[7] Matejić M. (2019). A new approach to the design and optimization of cycloidal power transmissions, PhD thesis, Faculty of Engineering, University of Kragujevac, Kragujevac.
[8] Tonoli A., Amati N., Impinna F., Detoni J., Ruzimov S., Gasparin E., Abdivakhidov K. (2013). Influence of Dry Friction on the Irreversibility of Cycloidal Speed Reducer, World Tribology Congress 2013, September 8-13, 2013, Torino, Italy.
[9] Huang C.H., Tsai S.J. (2017). A Study on Loaded Tooth Contact Analysis of a Cyloid Planetary Gear Reducer Considering Friction and Bearing Roller Stiffness, Journal of Advanced Mechanical Design, Systems, and Manufacturing, Vol. 11, No. 6, pp. 1-17.
[10] Concil F., Maccioni L., Gorla C. (2020). Development of a Computational Fluid Dynamics Simulation Tool for Lubrication Studies on Cycloidal Gear Sets, International Journal of Computational Methods and Experimental Measurements, Vol. 8, No. 3, pp. 220-232.
[11] Kudryavcev V. N. (1966). Planetarnye peredachi, Masinostroenie, Moscow.
[12] Lehmann M. (1976). Calculation and measurement of forces acting on cycloidal speed reducer, Doktorska disertacija, The Technical University of Munich, Munich.
[13] Malhotra S. K., Parameswaran M. A. (1983). Analysis of a cycloid speed reducer, Mechanism and Machine Theory, Vol. 18, No. 6, pp. 491-499.
[14] Davoli P., Gorla C., Rosa F., Longoni C., Chiozzi F., Samarani A. (2007). Theoretical and experimental analysis of a cycloidal speed reducer, International Design Engineering Technical Conferences and Computers and Information in Engineering Conference, , Vol. 7, pp. 1043-1051.
[15] Pham A.D., Ahnb H. J. (2017). Efficiency Analysis of a Cycloid Reducer Considering Tolerance, Journal of Friction and Wear, Vol. 38, pp. 490–496.
[16] Bednarczyk S.,(2019). Determining Power Losses in the Cycloidal Gear Transmission Featuring Manufacturing Deviations, Proceedings of the 14th International Scientific Conference: Computer Aided Engineering, pp. 55-63.
[17] Bednarczyk S. , Jankowski L., Krawczyk J. (2019). The influence of eccentricity changes on power losses in cycloidal gearing, Tribologia, Vol. 3, pp. 19-29.
[18] Blagojevic M., Kocić N., Marjanović M., Stojanović B., Đordevic Z., Ivanović L., and Marjanović N., 2012, “Influence of the Friction on the Cycloidal Speed Reducer Efficiency,” J. Balkan Tribol. Assoc., 18(2), pp. 217–227.
[19] Mihailidis A., Athanasopoulos E., Agouridas K. (2016). EHL film thickness and load dependent power loss of cycloid reducers, Proceedings of the Institution of Mechanical Engineers Part C Journal of Mechanical Engineering Science, Vol. 230, pp. 1303-1317.
[20] Mackić, T., Blagojević M., Babić Z., and Kostić N., (2013). Influence of Design Parameters on Cyclo Drive Efficiency, J. Balkan Tribol. Assoc., 19(4), pp. 167–179.
[21] Matejić M., Blagojević M., Kostić N., Petrović N., Marjanović N. (2019). Analysis of efficiency of a new two stage cycloid drive concept, 16th International Conference on Tribology SERBIATRIB 2019, pp. 335-340.

[22] Sensinger J. (2010). Unified Approach to Cycloid Drive Profile, Stress, and Efficiency Optimization. Journal of Mechanical Design, Vol. 132, No. 2.
[23] Olejarczyk K., Wiklo M., Kolodziejczyk K. (2018). Change of the cycloidal gearbox efficiency for different kind of bearings, sleeves vs. needle bearings, INTERNATIONAL GEAR CONFERENCE 27th-29th August 2018 Lyon Villeurbanne, pp. 87-97.
[24] Olejarczyku K., Wiklo M., Krol K., Kołodziejczyk K. (2017). Obliczenia teoretyczne oraz pomiary stanowiskowe sprawności przekładni cykloidalnej, Modelowanie inżynierskie, Vol. 33, No. 64, pp. 74-81
[25] Chmurawa M., John A., (2000). FEM in Numerical Analysis of Stress and Displacement Distributions in Planetary Wheel of Cycloidal Gear, International Conference on Numerical Analysis and Its Applications, pp. 772-779.
[26] Chmurawa M., Lokiec A. (2001). Distribution of Loads in Cycloidal Planetary Gear (CYCLO) Including Modification of Equidistant, 16th European ADAMS User Conference, Berchtesgaden, Germany.
[27] Blagojević M. (2003). Kinematic and Dynamic Analysis of One-Stage Cycloidal Speed Reducer, Master Thesis, Faculty of Mechanical Engineering, Kragujevac.
[28] Efremenkov E.A., Bonnard E. (2019). Power Parameters Automated Calculation for Transmission with Intermediate Rolling Bodies and Free Cage, MEMT-2019, IOP Conf. Series: Materials Science and Engineering 795.
[29] Tsai S.J., Chang L.C., Huang C.H. (2017). Design of Cycloid Planetary Gear Drives with Tooth Number Difference of Two, Forsch Ingenieurwes, Vol. 81, pp. 325-336.
[30] Wiklo M., Krol R., Olejarczyk K., Kolodziejczyk K. (2019). Output Torque Ripple for a Cycloidal Gear Train, Journal of Mechanical Engineering Science, pp. 1-12.
[31] Xu L.X. (2018). A dynamic Model to Predict the Number of Pins to Transmit Load in a Cycloidal Reducer with Assembling Clearance, Journal of Mechanical Engineering Science, pp. 1-23.
[32] Zhang T., Li X., Wang Y., Sun L. (2020). A Semi-Analytical Load Distribution Model for Cycloid Drives with Tooth Profile and Longitudinal Modifications, Applied Sciences, Vol. 10, pp. 1-19.
[33] Blagojević M., Marjanović N., Djordjević Z., Stojanović B., Marjanović V., Vujanac R., Disić A. (2014). Numerical and experimental analysis of the cycloid disc stress state, Tehnički vjesnik, Vol. 21, No. 2, pp.377-382.
[34] Lixing L., Xin L., Weidong H., Yuanmei Q. (1997). Accurate force analysis in cycloid drive, International Symposium "Machines and Mechanisms", Belgrade, Serbia, pp.1-4.
[35] Jankevich M., Lazurenko Y. (2003). The analysis of loads and selection of efficient geometrical parameters of cicloid gearboxes, International conference Power transmissions.
[36] Sumitomo catalogue
[37] ATB Sever catalogue
[38] SKF Catalogue (2015). Needle roller bearings.
[39] Zhu C., Liu M., Du X., Xiao N., Zhang B. (2010). Analysis on Transmission Characteristics of New Axis-fixed Cycloid Gear, Conference Advanced Materials Research, Vol. 97-101, pp. 60-63
[40] Mačkić T., Babić Ž., Kostić N., Blagojević M. (2013), Cyclo drive efficiency, 13th International Conference on Tribology - Serbiatrib'13, pp. 230-233.
[41] Shipley E. F. (1958). How to Predict Efficiency of Gear Trains, Product Engineering, Vol. 29, No. 31.

COMETa 2022
6th INTERNATIONAL SCIENTIFIC CONFERENCE
17th - 19th December 2022
Jahorina, B&H, Republic of Srpska
University of East Sarajevo
Faculty of Mechanical Engineering
Conference on Mechanical Engineering Technologies and Applications

ANALYSIS OF THE CLEARANCE INFLUENCE ON THE FOUR POINT CONTACT BALL BEARING DYNAMIC BEHAVIOR

Mirjana Bojanić Šejat[1], Ivan Knežević[2], Aleksandar Živković[3], Milan Rackov[4], Imre Kiss [5]

Abstract: The research of dynamic behavior bearing is motivated by the desire to reduce noise and vibration in their useing, as well as to increase the life, stiffness, speed and accuracy of rotation, and the development of methods for diagnostics and monitoring of bearings. The dynamic behavior of the bearing is regulated by the dynamic behavior of its structural elements.Vibrations that occur in the operation of ball bearings are a phenomenon that cannot be avoided. The clearance is of great importance if satisfactory bearing operation is to be achieved. The clearance designed to compensate the thermal expansion of the bearing elements is a source of vibration and creates nonlinearity in dynamic behavior. It is difficult for mathematical models to take into account certain factors, related to manufacturing error, geometric imperfections of rolling paths (especially wavines and roughness) and assembly of bearing elements, which indicates the need for experimental testing of real systems. Within this paper, an experimental study was conducted the influence of the clearance on the dynamic behavior of the four contact ball bearing FKL LSQFR 308 was observed.

Key words: Bearing, Clearance, Dynamic behavior, Four point contact ball bearing

[1] PhD, Mirjana Bojanić Šejat, University of Novi Sad, Faculty of Tehnical Sciences, Novi Sad, Serbia, bojanicm@uns.ac.rs (CA)
[2] Phd, Ivan Knežević, University of Novi Sad, Faculty of Tehnical Sciences, Novi Sad, Serbia, ivanknezevic@uns.ac.rs
[3] PhD, Aleksandar Živković, University of Novi Sad, Faculty of Tehnical Sciences, Novi Sad, Serbia, acoz@uns.ac.rs
[4] PhD, Milan Rackov, University of Novi Sad, Faculty of Tehnical Sciences, Novi Sad, Serbia, racmil@uns.ac.rs
[5] Prof. PhD. Eng. Imre Kiss, University Politehnica Timisoara, Faculty of Engineering, Hunedoara, Romania, imre.kiss@fih.upt.ro

1 INTRODUCTION

The complexity of assemblies such as bearings, and their undoubtedly great influence on the behavior of the assembly in which it is incorporated as a whole, influenced the focus of the research in this paper on the analysis of the dynamic behavior on four contact point ball bearings. These bearings can transfer radial and axial loads in both directions. Nowadays, they are most often used in agricultural machinery, machine tools, as well as in the transmission of motor vehicles.

Many authors have analyzed the theoretical and experimental static behavior on four point contact ball bearings, however, the dynamic behavior of these bearings is rarely found in the literature. Yao et al. [1] proposed a dynamic model of four point contact ball bearings with three degrees of freedom taking into account the influence of the clearance and the tolerance of the diameter of the rolling elements. They conducted an analysis for contact forces, impact forces and a bearing map of stability under the influence of radial, axial and combined loads. The clearance has a significant influence on the dynamic behavior and the creation of disruptive forces that cause oscillatory movement and vibrations of the bearing elements. The size of the radial clearance does not affect the own frequency of the bearing [2, 3], neither on the rotation frequency of the bearing elements [4]. Harsha [2] presented a model for studying the structure of vibrations in bearings depending on the clearance. A mathematical model is defined for the tangential motion of the rolling elements, as well as the inner and outer rings, using non-linear sources, such as the Hertzian contact force and radial clearance. Depending on the size of the radial clearance and the combination of the external radial load, the size of the relative displacement of the bearing center due to contact deformations also changes, and this further leads to a change in the number of rolling elements participating in the transmission of the external load, which has an impact on the change in the distribution of the external load between the rolling elements and rings. With these changes, the dynamic response of the rolling elements and the outer ring are changes. The displacement amplitude on the rolling elements decreases slightly, and the displacement amplitude on the outer ring increases with increasing clearance [3, 5, 6]. The change in the displacement amplitude of the outer ring (in the case when the inner ring is rotating) can be taken as an important diagnostic parameter for assessing the size of the radial clearance in the bearing. According to Liquin-u [5] the optimal sizes of the radial clearance under the action of an external load of 5000 N range from 1 to 26 μm and from 30 to 58 μm when the load is uniformly transmitted over the rolling bodies, which leads to an even distribution of contact deformations and periodic movement bearing center.

The subject of research in this paper is the analysis of the influence of structural (positive/negative clearence) on the dynamic characteristics of four point contact ball bearing.

2 EXPERIMENTAL TESTING OF VIBRATION OF FOUR POINT CONTACT BALL BEARING

The LSQFR 308 bearing is used for housing agricultural machinery, i.e. for housing the seed drill discs. Figure 1 shows the experimental stand schematically, on which the vibrations of the FKL LSQFR 308 bearing were tested. The electric motor via the coupling (1) and the flange (2) transmits the torque to the shaft (8), which is fitted with the tested bearings (5). On the shaft there is a drum (4) that simulates the seed drill disc and that rotates together with the shaft (8). The bearing is loaded with radial

and axial forces of 27 000 N and 13 400 N, respectively, via the hydraulic installation for external loading (7). The acceleration sensor (3) is connected to the A/D card (9), which sends the collected data directly to the computer (10).

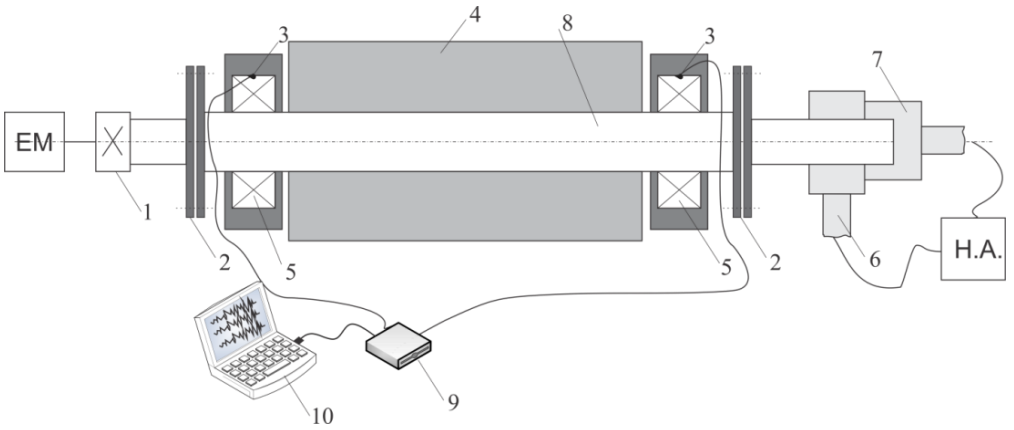

Figure 1. Schematic of the experiment for determination of bearing vibration

Figure 2. Experimental analysis for bearing FKL LSQFR 308

Figure 2 shows the experimental stand at the rolling bearing factory (FKL), where this bearing was tested. In order to simulate real conditions of exploitation, the inner ring of the bearing is loaded with radial and axial force of constant intensity. Radial and axial loading is achieved through levers (6), (7) hydraulically using hydraulic cylinders and hydro aggregates. The external load is transferred to the inner rings of the bearing via the shaft (8). PCB 352C33 and DYATRON P22 acceleration transmitters were used to measure vibrations on the bearing housing (5). The sensitivity of this transmitter is 10 mV/g and it registers vibrations in the frequency range of 1-20000 Hz. The experimental setup of this test was used to analyze the effect of clearance on the dynamic behavior of the same LSQFR 308 bearing.

3 ANALYSIS OF THE RESULTS OF EXPERIMENTAL TESTING OF THE LSQFR 308 BEARING

When examining the influence of clearance, bearings with a clearance of 10 to 40 μm were selected for the experimental test. The analysis of the impact of the clearance was performed under a combined load, with the number of revolutions being 200 rpm. The load and number of revolutions is determined based on the operational conditions of the considered bearing. During the experimental testing, it was established that the maximum acceleration amplitudes occur in the radial direction, and the results of the change in the acceleration amplitudes in the radial direction in the vertical plane of the bearing are presented below [7].

Figure 3 shows the frequencies of individual bearing elements at a clearence of 10 μm under load. The outer ring frequency (f_o) of 13.5 Hz is shown with a harmonic of 3x at 40.5 Hz and 4x at 54 Hz. The acceleration amplitude at these frequencies is 0.21 m/s^2, 0.33 m/s^2 and 0.35 m/s^2, respectively. The spectral line of 4.5 Hz with acceleration amplitudes of 0.49 m/s^2 corresponds to the frequency of the rolling elements (f_b). To the right of the spectral line corresponding to (f_o) is a frequency of 19.1 Hz which represents the sum of the frequency of the inner ring and the fundamental frequency of the spindle rotation (f_r = 6.66 Hz). The spectral line of 32.08 Hz with acceleration amplitudes of 0.4 corresponds to the frequency of the inner ring (f_i). The vibration spectrum in the frequency domain for a gap of 20 μm under load is shown in Figure 4. As in the previous case, the inner ring frequency of 13.5 Hz is shown with harmonics at 40.5 Hz and 54 Hz. The acceleration amplitude at these frequencies is 0.22 m/s^2, 0.47 m/s^2 and 0.38 m/s^2, respectively. To the right of the spectral line corresponding to (f_o) is a frequency of 19.1 Hz which represents the sum of the frequency of the inner ring and the fundamental frequency of the spindle rotation (f_r = 6.66 Hz).

Figure 3 shows the frequencies of individual bearing elements at a clearence of 10 μm under load. The outer ring frequency (f_o) of 13.5 Hz is shown with a harmonic of 3x at 40.5 Hz and 4x at 54 Hz. The acceleration amplitude at these frequencies is 0.21 m/s^2, 0.33 m/s^2 and 0.35 m/s^2, respectively. The spectral line of 4.5 Hz with acceleration amplitudes of 0.49 m/s^2 corresponds to the frequency of the rolling elements (f_b). To the right of the spectral line corresponding to (f_o) is a frequency of 19.1 Hz which represents the sum of the frequency of the inner ring and the fundamental frequency of the spindle rotation (f_r = 6.66 Hz). The spectral line of 32.08 Hz with acceleration amplitudes of 0.4 corresponds to the frequency of the inner ring (f_i). The vibration spectrum in the frequency domain for a gap of 20 μm under load is shown in Figure 4. As in the previous case, the inner ring frequency of 13.5 Hz is shown with harmonics at 40.5 Hz and 54 Hz. The acceleration amplitude at these frequencies is 0.22 m/s^2, 0.47 m/s^2 and 0.38 m/s^2, respectively. To the right of the

spectral line corresponding to (f_o) is a frequency of 19.1 Hz which represents the sum of the frequency of the inner ring and the fundamental frequency of the spindle rotation (f_r = 6.66 Hz).

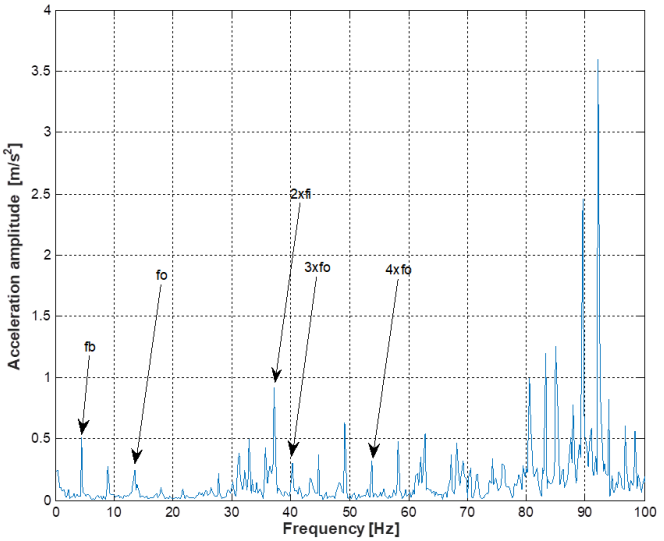

Figure 3. Display of the vibration spectrum in the frequency domain for the clearance G_r = 10 μm

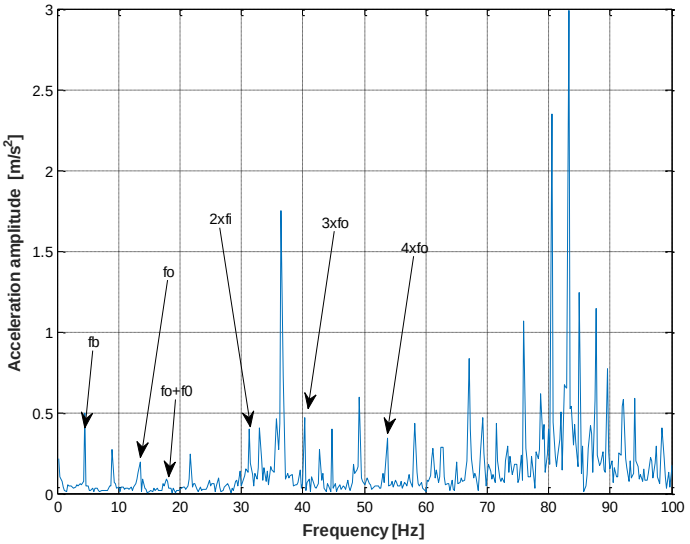

Figure 4. Display of the vibration spectrum in the frequency domain for the clearance G_r = 20 μm

Figure 5 shows the frequencies of individual bearing elements at a clearance of 30 μm. When the clearence is further increased to 30 μm, the acceleration amplitude increases to 0.26 m/s^2 at the frequency of the outer ring, while the amplitudes of its harmonics also increase to 0.85 and 0.58 m/s^2. In this case, the amplitude of the acceleration at the frequency of the rolling elements changes very little, while the amplitude at the inner ring decreases.

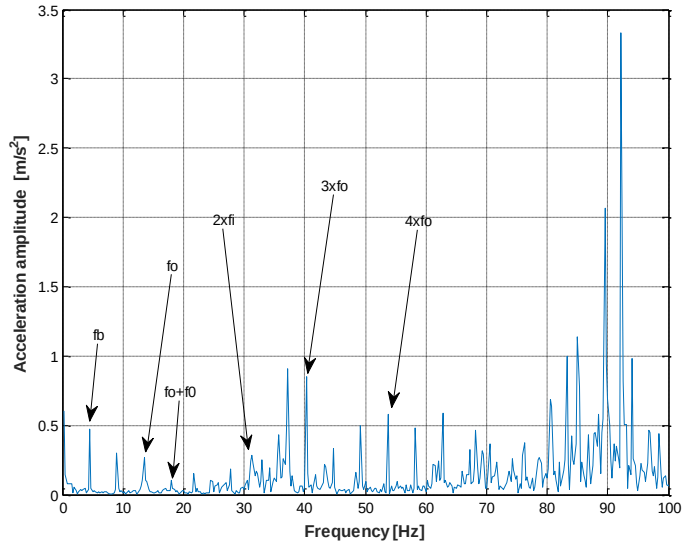

Figure 5. Display of the vibration spectrum in the frequency domain for the clearance G_r = 30 μm

The spectrum of vibrations in the frequency domain for a clearence of 40 μm under load action is shown in Figure 6. At a clearence of 40 μm, there is a significant increase in acceleration vibrations at the third and fourth harmonics of the frequency of the outer ring to 1.51 and 0.96 m/s^2, respectively, in which case the acceleration amplitude at the basic frequency of the outer ring increases to 0.86 m/s^2. In addition to the previous one, an acceleration amplitude of 0.49 m/s^2 at the second harmonic of the frequency of the outer ring can also be observed in the spectrum.

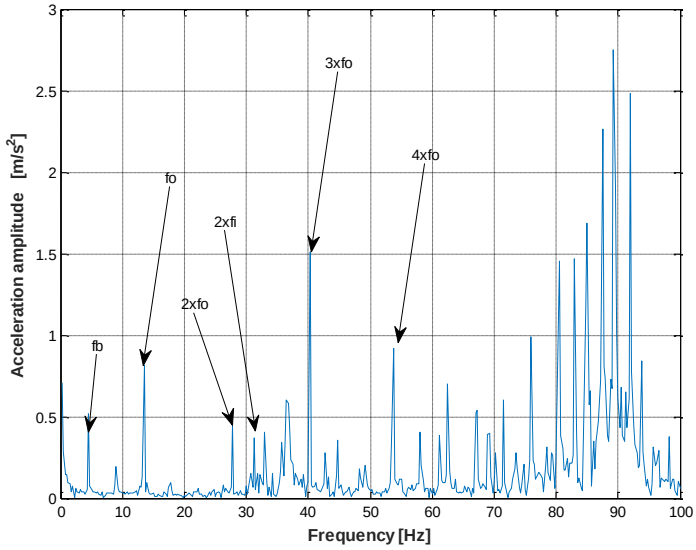

Figure 6. Display of the vibration spectrum in the frequency domain for the clearance G_r = 40 μm

4 CONCLUSION

By detecting the existing frequency components of the bearing elements in the frequency spectrum, their amplitude, the presence of their harmonics (integer multiples) and modulation components, a conclusion is reached about the influence of certain parameters on its dynamic behavior. On the other hand, in many scientific works, it is stated that bearing failure occurs when the amplitude of the acceleration at one of the characteristic frequencies exceeds 30% of its initial value in the frequency spectrum.

When analyzing the results obtained by experimental testing, it was concluded that the maximum acceleration amplitudes occur at the frequency of the outer ring, and that the acceleration amplitudes at other frequencies of the bearing elements are significantly smaller. On the other hand, there was no change in the frequencies of the bearing elements due to the change in clearance.

By analyzing the results of the research of the static and dynamic behavior of radial bearings and four point contact ball bearing, based on available literature information, as well as on the basis of own experiences and results, it is possible to propose some directions for future research, such as: defining a mathematical model for analysis of the impact of the clearance on the dynamic behavior of the four point contact ball bearing and its experimental verification, as well as the development of an appropriate software solution.

Finally, it should be noted that the development of four point contact ball bearing is still a current and insufficiently researched area, therefore, the analysis and examination of the influence of any parameter of this bearing, on its static and dynamic behavior, may represent the direction of future research.

ACKNOWLEDGEMENTS

This research (paper) has been supported by the Ministry of Education, Science and Technological Development through the project no. 451-03-9/2022-14/200156: “Innovative scientific and artistic research from the FTS (activity) domain”.

NOMENCLATURE

f_b frequency of the rolling elements [Hz]
f_i the frequency of the inner ring [Hz]
f_o the frequency of the out ring [Hz]
f_r the frequency of rotation [Hz]

REFERENCES

[1] Yao, T., et al. (2020). Multibody dynamics simulation of thin-walled four-point contact ball bearing with interactions of balls, ring raceways and crown-type cage. *Multibody System Dynamics*, 48(3): p.p. 337-372.
[2] Harsha, S. (2006). Nonlinear dynamic response of a balanced rotor supported by rolling element bearings due to radial internal clearance effect. *Mechanism and Machine Theory*, 41(6): p.p. 688-706.

[3] Upadhyay, S., S. Harsha, and S. Jain. (2010). Analysis of nonlinear phenomena in high speed ball bearings due to radial clearance and unbalanced rotor effects. *Journal of Vibration and Control*, 16(1): p.p. 65-88.
[4] Tomović, R. (2012). Calculation of the boundary values of rolling bearing deflection in relation to the number of active rolling elements. *Mechanism and machine theory*, 47: p.p. 74-88
[5] Liqin, W., et al. (2008). Nonlinear dynamics behaviors of a rotor roller bearing system with radial clearances and waviness considered. *Chinese Journal of Aeronautics*, 21(1): p.p. 86-96.
[6] Villa, C., J.-J. Sinou, and F. Thouverez. (2008). Stability and vibration analysis of a complex flexible rotor bearing system. *Communications in Nonlinear Science and Numerical Simulation*, 13(4): p.p. 804-821.
[7] Bojanić Šejat, M. (2021). *Modelovanje mehaničkog ponašanja kugličnih ležaja*, Doktorska disertacija, Fakultet tehničkih nauka, Univerzitet u Novom Sadu.

COMETa 2022
6th INTERNATIONAL SCIENTIFIC CONFERENCE
17th - 19th November 2022
Jahorina, B&H, Republic of Srpska
University of East Sarajevo
Faculty of Mechanical Engineering
Conference on Mechanical Engineering Technologies and Applications

MECHANICAL TRANSMISSIONS DIVISION SHOWING THE BASIC CONCEPTUAL SOLUTIONS OF UNIVERSAL MOTOR GEAR REDUCERS WITH HELICAL GEARS

Milan Rackov[1], Siniša Kuzmanović[2], Vojislav Miltenović[3], Ivan Knežević[4], Milan Banić[5], Aleksandar Miltenović[6], Sandor Bodzas[7]

Abstract: The paper presents the division of mechanical transmissions, with special reference to universal helical motor gear reducers. It gives the basic conceptual solutions of these reducers. There is an extremely large group of mechanical transmissions and within it, a large group of gear reducers with a large variety of different conceptual solutions by which reducer manufacturers try to provide a certain advantage to their products over the competition. Within this work, the advantages and disadvantages of individual solutions are presented to point out the possible directions for their further development.

Key words: Gear reducers, Helical Gears, Mechanical transmissions.

1 INTRODUCTION

Mechanical transmissions represent one of the most exploited groups of mechanisms within mechanical engineering. They are used for the transmission of mechanical energy and movement from the driving machine to the working machine, whereby they are usually used to change the number of revolutions, and thus the torque, and only in certain cases the direction of rotation, or the position, or the direction of the axis of rotation of the output shaft. They can be divided in different ways, but they are most often divided, depending on the size of the transmission ratio, into reducers (i > 1), which reduce the rotation number, multipliers (i < 1), which increase the rotation number, and simple transmissions (i = 1), which do not change

[1] Prof. PhD. Milan Rackov, Faculty of Technical Sciences, Univ. of Novi Sad, Serbia, racmil@uns.ac.rs (CA)
[2] Prof. PhD. Siniša Kuzmanović, Faculty of Technical Sciences, Univ. of Novi Sad, Serbia, kuzman@uns.ac.rs
[3] Prof. PhD. Vojislav Miltenović, , Research Center, University of Niš, Serbia, vojamiltenovic@yahoo.com
[4] Ass. PhD. Ivan Knežević, Faculty of Technical Sciences, Univ. of Novi Sad, Serbia, ivanknezevic@uns.ac.rs
[5] Prof. PhD. Milan Banić, Faculty of Mechanical Eng., University of Niš, Serbia, milan.banic@outlook.com
[6] Prof. PhD. Aleksandar Miltenović, Faculty of Mechanical Eng., University of Niš, Serbia, amiltenovic@yahoo.com
[7] Prof. PhD. Sandor Bodzas, Faculty of Engineering, Univ. of Debrecen, Hungary, bodzassandor@eng.unideb.hu

the velocity, but only the direction of rotation, and/or the position of the axis of rotation, and/or the direction of the axis of rotation.

Only reducers will be considered here and they are further divided into ordinary reducers, where the gear ratio is constant (i = const.) and variators, where the gear ratio changes gradually ($i \neq$ const.), and gearboxes, in which the gear ratio changes stepwise ($i \neq$ const.) and which, especially today, have an extremely large application within motor vehicles. Due to the volume of the matter, only ordinary reducers will be considered in the following. [1]

Depending on the method of realisation, i.e., applied transmission elements, there are geared, friction, belt and chain reducers. Only geared reducers will be considered which can be further divided depending on the way of making the gear pairs into reducers with cylindrical, conical, worm and special gear pairs. All these reducers are used to a large extent, as well as complex reducers created by their combination, so the number of these reducers is extremely large. Only reducers with cylindrical gears will be considered further. [2]

Gear reducers can be manufactured with normal or reduced arc clearance ($\Delta\varphi<10'$), as so-called zero-backlash gear reducers, which are used in modern mechanical engineering in robotics, machine tools and military technology, as motion transmitters for accurate positioning [3]. Within this paper, they will not be considered separately, although they represent an extremely large group of transmissions. So, only normal, so-called industrial reducers will be considered. Depending on the method of use, industrial reducers are divided into universal and special. Universal ones have slightly more parts and are adapted for different shapes and positions of installation, different powers and different speeds. So they are more complex and somewhat more expensive than special reducers, which are intended for a specific purpose and do not have any redundant parts or manufacturing, but even so, for smaller series, universal reducers are cheaper than special reducers.

2 APPLICATION OF UNIVERSAL GEAR REDUCERS

Universal reducers are further divided into motor reducers, which are delivered together with the motor (as a rule, with a four-pole asynchronous electric motor, because it is still small and cheap enough and does not create big shocks when starting like two-pole motors) and gear units without electric motor with a classic input shaft. The application of motor reducers comes from the desire to avoid the need to base the electric motor and axis align of the electric motor shaft and the input shaft of the reducer, as well as the possibility of avoiding the use of a coupling between the motor and the reducer. Application of motor reducers is possible only with smaller and medium sizes of reducers because reducer housings are not able to carry large and heavy electric motors.

Universal helical motor gear reducers with external gearing are produced with coaxial, or almost coaxial, shafts and with parallel shafts. They are made as flat reducers with one-part or two-part housing. In the beginning, there was a tendency to make reducers as coaxial reducers. [3]

However, in order to increase the gear ratios, within each reducer axis height, the axial distances were increased, especially of the output pair, in order to reduce the load on the gears and other components within the reducer [3], which is why the axis was lowered of the input shaft, so as not to reduce the gear ratio of the first pair (Fig. 1).

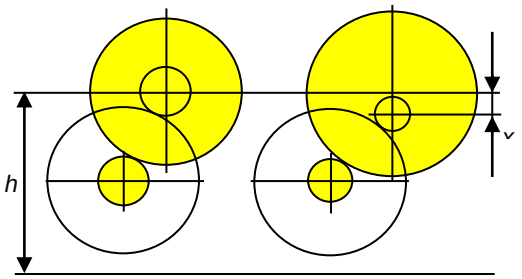

Figure 1. *Schematic explanation of leaving the classic solution of the helical two-stage gear reducer with aligned input and output shaft (1) and solution with misaligned input and output shaft which allows increasing the diameter of the output gear (2)*

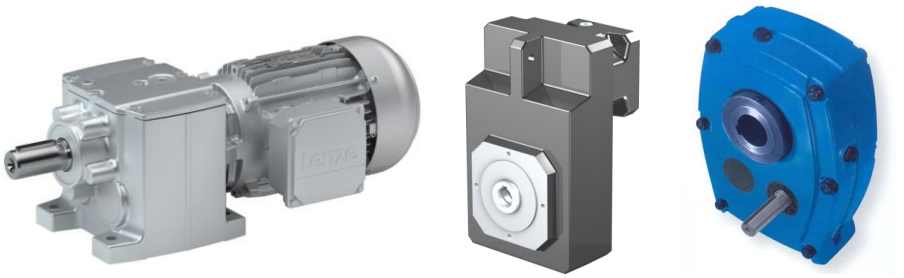

Figure 2. *Characteristic solutions of two-stage gear reducers with (1) almost coaxial shafts LENZE [6], (2) parallel shaft gear reducer with one-part housing STOBER [7] and (3) parallel shaft gear reducer with two-part housing RENOLD [8]*

Flat reducers with parallel shafts were developed to save space, so that gear reducers could be made in the form of plug-in reducers (Fig. 2-2, 2-3) [4,5]. The use of plug-in reducers avoids the classic foundation of the reducer. Although, it is still necessary to be fixed in some way to prevent its rotation. Also, there is no need to align the output shaft of the reducer and the input shaft of the working machine. Additionally, the application of a large and often expensive coupling that connects the reducer to the working machine is avoided. These are certainly the big advantages of flat-mounted reducers. They can be made in one-part and two-part housing variants. With one-piece housings, it is easier to align the opening of the bearing supports, although the assembly is much more complicated, while it is vice versa with two-part housings. In the case of plug-in reducers, a problem may arise due to the rigid connection between the motor reducer and the working machine, so, in the case of the need for an elastic connection, the electric motor is connected to the reducer by means of a belt transmission.

Gear reducers can be made as single-stage, two-stage, three-stage and multi-stage reducers depending on the required gear ratio or depending on the required speed of the output shaft. Today, all solutions are used, however, two-stage and three-stage reducers are the most implemented, because those gear ratios (revolution numbers) are most often required.

Electric motors can be joined to gear reducer in different ways. The most common

and simplest solution is when the electric motor is directly connected to the reducer and thus delivered to the customer as a motor gear reducer (Fig. 3-1). Sometimes, the customer wants to install electric motors by himself, so he wants a reducer without a motor, or to join an adapter for standard IEC motors, with a B5 or B14 flange (Fig. 3-2). This is usually when the customer is the manufacturer of electric motor and wants to use his own motors, or when the customer considers that in the event of a motor failure, he could more easily and quickly obtain a new electric motor. There are also cases when the customer, due to space limitations or the need for an elastic drive, wants a reducer where the motor is connected to the reducer using a belt transmission (Fig. 3-3). Most manufacturers today can fulfil all these customer requirements very simply.

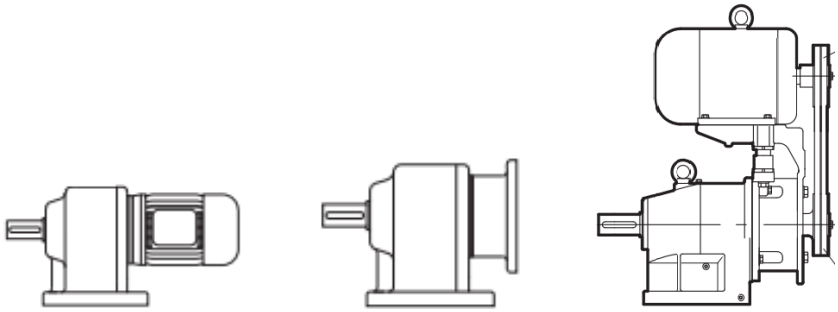

1 2 3

Figure 3. *Characteristic ways of connecting the motor and reducer (1) direct connection, (2) indirect, using an adapter for IEC motors, and (3) indirect, using a NORD belt transmission [9]*

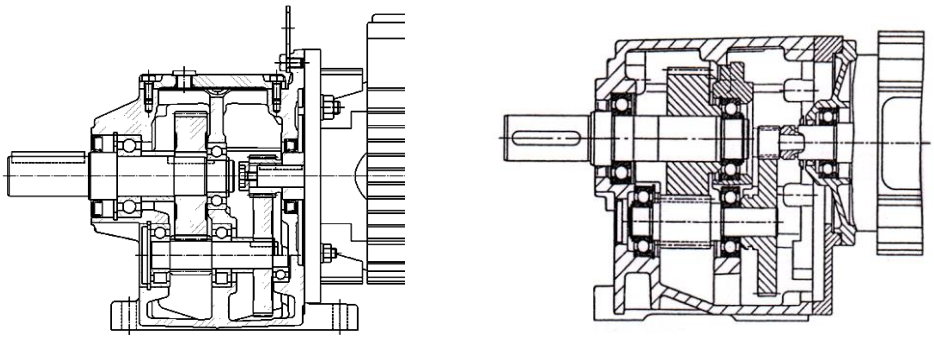

1 2

Figure 4. *Characteristic gear motor solutions (1) with standard IEC motor ROSSI [10] and (2) special gear motor LENZE [6]*

The motor gear reducers can use standard IEC motors (Fig. 4-1) or special reducer electric motors (Fig. 4-2). Special reducer electric motors have a special shape of the shaft, so they can accept the installation of smaller pinions and thus achieve higher gear ratios. [2] They have installed stronger bearings and thus can accept greater radial and axial forces that occur on the gears. They also have a better sealing solution so that direct connections between the motor and the reducer prevent oil from leaking from the reducer into the electric motor housing. In addition, reducer electric motors can be supplied with a greater number of different flanges, which enable easier connection with different sizes of reducers and provide a much more compact construction of the motor

reducer. All electric motors can be delivered with an electromagnetic brake, or only with a one-way brake, but only with less responsible constructions because the components within the reducer also affect the reliability of the system.

Motor reducers with coaxial shafts can be installed in different ways: with feet, with a small or large flange, with a mixer flange, or with feet and a flange, and all of them can be mounted in different positions (M1 to M6). [3] In order to ensure the possibility of different installation positions, the holes for filling, level control and draining oil are placed in such positions as to allow this. The breather valve is usually placed in the place of the oil filler opening. Medium and large reducers are supplied with a hanging hook to simplify the lifting and lowering of the reducers, while small reducers can be lifted and moved manually.

3 THE PROBLEM OF CHOOSING A CONCEPT WITHIN A LARGE NUMBER OF DIFFERENT SOLUTIONS

It is indisputable that the main problem with all reducer manufacturers is which concept of reducer housing to adopt. Some manufacturers make only housings for single-stage reducers and add another special single-stage reducer housing and thus build two-stage reducers, or by adding another special two-stage reducer housing, they build three-stage reducers (Concept 1). Of course, all these reducers do not have coaxial shafts, and the main advantage is given only to single-stage reducers.

Some manufacturers make housings for single-stage and two-stage reducers and, by connecting them, build three-stage and four-stage reducers. With this concept, they provide the basic advantage of their single-stage, two-stage and four-stage reducers (Concept 2).

There are many manufacturers who make single-stage reducers in their own housing and two-stage and three-stage reducers in the universal housing for two-stage and three-stage reducers. By connecting these housings, it is possible to obtain four-stage, five-stage and six-stage reducers (Concept 3). It should be pointed out that almost all large manufacturers of reducers use this concept because it enables coverage of almost the entire area of transmission ratios.

Some manufacturers produce two-stage reducers and add special single-stage housing and thereby building three-stage reducers, or add another two-stage and build four-stage gear units (Concept 4).

Some manufacturers make only two-stage and by their combination four-stage reducers. It is indisputable that their costs are very low and that they do not rationally cover the entire area of transmission ratios, but it is indisputable that in the area of two and four-speed reducers they have a great advantage over the competition (Concept 5).

There are manufacturers who make only universal housings for two-stage and three-stage reducers and in that area they achieve the greatest advantage (Concept 6). They certainly have slightly higher production costs than the previous solution, but they enable a more rational offer in the area of the most required three-stage reducers, although they do not offer gear ratios in the area of four-stage reducers.

Certainly, the reducers of the previous concept can provide a mutual connection of two-stage and three-stage universal reducers, which can also cover the area of transmission ratios of four, five and six-stage reducers, which are normally less required, but some manufacturers also offer such solutions (Concept 7).

4 PROBLEM SOLUTION

The choice of the accepted concept of the reducer largely depends on the selected area of gear ratios and torques (Fig. 5), which has to be covered with a universal gear reducer, and on the defined powers (sizes) of the connected electric motors. That area certainly depends on market requirements, existing competition, the manufacturer's plans and its technological capabilities.

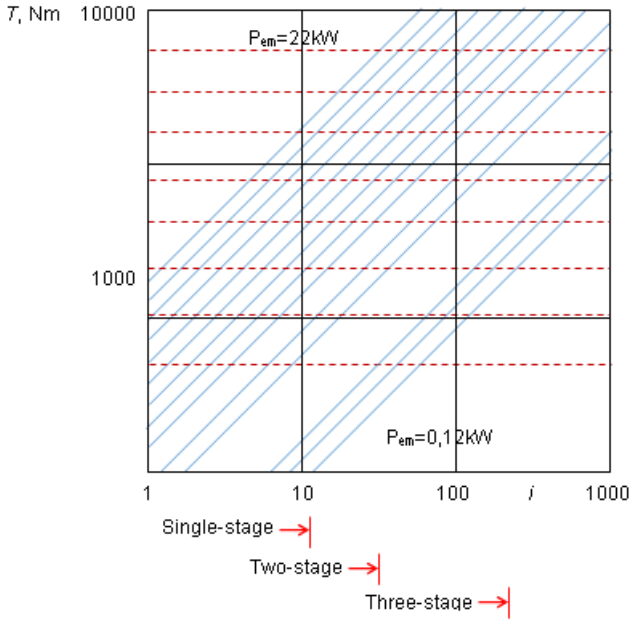

Figure 5. *Power diagram showing the torque developed by the electric motor at a certain gear ratio (number of revolutions of the output shaft) of the reducer if it is considered that the four-pole asynchronous electric motor operates with speed 1400 min^{-1}*

When adopting the nominal torque value, it should start from a projected value for a certain axis height of the reducer, which must be competitive. It is the same for all gear ratios, but the actual torque values are slightly different from the nominal value and have a different values for each ratio. They mainly depend on gear load capacity, as the most expensive components within the reducer. Since the highest value of the service factor is usually 2, the same value is adopted for the torque increase factor, i.e. $q_T = 2$, which corresponds to the standard row R20/6. Since the length factor depends on the torque increase factor $q_L = q_T^{1/3}$, it follows that the length factor increase is $q_L = 2^{1/3} = 1.25$, which means that the length measures, primarily the axis height of the reducer, should be increased according to the standard row R10 or R20/2. Previously, the row R10 (63, 80, 100, ...) was used to increase the axis height, but due to the tendency to increase the highest values of the gear ratios, the axis height was increased and the raw R20/2 (71, 90, 112, ...) is used. In the area of the most required gear ratios, some manufacturers also produce intermediate sizes so that the axis heights of the reducers, for some manufacturers, increase in the combined row of R20/2 - R20 - R20/2.

When defining the operation area of the reducer, it is calculated that each reducer covers a certain area depending on the size of the nominal torque (T_{2N}), extreme values of the service factor ($f_{B\min}$ and $f_{B\max}$) and the area of gear ratios.

If the projected values of nominal torques are adopted numbers according to the standard row R20/6, for example, numbers (50, 100, 200, 400, 800, 1600, 3200, 6300, ...), based on the diagram in Fig. 5, it can be concluded that in the area of small reducers there is no need for multi-stage reducers, while in the area of large reducers there is no need for single-stage reducers. It should be noticed that there are manufacturers who make reducers with lower load values and on account of that achieve higher gear ratios. Also, some do the opposite, and even those who are within certain axis heights have both variants of reducers, with higher and lower load capacities.

If the reducers are made according to concept 1, the main problem is that large reducer sizes need large and expensive gears, due to the large number of different gear ratios of single-stage reducers. So, this concept is recommended only for smaller reducers, while with medium-sized reducers, one-stage reducers should not be made, but only two-stage and three-stage, in which, gears from the first pair should use gears from smaller sizes of single-stage reducers.

If the reducers are made according to concept 2, it is evident that the reducers of this concept are suitable for all sizes of reducers, although their main advantage is in the area of single-stage, two-stage and four-stage reducers. In this concept, gears from single-stage reducers are used as the first pairs, in the two-stage variant.

Reducers made according to concept 3 are the most suitable because they cover the entire range of transmission ratios, and their main advantage is in the area of single-stage, three-stage, five-stage and six-stage reducers. This concept is particularly suitable for large reducers. In this concept, the same output pairs are used in the two-stage and three-stage variants, and the first pairs are adopted from single-stage reducers.

Reducers made according to concept 4 are suitable for smaller and medium sizes because they do not cover the entire range of gear ratios.

Reducers made according to concept 5 are very easy to manufacture, but they have a certain disadvantage because they do not cover the entire area of gear ratios. However, in the covered area, they can offer a cheap solution. The main priority was placed on the area of two-stage and four-stage reducers.

Reducers made according to concept 6 also represent an economical solution. Their emphasis is on three-stage reducers, although they very successfully cover the area of two-stage reducers as well.

Reducers made according to concepts 6 and 7 are very similar to reducers made according to concept 3 but without single-stage reducers. They can be partially covered by two-stage reducers, and smaller gear ratios are less often required and usually can be covered by belt transmissions. Therefore, single-stage gear reducers are not so important.

In order to achieve large gear ratios, reducer manufacturers use large driven gears, which are installed in the reducer through large openings on the top of the housing. Previously, it was impossible to install such large gears through the front openings.

5 CONCLUSION

Based on the conducted analysis, it is evident that each of the conceptual solutions applied today has its advantages and disadvantages. Large manufacturers, with the concept of reducers marked with 3, cover the entire area of gear ratios. Smaller manufacturers and, in general, the competition, want to ensure, in a certain segment of gear ratios and torques the advantage of their reducers with some of the different conceptual solutions. They mostly succeed in this, so they can remain on the market, although the competition is extremely strong. There are many manufacturers because universal motor gear reducers with helical gears are relatively simple products and relatively easy to make.

It is interesting that none of the reducer manufacturers has tried to make gear reducers in a universal housing for single-stage and two-stage reducers, which could be connected to make three-stage and four-stage reducers. These reducers, of course, would not be with coaxial shafts, but they would be relatively simple to manufacture and would probably be required in the reducer market of small gear units.

REFERENCES

[1] Rackov, M., Knežević, I., Čavić, M., Penčić, M., Čavić, D., Kuzmanović, S., Design Solutions Overview of Universal Motor Gear Drives with Helical Gears. *Proceedings of the 10th International Symposium on Graphic Engineering and Design (GRID 2020)*, Novi Sad, Serbia, 12-14 November 2020, p.p. 597-608.

[2] Kuzmanović, S., Miltenović, V., Rackov, M. (2020) Innovative design solutions of universal motor gearbox with helical gears. *International Scientific Journal Machines. Technologies. Materials*., ISSN 1313-0226, vol.14, no. 4, p.p. 137-141.

[3] Rackov, M., Kuzmanović, S., Blagojević, M., Đorđević, Z. (2019). *Motor Gear Reducers with Cylindrical Gears (in Serbian)*. Faculty of Technical Sciences, Novi Sad.

[4] Rackov, M., Kuzmanović, S., Knežević, I., Čavić, M., Penčić, M., Algin, V.B., Starzhinsky, V.E., Shil'ko, S.V. (2020). Design Solutions Overview of Single-Stage Universal Gear Reducers. *MATEC Web of Conferences*, ISSN: 2261-236X, vol. 317, no. 1, p.p. 01005-1–01005-10.

[5] Rackov, M., Knežević, I., Kuzmanović, S., Čavić, M., Penčić, M., Analysis of Housing Models of Modern Two-Stage Universal Gear Reducers. *Proceedings of the 4th International Scientific Conference on Mechanical Engineering, Technologies and Applications (COMETa 2018)*, Jahorina, B&H, 27-30 November 2018, p.p. 450-457.

[6] Lenze, L-force, Geared Motors, Effizient un passgenau, 01/2020, Version 1.2 de

[7] SMS/MGS Gearunits, Catalogue 11, STÖBER Antriebstechnik GmbH & Co. KG

[8] https://www.renold.com/products/gears-gearboxes/

[9] NORD Drivesystems, Standard Helical Gearboxes, G 2018, Getriebebau Nord, Hamburg

[10] Rossi parallel shaft gear reducers catalogue, 004BRO.GPR-de1105HQR

COMETa 2022
6th INTERNATIONAL SCIENTIFIC CONFERENCE
17th - 19th November 2022
Jahorina, B&H, Republic of Srpska
University of East Sarajevo
Faculty of Mechanical Engineering
Conference on Mechanical Engineering Technologies and Applications

MEZZANINE FLOORS AS A PART OF RACKING SYSTEM

Rodoljub Vujanac[1], Nenad Miloradovic[2], Snezana Vulovic[3]

Abstract: Mezzanine floors are additional floors above the ground floor slab level that multiplying the surface area and enabling it to be fitted out as an additional storage area, workshop or walkways. They can be free standing or attached to the building structure or racking system. The installation of a mezzanine is an ideal solution to maximize the space available by taking advantage of the height of the building. Mezzanine floors are usually totally dismountable and re-usable, and their structure, dimensions and location are easily modified to achieve the specific needs of the client. In this paper special consideration was given to the conditions on the mezzanine floor directly supported by the shelf or rack uprights or complemented with a variety of racking and shelving system.

Key words: Mezzanine, Pallet Racking, Regulation, Standard, Warehouse

1 INTRODUCTION

As businesses grow and expand, there is always the problem of limited space. In the past, the solution was to rent, purchase or build a new property. Beside the lack of the free space, adding infrastructure and building is a major investment and can tie up significant funds. The lower cost option to space expansion can be a mezzanine floor, also called mezzanine platform, or simply mezzanine or platform. It becomes cost-effective method for adding extra, valuable space at an extremely low cost. A mezzanine floor (or floors) is an intermediate floor between main floors of a building or between the ground floor and the ceiling, and therefore does not count as one of the floors in a building. So, mezzanine level flooring utilizes the otherwise unused vertical space below the ceiling and above the floor providing extra, affordable space with minimal investment. The word mezzanine comes from Italian “mezzo” which means “middle". Mezzanine floors may serve a wide variety of functions as shown in figure 1, from the primary purpose to provide extra space for storage, they are also used for manufacturing and

[1] Ph. D., Rodoljub Vujanac, Faculty of Engineering University of Kragujevac, Kragujevac, Serbia, vujanac@kg.ac.rs
[2] Ph. D., Nenad Miloradovic, Faculty of Engineering University of Kragujevac, Kragujevac, Serbia, mnenad@kg.ac.rs
[3] Ph. D., Snezana Vulovic, Institute for Information Technologies, University of Kragujevac, Kragujevac, Serbia, vsneza@kg.ac.rs

assembly operations, distribution, modular office space, and the expansion of retail space. The normal design for a mezzanine floor is just a part of the flooring of a building, usually less than a half of available area. Surely the uses and configurations of mezzanine floors vary depending on the goals and objectives of an end user. The many styles and varieties of mezzanine floor can be added to any type of building. Sometimes they are not required to be attached to the walls or ceiling which means they can be completely freestanding. Access of the personnel to the each floor is achieved by stairs or integrated lifts while the goods are lifted onto the platform usualy by a forklift or by means of some conveyor systems, possibly by means of an vertical conveyor (lifter) [1]. People on the mezzanine floor are further protected by placing the sides' railings that meet all current European standards and regulations. Beside the discussion on all types and constructions of mezzanine floors, this paper deals in more details with rack or shelves supported mezzanine floor.

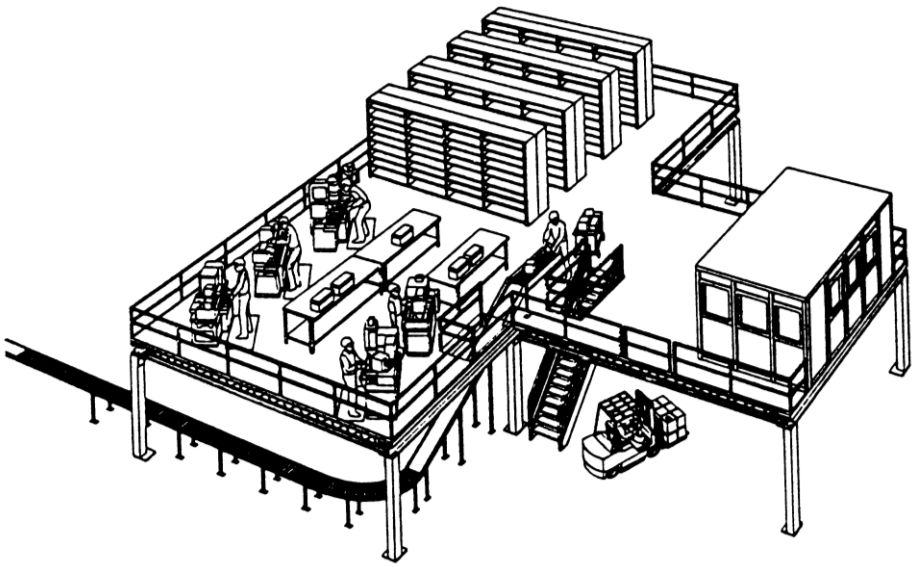

Figure 1. *Mezzanine floor [2]*

2 MEZZANINE FLOOR CLASSIFICATION

Mezzanine floors can be classified according to the following criterias:

- Application,
- Type of the mezzanine decking/flooring,
- Type of the structure and design.

2.1 Mezzanine Floor Application

Designs of mezzanine floors can be classified by their use. Storage is one of the most common use of a mezzanine floors, figure 2 a). A storage mezzanine offers flexibility to make adjustments through added shelving or racking and/or block stacking. Sometimes businesses will use one level of the mezzanine floors for the purpose of additional office space, i.e. for the modular offices and/or extra locker rooms for employees, figure 2 b). Mezzanines are often used in retail to increase the selling space and or the storage back of store, figure 2 c). Access points, staircases, railings and

gates are designed in such a way as to allow the movement of operators and goods, ensuring high safety standards. Other mezzanine uses include increasing space for production, packing, sorting etc. like shown on figure 2 d).

(a)

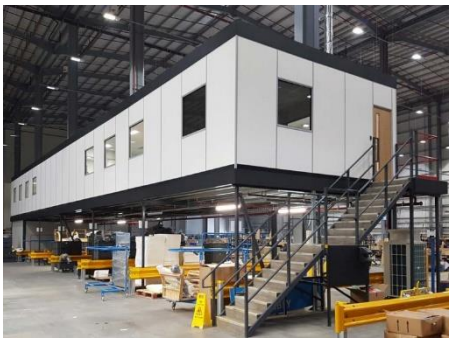

(b)

(c)

(d)

Figure 2. *Mezzanine floor application: a) warehouse, b) offices , c) retail, d) workshop.*

2.2 Mezzanine Flooring

The quality and adequate usage of a mezzanine depends primarly on choosing the correct flooring type. The flooring, on the other hand, depending on the means of handling and usage, can be provided by mezzanine manufacturers as following [3]:

a) ***Metal grating*** are usually made of steel or aluminium bars or sheets joining to form a strong anti-slip grid according to the required measures which allow passage of lights, air or liquid from anti-fire system.

b) ***Steel checked plate*** flooring made of thick sheet metal supported directly by steel tube or I, H beams is ideal for large, heavy storage racks, equipment storage or constant traffic.

c) ***Metal profiled patterned*** flooring made of steel or aluminium sheets can be with closed or punched surface. Due to the patterned surface, the structure of profile is more solid, in addition to its anti-slip effect. The characteristic holes pattern in case of punched surface, even assuring the appropriate light and/or air passage is maintaining the high structural rigidity.

d) ***Wood or playwood mezzanine flooring*** similar in term of installation with steel checked plate due to its beauty, warmth, and elegance is suitable for offices or retail space. But that does not exclude their application in the storage of goods too because of their slip resistant, good load strength and cost effectiveness.

e) ***Laminated panel floorig*** has a plywood structure substrate with a textured high density polyethylene (HDPE) face. It is ideal for environments where there is constant and continuous wheel or foot traffic due to its abrasion resistance because of its thick poly laminate finish that disperses weight evenly.

f) ***Resin composite flooring*** which can be worked much like wood is able to hold up to the abuse of pallet jacks, carts, dollies, and other heavy traffic.

g) ***Concrete flooring*** can be used in humid manufacturing and warehousing conditions with intensive mechanical traffic, heavy loads with potentially wet, combustible or volatile materials. Adventages are high load capacity, durability and longevity and disadvantegs are immobility and cost.

2.3 Mezzanine Structure

According to its supported structure mezzanine floor can be attached to the walls or ceiling of the building, to be completely freestanding or rack supported. Thus, without or with supporting steel columns (1) or racking columns/frames, other main mezzanine elements are as shown in figure 3: secondary beam (2), primary or main beam (3), buckling support (4), vertical bracing (5), mezzanine flooring/decking (6), uniformly distributed load (7), concentrated load (8), material handling equiment (9). Beside these main elements mezzanine floor accessories can be staircases (10), handrails (11), pallet transfer system (12), collision safety device (13), etc...

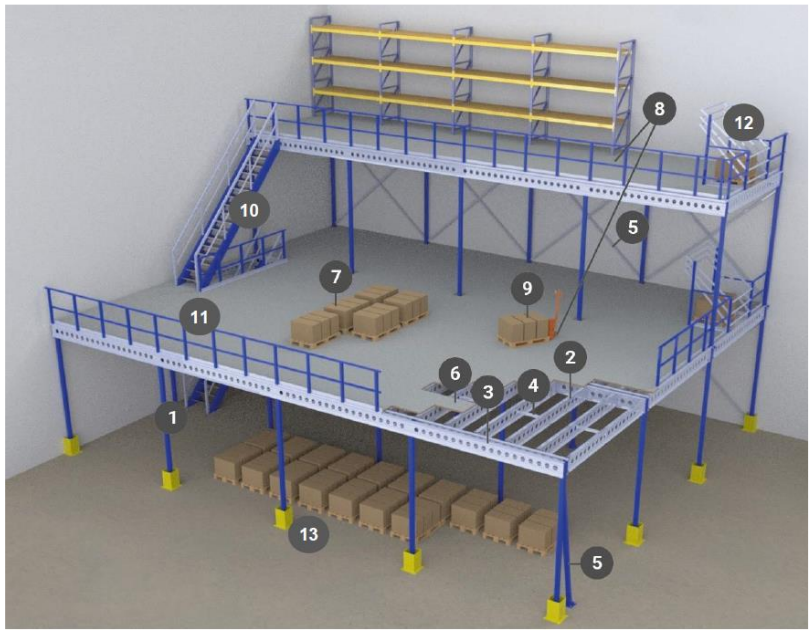

Figure 3. *Elements of mezzanine structure*

Most of the steel mezzanine parts are made from hot-rolled steel or cold-rolled sheet metal. Depending on the purpose the entire structure of the mezzanine floors can be [4]:

- Up to 12 m span lengths between supports;
- Up to 5 levels and more can be realised;
- Up to 2 t/m^2 load capacity;
- Completely bolted construction, expandable and easy to relocate at any time;
- With rack systems on the steel platform (highly concentrated loads);
- Can be driven over with electric lift truck (dynamic loads);
- Different shapes and layouts.

3 RACK SUPPORTED MEZZANINE FLOOR

Rack or shelf supported mezzanine floors are fully or partially supported by structures of racking or shelving system. As shown on the figure 4 the closely spaced upright frames or beam levels that supports the mezzanine floor provides a load capacity that exceeds other mezzanine structural designs above mentioned. Primarly use of rack supported mezzanine floor is extra storage area both for block stacking and/or aditional racking and/or shelving system. The exceptional strength of rack supported mezzanine floor provides in some cases an opportunity for the use of electric fork lift trucks.

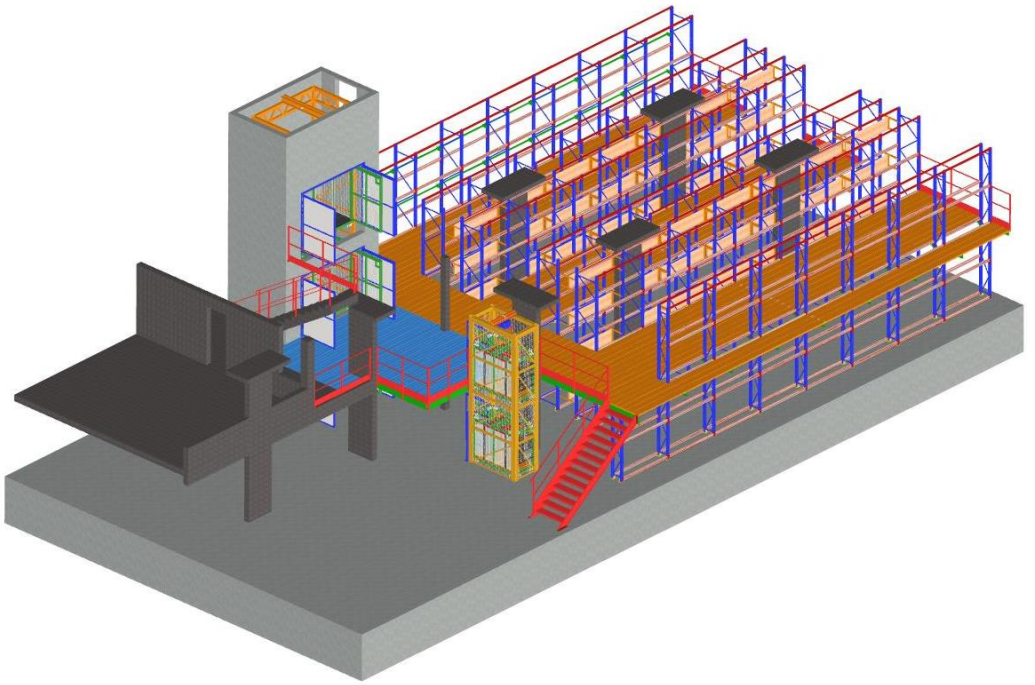

Figure 4. *Rack supported mezzanine floor [4]*

Figure 5 shows examples of a rack or shelf supported mezzanine or walkway floors.

The following additional information shall be provided by the specifier for floors that are supported by storage equipment, such as floors over racks or shelving suspended walkways and mezzanines [5]:

a) intended use of the floor, e.g. for office, storage, walkway, etc.;
b) maximum uniformly distributed load over the floor area not occupied by storage equipment;
c) maximum local loads that can occur, e.g. at lift truck loading and/or unloading areas;
d) maximum concentrated loads may be caused by wheeled traffic such as pallet trucks or trolleys or by shelving standing on the floor decking (see below) imposed on the floor or mezzanine;
e) additional requirements such as anti-slip, wear and tear resistance, ceiling light reflection etc.;
f) requirement imposed due to fire safety regulations.

Special consideration must be given to the point load conditions on the mezzanine floor of figure 5 (b) where the shelf or rack uprights on the mezzanine floor are not directly supported by the shelf or rack uprights of the mezzanine floor structure. The point loads imposed on the mezzanine floor decking can be relatively high and load spreaders may be necessary [5].

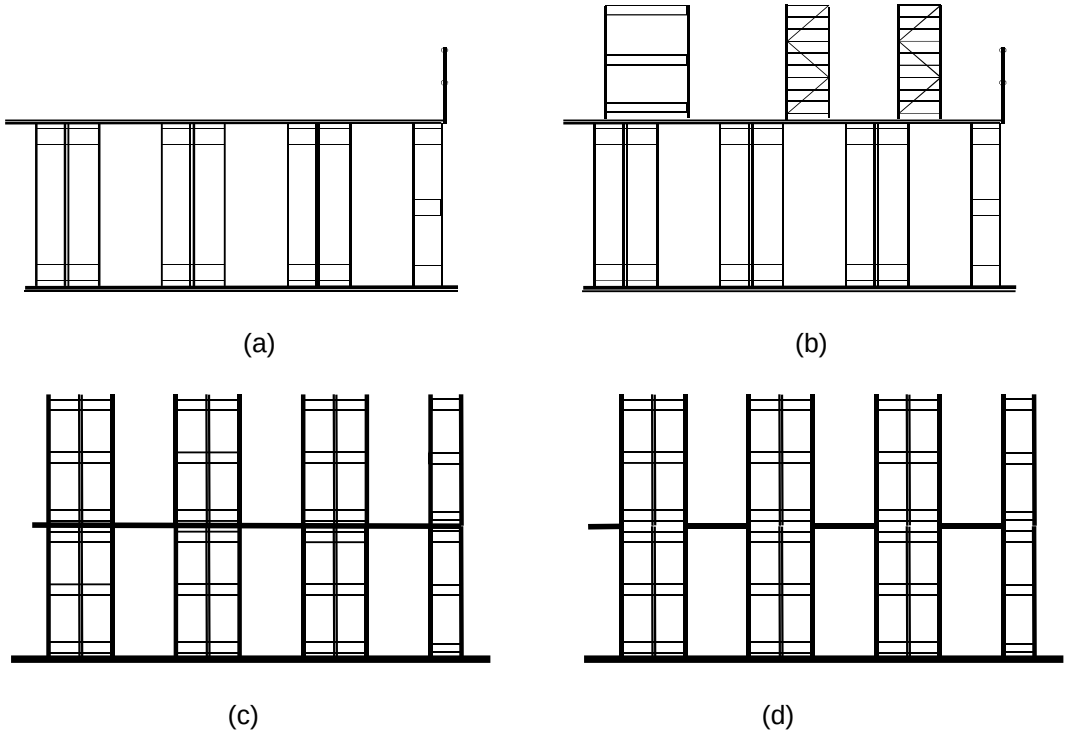

Figure 5. *Rack supported floor: a) over-rack mezzanine floor, b) over-rack mezzanine floor supporting shelving, c) multi-tier shelf racking d) walkways suspended between the upright frames [5]*

4 CONCLUSION

The many different options of mezzanine floors are a quick way to gain additional space at height of the building without having to make costly structural changes to the floor area. Attached to the walls, ceiling or racking structure, or completely freestanding on steel columns they provide optimal utilisation of the entire height of the building for the additional storage space, production or assembly area, office premises or selling space. That means the construction of a mezzanine floor primrarly is dependent on how the mezzanine will be used. Mezzanine floor structure designed to solve the problem of usage of additional space in warehouse with racking system is able to assemble to various racking levels. The benefit of this type of mezzanines is that they are designed for very easy, fast assembly and made with specially engineered components that quickly joined together wtih racking system to form a strong and secure spatial structure. Another advantage is that they are designed for heavy duty loads. Only one special consideration must be given to the concntrated loads when the shelf or rack uprights on the mezzanine floor are not directly supported by the shelf or rack uprights of the mezzanine floor structure.

LITERATURE

[1] Vujanac, R., Slavkovic, R., Miloradovic N., Blagojevic M. (2013). Vertical Reciprocating Conveyor as a Part of Fully Automated Multi Depth Pallet Rack Storage System, *Proceedings – 11th International Conference on Accomplishmnets in Electrical and mechanical Engineering and Information technology DEMI 2013*, p.p. 1105–1112.

[2] FEM 10.2.03: SPECIFIER'S CODE - Guidelines for Specifier's of Static Steel Racking and Shelving, *Section X of FEM, 2000.*

[3] Industrial Quick Seaech Articles, http:// www.iqsdirectory.com/articles/mezzanine/mezzanine-floor.html, accessed on 19.10.2022.

[4] IC INZENJERING D.O.O., Technical Handbook of Steel Mezzanine Floor, 2020.

[5] EN 15629:2008. Steel static storage systems - Specification of storage equipment, *European Sommittee for Standardization, 2008*.

COMETa 2022
6th INTERNATIONAL SCIENTIFIC CONFERENCE
17th - 19th December 2022
Jahorina, B&H, Republic of Srpska
University of East Sarajevo
Faculty of Mechanical Engineering
Conference on Mechanical Engineering Technologies and Applications

DETERMINING THE NUMERICAL VALUES OF THE POTENTIAL AT THE MEASURING POINTS

Snežana Vulović[1], Miroslav Živković[2], Rodoljub Vujanac[3], Ana Pavlović[4], Marko Topalović[5]

Abstract: In order to calibrate material parameters, a comparison of experimentally measured values and numerically predicted values is necessary. With complex FEM models, it is often impossible to create a mesh where the node of the element coincides with the position of the measuring point. The paper presents the procedure for determining the numerical values of the potential at the location of the measuring point. The first step is determining the element in which the measuring point is located and calculating the local coordinates of the measuring point in the element. The program (PAK-V) loads a file that contains the label of the measuring point, the element in which the measuring point is located and the local coordinates. Numerical values at the measuring points are calculated based on the nodal values of the element and the local coordinates. These extrapolated values are afterwards printed in a separate file for easier comparison with the measured values. After several iterations material parameters are obtained that accurately simulate geomechanical properties of a dam surroundings, facilitating structural analysis.

Key words: extrapolation, local coordinates, finite element, measuring point

[1] PhD, Snežana Vulović, Institute of Information Technologies (CA), University of Kragujevac, Kragujevac, Srbija, vsneza@kg.ac.rs
[2] PhD, Miroslav Živković, Faculty of Engineering, University of Kragujevac, Kragujevac, Srbija, miroslav.zivkovic.mfkg@gmail.com
[3] PhD, Rodoljub Vujanac, Faculty of Engineering, University of Kragujevac, Kragujevac, Srbija, rvujanac@gmail.com
[4] PhD, Ana Pavlović, Department of Industrial Engineering, University of Bologna, Bologna, Italy, ana.pavlovic@unibo.it
[5] PhD, Marko Topalović, Institute of Information Technologies, University of Kragujevac, Kragujevac, topalovic@kg.ac.rs

1 INTRODUCTION

Dams are objects that by their nature carry a certain risk, a potential danger to the surrounding area. That risk can never be completely removed, so the question of the safety of the dam, as well as the associated facilities, is of utmost importance. The safety of the dam implies that the dam is always in a condition in which it can fulfil all its designed functions without adverse consequences for people, the environment or property. Over time the exploitation conditions of the dam vary as the characteristics of the materials from which the objects were built, and the properties of the geotechnical environments upon which the objects were built change. Also, over time, the professional and social views of the safety criteria and risks (hydrological, seismotectonic, and others), evolve with occasional changes in standards and legal norms. Practically, the safety of dams is managed during their entire operational life.

During the construction, in order to monitor the condition of the dam and facilities, a system of technical observation is designed with a significant number of various instruments and measuring tools. The aim of data collection is to ensure relevant information on which identification and timely detection of the process that can cause threaten the security of the dam and facilities. The technical observation system changes and evolves during time. In recent years, the safety management system (SMS) for dams was formed with the aim of combining and standardizing collection, acquisition, archiving, processing and using data on technical observation.

The concept of dam safety management implies a series of procedures that are physically based, and supported with software system, which will ensure collection of the all data that are important for determination of current dam condition. Analysis of these data means engineering interpretation through mathematical models of relevant processes that are crucial for dam safety. Based on the conclusions of these predictive models, appropriate measures are adopted and implemented [1].

As a part of the dam SMS for filtration analysis and the stress-strain analysis, a finite element (FE) model of the dam and the surrounding rock mass is created. Inclusion of the position of measuring points in the FE model (i.e. matching the position of the measuring point with the FE node), results in the significant increase of the number of elements and nodes of the model. Also, the position of all of the measuring points at the time of the model creation is unknown, or the new measuring points are subsequently added. For these reasons, the process of calculating the numerical value (potential, strain...) when the position of the measuring point does not match the node in the model was developed, which is presented in this paper.

2 NATURAL COORDINATE SYSTEM IN TETRAHEDRAL ELEMENTS

The Finite Element Method (FEM) is the most common numerical methods that has implementation in almost all areas of science and technology. The basic idea of the FEM analysis is a spatial domain discretization to the subdomains on which the general laws of the continuum mechanics and numerical mathematics apply. These subdomains are terminologicaly denoted as the Finite Elements. The analysis of the system of coupled Finite Elements, obtained by discretizing continuum, enables the numerical simulation of the continuum response to the given excitation. The physical values included in the model are obtained in discreet form, i.e. in points derived from the discretization. These points are called nodes. Based on discretization of physical problem, and implementation of interpolation functions, with the introduction of natural (local) coordinate system, equilibrium equations are established for elements, and stored in the matrix form. Subsequently, element matrices are combined into a system

matrix for the entire structure. Characteristic of the natural coordinate system is that it is tied to the element, that the coordinate origin is in the center of the element and that the coordinates of the nodes are 1 or -1 [2-3].

A three-dimensional (3D) finite element is used for modelling three-dimensional bodies of general shape. A three-dimensional finite element can have a different number of nodes - the usual number is from 8 to 21. For modelling complex, irregular shapes, tetrahedral finite elements with midside nodes are used. Figure 1 shows a tetrahedral element with midside nodes with an arbitrary position of the Measuring Point (M_P).

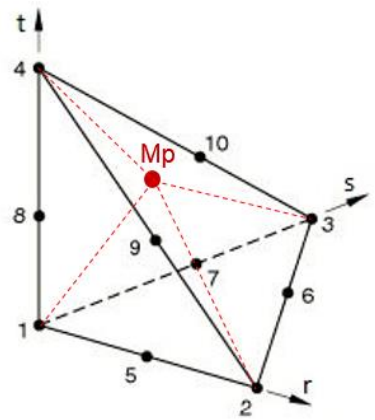

Figure 1. *Tetrahedral element with 10 nodes and the arbitrary position of the measuring point*

Geometry interpolation functions have the following form:

$$\mathbf{x} = \begin{Bmatrix} x_1 \\ x_2 \\ x_3 \end{Bmatrix} = \begin{Bmatrix} x \\ y \\ z \end{Bmatrix} = \mathbf{HX}\,, \tag{1}$$

where: $\mathbf{x}$ represents the coordinate vector of the material point in the element; while $\mathbf{H}$ is the interpolation matrix. Vector of node coordinates $\mathbf{X}$ is given with:

$$\mathbf{X}^T = \lfloor X_1\ Y_1\ Z_1\ X_2\ Y_2\ Z_2 .....X_N\ Y_N\ Z_N \rfloor. \tag{2}$$

For the interpolation matrix:

$$\mathbf{H} = \begin{bmatrix} h_1 & 0 & 0 & h_2 & 0 & 0 & ..... & h_N & 0 & 0 \\ 0 & h_1 & 0 & 0 & h_2 & 0 & ..... & 0 & h_N & 0 \\ 0 & 0 & h_1 & 0 & 0 & h_2 & ..... & 0 & 0 & h_N \end{bmatrix}, \tag{3}$$

the interpolation functions for the tetrahedral finite element are given in the Table 1.

Table 1. *Interpolation functions for the tetrahedral finite element*

		$i=5$	$i=6$	$i=7$	$i=8$	$i=9$	$i=10$
h_1	$1-r-s-t$	$-\frac{1}{2}h_5$		$-\frac{1}{2}h_7$	$-\frac{1}{2}h_8$		
h_2	r	$-\frac{1}{2}h_5$	$-\frac{1}{2}h_6$			$-\frac{1}{2}h_9$	
h_3	s		$-\frac{1}{2}h_6$	$-\frac{1}{2}h_7$			$-\frac{1}{2}h_{10}$
h_4	t				$-\frac{1}{2}h_8$	$-\frac{1}{2}h_9$	$-\frac{1}{2}h_{10}$
h_5	$4r(1-r-s-t)$						
h_6	$4rs$						
h_7	$4s(1-r-s-t)$						
h_8	$4t(1-r-s-t)$						
h_9	$4rt$						
h_{10}	$4st$						

The coordinates of the measuring point M_P (x, y, z) can be expressed using the coordinates of the element in which it is located, according to the equation (1), as:

$$\begin{aligned} x &= (1-r-s-t)X_1 + rX_2 + sX_3 + tX_4 \\ y &= (1-r-s-t)Y_1 + rY_2 + sY_3 + tY_4 \\ z &= (1-r-s-t)Z_1 + rZ_2 + sZ_3 + tZ_4 \end{aligned} \quad , \tag{4}$$

where $X_1, Y_1, Z_1;\ X_2, Y_2, Z_2;\ X_3, Y_3, Z_3;\ X_4, Y_4, Z_4$ are the coordinates of the nodes of the tetrahedral element (Figure 1.), while r, s, t are the local coordinates of the measuring point M_P given by the equations 5-7:

$$r = \frac{\left\{\begin{array}{l} x\left[Z_1(Y_3-Y_4)+Z_3(Y_4-Y_1)+Z_4(Y_1-Y_3)\right]+X_1\left[Y_3(Z_4-z)+y(Z_3-Z_4)+Y_4(z-Z_3)\right]+ \\ X_3\left[Y_4(Z_1-z)+y(Z_4-Z_1)+Y_1(z-Z_4)\right]+X_4\left[Y_3(z-Z_1)+y(Z_1-Z_3)+Y_1(Z_3-z)\right] \end{array}\right\}}{\left\{\begin{array}{l} X_2\left[Z_1(Y_3-Y_4)+Z_3(Y_4-Y_1)+Z_4(Y_1-Y_3)\right]+X_1\left[Y_3(Z_4-Z_2)+Y_2(Z_3-Z_4)+Y_4(Z_2-Z_3)\right]+ \\ X_3\left[Y_4(Z_1-Z_2)+Y_1(Z_2-Z_4)+Y_2(Z_4-Z_1)\right]+X_4\left[Y_3(Z_2-Z_1)+Y_2(Z_1-Z_3)+Y_1(Z_3-Z_2)\right] \end{array}\right\}} \tag{5}$$

$$s = \frac{\left\{\begin{array}{l} x\left[Z_1(Y_4-Y_2)+Z_2(Y_1-Y_4)+Z_4(Y_2-Y_1)\right]+X_1\left[Y_2(z-Z_4)+y(Z_4-Z_2)+Y_4(Z_2-z)\right]+ \\ X_2\left[Y_4(z-Z_1)+y(Z_1-Z_4)+Y_1(Z_4-z)\right]+X_4\left[Y_2(Z_1-z)+y(Z_2-Z_1)+Y_1(z-Z_2)\right] \end{array}\right\}}{\left\{\begin{array}{l} X_2\left[Z_1(Y_3-Y_4)+Z_3(Y_4-Y_1)+Z_4(Y_1-Y_3)\right]+X_1\left[Y_3(Z_4-Z_2)+Y_2(Z_3-Z_4)+Y_4(Z_2-Z_3)\right]+ \\ X_3\left[Y_4(Z_1-Z_2)+Y_1(Z_2-Z_4)+Y_2(Z_4-Z_1)\right]+X_4\left[Y_3(Z_2-Z_1)+Y_2(Z_1-Z_3)+Y_1(Z_3-Z_2)\right] \end{array}\right\}} \tag{6}$$

$$t=\frac{-\left\{\left[X_3(Y_1-Y_2)+X_1(Y_2-Y_3)+X_2(Y_3-Y_1)\right]\left[X_2(Z_1-z)+X_1(z-Z_2)+x(Z_2-Z_1)\right]-\right.}{\left.\left[X_2(Y_1-y)+X_1(y-Y_2)+x(Y_2-Y_1)\right]\left[X_3(Z_1-Z_2)+X_1(Z_2-Z_3)+X_2(Z_3-Z_1)\right]\right\}}$$
$$\frac{\left\{-\left[X_4(Y_1-Y_2)+X_1(Y_2-Y_4)+X_2(Y_4-Y_1)\right]\left[X_3(Z_1-Z_2)+X_1(Z_2-Z_3)+X_2(Z_3-Z_1)\right]\right\}}{\left\{+\left[X_3(Y_1-Y_2)+X_1(Y_2-Y_3)+X_2(Y_3-Y_1)\right]\left[X_4(Z_1-Z_2)+X_1(Z_2-Z_4)+X_2(Z_4-Z_1)\right]\right\}} \quad (7)$$

2.1 Algorithm for determination of local coordinates

In order to determine the exact element in the whole model in which a measuring point is located, and to determine local coordinates of that measuring point, Application Programming Interface (API) for program Femap [4] was developed. The algorithm for determining local coordinates is shown in the Figure 2.

When the model of the dam and the surrounding rock mass is completed, another file is loaded that contains the positions of the measuring points. When the API is started, the user must first select the measuring points and the appropriate elements in the model. API then determines in which element in the model the measuring point is located. Based on the coordinate of nodes, the volume of the element is calculated, and the volume of »virtual« elements formed with the measuring point and the nodes of the observed element (nodes 1,2, 3,4), Figure 1. are calculated.

»Virtual« elements are: 1,2,3,M_P; 1,3,4,M_P; 1,2,4,M_P and 2,3,4,M_P. If the measuring point is located in the observed element, local coordinates are calculated according to Eqs. (5-7). API creates ASCII file PIJEZ.DAT that has an ID of measuring point, ID of element, and local coordinates of the measuring point in the element.

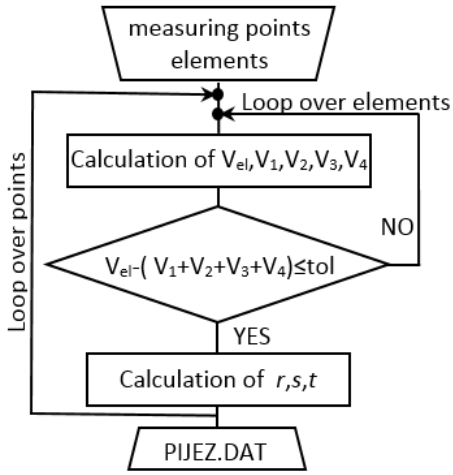

Figure 2. *Algorithm for calculation of the local coordinates*

3 CALCULATION OF POTENTIAL

The PAKV program [5] is used for the analysis of groundwater flow through porous materials. The PAKV program has been modified to calculate and print potential values at the measuring points, Figure 3. PAKV loads the input file pakp.dat from which it reads the identifier for (not) reading the measuring points, i.e. PIJEZ.DAT

file. In the PAKV program, in the phase of printing the results, the potential at the measuring point is calculated by extrapolation based on the nodal values of the potential in the element and the local coordinates of the measuring point according to equation (1). The potential values at the measuring points are printed in the file pijeznivoPAK.csv. Numerically calculated values are compared with measured values and the model is calibrated, i.e. correction of the filtration coefficients in the model with the aim of obtaining the best match between measured and numerically obtained values.

Figure 3. *Flow chart of the program PAKV*

4 CONCLUSIONS

The presented procedure was developed for the Đerdap dam model. Dam and surrounding rock mass are modeled with 3D tetrahedral elements. During the creation of the finite element model, the position of the measuring points was not considered. When the model was completed, the API was used to determine the final element in which the measuring point is located and to determine the natural (local) coordinates of the measuring point in the element; an ASCII file is created, which is one of the input files for the PAKV program. Using the extrapolation, the PAKV program calculates the potentials at the measuring points.

ACKNOWLEDGEMENTS

This research is supported by the Ministry of Education, Science and Technological Development, Republic of Serbia, Grant TR32036 and 451-03-9/2021-14/200378.

This research was promoted by the Central Europe Initiative as a part of the project ATC EVO technology transfer action.

REFERENCES

[1] Institut za vodopriverdu “Jaroslav Černi”, SUB HE “Đerdap”
[2] M. Kojić, R. Slavković, M. Živković, N. Grujović, (2010) *Metod konačnih elemenata 1 – Linearna analiza*, Kragujevac: Univerzitet u Kragujevcu, Mašinski fakultet.
[3] K. Bathe, (2006) *Finite element procedures*, Prentice Hall: Pearson Education, Inc,.
[4] Siemens Digital Industires Software Inc. Femap API reference version 12.
[5] M. Živković, S. Vulovic, N. Busarac, M. Kojić, R. Slavković, N. Grujović PAKV – program for analysis fluid flow through porous media

COMETa 2022
6th INTERNATIONAL SCIENTIFIC CONFERENCE
17th - 19th November 2022
Jahorina, B&H, Republic of Srpska
University of East Sarajevo
Faculty of Mechanical Engineering
Conference on Mechanical Engineering Technologies and Applications

IMPLEMENTATION OF MATHEMATIC MODELS IN DESIGN AUTOMATION

Miloš Matejić[1], Marija Matejić[2], Ljubica Mudrić-Staniškovski[3], Ivan Miletić[4]

Abstract: In this paper will be given an example of a mathematical model implementation in the design automation process. The introductory part of the paper shows the current commercial solutions for design automation. The critical overview of this field is given all along with the good and bad sides of design automation. The practice example of design is chosen for this investigation. Before the design model is made, the design is translated to mathematics parameters and the algorithm for user communication is solved. Special attention to the user communication interface is paid to minimize errors that can happen by human mistakes. The paper concludes with mathematical model advances in design automation as well as the bad sides of this approach. Also, further research directions are pointed out.

Key words: mathematic modelling, problem formulation, design automation

1 INTRODUCTION

Nowadays, the industry is growing very fast and as a consequence of that, it is faced with a new generation of fully digitalized production companies. With development of process automation and internet of things industry started to growing even faster. With those new features the today's industry is called Industry 4.0. The digitalization and automation ensures industry and its competitive development in modern conditions. One of the most important part of industry digitalization is communication between customers and manufacturing facilities via product developers and product designers. Today, many products, especially the families of products, can be automatically designed and put to manufacturing automatically between customers and production design automation systems. In this modern systems the role of product

[1]PhD, Miloš Matejić, University of Kragujevac Faculty of Engineering, Kragujevac, Serbia, mmatejic@kg.ac.rs (CA)
[2] PhD, Marija Matejić, University of Priština with temporary settlement in Kosovska Mitrovica Faculty of Technical Sciences, Kosovska Mitrovica, Kosovo, marija.matejic@pr.ac.rs
[3] MsC, Ljubica Mudrić-Staniškovski, University of Kragujevac Faculty of Engineering, Kragujevac, Serbia, ljubica.mudric.staniskovski@fink.rs
[4] PhD, Ivan Miletić, University of Kragujevac Faculty of Engineering, Kragujevac, Serbia, imiletic@kg.ac.rs

developer-product designer is to make an automatic bridge between customers and company production facilities. These systems are very suitable for typical products such as: furniture, transportation systems, process equipment, workshop tools etc.

Automation in CAD design assembly process is very interesting since first CAD packages appeared. *Dinev* et. al [1] has presented in their investigation how the components of an assembly are automatically related in function of chosen assembly variant. On the other investigation *Dinev* [2] went further and showed how the FEM analyses can be automatically performed. *Tarkian* [3] in his PhD dissertation showed examples of optimization in design automation in order to gain fast and optimal solution for the problem of frame loader. A very interesting research about design automation [4] was shown by giving examples of automation of design of transport aircraft, industrial robots, and micro air vehicles. Some authors went further from design automation and tried to get fully automated design drawings, [5]. Design automation can also be based on modular blocks of the design, [6]. Some CAD packages are not parametric base yet, so the easiest automation which can be done there is commands by scripts [7]. This is mostly AutoCAD related. An interesting design automation problem is shown in paper [8], which present how the curves of the second order can be automatically designed. Special attention is given to communication between CNC machines and designer in order to create a special bridge to accelerate manufacturing. Investigation like this is shown in the paper [9], and these examples was feature based from model to manufactured part. The communication between different design users which can accelerate design automation is shown in the paper, [10]. The interesting problem is applying a configurators in the design automation, which is shown in papers, [11]. An interesting review paper shows [12] how far is field of configurators went. The latest research in this field are data driven automation which accelerates the design process in big amount, [13-15].

An example of an automated design example is shown in this paper. The aim of the paper is to show advantages and disadvantages of mathematical modelling in design automation on the simple problem.

2 MATHEMATIC MODELS AND PARAMETERS IN DESIGN AUTOMATION

Modern CAD packages offers a variety of tools and commands to increase the flexibility of geometric models. However, to utilize them in efficient way, there is a need for tool-independent, generic modeling techniques. Mastering these techniques in the most cases eases the way towards design automation, since it represents:

1. A basis for solving tasks that involving geometry design automation.
2. A helpful tool to consult when is necessary to reach fast solutions.
3. An algorithm to locate the required geometric design automation level more easily.

To achieve design automation, knowledge based engineering methods can be employed to effectively capture knowledge by storing rules, relations, and facts in a functional mathematic model. In this paper, knowledge based engineering and mathematic modeling is used to support High Level CAD modeling by creating High Level CAD templates (HLCts) i.e automated CAD design. These methods are higher abstraction geometries that can be automatically instantiated in the design of new products. In the presented paper, it has been chosen to divide geometry transformations into two categories and include them step by step. The first category will describe the morphological levels of geometric modeling while the second will reflect on how to effectively increase, reuse or replace the number of geometric objects, hence its topology. Morphological changes are transformations that occur within the same instance of a given class, i.e. it is enough to re-evaluate the instance.

Topological changes are the ones that require instances of classes to be added, replaced or removed.

2.1 Morphological transformations

During a morphological transformation, the object will change continuously in the scope of the dimensions. Different morphological levels are shown in Figure 1, with increasing modeling complexity for each step by leveling up. The higher the level, the higher the knowledge content in the method described. Morphological geometric objects can be divided into four levels:

1. Fixed Objects are essentially objects that cannot change shape. These objects are intentionally or non-intentionally static and therefore have a fixed set of geometric output. This stage has zero morphological value.
2. Parameterization is made on geometric objects of which the values can change and hence do not have a static set of output. Because of the lack of relations between the various geometric objects, it is not realistic to use models based only on parameterization other than cases of non-complex geometries.
3. An effective way to decrease the number of input parameters is to set up relations between a model's geometric objects. This can be done strictly mathematically, referred to as Equation Based Relations in Figure 1.
4. Script Based Relations are created by writing the relations using the various programming languages provided by the CAD system, described in Figure 1. Both equation and script based relations are of course rule-based, but the use of the latter allows logic reasoning to be included in a more user-friendly manner, not necessarily mathematical.

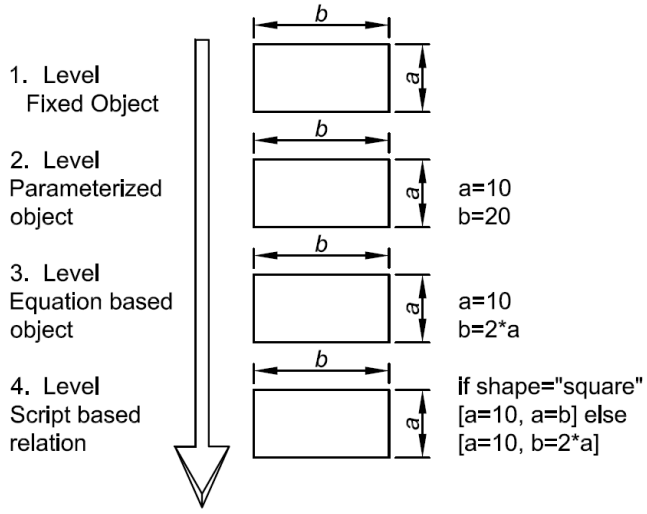

Figure 1. *Morphological transformation*

2.2 Topological transformations

As stated previously, there are three types of events that can take place during topological transformations:

- Adding an instance; an object is placed in a desired position;

- Removing an instance; an object is removed from a chosen position;
- Replacing an instance; an object is removed and one from a different class is added.

The main shortcoming of only using morphologically based models in the automatic design process is that the number of objects cannot be changed. For instance, in a structural optimization that uses morphological transformations only, the number of structure elements needs to be known in advance or alternatively the optimization must be repeated several times with different configurations. To describe the topological process the following terms are important: template, constraint and context. A template refers to an initial model to be re-instantiated; constraints are conditions which have to be satisfied by the instantiated instances; context is the geometric surroundings of an instance to which the constraints are referring to. The various levels of topological instantiation are pictured in the pyramid in Figure 2.

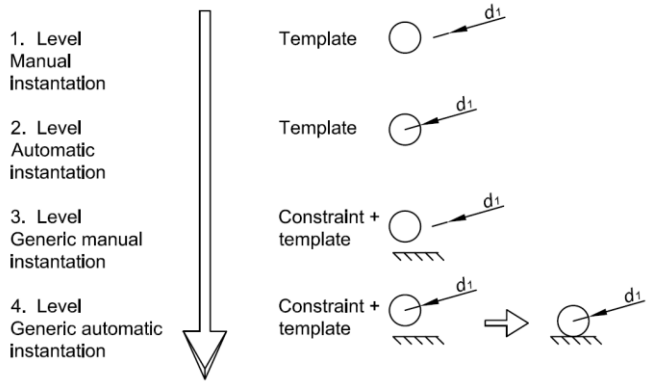

Figure 2. *Topological transformation*

The topological pyramid consists of the following stages:

1. Manual Instantiation: by performing copy and paste functions on various objects, manual instantiation is performed. However, the instances made are not context-dependent upon creation.
2. Automatic Instantiation: though only the template is defined, the instances created will follow the template model slavishly and cannot be context-dependent due to missing constraint definitions. The number of instances is parametrically modified.
3. Generic Manual Instantiation: context dependency for initiated instances is achieved by producing template and constraint manuals. These contain complete construction procedures of objects within the template and to which geometric features they are constrained. These definitions enable the template to be manually instantiated into different contexts. This increases the level of reusability in a geometric model.
4. Generic Automatic Instantiation: this stage is achieved when pre-defined functions can automatically generate or delete the instances depending on user input. The instances are both context- dependent and able to vary parametrically, hence full reuse and automation are achieved.

2.3 Dynamic top-down modeling

Traditionally, CAD design is divided into top-down and bottom up approaches. These design strategies could be associated to analysis and synthesis respectively. Top-down design requires ‘‘thinking and problem solving before integration, rather than afterwards’’. Hence, in the top-down approach, the critical information is placed on a hierarchal top level and branches down to all lower component levels in the product. When applying a dynamic top-down development process, the actual CAD models can be generated from pre-described High Level CAD templates (HLCt). The critical information on how the HLCt should be instantiated is stored in the knowledge base and used by the inference engine.

3 EXAMPLE OF MATHEMATICAL MODEL IMPLEMENTED IN DESIGN AUTOMATION

For an example of design automation using High Level CAD templates and mathematic modeling it is chosen a workshop table. Before the solution is done the following procedure is used:

1. Determination of input parameters;
2. Mathematical model of input dependent parameters is made in order to fully describe whole product;
3. The High Level CAD template is created (automated design);
4. The testing of created automated design is performed;

Input parameters for workshop table are given in Table 1.

Table 1. *Input parameters for workshop table*

Par. no.	Parameter name	Par. description	Unit
1.	Table length	Geometric	mm
2.	Table width	Geometric	mm
3.	Table height	Geometric	mm
4.	Frame section dimension	Geometric	mm
5.	Frame section wall thickness	Geometric	mm
6.	Frame color	Characteristics variable	ul
7.	Table surface paint	Characteristics variable	ul
8.	Wheels	True/False	ul

Next step in preparation for automated design is dependence definition between parameters. Dependence definition is regulated by mathematic relations, and because better overview it is shown by diagram in Figure 3.

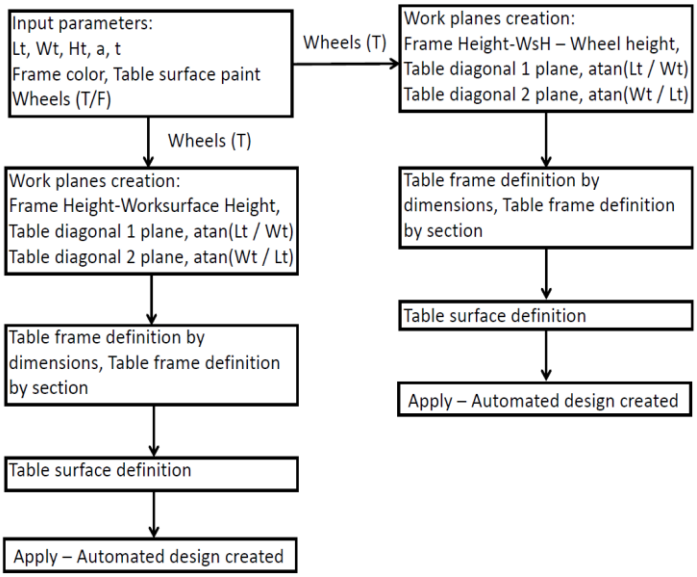

Figure 3. *Dependence between input parameters*

Before the High Level CAD template (automatic design) is created it is determined that top-down strategy is much better to be used. In this case the workplanes that will limit workshop table features must be created and parameterized. Other features will be limited to those se planes, and via future communication form the customization of workshop table will be performed.

In Figure 4 and Figure 5 are shown relation between parameters in used CAD software and model state with user communication form, respectively.

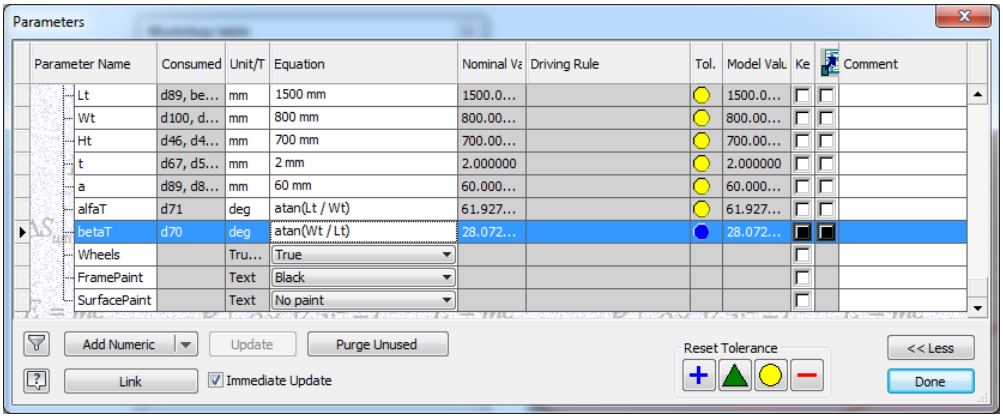

Figure 4. *Relation between parameters in CAD software*

The parameters which are previously defined by mathematic model must be defined in automated design High Level CAD template as well. All of the mathematic relations must be connected parameters to user parameters. User parameters will later appear in a communication form. Some of parameters are physical values, some are text parameters (such as table characteristics) and some of them are logical (True/False) parameters.

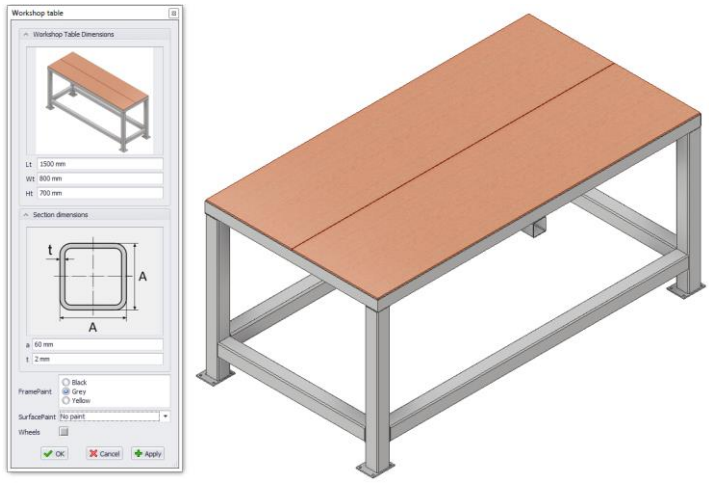

Figure 5. *Model state with user communication form*

Communication user form is a bridge between user and automated design. In the engineers scope is to limit the user form in order not to allow the user to create impossible designs.

4 CONCLUSION

The presented example of the automated design has some advantages and as well some disadvantages. Main advantages are:

- the presented model is very good for products which are manufactured as product families;
- when the system is built, the amount of necessary administrative and engineering staff can be significantly decreased, which is very positive for big companies;
- the mistakes in product design and documentation is fully avoided;
- the customer has a full control on the offered product options;
- the deals between enterprises and customers has a much easier flow etc.

However, the presented approach of automated design has a general disadvantages such as:

- the implementation of the presented approach to design automation is time consuming process;
- the design automation solutions are not suitable for small businesses because its price can be high;
- the adding of new products to the design automation system can be expensive, time consuming and potentially it can cause problems in solution working;
- the presented design automation approach is not suitable for all types of products, especially in products which is not supporting modularity.

The usage of these systems, its type choice must be based on company size, turnover, products customization level and so on. The future authors work in this field will be related to implementation of these tools into advanced CAD courses at their Institutions as a very perspective and attractive tool, which can be very successfully used in practice.

REFERENCES

[1] Dinev, G., Malakov, I. and Dotsev, D. (2012). CAD optimal design, documentation and automated assembly of mechanical product, Advanced Materials Research, pp. 463–464.

[2] Dinev, G. (2012). An approach for simulation design of mechanical assembled units, Advanced Materials Research, 463–464, pp. 1085–1088.

[3] Tarkian, M. (2012). Design Automation for Multidisciplinary Optimization A High Level CAD Template Approach, Available at: http://liu.diva-portal.org/smash/get/diva2:556208/FULLTEXT03, accessed in October 2022.

[4] Amadori, K. et al. (2012). Flexible and robust CAD models for design automation, Advanced Engineering Informatics, 26(2), pp. 180–195.

[5] Shah, D. B. (2013). Parametric Modeling and Drawing Automation for Flange Coupling using Excel Spreadsheet, International Journal of Research in Engineering and Technology, 1(2), pp. 187–192.

[6] Frank, G. et al. (2014). Towards a Generic Framework of Engineering Design Automation for Creating Complex CAD Models Human Robot Cooperation View project COMET K-Project-Advanced Engineering Design Automation (AEDA) View project Towards a Generic Framework of Engineering Design, (September 2014). Available at: www.iaria.org, accessed in October 2022.

[7] Moreno, R. and Bazán, A. M. (2017). Design Automation Using Script Languages. High-Level CAD Templates in Non-Parametric Programs, IOP Conference Series: Materials Science and Engineering, 245(6). doi: 10.1088/1757-899X/245/6/062039.

[8] Nesterenko, M. A. and Strashnov, S. V. (2019) 'Design automation based on parametrization of second order curves in CAD software', 11th IEEE International Conference on Application of Information and Communication Technologies, AICT 2017 - Proceedings, pp. 1–4. doi: 10.1109/ICAICT.2017.8686933.

[9] Wei, B. and Lv, M. (2020) 'Cad integration of mechanical numerical control board parts based on machining features', Computer-Aided Design and Applications, 18(S3), pp. 176–187. doi: 10.14733/cadaps.2021.S3.176-187.

[10] Matejic, M., Ivanovic, L., Stojanovic, B. (2020) 'Modern systems in technical documentation', in modern systems in technical documentation, Conference proceedings, COMETa 2020, pp. 339–346.

[11] Matejić, M., Pantić, M. and Blagojević, M. (2020) 'Comparative analysis between cpq systems', Conference proceedings, COMETa 2020, pp. 267–273.

[12] Shafiee, S. et al. (2021) 'Evaluating the benefits of a computer-aided software engineering tool to develop and document product configuration systems', Computers in Industry, 128, p. 103432. doi: 10.1016/j.compind.2021.103432.

[13] Heikkinen, T. (2021) 'Transparency of design automation systems using visual programming – within the mechanical manufacturing industry', Proceedings of the Design Society, 1(August), pp. 3249–3258. doi: 10.1017/pds.2021.586.

[14] Machchhar, R. J. and Bertoni, A. (2021) 'Data-driven design automation for product-service systems design: Framework and lessons learned from empirical studies', Proceedings of the Design Society, 1(August), pp. 841–850. doi: 10.1017/pds.2021.84.

[15] Vidner, O., Wehlin, C. and Wiberg, A. (2022) 'Design Automation Systems for the Product Development Process: Reflections from Five Industrial Case Studies', Proceedings of the Design Society, 2, pp. 2533–2542. doi: 10.1017/pds.2022.256.

COMETa 2022
6th INTERNATIONAL SCIENTIFIC CONFERENCE
17th - 19th December 2022
Jahorina, B&H, Republic of Srpska
University of East Sarajevo
Faculty of Mechanical Engineering
Conference on Mechanical Engineering Technologies and Applications

TRANSPORTATION OPTIMIZATION WITH EXCEL SOLVER

Nenad Kostić[1], Nenad Petrovic[2], Nenad Marjanović[3], Jelena Petrović[4]

Abstract: This article is dedicated to transportation efficiency and the related problems. Its main goal is to analyse the effects that optimization can have on transportation efficiency and its ecological performances. This problem essentially refers to determining the most lucrative maximum quantity of commodity that can be loaded in a transportation vehicle. We used evolutionary algorithm in Excel solver to observe three different case studies. In all case studies a loading capacity of a transportation vehicle is limited and different constraints are set on an allowed and a required number of parcels to be transported. Moreover, the packages to be loaded on the given vehicle are divided into three categories based on their weight and price. The results obtained through this analysis indicate that the optimization can result in significant logistic, economic, and ecological effects. The optimization leads to maximum utilization of available loading capacities and maximum profit. When conducted in such a manner, transportation of goods becomes more efficient and thus environment-friendly. Furthermore, the model developed here is general in its nature so it can be employed to solve any transportation problem of the similar nature with minimum adjustments. Thus, it can find a wide-spread practical application.

Key words: ecology, efficiency, excel solver, optimization, transport problem

1 INTRODUCTION

By concurrently striving to facilitate the negative effects and to generate as many positive ones as possible, the global market has been constantly posing new challenges to engineers. Among all negative effects, the main focus of the market is to increase their profit and reduce their current costs. From an engineering point of view,

[1] PhD, Nenad Kostić, University of Kragujevac Faculty of Engineering, Kragujevac, Serbia, nkostic@kg.ac.rs
[2] PhD, Nenad Petrović, University of Kragujevac Faculty of Engineering, Kragujevac, Serbia, npetrovic@kg.ac.rs (CA)
[3] PhD, Nenad Marjanović, University of Kragujevac Faculty of Engineering, Kragujevac, Serbia, nesam@kg.ac.rs
[4] MSc, Jelena Petrović, University of Kragujevac Faculty of Engineering, Kragujevac, Serbia, jelenapetrovic4b@gmail.com

costs are tightly knit to efficiency, degree of utilization, quality, etc. Hence, these must be improved in order to generate more profit.

Transportation efficiency is seen today as one of the most massive and widespread problems that has to be tackled. Consequently, it can be observed as one of the most demanding engineering challenges. The transportation problems include, inter alia, transport organization and management, packaging and loading goods, cost analyses, energy savings, and environmental impact. They also pose huge challenges for researchers.

The topic of transport logistics is nowadays the main focus of a large number of researchers and this field of study has been expanding rapidly. The roots of the transportation problems spread across different areas. The problem of goods packaging [1-3], for instance, is one of the most complex challenges. Moreover, transmission optimization designs and the positioning of transmission elements are compatible with transportation problems [4,5]. In order to solve such complex issues, it is necessary to apply optimization methods since without optimization, it is impossible to reach high-quality solutions today. One of the most important and widespread methods is the Genetic algorithm [6,7]. Excel is the most frequent software used for solving complex problems via optimization. It includes the Evolutionary algorithm [8] which relies on the principles of the genetic algorithm.

This paper aims at providing the mathematical model for solving one of the most widespread transportation problems – efficient organization. We use the software solution and the methods which are frequently used for the optimization of such complex problems nowadays. However, this general mathematical model is used here to measure the effects in three specific scenarios in order to prove its effectiveness in different circumstances. The primary goal in doing so is to identify the impact of the optimal transport organization and the benefits that can be thus achieved. Moreover, the model can be adapted to solve any problem of the similar nature.

2 DEFINING A PROBLEM

The transportation problem can be viewed as the issue of how to provide the optimal utilization of transportation capacities. For transportation to be as efficient as possible, the main task is to organize it in a way that allows economic benefits. In other words, loading capacities should be fully utilized. Packages, however, differ in both their masses and prices. In order to find the best loading solutions for every given scenario, we must use good mathematical optimization models.

The objective function in this model is the profit maximization while the main constraint is a transportation capacity. It is adopted here as 20t in all case studies. The additional constraint adopted in case studies is the mass of parcels to be loaded on a transportation vehicle. A number of packages refers to a minimum and a maximum number of parcels that ought to be transported.

In this general mathematical model, it is possible to define the objective function as presented in the Equation 1:

$$\sum_{i=1}^{n} p_i \cdot x_i \tag{1}$$

, where *p* stands for profit and *x* stands for a number of packages of a given type.

In the Equation 2, *m* stands for a mass of each package while *w* is the total transportation capacity that cannot be surpassed:

$$\sum_{i=1}^{n} m_i \cdot x_i \leq w \tag{2}$$

There are certain constraints concerning the variables. The variables *x*, as stated above, represent numbers of parcels of a given type. A minimum number that must be transported (size *a*), as well as the total availability of packages (size *b*), must be defined for each type of packages. This is shown is the Equation 3:

$$a \leq x_i \leq b \tag{3}$$

The value of x_i must be a positive integer number, as defined in the Equation 4:

$$x_i \geq 0 - integer. \tag{4}$$

Due to the limited capacity of a transportation vehicle, packages weights must be taken into consideration. In addition to specific masses, packages have different prices. Since the main goal is to optimize profits, packages should be selected and loaded in a way that will enable highest possible profits.

2.1 Excel solver – Evolutionary algorithm

This paper uses Excel solver. The optimization Evolutionary algorithm belongs to the group of heuristic optimization algorithms and relies on the principles of the Genetic algorithm. This software solution is chosen here due to its commercial availability and its wide-spread application, as well as its good performances.

Evolutionary algorithm can be used to solve complex optimization problems with constraints [8]. The user interface requires users to define an objective function, constraints, and variable constraints, as shown in Figure 1.

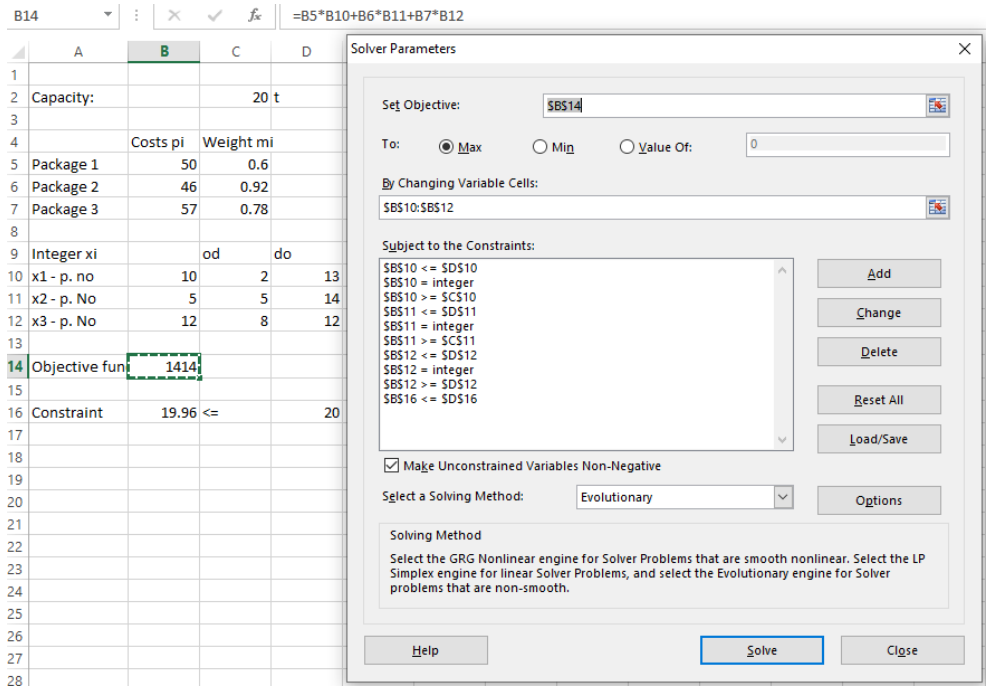

Figure 1. *User interface for an optimization configuration*

Evolutionary algorithm can be set based on the nature of a problem that is to be solved in a given situation. The general settings are presented in Figure 2.

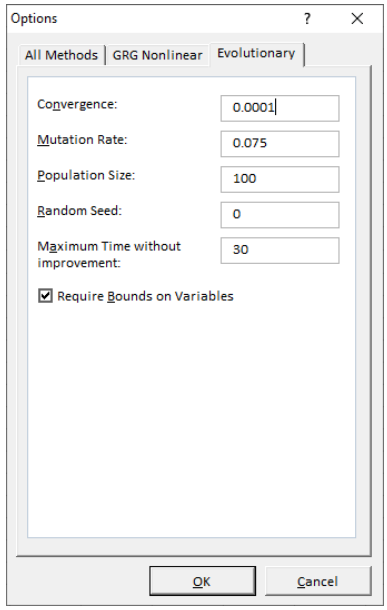

Figure 2. *Evolutionary algorithm settings*

This software provides operational security and precise solutions. It is user-friendly and very efficient in practical applications.

2.2 Case studies

For the sole purpose of verifying the results, three case studies are presented here with specific quantitative values. The main constraint is the maximum transportation capacity that is adopted here as 20t in all case studies. The same three types of packages are used. Their masses and prices are presented in Table 1.

Table 1. *Types of packages with their weights and prices*

	Package price – p_i	Package weight – m_i (t)
Package 1	50	0.6
Package 2	46	0.92
Package 3	57	0.78

The mathematical model for this specific problem can be presented as follows (Equations 5 and 6):

$$p_1 \cdot x_1 + p_2 \cdot x_2 + p_3 \cdot x_3 \tag{5}$$

$$m_1 \cdot x_1 + m_2 \cdot x_2 + m_3 \cdot x_3 \leq 20 \tag{6}$$

Case study 1 determines the optimal selection of parcels to be loaded in order to enable the highest profit when the adopted transportation capacity is fully occupied. Case study 2 determines the optimal selection of packages when there are constraints on the maximum number of packages (of all three types). Case study 3 evaluates the maximum and the minimum number of parcels of each type that ought to be loaded and transported. The optimization objective for the case studies is to generate as much profit as possible.

In Case study 1, the variables that define the number of parcels from three different package categories must be higher than zero which indicates that the given type exists. These values are integer numbers and there are no constraints in terms of the maximum number. In other words, it is possible to use as many packages as necessary despite their mass or price. The range for the variables in Case study 1 can be presented by the Equations 7:

$$\begin{aligned} x_1 &\geq 0 \\ x_2 &\geq 0 \\ x_3 &\geq 0 \end{aligned} \tag{7}$$

The range for the variables in Case study 2 can be presented with the Equations 8. In this case, the maximum number of packages from the given categories is defined based on their hypothetical availability.

$$\begin{aligned} 0 \leq x_1 &\leq 13 \\ 0 \leq x_2 &\leq 14 \\ 0 \leq x_3 &\leq 12 \end{aligned} \tag{8}$$

In Case study 3, the minimum numbers are also given in addition to the maximum ones. The minimum numbers are the numbers of packages of each type that have to be transported. The values for the variables can be presented by the Equations 9:

$$\begin{aligned} 2 \leq x_1 \leq 13 \\ 5 \leq x_2 \leq 14 \\ 8 \leq x_3 \leq 12 \end{aligned} \tag{9}$$

The values used here are hypothetical and arbitrarily selected because the goal of this paper is to demonstrate the practical application of the optimization model in different circumstances. This is most efficiently achieved by using specific values. The model developed here is flexible in terms of the number of variables and constraints so it can be easily applied to all similar transportation problems.

3 RESULTS

Excel solver and Evolutionary algorithm are used for the optimization in all case studies. The results indicate that high performances of transportation can be accomplished with this methodology. The transportation capacities can be employed to the maximum degree with the highest possible profit, while the costs are minimized and negative ecological impacts facilitated.

Figure 3 shows the number of parcels from three different package categories in all case studies.

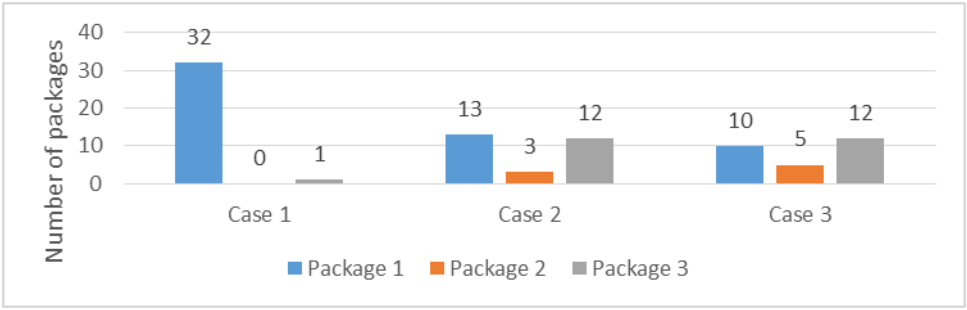

Figure 3. *The number of parcels from each category*

Case study 1 demonstrates that when there are no limitations in quantity of specific packages types that ought to be transported, the optimal model is to load 32 parcels of the Type 1, 0 parcels of the Type 2, and 1 parcel of the Type 3. The same values obtained for Case study 2 are 13, 3, and 12, respectively. In case of the third scenario tested here, those values are 10, 5, and 12, respectively. The economic indicators, i.e. the positive financial effects obtained by optimization are presented in Figure 4.

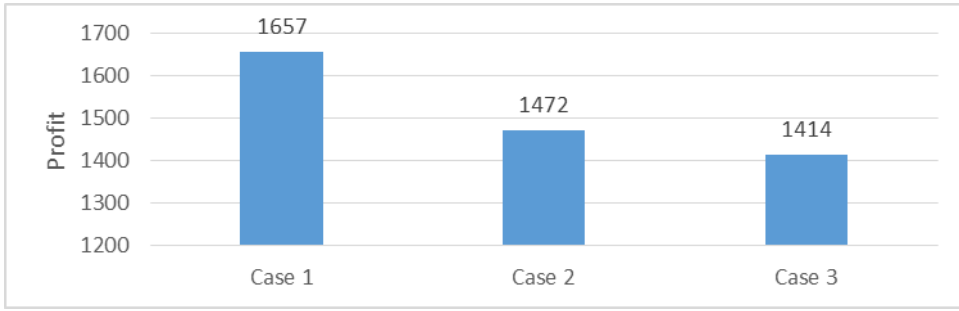

Figure 4. *The estimated profit*

It is evident from the figure above that the most profit is generated with the first scenario. This is not surprising taking into consideration that in this case there are fewest constraints. The second and the third tested scenarios follow in this particular order. The maximum difference between these case studies amounts to 15%, depending on the number of limitations. The results also indicate that there are differences in terms of the level of utilization of the given loading capacity, but they are slight – less than 0.5%. In general, the utilization of the loading capacity in all tested cases can be considered as very high (ranging from 19.92t to 19.98t). The obtained values are presented in Figure 5.

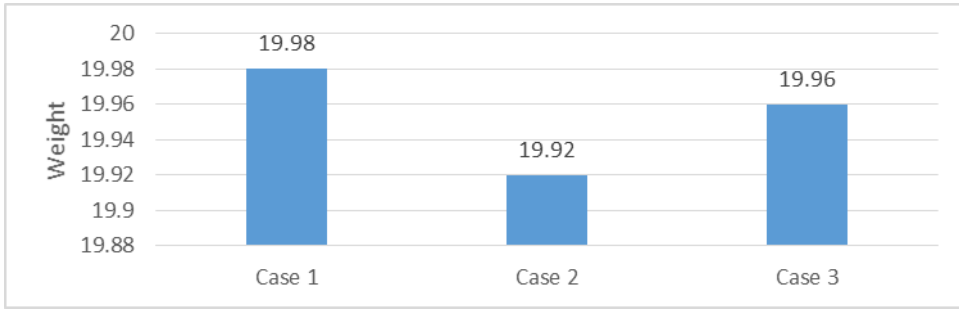

Figure 5. *The total mass of transported parcels – occupancy of the transporting capacities*

This problem is practically oriented. It is crucial for the organization of parcel-loading and transportation itself. The results obtained in this research verify the optimization model developed here by demonstrating that it helps accomplish maximum utilization of available loading capacities and maximum value of goods in different pre-set conditions. The effects of optimization are logistic, economic, and ecological. These are the main goals of the transport optimization.

4 CONCLUSION

This study focused on solving the complex problem of transportation optimization. The optimization was conducted in Excel solver via its Evolutionary optimization algorithm. With the set objective function (i.e. maximum profit), one can determine a quantity and a type of packages that can be transported in the most efficient way when the loading capacity is limited. The mathematical model developed here is general in its nature so it can be applied to all similar transportation problems.

The paper presents the results obtained for three case studies. The results indicate that the optimization can lead to maximum profit. The differences across tested scenarios amount to 15% depending on the number of different constraints. These limitations also impact the choice of packages to be loaded. The optimization also allowed the transportation capacities to be used to the maximum degree. The total capacity of a transportation vehicle in case studies was adopted as 20t, and the occupancy for different scenarios varied from 19.92t to 19.98t.

LITERATURE

[1] Wang, Y., and Chen, L. (2015). Two-dimensional residual-space-maximized packing, *Expert Syst. Appl.,* 42, p.p. 3297-3305.
[2] He, K., Huang, M., and Yang, C. (2015). An action-space-based global optimization algorithm for packing circles into a square container, *Comput. Oper. Res.,* 58, p.p. 67-74.
[3] Li, Z., Tian, Z., Xie, Y., Huang, R., and Tan, J. (2013). A knowledge-based heuristic particle swarm optimization approach with the adjustment strategy for the weighted circle packing problem, *Comput. Math. Appl.,* 66, p.p. 1758-1769.
[4] Marjanovic, N., Kostic, N., Petrovic, N., Blagojevic, M., and Matejic, M. (2017). Volume optimization of gear trains with spur gears using genetic algorithm, *MATEC Web Conf.,* 121, p.p. 01007.
[5] Kostic, N., Marjanovic, N., and Petrovic, N. (2016). A novel approach for solving gear train optimization problem, *Mobility Vehic. Mech.,* 45, p.p. 2 67-74.
[6] Shopova, E. G., and Vaklieva-Bancheva, N. G. (2006). BASIC—A genetic algorithm for engineering problems solution, *Comput. Chem. Eng.,* 30, p.p. 1293-1309
[7] Tang, P. H., and Tseng, M. H. (2013). Adaptive directed mutation for real-coded genetic algorithms, *Appl. Soft Comput.,* 13, p.p. 600-614.
[8] Chandrakantha, L. (2008). Using excel solver in optimization problems, *Math. Comp. Science Depart.*

COMETa 2022
6th INTERNATIONAL SCIENTIFIC CONFERENCE
17th - 19th December 2022
Jahorina, B&H, Republic of Srpska
University of East Sarajevo
Faculty of Mechanical Engineering
Conference on Mechanical Engineering Technologies and Applications

ON DESIGN AND CALCULATION OF LEVER TYPE LIFTING MECHANISM MULTIPLIERS

Svetomir Simonović[1]

Abstract: The paper represents characteristic designs of lever type lifting mechanism multipliers in relation to their use. Nonlinear displacement ratio of a lever based multiplier with relation to its levers inclination angles is deduced and considered. Also, working force applied by the piston of the hydraulic cylinder with relation to liftign mechanism platform position is deduced and analyzed. In addition, efficiency factors of a lever based multiplier are deduced and analyzed. Finally, the design and calculation of hydraulic cylinders with regard to their use with lifting mechanism multipliers and international regulations are considered.

Key words: Efficacy, Hydraulic Cylinder, Lever, Nonlinear

1 INTRODUCTION

The work takes in consideration nonlinear kinematic and dynamic of the lever based multipliers, [1]. The lever based multipliers are depicted at Figure 1. The kinematical schema depicted at figure 1a is used for freight hydraulic platform with lifting height up to 2 m. To enlarge the lifting height sequential lever based multiplier depicted at figure 1b. is used. Hydraulic platform with greater width and greater applied load capability is constructed according to kinematical schema shown at figure 1c, [1].

[1] Dr Svetomir Simonović, Akademija tehničkih strukovnih studija Beograd, Katarine Ambrozić br. 3, Beograd, Srbija, e-mail: svetomir.simonovic@visokatehnicka.edu.rs

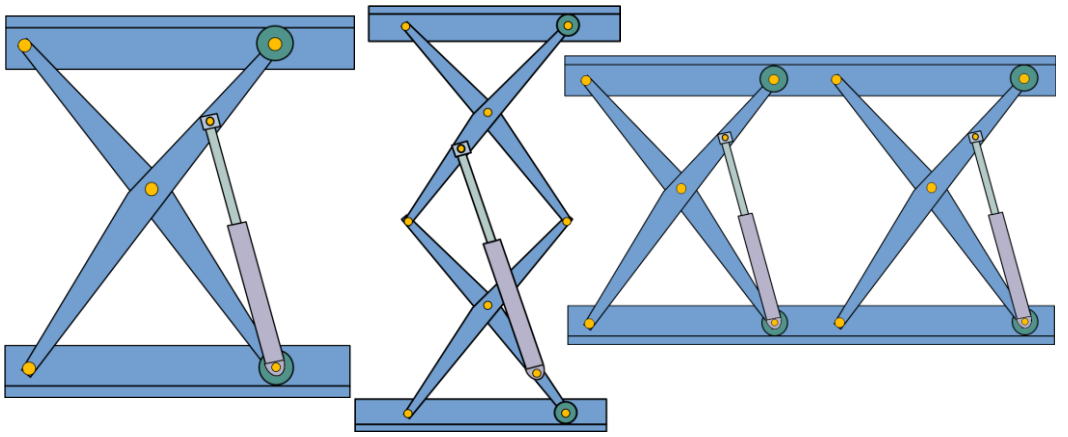

(a) (b) (c)

Figure 1: *(a) A levers based multiplier; (b) A sequential levers based multiplier; (c) A parallel levers based multiplier*

2 DISPLACEMENT RATIO OF LEVER BASED MULTIPLIERS

Levers based multipliers are applied with hydraulic freight platform for obtaining working force enlargement and for obtaining initial state compactness (figure 2) **, [1]**. The figure numbers denote: 1-hinge to fix lever to supporting frame and load bearing platform ; 2-central hinge; 3-hinge to fix hydraulic cylinder piston to lever; 4-hinge to fix lever to supporting frame and load bearing platform; 5-supporting roler; 6-supporting frame; 7-hydraulic cylinder; 8-supporting roler.

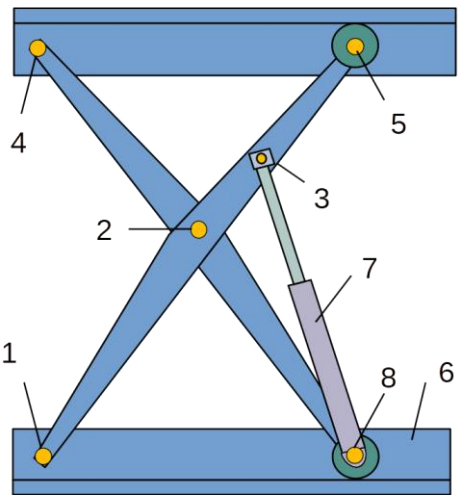

Figure 2*: A levers based multiplier;*

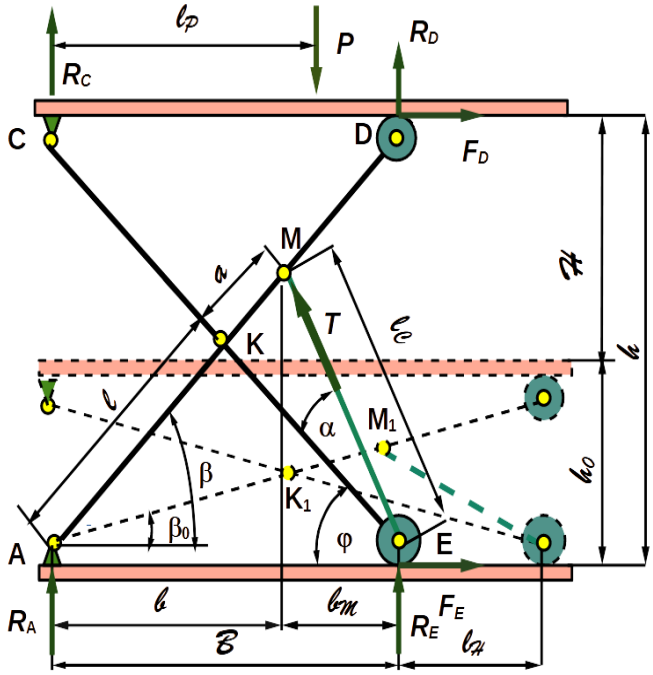

Figure 3*: Calculating diagram*

Displacement ratio of lever based multipliers n is

$$n = \frac{H}{L_p} \tag{1}$$

where H– elevating hight; L_p – working displacement of cylinder piston

Meaning of the Figure 3 symbols are*: P*- calculating load involving weight of the platform; R_A – vertical reaction applied at point A; R_C – vertical reaction applied at point C; R_D – vertical reaction applied at point D; R_E – vertical reaction applied at point E; F_D – roller resistant force applied at point D; F_E – roller resistant force applied at point E; T – current value of the force produced by the piston; β – inclination angle of the lever; φ – inclination angle of the piston; α – inclination angle between the piston and the lever; *H* – current height of the platform; h_0 – initial height of a roller hinge; *h* - current height of a roller hinge corresponding to *H*

Working displacement of the piston of the hydraulic cylinder that corresponds to the platform height *H* is

$$L_P = l_C - l_0 \tag{2}$$

where l_C – distance between piston hinge and the cylinder hinge that corresponds to the platform height H; l_0 - distance between piston hinge and the cylinder hinge that corresponds to the minimal platform height *H* = 0

Distance between the piston and cylinder hinges axis is

$$l_c = \sqrt{(l+a)^2(\sin\beta)^2 + (l-a)^2(\cos\beta)^2} \tag{3}$$

Combination of (2) and (3) yields

$$L_P = \sqrt{(l+a)^2(\sin\beta)^2 + (l-a)^2(\cos\beta)^2} - \sqrt{(l+a)^2(\sin\beta_0)^2 + (l-a)^2(\cos\beta_0)^2} \tag{4}$$

If platform traveling height H is expressed thtough geometrical parameters of the mechanism, it is obtained

$$H = 2l(\sin\beta - \sin\beta_0) \tag{5}$$

Taking into consideration expressions (2), (4) and (5) one obtains

$$n = \frac{2l(\sin\beta - \sin\beta_0)}{\sqrt{(l+a)^2(\sin\beta)^2 + (l-a)^2(\cos\beta)^2} - \sqrt{(l+a)^2(\sin\beta_0)^2 + (l-a)^2(\cos\beta_0)^2}} \tag{6}$$

Displacement ratio of a lever based multiplier n is nonlinear function of its levers inclination angles, so its value should be determined for fixed extremal traveling height. Taking into consideration presented calculation diagram and expression (6) one can conclude that displacement of the piston, when platform travesl from h_0 to h, is proportional to the distance between central hinge K and piston hinge M. So, approximate value of displacement ratio of a lever based multiplier n can be determined according to expression:

$$n = \frac{2l(\sin\beta - \sin\beta_0)}{a} \cdot 1{,}4 \tag{7}$$

Tvo level lever multiplier has doubled displacement ratio:

$$n = \frac{4l(\sin\beta - \sin\beta_0)}{a} \cdot 1{,}4 \tag{8}$$

3 WORKING FORCE APPLIED BY THE PISTON OF THE HYDRAULIC CYLINDER

Now, one can determine working force applied by the piston of the hydraulic cylinder, [1]. For it to be done one must preliminaru determine hinge reactions and rollers friction forces, as are shown at figure 3. It can be remarked here that horizontal components of reaction forces applied at hinges A and C are equal to zero, because of its combination with rolling resistance forces at points D and E.
Moment equilibrium equation for point D is

$$\sum M_D = 0 \Rightarrow P \cdot 2l(\cos\beta - l_p) - R_C \cdot 2l \cdot \cos\beta = 0 \tag{9}$$

Expression (9) yields values of reacton forces in lefthand supports as

$$R_C = R_A = P\left(1 - \frac{l_P}{2l\cos\beta}\right) \tag{10}$$

Analogically

$$\sum M_C = 0$$

yields values of reacton forces at righthand supports as

$$R_D = R_E = \frac{Pl_P}{2l\cos\beta} \tag{11}$$

The forces opposing rolling movement are

$$F_D = F_E = R_D\,\omega \tag{12}$$

where

$$\omega = \frac{2}{D_R}\left(f_k + \mu D_F\right)$$

ω – rolling resistance factor; D_R – roller diameter; d_F – roller bearings friction diameter; μ – bearing friction coefficient; f_k – rolling friction coefficient for plane surfaces

If hinge friction moment is neglected, piston force can be determined from the equlibrium equation of lever AD in regard to hinge K as

$$T = \frac{R_A l\cos\beta + R_D l\cos\beta + F_D l\sin\beta}{r} \tag{13}$$

where r = l cos α

Equations (9), (10) and (11) and (13)yield

$$T = \frac{P\left(l\cos\beta + \omega\frac{l_p}{2}tng\beta\right)}{l\cos\alpha} \tag{14}$$

where

$$\alpha = \left(\arccos\frac{l-a}{l_C} - \beta\right)$$

α - angle between the cylinder axle and the lever, [1].

4 LEVER MULTIPLIER EFFICIENCY FACTOR

Taking into consideration nonlinear relationship between force parameters and kinematic parameters of a lever multiplier system, an energetic approach is applied to deduction of a lever multiplier efficiency factor η as ratio between the efficient work to lift a load and total work including work to overcome internal resistances such as rolling resistance and hinge rotating friction,[1]. That is

$$\eta = \frac{A_H}{A_H + A_R + A_F} \tag{15}$$

where: A_H – work to lift load at height H; A_R - work to overcome rolling resistance; A_F – work to overcome hinge rotating friction.

Work to lift load is expressed as

$$A_H = P \cdot H = 2Pl\left(\sin\beta - \sin\beta_0\right) \tag{16}$$

Work to overcome rolling resistance is expressed as

$$A_R = \int_{\beta_0}^{\beta} dA_R(\beta) \tag{17}$$

where

$$dA_R(\beta) = 2F_D dx = 2R_D \omega dx$$

Differential of a roller trajectory is

$$\frac{dx}{d\beta} = \frac{d\left(2l\cos\beta_0 - 2l\cos\beta\right)}{d\beta} = 2l\sin\beta \tag{18}$$

so $dx = 2l\sin\beta d\beta$

Now, work to oveccome rolling resistances is

$$A_R = 2P \cdot \omega \cdot l_p \int_{\beta_0}^{\beta} \frac{\sin\beta}{\cos\beta} d\beta = 2P \cdot \omega \cdot l_p \left(-\ln\left|\cos\beta\right| + \ln\left|\cos\beta_0\right|\right) \tag{19}$$

Work to overcome rotating friction of hinges A and C is

$$A_F^{AC} = 2\mu \cdot r \int_{\beta_0}^{\beta} R_A d\beta = 2\mu \cdot r \int_{\beta_0}^{\beta} \left(1 - \frac{l_p}{2l \cdot \cos\beta}\right) d\beta \tag{20}$$

Work to overcome rotating friction of hinges E and D is

$$A_F^{ED} = 2\mu \cdot r \int_{\beta_0}^{\beta} \frac{Pl_p}{l\cos\beta} d\beta \tag{21}$$

Work to overcome rotating friction of hinge K is

$$A_F^K = \mu \cdot r \int_{\beta_0}^{\beta} P d\beta = P\mu r\left(\beta - \beta_0\right) \tag{22}$$

Expressions (20) and 21) contain standard integral having solution

$$\int_{\beta_0}^{\beta} \frac{d\beta}{\cos\beta} = \ln\left|tg\left(\frac{\beta}{2}+\frac{\pi}{4}\right)\right| - \ln\left|tg\left(\frac{\beta_0}{2}+\frac{\pi}{4}\right)\right| \tag{23}$$

If rolling bearings are used with hinges main losses are due to rolling resistance, so simplified Lever multiplier efficiency factor expression can be stated as

$$\eta = \frac{\sin\beta - \sin\beta_0}{\sin\beta - \sin\beta_0 + \frac{\omega l_p}{l}\left(-\ln|\cos\beta| + \ln|\cos\beta_0|\right)} \tag{24}$$

5 ON LEVER MULTIPLIERS HYDRAULIC CYLINDERS

The cylinder and connecting couplings for the cylinder should be made of materials satisfying the following:

- For tensile, compressive, bending, and torsional loading the cylinder and connecting couplings should have a value of safety factor that is not less than 5 based on ultimate strength, [2-8].
- For pressure calculations the cylinder and connecting coupling should have a safety factor value not less than that calculated while using prescribed methods. Also, cylinders should be designed in agreement with the prescribed method, [2-8].

Dished seamless cylinder and plunger heads, convex to pressure if used on plungers, should have a maximum allowable working pressure of not more than 60% of that for heads of the same dimensions with pressure on the concave side, [2-8].

Reinforced cylinder and plunger heads should be designed and so that the maximum stress at rated capacity should not exceed 83 MPa for mild steel and 1/5 of the ultimate strength of the material for other metals, [2-8].

The plunger and connecting couplings for the plunger should be made of materials in compliance with the following:

- For tensile, compressive, bending, and torsional loading the plunger and connecting couplings should have a safety factor value of not less than 5 based on ultimate strength, [2-8].
- For pressure calculations the plunger and connecting coupling should have a safety factor value not less than that calculated as specified by international or national rules, [2-8].

Plungers should be designed and constructed in accord with the applicable formula in national or international rules for calculation of elastic stability, bending, and external pressure, [2-8].

Plungers subject to internal pressure shall also be designed and constructed in accordance with Cylinder Design formulas provided by national or international rules, [2-8].

6 CONCLUSION

The kinematic and dynamic of a lever based multiplier is highly nonlinear in terms of its input and output motions or forces. From equation (6) can be concluded that displacement ratio of a lever based multiplier is nonlinear function of its levers inclination angles, so its value is determined for fixed extremal traveling height.

From equation (14) can be concluded nonlinear relations betwen force aplied by piston and the lever inclination angle, wich is at maximum when platform is at the lower limit position, that is when $\beta = \beta_0$

Under supposition that $l \approx l_p$, $\omega = 0{,}1$ and that inclination angle of the levers changes from 10^0 to 60^0 than if l / l_p ratio of lever based multiplier rise its efficiency factor diminish.

With lever type multiplier use of single acting and double acting types of piston type hydraulic cylinders are in common use because they do not need the head of the piston guiding elements.

REFERENCES

[1] Архангельский, Г.Г., Бабичев, С.Д., Ваксман, М. А., Котельников В.С. (2002). *Гидравлические лифты*, Издательство Ассоциации строительных вузов, Москва.

[2] Strakosch, G.R., Caporale, R. S. (2010). *The Vertical Transportation Handbook*, 4th ed., John Wiley & Sons, Inc., New York.

[3] Bangash, M.Y.H., Bangash, T. (2007). *Lifts, elevators, escalators and moving walkways / travelators /*, Taylor & Francis, London.

[4] Unger, D. (2021). *Aufzüge und Fahrtreppen Ein Anwenderhandbuch*, Springer-Verlag Berlin Heidelberg. Timoshenko, S., Young,D.H., Weaver, W. (1974*). Vibration problems in engineering*, John Wiley&Sons, New York.

[5] Tošić, S. (2004). *Liftovi*, Mašinski fakultet, Centar za mehanizaciju, Beograd.

[6] BSI. (1995). *Safety Rules for the Construction and Installation of Escalators and Passenger Conveyors*, BSEN 115:

[7] ASME. (2019). *Safety Codes for Elevators and Escalators*. A17.1, ASME.

[8] EN 81-3:2001+A1:2008. *Safety rules for the construction and installation of lifts - Part 3: Electric and hydraulic service lifts,* CEN.

PRODUCT DEVELOPMENT AND MECHANICAL SYSTEMS

COMETα 2022
6th INTERNATIONAL SCIENTIFIC CONFERENCE
17th - 19th November 2022
Jahorina, B&H, Republic of Srpska
University of East Sarajevo
Faculty of Mechanical Engineering
Conference on Mechanical Engineering Technologies and Applications

OBRAZOVANJE ZA INDUSTRIJU 4.0, SITUACIJA I IZAZOVI – STUDIJA STANJA SREDNJOŠKOLSKOG NIVOA

Biljana Marković[1], Aleksija Đurić[2]

Rezime: U inženjerstvu se svakodnevno pominje termin Industrija 4.0, te pojam digitalne transformacije preduzeća, tehnike i industrije u cjelini, kao pripreme za ulazak u novu indsutrijsku revoluciju. Bez transformacije obrazovnog sistema, na svim niovima obrazovanja, te bez saradnje na relaciji industrija – obrazovni sistem - vlada, kao relevantan nivo za donošenje odluka, neće biti moguće odgovoriti izazovima i promjenama koje neminovno donosi Industrija 4.0. Rad govori o intertnosti tradicionalnog obrazovnog sistema koji je još uvijek dominantan u BiH, te potrebi bržih promjena nastavnih programa i planova, sa akcentom na srednjoškloski nivo obrazovanja, kao pripremu za visoko obrazovanje.

Ključne riječi: industrija 4.0, srednjoškolsko obrazovanje, digitalna transformacija, promjene

EDUCATION FOR INDUSTRY 4.0, SITUATION AND CHALLENGES – STUDY OF THE STATE OF SECONDARY SCHOOL LEVEL

Abstract: In engineering, the term Industry 4.0 is mentioned every day, and the concept of digital transformation of companies, technology and industry as a whole, as preparation for entering a new industrial revolution. Without the transformation of the education system, at all levels of education, and without cooperation in the relationship between industry - education system - government, as a relevant level for decision-making, it will not be possible to respond to the challenges and changes that Industry 4.0 inevitably brings. The paper talks about the relevance of the traditional education system, which is still dominant in Bosnia and Herzegovina, and the need for faster changes in teaching programs and plans, with an emphasis on the high school level of education, as a preparation for higher education.

Keywords: industry 4.0, secondary education, digital transformation, changes

[1] Dr, Biljana Marković, Mašinski fakultet Univerzitet u Istočnom Sarajevu, Istočno Sarajevo, RS, BiH, biljana.markovic@ues.rs.ba (CA).
[2] Dr, Aleksija Đurić, Mašinski fakultet Univerzitet u Istočnom Sarajevu, Istočno Sarajevo, RS, BiH, aleksija.djuric@ues.rs.ba

1 UVOD

Dok se u razvijenim zemljama Evrope i svijeta uveliko govori o digitalnim transformacijama društva, u svim segmentima, počevši od osnovnih nivoa obrazovanja, preko srednjeg, univerzitetskog, do procesa primjene znanja, odnosno kreiranju novih radnih mjesta, razvoju malih i srednjih preduzeća, najveći broj mladih u Bosni i Hercegovini ne zna ili nema pristup osnovnim i neophodnim tehnološkim uređajima za digitalno obrazovanje. Novi, odnosno inovirani modeli visokog obrazovanja, koji moraju doživjeti digitalnu transformaciju, uveliko su uslovljeni ne samo izmjenom nastavnih planova i programa, odlukama koje se donose na nivou ministarstava i vlada, već i neizostavnim promjenama koje je potrebno provesti i u srednjem i osnovnom obrazovanju. Da bi se u BiH, kao i ostalim zemljama zapadnog Balkana postavile osnove budućeg ekonomskog razvoja, novih modela organizacije društva i privrede, otvorila nova tržišta, uspostavili novi izvori nabavke (posebno u okonostima Covida i ratnih dešavanja), koji treba da vode ka postulatima Industrije 4.0, neophodno je napraviti bar prve korake u izmjenama načina učenja, sticanja i prezentovanja potrebnih znanja na svim niovima obrazovanja. Ovdje je akcenat stavljen na srednjoškloski nivo obrazovanja, kao pripremu za visoko obrazovanje. U radu je prikazana analiza nastavnih planova i programa za srednje škole za zanimanja iz struke elektrotehnika i mašinstvo, koje su, osim IT, najviše involvirane u Industriju 4.0. Takođe, u radu su prikazani rezultati anketnog ispitivanja učenika srednje škola „28. juni“ iz Istočnog Novog Sarajeva.

Ako se govori o industrijskim revolucijama (Slika 1), počevši od Industrije 1.0, (pronalska parne mašine), preko ostale dvije industrijske revolucije, vezane za pronalazak struje, te robotizaciju kasnije, do Indusutrije 4.0, obrazovni sistem je, u stvari, bio odgovor na potrebe tih revolucija. Industrijskom podjelom rada, odnosno podjelom proizvodnih procesa na segmente, od ulaza do izlaza iz svih dijelova procesa, od nabavke, ulazne kontrole, proizvodje, održavanja, izlazne kontole, prodaje, obrazovanje se dijelilo na dijelove, odnosno otvarala su se različite stručne škole, kao nastavak obuke za zanatska zanimanja, a univerzitetsko obrazovanje dijelilo na godine, semestre, nastavne predmete, te prilagođavalo zahtjevima indsutrije.

Obzirom da je najvećim dijelom naše društvo tradicionalno, te vrlo sporo prati promjene, tako i danas, čak i su situaciji kad se masovno koriste pametni telefoni, računari, projektuju pametne kuće, priča o energetskim uštedama i korištenju alternativnih izvora energije, naše obrazovanje vuče teret konvencionalnog obrazovanja čiji je cilj bio isključivo sakupljanje i reprodukovanje informacija, a ne kreativno i inovativno razmišljanje bez koga nema budućnosti. Ovaj rad je nastao sa ciljem skretanja pažnje na sporost u transformaciji obrazovanog sistema u BiH, na svim nivoima, a posebno srednjoškolskog, te strahom da će mladi ljudi, koji uviđaju potrebu za sticanjem novih oblika znanja, napuštati ove prostore više i masovnije nego danas, u traženju zemalja i obrazovnih sistema koji im omogućavaju konkurentnost u poslu, na polju novih zanimanja koje se pojavljuju na tržištima razvijenih zemalja. Istraživanja su pokazala da 96% mladih u BiH smatra da ih formalno obrazovanje ne podučava potrebnim znanjem i praktičnim vještinama za tehnologije Industrije 4.0, ukoliko čak i znaju šta te vještine i znanja podrazumijevaju [1]. Neohodno je da svi u lancu odlučivanja o aspektu obrazovanja shvate da se paradigma promjenila, te da obrazovani sistem ne odgovara trenutku i nije usaglašen sa njim.

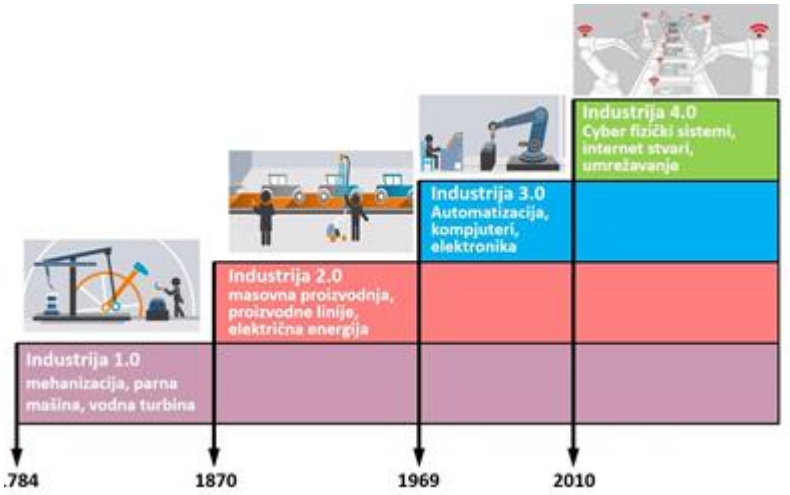

Slika 1. *Od industrije 1.0 do industrije 4.0 [3]*

U radu koji je objavljen 2021. god., na bazi provedenih istraživanja koja su prezentovana [2], vezana su za kompetencije potrebne za Industriju 4.0, a koje poseduju mašinski inežnjeri koji nisu na početku karijere, su u okvirima očekivanih, u odnosu na trenutnu opremljenost indsutrijskih kapaciteta neophodnom opremom, mašinama i uređajima, te savremnom IT podrškom. Takođe, rezultati su primjereni i u skladu su sa rezultatim preliminarnih istraživanja studijskih programa na mašinskim fakultetima u BiH, koji ne nude dovoljno znanja u mogućnosti za sticanje neophodnih kompetencija potrebnih za tehnologije vezane za Industriju 4.0. Dakle, visoko obrazovanje koje nije prilagođena očekivanim zahtjevima, kao preduslovima za ulazak u treću, a zatim četvrtu industrijsku revoluciju, ne daje adekvatan kadar koji bez pripreme i dodatane edukacije može pokrenuti promjene u privredi i automatsko prilagođavanje Industriji 4.0. Dakle, pred obrazovnim sistemom u BiH, kao i neposrednom okruženju ima mnogo prostora za transformaciju i razvoj metodologije obrazovanja, zasnovane na primjerima dobre prakse uspješnih zemalja, koje mogu biti primjenjenje u različitim industrijskim oblastima [2].

Univerzitetska praksa pokazuju da radoznalost i otvorenost studenata, sloboda i širina uma, mogu biti adekvatno iskorišteni samo ukoliko postoji prethodno struktuisano i utemeljeno znanje, koje se prenosi iz srednje škole, jer mogućava građenje novih spratova znanja na dobrim temeljima, te ukoliko ste kao predavač inventivni, interesantni, zanimljivi i vladate alatima koji mogu pokrenuti njihovo zanimanje, maštu, razmišljanje ka inovativnim stvarima, čak i ukoliko na raspolažate potrebnom opremom koja podstiče takav rad.

Najbolji način da se utoli »glad« za novim znanjima, za kojim mladi vape, ukoliko se govori o onima koji istinski imaju želju da uče i žive od svoga rada, je kreiranje sredine u okviru realizacije nastavnih programa, koja simulira realan radni prostor i okruženje koje odgovara okolnostima i uslovima indsutrijskog rada. To podrazumijeva timski, a ne individualan rad i mnogo interakcije između nastavnika (profesora) i studenata. Sistem prenošenja znanja koji se danas, uglavnom sastoji se iz predavanja, vježbi, testova, koji treba da pokažu koliko je tog znanja i informacija, koje je smješteno u literaturi, »preseljeno« u pamćenje, a često ne koliko je to znanje upotrebljivo za rješavanje konkretnih problema sa kojima se suočavamo u praksi.

Očigledno je neophodno mijenjati pristup, način, metoda rada, alate koji se koriste u te svrhe, kako bi se kod mladih ljudi stvarale vještine i sposobnosti koje im omogućavaju što bržu adaptaciju i uključivanje u realan svijet već prvog dana na poslu.

Zahtjevi za obrazovanjem u cilju adekvatne primjene za Industriju 4.0 podrazumijevaju korištenje savremnih tehničkih uređaja i pomagala. Ono što se koristi u svakodnevnom životu (telefoni, daljinski upravljači, tableti, laptopi, sotweri za igrice) treba usmjeriti u kreativno promišljanje i osmišljavanje novih rješenja za postojeće probleme. Sa takvom praksom treba krenuti vrlo rano, od prvog nivoa obrazovanja, preko srednjoškolskog, kao pripremu za visoko obrazovanje ili realni sektor.

2 EVROPSKI OKVIR ZA OBRAZOVANJE

Prepoznata potreba za promjenom i uvođenje digitalnih kompetencija u obrazovni sistem, mora biti vođena dobrim praksama i preporuka od strane svjetskih organizacija. UNESCO je definisao *Competency Framework for Teachers* (UNESCO. 2018.) kao odgovor na potrebe Agende održivog razvoja za 2030. godinu, a koja prepoznaje značajan potencijal informacionih i komunikacionih tehnologija u procesu ubrzanja napretka i povećanju globalne digitalne pismenosti [6]. Kao potencijalni izazovi u ovom procesu, prepoznati su koncepti: slobodno dostupnih edukativnih resursa, socijalne mreže, mobilne tehnologije, internet stvari, vještačka inteligencija, virtuelna i proširena stvarnost, obrada velikih skupova podataka, programiranje, te etika i zaštita privatnosti [5]. *Joint Research Center* Evropske komisije, 2013.-te godine definiše Evropski okvir za razvoj i razumijevanje digitalne kompetencije – DIGCOMP [7] koji predstavlja 21 kompetenciju razvrstanu u pet grupa (Slika 2.).

Kao što je prethodno pomenuto, za razliku od dobro poznatog tradicionalnog obrazovnog sistema, koji se razvijao postupno sa industrijskim revolucijama, obrazovanje digitalnih vještina i znanja (kompetencija) nije imalo adekvatan vremenski period koji je potreban za promjenu i prilagođavanja inertnih obrazovnih sistema. Prema [8], [9] digitalna transformacija obrazovnog sistema može da se posmatra na dva načina: prvi - uvođenje digitalnih tehnologija u proces obrazovanja (primjena softverskih i aplikativnih rješenja u procesu edukacije u cilju boljeg savladavanja gradiva, najčešći pristup), te drugi, kao izučavanje digitalnih vještina u okviru obrazovnog procesa (uz oslonac na digitalne tehnologije). Uzimajući u obzir prethodno, neophodno je na svim nivoima obrazovanja (predškolski odgoj i obrazovanje, osnovno obrazovanje, srednjoškolsko obrazovanje, visoko obrazovanje, kao I cjeloživotno učenje) uključiti razvoj i obuku digitalnih vještina koje prate tehnološki razvoj, odnosno učenje i savladavanje vještina i znanja koje danas čine digitalnu pismenost. Digitalna pismenost se može definisati kao sposobnost korištenja računara, softverskih i aplikativnih programa za manje složene praktične zadatke ili sposobnost pojedinca da na efikasan način koristi računar u svakodnevnom obavljanju poslovnih zadataka [10].

	Dimenzija 1	Dimenzija 2	Dimenzija 3
	5 Oblasti	21 Kompetencija	Razina/Nivo kompetencije
	OBLAST	**KOMPETENCIJE**	
Osnovne	**1. INFORMACIJE**	1.1 **Pregled, pretraga** i **filtriranje** informacija 1.2 **Evaluacija** informacija 1.3 **Upravljanje** informacijama i digit. sadržajem	
Osnovne	**2. KOMUNIKACIJA**	2.1 **Interakcija** posredstvom digitalnih tehnologija 2.2 **Dijeljenje sadržaja** posredstvom digitalnih teh. 2.3 Uključivanje u **digitalno državljanstvo** 2.4 **Kolaboracija** putem digitalnih tehnologija 2.5 **Ispravan i prihvatljiv način komunikacije** 2.6 Upravljanje **digitalnim identitetom**	
Osnovne	**3. KREIRANJE SADRŽAJA**	3.1 **Razvoj digitalnog sadržaja** 3.2 **Integracija i prerada digitalnih sadržaja** 3.3 **Autorska prava** i licenciranje 3.4 **Programiranje**	
Transverzalne	**4. SIGURNOST**	4.1 Zaštita **uređaja** 4.2 Zaštita **personalnih podataka** i **privatnosti** 4.3 Zaštita **zdravlja** i **dobrobiti** 4.4 Zaštita **životne sredine**	
Transverzalne	**5. RJEŠAVANJE PROBLEMA**	5.1 Rješavanje **tehničkih problema** 5.2 Identifikovanje **potreba** i **odogovornost teh.** 5.3 **Kreativna primjena** digitalnih tehnologija 5.4 Identifikovanje **nedostataka digitalnih komp.**	

Slika 2. *Evropski okvir za razvoj i razumijevanje digitalne kompetencije – DIGCOMP [7]*

3 STUDIJA SLUČAJA

Prelazak na Industriju 4.0 u BiH neće biti lagan i brz. Glavni razlozi za to su veliki troškovi i nedostatak kvalifikovanih radnika. Pod kvalifikovanim radnicima pored inženjera podrazumjevaju se i tehničari sa završenom srednjom školom. Andrea Benešová i Jiří Tupa u studiju objavljenoj 2017. godine [11] identifikovali su vještine i kvalifikacije koje trebaju imati svršeni srednjoškolci za rad u proizvodnji usklađenom sa Industrijom 4.0. Osnova dva izlazna profila koje se navode u studiji su tehničar elektrotehnike i tehničar mašinstva. Okvirno posmatrano, vještine koje se očejuju da steknu učenici srednjih škola date su u Tabeli 1.

Prema izvještaju Svjetskog ekonomskog foruma “Budućnost radnih mjesta” [12], uticaj automatizacije i COVID-19 će do 2025. godine izbaciti 85 miliona radnih mjesta. Međutim, među poslovima za koje je predviđeno da ostanu, 50% će zahtijevati prekvalifikaciju do 2025. Trenutni nesrazmjer između vještina koje posjeduju današnja generacija mladih ljudi i onoga što je potrebno tržištu je u opasnosti da se još više proširi, jer Industrija 4.0 konstantno zahtijeva nova znanje i vještine koje ljudi mogu pratiti.

Tabela 1. *Potrebne izlazne vještine učenika srednjih škola za primjenu tehnologija Industrije 4.0*

Meke vještine (Soft skils)	Odgovornost, Kreativnost, Samostalnost u radu, Komunikacione vještine (poznavanje stranih jezika), Timski rad, Kritičko razmišljanje, Emocionalna inteligencija, Socijalne vještine.
Tehničke vještine (hard skills)	Osnovne tehničke vještine: - Osnove elektrotehnike i mašinstva; - Poznavanje bezbjednosnih standarda; - Sposobnost održavanja novih mašina; - Poznavanje tehničke dokumentacije; - Poznavanje sistema kvaliteta; - Poznavanje multimedije; - Poznavanje programskih jezika Napredne tehničke vještine: - Internet stvari (IoT); - Poznavanje rada sa PLC kontrolerima; - Poznavanje elektronike za napajanje i upravljanje; - Poznavanje upravljanja robotima; - Poznavanje mrežnih sistema; - Vještačka inteligencija i mašinsko učenje; - Zaštita informacionih sistema; - Obrada podataka.

Obrazovanje tehničara mašinstva i elektrotehnike potrebnih kompanijama koje će u bliskoj budućnosti u potpunosti preći na Idustriju 4.0 je veliki izazov za obrazovni sistem u Republici Srpskoj. Sa jedne strane, potrebno je prilagoditi nastavne planove i programe potrebama Industrije 4.0, a sa druge strane je potrebno obučiti nastavni kadar. Kada su u pitanju struke elektrotehnika i mašinstvo u Tabeli 2 dat je pregled izlaznih profila sa godišnjim brojem časova stručnih predmeta za navedene srednje škole u Republici Srpskoj. Svi izlazni profili imaju 1882 časa godišnje opšteobrazovnih predmeta, što u prosjeku predstavlja oko 45% ukupne nastave. Generalno posmatrano iz tabele se može zaključiti da je broj časova teorije i vježbi (praktični dio predmeta) za stručne predmeta podjednak, nešto veći broj vježbi se može uočiti za zanimanje Tahničar informacionih tehnologija. Na osnovu prethodnog, u prosjeku oko 25% (približno 1000 časova/godini ili 30 časova/sedmici) nastave učenici bi trebalo da potroše na sticanje praktičnih znanja. Navadeni broj časova je definisan nastavnim planom i programom, te se može smatrati zadovoljavajućim, ali opremljenost i stručnost nastavnog kadra da učenicima prenesu znanje iz oblasti potrebnih Indsutriji 4.0 je posebna problematika.

U nastavku rada je prikazana analiza nastavnih planova i programa za sledeća zanimanja: Tehnčar informacionih tehnologija, Tehničar računarstva i programiranja, Mašinski tehničar za kompjutersko konstruisanje i Tehničar mehatornike. Ova četri izlazna profila u potpunosti odgovaraju potrebama Industrije 4.0. U Tabeli 3 dat je popis predmeta definisanih nastavnim planom i programom za nevedene izlazne profile koji omogućavaju sticanje naprednih tehničkih vještina potrebnih Indsutriji 4.0. Za očekivati je da učenici meke vještine stiču kroz opšteobrazovne predmete, a da osnovne tehničke vještine stiču kroz opšte stručne predmete. Analiza navedenih podataka urađena je na osnovu podataka dostupnih na web stranici Republičkog pedagoškog zavoda. Podaci iz tabele pokazuju da je broj časova koji je predviđen za predmeta koji omogućavaju sticanje naprednih znanje potrebnih Industriji 4.0 za navedene struke se kreće od 328 do 528 časova godišnje, odnosno od 7,7 do 13,2 %

od ukupnog broja časova. Za društvo u tranziciji, kakvo je u BiH, ovaj broj predmeta, kao i broj časova može se smatrati zadovoljavajućim, što bi značilo da u ovom trenutku treba raditi na usavršavanju nastavnog kadra i opremanju srednjih škola, kako bi plan i program rada mogli u potpunosti da budu primjenjeni.

Tabela 2. *Pregled izlaznih profila sa godišnjim brojem časova stručnih predmeta za struke elektrotehnika I mašinstvo*

Struka	Zanimanje	Godišni broj časova stručnih predmeta	
		Teorijski dio	Praktični dio (vježbe)
Elektrotehnika	Tehničar elektroenergetike	1268	972
	Tehničar elektronike	1098	1040
	Tehničar računarstva i programiranja	968	1170
	Tehničar telekomunikacija	1202	936
	Tehničar informacionih tehnologija	662	1576
	Tehničar multimedije	838	1266
Mašinstvo i obrada metala	Mašinski tehničar za kompjutersko konstruisanje	1196	1176
	Tehničar mehatronike	1240	1300
	Tehničar mašinske energetike	1492	912
	Tehničar CNC tehnologija	1100	1206

Tabela 3. *Popis predmeta definisanih nastavnim planom i programom srednjih škola za karakteristične izlazne profile koji omogućavaju sticanje naprednih tehničkih vještina potrebnih indsutriji 4.0*

Zanimanje	Naziv predmeta	Broj časova/godini	Procenat od ukupnog broja časova
Tehničar računarstva i programiranja	Digitalna tehnika	102	2,5%
	Računarske mreže	132	3,3%
	Automatika	132	3,3 %
	Baze podataka	132	3,3%
	=	498	12,4%
Tehničar informacionih tehnologija	Aplikativni programi	136	3,3%
	Računarske mreže i komunikacije	166	4,0 %
	Informacioni sistemi i baze podataka	102	2,5%
	Zaštita informacionih sistema	64	1,5%
	=	468	11,3%
Mašinski tehničar za kompjutersko konstruisanje	Modelovanje I simulacije pomoću računara	200	4,7%
	Automatizacija i robotika	64	1,5%
	CAD – CAM sistemi	64	1,5%
	=	328	7,7%
Tehničar mehatronike	Pneumatsko i relejsko upravljanje	102	2,3%
	Mehatronički sistemi	128	2,9%
	Sistemi automatskog upravljanja	128	2,9%
	Programabilni logički kontroleri	128	2,9%
	Dijagnostika i održavanje mehatroničkih uređaja i sistema	96	2,2%
	=	582	13,2%

Koliko učenici srednjih škola poznaju termine iz oblasti industrije 4.0 analizirano je kroz anketu koja je spovedena u Srednjoj školi "28. juni" u Istočnom Novom Sarajevu, među učenicima koji se školuju za zanimanja iz struke elektrotehnika i mašinstvo. Cilj navedne ankete bio je utvrditi trenutno stanje u obrazovanom sistemu na primjeru srednje škole koja obrazuje tehničera izlaznog profila koji potencijalno odgovara industriji 4.0. Anketu je popunilo ukupno 125 učenika svih godina. Na pitanje "Navedite tri primjera mekih vještina", 32% učenika je odgovorilo uspješno na pitanje, a najčešće nabrojane meke vještine su: komunikacija, javni nastup, prezentacija. Od ukupno anketiranih, 23 učenika ili 18,4% nije napisalo šta ih to asocira na robotiku i amutomatizaciju, vještačku inteligenciju i 3D tehnologije. Najčešći odgovori vezani na asocijaciju na prethodno navedene segmente Idustrije 4.0 su bili: robot, film, igrica, 3D štampanje, telefon i programiranje. Samo 5 učenika (4 %) je pokušalo da da odgovor na sledeća pitanja:

- Da li vam je poznat termin Industrija 4.0?
- Da li vam je poznat termin IoT – Internet of things (Internet stvari)?
- Da li vam je poznat termin mašinske učenje (Machine learning)?

Dijagram prikazan na Slici 3a pokazuje da 28% anketiranih učenika smatra da su tokom obrazovanja imali dvoljno praktične nastave koja podrazumjeva rad na računarima ili rad na mašinama, dok je dijagram na Slici 3b pokazuje da je 31,2% anketiranih učenika imalo priliku da tokom obrazovnog procesa posjeti proizvodne kompanije.

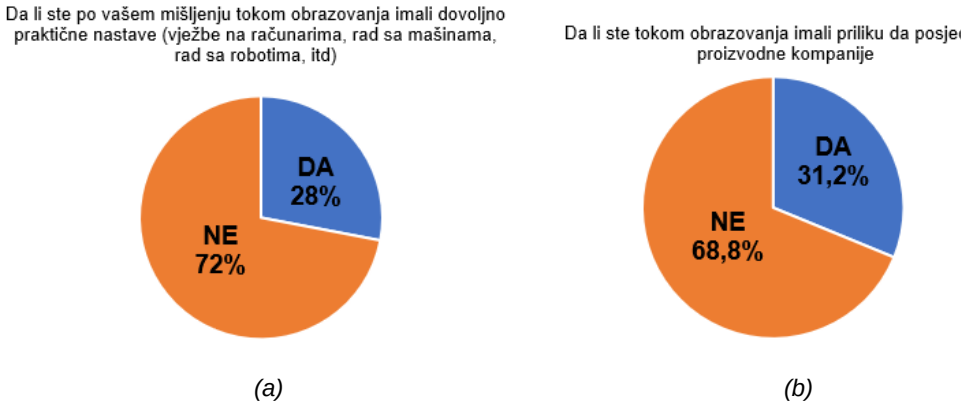

(a) *(b)*

Slika 3. *Prikaz rezultat anketnog ispitivanja učenika*

Prikazani rezultati ankete su očekivani, učenici se još nisu susreli sa terminima vezanim za Industriju 4.0, oprema koje škole posjeduju ne prati u potpunosti nastavne planove i programe, te su jasni pokazatelji da ne postoji sistemski pristup obrazovanju u cilju sticanja potrebnih znanja za primenu tehnologija Indsutrije 4.0.

U prilog prikazanim rezultatima istraživanja, zanimljivo je navesti vrlo aktuelne rezultate studije koju je proveo tim istraživača akademske zajednice BiH, a činili su ga 12 profesora iz Bihaća, Sarajeva, Tuzle i Mostara, sa tehničkih i ekonomskih fakulteta, u cilju istraživanja spremnosti za edukaciju i implementaciju Industrije 4.0 u obrazovnim ustanovama I preduzećima. U periodu istraživanja maj 2021.- februar 2022., na populaciji od 719 (47,3% učenika i studenata) ispitanika, 56 mjesta (177 menadžera i 542 ostalih), te uzorku od 176 preduzeća, iz 36 mjesta, dobijeni su

rezultati koji pokazuju da je koncept Indsutrije 4.0 prisutan u BiH, ali nedovoljno zastupljen u poslovnoj praksi, te da ne postoji dovoljno razumijevanje pojma i fenomena, kao ni mogućnosti koje svojim tehnologijama Industrija 4.0 pruža. Takođe, interesantno je pomenuti da 72,3% menadžera, kao i 86,2% zaposlenih smatra da su tehnologije Indsutrije 4.0 prijetnja postojećim radnim mjestima, ali istovremeno i prilika za otvaranje novih (98,35 menadžera I 95,9% zaposlenih).

Značajan dio ispitanika obuhvaćen istraživanjem ne poznaje adekvatno sadržaj pojma Industrija 4.0 (46% ispitanika je odgovorilo da ne zna šta je Industrija 4.0), oni koji su se susreli sa pojmom navode da su saznanja o tome sticali i formalno i neformalno, dok je svega ¼ ispitanika prijavilo da su znanja o Industriji 4.0 i njenim tehnologijama sticali kroz formalno obrazovne sisteme [13].

4 ZAKLJUČCI

Proces transformacije, odnosno ulazak u digitalni svijet, se dešava jako brzo, pri čemu tradicionalni obrazovni sistemi, na svim nivoima, nisu u mogućnosti da pruže adekvatan odgovor na postavljene izazove. Iz toga razloga je neophodna temeljna promjena, koja mora da krene od početnih nivoa obrazovanja, spajanjem najboljih elemenata iz oba svijeta: tradicionalnog (konvencionalnog) i digitalnog, kako bi se osigurale adekvatne kompetencije potrebne za novo digitalno doba. Dakle, naglašena je potreba modernizacije edukativnih procesa, vođena dobrim praksama, putem interdisciplinarnih principa u obrazovanju, u kontekstu Industrije 4.0 i digitalne transformacije, za koju moraju biti spremni svi akteri obrazovnog procesa, edukatori, djeca (učenici, student), roditelji, a za to je potrebna strategija. U izradi strategije moraju učestvovati svi, država, poslovna i akademska zajednica. Na transformaciju se ne smije gledati kao process budućnosti, već kao sadašnji trenutak, jer privreda traga za stručnim i kvalifikovanim ljudima koji enormno brzo mogu prihvatiti promjene i implementirati nove tehnologije, posebno one koje su integrativni dio Industrije 4.0.

ZAHVALNOST

Ovaj rad realizovan je zahvaljujući podršci uprave, profesora i učenika JU SŠ »28.juni« Istočno Novo Sarajevo.

LITERATURA

[1] Švraka, A. (2020), Kako je nastalo obrazovanje koje danas poznajemo? Glossa Centar, prostupljeno septembar 2022.
[2] B. Marković, A. Đurić, (2022). Education 4.0 for Industry 4.0. In: Rackov, M., Mitrović, R., Čavić, M. (eds) Machine and Industrial Design in Mechanical Engineering. KOD 2021. Mechanisms and Machine Science, vol 109. Springer, Cham. DOI:10.1007/978-3-030-88465-9_74.
[3] Miltenović, V., Antić, D. (2020): Inženjering pametnih proizvoda I usluga, Univerzitet u Nišu, ISBN 978-86-7181-112-5.
[4] Tadić, D. (2022), Uticaj Industrije 4.0 na promjene u obrazovanju, Tehnika-Kvalitet IMS, standardizacija i metrologija 22, DOI:10.5973/tehnika 2202257T
[5] Vujović,V. (2020), Digitalna trafnsformacija i visokom obrazovanju: pregled, razlozi i očekivanja, Jahorina Bussines Forum 2020.

[6] UNESCO (2018.) "UNESCO ICT Competency Framework for Teachers", Published in 2018 by the United Nations Educational, Scientific and Cultural Organization.
[7] Carretero, S., Vuorikari, R., Punie, Y. (2017.): DigComp 2.1 – The Digital Competence Framework for Citizens: With eight proficiency levels and examples of use, Luxembourg: Publications Office of the European Union.
[8] Balyer, A., & Öz, Ö. (2018.) Academicians' views on digital transformation in education, International Online Journal of Education and Teaching, 5(4), pp. 809-830.
[9] Hiltz, S. R., Turoff, M. (2005.) Education goes digital: The evolution of online learningand the revolution in higher education, Communications of the ACM,48(10), pp. 59−64.
[10] Savage, M., Barnett, A. (2015.) Digital literacy for primary teachers, Northwich: Critical Publishing Ltd.
[11] Benešová, A., Tupa, J. (2017.) Requirements for Education and Qualification of People in Industry 4.0, 27th International Conference on Flexible Automation and Intelligent Manufacturing, FAIM2017, 27-30 June 2017, Modena, Italy.
[12] https://www.edarabia.com/top-career-skills-prepare-industry - pristupljeno 25.10.2022.
[13] Karabegović, I., ostali (13 autora), (2022.) Industrija 4.0- nova poslovna stvarnost: spremnost za edukaciju i mogućnost za implementaciju u preduzećima u BiH, Zbornik implementacija Industrije 4.0 u budućnost, ISBN 978-9926-426-05-7

COMETa 2022
6th INTERNATIONAL SCIENTIFIC CONFERENCE
17th - 19th November 2022
Jahorina, B&H, Republic of Srpska
University of East Sarajevo
Faculty of Mechanical Engineering
Conference on Mechanical Engineering Technologies and Applications

IDENTIFICATION DESIGN PARAMETERS OR LOAD CAPACITY IN MANUAL GEARBOX FOR DIFFERENCE WORKING CONDITIONS

Miroslav Milutinović[1], Madina Isametova[2], Spasoje Trifković[3], Sanjin Troha[4], Milan Tica[5], Kulwant Singh[6]

Abstract: Manual gearbox work in different working condition. These conditions affect the reliability of the gearbox. The overall reliability of the gearbox includes the elemental reliability of gears, bearings, couplings, seals and lever mechanism. In this paper is presented a methodology for identifying design parameters based on torque results measured in exploitation on mountain conditions, flat conditions and combinations of flat and mountain conditions. For this conditions it is possible to determine elementary reliability of all components. Methodology is presented on manual six speed gearbox. Based on this methodology is developed computer software DRAG which can calculate design parameters or load capacity for given design parameters and desired working conditions.

Key words:gearbox, design parameters, load capacity, reliability

1 INTRODUCTION

Increasing global competition on the market, development of technical and technological achievements and increasing customer expectations force manufacturers to improve product flexibility, reduce development time and physical realization of products, without affecting economic effects, functional characteristics or quality. One of the basic parameters that affects these indicators is the operating conditions, and each product must be compatible with the environment in order to ensure functionality during its working life [1]. Looking at the product from the customer's point of view, the

[1] PhD Miroslav Milutinović, University of East Sarajevo Faculty of Mechanical Engineering, East Sarajevo, B&H RS, miroslav.milutinovic@ues.rs.ba(CA)
[2] PhD Madina Isametova, Satbayev University, Almaty, Kazakhstan, isametova69@mail.ru
[3] PhD Spasoje Trifković, University of East Sarajevo Faculty of Mechanical Engineering, East Sarajevo, B&H RS, spasoje.trifkovic@ues.rs.ba
[4] PhD Sanjin Troha, Faculty of Engineering, University of Rijeka, Rijeka, Croatia, sanjin.troha@riteh.hr
[5] PhD Milan Tica, Faculty of Mechanical Engineering, University of Banja Luka, Banja Luka, Bosnia and Herzegovina, milan.tica@mf.unibl.org
[6] Kulwant Singh,TriTed Inovations, Cambridge, Ontario, Canada, kulwant@trited.com

failure of the product during operation is undesirable, while from the manufacturer's point of view it is inadmissible.

The basis for the development of a reliable product is knowledge of how similar products function, as well as potential errors that occurred in the development and exploitation process, so that they do not repeat themselves. Different methods were used to define reliability. The methodology for defining a reliable system, insensitive to variations in operating conditions, in the first attempt is known as robust design. Although there were several authors [2,3] who wrote about the concept of robust design, the originator of this idea is considered to be Taguchi [4], who popularized this methodology a lot. The essence of the Taguchi idea was described in a more comprehensible and comprehensive way by the authors of the papers [5] and [6].

In order to achieve the insensitivity of the product or process in the construction phase, the authors of the works [29] have given an overview of the literature and a number of practical examples that have applications in the industry. The robust design methodology is achieved using Axiomatic design, which is applied to define design parameters or functional needs. The originator of axiomatic design is considered to be Sux [8,9] whose idea was to create a scientific basis for constructors, especially in the stages of product development. According to the authors of the papers [8,9,10,11] the Axiomatic design procedure is based on two generally accepted axioms. The relationship between functional requirements and design parameters can be represented by a relation [10].

$$\{FR\} = [A]\{DP\}$$

Where *FR* are the functional requirements, *DP* the design parameters and [*A*] correlation matrix. On the examples of a passenger car [12], thickness of the oil film at the ball bearing [13], setting the parking mode in the automatic transmission [14], сложених система [15] a number of optimal construction methodologies based on the principles of Axiomatic design were developed.

These methodologies are applied to elementary functions, which were arrived at by the method of decomposing the system to new elementary functions. The decomposition procedure can be divided into four levels [16,17,18], while the final number of decomposed components is not final and depends on the needs of the construction. In the paper [19,20,21] strategies for decomposing complex systems consisting of a large number of subsystems and components are proposed. Complex structures, such as vehicles [22] they can be decomposed into multiple subsystems such as the engine [23], gearbox [24,25,26], steering system, braking system, etc., and then to lower-order subsystems (gears, bearings, couplings, etc.) down to elementary components. Based on previously defined methodologies, the authors of the works [24,25,26] performed the decomposition of the manual six-speed gearbox for heavy-duty motor vehicles. Proper decomposition of the system plays an important role in optimizing design parameters. On the example of a five-speed gearbox, the authors of the papers [27,28], they optimized parameters with the aim of reducing noise during operation. Proper optimization of the parameters also affects the price of the product. In the paper [31], the authors searched for the optimum between the level of reliability, price and needs, depending on the new investment in the development of reliability. There are two levels of decision making that affect the price. The first level is deciding on the required level of reliability and it was processed by the authors [29], while the second level, which refers to the specifications of the components that provide it, was processed by the authors in the paper [30]. Each component must satisfy a certain

new level of reliability, so that the complete system has satisfactory operational reliability. The authors dealt with this problem in their papers [29,30,31].

During the operation of the gearbox, damage often occurs to the gears, bearings, couplings, seals, etc. Through long-term research, the authors of the paper [32] came to the data that as much as 49% of damage occurs on bearings, 41% on gears, while all other damage is 10%. Taking into account that bearing damage is influenced by several factors and that destruction is of a stochastic character, paper [33] shows a diagram of the probability of gear destruction for hardened gears, on which you can clearly see a decrease in durability with an increase in the number of changes.

2 EXPLOITATIONS MANUAL GEARBOX

Gearbox can be installed in different types of vehicles. Consequently, the conditions in which exploitations vary are stochastic in nature. The stochasticity of conditions is influenced by several parameters:

- Type of vehicle (the same transmission is installed in trucks of different capacities, for transmission in buses, in work machines, for internal transport, etc.)
- Vehicle operation (the same type of transmission is operated in difficult working conditions, light working conditions (highway) or variable (partially heavy and partially light))
- Handling the vehicle (the user of the vehicle influences the driving conditions with his experience)

Based on these parameters and the desired service life, the same construction of the gearbox will have a different load capacity for different input parameters (torque at the entrance to the gearbox). On the other hand, data on the loads to which the gearbox is exposed can be collected in different ways. One of the ways is to keep records of vehicle servicing with a clear indication of the type of vehicle and working conditions, the other way is information from the user (driver) and, as the most important and most reliable, is load measurement in the process of work. On the basis of the mentioned methods, the percentage participation of the transmission stages for different types of gearboxes was obtained, and the results for the manual six-speed ZF gearboxes will be presented in the paper. On the basis of the user survey, the results of the percentage participation of the terrain on which the vehicle was exploited were obtained (Figure 1).

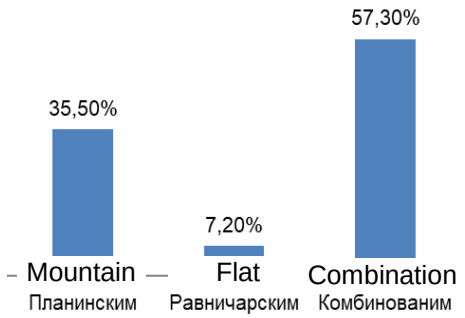

Figure 1. *Percentage share of the terrain where the vehicle was used*

For the mentioned conditions of exploitation, torque measurements were made at the output of the gearbox (on the cardan shaft) when driving the freight motor vehicle in unloaded and loaded conditions. The exploatatiion was carried out for approximately the same percentage participation of the transmission stages for loaded and unloaded vehicles. In Figure 2.a. a diagram of the percentage participation of the gear pairs , as well as the measured torque values for driving an unloaded vehicle in mountain conditions. Figure 2.b shows a diagram for the same working conditions, but when driving a loaded vehicle.

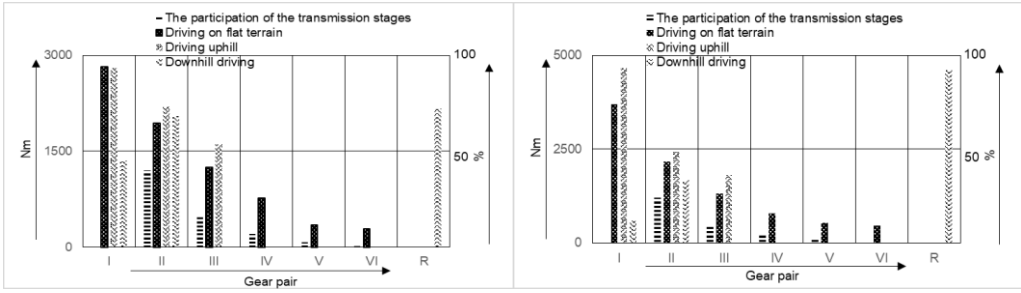

a) unloaded vehicle b) loaded vehicle

Figure 2. *The percentage share of the gear ratio and the measured value of the torque at the output of the gearbox when driving in mountainous conditions*

The vehicle is operated not only in mountainous conditions, but also in plains. Figures 3.a and 3.b show the diagrams of the proportional participation of the gear paris in plain conditions, with the values of the measured torques for the unloaded and loaded vehicle.

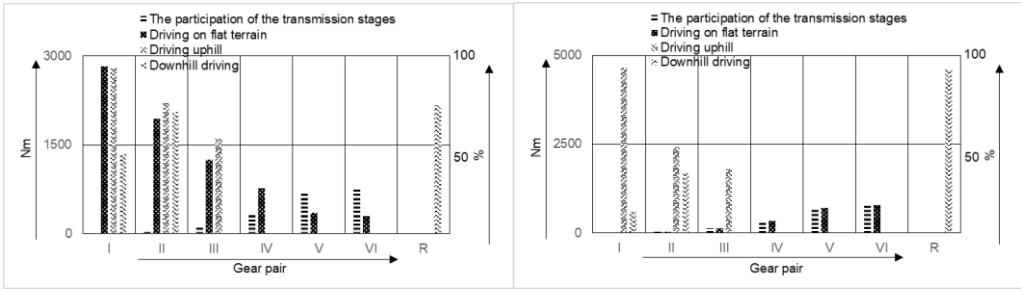

a) unloaded vehicle b) loaded vehicle

Figura 3. *The percentage share of gear ratios and the measured value of the torque at the output of the gearbox when driving in flat conditions*

The measured torque values can be used to define the load capacity for certain exploitation conditions. Taking into account that vehicles are used on different terrains, it is necessary to collect results for variable driving conditions as well. For the combined conditions of exploitation with the percentage participation of gear paris (table 1), torque values were measured for identical loads as in the previous tests, the values of which are given in Figure 4. The maximum torque of 4660Nm was measured when driving a loaded motor vehicle with an incline first , gear, while the minimum torque was measured when driving in sixth gear on flat terrain in the amount of 529Nm.

Other values varied, depending on the changing characteristics of the terrain on which the visilo was exploited.

Table 1. *Percentage share of transmission levels for combined exploitation conditions*

Gear pair	*I*	*II*	*III*	*IV*	*V*	*VI*	*R*
Percentage participation	*0,2*	*23,33*	*21,10*	*19,27*	*18,27*	*17,63*	*0,2*

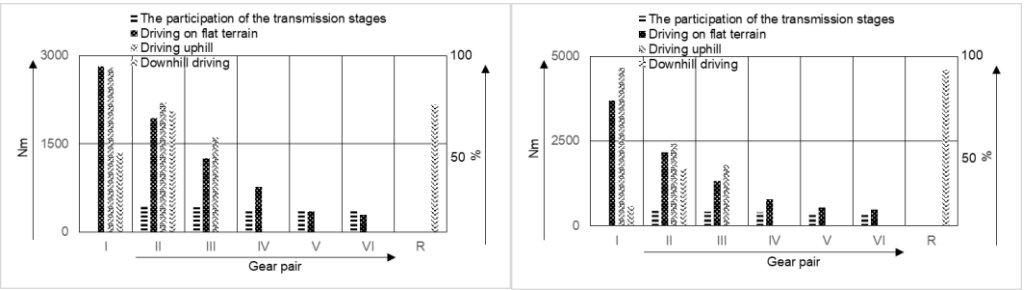

a) unloaded vehicle b) loaded vehicle

Figure 4. *The percentage share of the gear ratios and the measured value of the torque at the output of the gearbox when driving in combined conditions of exploitation*

3 RELIABILITY OF THE MANUAL GEARBOX

The total reliability of the gearbox consists of the partial reliability of the components that are built into the structure. Therefore, it is necessary to know the number of gears, coupling bearings, seals, etc. installed in the transmission. The reliability of the manual gearbox (Figure 5) consists of the product of the elementary reliability of the gear R_Z, bearing reliability R_L, the reliability of the sealer R_{ZP} and the reliability of the lever mechanism R_P [24,25,26].

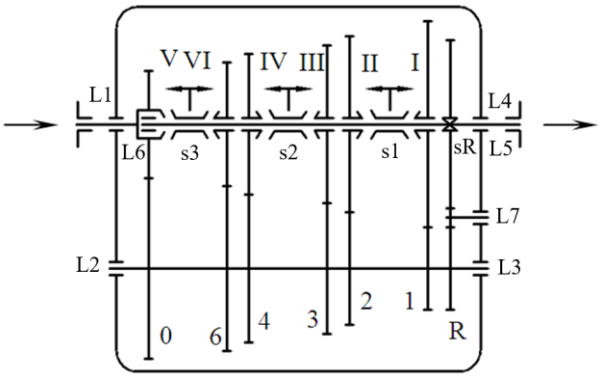

Figure 5. *Gearbox scheme*

$$R = R_z R_L R_s R_{zp} R_p \tag{1}$$

Considering that the gearbox has 6 gears for forward driving and one gear for reverse, its functioning is realized by the function of 4 spinhro-couplings, 7 bearings, 2 seals and a lever mechanism..

Assuming that the elementary reliabilities of the components are equal, the total reliability can be expressed:

$$R_j = \sqrt[r]{R} \tag{2}$$

So it is: $r=z+L+s+zp+p=7+7+4+2+1=21$ (3)

On the basis of equation 2, the obtained reliability values for each gear pairs R_{z0}, R_{zI}, R_{zII}, R_{zIII}, R_{zIV}, R_{zVI}, R_{zR} are the same values and they change in pairs when damage occurs. There are 7 bearings installed in the gearbox, so decomposition equation 2 and the elementary reliability of the bearings R_{L1}, R_{L2}, R_{L3}, R_{L4}, R_{L5}, R_{L6} and R_{L7} they should be equal. In an identical way to the reliability of synchro-couplings R_{s1}, R_{s2}, R_{s3} and R_{sR} they should have the same reliability as the reliability of the sealant R_{zp1} and R_{zp2}.

4 DETERMINATION OF THE PARAMETERS OF THE COMPONENTS INSTALLED IN THE GEARBOX

4.1 Determination of bearing capacity and design parameters of gears

The bearing load of the gear pair is determined based on the highest torque value in the load spectrum defined on the small gear during the expected working life. For each gear pair, the permissible stress on the flanks of the gear teeth is determined, and from the condition that the stress on the flanks is less than or equal to the permissible stress, the value of the bearing capacity of the gear is obtained:

$$T_x = \frac{\left(\sigma_{Hdoz}\right)_x^2 b_x d_x^2}{2Z^2 K} \frac{u_x}{u_x + 1} \tag{4}$$

Where is b_x – gear width

d_x – gear diameter

u_x – gear ratio of the gear pair

x=0, I, II, III,..,R – gear pari

To define the torque on the small gear of each gear pair, it is necessary to know the transmission ratio from the input or output to the small gear, as well as the degree of utilization, so that the value of the torque can be expressed as:

$$T_{ul} = \frac{T_x}{i_0 i_x \eta^2} \text{ respectively } T_{izl} = T_{x1} i_x \eta \tag{5}$$

Where are they: T_{ul} – torque at the input to the gearbox

T_{izl} – torque output from the gearbox

i_0 , i_x– working transmission ratio of the corresponding gear pairs

η – degree of gear pair utilization

The connection between functional needs and design parameters can be made by varying the width of the gear. Thus, on the basis of equation 5, for known values of the torque to the gear, the width of the gear can be determined as:

$$b_x = \frac{2T_{x1}}{\left(\sigma_{Hdoz}\right)_x^2 d_{x1}^2} \frac{u_x + 1}{u_x} Z^2 K \tag{6}$$

4.2 Determination of bearing reliability

A suitable bearing with satisfactory reliability is installed in each of the supports. Its reliability or unreliability depends on the spectrum of loads to which it is exposed during its working life. For each of the load levels from the load spectrum, it is possible to determine the Weibull function of the probability of destruction, for which the unreliability of the bearing can be expressed as:

$$F_p = \sum_{i=1}^{k} p_i\left(F_i\right) P_{Ri}\left(F_i\right) \tag{7}$$

So the reliability of the corresponding bearing is expressed as: R_{Ly}=1-F_{pLy} of each of the bearings y=1...7

4.3 Determining the reliability of synchro couplings

The number of synchro couplings that are installed also depends on the number of gears of the gearbox. Three synchro couplings and one toothed coupling are installed in the subject manual transmission, so their reliability should be identical. The reliability of the synchro coupling is affected by the number of times the two gears are turned on or off, so the sum of changes in both gears is calculated in the final form. Weibull's function for the potential destruction of couplings can be rewritten as:

$$F_{pz} = P_{Rz}\left(n_{\Sigma sz}\right) = 1 - e^{-\left(\frac{n_{\Sigma sz}}{\eta_z}\right)^{\beta_z}} \tag{8}$$

Where the parameters η_z and β_z depend on the appropriate coupling.

4.4 Determining the reliability of the sealant

The reliability of the seal is affected by the number of revolution of the shaft on which the seal is installed and depends on its service life. For the intended number of changes, the Weibull function for sealants can be expressed as:

$$F_{pzp} = P_{Rzp} = 1 - e^{-\left(\frac{n_{\Sigma zp}}{\eta_{zp}}\right)^{\beta_{zp}}} \tag{9}$$

Where the parameters η_{zp} and β_{zp} depend on the appropriate sealant.

4.5 Conditions for the selection of parameters

To define the number of changes (revolutions) of shafts and gears, it is necessary to know the number of revolutions at the input or output of the gearbox. A convenient way to determine the number of revolutions is to define the number of kilometers driven by a vehicle in which a suitable transmission is installed. The number of point changes (revolutions) can be expressed as:

$$S = n_{\Sigma} \cdot O_t \tag{10}$$

Where is *S*- Route

n_{Σ} - Number of wheel revolutin in route

O_t – Bulk of the drive wheel of vehicle

On the basis of which the participation of all transmission stages in the number of point-to-base changes can be determined

$$f_i = \frac{n_{\Sigma i}}{n_{\Sigma}} \tag{11}$$

Where is $n_{\Sigma i}$ - number revolution at all speed at wheel and on the basis of which the number of changes on the small gear can be determined

$$n_{\Sigma ij} = n_{\Sigma i} \cdot i \tag{12}$$

Where is *i* gear ratio from wheel to small gear.

5 SOFTWARE FOR IDENTIFICATION OF DESIGN PARAMETERS

On the basis of the previously defined procedure, software was developed for determining the design parameters and load capacity of the gearbox. The software consists of several stages in which the user makes some decisions and writes them in certain blocks. The data entered once configures the entire budget and the user does not have to enter them again. If necessary, the user can go back and correct the entered values.

The first step represents the definition of the desired reliability of the gearbox for a certain distance traveled by the vehicle. In this step, the user enters the bulk of the drive wheel of vehicle intended for installation on the vehicle, as well as the number of gear pairs, the number of bearings installed in the gearbox in question, the number of synro-couplings with the number of teeth (if installed), the number of seals and the number of lever mechanisms (Figure 6). Keeping in mind that all elemental reliability should be equal, by activating the command “ДЕКОМПОНОВАЊЕ ПОУЗДАНОСТИ“ elemental reliability is automatically determined, as well as the total reliability of a set of components (gears, bearings, synchro couplings, ...). If the user has doubts about any of the values he should enter in the empty fields, by activating the command “ПОМОЋ“ a field with appropriate explanations opens. By completing the first step and activating the command “ДАЉЕ“ it is moved to the next phase in which it is necessary to enter the basic parameters related to the smaller gear with the appropriate transmission ratio (Figure 7). The desired maximum torque values are entered in the same form. The

continuation of the process is executed with the command "ДАЉЕ". The load calculation is carried out in an identical way on software form 3 (Figure 8), where the percentage of the load in the gear load spectrum is also entered. In the next phase, elemental reliability is determined for a given load spectrum, with the parameters of the Weibull distribution defined η i β.

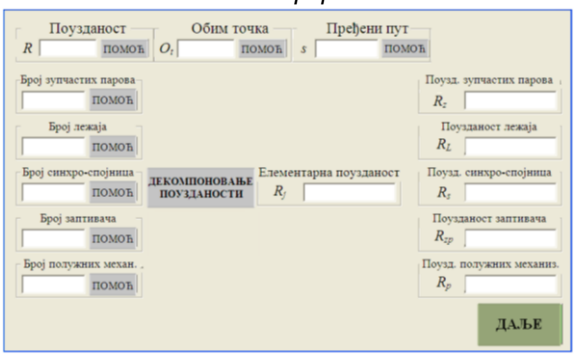

Figure 6. *Software form 1*

Figure 7. *Software form 2*

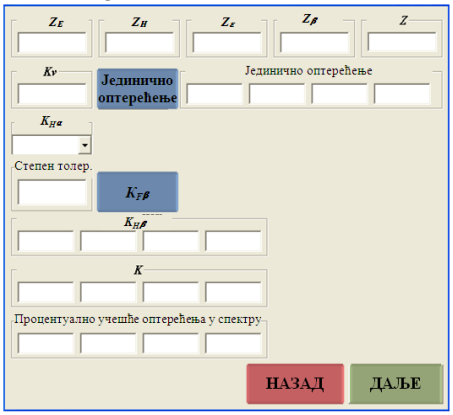

Figure 8. *Software form 3*

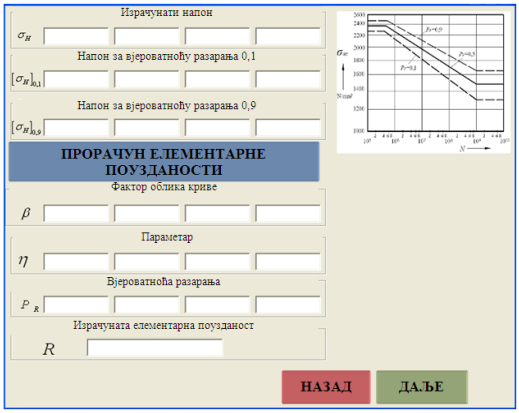

Figure 9. *Software form 4*

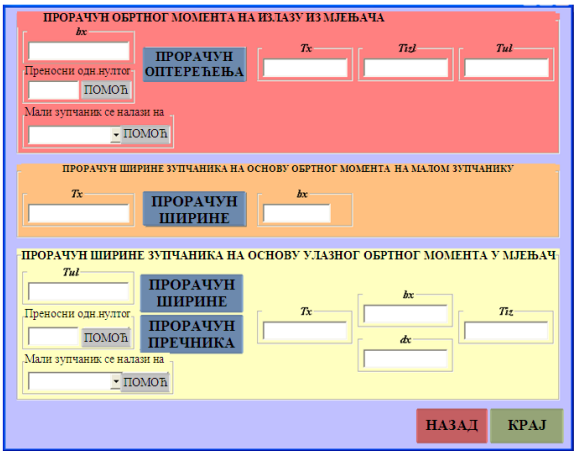

Figure 10. *Software form 5*

The procedure is iteratively repeated until the calculated reliability coincides with the desired reliability (Figure 9). The calculated value of the highest voltage for the elemental reliability thus calculated represents the permitted voltage. Based on the previously defined procedure, it is possible to determine the load capacity of the gear pair or the width of the gear, depending on the requirements. Through the software form, it is also possible to perform a check the calculated results (on the basis of the calculated load capacity, determine the width of the gears)

Taking into account that gear transmissions are defined on the basis of input torque, it is a variant made that it is possible to calculate the gear tooth width for defined values of input torque (Figure 10).

6 CONCLUSION

During their working life, gearboxes operate under stochastic working conditions. In order to harmonize the defined load capacity with the expected conditions of exploitation, as well as the harmonization of design parameters with the expected conditions of exploitation, a methodology was developed on the basis of which the DRAG software was created. The software is based on the data obtained in the exploitation process and the results of user analysis. In this way, rapid variations of the input parameters are enabled, with the aim of defining design parameters or load capacity based on the predicted reliability of the gearbox for a defined working lifeThe software makes it possible to define an optimal model, which will be used for the development of a new construction, by varying the exploitation parameters and known desing parameters.

REFERENCES

[1] Birolini, A.(2010): Reliability Engineering: Theory and Practice, 6th Edition, (Springer Verlag).
[2] Maier JRA, Fadel GM (2003): Affordance-based methods for design.In: Proceedings of ASME design theory and methodologyconference, Chicago, IL. Paper no. DETC2003/DTM-48673.
[3] Michaels, S.E. (1964): The usefulness of experimental design. Applied Statistics, Journal of the RoyalStatistical, Series C, 13, pp.221–235Real-Time Control Systems Library – Software and Documentation, http://www.isd.mel.nist.gov/projects/rcslib/.
[4] Arvidsson M., Gremyr I. (2007): Principles of Robust Design Methodology, quality and reliability engineering international, Published online in Wiley InterScience, pp 23-35.
[5] Hunter JS (1985). Statistical design applied to product design. Journal of Quality Technology; 17: pp.210–221.
[6] Kackar RN (1985).: Off-line quality control, parameter design, and the Taguchi method. Journal of QualityTechnology; 17:pp.176–188.
[7] Hasenkampa T., Arvidssonb M., Gremyra I. (2009): A review of practices for robust design methodology, Journal of Engineering Design, Vol. 20, No. 6, pp.645–657.
[8] Suh, N. P. (1990): Design of thinking design machine. Annals of the CIRP, 39(1), pp.145–149.
[9] Suh, N. P. (1990): The Principles of Design. Oxford University Press., New York.
[10] Suh N. P. (2007): Ergonomics, axiomatic design and complexity theory, Theoretical Issues in Ergonomics Science, Vol. 8, No. 2, pp.101–121.

[11] Suh, N. P. (2001): Axiomatic design: Advances and Applications. Oxford University Press.,New York.
[12] Lee, H., Seo, H., Park, G. J.(2003): Design enhancements for stress relaxation in automotive multi-shell-structures. International Journal of Solids and Structures,pp.5319–5334.
[13] Hirani, H., Suh, N. P. (2005):Journal bearing design using multiobjective genetic algorithm and axiomatic design approaches. Tribology International, 38, pp.481–491.
[14] Park G. (2007): Analytic Methods for Design Practice, Springer-Verlag London, ISBN 978-1-84628-472-4, e-ISBN 978-1-84628-473-1.
[15] Thielman J., Ge P.(2006): Applying axiomatic design theory to the evaluation and optimization of large-scale engineering systems, Journal of Engineering Design, Vol. 17, No. 1, pp.1–16.
[16] Osteras T., Murthy D.N.P. (2004): Rausand M.: Reliability Performance and Specificationsin New Product Development, ISBN 82-91917-17-5.
[17] Pimentel A. R., Stadzisz P. C. (2006):Aplication of the Indepedence Axiom on the Design of Object-oriented Software Using the Axiomatic Design Theory, Society for Design and Process Science, Vol. 10, No. 1, pp. 57-69.
[18] Jauregui-Becker J. M., Schotborgh W. O. (2011): A Decomposition Algorithm for Parametric Design, International Conference on Engineering Design, ICED11 15 – 18.
[19] Haftka R., Watson L.(2006): Decomposition theory for multidisciplinary design optimization problems with mixed integer quasiseparable subsystems, Optimization and Engineering, Volume 7, Issue 2, pp. 135-149.
[20] Haftka R., Watson L. (2005): Multidisciplinary Design Optimization with Quasiseparable Subsystems, Optimization and Engineering, Volume 6, Issue 1, pp. 9-20.
[21] Schutte JF, Haftka RT, Watson LT (20014): Decomposition and two-level optimization of structures with discrete sizing variables. Proc. AIAA/ASME/ASCE/AHS/ASC Structures, Structural Dynamics and Materials Conference. Palm Springs CA, USA, pp.349–353.
[22] Li S (2011): A matrix-based clustering approach for the decomposition of design problems, Research in Engineering Design 22,: pp.263–278.
[23] Arcidiacono G., Campatelli G. (2004): Reliability Improvement of a Diesel Engine Using theFMETA Approach, Quality and Reliability Engineering. pp.143-154.
[24] Milutinovic M., Ognjanovic M. (2009): Failure Probability of Gear Drive and Reliable Life Time Estimation, POWER TRANSMISSIONS '09, Chalkidiki, Greece pp. 285-291.
[25] Ognjanovic M., Milutinovic M. (2010): Carrying Capacity Model of Automotive Gearboxes Based on Reliability as Design Constraint, International Conference on Gears, (pp.1377 - 1380) ISBN: 978-3-18-092108-2.
[26] Ognjanovic M., Milutinovic M. (2011):Design for reliability of automotive gearboxes, International Scientific Conference, pp.225-230.
[27] Bozca M., Fietkau P. (2010): Empirical model based optimization of gearbox geometric design parameters to reduce rattle noise in an automotive transmission, Mechanism and Machine Theory, pp 1599–1612.
[28] Bozca M. (2012): Torsional vibration model based optimization of gearbox geometric design parameters to reduce rattle noise in an automotive transmission, Mechanism and Machine Theory 45, pp.1583–1598.

[29] Murthy D.N.P., Hagmark P.-E., Virtanen S. (2009): Product variety and reliability. Reliability Engineering and System Safety 94,pp.1601–1608.
[30] Murthy D.N.P., Østera T. (2009), Rausand M.:Component reliability specification. Reliability Engineering and System Safety 94, pp.1609–1617.
[31] Murthy, D.N.P et. Al. (2009): Investment in new product reliability, In Reliability Engineering and System Safety, Volume 94, Issue 10, pp 1593 – 1600.
[32] Collins J.A. (1981): Failure of Materials in Mechanical Design Analysis, Prediction, Prevention, John Wiley&Sons, New York.
[33] Ognjanovic M.: Failure Probability of Gear Teeth Wear, Fracture of Nano and Engineering Materials and Structures, C., 19., 2006, pp 1059-1060

COMETa 2022
6th INTERNATIONAL SCIENTIFIC CONFERENCE
17th - 19th November 2022
Jahorina, B&H, Republic of Srpska
University of East Sarajevo
Faculty of Mechanical Engineering
Conference on Mechanical Engineering Technologies and Applications

OPTIMIZATION AND EFFICIENCY ANALYSIS OF MUZZLE BRAKE FOR SNIPER RIFLE

Miloš Pešić[1], Marko Miljaković[2], Vladimir Kočović[3], Živana Jovanović Pešić[4], Nikola Jović[5], Jasmina Miljojković[6], Aleksandar Bodić[7]

Abstract: Muzzle brakes have a significant effect on reducing the recoil force of weapons during firing. In this paper, muzzle brake as recoil compensator and recoil force for sniper rifle with and without muzzle brake are considered. The objective is to obtain the optimum inclination angle for the blades (side openings) of the muzzle brake in order to reduce recoil force. The calculation of the muzzle brake was performed according to the methods of Ratto and Orlov-Tolockov. Based on the obtained input data for the calculation of muzzle brakes according to the Orlov-Tolockov method, a software solution was made in the Matlab software package. Based on the performed simulations, the optimal value of the side openings angle of the muzzle brake was determined in order to improve efficiency. The advanced muzzle brake model was created in the CATIA V5 software package. The prototype solution was produced using a 3D printer. After that, the muzzle brake prototype was made by processing the semi-finished product. Experimental testing of prototype and a comparison with the existing muzzle brake solution was performed. Based on the presented results, it can be concluded that the new muzzle brake design is more efficient than the existing one.

Key words: Muzzle brake, Recoil force, Sniper rifle, Experiment

[1] Miloš Pešić, Institute for Information Technologies – National Institute of the Republic of Serbia (CA), University of Kragujevac, Kragujevac, Serbia, milospesic@uni.kg.ac.rs
[2] Marko Miljaković, Faculty of Engineering University of Kragujevac, Kragujevac, Serbia, markomiljakovic@yahoo.com
[3] PhD Vladimir Kočović, Faculty of Engineering University of Kragujevac, Kragujevac, Serbia, vladimir.kocovic@kg.ac.rs
[4] Živana Jovanović Pešić, Faculty of Engineering University of Kragujevac, Kragujevac, Serbia, zixi90@gmail.com
[5] Nikola Jović, Faculty of Engineering University of Kragujevac, Kragujevac, Serbia, njovic1995@gmail.com
[6] Jasmina Miljojković, Faculty of Engineering University of Kragujevac, Kragujevac, Serbia, jasmina.miljojkovic@fink.rs
[7] Aleksandar Bodić, Faculty of Engineering University of Kragujevac, Kragujevac, Serbia, abodic@uni.kg.ac.rs

1 INTRODUCTION

During the previous few decades many improvements in small weapons technology were performed. Recoil management has always been the main concern with all small weapons varieties currently in use. Muzzle brakes are most often used devices for this purpose. A muzzle brake is a device that is attached to the muzzle of the barrel designed to reduce the barrel recoil energy or the entire weapon. They divert hot gases with high pressure and high velocity through ports at the sides, creating a force that is directed forward and reduces recoil.

In this paper, the existing and improved muzzle brake efficiency, as well as the sniper rifle recoil force, were investigated. The experimental tests were conducted by measuring the recoil force when firing a sniper rifle without a muzzle brake, with an existing muzzle brake and with a improved muzzle brake. The muzzle brake model was created in the CATIA V5 software package. According to the Orlov - Tolochkov method, the program solution was implemented in the Matlab software. Calculation and experimental results are presented for the existing and improved muzzle brake.

2 THEORETICAL BASIS

Fig. 1 defines the impulse and moment of momentum of the mass system (projectile, powder gases, and recoil mass for barrels with and without muzzle brakes) [1].

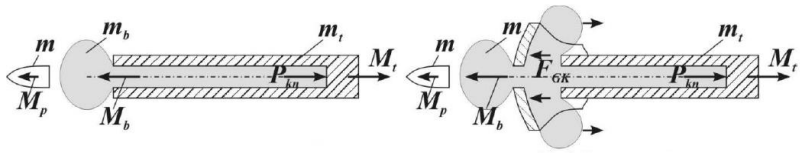

Figure 1. *Barrel without muzzle brake – left, and barrel with muzzle brake – right [1]*

In accordance with the moment of momentum law, barrel recoil moment without a muzzle brake is defined as

$$\int_0^{t_k} P_{kn} dt = M_t \ .$$

The force impulse on the bolt can be calculated from the force/time diagram in Fig. 2 based on the behavior of the powder gas forces on the barrel with and without a muzzle brake

$\int_0^{t_k} P_{kn} dt = I_g$ and on the muzzle brake $\int_0^{t_n} F_{gk} dt = I_{gk}$ [1].

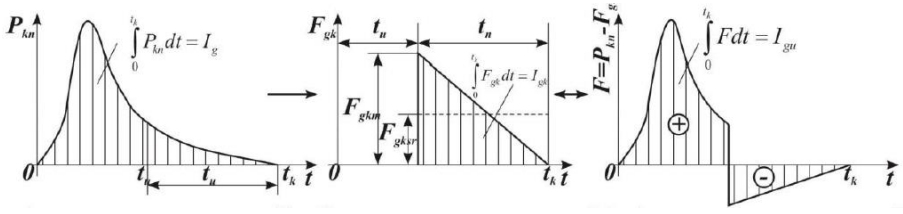

Figure 2. *Impulse forces of gunpowder gases on the barrel [1]*

2.1 Muzzle brake efficiency calculation by Ratto

The effectiveness of the muzzle brake during firing can be defined using the Ratto method [2]. In order to calculate the efficiency of the muzzle brakes, it is necessary to know its efficiency coefficient λ which is:

$$\lambda = \frac{W'_{\max} - W_{GK}}{W'_{\max}} = 1 - \frac{W_{GK}}{W'_{\max}} \tag{1}$$

where: $W'_{\max}$ represents free recoil velocity of the barrel without muzzle brake, W_{GK} is free recoil velocity of the barrel with the muzzle brake.

Efficiency of the muzzle brakes λ_E is given by the equations (2) and (3):

$$\lambda_E = \frac{W'^2_{\max} - W^2_{GK}}{W'^2_{\max}} = 1 - \frac{W^2_{GK}}{W'^2_{\max}} = 1 - \left(\frac{W_{GK}}{W'_{\max}}\right)^2 \tag{2}$$

$$\lambda_E = \lambda \cdot (2 - \lambda) \tag{3}$$

It is clear that the different labels ΔE, λ_E, and η_{gk} represent the same quantities. From here it can be concluded that, in order to calculate the efficiency of the muzzle brake λ_E it is necessary to calculate λ beforehand, because $\lambda_E = f(\lambda)$. Calculating the value of λ as a function of the weapon ballistic characteristics and the geometric shape of the muzzle brakes is reduced to the calculation of the $W'_{\max}$ and W_{GK} [2].

The recoil mass velocity without muzzle brake is given by the equation:

$$Q_{tr} \cdot W'_{\max} = q \cdot V_0 + \omega \cdot W_{sr} \tag{4}$$

where: Q_{tr} represents the recoil mass, V_0 is the initial velocity of the projectile, $r \cdot \omega$ is the the mass of gases passing through the blades (side openings), $(1-r) \cdot \omega$ is the the mass of gases passing through the muzzle brake, q is the projectile mass, and W_{sr} is the mean velocity of the gass flowout.

The equation for the side openings inclination angle of the muzzle brake by Ratto is [2]:

$$\rho = 0.65 + 0.35 \cdot \sin\left(45^\circ - \frac{\alpha + 3^\circ}{2}\right) \tag{5}$$

In the equation (5) ρ represents the friction coefficient of the gases on the muzzle brake blades. This coefficient is used to correct the obtained results in order to achieve better match with the experimental results.

2.2 Calculation of efficiency of the muzzle brake by Orlov-Tolockov

Unlike the Ratto method, this method considers the amount of gas taken through the side openings, the separation of the gas stream from the side channel axis, the shape of the muzzle brake cavity entrance and the angle of the entrance cone. In this way, a more precise match with the experimental results can be achieved [2,3].

Muzzle brake efficiency is expressed by the coefficient ΔE. This coefficient is critical for the free recoil velocity at the end of the gas flowout:

$$W_{GK} = W_{\max} \cdot \sqrt{1-\Delta E} \tag{6}$$

Replacing expressions for W_{GK} and $W_{\max}$ efficiency coefficient ΔE is defined as:

$$\Delta E = 100 \cdot \left[1 - \left(\frac{1+\alpha \cdot \frac{\beta \cdot \omega}{q}}{1+\frac{\beta \cdot \omega}{q}} \right)^2 \right] \tag{7}$$

Coefficient α represents:

$$\alpha = \frac{R_H}{R} \tag{8}$$

where: R represents the reaction of currents at the muzzle brake entrance, and R_H is the horizontal component of the current reaction at the the muzzle brake exit.

The functional dependence of the parameter α on the dimensions and shape of the muzzle brake can be determined assuming that the flow of powder gases is critical and isotropic.

For a muzzle brake with n rows, coefficient α is given as:

$$\alpha = K\sigma_1\sigma_2...\sigma_n + \sum_{i=1}^{n} \sigma_1\sigma_2...\sigma_{i-1}\left(1-\sigma_i\right)K_i\xi_i \cos\psi_i \tag{9}$$

where: K is the coefficient that characterizes the relative increase in the momentum of the powder gases in the muzzle brake cavity, σ_i is the relative amount of unused powder gases of the muzzle brake chamber, K_i is the coefficient of reactivity of the muzzle brake side channels; ξ_i is the coefficient that defines gas stream separation from the direction of the side channel axis due to the influence of the oblique section and is:

$$\xi_i = \frac{\cos\left(\psi_i \pm \Delta\psi_i\right)}{\cos\Delta\psi_i \cdot \cos\psi_i} = 1 \pm tg\psi_i \cdot tg\Delta\psi_i \tag{10}$$

where: $\Delta\psi_i$ is the jet deflection angle due to the influence of the oblique section.

3 RECOIL FORCE – SIMULATION

Muzzle brake model is created in CATIA V5 software package based on the measured dimensions of the existing muzzle brake (Fig.3). Based on the created model, input parameters required for the efficiency, as well as the recoil force calculation in Matlab software are obtained.

Figure 3. *Muzzle brake 3D model*

3.1 Software solution

Based on the Orlov - Tolochkov method for calculating muzzle brake efficiency, the software solution "AnalizaGK.m" was developed in the Matlab software package. The algorithm for the software solution "AnalizaGK.m" is shown in Fig. 4.

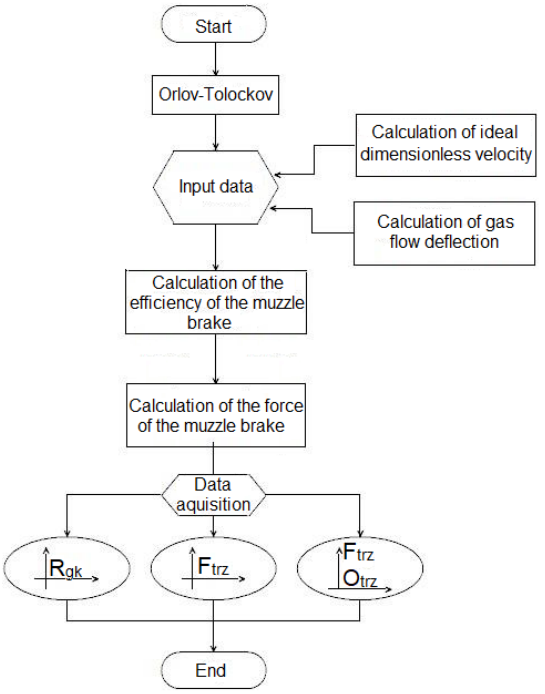

Figure 4. *Algorithm for the software solution "AnalizaGK.m"*

The software solution calculates ideal dimensionless velocity and the deflection of the gas stream. The software solution, apart from the efficiency of the muzzle brake, also provides the value of the calculated structural characteristic as an output data. The structural characteristic (α) calculated in this way is used as one of the input data in the program that solves the recoil force. By applying this software solution, the impact of the muzzle brake on the reduction of the recoil force, as well as the recoil process, can be analyzed.

4 MUZZLE BRAKE EFFICIENCY ANALYSIS

The dependence of the muzzle brake force on the inclination angle of the side openings is shown in Fig. 5 – left. An interval from 100° to 150° was used to analyse the influence of the inclination angle of the side openings. It can be concluded that with an increase in the inclination angle, higher force values are obtained.

Fig. 5 - right shows the dependence of the muzzle brake efficiency on the angle ψ. From the Fig. 5 – right can be concluded that with an increase in the inclination angle, higher efficiency values are obtained. For an angle value of 120° (production measure), the efficiency of the muzzle brake is 47.8%, and the force of the muzzle brake is 10.22 kN.

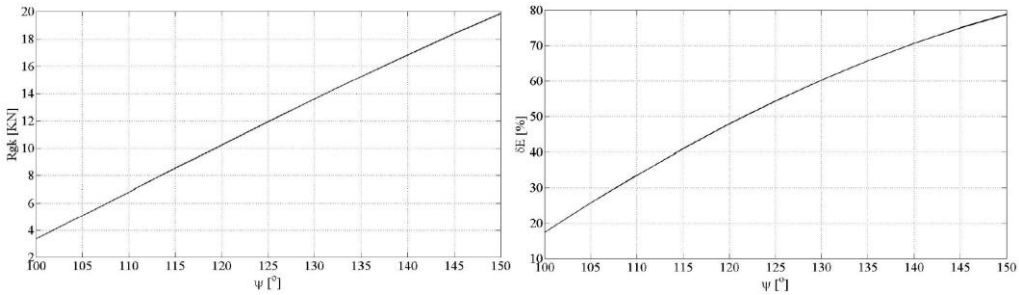

Figure 5. *Dependence of the muzzle brake force on the angle of the side openings – left and efficiency of the muzzle brake on the angle of the side opening – right*

Fig. 6 shows dependance of the muzzle brake force on time.

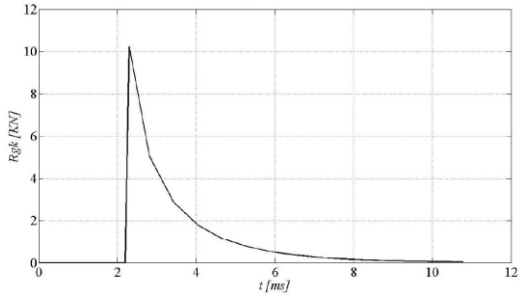

Figure 6. *Muzzle brake force-time dependance*

At the time interval from 0 to 2.2 ms, no pressure is applied to the muzzle brake, because the projectile is still moving in the barrel. After 2.2 milliseconds the muzzle brake starts to take effect. The muzzle brake has a maximum force value of 10.22 kN, after which it slowly decreases.

4.1 Analysis of the recoil process

The following forces act within the recoil process of a sniper rifle: the pressure force of powder gases – P, and the force of the muzzle brake – F_{gk}. On Fig. 7 – left is shown a comparison of the recoil force and the recoil resistance force on time.

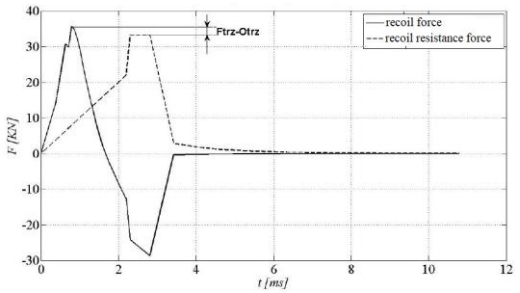

Figure 7. *Recoil force and recoil resistance force – left; Recoil force in dependance of time - right*

The difference between the maximum recoil force and the recoil resistance force represents the force exerted by the sniper rifle on the shooter. The maximum recoil force is 35.64 kN, and the recoil resistance force is 33.2 kN. The force exerted by the sniper rifle on the shooter is 2.48 kN.

5 EXPERIMENTAL TESTING

Based on the results obtained using a mathematical method improved muzzle brake was constructed. A comparative experimental analysis of the existing muzzle brake and improved muzzle brake effectiveness for the sniper rifle was done. During the experiment, the following forces were measured: recoil force without a muzzle brake, recoil force with the existing muzzle brake and recoil force with with the improved muzzle brake.

In order to obtain the experimental analysis results of the muzzle brake effectiveness, improved muzzle brake is constructed. Improved muzzle brake has retained the assembly and dimensional characteristics of the existing muzzle brake, while inclination angle of blades was changed. Improved muzzle brake should enhance efficiency, reduce the recoil force on the shooter and increase precision.

During the experiment, it is necessary to ensure operators safety. It was necessary to provide a secure grip for the sniper rifle in order to achieve a rigid connection. Rigid connection was established between the sniper rifle and the support on which the linear strain gauges were placed. In order to ensure a safe grip, it was necessary to produce an adapter that was tied to the rifle, instead of the sniper rifle stock. The other end of the rifle was tied to a fixed stand [4,5]. The prototype muzzle brake was obtained by 3D printing. The prototype muzzle brake and experimental setup are shown on Fig. 8.

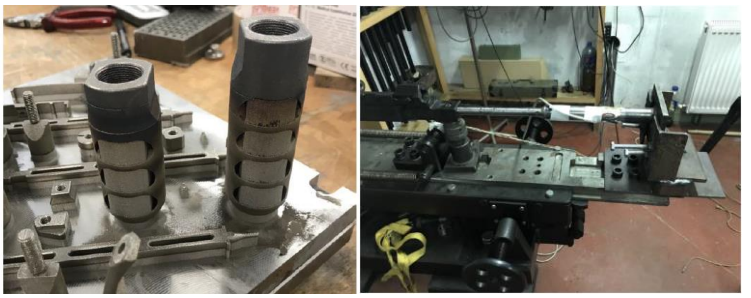

Figure 8. *Muzzle brake prototype – left and experimental measuring of recoil force – right*

The difference between the recoil force without the muzzle brake and the recoil force with the muzzle brake is the muzzle brake force. The obtained results of experimental testing are shown in Table 1.

Table 1. *Results of the experimental testing*

Recoil force without muzzle brake	Recoil force with the existing muzzle brake	Recoil force with the improved muzzle brake	Force of the existing muzzle brake solution	Force of the improved muzzle brake
23509 N	17033 N	15435 N	6476 N	8074 N

Deviation of the results obtained by calculation using Orlov-Tolochkov method from the experimental results is a consequence of the calculation method imperfection. For the calculation it was assumed that the side openings are circular in shape and have equal cross-sectional areas. In addition to the imperfection of the calculation, the influence of the recoil pad and the influence of the rifle stand were not taken into consideration. Based on the above, it can be concluded that the mentioned method of the muzzle brake efficiency calculation gives satisfactory results.

6 CONCLUSIONS

This paper presents a theoretical and experimental analysis of improved muzzle brake of the sniper rifle. Theoretical basis of Ratto and Orlov-Tolochkov methods are given. Calculation of improved muzzle brake was performed according to Orlov-Tolochkov method, because it gives more accurate results. Improved muzzle brake model is created in CATIA V5 software package based on existing muzzle brake dimensions and characteristics. Based on the created model, input parameters required for the efficiency and the recoil force calculation are obtained. The improved muzzle brake efficiency calculation was performed in the Matlab software. Using the "AnalizaGK.m" software solution, the muzzle brake efficiency and the sniper rifle recoil force are analyzed. Initial data within software solution were changed and varied in the desired interval. This provided different values at the output of the program. By varying the initial data, optimal values were determined and used for the construction of improved muzzle brake. The efficiency and recoil force is most affected by the angle of inclination of the side openings. On the basis of ballistic parameters, constructional dimensions and characteristics using aforementioned software solution, the obtained value of the new muzzle brake efficiency was 47.8% and the muzzle brake force was 10.22 kN. Based on the calculation results, improved muzzle brake was produced. Experimental tests of new muzzle brake were performed. Value of the muzzle brake force obtained by experimental testing of the new muzzle brake was 8.074 kN. It can be concluded that the presented calculation gives satisfactory results. These results can be used as a starting point for designing, construction and analyzing the parameters that affect the efficiency of muzzle brakes.

ACKNOWLEDGEMENT

This research is partly supported by the Ministry of Education and Science, Republic of Serbia, Grant 451-03-68/2022-14/ 200378, and Grant TR32036.

REFERENCES

[1] M. Petrović (2006), *Mehanika automatskog oružja*, Vojna akademija, Beograd.
[2] A. Kari, S. Ilić (2014), *Osnovi konstrukcije naoružanja*, Medija centar Odbrana, Beograd
[3] N.B. Ahmed, D. Jerković, N. Hristov, W. B. Abaci (2022), Analytical and experimental investigation of the muzzle brake efficiency, *Facta universitatis Series: Mechanical engineering*
[4] T.S. Davis (2021), *Improved Strain Gage Instrumentation Strategies for Rotorcraft Blade Measurements*, Doctoral dissertation, Old Dominion University, Norfolk VA.
[5] S. Procházka, P. Seman, M. Vondráček (2011), Additional Effect of Gases on Strain Gauges at Barrel Muzzle, *Advances in Military Technology*, 6/2, p.p. 29-38

COMETa 2022
6th INTERNATIONAL SCIENTIFIC CONFERENCE
17th - 19th November 2022
Jahorina, B&H, Republic of Srpska
University of East Sarajevo
Faculty of Mechanical Engineering
Conference on Mechanical Engineering Technologies and Applications

DESIGN AND TESTING OF ABRASIVE BELT GRINDER

Marija Matejic[1], Milos Matejic[2], Jovana Zivic[3], Lozica Ivanovic[4]

Abstract: The belt grinding machine, presented in this paper, was designed and tested for grinding any shape of object like circular, rectangular, or polygon. In this project, the work abrasive belt is used to grind the various types material of material such as metal, plastic, wood etc. The abrasive belt is rotated by a three-phase induction motor. The particular abrasive belt grinding machine has been developed for the purposes of experimental research. Hence this project namely adjustable belt grinder. The machining accuracy and surface quality of workpieces are the key factors that ultimately determine the performance of the equipment. The test workpieces are presented in the paper and their characteristics are commented. The paper concludes with comments on achieved results and directions for further research on this topic.

Key words: Belt grinder, Industrial design, Surface quality, Wear

1 INTRODUCTION

In the modern industry, there are still some pieces of the equipment that are attractive for various types of the research. One of those examples which is attractive for various type of investigation is grinding machines and wider grinding process. One of the most spread machines used for grinding are belt grinders. Belt grinding machines have their own advantages in lots of types of work, such as preparation parts for welding, sharpening tools, cleaning parts from rust, parts free form shaping and etc. The development of belt grinding in aspect of modularity to cover more production operations is necessary. This is because if a belt grinder in that way can gain more functions. Belt grinder modularity will certainly make the attraction of wider range of

[1] PhD, Marija Matejić, University of Priština with temporary settlement in Kosovska Mitrovica Faculty of Technical Sciences, Kosovska Mitrovica, Kosovo, marija.matejic@pr.ac.rs (CA)
[2] PhD, Miloš Matejić, University of Kragujevac Faculty of Engineering, Kragujevac, Serbia, mmatejic@kg.ac.rs
[3] MsC, Jovana Živič, University of Priština with temporary settlement in Kosovska Mitrovica Faculty of Technical Sciences, Kosovska Mitrovica, Kosovo, jovana.d.zivic@pr.ac.rs
[4] PhD, Lozica Ivanović, University of Kragujevac Faculty of Engineering, Kragujevac, Serbia, lozica@kg.ac.rs

users. Using the belt grinder, user can gain very good efficiency in certain operations [1].

The process of industrialization and modernization of life is accompanied by the increasingly widespread application of advanced technology, which among others is increasing rapidly using a variety of machines and mechanical work equipment that is run by electric motor drives [2]. In all technological processes huge and important role is reserved for surface quality. Surface quality directly effects on further production processes, like is quality and strength of boned elements [3-4]. The surface profile and roughness of a machined workpiece are two of the most important product quality characteristics and in most cases a technical requirement for mechanical products. Achieving the desired surface quality is of great importance for the functional behaviour of a part. The process-dependent nature of the surface quality mechanism along with the numerous uncontrollable factors that influence pertinent phenomena, make it important to find a straightforward solution and an absolutely accurate prediction model. Belt grinding machine is technical equipment that has effectiveness and efficiency that is quite good in the process so that it can produce a smooth surface of the workpiece [5-9].

Abrasive grinding is a widely employed finishing process, with abrasive grains being used as the cutting edge to accomplish close tolerances and excellent dimensional correctness and surface integrity. Abrasive belt grinding is a modification of the traditional grinding processes in which the contact wheel is made of polymer backing material. The grinding belt is formed of abrasives coated on a backing material and fastened around at least two rotating polymer contact wheels, which make it a compliant tool. A compliant belt grinding resembles an elastic grinding in its operating principle, and it offers some potentials like milling, grinding and polishing applications. The abrasive belt grinding process essentially is a two-body abrasive compliant grinding processes wherein the abrasive belt is forced against the components to remove undesired topographies, such as burrs and weld seams, to achieve the required material removal and surface finish [10-11]. In order to understand the process and achieve a good result of the final processing, it is necessary to take care of the details and parameters of the process as they are abrasive type of grinding belt, belt speed, contact wheel hardness, serration, and grinding force. Changing these process variables will affect the performance of the process [12-13].

The goal of this paper is for the future product to have good features, to be useful, safe and innovative. That's why the authors are focused a lot on product quality, functionality and modularity. The quality of the product is more and more considered a decisive factor every day competitiveness, which concerns the survival and development of every industrial enterprise, industrial branches, that is, industry as an economic activity [14-15].

2 BELT GRINDER DESIGN

In this study the new concept of belt grinder was developed. The most influential factor in concept developing was the belt grinder frame rigidity. The frame rigidity is necessary in order to get the best grinding results. Before the concept developing the main functions of the future product was determinated such as:

- the grinder work table must have ability to rotate from 0 degree to 180 degree,
- the work table must have adjustable height,

- the grinder must have ability to accept various sizes of grinding belts (papers),
- easy change of the grinding belts (papers)
- safety of operator must be fulfilled and
- future product must have enough rigidity.

After main functions the part of grinder was listed:

- driving unit (electric motor),
- driving pulley,
- driven pulley,
- belt tensioning mechanism,
- grinder frame and
- work table.

The belt grinder was designed and fabricated to be very simple for usage, with improved rigidity and numerous abilities for adjustments, as previously requested. The belt grinder presented in this paper has abilities to be used for grinding any shape of object like circular, rectangular and polygon. In this project the abrasive belt is used to grinding the material. In presented design it was paid attention that belt grinder has the ability to use various lengths of abrasive belts. The abrasive belt is rotated by three phase induction motor.

Frame of the presented solution was done from steel plate with 10 mm thickness. Steel plate was cut on laser cutting machine. Frame of the belt grinder is shown in Figure 1.

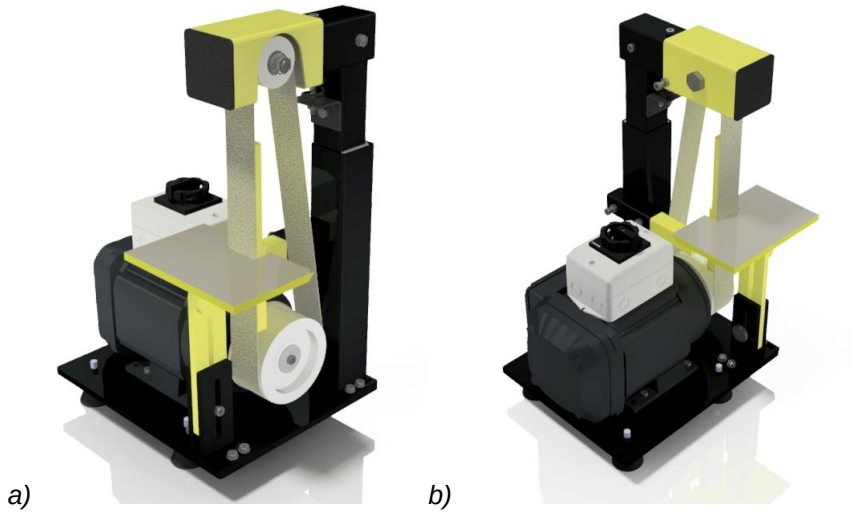

a) *b)*

Figure 1. *Frame of the solution a) front view; b) back view*

The frame of the presented solution has much better rigidity related to the frames of the other belt grinders that could be found on the market. Frame of the presented belt grinder is easy to be made, because of the big amount of the steel plates and square steel pipe. However, it is more expensive than solutions that could be found on the market, because a bigger amount of steel is used.

Worktable of the belt grinder is given in Figure 2a. The only difference between given worktables that could be found on the market is easier ability for the adjusting. The belt tension solution is acceptable and durable. The belt tension solution is given in Figure 2b.

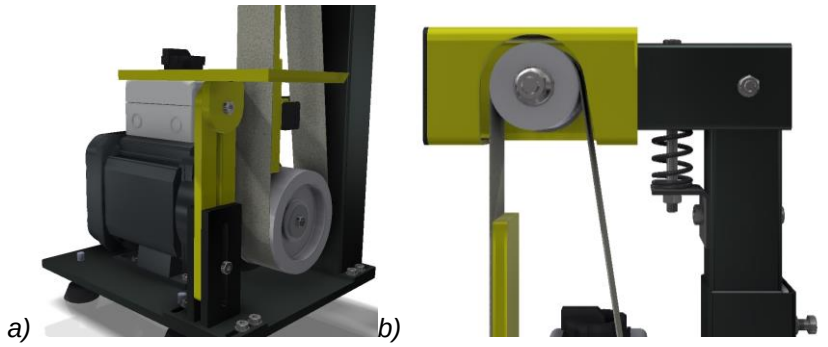

a) *b)*

Figure 2. *a) Work table of the belt grinder; b) Tension mechanism of the abrasive belt*

The state of the produced and assembled belt grinder is given in Figure 3. As in model the parts that is movable is painted in yellow color to give the user the additional attention on the work process and possible machine adjustments.

Figure 3. *The fabricated belt grinder from different angles*

The special attention is paid to have the electric switch moved away from worktable, but still close enough for turning machine on and shutting down.

3 BELT GRINDER TESTING

As material samples for belt grinder testing are given in table 1.

Table 1. *Materials used for belt grinder testing*

No.	Material	Dimensions
1.	Pine wood	30 x 50 mm
2.	Plastic PA6	Φ 60 mm
3.	Steel square profile S235JRG2	40 x 40 x 2 mm
4.	Steel angle S235JRG2	20 x 20 x 3 mm

The surface preparation before grinding was done on the portable band-saw. The band-saw make surface roughness between R_a=100µm and R_a=400µm [16], which is not acceptable surface finish for the most positions in mechanical engineering. From that fact, there was a need for fast and efficient surface treatment before the further processing. The ideal solution for that is a grinding with belt grinder. Belt grinder presents a very acceptable solution in aspects of efficiency, machine and reproduction material (abrasive belts) costs. The band-saw which is used for samples preparation in this paper is shown in Figure 4.

Figure 4. *Band-saw used for samples preparation*

After samples preparation the grinding on the belt grinder machine is performed. Because the different types of the materials is used (wood, steel and plastics), it is chosen to have a lower speed of the abrasive belt. The speed of abrasive belt was $v \approx 6$ m/s. The electric motor RPM was $n_{EM} = 1400$ min^{-1}, and diameter of the driving pulley was $d = 80$ mm. The grinding operation is shown in Figure 5.

a)  b) 

c) 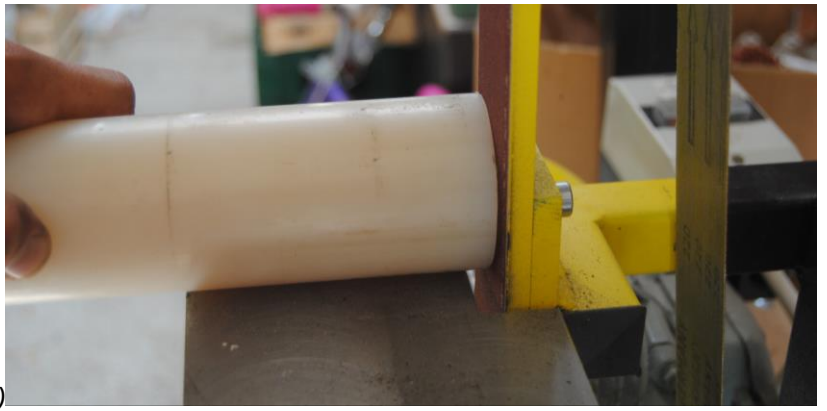

Figure 5. *Grinding operation a) pine wood; b) steel angle and c) plastics*

The abrasive belt on belt grinder had a granulation P80, [17]. The abrasive belt wears designation LS 309 and it has aluminium oxide grain and cotton cloth. According to the producer this abrasive belt is good for polishing ferrous or non-ferrous metals and hardwoods where belt conformability to the work piece is required. The grinded and un-grinded samples is shown in Figure 6 and figure 7.

Figure 6. *Grinded and un-grinded samples – comparative view*

a) 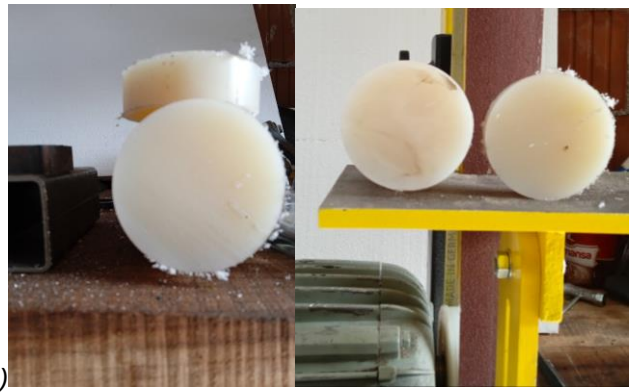

b) 

Figure 7. *Grinded and un-grinded samples a) plastics and b) metal square pipe*

According to literature sources [18] the surface roughness after grinding with P80 abrasive belt should be around R_a=20µm. The visual inspection of the shown samples can ensure the viewer that surface has much less roughness related to the band-sawed parts. In the further examination the surface profile will be measured after grinding.

4 CONCLUSIONS

The presented paper shows a multiple approach to the efficient grinding processes in the small workshops. Firstly, the design of novel belt grinder has been made, and later the actual grinding machine was fabricated. Before the worksamples is processed the functionality of the machine was tested. After that, the samples was prepared on band-saw, and processed on the belt grinder. Visual inspection has been made and it is determined that surface roughness after the hand grinding process is improved very much. In the further work, the authors will vary the grinding speeds and make a surface profile measurement in order to determinate acceptable grinding speeds for various types of the materials.

REFERENCES

[1] Setiawan, S., Arwizet, K., Syahri, B., Ambiyar, A., Darmawi, D., & Yufrizal, A. (2018). Design and Testing of Belt Grinding Development. Teknomekanik, 1(2), p.p. 38-42.

[2] Zulmaidas, I., Syahrul, S., Ambiyar, A., & Yufrizal, A. (2019). Manufacture and Testing of Belt Grinding Development. Teknomekanik, 2(1), p.p 20-23.

[3] AYDIN, İ., & Çolakoğlu, G. (2011). Roughness on wood surfaces and roughness measurement methods. Artvin Çoruh Üniversitesi Orman Fakültesi Dergisi, 4(1), p. p. 92-102.

[4] Smajic, S., & Jovanovic, J. (2021). Influence of Different Machining on the Roughness of Oak Wood. Bulletin of the Transilvania University of Brasov. Series II: Forestry• Wood Industry• Agricultural Food Engineering, p. p.101-108.

[5] Darmawi, D. (2018). Pengaruh Fraksi Penguat pasir Terhadap Sifat Mekanik Polimer Matrik Komposit (Similarity).

[6] Muhammad Saiful Hidayat, (2017) “Paparan Getaran Mesin Gerinda Dan Keluhan Subyektif (Hand Arm Vibration Syndrome) Pada Tenaga Kerja Di Abadi Dental Laboratorium Gigi Surabaya,” vol. 91, p. p. 399–404.

[7] R. R. Runtu, J. Soukotta, and R. Poeng, (2014) “Melalui Pengujian Karakteristik Statik Menurut Standar Iso 1708,” vol. 4, p. p. 63–75.

[8] A. M. Sakti, (2010) “Optimalisasi proses gerinda untuk permukaan,” J. Tek. Ind., vol. 11, p. p. 26–30.

[9] Lu, Chen. (2008) "Study on prediction of surface quality in machining process." Journal of materials processing technology 205.1-3, p. p.439-450.

[10] Wang, S.; Li, C. (2012) Application and development of high-efficiency abrasive process. Int. J. Adv. Sci. Technol., 47, p. p. 51–64.

[11] Pandiyan, V.; Tjahjowidodo, T. (2017), In-process endpoint detection of weld seam removal in robotic abrasive belt grinding process. Int. J. Adv. Manuf. Technol., 93, p. p. 1699–1714.

[12] Zhang, X., Kuhlenkötter, B., & Kneupner, K. (2005). An efficient method for solving the Signorini problem in the simulation of free-form surfaces produced by belt grinding. International Journal of Machine Tools and Manufacture, 45(6), p. p. 641-648.

[13] Pandiyan, V., Caesarendra, W., Tjahjowidodo, T., & Praveen, G. (2017). Predictive modelling and analysis of process parameters on material removal characteristics in abrasive belt grinding process. Applied Sciences, 7(4), 363.

[14] Bošković, G., Gligorijević Ž., Kvalitet proizvoda i konkurentnost preduzeća u industriji, Ekonomski fakultet Niš.

[15] Rade Ivanković , Zdravko Krivokapić , Đurđica Kučinar; Impact of product quality on company profitability by means of expert systems; 2012.

[16] Orlowski, K. A., Dobrzynski, M., Gajowiec, G., Lackowski, M., & Ochrymiuk, T. (2020). A Critical Reanalysis of Uncontrollable Washboarding Phenomenon in Metal Band Sawing. Materials, 13(20), 4472.

[17] https://www.klingspor.com/Product-Catalog/ , accessed in October 2022.

[18] Ghumatkar, A., Sekhar, R., & Budhe, S. (2017). Experimental study on different adherend surface roughness on the adhesive bond strength. Materials Today: Proceedings, 4(8), 7801-7809.

COMETa 2022
6th INTERNATIONAL SCIENTIFIC CONFERENCE
17th - 19th November 2022
Jahorina, B&H, Republic of Srpska
University of East Sarajevo
Faculty of Mechanical Engineering
Conference on Mechanical Engineering Technologies and Applications

APPROPRIATE ERGONOMIC DESIGNS TO IMPROVE THE SAFETY OF THE CRANE CABIN

Anita Vasileva[1], Elena Angeleska[2], Kristina Jakimovska[3], Sofija Sidorenko[4]

Abstract: Cranes are an essential part of the load handling equipment in industrial workplaces but they are high risk machines that can cause a great deal of material damage or injury which commonly occurs due to human error. In response to new design challenges, growing trend of focusing on user needs, such as body positions of the operator, unintuitive interactions in the work stations, disturbed field of view, and other issues that affect the operator's well-being and productivity, this research suggests principles, guidelines, and methods for designing and evaluating crane cabins with improved comfort and safety for the operator. In that aim firstly, the main ergonomic issues that exist of existing crane cabins are identified using correlating of data from ergonomics, design, construction and safety aspects, and a survey for collecting the user's opinions and experiences. After that, the research highlights a list of relevant anthropometric data need for designing crane cabins and existing standards regarding: the minimum operator envelope, zones of comfort and reach of controls, as well as requirements related with the operator's seat. Based on all collected and systematized data, in the end a design approach for developing crane cabins is suggested and solution is proposed. The generated concept is examined using software tools for virtual ergonomics. Finally, the issue of this paper is to provide baseline information that helps to upgrade the crane cabin ergonomics and avoid crane related fatalities and injuries.

Key words: crane cabin, ergonomic, human-centric design, safety

[1] Assistant MSc, Anita Vasileva, Ss. Cyril and Methodius University in Skopje, Faculty of Mechanical Engineering, Skopje, N. Macedonia, e-mail anita.vasileva@mf.edu.mk
[2] Assistant PhD, Elena Angeleska, Ss. Cyril and Methodius University in Skopje, Faculty of Mechanical Engineering, Skopje, N. Macedonia, e-mail elena.angeleska@mf.edu.mk
[3]Assoc. Prof. PhD, Kristina Jakimovska, Ss. Cyril and Methodius University in Skopje, Faculty of Mechanical Engineering, Skopje, N. Macedonia, e-mail kristina.jakimovska@mf.edu.mk
[4]Professor PhD, Sofija Sidorenko Ss. Cyril and Methodius University in Skopje, Faculty of Mechanical Engineering, Skopje, N. Macedonia, e-mail sofija.sidorenko@mf.edu.mk

1. INTRODUCTION

Cranes are one of the most widely used equipments, but followed by a high accident rate. A large number of studies about accident causes exist [1-3], which analyse the construction and the components of a crane safety system, but in most of the research the body positions of the operator, disturbed field of view, the operator's well-being and productivity are almost neglected. To bride the current "gap" in the field, this research conducts both a literature review and applied research.

The research is supported by a review of previous surveys in the field of the crane's safety, and the analyzed need for reducing errors in the operator-machine interactions which can consequently reduce possible damages or injuries. Moreover, in order to fully understand the problematic, an additional survey was conducted among crane operators in North Macedonia aiming to withdraw additional information about their specific requirements. This was done with the goal of finding a way to improve the process of designing crane cabins using a human-centric approach that has the potential to reduce the risk of operator discomfort or distraction. The human-centric design strategy is one segment of the product ergonomics methodology that involves fitting the equipment to the users. This means that the user is analyzed as a part of the system which is being designed that is consisted of the human, the product or equipment and the environment. Despite the growing trend of focusing on user needs and applying these human-centric strategies when developing industrial machines and equipment, ergonomic issues continue to exist in crane cabins resulting with unnatural body positions of the operator, unintuitive interactions in the work stations, disturbed field of view, and other issues that affect the operator's well-being and productivity such as: poor insulation, inappropriate heating/cooling, ventilation, vibrations, noise, etc.

According to reference [4] crane operators have the most direct consequence on how safely cranes are handled. An operator must never menage a crane in conditions that could compromise proper operation or mechanical integrity of the crane. As stated in reference [5], where crane cabin types are examined regarding characteristic divided in three groups: (1) operator-control devices interaction, (2) safety and (3) anthropometric adjustment, results show that all examined crane cabins only 52.5% of operator-control devices interaction, 75% of safety and 60% of anthropometric adjustment issues are satisfied in current designs.

There are several similar researches which indicate that contemporary crane cabins still contain significant ergonomic and safety flaws and do not satisfy the operator's needs entirely. The main challenge in designing the crane cabins is to adjust them according to the nature of the work. The crane operator's tasks require a static sedentary position with both hands constantly positioned on controls and frequent head and neck bending and body twisting while under the continuous influence of strong vibrations. Therefore, authors aim to propose some suggestions and guidelines to overcome the design flaws and offer more ergonomic solutions. For instance, in [6] the author's content analysis is to identify the crane operator's biomechanical and visual problems and to present certain design suggestions and changes to existing standards on the path to improved safety of crane cabins. In addition, [7] demonstrates a modification of a crane cabin through ergonomic analysis. Reference [8] on the other hand, gives an overview of strategies how to reduce whole-body vibration exposure on drivers. This paper also aims to analyze and systematize the main crane cabin issues related with ergonomics and propose a human-centric design method which can be applied for constructing safer crane cabins.

2. RESEARCH METHODOLOGY

As elaborated in the introduction, the main goal of this paper is to provide a thorough understanding of the crucial ergonomic issues in crane cabins based on background information and suggest principles, guidelines, and methods for designing and evaluating crane cabins with improved comfort and safety for the operator. The study goes through several stages (Figure 1). It is based on data which is extracted chiefly from academic literature and publications through attentive content analysis.

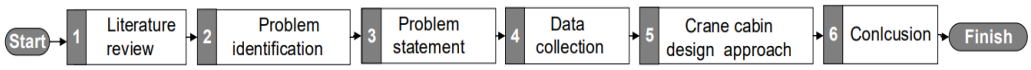

Figure 1. *Research methodology*

3. COLLECTION

In order to fully understand the problematic and pinpoint the main aspects and components of crane cabins that require an improved design approach for increasing the ergonomics, the initial step was to collect relevant data through a literature review and a survey. The data collection and analysis helped to understand and rate the main crane cabin interior issues. Once the main problems were established, the data collection process continued with withdrawing anthropometric data, ergonomic recommendations and existing standards which are directly related with the defined crane cabin interior components that cause those main problems.

3.1. Main crane cabin ergonomic issues according to a literature review

Based on information from several sources, the most common crane cabin issues are related to the seat, visibility, noise and commands/controls. In the review of cabin problems done in [6] it is stated that the placement of controls poses a great issue, as well as the positioning and visibility of indicators and displays, and the understandability of the signals and symbols. Furthermore, the authors elaborate that among the largest problem-causing factors are the seat and armrests. The issue lies in: the placement of the armrests at appropriate height, the options for adjustability of the armrests, the options for adjustability of the seat positions (horizontal and vertical adjustment), and the positioning and adjustments of the lumbar support of the seat (options for tilting and swiveling). In addition, the challenges of positioning the controls and levers to be within reach zones and easily operated, as well as allowing sufficient overview of the ground zone by removing obstructions from the field of view and distracting reflections are emphasized. According to [5] based on the evaluation of several crane cabin models, even the best-rated crane cabin models still have a 20% room for improvement. The main identified problems in the research are the interactions between the crane operator and controls, requiring a better placement of indica¬tors and regulators and adjustable work posutures. Similarly, in [9], authors pinpoint the following causes of driving discomfort: uncomfortable reach of controls, poor vision and poor seat adjustment (support, suspension, height), and in [10] authors also highlight the statement that the highest inconvenience is caused by armrests and inappropriately designed seat.

3.2. User requiremnts

With the goal to withdraw more information directly from crane operators and understand their problems and requirements, a short survey was conducted among 11 crane operators in North Macedonia. The survey questions are presented in Table 1.

Table 1. *List of questions*

Question	Offered answers
Age	18-25; 26-35; 36-45; 46-55; >56
Average daily hours operating in the crane cabin	
Rate the comfort of the work in the crane cabin	1-Extremely uncomfortable 2-Uncomfortable 3-Not so uncomfortable 4-Comfortable 5-Extremely comfortable
Usually in which part of your body do you feel pain at the end of your workday?	Hands; Shoulders; The Neck; The Back; Legs; Feet; Knees; Eyes ;Other
What do you consider to be the biggest disadvantage of the crane cabin?	Disturbed field of view; Dimension of the seat; The position of the seat; The position of the armrest; The position of the joysticks; Other

3.3. Anthropometric data, ergonomic recommendations and standards

In order to properly position the operator in the crane cabin, the crucial data that needs to be considered are the physical dimensions of the operator which then define the minimum operator envelope and seat dimensions. In that sense, for designing the crane cabin the key anthropometric dimensions required are the basic body dimensions of a male individual of the 5th and 9th percentile in a seated position which according to an anthropometric chart by [11] are: popliteal height, buttock-popliteal height, elbow rest height, shoulder height, sitting height normal, elbow-to-elbow breadth, hip breadth, shoulder breadth and lumbar height [10].

Additionally, in ISO 3411:2007, the physical dimensions of small, medium and large operators in a seated position are also provided. The standard refers to earth-moving machinery operators, but is equally applicable in the case of crane cabins due to the similar characteristics of the operators and the cabins. The same ISO standard contains guidelines for dimensioning the minimum operator envelope. Based on the reviewed ISO standard, simple illustrations were prepared to graphically illustrate the required operator space which can be used as a reference for dimensioning the crane cabin (Figure 2). The physical dimensions of the small and large operators were selected since they are to be used for defining the required adjustable elements in the cabin: the horizontal and vertical seat adjustment dimensions, the horizontal and vertical armrest adjustment dimensions, as well as the armrest tilting adjustment angles, and the backrest adjustment angles. The operator envelope dimensions, on the other hand, were also included in the illustration for describing the minimum clearances around the body of the operator in a seated position. Standard ISO 6682:1986 is also relevant, containing information regarding the zones of comfort and reach of controls. A similar approach was used for describing the comfortable reach zones through the same illustration using color marks of the comfortable reach areas around the reference hip point of the operator (yellow for hand reach zone, orange for feet reach zone). This was done to serve as a simple reference for fitting all the equipment in the crane cabin interior according to the user characteristics (Figure 2). The background grid on the illustration helps to identify the dimensions around the operator, one square of the grid represents a 100x100mm area.

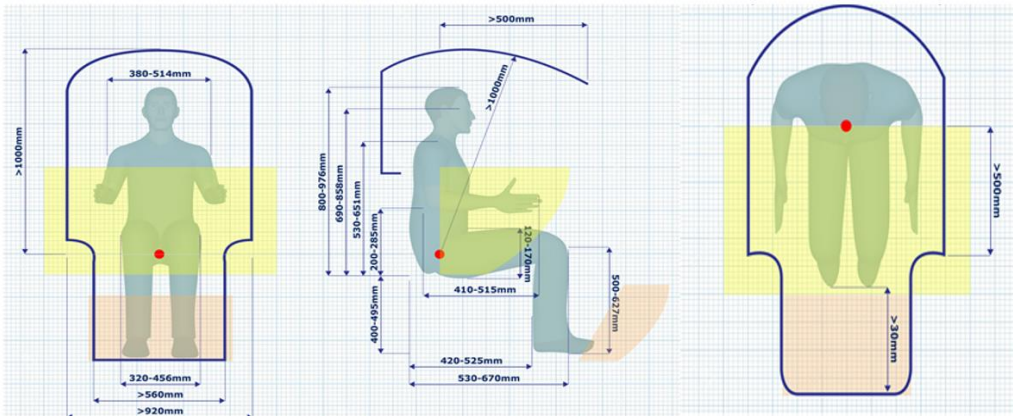

Figure. 2 *Anthropometric dimensions of a small and large male operator in a static seated position and operator envelope, according to ISO 3411:2007; and zones of comfortable reach (marked yellow and orange), according to ISO 6682:1986*

4. CRANE CABIN DESIGN APPROACH

4.1. Human-centric design method

The qualitative analysis and classification of the weaknesses of crane cabins was aggregated as per literature [4-9]. Finally, the verification of this literature analysis was made through a questionnaire. The goal was to conduct the questionnaire with 10 users and to get their feedback about the problems in crane cabins. Data was collected from October 2022 to November 2022 in Skopje. The questionnaire was completed online, using Google Forms. The Likert scale [12] was used in the questionnaire that converted it into points (1- being the least important, 5- being the most important). Summary, the results of the literature review and survey is shown on Table 2. In Table 2, the main users' health problems and the elements in a crane that contributed to them are indicated.

Table 2 *Data collection by literature review [5-7], [13-17] and survey*

Problem identification (by literature)	Resulted of
Increased force requirements of the joysticks Wrist/hand pain	Arm rest and joystick
White fingers when cold Disturbed field of view Neck pain and shoulder pain Shoulder pain Low back pain and lowe back Knee	seat position
Problem identification (by survey)	**Resulted of**
Position of the joysticks Wrist/hand pain	Arm rest and joystick
disturbed field of view Neck pain and shoulder pain Low back pain and lowe back	seat position
Cleaning of the windows	Cabin design

4.2. Concept generation for improved safety and ergonomics

Based on the inputs from (Table 2) a concept design of crane cabin was developed. The most important cabin issue which needs redesign of the ergonomic aspect is the crane seat. The common crane seats require people to actively fit the waist and back with the backrest when sitting, so that the backrest can provide enough support for the waist. However, due to the long-term attention to the workspace, users tend to subconsciously lean forward due to blurred vision and waist fatigue, and thus form a bad sitting posture, resulting in further waist and back pain. Issues of crane seat that need to be improved are: trunk flexion (>20°) position required to adequately view the workspace and place for knee rest when trunk flexion is more than 20°. According to [17] and [18] the basic concept for improved safety and ergonomics in the crane's cabin is generated. The crane chair consists of the knee-rest and the flexibility seat, whose surface can be tilted by an angle (Figure 3).

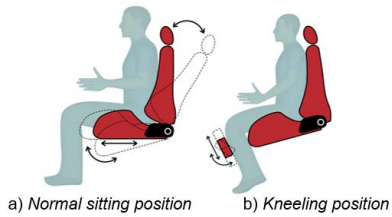

Figure. 3 *Schematic diagram of different use postures*

The arrows shown on Fig. 4 present the concept of fore-aft seat movement, the angle of the backrest, and knee position movement, as well as seat and knee rest lifters. It should be emphasized that the anthropometric data in Figure 2 was analyzed to obtain the height of the knee rests as well as their distance from each other. Additionally, the knee rest removal option or their comfort distancing is possible if the users do not want to use them.

4.3. Proposed model

Derived from the schematic diagram (Figure 3) a 3D model in SolidWorks was made of the proposed concept (Figure 4). In the 3D model the main components, such as high back, headrest, mechanical suspension, knee-rest, armrest, including their shape and anthropometric dimensions are defined.

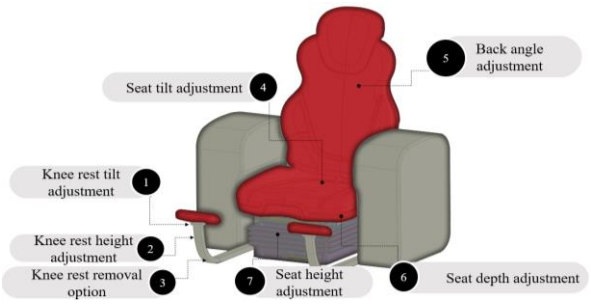

Figure 4. *The proposed model*

On Figure 4 the main tilt mechanisms of the proposed model are illustrated. In this paper, the mechanical elements that will be used are not considered. To verify the proposed model, the Siemens Jack software was used. The virtual mannequin which was used has a stature of nearly 175 cm and weight of 77.7 kg. In this study, the verification is made by positioning the upper-limb, back, shoulderes and joint angles of the down-limbs and knees. The proposed model has appropriate ergonomics according to the results of the simulation. The results by simulation are illustrated on Figure 5.

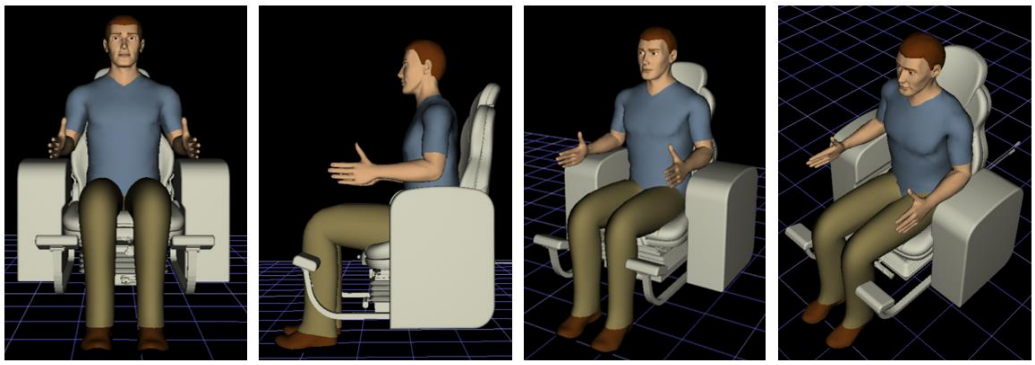

Figure 5 *Simulation for verification*

5. CONCLUSION

This research paper examines the ergonomic weaknesses of crane cabins and the ways in which they can be improved. The results of the conducted survey via a tailor-made questionnaire and data collection through literature give guidance on the current state and the desired future state. According to the results of the data analysis, the most important crane cabin issue that needs to be redesigned is the seat. Choosing the right crane cabin seat tilt mechanism can improve the operator's comfort. Hence, the proposed model of the crane seat was composed. The proposed model allows the operator to control exactly how much lumbar support is needed to maintain a healthy sitting posture as well as to improve the visual field. Further, the generated concept is analyzed using software tools for virtual ergonomics. However, the complexity of the issues considered has shortcomings in aspects such as mechanical design, material, the need to incorporate more experts and users, and the need for experimental investigations.

REFERENCES

[1] Lingard, H., Cooke, T., Zelic, G., & Harley, J. (2021). A qualitative analysis of crane safety incident causation in the Australian construction industry. *Safety Science*, *133*, 105028.

[2] Milazzo, M. F., Ancione, G., & Brkic, V. S. (2015, September). Safety in crane operations: An overview on crane-related accidents. In *6th International Symposium on Industrial Engineering (Belgrade, Serbia, 24-25 September 2015)*.

[3] Sadeghi, S., Soltanmohammadlou, N., & Rahnamayiezekavat, P. (2021). A systematic review of scholarly works addressing crane safety requirements. *Safety Science*, *133*, 105002.

[4] Neitzel, R. L., Seixas, N. S., & Ren, K. K. (2001). A review of crane safety in the construction industry. *Applied occupational and environmental hygiene*, *16*(12), 1106-1117.
[5] Spasojević-Brkić, V. K., Veljković, Z., & Brkić, A. (2015). CRANE CABINS'SAFETY AND ERGONOMICS CHARACTERISTICS EVALUATION BASED ON DATA COLLECTED IN SWEDEN PORT. *Journal of Applied Engineering Science*, *13*(4).
[6] Brkić, V. S., Klarin, M. M., & Brkić, A. D. (2015). Ergonomic design of crane cabin interior: The path to improved safety. *Safety science*, *73*, 43-51.
[7] Kushwaha, D. K., & Kane, P. V. (2016). Ergonomic assessment and workstation design of shipping crane cabin in steel industry. *International journal of industrial ergonomics*, *52*, 29-39.
[8] Tiemessen, I. J., Hulshof, C. T., & Frings-Dresen, M. H. (2007). An overview of strategies to reduce whole-body vibration exposure on drivers: A systematic review. *International Journal of Industrial Ergonomics*, *37*(3), 245-256.
[9] Wang, X., Dolivet, C., Brunel, N., & Minguy, J. L. (2000). Ergonomic evaluation of a crane cabin using a computerized human model. *Age*, *40*, 8-15.
[10] Brkić, V. S., Veljković, Z., & Brkić, A. (2019). Crane Cabins Development-Are there Innovations Needed?. In *E3S Web of Conferences* (Vol. 95, p. 01006). EDP Sciences.
[11] Panero, J. U. L. I. U. S., Dimension, M. Z. H., & Space, I. (1979). A Source Book of Design Reference Standards.
[12] Joshi, A., Kale, S., Chandel, S., & Pal, D. K. (2015). Likert scale: Explored and explained. *British journal of applied science & technology*, *7*(4), 396.
[13] Oliver, M. L., Northey, G. W., Murphy, T. A., MacLean, A., & Sexsmith, J. R. (2012). Joystick stiffness, movement speed and direction effects on upper limb muscular loading. *Occupational Ergonomics*, *10*(4), 175-187.
[14] Nourollahi-Darabad, M., Mazloumi, A., Saraji, G. N., Afshari, D., & Foroushani, A. R. (2018). Full shift assessment of back and head postures in overhead crane operators with and without symptoms. *Journal of occupational health*, *60*(1), 46-54.
[15] Brookham, R. L., Wong, J. M., & Dickerson, C. R. (2010). Upper limb posture and submaximal hand tasks influence shoulder muscle activity. *International journal of industrial ergonomics*, *40*(3), 337-344.
[16] Khademian, F., Afshari, D., Shahryari, M., & Jazaeri, S. A. (2018). Working Postures and Musculoskeletal Disorders Among Overhead Crane Operators in a Steel Industry. *Jundishapur Journal of Health Sciences*, *10*(2).
[17] Baskaran, T., Sankaranarayanasamy, K., & Gopanna, K. (2021). Assessment of Musculoskeletal discomfort for mobile crane operators. *Materials Today: Proceedings*, *46*, 10459-10463.
[18] Bettany-Saltikov, J., Warren, J., & Jobson, M. (2008). Ergonomically designed kneeling chairs are they worth it?: Comparison of sagittal lumbar curvature in two different seating. *Stud Health Technol Inform*, *140*, 103-106.

COMETa 2022
6th INTERNATIONAL SCIENTIFIC CONFERENCE
17th - 19th November 2022
Jahorina, B&H, Republic of Srpska
University of East Sarajevo
Faculty of Mechanical Engineering
Conference on Mechanical Engineering Technologies and Applications

THERMAL MODEL OF HIGH SPEED MOTORIZED SPINDLE

Miloš Knežev[1], Aleksandar Živković[2], Hasan Smajić[3] Aleksander Stekolschik[4] Clemens Feller[5] Cvijetin Mlađenović[6], Dejan Marinković[7]

Abstract: Market conditions imposed the need to significantly shorten the time cycle of the product development phase, with increasingly caused demands for the lowest possible price and highest possible quality. One of the main components of a machine tool that affects the accuracy and productivity of processing is the main spindle, that is, the motorized spindle. The integrated motorized spindle assembly is already widely used as the main spindle of machine tools. Among machine tool manufacturers, especially with precision machine tools, there is a tendency to predict thermal errors through numerical simulations. Correctly predicted errors are the basis for their efficient and easy compensation. The integrated FEM model enables effective improvement of the thermal performance of the entire machine tool, i.e. minimizing thermal errors and accurately predicting thermal errors for the purpose of error compensation

Key words: Finite element method, Motorized spindle, Thermal behaviour

1 INTRODUCTION

The behavior of machine tools while in exploitation is conditioned by the behavior of certain vital assemblies [1]. One of the main machine tool components affecting the accuracy and productivity of machining is the spindle unit. High-speed spindles are key components in machining dies, mold and aerospace parts. The heat generated in bearings and the motor are transferred through the spindle elements, causing linear, and non-linear thermal expansion [2].

[1] MSc, Miloš Knežev,Faculty of Technical Science, Novi Sad, Serbia, knezev@uns.ac.rs (CA)
[2] PhD, Aleksandar Živković, Faculty of Technical Science, Novi Sad, Serbia, acoz@uns.ac.rs
[3] PhD, Hasan Smajić, Faculty of Automotive Systems and Production, Cologne, Germany, hasan.smajic@th-koeln.de
[4] PhD, Aleksander Stekolschik, Faculty of Automotive Systems and Production, Cologne, Germany, alexander.stekolschik@th-koeln.de
[5] PhD, Clemens Feller, Bochum University of Applied Sciences, Bochum, Germany, clemens.faller@hs-bochum.de
[6] PhD, Cvijetin Mlađenović, Faculty of Technical Science, Novi Sad, Serbia, mladja@uns.ac.rs
[7] Msc, Dejan Marinković, Faculty of Technical Science, Novi Sad, Serbia, dejan.marinkovic@uns.ac.rs

The speed, power, torque, dynamic stiffness and thermal properties of the spindle determine the productivity and quality of machining operations [3]. The thermal model predicts generated heat in the whole motorized spindle structure due to heat flow from both internal and external sources. The majority of high-speed machine tools employ spindles with hybrid rolling element bearings. The higher operating speed of spindle generates high heat in the spindle system which has a significant influence on the working capability and machining accuracy [4] .The thermally induced errors can account for as much as 70 % of the dimensional errors on a machined workpiece. If thermal errors can be predicted, they can be removed in real time by the machine controller [5]. In this paper, the finite element method is used to simulate the temperature distribution of high speed spindle. This model includes the major heat sources, the heat transfer between spindle elements for a transient analysis of the thermal behavior.

2 HIGH SPEED MOTORIZED SPINDLE

The aim of this research is to analyze the temperature fields of the GMN TSSV 90000 high-speed motorized spindle assembly, whose cross-section is shown in figure 1. The shaft is fitted with two pairs of high precision ball bearings with angular contact, the front bearing is EX 12 7C1 DUL SNFA while the rear is EX 10 7C1 DUL SNFA, mounted in a "tandem" arrangement in pairs, so that the entire bearing forms an "O" arrangement. The high-speed motorized spindle assembly is designed as an asynchronous electric motor, so the stator is mounted in the housing, and the rotor is integrated with the shaft. One of the sources of generated heat is the asynchronous motor, while the other source is the bearings. For this reason, the stator is mounted in a sleeve with a channel around it, through which the cooling fluid flows, while the cooling of the bearing is done by pressurized air and oil, i.e. oil mist flowing through the bearings and in the gap between the rotor and the stator.

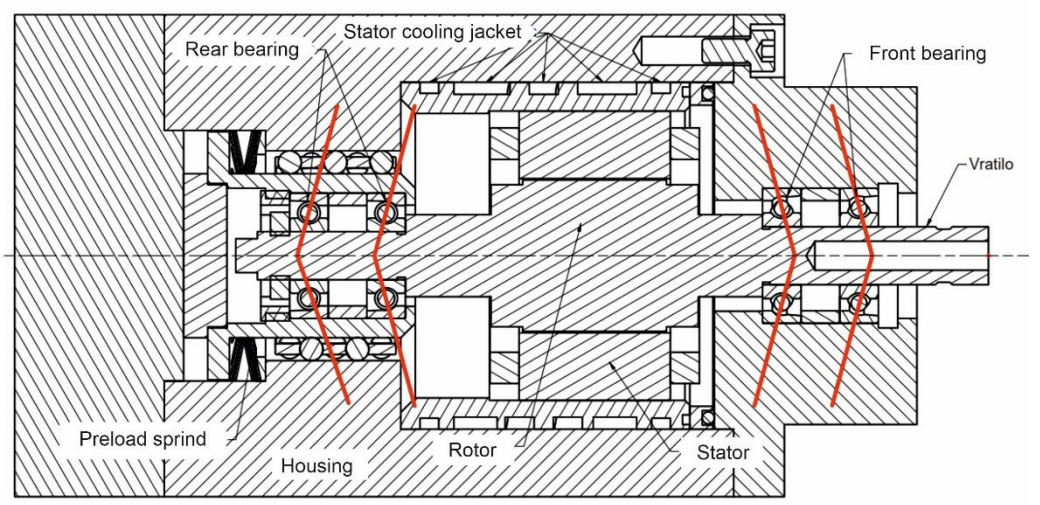

Figure 1. *Cross section of GMN TSSV 90000 high-speed motorized spindle assembly*

3 THERMAL FEM MODEL OF THE HIGH SPEED MOTORIZED SPINDLE

The model of high speed motorized spindle is built by using Inventor and the structure such as thread hole, keyhole, chamfer, fillet and so on are simplified. This structure has no significant effects on the analysis result. FEM model of the spindle has been importing to ANSYS Workbench. In defining the thermal model of the motorized spindle: the spindle shaft, bearings (rings and balls), housing, and other structure parts PLANE 188 element is used. Model consists of 7580 finite elements total.The finite elements CONTA 174 and TARGET170 were used to simulate contact joints. To simulate contact joints, contact pairs have been created at the joints, and the real constant TTC has been defined, i.e. the thermal contact conductivity ball, as well as for contact between the outer ring/housing, inner ring/spindle shaft, stator/cooling jacket, as a most important. In addition to these contacts, contacts between other parts of the structure are also defined. The finite element thermal model is shown as figure 2. Some assumptions are made for the thermal analysis:

- The motorized spindle model is axisymmetrical and assumes a uniform clearance between the outer ring and the housing around the entire perimeter.
- The thermal resistance in the axial direction, as well as axial conduction between contact elements is not considered.
- The flow rate of the cooling fluid is large enough so that the fluctuating temperature of the fluid is not considered.

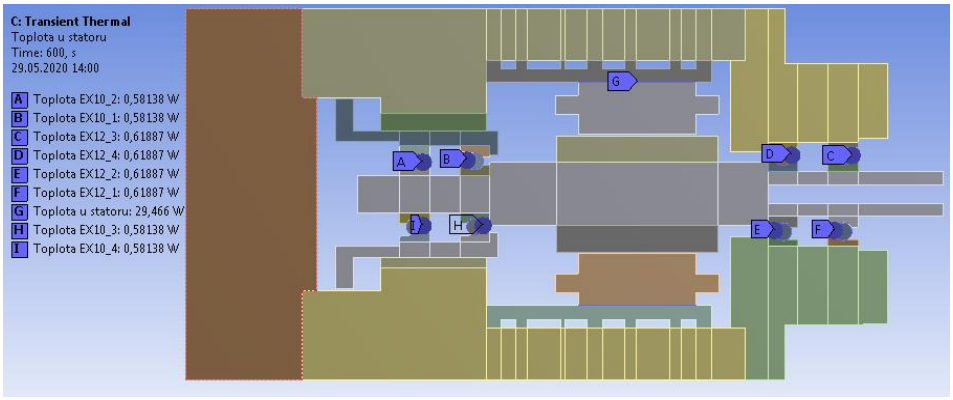

Figure 2. *FEM model of the high speed motorized spindle*

3.1 Heat generation in the motor

The electrical motor of a motorized spindle is a significant source of heat. The power losses occurring in the permanent magnet synchronous motor are armature winding losses, armature and rotor core losses. Motorized spindles typically use AC induction motors, and the effective input power of the motor is given by Eq. (1)

$$P=\sqrt{3}\cdot U\cdot I\cdot \cos\varphi, \tag{1}$$

where U is input voltage, I – current through each lead. The phase angle ‘φ’ between voltage and current determines the relative amount of effective power versus the measured apparent power. The effective electric input power is converted into mechanical output power and losses. The major portion of the losses is converted into heat [6]. The motor heat generation is estimated with the knowledge of speed and torque

and is given by Eq. (2).

$$Q_{motor}=2\cdot\pi\cdot f_{motor}\cdot M_{motor}\cdot\frac{1-\eta_{motor}}{\eta_{motor}}, \quad (2)$$

where the f_{motor} is themotor frequency, while torque T_{motor} is determined from the sum of torques related to actual bearing friction, windage losses, acceleration, and η_{motor} is the motor efficiency.

3.2 Heat generation in the bearings

Bearings are another important source of heat. The generated heat of a ball bearing is caused by three types of friction torque: friction torque due to load, friction torque due to the viscosity of the lubricant, and friction torque due to sliding. Therefore, the friction moment due to loading and lubrication for the outer and inner raceways can be defined as:

$$M_{1(i,o)}=\sum_{j=1}^{Z}\left\{f_1\left(\frac{Q_{i,o,j}}{Q_{(max)_{i,j}}}\right)^{1/3}Q_{i,o,j}d_b+10^{-7}f_0(v_o n)^{2/3}d_m{}^3\right\} \quad (3)$$

j=1,2...Z; for $v_o n>2000$[o/min]

where: f_1 – a parameter that depends on the bearing type and is defined as: $f_1=0.0013\,(P_0/C_0)$^0.33, $P_0=X_S F_r+Y_S F_a$. Parameters X_S and Y_S depending on the contact angle. $Q_{m(max)}$ – maximum contact load on the outer or inner raceways; f_0 – factor depending on the lubrication method; v_o – kinematic viscosity of the lubricant. In this case, an oil with a kinematic viscosity of 22 mm^2/s at 40 °C was considered.

The third component that affects heat generation on the bearing is the sliding moment, which is determined for each contact with the inner and outer raceways based on [7].

$$M_{S,i,o(j)}=\sum_{j=1}^{Z}\frac{3\mu Q_{i,o(j)}a_{i,o(j)}E'}{8} \quad (4)$$

The main axis of the elliptical contact for each position of the rolling body $a_{i,o}(j)$ has been calculated by Hertzian contact theory. According to (3) and (4), the heat generated in the bearings can be calculated as:

$$Q_b=1.047\cdot10^{-4}\cdot n(M_1+M_S) \quad (5)$$

3.3 Convection Boundary Condition

Heat transfer coefficient at spindle rotation, assumed that the temperature difference is minor, can be calculated. In this case, there is an exchange of heat between the rotor and the environment due to the rotation of the rotor, as well as the rolling path and the surrounding air due to the rotation of the internal rolling path. The heat transfer coefficient is generally defined according to [8]:

$$h=\frac{N_u k_a}{D} \quad (6)$$

where k_a is the heat conductivity of fluids, N_u is Nusselt's number and d_v is the diameter of the rotational part. In case of annular gap of the spindle, d_v changes to the size of gap $d_{gap.}$ Another forced convection takes place by means of a stator cooling fluid flowing through a spiral groove (Figure 3), the geometry of which is first reduced to an

equivalent stretched fluid channel with a rectangular cross-section. Also forced convection occurs when cooling and lubricating the bearing with oil mist.

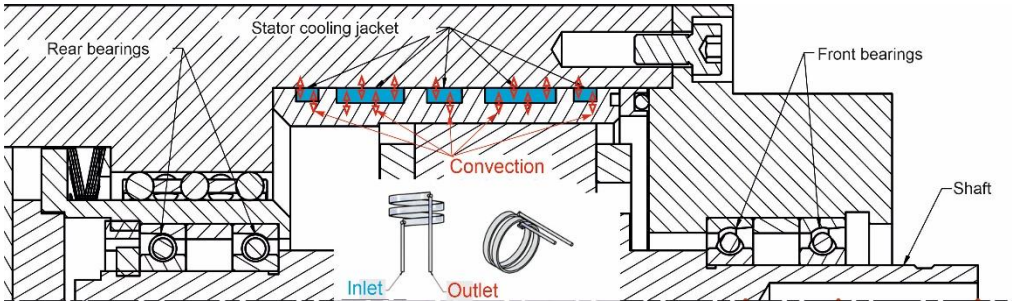

Figure 3. *Forced convection due to fluid flow through the motorized spindle housing*

3.4 Conduction between balls and raceways

The thermal contact conductance between balls and raceways is obtained empirically in function of the rotation speed [9]:

$$h_b = \frac{Z\sqrt{14+2lnv-2lnd_b}d_b^2}{2400} \tag{7}$$

$$v = \frac{n(d_m+d_b)}{19099} \tag{8}$$

The thermal resistance is obtained as [10]:

$$R_b = \frac{d_b}{h_b A} \tag{9}$$

3.5 Conduction between structure parts

In the thermal resistance of the contact between parts of the structure, it is assumed that the cross sections do not change. Also, it was assumed that the gap (hgap) is uniform. The thermal resistance of the contact between the outer ring and the housing is :

$$R = \frac{\ln(R_o/R_i)}{2\pi Lk} \tag{10}$$

where Ro and Ri are the inner and outer section radii which are observed in the inner or outer cilyndrical part, and L the length according section. Heat conductivity (k) for steel is 46.6 W/m-K and it is valid for 20-200 °C [11].

4 RESULTS AND DISCUSSION

The thermal characteristics analysis of the hihg-speed motorized spindle includes stationary change for different rotation speeds. Modeling results are shown in several ways: in graphic form (temperature increase depending on time and number of revolutions) and in numerical form, in the form of stationary temperatures of certain nodes of the finite element network, on the elements of the motorized spindle assembly. The analysis was carried out for the following conditions on oil flow through the housing Qk = 4 l/min and oil mist flow of Ql = 235.2 ml/h through the bearings at a constant air pressure of 0.5 bar and flow Qvazd = 50 l/min.

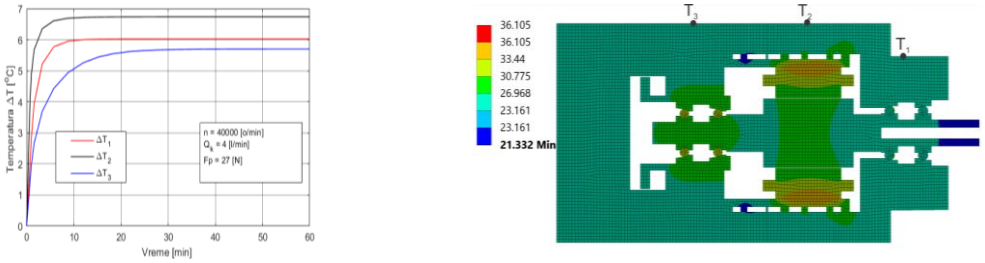

a) b)

Figure 4. *a) Temperature rise b) Layout of temperature fields in steady state at n=40000 rpm and cooling the housing with oil*

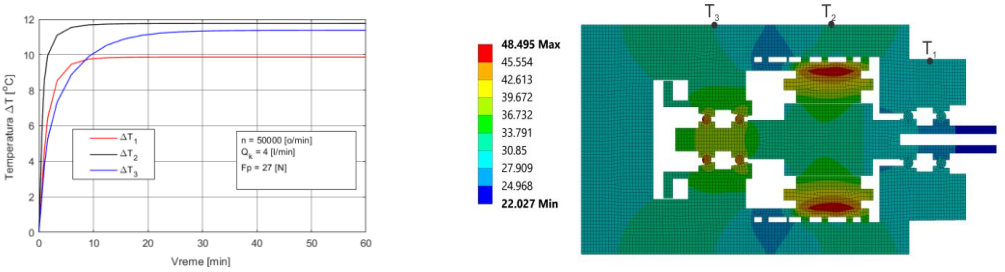

a) b)

Figure 5. *a) Temperature rise b) Layout of temperature fields in steady state at n=50000 rpm and cooling the housing with oil*

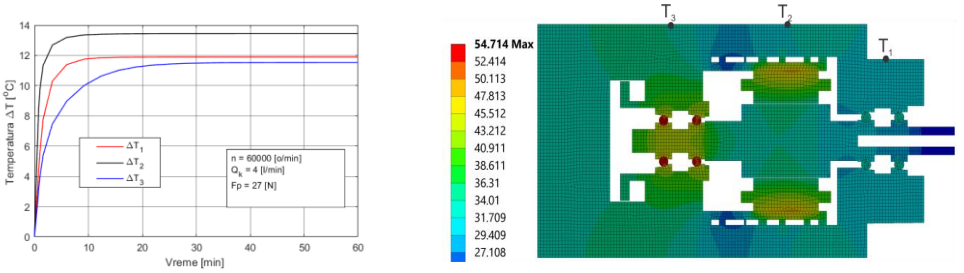

a) b)

Figure 6. *a) Temperature rise b) Layout of temperature fields in steady state at n=60000 rpm and cooling the housing with oil*

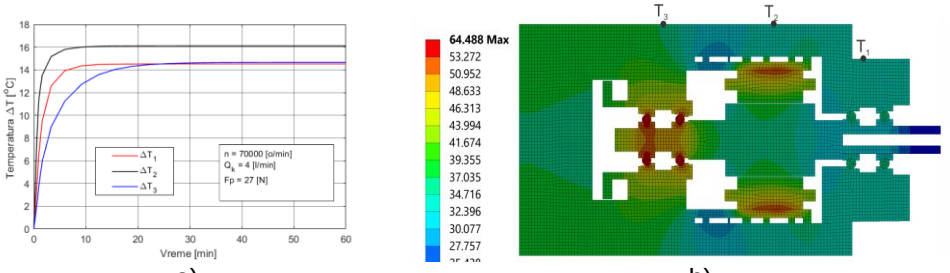

a) b)

Figure 7. *a) Temperature rise b) Layout of temperature fields in steady state at n=70000 rpm and cooling the housing with oil*

From the previous pictures, it can be concluded that the highest temperature increase is in the first time period of spindle operation (after t=10 min) and that it amounts to T=6.7 °C (for n=40000 rpm) up to T =17 °C (for n=70000 rpm). From the computer analysis, it can be concluded that the temperatures on the outer surface of the outer ring are higher by 3 to 5 °C than the temperature on the outer surface of the housing at the insertion point (T1 and T3 images from Figure 4 to Figure 7). Also, it can be observed that the temperature on the stator is higher by 11 °C (at n=40000 rpm) to 19 °C (at n=70000 rpm) than the temperature T2 (temperature on the casing near the stator as shown from (Figure 4 to Figure 7).The maximum temperatures occur at the stator of the electric motor and range from 31 °C at n=40000 rpm, to about 64 °C at n=70000 rpm. Temperatures on the bearings range from about 25 °C for n=40000 rpm, to 40 °C for n=70000 rpm.

In order to verify the developed mathematical model and to better understand the influence of certain system parameters on the thermal-mechanical behavior of the motorized spindle, an experimental test was carried out. During the experiment, the temperature was measured using a thermal imaging camera. The layout of the temperature fields recorded with a thermal imaging camera and determined by mathematical modeling is shown in Figures 8.

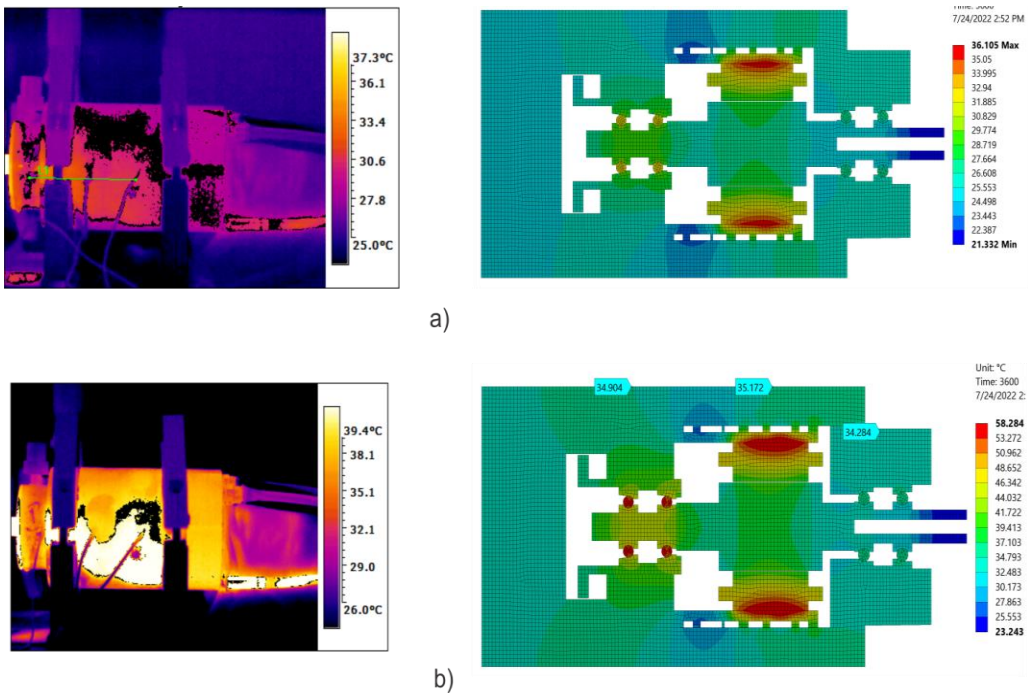

Figure 8. *Distribution of temperature fields in the stationary state during cooling of the housing with oil for Qk = 4 l/min and Ql = 235.2 ml/h at: a) n=40000 rpm; b) n=70000 rpm*

5 CONCLUSION

Summarizing the presented research and research results, it can be stated that the paper presents a mathematical model for predicting the study state thermal behavior of a high-speed motorized spindle. In this paper, the thermal model was created by using

the finite element approach by means allows to predict the behavior of the high-speed motorized spindle, in operation even in the design phase. Additionally, diference beetwean the simulated and experimentaly measured temperature fields, are less than 10%, which confirms the developed model's adequacy.

ACKNOWLEDGE

This research (paper) has been supported by the Ministry of Education, Science and Technological Development through project no. 451-03-68/2022-14/ 200156 “Innovative scientific and artistic research from the FTS (activity) domain”.

REFERENCES

[1] A. Živković, M. Zeljković, and M. Knežev, “Thermal model of high speed main spindle,” in *3th International Scientific conference, Conference on Mechanical Engineering Technologies and Applications - COMETa 2016*, 2016, pp. 215–220.
[2] A. Zivkovic, M. Zeljkovic, C. Mladjenovic, S. Tabakovic, Z. Milojevic, and M. Hadzistevic, “A study of thermal behavior of the machine tool spindle,” *Therm. Sci.*, vol. 23, no. 3 Part B, pp. 2117–2130, 2019, doi: 10.2298/TSCI180129118Z.
[3] T. Holkup, H. Cao, P. Kolář, Y. Altintas, and J. Zelený, “Thermo-mechanical model of spindles,” *CIRP Ann. - Manuf. Technol.*, vol. 59, no. 1, pp. 365–368, 2010, doi: 10.1016/j.cirp.2010.03.021.
[4] A. Segida, “Calculation of the temperature field and thermal dis- tortions of spindle assemblies and boxes,” *Sov. Eng. Res.*, vol. 4, pp. 72–74, 1984.
[5] D. A. Krulewich, “Temperature integration model and measurement point selection for thermally induced machine tool errors,” *Mechatronics*, vol. 8, no. 4, pp. 395–412, Jun. 1998, doi: 10.1016/S0957-4158(97)00059-7.
[6] V. P. Raja and R. S. Moorthy, “Prediction of Temperature Distribution of the Spindle System by Proposed Finite Volume and Element Method,” *Arab. J. Sci. Eng.*, vol. 44, no. 6, pp. 5779–5785, Jun. 2019, doi: 10.1007/s13369-019-03732-x.
[7] T. A. Harris and M. N. Kotzalas, *Essential Concepts of Bearing Technology*. CRC Press, 2006.
[8] H. Hertz, “Über die Berührung fester elastischer Körper,” *J. für die reine und Angew. Math.*, vol. 92, pp. 156–171, 1882.
[9] E. Uhlmann and J. Hu, “Thermal Modelling of a High Speed Motor Spindle,” *Procedia CIRP*, vol. 1, no. 1, pp. 313–318, 2012, doi: 10.1016/j.procir.2012.04.056.
[10] S.-M. Kim and S.-K. Lee, “Prediction of thermo-elastic behavior in a spindle–bearing system considering bearing surroundings,” *Int. J. Mach. Tools Manuf.*, vol. 41, no. 6, pp. 809–831, May 2001, doi: 10.1016/S0890-6955(00)00103-6.
[11] M. YOVANOVICH, “Thermal constriction resistance between contacting metallic paraboloids - Application to instrument bearings,” Jun. 1970, doi: 10.2514/6.1970-857.

COMETa 2022
6th INTERNATIONAL SCIENTIFIC CONFERENCE
17th - 19th November 2022
Jahorina, B&H, Republic of Srpska
University of East Sarajevo
Faculty of Mechanical Engineering
Conference on Mechanical Engineering Technologies and Applications

MODELING OF THE MACHINE TOOL SLIDERS MOVEMENT USING ARTIFICIAL INTELLIGENCE

Dejan Marinković[1], Aleksandar Živković[2], Cvijetin Mlađenović[3], Miloš Knežev[4], Dejan Lukić[5], Nicolae Ungureanu[6]

Abstract: This paper presents the analysis of experimental results using artificial intelligence. Based on the obtained experimental plan according to Taguchi, the experiment was performed on a test device. After that, the results were processed using a system of artificial neural networks with a varied number of inputs and one output.

Key words: Artificial intelligence, Artificial neural networks, NC machine tools

1 INTRODUCTION

The term Artificial intelligence first appears a few years after the research of Alan Turing and his test for machines ("Turing Test for machines"). Officially, this term was mentioned at a scientific conference in 1956 at Darmouth College, by scientist John McCarthy, who is considered as the originator of this discipline. The term artificial intelligence ("Artificial Intelligence") was defined as a field of computer sciences that aims to develop computer programs and applications that would have abilities similar to human cognitive abilities [1]. Researches of artificial neural networks ("Artificial neural networks") as one of the disciplines of artificial intelligence began in the fifties of the last century. The basic idea was to create a system that works on the principles of the human nervous system. As far as we know, human nerve cells have the ability to

[1] MSc, Dejan Marinković, University of Novi Sad, Faculty of Technical Sciences, Novi Sad, Serbia, dejan.marinkovic@uns.ac.rs (CA)
[2] PhD, Aleksandar Živković, University of Novi Sad, Faculty of Technical Sciences, Novi Sad, Serbia, acoz@uns.ac.rs
[3] PhD, Cvijetin Mlađenović, University of Novi Sad, Faculty of Technical Sciences, Novi Sad, Serbia, mladja@uns.ac.rs
[4] MSc, Miloš Knežev, University of Novi Sad, Faculty of Technical Sciences, Novi Sad, Serbia, knezev@uns.ac.rs
[5] PhD, Dejan Lukić, University of Novi Sad, Faculty of Technical Sciences, Novi Sad, Serbia, lukicd@uns.ac.rs
[6] PhD, Nicolae Ungureanu, Technical University of Cluj-Napoca, Department of Engineering and Technologic Management, nicolae.ungureanu@cunbm.utcluj.ro

remember, so the development of artificial neural network systems was based on the same. Artificial neural networks were not developed for application in one area, but have many different purposes, functions and capabilities [2].

2 DEFINING THE PARAMETERS THAT AFFECT ON THE APPEARANCE OF UNEVEN MACHINE TOOL SLIDERS MOVEMENT

During the experimental examination of the smoothness of the movement of machine tool sliders, the following influential parameters were varied:

- slider material,
- type of lubricating oil,
- slider speed (v),
- surface pressure (p),
- stiffness of system (C).

While performing the experiment, the aforementioned factors were taken into account, which does not mean that they are the only one that influence on the occurrence of stick-slip. Factors such as the roughness of the sliding surfaces, the mass of the sliders can have a great influence on the results of the experiment, while gray cast iron is often used as the material of the sliders in exploitation, which was not available to use while performing this experiment [8].

When talking about mechanical engineering, uneven movement occurs in the movement of machine tool slides. In many works, it is explained that the creation of uneven motion is most often related to the appearance of self-oscillating machines, when the stiffness of the mechanism is not sufficient and the difference in the friction coefficients of rest and motion, which occurs in mixed friction. In order for the system to be reliable even at high accelerations of the slider, there must be appropriate characteristics of the drive motor, while the positioning accuracy at certain external factors depends on the characteristics of the system for transferring the movement of the drive motor to the slider, as well as on the characteristics of the machine's leading elements. Therefore, the design solution should provide the least load on the system by internal forces that arise due to the occurrence of friction on surfaces with relative movement [3].

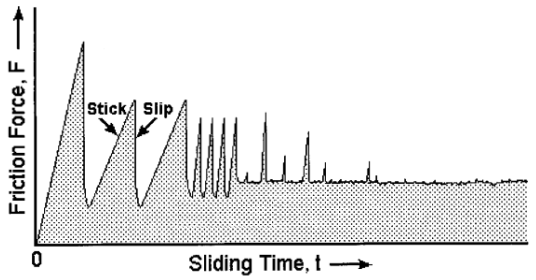

Figure 1. *Diagram of the occurrence of uneven movement (stick-slip) during sliding [4]*

3 THE EXPERIMENTAL DEVICE AND EXPERIMENT PLAN ACCORDING TO THE TAGUCHI METHOD

After defining the parameters of the experiment and their levels, the plan of the experiment was determined according to the Taguchi method. While performing the experiment, there are controlled and uncontrolled parameters. Managed parameters are those that can be controlled, and unmanaged parameters, are the so-called, noise parameters that represent parameters that are difficult to identify and control. Table 1 shows the input controlled parameters and their levels on the basis of which the experimental plan, orthogonal array according to Taguchi, L_{36} (2^2 and 3^3) was defined. The experimental plan was obtained using appropriate software [8].

Table 1. *Input parameters and their levels*

Parameters	**Levels**		
	1	***2***	***3***
Slider speed *v* [mm/min]	2	10	18
Surface pressure *p* [N/mm^2]	0,0266	0.1133	0.2
Stiffness of system *C* [N/mm]	200	300	400
	1	***2***	
Slider material	Tarcit	Č.1530	
Type of lubricating oil	Fampol KS 68	Famcirkol 3	

The following instrumentation, shown in Figure 2, was used to measure and detect the uneven movement of the machine tool slider:

A. measuring signal amplifier Hottinger Baldwin Messtechnik KWS/6A-5
B. PC for data processing
C. Hottinger Baldwin Messtechnik W1T/2 inductive position sensor
D. Hottinger Baldwin Messtechnik Q3 dynamometer
E. frequency regulator – Danfoss FC302
F. A/D conversion card- National Instruments NI USB-6281

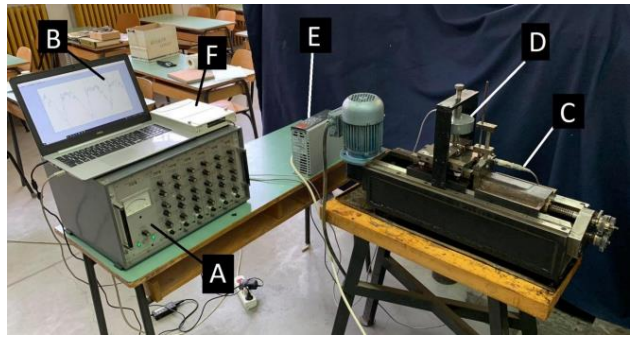

Figure 2. *Complete measuring instrumentation*

When the experiment is planned according to the Taguchi plan, the manipulation of the noise factor is carried out in order to cause a change, using the

obtained result, to recognize the optimal settings of the managed factors that make the process or the product itself resistant to changes caused by the noise factors. The experiment plan was obtained using the Minitab software and is shown in Table 2. The columns in Table 2 indicate the input parameters and their levels, on the other hand, the rows show the number of experiments [8].

Table 2. *Taguchi orthogonal array L_{36} (2^2 i 3^3)*

Number	Factor level				
	Material (M)	**Oil (O)**	**Speed (v)**	**Pressure (*p*)**	**Stiffness (*C*)**
1	1	1	1	1	1
2	1	1	2	2	2
3	1	1	3	3	3
4	1	1	1	1	1
5	1	1	2	2	2
6	1	1	3	3	3
7	1	1	1	1	2
8	1	1	2	2	3
9	1	1	3	3	1
10	1	2	1	1	2
11	1	2	2	2	1
12	1	2	3	3	3
13	1	2	1	2	3
14	1	2	2	3	1
15	1	2	3	1	2
16	1	2	1	2	3
17	1	2	2	3	1
18	1	2	3	1	2
19	2	1	1	2	1
20	2	1	2	3	2
21	2	1	3	1	3
22	2	1	1	2	2
23	2	1	2	3	3
24	2	1	3	1	1
25	2	1	1	3	2
26	2	1	2	1	3
27	2	1	3	2	1
28	2	2	1	3	2
29	2	2	2	1	3
30	2	2	3	2	1
31	2	2	1	3	3
32	2	2	2	1	1
33	2	2	3	2	2
34	2	2	1	3	1
35	2	2	2	1	2
36	2	2	3	2	3

After analyzing the results of the experimental test according to the Taguchi method, the percentage influence of the sliding material, surface pressure, speed of

the slider, stiffness of the drive-transmission system and the type of lubricating oil was determined. The mentioned influence individually amounts to 46.42% respectively; 18.59%; 5.76%; 4.23%, 0.09%; while the experimental error is 24.91%. The relatively large error of the experiment indicates a possible need to improve the experimental device. One of the possibilities that is causing larger error is spiral spindles that have a sliding connection with the nut, to install spiral spindles and nuts with ball recirculation. In this way, the occurrence of experimental noise caused by the coupling between the nut and the spiral spindle will be reduced [5].

4 SETTING THE ARTIFICIAL NEURAL NETWORK MODEL

4.1 Defining input parameters

In this work, a multi-layer neural network (MLP) with feedforward signal spreading and backpropagation error spreading was used. A large number of neural networks were trained, after which those with the best performance were selected. Training was conducted for different training algorithms, namely Levenberg – Marquardt (LM), Bayesian Regularization (BR), Scaled Conjugate Gradient (SCG). The structure of the input parameters is defined by the problem to be investigated. The input parameters are defined in Table 1, and the output parameter is the maximum displacement amplitude (Y). When forming a neural network, one of the steps requires choosing a way to distribute the data into sets. The data should be divided into training set, validation set and test set. In this work, groups were formed according to the experiment plan (Table 1 and Table 2). The total number of experiments was 36, with 4 set aside for post-training testing and network performance evaluation. The remaining 32 experiments were divided into 22 for training, 5 for validation and 5 for testing. From data in Table 1, the experiments were selected under the row. no. 2, 14, 21 and 34, so that the network would not see them and which were later used for model verification. Table 3 shows the defined structure and training sets of the neural network. The total available number of training pairs is 165. It was adopted that training is performed with the first 110 training pairs (22 experiments), the next 25 training pairs (5 experiments) are intended for validation, the remaining 25 (5 experiments) are intended for testing during training. The test (verification) set after training contains 20 training pairs (4 experiments).

4.2 Architecture of the neural networks

Artificial neural networks (ANNs) are built in layers, where the input and output layers are necessary, the number of neurons in the input and output layers depends on the number of parameters at the input and output of the network. Hidden layers are added between input and output. Most often, the initial number of layers is one, and if it is determined that it is not enough to solve the problem, new layers are added.

Table 3. *Structure of input data and training sets of artificial neural network*

Number	Factor levels					
	M	**O**	**v**	***p***	***C***	
1	1	1	1	1	1	TRAINING
2	1	1	3	3	3	
3	1	1	1	1	1	
			. . .			
21	2	1	3	1	1	
22	2	1	1	3	2	
23	2	1	2	1	3	VALIDATION
24	2	1	3	2	1	
25	2	2	1	3	2	
26	2	2	2	1	3	
27	2	2	3	2	1	
28	2	2	1	3	3	TESTING
29	2	2	2	1	1	
30	2	2	3	2	2	
31	2	2	2	1	2	
32	2	2	3	2	3	

The number of hidden neurons depends on many different factors, from the number of inputs and outputs, the number of pairs to be trained, the size of the noise and the error of the experiment in the training pairs, the complexity of the error function, the structure and the algorithm used to train the artificial neural network. The number of neurons (n) in the hidden layers can be determined in several different ways, some of which are [6]:

$$n \in [1, N_y]$$

$$n = \frac{2(N_x + N_y)}{3}, \tag{1}$$

$$n < 2N_x, \tag{2}$$

$$n = \sqrt{N_x N_y}, \tag{3}$$

where Nx is the number of input parameters and Ny is the number of output parameters. In neural networks with a larger number of hidden layers, funnel-shaped architectures are often applied, where the number of neurons in the hidden layers decreases from the input to the output of the network. According to the previous recommendations for the specific case of the performed experiment, the recommended number of neurons (n) in the hidden layers is from 1 to 10.

5 ANALYSIS OF RESULTS

Table 4 shows a comparison of the results of an artificial neural network with two neurons in one hidden layer and the results of experimental tests. As it was already

said from table 1, the experiments are separated under the row. no. 2, 14, 21 and 34, so the network did not see them during training and testing. The deviation error is determined by the formula:

$$\varepsilon = \frac{y_{exp} - y_{nm}}{y_{exp}} 100\% \quad (4)$$

Table 4. *Comparison of ANN results and experimental test results*

Num. of experiment from Table 1	Max. ampl. of Y [µm]		ε [%]
	Experimental	ANN	
2	15	17.25	-15
14	24	25.19	-4.95
21	22	23.18	-5.36
34	95	76.53	19.44
Deviation error ε_{sr}%			**11.19**

The presented results lead to the conclusion that the network with 2 neurons in one layer provides an average prediction error of 11.1%, which is enough to apply the mentioned model for the analysis of the smoothness of the slide movement in machine tools.

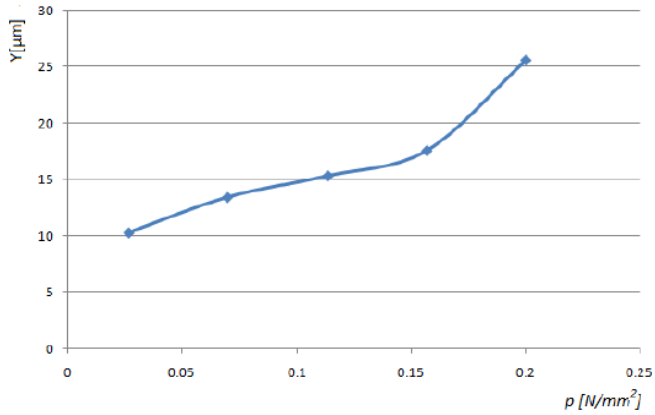

Figure 3. *The effect of surface pressure on the output value of Y – tarcite [9]*

Figure 3 shows the dependences of the output quantity Y on the surface pressure, when the slide material is tarcite. It can be observed that as the pressure increases, the magnitude of the amplitude of the occurrence of uneven motion also increases, while the stiffness and speed are kept constant. In Figure 4, you can see the change of Y depending on the pressure for the slide material - steel. As in the previous case, when the pressure increases, the size of Y also increases. The range of movement of the value of Y is greater than that of tarcite, which also corresponds to the experimental results from the test device [9].

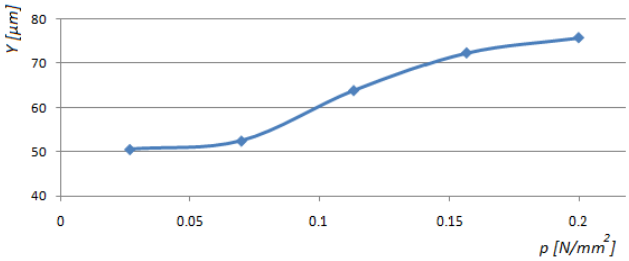

Figure 4. *The effect of surface pressure on the output value of Y – steel [9]*

6 CONCLUSION

This paper represents an attempt to predict the physically measured results of machine tool slider movements using artificial intelligence, i.e. using artificial neural networks. The models that analyze the smoothness of machine tool slide movements achieve a minimum average prediction error of about 11%, which can be considered a satisfactory result, if we take into account the currently available measurement technology whose accuracy, due to the sensitivity of sensors and external influences, is not significantly higher.

REFERENCES

[1] Kumar, R.: *Artificial Intelligence – Basics*, Machine Learning and Cognition in Enterprises, pp. 33-49, 2017.
[2] Zupan, J.: *Basics of artificial neural networks*, Nature-Inspired Methods in Chemometrics: Genetic Algorithms and Artificial Neural Networks, pp. 199-229, 2003.
[3] Marić, V. M.: *Examination of the smoothness of the movement of machine tool sliders*, Master thesis, University of Novi Sad, Faculty of Technical Sciences Novi Sad, 86 str, 1977
[4] Alan, D. B., William, A. D., Jacob, N. I.:*Origin and Characterization of Different Stick-Slip Friction Mechanisms*, Langmuir, Vol. 12, pp. 4559-4563, 1996.
[5] Poll, G.W.: *Life Cycle Engineering and Virtual Product Development – the Role of Trybology*, Tribology and Interface Engineering Series, Vol 48, pp. 15-28, 2005.
[6] Miljković, Z., Aleksendrić, D.: *Artificial neural networks*, A collection of solved problems with excerpts from the theory, University of Belgrade, Faculty of Mechanical engineering, 2009.
[7] Macukow, B.: *Neural Networks – State of Art, Brief History, Basic Models and Architecture,* Authorized lecture manuscript, Faculty of Applied Mathematics and Information Science, Warsaw University of Technology, Poland.
[8] Marinković, D.: *Analiza uzicaja pojedinih parametara na ravnomernost kretanja klizača mašina alatki*, Bachelor thesis, University of Novi Sad, Faculty of tecnical sciences, Novi Sad, Serbia, 2021.
[9] Marinković, D.: *Application of artificial neuron networks in modeling the uniformity of the machine tools sliders movement*, Master Thesis, University of Novi Sad, Faculty of tecnical sciences, Novi Sad, Serbia, 2022.

COMETa 2022
6th INTERNATIONAL SCIENTIFIC CONFERENCE
17th - 19th November 2022
Jahorina, B&H, Republic of Srpska
University of East Sarajevo
Faculty of Mechanical Engineering
Conference on Mechanical Engineering Technologies and Applications

KREIRANJE MODELA KOŠA POTKOLJENE PROTEZE KORIŠTENJEM 3D SCAN/CAD TEHNOLOGIJA

Sara Jerkić[1], Fuad Hadžikadunić[2], Mirza Oruč[3], Kenan Varda[4]

Rezime: Predmet razmatranja rada jeste iz domena specifičnih biomehaničkih istraživanja. Savremena naučno-stručna razmatranja i istraživanja se bave primjenom najpovoljnijih idejnih rješenja i tehnologija za formiranje funkcionalnih, sigurnih i konformnih rješenja i vrsta protetskih pomagala prema specifičnim namjenama i potrebama svakog pacijenta. U radu se prikazuje samo jedan dio složenog procesa, a koji se odnosi na dio primjene savremenih metroloških SCAN tehnologija, te metodologija CAD/CAE dizajniranja i analize u cilju kreiranja koša, kao dijela konstrukcije potkoljenog protetskog pomagala koji je direktno u kontaktu sa ostatkom ekstremiteta/residuuma korisnika. Istraživanja su pokazala da se na bazi korištenja savremenih tehnika mjerenja optičkih skeniranja vrlo složenih površina, razvijanja CAD modela koša proteze na principu 'surface modelling-a', može potvrditi uspješnost korištenja savremenih metoda u izradi koša proteze sa aspekta funkcionalnosti i konformiteta korištenja iste kod ispitanika.

Ključne riječi: koš, potkoljeno protetsko pomagalo, 3D SCAN/CAD tehnologije

DESIGNING OF A SOCKET MODEL OF A LOWER LIMB PROSTHESIS USING 3D SCAN/CAD TECHNOLOGIES

Abstract: The subject of consideration of the paper is in the domain of specific biomechanical research. Modern scientific and professional considerations and research deal with the application of the most favorable conceptual solutions and technologies for the formation of functional, safe and compliant solutions and types of prosthetic device according to the specific purposes and needs of each patient. The paper shows only one part of the complex process, which refers to the application of modern metrological SCAN technologies, and the CAD/CAE design and analysis methodology in order to create a socket, as part of the construction of a lower leg prosthetic device that is in direct contact with the rest of the limb/of the user's residue.

[1] Dipl. inž. maš., Sara Jerkić, Mašinski fakultet UNZE, Zenica, BiH, sara.jerkic@unze.ba
[2] V. prof. dr., Fuad Hadžikadunić, Mašinski fakultet UNZE, Zenica, BiH, fuad.hadzikadunic@unze.ba
[3] Doc. dr., Mirza Oruč, Medicinski fakultet UNZE, Zenica, BiH, mirza.oruc@unze.ba
[4] Mr., Kenan Varda, Mašinski fakultet UNZE, Zenica, BiH, kenan.varda@unze.ba

Research has shown that based on the use of modern measuring techniques of optical scanning of very complex surfaces, development of CAD models of the prosthesis socket based on the principle of 'surface modeling', it is possible to confirm the success of the use of modern methods in the production of the prosthesis socket from the aspect of functionality and conformity of its use by the examinees.

Key words: lower leg prosthetic device, socket, 3D SCAN/CAD technologies

1 UVOD

Tijelo čovjeka predstavlja veoma složenu ‘konstrukciju’ savršenog djelovanja u uslovima kada je integritet iste nenarušen u bilo kom smislu. Međutim, katkada su potrebne određene ‘korekcije’, uzrokovane različitim uslovima, kada se određeni dijelovi tijela nadoknađuju, koriguju ili uklanjaju, a što generalno utječe na ukupne performanse ljudskog tijela. U dijelu koji se odnosi na amputacije, ista se najjednostavnije opisuje kao hirurško uklanjanje ekstremiteta ili dijela tijela. Različiti su razlozi zašto ljekari predlažu amputacije kod određenih pacijenata, a neki od tih razloga su: zdravstveni problemi - dijabetes ili vaskularne bolesti, posljedice povreda u radnim uslovima, posljedice saobraćajnih i drugih nezgoda, posljedice ratnih djelovanja, itd. Zanimljivo je napomenuti da je amputacija kao jedno od medicinskih rješenja raširena tek u 20. stoljeću tokom Drugog svjetskog rata.

Razvoj nauke i tehnike, donio je nova i interesantna dostignuća u oblasti medicine. Tokom druge polovine 21. stoljeća započela je upotreba aditivnih tehnologija izrade u skoro svim segmetnima života. S razlogom se 21. stoljeće smatra početkom nove revolucije u oblasti tehnike. U zadnjih 30 godina došlo je do ubrzanog razvoja biomedicinskog inženjerstva i biotehnologije. Kao pozitivan primjer iz oblasti biomedicinskog inženjerstva, pored mnogih drugih, može se smatrati razvoj i izrada protetskih pomagala, slika 1. Način razvoja i izrade protetskih pomagala se vremenom mijenjao i razvijao, [1].

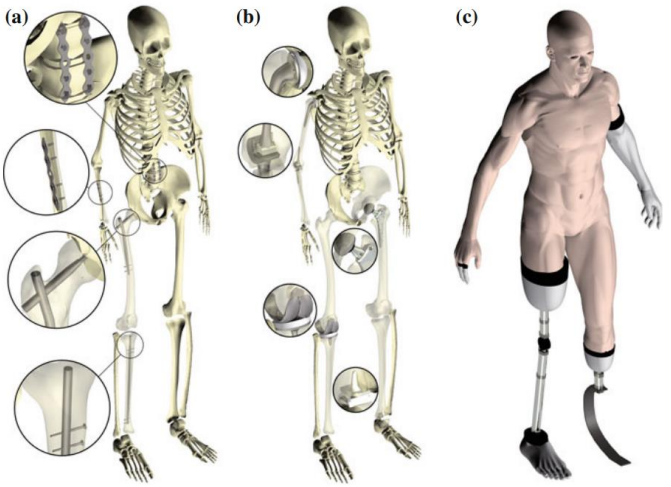

Slika 1. *Primjeri ortopedskih pomagala: a) fiksatori preloma: spinalna fiksacija, radijalne ploče i vijci, femoralni vijak i ploča, tibijalna intramedularna šipka, b) artikularne proteze: cjelokupno rame, lakat, kuk, koljeno, zglob, c) eksterne proteze: ruka, prst, noga iznad i ispod koljena, [1]*

Izrada protetskih pomagala predstavlja spregu više naučnih disciplina, kao i primjenu modernih metoda dijagnostike i protetike. Jedna od najvećih promjena u oblasti izrade protetskih pomagala je uvođenje tehnologije dizajniranja korištenjem CAD tehnologija. Druga značajna promjena se desila u oblasti primjene materijala, gdje se počelo sa aktivnim korištenjem "light-weight" materijala. Cilj korištenja i izrade protetskih pomagala je obezbijediti što sigurniju i što bolju mobilnost osoba sa amputiranim ekstremitetima.

Različita su područja ljudskoga tijela u kojima se mogu pojaviti potrebe za izradu protetskih pomagala: za donje ekstremitete, npr. potkoljenična ili nadkoljenična protetska pomagala, zatim za gornji dio tijela podlaktična ili nadlaktična protetska pomagala, itd. Način izrade protetskih pomagala je veoma bitna karika za postizanje ovog humanog cilja olakšavanja funkcionalnosti i konformnosti korisniku u posebnim uslovima djelovanja ljudskog tijela.

2 DOSADAŠNJA ISTRAŽIVANJA

Kreiranje modela 'koša' potkoljenične proteze danas je moguće uz dva moguća pristupa: praktičnim uzimanjem uzorka i fizičkog kreiranja modela na osnovu pravila protetske prakse; korištenjem savremenih tehnika skeniranja/mjerenja i modeliranja, kao baze za optimizaciju u saradnji s protetskom praksom, uz mogućnosti korištenja i numeričkih simulacija za ukupno postizanje funkcionalnosti i konformiteta proteze.

Istraživanjem dosadašnjih radova i naučnih studija iz oblasti bioimedicinskog inženjerstva, a naročito radova koji su naglasak stavili na izradu 3D modela koša primjenom CAD tehnologija, može se zaključiti da se veliki broj istraživanja uglavnom svodi na izradu 3D modela primjenom metoda konačnih elemenata korištenjem različitih softvera. Autori u većini radova stavljaju naglasak na način modeliranja 3D modela koji je specifične geometrije korištenjem metode "free surface modeling". Pored toga, rađena su istraživanja koja se odnose na poređenje modela koji se dobijaju tradicionalnim načinom izrade sa modelom koji je izrađen korištenjem novih tehnologija. U jednoj skupini radova fokus je stavljen na način izrade modela koša primjenom savremenih tehnologija, dok su u drugoj skupini radova obrađeni virtualni načini dobijanja CAD modela i svi faktori koji utiču na to.

Neka od istraživanja su prikazana u daljem tekstu. Cilj istraživanja koji je proveden od strane Engsberg, J. R., Clynch, G. S., Lee, A. G., Allan, J. S. i Harder, J. A. bio je da se pokuša razviti numerička metoda za izradu koša, [2]. Ali, I., Kumar, R. i Singh, Y. su koristili metod konačnih elemenata uz korištenje niza različitih kompozitnih materijala, kako bi se uz korištenje softvera Ansys utvrdio raspored napona i deformacija prilikom opterećenja, [3]. U istraživanju autora Colombo, G., Filippi, S., Rizzi, C., Rotini, F. opisan je postupak izrade 3D modela koša, korištenjem novih različitih metoda izrade kao što su reverzibilno inženjerstvo, virtualno izrađivanje prototipa i brza izrada prototipa, [4]. U radu autora Oldfrey, B., Miodownik, M., Barbareschi, G., Williams, R., Holloway, C. je prikazan postupak dobijanja CAD modela koša i njegova izrada korištenjem savremenih tehnologija, [5]. Krajňáková, V. je sa grupom autora opisala jednu od trenutno najpouzdanijih metoda za dobijanje CAD modela, a to je skeniranje, [6]. Oberrg, T., Lilja, M., Johansson, T. i Karsznia, A. su proveli istraživanje u kojem su poredili modele koji su dobijeni korištenjem CAD/CAM tehnologija i konvencionalnim metodama, [7]. Sanders, J.E. sa grupom autora je u radu proveo istraživanje na košu koji je izrađen primjenom CAD tehnologija, [8].

3 PROTETSKA POMAGALA

Tokom posljednjih 30 godina došlo je do razvoja i novih dostignuća u amputacijskoj hirurgiji, rehabilitaciji i protetskoj tehnologiji. Na taj način se omogućava osobama sa amputacijom da se na što brži i bolji način vrate svakodnevnim obavezama i aktivnostima. Razvojem tehnike i nauke povećala se raznolikost komponenti protetskih pomagala, ali i kako je ranije spomenuto uvedene su izmjene u tehniku izrade protetskih pomagala. Cilj je prije svega da se izrade protetska pomagala, kako bi korisnici istih mogli postići maksimalnu pokretljivost. Protetska pomagala ili proteze spadaju u ortopedska pomagala uz pomoć kojih se nadoknađuje amputirani ekstremitet ili samo dio ekstremiteta. Proteze prije svega imaju funkcionalnu ulogu, a zatim i estetsku. Kroz historijski razvoj protetskih pomagala, kao materijali za izradu su se koristili drvo, koža, metal, plastika, dok danas se pojavljuju bio-polimeri ili "light-weight" materijali.

Dio proteze koji je najvažniji za stabilnost i funkcionalnost proteze je koš. Da bi se postigao željeni rezultat koš mora da odgovara obliku dijela ekstremiteta koji je potrebno nadomjestiti. Uz to je obavezno potrebno voditi računa o izboru materijala, tako da nošenje protetskog pomagala bude ugodno, bez osjećaja hladnoće, bez iritacije kože uslijed znoja, ali i bez pojave bolova u amputiranom predjelu. Ne manje značajan faktor koji utiče na stabilnost protetskog pomagala, jeste i težina pomagala koja se potrebna da se postigne kako ne bi došlo do naglih kretanja ili zakretanja proteze. Dvije glavne podgrupe amputacije za koje se izrađuju protetska pomagala su transfemoralna i transtibijalna amputacija, slika 2 a).

Transfemoralna amputacija se odnosi na amputacije kod kojih je presječena bedrena kost ili urođene anomalije pri čemu nedostaje femur. Sa druge strane transtibijalna amputacija se odnosi na amputaciju prilikom koje je presječena kost tibije ili postoji urođeni nedostatak tibije. Podjela protetskih pomagala, u nastavku proteza, zavisi od nivoa amputacije donjih ekstremiteta. Za svaki od prethodno navedenih nivoa amputacije postoji odgovarajuća proteza, slika 2 b), [9].

Slika 2. *Protetska pomagala: a) vrste prema nivou amputacije, b) transtibijalna i transfemoralna proteza, [9]*

3.1 Koš protetskog pomagala

Proteze za pacijente sa amputiranim donjim ekstremitetima se sastoje iz četiri osnovne komponente: 1 - koš, 2 - koljeno, 3 - potkoljenični dio ili pilon, 4 - stopalo sa člankom, slika 2 a). U zavisnosti od toga da li se radi o transtibijalnoj ili transfemoralnoj amputaciji ove komponente se mogu modifikovati i nadograđivati. Sve komponente se

biraju ili izrađuju na osnovu potreba i stanja pacijenta. Osnovni i najvažniji zadatak komponenti proteze je da najbolje moguće oponašaju kompleksni mehanizam prirodne noge i pokrete noge. Koš (engl. 'prosthetic socket') je istovremeno primarna, ali i najkritičnija veza između dijela ekstremiteta koji je ostao nakon amputacije i ostatka proteze. Ovaj dio proteze, prikazano na slici 2 b), predstavlja vezu čija je glavna uloga osiguranje stabilnosti i kontrole. Stabilnost je moguće postići samo uz pravilnu i dobru izradu koša da bi se postiglo udobno prijanjanje na ostatak amputirane noge, što je vrlo bitno za postizanje pozitivnih rezultata tokom rehabilitacije.

Prilikom izrade koša, mora se izuzetno voditi računa o preostalom dijelu ekstremiteta. Najčešće se dešava da koš svojom zadnjom stranom treba da bude naslonjen na kost pelvisa. Ovome posebnu pažnju daju protetičari prilikom izrade i uzimanja otiska, kako bi se na ispravan način kreirao prepust za oslanjanje na kost. To je bitna stavka prilikom izrade koša tradicionalnim načinom izrade. Postoje i savremeni načini, a jedan od pouzdanijih načina izrade je lasersko skeniranje

4 PRIMJENA 3D SCAN/CAE METODA KREIRANJA KOŠA PROTEZE

U današnjoj modernoj tehnologiji 3D skeniranje sve više postaje obavezan postupak mjerenja koji se koristi kako u tehničkim tako i u prirodnim naukama. Razlog ovako velike ekspanzije tehnologije 3D skeniranja pored ubrzavanja procesa izrade je i povećana efikasnost, tačnost i ekonimičnost postupka. Sve navedeno posebno dolazi do izražaja kada se radi o tretiranju vrlo složenih elemenata ili prototipima, a posebno nivoa složenih prostornih krivulja i zakrivljenih ploha. U ovom slučaju, kada se radi o definiranju složene prostorne površine i volumena residuuma korisnika proteze, isto je praktično nemoguće 'snimiti' bez korištenja modernih 3D scan tehnologija.

Postupak 3D skeniranja sastoji se od dva različita i odvojena procesa. Prvi korak je prikupljanje podataka u nekom od oblika, a najčešće se radi o oblaku tačaka. U procesu 3D skeniranja ovaj prvi korak prikupljanja podataka, slobodno se može reći, jednostavniji i kratkotrajniji dio čitavog procesa. Nakon priupljenih podataka uz pomoć 3D skenera, vrši se obrada velike količine podataka. Još jedna od prednosti 3D skeniranja u procesu postprocesiranja je i mogućnost korištenja više različitih software-a kako bi se izvršila obrada potadaka i kreiranje modela. Za model koji je predmet rada korišten je 3D skener Artec Eva i izvršeno je ukupno 6 mjerenja. Na taj način se dobilo više "oblaka tačaka". Time se povećava period post-procesuiranja, ali se dobija precizno skeniran i izrađen prostorni složeni model

4.1 Kreiranje CAD modela koša korištenjem softverskih rješenja ArtecStudio i Mashmixer

Artec Studio je softver koji je omogućio učitavanje više STL fajlova dobijenih skeniranjem, pri čemu je svaki od skenova neovisan za sebe. Ono za što je korišten ovaj softver jeste da se svi dobijeni skenovi iz različitih položaja dovedu u jedan isti položaj i da se kreira oblak tačaka koji će zapravo predstavljati osnovu za kreiranje 3D modela residumma, slika 3 a). Na osnovu tog residuuma kasnije će se kreirati koš, slika 3 b).

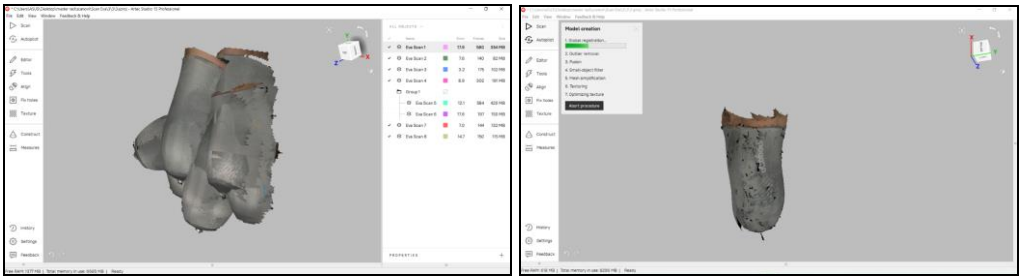

a) b)

Slika 3. *Prikaz skenova: a) za različite položaje, b) proces sjedinjavanja scan-ova i kreiranje polaznog modela reziduuma*

Prethodno dobijeni 3D model residuuma u softveru Artec Studio se učitava u MeshMixer. Na ovakvim modelima koji imaju slobodne površine, obično mreža elemenata zahtjeva određene dorade u pojedinim zonama. Na slici 4 a) je prikazan 3D model residuuma sa mrežom. Jasno se vidi da se u pojedinim zonama modela zahtijevaju određene korekcije mreže. Da bi se sa sigurnošću moglo odrediti o kojim zonama je riječ uz pomoć alatki unutar softvera, na modelu su različitim bojama određena kritična područja, slika 4 b).

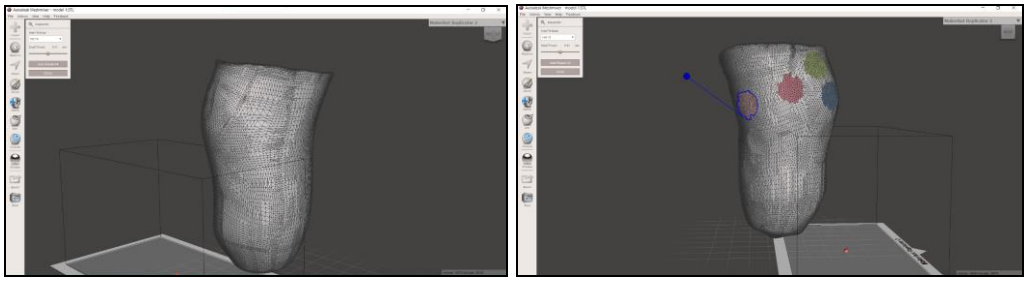

a) b)

Slika 4. *3D model residuuma: a) sa mrežom, b) područje sa kritičnom mrežom*

Nakon procesa kreiranja nove mreže, odnosno poboljšavanja postojeće mreže, dobija se 3D model residuuma koji na sebi nema zone sa “kritičnom” mrežom. Na slici 5 a) je prikazan model nakon procesa poboljšavanja mreže.

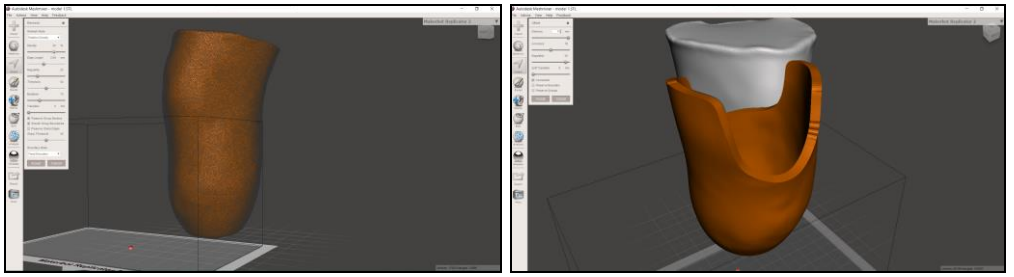

a) b)

Slika 5. *Mreža residuuma: a) nakon poboljšanja, b) sa modeliranim košem*

Nakon procesa poboljšavanja stanja površine residuuma, može se preći na naredni korak, a to je izrada 3D modela koša. Prilikom izrade 3D modela koša potrebno je voditi računa da taj model koša treba čvrsto da naliježe na reziduum, a da pri tome ne utiče na cirkulaciju krvi i da ne izaziva iritaciju ili druga nelagodna stanja kože. Da bi se ispravno označila površina preko koje će doći model koša, potrebno je znati da se koš zadnjom stranom mora oslanjati na kost pelvisa i na tom mjestu je potrebno ostaviti prepust za oslanjanje, slika 5 b).

Kako bi se dobio konačan 3D model koša, na koji je moguće kasnije dodavati ostale komponetne, potrebno je model spojiti sa adapterom. Na slici 6 a) je prikazan postupak spajanja modela koša sa adapterom, a na slici 6 b) konačan izgled modela nakon spajanja.

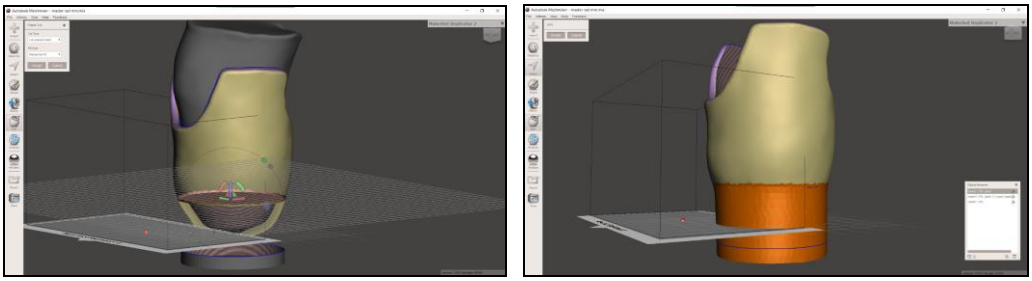

a) b)

Slika 6. *Model koša sa adapterom: a) spajanje, b) nakon spajanja*

Koš proteze treba da bude dizajniran tako da smanji pritisak u distalnom području, obavezno vodeći računa da post-operacijska rana i ožiljci na residuumu ne budu oštećeni. Istovremeno koš treba da ima takav dizajn da se preostali dio ekstremiteta u potpunosti uklopi u koš. Na slici 7 a) je prikazani konačan 3D model koša, a na slici 7 b) prikazan je kontakt modela reziduuma i modela koša.

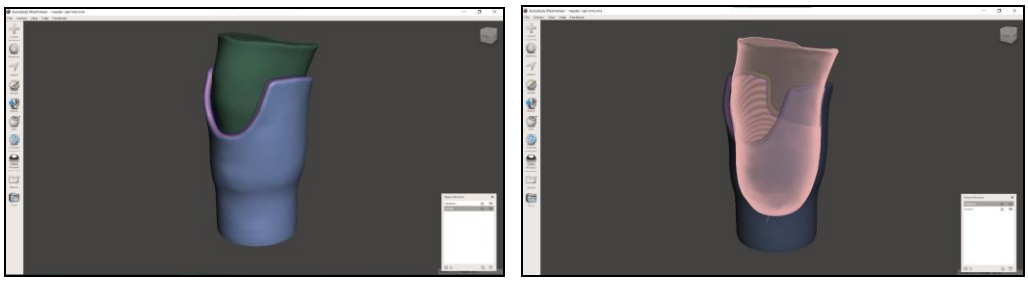

a) b)

Slika 7. *Konačan izgled: a) modela koša, b) veze modela reziduuma i modela koša*

5 ZAKLJUČCI

Predmet analize i razmatranja u ovom radu je bila primjena savremenih metroloških SCAN tehnologija, metodologija CAD dizajniranja i analize u cilju kreiranja dijela konstrukcije protetskog pomagala koji je direktno u kontaktu sa ostatkom ekstremiteta/residuuma korisnika i postizanje maksimalno mogućeg funkcionalnog komformiteta i sigurnosti pri korištenju.

Osnovni cilj rada je bio da se na bazi korištenja savremenih tehnika mjerenja tj. tehnika optičkih skeniranja vrlo složenih prostorno krivuljnih površina, razvijanja CAD modela na principu 'surface modelling-a', utvrdi uspješnost korištenja savremenih metoda u izradi koša proteze sa aspekta funkcionalnosti i konformiteta korištenja iste kod ispitanika. U ovom radu je prikazan samo dio kompleksnog procesa, koji je osnova za kreiranje polaznog modela koša primjenom 3D print tehnologija, a zatim i optimizacije modela koji se provode u daljim istraživanjima.

Na osnovu provedenih odgovarajućih koraka prilikom istraživanja, odnosno primijenjenih metodologija utvrđeno je da je kod definiranja pouzdanog polaznog modela koša, jedino moguće primijeniti mjernu tehnologiju skeniranja, koja je najpouzdanija za složene prostorne krivuljne površine, koje se ne mogu detaljno definirati niti jednom od klasičnih metoda, a za potrebe daljeg kreiranja 3D modela. Nakon toga, moguće je 'surface modelling' metodom izvršiti korekcije skenirane površine za dobijanje polaznog kvalitetnog i tačnog modela početne površine, kao osnove za dalje kreiranje koša protetskog pomagala.

LITERATURA

[1] Alessandro, F., Giorgio, O., Cristofolini, L. (2015). Experimental Stress Analysis for Materials and Structures, *Springer International Publishing Switzerland*

[2] Engsberg, J. R., Clynch, G. S., Lee, A. G., Allan, J. S., Harder, J. A. (1992). A CAD-CAM method for custom below-knee sockets, *Prosthetics and Orthotics International, vol 16, pp. 183-188*

[3] Ali, I., Kumar R., Singh Y. (2014). Finite Element Modelling and Analysis of Trans-Tibial Prosthetic Socket, *Global Journal of Researches in Engineering: A Mechanical and Mechanics Engineering Volume 14 Issue 4 Version 1.0, pp. 43-50*

[4] Colombo, G., Filippi, S., Rizzi, C., Rotini, F. (2010). A new design paradigm for the development of custom-fit soft sockets for lower limb prostheses, *Computers in Industry Computers in Industry vol 61, pp. 513–523*

[5] Oldfrey, B., Miodownik, M., Barbareschi, G., Williams, R., Holloway, C. (2020). *Digital Fabrication of Lower Limb Prosthetic Sockets, AT2030 Innovation Insights*

[6] Krajňáková, V., Michalíková, M., Hudák, R., Živčák, J., Barcalová, M. (2019). Application of the ACTEC EVA scanner for orthotics in practice, *Lekar a technika – Clinician and Technology, Vol 49, No. 3, pp. 92-96*

[7] *Oberrg, T., Lilja, M., Johansson, T. Karsznia, A. (1993). Clinical evaluation of trans-tibia prosthesis sockets: a comparison between CAD CAM and conventionally produced sockets, Prosthetics and Orthotics International, Vol. 17, pp. 164-171*

[8] Sanders, J. E., McLean, J. B., Cagle, J. C., Gardner, D. W., Allyn, K. J. (2016). Technical Note: Computer-Manufactured Inserts for Prosthetic Sockets, *Med Eng* Phys., 38 (8), pp. 801- 806.

[9] Mujkanović, A. (2020). *Numerička analiza integriteta konstrukcije na primjeru potkoljenog protetskog pomagala*, diplomski rad, Mašinski fakultet Univerziteta u Zenici.

ENERGY AND THERMOTECHNIC

COMETa 2022
6th INTERNATIONAL SCIENTIFIC CONFERENCE
17th - 19th November 2022
Jahorina, B&H, Republic of Srpska
University of East Sarajevo
Faculty of Mechanical Engineering
Conference on Mechanical Engineering Technologies and Applications

ODREĐIVANJE TEŽINA KRITERIJUMA U PROCESIMA OPTIMIZACIJE ENERGETSKIH LANACA GORIVA BAZIRANIH NA DRVNOJ BIOMASI

Srđan Vasković[1], Petar Gvero[2], Stojan Simić[3], Gojko Krunić[4] Velid Halilović[5] Slavenko Popović[6] Maja Mrkić Bosančić[7]

Rezime: Vrednovanje procesa proizvodnje energije iz različitih resursa predstavlja kompleksan zadatak. Taj zadatak mora uzeti u obzir različite tehnologije, manje ili veće proizvodne i investicione troškove, štetne uticaje na životnu sredinu (obnovljivi ili fosilni izvori energije), zatim energetske specifikacije posmatranih lanaca snabdijevanja gorivima i energijom. Višekriterijumska analiza i optimizacija je metodologija koja se bavi u opštem slučaju vrednovanjem skupova različitih alternativa. Kao takva, ova metodologija je idealna za pronalaženje optimalnih varijanti snabdijebanja energijom za usvojeni set kriterijuma prema kojima se vrši proces optimizacije. Za izbor optimalne varijante potrebno je ustanoviti adekvatne težine kriterijuma iz postojećeg skupa alternativa. Postoje različite metode za izbor težinskih faktora koje su uglavnom svedene na subjektivne i objektivne metode ili njihovu kombinaciju. U ovom radu koristiće se objektivna Metoda Entropije za određivanje težina kriterijuma za proces višekriterijumske optimizacije i njen uticaj na izbor optimalnog lanca snabdijevanja u odnosu na varijantu ujednačenih težinskih koeficijenata. Razlog za njenu primjenu se svodi na objektivnost prilikom donošenja odluka i isključivanje donosioca odluke iz tog procesa.

Ključne riječi: Entropijska metoda, MCDM analiza, snabdijevanje energijom, energetska efikasnost, zaštita okoline

[1] PhD, Srđan Vasković, University of East Sarajevo, Faculty of Mechanical Engineering, East Sarajevo, B&H, e-mail: srdjan.vaskovic@ues.rs.ba (CA)
[2] PhD, Petar Gvero, University of Banja Luka, Faculty of Mechanical Engineering, Banja Luka, B&H, e-mail: petar.gvero@mf.unibl.org
[3] PhD, Stojan Simić, Oil refinery Modriča, Modriča, B&H, e-mail: stojans@modricaoil.com
[4] PhD, Gojko Krunić, University of East Sarajevo, Faculty of Production and Management, Trebinje, B&H, e-mail: gojko.krunic@fpm.ues.rs.ba
[5] PhD Velid Halilović, Faculty of Forestry, Zagrebačka 20, Sarajevo, BiH, e-mail: v.halilovic@sfsa.unsa .ba
[6] Slavenko Popović, Termoelektrana Ugljevik, B&H, e-mail: slavenko_popovic@hotmail.com
[7] Mr. Maja Mrkić Bosančić, Ministarstvo energetike i rudarstva Republike Srpske, B&H, e-mail: mm.bosancic@mier.vladars.net

DETERMINATION OF THE WEIGHTS OF THE CRITERIA IN THE OPTIMIZATION PROCESSES OF ENERGY CHAINS OF FUELS BASED ON WOOD BIOMASS

Abstract: Evaluating the process of energy production from different resources is a complex task. That task must take into account different technologies, lower or higher production and investment costs, harmful effects on the environment (renewable or fossil energy sources), then the energy specifications of the observed fuel and energy supply chains. Multi-criteria analysis and optimization is a methodology that generally deals with the evaluation of sets of different alternatives. As such, this methodology is ideal for finding optimal variants of energy supply for the adopted set of criteria according to which the optimization process is carried out. In order to choose the optimal variant, it is necessary to establish adequate criteria weights from the existing set of alternatives. There are different methods for choosing weighting factors, which are mainly reduced to subjective and objective methods or their combination. In this paper, the objective Entropy Method will be used to determine the weights of the criteria for the multi-criteria optimization process and its influence on the choice of the optimal supply chain in relation to the variant of equal weight coefficients. The reason for its application comes down to objectivity when we are making decisions and excluding the decision maker from that process.

Key words: Entropy Method, MCDM analysis, Energy Supply, Energy Efficiency, Environmental Protection

1. UVOD

Težina kriterijuma pokazuju njihov značaj u procesu višekriterijumske optimizacije (MCDM) i ako su njihove vrednosti dobro određene rezultat ovakve analize će biti dobar. Najjednostavniji metod koji se koristi u mnogim MCDM studijama je korišćenje jednakih vrednosti kriterijuma [1], što naravno nije adekvatan i tačan pristup za konačnu evaluaciju u svim ozbiljnijim pristupima vezanim za MCDM [2]. Postoji nekoliko metoda za određivanje težine kriterijuma i one su klasifikovane u tri grupe: subjektivne, objektivne i hibridne (integrisane) metode. U subjektivnim metodama, određivanje težine kriterijuma zavisi od donosilaca odluka i kao takve ne uzimaju u obzir objektivne uslove [3]. Glavni nedostatak ovih metoda je što nisu dovoljno efikasni kada se broj kriterijuma povećava. U metodama objektivnog određivanja težina kriterijuma, preferencije donosilaca odluka nemaju ulogu u određivanju vrijednosti kriterijuma [3]. Težine su u ovom slučaju određene prema informacijama iz originalnih podataka sadržanih u optimizacionoj matrici. U poređenju sa subjektivnim metodama, objektivne metode određivanja težina kriterijuma imaju bolji matematički pristup u objektivnom određivanju vrijednosti težina, ali lošiju interpretabilnost. Stoga, njihovi zaključci ponekad nisu u skladu sa stvarnim značajem kriterijuma [4]. Da bi se prevazišli nedostaci subjektivnih i objektivnih metoda za određivanje težina, poslednjih godina se koriste metode koje kombinuju subjektivno i objektivno ponderisanje (određivanje težina kriterijuma) [5].

U ovom radu je dat prikaz primjene Entropijske metode kao objektivnog pristupa u određivanju težina kriterijuma energetskih lanaca baziranih na biomasi. Objektivnim pristupom određivanju težina kriterijuma, kriterijumi se posmatraju kao izvori informacija i relativna važnost kriterijuma reflektuje količinu informacija sadržanu u svakom od njih.

2. MATERIJALI I METODE

U ovom radu iskorišćeni su podaci i materijali iz prethodnih proračuna koji se odnose na tri lanca snabdijevanja drvnim gorivom od biomase i to: proizvodnja drvne sječke na terminalu-varijanta 1, proizvodnja peleta-varijanta 2 i proizvodnja sječke mobilnim iveračem u šumi-varijanta 3. To su podaci prikazani i tabeli 1., koji se odnose na kriterijume prethodno pomenuta tri lanca snabdijevanja gorivo i to: energetsku efikasnost, specifični investicioni trošak, specifični proizvodni trošak i specifičnu emisiju CO_2.

Tabela 1. *Kriterijumi energetskih lanaca za proizvodnju čvrstih biogoriva [6]*

Kriterijumi za izbor optimalne varijante lanca snabdijevanja gorivom			
	Alternativa1: proizvodnja drvne sječke na terminalu	**Alternativa2:** proizvodnja peleta	**Alterntiva3:** proizvodnja sječke mobilnim iveračem u šumi
energetska efikasnost (K_1)	0.94	0.68	0.97
specifični investicioni trošak u energetski lanac EUR/kW (K_2)	5.329×10^3	5.263×10^3	2.347×10^3
specifični proizvodni trošak EUR/ kWh (K_3)	17.248×10^{-3}	22.37×10^{-3}	12.867×10^{-3}
specifična emisija CO_2 kg/kWh (K_4)	12.365×10^{-3}	51.695×10^{-3}	4.342×10^{-3}

Entropijski metod (ENTROPY WEIGHT METHOD EWM) određivanja objektivnih težina kriterijuma zasniva se na mjerenju neodređenosti informacije koju sadrži matrica odlučivanja i direktno generiše skup težinskih vrednosti kriterijuma na osnovu međusobnog kontrasta pojedinačnih kriterijumskih vrednosti varijanti za svaki kriterijum i zatim istovremeno za sve kriterijume [7]. EWM metoda tretira nesigurnost u informacijskoj strukturi matrice odluke, poznatu kao Šenonova entropija [8]. Težine kriterijuma se generišu direktno na osnovu rejtinga alternativa i eliminišu problem subjektivnosti, nekompetentnosti ili odsustva donosioca odluke. Vrijednost entropije se kreće u rasponu [0,1] . Što je veća vrijednost Ei, to je veći stepen diferencijacije indeksa i, daje mu se veća težina. Težina i indikatora je data:

$$w_i = \frac{1-E_i}{\sum_{i=1}^{m}(1-E_i)} \quad (1)$$

Ono što treba još naglasiti kod ove metode jeste da takođe, nisu bitni ni priroda i tip kriterijuma.

VIKOR MCDM metoda nakon toga utvrđuje kompromisnu rang listu i kompromisno rešenje koje je najbliže idealnom rješenju [9]. Izlaz iz proračuna VIKOR metodom je mjera (Qi) za višekriterijumsko rangiranje alternativa. VIKOR ima opcije verifikacije: prihvatljivu prednost i prihvatljivu stabilnost. Na ovaj način smo ostvarili povratnu informaciju u smislu postizanja kompromisnog rješenja korekcijom težinakriterijuma za optimizaciju, kako bi se ispunili uslovi stabilnosti i prihvatljivih

prednosti rješenja u rangiranju alternativa (u našem slučaju opcija proizvodnje čvrstih biogoriva.

Mjera za višekriterijumsko rangiranje Q_i, prema VIKOR metodi, za *i=1,2,...n*, slijedi data je:

$$Q_i = \nu \frac{\left(S_i - S^*\right)}{S^- - S^*} + \left(1-\nu\right)\left(\frac{R_i - R^*}{R^- - R^*}\right) \tag{2}$$

$$S_j = \sum_{i=1}^{n} w_i \left| \frac{f_i^+ - f_{ij}}{f_i^+ - f_i^-} \right| \tag{3}$$

$$R_j = \max_i \left(w_i \left| \frac{f_i^+ - f_{ij}}{f_i^+ - f_i^-} \right| \right) \tag{4}$$

$$S^* = \min_j S_j, \quad S^- = \max_j S_j, \quad R^* = \min_j R_j \quad \text{i} \quad R^- = \max_j R_j \tag{5}$$

Gdje su : f_i^*najbolje i f_i^-najgore vrijednosti svih kriterijuma funkcija, i = 1,2,. . ,n

$f_i^* = \max_j f_{ij}$ $\quad f_i^- = \min_j f_{ij}$ ako *i*-ta funkcija predstavlja max atribut (6)

$f_i^* = \min_j f_{ij}$, $f_i^- = \max_j f_{ij}$ ako *i*-ta funkcija predstavlja min atribut (7)

w_i je težina kriterijuma,ν je "strateški koeficijent" koji uvjek pripada intervalu [0,1].

S_i -predstavlja mjeru odstupanja kojom seizražava zahtjev za maksimalnom grupnom koristi.

R_i-predstavlja mjeru odstupanja kojom se izražava zahtjev za minimizacijom maksimalnog rastojanja neke alternative od “idealnog”rješenja.

Veličina Qi predstavlja uspostavljanje kompromisne rang liste koja objedinjuje veličine Si i Ri. U osnovi prethodno izneseno predstavlja osnovne pretpostavke sa kojima se ušlo u proračun i analizu težinskih kriterijuma za lance snabdijevnja drvnim biogorivom. VIKOR metoda kao predstavnik MCDM metoda služi za ispitivanje uticaja na rangiranje varijanti snabdijevanja drvnim gorivima.

3. UPOREDNA ANALIZA UTICAJA TEŽINA KRITERIJUMA ZA SLUČAJ TEŽINA DOBIJENIH METODOM ENTROPIJE I SLUČAJ JEDNAKIH TEŽINA PRILIKOM IZBOR OPTIMLNE VARIJANTE LANCA SNABDIJEVANJA GORIVOM

Uzimajući u obzir kompletnu proceduru proračuna težina kriterijuma uz pomoć entropijske metode a za matricu odlučivanja datu u tabeli 1. imamo da je vrijednost težina distribuirana kao tabeli 2.

Tabela 2. *Kriterijumi energetskih lanaca za proizvodnju čvrstih biogoriva prema metodi entropije*

energetska efikasnost (K1)	specifični investicioni trošak u energetski lanac EUR/kW (K2)	specifični proizvodni trošak EUR/ kWh (K3)	specifična emisija CO2 kg/kWh (K4)
w_1=0,024	w_2=0,116	w_3=0,050	w_4=0,81

Iz tabele 2. zaključuje se da je kriterijum specifične emisije CO_2 sa najviše dodijeljenim težinskim koeficijentom, za njim slijedi specifični investicioni trošak, specifični proizvodni trošak i na kraju energetska efikasnost lanca. Uzimajući u obzir drugu opciju najjednostavijeg pristupa jednakosti svih težinskih faktora ($w_1=w_2=w_3=w_4=0,25$) na istom slučaju optimizacione matrice iz tabele 1. u nastavku slijedi uporedna analiza u traženju optimalne opcije za oba slučaja (težinskih faktora izračunatih EWM metodom i jednakih težinskih fakora) uz pomoć metode VIKOR.

VIKOR tehniku je prvi uveo Opricović 1998. godine kako bi rešio probleme višekriterijumskog odlučivanja (MCDM) i dobio najbolje kompromisno rešenje. Ovaj metod se fokusira na rangiranje i izbor iz skupa alternativa u prisustvu suprotstavljenih kriterijuma. Glavni cilj VIKOR metode je da se izabere rešenje koje je najbliže idealnom nivou u svakom kriterijumu, tako da su alternative zasnovane na određenoj meri „blizine" „idealnog" rešenja.

U našem slučaju postoje 4 kriterijuma i 3 alternative koje su rangirane na osnovu VIKOR metode. Tabele ispod prikazuje tip kriterijuma i težinu koja je dodeljena svakom kriterijumu, kao i kretanje kroz proračun.

Tabela 3. *Karakteristike kriterijuma energetskih lanaca za proizvodnju čvrstih biogoriva*

	Ime	tip	težina
1	kriterijum1	+	0.024
2	kriterijum2	-	0.116
3	kriterijum3	-	0.05
4	kriterijum4	-	0.81

Tabela 4. *Matrica odlučivanja*

	kriterijum1	kriterijum2	kriterijum3	kriterijum4
alternativa1	0.94	5329	0.0172	0.01237
alternativa2	0.68	5263	0.02237	0.0517
alternativa3	0.97	2347	0.01287	0.00434

Tabela 5. *Normalizovana matrica odlučivanja*

	kriterijum1	kriterijum2	kriterijum3	kriterijum4
alternativa1	0.622	0.679	0.555	0.232
alternativa2	0.45	0.671	0.721	0.969
alternativa3	0.641	0.299	0.415	0.081

Tabela 6. *Proračunske vrijednosti R i S*

	R	S
alternativa1	0.137	0.279
alternativa2	0.81	0.997
alternativa3	0	0

Tabela 7. *Vrijednosti Q*

	Q
alternativa1	0.224
alternativa2	1
alternativa3	0

Tabela 8. *Rangiranje alternativa*

	R vrijednost	Rang po R	S vrijed.	Rang po S	Q vrijednost	Rang po Q
alternativa1	0.137	2	0.279	2	0.224	2
alternativa2	0.81	3	0.997	3	1	3
alternativa3	0	1	0	1	0	1

Prijedlog kompromisnog riješenja daje se na osnovu:

Alternative ($A^{(1)}$), koja je najbolje rangirana po mjeri Q (minimum) ako zadovoljava sljedeće uslove:

Uslov 1. Prihvatljiva prednost: $Q(A^{(2)}) - Q(A^{(1)}) \geq 1/(m-1)$ gdje $A^{(1)}$ je alternativa na prvoj poziciji i $A^{(2)}$ je alternativa na drugoj poziciji mjereno po veličini Q, dok m je broj alternativa.

Uslov 2. Prihvatljiva stabilnost u odlučivanju: Alternativa $A^{(1)}$ mora biti takođe najbolje rangirana po S ili/i R.

Ukoliko jedan od uslova nije ispunjen, onda se predlaže set kompromisnih rešenja koji se sastoji od:

Riješenje 1. Alternative $A^{(1)}, A^{(2)}, \ldots, A^{(M)}$ ako **uslov 1** nije zadovoljen; Alternativa $A^{(M)}$ je određena $Q(A^{(M)}) - Q(A^{(1)}) < 1/(m-1)$ za maximum m (pozicije onih alternativa koje su ‘‘najbliže optimumu’’).

Riješenje 2. Alternative $A^{(1)}$ i $A^{(2)}$ ako **uslov 2** nije zadovoljen.

Riješenje 3. Alternative sa minimum Q vrijednosti biće izabrate kao najbolje alternative ako su oba uslova zadovoljena.

Prikaz rezultata izbora optimalne varijante dat je u sledećoj tabeli 9.

Tabela 9. *Prikaz rezultata ispunjenosti uslova optimalne varijante*

Uslov 1	Non acceptance
Uslov 2	**-**
Izabrato rješenje	**Rješenje 1**

Stoga su: alternativa3 i alternativa1 izabrane kao konačne optimalne alternative. Sličnom procedurom i u drugom slučaju jednakih kriterijuma dolazimo do rješenja da je alternativa 3 zadovoljila uslove optimalne varijante. Što znači da smo u oba slučaja dobili poklapanje varijantnog rješenja alternative3 koja se odnosi na proizvodnju drvnog čipsa uz pomoć mobilnog iverača u šumi.

4. ZAKLJUČAK

U ovome radu izvršen je prethodni proračun težinskih faktora kriterijuma lanaca proizvodnje drvnih goriva za tri varijante: proizvodnja drvne sječke na terminalu-varijanta 1, proizvodnja peleta-varijanta 2 i proizvodnja sječke mobilnim iveračem u šumi-varijanta 3. Proračun težinskih faktora za optimizaciju urađen je uz pomoć metode entropije koja spada u grupu objektivnih metoda. Da bi uporedili koliko težine kriterijuma utiču na izbor optimalne varijante određenog lanca snabdijevanja gorivima, koristili smo VIKOR metodu za dalju njihovu optimizaciju. Kao drugi slučaj za komparaciju sa dobijenim rezultatima kombinacije entropijske metode sa VIKOR metodom, koristili smo ujednačene vrijednosti težinskih koeficijenata sa kojima smo takođe ušli u proračun u VIKOR. Rezultati su pokazali da je varijantno rješenje br 3. koje se odnosi na proizvodnju drvne sječke mobilnim iveračem u šumi, optimalno rješenje prema oba slučaja i izrazilo izuzetno poklapanje u rangu alternativa. Međutim, s druge strane, ako bi iz nekih razloga vrijednosti faktora Q koji se dobija prilikom izračunavanja iz VIKOR metode, koristili kao pokazatelj koji bi mogao dati procjenu učešća od pojedinih varijantni u njihovom ukupnom zbiru, dobili bi skroz drugačije vrijednosti. Ovo u osnovi odnosi se na procejnu procenata miksa pojedinih alternativa u zbiru i može da bude jako primjenjivo u proračunu optimalnog energetskog miksa. Zbog toga, jako je bitno uraditi relevantnu procjenu i proračun težinskih fakotra prethodno prije procesa MCDM analize. Iz tih razloga procjene težinskih faktora uključuju i višestruke kombinovane pristupe različitih metoda da bi se konvergiralno njihovoj relevantnoj vrijednosti.

LITERATURA

[1] Wang et al. (2009). "Review on multi-criteria decision analysis aid in sustainable energy decision-making", Renewable and Sustainable Energy Reviews, Volume 13, Issue 9,Pages 2263-2278.

[2] Ginevičius. (2011). A new determining method for the criteria weights in multicriteria evaluation. International Journal of Information Technology & Decision Making, 10(6), 1067–1095.

[3] Zardari et al. (2015). Weighting Methods and their Effects on Multi-Criteria Decision Making Model. Springer International Publishing.

[4] Wang and Parkan. (2005). Multiple attribute decision making. Fuzzy Sets and Systems, 331–346.

[5] Meng and Chi. (2015). New combined weighting model based on maximizing the difference in evaluation results and its application. Mathematical Problems in Engineering, 9 pages.

[6] Vasković. (2016). „Razvoj modela za ocjenu prihvatljivosti energetskih lanaca pri proizvodnji energije i energenata iz biomase“. doktorska disertacija – Univerzitet u Istočnom Sarajevu, Mašinski fakultet.

[7] Srđević, B., Medeiros Y.D.P., Faria, A.S., Schaer, M., Objektivno vrednovanje kriterijuma performanse sistema akumulacija. Vodoprivreda, 35, 163-176, Novi Sad, 2003.

[8] Shannon, C.E. A mathematical theory of communication. Bell Syst. Tech. J. 1948, 27, 379–423.

[9] Opricović S., "Multicriteria Optimization of Civil Engineering Systems", Faculty of Civil Engineering, Belgrade, Serbia., 1998.

COMETa 2022
6th INTERNATIONAL SCIENTIFIC CONFERENCE
17th - 19th November 2022
Jahorina, B&H, Republic of Srpska
University of East Sarajevo
Faculty of Mechanical Engineering
Conference on Mechanical Engineering Technologies and Applications

COMPARATIVE ANALYSIS OF HEAT PUMP OPERATION USING GEOTSOL SOFTWARE

Nemanja Dobrnjac[1], Sasa Savic[2], Nemanja Koruga[3], Mirko Dobrnjac[4], Izet Alić[5]

Abstract: This paper describes the basic principle on which the operation of a heat pump is based, the heat sources it uses and comparative analysis through simulation of different types of heat pumps used for heating and preparation of domestic hot water in a residential building. The analysis was performed through the use of GeoTSOL software as an aid for simulation, with an accent on efficiency and influence on the environment.

Key words: heat pumps, GeoTSOL software, energy analysis

1 INTRODUCTION

Heat pumps as a renewable source of energy experienced a sudden expansion in the heating and air conditioning market thanks to technologies that enable the rational use of energy sufficient to achieve and maintain comfortable temperature conditions. It can be said that a heat pump is as good as its heat source. So, for the efficient and long-term operation of the heat pump, a heat source is needed that has a sufficient amount of heat with an appropriate temperature level. The higher the temperature of the heat source, the more efficient the operation of the heat pump in the case of heating. [1] For this purpose, three renewable heat sources (air, water or earth) are most often used for residential premises. [2] Depending on the type of heat source, heat pumps can be divided into:

[1] BSc Nemanja Dobrnjac, University of Belgrade, Faculty of Mechanical Engineering, Belgrade, Serbia, nemanjadobrnjac1@outlook.com (CA)
[2] BSc Saša Savić, University of Banja Luka, Faculty of Mechanical Engineering, Banja Luka, Bosnia and Herzegovina, ssavke994@gmail.com
[3] MSc Nemanja Koruga, University of Banja Luka, Faculty of Mechanical Engineering, Banja Luka, Bosnia and Herzegovina, nemanjakoruga@yahoo.com
[4] PhD Mirko Dobrnjac, University of Banja Luka, Faculty of Mechanical Engineering, Banja Luka, Bosnia and Herzegovina, mirko.dobrnjac@mf.unibl.org
[5] PhD Izet Alić, University of Tuzla, Faculty of Mechanical Engineering, Banja Luka, Bosnia and Herzegovina, izet.alic@untz.ba

- Air-to-water heat pumps
- Water-to-water heat pumps
- Ground-to-water heat pumps

2 GEOTSOL SOFTWARE

GeoTSOL software is a professional tool for planning and designing heat pump systems. With it, we can select different types and components of the system that go with the heat pump, calculate the required energy and see how much energy savings we have achieved based on the value of the seasonal performance factor. In the GeoTSOL software, it is also possible to select different heat sources (air, water or earth) and heat pump modes (monovalent, monoenergetic and bivalent) for a given location. In this paper, three types of heat pumps are discussed, which are shown for a residential building (family house) that has 193 m² of heated space, and the heat losses for the total building are approximately 11 143 W or 11,143 kW. Based on the calculation of the required heating elements, it was found that the total power of the installed heating elements (radiators, underfloor heating and pipe registers) in the mentioned building is 13.77 kW. [3] It is important to distinguish the SPF for the heat pump and the SPF for the entire system. A heat pump SPF includes only the heat pump equipment (ie, compressor and controls), while the entire system includes a ground loop, supplementary heating, space heating and heating of domestic hot water. [4]

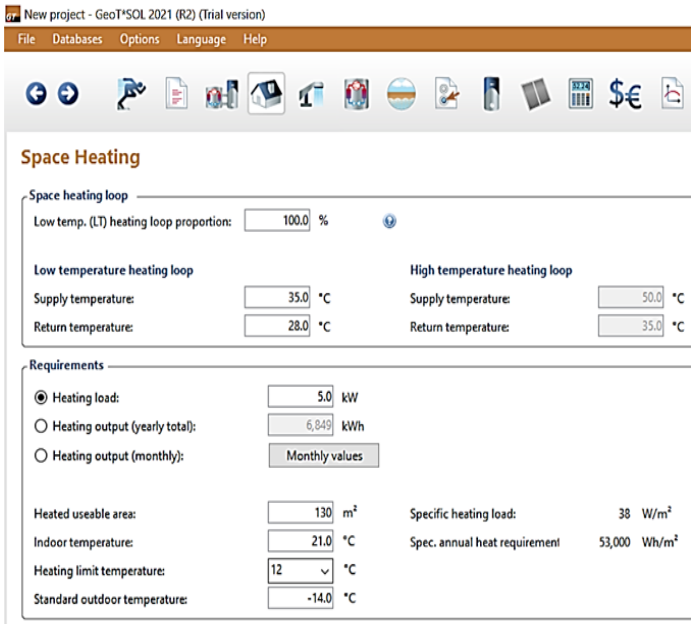

Figure 1. *Display of work in GeoTSOL software*

2.1 Air-to-water heat pump in GeoTSOL

The simulation of the air-to-water heat pump for the mentioned object was done so that the Viessmann heat pump was chosen, which has an installed power of

14.5 kW. The heat consumption of domestic hot water was also taken into the simulation. [5]

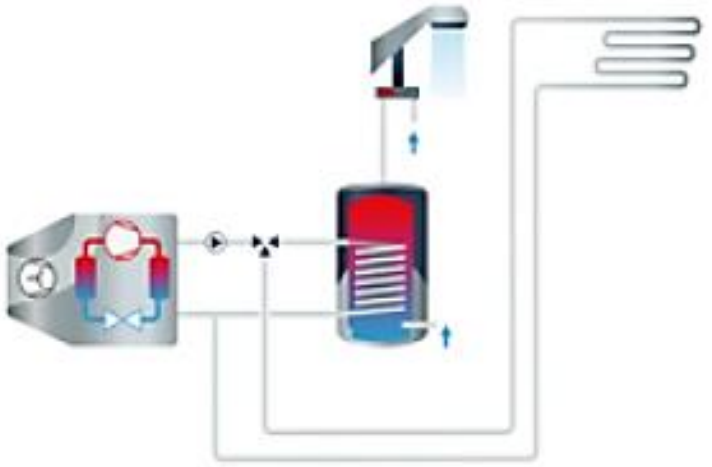

Figure 2. *Air-to-water heat pump system for space heating and DHW*

In the further part of the performance analysis for this type of heat pump, the data obtained by simulation in the GeoTSOL software will be presented.

Table 1. *Simulation results for the specified air-to-water heat pump in GeoTSOL software*

Used energy/yr.	
Energy required for heating the building	17,895 kW
Energy required for domestic hot water	7,225 kW
Generated energy/yr	
Energy supplied by a heat pump	25,249 kW
Factors of seasonal thermal performance	
Seasonal performance factor of the heat pump SPF	3.4
Seasonal performance factor of the entire heat pump system SPF	3.4
Electricity consumption/yr.	7,436 kW
Tank losses (boiler)/yr.	326 kW
Primary energy saving	20,342 kW
Reduction of CO_2 emissions	5,035 kg

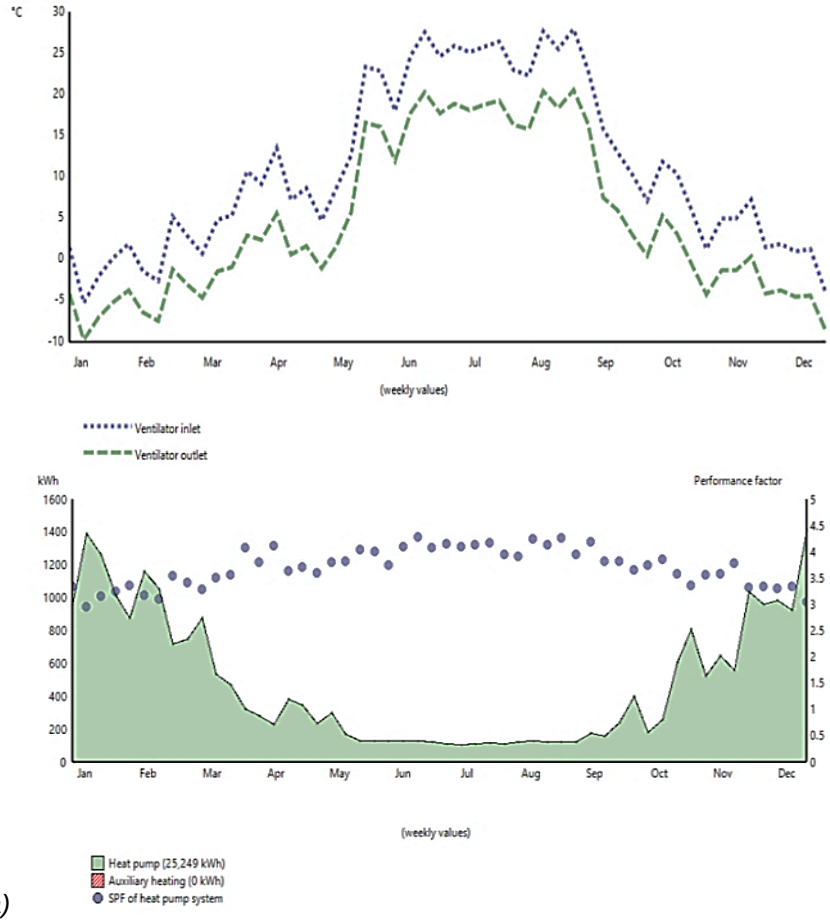

a)

b)

Figure 3. *a) Temperature diagram for case 1; b) Energy diagram and change of SPF factor during the year for case 1*

2.2 Water-to-water heat pump in GeoTSOL software

The simulation of the water-to-water heat pump for the mentioned facility was done so that a Vaillant heat pump with an installed power of 14 kW was chosen. The simulation of hot water consumption was also done according to the choice of the tank produced by the company Vaillant.

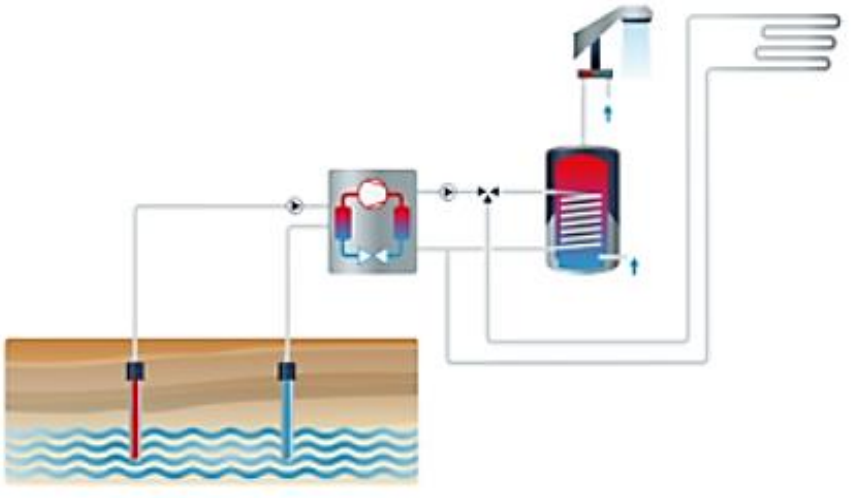

Figure 4. *Water-to-water heat pump system for space heating and DHW*

In the further part of the work analysis for this type of heat pump, the data obtained by simulation in the GeoTSOL software will be presented.

Table 2. Simulation results for the specified water-to-water heat pump in GeoTSOL software

Used energy/yr.	
Energy required for heating the building	17,531 kW
Energy required for domestic hot water	7,229 kW
Generated energy/yr	
Energy supplied by a heat pump	25,250 kW
Factors of seasonal thermal performance	
Seasonal performance factor of the heat pump SPF	5.0
Seasonal performance factor of the entire heat pump system SPF	4.7
Electricity consumption/yr.	5,040 kW
Tank losses (boiler)/yr.	683 kW
Primary energy saving	25,450 kW
Reduction of CO_2 emissions	6,299 kg

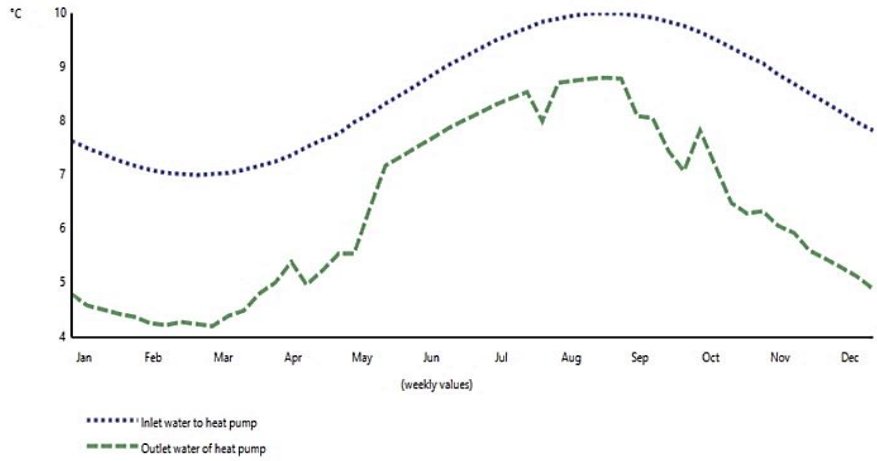

a)

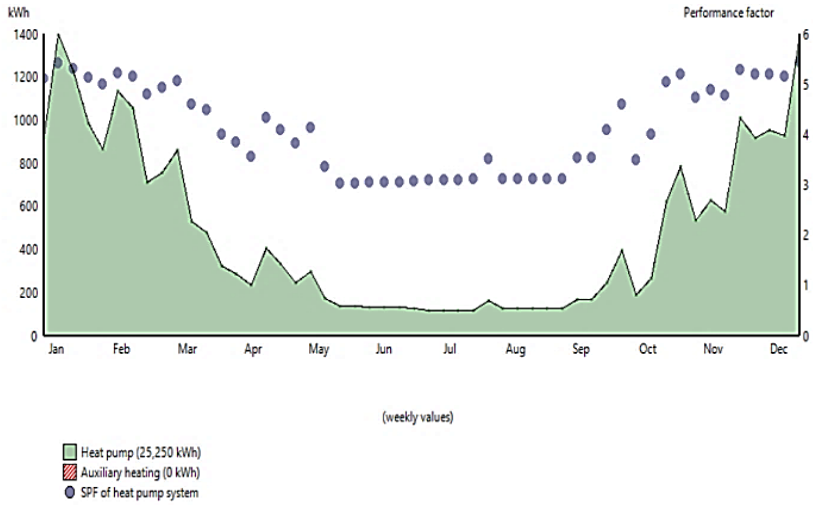

b)

Figure 6. *a) Temperature diagram for case 2 b) Energy diagram and change of SPF factor during the year for case 2*

2.3 Ground-to-water heat pump in GeoTSOL software

As for the ground-water heat pump, the considered case of its application for heating a residential building (family house) refers to the application of horizontal collectors through which the heat from the ground is transferred to the heat pump. The Vaillant heat pump with a power of 14 kW was chosen here. The simulation of the consumption of domestic hot water was carried out in this case as well as in the previous two cases of heat pumps that use air and water as a heat source.

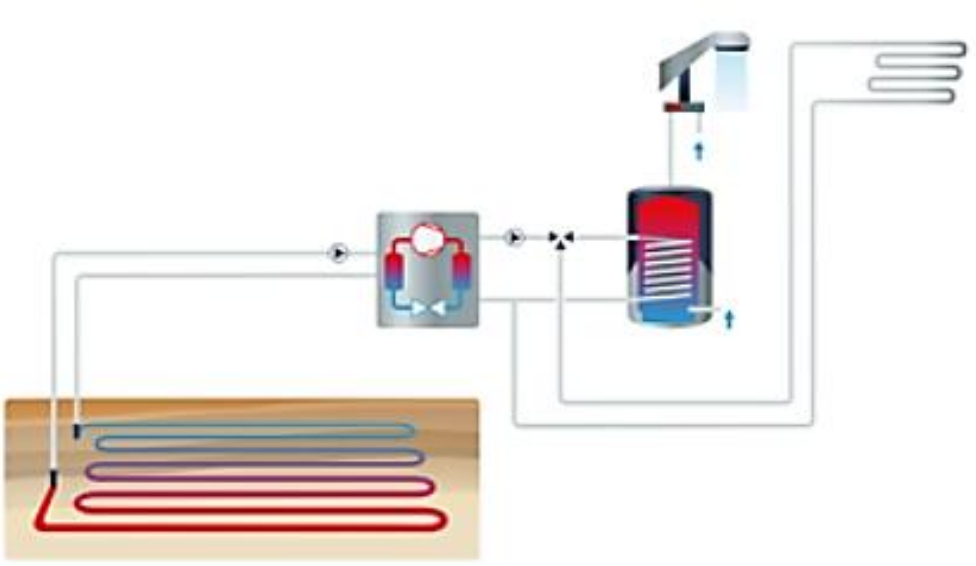

Figure 7. *Ground-to-water heat pump system (horizontal collectors) for space heating and DHW*

In the further part of the work analysis for this type of heat pump, the data obtained by simulation in the GeoTSOL software will be explained.

Table 3. *Simulation results for the specified ground-to-water heat pump in GeoTSOL software*

Used energy/yr.	
Energy required for heating the building	17,490 kW
Energy required for domestic hot water	7,155 kW
Generated energy/yr	
Energy supplied by a heat pump	25,126 kW
Factors of seasonal thermal performance	
Seasonal performance factor of the heat pump SPF	4.5
Seasonal performance factor of the entire heat pump system SPF	4.3
Electricity consumption/yr.	5,571 kW
Tank losses (boiler)/yr.	673 kW
Primary energy saving	24,003 kW
Reduction of CO_2 emissions	5,941 kg

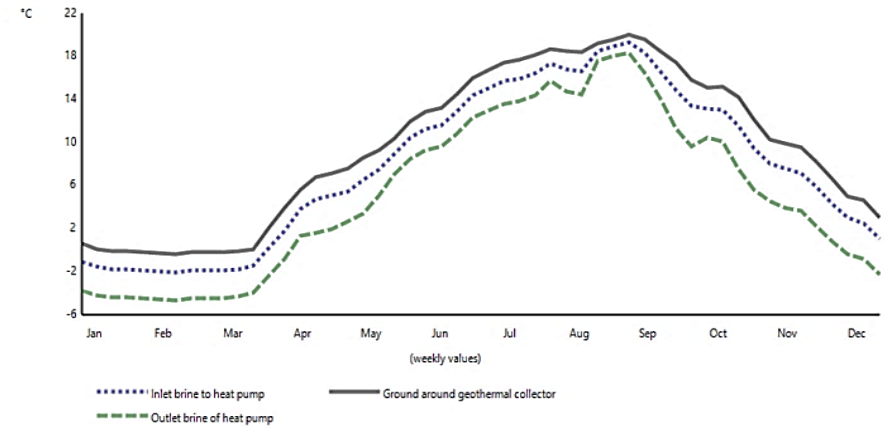

a)

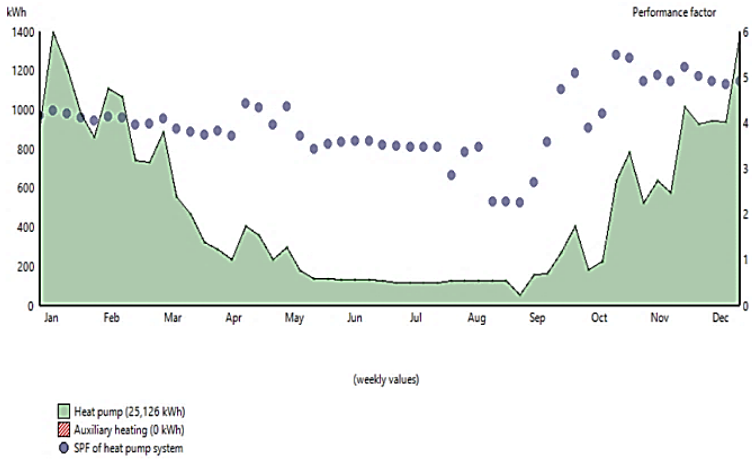

b)

Figure 8. *a) Temperature diagram for case 3 b) Energy diagram and change of SPF factor during the year for case 3*

3 CONCLUSION

Heat pumps represent a revolutionary solution in the field of renewable energy sources used for heating because they use natural resources (their heat energy) to meet the energy (heat) needs of end users. Based on the simulation carried out in the GeoTSOL software, it can be concluded that the best solution for the mentioned building (family house) would be a water-to-water heat pump, because it has the highest seasonal performance factor. This means that by using this type of heat pump, the greatest energy savings would be obtained, and with it, you would have the lowest consumption of electricity. Also with this type of heat pump we have the biggest annual reduction in CO_2 emissions.

REFERENCES

[1] Guzović, Z.: *Geotermalna energija i dizalice topline*, Fakultet strojarstva i brodogradnje, Sveučilište u Zagrebu.
[2] Dobrnjac, M. (2008) *Termodinamika*, Univerzitet u Bihaću – Tehnički fakultet, Bihać.
[3] Savić, Š*. Optimizacija grijanja porodične kuće sa toplotnom pumpom*, Mašinski fakultet Banja Luka, Diplomski rad, Banja Luka.
[4] GeoTSOL softver za proračun toplotnih pumpi
[5] Gutović D. (2019) P*rimjena toplotnih pumpi kod objekata različite energetske efikasnosti,* Fakultet tehničnih nauka, Novi Sad.

COMETa 2022
6th INTERNATIONAL SCIENTIFIC CONFERENCE
17th - 19th November 2022
Jahorina, B&H, Republic of Srpska
University of East Sarajevo
Faculty of Mechanical Engineering
Conference on Mechanical Engineering Technologies and Applications

UPOREDNA ANALIZA ISPLATIVOSTI ENERGENATA ZA GRIJANJE PORODIČNIH KUĆA I STANOVA

Aleksandar Luketa[1], Jelena Perišić[2], Srđan Vasković[3], Gojko Krunić[4]

Rezime: Potrebe za grijanjem u zimskom periodu, u mjestima gdje su temperature veoma niske su velike. Zbog toga je neophodno da se izabere što bolji način grijanja, sa što ekonomičnijim energentom. Veliki problem u svijetu danas predstavlja nedostatak pojedinih energenata, velike krize, kao i cijena energenata. Tema ovoga rada bazirana je na upoređivanju energenata na osnovu njihove isplativosti. Za proračun isplativosti uzet je primjer jedne porodične kuće. Za tu porodićnu kuću urađen je proračun gubitaka, te je za upoređivanje energenata uzeta: struja, pelet, gas i ugalj. Još jedna tema ovoga rada je upoređivanje isplativosti grijanja na 3 vrste energenata u zgradama. Upoređivanje je vršeno u zgradama starije i novije izgradnje na području Istočnog Sarajeva. Na bazi svega pomenutog urađene su komparativne analize svih slučajeva koje su pokazale međusobnu ujednačenost između cijena energenata, što ubrzo neće biti tako.

Ključne riječi: komparativna analiza, utrošak topote, energenti, isplativost.

COMPARATIVE ANALYSIS OF HEATING CONSUMPTION OF FAMILY HOUSES AND APARTMENTS IN VIEW OF DIFFERENT ENERGY SOURCES

Abstract: The energy need for heating in the winter period, in places where the temperatures are very low, is very high. That is why it is necessary to choose the best possible heating method, with the most economical energy source. A big problem in the world today is the lack of certain energy sources, major crises, as well as the price of energy sources. The topic of this paper is based on the comparison of energy sources based on their profitability in economic term. An example of a single-family house was taken to calculate profitability. A loss calculation was made for that family house, and the following energy sources were used to compare: electricity, pellets, gas and coal. Another topic of this paper is comparing the profitability of heating with 3

[1] Aleksandar Luketa, MSc student, Mašinski fakultet, Istočno Sarajevo, BiH, aleksandar.luketa96@gmail.com (CA)
[2] Jelena Perišić, MSc student, Mašinski fakultet, Istočno Sarajevo, BiH, jelenaperisic997@gmail.com
[3] Prof. dr, Srđan Vasković, van. prof, Mašinski fakultet, Istočno Sarajevo, BiH, srdjan.vaskovic@ues.rs.ba
[4] Dr Gojko Krunić, docent,Fakuletet za proizvodnju i menadžment, Trebinje, BiH, gojko.krunic@ues.rs.ba

types of energy sources in buildings. The comparison was made in buildings of older and newer construction in the area of East Sarajevo. On the basis of everything mentioned, comparative analysis of all cases are presented, which showed mutual uniformity between energy prices, which will not be the case very soon.

Key words: comparative analysis, heating consumption, energy sources, cost effectiveness.

1 UVOD

Globalna energetska kriza čiji smo svjedoci, pokazala je ranjivost razvoja savremenog društva u sektoru energetike i snabdijevanja energijom. Uzimajuću u obzir savremene trendove koji su promovisali zelenu i obnovljivu energiju, stvari su izgledale vrlo pozitivno u smislu napretka u njihovom korišćenju. Međutim, kada se desilo smanjenje isporuka ruskog gasa kojim su se mahom zadovoljavale potrebe evropskih zemalja, ispostavilo se da to baš i nije tako i da je sve bilo uglavnom vezano za profit i ucjenjivanje zemalja u tranziciji megalomanskom politikom smanjenja štetnih emisija i njihovom trgovinom kroz različite tržišne mehanizme. Ovaj rad neće se baviti globalnim energetskim prilikama već će napraviti komprativnu analizu troškova za dvije opcije i to za grijanje porodičnih kuća i stanova na teritoriji opštine Istočno Sarajevo. Analiza je rađena na osnovu stvarnih evidencija o utrošku različitih tipova energenata korišćenih za zagrijavanje objekata.

2 PRORAČUN GODIŠNJE POTROŠNJE TOPLOTE ZA PORODIČNU KUĆU

Proračun gubitaka toplote je vršen prema Njemačkom DIN 4701 iz 1959 [1]. Porodična kuća za koju se vrši proračun grijanja, kao i upoređivanje najekonomičnijeg energenta sastoji se od prizemlja i jednog sprata i od sledećih prostorija: dnevnog boravka, pet spavaćih soba, dva hodnika i tri kupatila. Površina objekta je 148.5 m^2.

Proračunom su dobijeni toplotni gubici od 15648.18 W, a instalisani kapacitet grejnih tijela je 17162 W. Radijatori u objektu su tipa ORION 600/95, jednocijevna razvodna mreža. Nakon proračuna gubitaka izvršen je proračun pada pritiska u instalaciji i iznosi 16293 Pa.

Proračun godišnje potrošnje toplote uz pomoć metode stepen dan dat je na osnovu sledećeg obrazca:

$$Q_{god} = \frac{24 \cdot Q_{gub} \cdot e \cdot y \cdot SD}{\left(t_u - t_s\right)} \left[Wh / god\right], \tag{1}$$

pri čemu je:

- Q_{god} [Wh/god] – godišnja potrebna količina toplote,
- $e = e_t \cdot e_b = 0.9 \cdot 1 = 0.9$ – *korekcioni faktor koji uzima u obzir prekid u zagrijavanju,*
- $y = 0.6$ – *korekcioni faktor koji uzima u obzir jednovremenost svih nepovoljnih uticaja,*
- $SD = 3077$ – vrijednost stepen – dana za Sarajevo,
- $t_u = 20\ ^{o}\mathrm{C}$ – unutrašnja projektna temperatura,
- $t_u = -18\ ^{o}\mathrm{C}$ – spoljnja projektna temperatura [1].

$$Q_{god} = \frac{24 \cdot 15648 \cdot 0.9 \cdot 0.6 \cdot 3077}{\left(20 - \left(-18\right)\right)} = 16421496.58 \left[Wh / god\right].$$

Pelet kao gorivo je jako zanimljiva kategorija, međutim sa turbulencijama na tržištu cijena energenata doživio je veliko poskupljenje što mu je dovelo pod upitnik konkurentnost u upotrebi kod nas ali i šire. Karakteristike drvnih peleta, kako navodi Glavonjić [2], zavise od više faktora među kojima se posebno izdvajaju vrsta drveta, oprema za proizvodnju, vlažnost i druge karakteristike polazne sirovine. Osnovne karakteristike drvnih peleta koje se najčešće mogu naći u ponudi na tržištu su sledeće:

- Energetska vrijednost: 4.3 - 4.9 kWh/kg [3],
- Zapreminska težina: 500 - 700 kg/m3 u zavisnosti od drvne vrste koja je korišćena za njihovu proizvodnju,
- Sadržaj vlage: 8% - 10%,
- Saržaj pepela: 0.5% - 6%,
- Prečnik: 6mm - 12mm,
- Dužina: 10mm - 30mm.

Prema tome orjentaciona potoršnja goriva, primjer pelet:

$$B = \frac{3.6 \cdot Q_{god}}{\eta \cdot H \cdot d} = \frac{3.6 \cdot 16421496.58}{0.75 \cdot 18000} = 4379.06 \text{ kg/god [1].}$$

3 UPOREĐIVANJE POTROŠNJE ENERGENATA ZA ZAGRIJAVANJE PORODIČNE KUĆE U TOKU SEZONE GRIJANJA

3.1 Pelet

Na osnovu proračuna gubitaka toplote i dobijene vrijednosti 15648.18 W, i procjenom odnosno deklaraciji proizvođača peleta dobije se sledeći proračun potrošnje peleta po kW.

U ne baš jakoj zimi potrebno je 50 W za grijanje 1m^2 za 1 sat, dok u uslovima jake zime potrebno je otprilike 60 W za grijanje 1 m^2 za 1 sat [1]. Za ovaj rad uzimamo period grijanja od 12 h. Pa nam je za taj period potrebno 12 h* 60 W=720 W.

Količina peleta koji treba da sagori za proizvodnju toplote za 1 m^2 dnevno biti će:

- 0.72 kW / 4.25 kW / kg = 0.169 kg,
- po danu: 0.169 kg · 148.5 m2 = 25.09 kg,
- mjesečno: 25.09 kg · 30 dana= 752.7 kg.

Na osnovu proračuna dobili smo da je za grijanje ovoga objekta po danu potrebno približno 25.09 kg peleta, dok je za jedan mjesec od 30 dana potrebno blizu 752.7 kg peleta. Pa tako za jednu grejnu sezonu koja traje otprilike 6 mjeseci (15.10.-15.04.) potrebno je 6 · 752.7 = 4516.2 kg peleta.

Po cijenam peleta u avgusta mjeseca ove godine od 480 KM/t bez pdv-a, sa pdv-om 561.6 KM/t. [4].

Za grijanje ove kuće potrebno je 561.6 KM/t · 4.51 t = 2536.29 KM.

3.2. Električna energija

Za grijanje pomoću električne energije biramo kotao od 18 kW, za proračun potrošnje uzimamo da kotao radi prvih sat vremena punim kapacitetom od 18 kW, dok

za narednih 11 h uzimamo da kotao radi sa 30% kapaciteta [5].

Količina električne energije koja je potrebna za zagrijavanje kuće:

- 18 kW · 1 h= 18 kWh,
- 18 kW · 0.3 · 11 h = 59.4 kWh,
- po danu: 18 + 59.4 = 77.4 kWh,
- mjesečno: 77.4 kWh · 30 dana= 2322 kWh.

Na osnovu proračuna dobili smo da je za grijanje ovoga objekta po danu potrebno približno 77.4 kWh, dok je za jedan mjesec od 30 dana potrebno blizu 2322 kWh. Pa tako za jednu grejnu sezonu koja traje otprilike 6 mjeseci (15.10.-15.04.) potrebno je 6 · 2322 = 13932 kWh.

Po cijenama električne energije u zimskom period od 0.169 KM/kWh [6], za grijanje ove kuće potrebno je:

- 13932 · 0.169 = 2354.50 KM.

3.3. Grijanje na ugalj

Za grijanje pomoću uglja biramo kotao od 18 kW, za proračun potrošnje uzimamo da kotao radi prvih sat vremena sa maksimalnim kapacitetom, dok za narednih 11 h uzimamo da kotao radi sa 30 % kapaciteta [5].

Količina uglja koja je potrebna za zagrijavanje kuće:

- 1 kWh= 0.25 kg uglja.

Za prvi sat rada sa maksimalnim kapacitetom potrošnja iznosi:

- 18 kW · 1 h= 18 kWh,
- 18 kW · 0.25 kg = 4.5 kg.

Za 11 h rada sa kapacitetom 30 %:

- 18 kW · 0.3 · 11 h= 59. 4 kW,
- 59.4 · 0.25 = 14.85 kg,
- po danu: 4.5 + 14.85 = 19.35 kg,
- mjesečno: 19.35 kg · 30 dana= 580.5 kg.

Za sezonu grijanja koja traje otprilike 6 mjeseci (15.10.-15.04.) potrebno je:

- 6 · 580.5= 3483 kg=3.48 t uglja.

Za grijanje ove kuće na ugalj, po cijeni uglja od 210 KM/t + pdv, potrebno je [7]:

- 245 .7 KM/t · 3.48 t= 855.036 KM.

3.4. Grijanje na prirodni gas

Za grijanje objekta pomoću prirodnog gasa biramo kotao od 28 kW, za proračun potrošnje uzimamo da kotao radi prvih sat vremena sa maksimalnim kapacitetom, dok za narednih 11 h uzimamo da kotao radi sa 30 % kapaciteta [5].

Količina uglja koja je potrebna za zagrijavanje kuće:

- 1 kWh= 0.25 kg uglja.

Za prvi sat rada sa maksimalnim kapacitetom potrošnja iznosi:

- 28 kW · 1 h= 28 kWh,

- 28 kWh= 2.8 m^3.

Za 11 h rada sa kapacitetom 30 %:

- 28 kW · 0.3 · 11 h= 92.4 kW,
- 92.4 kW= 9.24 m^3,
- po danu: 2.8 + 9.24 = 12.04 m^3,
- mjesečno: 12.04 m3 · 30 dana= 361.2 m^3.

Za sezonu grijanja koja traje otprilike 6 mjeseci (15.10.-15.04.) potrebno je:

- 6 · 361.2 m^3= 2167.2 m^3.

Za grijanje ove kuće na prirodni gas,po cijeni gasa od 1.35 KM/m^3, potrebno je:

- 2167.2 m^3 ·1.35 KM/ m^3= 2925.72 KM.

3.5. Tabela potrošnje energenata

Upoređivanja cijena energenata predstavljena su u tabeli 1. Prikazane cijene sus sa uračunatim pdv-om.

Tabela 1. *Upoređivanja cijena energenata u toku grejne sezone*

Naziv energenta	Cijena grijanja [KM]
Pelet	2536.29
Električna energija	2354.50
Ugalj	855.03
Prirodni gas	2925.72

Na osnovu proračuna potrošnje dobili smo tabelu 1. prema kojoj najisplativiji energent je ugalj, a najskuplji prirodni gas.

4 PREDNOSTI I NEDOSTACI ENERGENATA OBUHVAĆENIH U RADU

U tablama 2. - 5. navedene su neke od prednosti i nedostataka korišćenih energenata u sistemima grijanja.

Tabela 2. *Prednosti i nedostaci peleta u sistemima grijanja [1]*

Prednosti	Nedostaci
Čisto gorivo	buka
Rijetko loženje	komfor
Ugljenična neutralnost	zavisno od električne energije
Visoka kalorijska moć	komplikovano održavanje

Tabela 3. *Prednosti i nedostaci električne energije u sistemima grijanja [1]*

Prednosti	Nedostaci
Energetski učinkovito grijanje	Instalacijski trošak
Jednostavno grijanje	Vrijeme istalacije
Sigurnost i udobnost	Grijanje treba prilagoditi loklanim uslovima

Tabela 4. *Prednosti i nedostaci uglja u sistemima grijanja [1]*

Prednosti	**Nedostaci**
Pouzdanost	Oslobađa otrovne supstance
Dostupnost	Emitovanje gasova staklene bašte
Bezbijednost	Problem skladištenja

Tabela 5. *Prednosti i nedostaci prirodnog gasa u sistemima grijanja [1]*

Prednosti	**Nedostaci**
Mali troškovi održavanja	Toksičan
Jednostavan za korišćenje	Zapaljiv
Ekološki prihvatljiv	Neobnovljiv izvor

5 PREGLED ISPLATIVOSTI POTROŠNJE ENERGENATA U STANOVIMA

5.1. Stanovi novije gradnje

Za proračun potrošnje i isplativosti energenata uzeti su stanovi novije gradnje. Od energenata su uzeti struja, toplane i prirodni gas. U tabeli 6. je prikazan odnos utošenih količina i cijene grijanja pomoću tri energenta u stanovima novije gradnje.

Tabela 6. *Odnos utošenih količina i cijene grijanja pomoću tri energenta u stanovima novije gradnje [7].*

АНАЛИЗА ТРОШКОВА ГРИЈАЊА СТАНОВА М.М.Капора 2			Период 2021		Властити системи етажног грijања са гасним комбинованим загрijачем воде			Топлане И.Сарајево		Властити системи етажног грijања са електроблоковима		
					Годишњи трошак		Цијена грijања	Цијена грijања	Годишњи трошак грijања	Годишњи трошак		Цијена грijања
Ред. Бр	Адреса стана	Површина	Потрошња природног гас	Утрошена Енергија	Укупно	Грijање				Укупно	Грijање	
		[m2]	[Sm3]	[kWh]	[KM]	[KM]	[KM/m2]	[KM/m2]	[KM]	[KM]	[KM]	[KM/m2]
1	**2**	**3**	**4**	**5**	**6**	**7**	**8**	**9**	**10**	**11**	**12**	**13**
1	Стан бр. 4	57.00	438	3650	438	591	0.86	1.5	1026	617	617	0.902
3	Стан бр. 5	57.00	591	4925	591	798	1.17	1.5	1026	832	832	1.217
5	Стан бр. 29	37.00	404	3367	404	545	1.23	1.5	666	569	569	1.282
6	Стан бр. 49	57.00	533	4442	533	720	1.05	1.5	1026	751	751	1.098
7	Стан бр. 37	37.00	421	3509	421	568	1.28	1.5	666	593	593	1.335
8	∑	49.00				644	1.12		882		672	1.167
9												
10												
			8.334									
	domaćinstva cijena struje		0.169	KM/kwh								
	domaćinstva cijena gasa		1.35	KM/Sm^3								
	Toplane cijena grijanja		1.5	KM/m2								

Na osnovu gore navedenog proračuna možemo viditi da je u stanovima novije gradnje najisplativiji energent prirodni gas. Prosjek kvadrature izabranih stanova je 49 m^2. Prosjek cijena energenata prikazan je u tabeli 7. Prosjek cijena grijanja u stanovima novije gradnje predstavljen je u tabeli 7. Prikazane cijene sus sa uračunatim pdv-om.

Tabela 7. *Prosjek cijena grijanja u stanovima novije gradnje*

Naziv energenta	Prosjek cijena grijanja [KM]
Prirodni gas	644
Toplane	882
Električna energija	672

5.2. Stanovi starije gradnja

Za proračun potrošnje i isplativosti energenata uzeti su i stanovi starije gradnje. Od energenata su uzeti struja, toplane i prirodni gas. U tabeli 8. je prikazan odnos utošenih količina i cijene grijanja 3 energenta u stanovima starije gradnje.

Tabela 8. *Odnos utošenih količina i cijene grijanja pomoću tri energenta u stanovima starije gradnje [7].*

АНАЛИЗА ТРОШКОВА ГРИЈАЊА СТАНОВА Spasodanska br. 25 "B"			Период 2021		Властити системи етажног гријања са гасним комбинованим загрijачем воде			Топлане И.Сарајево		Властити системи етажног гријања са електроблоковима		
					Годишњи трошак		Цијена гријања			Годишњи трошак		Цијена гријања
Ред. Бр	Адреса стана	Површина	Потрошња природног гас	Утрошена Енергија	Укупно	Грijање		Цијена грijања	Годишњи трошак грijања	Укупно	Грijање	
		[m2]	[Sm3]	[kWh]	[KM]	[KM]	[KM/m2]	[KM/m2]	[KM]	[KM]	[KM]	[KM/m2]
1	**2**	**3**	**4**	**5**	**6**	**8**	**10**	**11**	**12**	**13**	**15**	**17**
1	Стан бр. 1	58.10	845	7042	542	1141	1.64	1.5	1046	1190	1190	1.707
2	Стан бр. 10	64.06	764	6367	1031	1031	1.34	1.5	1153	1076	1076	1.400
3	Стан бр. 12	77.38	1019	8492	1376	1376	1.48	1.5	1393	1435	1435	1.546
4	Стан бр. 64.04	64.06	905	7542	1222	1222	1.59	1.5	1153	1275	1275	1.658
5	Σ	65.90				1192	1.51		1186		1244	1.578
6												
7												
			8.334									
	domaćinstva cijena struje		0.169	KM/kwh								
	domaćinstva cijena gasa		1.35	KM/Sm3								
	Toplane cijena grijanja		1.5	KM/m2								

Na osnovu ovoga proračuna možemo da vidimo da u stanovima starije gradnje kao najisplativiji energent je grijanje na gradske toplane tj. na mazut. Prosjek kvadrature izabranih stanova je 65.9 m^2. Prosjek cijene energenata u stanovima starije gradnje prikazan je u tabeli 9. Prikazane cijene sus sa uračunatim pdv-om.

Tabela 9. *Prosjek cijena grijanja u stanovima starije gradnje*

Naziv energenta	Cijena grijanja [KM]
Prirodni gas	1192
Toplane	1186
Električna energija	1244

6 ZAKLJUČAK

U ovome radu izvršen je proračun gubitaka toplote za jednu porodičnu kuću. Na osnovu tih gubitaka izabrani su kotlovi za različite tipove energenata. Za poređenje potrošnje i cijene energenata uzeti su u obzir četiri vrste energenata: pelet, električna

energija, ugalj i prirodni gas. Za kuću površine 148.5 m2 kao najisplativiji energent se pokazao ugalj, dok najskuplji energent je prirodni gas.

Takođe u ovome radu urađeno je i poređenje isplativosti energenata u stanovima novije i stanovima starije gradnje. Uzet je prosjek stanova na različitim vertikalama i uzet je prosjek površina. U zgradama novije gradnje najisplativiji energent je prirodni gas dok je najskuplje grijanje na toplane. U zgradma starije gradnje najisplativiji energent je mazut odnosno grijanje na toplane, dok je najskuplje grijanje na električnu energiju.

Za porodične kuće naisplativiji energent je definitivno neko čvrsto gorivo, zbog velike površine vrlo je neispativo grijati na struju i na prirodni gas, dok za stanove najisplativiji energent je prirodni gas (trenutno mu je visoka cijena zbog krize).

Uzimajući u obzir energetsko siromaštvo ove države i generalno jako nizak standard života koji je još više poljuljan sa globalnom energetskom i ekonomskom krizom, ono od čega treba najviše strahovati stanovništvo ove države jeste poskupljenje električene energije koje je neminovno po svim pokazateljima na tržištu energije. Dosadašnja cijena elektične energije bila je socijalna kategorija i rušila je sve ekonomske računice ostalih energenata. Vrlo lako, tj uskoro, električna energija na ovom prostoru će postati luksuz, ne zato što to želi politika, već zato što mora električna energija poskupiti da bi bila ekonomski održiva na tržištu energije.

7 LITERATURA

[1] Todorović, B. (2005). Projektovanje postrojenja za centralno grijanje, Mašinski fakultet, Beograd.
[2] Glavonjić, B. (2011): Drvna goriva: vrste, karakteristike i pogodnosti za grejanje, Priručnik, Podgorica, str 1-61. Dostupno na: (file:///C:/Users/Korisnik/Downloads/Drvna%20goriva.pdf)
[3] Stelte, W. (2011): Fuel Pellets from Biomass - Processing, Bonding, Raw Materials, Risø-PhD-90 (EN), 1–47.
[4] https://faktor.ba/vijest/hoce-li-tona-peleta-u-bih-biti-1000-km-koliko-sada-kosta-u-hrvatskoj-bh-firmama-stizu-bezobrazne-ponude-iz-eu/171235
[5] Smjernice za upravljanje i održavanje termo-energetskih sistema u javnim objektima, Fond za zaštitu okoliša Federacije BiH, Fond za zaštitu životne sredine i energetsku efikasnost Republike Srpske, UNDP, 2014.
[6] https://elektrobijeljina.com/kalkulator/projekat/pripravnicki.html
[7] https://sarajevogas.com/

COMETa 2022
6th INTERNATIONAL SCIENTIFIC CONFERENCE
17th - 19th December 2022
Jahorina, B&H, Republic of Srpska
University of East Sarajevo
Faculty of Mechanical Engineering
Conference on Mechanical Engineering Technologies and Applications

PERSPECTIVES FOR ENERGY GENERATION IN SOUTHEAST EUROPE USING CLEAN COAL TECHNOLOGIES

Kristina Paunova[1], Vlatko Cingoski[2]

Abstract: Fossil fuels, especially coal, due to their unique composition and characteristics, are indispensable sources of electricity generation, especially in the Southeast European countries, North Macedonia, Serbia,and Bosnia and Herzegovina, among others. Strict environmental regulations, together with the tendency to continue with coal utilization,the long period needed for energy transition are the main reasons for the development of various concepts for clean use of coal. This paper addresses some technologies for clean coal utilization, a detailed description of the principle of operation and how they contribute to the environment and reduce pollution. The traditional process of burning coal in powder coal power plants is used as a comparison model and the new energy generation technologies using supercritical and ultra-supercritical power plants are presented. A description of the gasification process, integrated gasification in a combined cycle, and the types of gasifiers used are also given. Because each of these processes is accompanied by carbon dioxide emissions, the procedure for capturing and storing carbon in the long run is also considered.

Keywords: clean coal technologies, coal gasification, carbon capture.

1 INTRODUCTION

Energy needs are currently mostly satisfied by fossil fuels such as oil, coal, and natural gas. Fossil fuels belong to the group of non-renewable energy sources, thus their reserves are limited, so it's necessary to consider the possibility of their depletion in the future. Coal is the most widespread fossil fuel in the world. Around 27% of the needs for primary energy and 37% for electricity are obtained based on coal [1]. Some countries that heavily rely on coal, among other energy sources, for energy generation such as Southeast European countries, where most of the power plants are old and extremely polluting. Also, this region is home to 7 of the 10 most polluting power plants

[1] Student, Kristina Paunova, Faculty of Electrical Engineering, University "Goce Delcev"- Shtip, RN Macedonia, kristina.20609@student.ugd.edu.mk
[2] Prof. D-r Vlatko Chingoski, Faculty of Electrical Engineering, University "Goce Delcev"- Shtip, RN Macedonia, vlatko.cingoski@ugd.edu.mk

based on coal in Europe. On an average level, power plants situated in the Western Balkans (Albania, Bosnia and Herzegovina, Montenegro, Kosovo, North Macedonia, Serbia) emit 20 times more sulfur dioxide than European Union power plants. In 2016, 16 coal-fired power plants in Western Balkans produced as much pollution as the 250 active power plants in the European Union [2]. To ensure a secure energy future, researches are being done in the field of theoretical possibilities and the real rational application of energy sources. These researches go in two directions: extending the life of non-renewable energy sources and organization of energy sources and technological procedures that have minimal impact on pollution. This is when clean coal technologies come into play. Clean technologies are designed to improve the efficiency and environmental acceptability of coal throughout its life cycle stages. In the current scenario of accelerated global warming and the global need for energy security, these technologies are of great importance. In what follows some of these technologies that can be implemented in Southeast European power plants will be presented.

2 PULVERIZED COAL COMBUSTION

Combustion of pulverized coal is the most commonly used process to generate electrical energy. Approximately 97% of the coal-fired capacity in the world is produced by pulverized coal power plants [3]. This technology is not considered clean, unless it's combined with some advanced modern technologies. In these power plants, pulverized coal is placed in a boiler with air where is burned, releasing the chemical energy of the coal into heat. Then, the heat is used to generate steam from the water that flows through the tubes placed in the walls of the boiler. Next, the high-pressure and high-temperature steam is transmitted to the steam turbine, which is connected to an electrical generator for electricity production. After passing to the turbine, the steam is cooled and condensed back into a liquid and then it returns to the boiler's tubes to start the cycle over again. A pulverized coal system can burn a variety of coal types, but systems made to burn various types of coal are more sophisticated and expensive [4]. This process is presented in Figure 1.

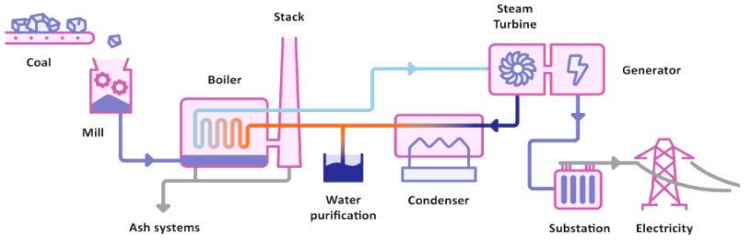

Figure 1. *Pulverized coal power plant [5]*

3 SUPERCRITICAL AND ULTRA-SUPERCRITICAL POWER PLANTS

Supercritical power plants are a new generation of coal-fied power plants. The difference between supercritical power plants and traditional power plants is that in supercritical plants the water flowing through them operates as a supercritical fluid, meaning it's neither a liquid nor a gas. This happens when water reaches its critical

point at high temperatures and high pressures, especially at 22 MPa and 374ºC. As the liquid approaches its critical point, its heat of vaporization begins to decrease until it reaches zero. This means that the amount of energy required to convert water to steam decreases over time, until the transition to the vapor phase is instantaneous. This reduces the amount of heat transfer to water that is usually required in conventional coal-fired power plants, requiring less coal to heat the same amount of water. This significantly improves the plant's thermal efficiency. These plants are the gold standard for new coal-fired plants because their efficiency can reach around 44%, compared to older coal-fired plants, which operate at 33%. Also, higher temperature and pressure coal-fired power plants, known as *ultra-supercritical*, are being studied and developed, with the potential to achieve efficiency of nearly 50%. Higher efficiency results in lower greenhouse gas emissions along with pollutants such as sulfur dioxide, nitrogen oxides, and particles that are dangerous to people's health [6].

4 FLUIDIZED BED COMBUSTION

Fluidized bed combustion is a method of burning solid fuels, like coal. Fluidization of the layer of solid particles occurs when a pressurized fluid (liquid or gas) passes through the medium and causes, under certain circumstances, the solid particles to behave like a fluid. As a result of fluidization, the state of the particles changes, from static to dynamic. [7]. Fluidized bed combustion is classified into two types: atmospheric fluidized bed combustion and pressurized fluidized bed combustion. Each type includes bubbling fluidized bed combustion and circulating fluidized bed combustion [8]. The working principle of fluidized bed combustion is shown in Figure 2.

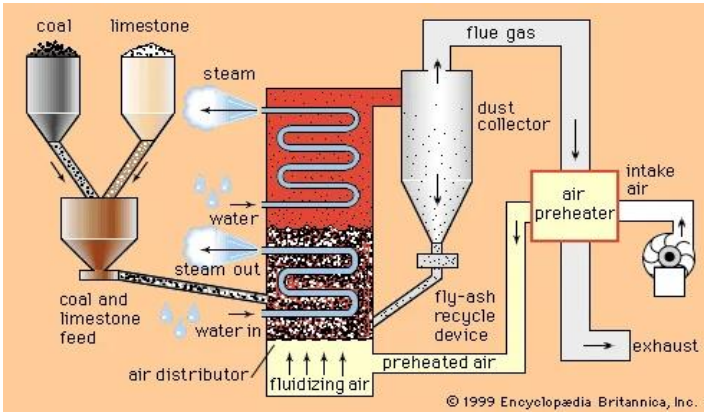

Figure 2. *Schematic diagram of fluidized bed combustion boiler [9]*

The layer of solid particles is formed by mixing coal and limestone. Evaporation pipes are placed directly in the layer itself. From the air preheater, the warm air is transferred from the bottom, up to the finely divided layer of solid particles. When the air flows at a low speed, the particles remain undisturbed, if the speed gradually increases the particles become suspended in the airflow. With a further increase in the air speed, the layer becomes very turbulent, and mixing of the particles occurs, which resembles the formation of bubbles in a boiling liquid. The velocity of the air that causes fluidization depends on parameters such as the particle size of the coal and the density of the air-coal mixture. Since the evaporation tubes are directly placed in the

layer of solid particles, they are in direct contact with the burning coal and produce high heat transfer rates. Due to this, the size of the unit is reduced to a great extent, and it also produces combustion with very high efficiency. Fluidized bed combustion systems are particularly suitable for low-quality, high-sulfur coal because of their capacity to retain sulfur dioxide in the bed as well as their ability to burn coal with high or variable ash content [10]. This technology offers many advantages such as:

- High thermal efficiency,
- Simple ash removing system,
- Fully automated process that ensures safe operation,
- Possible operation at temperatures as low as 150ºC,
- Decreased coal crushing, because pulverized coal is not a necessity,
- The system can quickly respond to changes in load demand,
- Lowering the temperature of the fluidized bed furnace helps to reduce air pollution.

5 COAL GASIFICATION

Coal gasification is the process of producing syngas (synthetic gas), a mixture primarily consisting of carbon monoxide, carbon dioxide, and hydrogen. Gasification can be defined as the transformation of solids into flammable gases in the presence of steam and air, oxygen or carbon dioxide. The gasification process consists of several steps, as shown in Figure 3.

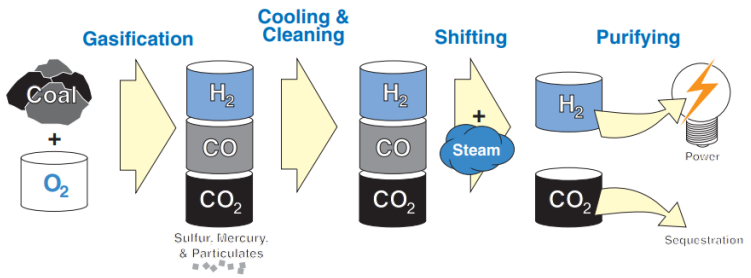

Figure 3. *Gasification process [11]*

Gasification is the process by which coal is converted into a very hot (up to 1800°C) synthesis gas, or syngas, which contains carbon monoxide, carbon dioxide, and hydrogen, as well as trace amounts of other gases and particles. This is accomplished by combining pulverized coal with an oxidant, most commonly steam, air, or oxygen. The syngas is then cooled and cleaned to remove any remaining gases and particles, leaving only carbon monoxide, carbon dioxide, and hydrogen. Syngas emissions are less difficult to clean up than pulverized coal power plant emissions. Mercury, sulfur, trace pollutants, and particulates are all removed during syngas cleaning. The syngas is then routed to a "shift reactor." By mixing with steam, carbon monoxide is converted into more carbon dioxide and hydrogen during the shift reaction. Then there's syngas, which is mostly hydrogen and carbon dioxide. After the syngas is shifted, it is separated into streams of hydrogen and carbon dioxide. The hydrogen, once purified, is ready for use. Carbon dioxide can be captured and sent for sequestration [11].

5.1 Types of gasifiers

Coal gasifiers come in three varieties, and each one is shown in Figure 4.

- Entrained flow gasifier,
- Moving bed gasifier,
- Fluidized bed gasifier.

The most aggressive form of gasification is *entrained flow*, in which pulverized coal and oxidizing gas flow concurrently. Optionally, the pulverized coal can be fed into the gasifier as a slurry with water, which serves as a source of steam for the reaction. Under high pressures and high temperatures, almost complete gasification is obtained with little formations of tars and char. These gasifiers are designed for coal with low reactivity and high throughput. *Moving-bed gasifiers* operate at 3 MPa and are very similar to blast furnaces. In a refractory-lined vessel, crushed coal with fine particles removed is placed on the top of a descending bed. The primary requirement for moving-bed gasifiers is high bed permeability to avoid pressure drops and channel burning. The coal is gradually heated as it moves downward and comes into contact with steam and oxygen-enriched air flowing upward counter-currently. The Lurgi moving-bed gasifier is the oldest and most well-known type of gasifier of this type, although some different kinds have also been developed. A *fluidized bed gasifier* is a vessel in which fine solids are suspended by an upwardly flowing gas, causing the entire bed to behave fluidically. Finely grounded coal is injected into a bed of inert particles that is fluidized at high pressure with steam and air (or oxygen). At a temperature of 1,223 – 1,373 K and a pressure of 2-3 MPa, the rising oxygen-enriched gas reacts with the coal [12].

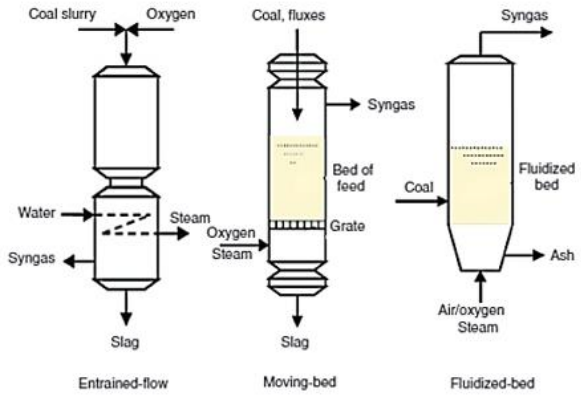

Figure 4. *Schematic representation of coal gasifier types [12]*

6 INTEGRATED GASIFICATION COMBINED CYCLE

The use of solid and liquid fuels in a power plant which has the environmental advantages of a gas power plant and the thermal properties of a combined cycle is possible with Integrated gasification combined cycle technology. After gasifying a solid or liquid fuel with oxygen, the resulting gas, called syngas is cooled and cleaned, then released into a gas turbine. The hot air from the gas turbine is routed to a heat recovery steam generator, which generates steam to power the steam turbine. Both gas and steam turbines generate power. This IGCC scheme has many different variants, most notably in the level of integration. Usually, boiler feed water is warmed in

a heat recovery steam generator (HRSG) and then passed to the gasification section where saturated steam is generated by cooling the syngas. The saturated steam is superheated and reheated in the HRSG, before being introduced to the steam turbine for power generation. The most common integration design is the level of integration of the gas turbine with the air separation unit. This unit is critical to increasing the efficiency, accessibility and functionality of an oxygen-fed IGCC power plant. The following figure shows a schematic representation of an IGCC power plant [13].

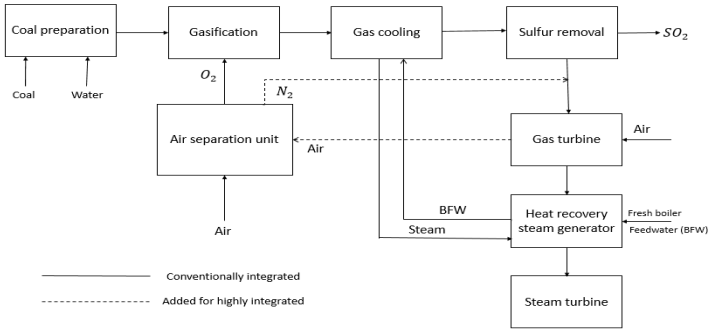

Figure 5. *Integrated gasification combined cycle block diagram [13]*

7 CARBON CAPTURE AND STORAGE

Carbon dioxide capture and storage (CCS) is a method that entails separating carbon dioxide from industrial and power sources, transporting it to a storage location, and isolating it from the atmosphere for an extended period of time. Carbon dioxide is captured from the places where it is produced such as thermal power plants or other industrial facilities.

7.1 Carbon capture systems

There are three basic systems for carbon capture: post-combustion capture, pre-combustion capture, and oxyfuel combustion capture.

7.1.1 Post-combustion capture

Post-combustion capture is a technique used to separate carbon dioxide from flue gas produced by the combustion of fossil fuels. The flue gas, a mixture of carbon dioxide, nitrogen, and some oxygenated compounds, is first processed in order to remove particles, nitrogen, and sulfur oxides. In most cases, they come into contact with a liquid solvent, usually a liquid amine solution. Carbon dioxide is selectively absorbed by the amine solution, capturing more than 85% of the carbon dioxide, allowing for the release of oxygen and nitrogen in the atmosphere. Furthermore, an amine rich in carbon dioxide is regenerated by using steam to remove the carbon dioxide from the liquid, enabling the amine to be reprocessed to the absorber while generating a concentrated carbon dioxide stream. The carbon dioxide is compressed and cooled as a liquid [14]. The advantages of this process are:

- Can usually be built into existing industrial facilities and power plants without requiring important changes to the original plant,
- Can be incorporated into new plants to accomplish reduction of greenhouse gasses close to zero-emission,

- It has a high level of operational flexibility (partial retrofit, zero to full capture operation) and therefore can fit market conditions for both current and new power plants,
- This process allows the integration of renewable technologies [14].

7.1.2 Pre-combustion capture

In pre-combustion capture, the carbon dioxide is removed prior to combustion. The capture procedure is divided into three stages:

1) The hydrocarbon fuel, usually gasified coal, is transformed into carbon monoxide and hydrogen in order to produce syngas,
2) The carbon monoxide is then transformed into carbon dioxide by a water gas shift reaction,
3) The resulting carbon dioxide is separated from the hydrogen, which can be burned safely. Carbon dioxide can be compressed into a liquid and transferred to a storage location [14].

7.1.3 Oxyfuel combustion

Oxyfuel combustion involves the process of burning a hydrocarbon fuel such as coal with almost pure hydrogen instead of air. In order to regulate the temperature, the oxygen is diluted with exhaust gas instead of nitrogen. The primary reason for using oxy-fuel combustion in a coal power plant is to produce flue gas with extremely high concentration levels of carbon dioxide and water vapor, allowing the carbon dioxide to be separated or captured purely through dehydration and desulfurization processes. The advantages of this type of combustion are lowered NOx emissions, high carbon dioxide pureness, and lower gas volume caused by increased density.

7.2 Carbon transport

Pipelines are preferable for transporting large quantities of carbon dioxide over long ranges up to 1,000 kilometers. Ships, where applicable, may be more economically appealing for amounts below a few million tons of carbon dioxide per year or longer distances abroad [16]. Transport of carbon dioxide by truck and railway is possible for small quantities. Trucks are used at some sites, moving carbon dioxide from the capture site to a nearby storage site. For quantities of less than a few million tonnes of carbon dioxide per year or longer distances overseas, the use of ships, where applicable, could be more economically attractive [17].

7.3 Carbon storage

Geologic formations, especially depleted oil and gas reservoirs, have been considered the best possible option for carbon dioxide storage because the environmental risks and uncertainties related to geologic storage are much lower when compared with ocean storage. EOR (Enhanced Oil Recovery) companies transfer and store the liquefied carbon dioxide for tertiary recovery by reducing the density of the oil and thus mobilizing the oil. According to current research, storing carbon dioxide in depleted oil and gas reservoirs poses the least environmental risk. It has already been attempted, and the locations have proven their ability to retain fluids (under pressure) for millions of years. Aside from depleted gas and oil reservoirs, deep aquifers are a long-term viable option. Furthermore, the transport costs for this kind of storage are relatively low [16]. Geological storage is shown in Figure 6.

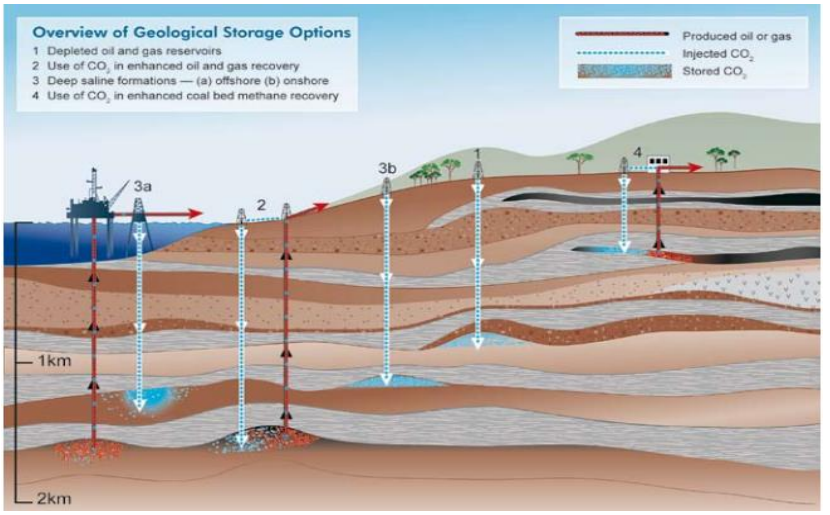

Figure 6. *Geological storage options [17]*

According to capacity, the ocean is by far the best location to store captured carbon. The direct injection of the captured carbon dioxide causes increased acidity of the ocean, but at such a slow speed which allows the marine organisms to adapt. Some researchers verify that injecting carbon dioxide at a depth of 1,000-1,500 m via a pipeline producing a jet of carbon dioxide can be absorbed in the surrounding water. As stated in another study, if carbon dioxide is injected at depths larger than 3,000 m, it will overcome the density of the ocean water followed by sinking at the ocean bottom and creating a securely isolated lake, as shown in Figure 7 [16].

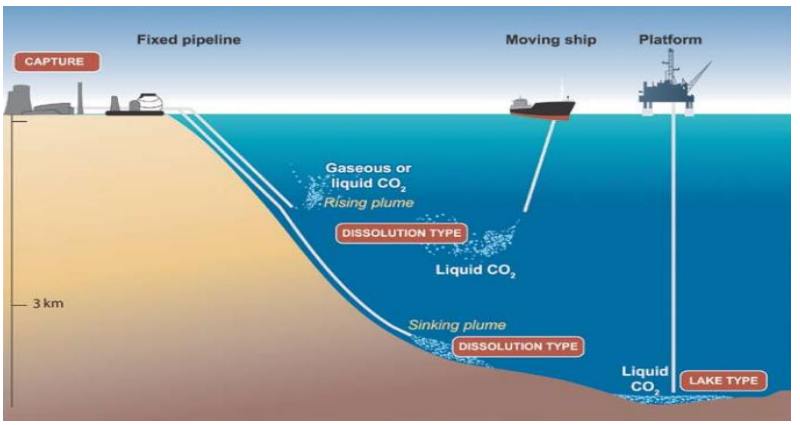

Figure 7. *Ocean storage of carbon dioxide [17]*

8 CONCLUSION

Considering that large amounts of coal are still available, it will continue to be the main source for generating electricity in the future. The important thing is to aim for the use of clean coal technologies to reduce the impact of climate changes on the environment and the health of living organisms. The classic burning of coal in power plants could be replaced by supercritical and ultra-supercritical technologies, which

reduce emissions of sulfur and nitrogen oxides. Gasification is also a technology that significantly reduces pollutants compared to conventional coal burning. The higher pressures and temperatures used in the gasification process allow for easier removal of carbon dioxide, for its further capture and geological storage. The future of clean coal technologies is bright and they will play a key role in global efforts to reduce the environmental impacts of electricity production.

REFERENCES

[1] Hannah Ritchie, Max Roser and Pablo Rosado (2020) - "Energy". *Published online at OurWorldInData.org.* Available: https://ourworldindata.org/energy

[2] Maria Giulia Anceschi (2019), *The Balkans (and Europe) are choking on coal pollution*, Available: https://www.balcanicaucaso.org/eng/Areas/Balkans/The-Balkans-and-Europe-are-choking-on-coal-pollution-193459

[3] CTCN, *Pulverised coal combustion with higher efficiency*, Available: https://www.ctc-n.org/technologies/pulverised-coal-combustion-higher-efficiency

[4] State utility forecasting group, *Clean Coal Technologies,* Purdue University,2007 Available:https://www.purdue.edu/discoverypark/energy/assets/pdfs/SUFG-CleanCoalTechnologiesReport.pdf

[5] World Coal Association, https://www.worldcoal.org/coal-facts/coal-electricity/

[6] J.M.K.C. Donev et al. (2018). Energy Education - Supercritical coal plant [Online]. Available: https://energyeducation.ca/encyclopedia/Supercritical_coal_plant

[7] Energy purse, Fluidized bed combustion boilers, Available: https://www.energypurse.com/why-fluidized-bed-combustion-boilers/

[8] Dipak K. Sarkar, Chapter 5 - Fluidized-Bed Combustion Boilers, Editor(s): Dipak K. Sarkar, *Thermal Power Plant, Elsevier,* 2015, pp. 159-187.

[9] Sarma V.L.N Pisupati, Alan W. Scaroni, fluidized-bed combustion, Available: https://www.britannica.com/technology/fluidized-bed-combustion

[10] Electrical 4 U, *Fluidized Bed Combustion | Types and advantages* (2020), Available: https://www.electrical4u.com/fluidized-bed-combustion-types-and-advantages-of-fluidized-bed-combustion/

[11] Fact sheet, *Hydrogen production from coal*, Available: file:///C:/Users/User/Downloads/factSheet_productionCoal%20(2).pdf

[12] Rand. D, Coal Gasification (2009), CSIRO Energy Technology, Clayton, VIC, Australia.

[13] Nevile. A.H. Holt, Integrated Gasification Combined Cycle Power Plants, *Encyclopedia of Physical Science and Technolgy, Academic Press,* 2001.

[14] A. Basile, A. Gugliuzza, A. Iulianelli, P. Morrone, 5 - Membrane technology for carbon dioxide (CO2) capture in power plants, In Woodhead Publishing Series in Energy, *Advanced Membrane Science and Technology for Sustainable Energy and Environmental Applications*, Woodhead Publishing, 2011, pp. 113-159.

[15] Steven M. Carpenter, Henry A. Long, 13 - Integration of carbon capture in IGCC systems, Editor(s): Ting Wang, Gary Stiegel, *Integrated Gasification Combined Cycle (IGCC) Technologies*, *Woodhead Publishing*, 2017, pp. 445-463.

[16] Shubham Das, Jayant Kumar, Carbon Capture and Storage, *International Journal of Scientific & Engineering Research,* Volume 7, Issue 10, October 2016.

[17] IPCC, 2005: IPCC Special Report on Carbon Dioxide Capture and Storage. Prepared by Working Group III of the Intergovernmental Panel on Climate Change [Metz, B., O. Davidson, H. C. de Coninck, M. Loos, and L. A. Meyer (eds.)]. *Cambridge University Press*, *Cambridge, United Kingdom and New York, NY, USA.*

COMETa 2022
6th INTERNATIONAL SCIENTIFIC CONFERENCE
17th - 19th November 2022
Jahorina, B&H, Republic of Srpska
University of East Sarajevo
Faculty of Mechanical Engineering
Conference on Mechanical Engineering Technologies and Applications

DILLEMA ABOUT INFLUENCE OF SPLITTER VANES ON HYDRAULIC CHARACTERISTIC AT RECTANGULAR RADIUS ELBOW

Valentino Stojkovski[1], Marija Lazarevikj[2], Viktor Iliev[3]

Abstract: Elbows are fittings in rectangular ducts which change the direction of the air stream without changing the air quantity or average velocity. When there is a change in direction in a duct then duct walls must absorb the sudden impact of the air in order to redirect the airflow to the desired direction. Splitter vanes assist the airflow in making a smoother and more gradual change in direction, thus transferring less impact and less force to the duct walls. While the splitter vane surfaces do add a small amount of friction, the amount of energy loss due to friction from the vanes is very little compared to the energy loss resulting from the airflow taking an abrupt change in direction. Splitter vanes in rectangular elbow are perhaps one of the greatest sources of conflict between the state that splitter vanes can cause the ductwork to become less efficient by increasing the pressure drop in the system and contrary that the obtaining a uniformity of the airflow into the rectangular ducts give better efficiency and lower pressure drop.

This paper presents results of experimental and numerical research of hydraulic characteristic at rectangular radius elbow without and with splitter radial vanes at different relative position in the domain of elbow. The results are presented through the loss coefficient of elbows which is function of the elbow radius, duct dimensions, angle of turn and Reynolds number. The numerical results of fluid flow domain are comparatively used for presenting the influence of splitter vane on uniformity of discharge distribution in the space of the elbow and on uniformity of fluid flow velocity profile.

The results show that the splitter vanes are proven very valuable for reducing pressure losses and increasing system efficiencies. Designers should add or remove turning

[1] Professor Dr. Valentino Stojkovski, Faculty of Mechanical Engineering, Skopje, North Macedonia, valentino.stojkovski@mf.edu.mk
[2] Assistant Marija Lazarevikj, PhD, Faculty of Mechanical Engineering, Skopje, North Macedonia, marija.lazarevikj@mf.edu.mk
[3] Professor Dr. Viktor Iliev, Faculty of Mechanical Engineering, Skopje, North Macedonia, viktor.iliev@mf.edu.mk

vanes from the design with aim to specify fittings with the highest possible efficiency and to increase system efficiency at every available opportunity.

Key words: rectangular radius elbow, splitter vane, loss coefficient, CFD calculation

1 INTRODUCTION

Ducts are mostly used in air distribution systems to supply or return air. Their shape can be round, square, rectangular or oval. Even though round ducts are most efficient, square/rectangular ducts fit better to building construction – above ceilings and into walls. Moreover, they are much easier to install between joists and studs. The system resistance in ductwork has three components: friction, dynamic and equipment pressure losses. Friction losses depend on air velocity, duct length and diameter (size), and material roughness, whereas dynamic losses are caused by change in air direction from elbows, restrictions or obstructions in the air stream stream such as dampers, filters and coils [1,2,3].

Duct losses occur across fittings and transitions and in order to mitigate them, radius elbows are desirable over square ones if the space allows. When a full radius elbow cannot fit, a part-radius elbow or square elbow with one or more splitters is recommended. A splitter vane is a curved fin placed in an air ductwork at a point of duct direction change. It is used to obtain more uniform flow and to reduce pressure drop [4,5]. Recommendation is to use them in low velocity systems.

In a duct without splitter vanes, the duct walls must absorb the sudden impact of air flow in order to reorient it to the desired direction. Splitter vanes assist in making a smoother and more gradual change in direction resulting in less force transferred. The splitter vanes presence add a small amount of friction, but losses originating from it are negligible compared to the energy lost due to abrupt or significant change in direction [6].

Some research show higher efficiency of square elbow when splitter vanes are added, i.e. more gradual decrement airflow direction change is achieved which causes pressure drop decrease and consequently the required fan power to supply the desired air flow rate is smaller [7].

In this paper, experimental and numerical investigation of the hydraulic characteristic of radius elbow in a rectangular duct with and without splitter vanes is performed. Three cases are compared: empty elbow, elbow with one vane and elbow with two vanes. In addition, the position of the vane in the elbow is changed to gain knowledge of its influence in the flow domain.

2 EXPERIMENTAL SETUP

2.1 Experimental installation

For conducting the experimental research, a physical model of a horizontal closed rectangular duct with radius elbows is manufactured. The measurements are performed in the Laboratory for Fluid Mechanics and Hydraulic Machines at the Faculty of Mechanical Engineering – Skopje. The experimental installation consists of centrifugal fan; reducer and two rectangular ducts connected by an elbow. The reducer is 1m long and decreases the channel height from 400mm to 270mm. The two rectangular conduits have a square cross-section with dimensions 270X270mm and a length of 1m each. The elbow is defined by internal radius (R1) of 150mm and external radius (R2) of 420mm; it changes the air direction from one to other rectangular duct.

The air flow is provided by a centrifugal fan. The experimental setup is shown in Figure 1.

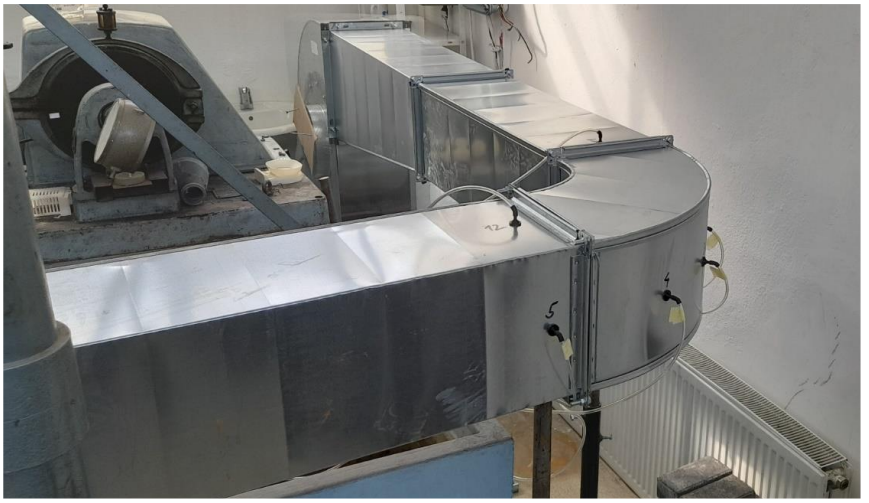

Figure 1. *Experimental setup: fan, reducer, duct and elbow*

2.2 Measuring equipment and procedure

Pressure drop in the elbow and air flow rate in the duct are determined based on pressure and velocity measurement by using adequate measuring equipment and data acquisition system (Figure 2).

Figure 2. *Measuring equipment and data acquisition system*

The pressure is measured in 12 measuring points along the internal and external curved side of the elbow (Figure 3 left) by using a set of 10 digital sensors with with a range of ± 1000 Pa and with U-tubes with manometric liquid – water. For each

given measuring point, the corresponding digital sensor and U-tube are connected in parallel. The digital sensors are connected to a pressure acquisition system with the ability to change the sampling time, monitor the pressure values at the measuring points in real time, and archive the data obtained from all sensors simultaneously in a tabular overview.

Two different modes of airflow through the duct are achieved by dimming the suction side of the fan. Velocity is measured in 9 points on the inlet cross-section (Figure 3 right) by the application of anemometer. The methodology of determining volume flow rate of air flowing in the duct is based on measured velocity and therefore computing the flow rate by velocity integration.

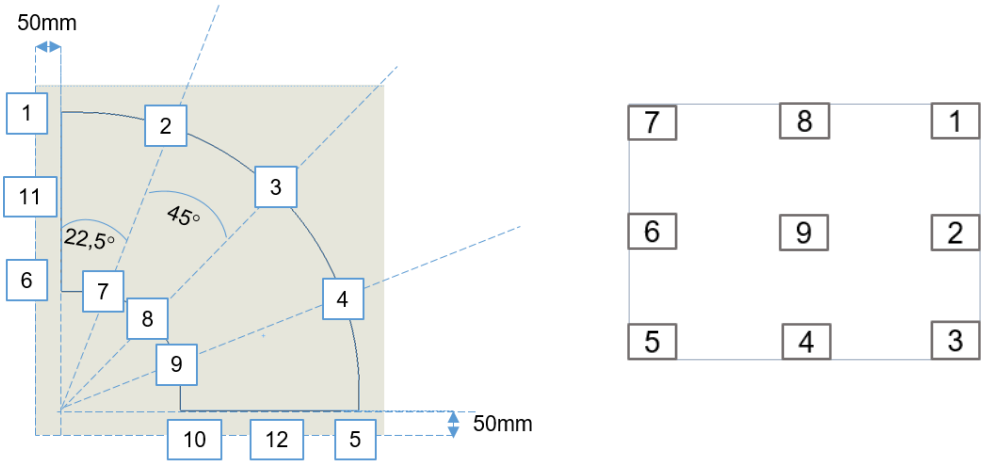

Figure 3. *Location of measuring points in elbow (left) for pressure measurements and in the inlet section (right) for velocity measurements*

Three different elbow constructions are used, i.e. empty elbow – without splitter vanes, elbow with one vane and elbow with two vanes (Figure 4).

Figure 4. *Elbow with one splitter vane (left) and two vanes (right)*

3 NUMERICAL SETUP

3.1 Numerical model and boundary conditions

Steady state flow of air through the rectangular ducts with elbow is modeled and simulated. Air is taken as a compressible fluid with density varying according to the law of ideal gas state, while its other thermophysical properties are constant throughout the domain. The turbulent flow of air is described by the k-ε turbulence model. One flow domain consisting of reducer, two ducts and elbow is present. Mass flow of air at inlet and atmospheric pressure at outlet are applied as boundary conditions in the model (Figure 4).

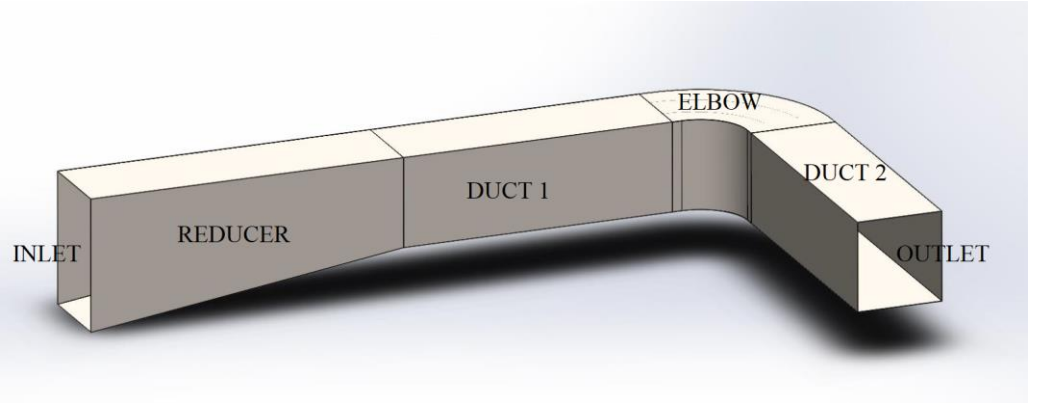

Figure 4. *Numerical model with boundary conditions*

Three geometrical models with different elbow configurations are used, i.e. without splitter vanes (Figure 5a), with one vane (Figure 5b) and with two vanes (Figure 5c). Four flow regimes (air mass flow of 0,3kg/s, 0,6kg/s, 0,9kg/s and 1,2kg/s) are simulated for each configuration.

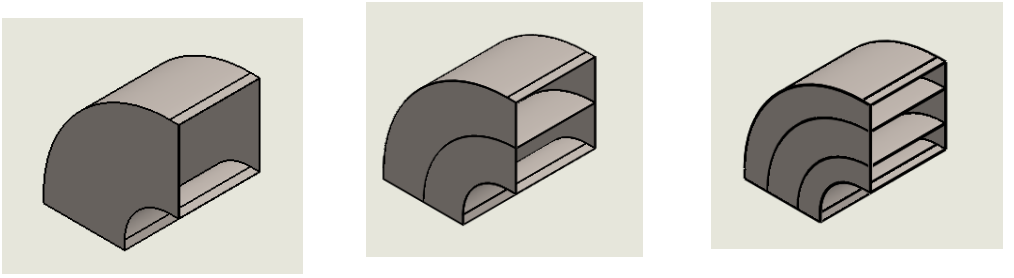

a) b) c)

Figure 5. *Different elbow configurations: a) no vanes, b) one vane, c) two vanes*

3.2 Numerical mesh

The geometrical model is based on the elbow with two vanes. For the configuration with two vanes, the vanes are taken as walls, while for the empty elbow, the vanes are assigned to interiors. This is in order to have the same numerical mesh in each case so that the comparison is made on equal basis. The numerical grid consists of above 2 million cells. The mesh is structural with hexagonal elements and a

boundary layer is placed around walls. The numerical mesh at the elbow and ducts is shown in Figure 6a, while the mesh at the inlet and outlet is given in Figure 6b and 6c, respectively.

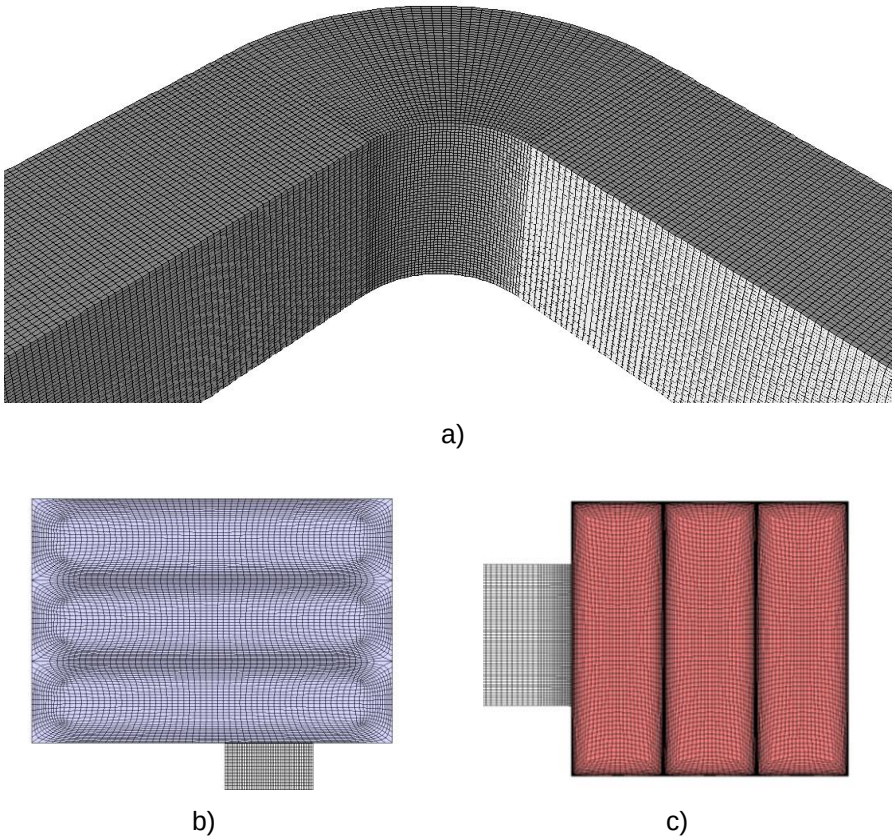

Figure 6. *Numerical grid: a) elbow, b) inlet and c) outlet*

4 RESULTS AND DISCUSSION

4.1 Experimental and numerical results comparison

Experimental measurements are performed using the laboratory installation with elbow without vanes (model 2-0), model with one vane centrally positioned (model 1-0) and model with two vanes (model 2-2).

The experimental values of pressure (p-st) measured in points at the internal and external side of the elbow which position is defined by the angle (0°-inlet and 90°-outlet) for the three geometrical models in similar operating mode (flow velocity from 7,6-7,7 m/s) are given in Figure 7.

Vacuum pressure is obtained on the internal wall (R1) and gauge pressure on the external wall (R2) in all three configurations. Highest underpressure and highest overpressure are obtained at angle of 45°.

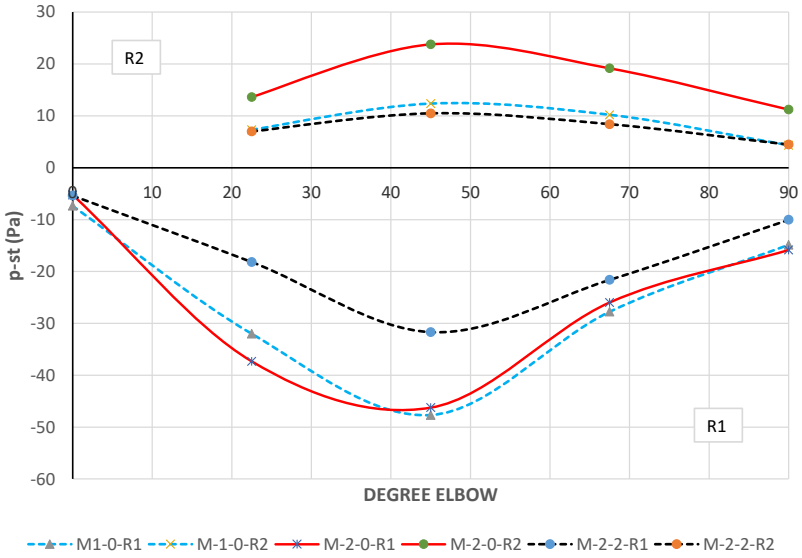

Figure 7. *Experimental results of pressure in measuring points positioned on the internal (R1) and external (R2) wall of the elbow*

The comparison between experimental and numerical results for pressure distribution on external and internal wall are given as relative values (p-11) to the pressure measured with the probe at angle of 45° (Figure 8). The length of external/internal wall of the elbow in direction from the first to the last measuring point is given on x-axis. Numerical results are given with dashed line, while symbols are used for relative values of measured pressure.

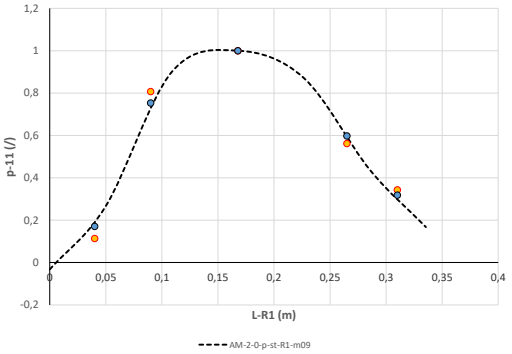

model 2-0: no vanes-на R1

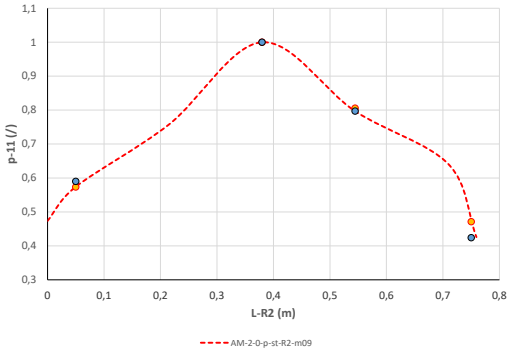

model 2-0: no vanes- R2

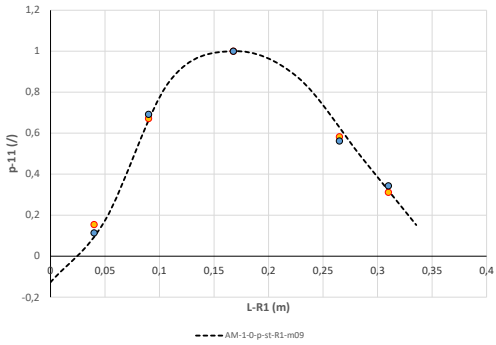

model 1-0: one central vane- R1

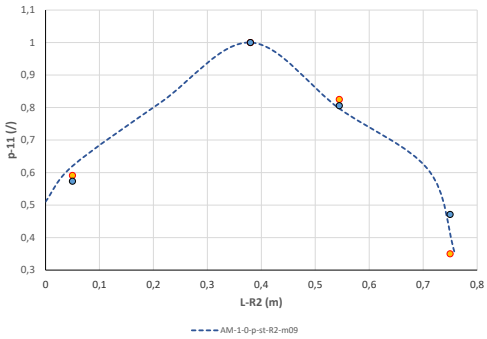

model 1-0: one central vane - R2

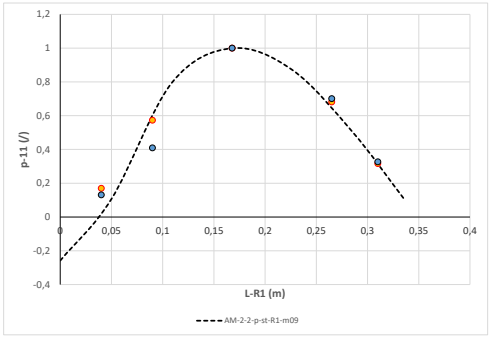

model 2-2: two vanes- R1

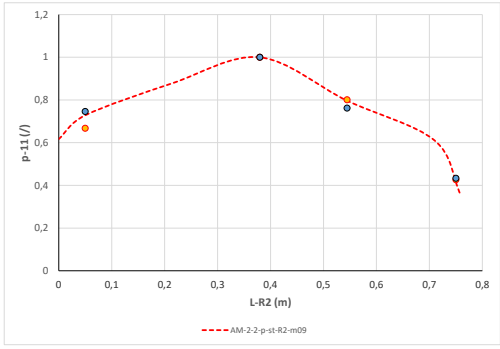

model 2-2: two vanes- R2

Figure 8. *Numerical and experimental results comparison*

The graphs show alignment of experimental and numerical results for pressure distribution along the external and internal side of the elbow. Thus, the numerical model is validated.

4.2 Influence of splitter vanes

Numerical resuls are used to compare the influence of the splitter vanes position as shown in Figure 9.

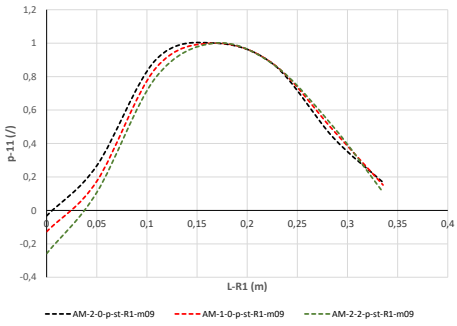

a) Pressure distribution along R1

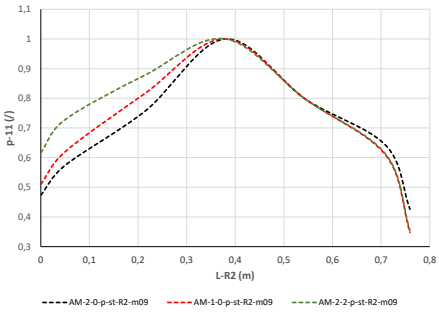

b) Pressure distribution along R2

Figure 9. *Influence of the splitter vanes position in the elbow pressure distribution*

Numerical resuls are used to compare the influence of the splitter vanes position on the elbow pressure distribution as shown in Figure 9. The influence is dominant at the elbow inlet until angle of 45°. The presence of vanes negatively affects the pressure distribution on the internal side, while it contributes to more uniform distribution on the external side of the elbow.

Measured values of pressure in probe no.11 (denoted as MM-11) at the elbow inlet and probe no.12 (denoted as MM-12) at the elbow outlet give the influence of splitter vanes addition on the pressure frequency (determined by FFT analysis) and pulsations intensity (given by the PtP values). The x-axis gives the number of vanes.

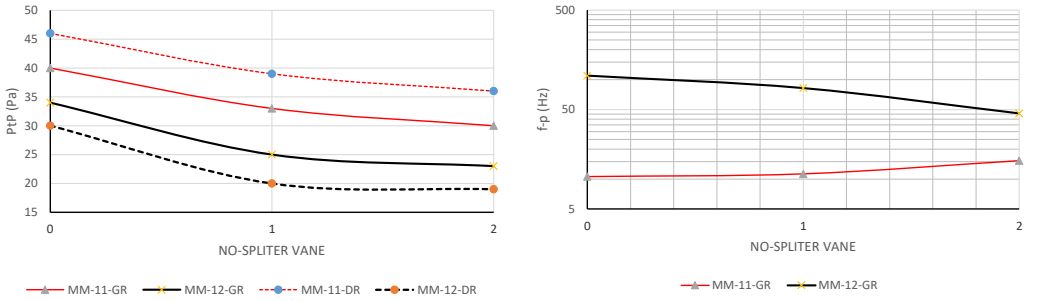

a) PtP values of pressure – pressure pulsations intensity

b) Pressure pulsations frequency

Figure 10. *Pressure pulsations intensity and frequency in probes 11 and 12*

The addition of splitter vanes reduces the pressure pulsations intensity both at elbow inlet and outlet. The pressure pulsations frequency is increasing at inlet by adding splitter vanes, but more significant influence of the added splitter vanes is noticed at the outlet where the pulsations frequency is quite decreased.

Two additional numerical models are developed to investigate the influence of vanes position in the elbow, i.e. model 2-1 with one vane closer to the external wall and model 2-3 with one vane closer to the internal wall.

The velocity field in the central plane covering the domain from the elbow inlet to the duct outlet obtained for the different numerical models is given in Figure 11.

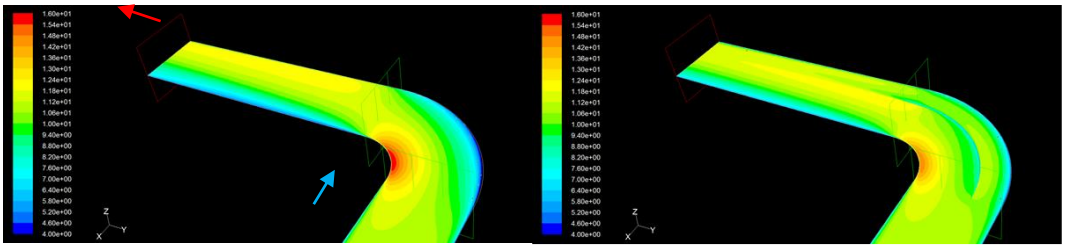

a) model 2-0: no vanes

b) model 2-1: one vane closer to external wall

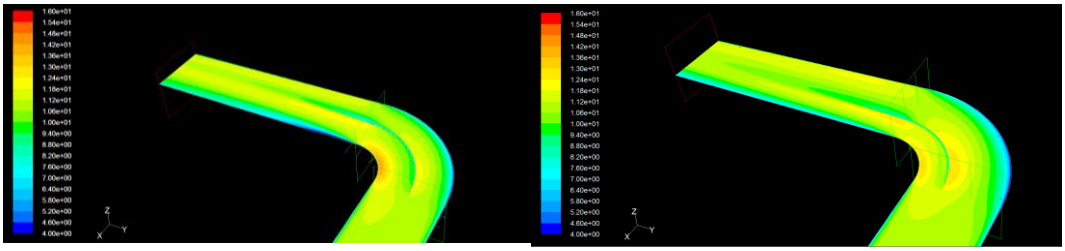

c) model 1-0: one central vane

d) model 2-3: one vane closer to internal wall

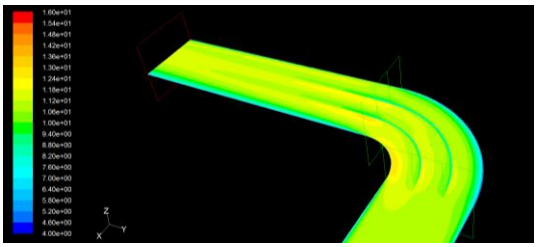

e) model 2-2: two vanes

Figure 11. *Flow field (vectors of velocity) of numerically investigated models of elbow*

It can be seen that when there is no vane, the flow is sticking to the external wall of the elbow, with maximal local velocity magnitudes on the internal side. By adding two vanes, there is no flow sticking to the external wall so the flow field is more uniform.

The influence of the splitter vane on the velocity profile uniformity at elbow inlet and outlet (50mm before inlet section and 50mm behind outlet section)-central horizontal section is given in Figure 12.

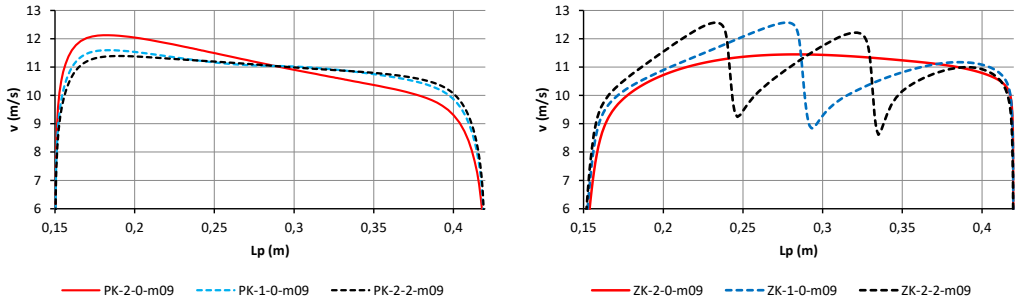

a) 50 mm before elbow inlet

b) 50 mm behind elbow inlet

Figure 12. *Velocity profile at elbow inlet and outlet*

The addition of splitter vanes gives more uniform velocity profile at elbow inlet contributing to more favorable flow conditions. Velocity profile at elbow outlet are significantly different for each configuration because of the vane influence on the channel outflow.

4.3 Influence of splitter vane position on pressure distribution and hydraulic characteristic of the elbow

Numerically obtained pressure distribution along the external and internal wall of the elbow with splitter vane in different position at constant mass flow rate is given in Figure 13.

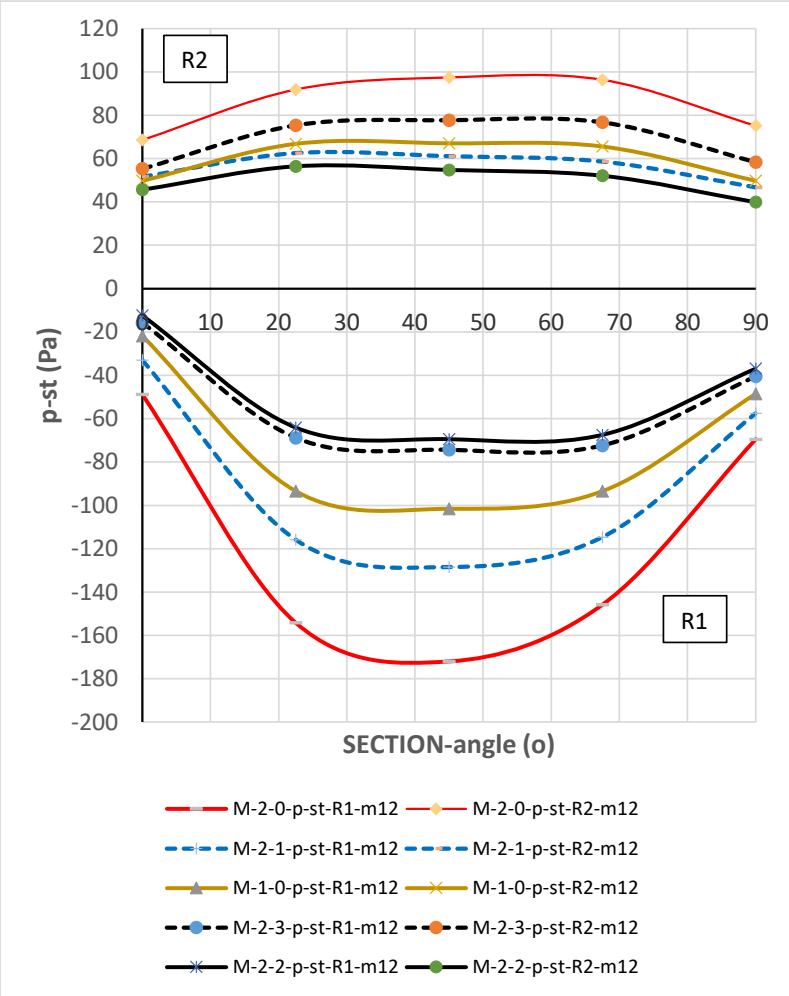

Figure 13. *Pressure distribution along external and internal wall of elbow*

The comparison of different splitter vane positions so as the number of vanes in the elbow emphasizes the changes in pressure intensity.

Smallest difference in pressure between the external and internal wall of the elbow and more uniform pressure distribution is obtained by adding two splitter vanes in the elbow.

Hydraulic losses of elbow are defined as difference between average pressure at 50mm before elbow inlet and average pressure at 50mm behind elbow outlet. The elbow hydraulic losses are calculated at different air mass flow rates (0,3; 0,6; 0,9; 1,2 kg/s) and given in Figure 14.

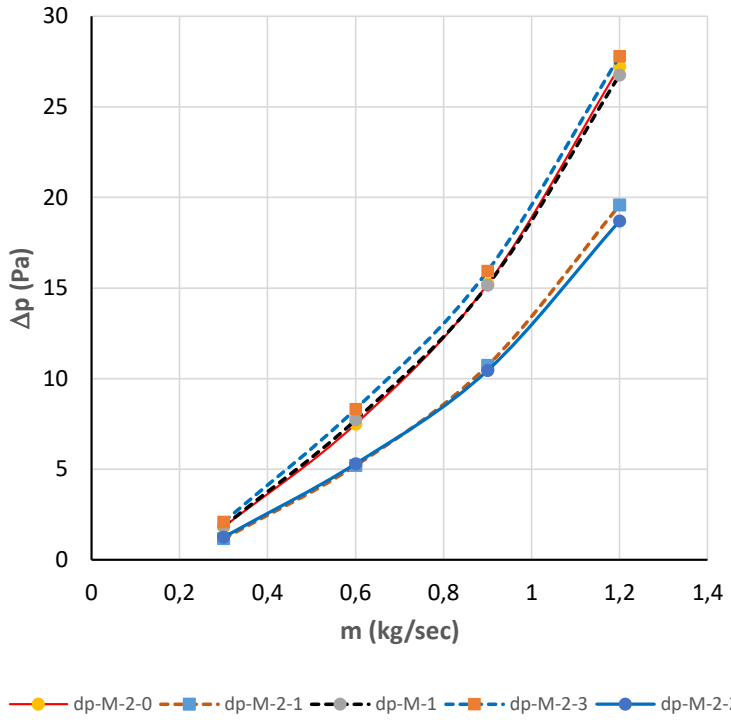

Figure 14. *Elbow hydraulic losses for different elbow configurations*

It can be seen that if one vane is added in the elbow, its position significantly affects the hydraulic characteristic, i.e. hydraulic losses are higher when the vane is closer to the internal wall of the elbow and hydraulic losses are lower when the vane is closer to the external wall. Moreover, if the vane is centrally positioned, there is almost no difference in the hydraulic characteristic compared to the elbow without vanes. The addition of two vanes reduces hydraulic losses in the elbow.

5 CONCLUSIONS

In this paper, exeperimental and numerical analysis of the number of splitter vanes and the vane position in the elbow is performed. The numerical model is validated by verifying the numerical results by comparison with the measurements. It was obtained that the splitter vane position affects the hydraulic characteristic.

The experimental and numerical investigation of the influence of the vane position in the elbow connecting two ducts with square cross-section show that locating a vane close to the external wall contributes to reducing hydraulic losses so as the addition of two vanes symmetrically in relation to the elbow boundary walls.

The experimental and numerical analysis is performed to resolve the dillema about the influence of the splitter vane position in the elbow. Further steps need to be taken in this research to improve the effects of adding the vane.

REFERENCES

[1] http://ibse.hk/MECH3423/MECH3423_1516_07-airside02.pdf
[2] Bhatia, A., HVAC How to size and design ducts, https://www.cedengineering.com/userfiles/HVAC%20-%20How%20to%20Size%20and%20Design%20Ducts%20R1.pdf
[3] https://energy-models.com/ductwork-design-program
[4] https://encyclopedia2.thefreedictionary.com/turning+vane
[5] Rasuo B., Dinulovic M., Trnicic M., Stamenovic M., Milosevic M., Curcic M., (2021). A study of aerodynamic noise in air duct systems with turning vanes, FME Transactions, vol. 49, no. 2, p.p. 308-314
[6] http://www.sheetmetaljournal.com/?p=690
[7] https://buildingengineer.wordpress.com/2009/12/11/turning-vanes-necessary-component-or-efficiency-reduction-device/

COMETa 2022
6th INTERNATIONAL SCIENTIFIC CONFERENCE
17th - 19th November 2022
Jahorina, B&H, Republic of Srpska
University of East Sarajevo
Faculty of Mechanical Engineering
Conference on Mechanical Engineering Technologies and Applications

АНАЛИЗА ПРОБЛЕМА И ПРИЈЕДЛОГ МЈЕРА ЗА ОПТИМИЗАЦИЈУ ПОТРОШЊЕ ТОПЛОТНЕ ЕНЕРГИЈЕ У ИНДУСТРИЈСКИМ ТЕРМОЕНЕРГЕТСКИМ ПОСТРОЈЕЊИМА

Давор Милић[1], Стојан Симић[2], Душан Голубовић[3], Горан Орашанин[4], Радомир Жугић[5]

Резиме: У прошлости се приликом пројектовања индустријских термоенергетских система није водило рачуна о потрошњи топлотне енергије. Усљед смањења залиха и пораста цијена фосилних горива, ограничења емисија отпадних гасова у атмосферу и смањења трошкова производног процеса у посљедњих двадесетак година све већа пажња се посвећује оптимизацији потрошње топлотне енергије. У циљу оптимизације потрошње топлотне енергије проводе се техничке, технолошке и организационе мјере: рекуперација топлоте из технолошког процеса, искоришћење отпадне топлоте димних гасова, повратак отпадног кондензата, замјена неисправних одвајача кондензата, замјена и поправка оштећене топлотне изолације и др. Детаљна анализа је показала да свака од примјењених мјера доприноси оптимизацији потрошње топлтне енергије у виду смањења потрошње топлотне енергије и искоришћења отпадне топлоте. Дефинисање удјела мјере са више аспеката (енергетски, еколошки, економски и др.) на смањење потрошње топлотне енергије у индустријским термоенергетским постројењима је од посебног значаја.

Кључне ријечи: енергетска ефикасност, индустријски термоенергетски системи,мјере за смањење потрошње енергије, топлотна енергија

ANALYSIS OF THE PROBLEM AND PROPOSED MEASURES FOR OPTIMIZING HEAT ENERGY CONSUMPTION IN INDUSTRIAL THERMAL ENERGY PLANTS

Abstract: In the past, the thermal energy consumption was not taken into account, within designing industrial thermal energy systems. Due to the decrease in stocks and

[1] Др Давор Милић, Машински факултет Источно Сарајево, БиХ, davor.milic@ues.rs.ba
[2] Др Стојан Симић, Машински факултет Источно Сарајево, БиХ, stojan.simic@ues.rs.ba
[3] Др Душан Голубовић, Машински факултет Источно Сарајево, БиХ, dusan.golubovic@ues.rs.ba
[4] Др Горан Орашанин, Машински факултет Источно Сарајево, БиХ, goran.orasanin@ues.rs.ba
[5] Мр Радомир Жугић, Blue-Air Systems GmbH, Achenfeldweg 8A, 6250 Kundl, Austria, r.zugic@blue-air.at

the increase in the price of fossil fuels, the limitation of emissions of waste gases into the atmosphere and the reduction of the production process costs, more and more attention is paid to the optimization of thermal energy consumption in the last twenty years. In order to optimize the consumption of thermal energy, technical, technological and organizational measures are implemented: heat recovery from the technological process, use of waste heat from flue gases, return of waste condensate, replacement of defective condensate separators, replacement and repair of damaged thermal insulation, etc. The detailed analysis showed that each of the applied measures contributes to the optimization of thermal energy consumption in the form of reduction of thermal energy consumption and utilization of waste heat. Defining the share of the measure from several aspects (energy, ecological, economic, etc.) to reduce thermal energy consumption in industrial thermal energy plants is of particular importance.

Key words: energy efficiency, industrial thermal energy systems, measures to reduce energy consumption, thermal energy

1 УВОД

Када је ријеч о енергији, у многим индустријским предузећима трошкови за енергију представљају значајан трошак пословања. Енергија се често погрешно сматра фиксним режијским трошком, мада је заправо један од трошкова којима се најлакше управља. И заиста, у многим земљама Европске уније искуство је показало да многе фабрике могу смањити трошкове за енергију и до 20 % без озбиљног улагања, те да је често лакше да се профит предузећа повећа смањењем трошкова за енергију него повећањем производње. Према томе циљ управљања енергијом је да се смање трошкови за енергију и да се предузећу донесе непосредна корист повећањем профитабилности односно конкурентности. Управљање енергијом представља примјену различитих техника управљања које омогућују да се идентификује и примјене мјере за смањење потрошње енергије и трошкова за енергију.

Мјере енергетске ефикасности у индустријским и енергетским постројењима подразумијевају широк спектар активности којима је крајњи циљ смањење потрошње енергије, при чему се истовремено смањује емисија загађујућих компонената у животну средину.

Ефекти смањења потрошње топлотне енергије у процесу производње могу се остварити:

- рационалним коришћењем материјала односно повећањем искоришћења материје, тј. смањењем губитака који неминовно носе и дио енергије унијете у процес;
- побољшањем постојећих технолошких процеса;
- рационалним коришћењем отпадне топлоте у циљу повећања термичког степена искоришћења посматраног производног постројења – сложеног система.

Реализација мјера управљања топлотном енергијом у индустријским предузећима подразумијева:

- оптимално коришћење производних капацитета;
- увођење критеријума енергетске ефикасности при избору технологије;
- ограничење изградње инвестиционих објеката, тј. индустријских погона са високом потрошњом енергије;
- коришћење енергије из отпадних материјала и отпадне топлоте;

- правилно коришћење расположиве енергије водене паре (параметре паре прилагодити захтјевима процеса, ријешити питање враћања кондензата, правилног одржавања арматуре и размјењивачких површина).

Енергетска ефикасност се не посматра као уштеда енергије, већ рационално коришћење и управљање енергијом при чему се не нарушавају услови рада и живота.

2 ПРЕГЛЕД И АНАЛИЗА МЈЕРА ЗА ПОБОЉШАЊЕ ЕНЕРГЕТСКЕ ЕФИКАСНОСТИ ТЕРМОЕНЕРГЕТСКИХ ПОСТРОЈЕЊА

Многе мјере повећања енергетске ефикасности усмјерене су првенствено ка унапређењу техника управљања перформансама, међутим у конкретној анализи укључене су и технике управљања процесима. На тај начин обезбјеђује се достизање жељеног стања појединих подсистема и остварење бољих енергетских перформанси, истовремено. Најприје се изврши шири преглед могућих мјера побољшања енергетске ефикасности, којим су обухваћене оне мјере које су примјерене стању и потребама термоенергетски постројења пројектованим прије више од тридесет година. То је шира листа мјера и неке од њих су већ успјешно имплементиране у појединим погонима. Међутим, поједине мјере још увијек нису у потпуности имплементиране. На основу ове листе могуће је конципирати ужу листу одговарајућих мјера. Дакле, листа мјера приказана је најприје у најширем контексту, а затим је избор редукован према потребама термоенергетских постројења пуштеним у погон седамдесетих и осамдесетих година прошлог вијека. Листа могућих мјера обухвата:

- побољшање процедура и квалитета одржавања котла,
- побољшање хемијске припреме воде (ХПВ),
- замјена/реконструкција горионика,
- контрола садржаја кисеоника у продуктима сагоријевања (контрола вишка ваздуха),
- рекуперација топлоте из димних гасова (предгријавање ваздуха за сагоријевање),
- рекуперација топлоте из димних гасова (повишење температуре напојне воде),
- побољшање топлотне изолације котловског постројења, дистрибутивне мреже, прирубница и цијевне арматуре,
- побољшање система поврата кондензата и подизање температуре рекуперацијом,
- замјена неисправних сабирника паре и одвајача кондензата,
- рекуперација топлоте из процеса одмуљивања котла,
- примјена интегрисаног система аутоматског управљања и др.

Како се на први поглед може закључити, коришћење енергије могуће је рационализовати на више различитих начина, али које су мјере приоритетније и исплативије предмет су специфичне и конкретне анализе. На слици 1. приказани су главни извори енергетских губитака и простор у оквиру кога треба покушати са побољшање.

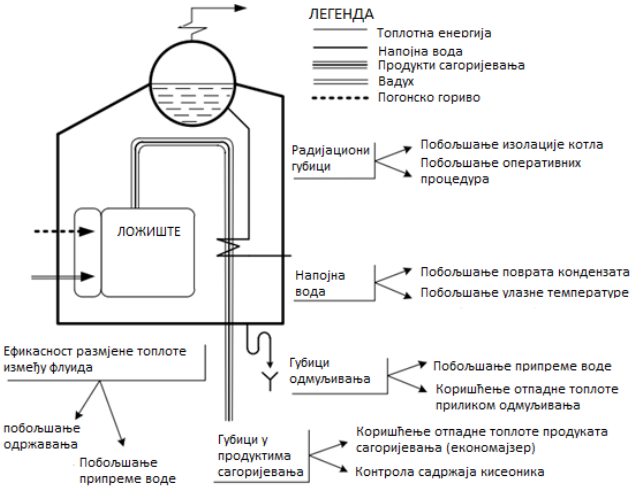

Слика 1. *Извори енергетских губитака и простор за побољшање енергетске ефикасности [1].*

У табели 1 приказане су потенцијалне могућности за уштеду енергије код котловских постројења [1].

Табела 1. *Могућности уштеде енергије код котловских постројења [1].*

Технике/методе	Потенцијал за уштеду [%]
Побољшање оперативних процедура и квалитета одржавања	до 5
Побољшање хемијске припреме воде	до 2
Контрола процеса одсољавања и одмуљивања	до 2
Коришћење отпадне топлоте процеса одмуљивања	до 3
Контрола процеса сагоријевања и садржаја кисеоника у продуктима сагоријевања	до 3
Контрола затварања пригушног елемента	до 1,5
Коришћење отпадне топлоте продуката сагоријевања	до 5
Предгријавање ваздуха за сагоријевање	до 5
Управљање распоредом оптерећења унутар котловнице	до 5
Примјена интегрисаног система аутоматског управљања	зависи од начина управљања

3 АНАЛИЗА ПРОБЛЕМА КОЈИ УТИЧУ НА ПОТРОШЊУ ТОПЛОТНЕ ЕНЕРГИЈЕ У ТЕРМОЕНЕРГЕТСКИМ ПОСТРОЈЕЊИМА

Како би се активности за побољшање енергетске ефикасности на микро плану могле боље сагледати, неопходно је познавати стање у термоенергетским постројењима. Познавањем прилика могу се боље препознати типични проблеми које су у мањој или већој мјери заједнички за све термоелектране, сличних карактеристика и услова експлоатације.

3.1 Оптимизација процеса сагоријевања

Уколико је императив да котловница функционише и у складу са важећом законском регулативом из области заштите животне средине (минимална емисија штетних гасова) неопходно је вршити контролу процеса сагоријевања. Регулација

процеса сагоријевања подразумјева контролу протока горива и ваздуха у циљу постизања највише могуће ефикасности процеса сагоријевања. Она се врши путем контроле температуре продуката сагоријевања на излазу из ложишта и контроле састава продуката сагоријевања, конкретно садржаја кисеоника. Удио кисеоника је параметар који пружа информацију о квалитету сагоријевања и самим тим представља веома добар показатељ ефикасности процеса сагоријевања. Примјеном ове мјере постиже се сталан процес сагоријевања што резултира уштедом енергије, чији се износ креће у границама до 3 % [2].

3.2 Одсољавање

Код испаривача са циркулацијом (природном или принудном) котловска вода кружи, па се због тога у њој повећава концентрација соли, тако да се садржај растворених материја у котловској води не повећава, због чега се мора водити рачуна о квалитету напојне воде. Код котлова са природном или принудном циркулацијом у добошу се врши раздвајање водене и парне фазе, при чему се паром одводи знатно мања количина примјеса, него напојном водом, што изазива повећање њихове концентрације у води која кружи у испаривачу. Ово може да доведе до повећања концентрације изнад дозвољених вриједности и стварања чврстих наслага на цијевима испаривача (слика 2а) које смањују ефикасност размјене топлоте, протоке и узрокују буку при раду котла. Због тога је потребно организовати непрекидно одвођење примјеса из ових испаривача што се назива континуалним одсољавањем. Континуално одсољавање врши се из воденог простора добоша, јер се тако смањује количина воде коју треба одвести. На слици 2б приказан је биланс континуалног одсољавања котла.

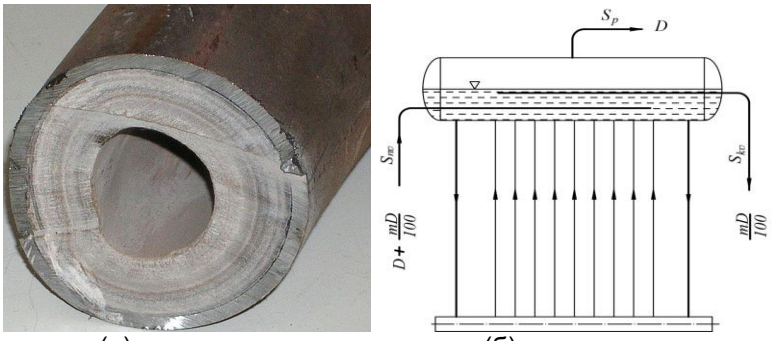

(а) (б)

Слика 2: *(а) чврсте наслаге на цијевима испаривача, (б) биланс континуалног одсољавање*

3.3 Одмуљивање котла

При производњи паре у парним котловима настаје чврсти талог (супстанце које су се налазиле у напојној води и оксиди гвожђа са унутрашње површине котла) који се нагомилава у унутрашњости котла и потребно га је одвести из добоша котла. Уколико се овај талог не одводи, он се нагомилава и тиме ремети правилан рад котла, што може довести и до хаварије.

Коришћење отпадне топлоте у процесу одмуљивања може смањити губитке одмуљивања до 50 %, што доводи до смањења потрошње топлотне

енергије од 0,5 до 2,5%. Уколико се користи и течни остатак из процеса одмуљивања може се остварити додатних 25 % чиме се остварује уштеда топлотне енергије од 0,75 до 3,75 % (за постројења која поседују ХПВ) [].

3.4 Замјена котлова

Под мјером замјена система за снабдијевање топлотом подразумијева се замјена котлова због:

- истеклог радног вијека, дотрајалости, неисплативости оправке и сл.,
- предимензионисаности у односу на тренутне потребе и дуготрајног рада при парцијалним оптерећењима
- преласка на друго гориво, и
- лошег стања, угрожене сигурности људи и опреме, и сл.

Старији котлови имају ефикасност од 56 до 70%, а савремени котлови могу да достигну ефикасност и преко 95%. Замјеном старих котлова и котловских инсталација, котловима новије генерације могу се смањити трошкови производње топлотне енергије и до 50%. Поред тога, прелазак на горива која при сагоријевању имају мању емисију штетних гасова и гасова који узрокују ефекат стаклене баште представљају додатну корист у смањењу загађења.

3.5 Замјена горионика

У горионицима долази до мијешања горива (течног или гасовитог) са ваздухом који је неопходан за сагоријевање. Од квалитета овог мијешања зависи и ефикасност сагоријевања, а тиме и рад котла (степен искоришћења котла као и састав димних гасова, односно емисија штетних продуката сагоријевања у животну средину). Код горионика новије генерације аутоматски се одржава одговарајући однос горива и ваздуха у мјешавини која сагоријева. Замјена постојећих горионика врши се: усљед завршеног радног вијека, неисплативости оправке, знатно веће потрошње горива у односу на номиналну и сл. Уградњом савремених горионика се смањују топлотни губици у котловском постројењу и остварују повољни ефекти са аспекта заштите животне средине.

3.6 Топлотна изолација котла и цијеви за развод топлотне енергије

Због високе температуре сагоријевања у котлу, висока је и температура плашта (оплате) котла. Постављањем топлотне изолације испод лимене оплате смањују се губици топлоте у околину. Под овом мјером се подразумијева [3]:

- постављање топлотне изолације плашта котла,
- постављање топлотне изолације резервоара на повишеној температури,
- замјена топлотне изолације опреме у котловници (цјевоводи, вентили, котао),
- замјена топлотне изолације паровода и резервоара паре,
- замјена топлотне изолације цјевовода за врелу (топлу) воду и резервоара за воду,
- замјена топлотне изолације резервоара мазута,
- замјена топлотне изолације осталих посуда на температури вишој од температуре околине,
- замјена топлотне изолације на опреми и цјевоводима (за воду, пару, мазут и др.) који се налазе ван котловнице.

Замјеном оштећене и постављањем нове изолације смањују се губици топлоте, а самим тим се повећава укупна енергетска ефикасност система. Постављање топлотне изолације представља један од најекономичнијих начина повећања енергетске ефикасности у индустрији и енергетици. У посљедње вријеме развијени су изолациони материјали чијом се примјеном обезбјеђује готово идеална топлотна изолација, код које су топлотни губици готово сведени на нулу.

3.7 Одвајачи кондензата

Одвајачи кондензата су уређаји који служе за одвајање кондензата или гасова који се не могу кондензовати (нпр. ваздуха) из тока паре, уз истовремено спречавање истицања паре. Неисправни одвајачи кондензата код којих је пригушни отвор отворен, пропуштају пару и беспотребно троше енергију, а у случају да се кондензат не враћа, губи се и топла вода.

Резултати неколико истраживања која се односе на одвајаче кондензата указују да неисправни одвајачи код којих се не спроводи програм проактивног одржавања, губе око 20 % паре која излази из котла. Исти извори наводе да се примјеном оваквог програма поменути губици могу редуковати, у просјеку, на око 6 % и да се овакви програми исплаћују за око 6 мјесеци [4].

3.8 Искоришћење топлоте димних гасова

Због неправилног рада котла и лоше размјене топлоте, температура димних гасова на излазу из котла је често изнад прописане за одређену врсту котлова. Уколико је температура димних гасова, изнад 200°C, топлота димних гасова могла би да се искористи, примјера ради, за загријавање воде или ваздуха за потребе гријања.

Под овом мјером се подразумијева уградња размјењивача топлоте у канале димних гасова у котлу, непосредно прије уласка гасова у димњак, ради загријавања воде или ваздуха топлотом димних гасова. На овај начин се знатно смањују топлотни губици котла усљед емитовања врелих гасова у атмосферу. Повећава се степен корисности котла и доприноси се бољем искоришћењу енергије, а самим тим и повећању енергетске ефикасности. Повећање температуре напојне воде за 10°C доводи до повећања ефикасности за 2%. У већини случајева, период поврата улагања у израду економајзера износи од 2 до 5 година. Повећавањем температуре ваздуха за 20°C, који се потом користи за сагоријевање горива, повећава се ефикасност сагоријевања за око 1%. За загријавање улазног ваздуха продуктима сагоријевања, обично се користе ротациони размјењивачи топлоте, а период поврата инвестиције је од 3 до 6 година.

3.9 Рекуперација топлоте из технолошких процеса

Процјена је да се у индустрији више од 50 % улазне енергије трансформише у отпадну топлоту, код котлова, хладњака, разних врста погона, мотора, пећи за разне материјале (стакло, метал, керамика и др.), сушара и сл. Потенцијал за уштеде кроз искоришћење ове отпадне топлоте (рекуперацију) у разним гранама индустрије је релативно велики. Циљ рекуперације је да се отпадна топлота искористи до најнижег остваривог нивоа температуре.

Искоришћење отпадне топлоте из технолошких процеса у сваком случају представља важну мјеру енергетске ефикасности, али је потребно детаљно провјерити изводљивост и исплативост прије доношења одлуке о провођењу овакве мјере. Рекуперација топлоте се може вршити на сљедеће начине:

- искоришћењем отпадне топлоте врелог ваздуха или гасова,
- искоришћењем отпадне топлоте расхладног постројења – коришћење топлоте кондензатора, итд.
- искоришћењем топлоте отпадних вода,
- искоришћењем топлоте при одмуљивању котла, и
- искоришћењем топлоте воде којом се хладе компресори.

4 ЗАКЉУЧЦИ

У посљедње вријеме активности које се проводе у циљу оптимизације потрошње топлотне енергије добијају све више на значају у свим областима човјекове дјелатности. Оптимизација потрошње топлотне енергије је значајна са енергетског, економског и еколошког аспекта. Управљање топлотном енергијом је посебно значајно у индустријским термоенергетским системима. У прошлости се приликом пројектовања индустријских и термоенергетских постројења није водило рачуна о потрошњи топлотне енергије за потребе производног процеса. Усљед смањења залиха и пораста цијена фосилних горива, ограничења емисија отпадних гасова у атмосферу и смањења трошкова производног процеса у посљедњих двадесетак година све већа пажња се посвећује оптимизацији потрошње топлотне енергије. Да би се смањила потрошња топлотне енергије у индустријским термоенергетским системима предузимају се неке од сљедећих активности: замјена застарјеле и енергетски неефикасне опреме у котловницама, побољшања на цијевној мрежи за дистрибуцију топлотне енергије до потрошача, искоришћење отпадне топлоте примјеном различитих техничких рјешења и др.

У раду је извршен детаљни приказ мјера којима се постиже оптимизација потрошње топлотне енергије и извршена анализа очекиваних уштеда топлотне енергије примјеном наведених мјера. Анализирана је могућност примјене савремених техничких рјешења у циљу уштеде примарне енергије, смањења емисије гасова стаклене баште, и повећања укупне енергетске ефикасности индустријских термоенергетских система.

ЛИТЕРАТУРА

[1] Милић, Д. (2022). Прилог истраживању потрошње топлотне енергије у индустријским термоенергетским постројењима, *Докторска дисертација*, Источно Сарајево.

[2] Thollander, P., Palm, J.: (2013). Improving Energy Efficiency in Industrial Energy Systems, London, *Springer*.

[3] Симић, С., Орашанин, Г., Голубовић, Д., Благојевић, Ј., Милић, Д.: (2017) Утицај топлотне изолације на смањење губитака енергије у индустријским и енергетским системима, *30. Procesing*, Београд.

[4] Јанкес, Г., Стаменић, М., Јовановић, А.: Повећање енергетске ефикасности у индустријским системима за снабдјевање паром и поврат кондензата, *Мрежа за енергетску ефикасност у индустрији Србије*, Београд.

COMETa 2022
6th INTERNATIONAL SCIENTIFIC CONFERENCE
17th - 19th December 2022
Jahorina, B&H, Republic of Srpska
University of East Sarajevo
Faculty of Mechanical Engineering
Conference on Mechanical Engineering Technologies and Applications

MEASURING NOZZLE TIP GEOMETRY INFLUENCE ON THE PNEUMATIC COMPARATOR PERFORMANCE

Jela M. Burazer[1], Dragiša M. Skoko†[2], Đorđe M. Novković[3], Milan R. Lečić[4], Goran S. Vorotović[5]

Abstract: Differential pneumatic comparators are devices that have great importance in todays production lines. Using the flapper-nozzle effect, these devices can control in an easy and quick way the dimensions of a produced machine part. The drawback of this method is the accumulation of impurities in the flapper-nozzle area that in time leads to narrowing the width of the zone between the nozzle and the workpiece. This is a consequence of a vacuum formation in the flapper-nozzle area. In this paper we present two different geometries of the measuring nozzle head. This new geometry is obtained by cuting out the nozzle from the inner side by two different angles: 45^o and 60^o. In that way we have obtained two new measuring nozzles that we can use for pneumatic control. It was already shown that this nozzle geometry is better compared to the standard nozzle. This paper tries to examine the effects that different cut out angles of the measuring nozzle head have on the behavior of the pneumatic comparator in the control process. This is done through presenting experimental results of pressure distributions in radial direction on the surface of the workpiece for different supply pressures p_o and different axial distances between the nozzle's front surface and the workpiece. It is demonstrated that higher cut out angle has better results in reduction of fouling of measuring nozzle head.

Key words: Measuring nozzle tip geometry, Pneumatic comparator, Pressure distribution.

[1] Jela Burazer, PhD, University of Belgrade, Faculty of Mechanical Engineering, Belgrade, Serbia, jburazer@mas.bg.ac.rs (CA)
[2] Dragiša Skoko†, PhD, University of Belgrade, Faculty of Mechanical Engineering, Belgrade, Serbia, dskoko@mas.bg.ac.rs
[3] Đorđe Novković, PhD, University of Belgrade, Faculty of Mechanical Engineering, Belgrade, Serbia, dnovkovic@mas.bg.ac.rs
[4] Milan Lečić, PhD, University of Belgrade, Faculty of Mechanical Engineering, Belgrade, Serbia, mlecic@mas.bg.ac.rs
[5] Goran Vorotović, PhD, University of Belgrade, Faculty of Mechanical Engineering, Belgrade, Serbia, gvorotovic@mas.bg.ac.rs

1 INTRODUCTION

Measurement and control of products, tools and devices represents a very important technological operation in the process of production, control and maintenance. In contrast to measurement, control is a comparison of one or more quantities simultaneously with another quantity of the same type. The control determines whether the actual measure is within the tolerance field. Devices used to control the dimensions of machine parts are called comparators, and according to the principle on which their work is based, comparators can be mechanical, optical, electrical, pneumatic, hydraulic.

Pneumatic comparators have found wide application in the control of machine products, both in small-scale and large-scale production. They are characterized by high precision [1], with the ability to clean the surface of the machine part being controlled by the pressurized air stream coming out of the measuring nozzle. In this way, the possibility of a control error is reduced. One of the problems that occurs in the operation of a pneumatic comparator is the accumulation of impurities on the tip of the measuring nozzle. This is due to the formation of a vacuum in the microchannel that is formed between the front surface of the measuring nozzle and the controlled machine part – the so called flapper-nozzle area. The influence of the measuring nozzle type geometry was the subject of [2-6]. It was shown in these papers that fouling of the measuring nozzle head can be reduced by altering the geometry of the nozzle's head. In the present research we will examine the influence of the angle at which the measuring nozzle is cut out on the performance of the pneumatic comparator. For this we will use two measuring nozzles with different cut out angles.

2 EXPERIMENTAL RIG

The experimental rig presented in *Figure 1*, comprises of several parts. The first part represents the supply of pressurized air, and it consists of: compressor AL, pressure regulator RP, manometer M and compressed air vessel.

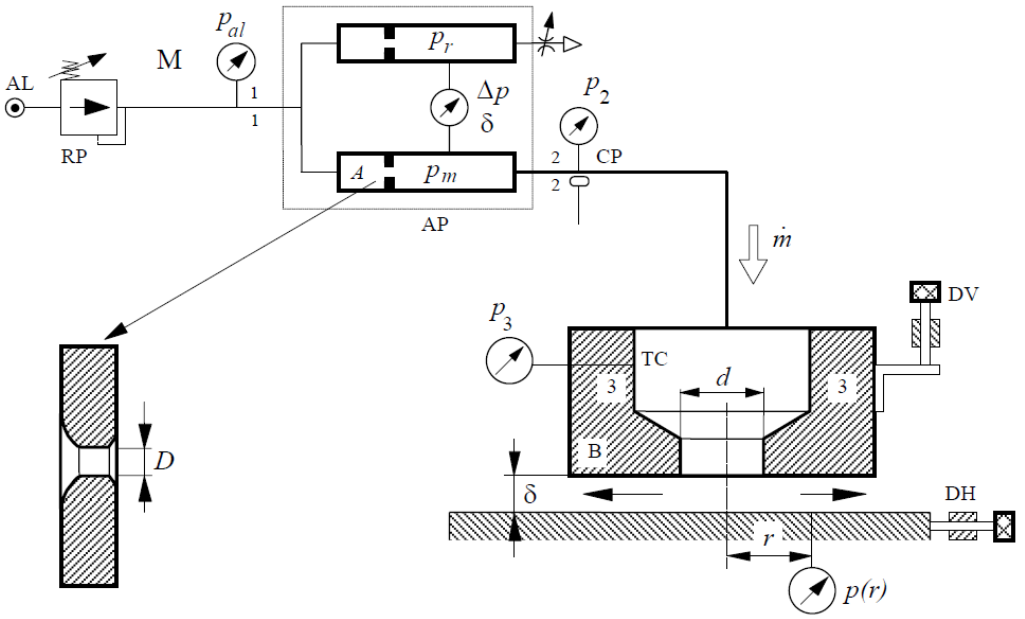

Figure 1. *Schematic of experimental rig.*

The second part is a differential pneumatic device AP, which has a working and measuring chamber connected by a membrane. The pressure difference between the measuring and working chambers, $\Delta p = p_m - p_r$, causes the movement of the membrane, which is detected as a pressure value on the manometer. There is an orifice inside the measuring chamber. This can be replaced with another that has different value of diameter. However, this is not done in the presented research. The orifice diameter D is not changed.

The third part is the nozzle positioner. The positioner is a mechanical micrometer device composed of three micrometers placed on all three axes, which enables the nozzle to be brought to the required point with an accuracy of 1 μm. When performing the experiment, the nozzle is translated vertically and horizontally. The positioner is attached to the pressure measuring stand. A hole with a diameter of D = 0.7 mm is drilled through the flat surface of the base, and on the bottom side is a connection for pressure measurement.

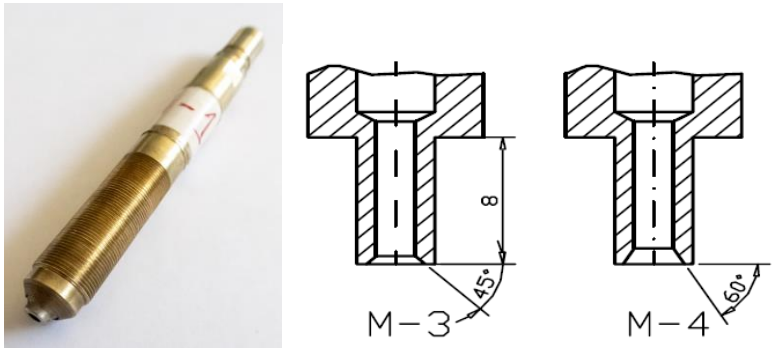

Figure 2. *Photograpy of a measuring nozzle and schematic of M3 and M4 nozzle tip geometry.*

The measuring nozzles used in these experiments are obtained when the standard nozzle with flat front surface of the head is cut out by two different angles on its inner side (see Figure 2). The cut out angle of the first nozzle M-3 is 45°, while the cut out angle for the other nozzle is 60°. The inner diameter of both nozzles bodies is 4 mm, and it changes to 2 mm near the nozzle's outlet. The outer diameter of the measuring nozzle's head is 4 mm.

3 RESULTS AND DISCUSSION

Figure 3 shows the distribution of pressure in the radial direction for nozzles M-3 and M-4 for two distances in the flapper-nozzle area at different values of supply pressure p_a. It is immediately noticeable that for the M-4 nozzle, the zone of approximately constant pressure is larger for a smaller axial distance. Also, for both values of the axial distance, for the M-4 nozzle, the negative pressure zone moves away from the nozzle axis, which is favorable. Also, the negative pressure values achieved for this nozzle are smaller for both shown axial distances. Practically, if we are talking about a smaller axial distance of 100 μm, at the highest supply pressure of 5 bar, a negative pressure occurs in the flapper-nozzle area for the M-3 nozzle. With the M-4 nozzle, for the same values of axial distance and supply pressure, there is no vacuum, even for the highest value of the supply pressure. On the other hand, the value of the negative pressure that occurs for p_a = 5 bar and 100 μm at the nozzle M-3

is small enough not to interfere with the proper operation of the pneumatic comparator. It is interesting to note that with nozzle M-4, both for a distance of 100 μm and for a distance of 250 μm, the linear part of the curve in the zone of lower pressure values is practically common for all supply pressures, while this is not the case with nozzle M3. There is some dispersion of values. The previous analysis shows us that M-4 nozzle can be used for higher supply pressures if the axial distance is smaller.

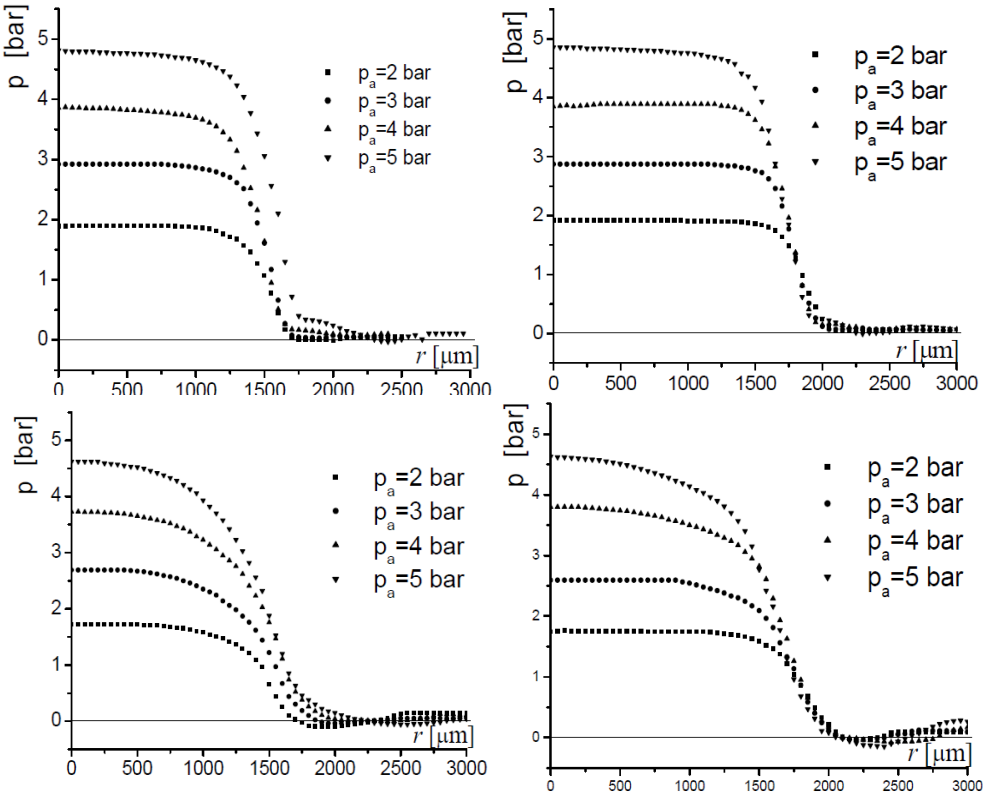

Figure 3. Pressure distribution for two different axial distances δ and variable supply pressures p_a.

Figure 4 shows the distribution of pressure in the radial direction for nozzles M-3 and M-4 for supply pressures p_a = 2 bar and p_a = 4 bar, at different values of the axial distance between the entire nozzle and the surface of the machine part being controlled. It is characteristic for both nozzles that as the distance δ increases, there is an underpressure in the flapper-nozzle area. For lower supply pressure, i.e. p_a = 2 bar, with nozzle M-4, the underpressure zone moves away from the nozzle axis in relation to nozzle M-3 under the same conditions, p_a and δ. It is characteristic that at the largest axial distance the vacuum zone moves away from the nozzle axis for both nozzles at higher supply pressure, while at lower pressure this is the case only for nozzle M-4. Practically, considering the dimensions of the nozzle (outer diameter 4 mm), it is clear that at a higher supply pressure, vacuum zone will not occur under the entire nozzle for any axial distance δ.

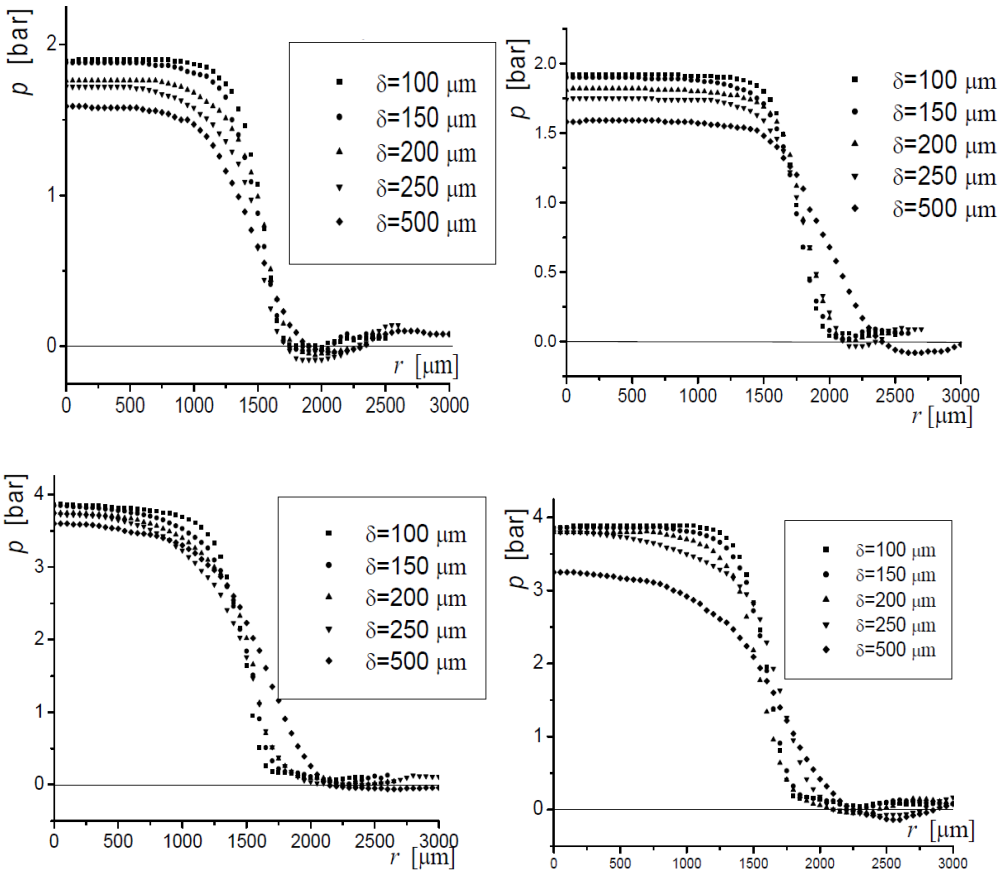

Figure 4. Pressure distribution for nozzles M-3 and M-4 for two different supply pressures and variable axial distance in the flapper-nozzle area.

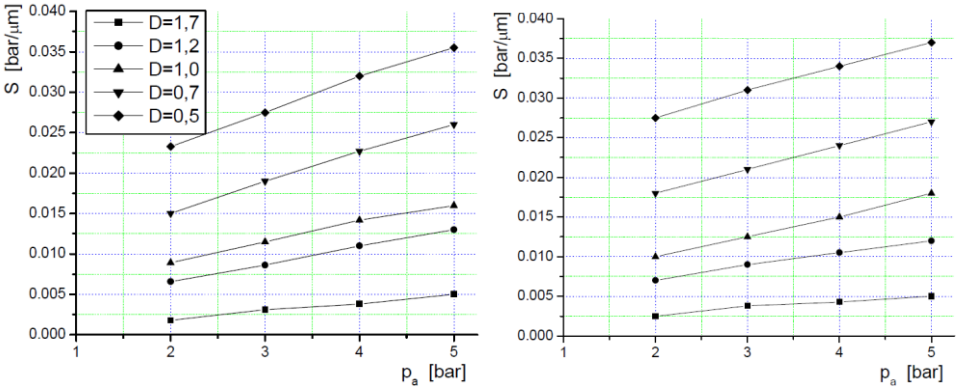

Figure 5. Changes in pneumatic sensitivity for nozzles M-3 and M-4, for different supply pressures p_a and orifice diameter D.

Figure 5 shows the dependences of the pneumatic sensitivity for nozzles M-3 and M-4 on the supply pressure, at different diameters of the throttle nozzle in the working chamber of the pneumatic comparator. This dependence is linear for both

nozzles, as expected. The pneumatic sensitivity of the M-4 nozzle is higher compared to the M-3 nozzle, for the same conditions of supply pressure and orifice diameter D. However, the influence of the nozzle type is more pronounced for smaller values of the diameter D and smaller supply pressure values. In other words, for one value of the orifice nozzle diameter, the influence of the nozzle type is greater for a lower supply pressure. On the other hand, if we observe the same supply pressure, the smaller the orifice diameter, the greater is the increase in pneumatic sensitivity in favor of the M-4 nozzle.

4 CONCLUSIONS

In the paper, the influence of the cut out angle of the nozzles of the pneumatic comparator on the pressure conditions that occur in the flapper-nozzle area is discussed. Two nozzles M-3 and M-4 were considered, whose cutting angles are 45^o and 60^o, respectively. In relation to the position of the negative pressure zone that occurs between the entire nozzle and the surface of the controlled part, we can conclude that the M-4 nozzle is more favorable, given the fact that the vacuum zone moves away from the axis of the nozzle. For smaller supply pressure values, even at a larger axial distance δ, the vacuum zone of the M-4 nozzle practically does not exist. When we talk about pneumatic sensitivity, the M-4 nozzle has a higher pneumatic sensitivity compared to the M-3 nozzle, for different values of the throttle diameter in the working chamber of the comparator. The influence of the type of nozzle is more pronounced at a lower supply pressure and a smaller diameter of the orifice D.

ACKNOWLEDGMENT

The results presented in this paper are from the research funded by the Ministry of Education, Science and Technological Development, Republic of Serbia, contract No. 2022451-03-68/2022-14/200105 (subproject TR35046, TR35045, TR35040).

REFERENCES

[1] Evans J.C, Morgan I.G. (1956). The application of pneumatic gauging to high precision linear measurement, J. *Scienti c instruments* 33, p.p. 388-390.

[2] Roy G, Crnojević C, Bettahar A, Florent P, Vo-Ngoc D. (1994). Influence of nozzle geometry in pneumatic metrology applications, *International Conference on fluid and thermal energy conversion*, Proc. Vol. 1, p.p. 363-368, Bali, Indonesia.

[3] Jermak Cz. J, Rucki M. (2001). The advantageous statistical metrological properties of the pneumatic sensor with two skewed nozzles, *Measurement Science Review*, Vol. 1, No. 1.

[4] Jermak Cz. J, Barišić B, Rucki M. (2010). Correction of the metrological properties of the pneumatic length measuring gauges through changes of the measuring nozzle head surface shape, *Measurement* Vol. 43, No. 9, p.p. 1217-1227, https://doi.org/10.1016/j.measurement.2010.06.001

[5] Jermak Cz. J, Jakubowicz M. (2012). Evaluation of properties of static air length gauges with slotted nozzles, Department of metrology and measurement systems, Institute of mechanical technology, Poznan University of technology Vol. 58, No. 11, p.p. 994-996.

[6] Jakubowic M. (2020). Accuracy of roundness assessment using air gauge with the slot-shaped measuring nozzle, *Measurement*, Vol. 155, 12 pages, https://doi.org/10.1016/j.measurement.2020.107558

COMETa 2022
6th INTERNATIONAL SCIENTIFIC CONFERENCE
17th - 19th December 2022
Jahorina, B&H, Republic of Srpska
University of East Sarajevo
Faculty of Mechanical Engineering
Conference on Mechanical Engineering Technologies and Applications

OPTIMIZATION OF WIND TURBINE ACTIVE POWER BY ADAPTIVE NEURO FUZZY ALGORITHM BASED ON TURBINE ATTRIBUTES

Dalibor Petkovic[1] Milos Milovancevic[2]

Abstract: Control methodologies could enable the wind turbine *active power regulation. Since short-term wind power prediction could be challenging due to the chaotic characteristics of wind speed in this paper was applied adaptive neuro fuzzy algorithm in order to determine the most important attributes the active power of wind turbine. Rotor RPM has the strongest influence on the active power of wind turbine. Hub temperature has the smallest impact on the active power of wind turbine. Combination of rotor RPM and generator winding 2 temperature is the optimal combination of two factors for the active power of wind turbine. The obtained results could be of practical importance to improve optimization of wind turbine power prediction as a key factor for successful business.*

Keywords: wind turbine; active power; feature selection; ANFIS.

1 INTRODUCTION

Renewable energy remains one of the most important topics for a sustainable future. Wind, being a perennial source of power, could be utilized to satisfy our power requirements. With the rise of wind farms, wind power forecasting would prove to be quite useful. However, the complexity and limited availability of wind resources create challenges that need to be addressed in order to continue improving wind energy harvesting. Control methodologies could enable the wind turbine power output regulation. Short-term wind power prediction is challenging due to the chaotic characteristics of wind speed.

In paper [1] has been investigated a classical control methodology for output power regulation for a turbine known that has been widely used for the twin problems of output regulation and disturbance rejection and simulations have been shown that the proposed methodology can substantially improve the output power regulation, reduce fatigue loads and also reduce actuator usage, relative to the baseline controllers. Model predictive control of a wind turbine-generator system is developed to stabilize power output and platform motion and reduce dynamic loads at mechanical

[1] University of Niš, Pedagogical Faculty in Vranje, Serbia
[2] University of Niš, Faculty for mechanical engineering, Serbia

and supporting components at high wind speeds [2]. A deep learning-based evolutionary approach for accurate forecasting of the power output in wind-turbine farms was developed in article [3] and the framework allows us to model the power curve of a wind turbine on a farm. A general framework for estimating annual averaged power output generation of wind turbines has been developed in article [4] where comparison of semi-empirical power output predictions and estimated power output predictions showed that Kappa and Wakeby distributions are superior to two-parameter Weibull distributions. Fatigue load could affect the secure and stability of wind turbine operation [5]. In paper [6] has been proposed a novel deep and transfer learning (DETL) framework, which enables a more efficient development of data-driven wind power prediction models for a group of wind turbines and computational experiments validate that the DETL outperforms conventional training methods on developing a batch of prediction models with a higher prediction accuracy and faster training speed. A new concept to modify wind farm's layout by deactivating selected wind turbines to maximize its total power output under different wind conditions has been developed in article [7]. Careful selection of data clustering technique for wind turbine is very essential as it has a significant impact on the accuracy of the prediction [8]. Various models based on measure-correlate-predict (MCP) methods have been used to estimate the long-term wind turbine power output (WTPO) at target sites for which only short-term meteorological data are available [9]. Accurate power prediction of a wind turbine under wake is important for wake suppression control, which is of great significance to reduce the energy loss of a wind farm [10].

The main goal of the study is to establish a model for estimation of the active power of the wind turbine. For such a purpose adaptive neuro fuzzy inference system (ANFIS) [11] is used since the methodology is suitable for the nonlinear data samples. The used wind turbine attributes are: ambient temperature, bearing shaft temperature, three blade pitch angles, gearbox bearing temperature, gearbox oil temperature, generator RPM, two generator winding temperatures, hub temperature, main box temperature and rotor RPM.

2 METHODOLOGY

2.1 Wind turbine dataset

In this investigation was used data of a certain windmill. The aim was to predict the wind power that could be generated from the windmill for the next 15 days. A long-term wind forecasting technique is thus required.

The dataset contains various weather, turbine and rotor features. Data has been recorded from January 2018 till March 2020. Readings have been recorded at a 10-minute interval. Table 1 shows input parameters and an output which is active power of the wind turbine.

Table 1: *Statistical information of input attributes and output power of wind turbine*

	Input/output parameters	*Minimum*	*Maximum*	*Standard deviation*
	Ambient Temperature	*21.08764*	*41.89491*	*3.456316*
	Bearing Shaft Temperature	*16.11988*	*55.08866*	*3.861263*
	Blade 1 Pitch Angle	*-1.57665*	*85.00029*	*9.153621*
	Blade 2 Pitch Angle	*-0.86433*	*85.00044*	*9.06482*

	Blade 3 Pitch Angle	*-0.86433*	*85.00044*	*9.06482*
	Gearbox Bearing Temperature	*23.00795*	*82.10266*	*8.481836*
	Gearbox Oil Temperature	*40.10956*	*70.70745*	*4.975482*
	Generator RPM	*8.51436*	*1809.942*	*406.2064*
	Generator Winding 1 Temperature	*38.62382*	*126.773*	*23.00673*
0	*Generator Winding 2 Temperature*	*38.28057*	*126.043*	*23.05384*
1	*Hub Temperature*	*13.6654*	*47.99619*	*3.509245*
2	*Main Box Temperature*	*15.22917*	*53.94978*	*4.15287*
3	*Rotor RPM*	*0*	*16.2735*	*3.633782*
	Active Power	*-10.7485*	*1779.032*	*632.5655*

2.2 ANFIS methodology

ANFIS network has five layers as it shown in Figure 1. The main core of the ANFIS network is fuzzy inference system. Layer 1 receives the inputs and convert them in the fuzzy value by membership functions. In this study bell shaped membership function is used since the function has the highest capability for the regression of the nonlinear data.

Figure 1: *ANFIS layers*

Bell-shaped membership functios is defined as follows:

$$\mu(x) = bell(x; a_i, b_i, c_i) = \frac{1}{1+\left[\left(\frac{x-c_i}{a_i}\right)^2\right]^{b_i}} \quad (1)$$

where $\{a_i, b_i, c_i\}$ is the parameters set and x is input. Second layer multiplies the fuzzy signals from the first layer and provides the firing strength of as rule. The third layer is the rule layers where all signals from the second layer are normalized. The fourht layer provides the inference of rules and all signals are converted in crisp values. The final layers sumarized the all signals and provied the output crisp value.

3 RESULTS

Feature selection represent a task of identification of the most important factors in order to improve prediction accuracy. This is useful preprocessing task before prediction process. ANFIS methodology was used for feature selection of the active power of wind turbine. The feature selection is important as preprocessing of the input parameters in order to remove unnecessary inputs. Data samples are divided in two groups for analyzing purpose. 50% data is used for training and remaining 50% is used for testing of the ANFIS network. ANFIS network is trained based on input and output pairs in Table 1.

Figure 2 and Table 2 shows single factors' influence on the active power of wind turbine. The input with the smallest training error has the strongest influence on the active power of wind turbine. As can be seen in Figure 2 the rotor RPM (input 13) has the strongest influence on the active power of wind turbine. On the other hand, hub temperature has the smallest impact on the active power of wind turbine.

Figure 3 shows combination of two factors influence on the active power of wind turbine. One can see that the combination of generator winding 2 temperature and rotor RPM is the optimal combination of two factors for the active power of wind turbine. On other words if one change in the same time the generator winding 2 temperature and rotor RPM then the active power of wind turbine could be the highest.

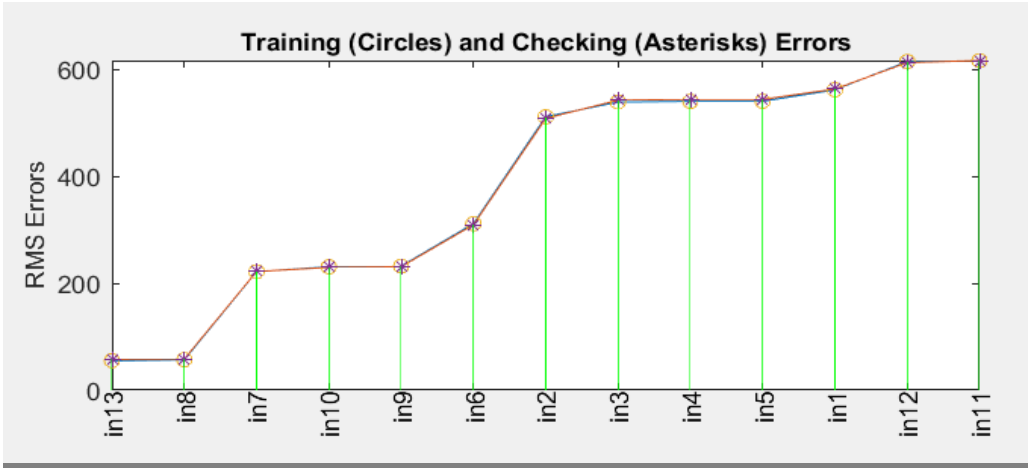

Figure 2: *Single factor influence on the active power of wind turbine*

Table 2: *Training and testing RMSE of single factor influence on the active power of wind turbine*

	Input parameters	*Training RMSE*	*Testing RMSE*
	Ambient Temperature	*561.3820*	*562.8017*
	Bearing Shaft Temperature	*511.0966*	*507.8864*

	Blade 1 Pitch Angle	*538.4638*	*541.9326*
	Blade 2 Pitch Angle	*539.8116*	*543.4384*
	Blade 3 Pitch Angle	*539.8116*	*543.4384*
	Gearbox Bearing Temperature	*311.2694*	*309.1802*
	Gearbox Oil Temperature	*221.4718*	*221.7888*
	Generator RPM	*56.8365*	*58.4045*
	Generator Winding 1 Temperature	*231.9365*	*230.8254*
0	*Generator Winding 2 Temperature*	*230.6122*	*229.5155*
1	*Hub Temperature*	*615.9637*	*616.0648*
2	*Main Box Temperature*	*614.1134*	*612.2216*
3	*Rotor RPM*	*54.9171*	*57.6749*

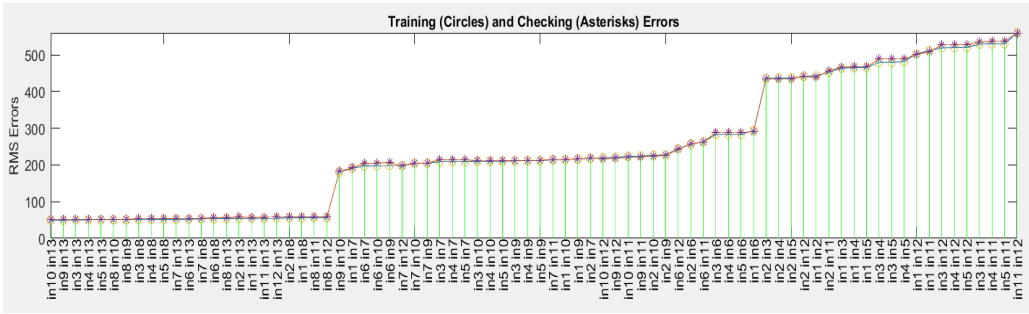

Figure 3: *Two factors influence on the active power of wind turbine*

Figure 4 an Table 3 shows three optimal combinations for prediction of the active power of wind turbine. One can note the blade 2 pitch angle is the third parameter which has impact if it is combined with generator winding 2 temperature and rotor

RPM. However, the training and checking RMSEs do not decreased significantly for more parameters hence it is suitable to use combination of two factors.

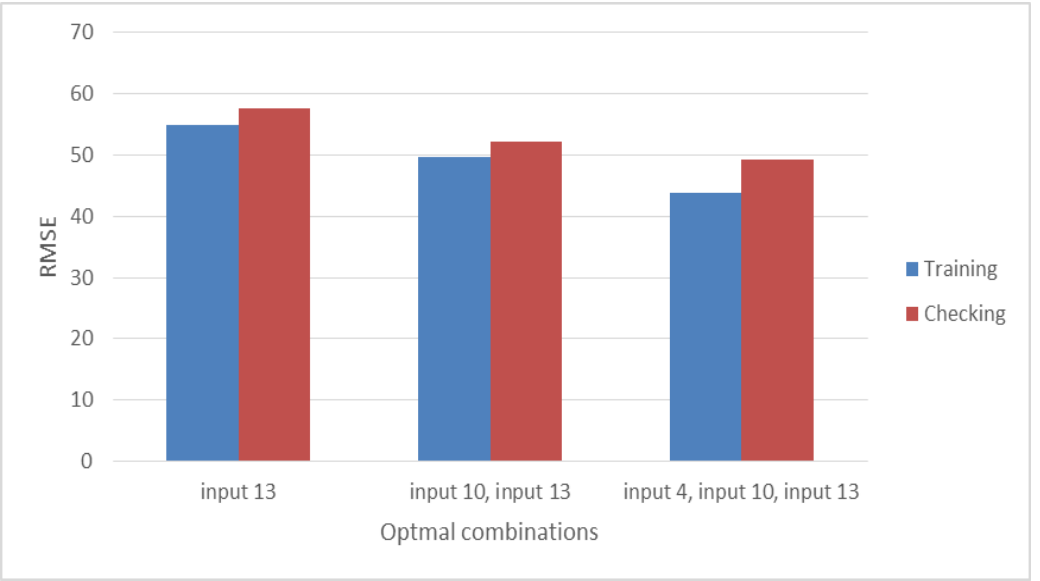

Figure 4: *Three optimal combinations for prediction of the active power of wind turbine*

Table 3: *Three optimal combinations for prediction of the active power of wind turbine*

	Optimal combinations	*Training RMSE*	*Testing RMSE*
one input	*Rotor RPM*	*54.9171*	*57.6749*
two inputs	*Generator Winding 2 Temperature, Rotor RPM*	*49.5976*	*52.1961*
three inputs	*Blade 2 Pitch Angle, Generator Winding 2 Temperature, Rotor RPM*	*43.8055*	*49.2135*

Two selected parameters are extracted and new ANFIS model is created and trained in 100 epochs. Figure 5 shows training and validation error curves for two selected parameters. One can note the minimal training errors occurs at 100th epoch.

Figure 6 shows decision surface for active power of wind turbine based on the created ANFIS model for two parameters. One can note the output value is the highest for highest rotor RPM. However, it is not real in practice while generator winding 2 temperatures does not have impact on the active power of wind turbine if the rotor

RPM has the highest value. Figure 7 presents the data distribution for two selected parameters and one can note the solid data distribution hence the obtained results are relevant.

Figure 5: *Training and validation error curves for two selected parameters*

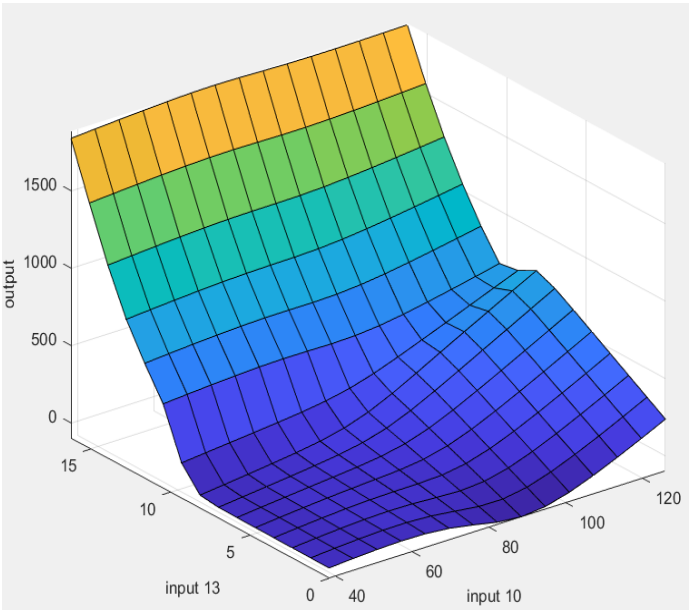

Figure 6: *Decision surface for e active power of wind turbine based on two selected parameters*

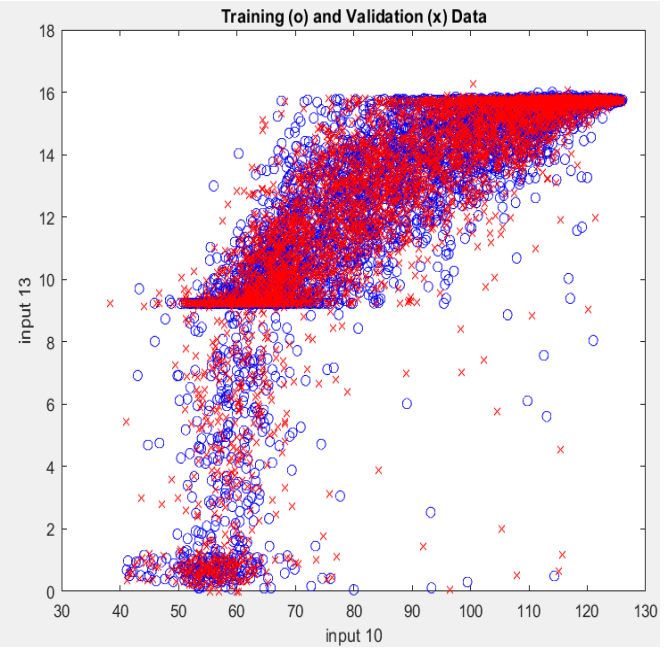

Figure 7: *Data distribution for two selected parameters*

4 CONCLUSION

Wind energy represents an important future energy source due to rising global interest in renewable energies. For this reason, power output prediction of wind turbines is a prominent task for supporting decisions regarding future sites.

The emergence of new sites for wind energy exploration requires an accurate prediction of the potential power output of a typical utility-scale wind turbine in such areas. This study aims to conceptualize the multiple key facets of power output of wind turbine and identify the most important attributes. To do so the most advanced machine learning techniques cold be used to study wind turbine. The main concluding remarks are:

- Rotor RPM has the strongest influence on the active power of wind turbine.
- Hub temperature has the smallest impact on the active power of wind turbine.
- Combination of rotor RPM and generator winding 2 temperature is the optimal combination of two factors for the active power of wind turbine.

REFERENCES

[1] Karimpour, M., Schmid, R., & Tan, Y. (2021). Exact output regulation for wind turbine active power control. *Control Engineering Practice*, *114*, 104862.\.

[2] Wakui, T., Nagamura, A., & Yokoyama, R. (2021). Stabilization of power output and platform motion of a floating offshore wind turbine-generator system using model predictive control based on previewed disturbances. *Renewable Energy*, *173*, 105-127.

[3] Neshat, M., Nezhad, M. M., Abbasnejad, E., Mirjalili, S., Groppi, D., Heydari, A., ... & Wagner, M. (2021). Wind turbine power output prediction using a new hybrid neuro-evolutionary method. *Energy*, *229*, 120617.
[4] Wacker, B., Seebaß, J. V., & Schlüter, J. C. (2020). A modular framework for estimating annual averaged power output generation of wind turbines. *Energy Conversion and Management*, *221*, 113149.
[5] Peng, C., Zou, J., Li, Y., Geng, H., & Zhang, Z. (2020). Optimization Control for Flapping Load Mitigation and Output Power Levelling of Wind Turbine. *IFAC-PapersOnLine*, *53*(2), 12121-12126.
[6] Liu, X., Cao, Z., & Zhang, Z. (2021). Short-term predictions of multiple wind turbine power outputs based on deep neural networks with transfer learning. *Energy*, *217*, 119356.
[7] Haces-Fernandez, F., Li, H., & Ramirez, D. (2019). Improving wind farm power output through deactivating selected wind turbines. *Energy Conversion and Management*, *187*, 407-422.
[8] Adedeji, P. A., Akinlabi, S., Madushele, N., & Olatunji, O. O. (2020). Wind turbine power output very short-term forecast: a comparative study of data clustering techniques in a PSO-ANFIS model. *Journal of Cleaner Production*, *254*, 120135.
[9] Díaz, S., Carta, J. A., & Matías, J. M. (2018). Performance assessment of five MCP models proposed for the estimation of long-term wind turbine power outputs at a target site using three machine learning techniques. *Applied Energy*, *209*, 455-477.
[10] Li, X., Qiu, Y., Feng, Y., & Wang, Z. (2021). Wind turbine power prediction considering wake effects with dual laser beam LiDAR measured yaw misalignment. *Applied Energy*, *299*, 117308.
[11] Jang, J.-S.R, ANFIS: Adaptive-Network-based Fuzzy Inference Systems, IEEE Trans. On Systems, Man, and Cybernetics (1993), Vol.23, 665-685.

COMETα 2022
6th INTERNATIONAL SCIENTIFIC CONFERENCE
17th - 19th December 2022
Jahorina, B&H, Republic of Srpska
University of East Sarajevo
Faculty of Mechanical Engineering
Conference on Mechanical Engineering Technologies and Applications

PREDVIĐANJE DOTOKA PRIMJENOM VJEŠTAČKIH NEURONSKIH MREŽA SA RAZLIČITIM STRUKTURAMA MREŽA

Marina Milićević[1], Budimirka Marinović[2]

Rezime: Predviđanja u hidrologiji igraju ogromnu ulogu u upravljanju vodnim resursima. Ona su se u prošlosti uglavnom oslanjala na statističke modele vremenskih serija. U ovom radu je predstavljena izrada i analiza više vještačkih neuronskih mreža različitih arhitektura kojima se predviđa dotok u akumulaciju. U izradi modela poseban naglasak je stavljen na određivanje broja neurona u skrivenim slojevima.

Analizirani modeli mreža sastoje se od ulaznog sloja veličine 4, izlaznog sloja veličine 1 i jednog, odnosno dva skrivena sloja u kojima je broj neurona variran. Izlazni sloj predstavlja dotok u akumulaciju, a ulazni slojevi predstavljaju količinu padavina sa 4 lokacije koje su značajne za posmatrani dotok. Modeli su razvijeni u programskom paketu MATLAB, koristeći Levenberg-Marquardt algoritam (MATLAB-ova funkcija fitnet), kao jedan od najčešće korišćenih algoritama u hidrološkim predviđanjima, dok su kao kriterijumi za procjenu performansi neuronskih mreža posmatrani statistički kriterijumi: srednja kvadratna greška (RMSE), srednja relativna greška (MRE) i koeficijent korelacije (R^2).

Ključne riječi: neuronske mreže, neuroni, skriveni sloj, dotok.

PREDICTION OF INFLOW USING ARTIFICIAL NEURAL NETWORKS WITH DIFFERENT NETWORK STRUCTURES

Abstract: Realiable and accurate forecasts play a huge role in water resource management. In the past, they mainly relied on statistical time series models. This research aims to develop neural network for wathe inflow selecting an optimum number of neurons in the hidden layer.

The created network models consist of an input layer of size 4, an output layer of size 1 and one or two hidden layers in which the number of neurons is varied. The output layer

[1] doc. dr, Marina Milićević, Fakultet za proizvodnju i menadžment Trebinje, Univerzitet u Istočnom Sarajevu, Trebinje, Bosna i Hercegovina, marina.milicevic@fpm.ues.rs.ba
[2] prof. dr, Budimirka Marinović, Fakultet za proizvodnju i menadžment Trebinje, Univerzitet u Istočnom Sarajevu, Trebinje, Bosna i Hercegovina, budimirka.marinovic@fpm.ues.rs.ba

represents the inflow into the reservoir, and the input in neural network are the amount of precipitation from 4 locations that are significant for the observed inflow. The models were developed in the MATLAB software package, using the Levenberg-Marquardt algorithm (MATLAB's fitnet function), as one of the most frequently used algorithms in hydrological predictions. In order to evaluatethe quality of the prediction of neural network we used evaluation criteria: root mean square error (RMSE), mean relative error (MRE) and coefficient of determination (R^2).

Key words: neural network, neurons, hidden layer, inflow.

1 UVOD

Optimalna struktura neuronske mreže u velikoj mjeri zavisi od broja skrivenih slojeva i broja neurona u skrivenim slojevima. Broj neurona u skrivenom sloju jednoznačno određuje broj težinskih koeficijenata koje je potrebno odrediti. Međutim, broj neurona koji će ostvariti željeno preslikavanje nije tako jednostavno odrediti s obzrirom da je on funcija velikog broja poznatih parametara, ali i potpuno nepoznatih parametara. Tako, optimalan broj neurona zavisi od broja ulaza i izlaza, broja obučavajućih parova, veličine šuma u obučavajćim parovima, složenosti funkcije greške, arhitekture neuronske mreže i algoritma obučavanja [1]. U tom smislu ne postoji opšti algoritam čija bi primjena tokom procesa obuvačavanja vještačke mreže dovela do optimalnog broja neurona za postmatrani problem [2].

U ovom istraživanju su razmatrane različite strukture vještačkih neuronskih mreža za predviđanje dotoka u akumulaciju. Razmatrane su neuronske mreže sa jednim i dva skrivena sloja. Najprije je izvršena analiza neuronskih mreža sa jednim skrivenim slojem pri čemu je broj neurona u njemu variran od 1 do 100, a nakon toga mreža sa dva skrivena sloja u kojima je broj neurona variran u slojevima od 1 do 10. Ocjena performansi je vršena na osnovu vrijednosti kriterijuma srednje kvadratne greške (RMSE), srednje relativne greške (MRE) i koeficijenta korelacije (R^2).

2 VJEŠTAČKE NEURONSKE MREŽE

Neurnoska mreža predstavlja skup algoritama koji nastoje da prepoznaju odnose u skupu podataka kroz proces koji oponaša način rada ljudskog mozga. Pogodne su za modeliranje i predviđanje promjene funkcionalnih karakteristika posmatranih sistema ili procesa, s obzirom da mogu biti obučavane da nađu rješenje, prepoznaju modele ponašanja, klasifikuju podatke i predvide buduće događaje [2].

2.1 Ocjenjivanje predviđanja dotoka

Za ispitivanje modela uopšteno se koriste grafičke i numeričke metode. Grafičke metode omogućavaju vizuelno poređenje odziva modela i mjerenih vrijednosti dok numeričke metode kvantiziraju odstupanje modela od stvarnih vrijednosti na osnovu statističkih mjera kvaliteta.

Za određivanje kvaliteta modela neuronskih mreža kao kriterijum za izbor arthitekture neuronske mreže koja daje nabolje rezultate kao kriterijumi kvaliteta modela koristila se [3]:

- srednja kvadratna greška (RMSE),
- srednja relativna greška (MRE) i
- koeficijent korelacije (R^2).

Srednja kvadratna greška (poznata i pod nazivom standardna devijacija) je najčešći metod za ocjenjivanje učinka vještačke neuronske mreže. Određuje se na osnovu razlika pojedinačnih rezultata mjerenja i srednje vrijednosti istih:

$$RMSE = \sqrt{\frac{1}{n}\sum_{i=1}^{n}(y_i - \overline{y_i})^2}$$

Srednja relativna greška određuje grešku napravljenju u predviđanju u odnosu na stvarne dimenzije i veličinu koja se mjeri.

$$MRE = \frac{1}{n}\sum_{i=}^{n}\frac{y_i - \overline{y_i}}{y_i}$$

Koeficijent korelacije određuje međusobnu povezanost dvaju podataka (u ovom slučaju stvarnih i predviđenih vrjednosti izlaza). Može uzeti vrijednosti iz intervala (0,1) i što je R^2 veći, povezanost posmatranih podataka je veća. Definiše se kao:

$$R^2 = 1 - \frac{\sum_{i=1}^{n}(y_i - \hat{y}_i)^2}{\sum_{i=1}^{n}(y_i - \overline{y}_i)^2}$$

U navedenim izrazima su: y_i vrijednost iz mjerenja; $\hat{y}_i$ vrijednost koju je mreža predvidila; $\overline{y_i}$ prosječna vrijednost podataka iz mjerenja; n ukupan broj mjerenja (broj podataka).

Modeli sa manjom vrijednošću RMSE i MRE ukazju na veći kvalitet algoritma, a vrijednost ovog parametra varira od 0 do ∞. Koeficijent R^2 se koristi za određivanje stepena sličnosti između predviđene vrijednosti i njene posmatrane vrijednosti. Najbolje vrijednost za R^2 je 1 što ukazuje na visoke performanse modela.

3 EKSPERIMENTALNI REZULTATI

U radu je izvršen postupak određivanja optimalnog broja skrivenih neurona na osnovu eksperimenta nad samim modelom. Kao ulazi u neuronsku mrežu odabrano je 4 neurona, količina padavina sa 4 različite lokacije, dok je izlaz iz mreže dotok u akumulaciju. Za trening je iskorišćeno 1278 podataka (70% ulaznih podataka), za validaciju 365, a za testiranje 183 podatka. U tabeli 1 su prikazane minimalne, maksimalne i srednje vrijednosti ulaznih vrijednosti i izlaznog podatka. Podaci korišteni u modelu su najprije normalizovani.

Tabela 1: Rang podataka korišenih u neuronskoj mreži

	minimum	*maksimum*	*Srednja vrijednost*
Lokacija 1	*0*	*118.700*	*4.425*
Lokacija 2	*0*	*177.300*	*4.663*
Lokacija 3	*0*	*150.700*	*4.644*
Lokacija 4	*0*	*145*	*4.335*
Izlazni podatak	*-12.93*	*501.04*	*59.718*

Razmatrane mreže se sastoje od ulaznog sloja veličine 4, izlaznog sloja veličine 1 i jednog, odnosno dva skrivena sloja u kojima je broj neurona variran. Ukupan broj neuronskih mreža koji je u eksperimentu obrađen je 200 od čega 100 sa jednim skrivenim slojem i 100 sa dva skrivena sloja. Prethodno pomenute greške su izračunate za svaki od slučajeva, a zatim su analizirane i prikazane tabelarno i grafički. Ulazni podaci podjeljeni su u tri međusobno disjunktne grupe u odnosu 70:20:10 i to na podatke za trening mreže, podatke za validaciju i podatke za testiranje, redom. Modeli su razvijeni u programskom paketu MATLAB, koristeći Levenberg-Marquardt algoritam

(MATLAB-ova funkcija fitnet). Ovo je jedan od najčećće korištenih algoritama u hidrološkim predviđanjijma [4, 5].

3.1 Neuronske mreže sa jednim skrivenim slojem

U neuronskim mrežama sa jednim skrivenim slojem broj neurona je variran od 1 do 100. Dobijene greške mjerenja su prikazane u tabeli 2.

Tabela 2.: Greške mjerenja za različit broj neurona u neuronskoj mreži sa jednim skrivenim slojem

Broj neu	Tip greške	Vrjednost greške									
1 - 10	RMSE*	0.1321	0.1261	0.1293	0.1304	0.1264	0.1279	0.1354	**0.1253**	0.1310	0.1296
	RMSE	0.1307	0.1323	0.1370	0.1293	0.1382	0.1329	0.1368	0.1256	0.1272	0.1211
	R^2	0.2439	0.1950	0.2740	0.3338	0.2632	0.1893	0.2779	0.1978	0.2198	0.2920
	MRE*	0.026	-0.010	-0.008	0.136	-0.000	-0.023	0.0432	0.018	-0.011	-0.083
	MRE	0.0504	0.022	-0.058	0.072	-0.049	-0.051	0.0555	-0.050	0.058	0.029
11 - 20	RMSE*	0.1327	0.1292	0.1276	0.1295	0.1272	0.1299	0.1276	0.1319	0.1298	0.1332
	RMSE	0.1242	**0.1159**	0.1388	0.1279	0.1384	0.1336	0.1412	0.1309	0.1267	0.1299
	R^2	0.3073	**0.4215**	0.3225	0.2886	0.1887	0.2908	0.1864	0.2590	0.2042	0.2465
	MRE*	-0.017	-0.013	-0.0012	0.017	-0.013	0.105	**-0.005**	0.048	-0.036	-0.265
	MRE	0.087	0.071	0.0112	-0.202	-0.054	0.130	**0.001**	0.034	0.059	-0.122
21 -30	RMSE*	0.1253	0.1290	0.1238	0.1229	0.1281	0.1305	0.1270	0.1291	0.1216	0.1285
	RMSE	0.1293	0.1350	0.1293	0.1402	0.1367	0.1456	0.1325	0.1421	0.1305	0.1341
	R^2	0.2536	0.2324	0.2927	0.2996	0.2621	0.1042	0.2726	0.3044	0.2472	0.2546
	MRE*	0.002	-0.037	0.036	0.081	-0.0756	-0.087	-0.104	-0.016	0.000	0.071
	MRE	-0.034	-0.067	-0.073	-0.024	-0.1406	0.034	-0.103	-0.043	0.022	0.131
31 -40	RMSE*	0.1249	0.1258	0.1284	0.1267	0.1269	0.1290	0.1247	0.1285	0.1266	0.1280
	RMSE	0.1347	0.1357	0.1341	0.1405	0.1273	0.1487	0.1298	0.1325	0.1421	0.1327
	R^2	0.2335	0.2127	0.3494	0.2926	0.2947	0.2025	0.3241	0.1414	0.3064	0.2798
	MRE*	0.0094	-0.040	0.077	0.048	-0.045	0.128	0.0315	0.020	0.030	-0.146
	MRE	-0.0359	0.014	0.046	-0.026	0.097	0.126	0.0423	0.122	0.004	-0.149
41 -50	RMSE*	0.1255	0.1260	0.1249	0.1261	0.1276	0.1443	0.1231	0.1219	0.1249	0.1233
	RMSE	0.1238	0.1412	0.1364	0.1412	0.1457	0.1708	0.1385	0.1344	0.1321	0.1366
	R^2	0.2952	0.2609	0.3449	0.2835	0.2037	0.0808	0.1900	0.3485	0.3056	0.3159
	MRE*	0.100	0.006	-0.0816	-0.049	-0.027	0.286	0.026	-0.016	-0.0590	-0.046
	MRE	-0.016	-0.045	-0.2890	0.007	-0.168	0.303	-0.109	-0.121	-0.0290	-0.053
51 -60	RMSE*	0.1273	0.1326	0.1220	0.1264	0.1254	0.1274	0.1206	0.1213	0.1205	0.1233
	RMSE	0.1221	0.1481	0.1346	0.1353	0.1348	0.1315	0.1534	0.1408	0.1368	0.1532
	R^2	0.2864	0.1419	0.2577	0.1299	0.1102	0.1091	0.2641	0.2104	0.3274	0.0204
	MRE*	0.009	-0.288	-0.059	-0.148	-0.0275	-0.019	-0.077	-0.001	0.002	-0.093
	MRE	0.008	-0.289	-0.009	0.013	0.0721	-0.792	-0.053	-0.073	-0.089	0.095
61 -70	RMSE*	0.1199	0.1372	0.1240	0.1265	0.1267	0.1233	0.1233	0.1212	0.1240	0.1215
	RMSE	0.1419	0.1267	0.1329	0.1469	0.1457	0.1471	0.1320	0.1375	0.1344	0.1335
	R^2	0.1877	0.2430	0.2492	0.1461	0.3105	0.0962	0.3000	0.1671	0.2654	0.3101
	MRE*	-0.0325	0.007	0.008	0.114	-0.043	0.006	-0.5990	0.020	0.008	0.127
	MRE	-0.0298	-0.060	-0.007	0.092	-0.059	-0.029	0.0004	-0.231	0.020	0.019
71 -80	RMSE*	0.1227	0.1250	0.1219	0.1219	0.1262	0.1222	0.1292	0.1229	0.1153	0.1202
	RMSE	0.1343	0.1349	0.1508	0.1449	0.1632	0.1453	0.1303	0.1500	0.1410	0.1338
	R^2	0.2974	0.0172	0.1854	0.0760	0.0972	0.2460	0.2359	0.1473	0.2872	0.1400
	MRE*	-0.036	-0.144	-0.0091	0.014	-0.067	0.002	0.077	0.001	-0.0101	-0.063
	MRE	0.142	-0.046	-0.0376	-0.025	-0.182	-0.068	0.102	-0.137	-0.0719	-0.043
81 -90	RMSE*	0.1216	0.1264	0.1200	0.1264	0.1202	0.1188	0.1215	0.1257	0.1250	0.1237
	RMSE	0.1316	0.1772	0.1507	0.1308	0.1466	0.1699	0.1542	0.1432	0.1472	0.1535
	R^2	0.1878	0.1166	0.1628	0.1499	0.1494	0.0103	0.0949	0.1210	0.1976	0.1567
	MRE*	0.002	-0.051	-0.006	0.008	-0.0005	-0.026	-0.033	-0.003	-0.010	0.151
	MRE	-0.034	-0.055	0.069	0.124	-0.0908	-0.080	-0.035	0.069	0.123	0.087
91 -100	RMSE*	0.1143	0.1218	0.1351	0.1252	0.1173	0.1250	0.1413	0.1233	0.1224	0.1284
	RMSE	0.1605	0.1572	0.1594	0.1239	0.1528	0.1508	0.1426	0.1275	0.1331	0.1496
	R^2	0.0884	0.0663	0.1086	0.3082	0.1369	0.1373	0.0467	0.2158	0.3847	0.0532
	MRE*	0.0381	0.044	0.338	0.172	-0.012	-0.023	-0.4383	-0.023	0.008	0.029
	MRE	-0.0148	0.137	0.259	-0.334	-0.138	-0.108	-0.2656	-0.007	0.261	0.002

Srednja kvadratna greška izračunata je posebno na podacima za validaciju (RMSE) i na podacima za treniranje (RMSE*). RMSE* je dostigla najveću vrijednost od 0,1443 za mrežu sa 46 neurona u skrivenom sloju, a najmanju vrijednost od 0.1253 za 8 neurona u skrivenom sloju. Slično je i RMSE najmanju vrijednost od 1.1159 dostigla za 12 neurona u skrivenom sloju. Takođe iz tabele 2 i slike 1 se vidi da su za 8 neurona

RMSE*=0.1253 i RMSE=0.1256 skoro identične, a nakon 8 neurona grafici ovih grešaka prikazuju veća odstupanja, pa se zaključuje da po kriterijumu srednje kvadratne greške, mreža sa 8 neurona u jednom skrivenom sloju daje najbolje rezultate.

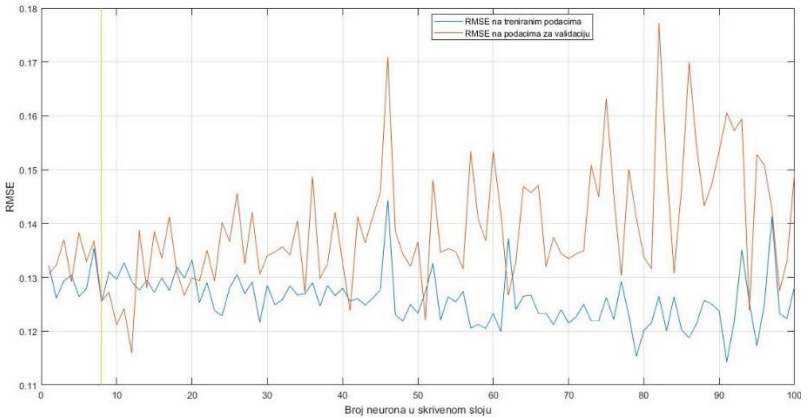

Slika 1: *Srednja kvadratna greška za podatke za validaciju i podacima za treniranje za neuronsku mrežu sa jednim skrivenim slojem*

Koeficijent korelacije R^2 ima najveću vrijednost 0.4215 za mrežu sa 12 neurona (slika 2), pa po ovom kriterijumu ova mreža daje najbolje rezultate. Po kriterijumu relativne greške, mreža sa 17 neurona u skrivenom sloju, daje najbolje rezultate, grafik na slici 3.

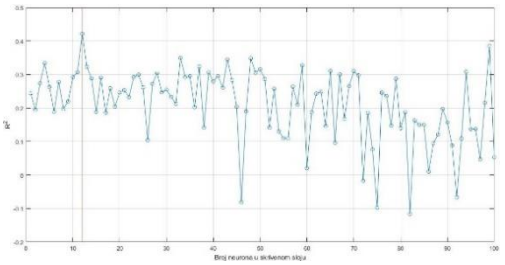

Slika 2: *Koeficijent korelacije R^2 za različit broj neurona u skrivenom sloju*

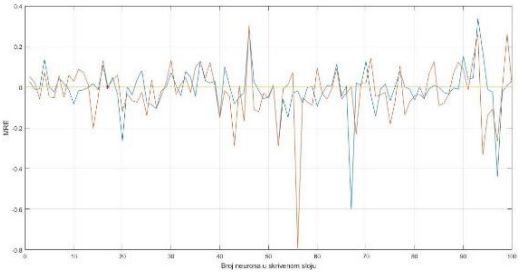

Slika 3*: Vrijednosti relativne greške u zavisnosti od broja neurona u skrivenom sloju*

Na osnovu navedenog može se zaključiti da u mreži sa jednim skrivenim slojem broj neurona u tom sloju ne bi trebao prelaziti 17. Na slici 4 dat je uporedn prikaz stvarnih vrijednosti dotoka i vrijednosti dobijenih neuronskom mrežom za čitav domen od 1826 podataka (lijevo) i samo za podatke korišćene za testiranje (desno) koji ima 10% od ukupnog broja podataka (tačno 183 podatka za testiranje mreže), i to na mreži arhitekture 4 – 8 – 1.

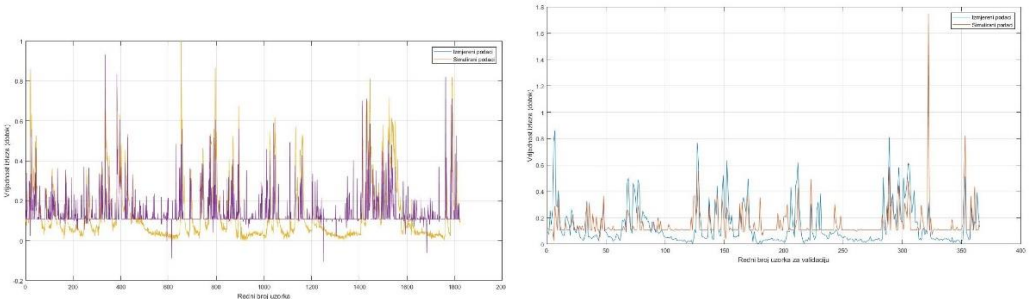

Slika 4: *Uporedni prikaz stvarnih vrijednosti i vrijednosti dobijenih simulacijom neuronske mreže, lijevo čitav domen, desno podaci korišćeni za testiranje neuronske mreže*

3.2 Neuronske mreže sa dva skrivena sloja

U neuronskim mrežama sa dva skrivena sloja broj neurona je variran u opsegu 1 do 10 u oba sloja. Tako je obuhvaćeno ukupno 100 mreža sa dva skrivena sloja. Slika 5, lijevi 3D prikaz, prikazuje vrijednosti srednje kvadratne greške RMSE i RMSE*. Opseg RMSE kreće se od 0.1126 za mrežu sa arhitekturom 17 – 2 – 3 – 1 do 1.1530 za mrežu sa arhitekturom 17 – 1 – 8 – 1.

Na slici 5 dat je i 2D prikaz (desno) ovih grešaka za broj neurona od 1 do 100 raspoređenih po slojevima, gdje prvih 10 tačaka predstavlja grešku za mrežu u kojoj je u drugom sloju uvijek 1 neuron, a u prvom sloju broj neurona varira od 1 do 10, zatim drugih 10 tačaka predstavlja podatke za grešku kad je u drugom sloju broj neurona fiksiran na 2, a u prvom opet varira od 1 do 10, itd.

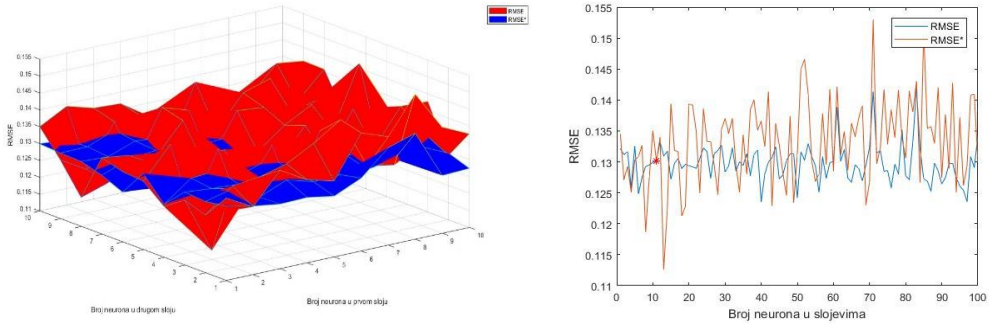

Slika 5: Vrijednosti srednje kvadratne greške RMSE i RMSE u neuronskoj mreži sa dva skrivena sloja, lijevo 3D prikaz, desno – 2D prikaz*

Analizirajući dobijene podatke prikazane na grafiku na slici 5, može se vidjeti da su za mrežu sa 17 – 1 – 2 – 1 rasporedom neurona RMSE*=0,1301 i RMSE=0,1303 skoro identične, nakon čega grafici ovih grešaka prikazuju veća odstupanja, tako da po kriterijumu srednje kvadratne greške, mreža sa 1 i 2 neurona u prvom i drugom skrivenom sloju daje najbolje rezultate.

Koeficijent korelacije R^2 dat je na slici 6. Po ovom kriterijumu mreža sa arhitekturom 17 – 7 – 10 – 1 daje najbolje rezultate.

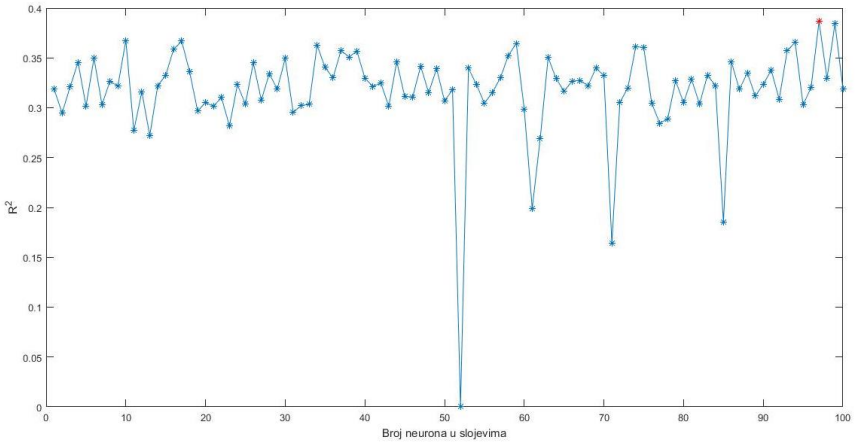

Slika 6*: Koeficijent korelacije neuronskoj mreži sa dva srivena sloja, broj neurona variran u opsegu 1 do 10 u oba sloja*

Kada se razmatra relativna greška MRE, slika 7, posebno za podatke za trening, a posebno za podatke za validaciju, vidi se da je najbolja mreža sa rasporedom neurona u skrivenim slojevima 17 – 9 – 2 – 1.

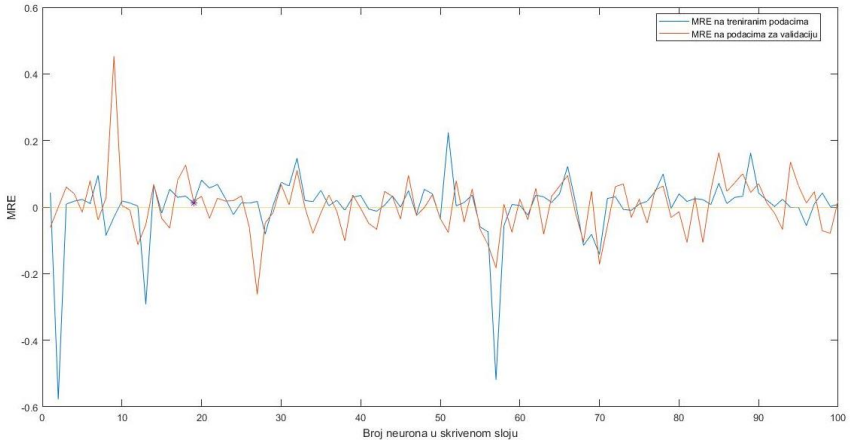

Slika 7: Relativna greška MRE na treniranim i podacima za validaciju

Analiza podatuje da u slučaju mreže sa dva skrivena sloja, broj neurona u skrivenim slojevima u zavisnosti od posmatranog kriterijuma.

Na slici 8 prikazan je uporedni grafik prikaz tačnih i predviđenih vrijednosti izlaza za svih 1826 ulaznih podataka za mrežu sa arhitekturom 17 – 9 – 2 – 1, kod koje su RMSE=0.1228, RMSE*=0.1296, R^2=0.3909 i R^2*=0.2967.

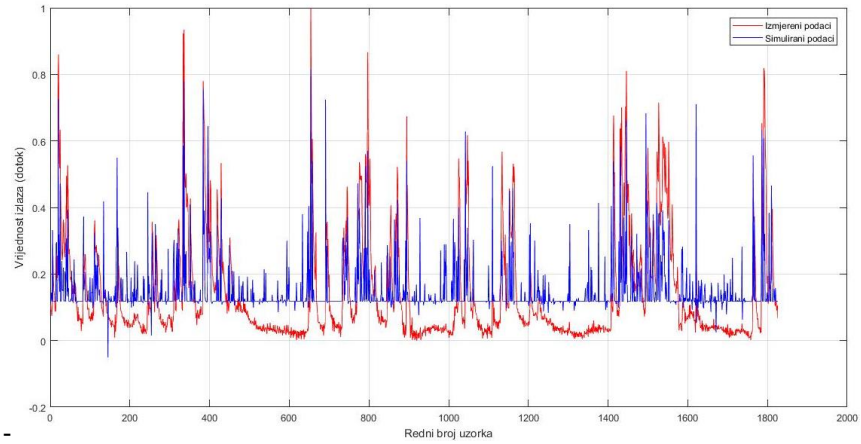

Slika 9: Uporedni grafik tačnih i predviđenih vrijednosti izlaza za svih 1826 ulaznih podataka za mrežu sa arhitekturom 17 – 9 – 2 – 1

4 ZAKLJUČCI

U ovom radu je razvijen model vještačih neuronskih mreža za prognozu predviđanja dotoka. Naglasak u radu je stavljen na izbor strukture neuronske mreže u smislu optimalnog izbora broja skrivenih slojeva i broja neurona u skrivenim slojevima. Levenberg-Marquardt metod sa četiti neurona u ulaznom sloju i jedan u izlaznom sloju je razvijen dok je broj neurona u jednom i dva skirvena sloja variran kako bi se dobila neuronska mreža sa optimalnom strutkurom. Kao kriterijumi za ocjenu modela korištene su srednja kvadratna greška (RMSE), srednja relativna greška (MRE) i koeficijent korelacije (R^2). Analiza modela sa jednim skrivenim slojem pokazuje da je optimalni broj neurona u ovom slučaju 8 dok je u slučaju sa dva skrivena sloja mreža sa strukturom 17 – 9 – 2 – 1usvojena kao najbolja mreža.

LITERATURA

[1] Philippides A. (2003). Introduction to Neural networks, *Centre for Computitional Neuroscence and Robotics*.
[2] Miljković, Z., Aleksandrić D. (2009). Vještačke neuronske mreže, *Univerzitet u Beogradu, Mašinski Fakultet*
[3] Elsheikh, A. H., Sharshir, S. W., Abd Elaziz, M., Kabeel, A. E., Guilan, W., & Haiou, Z. (2019). Modeling of solar energy systems using artificial neural network: A comprehensive review. *Solar Energy,* 18.
[4] Othman, F. (2011). Reservoir Inflow Forecasting Using Artificial Neural Network. *International Journal of the Physical Sciences,* 6, 434–440.
[5] Cobaner M, Information C, Haktanir T, Kisi O. (2008). Prediction of Hydropower Energy Using ANN for the Feasibility of Hydropower Plant Installation to an Existing Irrigation Dam. *Water Resour. Manage*., 22: 757-774.

COMETa 2022
6th INTERNATIONAL SCIENTIFIC CONFERENCE
17th - 19th November 2022
Jahorina, B&H, Republic of Srpska
University of East Sarajevo
Faculty of Mechanical Engineering
Conference on Mechanical Engineering Technologies and Applications

POBOLJŠANJE ENERGIJSKE EFIKASNOSTI KROZ ESCO MODEL

Meho Kulovac[1], Krsto Batinić[2], Dušan Golubović[3], Azrudin Husika[4], Nihad Harbaš[5]

Rezime: ESCO (Energy Service Company) je fizička ili pravna osoba koja pruža energijske usluge u svrhu poboljšanja energijske efikasnosti i pri tome preuzima finansijski rizik za takva ulaganja. ESCO kompanija svojim sredstvima finansira projekat umjesto krajnjeg korisnika. Provedeni projekat svojim tehničkim rješenjima ostvaruje uštede iz kojih krajnji korisnik otplaćuje sredstva koja je ESCO kompanija uložila. Činjenica je da je zgradarstvo u BiH veliki potrošač energije i u dosta lošem građevinskom stanju. Isto tako, činjenica je da javni i privatni sektor svojim kapacitetima nisu u stanju finansirati sve potrebe koje imaju u smislu povećanja energijske efikasnosti. To potvrđuje dosadašnja dinamika finansiranja projekata energijske efikasnosti sopstvenim sredstvima. Sve ovo ukazuje da je pravo vrijeme da se javnom ali i privatnom sektoru omogući provođenje energijske usluge, koja bi pomogla u naporima prevazilaženja nedostatka finansijskih sredstava. U radu je dat prikaz ESCO koncepta kao i trendovi njegove upotrebe u BiH.

Ključne riječi: energijska efikasnost, ESCO (Energy Service Company) koncept, potrošnja energije

IMPROVEMENT OF ENERGY EFFICIENCY TROUGHT ESCO MODEL

Abstract: ESCO (Energy Service Company) is a natural or legal entity that provides energy services for the purpose of improving energy efficiency and thereby assumes the financial risk for such investments. The ESCO company finances the project instead of the end user. The implemented project achieves savings with its technical solutions from which the end user repays the funds invested by the ESCO company. The fact is that the building industry in Bosnia and Herzegovina is a large consumer of energy and is in a rather poor state of construction. Likewise, it is a fact that the public and private sectors are not able to finance all the needs they have in terms of

[1] MSc, Meho Kulovac, nLogic Advisory, Sarajevo, Bosna i Hercegovina, meho.kulovac@nlogic.ba
[2] dipl.inž.maš. Krsto Batinić, Mašinski fakultet Istočno Sarajevo, BiH, krsto.batinic@ues.rs.ba
[3] prof. dr Dušan Golubović, Mašinski fakultet Istočno Sarajevo, BiH, dusan.golubovic@ues.rs.ba
[4] prof. dr Azrudin Husika, Mašinski fakultet Sarajevo, BiH, husika@mef.unsa.ba
[5] MSc, Nihad Harbaš, nLogic Advisory, Sarajevo, Bosna i Hercegovina

increasing energy efficiency with their capacities. This is confirmed by the current dynamics of financing energy efficiency projects with own funds. All this indicates that it is the right time to enable the public and private sector to implement energy services, which would help in efforts to overcome the lack of financial resources. The paper presents the ESCO concept as well as trends in its use in Bosnia and Herzegovina. n the past, the thermal energy consumption was not taken into account, within designing industrial thermal energy systems. Due to the decrease in stocks and the increase in the price of fossil fuels, the limitation of emissions of waste gases into.

Key words: energy efficiency, ESCO (Energy Service Company) concepts, energy consumption

1 UVOD

Veliki potencijal za uštede energije i doprinos dekarbonizaciji zemalja u Evropi može se ostvariti na polju javnih zgrada. Sektor zgradarstva (domaćinstva, javne i poslovne zgrade) je odgovoran za potrošnju približno 40% od ukupne potrošnje energije, kao i za 36% ukupnih emisija čestica CO2 [1]. Shodno visokom procentu udjela potrošnje energije i emisija čestica, sektor zgradarstva je prepoznat kao jedan od primarnih sektora u kojima je potrebno primjenjivati mjere energijske efikasnosti i raditi na unapređenju procesa koji se tiču proizvodnje, distribucije i iskorištavanja električne i toplotne energije. Pored zgradarstva, sektor koji je trenutno odgovoran za do 50% troškova za energiju na nivou opština i/ili kantona je sektor javne rasvjete. Potencijal uštede energije koji se može ostvariti renovacijom sistema javne rasvjete iznosi približno 80%, kada se implementiraju sistemi bazirani na LED tehnologiji i sistemu automatskog upravljanja, te se postižu energijske i finansijske uštede. Posvećenost javnog sektora renoviranju i poboljšanju perfomansi svojih zgrada i sistema je fundamendalna i krucijalna ukoliko se teži postići zacrtane ciljeve po pitanju dekarbonizacije Europe.

Prihvatanjem Ugovora o energetskoj zajednici, jula 2006. godine, Bosna i Hercegovina (BiH) postala je članica Energetske zajednice. Navedenim se, između ostalog, obavezala prenijeti direktive Europske unije (EU) i stvoriti pravno-regulatorni i institucionalni okvir za unaprijeđenje okoliša, energetike i ostalih oblasti. Na temelju postojećeg zakonodavnog okvira, institucije BiH provode projekte u oblastima, između ostalih, energijske efikasnosti (EE) i obnovljivih izvora energije (OIE). Kako bi se postigli svi zacrtani ciljeve, trenutno raspoloživa sredstva nisu dovoljna, kako za povećanje EE, tako i udio OIE, ali i smanjenja emisije stakleničkih plinova iskazanih kroz strateške i akcione planove. S tim u vezi, potrebno je iznaći nove izvore finansiranja.

Implementacija programa i projekata iz oblasti energijske efikasnosti može dovesti do značajnih potencijalnih smanjivanja radnih troškova u javnim institucijama, preduzećima i domaćinstvima, ali postoje barijere koje dovode do slabe realizacije aktivnosti upravljanja potrošnjom energijom, a neke od barijera su:

- Nedostatak iskusnog rukovodećeg kadra, i/ili nedostatak vremena koje se treba uložiti i posvetiti u poboljšanje procesa potrošnje energijom;
- Nedostatak sigurnosti da će resursi koji će se utrošiti na upravljanje potrošnjom energije isplatiti i ostvariti finansijsku i energijsku korist
- Poteškoće nabavke potrebnih sredstava za implementaciju projekata upravljanja potrošnjom energije

Suštinski, građani i korisnici objekata raznih namjera nisu u potrazi i potrebi za

energijom, već traže potrebe za energijom. Najčešće se to ogleda kroz potrebe za grijanjem objekata, grijanjem potrošne tople vode, hlađenjem, rasvjetom i slično. Istraživanja pokazuju da korisnici energije prihvataju manji broj opcija energijske efikasnosti nego što je to u njihovom finansijskom interesu. Najčešći razlozi su trenutno još uvijek relativno jeftina cijena energenata (te samim tim i njihovi troškovi), nedostatak informacija, vremena i znanja da se prepozna interes građana i korisnika u korištenju energijski efikasnih tehnologija i obnovljivih izvora energije. Shodno vremenu energetske krize, te povećanju cijena svih energenata (a sa tim i ukupnim troškovima), interes građanstva, privrede i službenika javnih institucija je povećan za načine smanjivanja troškova. Velika površina objekata javnih sektora, loše stanje (ili nepostojanje) termoizolacionih materijala, dotrajalost stolarije i bravarije, neefikasnost postojećih sistema te manjak automatizacije i regulacije uzrokuju visoku potrošnju energije i energenata čiji je niski stepen efikasnosti posebno vidljiv u vremenima visoke cijene energenata, te čine da su projekti energijske efikasnosti u ovom sektoru veoma isplativi (po pitanju uštede energije i novca), ali i investiciono početno veoma visoki.

Ukoliko nisu grantovski finansirani, projekti EE iz javnog sektora se baziraju na komercijalnom finansiranju i relativno su skromnog obima. Vrlo je afirmativan pristup da se kreira održiv finansijski mehanizam i to naročito za javni sektor. Na taj način omogućava se smanjivanje potrebe za inostranim kreditima i zaduživanjima, te se jačaju sopstvene institucije i stvara mogućnost realokacije sredstava. Stoga, slijedeći praksu razvijenih zemalja u rješavanju ovakvih problema, Zakonima o EE u oba entiteta u BiH postavljena je osnova za ugovaranje energijske usluge, kao jednog od mogućih načina rješavanja problema potrebnih sredstava, koji bi dijelom mogao doprinijeti boljoj, odnosno intenzivnijoj dinamici investiranja. Ovim bi se nedostatak javnih finansijskih sredstava rješavao putem investicija od strane tzv. ESCO kompanija.

2 ELEMENTI ESCO-A

Prema definiciji, ESCO (Energy Service Company) je fizička ili pravna osoba koja pruža energijske usluge u svrhu poboljšanja energijske efikasnosti u objektu i pri tome preuzima finansijski rizik za takva ulaganja. Plaćanje pruženih usluga temelji se na postignutim poboljšanjima, odnosno ostvarenim uštedama. ESCO kompanija svojim sredstvima finansira projekat, umjesto krajnjeg korisnika, koji implementiranim mjerama i tehničkim rješenjima ostvaruje uštede iz kojih krajnji korisnik vraća, odnosno otplaćuje, sredstva koja je ESCO kompanija uložila.

Počeci pružanja energijskih usluga kreću od 1970tih godina, i vežu se za energetsku krizu koja se javila u tom periodu, Energijske usluge su se prvo počele nudit u zemljama Zapadne Evrope i Sjedinjenih Američkih Država, na čijem tržištu se javljaju firme koje su se specijalizovale za rad sa klijentima radi savladavanja barijera koje se suprostavljaju razvoju i implementaciji projekata iz oblasti energijske efikasnosti. Firme koje se suštinski bave projektima i uslugama iz oblasti energije, nude klijentima inovacijske elemente poput:

- Razvoja projekata koje potpomaže treća osoba;
- Garancije efikasnosti u radu i isporuci energije;
- Implementacije projekata na temelju trenutnog godišnjeg budžeta za energiju;
- Isporuku energije, servis i održavanje instalacija te preuzimanje odgovornosti za kompletan sistem.

Prednosti ESCO kompanija u odnosu na ostale kompanije koje su standardno uključene u projekte vezane za električnu i toplotnu energiju su te da ESCO kompanije daju kompletna integrisana rješenja, te povezuju plaćanje sa izvršenjem projekta.

3 ESCO KONCEPT

Kao jedan od najatraktivnijih aspekata ESCO modela sa stanovišta klijenta (Javne institucije, preduzetnika, zajednice stanara u zgradi kolektivnog stanovanja i slično) je taj što ESCO kompanija odgovara za sve faze projekta, od izrade idejnog i glavnog projektnog rješenja (za novoplanirani sistem), komunikaciju sa distribiterima energije, proizvođačima opreme, finansijskim institucijama, državnim organima (potrebnim za izdavanje dozvola i odobrenja i slično). Ovaj koncept „ključ u ruke“ smanjuje finansijske troškove klijenta, kao i vrijeme potrebno da se uloži u prikupljanje kompletne dokumentacije koje često bude krucijalni razlog neprihvatanja i odbijanja ulaganja u projekte energijske efikasnosti. Na slici 1. je prikazan tradicionalni pristup kada klijent želi da implementira projekte iz oblasti energijske efikasnosti, a na slici 2. je prikazan ESCO pristup pri postizaciju istih efekata (implementiranja projekata EE i korištenja OIE).

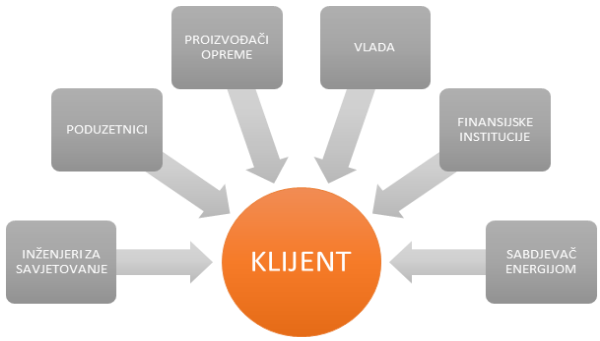

Slika 1. *Tradicionalni pristup implementaciji projekata EE i OIE*

Slika 2. *ESCO pristup implementaciji projekata EE i OIE*

4 ESCO KLIJENTI

ESCO kompanija u principu može da radi sa klijentima iz bilo kojeg sektora ili tržišta, međutim u praksi se pokazalo da postoje određene prepreke i barijeje koje se za svaki sektor moraju uzeti u obzir:

- Individualno stambeno tržište (rezidencijalni sektor) generalno nije interesantan za ESCO modele iz razloga niskih investicija, te malih ugovora koji se potpisuju sa svakim domaćinstvom posebno;
- Kolektivno stambeno tržište je prihvatljivije za ESCO kompanije shodno većim površinama objekata i generalno većim potrebama za energijom, ali ovisi o tipu i načinu trenutne naplate energenata, te da li je moguće izvesti moguće prepravke sistema i instalacija;
- Sektor javnih zgrada (zgrade institucija vlada, bolnice, vrtići) su suštinski najinteresantniji i zanimljiviji za ESCO kompanije radi niskog finansijskog rizika, velikog broja zgrada i visokog potencijala energijske uštede. Objekti u javnom vlasništvu su suštinski najveći potrošači energije, te imaju najveći prostor da se smanji potrošnja energije i troškovi za energente nakon provedbe energetske obnove. Sigurnost u plaćanju mjesečnih/godišnjih troškova za ESCO uslugu je obezbjeđena ugovorom, te ESCO kompanije najviše investiraju u ovaj sektor;
- Komercijalno tržište: velike zgrade kompanija, velika područja i hoteli su veoma atraktivni ESCO kompanijama jer imaju ogroman potencijal energetske uštede, ali i zbog toga što vlasnici ovih tipova objekata često nemaju odgovarajući kadar niti tehničke resurse sposobne za realizaciju projekata iz oblasti energijske efikasnosti. Jedna od najvećih prepreka i barijera jeste sigurnost finansiranja odnosno plaćanja mjesečnih/godišnjih ESCO faktura prema klijentu
- Industrijsko tržište je također jedan od najvećih potrošača energije, ali generalno velika industrijska postrojenja često imaju tehničko osoblje i kapital potreban za ulaganje u projekte energetske obnove, pa ovo tržište nije standardno tržište za ESCO kompanije.

5 MODELI ESCO UGOVORA

Bitna komponenta u definiciji ESCO-a je povezanost ESCO-ve naplate sa izvršenjem projekta. Ovu vezu predstavlja ugovor o izvršenju projekta sklopljen između ESCO-a i klijenta. Ugovor o izvršenju može da se shvati kao ugovor o vršenju usluga gdje ESCO daje djelomičnu ili potpunu uslugu u pogledu realizacije uštede u jednoj zgradi ili preduzeću, uz garanciju da će ušteda energije koja je rezultat projekta biti adekvatna za kompenzaciju ESCO-a tokom određenog vremenskog perioda. Ovaj period je obično 3-10 godina, iako u principu nema ograničenja, mada prekratak vremenski period ne bi omogućio ESCO-u da nadoknadi svoje troškove.

Modeli ugovora mogu biti:

- Ugovaranje sa garantovanim uštedama
- Ugovaranje sa podjelom ušteda
- „Chauffage“ ugovori

5.1 Ugovaranje sa garantovanim uštedama

U skladu sa ugovorom kojim se garantuje ušteda po izvršenju, ESCO garantuje

da će mjere, koje će se implementirati u pogledu instalacija za efikasno korištenje energije, doprinjeti dovoljnim uštedama da projekat bude isplativ. Projekat je zamišljen i projektovan tako da finansijska vrijednost garantovanih ušteda iz energije bude veća od iznosa naknade za ESCO, plus otplate bilo kakvog kredita/pozajmice vezane za ovaj projekat. Na taj način klijent odmah realizuje određenu gotovinsku pogodnost i to od trenutka kada je projekat implementiran, iako će ta ušteda biti relativno mala tokom početnih godina projekta, dok se projekat još uvijek isplaćuje (povrat pozajmice plus i naknada za ESCO uslugu). Kada ugovor između ESCO i klijenta istekne, gotovinska pogodnost koju klijent uživa je veća.

Ukoliko energijska ušteda ne bude na nivou koji je specificiran garancijom, ESCO kompanija je odgovorna za nadoknadnu razlike i to na način da se ta razlika do garantovanog nivoa isplati klijentu. U slučaju da energijska ušteda prevalizazi garantovani iznos, dodatna ušteda se dodjeljuje ESCO kompaniji. Zato je i svrha i rezultat ugovora o garantovanoj uštedi zaštiti klijenta od svih rizika u izvršenju projekta. Obzirom da ESCO kompanija sa ovim modelom snosi cijeli rizik sprovođenja projekta, ovim modelom veći dio kreditnog rizika snosi klijent. Iz tog razloga nije uobičajeno da se ugovor garantovanog izvršenja projekta veže sa aranžmanom finansiranja od treće strane. Ukoliko se koristi model ugovora garantovanje uštede po izvršenju projekta, za finansiranje je obično odgovoran klijent.

5.2 Ugovaranje sa podjelom ušteda

Ugovor o podjeli uštede koja proizilazi iz izvršenja projekta je ugovor kojim se dijeli ušteda između ESCO kompanije i klijenta. Ukoliko projekat ostvari veću uštedu nego što se očekuje, i klijent i ESCO dobijaju dodatne vrijednosti, i obrnuto – ukoliko ostvari manju uštedu oba člana su na gubitku. Obzriom da u ovom slučaju klijent snosi dio rizika izvršenja projekta, ovaj tip projekta je najčešće povezan sa finansiranjem od treće strane, odnosno kombinacijom između finansiranja iz budžeta klijenta i budžeta ESCO-a.

5.3 „Chauffage“ ugovori

Jedan od ekstremnih oblika upravljanja potrošnjom energije je aranžman "chauffage", gde ESCO preuzima kompletnu odgovornost za klijenta u pogledu jedne energetske cjeline (npr. grijanje prostora, javna rasvjeta itd.) Tamo gde je tržište energije konkurentsko, ESCO u aranžmanu grijanja takode preuzima i punu odgovornost za kupovinu goriva. Naknada koju klijent plaća u takvom aranžmanu obračunava se na osnovu postojećeg utroška energije, minus postotak uštede (što je često u opsegu od 5-10%). Na taj se način klijentu garantuje trenutna ušteda u odnosu na dosadašnji račun. ESCO preuzima odgovornost za davanje na raspolaganje odredenog nivoa energetske usluge – te ako se to može uraditi efikasnije i jeftinije, tim su zarade veće.

5.4 EnPC

EnPC (Energy Performace Contracting) odnosno Energetski ugovor o djelovanju/efektu prestavlja finansiranje projekata na račun štednje energije i ESCO kompanija garantuje da će uštede biti realizovanje u određenom vremenskom roku.

6 PROCES UGOVARANJA I REALIZACIJE UGOVORA O ENERGIJSKOM EFEKTU

Energijska usluga je provođenje projekta energijske efikasnosti i ostalih povezanih aktivnosti od strane pružatelja energijske usluge temeljena na ugovoru o energijskom efektu sa garancijom da u referentnim uslovima vodi do provjerljivog i mjerljivog ili procjenjivog poboljšanja energijske efikasnosti i/ili ušteda energije i vode.

Ugovorom o energijskom efektu pružatelj energijske usluge se obavezuje provesti ulaganja (radove ili usluge) kroz energijske obnove zgrada ili sistema javne rasvjete putem mjera energijske efikasnosti kojima se postiže garantovana ušteda energije i/ili ušteda vode i/ili ušteda pripadajućih troškova u odnosu na referentnu potrošnju energije i/ili pripadajućih troškova, na način da rizik i koristi takvog ugovaranja preuzme pružatelj energijske usluge, a naručitelj se pružatelju energijske usluge obavezuje za vrijeme trajanja ugovora plaćati naknadu temeljenu na ugovorenoj novčanoj vrijednosti energijskih ušteda koje su ostvarene i utvrđene. Energijsku uslugu subjektu iz javnog sektora pružaju pravne osobe na osnovu ugovora o energijskom efektu koji se sklapa nakon provedenog postupka javne nabavke, a u skladu s posebnim zakonom kojim se uređuju obligacioni odnosi. Nabavka energijske usluge za subjekte javnog sektora provodi se primjenom Zakona o javnoj nabavci uz primjenu kriterija ekonomski najpovoljnije ponude, a u skladu sa zakonom koji uređuje područje energijske efikasnosti.

Nakon što se od strane naručitelja izvrši izbor objekata po osnovu utvrđenih kriterija, shodno odredbama prijedloga Pravilnika i Ugovora o energijskom efektu, pristupa se pribavljanju i realizaciji energijske usluge, što podrazumjeva sljedeće korake:

- Naručitelj izrađuje tendersku dokumentaciju, provodi postupak javne nabavke i donosi odluku o odabiru prema kriteriju Ekonomski najpovoljnije ponude.
- Naručitelj i pružatelj usluge sklapaju Ugovor o energijskom efektu.
- Pružatelj izrađuje projektnu dokumentaciju (Projekt) kojom mora obuhvatiti i razraditi sve mjere kojima namjerava postići uštede, te dokazati postizanje svih vrijednosti iz ponude, a sve u skladu sa posebnim zakonom kojim se uređuje područje energijske efikasnosti i drugim propisima.
- Pružatelj usluge dostavlja Projekat naručitelju koji imenuje stručnu komisiju. Stručna komisija provjerava usklađenost Projekta sa propisima, te provjerava jesu li Projektom dokazive vrijednosti koje je pružatelj iskazao u ponudi. Stručna komisija izdaje Izvještaj o verifikaciji Projekta. Ukoliko Stručna komisija utvrdi da Projekat ima nedostatke, predložit će rok za uklanjanje istih.
- Pružatelj ima obavezu da ishoduje akt kojim se dozvoljava gradnja ukoliko za to postoji obaveza prema važećim propisima koji uređuju tu oblast.
- Pružatelj izvodi radove energijske obnove zgrade u skladu sa verificiranim projektom. Izvođenje radova nadzire stručni nadzor angažovan od strane pružatelja. Naručitelj ima pravo nadzora nad provedbom energijske obnove o vlastitom trošku.
- Pružatelj usluge naručitelju dostavlja završni izvještaj stručnog nadzora da su radovi energijske obnove dovršeni i da su otklonjeni svi vidljivi nedostaci. Pružatelj prilaže kompletnu atestno-tehničku dokumentaciju, saglasnosti, i dozvole (naročito upotrebnu dozvolu), ako propisi predviđaju dozvole i svu dokumentaciju koju je po opštim propisima vlasnik građevine dužan imati o izvedenim radovima.

- Pružatelj po provođenju energijske obnove ishodi energijski certifikat.
- Naručitelj i pružatelj provode primopredaju radova o čemu sačinjavaju zapisnik.
- Naručitelj u roku od 15 dana donosi Odluku o verifikaciji obnove kojom potvrđuje da je pružatelj izvedbom u skladu s verificiranim projektom postigao stanje zgrade kojim se osiguravaju preduslovi najmanje za ostvarenje garantovanih ušteda iz ponude, te da su izvedeni radovi energijske obnove u potpunosti u skladu s verificiranim projektom. Odlukom se utvrđuje datum završetka obnove, odnosno datum od kojeg se ostvaruju uštede.
- Od datuma završetka obnove počinju se ostvarivati uštede i nastupaju obaveze naručitelja u smislu plaćanja naknada po ugovoru o energijskom efektu. Tokom cijelog vijeka trajanja Ugovora, pružatelj provodi mjere praćenja i kontrole ušteda (obuka korisnika, redovni pregledi sa tromjesečnim zapisnicima o ostvarenju ušteda, investicijsko održavanje elemenata zgrade i ugrađene opreme koji su bili predemet energijske obnove).
- Po isteku ugovora, naručitelj i pružatelj sačinjavaju Zapisnik i time formalno okončavaju ugovor. Zapisnik mora minimalno sadržavati informaciju o ostvarenoj uštedi, o izmirenim potraživanjima strana te ispunjenju svih ostalih ugovornih obaveza.

U nastavku hodogram gore opisanih aktivosti koje se trebaju provesti od strane naručitelja i pružatelja.

Slika 3. *Hodogram opisanih aktivnosti*

7 ZAKLJUČAK

U BiH se već duži vremenski period nastoji uspostaviti ESCO tržiše, te kroz razne projekte su se pokušale izvršiti konkrente aktivnosti prije svega formalno-pravne, ali bez posebnog uspjeha. Ovaj princip poslovanja i finansiranja projekata energijske efikasnosti već dugo egzistira u zemljama okruženja. Sve zemlje su, kao što treba i

BiH, prošle kroz formalno-pravno usklađivanje sa „novim“ poslovnim modelom. Isto tako, sve zemlje su imale istu motivaciju, povećati ulaganje u projekte energijske efikasnosti. Obzirom na ograničene sopstvene finansijske kapacitete, jedan od mogućih načina iznalaženja dodatnih finansijskih sredstava je angažovanje privatnog kapitala. Međutim, da bi se privatni sektor lako odlučio za ulaganje u tuđu imovinu, mora se kreirati prvo siguran pravi ambijent, a onda i profitabilnost istih.

Ono što ohrabruje je da na našem tržištu postoji interes za ovakvim poslovnim modelima. Određeni broj kompanija se bavi jednim segmentom pružanja energijske usluge, odnosno snabdijevanjem toplotnom energijom. U Federaciji BiH nalazimo veliki broj javnih objekata koji imaju ugovorenu ovakvu uslugu, uključujući i javni sektor iz Srednjebosanskog kantona.

Činjenica je da je zgradarstvo javnog sektora veliki potrošač i u dosta lošem građevinskom stanju. Isto tako, činjenica je da javni sektor svojim kapacitetima nije u stanju finansirati sve potrebe koje ima u smislu povećanja energijske efikasnosti. To potvrđuje dosadašnja dinamika finansiranja projekata. Sve ovo ukazuje da je pravo vrijeme da se javnom sektoru omogući provođenje energijske usluge, koja bi jednim dijelom pomogla u naporima prevazilaženja nedostatka finansijskih sredstava.

ESCO model ugovora je, neupitno, koristan. Vrijednost samog modela se najviše ogleda u činjenici da su obje ugovorne strane u konačnici zadovoljne. Naručitelj, koji u konačnici završi sa saniranim objektima o kojima ne treba da brine u narednih 25-30 godina i uživa u svim benefitima nakon izlaska ESCO kompanije iz ugovora i pružatelja, koji nakon inicijalnog ulaganja, kroz godine povrata ostvaruje dogovorene prihode.

LITERATURA

[1] Moles-Grueso, S., Bertoldi, P. and Boza-Kiss, B., Energy Performance Contracting in the Public Sector of the EU – 2020, EUR 30614 EN, Publications Office of the European Union, Luxembourg, 2021, ISBN 978-92-76-30877-5, doi:10.2760/171970, JRC123985
[2] Principi Esco operacija - Balkan Energy Solutions Team
[3] UNDP, Studija izvodljivosti za ESCO pilot projekat, mart 2021
[4] http://www.see-institute.org/srpski/esco-kompanije - pristupljeno 25.10.2022.
[5] https://fmeri.gov.ba/media/1819/okvirna_energetska_strategija_bosne_i_hercegovine_do_2035_bih_finalna.pdf - pristupljeno 20.10.2022.
[6] https://www.vladars.net/sr-SP-Cyrl/Vlada/Ministarstva/mgr/Documents/1_ESCO_konacno_seminar_pitanja_RS_ECA_040927393.pdf - pristupljeno 20.10.2022.

COMETa 2022
6th INTERNATIONAL SCIENTIFIC CONFERENCE
17th - 19th December 2022
Jahorina, B&H, Republic of Srpska
University of East Sarajevo
Faculty of Mechanical Engineering
Conference on Mechanical Engineering Technologies and Applications

A BACK VIEW OF THE HISTORY OF THERMODYNAMICS

Jovan Mitrovic[1], Mitar Perusic[2]

Abstract: It is believed that the history of thermodynamics as a scientific branch began with the work published by Sadi Carnot (1796-1832) in 1824. For the first 10 years, the work went unnoticed in scientific circles, and after that in many papers it was interpreted as the foundations of thermodynamics. In this paper is shown that James Watt (1736-1819), more than 50 years before Carnot, significantly contributed to the formulation of thermodynamics as a science. Watt is well-known as the mechanical creator of the steam engine that enabled the first industrial revolution in the late 18th century. However, he is less known as the author of numerous ideas in modern thermodynamics, including also the first law of thermodynamics as a branch of physics. In this paper, special attention is paid to the Watt's formulation of the first law of thermodynamics as a postulate on the conversion of one type of energy into another.

Keywords: Energy transformation, energy conservation, the first law of thermodynamics.

1 INTRODUCTION

It is known that the generation of fire based on mechanical friction represents conversion of mechanical energy into heat. Count Rumford (1753-1814) well known Benjamin Thompson, (Thompson, 1798) is usually reported to be the first who conducted experiments in this area of energy conversion. More than a century prior to Rumford, in 1675, Robert Boyle (1627-1691) described several methods of mechanical generation of heat (Boyle, 1675). Boyle recognized two important properties of heat:

a) heat can be understood as motion of smallest parts of bodies,
b) heat is produced by mechanical action.

Consequently, heat cannot be of substantial origin, Boyle concluded, it is the magnitude of the process. Contribution to the principle, has been made by Leibniz research (G.W. Leibniz, 1646-1716), and he provided (Leibniz, 2017) a relationship between the mechanical work and heat as equivalence of different kinds of energy. This allows application of Leibniz's idea of conservation of energy- vis viva- of 1692 in an

[1] Prof. dr Jovan Mitrovic, Stuttgart, Germany, mitrovic@tebam.de
[2] Prof. dr Mitar Perusic, University of East Sarajevo, Faculty of Technology Zvornik, Republic of Srpska, B&H, mitar.perusic@tfzv.ues.rs.ba

inelastic impact (Spector, 1975). Leibniz assumed that vis viva in an inelastic collision of gross bodies is not conserved and that the obvious loss of this quantity is caused by its distribution among the small elements of impacting bodies, which is in agreement with the Boyle's experiment published in 1675, more than two decades earlier.

The works on the equivalence of heat and work cover an important period in the history of thermodynamics. The works appeared in this period can be viewed as an introduction to the first law of thermodynamics. The papers by Kuhn (Kuhn, 1959) and Smith (Smith, 2003) provided overviews on the development of thermodynamic thoughts. This period is followed by the period of formulation of the laws of thermodynamic in 19th century; the boundary between them is smooth. Of the numerous papers on the laws of thermodynamics the original contributions by Mayer and Joule (Joule, 1843; Mayer, 1839) are mentioned. Details of these fundamental formulation have been permanently deepened e.g., in (Cardwell, 1967; Collins, 2015; Newburgh & Leff, 2011; Sarton et al., 1929; Wisniak, 2008). Interestingly, none of the authors mentioned James Watt's contributions to the foundations of thermodynamics.

In the history of thermodynamics, there is undisputable agreement that the first law of thermodynamics was formulated by Julius Robert Mayer and James Prescot Joule at about the same time, in the 1840s (Newburgh & Leff, 2011). In this work are presented some evidences (*Fig.1*) which show that James Watt (1736-1819) developed in 1760s clear ideas about the conservation and conversion of energy which he stated in his patent of 1769 (*File:James Watt Patent 1769 No 913.Pdf - Wikimedia Commons*, n.d.) and formulated the first law in 1774.

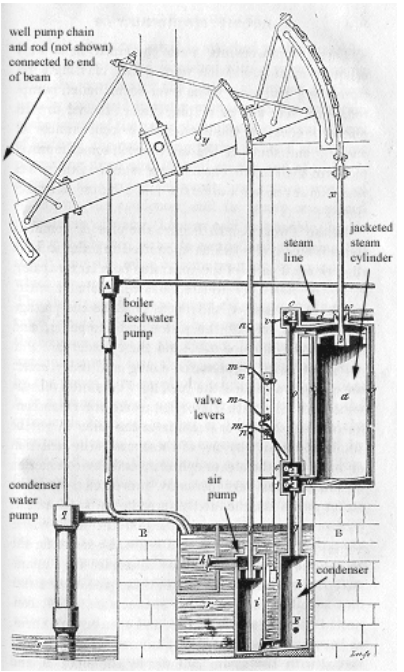

Figure 1. *Watt's steam engine with separate condenser (h) as described in his patent of 1769, built in 1774; the water boiler is not shown in the drawing. The original drawing in Stuart's book* (Stuart, 1829) *is without any text; Prof. Lyra, Michigan State University, presents the figure with text without mentioning the author, https://www.egr.msu.edu/~lira/supp/steam/wattengine.htm.*

But Watt did not publish any text about this law and presented his ideas in the form of a technical drawing. Naturally, his ideas could be understood only by the scientists, who viewed sketches and drawings as a way of spreading the knowledge. In 1778 Watt provided a proposal in this context. Some details can be taken from earlier publications (Mitrovic, 2022b, 2022a; Митрович & Смык, 2021).

2 UNDERSTANDING THE CONVERSION OF HEAT INTO WORK

The Watt's understanding of the conversion of heat into work is illustrated in *Fig. 1* which shows a drawing of the steam engine as described in his patent of 1769. The steam cylinder (*a*), enveloped by a layer of steam, is connected to the boiler (not shown in the drawing). The steam layer was devised to prevent heat losses to surroundings and condensation of steam prior to performing the work. This construction almost completely prevented heat losses to the environment. The separate condenser (*h*), situated below the steam cylinder, is immersed in cooling water. In comparison to Newcomen's installation, the Watt's arrangement increased the performance of the engine substantially. The figure contains all the important details of the working principle of a steam engine and can be read like a book on thermodynamics.

2.1 THE EQUIVALENCE OF HEAT AND WORK

For some 40 years, around the transition from the 18th to the 19th century, Watt's steam engine was the main industrial facility for converting thermal energy (heat) into mechanical work. Watt practiced this kind of energy conversion several decades before the "official" development of thermodynamics began in the first half of the 19th century. On page 337 John Farey (Farey, 1827) states (see also p. 330):

In 1778, when Mr. Watt first established his engine, his proposals were to raise 500,000 ft³ of water 1 ft high by the consumption of one hundred weight (= 112 lbs.) of Wednesbury coals.

This proposal is important for understanding the equivalence and mutual convertibility of different energy forms. Its greatest value consists in showing the profound connection between heat that "disappears and reappears" as work. This interconnection became later a pillar of the foundation of the dynamical theory of heat (Thomson, 1852). Watt's proposal expresses the energy balance of a set of real processes connected in series, spanning three modes of energy conversion (*Chemical energy of coal* $\rightarrow$ *Heat* $\rightarrow$ *Mechanical energy of steam* $\rightarrow$ *Useful mechanical work*), taking into account all the energy losses of the engine's installation.

Multiplying the mass, *m*, of coal consumed in the reaction by the heat of this reaction, *H*, Watt's proposal can be cast in the quantitative energy equation:

$$Hm = V\rho gh + E_{loss} \tag{1}$$

where are:

V-volume, ρ -mass density, h-elevation height of water, m- mass of coal consumed, g-acceleration of gravity, E_{loss}-sum of all energy losses.

Eq. (1) specifies the quantity of heat (coal) required to produce a quantity of mechanical work by using Watt's steam engine. The quantity E_{loss} encompasses all losses of the energy conversion process, i.e., friction and heat losses, including also the heat of steam condensation in the condenser. Consequently, Watt's proposal states the equivalence

of heat and work and measured the heat in terms of the mechanical units.[3] The conversion of energy from one form into the other, does not contradict to the idea of its conservation, hence the Watt's proposal expresses also the principle of energy conservation. On its basis Cardwell guessed that a given amount of heat must correspond to a given amount of work (Cardwell, 1967). Because of the clarity of the Watt's proposal, it is possible that later research into the mechanical equivalent of heat, such as those of Joule, have been motivated by Watt's ideas (Joule, 1843).

2.2 THE FIRST LAW OF THERMODYNAMICS

Eq. (1) leads to an important relationship of thermodynamics if the energy (heat) losses are assumed to arise only from steam condensation in the condenser and set, $E_{loss} = Q_C$, where Q_C denotes that wasted heat. The product $H \cdot m$ is equal to the heat Q_B, the working substance receives in the boiler. Denoting, in addition, by W the elevation work, $V \rho g h = W$, Eq. (1) takes the form

$$Q_B = W + Q_C \tag{2}$$

The heat Q_B is converted in the work W and wasted heat Q_C. This equation is well-known from literature as the ***First Law of Thermodynamics***. It's formulation by James Watt in 1778 preceded by more than 6 decades the next generation of similar works, starting with J.R. Mayer and J.P. Joule in the 1840s. Collins names it *the Mayer–Joule Principle* (Collins, 2015), without mentioning James Watt. The meaning of the terms Q_B and W are mentioned in the Watt's proposal, while the term Q_C follows from the fact that steam engine was used for energy conversion. In his 1769 patent, Watt described the principle of the steam engine and identified the heat of condensation of the steam Q_C as wasted heat.

Eq. (2) is suitable for quantifying the consequence of the idea that heat is transported from the boiler to the condenser without consumption, $Q_B = Q_C$, as S. Carnot and W. Thomson (Lord Kelvin) originally thought; in this case no work is won, $W = 0$!

Energy splitting in the steam engine. The energy splitting shown in *Eq. (2)* is an important step of the energy conversion process. This step is illustrated in Figure 2. It shows a section of *Fig.1* surrounding the steam cylinder and visualize some details of the first law of thermodynamics. The splitting of the energy Q_B, satisfying Eq. (2), occurs on the piston as it moves down the cylinder. Literally, the piston acts as a permeable device, allowing only the mechanical energy pdV of the vapor to leave the cylinder and do the work W,

$$W = \int_{Vi}^{Vf} pdV \tag{3}$$

The transfer of the work from the piston to the water pump q takes place via the vertical rod, (*Fig. 1*), and the massive rocker (beam), which can perform small angular movements in the plane of the drawing around its suspension point. The heat Q_C leaves the cylinder mainly as latent heat of steam; after the steam condensation in the separate condenser, it becomes absorbed by cooling water and wasted as sensible heat.

[3] Eq. (1) does not contain the coefficients of energy equivalence which would be necessary if the terms were measured in different units.

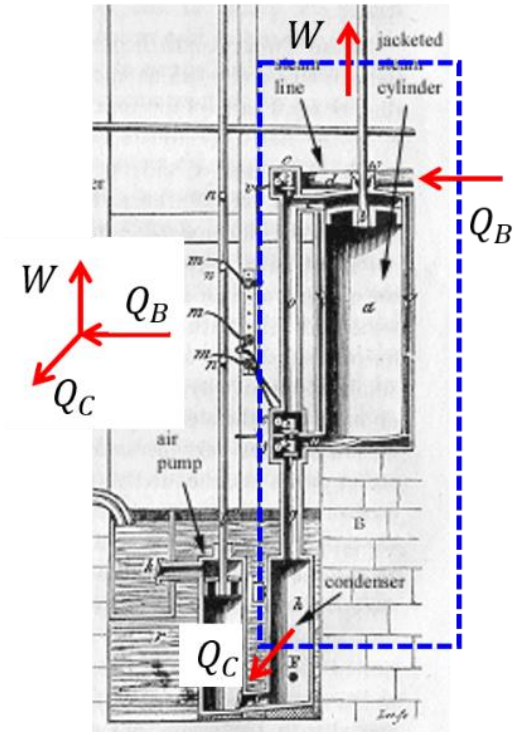

Figure 2. *Visualization of the first law according to James Watt or splitting the energy in the Watt's steam engine* (Mitrovic, 2022b)*, excerpt from Fig. 1.*

3 FLOW SHEET OF WATT'S ENERGY CONVERSION PROCESS

The drawing of Watt's installation (*Fig. 1*) is too complex for a quick overview of the whole energy conversion process. On the basis of this drawing and Watt's patent of 1769, a simple flow sheet is generated, as shown in *Fig. 3*, that will be used for a brief description and comparison with modern installations. The main elements are the water boiler, the steam cylinder, the separate condenser and the feed pump. These components constitute the Watt's cycle. The working substance changes its potential (state) mainly in the boiler and in the steam cylinder; the changes in the feed pump and the condenser are not separately illustrated. With this assumption the change of potential in the boiler is equal and opposite to that in the steam cylinder. The term potential used here shall account for Watt's idea stated in his patent of 1769 that the power of steam drives the engine (*File:James Watt Patent 1769 No 913.Pdf - Wikimedia Commons*, n.d.).

The *Fig. 3* is corresponding to the Watt's drawing in *Fig. 1* and constitutes the skeletons of several modern energy conversion plants. For instance, replacing in Watt's installation the steam cylinder by a steam turbine with an electric-generator, it becomes identical to the flow sheet of a contemporary power plant operating with saturated steam. The flow sheet (on the left) not only shows the implementation of *Eq. 2*., but also the temperature range covered by the steam engine. The steam has the highest temperature in the boiler and the lowest in the condenser. Watt recommended keeping the temperature in the condenser as low as possible (depending of cooling water). He did

not limit the temperature in the boiler directly, but for safety reasons (boiler explosion) via the steam pressure, which he determined himself as a function of the temperature.

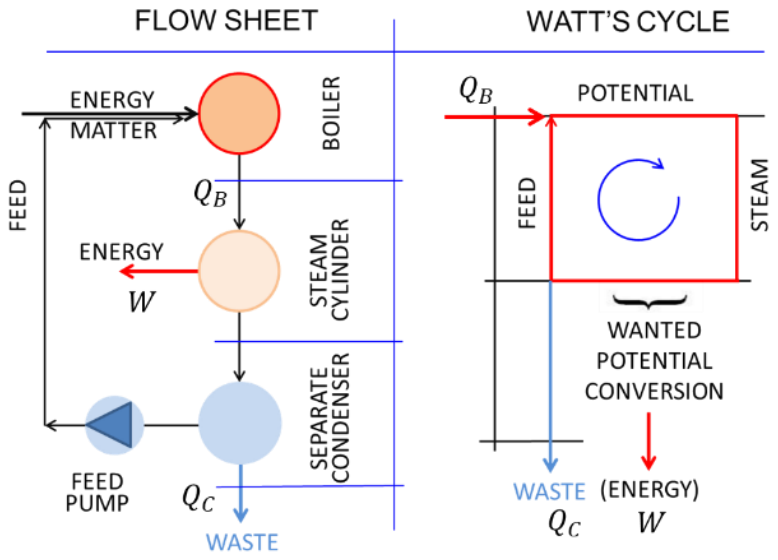

Figure 3. *Simplified flow sheet of Watt's energy conversion process* (Mitrovic, 2022a). *For the meaning of Q_B, W and Q_C see Eq. (2).*

Because of $T = f(p)$ he clearly defined the temperature of the working substance in the boiler and thus also the temperature range of the steam engine. The temperature range Watt defined corresponds exactly to the definition that Sadi Carnot published in his 1824 dissertation (Bradu, 2009). Carnot's definition is known in the literature as Carnot's postulate, while James Watt is never mentioned as the originator of this idea. Further details are given in (Mitrovic, 2022a).

4 CONCLUSIONS

In modern science, Julius Robert Mayer and James Prescot Joule are generally considered to be the creators of the first law of thermodynamics in 1840s. The paper presents some facts that James Watt established and applied this law already in his patent of 1769. However, Watt's ideas remained unrecognised and were not adequately mentioned in the history of thermodynamics. Mostly for the reason that Watt never published his work in a research or academic paper, but mainly as technical sketches or drawings which were considered as work of practician without a scientific value at the time (Mitrovic, 2022b).

REFERENCES

[1] Boyle, R. (1675). Experiments, notes, &c., about the mechanical origine or production of divers particular qualities: among which is inserted a discourse of the imperfection of the chymist's doctrine of qualities; *Printed by E. Flesher for R. Davis Oxford.*

[2] Bradu, B. (2009). Réflexions sur la puissance motrice du feu, de Sadi Carnot. Bibnum. *Textes Fondateurs de La Science.*

[3] Cardwell, D. S. L. (1967). Some factors in the early development of the concepts of power, work and energy. *The British Journal for the History of Science*, *3*(3), 209–224.
[4] Collins, M. W. (2015). The first law of thermodynamics: 2. The Joule–Mayer controversy. *Kelvin, Thermodynamics and the Natural World*, 231–236.
[5] Farey, J. (1827). A treatise on the steam engine: Historical, practical, and descriptive. *Longman, Rees, Orme, Brown, and Green*.
[6] File:James Watt Patent 1769 No 913.pdf - Wikimedia Commons. (n.d.). Retrieved May 19, 2022, from https://commons.wikimedia.org/wiki/File:James_Watt_Patent_1769_No_913.pdf
[7] Joule, J. P. (1843). On the calorific effects of magneto-electricity, and on the mechanical value of heat. *The London, Edinburgh, and Dublin Philosophical Magazine and Journal of Science*, *23*(152), 263–276. https://doi.org/10.1080/14786444308644730
[8] Kuhn, T. (1959). Energy Conservation as an Example of Simultaneous Discovery: Critical Problems in the History of Science. *University of Wisconsin Press Madison.*
[9] Leibniz, G. W. (2017). Essay in Dynamics showing the wonderful laws of nature concerning bodily forces and their interactions, and tracing them to their causes.
[10] Mayer, R. (1839). Bemerkungen über die Kräfte der unbelebten Natur.
[11] Mitrovic, J. (2022a). Some Ideas of James Watt in Contemporary Energy Conversion Thermodynamics. *Journal of Modern Physics*, *13*(4), 385–409.
[12] Mitrovic, J. (2022b). Who Established the First Law of Thermodynamics? *Chemie Ingenieur Technik*, *94*(6), 1–5.
[13] Newburgh, R., & Leff, H. S. (2011). The Mayer-Joule principle: The foundation of the first law of thermodynamics. *The Physics Teacher*, *49*(8), 484–487.
[14] Sarton, G., Mayer, J. R., Joule, J. P., & Carnot, S. (1929). The discovery of the law of conservation of energy. *Isis*, *13*(1), 18–44.
[15] Smith, C. (2003). Force, energy, and thermodynamics. *Cambridge History of Science*, 289–310.
[16] Spector, M. (1975). Leibniz vs. the Cartesians on Motion and Force on JSTOR. *Stidia Leibnitiana*, *7*(1), 135–144. https://www.jstor.org/stable/40693764
[17] Stuart, R. (1829). Stuart's Descriptive History of the Steam Engine: A New Edition with a Supplement, Continuing the Subject to the Year 1829. *Whittaker, Treacher, and Arnot.*
[18] Thompson, B. (1798). An inquiry concerning the source of the heat which is excited by friction. *Philosophical Transactions of the Royal Society of London*, *88*, 80–102. https://doi.org/10.1098/RSTL.1798.0006
[19] Thomson, W. (1852). II. On the dynamical theory of heat, with numerical results deduced from Mr. Joule's equivalent of a thermal unit, and M. Regnault's observations on steam. *The London, Edinburgh, and Dublin Philosophical Magazine and Journal of Science*, *4*(22), 8–21.
[20] Wisniak, J. (2008). Conservation of energy: readings on the origins of the first law of thermodynamics. Part I. *Educación Química*, *19*(2), 159–171.
[21] Митрович, Й., & Смык, А. Ф. (2021). Термодинамика Джеймса Уатта-проигнорирована или не понята? *Вопросы Истории Естествознания и Техники*, *42*(3), 397–442.

RENEWABLE ENERGY AND ENVIRONMENTAL PROTECTION

COMETa 2022
6th INTERNATIONAL SCIENTIFIC CONFERENCE
17th - 19th November 2022
Jahorina, B&H, Republic of Srpska
University of East Sarajevo
Faculty of Mechanical Engineering
Conference on Mechanical Engineering Technologies and Applications

OSNOVNI ASPEKTI PROIZVODNJE ENERGIJE SPALJIVANJEM OTPADNE POLJOPRIVREDNE BIOMASE U LOŽIŠTIMA

Stojan Simić[1], Goran Orašanin[2], Davor Milić[3], Srđan Vasković[4], Jovana Blagojević[5], Krsto Batinić[6]

Rezime: Otpadna poljoprivredna biomasa predstavlja izuzetno veliki energetski potencijal, koji trenutno nije dovoljno iskorišćen. Pri sagorijevanju biomase ne dolazi do povećanja sadržaja ugljen-dioksida u atmosferi što je od posebnog značaja sa aspekta zaštite životne sredine. Kada se otpadna poljoprivredna biomasa koristi kao energent najprihvatljivija su kogeneracijska postrojenja, koja u jednom tehnološkom procesu istovremeno proizvode toplotnu i električnu energiju. Ovaj otpadni materijal već danas ima, a i u narednom periodu će imati značajno mjesto u razvoju ekologije, poljoprivrede i energetike svakog regiona koji se opredijeli za njegovu upotrebu za proizvodnju energije. U radu se sa više aspekata razmatraju postupci dobijanja energije iz otpadne poljoprivredne biomase, kao i postupci njenog iskorišćenja za proizvodnju toplotne i električne energije.

Ključne riječi: poljoprivreda, biomasa, energija, proizvodnja.

BASIC ASPECTS OF ENERGY PRODUCTION BY BURNING WASTE AGRICULTURAL BIOMASS IN BURNES

Abstract: Agricultural biomass waste is extremely high energy potential, which is not sufficiently utilized. The burning of biomass is not an increased content of carbon dioxide in the atmosphere which is very important in environmental protection. When

[1] Dr Stojan Simić**,** Mašinski fakultet Istočno Sarajevo, Vuka Karadžića 30, Istočno Sarajevo, BIH stojan.simic@ues.rs.ba
[2]Dr Goran Orašanin, Mašinski fakultet Istočno Sarajevo, Vuka Karadžića 30, Istočno Sarajevo, BIH goran.orasanin@ues.rs.ba
[3]Dr Davor Milić, Mašinski fakultet Istočno Sarajevo, Vuka Karadžića 30, Istočno Sarajevo, BIH, davor.milic@ues.rs.ba
[4],Dr Srđan Vasković, Mašinski fakultet Istočno Sarajevo, Vuka Karadžića 30, Istočno Sarajevo, BIH, srdjan.vaskovic@ues.rs.ba
[5] Jovana blagojević, ma , Mašinski fakultet Istočno Sarajevo, Vuka Karadžića 30, Istočno Sarajevo, BIH, jovana.blagojevic@ues.rs.ba
[6] Krsto Batinić, dipl.maš.inž. , Mašinski fakultet Istočno Sarajevo, Vuka Karadžića 30, Istočno Sarajevo, BIH, krsto.batinic@ues.rs.ba

the waste agricultural biomass used as fuel are acceptable cogeneration plants, which in the same technological process simultaneously generate heat and electricity. Waste agricultural biomass already has, and in the future will have a significant role in the development of ecology, agriculture and energy of each region to opt for its use to produce energy. This paper deals with several aspects of the methods of obtaining energy from agricultural biomass waste, as well as methods of its utilization for heat and electricity.

Key words: agriculture, biomass, energy, production.

1 UVOD

U svijetu neprekidno raste potreba za energijom. Zalihe fosilnih goriva su sve manje. Upravo zbog te činjenice treba se okrenuti drugim izvorima energije koji se nalaze u prirodi i koji su obnovljivi. U industrijski razvijenim zemljama već godinama se velika pažnja poklanja obnovljivim izvorima energije i zaštiti životne sredine. Poljoprivreda je veliki potrošač, ali istovremeno može postati i značajan proizvođač energije. Sa stanovišta poljoprivredne proizvodnje posebno je interesantno dobijanje energije iz biomase. Glavna prednost u korišćenju biomase kao izvora energije su veliki potencijal, ne samo u tu svrhu zasađene biljne kulture već i otpadnih materijala koji nastaju u poljoprivrednoj i prehrambenoj industriji.

U poljoprivredi postoje velike količine biljnih ostataka koje se mogu dijelom koristiti za proizvodnju energije. Poljoprivrednu biomasu čine ostaci jednogodišnjih kultura kao što su: slama žitarica, kukuruzovina, kukuruzni oklasak, stabljika, ljuska, koštice i dr. Nedopustivo je potpuno ukloniti sve biljne ostatke sa zemljišta da se ne osiromaši i poremeti prirodni ciklus kruženja supstance u njemu.

Danas se primjena biomase za proizvodnju energije pospješuje uvažavajući načelo održivog razvoja. Postoje razne procjene potencijala i uloge biomase u globalnoj energetskoj politici u budućnosti, ali se u svim strategijama predviđa njen značajan porast i mnogo veća uloga nego do sada. Glavna prednost biomase u odnosu na fosilna goriva je neuporedivo manja emisija štetnih gasova i otpadnih supstanci. Računa se da je opterećenje atmosfere sa ugljen-dioksidom pri korišćenju biomase kao goriva zanemarljivo, obzirom da je količina emitovanog ugljen-dioksida prilikom sagorijevanja jednaka količini apsorbovanog ugljen-dioksida tokom rasta biljke.

U radu se sa više aspekata razmatra upotreba otpadne poljoprivredne biomase za proizvodnju toplotne i električne energije kada se vrši njeno spaljivanje u ložištima različitih konstrukcija.

2 PREDNOSTI I NEDOSTACI UPOTREBE OTPADNE POLJOPRIVREDNE BIOMASE

Biomasa je organska supstanca biljnog ili životinjskog porijekla koja se različitim procesima pretvara u upotrebljivu energiju. Može se direktno pretvoriti u energiju sagorijevanjem i tako proizvoditi vodena para za grijanje i dobijati električna energija u malim termoelektranama. Biomasa je biorazgradljivi dio proizvoda, otpada i ostataka poljoprivredne proizvodnje (biljnog i životinjskog porijekla), šumarske i srodnih industrija. Ona predstavlja obnovljiv izvor energije i uopšteno se može podijeliti na drvnu, nedrvnu i životinjski otpad, gdje se razlikuje:

- drvna biomasa (ostaci iz šumarstva, otpadno drvo i dr.),
- drvna uzgojena biomasa (brzorastuće drveće),
- nedrvna uzgojena biomasa (brzorastuće alge i trave),
- ostaci i otpaci iz poljoprivrede,
- životinjski otpad i ostaci,
- gradski i industrijski otpad.

Najviše se koristi drvna biomasa koja je nastala kao sporedni proizvod ili otpad, kao i ostaci koji se ne mogu više iskoristiti. Takva se biomasa koristi kao gorivo u postrojenjima za proizvodnju toplotne i električne energije ili se prerađuje u tečna i gasovita goriva koja se koriste u industriji, domaćinstvima, motornim vozilima i dr.

Osnovni aspekt pri korišćenju biomase treba da bude održivost korišćenja. Održivost korišćenja, prije svega, podrazumijeva da količina biomase koja se koristi za dobijanje energije uvijek bude manja ili jednaka prirastu količine biomase. Kada su u pitanju poljoprivredne kulture, održivost korišćenja biomase podrazumijeva plansko i redovno vraćanje određene količine supstance u zemljište zaoravanjem (oko 30% biomase), jer se tako održava ravnoteža i postiže veća plodnost zemljišta.

Sa privrednog i ekološkog stanovišta postoji mnoštvo aspekata koji ukazuju na opravdanost primjene i korišćenja biomase kao energenta. Ekološki aspekti korišćenja biomase su:

- u zemljištu se za 28 dana razgradi oko 95% supstance biomase;
- biogoriva sadrže neznatne količine sumpora pa u produktima sagorijevanja nema sumpornih oksida;
- pri sagorijevanju biomase dobija se tzv. “čisti pepeo“;
- nema emisije ugljovodonika kao produkta nepotpunog sagorijevanja;
- biomasa je u potpunosti obnovljiv izvor energije;
- sva biomasa već postoji i nije je potrebno stvarati, već je treba samo planski iskoristiti i pomoći joj da se regeneriše.

U posljednje vrijeme biomasa dobija sve više na značaju kao resurs koji se koristi za proizvodnju "čiste energije". Privredni aspekti korišćenja biomase su:

- redukcija gasova koji izazivaju efekat staklene bašte;
- manja emisija štetnih komponenata u poređenju sa sličnim tehnologijama koje koriste fosilna goriva;
- smanjenje opasnosti od pojave požara;
- zaštita biljnog i životinjskog svijeta;
- otvaranje novih radnih mijesta;
- ekonomsko-komercijalni efekti u ruralnim sredinama.

Pored brojnih prednosti koje posjeduje kada se koristi u procesu proizvodnje energije, biomasa ima i neke nepogodnosti. U toku eksploatacije biomase najčešće se javljaju sljedeće nepogodnosti:

- manipulacioni i ekonomski problemi pri sakupljanju, pakovanju i skladištenju;
- periodičnost nastajanja;
- relativno mala zapreminska masa i toplotna moć svedena na jedinicu zapremine;
- razuđenost u prostoru;
- nepovoljan oblik i visoka vlažnost;
- visoke investicije u postrojenja za proizvodnju energije.

U poljoprivredi se pored glavnih proizvoda dobija i značajna količina otpadaka u obliku organske supstance. Među tim otpacima najvažnije su slama i kukuruzovina. Obzirom da je prosječan odnos zrna i mase, tzv. žetveni odnos 53% na prema 47%,

proizilazi da biomase ima približno koliko i zrna. Ako se razdvoje kukuruzovina i oklasak, njihov odnos je prosječno 82% na prema 18%, odnosno pri proizvodnji jedne tone zrna kukuruza dobija se 0,89 t otpadne biomase sa 0,71 t kukuruzovine i 0,18 t kukuruznog oklaska. Nesporno je da se nastala biomasa mora prvenstveno vraćati u zemljište. Preporučuje se zaoravanje 30 do 50% te mase, što znači da za energetsku upotrebu ostaje najmanje 30%. Ta količina predstavlja značajan potencijal za proizvodnju energije. Adekvatnim tretiranjem te količine biomase može se mnogo uštediti, ukoliko se ta energija iskoristi za ogrev ili za sušenje poljoprivrednih kultura. U tabeli 1. dato je koliko se dobije otpadne biomase pri uzgoju kukuruza na površini od jednog hektara.

Tabela 1. *Vrsta, količina i raspoloživost za energetske potrebe otpadne biomase od kukuruza*

Količina kukuruza, ha	Vrsta otpadne biomase	Količina otpadne biomase, t	Raspoloživo za energetske potrebe, %
1,0	kukuruzovina (komušina)	3,85	70
	kukuruzni oklasak	1,65	30

Pri proizvodnji jedne tone pšenice nastane jedna tona slame koja predstavlja otpadnu biomasu od koje je 35% raspoloživo za korišćenje za energetske potrebe, a pri proizvodnji jedne tone soje nastanu dvije tone slame od kojih se 60% može iskoristiti u energetske svrhe.

Zaoravanje slame i kukuruzovine usitnjene kombajnom prilikom žetve ili isjeckane nakon žetve, može biti korisno na zbijenim zemljištima i zemljištima siromašnim organskim supstancama. Nedostatak zaoravanja slame i kukuruzovine je u tome što smetaju finoj obradi zemljišta i kvalitetnoj sjetvi i što se pri njihovoj razgradnji pomoću mikroorganizama troši azot iz zemljišta. Pored toga, slama i kukuruzovina mogu biti smetnja prilikom nicanja usjeva.

Spaljivanje slame i kukuruzovine na njivi je najneprihvatljiviji način upotrebe ovog otpadnog materijala. Iz pepela ovih supstanci dobije se nešto kalijuma kao đubriva i to je jedina korist, pored uništavanja štetočina i uzročnika bolesti na njivi. Štete od spaljivanja su višestruke i ogledaju se u sljedećem:

- gubitak relativno velike količine organske supstance;
- isušivanje zemljišta;
- zagađivanje životne sredine dimnim gasovima i pepelom;
- opasnost od širenja požara, i dr.

Od slame i kukuruzovine na poljoprivrednom gazdinstvu može se proizvoditi vještački stajnjak, ali je to posao koji zahtijeva značajna finansijska ulaganja, mnogo vremena i radne snage. Bolji načini upotrebe slame i kukuruzovine su sljedeće:

- Obogaćivanje slame radi povećanja probavljivosti i hranljivosti pri ishrani stoke. To se postiže njenim tretiranjem sa NaOH bazom, amonijakom, benuralom (ureom) i pranjem vodenom parom.
- Od slame i kukuruzovine može se presovanjem dobiti briket za loženje.
- Slama i kukuruzovina mogu se koristiti za proizvodnju građevinskih ploča, iverice, celuloze i papira, izolacionih električnih materijala, vještačke smole i dr.
- Od ovog otpadnog materijala može se proizvoditi biogas i tečno gorivo.

3 POTENCIJAL OTPADNE POLJOPRIVREDNE BIOMASE U SVIJETU I ZEMLJAMA U REGIONU

U svijetu se godišnje proizvede preko dvije milijarde tona zrna žita, najviše pšenice, kukuruza i riže. Uz to se, kao sporedni proizvod, proizvode i oko tri milijarde tona slame i kukuruzovine. To je izuzetno velika količina i važno je da se korisno upotrijebi.

Danska je vodeća zemlja u Evropskoj Uniji po iskoristivosti otpadne biomase i proizvodnji energije od nje. Ova zemlja je nakon svjetske ekonomske krize sedamdesetih godina prošlog vijeka donošenjem više planova u sklopu svoje ekonomske politike, pokazala da je moguće iskoristiti potencijale u biomasi za proizvodnju toplotne i električne energije. Švedska posjeduje postrojenje koje koristi slamu od žitarica za proizvodnju toplotne energije. Sakupljena slama sa 120 ha je dovoljna da zagrije 130 domaćinstava. Ova investicija je iznosila 520 hiljada evra i isplatila se za nešto manje od sedam godina. U Švedskoj postoji jedna kompanija koja ima 30 ovakvih ili sličnih postrojenja, što ukazuje na riješenost države da ozbiljno investira u obnovljive izvore energije i na isplativost ovakvih projekata.

Srbija sa oko 45000 km^2 poljoprivredne površine posjeduje izuzetno veliki potencijal u biomasi. U Srbiji se u prosjeku svake godine proizvede oko 13 milina tona otpadne biomase, od toga samo u Vojvodini oko 9 miliona tona. Energija koja bi se mogla dobiti korišćenjem ovog izvora predstavlja 2,68 miliona tona ekvivalentne nafte. Na taj način bi se godišnje uštedilo oko 60 miliona evra koji se ulože za uvoz sirove nafte. Međutim, u Srbiji još uvijek nisu zadovoljavajući rezultati u korišćenju biomase kao energenta i pored postojećih potencijala.

U Bosni i Hercegovini, pored 1,2 miliona tona zrna žita, godišnje se dobija i oko 2 miliona tona slame i kukuruzovine. Jasno je da je potencijal otpadne poljoprivredne biomase relativno veliki. Međutim njeno iskorišćenje za proizvodnju toplotne energije je na niskom nivou. U predstojećem periodu potrebno je preduzeti odgovarajuće aktivnosti da bi se u što većem obimu ovaj otpadni materijal počeo koristiti kao energent za proizvodnju toplotne i električne enrgije.

4 TEHNIČKO-TEHNOLOŠKI ASPEKTI DOBIJANJA ENERGIJE IZ OTPADNE POLJOPRIVREDNE BIOMASE

Biomasa je prema svojstvima sličnija fosilnim gorivima nego obnovljivim izvorima energije, što je i razumljivo jer su fosilna goriva u stvari fosilni oblik biomase. Energija iz biomase može se dobiti na više načina:

- neposrednim spaljivanjem radi dobijanja toplotne energije;
- preradom stajnjaka od životinja u biogas (digestija);
- preradom biomase u alkohol (etanol) ili proizvodnjom biljnih ulja.

Na slici 1. prikazana je opšta šema proizvodnje energije iz uzgojne i otpadne biomase.

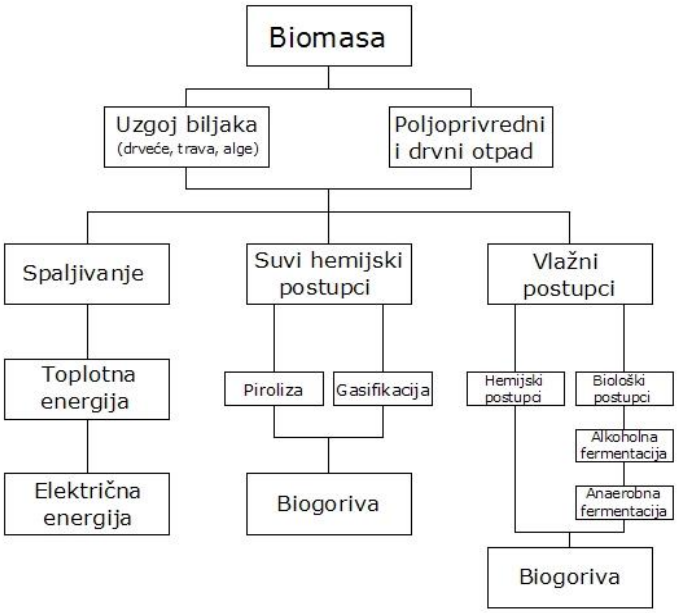

Slika 1. *Opšta šema proizvodnje energije iz biomase*

Prerada biomase se vrši u cilju dobijanja pogodnijeg oblika za transport, skladištenje i iskorišćenje. Primarne tehnologije prerade biomase su mehanička, biohemijska i termičko-hemijska prerada.

Mehanička prerada u suštini predstavlja briketiranje, odnosno peletiranje biomase. Tehnologija briketiranja-peletiranja je postupak prilikom kojeg se usitnjeni materijal pri visokom pritisku pretvara u kompaktnu formu relativno velike zapreminske mase pogodnu za dalju manipulaciju i korišćenje.

Pod biohemijskom preradom se podrazumijeva razgradnja biomase sa ili bez prisustva kiseonika uz oslobađanje manje ili veće količine toplote. Biohemijskom preradom se dobijaju gasoviti produkti (biogas), tečna goriva (bioetanol) i kompost koji se može upotrijebiti kao đubrivo u poljoprivredi.

Termičko-hemijska prerada biomase se vrši procesom sagorijevanja. U zavisnosti od vrste, sadržaja vlage i veličine komada razlikuju se tehnologije za pripremu i konstrukciona rješenja ložišta kotlova u kojima se vrši sagorijevanje otpadne biomase. Za sagorijevanje se uglavnom koriste klasične tehnologije sagorijevanja na rešeci (nepokretnoj, pokretnoj, kosoj i stepenastoj), sagorijevanje u letu i sagorijevanje u fluidizovanom sloju. Najčešće korišćena goriva za ovakva postrojenja su drvni otpaci iz šumarstva i drvne industrije, slama, kukuruzovina i drugi poljoprivredni otpad, komunalni i industrijski biorazgradljivi otpad. Prema načinu neposredne pripreme biomase za sagorijevanje, razlikuju se tehnologije kod kojih se vrši [1, 2]:

- neposredno sagorijevanje biomase u kotlovima sa ložištem klasične ili specijalne konstrukcije,
- gasifikacija biomase u predložištu, a zatim sagorijevanje gasa u kotlovima sa ložištem klasične konstrukcije za gasovita goriva.

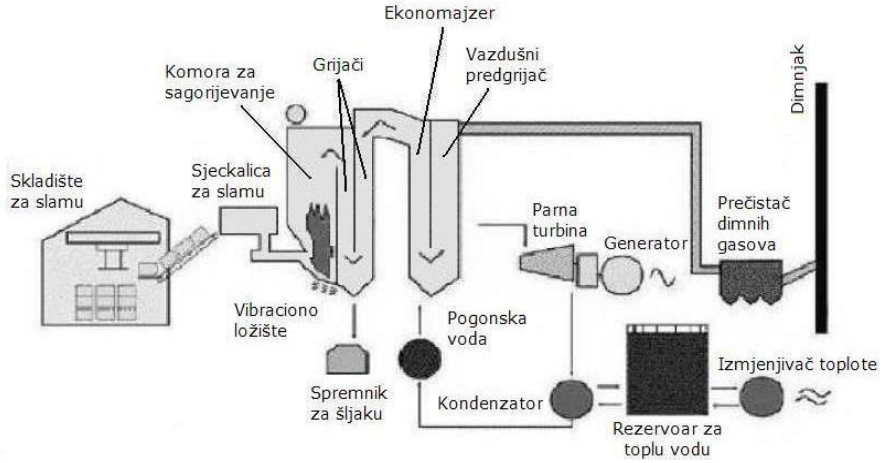

Slika 2. *Tehnološka šema termoelektrane-toplane na slamu*

Ove tehnologije se zasnivaju na proizvodnji vodene pare koja se koristi za zagrijavanje u industrijskim postrojenjima i stambenim jedinicama ili za dobijanje električne energije u malim termoelektranama koje kao gorivo koriste biomasu. Na slici 2. prikazana je tehnološka šema jedne termoelektrane-toplane koja kao gorivo koristi slamu od žitarica.

Pored neposrednog sagorijevanja često se koriste i različita tehnička rješenja za kosagorijevanje otpadne biomase sa nekim drugim gorivom. Na slici 3. prikazano je direktno i indirektno kosagorijevanje otpadne poljoprivredne biomase sa ugljem.

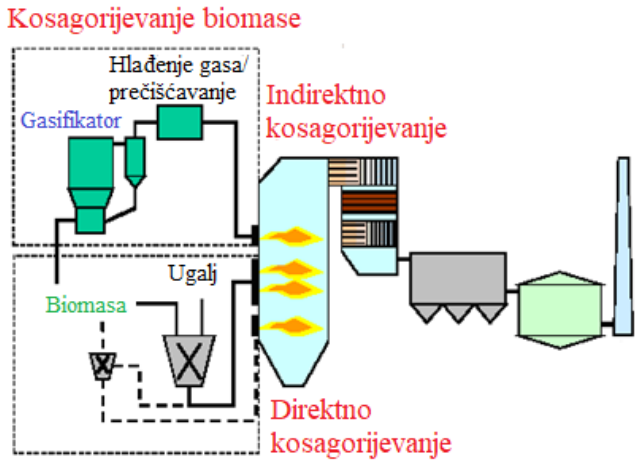

Slika 3. *Šematski prikaz direktnog i indirektnog kosagorijevanje otpadne poljoprivredne biomase sa ugljem*

Osnovni problem koji se javlja pri korišćenju biomase za proizvodnju toplotne i električne energije je relativno visok sadržaj vlage i mala toplota moć po jedinici mase. U tabeli 2. date su toplotne moći nekih vrsta goriva i gorivog otpada u poređenju sa otpadnom poljoprivrednom biomasom.

Tabela 2. *Toplotne moći nekih vrsta goriva, gorivog otpada i otpadne biomase*

Redni broj	Gorivo, gorivi otpad	Donja toplotna moć	Jedinica
1.	kameni ugalj	24-37,7	MJ/kg
2.	mrki ugalj	12,7-23,9	
3.	lignit	7,0-12,6	
4.	otpadna biomasa		
	slama pšenice i ječma (udio vlage 14%)	14,0	
	sojina slama (udio vlage 10%)	15,5	
	kukuruzni oklasak (udio vlage 10%)	14,5	
	ljuska od suncokreta (udio vlage 10%)	16,5	
	grane od voća, vinove loze i šumskog drveća (udio vlage 20%)	15,0	

Pored prisustva vlage, problem predstavlja količina pepela koja nastaje u toku sagorijavanja otpadne poljoprivredne biomase. Od ukupne količine biomase koja sagori nastane oko 20% pepela. U tabeli 3. prikazana je tehnička analiza raznih vrsta otpadne poljoprivredne biomase.

Tabela 3. *Tehnička analiza raznih vrsta otpadne poljoprivredne biomase*

Vrsta materijala	Vlaga, % ,	Pepeo, % ,	Koks, % ,	Volatili, % ,
Pšenična slama	7,21	5,45	22,50	70,29
Kukuruzovina	7,43	4,49	18,57	74,00
Kukuruzni oklasak	9,19	2,18	17,75	73,06
Ljuska suncokreta	7,20	2,93	15,50	77,30

Hemijski sastav otpadne poljoprivredne biomase varira u zavisnosti od tipa izvornih supstanci. Uglavnom se prosječan sastav sastoji od 25% lignina i 75% ugljenih hidrata, odnosno šećera. U tabeli 4. prikazan je hemijski sastav otpadne poljoprivredne biomase.

Tabela 4. *Hemijski sastav otpadne poljoprivredne biomase (osnovni elementi)*

Hemijski elemenat	Vrsta biomase		
	Slama žitarica, % ,	Kukuruzni oklasak, % ,	Ljuska suncokreta, % ,
Ugljenik (C)	44,84	48,31	50,57
Vodonik (H)	5,68	5,74	5,68
Kiseonik (O)	40,86	43,10	40,90
Azot (N)	0,62	0,66	0,60
Pepeo	8,00	2,19	2,25

Kada se biomasa koristi kao gorivo za proizvodnju električne energije pogodnije su zbog troškova transporta termoelektrane male snage, ali je problem što ta postrojenja imaju manji stepen iskorišćenja. Zbog toga se pribjegava izgradnji termoenergetskih postrojenja koja u jednom tehnološkom procesu istovremeno proizvode električnu i toplotnu energiju (kogeneracija). U većini kogeneracijskih sistema hemijska energija se pretvara u mehaničku i toplotnu energiju. Mehanička energija se koristi za proizvodnju električne energije, dok se toplotna energija koristi za proizvodnju tehnološke pare, grijanje vode ili vazduha. Osnovna prednost kogeneracije je veća iskoristivost energenta u odnosu na klasične elektrane koje služe samo za proizvodnju električne energije i industrijske sisteme koji služe samo za proizvodnju

pare ili tople vode za tehnološke procese. Jedan od glavnih razloga za izgradnju kogeneracijskih postrojenja je mogućnost proizvodnje jeftinije električne struje u odnosu na cijenu u elektro mreži, tako da se uložena finansijska sredstva u ova postrojenja počinju relativno brzo otplaćivati.

5 ZAKLJUČCI

U radu su objašnjeni postupci dobijanja energije iz otpadne poljoprivredne biomase, kao i postupci njenog iskorišćenja za proizvodnju toplotne i električne energije. Postrojenja za proizvodnju toplotne i električne energije iz otpadne poljoprivredne biomase već danas imaju, a i u narednom periodu će zauzimati značajno mjesto u razvoju ekologije, poljoprivrede, energetike i uopšte cijele ekonomije svakog regiona koji se opredijeli za njenu upotrebu i korišćenje.

Za zemlje u regionu karakterističan je nizak nivo iskorišćenja otpadne poljoprivredne biomase u energetske svrhe. Privatna gazdinstva često na njivama vrše spaljivanje otpadne biomase. Slamu od žitarica uglavnom koriste za prostirku u objektima gdje se uzgaja stoka. Otpadna poljoprivredna biomasa u zemljama u regionu prestavlja značajan energetski resurs kojeg treba u narednom periodu na adekvatan način iskoristiti.

LITERATURA

[1] Đonlagić, M.: (2010). Obnovljivi izvori energije*, Studija o obnovljivim izvorima energije u BiH*, Tuzla.

[2] Šljivac, D.: (2008). Obnovljivi izvori energije*, Energija biomase*, Osijek.

[3] Jordanović-Vasić, M.: (2009). Upotreba biomase iz poljoprivrednog otpada kao obnovljivog izvora energije, *Nauka i praksa*, str. 60-63.

[4] Šišić, I., Ćehajić, A., Rekanović, S.: (2013). Istraživanje optimalnih rješenja valorizacije poljoprivredne biomase u energetske i druge svrhe, 9th International Scientific Conference on Production Engineering, str. 645-650.

COMETa 2022
6th INTERNATIONAL SCIENTIFIC CONFERENCE
17th - 19th November 2022
Jahorina, B&H, Republic of Srpska
University of East Sarajevo
Faculty of Mechanical Engineering
Conference on Mechanical Engineering Technologies and Applications

NUMERIČKA ANALIZA UKUPNOG DOLAZNOG SOLARNOG ZRAČENJA NA POVRŠINU RAVNOG SOLARNOG PRIJEMNIKA SA JEDNOOSNIM PRIVIDNIM PRAĆENJEM SUNCA – SLUČAJ SA NAGNUTOM S-J OSOM I PRAĆENJEM U PRAVCU I-Z

Aleksandar Nešović[1]

Rezime: U ovom radu koristi se softver Energy Plus da bi se numerički analizirala moguća implementacija mehanizma jednoosnog (oko nagnute S-J ose u pravcu I-Z) prividnog praćenja kretanja Sunca na konstrukciju ravnog (pločastog, zastakljenog) solarnog prijemnika, sve sa ciljem da se maksimizira prikupljanje ukupnog dolaznog solarnog zračenja. Na osnovu velikog broja simulacija, napravljen je petomesečni (od juna do oktobra) uzorak, a potom su definisana tri osnovna obrasca ponašanja navedene solarne konstrukcije: pri izrazito vedrom (prvi slučaj), vedrom (drugi slučaj) i oblačnom vremenu (treći slučaj). Rezultati pokazuju opravdanost primene ovakvog solarnog dizajna, jer u prvom (16. avgust) slučaju na pokretni solarni prijemnik dospeva i do 50% više solarnog zračenja nego na fiksni solarni prijemnik iste aktivne površine. U drugom (26. jul) slučaju, ta razlika je nesto manja, tj. 35% u korist pokretnog solarnog prijemnika, da bi u trećem (6. septembar) slučaju ona bila najmanja (ispod 10%), ali i dalje u korist pokretnog solarnog prijemnika.

Ključne riječi: Jednoosno prividno praćenje Sunca, Numerička simulacija, Pokretni solarni prijemnik, Ukupno dolazno solarno zračenje, Fiksni solarni prijemnik.

NUMERICAL ANALYSIS OF THE TOTAL INCIDENT SOLAR RADIATION ON THE FLAT-PLATE SOLAR COLLECTOR WITH SINGLE-AXIS TRACKING – CASE WITH INCLINED N-S AXIS AND E-W TRACKING

Abstract: In this paper, the Energy Plus software was used to numerically analyze the possible implementation of the single-axis (around the inclined N-S axis in the E-W direction) tracking mechanism on the flat-plate solar collector, all with the aim of maximizing the collection of the total incident solar radiation. Based on a large number of simulations, a five-month (from June to October) sample was created, and then three basic behavior patterns of the mentioned solar structure were defined: extremely

[1] Mast. inž. maš., Aleksandar Nešović, Fakultet inženjerskih nauka Univerziteta u Kragujevcu, Kragujevac, Srbija, aca.nesovic@kg.ac.rs (CA).

clear (first case), clear (second case) and cloudy weather (third case). The results were showed the application justification of this solar design, because in the first case (August 16), up to 50% more solar radiation reaches the single-axis tracking flat-plate solar collector than the fixed flat-plate solar collector of the same active surface. In the second (July 26) case, that difference is somewhat smaller, i.e. 35% in favor of the single-axis tracking flat-plate solar collector, so that in the third (September 6) case it would be the smallest (below 10%), but still in favor of the single-axis tracking flat-plate solar collector.

Keywords: Fixed flat-plate solar collector, Numerical simulation, Single-axis tracking, Total incident solar radiation, Tracking flat-plate solar collector.

1 UVOD

U stambenom sektoru najveću primenu imaju ravni (pločasti, zastakljeni) solarni prijemnici, koji su, prema tradicionalnoj klasifikaciji, nekoncentrišući i nepokretni.Konstrukcija ravnih solarnih prijemnika prilično je jednostavna: određeni broj lamela sa integrisanim protočnim kanalima spaja se u aktivnu površinu za prikupljane solarne energije, tj. apsorbersku ploču (ravnu površinu), koja se sa gornje strane prekriva zastakljenjem (jednoslojnim ili višeslojnim), a sa donje strane štiti slojem izolacije. Time se toplotni gubici ravnog solarnog prijemnika smanjuju, a termički stepen korisnosti povećava.

Praksa je ipak pokazala da navedena konstrukcija ne mora uvek da bude nekoncentrišuća i nepokretna. Iako su sistemi za prividno praćenje kretanja Sunca više karakteristični za PV panele i neke druge tipove solarnih prijemnika, do danas je objavljen određen broj radova u kojima se ravni solarni prijemnik rotira oko jedne ili obe ose (Tab. 1). U tabeli 2, hronološki su prikazani radovi u kojima se kod ravnih solarnih prijemnika primenjuju razne koncentrišuće, odnosno reflektujuće površine.

Tabela 1. *Istorijski razvoj primene nekonvencionalnih ravnih solarnih prijemnika Prvi deo (od 1970. do 2000.)*

Godina	70	77	78	79	80	81	86	90	91	92	95
Reflektor	[1]	[2]	-	[3]	[4] [5]	-	[6]	-	-	[7]	[8]
Koncentrator	-	-	-	-	-	[17]	-	[18]	-	-	-
Prividno praćenje Sunca	-	-	[21] [22]	-	-	-	-	-	[23]	[24]	-

Tabela 2. *Istorijski razvoj primene nekonvencionalnih ravnih solarnih prijemnika Drugi deo (od 2000. do 2021.)*

Godina	12	13	14	15	17	18	20	21
Reflektor	[9]	[10]	[11]	[12] [13]	[14]	[15]	[16]	-
Koncentrator	-	-	[19]	-	-	-	[20]	-
Prividno praćenje Sunca	-	[25]	[26] [27] [28]	[29]	-	[30] [31]	[32]	[33]

U ovom radu napravljen je još jedan mali iskorak, koji se ogleda u primeni savremenih softverskih alata (u ovom slučaju programa Energy Plus) u termičkim analizama pokretnih (mobilnih) solarnih sistema. Autor se nada da će ovo istraživanje biti od značaja budućim istraživačima, još više, ako se u obzir uzme da pomenuti softver u sebi poseduje alate za istraživanje samo fiksnih ravnih solarnih prijemnika, sto znači da su uslovi istaživanja pokretnih ravnih solarnih prijemnika veštački kreirani od strane korisnika.

2 ENERGY PLUS MODEL UKUPNOG DOLAZNOG SOLARNOG ZRAČENJA

U softveru Energy Plus postoji model za proračun ukupnog dolaznog solarnog zračenja na proizvoljno orijentisanu fiksnu ravnu površinu, u ovom slučaju solarnog prijemnika I_{TOT} [W]. Proračun ovog zračenja je veoma složen, ali se u opštem slučaju može predstaviti kao zbir direktnog I_{DIR} [W], difuznog I_{DIFF} [W] i reflektovanog I_{REF} [W] solarnog zračenja Jed. (1):

$$I_{TOT} = I_{BEAM} + I_{DIFF} + I_{REFL} \tag{1}$$

Difuzno solarno zračenje na površinu solarnog prijemnika dospeva iz tri pravca: nebeske kupole (engl. *Sky Dome*) $I_{DIFF-SD}$ [W] i horizonta (engl. *Horizon*) I_{DIFF-H} [W], kao i uske oblasti koja se formira oko direktnog solarnog zraka (engl. *Circumsolar*) I_{DIFF-C} [W] Jed. (2):

$$I_{DIFF} = I_{DIFF-SD} + I_{DIFF-H} + I_{DIFF-C} \tag{2}$$

Reflektovano solarno zračenje nastaje odbijanjem solarnog zračenja (direktnog i difuznog) od zemlje I_{REFL-G} [W] i okolnih površina I_{REFL-S} [W] Jed. (3):

$$I_{REFL} = I_{REFL-G} + I_{REFL-S} \tag{3}$$

3 SCENARIO SIMULACIJA

Na narednoj slici prikazani su Energy Plus modeli fiksnog (Sl. 1a) i pokretnog ravnog solarnog prijemnika sa jedoosnim praćenjem kretanja Sunca u pravcu I-Z (Sl. 1b), oba sa istim S-J nagibom prema horizontali pod uglom od 34° (optimalni ugao za grad Kragujevac). Njihove geometrijske karakteristike prikazane su u Tab. 3.

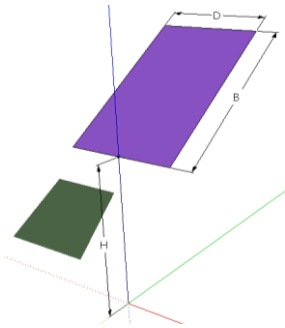

Slika. 1a. *Fiksni ravni solarni prijemnik*

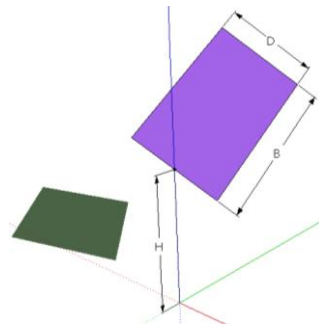

Slika. 1b. *Pokretni ravni solarni (jednoosno praćenje Sunca u pravcu I-Z)*

Tabela 3. *Geometrijske karakteristike analiziranih solarnih prijemnika*

Solarni prijemnik	Fiksni	Pokretni
B [mm]	800	
D [mm]	500	
H [mm]	700	
Broj simulacija	1	181
Lokacija	Kragujevac, Srbija	
Vremenske prilike	26. jul (vedar dan)	
	16. avgust (izrazito vedar dan)	
	6. septembar (oblačan dan)	

Kako u softveru Energy Plus ne postoje modeli za analizu pokretnih solarnih prijemnika, za potrebe ove studije, modeli su veštacki napravljeni. Naime, nizom simulacija, vršen je proračun ukupnog dolaznog solarnog zračenja tokom čitavog dana, za svaki ugao zakretanja ravne površine: od -90° (trenutak izlaska Sunca) do +90° (trenutak zalaska Sunca), pri čemu je korak zakretanja bio 1°. Da bi rezultati bili što precizniji, korišćen je vremenski fajl sa jednominutnim korakom. Nakon toga, maksimalna brojna vrednost ukupnog dolaznog solarnog zračenja (za dati ugao zakretanja u datom vremenskom trenutku) korišćena je za formiranje dnevne krive ukupnog dolaznog solarnog zračenja.

4 REZULTATI I DISKUSIJA

Intenzitet ukupnog dolaznog I_{TOT*} [W] solarnog zračenja na horizontalnu ravnu površinu za tri karakteristična slučaja (26. jul – vedar dan, 16. avgust – izrazito vedar dan i 6. septembar – oblačan dan) prikazan je na Sl. 2.

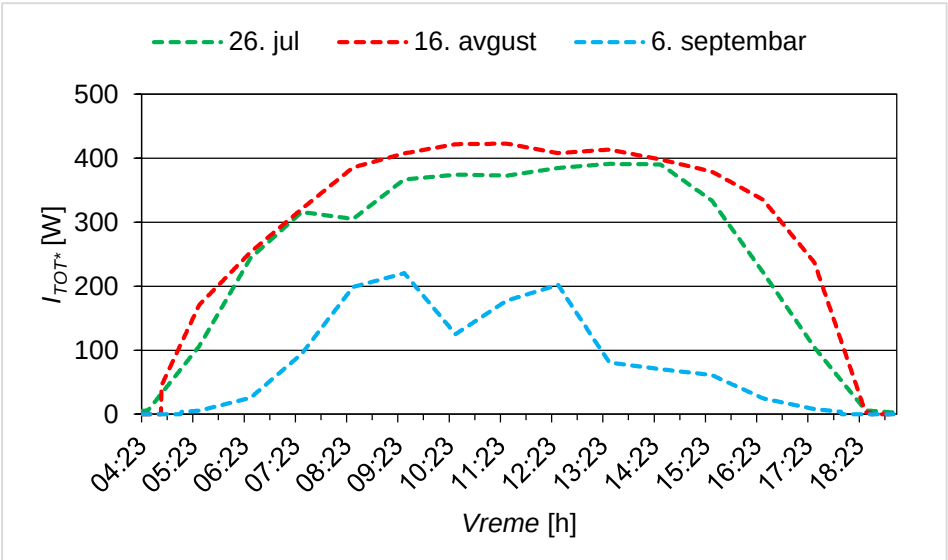

Slika. 2. *Ukupno dolazno solarno zračenje na horizontalnu ravnu površinu*

Za 26. jul (vedar dan, izlazak Sunca u 04:23 h, zalazak Sunca u 17:03 h) prosečan dnevni intenzitet I_{TOT*} = 267.05 W. Dijagram (Sl. 2) pokazuje blagi diskontinuitet (od 07:00h do 15:00 h), što se objašnjava prisustvom delimične oblačnosti. Vrednost I_{TOT*} najveća je u 13:30 h (391.2 W). Za 16. avgust (izrazito vedar dan, izlazak Sunca u 04:46 h, zalazak Sunca u 18:36 h) prosečna dnevna vrednost I_{TOT*} = 328.52 W, dok je maksimalna dnevna vrednost 385,2 W (10:30 h). Solarna kriva za 6. septembar (izlazak Sunca u 05:09 h, zalazak Sunca u 18:01 h) govori da se radi o oblačnom danu (prisustvo velikih solarnih fluktuacija). Tokom ovog dana (Sl. 2) prosečna dnevna vrednost ukupnog dolaznog solarnog zračenja na horizontalnu ravnu površinu je 100.34 W. Maksimalna vrednost solarnog zračenja zabeležena je u 09:30 h (220,4 W).

Na sledećim slikama (Sl. 3-5) prikazano je poređenje fiksnog i pokretnog ravnog solarnog prijemnika za pomenute (prema Sl. 2) dane.

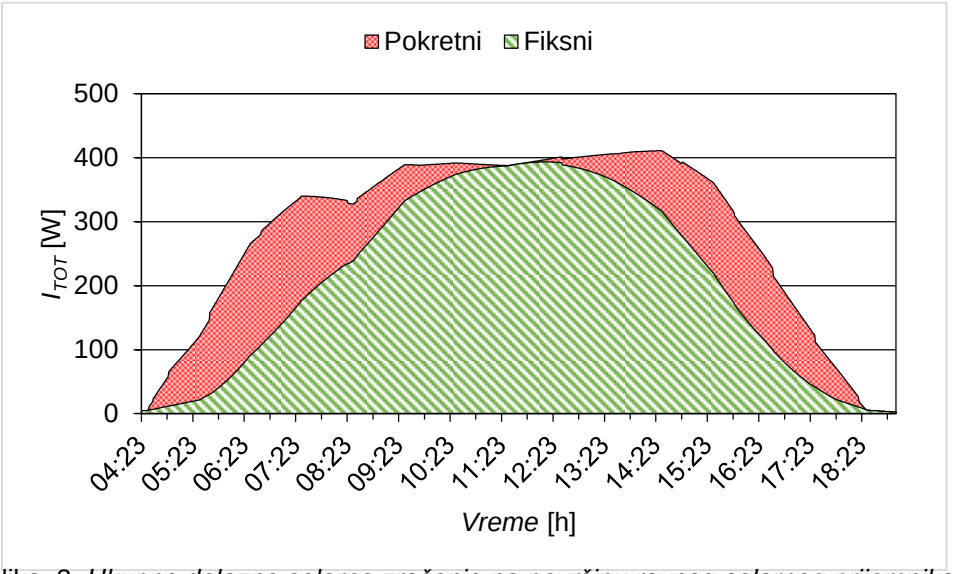

Slika. 3. *Ukupno dolazno solarno zračenje na površinu ravnog solarnog prijemnika (26. jul)*

Pokretni solarni prijemnik tokom vedrog dana (26, jul, Sl. 3) može postići do 35.92% bolje rezultate od fiksnog solarnog prijemnika, jer na njegovu površinu tada u proseku dospeva 284.41 W solarnog zračenja, dok na površinu fiksnog solarnog prijemnika dospeva 209.24 W. Kada su vremenske prilike još povoljnije (karakteristike izrazito vedrog vremena), pokretni solarni prijemnik u stanju je da prikupi i do 347.1 W, što je za 47.55% više od fiksnog solarnog prijemnika (Sl. 4). Tokom oblačnih dana, kada je udeo difuznog solarnog zračenja u ukupnom solarnom iznosu veći od udela direktnog solarnog zračenja, razlike između pokretnih i nepokretnih solarnih prijemnika se smanjuju, pa mogu pasti ispod 8% (slučaj prikazan na Sl. 5). U ovoj situaciji, ukupno prosečno dnevno dolazno solarno zračenje na površine fiksnog i pokretnog ravnog solarnog prijamnika redom su (6. septembar): 95.11 W i 101.88 W.

Bolji rezultati, koje ostvaruje pokretni ravni solarni prijemnik u odnosu na fiksni, leže u primeni jedoosnog sistema za prividno praćenje kretanja Sunca. Ovakvim mehanizmom obezbeđuje se minimalna vrednost solarnog upadnog ugla (ugao između vektora položaja Sunca, tj. direktnog solarnog zračenja i vektora normale na površinu ravnog solarnog prijemnika) u svakom trenutku, što je od posebne važnosti za

transferzalnu (poprečnu) ravan, koja ima prednost korišćenja u ovakvim termičkim analizama (karakteristične za pokretne solarne sisteme) u odnosu na još jednu – uzdužnu ravan.

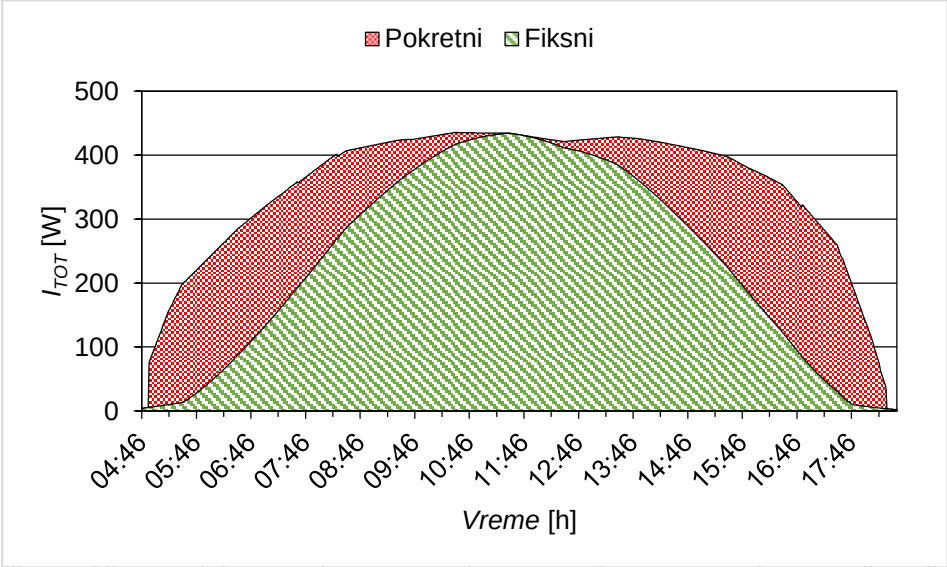

Slika. 4. *Ukupno dolazno solarno zračenje na površinu ravnog solarnog prijemnika (16. avgust)*

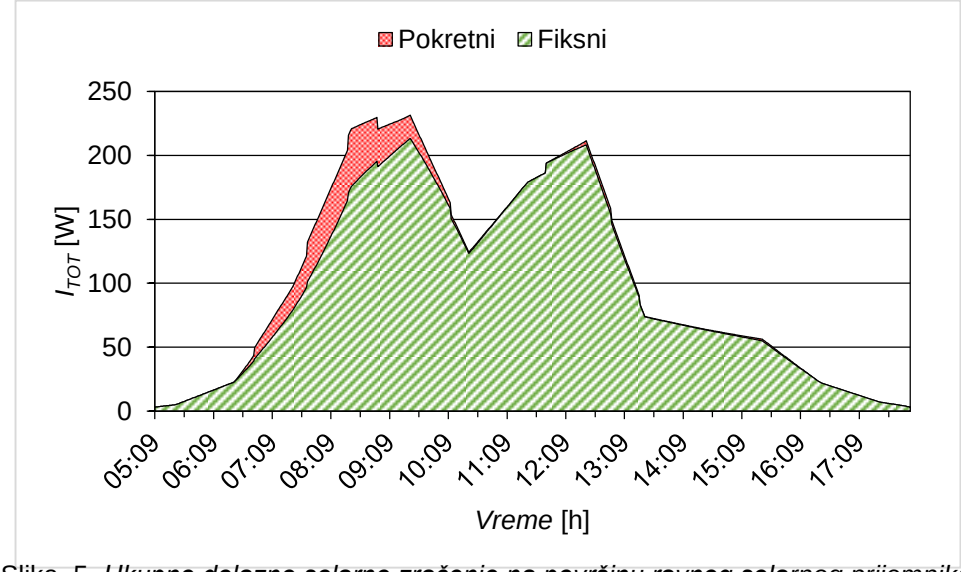

Slika. 5. *Ukupno dolazno solarno zračenje na površinu ravnog solarnog prijemnika (16. avgust)*

Primena ovakvog mehanizma tokom dana dolazi do punog izražaja pre i posle solarnog podneva, tj. pre i posle tzv. zenitnog položaja, kada se obezbeđuje "upravnost" direktnog solarnog zračenja (po intenzitetu slabijeg) na površinu solarnog

prijemnika. U trenutku solarnog podneva, ravni u kojima leže pokretni i fiksni solarni prijemnik međusobno su paralelne, a njiihove aktivne površine za prikupljanje solarnog zračenja jednake, pa su im i termičke karakteristike identične. Drugim rečima, u trenutku solarnog podneva, solarna kriva pokretnog solarnog prijemnika preklapa se sa solarnom krivom fiksnog solarnog prijemnika (Sl. 3-5).

5 ZAKLJUČAK

U ovom radu izvršeno je poređenje termičkih karakteristika pokretnog (oko nagnute S-J ose u pravcu I-Z) i fiksnog ravnog solarnog prijemnika (istih aktivnih površina i sa istim nagibom prema horizontali) korišćenjem savremenog softverskog paketa Energy Plus. Rezultati su pokazali opravdanost primene ovakvih solarnih sistema, jer se time može prikupiti 7-50% više solarne energije, zavisno od vremenskih prilika. Uloga numeričkih alata u ovakvim situacijama (kada eksperimentalna i svaka druga istraživanja mogu biti dosta skupa) može biti od presudnog značaja, jer se time štede i vreme i novac, pa bi softveri (poput Energy Plus programa), trebalo da zauzmu posebno mesto svim početnim fazama istraživanja svih mogućih tipova HVAC sistema. Da bi to bilo moguće, potrebno je da se neprestano radi na usavršavanju softvera kako bi se ispratile sve potrebe njihovih korisnika.

ZAHVALNOST

Ovo je rezultat rada u okviru dva projekta: projekat TR 33015 Tehnološkog razvoja Republike Srbije, projekat III 42006 Integralna i interdisciplinarna istraživanja Republike Srbije. Prvi projekat je pod nazivom "Istraživanje i razvoj Srpske kuće nulte neto potrošnje energije". Drugi projekat je pod nazivom "Istraživanje i razvoj energijski i ekološki visoko efikasnih sistema poligeneracije zasnovanoj na obnovljivim energijskim izvorima". Želim da se zahvalim Ministarsvu prosvete, nauke i tehnološkog razvoja Republike Srbije na njihovj finansijskoj podršci tokom ovog istraživanja.

LITERATURA:

[1] Safwat, H. H., Souka, A. F. (1970) Design of a new solar-heated house using double-exposure flat-plate collectors, *Solar Energy*, 13, pp. 105-119.
[2] Grassie, S. L., Sheridan, N. R. (1977) The use planar reflectors for increasing the energy yield of flat-plate collectors, *Solar Energy*, 19, pp. 663-668.
[3] Larson, D. C. (1979) Mirror enclosures for double-exposure solar collectors, *Solar Energy*, 23, pp. 517-524.
[4] O'gallagher, J. J., Rabl, A., Winston, R. (1980) Absorption enhancement in solar collectors by multiple reflections, *Solar Energy*, 24, pp. 323-326.
[5] Taha, I. S., Eldighidy, S. M. (1980) Effect of off-south orientation on optimum conditions for maximum solar energy absorbed by flat plate collector augmented by plane reflector, *Solar Energy*, 25, pp. 373-379.
[6] Arata, A. A., Geddes, R. W. (1986) Combined collector-reflector systems, *Energy*, 2, pp. 621-630.
[7] Chiam, H. F. (1992) Stationary reflector-augmented flat-plate collectors, *Solar Energy*, 29, pp. 65-69.
[8] Bollentin, J. W., Wilk, R. D. (1995) Modeling the solar irradiation on flat plate collections augmented with planar reflectors, *Solar Energy*, 55, pp. 343-354.

[9] Lertsatitthanakorn, C., Rungsiyopas, M., Therdyothin, A., Soponronnarit, S. (2012) Performance study of a double-pass thermoelectric solar air collector with flat-plate reflectors, *Journal of Electronic Materials*, 41, pp. 999-1003.
[10] Nikolić, N., Lukić, N. (2013) A mathematical model for determining the optimal reflector position of a double exposure flat-plate solar collector, *Renewable Energy*, 51, pp. 292-301.
[11] Pandolfini, J., Krothapallia, A. (2014) Thermodynamic modeling of the multiple parabolic reflector flat panel collector, *Energy Procedia*, 57, pp. 2762-2771.
[12] Baccoli, R., Mastino, C. C., Innamorati, R., Serra, L., Curreli, S., Ghiani, E., Ricciu, R., Marini, M. (2015) A mathematical model of a solar collector augmented by a flat plate above reflector: Optimum inclination of collector and reflector, *Energy Procedia*, 81, pp. 205-214.
[13] Nikolić, N., Lukić, N. (2015) Theoretical and experimental investigation of the thermal performance of a double exposure flat-plate solar collector, *Solar Energy*, 119, pp. 100-113.
[14] Bhowmik, H., Amin, R. (2017) Efficiency improvement of flat plate solar collector using reflector, *Energy Reports*, 3, pp 119-123.
[15] Baccoli, R., Frattolillo, A., Mastino, C., Curreli, B., Ghiani, E. (2018) A comprehensive optimization model for flat solar collector coupled with a flat booster bottom reflector based on an exact finite length simulation model, *Energy Conversion and Management*, 164, pp. 482-507.
[16] Abd, H. M., Alomar, O. R., Ali, F. A., Salih, M. M. M. (2020) Experimental study of compound parabolic concentrator with flat plate receiver, *Applied Thermal Engineering*, 166, pp. 114678.
[17] Chiam, H. F., Planar concentrators for flat-plate solar collectors, *Solar Energy*, 26, pp. 503-509.
[18] Tasdemiroglu, E., Arinc, F. (1990) Comparison of the available solar radiation on fiat-plate and concentrating solar collectors in Turkey, *Solar & Wind Technology*, 7, pp. 293-297.
[19] Pandolfini, J., Krothapalli, A. (2014) Thermodynamic modeling of the multiple parabolic reflector flat panel collector, *Energy Procedia*, 57, pp. 2762-2771.
[20] Qiu, G., Ma, Y., Song, W., Cai, W. (2021)Comparative study on solar flat-plate collectors coupled with three types of reflectors not requiring solar tracking for space heating, *Renewable Energy*, 169, pp. 104-116.
[21] Drago, P. (1978) A simulated comparison of the useful energy gain in a fixed and a fully tracking flat plate collector, *Solar Energy*, 20, pp. 419-423.
[22] Neville, R. C. (1978) Solar energy collector orientation and tracking mode, *Solar Energy*, 20, pp. 7-11.
[23] Gordon, J. M., Kreider, J. F., Reeves, P. (1991) Tracking and stacionary flat plate solar collectors: Yearly collectible energy correlations for photovoltaic applications, *Solar Energy*, 47, pp. 245-252.
[24] Reddy, T. A., Attalage, R. A. (1992) Annual collectible energy of a two-axis tracking flat-plate solar collector, *Solar Energy*, 48, pp. 151-155.
[25] García, A., Martin, R. H., Pérez-García, M. (2013) Experimental study of heat transfer enhancement in a flat-plate solar water collector with wire-coil inserts, *Applied Thermal Engineering*, 61, pp. 461-468.
[26] Föste, S., Giovannetti, F., Ehrmann, N., Rockendorf, G. (2014) Performance and reliability of a high efficiency flat plate collector – final results on prototypes, *Energy Procedia*, 48, pp. 48-57.

[27] Maia, C. B., Ferreira, A. G., Hanriot, S. M. (2014) Evaluation of a tracking flat-plate solar collector in Brazil, *Applied Thermal Engineering*, 73, pp. 953-962.
[28] Beikircher, T., Berger, V., Osgyan, P., Reuß, M., Streib, G. (2014) Low-e confined air chambers in solar flat-plate collectors as an economic new type of rear side insulation avoiding moisture problems, *Solar Energy*, 105, pp. 280-289.
[29] Yuan, G., Hong, L., Li, X., Xu, L., Tang, W., Wang, Z. (2015) Experimental investigation of a solar dryer system for drying carpet, *Energy Procedia*, 70, pp. 626-633.
[30] Hafez, A. Z., Yousef, A. M., Harag, N. M. (2018) Solar tracking systems: Technologies and trackers drive types – A review, *Renewable and Sustainable Energy Reviews*, 91, pp. 754-782.
[31] Samimi-Akhijahani, H., Arabhosseini, A. (2018) Accelerating drying process of tomato slices in a PV-assisted solar dryer using a sun tracking system, *Renewable Energy*, 123, pp. 428-438.
[32] Das, M., Akpinar, E. K. (2020) Determination of thermal and drying performances of the solar air dryer with solar tracking system: Apple drying test, *Case Studies in Thermal Engineering*, 21, pp. 10731.
[33] Rodríguez-Munoz, J. M., Bove, I., Alonso-Suarez, R. (2021) Novel incident angle modifier model for quasi-dynamic testing of flat plate solar thermal collectors, *Solar Energy*, 224, pp. 112-124.

COMETa 2022
6th INTERNATIONAL SCIENTIFIC CONFERENCE
17th - 19th November 2022
Jahorina, B&H, Republic of Srpska
University of East Sarajevo
Faculty of Mechanical Engineering
Conference on Mechanical Engineering Technologies and Applications

TOPLOTNI GUBICI ALUMINIJUMSKE RAVNE APSORBERSKE PLOČE U FUNKCIJI VEKTORSKIH KARAKTERISTIKA VETRA – NUMERIČKA ANALIZA

Aleksandar Nešović[1], Mladen Josijević[2], Nebojša Lukić[3], Novak Nikolić[4], Dušan Gordić[5]

Rezime: Ako se vodi dodeli uloga primara, a vazduhu uloga sekundara, tada se apsorberska ploča može tretirati i kao rekuperativni razmenjivač toplote tipa voda-vazduh, sa istosmernim (prvi slučaj), suprotnosmernim (drugi slučaj) ili unakrsnim (treći slučaj) strujanjem radnih fluida. U ovom radu koristi se softver Ansys Fluent da bi se odredili toplotni gubici aluminijumske ravne apsorberske ploče sa integrisanim protočnim kanalom kružnog poprečnog preseka sa njene donje strane, koji nastaju kao posledica uticaja vetra, uzimajući u obzir njegove vektorske karakteristike (pravac, smer i intenzitet). Prvi rezultati simulacija potvrđuju početnu pretpostavku da toplotni gubici apsorberske ploče (pomenutog dizajna) rastu zajedno sa brzinom vetra, bez obzira na pravac i smer strujanja radnih fluida. Uočava se da su toplotni gubici apsorberske ploče najveći u slučaju unakrsnog (intenzitet vetra do 1 m/s), odnosno suprotnosmernog strujanja (intenzitet vetra >1 m/s). Gledajući iz ugla korisnika toplotne energije, najveće benefite donosi istosmerno strujanje, i to pri brzinama vetra do 2 m/s. Nakon ove granične vrednosti, poželjno je da napadni ugao vetra bude normalan na položaj apsorberske ploče, odnosno protočnog kanala koji je sa njom integrisan.

Ključne riječi: Aluminijumska ravna apsorberska ploča, Numerička simulacija, Pravac i brzina vetra, Termička analiza, Toplotni gubitak.

HEAT LOSSES OF THE ALUMINUM FLAT ABSORBER PLATE AS A FUNCTION OF THE VECTOR WIND CHARACTERISTICS – NUMERICAL ANALYSIS

Abstract: Abstract: If water is the primary working fluid, and air the secondary working fluid, then the absorber plate can be treated as a recuperative heat exchanger (type: water-air), with concurrent (first case), countercurrent (second case) or cross (third

[1] Mast. inž. maš., Aleksandar Nešović, Fakultet inženjerskih nauka Univerziteta u Kragujevcu, Srbija, aca.nesovic@kg.ac.rs (CA).
[2] Dr, Mladen Josijević, Fakultet inženjerskih nauka Univerziteta u Kragujevcu, Srbija, mladenjosijevic@gmail.com.
[3] Dr, Nebojša Lukić, Fakultet inženjerskih nauka Univerziteta u Kragujevcu, Srbija, lukic@kg.ac.rs.
[4] Dr, Novak Nikolić, Fakultet inženjerskih nauka Univerziteta u Kragujevcu, Srbija, novak.nikolic@kg.ac.rs.
[5] Dr, Dušan Gordić, Fakultet inženjerskih nauka Univerziteta u Kragujevcu, Srbija, gordic@kg.ac.rs.

case) flow direction. In this work, Ansys Fluent software is used to determine the heat losses of the aluminum flat absorber plate with an integrated circular cross-section flow channel on its underside, which occur as a result of the wind, taking into account its vector characteristics (direction, head, and intensity). The first results of the simulations confirm the initial assumption that the heat losses of the absorber plate (mentioned design) grow together with the wind speed, regardless of the direction of the flow of the working fluid. It is observed that the heat losses of the absorber plate are the highest in the case of the cross (wind speed up to 1 m/s) or reverse (wind speed >1 m/s) flow. Looking from the point of view of heat energy users, the same direction of the current of the working fluids brings the greatest benefits, and that is at wind speeds of up to 2 m/s. After this limit value, the angle of attack of the wind should be normal to the position of the absorber plate, i.e. the flow channel that is integrated with it.

Keywords: Aluminum flat absorber plate, Heat loss, Numerical simulation, Thermal analysis, Wind direction, and speed.

1 UVOD

Apsorber predstavlja osnovnu jedinicu građe i funkcije svih solarnih prijemnika, zbog čega treba da ispuni niz sledećih zahteva: visok koeficijent toplotne provodljivosti, visok koeficijent prolaza toplote, visok koeficijent apsorpcije kratkotalasnog i nizak koeficijent emisije dugotalasnog zračenja, dug radni vek, otpornost na koroziju, otpornost na visoke radne temperature, nizak koeficijent hidrauličkog otpora, nisku cenu proizvodnje, malu masu, malu debljinu, itd.

U praksi, najveću primenu nalazi ravan apsorber sa protočnim kanalima raznih oblika (Sl. 1), što i potvrđuju numerička istraživana sprovedena u [1, 2].

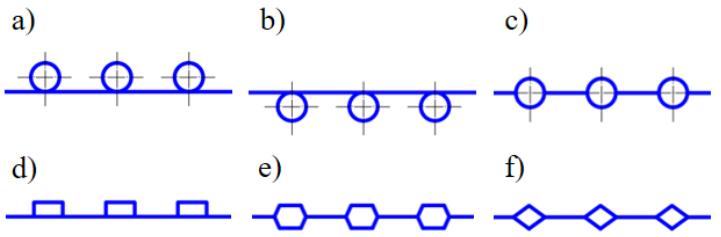

Slika 1. *Najčešće korišćeni tipovi ravnog apsorbera* [3-6].
a) *Kružni protočni kanali sa gornje strane,* b) *Kružni protočni kanali sa donje strane*, c) *Kružni protočni kanali u ravni*, d) *Pravougaoni protočni kanali sa gornje strane*, e) *Šestougaoni protočni kanali u ravni*, f) *Romboidni protočni kanali u ravni*.

Ravan apsorber nastaje spajanjem većeg broja (elementarnih) ravnih apsorberskih ploča (Sl. 2), izrađenih raznim tehnološkim postupcima, najčešće od bakra i aluminijuma [5-9].

Da bi se došlo do optimalne konstrukcije apsorbera, još u fazi projektovanja, u obzir treba uzeti veliki broj uticajnih parametara, podeljenih u tri osnovne grupe: grupa dizajnerskih parametara (geometrijske karakteristike, dimenzije, materijali izrade, itd.), grupa operativnih parametara (tip, maseni protok, brzina i temperatura radnog fluida na ulazu) i grupa meteoroloških parametara (intenzitet ukupno dolaznog solarnog zračenja, pravac i brzina vetra, ambijentalna temperatura, itd.).

U literaturi [10-17] postoje eksperimentalni, teorijski i numerički radovi u kojima se ispituje uticaj vremenskih prilika, tj. uticaj vetra, na performanse solarnih prijemnika.

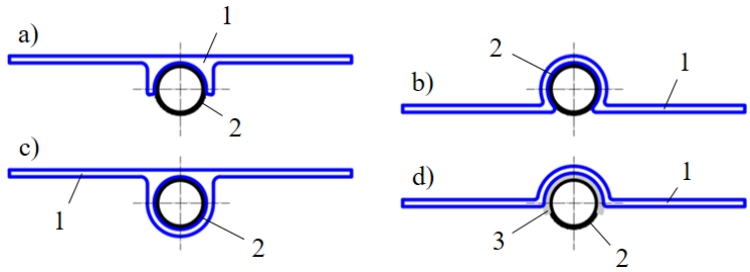

Slika 2. *Najčešće korišćene tehnologije spajanja ravne apsorberske ploče i protočnog kanala* [5-9].
1) *Ravna apsorberska ploča*, 2) *Protočni kanal*, 3) *Lem*.
a) *Pričvršćivanje,* b) *Mehaničko pričvršćivanje*, c) *Hladno izvlačenje*, d) *Lemljenje*.

Za razliku od pomenutih istraživanja, u ovom radu se aluminijumska ravna apsorberska ploča posmatra izolovano (ne u sklopu konstrukcije solarnog prijemnika), i to kao rekuperativni razmenjivač toplote tipa voda-vazduh, koji pritom nema jasno definisan tok strujanja radnih fluida, jer je on u funkciji od napadnog ugla vetra.

Da bi se složeni mehanizmi prostiranja toplote, tj. toplotni gubici, u kojima učestvuje apsorberska ploča, opisali u ovakvim situacijama, autori problem aproksimiraju, i to njenim izdvojenim posmatranjem, u slučaju istosmernog (prvi slučaj), suprotnosmernog (drugi slučaj) i unakrsnog (treći slučaj) proticanja radnih fluida. Istraživanje je sprovedeno u softveru *Ansys Fluent*, jer se savremeni solarni dizajn danas ne može zamisliti bez korišćenja simulacionih (numeričkih) alata.

2 ALUMINIJUMSKA RAVNA APSORBERSKA PLOČA

2.1 *CATIA* model

Ravna aluminijumska apsorberska ploča (dimenzija 800x100 mm i debljine 2 mm), poseduje protočni kanal kružnog poprečnog preseka (unutrašnjeg prečnika Ø15 mm) sa njene donje strane. Ravna ploča i protočni kanal međusobno su integrisani u postupku hladnog izvlačenja (Sl. 3).

Slika 3. *Izometrijski prikaz aluminijumske ravne apsorberske ploče.*

2.2 *ANSYS* model

Termičkoj analizi prethodi formiranje i definisanje sledećih domena (Sl. 4): dva fluidna (za vazduh i za vodu) i jedan solidni (za aluminijumsku ravnu apsorbersku ploču) domen.

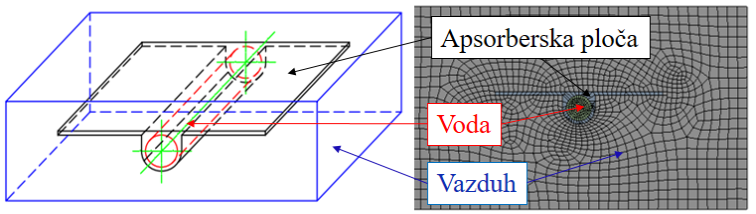

Slika 4. *Fluidni i solidni domeni.*

Globalni parametri mreže (metoda – opcija *automatska*) koriste se za stvaranje mreže diskretizacionih elemenata, tzv. kontrolnih zapremina (Sl. 4) sledećih dimenzija (veličina): relevantni centar – opcija *fino*, izglađivanje – opcija *visoko* i centar ugla raspona – opcija *fino*.

2.3 Principi konzervativnosti

Mehanizmi prostiranja toplote (zračenje je zanemareno), za slučaj turbulentnog režima strujanja (standardni model – opcija *k-ε*) radnih fluida (u ovom slučaju vode i vazduha), moraju biti u skladu sa Zakonima održanja, tj. Principima konzervativnosti. Termičke karakteristike korišćenih materijala (Sl. 4) prikazane su u Tab. 1.

Tabela 1. *Termičke karakteristike korišćenih materijala.*

Materijal	ρ [kg/m^3]	c_P [J/(kg·K)]	λ [W/(m·K)]	μ [Pa·s]
Vazduh	1,225	1006,43	0,0242	0,0000179
Aluminijum	2719	871	202,4	-
Voda	998,2	4182	0,6	0,001003

Zakon održanja mase (prvi Princip konzervativnosti) moze se opisati preko Jed. (1). Drugi Princip konzervativnosti, odnosno Zakon održanja momenta definiše se Navie-Stoksovim jednačinama, tj. Jed. (2)-(4), dok se treći Princip konzervativnosti odnosi se na Zakon održanja energije Jed. (5) [18]:

$$\frac{\partial \rho}{\partial t}+\frac{\partial(\rho u)}{\partial x}+\frac{\partial(\rho v)}{\partial y}+\frac{\partial(\rho w)}{\partial z}=0 \tag{1}$$

$$\rho\left(\frac{\partial u}{\partial t}+u\frac{\partial u}{\partial x}+v\frac{\partial u}{\partial y}+w\frac{\partial u}{\partial z}\right)=-\frac{\partial P}{\partial x}+\mu\left(\frac{\partial^2 u}{\partial x^2}+\frac{\partial^2 u}{\partial y^2}+\frac{\partial^2 u}{\partial z^2}\right)+X \tag{2}$$

$$\rho\left(\frac{\partial v}{\partial t}+u\frac{\partial v}{\partial x}+v\frac{\partial v}{\partial y}+w\frac{\partial v}{\partial z}\right)=-\frac{\partial P}{\partial y}+\mu\left(\frac{\partial^2 v}{\partial x^2}+\frac{\partial^2 v}{\partial y^2}+\frac{\partial^2 v}{\partial z^2}\right)+Y \tag{3}$$

$$\rho\left(\frac{\partial w}{\partial t}+u\frac{\partial w}{\partial x}+v\frac{\partial w}{\partial y}+w\frac{\partial w}{\partial z}\right)=-\frac{\partial P}{\partial z}+\mu\left(\frac{\partial^2 w}{\partial x^2}+\frac{\partial^2 w}{\partial y^2}+\frac{\partial^2 w}{\partial z^2}\right)+Z \tag{4}$$

$$\frac{\partial T}{\partial t}+u\frac{\partial T}{\partial x}+v\frac{\partial T}{\partial y}+w\frac{\partial T}{\partial z}=a\left(\frac{\partial^2 T}{\partial x^2}+\frac{\partial^2 T}{\partial y^2}+\frac{\partial^2 T}{\partial z^2}\right) \tag{5}$$

Sada se toplotni gubici, koji nastaju kao posledica hlađenja vode u aluminijumskoj ravnoj apsorberskoj ploči, mogu odrediti analitički, primenom Prvog

zakona Termodinamike za otvorene termodinamičke sisteme Jed. (6) [19]:

$$\dot{Q}_W = \dot{m}_W \cdot c_p \cdot \left|\Delta T_W\right| = \dot{m}_W \cdot c_p \cdot \left(\left|T_{W-out} - T_{W-in}\right|\right) \tag{6}$$

3 SCENARIO SIMULACIJA

U termičkoj analizi toplotnih gubitaka (početni granični uslovi ispitivanja dati u Tab. 2) apsorberske ploče koriste se dve ravni (Sl. 5): uzdužna *π1* i poprečna *π2*.

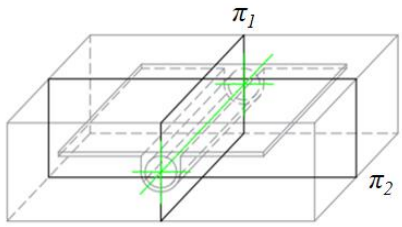

Slika 5. *Uzdužna i poprečna ravan.*

Tabela 2. *Početni granični uslovi numeričkog simuliranja.*

Scenario	$c_{W\text{-}in}$ [m/s]	$c_{A\text{-}in}$ [m/s]	$T_{W\text{-}in}$ [K]	$T_{A\text{-}in}$ [K]
Prvi slučaj	0,0068 Preporuka [5]: 0,015 kg/(s·m²)	0,5; 1; 1,5; 2; 2,5; 3	313	298
Drugi slučaj				
Treći slučaj				

U uzdužnoj ravni razmatraju se toplotni gubici koji nastaju u aluminijumskoj ravnoj apsorberskoj ploči pri rekuperativnom istosmernom (prvi slučaj, Sl. 6a) i suprotnosmernom (drugi slučaj, Sl. 6b) strujanju vode i vazduha. U poprečnoj ravni razmatra se rekuperativno unakrsno (treći slučaj, Sl. 6c) strujanje radnih fluida.

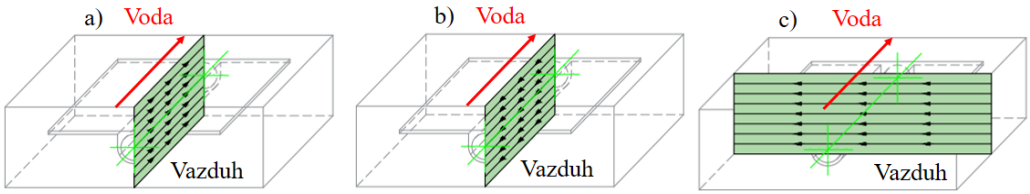

Sl. 6. *Šeme strujanja radnih fluida.*
a) *Istosmerno strujanje,* b) *Suprotnosmerno strujanje*, c) *Unakrsno strujanje.*

4 REZULTATI I DISKUSIJA

Na Sl. 7 prikazano je površinsko temperaturno polje aluminijumske ravne apsorberske ploče (slučaj istosmernog strujanja) u zavisnosti od brzine strujanja vazduha: $c_{A\text{-}in}$=1 m/s, $c_{A\text{-}in}$=2 m/s i $c_{A\text{-}in}$=3 m/s.

Sa priložene slike (Sl. 7) može se uočiti da, uzdužno gledano, temperaturni gradijent površine apsorberske ploče raste sa porastom brzine strujanja vazduha. Zbog toga je temperatura površine apsorberske ploče najneravnomernija za $c_{A\text{-}in}$=3 m/s

(najveća usvojena brzina strujanja vazduha). Bez izuzetka, isti zaključci se mogu izvesti i za preostale slučajeve (suprotnosmernog i unakrsnog) strujanja.

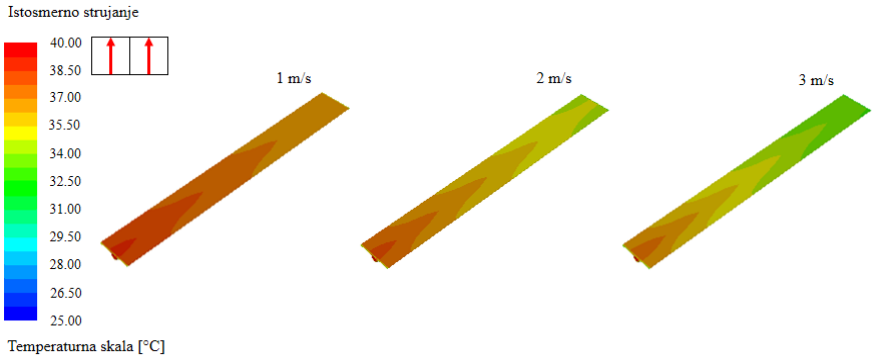

Slika 7. *Temperatura slobodne površine aluminijumske ravne apsorberske ploče (prvi slučaj – istosmerno strujanje).*

Na narednom dijagramu (Sl. 8) prikazano je poređenje toplotnih gubitaka rekuperativnog razmenjivača toplote sa istosmernim, suprotnosmernim i unakrsnim strujanjem vode i vazduha, za različite brzine strujanja.

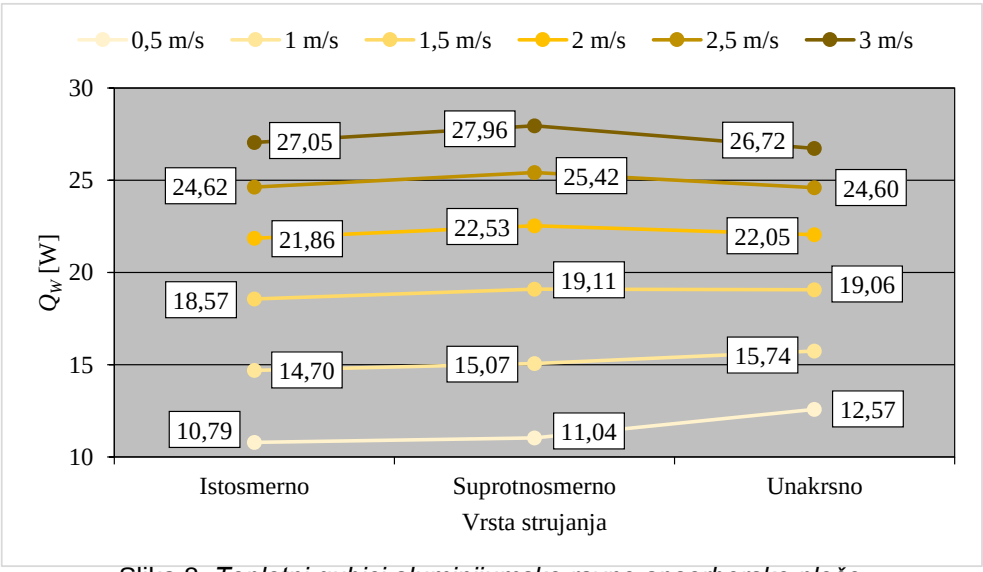

Slika 8. *Toplotni gubici aluminijumske ravne apsorberske ploče.*

Prvo što se može uočiti sa dijagrama (Sl. 8) je povećanje toplotnih gubitaka sa povećanjem brzine vazduha. Tako se pri istosmernom strujanju, toplotni gubici mogu povećati sa 10,79 W ($c_{A\text{-}in}$=0,5 m/s) na 27,05 W ($c_{A\text{-}in}$=3 m/s). U slučaju suprotnosmernog strujanja, toplotni gubici mogu biti veći do 2,53x (11,04 W kada je $c_{A\text{-}in}$=0,5 m/s i 27,96 W kada je $c_{A\text{-}in}$=3 m/s), dok je kod unakrsnog strujanja to povećanje 2,13x (u odnosu na 12,57 W za $c_{A\text{-}in}$ =0,5 m/s).

Kada je brzina vazduha 0,5 m/s, toplotni gubici su najmanji u slučaju istosmernog strujanja (10,79 W). Pri istoj brzini vazduha, za 2,29% su veći u slučaju suprotnosmernog strujanja (11,04 W). Kod unakrsnog strujanja, toplotni gubici su

najveći i iznose 12,27 W. To je za 13,92% i 16,53% više od suprotnosmernog i istosmernog, respektivno. Pri brzinama vazduha $c_{A\text{-}in}$=1 m/s, toplotni gubici su i dalje najveći kod unakrsnog strujanja (15,74 W), ali su oni sada za 4,45% veći u odnosu na suprotnosmerno, odnosno za 7,08% veći u odnosu na istosmerno strujanje. Drugim rečima, razlike među njima su umanjene.

Iako se u literaturi mogu pronaći (eksperimentalni) podaci da su mehanizmi prostiranja toplote najizraženiji kod suprotnosmernog, a najmanje kod istosmernog strujanja, numeričke analize su pokazale da u slučaju apsorberske ploče to važi kada je brzina vazduha 1,5-2,5 m/s (simulacioni korak).

Prvi „diskontinuitet“ uočava se pri brzinama vazduha do $c_{A\text{-}in}$=1,5 m/s. U ovom opsegu, toplotni gubici pri unakrsnom strujanju veći su od toplotnih gubitaka pri suprotnosmernom strujanju (13,92% za $c_{A\text{-}in}$=0,5 m/s i 4,45% za $c_{A\text{-}in}$=1 m/s). Drugi „diskontinuitet“ dešava se kada je ulazna brzina vazduha 2,5 m/s. Pri ovim, i većim brzinama (u ovom slučaju $c_{A\text{-}in}$=3 m/s), dijagram na Sl. 8 pokazuje da su toplotni gubici pri istosmernom strujanju veći od onih koji nastaju pri unakrsnom strujanju (0,09% za $c_{A\text{-}in}$=2,5 m/s i 1,22% za $c_{A\text{-}in}$=3 m/s). Toplotni gubici pri suprotnosmernom strujanju i dalje su najveći: 25,42 W ($c_{A\text{-}in}$=2,5 m/s) i 27,96 W ($c_{A\text{-}in}$=3 m/s).

Navedene pojave, tj. diskontinuiteti, mogu se objasniti specifičnim oblikom ravne apsorberske ploče, zbog čega se pri unakrsnom obstrujavanju vazduha, u prostoru između protočnog kanala i leve strane apsorberske ploče (smer strujanja, Sl. 6c), javlja tzv. zona recirkulacije (zona pada pritiska sa vazdušne strane). Ova zona pri manjim brzinama vazduha više učestvuje (i pospešuje) u razmeni toplote putem konvekcije. Kako brzina strujanja raste, količina (masa) „zarobljenog“ vazduha sve je veća, zona recirkulacije se povećava, a njeno učešće u konvektivnoj razmeni toplote opada.

5 ZAKLJUČAK

Upotreba softverskih alata u početnim fazama istraživanja danas je postala nezaobilana, jer se na taj način štede vreme i novac. Takođe se dolazi do prvih rezultata koji usmeravaju njegov dalji tok – prelazak na naredne faze koje mogu uključivati i dodatna (dopunska) eksperimentalna istraživanja, ili obustavljanje istih.

U ovom radu, predmet istraživanja bili su toplotni gubici aluminijumske ravne apsorberske ploče (veoma bitan deo u konstrukciji svakog solarnog prijemnika) koji nastaju kao posledica uticaja vetra. Korišćenjem softvera *Ansys Fluent* dobijeni su zanimljivi rezultati koji pokazuju da se apsorberska ploča različito ponaša u zavisnosti od vektorskih karakteristika vetra, što bi bilo zanimljivo eksperimentalno ispitati.

Naime, pri brzinama vetra do 1 m/s, toplotni gubici su najveći u slučaju unakrsnog strujanja. Pri većim brzinama, simulacije su pokazale da se isti efekat postiže pri suprotnosmernom strujanju. Sa druge strane, najmanji toplotni gubici dešavaju se pri istosmernom strujanju (brzina vetra do 2 m/s), odnosno pri unakrsnom strujanju (brzine >2 m/s).

ZAHVALNOST

Ovo je rezultat rada u okviru dva projekta: projekat TR 33015 Tehnološkog razvoja Republike Srbije, projekat III 42006 Integralna i interdisciplinarna istraživanja Republike Srbije. Prvi projekat je pod nazivom „Istraživanje i razvoj Srpske kuće nulte neto potrošnje energije“. Drugi projekat je pod nazivom „Istraživanje i razvoj energijski i ekološki visoko efikasnih sistema poligeneracije zasnovanoj na obnovljivim

energijskim izvorima“. Želim da se zahvalim Ministarsvu prosvete, nauke i tehnološkog razvoja Republike Srbije na njihovj finansijskoj podršci tokom ovog istraživanja.

LITERATURA:

[1] Fernando, T. L., Xavier, A. A., Sarzosa, Q. W. (2020) CFD Analysis of a solar flat plate collector with different cross sections, *Enfoque UTE*, 11, pp. 95-108.
[2] Ekramian, E., Etemad, S. G., Haghshenasfard, M. (2014) Numerical analysis of heat transfer performance of flat plate solar collectors, *Journal of Fluid Flow, Heat and Mass Transfer (JFFHMT)*, 1, pp. 38-42.
[3] Martinopoulos, G., Tsilingiridis, G., Kyriakis, N. (2013) Identification of the environmental impact from the use of different materials in domestic solar hot water systems, *Applied Energy*, 102, pp. 545-555.
[4] Vanek, F. M., Albright, L. D. (2008) *Energy systems engineering: Evaluation & Implementation*, New York.
[5] Lukić N., Babić, M. (2008*) Solar energy – Monograph*, Faculty of Engineering, Kragujevac.
[6] Pavlović, T. M., Čabrić, B. D. (2007) *Physics and technique of solar energy*, Construction book, Belgrade.
[7] Ekechukwu, O. V., Norton, B. (1999) Review of solar-energy drying system III: Low temperature air-heating solar collectors for crop drying applications, *Energy Conversion and Management*, 40, pp. 657-667.
[8] Weast, R. C. (1985) *Handbooks of Chemistry and Physics*, The Chemical Rubber, Cleveland.
[9] Harris, N., Miller, C., Thomas, I. (1985) *Solar energy systems design*, John Wiley, New York, 1985.
[10] Radu, A., Axinte. E. (1989) Wind forces on structures supporting solar collectors, *Journal of Wind Engineering and Industrial Aerodynamics*, 32, pp. 93-100.
[11] Kind, R. J., Gladstone, D. H., Moizer, A. D. (1983) Convective heat losses from flat-plate solar collectors in turbulent winds, 1, pp. 80-85.
[12] Sharples, S., Charlesworth, P. S. (1998) Full-scale measurements of wind-induced convective heat transfer from a roof-mounted flat plate solar collector, *Solar Energy*, 62, pp. 69-77.
[13] Fleck, B. A., R. M. Meier, Matović, M. D. (2002) A field study of the wind effects on the performance of an unglazed transpired solar collector, *Solar Energy*, 73, pp. 209-216.
[14] Kutscher, C., Christensen, C., Gawlik, K. (2003) A field study of the wind effects on the performance of an unglazed transpired solar collector-Reply, *Solar Energy*, 74, pp. 353-354.
[15] Chung, K., Chang, K., Liu, Y. (2008) Reduction of wind uplift of a solar collector model, *Journal of Wind Engineering and Industrial Aerodynamics*, 96, pp. 1294-1306.
[16] Kumar, S., Mullick, S. C. (2010) Wind heat transfer coefficient in solar collectors in outdoor conditions, *Solar Energy*, 84, pp. 956-963.
[17] Stathopoulos, T., Ioannis Z., Xypnitou, E. (2012) *Wind loads on solar collectors: a review*, Structures Congress.
[18] Munson, B. R., Okiishi, T. H., Huebsch, W. W., Rothmayer, A. P. (2013) *Fluid mechanics*, Wiley, Singapore.
[19] Bojić, M. (2011) *Thermodynamics*, Faculty of Engineering, Kragujevac.

COMETa 2022
6th INTERNATIONAL SCIENTIFIC CONFERENCE
17th - 19th November 2022
Jahorina, B&H, Republic of Srpska
University of East Sarajevo
Faculty of Mechanical Engineering
Conference on Mechanical Engineering Technologies and Applications

ANALIZA TEHNOLOGIJA I TEHNOLOŠKOG PROCESA ISKORIŠTAVANJA ŠUMA –STUDIJ SLUČAJA ZENIČKO-DOBOJSKI KANTON

Velid Halilović[1], Jusuf Musić[2], Muhamed Bajrić[3], Jelena Knežević[4], Maida Jaganjac[5], Dino Hadžidervišagić[6], Srđan Vasković[7], Gojko Krunić[8]

Sažetak: U radu se prikazuje analiza tehnologija i tehnološkog procesa iskorištavanja šuma na području Zeničko-dobojskog kantona. Ista se zasniva na podacima koji su dobijeni iz Kantonalnog javnog preduzeća ŠPD d.o.o Zavidovići, kojem se povjerava gazdovanje šumama i šumskim zemljištem u državnom vlasništvu na području Zeničko-dobojskog kantona. U radu su, također, analizirani podaci koji su dobijeni od privatnih izvođača radova, koji vrše usluge u procesu iskorištavanja šuma. U procesu iskorištavanja šuma na području Zeničko-dobojskog kantona utvrđeno je, također, koliko poslova u pojedinim fazama rada obavlja preduzeće u vlastitoj režiji, a koliko realizuju privatni izvođači radova. Proizvodnja šumskih drvnih sortimenata izvršena je kombinovano, odnosno jednim dijelom vlastitim radnim snagama u procentualnom iznosu od 32,96 % od ukupne realizacije, a drugim dijelom, putem privatnih izvođača radova izvršeno je u procentualnom iznosu 60,87 % i putem maloprodaje fizičkim licima u procentualnom iznosu 6,17 %. U svom vlasništvu preduzeće posjeduje 32 traktora, dok privatni izvođači radova posjeduju 18 traktora. U fazi daljinskog transporta drveta u 100% slučajeva kupac vrši utovar i daljinski transport šumskih drvnih sortimenata. Također, u radu se navode i povrede radnika koje nastaju prilikom procesa iskorištavanja šuma. Navodi se organizacija rada i broj zaposlenih radnika.

[1] Prof. dr. Velid Halilović, Šumarski fakultet u Sarajevu, Zagrebačka 20, Sarajevo, BiH, v.halilovic@sfsa.unsa.ba
[2] Prof. dr. Jusuf Musić, Šumarski fakultet u Sarajevu, Zagrebačka 20, Sarajevo, BiH, j.music@sfsa.unsa
[3] Prof. dr. Muhamed Bajrić, Šumarski fakultet u Sarajevu, Zagrebačka 20, Sarajevo, BiH, m.bajric@sfsa.unsa
[4] Doc. dr. Jelena Knežević, Šumarski fakultet u Sarajevu, Zagrebačka 20, Sarajevo, BiH, j.knezevic@sfsa.unsa
[5] Mr. Maida Jaganjac, Bosanski Petrovac, BiH, maida.jamakovic96@gmail.com
[6] Doc. dr. Dino Hadžidervišagić, Šumarski fakultet u Sarajevu, Zagrebačka 20, Sarajevo, BiH, d.hadzidervisagic@sfsa.unsa
[7] Prof. dr. Srđan Vasković, Mašinski fakultet u Istočnom Sarajevu, srdjan_vaskovic@yahoo.com
[8] doc. dr Gojko Krunić, Univerzitet u Istočnom Sarajevu, Fakultet za proizvodnju i menadžment, Trebinje, BiH, e-mail: gojko.krunic@fpm.ues.rs.ba

Ključne riječi: Šumarstvo, Korištenje strojeva, Tehnologija, Tehnološki proces, Motorna pila, Traktori.

ANALYSIS OF TECHNOLOGIES AND TECHNOLOGICAL PROCESS OF FOREST HARVESTING – CASE STUDY ZE-DO CANTON

Abstract: The paper analyzes the technology and technological process of forest exploitation in the area of Zenica-Doboj Canton. The foundations are based on data obtained from the Cantonal Public Company ŠPD doo Zavidovići, which has been entrusted with the management of forests and state-owned forest land in the Zaniško-dobojski Canton. The paper also analyzes the data obtained from subcontractors who provide services in the process of forest exploitation. In the process of forest exploitation in the area of Zeničko-dobojski Canton, it was also determined how many jobs in certain phases of work the company performs in its direction, how many private contractors. The production of forest wood assortments is performed in combination, ie. Partly by own labor in the percentage of 32.96% of total sales, in the second part through private subcontractors in the percentage of 60, 87% and through retail of individuals in the percentage of 6.17%. The company owns 32 tractors, while private contractors own 18 tractors. In the faze of remote transport, wood assortiments, customer alone does the load-on and remote transport in 100% cases. Company does not perform service of remote transport. In this paper also mentioned injuries that workers have gotten during the process of exploaiting the forest. Here is listed number of employess and the work organization.

Key words: Forestry, Utilisation of machinery, Technology, Technology process, ChainsaW, Tractors.

1 UVOD

Šuma je uvijek bila i ostat će jedan od najvažnijih prirodnih resursa ovog planeta. Iskorištavanje šuma predstavlja proces proizvodnje, koji obuhvata cjelokupni uloženi rad radi dobivanja i upotrebe materijalnih dobara šume.

Pod pojmom „mehanizacija“ podrazumijeva se sistematska primjena mašina u tehnološkom procesu rada sa ciljem: olakšanja ili humanizacije ljudskog rada, povećanja produktivnosti i kvaliteta rada i smanjenja troškova proizvodnje (Kulušić 1977).

U procesu iskorištavanja šuma od davnina se u velikoj mjeri koristila kako ljudska tako i životinjska radna snaga. Nakon pojave mehanizacije u velikoj mjeri je olakšan rad u procesu dobivanja drvne mase, jer se isti provodi u kombinaciji ljudskog i strojnog rada. Treba istaći da su vrlo značajne i 70-tegodine prošlog vijeka, jer su se tada po prvi puta upotrijebili specijalni šumski traktori za privlačenje drveta (Bedžula i Slabak 1974).

Prema nekim autorima u procesu razvoja šumske mehanizacije razlikuju se tri razvojne faze: faza djelomične mehanizacije, faza potpune mehanizacije i faza potpune mehanizacije sa djelomičnom automatizacijom.

Početkom 1977. godine radovi u fazi sječe i izrade, kao i oni u fazi prevoza drveta, su mehanizovani u 100 % iznosu, dok su radovi u fazi privlačenja drveta bili mehanizirani sa 33%, a kod utovara i istovara drveta taj iznos je bio oko 49% (Šumarska enciklopedija 1,1980).

Tematika istraživanja se odnosi na analizu tehnologije i tehnoloških procesa, zatim na kvalitet i kvantitet sredstava rada koji se trenutno koriste na području Zeničko-

dobojskog kantona.

Tehnologije faze sječe i izrade prema mjestu izrade djele se na: sječu i izradu na sječini; izradu sortimenata na traktorskom putu ili sabirnom mjestu na sječini; izradu na šumskom (pomoćnom) stovarištu; izradu na centralnom mehaniziranom stovarištu (CMS-u) (Gurda i dr. 2010).

Tokom privlačenja drveta, koje se još naziva i primarnim transportom (Poršinsky 2005), oblovina se dijelom ili u potpunosti transportira izvan izgrađenih šumskih puteva, pri čemu su moguća četiri temeljna načina: privitlavanje drveta (vuča drveta po tlu), privlačenje drveta (vuča drveta s jednim krajem odignutim od tla), izvoženje drveta (drvo na tovarnom prostoru vozila) i iznošenjem drva (drvo odignuto od tla).

Daljinski prijevoz drveta, iako važna dionica dobivanja drveta, istodobno vezana i uz značajne proizvodne troškove, najmanje je podložan utjecajima posebnosti i načina gospodarenja šumama u našim uvjetima (veliki se dio obavlja izvan šume), (Tomašić 2012).

Osnovni cilj ovog rada jeste da se izvrši detaljna analiza tehnologija i tehnološkog procesa iskorištavanja šuma na području Zeničko-dobojskog kantona, te da se dobije realno stanje o ovoj problematici.

U funkciji realizacije postavljenog cilja istraživanja definisani su određeni zadaci:

a) Utvrditi učešće sječe i izrade drvnih sortimenata po izvođačima radova,
b) Utvrditi učešće privlačenja drvnih sortimenata po izvođačima radova i
c) Utvrditi stanje zaštite na radu.

Prikupljanje podataka koji su bili neophodni za ovu analizu odvijalo se na dva načina.

Podaci o preduzeću šumarstva kojem je povjereno gospodarenje šumama u državnom vlasništvu na području Zeničko-dobojskog kantona dostavljeni su od strane nadležnih službi u sklopu JP „ŠPD-ZDK“ d.o.o. Zavidovići. Svi traženi podaci su u cijelosti dostavljeni, te nije bilo nikakvih problema sa pomenutim preduzećem što je u velikoj mjeri olakšalo samu analizu.

Radi stvarnog uvida u stanje mehanizacije na području ovog kantona, djelokrug rada je obuhvatao i privatna preduzeća koja vrše usluge sječe i izrade, te izvoza šumskih drvnih sortimenata.

Od službe KJP ŠPD ZE-DO kantona je dobijen kontakt od 15 privatnih poduzetnika koji najviše participiraju u ovim poslovima sječe i izvoza šumskih drvnih sortimenata. Međutim samo jedan manji broj, njih sedam, je ustupilo tražene podatke.

Kada su svi podaci prikupljeni pristupilo se njihovoj analizi na osnovu sličnih radova koji su se provodili na teritoriji Bosne i Hercegovine, sve dostupne literature, te su prikupljeni podaci usaglašeni i prikazani.

2 REZULTATI I DISKUSIJA

- Sječa šumskih drvnih sortimenata

Nakon prikupljenih podataka i provedene analize ustanovilo se da izradu šumskih drvnih sortimenata preduzeće i privatni izvođači radova vrše na sječini. Uglavnom preovladava sortimentni metod kako kod preduzeća šumarstva, tako i kod privatnih izvođača radova, a u rijetkim slučajevima primjenjuje se deblovni i

poludeblovni metod. Analiza sredstava rada koja su se koristila u fazama sječe i izrade, izvoza, te otpreme drvnih sortimenata zasnivala se na: broju i vrsti sredstava, vlasništvu i prosječnoj starosti.

Tabela 1. *Pregled izvršenja sječa po poslovnim jedinicama u m³ (neto drvna masa) (KJP ŠPD ZDK d.o.o. Zavidovići, Izvještaj o poslovanju za 2020. godinu*.

Redni broj	POSLOVNA JEDINICA	NETO DRVNA MASA m³			INDEX	
		Ostvareno I -XII 2019	Planirano I -XII 2020	Ostvareno I -XII 2020	5:3	5:4
1	2	3	4	5	6	7
1	ŠUMARIJA OLOVO	90.596	106.479	90.930	100,37	85,40
2	ŠUMARIJA VAREŠ	67.918	71.798	59.405	87,47	82,74
3	ŠUMARIJA VISOKO	11.705	12.041	10.953	93,58	90,96
4	ŠUMARIJA KAKANJ	33.199	26.605	17.724	53,39	66,62
5	ŠUMARIJA ZENICA	21.783	19.520	18.438	84,64	94,46
6	ŠUMARIJA ŽEPČE	18.952	17.440	13.213	69,72	75,76
7	ŠUMARIJA ZAVIDOVIĆI	78.057	61.699	62.857	80,53	101,88
8	ŠUMARIJA MAGLAJ	3.795	3.206	3.223	84,93	100,53
9	ŠUMARIJA TEŠANJ	12.879	12.010	10.083	78,29	83,96
JP ŠPD ZDK		**338.884**	**330.799**	**286.826**	**84,64**	**86,71**

Tabela 2. *Ostvarena sječa šumskih drvnih sortimenata po angažovanim kapacitetima (KJP ŠPD ZDK d.o.o. Zavidovići, Izvještaj o poslovanju za 2020. godinu).*

Redni broj	Poslovna jedinica	Sredstva preduzeća (m³)	Kooperanti (m³)
1	Šumarija Olovo	35.456	55.456
2	Šumarija Vareš	22.423	36.975
3	Šumarija Visoko	0	10.953
4	Šumarija Kakanj	8.860	8.860
5	Šumarija Zenica	5.465	12.971
6	Šumarija Žepče	0	13.213
7	Šumarija Zavidovići	23.162	39.687
8	Šumarija Maglaj	0	3.223
9	Šumarija Tešanj	0	10.083
10.	ŠPD ZDK	95.357	191.421
11.	%	33,2	67,7

Također su prikuplje ni podaci i za broj i starost motornih pila. Prilikom provedenog anketiranja utvrdilo se je da preduzeće posjeduje 177 motornih pila, a privatni poduzetnici 51 motornu pilu. Dakle, ukupno je analizirano 228 motornih pila. (preduzeće+privatni izvođači radova).

U sklopu preduzeća vijek trajanja motornih pila ne prelazi 2,5 godine, a kod privatnih preduzeća starost ne prelazi 3 godine.

Na slici koja slijedi prikazana je starost motornih pila koje su se koristile za navedeni period.

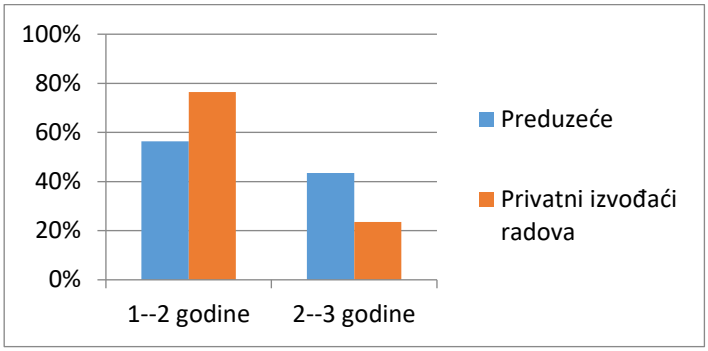

Slika 1. *Starost motornih pila u preduzeću šumarstva i kod privatnih izvođača radova*

Većina motornih pila koje su analizirane kako u preduzeću, tako i kod privatnih izvođača radova su tipa Husquarna 372 Xp.

- Privlačenje/izvoz šumskih drvnih sortimenata

Tabela 3. *Pregled izvršenja izvučenog drveta po šumskim upravama i ukupno u m³ (neto drvna masa) (KJP „ŠPD ZDK" d.o.o. Zavidovići , Izvještaj o poslovanju za 2020. godinu)*

Redni broj	SORTIMENT	NETO DRVNA MASA m³			INDEX	
		Ostvareno I -XII 2019	Planirano I -XII 2020	Ostvareno I -XII 2020	5:3	5:4
1	2	3	4	5	6	7
1	ŠUMARIJA OLOVO	92.510	106.479	89.200	96,42	83,77
2	ŠUMARIJA VAREŠ	67.023	71.798	58.532	87,33	81,52
3	ŠUMARIJA VISOKO	11.760	12.041	10.784	91,70	89,56
4	ŠUMARIJA KAKANJ	32.821	26.605	17.479	53,26	65,70
5	ŠUMARIJA ZENICA	21.992	19.520	18.137	82,47	92,92
6	ŠUMARIJA ŽEPČE	18.991	17.440	13.722	72,26	78,68
7	ŠUMARIJA ZAVIDOVIĆI	78.143	61.699	63.229	80,91	102,48
8	ŠUMARIJA MAGLAJ	3.355	3.206	3.136	93,47	97,82
9	ŠUMARIJA TEŠANJ	13.064	12.010	10.057	76,98	83,74
JP ŠPD ZDK		**339.659**	**330.799**	**284.276**	**83,69**	**85,94**

Analizirajući fazu izvoza u šumariji Olovo primjećuje se da je izvršena u količini od 89.200 m³ neto mase četinara i lišćara, što je 83,77 % u odnosu na plan poslovanja za 2020. godinu, a 94,42 % u odnosu na ostvareni učinak u 2019. godini. U ovoj fazi rada ostvaren je podbačaj u količini od 17.279 m³ u odnosu na plan poslovanja za 2020. godinu

Analiza ove faze u tabeli je predstavljena I za ostale šumarsije na području ŠPD-a.

U fazi izvoza drvnih sortimenata za period januar- decembar 2020. godine najbolje rezultate u odnosu na plan ostvarila je P.J.Šumarija Zavidovići u iznosu od 102,48 %, a najlošije rezultate je ostvarila je P.J.Šumarija Kakanj u iznosu od 65,70 %.

Tabela 4. *Izvoz šumskih drvnih sortimenata po angažovanim kapacitetima. (KJP „ŠPD ZDK“ d.o.o. Zavidovići, Izvještaj o poslovanju za 2020. godinu)*

Redni broj	Poslovna jedinica	Brigade (m^3)	Kooperanti (m^3)
1	Šumarija Olovo	32.600	56.600
2	Šumarija Vareš	20.899	37.632
3	Šumarija Visoko	0	10.784
4	Šumarija Kakanj	8.739	8.739
5	Šumarija Zenica	4.350	13.787
6	Šumarija Žepče	0	13.722
7	Šumarija Zavidovići	23.268	39.897
8	Šumarija Maglaj	0	3.136
9	Šumarija Tešanj	0	10.057
10	ŠPD ZDK	89.856	190.354
11	%	31,6%	68,4%

Kada su u pitanju mehanizirana sredstva rada u fazi privlačenja drveta, preduzeća šumarstva u svom vlasništvu posjeduje 32 traktora. Prilikom anketiranja došlo se i do podatka o broju traktora koje posjeduju privatni izvođači radova. Taj broj je cca 18 traktora, s tim da treba navesti da je analizirano 9 privatnih izvođača radova.

Analizom koja se provela došlo se do podataka da se uglavnom koriste specijalni šumski traktori u fazi privlačenja drveta.

U preduzeću posjeduju sljedeće tipove specijalnih šumskih trakotra:

Tabela 5. *Tipovi specijalnih traktora i njihov broj po šumarijama*.

Redni broj	**Šumarija Olovo**	**Šumarija Vareš**	**Šumarija Kakanj**	**Šumarija Zenica**	**Šumarija Zavidovići**
1.	Zglobni traktor LKT 81	Zglobni traktor Timberjack 240 C	Zglobni traktor Timberjack 240-b	Zglobni traktor Timberjack 350	Zglobni traktor Timberjack 225
2.	Zglobni traktor Timberjack 240 B	Zglobni traktor Timberjack 240 C	Buldozer Fiat Kobelco	Zglobni traktor Timberjack 240 C	Zglobni traktor Timberjack 380
3.	Zglobni traktor Hittner 140 V	Zglobni traktor Timberjack 240 C	Skip-case		Zglobni traktor Timberjack 380
4.		Zglobni traktor Timberjack 380-a	Utovarivač rd-130		Zglobni traktor Timberjack 350 A
5.		Zglobni traktor Hittner 120 V	Zglobni traktor Timberjack 240a		Zglobni traktor Timberjack 450 C
6.		Zglobni traktor Hittner 120 V	Zglobni traktor Timberjack 350 A		Zglobni traktor Hittner 120 V

Na osnovu gore navedenih podataka može se zaključiti da je najzastupljeniji traktor koji preduzeće koristi u fazi privlačenja drveta tipa Timberjack. Kada je u pitanju starost pomenutih traktora iz preduzeća navode da je vijek trajanja istih 6,5 godina. Prosječna starost traktora u preduzeća iznosi 13,50 godina i prikazana je na sljedećoj slici:

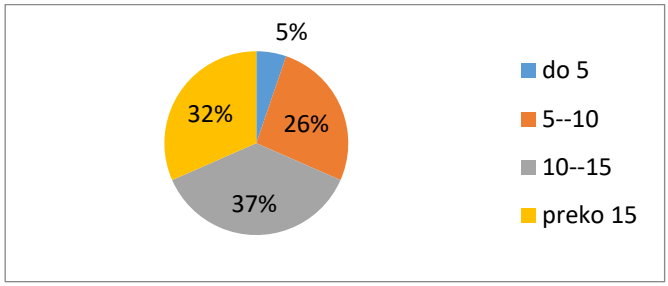

Slika 2. *Starost traktora u preduzeću*

Analizirano je 9 privatnih izvođača radova koji obavljaju poslove u fazi privlačenja drveta. U sljedećoj tabeli je prikazana brojnost traktora koji se nalaze u vlasništvu privatnih izvođača radova

Tabela 6. *Broj traktora kod privatnih izvođaća radova*

Naziv preduzeća	**Broj traktora**
Kepić d.o.o.	4
Ponar d.o.o.	3
Palež d.o.o	2
Brenta d.o.o.	3
Drvex d.o.o.	1
Selimanović d.o.o	3
Alajmović d.o.o	2

Ukupan broj analiziranih traktora kod privatnih izvođača radova je 18. Od tog broja 29 % su adaptirani šumski traktori, a 71% njih su specijalni šumski traktori. Od ukupnog broja traktora samo jedan je starosti do 5 godina, 7 njih je starosti 10-15 godina, 5 traktora je starosti 5-10 godina, a njih 6 je starosti preko 15 godina.

3 ZAKLJUČAK

Nakon provedene detaljne analize dostupnih podataka dolazi se do sljedećih zaključaka:

U fazi sječe i izrade drvnih sortimenata prema detaljno analiziranim podacima o obimu sječa za 2020. godinu, preduzeće vlastitim kapacitetima realizuje 33,2 % radova, a privatni poduzetnici realizuju 66,8 % radova. U svom vlasništvu preduzeće posjeduje 177 motornih pila, dok privatni izvođači radova u svom vlasništvu posjeduju 51 motornu pilu. Dakle, ukupan broj motornih pila (preduzeće + privatni izvođači radova) je 228. U sklopu preduzeća vijek trajanja motornih pila ne prelazi 2,5 godine, a kod privatnih preduzeća starost ne prelazi 3 godine.

Kada je u pitanju faza sječe i izrade šumskih drvnih sortimenata na nivou preduzeća sastavljena je u 100% slučajeva od 1+1 (sjekač i pomoćni radnik), dok kod privatnih izvođača radova u nekim slučajevima organizuje se i kao 2+0, odnosno dva sjekača, bez pomoćnih radnika.

U fazi primicanja i privlačenja drvnih sortimenata od panja na međustovarište, prema analiziranim podacima o obimu radova za 2020. godinu, preduzeće vlastitim kapacitetima realizuje 31,6 % radova, a privatni poduzetnici realizuju 68,4% radova.

Ukupan broj analiziranih traktora kod privatnih izvođača radova je 18. Od tog broja je 29 % su adaptirani šumski traktori, a 71% njih su specijalni šumski traktori. Od ukupnog broja traktora samo jedan je starosti do 5 godina, 7 njih je starosti 10-15 godina, 5 traktora je starosti 5-10 godina, a njih 6 je starosti preko 15 godina.

U fazama sječe i izrade, te primicanja i privlačenja drvnih sortimenata došlo je do smanjenja izvršenja radova. Kada su u pitanju privatni izvođači radova obim poslova je negdje skoro isti u proteklih par godina, dok se obim poslova koje preduzeće obavlja vlastitim kapacitetima smanjuje u zadnjih par godina.

U svrhu unapređenja tehnologije u procesu iskorištavanja šuma preduzeće je unaprijedilo službu zaštite na radu, te nabavilo novu mehanizaciju sa poslove u procesu iskorištavanja šuma.

LITERATURA

[1] Antolić, D., (2020): Diplomski rad “Mehanizirani sustav pridobivanja drva - trendovi razvoja i mogućnosti primjene”, Šumarski fakultet Sveučilišta u Zagrebu, Zagreb. 1-61.
[2] Gregur, J., (2015): Povijest mehanizacije u šumarstvu. Završni rad, Šumarski fakultet Sveučilišta u Zagrebu, 1–22.
[3] FIRMA (Fostering Interventions for Rapid Market Advancement)(2013): USAID Sida Project, Mogućnosti korištenja niskovrijednih drvnih sortimenata i konverzija izdanačkih šuma u Bosni i Hercegovini, Završni izvještaj. 1 – 97.
[4] 6. Halilović, V., (2017): Karakteristike i upotreba motornih pila, Šumarski fakultet Univerziteta u Sarajevu, 1-154.
[5] 7. Halilović, V., Mahmutović, Z., (2020): Zaštita na radu u šumarstvu, Samostalni sindikat šumarstva, prerade drveta i papira BiH, Sarajevo. 1-196.
[6] 8. Halilović V., Musić J., Gurda S., Topalović J., (2015): „Analisys of the means of forest harvesting in the Federation of Bosnia and Herzegovina“, Glasnik Šumarskog fakulteta, Beograd, Srbija.
[7] 9. Horvat, D., Šušnjar, M. (2005): Tehničke značajke skidera “Ecotrac 120V”. Istraživanje i studija u okviru projekta “Razvoj, izrada i ispitivanje specijalnog šumskog vozila –skidera mase 7t” u okviru programa RAZUM Ministarstva znanosti, obrazovanja i športa RH. Studija. Zagreb: Sveučilište u Zagrebu, Šumarski fakultet.
[8] 10. Malnar, M., (2000): Tehničko-tehnološki čimbenici prijevoza drva u brdsko gorskim uvjetima na primjeru šumarije Prezid. Magistarski rad, Šumarski fakultet Sveučilišta u Zagrebu. 1-124.
[9] 11. Metzinger, T. Č., Toth, M., (2020): Metodologija istraživačkog rada za stučne studije, Veleučilište Velika Gorica, Velika Gorica. 1-51.
[10] 12. Matić, S. (1983): Šuma i mehanizacija. Zbornik savjetovanja "Šumarska mehanizacija u teoriji i praksi" Opatija, 1983, str. 37-46.
[11] 13. Poršinsky, T., 2005: Djelotvornost i ekološka pogodnost forvardera Timberjack 1710 pri izvoženju oblovine iz nizinskih šuma Hrvatske. Disertacija, Šumarski fakultet Sveučilišta u Zagrebu, 1 – 170.
[12] 15. Tomičić, B., (1974): Iskorištavanje šuma na Bilogorsko-Podravskom području. Edicija "Sto godina šumarstva Bilogorsko-Podravske regije", Bjelovar.
[13] 16. Tomašić Ž., 2012: „Razvoj tehnologije i tehničkih sredstava u pridobivanju drva s obzirom na posebnost šuma i šumarstva u Republici Hrvatskoj“, Pregledni članak, Zagreb
[14] Internet: KJP ŠPD ZDK d.o.o Zavidovići, Dokumenti Izvještaj o poslovanju

COMETa 2022
6th INTERNATIONAL SCIENTIFIC CONFERENCE
17th - 19th November 2022
Jahorina, B&H, Republic of Srpska
University of East Sarajevo
Faculty of Mechanical Engineering
Conference on Mechanical Engineering Technologies and Applications

RESOURCE-SAVING TECHNOLOGIES AND ANALYSIS OF THE USE OF SECONDARY RAW MATERIALS EXTRACTED FROM SOLID MUNICIPAL WASTE DURING THE 2020 PANDEMIC IN THE PERM KRAY (RUSSIA)

Tatyana Sereda[1], Sergey Kostarev[2], Oksana Fotina[3]

Abstract: On the basis of the system analysis, established factors and conditions of Russia's economic development the authors have formed the conceptual Waste Today – Environmentally Safe, Sustainable Development Tomorrow scheme. It is shown that one of the most acceptable mechanisms to prevent the negative impact of waste causing a high level of environmental hazard to the natural environment and the life of the population is a new approach to the concept of waste as a subject of environmental, commodity-monetary and other types of legal relations and the transition of the entire system of treatment of used products to the technical and social-economic system "Resource consumers – Technology – Secondary and commodity resources (RTS) and management of this system using mechanisms of economic and legal regulation, where secondary resources and alternative energy sources will be the subject of public relations. The paper reflects the results of research on the morphological composition of municipal solid waste (secondary resources) conducted during the 2020 pandemic in Perm Kray of the Russian Federation.

Key words: Municipal solid wastes, Pandemic, Secondary resources, Morphological analysis of waste

1 INTRODUCTION

Depletion of natural resources for the functioning of production processes and meeting the needs of the population lead to environmental problems. One of the essential problems of ecology and mathematical ecology is the problem of ecosystems stability [1, 2]. Only stable systems can exist for a long time. On the other hand, the stability limits set those maximum loads on an ecosystem. Exceeding those limits will

[1] Perm State Agrarian-Technological University named after academician D N Pryanishnikov, Russia, (iums@dom.raid.ru)
[2] Perm Institute of the FPS of Russia, Russia,
[3] Perm State Agrarian-Technological University, Russia, oksanafotina@gmail.com

lead to destruction. This aspect acquires special urgency in connection with strengthening of anthropogenic influence [3], including at the expense of influence of the formed waste on ecosystems. A preliminary morphological and component analysis of the waste composition for the spring and summer period of 2020 was presented in [4]. The research concerning waste accumulation at the penitentiary facilities of Perm Krai was published in one of the works [5].

2 INSTRUMENTS AND EQUIPMENT

For waste sorting, 3 sizes of sieves with cells were used: 250x250 mm, 80x80 mm, 20x20 mm. The sieves were made of a wooden frame and reinforcing polymer rods, forming a grid. The screens were installed vertically, thus, fine fractions were sieved with distinguishing of 4 waste fractions: more than 250 mm, 80-250 mm, 20-80 mm, 0-20 mm. M-ER 333 AF/FARMER scales with a scale division of 0.01 kg were used to determine the total mass of the MSW arriving at the sorting. To determine the component composition of the waste we used MK-32.2-A20 scales with the scale division of 0,001 kg. Scales are verified by the manufacturer, the verification period of scales MK-32.2-A20 is valid for the entire period of the research.

The research was carried out in accordance with the Regulations developed on the basis of the federal environmental regulation «Solid domestic waste. Determination of the morphological composition by gravimetric method». The object of the study was the flow of solid municipal wastes from two groups of Perm Kray's settlements: settlements with a population over 500000 people – Perm, the capital city of Perm Kray, and settlements with a population under 300000 people – the Kondratovo village. The research methods included analysis, comparison, generalization, analogy, and statistical data processing.

3 RESEARCH RESULTS

3.1 Development of the structure of the technical-socio-economic *Resource Users – Technology – Secondary and Commodity Resources* system:

Many works are devoted to the problem of using secondary resources [6–9]. On the basis of the system analysis the structure of technical-socio-economic Resource Users – Technology – Secondary and Commodity Resources system (RTS system) was proposed and the main classes of its elements were determined.

The following elements are included in the system under consideration: *R* – resource users, including population and labor resources; *E* – economic resources; *P* – production resources (machinery and technology); *T* – commodity resources, including secondary commodity resources that have not lost their consumer properties (for example, glassware, clothes, shoes, furniture, etc.); *U* – controlling impacts (regulatory, economic, etc.) and *Z* – disturbing impacts (sanctions, pandemics, violation of environmental law, climatic factors, etc.).

The flow is composed of 3 flows: exhaustible natural resources: natural resources energy - exhaustible non-renewable: $PR_{EN\_ISH.}$ (oil, gas, coal, etc.); natural resources raw materials - exhaustible renewable: $PR_{N\ ISCH.}$ (forests, animal and plant origin, etc.) and natural resources non-exhaustible $PR_{NSC.}$ (solar, wind, hydro, tidal, etc.).

Δq – material and energy flows recycled within the RTS system, so-called recycled natural resources or secondary energy resources.

I – information flows of monitoring; *R* – relations reflecting relations of elements.

The output consists of 3 streams: q1 – secondary energy resources VR_E – recyclable (waste heat energy, gaseous products, steam, etc.), q2 secondary raw materials resources – recyclable: VR_S (glass, paper, textile, metal, plastic, etc.) and the output stream q3 – secondary non-recyclable resources (NR) – waste (including hazardous) (Figure 1). An article [10] is devoted to the construction of a waste sorting system.

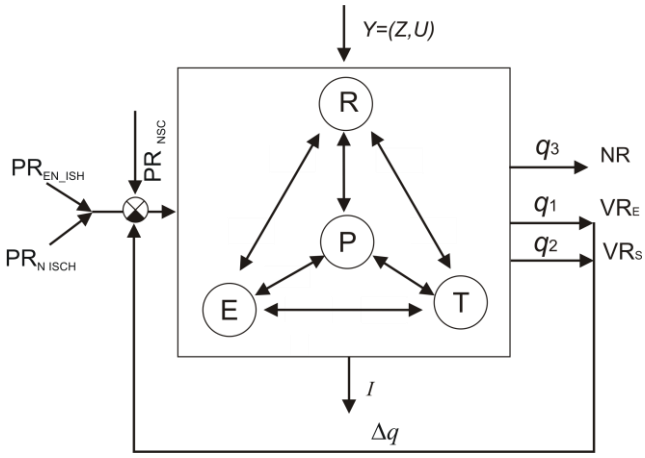

Figure 1. *Structure of the technical-socio-economic RTS system*

3.2 Research results of morphological analysis of secondary resources

In the research during 2020, 5144.71 kg were selected and sorted during 4 seasons (in spring – 1348 kg, in summer – 1184 kg, in autumn – 1313 kg, in winter – 1299.71 kg) in Perm.

The analysis of studies has shown that the recyclable components included in MSW, which can be used for recycling:

- waste paper not contaminated with food waste;
- polymer waste, in the form of PET and polycarbonate bottles (containers);
- metal, which includes mainly aluminum and tin cans;
- textiles, which includes clothing and other textiles;
- glassware.

The weighing of useful components showed that the main recyclable part of paper and cardboard are in the coarse (over 250 mm) and medium (250-80 mm) fractions, PET and polycarbonate bottles, glassware, metals are in the medium fraction, and textiles are in the large and medium fractions (figure 2).

Due to the fact that the main part of MSW is further utilized at MSW landfills, all the wastes have been conditionally divided into 3 constituent parts by the degree of biodegradation:

- biodegradable – food and vegetable waste (at landfills complete biodegradation of waste occurs from one to three years with the formation of biogas and leachate, with the introduction of control technologies at landfills);

- not easily degradable – waste paper, wood, textile, composite materials, siftings (biodegradation processes last for up to 25-30 years on the landfills);
- conditionally non-degradable – polymers, glass, metals, inert materials, other materials (natural process of waste biodegradation may last up to 100-1000 years).

Figure 2. *Photos of research on waste sorting*

The main components in the morphological composition of MSW traditionally processed as recyclable materials are the components presented in Table 1.

Thus, the percentage content of recyclable components in the studied samples of Perm Krai is:

- in the spring season 53.91%;
- in summer 50.142%;
- in autumn 40.19%;
- in winter 57.999%.

The percentage of organic waste. related to degradable components is:

- in the spring season 27.76%;
- in the summer season 28.746%;
- in the fall 41.741%;
- in winter 21.934%.

The percentage of hard-to-degrade components is:

- in the spring season was: waste paper 10.42%, wood 1.82%, textiles 6.2%, composite materials 1.30%, dropout 5.39%;
- in summer: wastepaper 10.446%, wood 1.323%, textile 8.106%, composite materials 1.991%, dropout 4.277%;

- in the fall season was: waste paper 9.094%, wood 1.371%, textiles 5.497%, composite materials 2.074%, dropout 5.735%;

- in winter season was: waste paper 13.746%, wood 0.662%, textile 6.011%, composite materials 3.928%, dropout 5.599% (Total – 29.946%).

Percentage content of conditionally non-degradable components of MSW is:

- in the spring season, respectively: polymers 21.32%, glass 11.90%, metals 2.25%, inert 2.88%, and others 8.71%;

- in summer season, respectively: polymers 13.171%, glass 14.675%, metals 2.421%, inerts 6.12%, and others 8.68%;

- in the fall season, respectively: polymers 12.082%, glass 10.831%, metals 1.315%, inerts 3.257%, and others 6.944%;

- in winter: polymers 20.63%, glass 14.43%, metals 2.52%, inerts 2.762% and others 7.71%. (Total – 8.052%).

Table 1. *Percentage content of recyclable components in the studied samples of MSW by seasons*

Components MSW for recyclables	Content of recyclable components of MSW, % by seasons				
	Spring	Summer	Autumn	Winter	Average annual
Waste paper	10.42	10.446	9.094	13.746	10.927
Polymers	21.32	13.171	12.082	20.63	16.801
Glass	11.90	14.675	10.831	14.430	12.959
Metals	2.25	2.421	1.315	2.52	2.127
Textiles	6.2	8.106	5.497	6.011	6.454
Wood	1.82	1.323	1.371	0.662	1.294
Total	53.91	50.142	40.19	57.999	50.56

4 CONCLUSION

On the basis of the experimental studies of the component (morphological) composition of the municipal solid wastes in two settlements of the Perm Kray, a settlement with a population under 300000 inhabitants – Kondratovo village and a settlement with a population over 500000 inhabitants – Perm city the following conclusions were made:

1. Experimental research was carried out in full according to the developed regulations. All in all 10073 kg of MSW were studied in Perm and Kondratovo during the entire studies.

2. The results of household solid waste measurements in the Perm Kray in the pandemic of 2020 showed the reduction of the annual norm of MSW from public places (administrations, offices, libraries, schools, kindergartens, temples, baths, hairdressing salons, beaches, parks, theaters and so on) by 70-80% on the average. Increase in 2.08 times the rate of solid municipal waste in the private sector in individual residential buildings (310.37 kg per person per year (in 2016 it was 149 kg of MSW per capita per year)). Increase in 1.5 times the rate of solid municipal waste in apartment buildings (became 0.073 m3 of MSW per person per year (in 2016 was 0.048 m^3 of MSW per capita per year)).

3. The average annual indicators of the morphological composition of solid municipal waste in Perm Kray's settlements are mainly represented by organic waste

(30.045%), polymers (16.803%), glass (12.96%), and waste paper (10.93%).

4. The analysis of the waste composition showed, that during 4 seasons the average annual mass of 10073 kg of MSW constituted 22.18% of all the solid municipal wastes with the fraction bigger than 250 mm, which contained the most recyclable part – cardboard, textile, rubber, etc. Other recyclable components are presented by the average fraction and amount to 63.24% per year, where a considerable part is constituted by waste paper and textiles and metal (in the form of aluminium and tin cans), polymers (in the form of PET bottles) and glass (in the form of glass containers). The fraction in the size range of 20-80 mm had an insignificant content (9.51%) on average over the year and practically no components suitable for HS. The 0-20 mm fraction (a mixture of food waste, pieces of soil, scraps of paper and film), was almost impossible to sort by hand. The sieve content averaged 9.51% over the year.

5. Despite the allocation of only MSW flow for analysis, hazardous waste was found in the composition of the studied waste, in particular medical waste, batteries, chemicals, fluorescent lamps, masks, syringes and gloves, which may pose some threat to personnel during waste processing and the environment during disposal of MSW in landfills, whose total content for the year averaged 0.053% in the averaged indicators of MSW composition in Perm Kray.

6. Calculations showed that the percentage content of recyclable components in the studied samples of Perm Krai averaged over the seasons of the year was 50.56%. The research showed that the extraction of components of MSW during sorting for recycling will allow reducing the hard-to-degrade and conditionally non-degradeable components of MSW transported to disposal sites by 20.72 % and 31.884 % on the average for a year correspondingly.

7. An increase in the morphological composition of MSW in the morphological composition of the heaviest fractions: food waste (1.9 times) and glass containers (1.5 times) compared to similar measurements in 2016 and an increase in waste in the period of self-isolation in the residential sector were noted in the pandemic. This led to an overestimated standard of MSW from the population. Therefore, it is necessary to make adjustments to the methodology for calculating the standards of MSW with the introduction of corrective indicators, taking into account the special periods of life of the population (pandemics, emergencies, etc.).

REFERENCES

[1] Elgizawy, S., El-Haggar, S., and Nassar, K. (2016). Slum Development Using Zero Waste Concepts: Construction Waste Case Study. *Procedia Engineering*, vol. 145, p.p. 1306–13.

[2] Domenech, T. and Bahn-Walkowiak, B. (2019). Transition Towards a Resource Efficient Circular Economy in Europe, *Policy Lessons from the EU and the Member States Ecological Economics*, vol. 155, p.p. 7–19.

[3] Kirchherr, J., Reike, D. and Hekkert M. (2017). Conceptualizing the circular economy: An analysis of 114 definitions, *Resources, Conservation & Recycling*, vol. 127, p.p. 9.

[4] Sereda T G 2021 Study of the morphological composition of municipal solid waste in the Perm region *IOP Conf. Ser.: Earth Environ. Sci.* , vol. 677, p.p. 042080.

[5] Sereda, T.G., Kostarev, S.N., Novikova Kochetova, O.V., Ivanova, I.E. Study of solid municipal waste accumulation rates in penitentiary facilities in Perm Krai during the pandemic of 2020 (2022), *IOP Conference Series: Earth and Environmental Science*, vol.1043, no. 1, p.p. 012005.

[6] Fernando, Silva Yimmy, et al. (2019). Effect of incorporation of masonry residue on the properties of self - compacting concretes *Constr. and Build. Mater* , vol.196, p.p. 277–83.
[7] Regidor, A. (2016). Proposals for public investment projects under the principle of sustainable development Nóesis: Revista de Ciencias *Sociales&Humanidades*, vol. 25, p.p. 23–48.
[8] Goldstein, B. and Rasmussen, F. (2018). LCA of Buildings and the Built Environment *Life Cycle Assessment. Theory and Practice*, vol. 28, p.p. 695–720.
[9] Kechichian, E. and Hoon, Jeong M. (2016). Mainstreaming Eco-Industrial Parks *The World Bank Group.*
[10] Sereda, T.G. and Kostarev, S.N. (2019). Development of automated control system for waste sorting *IOP Conference Series: Materials Science and Engineering*, vol.537(6), p.p. 062012.

COMETa 2022
6th INTERNATIONAL SCIENTIFIC CONFERENCE
17th - 19th November 2022
Jahorina, B&H, Republic of Srpska
University of East Sarajevo
Faculty of Mechanical Engineering
Conference on Mechanical Engineering Technologies and Applications

CITIES IN THE FIGHT AGAINST CLIMATE CHANGE USING RENEWABLE ENERGY SOURCES: CASE STUDY OF PRIBOJ MUNICIPALITY

Ana Radojević[1], Marko Janjušević[2], Danijela Nikolić[3], Jasmina Skerlić[4]

Abstract: Cities as the largest consumers of energy are at the same time places where action can be taken by applying energy efficiency measures and using renewable energy sources in order to reduce greenhouse gas emissions. In the Republic of Serbia, two key laws in the field of energy and climate were adopted in 2021 - the Law on Climate Change and the Law on the Use of Renewable Energy Sources. The adoption of these key regulations represents an important step in the energy transition, as well as the harmonization of the regulations of the Republic of Serbia with the acquis communautaire in the fight against climate change. Local governments are responsible for energy consumption in public buildings, public transport and public lighting. District heating, which is also the responsibility of local governments, is responsible for a large part of GHG emissions, if they use fuel oil or coal as fuel. The paper shows how much CO2 emissions are reduced when the existing lighting (mercury and sodium lamps) is replaced with LED lighting and when the fuel oil in the city heating plant is replaced with biomass.

Key words: biomass, CO2 emission reduction, energy consumption in the cities, LED lighting

1 INTRODUCTION

Cities as the largest consumers of energy are at the same time places where action can be taken by applying energy efficiency measures and using renewable energy sources in order to reduce greenhouse gas emissions. Local governments are responsible for energy consumption in public buildings, public transport and public lighting. District heating, which is also the responsibility of local governments, is

[1] Ana Radojević, energy manager of City of Kragujevac, Kragujevac, Serbia, radojevic.ana.kg@gmail.com
[2] Marko Janjušević, Public company "Heating plant Priboj", Priboj, Serbia, markojanjusevic@yahoo.com
[3] Associate professor, PhD Danijela Nikolić, University of Kragujevac, Faculty of Engineering, Kragujevac, Serbia, danijelan@kg.ac.rs
[4] Associate professor, PhD Jasmina Skerlić, University of Priština temporarily settled in Kosovska Mitrovica, Faculty of Technical Sciences, Kosovska Mitrovica, Serbia j.skerlic@pr.ac.rs

responsible for a large part of GHG emissions, if they use fuel oil or coal as fuel. The paper shows how much CO_2 emissions are reduced when the existing lighting (mercury and sodium lamps) is replaced with LED lighting and when the fuel oil in the city heating plant is replaced with biomass in the municipality of Priboj.

2 IMPACT OF USING LED LIGHTING AND BIOMASS IN DISTRICT HEATING SYSTEMS ON THE REDUCTION OF ENERGY CONSUMPTION IN CITIES

The international community has, by ratifying the Paris Agreement, agreed to take common action in order to hamper the greenhouse effect [1]. For instance, the European Commission has announced a “European Green Deal” [2], containing explicit goals to decarbonize energy sectors and increase renewable power generation, such as wind and solar power. The new Renewable Energy Directive 2018/2001 regulates the constitution of communities of renewable energy sources and promotes the exploitation of solid biomass, biofuels and biogas for district heating. The artificial lighting sector, which consumes more than a fifth of the world's electrical energy annually, remains a necessary condition for modern life, with 55% of it currently concentrated in urban areas, a rate that could reach 70% by 2050 for socio-economic reasons [3]. Public lighting connects hundreds of millions of streetlights with access to power across the globe, being responsible for 19% of global electricity usage, 30% - 50% of a typical city's energy bill and the already exceeding levels of CO_2 emissions. Consequently, this represents a priority issue for cities in their strategy towards sustainability [4].

2.1 Impact of using LED lighting on reducing energy consumption in cities

The strategy of public lighting is today a real urban issue: a well-lit city satisfies citizens and is a factor of development, attractiveness, safety and economy for communities. Urban authorities are challenged to define the right lighting, where it is needed, when it is needed, how it is needed and at the best cost. In the midst of economic and industrial growth and in the face of societal challenges, it is important to achieve ambitious energy independence targets while meeting its commitments to sustainable development [5].

By replacing street lighting, in addition to saving energy, visual comfort and safety are improved and of the most common measures is the replacement of light sources with more efficient LED lamps, which is increasingly becoming a satisfactory and cost-effective solution due to its low energy consumption, long life, reduced investment costs and maintenance costs, less environmental impact [6] and many other advantages [6].

Comparison of conventional (usually high-pressure sodium (HPS)) and LED luminaires in street/road lighting is not often based on photometrically equivalent lighting solutions and/or correct economic analysis, which may lead to either overestimation or underestimation of savings of any kind. Therefore, paper [7] presents a correct methodology for the determination of actual energy efficiency and cost indicators in street/road lighting. Analyzing optimal lighting solutions, characterized by the lowest installed power, it was shown that when considering mesopic effects the average energy savings achieved comparing LED (NW and WW) with HPS lighting solutions amounted to 41–62% and 29–59%, respectively, while the ratio between the total costs of the comparable LED (NW and WW) and HPS lighting solutions belonged to the ranges 0.59–1.26 and 0.61–1.14, respectively.

In most papers, one can come to the conclusion that greater savings are achieved both by the replacement of the existing luminaires with LED, and by combining that replacement with the installation of lighting control systems [8], [9].

The environmental impacts of energy-saving options in PLSs have been investigated in the literature. Researchers have investigated the most suitable, environmentally friendly and “green” solutions for the most commonly available PLS technologies [10]. Some other works have been conducted to investigate the equivalent CO_2 reduction by using LED luminaries for a case in Rome, Italy [11]., impact of different lighting technologies on CO_2 reduction in some cases in Italy [12], the use of LED technology and biomass for CO_2 reduction [13], switching time optimization for CO_2 reduction in a case in Italy [14], and impact of lighting optimization and replacing HPS fixtures by LED ones on greenhouse gas emission reduction [15].

In Serbia, the structure of existing lamps is dominated by lamps with high-pressure mercury (Hg lamps), as well as other types of less energy-efficient lamps, and in the last ten years, more efficient high-pressure sodium lamps (Na lamps) have been introduced more intensively.

The LED lamp is initially intended for ambient lighting of the street scene (road and sidewalk surfaces), urban intersections, squares, park areas, as well as other traffic facilities and areas (fuel supply stations, parking areas).

2.2 The impact of using biomass in district heating systems on the reduction of energy consumption in cities

The new Renewable Energy Directive 2018/2001 regulates the constitution of communities of renewable energy sources and promotes the exploitation of solid biomass, biofuels and biogas for district heating.

Serbia's energy policy is strongly aligned with EU energy acquis and strives to increase energy efficiency, greater use of renewable energy sources and reduction of greenhouse gases.Two systemic laws set the legislative framework to support sustainable energy management: the Law on Energy Efficiency and Efficient Use of Energy and the Law on the Use of Renewable Energy Sources.For the achievement of national energy and climate goals, the contribution of local partners, such as local governments, is of great importance.

District heating systems are one of the optimal solutions for the production, distribution and consumption of thermal energy.There is a wide range of energy sources that can be used in district heating systems: natural gas, solar energy, geothermal energy and combinations of renewable energy sources.As renewable energy sources, the following are used: wind energy, organic waste, biogas from wastewater treatment plants and forest or agricultural biomass.

Biomass district heating systems are the optimal economic and ecological solution for the production and distribution of thermal energy.These systems contribute significantly to mitigating climate change and controlling emissions.These are systems that use forest or agricultural biomass as fuel. They are mostly implemented in rural areas where there is a great biomass potential, as well as where there are no other sources of energy.The implementation of biomass in district heating contributes to the ecological sustainability of the field and the local circular economy.

In Serbia, biomass is used as a fuel in places where gas is not available, where there is security and stability of supply due to the large amount of forests, where fuel transportation costs are low, and where there is a large number of stakeholders - forest owners, companies for wood processing and pellet production.

The paper [16] shows biomass heating in four Spanish cities.The model includes technical and non-technical characteristics for assessing the sustainability of the biomass district system.

The use of biomass for heating can also be applicable for smaller communities in order to achieve energy independence, as described in the paper [16]. This paper has shown that CO_2 emissions are reduced by 55% in this way.

The impact of biomass use on climate in DHS was demonstrated by Hammar and Levihn [17] who measured how different biomass sources affect overall emission rates and net energy production.

In the framework of the energy strategy toward 2050, district heating systems offer a great flexibility in terms of heat generation technologies and renewable resources integration, resulting, in case of proper management and supply conditions, in fossil primary energy and greenhouse gases savings compared to conventional technologies. In Italy, only the 2.5% of the thermal final uses are satisfied by DHS and, although widely available over the territory, those fuelled by wooden biomass represent less than the half of the total [18].

3 CASE STUDY OF THE MUNICIPALITY OF PRIBOJ

3.1 The impact of using LED lighting on reducing energy consumption and reducing CO_2 emissions

The main characteristics of the public lighting system in the municipality of Priboj were mostly inefficiency and obsolescence, and as such, the system did not provide quality lighting. There were high costs for energy and maintenance. In addition, the function of the system was significantly impaired by years of insufficient or poor maintenance. The maintenance of the public lighting system carried out by the municipality included the replacement of light sources (bulbs) and other parts of lamps (ballasts, bulb sockets, glass protectors), replacement of damaged lamps, replacement of damaged poles and cable installations, replacement of damaged parts of control units (meters, contactors, photorelays, astronomical clocks, fuses) and, if necessary, system expansion. On the whole, the quality of maintenance of the public lighting system was insufficient, which resulted in insufficient quality of the lighting itself. This situation endangered the safety of all participants in traffic, and the problem of inadquate lighting particularly posed the problem for the traffic safety of children - pedestrians. The existing lighting was dominated by mercury bulbs with 49.05% and sodium with 28.14%.

Figure 1 shows the consumption of electricity for 2019 and 2021. Reduction of electricity consumption amounts to 42%. From a total of 1.306 MWh per year in 2019 to 762 MWh in 2021.

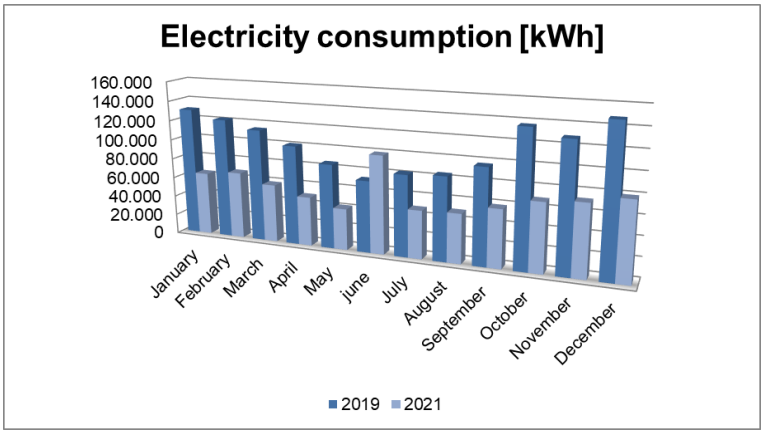

Figure 1. *Electricity consumption before and after the replacement of public lighting*

Figure 2 shows the reduction of CO_2 emissions for 2019 and 2021. The reduction of CO_2 emissions amounts to 42%. From a total of 1.188 t CO_2 per year in 2019 to 694 t CO_2 in 2021.

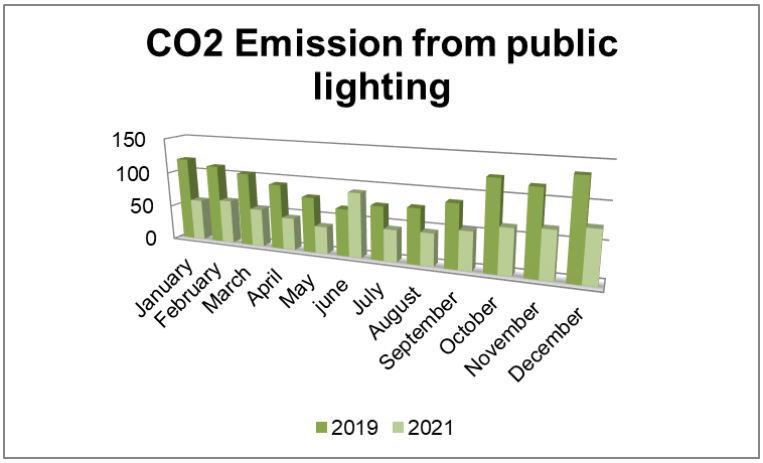

Figure 2. *CO_2 emission before and after the replacement of public lighting*

3.2 The impact of using biomass in the district heating system on reducing energy consumption and reducing CO_2 emissions

In 2021, in the municipality of Priboj, the first biomass boiler station used in the district heating system in Serbia was put into operation. This boiler house has a power of 23 MW, distributed in two heating oil boilers with a power of 2 x 7,5 MW and one wood chip boiler with a power of 8 MW. In the first heating season of 2021/2022, only the wood chip boiler worked, with a power of 8 MW.

Figure 3 shows the consumption of fuel oil in the 2020/2021 heating season and wood chips in the 2021/2022 heating season. In the 2020/2021 heating season, 1.800 tons of fuel oil were consumed, and after replacing the boilers, 33.000 m^3 of wood chips were used. When the consumption is converted into tons of equivalent oil, in order to be able to compare the consumption, it turns out that the consumption is higher after replacing the boilers. The reason for this is that the heating in the

2020/2021 season lasted 15 hours/day (6 am - 9 pm), while after the installation of new boilers, the heating was 24 hours a day. A survey conducted among district heating users showed that 75% of citizens are now satisfied with the quality of district heating.

The savings achieved in fuel costs are also significant. In the 2020/2021 heating season, the costs of fuel oil amounted to 1.780.000 euros, and in 2021/2022, they were 932.203 euros. Such big savings were achieved even with the price of wood chips jumping from 24 euros/t to 39 euros/t.

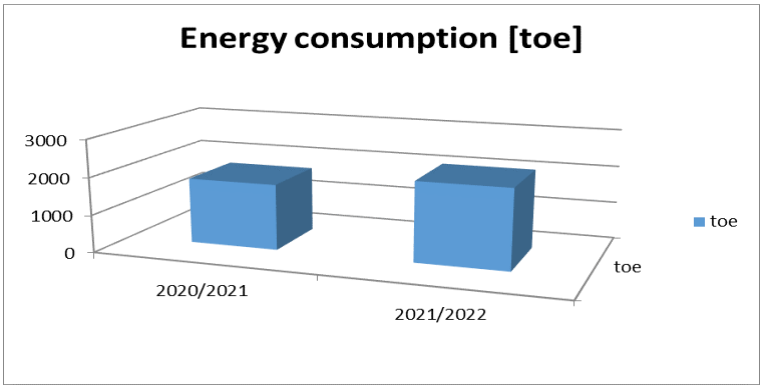

Figure 3. *Heat energy consumption for the heating seasons 2020/2021 and 2021/2022*

Figure 4 shows the reduction of CO_2 emission for 2020/2021 and 2021/2022 heating seasons. In the 2020/2021 heating season, when the city heating plant used fuel oil as fuel, the CO_2 emission was 5.544t, while the following year, when wood chips were used, the CO_2 emission was 524t, which led to 92% reduction in emissions.

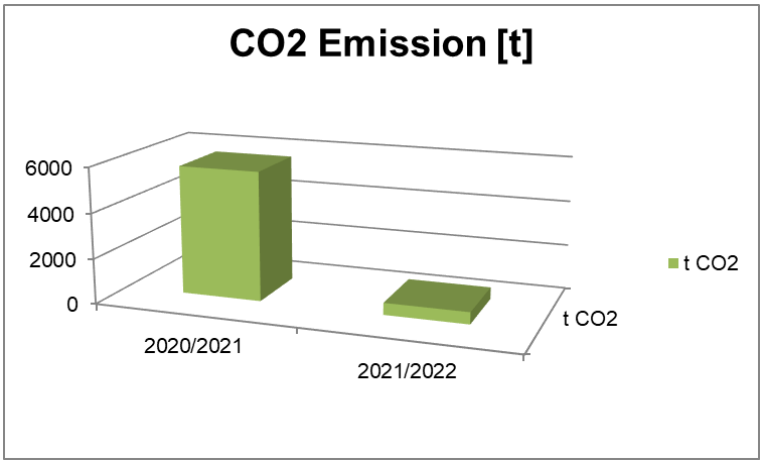

Figure 4. *Reduction of CO_2 emissions for the heating seasons 2020/2021 and 2021/2022*

4 CONCLUSION

Cities, as large energy consumers, have a great responsibility both for reducing energy consumption and for using renewable energy sources, all of which aim to reduce CO_2 emissions.

By using renewable energy sources - biomass in district heating systems and replacing lighting that uses sodium and mercury bulbs with modern LED bulbs in public lighting, it is possible to achieve significant savings in CO_2 emissions and this is a good way towards low-carbon cities.

The use of biomass in district heating systems in Serbia is still at the beginning, for now, out of a total of 51 heating plants, four heating plants have switched to the use of bimass wood chips, as well as the use of LED lighting in public lighting.

The paper presents a case study of the municipality of Priboj in which the use of LED lighting led to a reduction of CO_2 emissions by 42%, and the use of wood chips in the district heating system to a reduction of CO_2 emissions by 92%.

ACKNOWLEDGEMENTS

This research is part of the projects TR 33015 and III 42006. The authors would like to thank to the Ministry of Education, Science and Technological Development of Republic of Serbia for the financial support during this research.

LITERATURE

[1] Paris Agreement - Status of Ratification UNFCCC [WWW Document], n.d. URLhttps://unfccc.int/process/the-paris-agreement/status-of-ratification 09.14.2020, accessed on October 24, 2022

[2] EUR-Lex 52019DC0640 - EN - EUR-Lex [WWW Document], n.d. URLhttps://eur-lex.europa.eu/legal-content/EN/TXT/?uri=CELEX:52019DC0640 4.7.20, accessed on October 27, 2022

[3] R, Carli, M. Dotoli, R. Pellegrino (2018). A decision-making tool for energy efficiency optimization of street lighting*, Comput. Oper. Res.*, 96 , pp. 223-235

[4] Pardo-Bosch, F., Blanco, A., Sesé, E., Ezcurra, F., Pujadas, P. (2022). Sustainable strategy for the implementation of energy efficient smart public lighting in urban areas: case study in San Sebastian, *Sustainable Cities and Society*, vol. 76, 103454

[5] Kasseh, Y., Touzani, A., El Majaty, S. (2022). What public lighting governance model should be deployed in Moroccan cities for sustainable and efficient energy management?, Available online 19 July 2022, *In Press, Corrected Proof, materials-today-proceedings*

[6] Radojević, A., Janjušević, M., Nikolić, D., Bogdanović G., Ivanović, L., Skerlić, J., Palkova Z.(2022). Possibilities for reduction of energy conusuption by replacing public lighting with LED lighting: Case study of Priboj municipality, *Engineering TODAY*, vol. 1 / NO. 2 / 2022, p.p.19-29.

[7] Davidovic, M., Kostic, M. (2022). Comparison of energy efficiency and costs related to conventional and LED road lighting installations, *Energy*, vol. 254, Part B, 124299

[8] Sadeghian, O., Moradzadeh, A., Mohammadi-Ivatloo, B., Abapour, M., Anvari-Moghaddam, A., Shiun Lim, J., Pedro Garcia Marquez, F. (2021). A comprehensive review on energy saving options and saving potential in low

voltage electricity distribution networks: Building and public lighting, *Sustainable Cities and Society*, vol. 72, September 2021, 103064
[9] Fryc, I. , Czyżewski, D., Fan, J., Gălăţanu, C.D. (2021). The drive towards optimization of road lighting energy consumption based on mesopic vision—a suburban street case study, Energies, 14
[10] Shahzad, K., Čuček, L., Sagir, M., Ali, N. , Rashid, M.I. , Nazir, R. , ..., Ismail, I.M.I. (2018). An ecological feasibility study for developing sustainable street lighting system, Journal of Cleaner Production, 175 (2018), pp. 683-695
[11] Campisi, D., Gitto, S., Morea, D. (2018). Economic feasibility of energy efficiency improvements in street lighting systems in Rome, *Journal of Cleaner Production*, 175 (2018), pp. 190-198.
[12] Beccali, M., Bonomolo, M., Ciulla, G., Galatioto, A., Lo Brano V. (2015). Improvement of energy efficiency and quality of street lighting in South Italy as an action of Sustainable Energy Action Plans. The case study of Comiso (RG), *Energy*, 92 (Part 3) (2015), pp. 394-408,
[13] Molina-Moreno, V., Utrilla, P.N.C., Cortés-García, F.J., Peña-García A. (2018). The use of led technology and biomass to power public lighting in a local context: The case of baeza (Spain), Energies, 11 (7)
[14] Rossi, C., Gaetani, M., Defina A. (2016). AURORA: An energy efficient public lighting IoT system for Smart Cities, *Performance Evaluation Review*, 44 (2) , p.p. 76-81.
[15] Sędziwy, A. Basiura, A. Wojnicki I. (2018). Roadway lighting retrofit: Environmental and economic impact of greenhouse gases footprint reduction, *Sustainability (Switzerland)*, 10 (11)
[16] R.Volpe, Gonzalez, M., Alriols, Martelo Schmalbach, N., Fichera A. (2022). Optimal design and operation of distributed electrical generation for Italian positive energy districts with biomass district heating, *Energy Conversion and Management*, vol. 267, 115937
[17] Hammar, T., Levihn, F. (2020). Time-dependent climate impact of biomass use in a fourth generation district heating system, including BECCS, *Biomass Bioenergy,* 138 (2020), Article 105606.
[18] Ferla, G., Caputo P. (2022). Biomass district heating system in Italy: A comprehensive model-based method for the assessment of energy, economic and environmental performance, *Energy*, vol. 244, Part B,, 123105

COMETa 2022
6th INTERNATIONAL SCIENTIFIC CONFERENCE
17th - 19th December 2022
Jahorina, B&H, Republic of Srpska
University of East Sarajevo
Faculty of Mechanical Engineering
Conference on Mechanical Engineering Technologies and Applications

RESEARCH IN THE FIELD OF RENEWABLE ENERGY THROUGH THE APPLICATION OF MODERN ICT TECHNOLOGIES

Eleonora Desnica[1], Jasmina Pekez[2], Dalibor Dobrilović[3], Ljiljana Radovanović[4], Dragica Radosav[5], Luka Đorđević[6], Milica Mazalica[7], Siniša Mihajlović[8]

Abstract: Today's technological progress and new opportunities for humanity (information and communication technologies, new forms of renewable energy and energy efficiency, recycling) provide unimaginable opportunities for sustainable development. Sustainable development should be seen as a chance to create an opportunity for a better and more quality life from the emerging awareness and demands of the market to sustainability. In accordance with the development of the information society, educational institutions should enable and provide a basis for the existence and creation of knowledge and learning society, be accompanied by the development of knowledge and skills related to ICT, and thus strengthen the role of ICT in education. This paper aims to point out the potential of renewable energy sources, the importance of the application of ICT technologies in all spheres of life, within smart technologies, and the possibility of using renewable energy sources through the application of modern ICT solutions.

Key words: information and communication technologies (ICT), power sensor stations, renewable energy, sustainable development

[1] Full professor Eleonora Desnica, University of Novi Sad, Technical Faculty “Mihajlo Pupin”, Zrenjanin, Serbia, desnica@tfzr.uns.ac.rs (CA)
[2] Assoc. professor Jasmina Pekez, University of Novi Sad, Technical Faculty “Mihajlo Pupin”, Zrenjanin, Serbia jasmina.pekez@tfzr.rs
[3] Assoc. professor Dalibor Dobrilović, University of Novi Sad, Technical Faculty “Mihajlo Pupin”, Zrenjanin, Serbia, dalibor.dobrilovic@tfzr.rs
[4] Full. professor Ljiljana Radovanović, University of Novi Sad, Technical Faculty “Mihajlo Pupin”, Zrenjanin, Serbia, ljiljana.radovanovic@tfzr.rs
[5] Full professor Dragica Radosav, University of Novi Sad, Technical Faculty “Mihajlo Pupin”, Zrenjanin, Serbia, dragica.radosav@tfzr.rs
[6] Teaching assistant Luka Đorđević, University of Novi Sad, Technical Faculty “Mihajlo Pupin”, Zrenjanin, Serbia, luka.djordjevic@tfzr.rs
[7] Teaching assistant Milica Mazalica, University of Novi Sad, Technical Faculty “Mihajlo Pupin”, Zrenjanin, Serbia, milica.mazalica@tfzr.rs
[8] Teaching assistant Siniša Mihajlović, University of Novi Sad, Technical Faculty “Mihajlo Pupin”, Zrenjanin, Serbia, sinisa.mihajlovic@tfzr.rs

1 INTRODUCTION

The term renewable energy sources mean energy sources found in nature are renewable in whole or in part, especially energy from watercourses, wind, non-accumulated solar energy, biomass, geothermal energy, etc. The use of these sources contributes to more efficient use of own potentials in energy production, reducing »greenhouse gas emissions«, reducing fossil fuel imports, developing local industry, and creating new jobs. Renewable energy technologies are clean and have much less impact on the environment than conventional energy technologies [1,2].

The Republic of Serbia has passed many laws and documents in the field of renewable energy sources, which creates conditions for a significant increase in the production and use of these energy sources. Vojvodina is a region with significant natural potential in the field of renewable energy sources, and the national energy policy calls for increased use of renewable sources in order to meet the growing electricity needs [3]. Numerous laws and documents have been passed at the Government of AP Vojvodina level, but assistance in the use of renewable energy sources is still insufficient. Numerous researches in this field were conducted at the Faculty of Technical Sciences, the Faculty of Agriculture, and the Faculty of Technology in Novi Sad, as well as at the Technical Faculty "Mihajlo Pupin" in Zrenjanin, and the results were presented through numerous projects of these institutions [4].

The process of adopting new technologies is slow, with the main problem for the installation of new plants being the starting price, which raises the price of energy obtained in the first few years to the point of complete unprofitability compared to other commercially available energy sources. However, in the long run, the benefits of using renewable energy sources exceed the costs required for installation, so a significant increase in the share in the energy balance is expected, as they are imposed as a natural response to existing and upcoming climate problems [5,6].

At every step, the Internet and information technologies are changing many aspects of life, both in Serbia and elsewhere in the world. Information and communication technology (ICT) provides a good foundation for the creative and effective use of knowledge. The purpose of modern ICT technologies is in every economy segment, education, environmental protection, health care, science, and innovation.

The focus of this paper is solar resources as a form of renewable energy sources, the importance of ICT in all spheres of life, within smart technologies such as smart cities, smart agriculture (sensors monitor various parameters in a wide range, for example, from whether the containers are full and they need to be empty, the smart solar benches allow phones to be charged, the parking system based on IoT technology, use of IoT in agricultural areas - monitoring the humidity in vineyards and microclimatic condition in greenhouses, controlling humidity and temperature levels of hay, straw, etc.). Also, the goal is to point out the wider promotion of the importance and possibility of using renewable energy sources and modern ICT technologies in education.

2 APPLICATION AND MODELS OF SOLAR ENERGY USE

The use of solar energy is just one of the areas of renewable energy use. Therefore, the use of solar energy is a reflection and part of a global process, important in the field of protection and preservation of the environment. In the past decades, technologies have been developed to transform solar energy into electricity

or heat, and these technologies are used today with significantly more engagement in the total production of useful energy [7].

According to the method of conversion of solar radiation, active solar systems can be divided into two groups: systems in which solar radiation energy is directly transformed into electricity (e.g., photovoltaic systems) and systems in which solar radiation is directly transformed into heat, i.e., heat solar receivers energy [8].

Direct collection of solar energy can be done through:

- photovoltaic cells for obtaining electricity;
- solar collectors for water heating (solar energy), and
- mirrors for focusing sunlight (mirror power plant) [5].

3 OVERVIEW OF THE IMPORTANCE OF MODERN ICT SOLUTIONS

Information technology has recently been replaced by the term information and communication technology (ICT). Figure 1 is presented the architecture of modern ICT technologies: data collection and observation, the realization of new techniques of data analysis and control; encouraging automation, scalability, and process efficiency; reducing costs, and increasing revenue; based on cloud services and the Internet access.

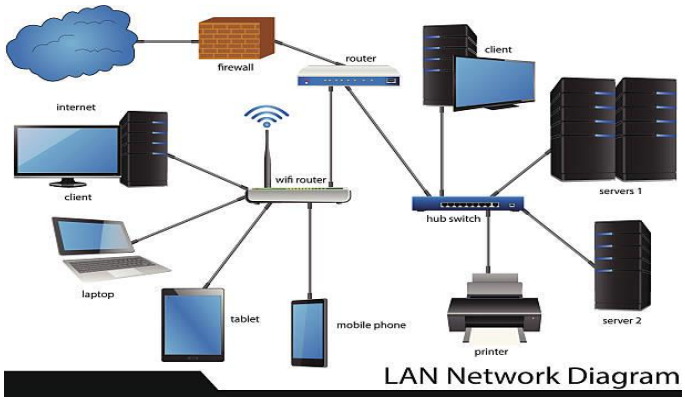

(a)

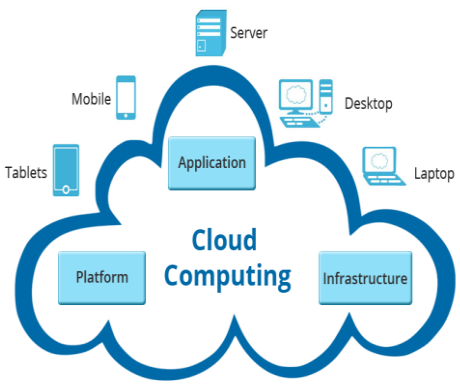

(b)

(c)

Figure 1. Modern ICT technologies – yesterday, today, tomorrow (a) LAN – Local Area Network [9], (b) Cloud service [10], (c) M2M, IoT [11]

This modern time in which we live and the jobs that are done in the process of education require us to be flexible, dexterous, quick to learn and adapt to the situation. Keeping in mind the constant progression of technology, the application of modern technological solutions includes all modern solutions applicable to the teaching process, including the possibility of artificial intelligence, process simulation, and virtualization of certain processes in education.

Following the development of the information society, educational institutions should enable and provide a basis for the existence and creation of a knowledge and learning society, be accompanied by the development of knowledge and skills related to ICT, and thus strengthen the role of ICT in education. The basis of this approach is the existence of staff who are trained to use the latest ICT.

Modern educational information and communication technologies introduce innovations in the way of realization of the teaching process to overcome many shortcomings and in the function of modernizing education, through greater application and development of methodological practice, with the support of information and communication technology [12].

3.1 Internet of things (IoT)

The possibilities of using the Internet of Things are wide, almost unlimited. According to predictions, this technology will be represented in every view in the near future. The term Internet of Things (IoT) has been mentioned as a concept for more than 20 years. In 1999 Kevin Ashton of Procter & Gamble, later MIT's Auto-ID Center brought this term, and thanks to advances in information and communication technology, this term has existed for the last few years [13].

One of the most important elements of the IoT system is the technologies for the transfer of collected data. Recently, more and more wireless technologies are being used. These technologies can be short-range or WPAN (RFID, Bluetooth, ZigBee, etc.), medium-range (Wi-Fi), or long-range, which include mobile systems (4G, 5G) and LP-WAN (LoRa, LoRaWAN, SigFox, NB-IoT, LTE-M, etc.). In paper [14] is given overview and description of these technologies.

The Internet of Things has a wide range of applications in other areas. His application has a range from personal use to control of the entire city. Each area in which it is applied can have the attribute "smart". The main feature of smart things is the possession of a unique identifier, a built-in system, and the ability to transfer data over the network. Considering that it is defined as a complex ecosystem that can be used to connect everything, everyone, any services, or business, it can be found in almost every aspect of life. For example - in the city (for traffic unloading, air pollution monitoring, efficient street lighting, water control), for personal use (various reminders), in agriculture (irrigation system control), in the food industry (for monitoring the origin and quality of food, product delivery, etc.), in electricity (for energy consumption, device control), in safety, for health, in the environment (for measuring of particulate emissions), etc.

4 USE OF SENSOR STATIONS THROUGH THE PROJECT AT THE TECHNICAL FACULTY "MIHAJLO PUPIN" ZRENJANIN

The use of sensor stations in the framework of smart technologies may include the installation of sensor stations in places without infrastructure, which is why they are mainly powered by batteries that have a limited capacity. This problem can be overcome by using photovoltaic cells to transform solar energy into electricity, which

would ensure their energy independence, and would allow for their even greater application. In this segment of the application, the research is focused on the possibility of supplying sensor cells with electricity using PV cells (photovoltaic cells).

The authors of this paper are currently working on this topic at the Technical Faculty "Mihajlo Pupin" Zrenjanin, University of Novi Sad, and within the project "Creating laboratory conditions for research, development, and education in the field of the use of solar resources in the Internet of Things". (project number 142-451-2684/2021-01/02). One of the goals of the project is to establish a research laboratory in the field of using solar panels to provide energy to sensor stations. The importance of this topic arises from the growing use of sensor technologies and stations in the various systems that surround us and have increasing applications. The formed laboratory equipment (Figure 2) would be used as portable for outdoor measurements under different influences of solar radiation on a direct power supply of sensor stations and the chargeability of their batteries. The sensor are voltage sensors for DMM, temperature sonde from DMM, BH1750, DHT-22 temperature and humidity. Current system power consumption is not measured. The reason is that Arduino board (the main component) of the system is powered directly from PC via US B, for data acquisition (sending data to PC), and while the monitoring the system consumption from baterry is not priority. The purpose of the system is to acquire solar panel system and ambient data as well as to analyze its dependence and to optimize sensor mode energy consumption (Arduino board).

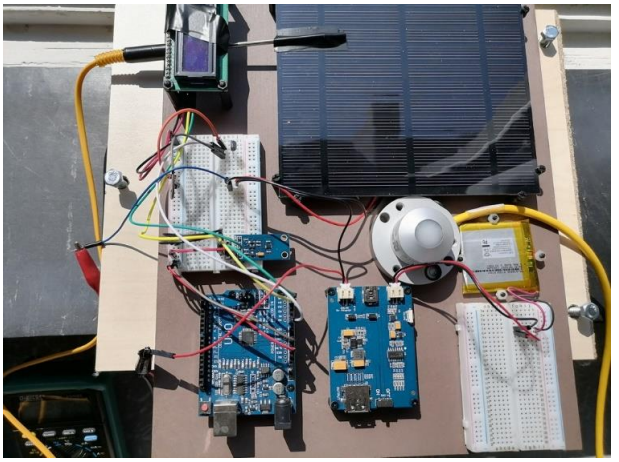

Figure 2. Prototype of the field measuring system

In addition to the intensity of solar radiation and determining the optimal dimensions of solar panels, the laboratory would be used to assess the impact of dust, atmospheric conditions, shadows, and other factors on electricity generation. The obtained measurements would be used to optimize the operation of solar stations and their design in terms of reducing consumption, duty cycle, composition, and types of components.

Research and experimentation, which simultaneously includes the area of development, optimization, and operation of sensor stations, but also their supply of solar energy, is not sufficiently represented in our scientific research institutions, especially not in the Banat region. Also, laboratory equipment that can be used in teaching the subjects of the profile of Information Technology and Mechanical

Engineering and which relates to the design, development, and programming of such systems is not represented at our higher education institutions. The introduction of such laboratory equipment and their use in teaching would raise the level of the teaching process and enable the training of a new profile of experts.

5 CONCLUSION

The European Union has a strategy to promote the use of renewable energy sources in the future, with a series of measures to encourage investment in renewable energy facilities.

Renewable energy sources are one of the areas that have experienced the greatest development in the last ten years. In the next ten years, we will surely have more exciting news.

Thanks to new technologies and their wide application, we are entering the era of an information society in which information and knowledge will replace the dominant influence of energy and capital. All this requires modern man to master new knowledge and technologies, so the basic requirement before all of us is using computers, that is, the need for basic computer literacy.

The Internet of Things (IoT), through the realization of a new dimension of connectivity, represents a revolution, both in industry and in everyday life. It is presented as a concept and paradigm which considers widespread objects that have wireless or wired connections, with the use of unique address schemes, have the ability to communicate and collaborate with each other (or with other things/objects) in order to create new applications and services.

Experimentation, research, and the possibility of creating a laboratory through a project, which includes this topic in their work with students, can significantly contribute:

- creation of new technical solutions in the field of solar power supply of sensor stations,
- creation of a larger number of qualified experts for the development of sensor stations and hardware-software systems in this field,
- significant improvement of the quality of domestic educational institutions and their study programs,
- significant increase in the number of domestic ICT companies and development of sensor systems for both domestic and foreign markets.

ACKNOWLEDGMENTS

The research is conducted through the project »Creating laboratory conditions for research, development, and education in the field of the use of solar resources in the Internet of Things«, at the Technical Faculty »Mihajlo Pupin« Zrenjanin, financed by the Provincial Secretariat for Higher Education and Scientific Research, Republic of Serbia, Autonomous Province of Vojvodina, Project number 142-451-2684/2021-01/02.

REFERENCES

[1] www.obnovljiviizvorienergije.rs
[2] Desnica, E., Letić, D., Gligorić, R. (2012). Educating engineers in harmony with nature - the usefulness of renewable energy sources, *Journal of Tractors and power machines*, vol.17, no.4, p.p. 87-93.
[3] https://rav.org.rs/sr/key-sectors/renewable-energy/

[4] Desnica, E., Nikolić, M. (2013). The place and role of universities in education for sustainable development, *Journal of Tractors and power machines,* vol.18, no.5, p.p. 43-47.
[5] Mikić Bojović, J. (2018). *Use of renewable energy sources in the function of environmental protection*, Master thesis, the University of Business Academy in Novi Sad, Faculty of Economics and Engineering Management, Novi Sad.
[6] Damjanović, D. (2010). *Rational use of energy in the function of local community development*, Palgo Center, Belgrade.
[7] Lambić, M. (2015). *Solar Energy*, Institute for Textbooks, Belgrade.
[8] Kosorić, V. (2007). *Active Solar Systems*, Construction Book, Belgrade.
[9] https://www.istockphoto.com/photos/local-area-network-diagram
[10] https://www.emphatictechnologies.com/cloud-app-development.php
[11] https://www.peerbits.com/blog/difference-between-m2m-and-iot.html
[12] Brzaković, M., Lalović, K., Jocić, G., Rajčević, D., Ivanović, S. (2017). Thoughts on the importance of applying advanced technology solutions in education, *Informacione tehnologije, obrazovanje i preduzetništvo ITOP 17*, p.p. 499-508.
[13] Božić, Ž. (2020). I*nternet of Things - vision, application and research challenges*, Master thesis, University of Sarajevo, Faculty of Economics, Sarajevo.
[14] Dobrilović, D. (2018). Networking technologies for smart cities: an overview, *INDECS*, vol. 16(3-A), p.p. 408-416, DOI 10.7906/indecs.16.3.13

COMETa 2022
6th INTERNATIONAL SCIENTIFIC CONFERENCE
17th - 19th November 2022
Jahorina, B&H, Republic of Srpska
University of East Sarajevo
Faculty of Mechanical Engineering
Conference on Mechanical Engineering Technologies and Applications

COMPUTATIONAL AERODYNAMIC ANALYSIS OF A SMALL WIND TURBINE

Jelena Svorcan[1], Dragoljub Tanović[2], Aleksandar Kovačević[3]

Abstract: The growing climate change issues and the ongoing energy crisis stipulate further exploitation of renewable energy sources and the development of systems capable to efficiently generate clean energy. Among the most promising are wind turbines, that come in different shapes and sizes. Small-scale wind turbines are economic and particularly suitable for small consumers and rural areas. They are not too common, and further research into their performance is necessary. This paper focuses on the design and aerodynamic performance of a small horizontal-axis wind turbine. Its rotor geometry is described while its basic aerodynamic coefficients, power and thrust coefficients, are computed by finite volume method in ANSYS Fluent. Flow is assumed as incompressible and viscous, while Reynolds-averaged Navier-Stokes (RANS) equations are closed by different turbulence models. Wind turbine aerodynamic performance is estimated, and different flow visualizations are provided, particularly focusing on the wind turbine wake.

Key words: Aerodynamic coefficients, CFD, RANS, Wind turbine

1 INTRODUCTION

One of the most important contemporary goals worldwide is to achieve greater generation of electric energy from renewables and alleviate some of the climate change challenges. Wind resource stands out as the one with the most potential because it is available almost everywhere, over both earth and water surfaces. The numbers of installed wind turbines grow annually, and much work is being done on their further advancement. With continuous development and cost reduction of wind turbine (WT) technology small-scale structures are also becoming more interesting and popular. Even though they contribute in small portions, they require very low

[1] Dr Jelena Svorcan, University of Belgrade, Faculty of Mechanical Engineering, Belgrade, Serbia, jsvorcan@mas.bg.ac.rs (CA)
[2] Dragoljub Tanović, University of Belgrade, Faculty of Mechanical Engineering, Belgrade, Serbia, dtanovic@mas.bg.ac.rs
[3] Aleksandar Kovačević, University of Belgrade, Faculty of Mechanical Engineering, Belgrade, Serbia, akovacevic@mas.bg.ac.rs

investments and can be put to use in both rural and urban environments. Many recent studies focused on small-scale WTs are available [1-8].

These research investigations address some of the open questions (challenges) to the operation of small WTs such as their lower aerodynamic performance in comparison to their larger counterparts, poor starting characteristics, optimal control, etc. The reduced values of power coefficient are mostly caused by the low Reynolds number (Re) flows (due to both smaller velocities as well as small chord lengths) that transition from laminar to turbulent. Since these flow phenomena still remain unresolved, further numerical and experimental studies are necessary.

A commercially available small-scale, horizontal-axis WT is studied here for two reasons. Firstly, we wish to understand the capabilities and limitations of usually employed computational approach (solving RANS equations) for low-to-medium Re rotational flows. Secondly, if we validate an appropriate numerical model, we can set the basis for further studies of possible WT enhancements through modified design and optimization that could lead to an increased power generation and more efficient exploitation of these WTs.

2 NUMERICAL MODELLING

The details of the employed numerical approach are provided below. We start with the most important wind turbine properties, and its rotor, and build an appropriate geometric model around it that adequately represents the outer domain. We then discretize this domain into cells and solve the governing flow equations in each cell.

2.1 Geometry

Basic properties of the investigated three-bladed WT are listed in Table 1.

Table 1. *WT properties*

Rated power [W]	300
Diameter [m]	1.35
Cut-in wind speed [m/s]	2
Rated wind speed [m/s]	13
Cut-out wind speed [m/s]	50
Blade material	Nylon fiber

The starting rotor geometry was extracted from the real product by 3D scanning which resulted in a more plausible but unsmooth (slightly rugged, uneven) model surfaces. Otherwise, the remainder of the geometric model was defined in accordance with the procedure described in [9]. The quasi-rotating zone encompassing the rotor is a cylinder with the following dimensions: radius 1 m, length 1.5 m where 0.5 m is fore and 1 m aft of the rotor plane. The outer cylinder (representing the

surrounding domain) stretches 3 m fore and 7 m aft of the coordinate beginning (10 m length in total) and 5 m in radial direction (cylinder radius). There is an interface surface between the two zones.

2.2 Mesh

Grid generation methodology and cell sizing are mostly defined from previous experience [9]. However, the slight ruggedness of the model surfaces somewhat limited the possibilities of further refining the mesh. Overall properties of the final unstructured mesh, that has approximately 3.5 million tetrahedral control volumes, are: 5 cm element size along the blades, additional refinement near the leading edge to better represent the curvature, 20 cm maximal face size in the whole domain, and cell growth rate 1.2 (from the blades towards the outer boundaries). A detail of the mesh around the blade is illustrated in Figure 1.

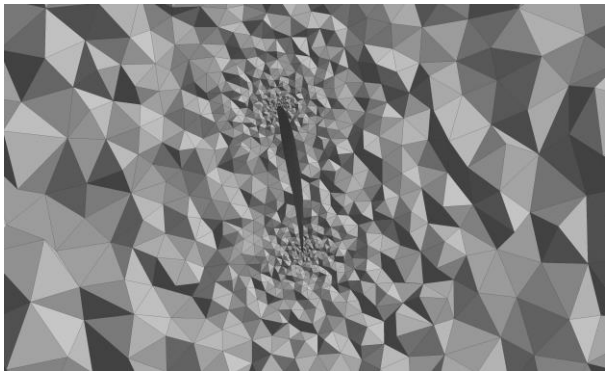

Figure 1. *Detail of the generated computational mesh*

2.3 Computational set-up

Three-dimensional, steady (quasi-rotational), incompressible, turbulent flow simulations were performed in the engineering software package ANSYS Fluent [10] by finite volume method. Reynolds-averaged Navier-Stokes (RANS) equations were closed by the:

- 1-equation Spalart-Allmaras [10] (although simple, solving just one transport equation for the kinematic eddy viscosity, it was developed for aerospace applications and performs well with turbomachinery), or,
- 2-equation *k-ω* shear stress transport (SST) [10] (widely employed with airfoils) turbulence model.

Even though the considered Reynolds numbers are low, and flow transition and laminar separation bubbles can be expected, transitional flow are extremely sensitive to outer disturbances. In real operation, when not ideally smooth surfaces rotate, the flow readily transitions and fully turbulent flows might be expected. Secondly, since it was not possible to achieve sufficiently fine mesh resolution in the wall vicinity to resolve transition, it was not necessary to employ more complex turbulence models that require extremely fine spatial and temporal scales.

Standard air properties are assumed. Velocity vector representing the oncoming wind is defined along the inlet boundary. The nominal wind speed of 10 m/s is assumed. Zero gauge pressure is assumed along the outlet. The rotation of the WT rotor is resolved by the moving reference frame (MRF) model where certain additional inertial terms are added to the flow equations withing the designated region. Different

operating points are achieved by changing the angular velocity Ω of the quasi-rotating zone. An interface surface separates the two zones, whereas the blade surfaces are no-slip and rotating.

Pressure-based solver with SIMPLEC coupling scheme of pressure and velocity fields is employed. All spatial derivatives are approximated by 2nd order schemes. Computations were performed until reaching the converged values of aerodynamic coefficients, usually 500-1000 iterations.

3 RESULTS AND DISCUSSION

Once the computations finish, we proceed with the post-processing of the obtained data. Some of the most important results are provided and examined below. We are primarily interested in the global values like the generated power and normal force acting on the blades, but also on local distributions along the blades (like pressure) or in the close vicinity of the blades (like velocity or vorticity).

3.1 Quantitative analysis

In order to perform a more general quantitative analysis, it is convenient to transform the absolute values of velocity V, thrust force T and power P to dimensionless aerodynamic coefficients:

$$TSR = R\Omega/V,\ C_T = T/(0.5\rho V^2 A),\ C_P = P/(0.5\rho V^3 A). \quad (1)$$

Reference values used for the computation of the tip-speed-ratio TSR, aerodynamic coefficients of thrust C_T and power C_P are: blade length R = 0.625 m, area A = 1.2272 m^2, air density ρ = 1.225 kg/m^3, and velocity V = 10 m/s.

Computed power and thrust coefficient curves with respect to tip-speed-ratio are presented in Figure 2. The value corresponding to the rated operation of the real WT is also drew in and marked by a black cross. It can be observed that both curves follow the expected trends and that there are no particular differences in the values produced by the two tested turbulence models (*k-ω* SST and SA) when the simplest MRF approach is used. More importantly, the correspondence of numerical results to the real operating point is quite satisfactory.

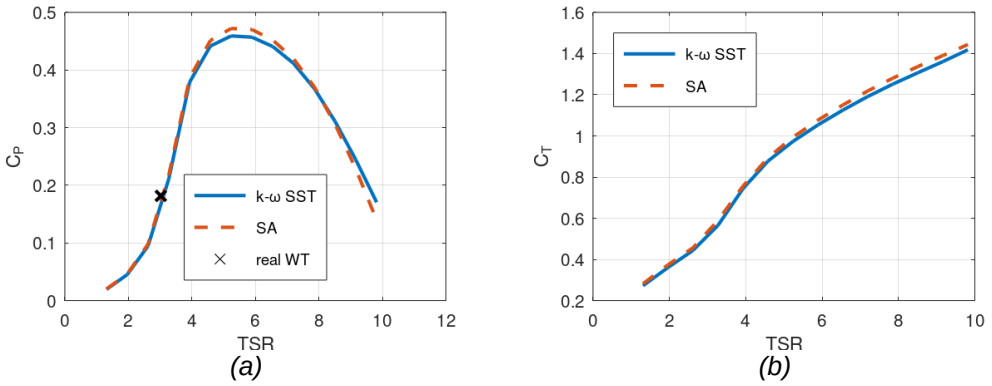

Figure 2. *(a) C_P(TSR), (b) C_T(TSR)*

3.2 Qualitative analysis

The computed flow fields can be further illustrated. Pressure contours over the upper blade surface are depicted in Figure 3. Negative gauge pressure values can be observed in the vicinity of the leading edge where the greatest velocity increase appears. It may also be noticed that the outer parts of the blades contribute the most.

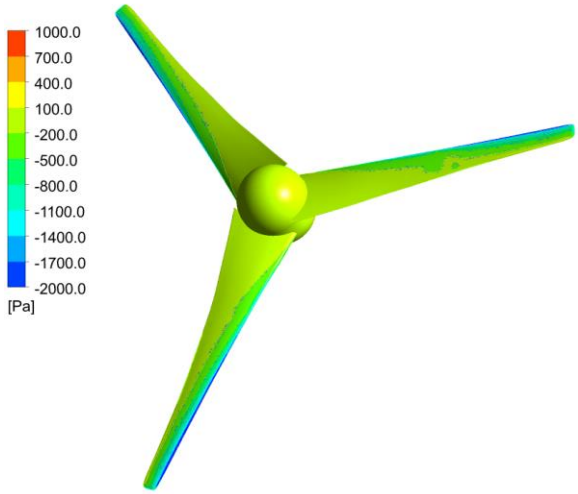

Figure 3. *Pressure contours over the blades at TSR = 3.93*

The changes in the oncoming wind speed caused by the rotor are presented in Figure 4. They are mostly limited to the streamtube encompassing the blades. The wake behind the rotor can be clearly differentiated by the reduced values of wind speed. And this is exactly how the WT affects the air flow. It extracts a portion of its kinetic (translation) energy and transforms it to rotating kinetic energy, and subsequently electric energy.

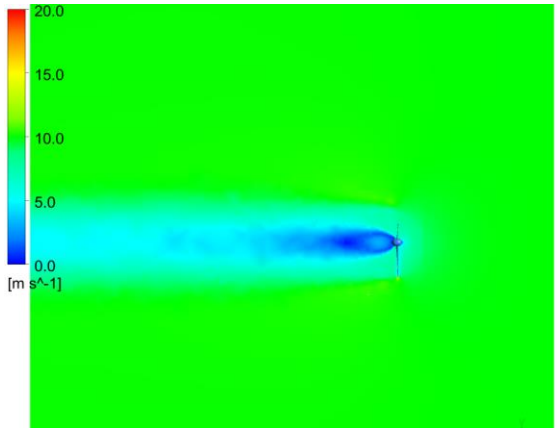

Figure 4. *Velocity in stationary frame at TSR = 3.93*

The actual (relative) flow around the blade cross-sections is illustrated in Figure 5. The velocity magnitude is much larger because relative velocity represents the

vector sum of (reduced) wind speed and rotating velocity component. Again, the acceleration of the flow along the suction side is apparent. Since a nominal operating point is analysed (*TSR* = 5.24) where maximal power coefficient is achieved, the flow along the complete blade is smooth and attached.

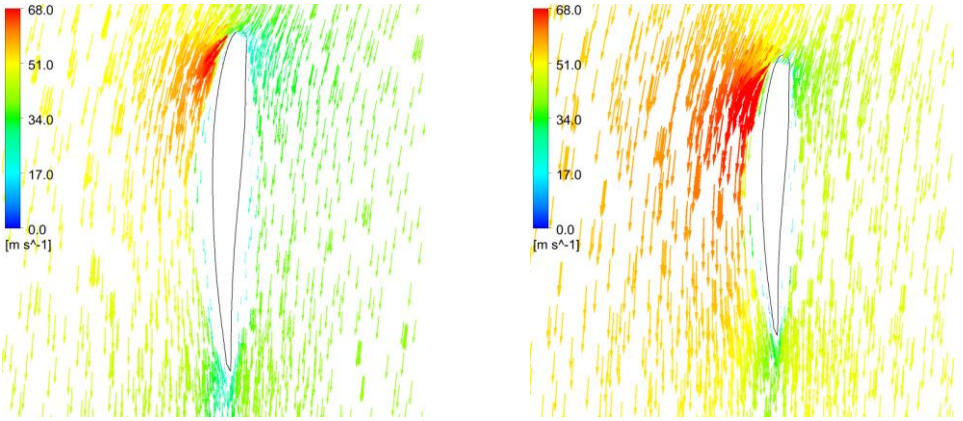

(a) *(b)*

Figure 5. *Relative velocity vectors at TSR = 5.24 at: (a) y = 0.5 m, (b) y = 0.6 m*

Finally, the vortical structures and the wakes detaching from the blade root and tips are depicted in Figure 6. Root section causes some losses but they are not significant, whereas blade tips act as a greater source of flow deficit. Some smaller flow detachments can be observed along the blades because a non-optimal regime is considered (at *TSR* = 3.93).

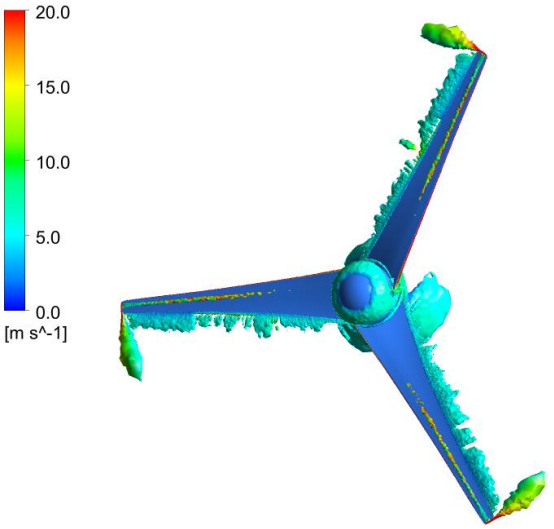

Figure 6. *Shed wakes at TSR = 3.93*

4 CONCLUSIONS

This paper describes the numerical study of flows appearing around a small-scale, commercially available horizontal-axis WT. Flows were considered 3D, incompressible and turbulent. A reasonable estimation of global aerodynamic performance is achieved by solving RANS equations coupled with MRF approach which is confirmed by comparison of numerical to real operation data. Also, the main flow features seem well captured. In the future, bigger and more refined meshes should be combined with more advanced turbulence modelling to gain more insight into the occurrences in the proximity of blades (within the boundary layer) as well as transient effects. Also, the validated numerical model can be used for future WT optimization studies.

ACKNOWLEDGEMENT

This research work is supported by the Ministry of Education, Science, and Technological Development of the Republic of Serbia through contract no. 451-03-68/2022-14/200105.

REFERENCES

[1] Giguère, P., Selig, M.S. (1997). Low Reynolds number airfoils for small horizontal axis wind turbines, *Wind Engineering*, 21/6, p.p. 367−380.
[2] Wiener, J.G., Koontz, T.M. (2010). Shifting winds: Explaining variation in state policies to promote Small-Scale wind energy, *Policy Studies Journal*, 38/4, p.p. 629−651.
[3] Tummala, A., Velamati, R.K., Sinha, D.K., Indraja, V., Krishna, V.H. (2016). A review on small scale wind turbines, *Renewable and Sustainable Energy Reviews*, 56, p.p. 1351−1371.
[4] Porto, H.A., Fortulan, C.A., Porto, A.J.V. (2022). Power performance of starting-improved and multi-bladed horizontal-axis small wind turbines, *Sustainable Energy Technologies and Assessments*, 53, 102341.
[5] Choe Wei Chang, C., Jian Ding, T., Jian Ping, T., Chia Chao, K., Bhuiyan, M.A.S. (2022). Getting more from the wind: Recent advancements and challenges in generators development for wind turbines, *Sustainable Energy Technologies and Assessments*, 53, 102731.
[6] Yossri, W., Ben Ayed, S., Abdelkefi, A. (2021). Airfoil type and blade size effects on the aerodynamic performance of small-scale wind turbines: Computational fluid dynamics investigation, *Energy*, 229, 120739.
[7] Yi-Nan, Z., Hui-Jing, C., Ming-Ming, Z. (2021). A calculation method for modeling the flow characteristics of the wind turbine airfoil with leading-edge protuberances, *Journal of Wind Engineering and Industrial Aerodynamics*, 212, 104613.
[8] Shahzad, Ali Q., Kim, M.-H. (2022). Quantifying impacts of shell augmentation on power output of airborne wind energy system at elevated heights, *Energy*, 239, 121839.
[9] Svorcan, J., Peković, O., Ivanov, T. (2018). Estimation of wind turbine blade aerodynamic performances computed using different numerical approaches, *Theoretical and Applied Mechanics*, 45/1, p.p. 53−65.
[10] ANSYS, ANSYS Fluent Theory Guide, Release 18.1, 2017.

MAINTENANCE AND TECHNICAL DIAGNOSTICS

COMETa 2022
6th INTERNATIONAL SCIENTIFIC CONFERENCE
17th - 19th November 2022
Jahorina, B&H, Republic of Srpska
University of East Sarajevo
Faculty of Mechanical Engineering
Conference on Mechanical Engineering Technologies and Applications

PREGLED STRATEGIJA ODRŽAVANJA

Bogdan Marić[1], Vlado Medaković[2]

Rezime: U savremenim tehničkim sistemima strateški pristup procesu održavanja je neophodan. Od prošlog vijeka potreba za održavanjem je sve veća, s toga su razvijene različite strategije održavanja, čije su osnovne karakteristike navedene u radu, kao i metode za izbor najpovoljnijih, takođe i problemi sa kojima se susrećemo prilikom izbora najpovoljnijih strategija održavanja. Pregledom datih strategija utvrđuju se karakteristike strategija, odnosno razlozi zašto je određena strategija pogodna, ili nije, za određeni tehnički sistem. Izborom pravilnih strategija mogle bi se ostvariti uštede u održavanju, kako sa aspekta ekonomskih pokazatelja uloženih sredstava, tako i sa aspekta rada mašina, odnosno tehničkih sistema u stanju u radu.

Ključne riječi:Strategija održavanja, tehnički sistem, metode, izbor, problemi.

OVERVIEW OF MAINTENANCE STRATEGIES

Abstract: In modern technical systems, a strategic approach to the maintenance process is necessary. Since the last century, the need for maintenance has been increasing, as a result, various maintenance strategies have been developed, the basic characteristics of which are listed in the paper, as well as the methods for choosing the most favorable ones, as well as the problems we face when choosing the most favorable maintenance strategies. By reviewing the given strategies, the characteristics of the strategies are determined, i.e. the reasons why a certain strategy is suitable, or not, for a certain technical system. By choosing the right strategies, maintenance savings could be achieved, both from the aspect of the economic indicators of the invested funds, and from the aspect of the operation of machines, that is, technical systems in working condition.

Key words: Maintenance strategy, technical system, methods, selection, problems.

1 UVOD

Potreba za održavanjem postoji od momenta kada je čovjek napravio prva

[1] Dr Bogdan Marić, vanr. prof., UIS, Mašinski fakultet I. Sarajevo, (e-mail: bogdan.maric@ues.rs.ba)
[2] Dr Vlado Medaković, vanr. prof., UIS, Mašinski fakultet I. Sarajevo, (e-mail: vlado.medakovic@ues.rs.ba)

materijalna dobra. Materijalna dobra koja su ljudi pravili prije industrijske revolucije, su bila jednostavne konstrukcije, često su bila predimenzionisana i predviđena za duži vremenski period korišćenja. Održavanje je tada imalo manji značaj i uglavnom se odnosilo na popravku polomljenih ili rashodovanih dijelova. Početkom dvadesetog vijeka, eskalirala je pojava fabrika sa ciljem zadovoljenja potreba masovne proizvodnje. Usložnjavanjem sredstava rada, fabrika iskazuje povećane potrebe za održavanjem[4]. Održavanje je veoma odgovoran zadatak. Angažovanjem specijalista iz različitih struka formira se tim čiji je osnovni zadatak ostvarivanje maksimalnog izlaznog efekta, u smislu proizvodnosti, profitabilnosti, uslova rada, za dati proizvodni sistem.

Cilj ovog rada je pregled strategije održavanja i prikaz načina izbora strategije održavanja primjenom metoda višekriterijumskog odlučivanja uz primjenu odgovarajućih specijalizovanih softverskih alata, radi iznalaženja najbolje prakse za konkretne poslovne procese. U radu će biti riječ uopšteno o strategiji održavanja, razlikama između tradicionalnih i savremenih strategija, te prednosti primjene savremenih strategija. Takođe, koji su problemi koji se javljaju prilikom uvođenja strategije održavanja, zašto je teško odabrati strategiju održavanja koja će biti prikladna za određen tehnički sistem i koje su metode odlučivanja prilikom izbora strategije održavanja.

2 STRATEGIJE ODRŽAVANJA TEHIČKIH SISTEMA

Održavanje predstavlja složeni funkcionalni sistem, objedinjen jedinstvenim ciljem i zadatom funkcijom kriterijuma. Sa inženjerskog aspekta, sama realizacija održavanja razmatranog tehničkog sistema može da se ostvari na više načina (varijanti). Svaka od varijanti je definisana koncepcijom, organizacijom i karakterom postupaka održavanja, kao i odnosom između pojedinih nivoa održavanja. Izabrana varijanta odražava definisanu strategiju ili politiku održavanja[1].

Strategijom održavanja naziva se skup pravila na osnovu kojih se donose odluke o tome kada i kakve operacije održavanja treba preduzeti u toku eksploatacije sistema[2]. Pojam strategija održavanja odnosi se na određivanje ili izbor akcija održavanja koje će biti sprovedene na nekim tehničkim sistemima da bi se na najbolji način iskoristila, odnosno da bi se maksimizirala njihova raspoloživost i pouzdanost. Pojam akcije održavanja odnosi se na sve moguće preventivne i korektivne radnje. Kod nas se uobičajeno strategijom podrazumijeva izbor pravca akcije, racionalna nabavka, i raspoređivanje akcija za postizanje ciljeva[3]

2.1 Podjela strategija održavanja

Danas se strategije održavanja grubo mogu svrstati u dvije grupe. Osnovna podjela strategija održavanja je na:

- Tradicionalne strategije
- Moderne strategije

Naknadno, preventivno i kombinovano održavanje danas spadaju u tradicionalne strategije održavanja. U moderne (savremene) strategije održavanja spadaju: proakt ivno, totalno preventivno, totalno produktivno, samoodržavanje.

2.1.1 Tradicionalne strategije održavanja

Tradicionalne strategije održavanja su naknadno, preventivno i kombinovano održavanje, pri čemu kombinovano predstavlja kombinaciju prethodna dva.

Kod naknadnog održavanja, aktivnosti održavanja se isključivo izvode nakon pojave zastoja na opremi, i to u obliku naknadne intervencije. Naknadno održavanje se može predstaviti kroz dva vida održavanja, a to su: čekanje na otkaz i korektivno održavanje[4].

Čekanje na otkaz je najprimitivniji oblik strategije održavanja, kvazi strategija u krajnjem obliku. Suština je u tome da se aktivnosti održavanja ne planiraju niti izvode dok ne dođe do pojave zastoja na opremi. Takav vid tretiranja tehničkog sistema može biti vrlo neracionalan, skup, naročito zbog gubitaka u proizvodnji izazvanih otkazima, rizikujući pri tome da sastavni dio, ili kompletan sistem pretrpi havariju, ali i da dođe do povreda rukovaoca mašine. Primjena ove politike bila je uglavnom aktuelna prije industrijske revolucije[4].

Pod korektivnim intervencijama se podrazumijevaju intervencije održavanja koje se sprovode nakon uočene neispravnosti ili otkaza sistema. Za razliku od strategije čekanja na otkaz, ovdje se uz aktivnosti otklanjanja zastoja, otklone i neke uočene slabosti ili problemi koji bi u bliskoj budućnosti ponovo doveli do zastoja [4].

Suštinska karakteristika naknadnog održavanja, bilo da je riječ o korektivnom održavanju ili strategiji „čekanje na otkaz“, sadržana je u činjenici da svi dijelovi sistema ostaju u sistemu do momenta otkaza.

Intenzivniji razvoj industrije posle drugog svjetskog rata zahtijevao je veću pouzdanost sve složenijih tehničkih sistema, što je dovelo do pojave preventivnog održavanja. Ovaj tip održavanja se zasniva na planiranim aktivnostima koje se sprovode prije pojave otkaza.

Preventivno održavanje može biti stihijsko preventivno održavanje, koje se i ne smatra kao oblik strategije održavanja. Spada u podgrupu preventivnog održavanja zbog toga što se pojedine aktivnosti održavanja tehničkih sistema praktikuju prije pojave zastoja na opremi. To su obično ustaljeni oblici njege sistema i izvode se bez organizovanog i sistematskog praćenja ponašanja mašine. Pored stihijskog, tu je i plansko preventivno održavanje, koje obuhvata sistem mjera i aktivnosti kojima se direktno utiče na sprječavanje nastanka kvarova, te se tako održava radna sposobnost tehničkog sistema. Planom se određuju sve održavačke aktivnosti i to po određenom tehnološkom i vremenskom redoslijedu, a pod preventivom se smatra sve ono što se preduzima da ne dođe do pojava koje nisu predviđene planom[4].

2.1.2 Savremene strategije održavanja

Savremenim strategijama održavanja se smatra proaktivno održavanje, totalno preventivno,totalno produktivno (TPM) održavanje i samoodržavanje, a često se pominje i prediktivno održavanje, E-održavanje, RCM itd. U nastavku ćemo se fokusirati na totalno produktivno (TPM) održavanje, kao najuticajnijeg predstavnika ove grupe održavanja. TPM nije kratkotrajan program za rješavanje problema i smanjenje troškova održavanja. To je proces koji mijenja poslovnu kulturu i trajno poboljšava i održava ukupnu učinkovitost opreme kroz aktivno učešće svih članova organizacije. Prema načelima TPM-a, u svakom proizvodnom procesu postoje tri obilježja čiji se gubici moraju nulirati, tj. obilježja se moraju unaprijediti do stanja “nula gubitaka“ (eng. Zero loss). Ta tri obilježja su: raspoloživost proizvodne opreme, kvaliteta izrade i brzina izrade. Mnogo pokušaja implementacije TPM-a rezultuje neuspjehom. Razloga za neuspjeh ima mnogo, poput nedostatka razumijevanja uticaja TPM-a, bez podrške uprave nema ni rezultata, nedovoljno edukovanih zaposlenika o TPM-u, sindikalni otpor nastao zbog nepoznavanja TPMa i njegovih mogućnosti i ciljeva, nedostatak upornosti i motivacije, loše razvijena strategija, odnosno krivi pristup implementaciji.

TPM je velika promjena u preduzeću te može imati uticaja na strukturu preduzeća, na podjele odgovornosti zaposlenika, način funkcionisanja samog proizvodnog procesa, na učinkovitost itd [5]. Na narednoj slici je dijagram vjerovatnoće otkaza u odnosu na vrijeme za tradicionalni pristup i savremeni pristup održavanja[3]:

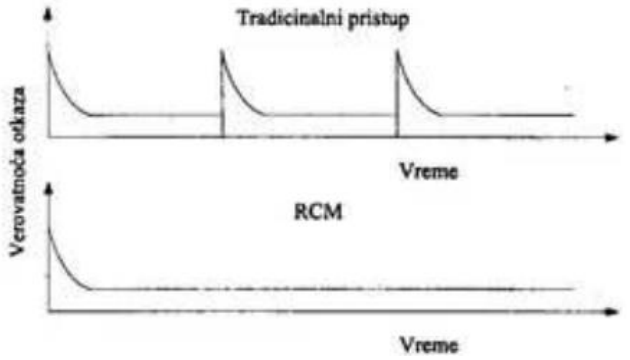

Slika 1. *Grafički prikaz vjerovatnoće otkaza u odnosu na vrijeme*

Iskustva pokazuju da je za prelazak s klasičnog na savremeno, potrebno vremensko razdoblje u trajanju od pet do osam godina. Promjena se odnosi na napuštanje kratkoročnih ciljeva i orijentaciju fabrike ka njenim dugoročnim ciljevima i strategijama. U narednoj tabeli su prikazane razlike u pristupima održavanja [1]:

Tradicionalni pristup održavanju	**Suvremeni pristup održavanju**
Orijentacija na popravke	Orijentacija na pouzdanost
Popravi	Unaprijedi
Majstor	Član poslovnog tima
Rješavaj otkazima	Eliminiraj otkaze
Smanji troškove održavanja	Povećaj vrijeme održavanja
„Akcija program mjeseca“	Kontinuirano unaprjeđivanje
Vjerovanje da su otkazi neizbježni	Vjerovanje da su otkazi samo izuzeci
Nizak udio planskih poslova	Visok udio planskih poslova
Mnogo reklamacija	Malo reklamacija
Niska pouzdanost	Visoka pouzdanost
Visoki troškovi održavanja	Niski troškovi održavanja
Kratkoročni planovi	Dugoročni planovi
Neprofitni karakter	Privlači investicije

Slika 2. *Prilazi u održavanju*

Kada je riječ o samoodržavanju bitno je pomenuti, da kako bi se kod tehničkih sistema spriječilo da njihov otkaz, zbog pojave kvara na nekom uređaju, uzrokuje nemogućnost sistema da obavlja svoj zadatak, proizvođači takve uređaje nastoje dizajnirati ne samo da su tolerantni na pojavu greške, nego da je mogu i otkloniti. Uređaj sa ugrađenim samoodržavanjem je uređaj koji može funkcionisati i u slučaju pojave greške. Pod tim pojmom se ne misli na popravak ili zamjenu neispravnih fizičkih dijelova, nego na popravak funkcionalnosti sistema. To znači da se u slučaju greške, tj.

primijećene razlike u funkciji uređaja, uređaj mora samoodržavanjem vratiti u ispravno funkcionalno stanje. Ovakvo održavanje se zove funkcijsko održavanje te je mnogo kompleksnije od fizičkog održavanja. Njegovom primjenom ne samo da se povećava raspoloživost sistema, poboljšava tolerantnost na greške, nego i smanjuju troškovi održavanja [6].

3 DONOŠENJE ODLUKA O STRATEGIJAMA ODRŽAVANJA

Prilikom donošenja odluke koja će se strategija održavanja primijeniti za konkretan tehnički sistem neophodan je detaljan pregled svih strategija održavanja. To nije nimalo lak posao. Potrebno je poznavati različite strategije održavanja, detaljnu analizu njihovih prednosti i nedostataka, kao i detaljnu dijagnostiku našeg preduzeća, i na osnovu toga, različitim metodama, implementirati najbolju strategiju održavanja u skladu sa mogućnostima preduzeća. Pri tome se mogu javiti različiti problemi o kojima će biti riječ u nastavku teksta.

Izbor strategije održavanja predstavlja jednu od najvažnijih odluka u procesu održavanja, budući da ne postoji jedinstvena strategija održavanja koja će biti jednako uspješna za sve poslovne procese. Zbog velikog broja kriterijuma, koji se moraju uzeti u obzir, prilikom izbora strategije održavanja taj problem se posmatra kao višekriterijumski. Višekriterijumsko odlučivanje predstavlja donošenje odluke kada je prisutno više kriterijuma, koji su često suprotstavljeni. Glavni cilj metoda višekriterijumskog odlučivanja je poduprijeti donosioce odluka kada postoji veliki izbor alternativa za problem koji je potrebno riješiti.

3.1 Dijagnostika pri održavanju

Dijagnostika je određivanje stanja određene mašine sa ciljem procjene pouzdanosti procesa i predlaganja načina servisiranja[7]. Uloga dijagnostike je otkrivanje kvarova mašine ili pojedinih njegovih dijelova u najranijoj mogućoj fazi. Nadzorom stanja ponašanja sistema, olakšava se planiranje održavanja i popravaka, čime se vrijeme zastoja pogona nastalo zbog zamjene i popravaka mašina, svodi na najmanju moguću mjeru. U slučajevima kada se nadzor kvalitetno sprovodi, izbjegnuta su mnoga nepotrebna zaustavljanja pogona. Osnova dijagnostike je poređenje stvarnih i željenih ponašanja odnosno parametara procesa. Osim teorijskog znanja vrlo je korisno i iskustveno poznavanje ponašanja mašine u pojedinim otkaznim periodima. Karakteristične su faze rada dijagnostike prikazane su na narednoj slici[7]:

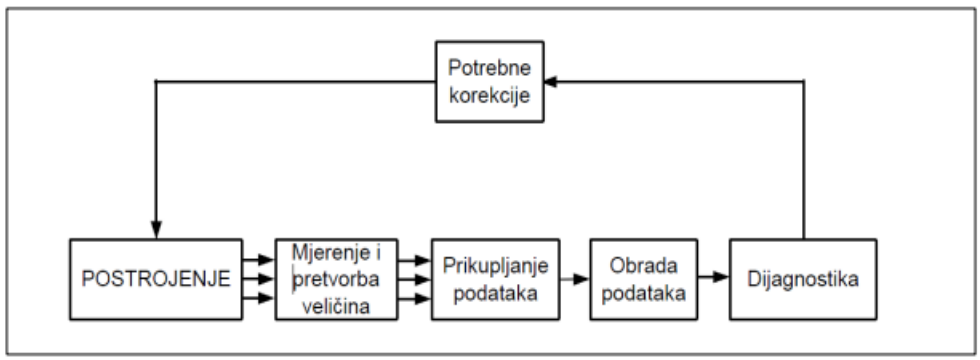

Slika 3. *Faze dijagnostike u održavanju*[7]

Osnovne dijagnostičke metode dijele se na subjektivne metode koje su vezane za čula vida i sluha, te na objektivne metode koje služe za mjerenje željenih parametara korišćenjem mjernih uređaja. Dijagnostičke metode su: vizuelne metode ili endoskopija, koja se dijele na direktne i indirektne metode, termografija koja predstavlja ispitivanje električnih sklopova i instalacija pomoću kontaktnog termometra ili IC kamere, zatim, mjerenje pritiska, spektrografska analiza ulja, ferografska analiza čestica, penetrantske metode, magnetne metode, ultrazvučni test, analiza vibracija, metoda udarnih impulsa i druge.

3.2 Problemi kod izbora strategije održavanja

Postoje različiti problemi koji otežavaju izbor strategije održavanja. Pri donošenju odluke treba znati odrediti osnovni cilj održavanja. Osim cilja održavanja, javlja se problem pri određivanju najvažnijih uticajnih elemenata za definisanje strategije. Na narednoj slici dat je prikaz svih uticajnih faktora koji utiču na izbor strategije održavanja[8]:

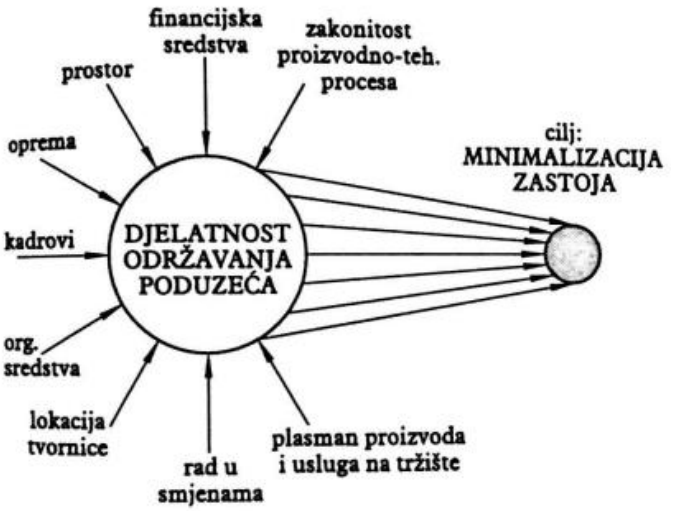

Slika 4. *Uticajni elementi na izbor strategije održavanja*[8]

Broj kriterijuma kod izbora strategije održavanja je jako veliki, što predstavlja problem prilikom rangiranja kriterijuma po važnosti. Kolika je težina pojedinog uticajnog elementa, odnosno proračunatih podataka, biće različita od preduzeća do preduzeća, ali važno je da ih treba razmotriti i vrijednovati, te izabrati onu strategiju održavanja koja će postići postavljeni cilj. Osim velikog broja kriterijuma pri odabiru, postoji i velik broj strategija tj. alternativa, samim tim, menadžer koji odabire moguće alternative, može napraviti pogrešnu odluku. Prilikom izbora potrebno je u obzir uzeti i druge parametre, od kojih se posebno ističu: rezultati analize važnosti opreme, zahtjevi za pouzdanost i raspoloživost u radu opreme, struktura uzroka oštećenja i otkaza, posljedice pojave oštećenja i otkaza, raspoloživi kadrovi i zahtjev za osiguranje minimalnih troškova [8]. Ukupna strategija održavanja zasniva se na "znanju o stanju" tehničkog sistema. Pri tome se koordinacija između kratkoročnog i dugoročnog održavanja pojavljuje kao jedan od kriterija za izbor strategije. Uzimajući obzir sve navedene kriterijume koje je potrebno razmotriti prilikom izbora strategije održavanja, može se zaključiti da se radi o problemu višekriterijumskog odlučivanja.

3.3 Metode odlučivanja

Nakon pregleda različitih pristupa, postavlja se pitanje šta izabrati za određeno preduzeće kao najprimjereniji oblik održavanja. Odlučivanje je stalan proces. Mnoge odluke traže puno vremena, priprema i znanja. Opšta podjela metoda višekriterijumskog odlučivanja ne postoji, već se one obično dijele prema nekim kriterijumima. Prema literaturi[9], postoje brojne metode odlučivanja: TOPSIS, DEA, AHP, ANP, AIRM, ELECTRE, ER, OCRA, WPM, GRA, SMART, PROMETHEE. Zbog velikog broja metoda u nastavku teksta će biti fokus na AHP i ANP metodama koje su veoma slične i nadovezuju se jadna na drugu.

ANP metoda omogućuje modelovanje funkcionalne interakcije kriterijuma i alternativa u modelu, te se time postiže veća stabilnost rezultata. Struktura povratnih veza koja postoji u ANP-u omogućuje mrežno definisanje problema, te se razlikuje od AHP-a jer ne predstavlja linearnu hijerarhiju već modeluje uticaje između elemenata mreže [9]. Metoda analitički mrežni proces (ANP) je novija metoda za odlučivanje te uključuje određenu nadogradnju u odnosu na AHP metodu.

AHP metoda koristi tipični tablični zapis za upoređivanje i rangiranje alternativa, pri odlučivanju u smislu prednosti jedne od alternativa u odnosu na ostale. Metoda upoređuje prednosti i nedostatke pojedinih alternativa te kao rezultat daje prioritete alternativa obliku brojčanih vrijednosti. Kriterijumi za izbor određene alternative mogu imati različite važnosti zbog čega im se dodjeljuju težine. Algoritam metode se temelji na tzv. upoređivanju alternativa u parovima.

Rješavanje problema AHP metodom sastoji se od sljedeća 4 koraka [9]: 1. Izrada hijerarhije modela problema (cilj, kriteriji, podkriterij), 2. Upoređivanje parova hijerarhijske strukture pomoću Saaty-eve skale, 3. Izračunavanje težinskih koeficijenata prioriteta elemenata hijerarhijske strukture i 4. Izračunavanje lokalnih prioriteta (težina) kriterija, podkriterija i alternativa

Prema[10], za izbor strategije održavanja, primjenom metoda AHP, predloženi su sljedeći koraci: Formiranje tima stručnjaka, Definisati cilj i svrhu, Identifikacija kriterijuma i podkriterijuma za izbor strategije održavanja, Ustanoviti alternativne pristupe održavanju, Konstruisati hijerarhijski okvir za analizu, Skupiti empirijske podatke i informacije, Napraviti parnu komparaciju za svaki nivo kriterijuma i podkriterijuma, Napraviti test stabilnosti, Izračunati uticaj svakog kriterijuma i podkriterijuma, Sinteza rezultata, Analiza osjetljivosti, Konačni poredak predloženih alternativa - Uzevši u obzir rezultate desetog koraka i rezultata analize osjetljivosti, može se ustanoviti konačno rješenje AHP metode.

Za izbor strategije održavanja AHP metodom koristi se softver ExpertChoice. ExpertChoice predstavlja način odlučivanja koji se usklađuje s ciljem donosioca odluke. Najprije se odrede najuticajniji parametri, odnosno hijerarhijski se poredaju cilj, kriterijumi, podkriterijumi i alternative za konkretan proizvodni proces, i unesu se u program. Unutrašnjom logikom program vrši poređenje kriterijuma sa drugim kriterijumima, i tako svaki sa svakim, takođe se istom logikom vrši poređenje podkriterijuma sa drugim podkriterijumima, u zavisnosti od navedenih alternativa. Program za svako poređenje odredi najpovoljniju strategiju, a onda na osnovu pojavljivanja strategija za pojedinačna poređenja određuje se najpovoljnija strategija za cjelokupan proces proizvodnje, kao što je prikazano na slici 5.[11].

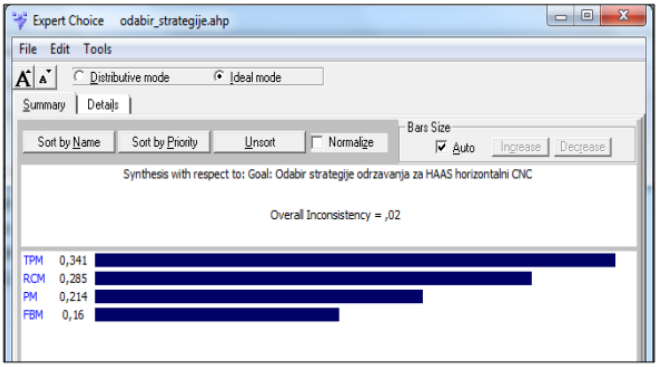

Slika 5. *Softverski izbor strategije održavanja s obzirom na cilj*

4 ZAKLJUČCI

U ovom radu obrađena je tema pregleda strategije održavanja. Cilj pregleda strategija održavanja je donošenje najboljih odluka za tehničke sisteme o kojima odlučujemo, odnosno postizanje najboljih rezultata poslovanja u smislu ostvarivanja dužih vremena u radu bez otkaza, odnosno povećanja raspoloživosti, proizvodnosti, a samim tim doći će i do povećanja profitabilnosti preduzeća, što predstavlja ključni cilj poslovanja svih poslovnih preduzeća, kao i obezbjeđivanje povoljnijih i bezbjednijih uslova rada. Da bi se cilj u najboljoj mjeri ostvario, potrebno je strateški pristupiti traženju optimalne politike održavanja, koja se može implementirati u skladu sa datim proizvodnim sistemom i koja će u zavisnosti od konkretnih uslova procesa ostvariti najbolje poslovne rezultate. Održavanje zahtjeva prije svega adekvatno izabranu strategiju održavanja, te racionalnu organizaciju održavanja dobro opremljenu sredstvima i ljudima.

LITERATURA

[1] Habul, A., Velić, A. (2010). *Menadžment održavanja u savremenom poslovanju*. Zenica
[2] Marić, B., Medaković, V. (2018). Izbor strategija održavanja, *Zbornik radova 5. Konferencije „ODRŽAVANJE 2018“,* Zenica, str. 147-151, ISSN 1986-583X
[3] Stanojević, P., Mišković, P. (2003). Strategije održavanja tehničkih sistema. Beograd. *Vojnotehnički glasnik*.
[4] Vukotić, V. (2009). Efektivnost i održavanje tehničkih sistema
[5] Hadžović, E. (2012). *Proces uvođenja TPM koncepta održavanja*. Fakultet strojarstva i brodogradnje. Zagreb. Završni rad.
[6] Tudor, M. (2007). Samoodržavanje brodskih sustava. Pomorstvo. 31. – 38. Str
[7] Miletić, A. (2002). Dijagnostičke metode i kriterijumi za ocjenu elektromehaničkog stanja asinhronog motora. Magistarski rad. Fakultet elektrotehnike i računarstva.
[8] Milovanović, Z. (2007). *Održavanje i pouzdanost zehničkih sistema*. Banja Luka.
[9] Dujmić, D. (2014). *Primjena višekriterijalnog odlučivanja u odabiru lokacije skladišta*. Diplomski rad. Fakultet strojarstva i brodogradnje. Zagreb.
[10] Lisjak, D. (2011). Primjena AHP metode kao alata za optimalni izbor opreme. Zagreb.
[11] Majača, S. (2015). *Izbor strategije održavanja primjenom metoda višekriterijalnog odlučivanja*. Diplomski rad. Fakultet strojarstva i brodogradnje. Zagreb. 70 str.

COMETa 2022
6th INTERNATIONAL SCIENTIFIC CONFERENCE
17th - 19th December 2022
Jahorina, B&H, Republic of Srpska
University of East Sarajevo
Faculty of Mechanical Engineering
Conference on Mechanical Engineering Technologies and Applications

AN OVERVIEW ON PORT MACHINERY PREDICTIVE MAINTENANCE

Deda Đelović[1]

Abstract: As per researches` results presented in different available references, in the overall port costs, significant share is related to the purchase, operation and maintenance of port machinery. Improper maintenance of port machinery can significantly decrease the productivity rates in the cargo handling process.

Predictive maintenance uses condition monitoring tools to detect various deterioration signs, anomalies, and equipment performance issues. There is a very wide range of preconditions which have to be fulfilled in order to implement predictive maintenance.

After theoretical considerations on general importance of port machinery, key features of the Predictive maintenance are analyzed. As well, key groups of positive effects of implementation of Predictive maintenance are identified. Special attention is given to identification of group of port machinery on which Predictive maintenance should be implemented. In that sense, a methodology for selecting "critical port machinery" is proposed. Concrete results of reserach shown in this paper are related to the cargo handling and port machinery maintenance systems in the Port of Bar (Montenegro).

Key words: Port machinery, Predictive maintenance.

1 INTRODUCTION

Maintenance probably started out as a need to fix machine when it broke down. The repairs were probably performed by the operator of a machine. As time progressed, however, equipment has became much more complex and downtime become more critical. In the present days, it takes many special skills, tools, equipment and materials to repair equipment. This modern complexity brought about the need for the trained operation, maintenance and repair craftsman.[1].

[1] Prof. dr Deda Đelović, "Luka Bar" AD, Obala 13.jula 2, 85 000 Bar, Crna Gora. djelovic.deda@gmail.com

The general purpose of maintenance is to maximize an asset's useful lifetime and minimize costs [2]. Improper maintenance can significantly decrease the productivity rates projected during an operational assessment [3].

Port machinery is one of the key technological elements of the port. The main aspects of its importance are (based on [4]): increasing efficiency of implementation of an appropriate variant of the goods supply chain; reduction of costs of an appropriate variant of the goods supply chain by reducing costs of handling operations in the port; increasing the total capacity of the port; increasing quality of provided port services; reduction of detention of means of transport in the port based on handling operations; improving level of utilization of means of transport (ships, wagons, trucks); increasing safety at work, reducing number of occupational diseases and accidents at work, etc.

A very high proportion of the capital and operation budget of a port is devoted to the purchase, operation and maintenance of mechanical handling equipment [5].

General objective of the port machinery maintenance can be defined as follows: "to improve the productivity and efficiency of the port by increasing equipment availability" [6].

Data published by some authors state that share of maintenance costs over lifetime of port machinery are at the level above 40% [7]. As well, it is illustrative to point out results presented in the study [8], where is stated that Mobile Harbor Crane maintenance cost were higher than operational cost.

There is no doubt that any single handling equipment that is not well maintained can affect all operations in the port. Sometimes the breakdown may cause huge losses for ports and shipping companies. Maintenance in a port is not only the process of fixing particular equipment, but rather is a system linking many activities together [5].

2 PREDICTIVE MAINTENANCE OF PORT MACHINERY

In the literature could be found that traditional components of a maintenance program often fall into following four categories [9]: Reactive maintenance (fix when broken), Planned maintenance (scheduled maintenance activities), Proactive maintenance (defect elimination to improve performance) and Predictive maintenance (advanced analytics and sensing data to predict machine reliability).

There are different definitions of the Predictive maintenance, depending on authors approach. Here are presented some of those definitions.

Predictive maintenance is a maintenance strategy that uses condition monitoring tools to detect various deterioration signs, anomalies, and equipment performance issues. The goal of predictive maintenance is to optimize the usage of maintenance resources. By knowing when a certain part will fail, maintenance system can schedule maintenance work only when it is actually needed, simultaneously avoiding excessive maintenance and preventing unexpected equipment breakdown [10].

Predictive maintenance: it is a technique aiming to help determine the condition of in service equipment in order to predict when maintenance should be preformed [11].

Predictive maintenance is using Artificial Intelligence (AI) technology and data analytics to predict when equipment is likely to fail before the breakdown actually occurs. Maintenance schedules are then updated based on these forecasts [12].

Predictive maintenance is based on a cycle of "data, insights, actions" and this cycle repeats over time making maintenance predictions faster and more precise [13].

2.1 Implementation of Predictive maintenance – expected results

When implemented successfully, predictive maintenance lowers operational costs, minimizes downtime issues, and improves overall asset health and performance [10].

Where there is deadline pressure and safety must be guaranteed, intelligent concepts in the form of predictive maintenance make the most sense [14].

The goals of Predictive maintenance are to reduce asset downtime, prevent unexpected failures, promote productivity and increase the safety of personnel. A predictive maintenance strategy seeks to reduce or completely eliminate unexpected failures. In a predictive scheme, both productivity and safety increase with the strategic scheduling of maintenance tasks [15]. Predictive maintenance goes beyond simply preventing equipment breakdown [16].

Predictive maintenance keeps equipment and assets running when you need them while also reducing the cost of maintenance and time-sensitive repairs [17].

Besides already mentioned, in reference [18] is stated that Predictive maintenance enables also and greater understanding of high-energy consumers and insights to potential areas of energy wastage

Benefits of implementing Predictive maintenance are quantified in [19]:

- Maintenance costs - down by 50%
- Unexpected failures - reduced by 55%
- Repair and overhaul time - down by 60%
- Spare parts inventory - reduced by 30%
- 30% increase in machinery mean time between failures (MTBF)
- 30% increase in uptime

Predicitive maintenance aims to prevent port machinery (crane, etc.) breakdown using Artificial Inteligence (AI). Incorporating AI on crane maintenance activities results on an increase in uptime and a decrease in repair costs. When an equipment breaks, it can have a significant domino effect on the terminal operation. Severe crane breakdowns requiring control system experts to get involved are costly. Consequential costs, e.g. resulting from delayed container and vessel shipment schedules, further boost the issue [12].

2.2 Preconditions to have Predictive maintenance introduced

The most important part of predictive maintenance (and, at the same time, the hardest one) is creating and appropriately introducing predictive algorithms. In fact, it is necessary to create a model that will consider many different variables and how they correlate and impact one another – with the final objective being able to predict machine failures. The main reason why predictive maintenance is currently not more widely adopted is because it has a relatively high barrier to be implemented.

It can require a sizeable upfront investment to buy and install condition monitoring equipment, develop predictive models, and pair everything up with a specialized software. On paper, predictive maintenance is clearly a better strategy. However, implementing condition monitoring technology and developing predictive models can be challenging and expensive [10].

However, it should be noted that the preconditions to fully introduce Predictive Maintenance recognized based on reference [20]:

- maintenance organization - which ensures the optimal application of selected methods of Predictive maintenance,
- work force capable to practically apply the chosen methods,

- necessary equipment and
- information system that will ensure timely disposal of management information,

have priority and could be defined as "prerequisites of prerequisites" for the effective introduction and application of Predictive Maintenance.

2.3 For which port machinery to implement Predictive maintenance?

Combining methods of “standard preventive” and methods of predictive maintenance is a recipe for success - start by identifying critical assets to be included in the Predictive maintenance program. Assets with high repair/replacement costs that are critical for working process realization are often the best candidates [10].

Critical assets are the organizational resources essential to maintaining operations and achieving the organization's mission. Critical Asset, in general, means facilities, systems, and equipment which, if destroyed, degraded, or otherwise rendered unavailable, would affect the reliability or operability [21].

Port equipment operators need to move towards predictive maintenance in order to optimize the useful life of their assets [3].

In order to establish bases to fully utilize benefits of the Predictive maintenance, in this chapter is proposed a methodology of “critical port machinery” selection on which this maintenance concept should be implemented. In a condensed way, it can be said that proposed methodology has following three principal segments:

- **segment A**: conducting analyses whose objective is to get answers (A_j) on the next ten questions (Q_i):
  - Q1 -What was throughput structure in the previous period?
    A1 – Throughput structure for the previous period;
  - Q2 – Which cargoes had dominant share in the overall throughput structure in the previous period?
    A2 – cargoes group and cargo type which had dominant share in the overall throughput in the previous period;
  - Q3 – Which port machinery classes were used per handling operations with priority cargo group (with the biggest share in the overall throughput structure) in the previous period?
    A3 – handling operations with priority cargo group; port machinery classes used in handling operations with priority cargo group (according to documented cargo handling technologies);
  - Q4 – What port machinery types are used in the process of loading/unloading ships with priority cargo group in the previous period?
    A4 - Port machinery types used in the loading/unloading process of ships with priority cargo group in the previous period;
  - Q5 – What were average hourly productivity rates per port machinery types in the process of loading/unloading ships with priority cargo group in the previous period?
    A5 – Hourly productivity rates per port machinery types in the process of loading/unloading ships with priority cargo group;
  - Q6 – What port machinery type is contributing the most to achieving contracted values of productivity/avoiding demurrage costs related to ships with priority cargo group in the previous period?

A6 – Port machinery type which is contributing the most to achieving contracted values of productivity in the previous period;

- Q7 – What is correlation between hourly operating costs and hourly productivity per port machinery types?
  A7 – Correlation between hourly operating costs and hourly productivity per port machinery types;
- Q8 – Are there any alternative port machinery type which could replace port machinery types which contributing the most to achieving contracted level of hourly productivity/avoiding demurrage costs related to ships with priority cargo group in the previous period?
  A8 – Yes, there are/No, there are not - alternative port machinery type;
- Q9 – What are cost components appeared when the loading/unloaing process of a ship with priority cargo group is interrupted due to port machinery downtime? What are registered or calculated values of those cost components?
  A9 – cost components appeared when the loading/unloading process of a ship with priority cargo group is interrupted due to port machinery downtime; registered or calculated values of those cost components;
- Q10 – What is character of expected customers demands in the next period (what is expected throughput structure)?
  A10 - Character of expected customers demands in the next period;

- **segment B**: defining selection criteria based on results on analyses performed within segment A;
- **segment C**: ranking port machinery by defined selection criteria;

3 CONCLUSIONS

The importance that ports have in the supply chain, the essence of the process of carrying out cargo handling operations and the role and importance of port machinery in that process enable a conclusion that the application of Predictive maintenance would have significant positive effects, which can definitely contribute to increasing the level of quality of port services provided. Achieving a satisfactory level of Predictive maintenance application is possible only if that process is carried out in accordance with a precisely defined methodology that respects all significant influencing factors. In this context, the primary task is the proper selection of “critical port machinery” where Predictive maintenance would be applied. In the paper, the structure of the methodology for the selection of the mentioned “critical port machinery” is presented. Also, it is essential to correctly identify and fulfill the prerequisites for the introduction of Predictive maintenance. According to plan of author`s engagement in this field, the next task is autmoatization of “critical port machinery” selection where Predictive maintenance should be implemented.

REFERENCES:

[1] Steps to effective equipment maintenance, United Nations, 1983.
[2] Regulation and Policy, the importance of planned maintenance. https://www.greenport.com/news101/, approached on 29/07/2022.
[3] How to maintain port equipment. https://blog.sennebogen-na.com/, approached on 30/07/2022.
[4] Stipanić, Lj. (1982): *Mehanizacija luka i lučkih terminala*, Istarska naklada, Pula.

[5] dos Barbosa, M.J.S. (1999), Equipment maintenance management in Cape Verde, Porto da Praia: toward an improvement, World Maritime University Dissertations. 414, https://commons.wmu.se/all_dissertations/414, approached on 31/07/2022.
[6] Maintenance-of-port-equipment. https://opms.com.sg/project/ , approached on: 01/08/2022.
[7] Steele, G. (2021), Port maintenance handbook. https://www.icevirtuallibrary.com/isbn/9780727764133, approached on: 02/08/2022.
[8] Gurning, R.O.S., Simatupang, E.J., Handani, D.W. (2019), The investigation of life cycle costs of Mobile Harbour Crane: a case study in Berlian Terminal at Tanjung Perak Seaport, Maritime Safety and Maritime Sustainable Islands Development Initiatives – International Conference. Indonesia.
[9] Coleman, C., Damodaran, S., Chandramouli, M., Deuel, E., Making maintenance smarter, Predictive maintenance and the digital supply network. : https://www2.deloitte.com/us/en/insights/focus/industry-4-0/using-predictive-technologies-for-asset-maintenance.html, approached on: 03/08/2022.
[10] A Complete Guide to Predictive Maintenance. https://limblecmms.com/predictive-maintenance/, approached on: 04/08/2022.
[11] Management of port equipment. https://www.slideshare.net/m7ammmedx/ , approached on: 04/08/2022.
[12] https://new.siemens.com/global/en/markets/cranes/harbor-cranes/predictive-maintenance.html, approached on: 05/08/2022.
[13] https://www.konecranes.com/service/predictive-maintenance-and-remote-monitoring/predictive-maintenance, approached on: 06/08/2022.
[14] https://www.igus.bg/info/predictive-maintenance-crane-industry, approached on: 07/08/2022.
[15] https://www.uesystems.com/how-predictive-maintenance-enhances-plant-safety-without-sacrificing-productivity/., approached on: 08/08/2022.
[16] https://www.shell.com/business-customers/lubricants-for-business/perspectives/the-benefits-of-predictive-maintenance.html, approached on: 09/08/2022.
[17] https://www.industryweek.com/technology-and-iiot/article/22026789/a-primer-on-predictive-maintenance-to-improve-asset-efficiency, approached on: 10/08/2022.
[18] https://news.hydac.com/, approached on: 11/08/2022.
[19] Mobley, K., Plant Engineer's Handbook. https://reliabilityweb.com/tips/article/the_top_6_benefits_of_predictive_maintenance
[20] Đelović, D. (2004), Održavanje po stanju u sistemu održavanja sredstava lučke mehanizacije – preduslovi uvođenja i potencijalni efekti primjene, Tehnička dijagnostika, vol. 3, br. 1, str. 42-47. In his book, approached on: 12/08/2022
[21] https://www.lawinsider.com/dictionary/critical-asset, approached on: 13/08/2022.
[22] World Cargo News, 1st May 2021. worldcargonews.com/in-depth/in-depth/assessing-life-cycle-costs, approached on: 14/08/2022.

QUALITY, MANAGEMENT AND ORGANIZATION

COMETa 2022
6th INTERNATIONAL SCIENTIFIC CONFERENCE
17th - 19th November 2022
Jahorina, B&H, Republic of Srpska
University of East Sarajevo
Faculty of Mechanical Engineering
Conference on Mechanical Engineering Technologies and Applications

A QUALITY CONTROL SCHEME FOR MULTISTAGE MANUFACTURING SYSTEMS WITH MULTIPLE DISRUPTIONS

Panagiotis Kolonelos[1], George Nenes[2], Konstantinos A. Tasias[3]

Abstract: In contemporary manufacturing processes, multiple, sequential, processing stages are required to complete a final product. The quality of the end product is crucial to ensure high customer satisfaction, necessitating effective statistical process monitoring (SPM) techniques for quality control and improvement. Nevertheless, due to the inherent complexity of multistage manufacturing, where the final product quality is often related to the quality output of the intermediate stages, conventional SPM tools, monitoring each production stage independently, may lead to inferior performance. In this light, a control scheme is proposed to monitor quality in univariate, multistage, production systems with multiple operational states. The critical-to-quality characteristic of the final product depends on the quality level of the previous workstations, and information regarding the process state is collected by inspection at all manufacturing stages. A two-dimensional Discrete Time Markov chain models the operation of the proposed control scheme, which is designed through an economic optimization criterion. Finally, a comparative analysis evaluates the economic performance of different process restoration policies.

Key words: Manufacturing processes, Multiple quality shifts, Multistage manufacturing, Quality control

1 INTRODUCTION

In the era of contemporary manufacturing, production processes involve multiple, serially concatenated, stages [1-2]. Multistage processes are common in practice and met in various industries including, inter alia, pharmaceutical manufacturing, and semiconductor manufacturing [1,3]. Although statistical process monitoring (*SPM*) is the most efficient method to monitor and control product quality, conventional *SPM* tools fail to capture the transmission of variation through the production stages [3-4]. To this effect, several researchers have proposed appropriate

[1] M.Sc., Panagiotis Kolonelos, University of Western Macedonia, Kozani, Greece, panoskol@gmail.com
[2] Full Prof., George Nenes, University of Western Macedonia, Kozani, Greece, gnenes@uowm.gr
[3] Asst. Prof., Konstantinos Tasias University of Western Macedonia, Kozani, Greece, ktasias@uowm.gr (CA)

SPM techniques for multistage processes (e.g., [5-6]). Nevertheless, the economic optimization of *SPM* tools for production systems with multiple stages has not received adequate attention. To this end, an economically designed control scheme for processes with two dependent production stages is developed. Moreover, the economic performance of the proposed scheme is evaluated for two different process investigation policies.

2 PROBLEM SETTING AND CONTROL SCHEME'S OPERATION

A two-stage production process is set up for infinite operation and produces a single type of product. The quality output of each stage is defined through a key quality characteristic, X_1, and X_2, respectively, which are normally distributed $\left(X_1 \sim N\left(\mu_{10},\sigma_1^2\right), X_2 \sim N\left(\mu_{20},\sigma_2^2\right)\right)$. The final product's quality is assessed through a critical-to-quality characteristic Y, equal to the sum of X_1 and X_2 $\left[Y \sim N\left(\mu=\mu_{10}+\mu_{20},\sigma^2=\sigma_1^2+\sigma_2^2\right)\right]$. Two independent assignable causes may occur, one affecting X_1 by shifting its mean from μ_{10} to μ_{11}, and the other affecting X_2 by shifting its mean from μ_{20} to μ_{21}. The elapsed time until the occurrence of each quality shift is assumed to be an exponentially distributed random variable.

The process operating state is estimated through a periodic sampling inspection, made every h time units, where two samples are collected from the output of each manufacturing stage. The process is monitored by two control charts, defined by the values of the following parameters: a. the sampling interval h; b. the sample size of each stage, n_1, and n_2; c. the control limits for each control chart, k_1 and k_2. Figure 1 illustrates the control scheme used to monitor the two-stage production process.

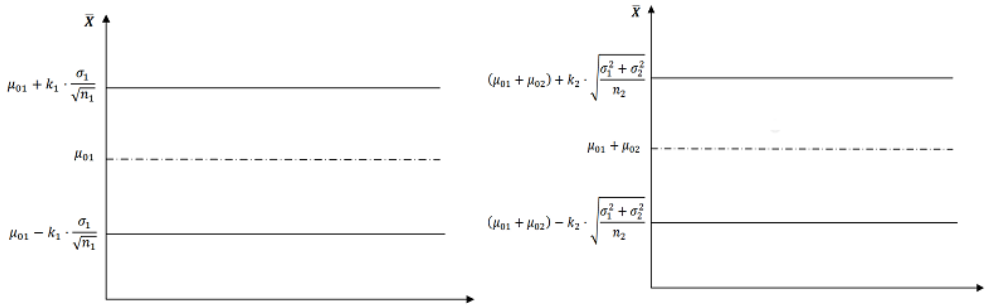

Figure 1. *Quality control scheme*

At each sampling instance t, the mean of X_1 and Y of the collected samples are computed, and then, compared to the respective control limits. Based on the comparison one of the following decisions is made:

(a) If the mean of both samples lies between the respective control limits, then, the process is considered in-control (*IC*) and continues its operation (α_t=0).

(b) If both the mean of X_1 and Y outreach the control limits, both manufacturing stages are investigated and a true alarm initiates process restoration actions (α_t=3).

(c) If the mean of X_1 outreaches the respective control limits (α_t=1), two different policies are considered, thereby formulating two different models: Either both stages

are investigated (Model A) or stage 1 is investigated (Model B). If the investigation reveals the effect of assignable cause 1, stage 1 is restored to the *IC* state.
(d) If the mean of *Y* outreaches the control limits, then, either both stages (Model A) or only stage 2 (Model B) are investigated, and if assignable cause 2 has occurred, it is restored to the *IC* state (α_t=2).
In Figure 2 the above-mentioned quality control policy is presented.

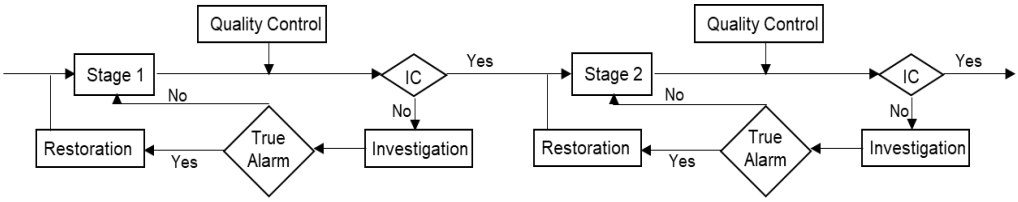

Figure 2. *Quality control policy*

3 MATHEMATICAL MODEL

The operation of the process is modeled through a two-dimensional discrete-time Markov chain. The process state at each sampling instance *t* is denoted by Y_t and has the following possible values: Y_t=0, if no assignable cause has occurred; Y_t=1, if the assignable cause that affects stage 1 has occurred; Y_t=2, if the assignable cause that affects stage 2 has occurred; Y_t=3, if both assignable causes have affected the process. Each process state along with each possible decision made at each sampling instance corresponds to a state in the formulated Markov chain. The transition probability matrix is shown in Figure 3.

$$
\boldsymbol{P} = \begin{array}{c} \\ 0,0 \\ 0,1 \\ 0,2 \\ 0,3 \\ 1,0 \\ 1,1 \\ 1,2 \\ 1,3 \\ 2,0 \\ 2,1 \\ 2,2 \\ 2,3 \\ 3,0 \\ 3,1 \\ 3,2 \\ 3,3 \end{array}
\begin{array}{c}
\begin{array}{cccccccccccccccc} 0,0 & 0,1 & 0,2 & 0,3 & 1,0 & 1,1 & 1,2 & 1,3 & 2,0 & 2,1 & 2,2 & 2,3 & 3,0 & 3,1 & 3,2 & 3,3 \end{array} \\
\begin{bmatrix}
P_{00}^{00} & P_{01}^{00} & P_{02}^{00} & P_{03}^{00} & P_{01}^{00} & P_{01}^{01} & P_{01}^{02} & P_{01}^{03} & P_{02}^{00} & P_{02}^{01} & P_{02}^{02} & P_{02}^{03} & P_{03}^{00} & P_{03}^{01} & P_{03}^{02} & P_{03}^{03} \\
P_{00}^{10} & P_{01}^{10} & P_{02}^{10} & P_{03}^{10} & P_{01}^{10} & P_{01}^{11} & P_{01}^{12} & P_{01}^{13} & P_{02}^{10} & P_{02}^{11} & P_{02}^{12} & P_{02}^{13} & P_{03}^{10} & P_{03}^{11} & P_{03}^{12} & P_{03}^{13} \\
P_{00}^{20} & P_{01}^{20} & P_{02}^{20} & P_{03}^{20} & P_{01}^{20} & P_{01}^{21} & P_{01}^{22} & P_{01}^{23} & P_{02}^{20} & P_{02}^{21} & P_{02}^{22} & P_{02}^{23} & P_{03}^{20} & P_{03}^{21} & P_{03}^{22} & P_{03}^{23} \\
P_{00}^{30} & P_{01}^{30} & P_{02}^{30} & P_{03}^{30} & P_{01}^{30} & P_{01}^{31} & P_{01}^{32} & P_{01}^{33} & P_{02}^{30} & P_{02}^{31} & P_{02}^{32} & P_{02}^{33} & P_{03}^{30} & P_{03}^{31} & P_{03}^{32} & P_{03}^{33} \\
P_{10}^{00} & P_{11}^{00} & P_{12}^{00} & P_{13}^{00} & P_{11}^{00} & P_{11}^{01} & P_{11}^{02} & P_{11}^{03} & P_{12}^{00} & P_{12}^{01} & P_{12}^{02} & P_{12}^{03} & P_{13}^{00} & P_{13}^{01} & P_{03}^{32} & P_{13}^{03} \\
P_{10}^{10} & P_{11}^{10} & P_{12}^{10} & P_{13}^{10} & P_{11}^{10} & P_{11}^{11} & P_{11}^{12} & P_{11}^{13} & P_{12}^{10} & P_{12}^{11} & P_{12}^{12} & P_{12}^{13} & P_{13}^{10} & P_{13}^{11} & P_{13}^{12} & P_{13}^{13} \\
P_{10}^{20} & P_{11}^{20} & P_{12}^{20} & P_{13}^{20} & P_{11}^{20} & P_{11}^{21} & P_{11}^{22} & P_{11}^{23} & P_{12}^{20} & P_{12}^{21} & P_{12}^{22} & P_{12}^{23} & P_{13}^{20} & P_{13}^{21} & P_{13}^{22} & P_{13}^{23} \\
P_{10}^{30} & P_{11}^{30} & P_{12}^{30} & P_{13}^{30} & P_{11}^{30} & P_{11}^{31} & P_{11}^{32} & P_{11}^{33} & P_{12}^{30} & P_{12}^{31} & P_{12}^{32} & P_{12}^{33} & P_{13}^{30} & P_{13}^{31} & P_{13}^{32} & P_{13}^{33} \\
P_{20}^{00} & P_{21}^{00} & P_{22}^{00} & P_{23}^{00} & P_{21}^{00} & P_{21}^{01} & P_{21}^{02} & P_{21}^{03} & P_{22}^{00} & P_{22}^{01} & P_{22}^{02} & P_{22}^{03} & P_{23}^{00} & P_{23}^{01} & P_{23}^{02} & P_{23}^{03} \\
P_{20}^{10} & P_{21}^{10} & P_{22}^{10} & P_{23}^{10} & P_{21}^{10} & P_{21}^{11} & P_{21}^{12} & P_{21}^{13} & P_{22}^{10} & P_{22}^{11} & P_{22}^{12} & P_{22}^{13} & P_{23}^{10} & P_{23}^{11} & P_{23}^{12} & P_{23}^{13} \\
P_{20}^{20} & P_{21}^{20} & P_{22}^{20} & P_{23}^{20} & P_{21}^{20} & P_{21}^{21} & P_{21}^{22} & P_{21}^{23} & P_{22}^{20} & P_{22}^{21} & P_{22}^{22} & P_{22}^{23} & P_{23}^{20} & P_{23}^{21} & P_{23}^{22} & P_{23}^{23} \\
P_{20}^{30} & P_{21}^{30} & P_{22}^{30} & P_{23}^{30} & P_{21}^{30} & P_{21}^{31} & P_{21}^{32} & P_{21}^{33} & P_{22}^{30} & P_{22}^{31} & P_{22}^{32} & P_{22}^{33} & P_{23}^{30} & P_{23}^{31} & P_{23}^{32} & P_{23}^{33} \\
P_{30}^{00} & P_{31}^{00} & P_{32}^{00} & P_{33}^{00} & P_{31}^{00} & P_{31}^{01} & P_{31}^{02} & P_{31}^{03} & P_{32}^{00} & P_{32}^{01} & P_{32}^{02} & P_{32}^{03} & P_{33}^{00} & P_{33}^{01} & P_{33}^{02} & P_{33}^{03} \\
P_{30}^{10} & P_{31}^{10} & P_{32}^{10} & P_{33}^{10} & P_{31}^{10} & P_{31}^{11} & P_{31}^{12} & P_{31}^{13} & P_{32}^{10} & P_{32}^{11} & P_{32}^{12} & P_{32}^{13} & P_{33}^{10} & P_{33}^{11} & P_{33}^{12} & P_{33}^{13} \\
P_{30}^{20} & P_{31}^{20} & P_{32}^{20} & P_{33}^{20} & P_{31}^{20} & P_{31}^{21} & P_{31}^{22} & P_{31}^{23} & P_{32}^{20} & P_{32}^{21} & P_{32}^{22} & P_{32}^{23} & P_{33}^{20} & P_{33}^{21} & P_{33}^{22} & P_{33}^{23} \\
P_{30}^{30} & P_{31}^{30} & P_{32}^{30} & P_{33}^{30} & P_{31}^{30} & P_{31}^{31} & P_{31}^{32} & P_{31}^{33} & P_{32}^{30} & P_{32}^{31} & P_{32}^{32} & P_{32}^{33} & P_{33}^{30} & P_{33}^{31} & P_{33}^{32} & P_{33}^{33}
\end{bmatrix}
\end{array}
$$

Figure 3. *Transition probability matrix*

The steady-state probabilities, which represent the long-term probability for the process being in state ($Y=l,\alpha=j$), denoted by π_{lj}, are computed by solving the following system of linear equations:

$$\pi_{lj} = \sum_{k=0}^{3}\sum_{i=0}^{3}\left(\pi_{ki}\cdot P_{ij}^{kl}\right), \forall l, j \quad \text{and} \quad \sum_{l=0}^{3}\sum_{j=0}^{3}\pi_{lj} = 1 \tag{1}$$

4 ECONOMIC MODELS

The expected cost per time unit (*ECT*) is evaluated as the ratio of the expected cost of a transition step (*EC*) over the expected duration (*ET*) (*ECT=EC/ET*). *EC* considers the inspection cost, the out-of-control (*OOC*) operation cost, the restoration cost, and the false alarm cost. *ET* considers the sampling interval *h* and the time delays required for process investigation and restoration.

4.1 Model A

The *EC* and *ET* of Model A, i.e., both stages are investigated in case of an alarm, are given from the following expressions:

$$\begin{aligned}
EC_A &= b + \left(c_1\cdot n_1 + c_2\cdot n_2\right) + \\
&+\left(\pi_{00} + \sum_{l=0}^{3}\sum_{j=2}^{3}\pi_{lj} + \sum_{l=0}^{1}\pi_{l1}\right)\cdot\left[\begin{array}{l} M_1\cdot\left(\dfrac{\lambda_1\cdot\left(1-\exp\left(-\lambda_2\cdot h\right)\right)-\lambda_2\cdot\exp\left(-\lambda_2\cdot h\right)\cdot\left(1-\exp\left(-\lambda_1\cdot h\right)\right)}{\lambda_2\cdot\left(\lambda_1+\lambda_2\right)}\right)+ \\ +M_2\cdot\left(\dfrac{\lambda_2\cdot\left(1-\exp\left(-\lambda_1\cdot h\right)\right)-\lambda_1\cdot\exp\left(-\lambda_1\cdot h\right)\cdot\left(1-\exp\left(-\lambda_2\cdot h\right)\right)}{\lambda_1\cdot\left(\lambda_1+\lambda_2\right)}\right)+ \\ +M_3\cdot\left(h-\dfrac{1-\exp\left(-\lambda_1\cdot h\right)}{\lambda_1}-\dfrac{1-\exp\left(-\lambda_2\cdot h\right)}{\lambda_2}\right)+\dfrac{1-\exp\left(-\left(\lambda_1+\lambda_2\right)\cdot h\right)}{\lambda_1+\lambda_2}\end{array}\right]+ \\
&+\pi_{10}\cdot\left[\begin{array}{l} M_1\cdot\left(\dfrac{1-\exp\left(-\lambda_2\cdot h\right)}{\lambda_2}\right)+ \\ +M_3\cdot\left(h-\dfrac{1-\exp\left(-\lambda_2\cdot h\right)}{\lambda_2}\right)\end{array}\right]+\left(\pi_{20}+\pi_{21}+\pi_{31}\right)\cdot\left[\begin{array}{l} M_2\cdot\left(\dfrac{1-\exp\left(-\lambda_1\cdot h\right)}{\lambda_1}\right)+ \\ +M_3\cdot\left(h-\dfrac{1-\exp\left(-\lambda_1\cdot h\right)}{\lambda_1}\right)\end{array}\right]+ \\
&+\pi_{30}\cdot M_3\cdot h+\left(\pi_{11}+\pi_{12}+\pi_{13}+\pi_{31}+\pi_{32}+\pi_{33}\right)\cdot L_1+\left(\pi_{22}+\pi_{23}+\pi_{32}+\pi_{33}\right)\cdot L_2+ \\
&+\left(\pi_{01}+\pi_{02}+\pi_{03}+\pi_{21}+\pi_{22}+\pi_{23}\right)\cdot L_{01}+\left(\pi_{02}+\pi_{03}+\pi_{12}+\pi_{13}\right)\cdot L_{02}
\end{aligned} \tag{2}$$

$$\begin{aligned}
ET_{\mathrm{A}} &= h+\sum_{l=0}^{3}\pi_{l1}\cdot T_{01}+\sum_{l=0}^{3}\sum_{j=2}^{3}\pi_{lj}\cdot T_{02}+ \\
&+\left(\pi_{11}+\pi_{12}+\pi_{13}+\pi_{31}\right)\cdot T_1+\left(\pi_{22}+\pi_{23}\right)\cdot T_2+\left(\pi_{32}+\pi_{33}\right)\cdot T_3
\end{aligned} \tag{3}$$

4.2 Model B

The *EC* and *ET* of Model B, i.e., only the stage whose quality characteristic issues an alarm is investigated, are computed from the following equations:

$$
\begin{aligned}
EC_B &= b+\left(c_1\cdot n_1+c_2\cdot n_2\right)+\\
&+\left(\begin{array}{l}\sum_{j=0}^{3}\pi_{0j}+\pi_{11}+\pi_{13}+\\ +\pi_{22}+\pi_{23}+\pi_{33}\end{array}\right)\cdot\left[\begin{array}{l}M_1\cdot\left(\dfrac{\lambda_1\cdot\left(1-\exp\left(-\lambda_2\cdot h\right)\right)-\lambda_2\cdot\exp\left(-\lambda_2\cdot h\right)\cdot\left(1-\exp\left(-\lambda_1\cdot h\right)\right)}{\lambda_2\cdot\left(\lambda_1+\lambda_2\right)}\right)+\\ +M_2\cdot\left(\dfrac{\lambda_2\cdot\left(1-\exp\left(-\lambda_1\cdot h\right)\right)-\lambda_1\cdot\exp\left(-\lambda_1\cdot h\right)\cdot\left(1-\exp\left(-\lambda_2\cdot h\right)\right)}{\lambda_1\cdot\left(\lambda_1+\lambda_2\right)}\right)+\\ +M_3\cdot\left(h-\dfrac{1-\exp\left(-\lambda_1\cdot h\right)}{\lambda_1}-\dfrac{1-\exp\left(-\lambda_2\cdot h\right)}{\lambda_2}\right)+\dfrac{1-\exp\left(-\left(\lambda_1+\lambda_2\right)\cdot h\right)}{\lambda_1+\lambda_2}\end{array}\right]+\\
&+\left(\pi_{10}+\pi_{12}+\pi_{32}\right)\cdot\left[\begin{array}{l}M_1\cdot\left(\dfrac{1-\exp\left(-\lambda_2\cdot h\right)}{\lambda_2}\right)+\\ +M_3\cdot\left(h-\dfrac{1-\exp\left(-\lambda_2\cdot h\right)}{\lambda_2}\right)\end{array}\right]+\left(\pi_{20}+\pi_{21}+\pi_{31}\right)\cdot\left[\begin{array}{l}M_2\cdot\left(\dfrac{1-\exp\left(-\lambda_1\cdot h\right)}{\lambda_1}\right)+\\ +M_3\cdot\left(h-\dfrac{1-\exp\left(-\lambda_1\cdot h\right)}{\lambda_1}\right)\end{array}\right]+\\
&+\pi_{30}\cdot M_3\cdot h+\left(\pi_{11}+\pi_{13}+\pi_{31}+\pi_{33}\right)\cdot L_1+\left(\pi_{22}+\pi_{23}+\pi_{32}+\pi_{33}\right)\cdot L_2+\\
&+\left(\pi_{01}+\pi_{03}+\pi_{21}+\pi_{23}\right)\cdot L_{01}+\left(\pi_{02}+\pi_{03}+\pi_{12}+\pi_{13}\right)\cdot L_{02}
\end{aligned}
\tag{4}
$$

$$
\begin{aligned}
ET_{\mathrm{B}} &= h+\sum_{l=0}^{3}\pi_{l1}\cdot T_{01}+\sum_{l=0}^{3}\pi_{l2}\cdot T_{02}+\sum_{l=0}^{3}\pi_{l3}\cdot T_{03}\\
&+\left(\pi_{11}+\pi_{31}\right)\cdot T_1+\left(\pi_{22}+\pi_{23}\right)\cdot T_2+\pi_{33}\cdot T_3
\end{aligned}
\tag{5}
$$

5 NUMERICAL ANALYSIS

The optimum design parameters and the minimum ECT of the two models are computed for 32 cases, with different parameters. The benchmark of scenarios that are used are presented in Table 1 (b=0, c_1=1, c_2=1.2, L_1=150, L_2=200, L_{01}=L_{02}=200, T_{01}=T_{02}=T_1=T_2=T_3=0, δ_0=0.5, M_3=M_1+M_2).

Table 1. *Parameter sets of the 32 cases*

Case	δ_2	λ_1	λ_2	M_1	M_2	Case	δ_2	λ_1	λ_2	M_1	M_2
1	1	0.005	0.005	100	150	17	2	0.005	0.005	100	150
2	1	0.005	0.005	100	750	18	2	0.005	0.005	100	750
3	1	0.005	0.005	500	150	19	2	0.005	0.005	500	150
4	1	0.005	0.005	500	750	20	2	0.005	0.005	500	750
5	1	0.005	0.01	100	150	21	2	0.005	0.01	100	150
6	1	0.005	0.01	100	750	22	2	0.005	0.01	100	750
7	1	0.005	0.01	500	150	23	2	0.005	0.01	500	150
8	1	0.005	0.01	500	750	24	2	0.005	0.01	500	750
9	1	0.01	0.005	100	150	25	2	0.01	0.005	100	150
10	1	0.01	0.005	100	750	26	2	0.01	0.005	100	750
11	1	0.01	0.005	500	150	27	2	0.01	0.005	500	150
12	1	0.01	0.005	500	750	28	2	0.01	0.005	500	750
13	1	0.01	0.01	100	150	29	2	0.01	0.01	100	150
14	1	0.01	0.01	100	750	30	2	0.01	0.01	100	750
15	1	0.01	0.01	500	150	31	2	0.01	0.01	500	150
16	1	0.01	0.01	500	750	32	2	0.01	0.01	500	750

The economic outcome of the control scheme for each case, and the optimum parameters, are presented in Tables 2 (Model A) and 3 (Model B).

Table 2. *Economic design for the 32 cases: Model A*

	k_1	k_2	n_1	n_2	h	ECT_A		k_1	k_2	n_1	n_2	h	ECT_A
1	2	2.6	24	13	8	16.26	17	2	3	25	5	6.3	14.29
2	2.2	2.7	9	7	2.6	22.61	18	2.1	3	21	5	6	23.22
3	1.9	2.6	32	17	5.5	27.10	19	2	3	32	6	4.7	23.79
4	2	2.6	24	14	3.5	33.64	20	2.1	3	22	5	2.8	29.20
5	2.1	2.6	17	13	5.6	20.78	21	2.1	3	15	5	4.5	18.09
6	2.3	2.7	5	6	1.6	29.19	22	2.4	3.1	6	3	1.5	24.78
7	1.9	2.5	31	19	5.3	31.35	23	2	3	29	7	4.2	27.39
8	2.1	2.6	18	14	2.5	41.82	24	2.1	3	16	5	2	35.66
9	2	2.5	27	10	6.6	19.87	25	2	3.1	25	5	5.8	17.70
10	2.1	2.7	14	8	3	26.26	26	2.2	3	13	3	2.5	23.17
11	1.9	2.6	35	15	4.3	35.55	27	1.9	3.1	33	6	3.8	31.63
12	2	2.6	29	13	3.1	40.97	28	2	3	26	5	2.6	36.23
13	2	2.6	22	13	5.5	24.19	29	2	3	20	5	4.6	21.46
14	3	2.7	10	7	2	33.20	30	2.3	3.1	8	3	1.5	28.75
15	1.9	2.6	33	17	4	39.59	31	1.8	3	20	6	2.8	35.89
16	2	2.6	24	14	2.5	48.90	32	2	3	21	5	2	42.63

Table 3. *Economic design for the 32 cases: Model B*

	k_1	k_2	n_1	n_2	h	ECT_B		k_1	k_2	n_1	n_2	h	ECT_B
1	2	2.4	22	11	7	15.27	17	2.1	2.9	21	5	6.1	13.38
2	2.3	2.5	9	6	2.4	21.12	18	2.2	2.9	9	3	2.5	18.45
3	1.9	2.4	34	16	5.5	26.08	19	2	2.8	33	6	4.8	22.84
4	2	2.4	24	12	3.3	32.40	20	2.1	2.9	21	5	2.7	28.15
5	2.1	2.4	17	12	5.3	18.83	21	2.1	2.9	15	5	4.3	16.26
6	2.5	2.4	6	4	1.4	26.57	22	2.4	2.8	4	2	1.1	22.46
7	2	2.3	33	17	5	29.51	23	2	2.8	29	6	4.1	25.57
8	2.1	2.4	18	12	2.4	39.46	24	2.1	2.9	16	5	2	33.64
9	2	2.5	27	11	6.5	18.84	25	2	2.9	26	5	5.9	16.83
10	2.2	2.5	13	6	2.5	24.91	26	2.2	2.9	13	3	2.5	22.09
11	1.9	2.4	34	13	4	34.52	27	1.9	2.8	32	5	3.6	30.68
12	2	2.4	29	11	3	39.74	28	2	2.9	26	5	2.6	35.22
13	2	2.4	21	11	5	22.37	29	2.1	2.9	21	5	4.4	19.72
14	2.3	2.5	8	6	1.7	30.56	30	2.3	2.9	8	3	1.5	26.64
15	1.9	2.4	34	16	4	37.72	31	2	2.9	32	6	3.3	33.16
16	2	2.4	24	12	2.4	46.66	32	2.1	2.9	21	5	1.9	40.66

By examining the optimum design parameters of the two models, it is immediately evident that larger values of *OOC* operation costs result in more frequent sampling and higher *ECT*s. This indicates that if the *OOC* operation cost is great,

sampling intervals should be smaller, to avoid a long-lasting *OOC* process operation. Similar conclusions are drawn for larger values of λ's. Moreover, the larger the magnitude of the shift of assignable cause 2, the smaller the sample sizes and the *ECT*, since it becomes easier to detect the shift.

The comparison of the economic outcome of Model A with Model B is given in Table 4.

Table 4. *Economic comparison between Model A and Model B*

	$\frac{ECT_A - ECT_B}{ECT_B}$ (%)		$\frac{ECT_A - ECT_B}{ECT_B}$ (%)		$\frac{ECT_A - ECT_B}{ECT_B}$ (%)		$\frac{ECT_A - ECT_B}{ECT_B}$ (%)
1	6.48	9	5.47	17	6.80	25	5.17
2	7.05	10	5.42	18	25.85	26	4.89
3	3.91	11	2.98	19	4.16	27	3.10
4	3.83	12	3.10	20	3.73	28	2.87
5	10.36	13	8.14	21	11.25	29	8.82
6	7.08	14	8.64	22	10.33	30	7.92
7	6.24	15	4.96	23	7.12	31	8.23
8	5.98	16	4.80	24	6.00	32	4.85

The percentage improvements presented in Table 4 indicate a significant economic improvement of Model B, compared to Model A, which varies between 2.87% and 25.85%.

6 CONCLUSIONS

A quality control scheme for two-stage manufacturing processes is proposed. The control scheme consists of two control charts, one for monitoring the first stage of the process, and the other, for the second one. The process is subject to multiple quality disruptions, affecting both production stages. Two different approaches/models are considered regarding the investigation of the process in case of an *OOC* signal issued by the control scheme: Model A: Both stages are investigated regardless of the control chart associated with the *OOC* indication; Model B only the stage whose control chart issued the alarm, is investigated. A discrete-time Markov chain is used to model the operation of the control scheme, and the optimal design parameters are derived through an economic optimization criterion. An extended numerical analysis led to utilitarian conclusions regarding the control scheme's operation, and a comparative study between Model A and Model B demonstrated the economic superiority of Model B in all examined cases.

NOMENCLATURE

α_t decision made at t^{th} inspection based on the last points plotted on the control charts

b fixed sampling cost

c variable sampling cost per unit

h sampling interval

L_i restoration cost for stage i

L_{0i} investigation cost for stage *i*

M_i *OOC* operation cost per time unit for stage *i*

k_i control limit of the control chart that monitors stage *i*

n_i sample size of stage *i*

P transition probability

T_i time required for the restoration of stage *i*

T_{0i} time required for the investigation of stage *i*

Y_t process state at t^{th} inspection

Greek symbols

δ_i magnitude of shift due to assignable cause *i*

λ_i occurrence rate of assignable cause *i*

μ_{10} *IC* mean of X_1 quality characteristic

μ_{11} *OOC* mean of X_1 quality characteristic

μ_{20} *IC* mean of X_2 quality characteristic

μ_{21} *OOC* mean of X_2 quality characteristic

μ *IC* mean of *Y* quality characteristic $\left(\mu = \mu_{10} + \mu_{20}\right)$

π steady-state probability

σ_1^2 variance of X_1 quality characteristic

σ_2^2 variance of X_1 quality characteristic

σ^2 variance of *Y* quality characteristic $\left(\sigma^2 = \sigma_1^2 + \sigma_2^2\right)$

REFERENCES

[1] Kim, J., Jeong, M.K., Elsayed, E.A. (2016). Monitoring multistage processes with autocorrelated observations. *International Journal of Production Research*, 55, p.p. 2385–2396.

[2] Sangahn, K.I.M. (2019). Variable selection-based SPC procedures for high-dimensional multistage processes. *Journal of Systems Engineering and Electronics*, 30, p.p. 144-153.

[3] Shi, J., Zhou, S. (2009). Quality control and improvement for multistage systems: A survey. *IIE Transactions*, 41, p.p. 744-753.

[4] Woodall, W.H., Montgomery, D.C. (1999). Research Issues and Ideas in Statistical Process Control. *Journal of Quality Technology*, 31, p.p. 376–386.

[5] Jin, M., Tsung, F. (2009). A chart allocation strategy for multistage processes. *IIE Transactions*, *41*, p.p. 790-803.

[6] Tsung, F., Li, Y., Jin, M. (2008). Statistical process control for multistage manufacturing and service operations: a review and some extensions. *International Journal of Services Operations and Informatics*, 3, p.p. 191-204.

COMETa 2022
6th INTERNATIONAL SCIENTIFIC CONFERENCE
17th - 19th November 2022
Jahorina, B&H, Republic of Srpska
University of East Sarajevo
Faculty of Mechanical Engineering
Conference on Mechanical Engineering Technologies and Applications

DETERMINATION OF ORGANIZATIONAL RESILIENCE LEVEL WITHIN BUSINESS PROCESSES IN PRODUCTION COMPANIES

Aleksandar Aleksic[1], Snezana Nestic[2], Danijela Tadic[3], Nikola Komatina[4]

Abstract: Ongoing business activities need to adapt to market conditions in a continuous manner but sometimes significant disruptions (pandemic of covid 19, geopolitical instability, inflation, etc.) may occur. In that case, adaptation is not enough so organizations must demonstrate resilience-ability to overcome the unwell present state and continue to function as before or even better. The motivation for conducting this research and project comes from the fact that more knowledge is needed about organizational resilience, as well as conditions for its development and enhancement. The objective of this research is to propose a model for the assessment of organizational resilience at the level of the business process of product/service realization. The model is based on the fuzzy Delphi method, and it is verified on the real-life data obtained in one medium production company. Future research should cover the examination of the relationship between the assessed level of organizational resilience and the time needed for performance recovery after significant disruptions.

Keywords: Organizational resilience, fuzzy sets, fuzzy Delphi

1 INTRODUCTION

From time to time, it may be considered that unpredicted events shape reality and business trends [1]. In the few past years, many of those manifested, such as covid 19 pandemic or unstable geopolitical situations in different parts of the world. In times of crisis and disruptions, organizational resilience (OR) is usually seen as a crucial feature of any organizational system such as enterprises and companies [2]. Although there is a significant number of papers in the literature, still there is no consensus on whether organizational resilience is a feature, ability, or capability of an organization, or

[1] PhD Aleksandar Aleksic, Faculty of Engineering, University of Kragujevac, Kragujevac, Serbia, aaleksic@kg.ac.rs
[2] PhD Snezana Nestic, Faculty of Engineering, University of Kragujevac, Kragujevac, Serbia, s.nestic@kg.ac.rs (CA)
[3] PhD Danijela Tadic, Faculty of Engineering, University of Kragujevac, Kragujevac, Serbia, galovic@kg.ac.rs
[4] MSc Nikola Komatina, Faculty of Engineering, University of Kragujevac, Kragujevac, Serbia, s.nestic@kg.ac.rs

something else [3]. In compliance with that, there are attempts to define it in a way that might be suitable for the assessment or even management. As a complex construct, organizational resilience is described through its indicators or resilience factors (RFs). Determining the level of the RFs value can be determined by using the Delphi technique, which has been extended with type 1 triangular fuzzy numbers (TFNs). The aggregation of the assessment of DMs into a single assessment can be obtained by applying the operator fuzzy geometric mean by analogy to existing research [4,5]. A referent literature analysis [6] indicates the existence of various research on the topic of determining if DMs have reached a consensus. One of the appropriate methods [7] suggests that it should be accomplished in the second round of the Delphi method. There are no suggestions if the obtained solution in the second iteration, without reaching a consensus, should be accepted, or rejected.

In the literature, there is a small number of works where the Delphi method with TFNs was developed, in which the determination of consensus is based on APMO [7]. At the same time, there are almost no papers that treat the resilience assessment at the business process level by using the fuzzy Delphi method. The motivation for this paper comes from those facts with a need to fully understand the condition of the organization regarding resilience since during a crisis or disruption, it can determine if an organization will survive in the market or not.

The wider objective of this research may be interpreted as a) introducing RFs according to the resilience literature [3], b) modeling the level value of the RFs at the level of business processes by the TFNs, c) modification of the method which is used for the reaching consensus developed by the management team, and d) definition of management actions which should lead to the enhancement of organizational resilience at the level of business processes.

The rest of the paper is organized as follows: Section 2 presents a relevant literature review. Section 3 presents the proposed model. A case study is presented in Section 4 and a conclusion is presented in Section 5.

2 LITERATURE REVIEW

This section presents a review of the literature that includes: (i) different models of resilience and performance evaluation systems, and (ii) the Delphi technique, which is extended with type 2 interval fuzzy numbers.

2.1 Organizational resilience models, their description and assessment

From the period of conceptualization [8] until these days, OR has been a point of interest for many scholars. The brief explanation of the concept may be summarized as follows. While the performance of an organization has an ongoing trend over time, during the disruption its values rapidly go down. As each company has some level of OR, it should recover in a certain amount of time or it will terminate. If one company has a stronger OR, its performance will bounce back in a shorter period. However, there is still little consensus on its main features, assessment, and management [9]. Different scholars describe OR as an ability of an organization, the capability of an organization, process, capacity, or emergent property [3]. This research treats OR as a complex construct that can be decomposed into RFs and further assessed and managed [10].

2.2 Delphi technique with type 1 fuzzy numbers

The Delphi technique can be defined as a structured process for the collection

and handling of data during several rounds of process execution. There are several decision-makers (DMs) with different specialties that participate in this process. There are numerous suggestions in the literature as to how much DMs should participate in the decision-making process. For instance, Somerville [11] believes that 5 to 10 experts should participate in the decision-making process. Other scholars believe that no more than 10 experts should participate in the decision-making process [12]. All scholars agree that there is the anonymity of DMs and that there should be no consultation between them during the evaluation process. In general, DMs express their assessments using precise numbers, interval ratings, measurement scales as well as linguistic expressions.

In the first round, a written questionnaire with precisely defined questions is sent to the DMs. They express their answers using a pre-defined measurement scale and return the completed questionnaire to the analyst in writing. Firstly, the analyst aggregates different assessments of DMs into a single assessment using one of the aggregation methods. In the Delphi technique, the key question is when consensus can be considered as reached. Then, it is checked whether a consensus has been reached. There are 15 developed methods for consensus checking defined by the literature [6]. Choosing a method for checking consensus can be seen as a task itself. If no consensus is reached, it is necessary to repeat the procedure in the second round. It is considered that DMs in the second round should correct their estimates respecting the aggregated value calculated in the first round. The evaluation and processing procedure is repeated as in the first round.

In practice, it is considered that the aggregated value obtained in the second round can be accepted as the final solution. Some scholars believe that a consensus [13] is reached definitely in the third round. In the literature, there are papers in which the procedures for checking consensus have been developed. Those are based on parametric hypothesis testing, the application of the variance test, and the student's distribution test.

There are several papers where the Delphi technique is enhanced with TFNs [13-15], as in this research. In the analyzed papers, DMs based their assessments on different measurement scales. For instance, Kumar et al. [16] used a nine-point scale, as in this research. Domains of used fuzzy numbers are defined at different intervals. In this research, the domains of TFNs are defined on the common scale numbers [1-9], by respecting the suggestion of different authors [17]. The aggregation of the DM opinions into a unique assessment can be given by using: (i) fuzzy geometric operator [4,5], or (ii) fuzzy averaging operator [18].

3 THE PROPOSED MODEL

The business processes under consideration can be formally described as a set $\{\mathbf{1}, \dots, \boldsymbol{p}, \dots, \boldsymbol{P}\}$. The total number of business processes is marked as $\boldsymbol{P}$. The business processes are determined in compliance with the APQC framework [19]. The index of the business process is denoted as $\boldsymbol{p}, \boldsymbol{p} = \mathbf{1}, .., \boldsymbol{P}$. The level of each RF should be assessed at the level of each business process. This represents the essence of the proposed research since DMs should be aware of the RFs level so they could manage it and enhance it continuously. The set of RFs is defined according to the referent literature [10]. Formally, the list of proposed RFs is represented by a formal set $\{\mathbf{1}, \dots, \boldsymbol{j}, .., \boldsymbol{J}\}$. The number of analyzed RFs is marked with $\boldsymbol{J}$ and $\boldsymbol{j}, \boldsymbol{j} = \mathbf{1}, .., \boldsymbol{J}$ is index of RF. The level of each RF $\boldsymbol{j}$, $\boldsymbol{j} = \mathbf{1}, .., \boldsymbol{J}$ at the level of each identified business process $\boldsymbol{p}, \boldsymbol{p} = \mathbf{1}, .., \boldsymbol{P}$ is assessed by each DM. They can be presented by a set of indices $\{\mathbf{1}, .., \boldsymbol{e}, .., \boldsymbol{E}\}$. Index of DM is marked as $\boldsymbol{e}, \boldsymbol{e} = \mathbf{1}, \dots, \boldsymbol{E}$ and $\boldsymbol{E}$ is total number of DMs. In

the treated problem, five DMs participate according to the recommendation provided by Somerville [11]. Those are the business owner, production manager, quality manager, logistic manager, human resource manager, and marketing and sale manager.

OR can be expressed by a certain value that is associated with a described level of activities that are implemented in a treated company [20]. Those levels could be examined to benchmark operational capacity, organizational resilience, and disaster risk reduction [21]. By analogy to Pescaroli et al. [21] which has employed a Likert scale to assess the level of OR, this research proposes a scale of seven pre-decided linguistic terms. It is worth mentioning that a company can be represented through a network of its business processes so the level of OR can be assessed can be determined for each business process. OR itself can be decomposed to the finite set of RFs, so each RFs can be assessed to be at a certain level within the company's business processes which is described in table 1. It is considered that DMs can express their assessments in a sufficiently good way using the pre-decided linguistic terms proposed within the proposed research. These linguistic expressions are modeled by TFNs.

Table 1. *The linguistic expressions defining the level of OR for each RFs*

The description of the OR level for each RFs	*The corresponding values of RFs*
There are no blueprints or plans for the construction of the OR, there is no awareness of the OR (B1)	(1,1,1.5)
there are drafts of activities for securing the OR (B2)	(1,2.5,4)
there are clear plans and activities for securing OR (B3)	(2.5,4,5.5)
competencies of all employees in the field of OR management are ensured (B4)	(3.5,5,6.5)
competencies of all employees in the field of OR management are ensured and there is a partially developed awareness of OR (B5)	(4.5,6,7.5)
competencies of all employees in the field of OR management are ensured and there is a fully developed awareness of OR (B6)	(6,7.5,9)
All needed competences are ensured and there is the absolute commitment of management and all employees regarding OR management (B7)	(8.5,9,9)

Furthermore, the proposed Algorithm for determining the value is presented RF $\boldsymbol{j}, \boldsymbol{j} = \mathbf{1},..,\boldsymbol{J}$ at the level of each business process $\boldsymbol{p}, \boldsymbol{p} = \mathbf{1},..,\boldsymbol{P}$.

The proposed Algorithm can be realized through the following steps.

Step 1. Each DM $\boldsymbol{e}, \boldsymbol{e} = \mathbf{1}, \ldots, \boldsymbol{E}$ is assessing the value of each RF $\boldsymbol{j}, \boldsymbol{j} = \mathbf{1},..,\boldsymbol{J}$ at the level of each identified business process $\boldsymbol{p}, \boldsymbol{p} = \mathbf{1},..,\boldsymbol{P}$ by using one of seven pre-defined linguistic expressions that have been modeled by TFNs, $\widetilde{\boldsymbol{b}}_{\boldsymbol{jp}}^{\boldsymbol{1e}}$.

Step 2. Let us determine the "Average Percent of Majority Opinions" (APMO) Cut off Rate [7] in the first round:

$$\widetilde{\boldsymbol{APMO}}^{\mathbf{1}} = \frac{\widetilde{\boldsymbol{b}}_{\boldsymbol{jp}}^{\boldsymbol{1min}} + \widetilde{\boldsymbol{b}}_{\boldsymbol{jp}}^{\boldsymbol{1max}}}{\sum_{\boldsymbol{e}=\mathbf{1},..,\boldsymbol{E}} \widetilde{\boldsymbol{b}}_{\boldsymbol{jp}}^{\boldsymbol{1e}}} \tag{1}$$

It should be checked if a consensus is reached in the first round:

$$\boldsymbol{defuzz}\left(\widetilde{\boldsymbol{APMO}}^{\mathbf{1}}\right) \leq \mathbf{0.7} \tag{2}$$

Defuzzification is performed by applying the Graded Mean Integration Representation - GRIM [22]. if the consensus is reached in the first iteration, then the value of $\widetilde{b}_{jp}^{1}$should be calculated by applying the operator of the fuzzy geometric mean. This value is described by TFN based on the rules of fuzzy algebra [23].

Step 3. Let us determine the Hamming distance between $\widetilde{b}_{jp}$ and TFNs that correspond to the pre-defined linguistic expressions $L_k, k = 1,..,K$, $d\left(\widetilde{b}_{jp}, L_k\right)$. Each RF $j, j = 1,..,J$ at the level of process $p, p = 1,..,P$ should be adjoined with one of the pre-defined linguistic expressions $L_k, k = 1,..,K$ according to the expression:

$$\min_{k=1,..,K} d\left(\widetilde{b}_{jp}, L_k\right) \quad (3)$$

Step 4. If the condition defined in Step 2 is not met, then the second round should be performed. DMs assess the level of each RF $j, j = 1,..,J$ at the level of business process $p, p = 1,..,P$ concerning $\widetilde{b}_{jp}$. Fuzzy ratings of DMs in the second round are denoted as $\widetilde{b}_{jp}^{2e}$.

Step 5. Let us check if the consensus is reached in the second iteration:

$$defuzz\left(\widetilde{APMO}^{1}\right) \leq 0.8 \quad (4)$$

The algorithm proceeds to Step 3.

Step 6. In case no consensus was reached in the second round, do not give recommendations on further execution of the Delphi technique. Here, the authors believe that the proposed procedure (Step 4 to Step 5) should be continuously performed until a consensus is reached.

Step 7. By applying GRIM, the representative scalar of aggregated RF fuzzy value is obtained at the level of each denoted sub-process, b_{ip}.

Step 8. By applying the Maxmin rule (Wald rule), the pessimistic approach is used to determine the rank of RFs:

$$\max_{j} \min_{p} b_{ip} \quad (5)$$

The RFs that are ranked last should be recognized as the most critical ones that should be improved immediately.

4 THE ILLUSTRATIVE EXAMPLE

The company that is used for the illustrative example is medium size company functioning as a part of a big supply chain producing scales and analytical instruments. For the purpose of calculations, the business processes are determined in compliance with the APQC framework [19]. The business processes under consideration can be formally described as a set $\{1, \ldots, p, \ldots, P\}$. The total number of business sub-processes is marked as P, and those are operating in the scope of a business process that embraces Produce/Assemble/Test product [19]: (1) Schedule production (subprocess - SP1), (2) Produce/Assemble product (subprocess - SP2), (3) Perform quality testing (subprocess - SP3), (4) Maintain production records and manage lot traceability (subprocess - SP 4).

The considered RFs which are significant for a production company are [10]: management commitment (1), reporting culture (2), learning (3), awareness (4), preparedness (5), flexibility (6), self-organization (7), teamwork (8), redundancy (9), and fault-tolerance (10).

According to the proposed Algorithm (Step 1) assessments of DMs are presented in Table 2.

Table 2. *The assessments of DMs*

	SP1	SP2	SP3	SP4
RF1	B4, B3, B5, B5, B5	B5, B5, B5, B4, B5	B6, B5, B5, B5, B4	B6, B5, B6, B6, B4
RF2	B6, B5, B6, B5, B4	B6, B6, B5, B5, B5	B6, B5, B6, B5, B4	B6, B6, B5, B5, B5
RF3	B6, B6, B5, B5, B7	B6, B5, B5, B5, B5	B6, B4, B4, B4, B6	B4, B3, B3, B5, B4
RF4	B4, B4, B5, B6, B4	B5, B4, B4, B6, B5	B5, B5, B4, B4, B3	B5, B6, B4, B4, B4
RF5	B4, B5, B3, B4, B4	B5, B5, B4, B5, B5	B3, B4, B5, B4, B2	B5, B5, B6, B4, B4
RF6	B7, B6, B5, B6, B7	B6, B6, B5, B6, B6	B6, B6, B5, B5, B6	B6, B4, B4, B5, B6
RF7	B5, B5, B6, B4, B5	B6, B5, B5, B7, B7	B6, B5, B7, B5, B6	B5, B5, B4, B5, B4
RF8	B7, B7, B6, B7, B7	B6, B5, B6, B5, B6	B4, B3, B5, B5, B4	B6, B7, B4, B5, B6
RF9	B1, B3, B3, B3, B1	B2, B1, B1, B1, B1	B5, B6, B4, B4, B5	B5, B5, B6, B4, B5
RF10	B6, B4, B5, B5, B7	B6, B5, B6, B5, B6	B7, B6, B7, B6, B6	B7, B7, B5, B6, B7

APMO, the aggregated values, and linguistic expressions are obtained by applying the proposed Algorithm (Step 2 to Step 7) and presented in Table 3.

Table 3. *APMO, the aggregated values of RFs, and appropriate linguistic expressions*

	SP1 APMO/the fuzzy aggregated values of RF/crisp	SP2 APMO/ the fuzzy aggregated values of RF/crisp	SP3 APMO/ the fuzzy aggregated values of RF/crisp	SP4 APMO/ the fuzzy aggregated values of RF/crisp
RF1	0.39/ (3.80,5.33,6.85)/5.33	0.40/ (4.28,5.79,6.85)/5.71	0.43/ (4.53,6.05,7.56)/6.05	0.39/ (5.09,6.61,8.13)/6.61
RF2	0.41/ (4.80,6.33,7.84)/6.33	0.42/ (5.05,6.56,8.07)/6.56	0.41/ (4.80,6.33,7.84)/6.33	0.42/ (5.05,6.56,8.07)/6.56
RF3	0.42/ (5.73,7.11,8.37)/7.09	0.45/ (4.77,6.27,7.78)/6.27	0.43/ (4.34,5.88,7.40)/5.88	0.45/ (3.22,4.74,6.26)/4.74
RF4	0.46/ (4.10,5.62,7.14)/5.62	0.44/ (4.31,5.83,7.35)/5.83	0.42/ (3.62,5.14,6.66)/5.14	0.46/ (4.10,5.62,7.14)/5.62
RF5	0.43/ (3.44,4.96,6.47)/4.96	0.40/ (4.28,5.79,7.29)/5.79	0.41/ (2.68,4.32,5.87)/4.30	0.44/ (4.31,5.83,7.35)/5.83
RF6	0.39/ (6.51,7.72,8.68)/7.68	0.39/ (5.66,7.17,8.68)/7.17	0.40/ (5.35,6.86,8.37)/6.86	0.42/ (4.57,6.10,7.62)/6.10
RF7	0.43/ (4.53,6.05,7.56)/6.05	0.40/ (6.15,7.38,8.37)/7.34	0.42/ (5.37,7.11,8.37)/7.03	0.41/ (4.07,5.58,7.08)/5.58
RF8	0.38/ (7.93,8.68,9)/8.61	0.40/ (5.35,6.86,8.37)/6.86	0.39/ (3.80,5.33,6.85)/5.33	0.40/ (5.45,6.86,8.13)/6.84
RF9	0.39/ (1.73,2.30,3.27)/2.37	0.58/ (1.00,1.20,1.83)/1.27	0.44/ (4.31,5.83,7.35)/5.83	0.43/ (4.53,6.05,7.56)/6.05
RF10	0.42/ (5.15,6.56,7.84)/6.54	0.40/ (5.35,6.86,8.37)/6.86	0.41/ (6.90,8.07,9)/8.03	0.40/ (6.98,8.00,8.68)/7.94

By applying step 8 of the proposed algorithm, the max of the min values at the level of the sub-processes is:

$\boldsymbol{Max}\,(\mathbf{5.33}, \mathbf{6.33}, \mathbf{4.74}, \mathbf{5.14}, \mathbf{4.30}, \mathbf{6.10}, \mathbf{5.33}, \mathbf{1.27}, \mathbf{6.54}) = \mathbf{6.54}$ so RF10 is the first in the rank.

RF 9 is ranked in the last place so the management should consider actions to enhance it. The results comply with usual business practices but taking into

consideration the global trends and ongoing energetic crisis, the company management should address redundancy lack in some of the critical activities that may impact the business continuity.

5 CONCLUSION

As there is an ongoing process of research in the domain of resilience, it may be noticed that it has been often treated as an outcome-when organization cope well during a crisis or bounce back from disruptions or interruptions. Over the few past years, many unpredicted events have occurred shaping the business in a way that could not be predicted. This means that companies oriented to business continuity will need to consider the analysis and enhancement of their organizational resilience.

The main contribution of the research is the proposed model for the assessment of the OR level of one production company to deliver a comprehensive analysis of it so it can be used as input for resilience enhancement.

The main constraint f the model is the need for a well-structured process of obtaining information during the sessions and a facilitator with the skills needed to deliver the fuzzy Delphi study. The main advantage of the proposed model is that it provides an answer to the assessed value of RFs in an exact manner. As such, it can be used for monitoring and managing organizational resilience over time.

Future research should be oriented to examining the relationship between the values of RFs and the time needed for performance recuperation after significant disruptions.

Acknowledgment

This research is supported by the grant of the University of Kragujevac, project: Coping with unpredictable disruptions in the domain of Engineering Management – Organizational resilience enhancement - CODEMO.

REFERENCES

[1] Stonehouse, G. H., Konina, N. Y. (2020, February). Management challenges in the age of digital disruption. *In 1st International Conference on Emerging Trends and Challenges in the Management Theory and Practice* (ETCMTP 2019) (pp. 1-6). Atlantis Press.

[2] Hepfer, M., Lawrence, T. B. (2022). The Heterogeneity of Organizational Resilience: Exploring functional, operational and strategic resilience. *Organization Theory*, vol. 3, no. 1.

[3] Hillmann, J., Guenther, E. (2021). Organizational resilience: a valuable construct for management research?. *International Journal of Management Reviews*, vol. 23, no. 1, p.p. 7-44.

[4] Khan, S., Haleem, A., Khan, M. I. (2020). Risk management in Halal supply chain: an integrated fuzzy Delphi and DEMATEL approach. *Journal of Modelling in Management*, vol. 16, no. 1, p.p. 172-214.

[5] Bui, T. D., Tsai, F. M., Tseng, M. L., Ali, M. H. (2020). Identifying sustainable solid waste management barriers in practice using the fuzzy Delphi method. *Resources, conservation and recycling*, vol. 154, 104625.

[6] Heiko, A. V. D. G. (2012). Consensus measurement in Delphi studies: review and implications for future quality assurance. *Technological forecasting and social change*, vol. 79, no. 8, p.p. 1525-1536.

[7] Islam, D. M., Dinwoodie, J., Roe, M. (2006). Promoting development through multimodal freight transport in Bangladesh. *Transport Reviews*, vol. 26, no. 5, p.p. 571-591.
[8] Holling, C. S. (1973). Resilience and stability of ecological systems. *Annual Review of Ecology and Systematics*, vol. 4, p.p. 1-23.
[9] Ma, Z., Xiao, L., Yin, J. (2018). Toward a dynamic model of organizational resilience. *Nankai Business Review International*, vol. 9, no. 3, p.p. 246-263.
[10] Macuzić, I., Tadić, D., Aleksić, A., Stefanović, M. (2016). A two step fuzzy model for the assessment and ranking of organizational resilience factors in the process industry. *Journal of Loss Prevention in the Process Industries*, vol. 40, p.p. 122-130.
[11] Somerville, J. A. (2008). Effective Use of the Delphi Process in Research: Its Characteristics, Strengths, and Limitations.
[12] Malone, D. C., Abarca, J., Hansten, P. D., Grizzle, A. J., Armstrong, E. P., Van Bergen, R. C., ... Lipton, R. B. (2005). Identification of serious drug-drug interactions: Results of the partnership to prevent drug-drug interactions. *American Journal of Geriatric Pharmacotherapy*, vol. 3, no. 2, p.p. 65–76.
[13] Singh, P. K., Sarkar, P. (2020). A framework based on fuzzy Delphi and DEMATEL for sustainable product development: A case of Indian automotive industry. *Journal of Cleaner Production*, vol. 246, 118991.
[14] Dawood, K. A., Sharif, K. Y., Ghani, A. A., Zulzalil, H., Zaidan, A. A., Zaidan, B. B. (2021). Towards a unified criteria model for usability evaluation in the context of open source software based on a fuzzy Delphi method. *Information and Software Technology*, vol. 130, 106453.
[15] Mabrouk, N. (2021). Green supplier selection using fuzzy Delphi method for developing sustainable supply chain. *Decision Science Letters*, vol. 10, no. 1, p.p. 63–70.
[16] Kumar, A., Mangla, S.K., Luthra, S., Rana, N.P., Dwivedi, Y.K. (2018). Predicting changing pattern: building model for consumer decision making in digital market. *Journal of Enterprise Information Management*, vol. 31, no. 5, p,p. 674-703.
[17] Habibi, A., Jahantigh, F. F., Sarafrazi, A. (2015). Fuzzy Delphi Technique for Forecasting and Screening Items. *Asian Journal of Research in Business Economics and Management*, vol. 5, no. 2, p.p. 130-143.
[18] Tsai, H.-C., Lee, A.-S., Lee, H.-N., Chen, C.-N., Liu, Y.-C. (2020). An Application of the Fuzzy Delphi Method and Fuzzy AHP on the Discussion of Training Indicators for the Regional Competition, Taiwan National Skills Competition, in the Trade of Joinery. *Sustainability*, vol. 12, no. 10: 4290.
[19] APQC, "Process Classification Framework V6.11", 2015
[20] Aleksić, A., Stefanović, M., Arsovski, S., Tadić, D. (2013). An assessment of organizational resilience potential in SMEs of the process industry, a fuzzy approach. *Journal of Loss Prevention in the Process Industries*, vol. 26, no. 6, p.p. 1238-1245.
[21] Pescaroli, G., Velazquez, O., Alcántara-Ayala, I., Galasso, C., Kostkova, P., Alexander, D. (2020). A likert scale-based model for benchmarking operational capacity, organizational resilience, and disaster risk reduction. *International Journal of Disaster Risk Science*, vol. 11, no. 3, p.p. 404-409.
[22] Sisman, B. (2016). Bulanık Moora Yöntemi Kullanılarak Yeşil Tedarikçi Geliştirme Programlarının Seçimi ve Değerlendirilmesi. *Journal of Yaşar University*, vol. 11, no. 44, p.p. 302-315.
[23] Dubois, D., Prade, H. (1980). *Fuzzy Sets and Systems: Theory and Applications*. *Academic Press*, Inc (London) Ltd.

COMETa 2022
6th INTERNATIONAL SCIENTIFIC CONFERENCE
17th - 19th November 2022
Jahorina, B&H, Republic of Srpska
University of East Sarajevo
Faculty of Mechanical Engineering
Conference on Mechanical Engineering Technologies and Applications

ZNAČAJ UMREŽAVANJA U KONTEKSTU OSTVARIVANJA POSLOVNE IZVRSNOSTI

Angela Fajsi[1], Slobodan Morača[2], Slaviša Moljević[3], Nenad Medić[4]

Rezime: Sve stroži zahtevi globalnog tržišta i rapidan tehnološki razvoj uslovljavaju organizacije da unapređuju odnose sa interesnim grupama u cilju postizanja izvrsnosti u poslovanju. Osnovni cilj ovog rada jeste da se ispita na kom nivou je uspostavljeno poslovno umrežavanje u organizacijama koje su osvojile sertifikate ili nagrade za poslovnu izvrsnost i koje se prednosti u tom kontekstu ostvaruju. Rezultati sprovedenog istraživanja dokazuju visok nivo poslovne saradnje koji ispitane organizacije ostvaruju i ukazuje na njen značaj, posebno posmatrajući u promenljivim uslovima nove industrijske revolucije.

Ključne riječi: kvalitet, poslovna izvrsnost, poslovno umrežavanje,

THE IMPORTANCE OF NETWORKING IN THE CONTEXT OF ACHIEVING ORGANIZATIONAL BUSINESS EXCELLENCE

Abstract: The increasingly strict requirements of the global market and rapid technological development require organizations to improve relations with interest groups to achieve business excellence. The paper's main aim is to examine at what level business networking is established in organizations that have won certificates or awards for business excellence and what advantages are realized in that context. The results of the conducted research indicate the positive impact that is being achieved between business excellence and networking, especially considering the changing conditions of the new industrial revolution.

Key words: business excellence, networking, quality

[1] M.Sc., Angela Fajsi, Univerzitet u Novom Sadu, Fakultet tehničkih nauka, Novi Sad, Republika Srbija, angela.fajsi@uns.ac.rs (CA)
[2] Dr, Slobodan Morača, Univerzitet u Novom Sadu, Fakultet tehničkih nauka, Novi Sad, Republika Srbija, moraca@uns.ac.rs
[3] Dr, Slaviša Moljević, Univerzitet u Istočnom Sarajevu, Mašinski fakultet, Istočno Sarajevo, Republika Srpska, slavisa.moljevic@ues.rs.ba
[4] Dr, Nenad Medić, Univerzitet u Novom Sadu, Fakultet tehničkih nauka, Novi Sad, Republika Srbija, medic.nenad@uns.ac.rs

1 UVOD

Organizacije se danas suočavaju sa sve strožim zahtevima na globalnom tržištu kako bi postale izvrsnije u svom poslovanju i na taj način održale ili poboljšale svoju konkurentsku poziciju. Ostvarivanje izvrsnosti u poslovanju danas nije uslovljeno isključivo internim faktorima, već je neophodno izvršiti integraciju neophodnih znanja, veština, metoda i tehnologije iz eksternog okruženja kako bi se zadovoljili sve stroži zahtevi tržišta po pitanju kvaliteta. Današnji poslovni zahtevi se razlikuju i očekuje se brzina, fleksibilnost, prilagodljivost, tačnost i lakoća izvođenja poslovanja sa performansama proizvoda i usluga koji zadovoljavaju ili čak prevazilaze zahteve za kvalitetom definisane od strane korisnika [1].

Saradnja sa ljudima i umrežavanje tehnologije omogućava razvoj znanja i kompetencija kako bi se povećale mogućnosti boljeg iskorišćenja i ponovne upotrebe resursa, kao i mogućnost učenja iz najboljih praksi [2], što dalje povećava mogućnost ostvarivanja izvrsnosti u procesima i rezultatima.

Osnovni cilj ovog rada jeste da se ispita značaj poslovnog umrežavanja u kontekstu ostvarivanja poslovne izvrsnosti organizacija. Na uzorku od 124 organizacije koje imaju dodeljen određen nivo priznanja ili nagrada za poslovnu izvrsnost definisanih od strane organizacije EFQM (engl. *European Foundation for Quality Management*) ispitivan je nivo saradnje koji ostvaruju sa ostalim interesnim grupama, tj. meren je njihov uticaj u odnosu na ostvaren nivo poslovne izvrsnosti. Očekivani doprinos ovog rada jeste da se kroz pregled literature i empirijsko istraživanje istraži nivo uticaja koje poslovno umrežavanje ostvaruje na poslovnu izvrsnost i shodno tome daju predlozi za dalja istraživanja.

Nakon uvodnog dela sledi drugo poglavlje rada u okviru koga je predstavljen oblast poslovna izvrsnost i njeni osnovni elementi. U trećem poglavlju rada pregledom literature je pojašnjena veza između poslovnog umrežavanja i poslovne izvrsnosti. Četvrto poglavlje rada predstavlja istraživački okvir gde se empirijskim metodama ispitivao uticaj poslovng umrežavanja na ostvarivanje izvrsnosti. Nakon toga, u petom poglavlju rada, sledi diskusija rezultata. U poslednjem poglavlju rada su data zaključna razmatranja i implikacije za buduća istraživanja.

2 POSLOVNA IZVRSNOST

Prema definiciji od strane EFQM organizacije poslovna izvrsnost podrazumeva „izvanredne nivoe performansi koje zadovoljavaju ili prevazilaze očekivanja svih interesnih grupa“ [3]. Poslovnu izvrsnost ne treba posmatrati kao kratkoročnu aktivnost organizacije, već kao filozofiju upravljanja, set principa, kriterijuma i prilaza koji omogućavaju ostvarivanje najboljih rezultata u srednjoročnom i dugoročnom periodu, pritom obezbeđujući podršku za održivi razvoj u budućnosti [4].

Osnovu koncepta poslovne izvrsnosti čine postojanje snažnog liderstva, fokus na kupca i na zaposlene, usklađivanje sa poslovnim strategijama, organizaciono učenje, inovacije i poboljšanja, razvoj partnerstava, fokus na postignute rezultate, socijalnu odgovornost i brigu o životnoj sredini [5]. Kako bi organizacije mogle izvršiti samoprocenu ili biti ocenjene prema navedenim kriterijumima uspostavljeni su modeli za procenu poslovne izvrsnosti koji su namenjeni svim organizacijama bez obzira na veličinu i tip delatnosti. Dva najviše citirana modela na globalnom nivou, ujedno i najzastupljenja u praktičnoj primeni jesu Malkolm Baldridž model, i EFQM model na osnovu čijih kriterijuma je sprovedeno istraživanje u okviru ovog rada.

EFQM model je prepoznat kao globalna struktura koja pomaže organizacijama da upravljaju promenama i poboljšaju organizacione performanse [6]. Iako je na

početku model prvenstveno bio namenjen industrijskim organizacijama, vremenom je njegova primena postala šira. U poslednjih nekoliko godina postoji sve veće interesovanje za implementaciju EFQM i ostalih modela poslovne izvrsnosti u različitim sektorima javne administracije, obrazovnih institucija i zdravstvenih organizacija [7]. Poslednja verzija modela EFQM 2020 je prilagođena globalnim zahtevima tržišta koje podrazumevaju digitalnu transformaciju i poslovno umrežavanje [8].

3 POSLOVNA IZVRSNOST I POSLOVNO UMREŽAVANJE

Prethodni poslovni sistemi su predstavljali statičko okruženje i podrazumevali su stabilan skup partnera i dobavljača. Međutim, moderne organizacije zahvaljujući razvoju virtuelnih platformi se povezuju kako bi formirale poslovni ekosistem u kojem je svaka organizacija složeno umrežena i zavisna od drugih [9]. Mnoge organizacije sve više usvajaju model zajedničkog stvaranja vrednosti. Poznati brendovi kao što su Guess, Reebok i mnogi drugi posluju po ovom principu i na taj način ostvaruju željene organizacione performanse i izvrsnost u poslovanju.

Terziovski [10] je u svom istraživanju zaključio da prakse umrežavanja imaju snažan pozitivan uticaj na poslovnu izvrsnost posebno u sektoru malih i srednjih organizacija. Umrežavanjem organizacije teže da iskoriste strateške resurse iz mreže partnera, omogućavaju im da integrišu i optimizuju različite ekspertize, sposobnosti i znanja koja se smatraju strateški značajnim za organizaciju. Sa tehnološkim napretkom došlo je do promena u strukturi povezivanja između organizacija i na porastu značaja međusobne saradnje i komunikacije.

Sa pojavom i razvojem nove industrijske revolucije pojavljuju se „povezani ljudi“ ili „profesionalci 4.0“, koji su odlikuje se efikasnijim, fleksibilnijim, bržim načinom rada zahvaljujući kome postaju konkurentniji i spremniji da odgovore izmenjenim zahtevima okruženja. Na ovaj način se ostvaruje veća povezanost između procesa i donosioca odluka, podstiče se razmena znanja i identifikuju se kanali za poboljšanja, problema, greške i rešenja, koje se direktno vezuju za finalni proizvod ili uslugu [11].

4 ISTRAŽIVAČKI OKVIR

4.1 Metodologija i opis uzorka

U radu je predstavljen deo istraživanja koje je sprovedeno u doktoratu prvog autora ovog rada. Istraživanje je sprovedeno u periodu od januara do marta 2021. godine, Upitnici su distribuirani ispitanicima u elektronskom formatu putem Gugl obrazaca (engl. *Google Forms*).

U istraživanju je učestvovalo 124 organizacije koje imaju dodeljena priznanja iili nagrade za poslovnu izvrsnost dodeljene od strane EFQM organizacije. Organizacije posluju u domenu proizvodnih i uslužnih delatnosti i imaju sedište u 27 različitih zemlja širom sveta. Kada se posmatra veličina organizacija, skoro 70% pripada sektoru malih i srednjih organizacija, dok preostali ispitanici čine velike organizacije.

U tabeli 1 je predstavljena struktura organizacija prema nivou ostvarenih priznanja I nagrada.

Tabela 1. *Struktura organizacija prema nivou priznanja ili nagrada za poslovnu izvrsnost*

Varijabla	Kategorija	Broj	Procenat (%)
Poslovna izvrsnost	Posvećen izvrsnosti	24	19.35
	Posvećen izvrsnosti 2 zvezde	19	15.32
	Priznat za izvrsnost 3 zvezde	12	9.68
	Priznat za izvrsnost 4 zvezde	30	24.19
	Priznat za izvrnsost 5 zvezdi	21	16.94
	EFQM Finalista za dobijanje nagrade	10	8.06
	EFQM Dobitnik nagrade za izvrsnost	8	6.45

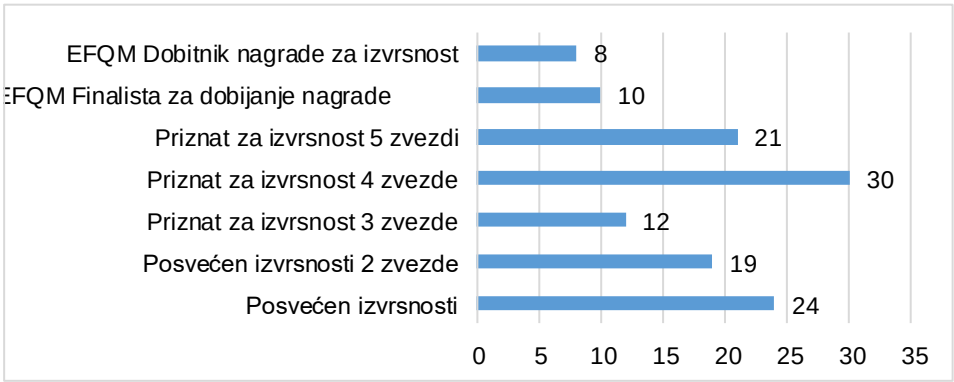

Slika 1. *Grafički prikaz osvojenih priznanja ili nagrada za poslovnu izvrsnost*

Najveći broj organizacija prepoznat je kao posvećen izvrsnosti sa četiri (24.19%), jednom (19.35%), pet (16.94%) ili dve (15.32%) zvezde.

4.2 Rezultati istraživanja

Rezultati istraživanja vezani za nivo međuorganizacione saradnje i broja zajedničkih aktivnosti je predstavljen tabelom 2 i grafički (slike 1 i 2).

Tabela 2. *Prikaz organizacija prema nivou poslovnog umrežavanja*

Varijabla	Kategorija	Broj	Procenat
Nivo međuorganizacione integracije	Saradnja ne postoji ili je na veoma niskom nivou	15	12.10
	Saradnja postoji, ali zavisi od poslovnih potreba i zahteva tržišta	60	48.39
	Postoji konstantna povezanost sa drugim organizacijama u procesu razvoja proizvoda i/ili usluga.	49	39.51
Broj zajedničkih aktivnosti sa partnerima u prethodne tri godine	Manje od 3	33	26.61
	Između 3 i 5	43	34.68
	Više od 5	48	38.71

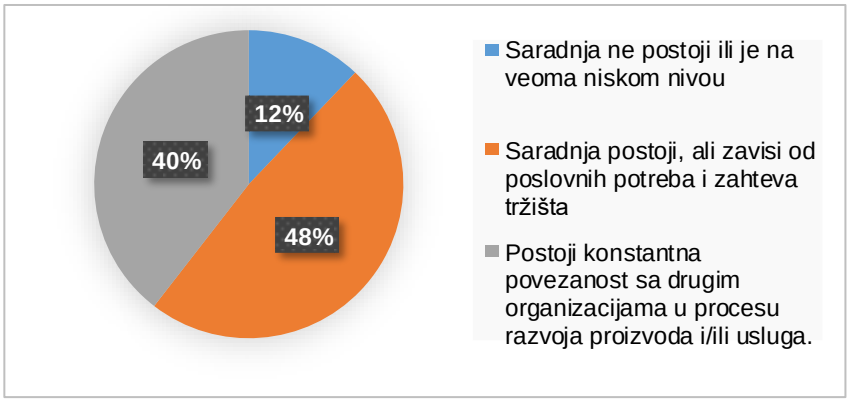

Slika 2. *Grafički prikaz nivoa međuorganizacione integracije*

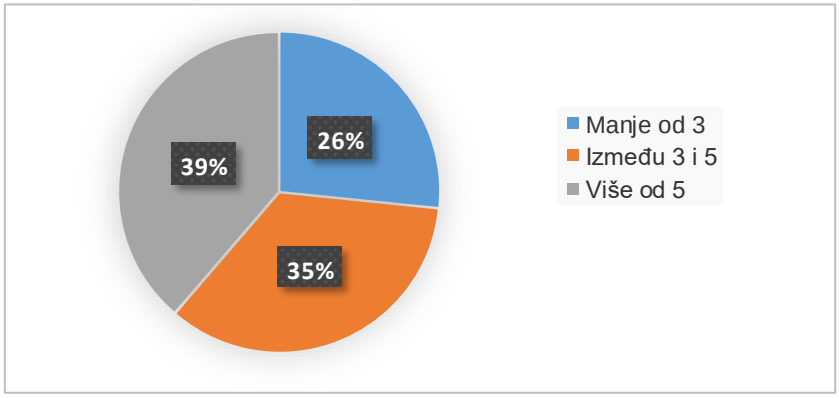

Slika 3. *Broj zajedničkih aktivnosti sa partnerima u prethodne godine*

Prilikom ocenjivanja nivoa poslovnog umrežavanja, 39.51% organizacija se izjasnilo da postoji konstantna povezanost sa drugim organizacijama u procesu razvoja proizvoda i/ili usluga, i u sličnom procentu, 38.71% su se izjasnili da su prethodne tri godine imali više od pet zajedničkih atkivnosti sa partnerima. Rezultati impliciraju postojanje visokog nivoa međurganizacione saradnje kod organizacija koje su prepoznate ili nagrađene za izvrsnost u poslovanju.

4 DISKUSIJA

Pretragom literaturnih izvora zaključeno je da postoji snažno teorijsko uporište kojim se dokazuje veza između poslovne izvrsnosti i poslovnog umrežavanja. Kroz empirijsko istraživanje ispitivao se nivo umrežavanja kod organizacija koje imaju osvojene nagrade ili priznanja za poslovnu izvrsnost. Zaključeno je da 87.8% od ukupnih ispitanika ostvaruje saradnju sa poslovnim partnerima, a skoro 40% je navelo da postoji kontinuitet u saradnji u procesu razvoja proizvoda/usluga. Prema EFQM modelu 2013 deo partnerstvo i resursi se ocenjuje kao zasebna celina, predstavlja preduslov za unapređenje na putu ka izvrsnosti [3], što su rezultati u ovom istraživanju i pokazali. Pretpostavka je da organizacije koje su se izjasnile da nemaju ostvarenu

saradnju imaju niže nivoe poslovne izvrsnosti i da je prilikom ocenjivanja deo partnerstvo i resursi identifikovan kao značajan prostor za poboljšanja.

Kada je u pitanju broj zajedničkih aktivnosti u prethodne tri godine, više od trećine ispitanika se izajsnilo da su imali više od 5 aktivnosti, što ukazuje dalje na intenzivnu saradnju i umrežavanje na različitim nivoima. Dve godine pre sprovedenog istraživanja je trajala pandemija virusa Kovid 19, mnoge organizacije su smanjile obim poslovnih aktivnosti ili čak privremeno obustavile, te se može pretpostaviti da bi pod normalnim uslovima procenat međusobne saradnje bio i veći.

5 ZAKLJUČCI

U okviru datog rada sprovedeno je ispitivanje se u kojem stepenu je razvijena saradnja kod organizacija koje imaju ostvarene nagrade ili priznanja za poslovnu izvrsnost i da li to ima uticaja na nivoe ostvarene poslovne izvrsnosti.

Teorijskim pregledom literature je izveden zakljucak da se poslovno umrežavanje ne posmatra više samo kao preporuka za razvoj poslovanja, već kao neophodni uslov da bi organizacije opstale i razvijale se na globalnom tržištu. Empirijskim istraživanjem je dokazano da većina organizacija koje su priznate ili nagradjene kao izvrsne u svom poslovanju, ostvaruju visok stepen međuorganizacione saradnje što implicira na postojanje pozitivne korelacije između dve posmatrane kategorije. Preporuka za dalja istraživanja obuhvata ispitivanje statističke značajnosti ove veze kako bi mogli da se identifikuju dalji prostori za poboljšanja u ovoj oblasti.

LITERATURA

[1] Nguyen, T., Tucek, D., & Pham, N. T. (2022). Indicators for TQM 4.0 model: Delphi Method and Analytic Hierarchy Process (AHP) analysis. Total Quality Management & Business Excellence, 1-15.
[2] Xu, X., Lu, Y., Vogel-Heuser, B., & Wang, L. (2021). Industry 4.0 and Industry 5.0—Inception,conception and perception. Journal of Manufacturing Systems, 61, 530-53.
[3] EFQM. (2013). EFQM Excellence Model 2013. EFQM Publications
[4] Sampaio, P., Saraiva, P., & Monteiro, A. (2012). A comparison and usage overview of business excellence models. The TQM Journal, 24(2), 181-20
[5] Porter, L., & Tanner, S. (2012). Assessing business excellence. Routledge
[6] Boulter, L., Bendell, T., & Dahlgaard, J. (2014). Total quality beyond North America: A comparative analysis of the performance of European Excellence. International Journal of Operations and Production Management, 33(2), 197-215.
[7] Đorđević, A., Klochkov, Y., Arsovski, S., Stefanović, N., Shamina, L., & Pavlović, A. (2021). The impact of ICT support and the EFQM criteria on sustainable business excellence in higher education institutions. Sustainability, 13(14), 7523
[8] EFQM. (2019). EFQM Excellence Model 2020. EFQM Publications
[9] Asif, M. (2020). Are QM models aligned with Industry 4.0? A perspective on current practice.Journal of Cleaner Production, 258, 120820
[10] Terziovski, M. (2003). The relationship between networking practices and business excellence: a study of small to medium enterprises (SMEs). Measuring business excellence, 7(2), 78-92.
[11] Hirman, M., Benesova, A., Steiner, F., & Tupa, J. (2019). Project management during the Industry 4.0 implementation with risk factor analysis. Procedia Manufacturing, 38, 1181-1188.

COMETa 2022
6th INTERNATIONAL SCIENTIFIC CONFERENCE
17th - 19th November 2022
Jahorina, B&H, Republic of Srpska
University of East Sarajevo
Faculty of Mechanical Engineering
Conference on Mechanical Engineering Technologies and Applications

PRODUCTION OF AUTOMOTIVE INDUSTRY IN THE WORLD

Branislav Dudić [1], Alexandra Mittelman[2], Pavel Kovač[3], Borislav Savković[4], Eleonóra Beňová[5], Dušan Golubović[6]

Abstract: Automotive industry has long and rich history in the world and it is very important for economic growth, industrial production, employment rate, direct investments, export and introducing new innovations. Automotive industry invests into research and development globally more than 90 billion EUR and this amount represents up to 19 percent of all global costs on research and development. Automotive industry has had the significant position in the Slovak economy since the beginning of the economic transformation of Slovakia. Slovakia has become one of the leading producers of automobiles in Central Europe mainly because of the presence of automobile companies Volkswagen in Bratislava, PSA Peugeot Citroën in Trnava, Kia Motors in Žilina Jaguar in Nitra. From the economic point of view, automotive industry has brought record investments and export to Slovakia. In the paper production of automobile industry in the world with sales and overview of production in Slovakia is presented. Estimated are the worldwide motor vehicle production from 2000 to 2020as well.
Key words: Automotive Industry, Automobile Production, Challenges of the Automotive Industry.

1 INTRODUCTION

History of automotive industry in the world, from the point of view of the beginning of the rise of an automobile, extends into far past. The invention of

[1] Dr, Branislav Dudić, Comenius University Bratislava, Faculty of Management, Slovakia and University Business Academy, Faculty of Economics and Engineering Management, Serbia, branislav.dudic@fm.uniba.sk
[2] Dr, Alexandra Mittelman, Comenius University Bratislava, Faculty of Management, Slovakia, alexandra.mittelman@fm.uniba.sk
[3] Dr, Pavel Kovač, University of Novi Sad, Faculty of Technical Sciences, Serbia, pkovac@uns.ac.rs
[4] Dr, Borislav Savković, University of Novi Sad, Faculty of Technical Sciences, Serbia, savkovic@uns.ac.rs
[5] Dr, Eleonóra Beňová, Comenius University Bratislava, Faculty of Management, Slovakia, eleonora.benova@fm.uniba.sk
[6] Dr, Dušan Golubović, University of East Sarajevo, Faculty of Mechanical Engineering, Lukavica, BIH, dusan.golubovic54@gmail.com

automobile can be considered as one of the most significant inventions in the history of humankind. It has become the essential part of life in the society, that approached to this invention very sceptically from the beginning [1]. The year 1839 brought the development of the vulcanising process that enabled the production of tyres and the beginning of the development of automobiles. The development of automotive industry is connected to Mr. Henry Ford who in 1903 established the company Ford Motor Company, that still works in present. Mr. Henry Ford was present at the beginning of the modern automotive industry that as the first one promoted the thought of an automobile as the mass means of transport.

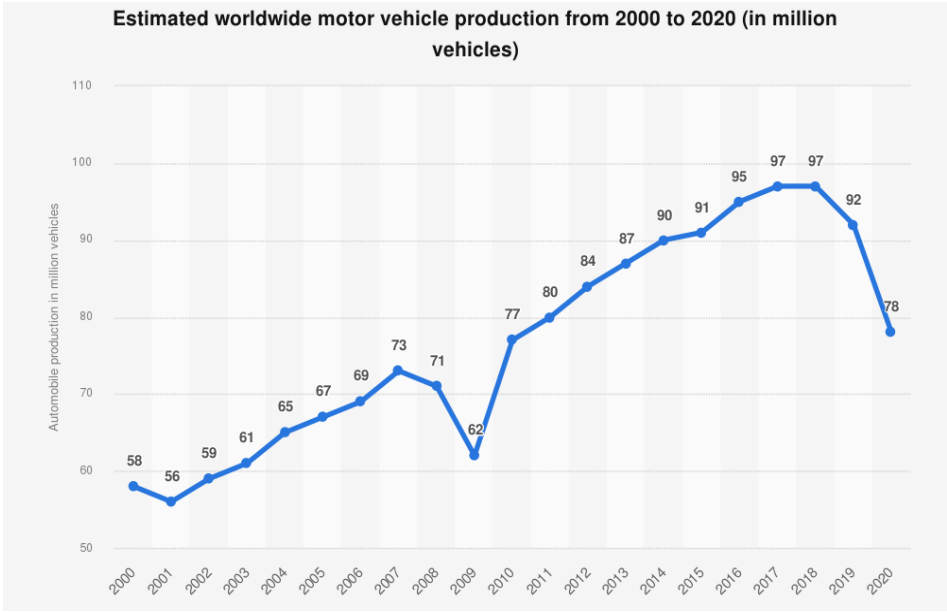

Figure 1. *Estimated worldwide motor vehicle production from 2000 to 2020 (in million vehicles) [2]*

The development of automotive industry in the world has long and rich history. The USA became the representative automobile market around 1913. The implementation of assembly line production in Ford company was the significant milestone, next milestone in the development of automotive industry was brought by the company Toyota, which came with the new, so-called LEAN system of production. American automobile companies kept the first place on the world market till the beginning of 80s, when they were advanced by Japanese producers of automobiles. Japanese automobile companies became well-known in 60s. In 70s, they managed to advance German producers and in 80s and 90s they produced more vehicles than USA. However, in 90s, the production of automobiles in China and India started to develop.

1.1 Worldwide motor vehicle production 2000-2020

In 2020, almost 78 million motor vehicles were produced worldwide. This figure translates into a decline of around 15 percent, compared with the previous year. China, Japan, and Germany were the largest producers of cars and commercial vehicles in 2020. China is ranked as the largest passenger car manufacturer in the world, having

produced more than 21 million cars in 2020, and accounting for almost one third of the world's passenger vehicle production. Over the past decades, China has emerged as one of the main growth markets for players in the global automotive industry. One of China's largest car manufacturing companies is the joint venture between General Motors and SAIC Motor Corporation Limited, known as Shanghai General Motors Company Ltd or simply Shanghai GM. GM produces and sells passenger vehicles under the Chevrolet and Cadillac brands, among others. Aside from manufacturing cars, the company also produces engines and transmission systems. Shanghai GM's production amounted to a little over 1.6 million units in 2019 [2-3].

1.2 Production of automobile industry in the world

Automotive industry is an industry that we range into secondary sector within the scope of four sectors in national economy and which generally significantly influences the level of development of economy and standard of living of population. It belongs into fast advances in technology and science, fast growth of work production and high investment opportunity. Its main function is production, marketing, and sale of vehicles.

All automobile companies and their sub-suppliers of spare parts belong into this industry. Automotive industry is closely connected to engineering industry, electronics, and chemical industry as well as with metallurgical industry. Passenger vehicles, trucks, buses, and motorbikes belong into the products of automotive industry. Automotive industry invests globally into research and development more than 90 billion EUR, and it represents with this amount up to 19 percent of all global costs on research and development [3-5].

Global sales in automotive industry are connected also to global economic development. The biggest producers of automobiles in the world can be considered European Union, USA, and Japan. They represent about 80%-90% of all production. Recently, mainly in China, the production has increased. China occupies fourth place with its 4.4million produced vehicles (2003), right after USA, Japan, and Germany – the biggest producer of automobiles in the world.

1.3 Worldwide car sales 2010-2021

Worldwide car sales are expected to grow to around 66 million automobiles in 2021, up from an estimated 63.8 million units in 2020. The sector experienced a downward trend on the back of a slowing global economy and the advent of the coronavirus pandemic in all key economies. It had been estimated pre-pandemic that international car sales were on track to reach 80 million. Although the latest figures show an improvement from previous estimates, the industry's economic woes continue, and demand for new motor vehicles declined in 2020. South America and Europe were among the hardest-hit regions, with auto sales in these regions contracting by about one-fourth year-on-year. After years of double-digit growth, China's economy began to lose steam. China was the largest automobile market based on sales with around 19.8 million units in 2020. However, monthly car sales in China were in free-fall in February 2020 due to the coronavirus outbreak in the country and fears over a looming recession. As a result of successful containment measures, the market started showing signs of recovery in April, providing a lifeline for major

manufacturers. By February 2021, figures had risen by around four times the February 2020 volume [6].

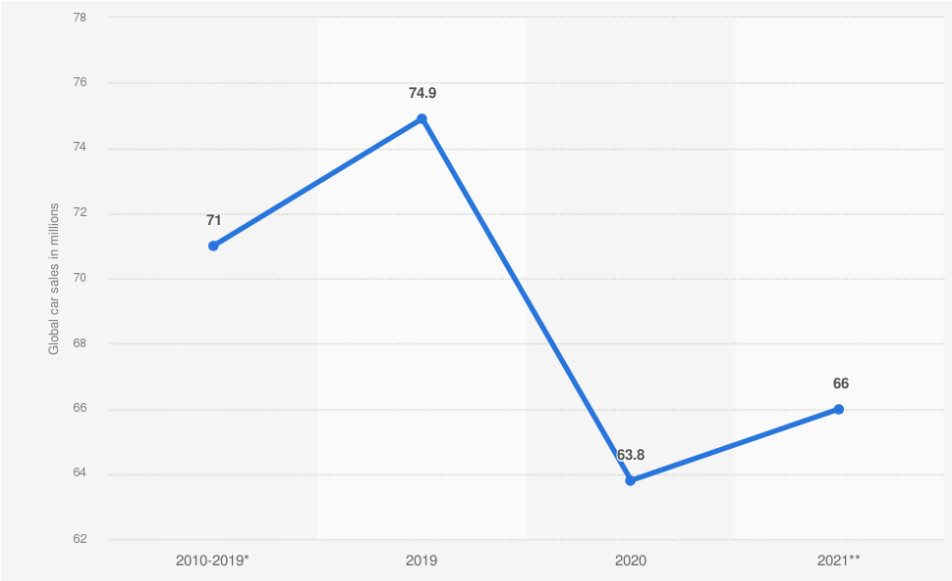

Figure 2. *Number of cars sold worldwide between 2010 and 2021 (in million units) [6]*

2 AUTOMOTIVE INDUSTRY AND PRODUCTION OF VEHICLES IN SLOVAKIA

Automotive industry has occupied the significant position in the Slovak economy since the beginning of the economic transformation of Slovakia. Currently, automotive industry is one of the main contributors to economic growth, employment rate and it plays the important role in the foreign trade of Slovakia.

2.1 Industry revenue of "manufacture of motor vehicles"in Slovakia 2012-2025

This statistic shows the revenue of the industry "manufacture of motor vehicles" in Slovakia from 2012 to 2018, with a forecast to 2025. It is projected that the revenue of manufacture of motor vehicles in Slovakia will amount to approximately 22.69 billion U.S. Dollars by 2025 [7].

Slovak automotive industry comprises 13% GDP, it has 35% share in industrial export, and it directly employs more than 154,000 people. The most significant automobile factories are Volkswagen in Bratislava, PSA Peugeot Citroën in Trnava, Kia Motors in Žilina and the newest brand is Jaguar Land Rover near Nitra. The production of automobiles increases every year, total production in 2019 was in the amount of 1,092,902 vehicles. The estimated production in the amount of 1,250,000 vehicles in 2020 by influence of the world pandemics did not fulfil expectations.

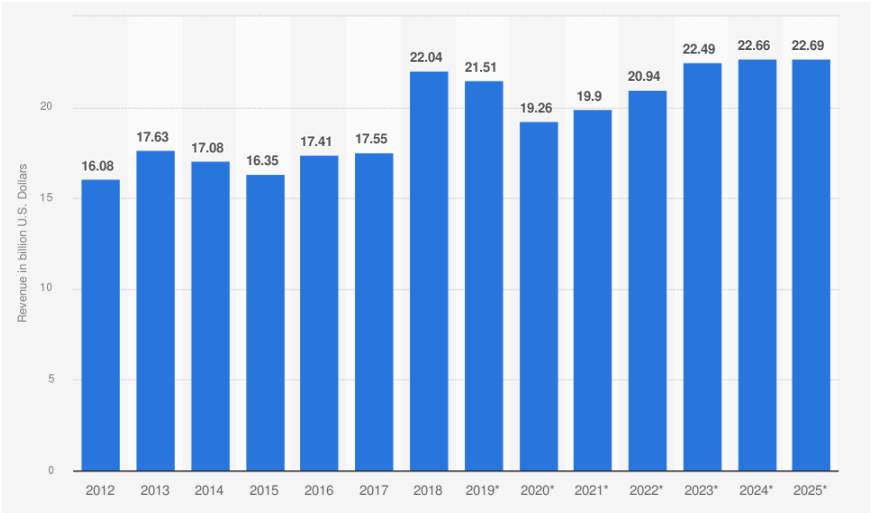

Figure 3. *Industry revenue of "manufacture of motor vehicles" in Slovakia from 2012 to 2025 (in billion U.S. Dollars) [7]*

2.2 Industry revenue of "wholesale and retail trade "in Slovakia 2012-2025

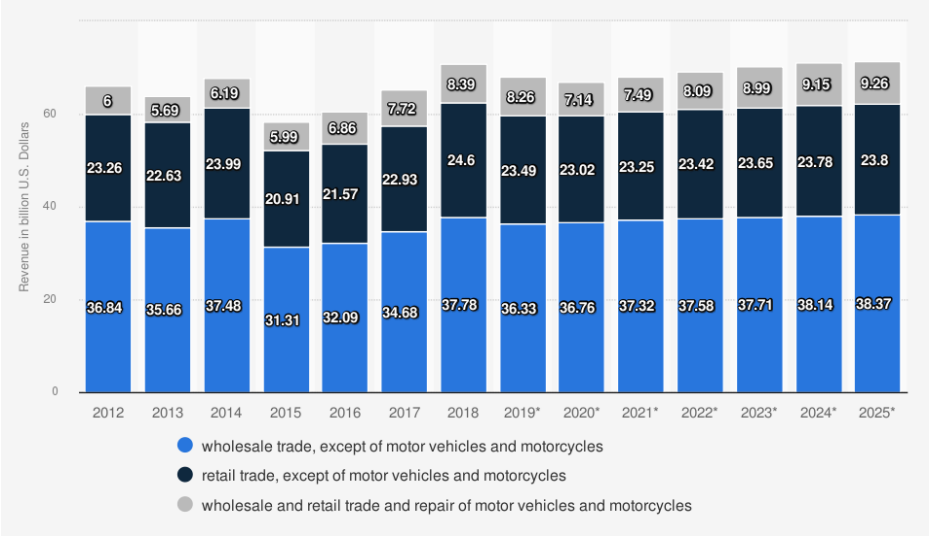

Figure 4. *Industry revenue of "wholesale and retail trade" in Slovakia from 2012 to 2025(in billion U.S. Dollars) [8]*

This statistic shows the revenue of the industry "wholesale and retail trade, repair of motor vehicles and motorcycles" in Slovakia by segment from 2012 to 2018, with a forecast to 2025. It is projected that the revenue of wholesale and retail trade, repair of motor vehicles and motorcycles in Slovakia will amount to approximately 9.26 billion U.S. Dollars by 2025 [8].

2.3 The impact of pandemics Covid-19 on automotive sector

The gradual spread of Covid- 19 had the consequence the slowdown and the freeze of the production in factories for vehicles all around the world. The lack of stock necessary to produce automobiles exported globally weakened the economy what resulted into breach of contracts with suppliers and sellers and certain tension on the market, where sale decreased as well as revenues from the sale of sold automobiles. The spread of pandemics COVID-19 had the negative consequences also on the automotive industry in Slovakia where slight decrease of export of automobiles into foreign countries was recorded due to the closing of borders of surrounding countries.

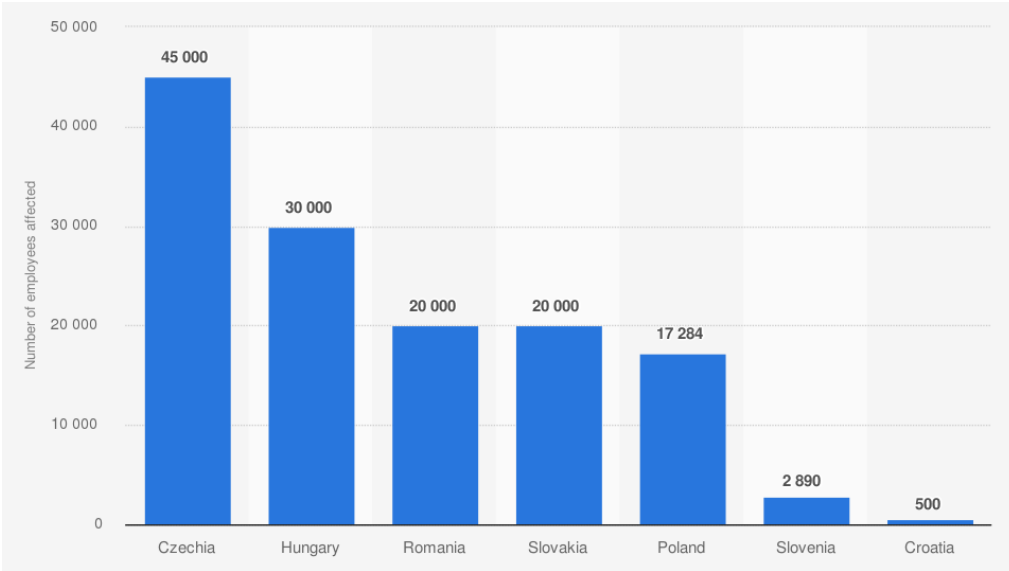

Figure 5. *Automotive industry losses due to downtime caused by the coronavirus (COVID-19) pandemic in Central and Eastern European countries in 2020*, by number of employees affected [9]*

2.3.1 COVID-19 impact on automotive industry in CEE 2020, by employees affected

Nearly 250 thousand cars were not manufactured in Central and Eastern Europe due to the downtime caused by the coronavirus outbreak. Nearly 136 thousand people working in the automotive factories in the CEE region were affected by the COVID-19 crisis. The actual number of affected employees was much higher. This is due to delays in data transfer and the unavailability of full reports from production plants. In 2020, the total fall by 85% in the sale of automobiles in Europe was recorded, due to the influence of the government's decree-law and quarantine measures to close borders to eliminate whatever connection with the surrounding world. The fall hit fully the market.

3 ANALISE

Slovakia with its four automobile companies is ranked among the countries with highly developed automotive industry that has the significant influence on economic results and total economic situation in the country. Automotive industry in Slovakia has

brought higher employment, has increased gross domestic product, has brought direct foreign investments and has improved export. All four automobile manufacturers in Slovakia have already begun to optimize their production processes and they must react on the global changes on automobile market. Slovak manufacturers must prepare for the industrial production of more ecological vehicles and automotive industry needs immediate investments into innovations, this has been agreed by various analytics.

4 CONCLUSIONS

Number of cars sold worldwide (in million units) has increasing trends between 2010 and 2021.

Industry revenue of “manufacture of motor vehicles “in Slovakia from 2012 to 2025 has increasing trends as well.

Automotive industry losses due to downtime caused by the coronavirus (COVID-19) pandemic in Central and Eastern European countries in 2020*, by number of employees affected is noticed.

COVID-19 impact on automotive industry in CEE 2020, by employees affected is noticed.

REFERENCES

[1] Jančura, M. (2016). Československá automobilová história v rokoch 1918 – 1948 a jej hospodárske, technicko- historické a kultúrno-spoločenské aspekty v českej a slovenskej historiografii. [online]. *In: ČLOVEK A SPOLOČNOSŤ. [cit. 2021-07-02].* ISSN 1335-3608.

[2] Statista. Retrieved November 28, 2021, from https://www.statista.com/statistics/262747/worldwide-automobile-production-since-2000/

[3] Hacker, Fl, Harthan, R, Matthes F, Zimmer, Wi. (2009). Environmental impacts and impact on the electricity market of a large scale introduction of electric cars in Europe : critical review of literature S.l., *The European Topic Centre on Air and Climate Change (ETC/ACC)*.

[4] Smokers, R, et al. Opportunities for the Use of Renewable Energy in Road Transport, Policy makers report S.L.*, IEA, Renewables in Transport (RETRANS)*, 2010

[5] Dyke, K,Schofield, N, Barnes, M. (2009). Analysis of Electric Vehicles on Utility Networks, *World Electric Vehicle Journal*, Vol. 3, pp.. 1-9.

[6] Statista Research Department, In *Statista*. Retrieved November 28, 2021, from https://www.statista.com/statistics/200002/international-car-sales-since-1990/

[7] In *Statista*. Retrieved November 28, 2021, from https://www.statista.com/forecasts/395999/manufacture-of-motor-vehicles-revenue-in-slovakia

[8] In *Statista*. Retrieved November 28, 2021, from https://www.statista.com/forecasts/907035/wholesale-and-retail-trade-revenue-in-slovakia

[9] In Statista. Retrieved November 29, 2021, from https://www.statista.com/statistics/1108739/cee-covid-19-impact-on-automotive-industry-by-affected-employees/

COMETa 2022
6th INTERNATIONAL SCIENTIFIC CONFERENCE
17th - 19th November 2022
Jahorina, B&H, Republic of Srpska
University of East Sarajevo
Faculty of Mechanical Engineering
Conference on Mechanical Engineering Technologies and Applications

BUSINESS MODELS IN TRANSITION - A CHANGE FOR PERFORMANCE ENHANCEMENT AND RESILIENCE

Michael Huber[1], Nikolina Ljepava[2], Aleksandar Aleksić[3]

Abstract: Business models are changing - more radically than ever before. Digital as well as societal influences, rapid changes in the market and competitive environment, and increasing customer dynamics are forcing traditional business models to change. Static considerations are changing into dynamic optimizations. In addition, reaction times are decreasing dramatically due to ever faster-changing conditions. This requires that the ability to change business models becomes a competence of companies in a dynamic market. More than ever, the resilience of the business model is thus inexorably coming into focus for all companies. However, these changes offer unique opportunities: they enable companies not only to respond proactively to change but also to actively drive change through business model innovation. The main contribution of this research appoints a case study at one of the world's largest manufacturers of weighing systems, highlighting how resilient business models can be built that are sustainably successful even in periods of turbulent upheaval.

Key words: Business Model, Business Model Design, Resilience Management, Resilient Business Models

1 INTRODUCTION

Considering that the performance of new computer chips doubles on average about every 20 months, the speed and extent of technological innovations are increasingly leading to a fundamental transformation of business, science and politics. Due to these constantly changing conditions, companies are faced with the challenge of maintaining their competitive advantages in the long term. According to Schwab [1], technologies such as artificial intelligence, the Internet of Things, autonomous driving, nana- and biotechnology will lead to the development of new business models or even the disruption of established companies in many industries in the coming decades.

Likewise, technological progress is increasingly changing the process of

[1] PhD Candidate, Michael Huber, University of Kragujevac, Uster, Switzerland, michael.huber@kg.ac.rs
[2] Prof., Nikolina Ljepava, American University in the Emirates, Dubai, UAE, nikolina.ljepava@aue.ae
[3] Prof., Aleksandar Aleksić, University of Kragujevac, Kragujevac, Serbia, aaleksic@kg.ac.rs

globalization. In addition to the tried and tested drivers such as trade and capital flows, the importance of data and information flows is growing. According to Schwab [1], studies show that value creation through the aforementioned data and information flows is already exerting a greater influence on global growth. At first glance, this reduces the importance of production and the exchange of physical goods, but this in no way means a slowdown or even a step backwards. Rather, it is a clear sign of ever closer economic networking.

Under these circumstances, companies in many sectors are faced with the problem of maintaining and, above all, expanding their competitive advantages in the long term. Under the understanding of classical economics, companies gain competitive advantages by minimizing costs and recognizing as well as serving customer preferences. In practice, it may be seen that the paradigm of cost reduction has been applied to the majority of companies [1]. However, the ability to innovate resiliently will become more relevant than ever for companies to recognize technological trends at an early stage and exploit them accordingly.

Interestingly, it should be noted that high investments in research and development as well as in the skills of employees no longer guarantee a competitive advantage [1]. From the point of view of the authors of this paper, this statement should be taken with extreme caution so it impacts the research motivation to find out if it apply universally or to a certain point to organizations all over the world. Nevertheless, accelerated technological development leads to rising product development costs as well as shorter product life cycles. Regrettably, this reduces the duration of economic usability. However, in order to secure sustainable competitive advantages for companies, it is necessary to further develop strategies, processes, products and services as well as resilient organizations - hence the transformation of entire business models [2].

The main idea of this research is to build resilient business models. According to Holling and Gunderson [3], resilience is an analytical category that describes the susceptibility of a system to failure. Although there is no consesus on the strict definiton on organoizational resilience, it may be described as the ability to withstand, shape and adapt to shocks and crises.

The first section focuses on the general challenges and the constantly changing framework conditions for companies. In the following chapter, there is a detailed literary discussion with regard to terminology and classifications in the context of business models. The third chapter describes on the one hand the development of the business models and on the other hand the conceptual frameworks and designs. Based on the previous chapters, a case study is conducted at one of the world's largest manufacturers of weighing systems. The findings from the substantive subsections of the paper are brought together in the fifth chapter. Possible takeaways and a critical outlook on developments will be presented.

2 LITERATURE REVIEW

The current digital and social changes are influencing companies faster and more radically than before [4]. In addition, corporate success is increasingly linked to the functionality of the entire business model. For this purpose, Tewes [4] analyzed the 50 most common definitions of business models in a study, which provide a first-class literary overview. However, a uniform framework regarding the exact design of business models does not exist in the literature. Nevertheless, the relevant building blocks for business success can be named. Undisputed in all respects is the relevance in the application of business models. As an indication of this, a study on the increase of

published articles on business models, in academic as well as non-academic journals, can be pointed out [5].

Basically, the description of business models should help to understand, analyze and communicate the decisive factors of the company's success as well as failure. In doing so, it shows the logical relationships of a company's business activities.

In summary, a business model can be used, among other things, to develop an in-depth understanding of the business idea, to work out differences compared with competitors, to understand the weaknesses of one's own company, to systematically demonstrate customer benefits, and to analyze the probability of success [6].

3 METHODOLOGY

3.1 Description of business models designs

The description approaches for business models [7] can be divided into two main categories. While the first category deals with generic description approaches for business models, the second concentrates on individual, selected business models. Accordingly various are the beginnings as well as goals to it. In the further elaboration of this present work the generic description beginnings stand in the foreground [7].

One goal of generic approaches to the structured description of business models is to improve the communication of business ideas to interested parties [12]. On the other hand, a structured representation allows an improvement of the methodical support of strategic management.

This raises the question of what elements a business model consists of and how these elements are designed and arranged.

3.2 Business models in companies

A study from 2013 on the current and future pressure on companies to change and act shows how much business models will change. The figure 1 shows that a total of 34 percent of the 350 respondents expect fundamental or at least very strong changes in their business model [8].

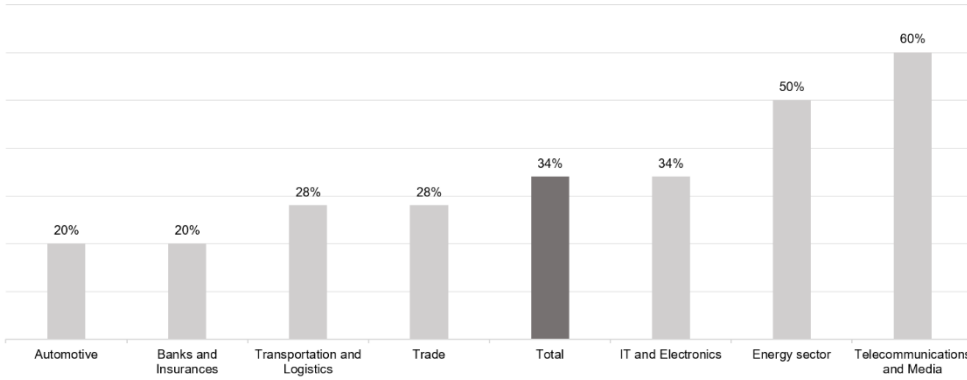

Figure 1. *An overview of the possible change in business models*

Business models today are no longer driven purely by products, but rather by customer experience, service and convenience. An excellent example of this is, among others, the company Nestlé with the Nespresso concept. While traditional coffee

manufacturers are operating with less growth in the market, Nestlé has revolutionized it. With Nespresso, Nestlé has developed a simple everyday item into a lifestyle product. The capsule system used for this is not only practical, but also quick and easy to use. In addition, it offers the customer a consumption experience that begins with the purchase of the capsules and is supported by the design of the machine, store and advertising [8].

3.3 Business model Canvas: Insights on the level of change in business models

The business model Canvas by Osterwalder and Pigneur [6] represents one of the most important approaches in the context of business model design. This is mainly due to the widespread use of the approach. In addition, the approach enjoys high reputation due to a high practical orientation and simplicity. This approach goes hand in hand with the objective: With the development of the business model concept, the complexity of companies should not be oversimplified, but still be built up as intuitively as possible [6].

Osterwalder and Pigneur clarify in their framework a kind of conceptual map of a visual language with associated grammar, which can be used to simplify the reality of the company, considering processes, structures and systems [6]. In addition to this common language, which can be understood by any company there is no assignment to a specific industry; thus, the approach is universally applicable.

In developing the approach, Osterwalder relied on the Balanced Scorecard according to Kaplan and Norton and his published Business Model Ontology. The four main areas of Product, Customer Interface, Infrastructure Management and Financial Aspects form the basic framework, along with nine building blocks, some of which are newly listed. Together with Pigneur, this was further developed into the concept of the business model Canvas [6].

The model template used to develop new business models and document existing ones does not require a strict sequence or processing of the building blocks. However, Osterwalder and Pigneur suggest working from the customer segments on the right to the cost structure on the left [6].

The strength of a *Canvas* lies primarily in the visualization and application of the tool in the team. By simply sticking or moving notes (post-its) and the resulting discussion, the business model indirectly supports the creation. In doing so, the method not only helps to show and analyze existing business models, but rather new possibilities in the design, implementation and development of new business models and ideas.

4 THE CASE STUDY

As explained in the previous chapters, the strength of the business model Canvas lies primarily in its visualization, simplicity of use, and approach. The successful implementation is also proven by a study from 2015. Strategyzer surveyed 1300 users and interviewed, among others, 35 Financial Times Global 500 companies from various industries, such as telecommunications, healthcare, manufacturing, IT or financial services. The results showed that 36 percent of the participants use the Canvas business model to develop new businesses and almost a quarter use it to implement new products and services within existing organizations. It seems that the approach has become a *global phenomenon* and an internationally recognized standard, which is perceived as practical and challenging [9]. Therefore, it makes sense to outline an example from METTLER TOLEDO that can be applied in practice in more detail.

METTLER TOLEDO is a global manufacturer of precision instruments for use in laboratories, industry and the food trade, with headquarters in Columbus, Ohio and main operational headquarters in Greifensee, Switzerland. In doing so, the world's largest manufacturer of weighing systems covers a weighing range from 0.1 micrograms to 1000 tons, making it the global market leader [10].

Microbalances that reach a maximum load of up to 10.1 g, provide readability of 0.1 µg, offer optimal draft shield for easy cleaning and ensure active temperature control? That's what METTLER TOLEDO's new and innovative XPR micro- and ultra-microbalance (hereafter referred to as XPR) offers [11]. In the table 1, the nine elements of the Canvas will be examined in more detail and explained using the example of the aforementioned microbalance.

At the beginning, the question about the customers, the **Customer Segments** (1/9), takes place. In this first step, these segments should be named as well as selected, which a company wants to reach, work on or even ignore if necessary [12]. The next step is to relate the customer segments just elaborated to the value propositions.

The next step is **The value proposition** (2/9), which describes the specific benefit or value that a package of selected products as well as services represents for exactly one customer segment. In this context, the values can be both quantitative (price, availability) and qualitative (design, specification) in nature [6].

The Channels (3/9) comprise the relevant communication, distribution and sales channels with which the identified customer segments are to be reached and addressed. This is how the value proposition is conveyed [12]. The channels form contact points between the customers and the company with the aim of making potential customers aware of the company, arousing interest, and ideally selling the products [13].

Customer Relationships (4/9) describe the relationship that a company develops and enters into with a specific customer segment. These include personal contact through to automated service [6, 12].

The revenue streams (5/9) describe the income that a company derives from each customer segment. To make revenue streams sustainable, companies should address the following guiding questions [12, 13]: How is the pricing model defined? What is the pricing strategy? What may the product or service cost?

The Key Activities (6/9) describe the most important strategic activities that a company must do. This results in the following guiding questions for companies [12, 13]: What does the company need to do to fulfill the value proposition for customers? What are the company's core areas or key activities?

The Key Resources (7/9) describe the relevant resources that are necessary for the business model to function. For the company, the following questions are derived to determine key resources [12, 13]: Which core areas does the company have? Are the competencies of the employees adequately defined and described?

The penultimate element, **Key Partners** (8/9), describes the network of suppliers and strategic partners that contribute to the success of the business model [12].

The **Cost Structure** (9/9), describes the important cost blocks that are incurred in a business model or in the company [12]. Here, too, the following guiding questions can be helpful in working out the cost structure [12,13]: How much does it cost the company to implement the Key Activities? What costs are incurred by the Key Resources and Key Partners? Which costs have a special relevance, for example raw materials?

Table *1. Canvas business model according to Osterwalder and Pigneur of METTLER TOLEDO's XPR micro- and ultra-microbalances*

<table>
<tr>
<td rowspan="2">Key Partners (8/9)

External suppliers; Internal suppliers; Know-how of internal development organizations; End customers involved in development; Global procurement; Global supply chain management

Due to the relevance of the XPR to the end customers, these are sometimes very closely involved directly in the development. This produces significant advantages for both sides. Above all, the very practice-oriented development of products, as is the case with XPR, strengthens these partnerships in the long term.</td>
<td>Key Activities (6/9)

Research and development; Production; Infrastructure (berths); Marketing; Sales

XPR's core competencies lie in the load cells it develops and builds itself. Load cells are force transducers used to build level weighing devices. Other essential elements of the product are sourced through external partners as well as through a strong and global supplier network.</td>
<td rowspan="2">Value Propositions (2/9)

Highest precision; High sensitivity; Weighing of sample quantities with a weight of up to 30 µg; Incredibly high resolution; Dosing of smallest quantities

The elements of the Customer Segments can be connected with those of the Value Propositions. For example, the precision as well as the sensitivity of the XPR are directly related to the quality.</td>
<td>Customer Relationships (4/9)

Events (in-house, on-site, trade fairs); Trainings; Direct service through field service; Digital communication (email campaigns, newsletter)

METTLER TOLEDO is in direct contact with end customers through its strong sales network as well as its complex applications and products. The relationship is strengthened primarily through on-site training and service for the products and services.</td>
<td rowspan="2">Customer Segments (1/9)

Product testing and quality assurance laboratory; Chemical laboratory; Mining; Medical technology

The customers are the heart of every company. In order to be able to serve customers adequately, they are segmented according to common needs, behaviors or other attributes.</td>
</tr>
<tr>
<td>Key Resources (7/9)

Research and development teams; Production (component manufacturing); Marketing (Strategic Product Group; Sales team; Service team; Bunks (climate chamber); Software development team; Product design team

METTLER TOLEDO is a technology leader and asserts the key competencies necessary for XPR with strong internal processes.</td>
<td>Channels (3/9)

E.g. Market Organizations (Direct Sales, Sales & Service); Sales International; Dealer; METTLER TOLEDO Experts; Online

METTLER TOLEDO pursues named channels with its own sales companies, the so-called market organizations. As a result, the company is directly represented in 40 countries. Countries where there is no direct representation are covered either by Dealer or Sales International.</td>
</tr>
<tr>
<td colspan="3">Cost Structure (9/9)

Wages and salaries; Raw materials; Manufacturing costs; Registration costs; Promotion costs

The cost structure should be homogeneous and balanced from an economic point of view, regardless of the XPR, i.e., of products and companies in general. It is therefore the goal of each individual company to keep costs as low as possible - this applies just as much to METTLER TOLEDO as it does to the XPR.</td>
<td colspan="2">Revenue Streams (5/9)

Fixed price per product sale; Service and installation fee; Training on excellent/efficient product application

A company must first and foremost generate sales and ultimately profit in order to survive on the market. Thus, in this element, the value propositions for the customers' problems are converted into financial inflows [13]. Or in other words, the company sells the product, the XPR.
METTLER TOLEDO drives a high price strategy due to its market leadership; especially in the segment of micro- and ultra-microbalances, as is the XPR.</td>
</tr>
</table>

Since no document of this kind is created as an end in itself, the business model should be subject to regular review according to Windolph [13], in which the following questions, among others, should be discussed and worked on:

- Does the business model Canvas for XPR still make sense? Do the individual elements still make sense when linked together?
- On which specific elements could the business model be improved or replaced by a new variant?
- Is the business model understood within the company?
- Can or do other ideas need to be incorporated?
- Which long-term advantages over, for example, the competition exist or can be newly expanded?

5 CONCLUSION

Success does not happen by chance and so it should be noted that there is almost no company that does not apply a business model. This is because the initial mindset as well as the idea generation are already the first essential elements on the journey to a successful business model [14]. The way and the framework or business model design used for this differ just as much as the variety of products or services offered.

Fast-moving startups as well as traditional companies find their common denominator in the business model. Only the characteristics in terms of depth, maturity or scope of the business model differ. Start-ups are not burdened by long-established processes, systems or procedures and thus have no technical legacy. Their talent is precisely tuned to the development of new approaches, as they are not (for the time being) bound to structures. As a result, they create new customer experiences because they focus on customer requirements - which changes expectations on the market side. Successful traditional companies have likewise understood how to respond to constantly changing market conditions by adopting new business model approaches. This allows them to remain successful [15] and continue to establish themselves which is in compliance with findings of the proposed research.

As simple as it sounds, the key to success is that the business model must remain in motion. The idea that a business model and thus also the corporate strategy are finalized is wrong. Therefore, it is important for companies to ensure that business models are continuously worked on and developed. Similarly, corporate success is not a linear process. This means that a chosen path may even have to be changed if there are good reasons for doing so. This is often the subject of literary discussion as to what extent changes should be made.

The main findings of the research presented in this paper are: Beyond the industry-specific pressure to change, it is necessary to pick up on various trends and adapt the business model accordingly as well as to develop new or complementary business models. For example, the steadily growing demand for a business model orientation *away from ownership* like it is presented in previosly conducted research [13]. Although cars have already been leased for decades, car subscriptions have been making it clear for some years that there are valid alternatives to pure ownership. This pattern of change can now be seen not only in the automotive industry, but from mechanical engineering to consumer goods and the pharmaceutical industry.

The challenges facing companies require not only the design of models, but also a flexible, dynamic and agile design of the infrastructure. Last but not least, this requires a positive and change-oriented corporate culture.

REFERENCES

[1] Schwab, K. (2016). Die Vierte Industrielle Revolution, *Pantheon Verlag.*
[2] Chesbrough, H. (2007). Business model innovation: It's not just about technology anymore, *Strategy and Leadership, pp.* 12-17.
[3] Holling, C. S. & Gunderson, L. H. (2002). Resilience and Adaptive Cycles, *Island Press, p.* 27.
[4] Tewes, S. (2018). Geschäftsmodelle entdecken: Die Bausteine des Erfolgs, *ZL Verlag Oberhausen, pp.* 11-17.
[5] Zott, C., Amit, R. & Massa, L. (2011). The business model: Recent developments and future research, *Journal of Management, p.* 1022-1023.
[6] Osterwalder, A. & Pigneur, Y. (2011). Business Model Generation: Ein Handbuch für Visionäre, Spielveränderer und Herausforderer, *Campus Verlag,* pp. 19-20, pp. 24-48, p. 34, p. 36, p. 38, pp. 40-44, p. 84, p. 156.
[7] Hedmann, J. & Kalling, T. (2003). The business model concept: Theoretical underpinnings and empirical illustrations, *European Journal of Information Systems*, p. 49-53.
[8] Ebert, D. & Deutsch, M. (2016). Business Model Guide: Ihr Weg zum neuen Geschäftsmodell, *KPMG,* p. 10, pp. 12-13., pp. 18-19, pp. 24-26, p. 46, pp. 48-49.
[9] Hanshaw, N. (2015). Studie: Business Model Canvas ersetzt traditionelle Businesspläne, https://innovators-guide.ch/2015/02/business-model-canvas-vs-businessplaene/, accessed 11.06.2021.
[10] MT (2021a). Investor Relations: Overview, https://www.mt.com/ch/de/home/site_content/investors.html?p=%2F, accessed 11.06.2021.
[11] MT (2021b). Laborwaagen und -wägelösungen: Mikrowaagen und Ultramikrowaagen, https://www.mt.com/ch/de/home/products/Laboratory_Weighing_Solutions/Micro_Ultra_Balances.html, accessed 11.06.2021.
[12] Reich, S. (2021). Business Model Canvas: Vorgehensweise, https://methodenpool.salzburgresearch.at/methode/business-model-canvas/, accessed 11.06.2021.
[13] Windolph, A. (2021). Business Model Canvas: Anleitung und Praxisbeispiel, https://projekte-leicht-gemacht.de/blog/pm-methoden-erklaert/business-model-canvas-anleitung-praxisbeispiel/, accessed 11.06.2021.
[14] Schächner, M. (2021). Geschäftsmodell: Fokus statt unternehmerischer Blindflug, https://www.starting-up.de/gruenden/beratung-coaching/geschaeftsmodell-entwickeln.html, accessed 22.04.2021.
[15] Hardy, J. (2019). Warum erfolgreiche Geschäftsmodell auch scheitern können, https://www.avanade.com/de-de/blogs/digital-business/application-development/warum-erfolgreiche-geschaeftsmodelle-auch-scheitern-koennen, accessed 21.04.2021.

COMETa 2022
6th INTERNATIONAL SCIENTIFIC CONFERENCE
17th - 19th November 2022
Jahorina, B&H, Republic of Srpska
University of East Sarajevo
Faculty of Mechanical Engineering
Conference on Mechanical Engineering Technologies and Applications

ISPITIVANJE RAVNOSTI GRANITNOG STOLA KMM PRIMENOM KONVENCIONALNE I KOORDINATNE METROLOGIJE

Miloš Ranisavljev[1], Andrej Razumić[2], Branko Štrbac[3], Biserka Runje[4], Amalija Horvatić Novak[5], Miodrag Hadžistević[6]

Rezime: Obezbeđenje ravnosti granitnog stola je ključni zadatak kako bi se postigla visoka pouzdanost rezultata merenja kod procedura kao što su kalibracija etalona, merne opreme, itd. Termička stabilnost i visoka tvrdoća karakterišu granit kao primarni materijal za izradu radnog stola kod koordinatnih mernih mašina (KMM). Prema veličini dozvoljenog odstupanja od ravnosti, granitni stolovi se razvrstavaju po klasama tačnosti na klase 0, 1, 2 i 3. U ovom radu je vršena procena greške ravnosti granitnog stola KMM pomoću dva merna instrumenta, koincidenc libele i KMM Carl Zeiss CONTURA G2 RDS. Koincidenc libela predstavlja konvencionalni uređaj za merenje nagiba sa visokom tačnošću, dok je KMM univerzalni merni sistem koji se koristi za merenje skoro svih dimenzionalnih i geometrijskih karakteristika kvaliteta na radnom predmetu. Rezultati merenja ravnosti su analizirani u dva nezavisna softvera i napravljena je komparativna analiza.

Ključne riječi: granitni sto, koincidenc libela, koordinatna merna mašina, ravnost.

FLATNESS INVESTIGATION OF THE CMM GRANITE TABLE VIA CONVENTIONAL AND COORDINATE METROLOGY

Abstract: bstract: Ensuring the flatness of the granite table is a crucial task to achieving high reliability of measurement results in procedures such as calibration of standards, measuring equipment, etc. Thermal stability and high hardness characterize granite as the primary material for making tables for Coordinate Measuring Machines (CMM). According to the size of the allowed deviation, granite tables are classified into several accuracy classes such as 0, 1, 2 and 3. In this paper, the flatness error of the CMM granite table was estimated using two measuring devices, the coincidence level, and

[1] M.Sc., Miloš Ranisavljev, Fakultet tehničkih nauka, Novi Sad, Srbija, mranisavljev97@uns.ac.rs
[2] Mag.ing, Andrej Razumić, Fakultet strojarstva i brodogradnje, Zagreb, Hrvatska, andrej.razumic@fsb.hr
[3] Doc. dr, Branko Štrbac, Fakultet tehničkih nauka, Novi Sad, Srbija, strbacb@uns.ac.rs
[4] Prof. dr, Biserka Runje, Fakultet strojarstva i brodogradnje, Zagreb, Hrvatska, biserka.runje@fsb.hr
[5] Dr, Amalija Horvatić Novak, Fakultet strojarstva i brodogradnje, Zagreb, Hrvatska, amalija.horvatic@fsb.hr
[6] Prof. dr, Miodrag Hadžistević, Fakultet tehničkih nauka, Novi Sad, Srbija, miodrags@uns.ac.rs

the Carl Zeiss CONTURA G2 RDS CMM. A coincidence level is a conventional device for measuring inclination with high accuracy. At the same time, CMM is a universal measuring system used to measure almost all dimensional and geometric quality characteristics on the workpiece. The results of flatness measurements were analyzed in two independent software and a comparative analysis was performed.

Key words: Coincidence Level, Coordinate Measuring Machine, Flatness, Granite surface plate

1 UVOD

Granitne površinske ploče (referentne ploče) predstavlju praktičnu realizaciju idealne ravni i obavezan su deo metrološke opreme u proizvodnim pogonima i u kalibracionim laboratorijama. Granitne površinske ploče su generalno napravljene od veoma finog zrnastnog crnog granita koji je oslobođen naprezanja u cilju maksimalne stabilnosti tokom procesa izrade. Gornja površina granitne ploče je referentna površina i obrađena je do granice ravnosti u zavisnosti od klase i veličine. Najtačnija je klasa 0 koja ima najmanju grešku ravnosti (do 5,5 μm) i naziva se često „laboratorijska klasa“. Klasa 1 se koristi kod mernih instrumenata za kontrolu a klase 2 i 3 u metrološkim laboratorijama proizvodnih preduzeća. Klase tačnosti i dozvoljene greška ravnosti granitnih ploča su predstavljene u standardu BS 817:1988 [1]. Pored klase tačnosti, dozvoljena greška ravnosti referentnih ploča zavisi i od dimenzija. Ispunjenje propisanih zahteva za ravnost granitnih ploča predstavlja neophodan uslov prilikom izvršavanja postupaka kalibracije etalona i merne opreme. Za definisanje dozvoljene greške ravnosti koristi se tolerancija ravnosti i ona označava prostor omeđen sa dve paralelne ravni u kojoj moraju biti sadržane sve nesavršenosti realne ravni [2]. Različite metode su razvijene za merenje ravnosti površina u zavisnosti od njihovih dimenzija i kvaliteta obrađene površine. Ravnost granitnih ploča se može meriti pomoću laserskih interferometara, libela (elektronskih, koincidenc), autokolimatorima i/ili koordinatnih mernih mašina (KMM) [3]. Granitni sto KMM se često koristi kao baza u formiranju koordinatnog sistema radnog predmata jer se u većini slučajeva tokom merenja radni predmet postavlja na sto. Međutim, ovu praksu treba izbegavati jer je gotovo sigurno da se naslona površina radnog predmeta značajno razlikuje od površine granitnog stola u pogledu greške ravnosti (greške oblika). Takođe, kada se vrši merenje dužine na KMM a pritom se koristi referentni koordinatni sistem mašine, greška ravnosti granitne ploče će značajno uticati na rezultat merenja jer neće biti ispunjen Abbe-ov princip. Ovo je slučaj kada se provera performansi KMM vrši korišćenjem graničnih merki prema standardu ISO 10360:2016 [4]. U eksploataciji, granitni sto KMM je često opterećen velikom težinom radnih predmeta koji mogu naneti mehanička oštećenja i narušiti specifiranu grešku ravnosti. Imajući ovu činjenicu u vidu bilo bi poželjno da se pre sprovođenja testova verifikacije KMM prema standardu ISO 10360-2016 ispita da li je greška ravnosti granitne ploče u specifikacijskim granicama. Međutim, za sada standard ovo ne uzima u obzir. S obzirom na sve navedene činjenice potrebno je periodično izmeriti grešku ravnosti granitnog (baznog) stola KMM. Najčešće korišćeni postupci za prikupljanje i analizu podataka sa granitne ploče jesu Union Jack i Moody-jev metod [5]. Ove metode govore o broju i redosledu pozicija na kome treba uzorkovati tačke sa granitne ploče.

U ovom radu, merena je greška ravnosti radnog stola koordinatne merne mašine pomoću dva merna instrumenta: koincidenc libele i koordinatne merne mašine čiji je radni sto predmet studije. Na osnovu uzorkovanih tačaka procenjena je greška

ravnosti pomoću dva softverska rešenja. Greška ravnosti na KMM je procenjena metodom rotacija kroz jednu tačku a kod koincidenc libele metodom čija se vrednost vertikalnog odstupanja dobija izračunavanjem poznatog koraka i izmerenog nagiba.

2 EKSPERIMENTALNO ISTRAŽIVANJE

Koordinatna merna mašina koja je korišćena u studiji je Carl Zeiss Contura G2 sa RDS obrtnom glavom i VAST XXT pasivnim mernim senzorom. Merni opseg mašine je 1000×1200×600 mm, a maksimalno dozvoljena greška je MPE_E=1,9 + *L*/330 µm, gde je *L* u mm. Drugi merni uređaj koji je korišćen u studiji jeste koincidenc libela, konvencionalni uređaj za merenje ugla nagiba u jedinicama mm/m. Tačnost očitavanja libele je 0,01 mm/m (približno jednako uglu od 2") a proširena merna nesigurnost kalibracije U=0,002 mm/m. Prilikom merenja, koincidenc libela je bila postavljena na nosač sa 3 tačke dodira. Potrebno je napomenuti da zbog postojanja magacina mernih pipaka na radnom stolu KMM, nije bilo moguće proceniti grešku ravnosti na čitavoj površini stola, ali da je onaj deo stola koji je najviše izložen uticajima habanja bio uključen u razmatranje. Ispitivana granitna ploča je klase 0 i prema standardu za ploču ovih dimenzija maksimalno dozvoljena greška ravnosti je 7,5 µm. Tokom merenja, u laboratoriji je bilo konstantnih 20 °C sa varijacijama od ±0.5 °C. Vlažnost vazduha nije bila praćena. Na slici 1. prikazana je KMM (a) i koincidenci libela (b).

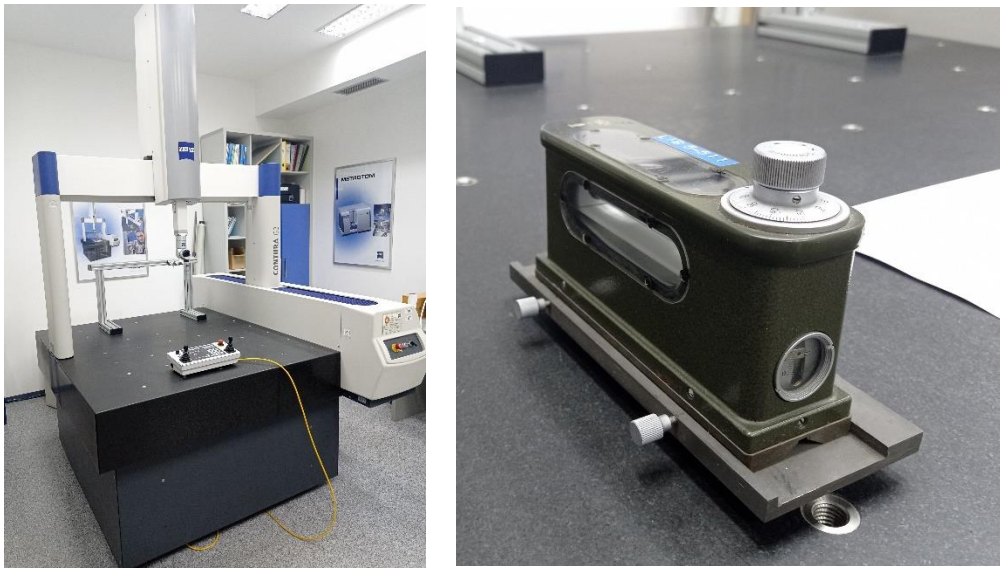

(a) (b)

Slika 1. *Carl Zeiss Contura G2 RDS (a), koincidenc libela (b)*

Prikupljanje rezultata merenja koincidenc libelom je izvršeno prema GRID strategiji. Ukupno je uzorkovano 40 mernih mesta sa po tri ponavljanja. Na slici 2 su prikazana merna mesta prema GRID strategiji i srednje vrednosti rezultata merenja su ispisane u elipse koje definišu položaj libele na granitnom stolu. Direktno merenje greške ravnosti pomoću KMM izvršeno je jednostrukim mernim pipkom sa vrhom od silicijum nitrida (SiN), prečnika 5 mm i dužine tela od 75 mm. Strategija za prikupljanje tačaka bila tačka-po-tačka i ukupno 40 tačaka, sa po tri ponavljanja, je uzorkovano.

Rezultati merenja (srednje vrednosti tri ponavljanja) na KMM su prikazani u *x*, *y*, *z* koordinatama, tabela 1. Ponavljanje je sprovedeno pri korišćenju oba merna instrumenta sa ciljem eliminisanja slučajnih grešaka u rezultatu merenja. Položaj tačaka kod direktog merenja je bio u približno istim oblastima u kojima su dobijeni rezultati sa koincidenc libele. Sva merenja su sprovedena u istom danu od strane jednog operatera.

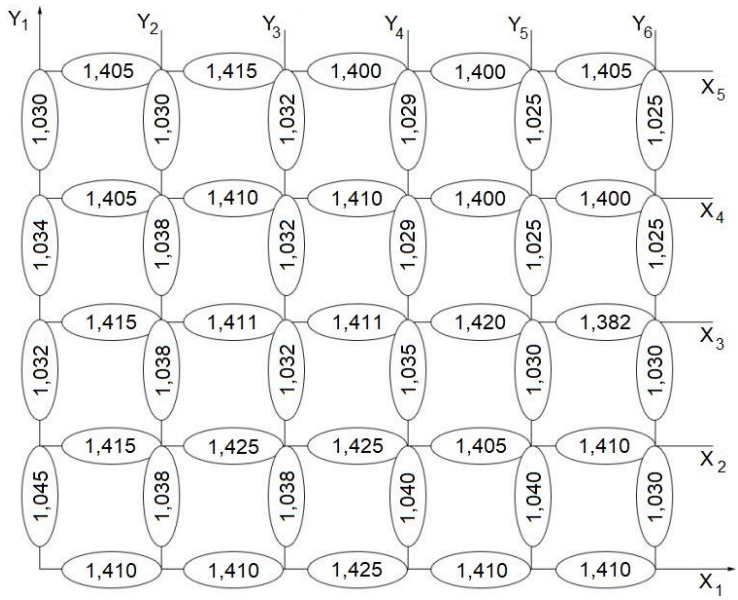

Slika 2. *Strategija za prikupljanje podataka pomoću koincidenc libele sa srednjim vrednostima rezultata merenja*

Tabela 1. *Koordinate uzorkovanih tačaka sa KMM*

x	*y*	*z*	*x*	*y*	*z*	*x*	*y*	*z*
12.5938	-1002.6854	-506.2920	412.3205	-601.1759	-506.2911	984.6031	-395.6776	-506.2896
11.70175	-788.8930	-506.2908	412.3208	-399.6198	-506.2912	984.7202	-605.1770	-506.2894
11.70381	-591.3090	-506.2911	611.0159	-399.6154	-506.2910	984.7228	-800.6996	-506.2896
11.70031	-397.4137	-506.2909	611.0099	-594.4614	-506.2906	984.7132	-999.3241	-506.2908
211.7358	-397.4074	-506.2908	611.0102	-790.5325	-506.2903	912.3834	-1086.1599	-506.2905
211.7393	-594.3643	-506.2909	611.0106	-1005.4086	-506.2915	711.0465	-1086.1432	-506.2915
211.7351	-798.9074	-506.2915	813.3193	-1005.4030	-506.2912	510.4545	-1086.1396	-506.2917
211.7381	-992.8912	-506.2919	813.3195	-796.8106	-506.2903	314.2541	-1086.1684	-506.2923
412.3180	-998.1997	-506.2918	813.3185	-590.7661	-506.2897	113.5029	-1086.1439	-506.2926
412.3209	-797.8211	-506.2910	813.3157	-395.6763	-506.2903	113.4991	-878.9448	-506.2912
310.0775	-878.9415	-506.2915	916.8035	-683.0735	-506.2891	309.5959	-683.0771	-506.2910
509.5570	-878.9452	-506.2904	713.1865	-683.0806	-506.2899	111.9715	-683.0815	-506.2910
716.0492	-878.9480	-506.2907	506.7671	-683.0822	-506.2900	111.9719	-475.8023	-506.2911
916.8035	-878.9433	-506.2896						

3 REZULTATI I DISKUSIJA

Principi rada dva razmatrana merna instrumenta za merenje greške ravnosti se značajno razlikuju. Oba merna instrumenta daju vrednosti koordinata od strane hardvera. Koincidenc libela je kao rezulat merenja dala vrednosti ugla nagiba na određenom koraku (*x*, *y*) dok KMM daje koordinate uzorovanih tačaka na mestu

kontakta vrha mernog pipka (vrši se korekcija radijusa vrha mernoh pipka i izražavaju se koordinate centra) i ispitivane granitne ploče. Za potrebe određivanja greške ravnosti razvijena su softverska rešenja za svaki merni instrument. Treba napomenuti da komercionalni softver KMM (Calypso) može da proračuna grešku ravnosti ali ne daje podatke o jednačini referentne ravni. Izlazne vrednosti iz oba softvera su slične: greška ravnosti, jednačina referentne ravni i grafički prikaz greške. Softver koji obrađuje podatke tačaka sa KMM ima mogućnost da odredi grešku ravnosti prema metodi minimalne zone i metode najmanjih kvadrata dok softver za koincidenc libelu određuje grešku ravnosti samo prema kriterijumu najmanji kvadrati. Ovo je nedostatak ovog softvera jer internacionalni standardni nalažu da se greška oblika određuje prema kriterijumu mininalne zone. Greška ravnosti se određuje kao zbir dve ekstremno udaljene uzorkovane tačke od referentne ravni. U nastavku su dati rezultati greške ravnosti korišćenjem softvera prilagođnih vrsti mernog instrumenta.

3.1 Softver za obradu rezultata koincidenc libele

Softversko rešenje za obradu rezultata koincidenc libele u cilju dobijanja greške ravnosti razvijeno je u programskon sistemu Matlab od strane Laboratorije za precizno merenje dužina Fakuteta strojarstva i brodogradnje iz Zagreba [6]. Kako je već rečeno koristi se metoda najmanjih kvadrata za definisanje jednačine referentne ravni. Metoda najmanjih kvadrata se bazira na regresiji i najbolje »fituje« ravan kroz uzorkovane tačke. Na slici 3.a prikazan je korisnični interfejs softvera i dobijena je vrednost greške ravnosti δ=0,00324 mm. Jednačina referentne ravni je: 0,00141531x + 0,00103165y – z + 0,000522302 = 0. Na slici 3.b prikaza dat je grafički prikaz referentne ravni i uzorkovanih tačaka.

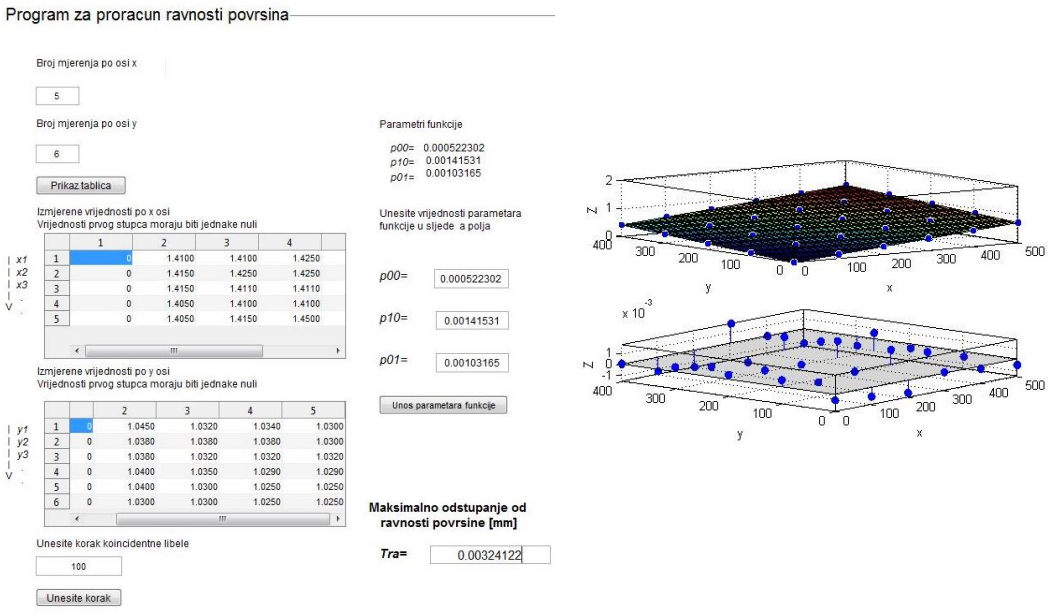

(a) (b)

Slika 3. *Korisnički interfejs softvera za obradu rezultata merenja koincidenc libelom (a), referentna ravan i uzorkovane tačke (b)*

3.2 Rotacija kroz jednu tačku-softver za obradu rezultata KMM

Za dobijanje greške ravnosti iz koordinatna uzorkovanih tačaka na KMM programsko rešenje je razvijeno u Excel-u na Fakultetu tehničkih nauka u Novom Sadu [7]. Softversko rešenje je prvenstveno razvijeno za određivanje greške ravnosti prema kriterijumu minimalne zone ali ima mogućnost određivanja greške ravnosti prema najmanjim kvadratima. Na bazi uzorkovanih tačaka određena je greška ravnosti δ=0,0019 mm i jednačina referentne ravni je $1{,}71\times10^{-6}x+1{,}715\times10^{-6}y - z-506{,}29043=0$. Na slici 4.a prikazan je korisnički interfejs softvera rotacija kroz jednu tačku a na slici 4.b dat je grafički prikaz referentne ravni i uzorkovanih tačaka. Treba napomenuti da je greška ravnosti dobijena prema kriterijumu minimalne zone manja i iznosi δ=0,00169 mm.

-506.292618	-0.000772507	28	35	min	-0.000918052
-506.289115	0.000926399	35	13	max	0.000987752
Ravnost(MZ)	0.001698906			Ravnost(LSM)	0.001905804
z	Rastojanje MZ			Z-MZ	Z-LSM
-506.292013	2.39719E-05		Rezultati	-506.2920371	-506.2921256
-506.290891	0.000913371	A	-1.81973E-06	-506.2918045	-506.2917605
-506.291161	0.000426901	B	-1.09557E-06	-506.291588	-506.2914217
-506.290964	0.000411483	C	1	-506.2913756	-506.2910892
-506.290827	0.000184465	D	506.2909615	-506.2910116	-506.2907475
-506.290925	0.000302238	Ravnost(MZ)	0.001698906	-506.2912274	-506.2910853
-506.291521	-6.96639E-05	Tacka1	28	-506.2914514	-506.291436
-506.291902	-0.000238147	Tacka2	35	-506.291664	-506.2917687
-506.291859	-0.000554333	count	16670	-506.2913048	-506.2914352
-506.291019	6.61341E-05	countmax	160000	-506.2910852	-506.2910916
-506.291111	-0.000241303	%fin.	100	-506.2908698	-506.2907544
-506.291205	-0.000556122	Coord X	498.2116023	-506.290649	-506.2904087
-506.291057	-0.000769698	Coord Y	-740.9223979	-506.2902874	-506.2900694
-506.290648	-0.00014722	Coord Z	-506.2908666	-506.2905009	-506.2904035
-506.290309	0.000406588	l	42	-506.2907157	-506.2907397
-506.291532	-0.000581001	m	270	-506.2909511	-506.2911082
-506.291277	-0.000694155	Tacaka	40	-506.290583	-506.2907626

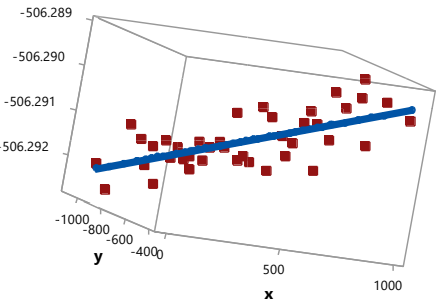

(a) (b)

Slika 4. *Korisnički interfejs softvera rotacija kroz jednu tačku (a), referentna ravan i uzorkovane tačke (b)*

Iz dobijenih rezultata se može zaključiti da je veća greška ravnosti dobijena pri merenju sa koincidenc libelom. Razlog treba tražiti u tačnosti i hardvera i softvera. Prvo, određivenje koraka (*x* i *y* koordinate) ne bazira se na preciznom merenju što znatno utiče na softversku obradu podataka. Drugo, treća decimalna kod rezultata prikazanih na slici 2 dobijena je procenom metrologa što nije uobičajena praksa. Sa druge strane, greška ravnosti dobijena na KMM odgovara maksimalno dozvoljenoj grešci MPE što je gotovo idealno. Softversko rešenje je verifikovano i poređeno sa nekoliko drugih nekomercionalnih softverskih rešenja ali i komercionalnih KMM softvera i pokazalo je veoma dobre rezultate [8]. Međutim, ono što je najvažnije jeste da su obe vrednosti greške ravnosti manje od specifirane greške ravnosti od 7,5 µm iz čega se može zaključiti da oba merna instrumenta sa predloženim metodama za ocenu greške ravnosti se mogu koristiti za ovaj metrološki zadatak. Takođe, može se zaključiti da ispitivana granitna ploča KMM zadovoljava specifikaciju proizvođača.

Pošto oba softvera daju matematički model merenja (jednačina referentne ravni) istraživanja bi trebalo proširiti na određivanje merne nesigurnosti rezultata

merenja greške ravnosti koristeći se upustvom za izražavanjem merne nesigurnosti (GUM) ili Monte Karlo simulacijom. U radu [8] dat je predlog metodologije za određivanje merne nesigurnosti KMM pri merenju ravnosti primenom GUM okvira a svakako bi bio izazov odrediti mernu nesigurnost predložene metode sa koincidenc libelom.

4 ZAKLJUČAK

U cilju postizanja tačnosti merenja mnogim metroloških zadataka potrebno je osigurati da referentne ploče zadovoljavaju specifikaciju sa aspekta dozvoljene greške ravnosti. Iako su napravljene od veoma čvrsto i otpornog materijala vremenom, usled raznih mehaničkih opretećenja i oštećenja, referentne ploče mogu izgubiti specifikacijsko ograničenje. Ovo istraživanje je pokazalo da se veoma uspešno greška ravnosti referentne ploče KMM može meriti samom KMM i koincidenc libelom. Isto tako je pokazano da granitna ploča kao deo hadverske strukture KMM zadovoljava specifikacijsku granicu proizvođača nakon trinaest godina ekspoatacije. Kao pravac budućih istraživanja predlaže se određivanje merne nesigurnosti predstavljenih metoda merenja.

ZAHVALNOST

Rezultati prezentovani u ovom radu su realizovani u okviru razvojnog projekta »Savremene proizvodne i informacione tehnologije u proizvodnom mašinstvu« čiji je nosilac Departam za proizvodno mašinstvo Fakulteta tehničkih nauka u Novom Sadu.

LITERATURA

[1] British Standard: BS 817:1988 Specification for Surface Plates.
[2] Zahwi, S. Z., Amer, M. A., Abdou, M. A., & Elmelegy, A. M. (2013). On the calibration of surface plates. Measurement, 46/2, p.p. 1019-1028.
[3] ISO 12781-1:2011 Geometrical product specifications (GPS) — Flatness — Part 1: Vocabulary and parameters of flatness.
[4] ISO 10360-12:2016 Geometrical product specifications (GPS) — Acceptance and reverification tests for coordinate measuring systems (CMS).
[5] Lakota, S., Görög, A. (2011). Flatness measurement by multi-point methods and by scanning methods. Ad Alta: Journal of interdisciplinary research, vol. 1, no. 1, p.p. 124-127.
[6] Runje, B., Marković, M., Lisjak, D., Medić, S., Kondić, Ž. (2013). Integrated procedure for flatness measurements of technical surfaces. Technical Gazette, 20/1, p.p.113-116.
[7] Radlovački, V., Hadžistević, M., Štrbac, B., Delić, M., Kamberović, B. (2016). Evaluating minimum zone flatness error using new method—Bundle of plains through one point. Precision Engineering, 43, p.p. 554-562.
[8] Štrbac, B., Mikó, B., Rodić, D., Nagy, J., & Hadžistević, M. (2020). Analysis of characteristics of non-commercial software systems for assessing flatness error by means of minimum zone method. Tehnički vjesnik, 27/2, p.p. 535-541
[9] Štrbac, B., Radlovački, V., Spasić-Jokić, V., Delić, M., Hadžistević, M. (2017). The difference between GUM and ISO/TC 15530-3 method to evaluate the measurement uncertainty of flatness by a CMM. Mapan, 32/4, p.p. 251-257

COMETa 2022
6th INTERNATIONAL SCIENTIFIC CONFERENCE
17th - 19th December 2022
Jahorina, B&H, Republic of Srpska
University of East Sarajevo
Faculty of Mechanical Engineering
Conference on Mechanical Engineering Technologies and Applications

KOMUNIKACIJA KAO KLJUČNI FAKTOR USPJEHA PROJEKTA

Mirjana Jokanović Đajić[1], Tanja Glogovac[2]

Rezime: Projekti i implementacija istih postali su dio svakodnevice. Uprkos tome, loša izvedba i neuspjeh projekata nešto je sa čim se organizacije i pojedinci često susreću. S tim u vezi, cilj je otkriti koji su to faktori koji imaju signifikantan uticaj na uspjeh projekta, te iste pokušati i unaprijediti. Gvozdeni trougao, vrijeme-opseg-budžet, odavno je proširen faktorima kao što su: ljudski resursi, kvalitet, produktivnost, profitabilnost, zadovoljstvo klijenta, efikasna komunikacija i sl.

Komunikacija je jedan od bitnijih procesa u svijetu upravljanja projektima, teško je savladati, ali je važno učiniti svaki napor kako bi se postigao njen uspjeh. Cilj rada jeste da se ukaže na važnost komunikacije prilikom implementacije projekata.

Ključne riječi: faktori uspjeha, komunikacija, projektni menadžment

COMMUNICATION AS A KEY FACTOR OF PROJECT SUCCESS

Abstract: Projects and their implementation have become part of everyday life. Despite this, poor performance and project failure is something that organizations and individuals often encounter. In this regard, the goal is to find out which factors have a significant impact on the success of the project, and to try and improve them. The golden triangle, time-scope-budget, has long been extended by factors such as: human resources, quality, productivity, profitability, client satisfaction, effective communication, etc.

Communication is one of the most important processes in the world of project management, it is difficult to master, but it is important to make every effort to achieve its success. The aim of the paper is to point out the importance of communication during the implementation of projects.

Key words: communication, project management, success factors

[1] Master, Mirjana Jokanović Đajić, Fakultet za proizvodnju i menadžment Trebinje, Univerzitet u Istočnom Sarajevu, Trebinje, BiH, mirjana.jokanovic@fpm.ues.rs.ba

[2] Master inženjer tehnologije, Tanja Glogovac, Mašinoprojekt kopring, Beograd, Srbija, tanja.glogovac@yahoo.com

1 UVOD

Uspjeh je dosta subjektivna stvar i različite osobe različito percipiraju prethodno navedeni pojam, ali se generalno smatra da je uspješan projekat onaj koji zadovoljava zahtjeve klijenta/naručioca projekta i ostalih zainteresovanih strana, a naročito dimenziju kvaliteta.

Ključni faktori uspjeha projekta mogu da posluže kao fundamentalni kriterijumi s ciljem preventivnog djelovanja kako ne bi došlo do neuspjeha projekta tokom njegove implementacije.

Različiti autori navode različite faktore kao uticajne, zavisno od područja u kome se projekt sprovodi, iskustva projektnog menadžera, znanja i sl. ali se većina slaže da se na listu signifikantnih faktora mogu uvrstiti i sljedeći: vrijeme, troškovi, kvalitet, održivost, ljudski resursi, jasni ciljevi, uspješna i efikasna komunikacija. Upravo je prethodno navedeno bilo i jedan od motivatora koji su doveli do teme ovog rada.

Komunikacija je sastavni dio života i čini preduslov bilo kakvih društvenih aktivnosti, budući da je to nezaobilazan i neprevaziđen proces koji traje, prilagođava se i mijenja, shodno datim okolnostima i vrijednostima, ne samo društvene zajednice, već i čovječanstva u cjelini.

Projektni menadžeri i članovi projektnog tima komuniciraju koristeći različite medije za prenos poruka. Važni faktori uključuju komunikaciju o tome kako će se projektom upravljati i kako će komunikacija teći u i iz projekta.

Ovaj rad dovodi u vezu komunikaciju i uspjeh projekta, odnosno daje prikaz faktora komunikacije koji imaju uticaj na uspjeh/neuspjeh projekta.

Rad je podijeljen u dva dijela. U prvom dijelu analizirana je komunikacija i sa njom povezani pojmovi, dok drugi dio daje prikaz faktora uspjeha projekta, baziranih na komunikaciji, odnosno u ovom dijelu dat je literaturni prikaz komunikacijskih faktora, prema različitim autorima, signifikantnih za uspjeh projekta. S tim u vezi, cilj ovog rada jeste da se na osnovu literaturnog pregleda da prikaz osnovnih komunikacijskih faktora koji imaju uticaj na uspjeh projekta. Metode koje su korištene prilikom obrade sekundarnih podataka su metoda analize, komparativna metoda, sinteza i dedukcija.

2 KOMUNIKACIJA, MODELI I METODE

Kada je upravljanje projektima u pitanju komunikacija između svih zainteresovanih strana je jedan od ključnih faktora za uspješno izvođenje projekta. Projektni menadžer je, između ostalog, zadužen za praćenje komunikacije kao i to da su potrebne informacije, odluke i slično, došle do svih zainteresovanih strana. Ovaj ciklus komunikacije i protoka informacija je iterativan i nastavlja se tokom čitavog trajanja projekta.

Komunikacija obuhvata efikasnu razmjenu i razumjevanje informacija između zainteresovanih strana. Efikasna komunikacija je od vitalnog značaja za uspjeh projekata, programa i portfelja; prave informacije moraju biti prenijete relevantnim stranama, tačno i doslijedno kako bi se ispunila njihova očekivanja. Komunikacija treba da bude korisna, direktna, jasna i blagovremena.

Pravovremeno proslijeđivanje informacija akterima projekta je veoma važno, posebno ako nešto utiče na obim, vrijeme, cijenu, rizik ili kvalitet zadatka, te zahtijeva blagovremenu eskalaciju putem odgovarajućih kanala komunikacije. Informacije koje će uticati na projekat – bilo dobre ili loše – su od vitalnog značaja za aktere projekta.

Komunikacija, odnosno razmjena informacija vezanih za projekat među zainteresovanim stranama može imati više oblika i to [1]:

- Štampani dokumenti, sistemi dosijea i elektronske baze podataka;

- Elektronska komunikacija i alati za konferencije, kao što su e-pošta, faks, govorna pošta, telefon, video i veb konferencije, veb stranice i veb izdavaštvo; i
- Elektronski alati za upravljanje projektima, kao što su veb interfejsi za softver za planiranje i upravljanje projektima, softver za podršku sastancima i virtuelnim kancelarijama, portali i alati za upravljanje saradničkim radom.

Osnovni model komunikacije podrazumjeva da je poruka razmjenjena između pošiljaoca i primaoca, a ključne komponente modela uključuju [1]:

- Kodiranje. Prevođenje misli, ideje na jezik koji primalac razumije.
- Poruka i povratna poruka. Izlaz kodiranja.
- Medij. Metod koji se koristi za prenošenje poruke.
- Buka. Sve što ometa prenos i razumijevanje poruke (npr. udaljenost, nepoznata tehnologija, nerazumjevanje konteksta).
- Dekodiranje. Prevođenje poruke nazad u smislene misli ili ideje.

Ono što je svojstveno za osnovni model komunikacije je potvrda poruke. Potvrda znači da primalac signalizira prijem poruke, ali ne nužno i saglasnost sa porukom. Druga radnja je odgovor na poruku, što znači da je primalac dekodirao, razumio i odgovara na poruku.

Komponente u komunikacionom modelu treba razumjeti i uzeti u obzir kada se govori o komunikaciji na projektu. Kao dio komunikacijskog procesa, pošiljalac je odgovoran da informacije budu jasne i potpune kako bi ih primalac mogao ispravno primiti i potvrditi da su pravilno shvaćene. Primalac je odgovoran da informacije budu primljene u cjelini, ispravno shvaćene i potvrđene. Ukoliko komunikacija nije uspješna to može negativno uticati na tok projekta.

Postoji nekoliko metoda komunikacije koje se koriste za razmjenu informacija među zainteresovanim stranama projekta. Ove metode se mogu široko klasifikovati na:

Interaktivna komunikacija. Između dvije ili više strana koje obavljaju višesmjernu razmjenu informacija. To je najefikasniji način da se osigura zajedničko razumjevanje svih učesnika o određenim temama, i uključuje sastanke, telefonske pozive, video konferencije itd.

Push komunikacija. Šalje se određenim primaocima koji treba da znaju informacije. Ovo osigurava da se informacije distribuiraju, ali ne potvrđuje da su zaista stigle ili da ih je razumjela namjenjena publika. Push komunikacija uključuje pisma, bilješke, izvještaje, mejlove, faksove, govornu poštu, saopštenja za štampu itd.

Pull komunikacija. Koristi se za veoma velike količine informacija ili za veoma široku publiku, što zahtjeva da primaoci pristupaju komunikacijskom sadržaju po sopstvenom nahođenju. Ove metode uključuju intranet sajtove, e-učenje i baze podataka itd.

Projektni menadžer odlučuje, na osnovu komunikacijskih zahtjeva kako i kada će se metode komunikacije koristiti u projektu. Komunikacija ne samo da drži sve u toku sa napretkom projekta, već takođe olakšava prihvatanje i vlasništvo nad glavnim projektnim odlukama i prekretnicama. Uspjeh projekta uveliko zavisi od toga da li su sve informacije, kao i očekivanja, ciljevi, potrebe, resursi, izvještaji o statusu, budžeti i zahtjevi za kupovinu redovno saopštavani svim važnim zainteresovanim stranama na projektu. Prekidi u komunikaciji su neprihvatljivi razlozi za kašnjenje projekta [1]. S obzirom na važnost komukacije planiranje komunikacije je veoma važan korak koji je potrebno sprovesti**.**

2.1. Plan komunikacije projekta

Upravljanje projektnom komunikacijom je oblast znanja koja koristi procese potrebne da bi se obezbjedilo pravovremeno i odgovarajuće stvaranje, prikupljanje, distribucija, skladištenje, pronalaženje i konačno raspolaganje projektnim informacijama. Za komunikaciju na projektu je odgovoran cijeli projektni tim. Projektni menadžer je, međutim, odgovoran za razvoj plana upravljanja komunikacijom projekta. Planiranje komunikacija je proces utvrđivanja potreba za informacijama zainteresovanih strana i definisanja pristupa komunikaciji tokom trajanja projekta.

Proces odgovara na potrebe informacija i komunikacija zainteresovanih strana u projektu; na primjer, kome su potrebne koje informacije, kada će im trebati, kako će im biti date i od strane koga. Dok svi projekti dijele potrebu za saopštavanjem informacija o projektu, informacione potrebe i metode distribucije se veoma razlikuju. Veoma važan faktor za uspjeh projekta je identifikovanje potreba za informacijama i određivanje odgovarajućih sredstava za zadovoljavanje istih. Nepravilno planiranje komunikacije će dovesti do problema kao što su kašnjenje u isporuci poruka, komunikacija osjetljivih informacija pogrešnim učesnicima u projektu ili nedostatak komunikacije sa nekim od potrebnih zainteresovanih strana.

Komunikacioni plan omogućava projektnom menadžeru da dokumentuje pristup za najefikasniju komunikaciju sa zainteresovanim stranama. Efikasna komunikacija znači da se informacije pružaju u pravom formatu, o čemu odlučuje projektni menadžer, u pravom trenutku i da se informacije dijele sa učesnicima projekta kojima su u datom trenutku potrebne za dalji rad. Efikasna komunikacija podrazumjeva pružanje samo informacija koje su potrebne. Rezultate ovog procesa planiranja treba redovno kontrolisati i revidovati tokom projekta kako bi se osigurala konstantna primjenljivost [1].

Efikasan komunikacioni plan treba da da odgovore na sljedeća pitanja:

- S kim treba da komuniciramo?
- Kada komuniciramo?
- Kako komuniciramo?
- Šta treba da se saopšti?
- Koliko često saopštavamo status?
- Kada se sastajemo kao tim?
- Kada komuniciramo sa ključnim zainteresovanim stranama i na koji način?
- Koju vrstu medija treba da koristimo i kada? U koju svrhu?
- Timska komunikacija, interni, eksterni, liderski timovi?

Zadovoljenje očekivanja stejkholdera je veoma važan faktor za uspjeh svakog projekta.

Komunikacioni plan treba da bude pripremljen na način da identifikuje sve stejkholdere i pripremi strategiju za upravljanje njihovim očekivanjima i percepcijama kroz pozitivnu komunikaciju. Takođe treba planirati angažovanje i uključivanje stejholdera putem pravih informacija pravim ljudima u pravo vrijeme [2].

2.2. Komunikaciona tehnologija

Ova stavka određuje koja pomagala ili metode će članovi projektnog tima koristiti za obavljanje neophodne komunikacije. Sa Internetom i e-poštom mogu se pronaći mnoga kreativna rešenja, kao što su serveri ili intranet projekti sa objavama, ažuriranjima i tablom. Prepreke sa kojima se susreću svi akteri projekta treba procijeniti prije nego što se razmotri koje sredstvo koristiti za svaku komunikacijsku stavku.

Metode koje se koriste za komunikaciju i prenos informacija među zainteresovanim stranama u projektu mogu se značajno razlikovati. Na primjer, projektni tim kao metode komunikacije može koristiti tehnike od kratkih razgovora pa sve do produženih sastanaka, ili od jednostavnih pisanih dokumenata do materijala (npr. rasporeda i baza podataka) koji su dostupni na mreži. Odabir metoda zavisi od primaoca informacije, vrste i hitnosti.

Analiza publike, vrsta informacija koje se saopštavaju i hitnost informacija treba da budu uračunati u metod. Tehnologija je donijela alate za saradnju i arhiviranje dokumenata za distribuciju komunikacije u vezi sa projektom. I sa odabirom alata za komunikaciju, plasiranje i arhiviranje informacija i dokumentacije treba biti pažljiv. Alati su odlični dodaci, koji omogućavaju pojedincima da „izvuku“ informacije. Međutim, nametanje tehnologije koja je neprikladna članovima na projektu ili samom projektu može kao rezultat dati nedostupne informacije, koje ostaju neaktivne. Pored toga, ono što je potrebno osigurati je da su alat i medij komunikacije odgovarajući za oblasti koje su već pomenute, alat mora već biti prihvaćen, snažno promovisan i potpuno integrisan u organizaciju pre upotrebe. U suprotnom implementacija alata na početku nekog projekta može dovesti do kašnjenja dok traje period adaptacije svih učesnika na novi alat za komunikaciju [1].

Uspješne studije slučaja donijele su neke zanimljive zaključke: bilo koji projekat ne može da se vodi bez efikasne komunikacije, a članovi tima treba da izaberu sopstvene fleksibilne, prilagođene korisniku i moderne komunikacione alate koji savršeno odgovaraju agilnim ili hibridnim metodologijama upravljanja projektima [3].

3 FAKTORI USPJEHA PROJEKATA

Svaki član projektnog tima može težiti različitim ili čak kontradiktornim ciljevima u projektu. Ovi oprečni pogledi na uspjeh mogu dovesti do lošeg cjelokupnog projektnog učinka. Kao odgovor na ove različite prioritete većina prethodne literature je identifikovala zajedničke ključne faktore uspjeha projekta i to [4]:

- troškovi,
- vrijeme,
- kvalitet.

Međutim, kako je polje uspjeha projekta postajalo sve više interesantno istraživačima, tako su se ključni faktori uspjeha projekta proširivali. Danas oni obuhvataju: motivaciju zaposlenih, vještine i znanja zaposlenih, radno okruženje, liderstvo, timski rad i sl., dok zasigurno značajno mjesto zauzima i komunikacija.

Esmail i dr. (2016) u svom radu navode da podrška, posvećenost višeg menadžmenta, konstruktivnost, timski rad, komunikacija (efikasna i otvorena), i povjerenje predstavljaju ključne faktore uspjeha većine projekata [4].

Čulo i Skenderović (2010) u radu pod nazivom “Važnost komunikacijskog menadžmenta u uspjehu projekata” zaključuju da je za menadžere projekata ključno da pravovremeno prenesu poruku, kako bi se izbjegli neuspjesi u procesu komunikacije. Takođe, autori naglašavaju da važni faktori uspjeha uključuju komunikaciju o tome kako će se upravljati projektom, kako ulaziti i izlaziti iz projekta [5].

Fajaz i dr. (2017) naglašavaju da je nesumnjivo ustanovljeno da efektivna komunkacija na projektu utiče na zaključak, te da je to faktor koji doprinosu uspjehu projekata [6].

Vu i dr. (2017) navode da efikasna komunikacija može poboljšati transparentnost informacija, tako da projektni tim može da razumije trenutni status

projekta, pravac budućih napora, te da poboljša koheziju tima, kako se bi osigurala uspješna realizacija projekta. Stoga, efikasna komunikacija pomaže u objedinjavanju koncepta projekta i ideja timova, jačanju njihovog prepoznavanja sadržaja rada, procesa zadataka i pravila i propisa, kooordinaciji ponašanja tima i na taj način doprinosi uspjehu projekta [7].

Belasi i Tukel (1996) navode da su za uspjeh projekta ključni: efektivna i jasna komunikacija, komunikacione vještine, sposobnost delegiranja autoriteta, sposobnost koordinacije, upravljačke vještine, itd. [8].

Montequin i dr. (2016) u svom istraživanju zaključuju da je za uspjeh projekta važna česta i jasna komunikacija, interna i eksterna [9].

Bril i dr. (2006) apostrofiraju da su izražene vještine verbalne komunikacije bitan faktor uspjeha projekta [10].

Fišer (2011) navodi da aktivnim slušanjem i provođenjem više vremena u neformalnim razgovorima (internim i eksternim) možemo biti na korak bliže do uspješne implementacije projekta [11].

Za uspjeh projekta bitno je uspostaviti kako formalne, tako i neformalne komunikacione kanale, imati prikladnu komunikaciju sa svim stejkholderima, te osigurati optimalan nivo razumijevanja komunikacije svih učesnika u projektu, navodi autor Nikolas Klark (2010) [12].

Sposobnost projektnog menadžera da objasni eventualne izmjene na projektu, odnosno izmjenu plana projekta smatra se jednim od bitnijih faktora uspjeha projekta, navodi se u radu, autora Ričarda Njutna (2009) [13].

Timska komunikacija, saradnja, koordinacija, klima, sukobi, te učinak tima, presudni su za uspjeh projekta, zaključuje se u radu pod nazivom ”Razumijevanja značenja uspjeh projekta” (Sudhakar, 2016) [14].

Sposobnost tima da upravlja projektnim resursima, komunikacija, unapređenje i postizanje ciljeva u svrhu promocije komunikacije kroz projekat, unapređenje znanja kroz dodatne edukacije i treninge, korišćenje pravih vještina, česti sastanci, kao i postojanje jasnih komunikacijskih kanali ključni su za projekat navode Oh i Choi (2020) [15].

Efikasno i efikasno angažovanje i komunikacija uključuje određivanje kako, kada, koliko često i pod kojim uslovima stejkholderi žele da budu – i treba da budu – uključeni. Komunikacija je ključni dio angažovanja; međutim, angažovanje ulazi dublje kako bi uključilo svijest o idejama drugih, asimilaciju drugih perspektive i kolektivno oblikovanje zajedničkog rešenja. Angažovanje uključuje izgradnju i održavanje čvrstih odnosa kroz čestu, dvosmijernu komunikaciju. Saradnja se može odvijati kroz interaktivne sastanke, sastanke licem u lice,neformalni dijalog i aktivnosti razmijene znanja [16].

Prethodno navedeni faktori uspjeha, sa akcentom na komunikaciju, prikazani su u tabeli 1.

Tabela 1. *Faktori uspjeha projekta, bazirani na komunikaciji*

FAKTOR USPJEHA	**NAZIV AUTORA I RADA U KOME SE NAVODI FAKTOR**
▪ efektivna komunikacija ▪ otvorena komunikacija	Esmaeilli, B., Pellicer, E., Molenaar, K. R. [4]
▪ sposobnost pravovremenog prenošenja poruke, ▪ komunikacija o načinu upravljanja projektom	Čulo, K., Skenderović, V. [5]

▪ efektivna komunikacija	Fayaz, A., Kamal, Y., Amin, S., Khan, S. [6]
▪ efikasna komunikacija	Wu, G., Liu, C., Zhao, X., Zuo, J. [7]
▪ efikasna komunikacija, ▪ jasna komunikacija, ▪ komunikacione vještine	Belassi, W., Tukel, O. I. [8]
▪ česta komunikacija, ▪ jasna komunikacija	Montequin, V. R., Cousillas, S. M., Alvarez, V., Villanueva, J. [9]
▪ izražene vještine verbalne komunikacije	Brill, J. M., Bishop, M. J., Walker, A. E. [10]
▪ aktivno slušanje, ▪ provođenje više vremena u neformalnim razgovorima	Fisher, E. [11]
▪ uspostavljanje formalnih komunikacionih kanala ▪ uspostavljanje neformlanih komunikacionih kanala, ▪ prikladna komunikacija sa svim stejkholderima, ▪ osiguranje optimalnog nivoa razumijevanja komunikacije svih učesnika u projektu	Clarke, N. [12]
▪ sposobnost projektnog menadžera da objasni eventualne izmjene na projektu	Newton, R. [13]
▪ timska komunikacija	Sudhakar, G. P. [14]
▪ postojanje jasnih komunikacijskih kanala, ▪ česti sastanci	Oh, M., Choi, S. [15]

4 ZAKLJUČCI

Upravljanje projektnom komunikacijom uključuje brojne procese, resurse i aktivnosti, potrebne kako bi se obezbijedilo blagovremeno i efikasno generisanje, prikupljanje, distribucija, skladištenje, preuzimanje i konačno raspolaganje projektnim informacijama.

Upravo zbog prethodno navedenog, menadžeri projekata koriste oko 90% svog vremena u internoj i eksternoj komunikaciji, bilo sa članovima tima ili sa ostalim zainteresovanim stranama projekta.

Efikasna komunikacija djeluje kao most koji spaja različite stejkholdere projekta, povezujući ih u jednu koherentnu cjelinu, a sve s ciljem uspjeha projekta.

Na osnovu pregleda literature autora današnjice i na osnovu uvida u veliki broj radova, što svjedoči o tome koliko je ova tematika zanimljiva i još uvijek neiscrpno polje istraživanja, jasno je vidljivo da faktori komunikacije (efikasna, jasna i česta komunikacija, jasni komunikacioni kanali, aktivno slušanje, česti sastanci i sl.) ima značajan uticaj na uspjeh projekata i da im treba posvetiti posebnu pažnju prilikom implementacije projekta, kako bi isti uspješno bio završen.

Jedan od glavnih doprinosa ovog rada je taj što će on da obezbijedi naučnoj i poslovnoj zajednici pregled raspoložive teorije iz oblasti koja je predmet rada. Takođe, rezultati istraživanja bi trebali da posluže kao okvir za adekvatno pozicioniranje novih instraživačkih aktivnosti. Konkretno, što se tiče budućih istraživanja autora, planirano je

da se sprovede primarno istraživanje s ciljem utvrđivanja podudarnosti primarnih i sekundarnih podataka.

LITERATURA

[1] Ksenija Čulo, Vladimir Skendrovic (2010). Communication management is critical for project succes, *Informatol*, 43, 2010., 3, 228-235

[2] Kirti Rajhans (2018). Effective Communication Management: A Key to Stakeholder Relationship Management in Project-Based Organizations, *The IUP Journal of Soft Skills*, Vol. XII, No. 4, 2018

[3] Matthew R. Ganis, Maïgorzata Waszkiewicz (2018). Digital Communication Tools as a Success Factor of Interdisciplinary Projects, *Problemy ZarzÈdzania – Management Issues*, vol. 16, no. 4(77): 85 –96

[4] Esmaeilli, B., Pellicer, E., Molenaar, K. R. (2014). Critical Success Factors for Construction Projects, *18th International Congress on Project Management and Engineering***,** p.p. 458-468.

[5] Čulo, K., Skenderović, V. (2010). Communication Management is Critical for Project Success, *Informatol*, vol. 43, p.p. 328-235

[6] Fayaz, A., Kamal, Y., Amin, S., Khan, S. (2017). Critical Success Factors in Information Technology Projects, *Management Science Letters*, vol. 7, p.p. 73-80

[7] Wu, G., Liu, C., Zhao, X., Zuo, J. (2017). Investigating the relationship between communication-conflict interaction and project success among construction project teams, *Internation Journal of Project Management*, vol. 35, p.p. 1466-1482

[8] Belassi, W., Tukel, O. I. (1996). A new framework for determining critical success/failure factors in projects, *International Journal of Project Management*

[9] Montequin, V. R., Cousillas, S. M., Alvarez, V., Villanueva, J. (2016). Success Factors and Failure Causes in Projects: Analysis of Cluster Patterns Using Self-organizing Maps, *Procedia Computer Science*, vol. 100, p.p. 440-448

[10] Brill, J. M., Bishop, M. J., Walker, A. E. (2006). The Competencies and Characteristics Required of an Effective Project Manager: A Web/Based Delphi Study, *Educational Technology Research and Development*, Vol 54, No 2, p.p. 115-140

[11] Fisher, E. (2011). What practitioners consider to be the skills and behaviours of an effective people project manager, *International Journal of Project Management*, Vol 29, No 8, p.p. 994-1002

[12] Clarke, N. (2010). Emotional Intelligence and Its Relationship to Transformational Leadership and Key Project Manager Competences, *Project Management Journal*, Vol. 41, No. 2, p.p. 5-20

[13] Newton, R. (2009). The Project Manager: Mastering the Art of Delivery, Financial Times Management, 2nd Edition, 2009, ISBN-10: 0273723421

[14] Sudhakar, G. P. (2016). Understanding the Meaning of „Project Success“, *Binus Business Review*, Vol. 7, No. 2, p.p. 163-169

[15] Oh, M., Choi, S. (2020). The Competence of Project Team Members and Success Factors with Open Innovation, *Journal of Open Innovation: Technology, Market and Complexity*, vol. 6. no. 51

[16] PMI (Project Management Institut, Global standard) (2021). The standard for project management and a guide to the project management body of knowledge (PMBOK® GUIDE), Seventh Edition

COMETa 2022
6th INTERNATIONAL SCIENTIFIC CONFERENCE
17th - 19th November 2022
Jahorina, B&H, Republic of Srpska
University of East Sarajevo
Faculty of Mechanical Engineering
Conference on Mechanical Engineering Technologies and Applications

COMPARATIVE ANALYSIS COMPETENCIES IN TRADITIONAL AND AGILE PROJECT MANAGEMENT APPROACHES

Marija Savković [1], Nikola Komatina [2], Snežana Nestić[3], Ranka Gojković[4]

Abstract: In order for the project to be successfully implemented, each individual involved in the project must possess appropriate competencies and skills. Competencies/skills have a great influence when assembling the project team itself and when deciding on the inclusion of new members in the existing project team. In particular, the competencies and skills of the project manager have an impact on the successful realization of the project's goals. The members of the project team must possess certain competencies/skills in order to successfully cooperate with each other and to successfully implement the tasks assigned to them. The main goal of this research paper is a comparative review and analysis of competencies/skills in traditional and agile project management approaches. Also, the paper highlights the roles, responsibilities and powers of each team member, both in the traditional and in the agile approach.

Key words: agile project management, competencies/skills, traditional project management

1 INTRODUCTION

Every individual involved in the project, be it a project manager, sponsor, member of the project team, must possess knowledge, skills and competences in order to successfully implement the project. Competencies represent an individual's underlying characteristic that is causally related to effective job performance. Skills/competencies have a great impact when assembling a project team and when including new members in an existing project team. Also, the success of project

[1] MSc, Marija Savković, University of Kragujevac, Faculty of Engineering, Kragujevac, Srbija, marija.savkovic@kg.ac.rs
[2] MSc, Nikola Komatina, University of Kragujevac, Faculty of Engineering, Kragujevac, Srbija, nkomatina@kg.ac.rs
[3] PhD, Snežana Nestić, University of Kragujevac, Faculty of Engineering, Kragujevac, Srbija, s.nestic@kg.ac.rs
[4] PhD, Ranka Gojković, University of East Sarajevo, Faculty of Mechanical Engineering, East Sarajevo, Bosnia and Herzegovina, ranka.gojkovic@ues.rs.ba

implementation largely depends on the competencies and skills of the project manager and other members of the project team. The members of the project team must possess certain competencies/skills in order to successfully cooperate with each other and to successfully implement the tasks assigned to them. New project management approaches require new skills/competencies (Kostić, 2017).

Traditional project management is a linear and sequential approach that is applied in the simplest situations when the project is short, when the goals and requirements of the users/clients are clear, if the initial requirements and goals of the project will not change to a large extent during the project implementation. Traditional projects are quite predictable and uncomplicated, they are implemented in a stable environment and are characterized by a very low rate of change in requirements (Wysocki, 2009). Also, these projects do not require a large involvement of end users in the implementation of the project (Fernandez, Fernandez, 2008).

Agile management as a new project management approach was developed to overcome the basic shortcomings of traditional project management such as: rigidity, non-responsiveness to changes and detailed planning. An agile project management approach is adequate in complex and uncertain situations when changes are frequent and unpredictable and when it is not possible to carry out precise assessments, early predictions and design solutions at the beginning. Unlike traditional projects, in agile projects the connection between the organization and the client is very strong and clients often change their requirements and expectations (in the sense of requiring additional functionalities) during the implementation of the project (Hass, 2007; Wysocki, 2009).

Both approaches to project management require the possession of certain skills/competencies. The purpose of the paper is to present key competencies which have particular importance in achieving project success both in the traditional and in the agile approach to project management. The paper provides a comparative overview of key competencies/skills in both approaches to project management.

2 SKILLS/COMPETENCIES IN TRADITIONAL PROJECT MANAGEMENT APPROACH

Traditional project management is a linear and sequential approach that is applied in the simplest situations when the project is short, when the goals and requirements of the users/clients are clear, if the initial requirements and goals of the project will not change to a large extent during the project implementation and when it is necessary to results are achieved within the defined time, scope and budget. According to the traditional understanding, any project that was completed on time, within the budget, with a high quality result was considered successful (Müller, Turner, 2007).

In the traditional approach, the project manager has a key role. He manages the implementation of the project in order to complete the project in the most efficient way. The basic and most important task of the project manager is to ensure that the project is realized in accordance with the available resources (in the planned time and with the planned costs). The project manager is simultaneously a leader, entrepreneur, resource allocator, integrator, negotiator (Cockburn, Highsmith, 2001**;** Colomo-Palacios et al., 2013). He leads the project team, coordinates the activities of all members of the project team and directs their activities in order to successfully implement the project (Hoda et al., 2013).

Edum-Fotve McCaffer (2000) believes that the most important skills and competencies of a project manager are: technical skills, time management,

presentation and written expression skills, decision-making ability, negotiation skills, task delegation skills, teamwork, computer skills, meeting management, stress management and problem solving skills. Pant and Baroudi (2007) list the following as the most important skills and competencies: communication skills, interpersonal skills, technical competencies, cognitive abilities, flexibility, ability to make decisions, ability to solve problems, reliability. Tohidi and Jabbari (2012) believe that the most important skills of a project manager are the motivation of team members, human resource management, leadership, correct attitude towards the environment, correct attitude towards co-workers. According to Madter et al. (2012), the most important skills of a project manager are: ability to work in a team, ability to manage people, self-confidence, problem-solving orientation, communication ability, interpersonal skills, conflict management and change management. Kerzner points out leadership abilities, ambition, creativity, flexibility and adaptability, personal commitment, vision, creating trust, ability to persuade, ability to make decisions, ability to identify problems, ability to organize work to subordinates as the main competences. El-Sabaa (2001) lists as the most important skills of project manager: human skill (mobilizing, communication, delegating authority, political sensitivity, high self-esteem, and enthusiasm), conceptual and organizational skill (planning, organizing, strong goal orientation, ability to see the project as a whole, ability to visualize the relationship of the project to the industry and the community, and strong problem orientation), technical skill (special knowledge in use of tools and techniques; project knowledge; understanding methods, processes, and procedures; technology required; and skills in use of computer).

The project sponsor is a person from top management or an organization that is responsible for the smooth implementation of the project. It ensures the financing of the project and provides the necessary material resources and protects the project from adverse influences and problems. He is the supervisor of the project manager. The sponsor helps the members of the project team in achieving the goals, but is not in charge of solving problems on the project. It points out project limitations, provides necessary advice and warns of any changes should they occur. Based on the analysis of the tasks performed by the sponsors, it can be concluded that they must possess the following skills: communication skills, flexibility, ability to negotiate, ability to manage changes, etc (Tohidi, Jabbari, 2012).

The members of the project team are directly involved in the implementation of the project. They must possess a full range of skills and competencies in order to effectively carry out the tasks assigned to them. A review of literature sources found that the most important skills and competencies that project team members must possess are: technical skills and competencies, communication skills, collaboration skills with other members of the project team, the ability to negotiate with other members of the project team, orientation to the efficient execution of tasks, the ability to continuous learning and improvement, etc (Chipulu et al., 2012). Also, members of the project team must be characterized by sociability, politeness, patience, compassion towards other members of the project team, the ability to communicate assertively and the ability to self-control (Colomo-Palacios et al., 2013). The most important personal qualities that project team members should possess are: professionalism, reliability, perseverance and consistency, ambition, flexibility, thoroughness in work and attention to details. Project team members must have good communication skills in order to maintain a harmonious relationship within the team (Tohidi, Jabbari, 2012).

3 SKILLS/COMPETENCIES IN AGILE PROJECT MANAGEMENT APPROACH

Agile approach to project management involves a permanent and active role of all actors involved in the implementation of the project (client, development team, stakeholders etc.). All actors involved in the implementation of the project must continuously communicate and exchange information in order to successfully implement the project. This approach focuses in particular on empowering and encouraging self-organized multi-functional teams to give their maximum contribution during project implementation (Augustine, 2005; Denning, 2015; Ismail, Mansor, 2018).

Unlike the traditional project manager, agile manager is less implemented by control and monitoring of the members of the development team. People orientation and focus on the overall picture of the project and its connection with the environment are the most essential skills of agile project managers. The Agile project manager focuses especially on the project team and takes over the role of mentors facilitator and intermediaries. Effective project managers should be good communicators. He provides support to team members and encourages cooperation and interaction within the team. It focuses especially on promoting teamwork and harmonious relationship between project team members. He leads, motivates and directs members of the project team to successfully implement the project. Agile project manager provides assistance to team members to make their tasks as efficiently and achieve the best possible effectiveness. It is more oriented to people and interactions between them, but on the plan. Also, agile project manager must possess the ability to adapt to changes, the ability to handle adverse, tiring and stressful issues and situations, must be comfortable and open with new ideas and approaches (Liikamaa, 2015).

Based on the analysis of scientific research papers, the most important skills and competencies of agile project manager are: organizational skills, orientation to results and continuous improvement, organization of meetings, communication skills, orientation to problems that may occur, analytical thinking and reasoning, critical thinking, knowledge and understanding of the organization environment (supplier, customers), the skill of flexible analysis of the situation, the observation of emergency situations, understanding of uncertain, complex and abstract situations, management of changes and effective problem solving (Banerjee, 2016; Sutling, 2014) (Table 1.). The most importatnt personal qualities of agile project managers are: leadership capabilities, emotional intelligence, professionalism, empathy and understanding, innovation, confidence, ability, efficient decision-making, harism and positive attitude, self-consciousness, flexibility, tacticality, reliability, ethical behavior (Sutling, 2014).

Two new roles appear in the agile approach to project management are Scrum Master and Product Owner. The tasks and roles of Product Owner and Scrum Masters are complementary because Product Owner is in charge of defining what needs to be done, and Scrum Master is in charge of finding the way it can be done (Schwaber, Sutherland, 2012). The Product Owner represents the interests of the client and its most important task is to manage the expectations and requirements of customers/clients (Fisher, 2011). Also, Product Owner is responsible for achieving results.

The Scrum Master is a mediator between the Product Owner and members of the development team. On the one hand, he helps the development team to overcome difficulties and on the other hand, it provides recommendations and suggestions to the product owner to bring the product's most efficient way to meet customer requirements (Deemer et al., 2012). With all that in mind, it can be concluded that the powers of Scrum Master are limited in relation to the authority of the traditional project manager (Adkins, 2015). He has no authority to control the members of the project team during

the performing of tasks. Scrum Master performs facilitation and coaching team (Thomas, Mengel, 2008). In order to successfully direct and lead the project team Scrum Master must possess good negotiating and communication skills (Cheng et al., 2005). Also, Scrum Master must be honest and correct to associates and must not have hidden intentions (Rubin, 2012), must possess a harism and be a positive and extrovert person.

The review of the literature can be concluded that the most important skills and competencies which must members of the agile project teams own are: communication skills, taking up in performing tasks, orientation on rules, orientation to problems, critical and abstract thinking, sociability, empathy, politeness, patience, ability of acertive communication and the ability of self-control (Rubin, 2012). Also, members of the project team must have the ability of self-development and ability to contain learning and improvement (Clarke, 2010). The most significant personal qualities that must have members of the project team are: professionalism, innovation, creativity, perseverance, consistency, enthusiasm, proactgiveness, reliability, flexibility, honesty etc. (Table 1.).

4 COMPARATIVE REVIEW AND ANALYSIS COMPETENCIES IN TRADITIONAL AND AGILE PROJECT MANAGEMENT

Table 1. provides a comparative overview of the most important skills/competencies in the traditional and agile approach to project management. The table represents the systematization of skills/competencies from twenty scientific research papers in this field.

Table 1. *Comparative overview of skills/competencies in traditional and agile approaches to project management*

Skills/ competencies	***A traditional approach***	***An agile approach***	***Skills/ competencies***	***A traditional approach***	***An agile approach***
personal characteristics			*coordination skills of team members*		✓
leadership skills		✓	*managing group dynamics*		✓
emotional intelligence		✓	*motivation of team members*		✓
innovation and creativity		✓	*stress management*		✓
perseverance and consistency	✓	✓	*conflict management*		✓
enthusiasm	✓	✓	*teaching/mentoring skills*		✓
ability to make decisions	✓	✓	***task-oriented skills/competencies***		
proactiveness		✓	*focusing on tasks*	✓	
flexibility		✓	*taking the initiative in the execution of tasks*		✓
communication skills	✓	✓	*ability to delegate tasks*	✓	
organizational/managerial skills/competencies			*orientation to problems that may arise*		✓
managing teams		✓	*rule orientation*	✓	
orientation to results	✓	✓	*critical thinking*		✓
negotiation skills with co-workers		✓	*the ability to think logically and reason*		✓
organization of meetings		✓	***skills related to self-development and***		

Skills/ competencies	***A traditional approach***	***An agile approach***	***Skills/ competencies***	***A traditional approach***	***An agile approach***
			development of associates		
analysis of the organizational structure	✓		*the ability of self-development*		✓
knowledge of organizational culture		✓	*self-development of competencies among associates*		✓
technical project management skills/competencies			*ability for continuous learning and improvement*		✓
understanding the goals and requirements of the project	✓		*performance evaluation*		✓
technical expertise	✓		***contextual skills/ competencies***		
specialized knowledge related to the application of project management tools and techniques	✓		*knowledge of the process*	✓	
knowledge of standards	✓		*knowledge and understanding of the organization's environment (suppliers, customers)*		✓
human resource management skills	✓		*customer/ stakeholder orientation*		✓
cost and financial management on the project	✓		*ability to negotiate with stakeholders*		✓
management of material resources	✓		*marketing and sales skills*	✓	
quality management	✓		***skills that enable system stabilization during crisis***		
project risk management	✓		*the ability to proactively analyze problems*		✓
documentation management	✓		*crisis situation management*		✓
time management	✓		*understand complex situation*		✓
people-oriented skills/competencies			*change management*		✓
analytical thinking		✓			

Particularly important skills in the traditional project management approach are: focus on the technical aspects of the project, rule orientation, understanding the goals and requirements of the project, technical expertise and possession of specialized knowledge related to the application of project management tools and techniques, delegation of tasks to associates. In contrast to traditional project management, in agile project management the most important skills/competencies that the project manager and other members of the project team must possess are: knowledge and understanding of the organization's environment, leadership skills, ability to think critically, the ability of self-development, ability to resolve conflicts, inclination towards teamwork. Also, openness, creativity, flexibility, enthusiasm, emotional intelligence etc are very important.

5 CONCLUSION

In order for contemporary organizations to ensure their survival in a turbulent environment, it is necessary to undertake strategic changes and overcome all the challenges they face. Organizations achieve these goals through the implementation of projects. The successful implementation of projects is largely determined by the skills/competencies of every individual involved in the project, be it a project manager or member of the project team.

In this paper literature review and analysis of key competencies is given. The table presents a systematic literature review of main competencies/skills that project managers and other members of the project team involved in project implementation must possess. These skills/competencies are taken into account when assembling the project team and when deciding whether to include new members in the existing project team.

By analyzing the table, it can be concluded that certain skills/competencies are of particular importance in the traditional and some in the agile approach to project management. Thus, skills such as focus on the technical aspects of the project, rule orientation, understanding the goals and requirements of the project, technical expertise and possession of specialized knowledge related to the application of project management tools and techniques, delegation of tasks to associates are characteristic of traditional project management and skills/competencies such as knowledge and understanding of the organization's environment, leadership skills, ability to think critically, the ability of self-development, ability to resolve conflicts, inclination towards teamwork, the ability to think logically and reason, openness, creativity, flexibility, enthusiasm, emotional intelligence etc. agile project manager and other members of the project team must possess an agile approach to project management. Some skills/competencies (such as orientation to results, ability to make decisions and communication skills etc.) are represented in both project management approaches.

LITERATURE

[1] Adkins, L. (2015). Coaching agile teams: a companion for Scrum Masters, agile coaches, and project managers in transition, Boston, MA: Addison-Wesly Pearson Education.

[2] Cheng, M., Dainty, A., Moore, D. (2005), What makes a good project manager?, *Human Resource Management Journal*, Vol. 15 No. 1, pp. 25–37.

[3] Chipulu, M. N., Ojiako, U., Williams, T. (2012). A Multidimensional Analysis of Project Manager Competences, *IEEE Transactions on Engineering Management*, vol. 60, no. 3.

[4] Clarke, N. (2010). Emotional intelligence and its relationship to transformational leadership and key project manager competences, *Project Management Journal*, vol. 4, no. 2, p.p. 5-20.

[5] Cockburn, A., Highsmith, J. (2001). Agile software development, the people factor, *Computer*, 34 (11), p. p.131-133.

[6] Colomo-Palacios, R., Aramo-Immonen, H., Bikfalvi, A., Mancebo, N., Vanharanta, H. (2013). Project Managers' Competence Identification, *Enhancing the Modern Organization through Information Technology Professionals*, p. p.17-31.

[7] Edum-Fotwe, F. T., McCaffer, R. (2000). Developing project management competency: perspectives from the construction industry, *International journal of project management*, 18 (2), p. p. 111-124.

[8] El-Sabaa, S. (2001). The skills and career path of an effective project manager, *International Journal of Project Management*, vol. 19, no. 1, p. p.1-7.
[9] Deemer, P., Benefield, G., Larman, C., Vodde, B. (2012), A lightweight guide to the theory and practice of scrum (version 2.0), *Technical report*,
[10] Fernandez, D. J., Fernandez, J. D. (2008). Agile project management- agilism versus traditional approaches, *Journal of Computer Information Systems*, 49 (2), p. p.10-17.
[11] Fisher, E. (2011), What practitioners consider to be the skills and behaviours of an effective people project manager, *International Journal of Project Management*, vol. 29, no. 8, p. p. 994-1002.
[12] Hass, K. B. (2007). The blending of traditional and agile project management, *PM world today*, 9 (5), p. p. 1-8.
[13] Hoda R., Noble J., Marshall S. (2011). The impact of inadequate customer collaboration on self-organizing Agile teams, *Inf. Softw. Technol.*, vol. 53, no. 5, p. p. 521-534.
[14] Kerzner, H. (2005). Project Management, 9th ed. New Jersey: John Wiley & Sons
[15] Kostić, M. (2017). Challenges of Agile Practices Implementation in The Medical Device Software Development Methodologies, European Project Management Journal, vol. 7, issue 2, pp. 36-44.
[16] Liikamaa, Kirsi. (2015). Developing a Project Manager's Competencies: A Collective View of the Most Important Competencies. *Procedia Manufacturing*, 3. p. p. 681-687.
[17] Madter, N., Bower, D. A., Aritua, B. (2012), Projects and personalities: A framework for individualising project management career development in the construction industry, *International Journal of Project Management*, 30 (3), p. p. 273-281.
[18] Müller, R., Turner, R. (2007), The influence of project managers on project success criteria and project success by type of project, *European management journal*, 25 (4), p.p. 298-309.
[19] Pant, I., Baroudi, B. (2008), Project management education: The human skills imperative, *International journal of project management*, 26 (2), p. p.124-128.
[20] Rubin, K. S. (2012). Essential Scrum: A Practical Guide to the Most Popular Agile Process (1st ed.), Addison-Wesley Professional.
[21] Schwaber, K., & Sutherland, J. (2012). Software in 30 days: how agile managers beat the odds, delight their customers, and leave competitors in the dust. John Wiley & Sons.
[22] Banerjee, S. (2016). Role of a Project Manager in Managing Agile Projects, *Journal of Business & Financial Affairs*. 5.
[23] Sutling, K., Mansor, Z., Widyarto, S. (2014). The Influence of Project Manager Behaviour in Determine Agile Software Development Project Success.
[24] Thomas, J., Mengel, T. (2008). Preparing project managers to deal with complexity - Advanced project management education, *International Journal of Project Management*, vol. 26, no. 3, p.p. 304-315.
[25] Tohidi, H., Jabbari, M. M. (2012). Role of human aspects in project management. *Procedia-Social and Behavioral Sciences*, *31*, p. p 837-840.
[26] Wysocki, R. K. (2009). Effective project management: traditional, agile, extreme. (5th ed.) Indianapolis: Wiley Publishing

COMETa 2022
6th INTERNATIONAL SCIENTIFIC CONFERENCE
17th - 19th November 2022
Jahorina, B&H, Republic of Srpska
University of East Sarajevo
Faculty of Mechanical Engineering
Conference on Mechanical Engineering Technologies and Applications

PROJECT METHODOLOGIES AND THEIR IMPACT ON THE PROJECT SUCCESS

Mirjana Jokanović Đajić[1], Soukaina El Hajjaji[2], Ranka Gojković[3]

Abstract: It is very difficult or even impossible to know precisely at the initial planning stage what are all the activities that need to be carried out in order to complete the project and what their cost and duration parameters are. Also, this could be less or more complex, depending on the project methodology. Traditional approach consists of five phases, which include the planning phase or activity, which means that with this approach planning is imperative. On the other hand, through agile methodology, projects are typically completed in cycles with the next cycle returning to the planning phase. Nowdays it isn't unknown that many organizations are using a combination of both agile and traditional methods (hybrib model) which may introduce more overhead in regards to additional project documentation. The purpose of this paper is to qualitatively express, based on a literature review, the influence of different project methodologies on the project success, with an emphasis on the application of the project methodologies in different branches of the economy. The results of this work should show which project methodology is best to use in which economic area, in order to more easily ensure the success of the project.

Key words: projects, project methodologies, project success

1 INTRODUCTION

The paradigm of traditional project management says: ”Plan first, execute second.” On the other hand, in the center of increased globalization is the need for project managers to have flexibility in a project system in order to be able to adjust constantly to emerging challenges and opportunities. The need to distribute responsibility and initiative in support of adaptation to change is familiar territory to agile approaches to projects. The paradigm of agile methodology is ”Adapt to change

[1] Master, Mirjana Jokanović Đajić, Fakultet za proizvodnju i menadžment Trebinje, Univerzitet u Istočnom Sarajevu, Trebinje, BiH, mirjana.jokanovic@fpm.ues.rs.ba
[2] dr Soukaina El Hajjaji, Faculty of juridic, economic and social sciences, Abdelmalek Essaâdi University, Tangier, Morocco, soukaina.elhajjaji@gmail.com
[3] doc. dr Ranka Gojković, Univerzitet u Istočnom Sarajevu, Mašinski fakultet Istočno Sarajevo, Istočno Sarajevo, BiH, ranka.gojkovic@ues.rs.ba

as you iterate." These competing and completely different methodologies represent two ends of a spectrum between linear and non-linear project management processes. Nowdays many development projects use combination of the previous mentioned two methodologies so-called hybrid methodology.

The paper analyzes the connection between project methodologies (traditional, agile, hybrid) and the project success. Also, the paper presents which methodology will easily and better lead project to its success, depending on the field of application, based on the literature review. The methods used in the processing of secondary data are analysis method, comparative method, synthesis and deduction.

2 PROJECT METHODOLOGIES

Since the end of the 1980s, project management has profoundly transformed the practices and performance of organizations. It has spread internationally in various sectors: services, mass industries, public companies, SMEs, Research & Development… Companies are always looking for new and improved ways to complete their projects more efficiently. This has led to the development of many new methodologies of project management, from traditional methodology to Agile and hybrid methodology. The essential objective of all these project management styles is to be able to bring value to the customer more quickly. It promotes adaptive planning, evolutionary development and early delivery and encourages continuous improvement. In this article, three different methodologies are presented (traditional, agile and hybrid) and the difference between them regarding project planning. According to Serrador P. [1], different industries may require different types of projects and have different project management needs which is may have an impact on the need for planning and the effect of planning on success.

2.1 Traditional Methodology

Traditional, or waterfall, project management is a legacy of industry and building construction, and its main phases were first modeled in 1956 by Herbert D. Benington. Traditional project management is an established methodology where projects are conducted in a sequential cycle. It follows a fixed sequence: initiation, planning, execution, monitoring and closure. The traditional approach to project management emphasizes linear processes, documentation, up-front planning and prioritization.

Due to its predictive nature, the traditional methodology has the advantage of offering a complete planning of the project from the start: clearly defined objectives, fixed execution times and deadlines, and a precise budget. From the traditional perspective, the goal of the planning phase of a project is to prepare the structure for project execution and control.

The impact of the planning process on project success has been demonstrated by various authors who have explored that planning and determination of the ideal project lifecycle for the project being embraced can significantly affect the success of that project [2] [3].

Al Nasseri and Aulin [4] highlighted and identified the following factors as enablers of successful project planning activities;

1. Proper understanding of the interrelationship between scope (alignment), Schedule
2. Rapid re-planning and recovery from unforeseen Baseline Schedule
3. Good recording of timetable delays in progress

4. Availability of alternate preparation approaches to fix problems with current methods
5. Maintain Quality Control schedule by eliminating unwanted organizational actions
6. Asset levelling performance in Scheduling
7. Efficiency of the motivational and educational programs administrative help
8. Focusing on a holistic approach rather than individual task completion
9. Detailed schedules are accurate
10. Cost-efficiency in the development and reworking of timetables and tasks
11. Unit expertise in handling planned operations, delays and remedial measures
12. Inputs, milestones and deliverables are recorded

2.2 Agile Methodology

Agile project management is defined by Wysocki as a non-linear, iterative or adaptive approach to project management. APM projects are typically completed in cycles with the next cycle returning to the planning phase prior to launching [1].

The principles of agile project methodology begin with the underlying principles and values of the Agile Manifesto and Declaration of Interdependence. Of particular importance are the emphases on people and the desire to remain flexible and adaptable in the fact of uncertainty and complexity. Agile project management approaches also emphasize a generative approach where only what is needed (processes, tools, procedures, documentation, etc) is required to be used in project [5].

Critical success factors of agile methods include [6]:

- culture,
- communication,
- people,
- delivery strategy,
- software engineering techniques,
- team capabilities,
- management support,
- customer involvement and
- strength of the process.

On the one hand, traditional project management is capable to cover the entire product life cycle, while on the other hand, agile project management typifies an alternative paradigm. “Agility is the project team’s ability to quickly change the project plan as a response to customer or stakeholders needs, market or technology demands in order to achieve better project and product performance in an innovative and dynamic project environment” [7].

2.3 Hybrid Methodology

Besides traditional and agile methodology, a third approach combining both methodologies is emerging and has been reported in various domains of literature by academics and practitioners. At its most general level, a hybrid project management approach combines methodologies and practices from more than one project management approach. To date, the combination of agile and traditional approaches and practices has been discussed in the software engineering, information systems,

and practitioner literature [8], but the effects of this hybrid approach on performance have only rarely been explored empirically in the literature [9].

In the context of hybrid project management, projects are planned using the traditional approach and a work flowchart known as the Water-Scrum-Fall [10]. This allows teams to better understand the tasks involved and the overall scope of the project. The projects are then executed using the Agile method, which provides enough leeway to manage changes and reassess the workload after short sprints. In addition to this approach, different other hybrid combination could be identified, such as Waterfall-Agile [11], Hybrid V-model [12] and Agile-Stage-Gate [13].

The aim of the hybrid project management approach is to bring together the best of the agile and traditional approaches. This is supposed to lead to achieving flexibility without unsettling project planning and to avoid the disadvantages of one approach with the help of positive elements from the opposite approach. An upstream project planning phase takes place in which the agile realization is prepared and plans for time, budget and scope management are set up [14].

The hybrid methodology requires specific planning according to the chosen approach, it is based on a complete project plan but the specific details of each sprint is not defined until the first sprint is completed [15].

2.4 Project Methodology Application

For decades, projects have been managed using collections of practices and methodologies that we refer to as the traditional approach, The Waterfall model is still the most commonly used project management method with goal oriented projects (clear goals) with no possibilities for future changes and can be implemented in **small and complex projects** such as **construction** [1]. The results of a study done by Faraji et al. [16] show that traditional project management principles and performance domains can be utilized for various types of projects in the **construction industry**.

Different industries may require different types of projects and have different project management needs. This may have an impact on the need for a specific management his impact project's success. Traditional project management is very comprehensive, and it has been proven to work in diverse project situations and fields.

There is wide evidence that traditional project management methodology is widely recognised and applied in companies' managerial practice in many industries besides IT, like **R&D**, **governmental**, **transportation**, **construction**, **higher education** or **power** [17].

In the last decade the research on Agile Project Management and its adoption beyond software industry has emerged expeditiously due to the fact that projects are being more complex with uncertain outcomes and goals changing over time. Generally, todays' business environment increasingly changes in every aspect. Competition is global, opportunities are dynamic, and business processes are highly complex. These circumstances were traditionally dealt by project experts that would attempt to predetermine every possible detail prior to implementation, but project managers are becoming aware of the relative shortcomings of traditional project-based structures to deal with the need to effect change and to take advantage of new or emerging opportunities. In order to be competitive organizations are forced to recognize changes and to be more flexible when they meet them. In this context, extending agile methods beyond software community is becoming desirable response to fast-changing and challenging business environment. Agility turned out to be a buzzword in a modern business world [18].

Baird and Riggins [6] say that while agile methods, including one particular agile method referred to as “Scrum” have been shown to be beneficial when used on projects where requirements changes are unavoidable, it is often reported that Agile works best with skilled developers working on small to medium sized projects in **environments** that facilitate communication.

Lehnen et al. [7] conclude that agile project management, in particular, turns out to be very effective in **lead user projects**. As Scrum is mostly used among agile methods, following model relies upon it.

The authors emphasize that the agile methodology is applicable in the following areas: **innovation management and product development, construction and real estate, education, services** [17].

The agile **software development** methodology is being widely accepted within the software development community. Agile provides multiple benefits over the previously used waterfall methodology. Agile attempts to simplify the software planning and estimation process by decomposing large requirements into small individual tasks. Analyzing small tasks allow the software development team to more accurately predict the level of effort required in order to implement the change. This allows the project manager to accurately depict the percentage complete of the software which allows them to continually track overall project progress against the originally planned progress [19].

Authors apostrophize that it can be concluded that Agile can and should be used in **information technology and research**. The key benefit of Agile is time, and as a consequence, the absence of lost profits [20].

In the paper [21], authors say that it is possible to identify that there is still a concentration of study on Agile Project Management in **software development activities**; however, it has become more widely used in different sectors recently.

To date, the combination of agile and traditional approaches and practices has been discussed in the **software engineering**, **information systems**, and practitioner literature [8], but the effects of this hybrid approach on performance have only rarely been explored empirically in the literature.

In the project management domain, analysis of the large, diverse sample of projects showed that 62% of projects were neither fully agile nor fully traditional [9]. They stated that the hybrid approach consisted of, “by far, the majority of projects and this phenomenon should be further investigated.” Hybrid approaches combining agile and traditional that stretch beyond software development are an important emergent methodology in **non software industries** [22], **education** [6] and **construction projects** [23].

Research done by Lalmi and al. [23] showed that a hybrid project management model for construction projects based on lean, agile and traditional approaches and the use of best practices from these approaches to increase the chances of project success by reducing costs, shortening project schedules, optimizing results, eliminating waste and increasing project satisfaction. This model aims to extract best practices from the three traditional, agile and lean design and construction approaches, the benefits that flow from the structure and predictability of traditional methods, adaptability and waste reduction to an agile model based on lean design and construction tools and methods and agile practices [5].

Table 1. Application of different project methodologies in different fields

METHODOLOGIES APPLICATION		
TRADITIONAL	*AGILE*	*HYBRID*
• *IT projects [24]*	• *Projects in software industry,* • *Innovation* • *Management and product development,* • *Construction and real estate,* • *Education,* • *Services [18]*	• *Non software industries [22]*
• *Software* • *Production* • *Communications* • *Services* • *Government [1]*	• *Projects in environment [6]*	• *Education [6]*
• *Construction and engeeering [1]*	• *lead user projects [7]*	• *Contruction projects [23]*
• *R&D* • *Transportation* • *Higher education Power [5]*	• *Software development [19] [21]*	• *Various industries [25]*
	• *Information technology and research [20]*	

3 CONCLUSION

Whether it is the traditional, agile or hybrid methodology with all their forms and models, project management has been proven to improve project success. Good project management enables a company to achieve the desired objectives and results; hence the importance of applying it appropriately, especially in this highly competitive context strongly marked by globalization. Nowadays, the increased use of the agile management method can be observed within companies. However, traditional methods that have existed for decades continue to be used until now.

This research set out to appraise the impact of project management methods on the performance and success of the project or project management based on literature review. All this depends on the type of organizations and the type of activities. A given method may have an influence on performance, but the level of influence may depend on the type of organizations or the type of activities in question.

Through the writing of this article, other research questions have emerged regarding wheather the use of a traditional method in the context of a decentralized organization have a positive impact on performance? And will the application of agile methods in decentralized environment have the same impact? Depending on the circumstances, the question arises whether to be “agile” or not. These are the main questions we will futher explore in our future research as it has been proven that an inappropriate choice of methods can have a negative impact on project performance, or even lead to project failure.

REFERENCES

[1] Serrador, P. (2013). The impact of planning on project success-a literature review. The Journal of Modern Project Management, 1(2).

[2] Rahrovani, Y., Chan, Y. E., & Pinsonneault, A. (2014). Determinants of IS planning comprehensiveness. Communications of the Association for Information Systems, 34(1), 59.

[3] Zwikael, O., Pathak, R. D., Singh, G., & Ahmed, S. (2014). The moderating effect of risk on the relationship between planning and success. International Journal of Project Management, 32(3), 435-441.

[4] Al Nasseri, H., & Aulin, R. (2016). Understanding management roles and organisational behaviours in planning and scheduling based on construction projects in Oman. Journal of Construction in Developing Countries, 21(1), 1.

[5] Fernandez, J. D., Fernandez (2008). Agile Project Management – Agilism Versus Traditional Approaches, Journal of Computer Information System, pp. 10-17

[6] Baird, A., Riggins, J. F. (2012). Planning and Sprinting: Use of a Hybrid Project Management Methodology within a CIS Capstone Course, Journal of Information Systems Education, vol. 23, no. 3, pp.243-257

[7] Lehnen, J., Schmidt, S. T., Herstatt, C. (2016). Bringing agile project management into lead user projects, International Journal of Product Development, Vol. 21, No.2/3, pp. 212-232

[8] Papadakis, E., & Tsironis, L. (2018). Hybrid methods and practices associated with agile methods, method tailoring and delivery of projects in a non-software context. Procedia computer science, 138, 739-746.

[9] Gemino, A., Horner Reich, B., & Serrador, P. M. (2021). Agile, traditional, and hybrid approaches to project success: is hybrid a poor second choice?. Project Management Journal, 52(2), 161-175.

[10] Wysocki, W., & Orłowski, C. (2019). A multi-agent model for planning hybrid software processes. Procedia computer science, 159, 1688-1697.

[11] Hassani, R., El Bouzekri El Idrissi, Y., & Abouabdellah, A. (2018, January). Digital project management in the era of digital transformation: Hybrid method. In Proceedings of the 2018 International Conference on Software Engineering and Information Management (pp. 98-103).

[12] Hayata, T., & Han, J. (2011, July). A hybrid model for IT project with Scrum. In Proceedings of 2011 IEEE International Conference on Service Operations, Logistics and Informatics (pp. 285-290). IEEE.

[13] Žužek, T., Kušar, J., Rihar, L., & Berlec, T. (2020). Agile-Concurrent hybrid: A framework for concurrent product development using Scrum. Concurrent Engineering, 28(4), 255-264.

[14] Reiff, J., & Schlegel, D. (2022). Hybrid project management–a systematic literature review. International journal of information systems and project management, 10(2), 45-63.

[15] Špundak, M. (2014). Mixed agile/traditional project management methodology–reality or illusion?. Procedia-Social and Behavioral Sciences, 119, 939-948.

[16] Faraji, A., Rashidi, M., Perera, S., & Samali, B. (2022). Applicability-Compatibility Analysis of PMBOK Seventh Edition from the Perspective of the Construction Industry Distinctive Peculiarities. Buildings, 12(2), 210.

[17] Spalek, S. (2016, May). Traditional vs. modern project management methods. Theory and practice. In Smart and Efficient Economy: Preparation for the Future Innovative Economy, 21st International Scientific Conference.

[18] Ciric, D., Lalic, B., Gracanin, D., Palcic, I., ZivLak, N. (2018). Agile Project Management in New Product Development and Innovation Processes: Challenges and Benefits Beyond Software Domain, IEEE International Symposium on Innovation and Entrepreneurship (TEMS-ISIE), pp. 156-163
[19] Edeki, C. (2015), Agile Software Development Methodology, European Journal of Mathematics and Computer Science, Vol. 2, No. 1, пп. 22-27
[20] Shavaliev, SH. A., Puryaev, S. A. (2018). Agile in project management system in mechanical engineering, IOP Conf. Series: Materials Science and Engineering 412
[21] Santos, P. O., Monteiro de Carvalho, M. (2020). Lean and Agile Project Management, Journal Modern PM, issue 24, vol. 08, no. 02, pp. 96-109
[22] Zasa, F. P., Patrucco, A., & Pellizzoni, E. (2020). Managing the hybrid organization: How can agile and traditional project management coexist?. Research-Technology Management, 64(1), 54-63.
[23] Lalmi, A., Fernandes, G., & Souad, S. B. (2021). A conceptual hybrid project management model for construction projects. Procedia Computer Science, 181, 921-930.
[24] Ahmad, G., Rahim Soomro, T., & Raza Naqvi, S. M. (2016). An overview: merits of agile project management over traditional project management in software development. Journal of Information & Communication Technology, 10(1), 105-120.
[25] Sithambaram, J., Nasir, M. H. N. B. M., & Ahmad, R. (2021). Issues and challenges impacting the successful management of agile-hybrid projects: A grounded theory approach. International Journal of Project Management, 39(5), 474-495.

STUDENT SECTION

COMETa 2022
6th INTERNATIONAL SCIENTIFIC CONFERENCE
17th - 19th November 2022
Jahorina, B&H, Republic of Srpska
University of East Sarajevo
Faculty of Mechanical Engineering
Conference on Mechanical Engineering Technologies and Applications

ANALIZA ENERGETSKE EFIKASNOSTI KOGENERACIJSKOG POSTROJENJA

Valentina Lulić[1]

Rezime: U ovom radu predstavljena je kombinovana proizvodnja toplotne i električne energije tj. kogeneracija. Najprije je definisan sam pojam kogeneracije i njene karakteristike a nakon toga prikazano je konkretno kogeneracijsko postrojenje sa svim potrebnim tehničkim podacima. U središtu pažnje našlo se poređenje kogeneracijskog sistema sa sistemima za odvojenu proizvodnju toplotne i električne energije i samim time izvršena je analiza energetske efikasnosti kogeneracijskog postrojenja.

Ključne riječi: kogeneracija, analiza, energetska efikasnost

ENERGY EFFICIENCY ANALYSIS OF COGENERATION PLANT

Abstract: The combined production of heat and electricity has been presented in this work. First, we talked about the concept of cogeneration and its characteristics, after that a specific cogeneration plant with all necessary technical data. The center of attention was the comparison of the cogeneration system with system for the separate production of heat and electricity, and complete analysis of the energy effectiveness of the cogeneration plant was also perfomed.

Key words: cogeneration, analysis, energy efficiency

1 UVOD

U 21 vijeku dobijanje energije iz obnovljivih izvora energije je zdravo upravljanje energijom i predstavlja koncept održivog razvoja. Postoji nekoliko osnovnih razloga za to, od kojih je svakako najvažniji svijest da opada dostupnost fosilnih goriva, ali i svijest da njihova konačna upotreba može imati štetne posljedice po životnu sredinu. Kombinovana proizvodnja električne i toplotne energije, je globalno prihvaćen, priznat i atraktivan način proizvodnje električne energije zbog niskih troškova ulaganja, kratkog perioda izgradnje, smanjene potrošnje goriva i zagađenja životne sredine.

[1] Dipl. inž. maš. Valentina Lulić, Mašinski fakultet Istočno Sarajevo, BiH, valentinalulic313@gmail.com

2 KOMBINOVANA PROIZVODNJA ELEKTRIČNE I TOPLOTNE ENERGIJE - KOGENERACIJA

Kombinovana proizvodnja električne i toplotne energije tj. kogeneracija je proces koji proizvodi električnu energiju i toplotu istovremeno iz jednog izvora energije. Koncept kogeneracije zasniva se na principu termalne kaskade, što znači da se električna energija proizvodi na lokaciji gdje se značajan dio proizvedene otpadne toplote regeneriše kako bi se zadovoljile potrebe potrošača u vidu grijanja ili hlađenja. Osnovni cilj kogeneracijskog postrojenja je proizvodnja toplotne energije u količini koja je potrebna. Ako posmatramo podjelu oblika energije uvjerićemo se da je na prvom mjestu električna energija jer se ona može prenositi na udaljene lokacije a toplotna energija to ipak ne može. Prema tome najvažnije je omogućiti što efikasniju proizvodnju toplotne energije a time i mehanički rad koji je potreban za proizvodnju električne energije. Dokazano je da se više od pola energije gubi i samim time ne iskoristi. Najviše izgubljene energije je iz kondezatora. Kogeneracijski sistemi imaju visok stepen korisnosti sto znači da pri svom radu emituju niske vrijednosti emisija štetnih čestica [1].

Elektrane kogeneracijskih sitema kao gorivo mogu da koriste biomasu, prirodni plin, vodonik ili drvenu građu. Kogeneracijska postrojenja imaju široku primjenu, koriste se u toplotnim sistemima gradova, industrije, fabrika, bolnica, zatvora, rafineriji nafte itd.

Velika prednost kogeneracijskih sistema ogleda se u tome da se sav višak proizvedene električne energije može predati mreži jer se za svaki predani kWh dobija subvencija. Međutim, moguće je da i u slučaju manjka električne energije kogeneracijsko postrojenje preuzme iz mreže kako bi podmirio svoje potrebe [2].

U skladu s tehnologijom koju koriste kogeneracijska postrojenja se mogu podijeliti na [3]:

- Sa parnom turbinom,
- Sa gasnom turbinom,
- Kombinovani ciklus,
- Sa SUS motorom,
- Gorive ćelije,
- Stirlingov motor.

3 KOGENERACIJSKO POSTROJENJE NA BIOMASU

U radu će biti prikazano kogeneracijsko postrojenje koje proizvodi električnu energiju snage 400 kW, dok se toplotna energija proizvodu u dva oblika. Prvi oblik je u vidu toplog zraka čija je temperatura 225-272 °C, u količini 6,3 kg/s, toplotnog učinka 1200 kW. Drugi oblik je u vidu tople vode čiji je toplotni učinak 944-1686 kW. Ova dva oblika mogu da se koriste za procese sušenja, za tehnološke potrebe kao i za grijanje.

Postrojenje je izvedeno modularno, neki dijelovi se proizvode u fabrici pa se naknadno sklapaju na lokaciji primjene, kao podloga koristi se betonski plato s montažnim temeljima čija je visina 600 mm. Rad postrojenja je u potpunosti automatizovan, projektovani radni vijek je 20 godina rada i u sklopu postrojenja se nalazi i pogonsko skladište za biomasu za autonoman rad od 40h.

Postrojenje koristi biomasu kao gorivo koja je usitnjena na veličinu od 50 mm a porijeklom može biti drvna ili poljoprivredna.

Slika 1. *Kogeneracijsko postrojenje na biomasu [4]*

U postrojenju se nalazi sistem za sušenje na osnovu vazduha koji nije iskorišten kako bi se omogućila što veća efektivnost iskorištenja biomase. Kod upotrebe šumske mase vrši se stepenasto sagorijevanje u ložištu dok kod poljoprivredne zbog povećanog prisustva kalijuma i natrijuma vrši se modifikovana tehnologija sa stepenastim sagorijevanjem. Osnovne karakteristike pogona prikazane su u tabeli 1.

Tabela 1. *Osnovne karakteristike pogona datog kogeneracijskog postrojenja [4]*

Parametri	*Iznosi*
Broj radnih dana postrojenja	*345 d godišnje*
Broj radnih sati	*8280 h godišnje*
Broj zaposlenih radnika u jednoj smjeni	*1*
Broj smjena pri smjenskom načinu zaposlenih	*4*
Ukupan broj potrebnih zaposlenih	*5*
Proračunski vijek trajanja postrojenja	*20 godina*
Instalirana snaga potrošača električne energije	*100 kW*
Potrebna priključna najveća snaga postrojenja	*100 kW*
Prosječna angažovana snaga potrošača električne energije	*40 kW*

Generator koji je ugrađen za proizvodnju električne energije je generator 630 kV A, 400 V, njegovo spajanje na srednjenaponsku mrežu 10 (20) kV vrši se pomoću transformatora. Spajanje postrojenja na srednjenaponsku mrežu vrši se uz odgovarajuću i sigurnosnu opremu u skladu s tehničkim uslovima za priključenje na elektroenergetsku mrežu malih elektrana. Uzimajući u obzir to da kogeneracijsko postrojenje koristi električnu energiju koja je niskog napona (380 V), za napajanje vlastite potrošnje, kod priključivanja na niskonaponsku mrežu mora se pripremiti trofazni priključak 0,4 kV i najveća snaga 100 kW. Generatorska jedinica se može priključiti na elektroenergetsku mrežu na dva načina.

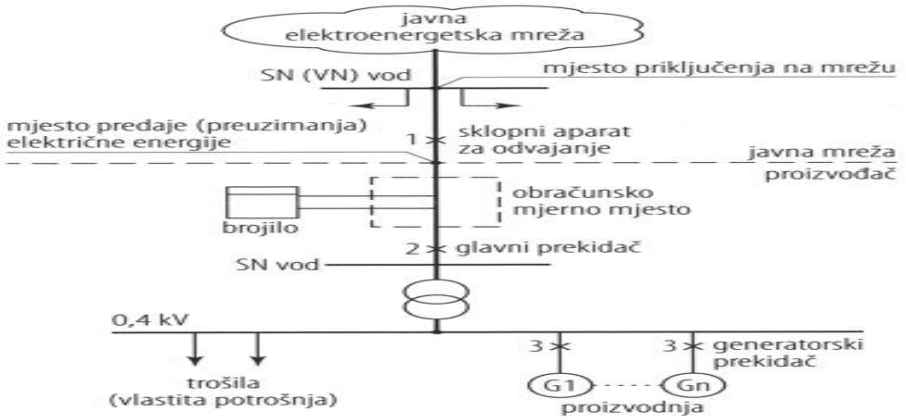

a) Priključenje na mrežu sa zajedničkim radom

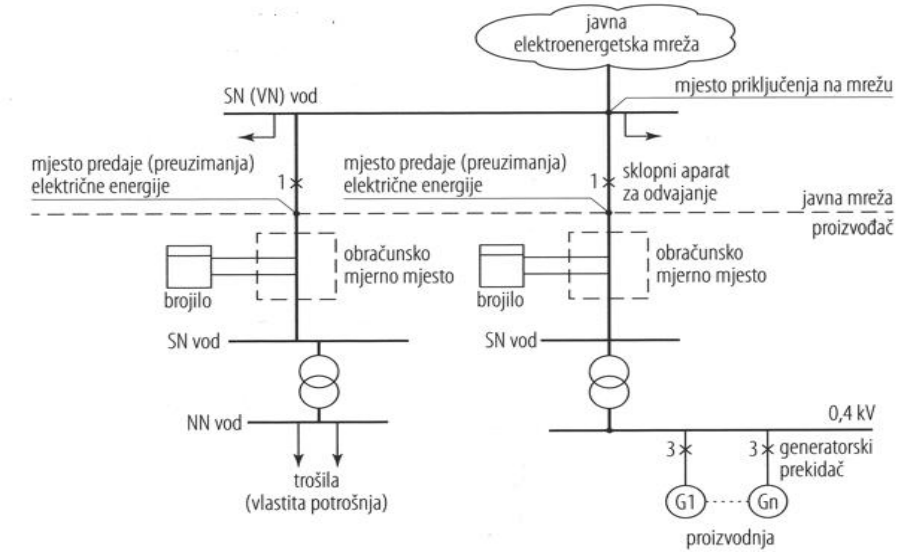

b) Priključenje na mrežu s odvojenim mjerenjem vlastite potrošnje

Slika 2. *Dva osnovna priključivanja kogeneracijskog postrojenja na elektroenergetsku mrežu [4]*

Kogeneracijsko postrojenje se sastoji od nekoliko glavnih dijelova, izdvojene su neke od osnovnih cjelina [4]:

- Sistem za snabdijevanje skladišta biomasom
- U užem smislu samo postrojenje,
- Stanica distribucije tople vode
- Sistem za iskorištavanje toplog vazduha s izduvnog sistema turbine
- Unutrašnja i vanjska infrastruktura
- Spoljašnje uređenje na lokaciji postrojenja

Kogeneracijsko postrojenje na biomasu je našlo svoju primjenu u procesima sušenja, u ciglanama, u lokalnim zajednicama, primjenjuje se za sušenje drvene piljevine i za proizvodnju pare i tople vode [4].

4 ANALIZA ENERGETSKE EFIKASNOSTI KOGENERACIJSKOG POSTROJENJA

Proces analize kogeneracije obuhvata samo bazne potrebe jer gledajući s ekonomske strane prednosti su vidljive tek nakon nekoliko godina. Što se tiče njegovog uticaja na životnu sredinu prednosti se najlakše mogu izdvojiti ukoliko se posmatraju na nivou regije.

Proizvodnja električne energije na lokalnom nivou preko kogeneracije umanjuje mogućnost da krajni potrošači ostanu bez električne i toplotne energije. Pored toga korištenjem obnovljivih izvora energije umanjuje se potreba za uvoznom energijom. Ovo je jedna od najvažnijih stavki za energetsku budućnost. Sam koncept kogeneracije raste ali iz brojnih političkih razloga ona se još uvijek ne koristi u svom punom potencijalu.

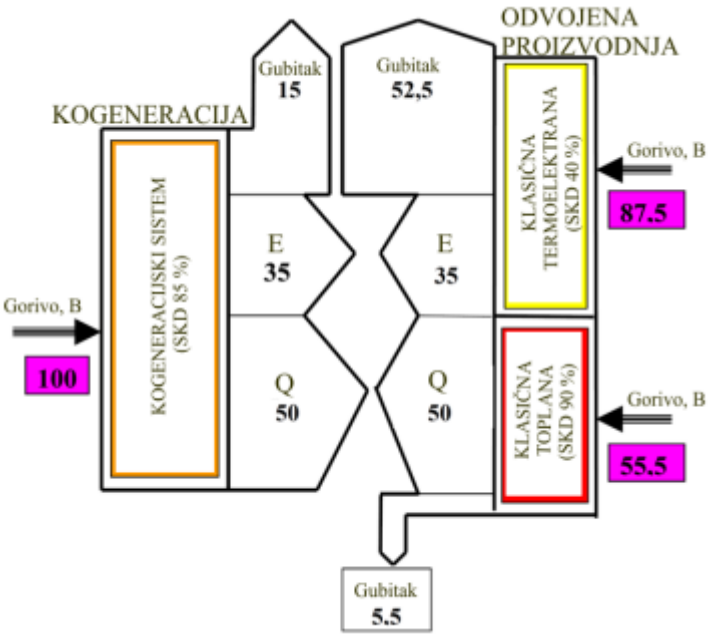

Slika 3. *Poređenje kogeneracijskog sistema sa sistemima za odvojenu proizvodnju toplotne i električne energije [5]*

Poređenje je izvršeno na sljedećim principima [5]:

- Za oba sistema je korištena ista vrsta goriva,
- Najbolja jedinica sistema kogeneracije poredila se s najboljom jedinicom sistema za odvojenu proizvodnju električne i toplotne energije, koja je raspoloživa na tržištu,
- Referentne vrijednosti efikasnosti kogeneriacije koje su starije od 10 godina utvrdile su se na osnovu vrijednosti jedinica starih 10 godina,
- Referentne vrijednosti jedinica sistema za odvojenu proizvodnju toplotne i

električne energije omogućiće, između potencijalnih članica Evprske Unije, njihove klimaske razlike.

Prema tome, za kogeneracijski sistem koji je prikazan na slici dobijeni su sljedeći rezultati [5]:

- Gubici u sistemi kogeneracije: 15%
- Gubici u sistemu odvojene proizvodnje električne i toplotne energije: 40,5%
- Razlika u potrošnji goriva: 43%
- Ušteda goriva: 30%.

Prednost je to što se mogu iskoristiti otpadne sirovine kao gorivo umjesto da se odlažu na deponije. Izgradnjom kogeneracijskog postrojenja otvaraju se i nove mogućnosti za radna mjeste, postiže se bolja konkurentska pozicija na tržištu [5].

5 ZAKLJUČAK

Energetska efikasnost postrojenja može se definisati kao visok stepen korisnog dejstva tog postrojenja. U ovom radu u pitanju je kogeneracijsko postrojenje čija je energetska efikasnost veoma visoka i koja iznosi 85%. Klasični načini proizvodnje toplotne i električne energije postižu energetsku efikasnost od 30-40% pri čemu ispuštaju veliku količinu otpadne energije u vidu toplote dok kogeneracijsko postrojenje koristi toplotu i može da dostigne vrijednost energetske efikasnosti od čak 90%. Odvojena proizvodnja električne i toplotne energije ima gubtike i pri prenosu energije od 15%. Emisije štetnih gasova su na minimalnom nivou. Potencijal izgradnje kogeneracijskog postrojenja se najbolje može vidjeti u sve većem porastu potražnje električne energije i u mogućnosti zaštite životne sredine. Teži se ka gradnji kogeneracijskog postrojenja pri širenju industrijskih zona i kapaciteta elektroenergetskog sistema. Što se tiče Republike Srpske, ona u potpunosti trenutno ne koristi potencijal kogeneracijskog postrojenja međutim teži se ka boljoj eksploataciji njegovog integrisanja na energetskom tržištu pa se može zaključiti da je budućnost kombinovane proizvodnje električne i toplotne energije veoma perspektivna.

LITERATURA

[1] Labudović B., Obnovljivi izvori energije, Energetika marketing, Zagreb, 2002
[2] https://hr.wikipedia.org/wiki/Kogeneracija#Karakteristike, pristupljeno: 15.10.2022.
[3] Urošević D., Razvoj modela za energetsko vrednovanje složenih kogenerativnih postrojenja, Novi Sad, 2014.
[4] Labudović B., Osnovne primjene biomase, Zagreb, 2012.
[5] Milovanović Z., Energetska efikasnost kogeneracije i kombinovane proizvodnje energije, Banja Luka, 2016.

COMETa 2022
6th INTERNATIONAL SCIENTIFIC CONFERENCE
17th - 19th November 2022
Jahorina, B&H, Republic of Srpska
University of East Sarajevo
Faculty of Mechanical Engineering
Conference on Mechanical Engineering Technologies and Applications

TEORIJSKE OSNOVE FOTONAPONSKIH SISTEMA

Stefan Adžić[1]

Rezime: U radu su opisane teorijske osnove fotonaponskih sistema. Govori o osnovnim odlikama sunčevog zračenja, globalnom i terestičkom zračenju, pretvaračima Sunčeve u električnu energiju i data je osnovna podjela.

Ključne riječi: Sunčeva energija, obnovljivi izvori energije, fotonaponski modul, solarni panel.

THEORETICAL FOUNDATIONS OF PHOTOVOLTAIC SYSTEMS

Abstract: The paper describes the theoretical foundations of photovoltaic systems. It talks about the basic characteristics of solar radiation, global and terrestrial radiation, solar energy converters into electricity and the basic division is given.

Key words: Solar energy, renewable source of energy, photovoltaic module, solar panel.

1 UVOD

Upotreba alternativnih, odnosno obnovljivih izvora energije je u stalnom porastu i trenutno igra veoma važnu ulogu u energetskim sistemima. Jedan od načina korišćenja sunčeve energije je primjena fotonaponskih sistema. Fotonaponske ćelije (*photovoltaic cells*) čine osnovni dio mnogih savremenih proizvoda, počevši od malih sistema pa sve do velikih sistema za snadbijevanje električnom energijom. Pri tome, veoma važno je napomenuti da fotonaponske ćelije pri transformisanju sunčeve u električnu energiju ne ispuštaju nikakve štetne materije što im daje veliku prednost u odnosu na klasične fosilne izvore energije.

Termin fotonapon (*photovoltaic)* je prvi put upotrijebljen krajem XIX vijeka. Fotonapon se može prevesti doslovce kao "svjetlosni elektricitet", a to je upravo ono što fotonaponski materijali i uređaji rade, pretvaraju svjetlosnu energiju u električnu. Ovu pojavu je otkrio devetnaestogodišnji francuski fizičar *Edmond Becquerel* 1839. godine. On je uspio da izazove pojavu napona kada je svijetleću metalnu elektrodu potopio u slab elektrolitski rastvor. Skoro 40 godina kasnije, Adams i Dej bili su prvi koji

[1] Dipl. inž. maš. Stefan Adžić, Mašinski fakultet, Istočno Sarajevo, stefanadzic73@gmail.com

su ispitivali efekte fotonaponskih pretvarača čvrstih tijela. Bili su u mogućnosti da naprave ćelije od Selena koje su imale efikasnost između 1% i 2%. Albert Ajnštajn je 1904. godine objavio teorijsko objašnjenje fotonaponskog efekta, što ga je 1923. godine dovelo do Nobelove nagrade. Otprilike u isto vrijeme poljski naučnik Jan Čokhralski počeo je da razvija metod za pravljenje savršenog silikonskog kristala, da bi se između 1940. i 1950. godine njegovim procesom počeli generisati jednokristalni fotonaponski pretvarači.

Prvo postojano generisanje energije iz fotonaponskog pretvarača bilo je 1958. godine, na satelitu Avangarda I.

Danas fotonaponski sistemi proizvode značajnu količinu električne energije koja se koristi širom svijeta. PV tehnologija će u budućnosti moći da pruži veliku podršku stopi rasta naprednih ekonomija, kao i zemalja u razvoju. PV moduli mnogih proizvođača su sada komercijalno dostupni, a na tržište je plasiran određen broj elektroenergetskih sistema za obradu električne energije proizvedene od PV sistema, posebno za sisteme povezane na mrežu. [5]

Solarne ćelije predstavljaju složenu strukturu čiji je glavni dio (aktivni sloj) napravljen od poluprovodničkih materijala. Fotonaponski elementi se mogu realizovati na mnogo različitih načina, o čemu svjedoči veliki broj različitih tehnoloških i proizvodnih procesa, od kojih su neki specijalno razvijani za ovu oblast. Fotonaponski sistemi generalno se sastoje od više fotonaponskih ćelija (obično grupisanih i upakovanih u skupove ćelija nazvanih moduli).

Solarna postrojenja mogu biti postavljenja na bilo kakvoj površini, ali je želja da se osigura nesmetan rad bez zasjenjenja od obližnih objekata, rastinja ali i od susjednih fotonaponskih modula. Osnova solarnog postrojenja su nosači na koje se postavljaju fotonaponski moduli, fotonaponski moduli kao i pretvarači. Ova tri elementa čine bazu funkcionalnosti solarnog postrojenja. [6]

2 TEORIJSKE OSNOVE FOTONAPONSKIH SISTEMA

2.1 Osnovne odlike sunčevog zračenja

Bitne odlike sunčevog zračenja (eng. solar radiation) posljedice su rotacije Zemlje, gdje imamo dvije vrste rotacije:

- oko Sunca (donosi 4 godišnja doba)
- oko vlastite ose simetrije u smjeru sjever-jug (donosi izmjene dana i noći).

Zemlja rotira oko Sunca po eliptičnoj putanji (ekliptici), koja je vrlo malog ekcentriteta (e=0,0167), pri čemu velika osa elipse iznosi 149 680 000 km, a mala 149 660 000 km, pa je elipsa svojim oblikom vrlo bliska kružnici. Vremenski period jedne rotacije Zemlje oko Sunca naziva se jednom godinom. Perihel je tačka u kojoj je Zemlja najbliža Suncu, šta se događa 2. januara, a afel tačka u kojoj je Zemlja najdalje od Sunca, što se dešava 02. jula. Gledajući sa sjevernog pola, Zemlja se okreće oko Sunca i oko vlastite ose u smjeru koji je suprotan kretanju kazaljke na satu. Jedan okret Zemlje oko vlastite ose traje jedan dan. Kao rezultat nagiba ekvatorijalne ravnine Zemlje u odnosu na ekliptiku nastaju četiri godišnja doba (slika 2.1).

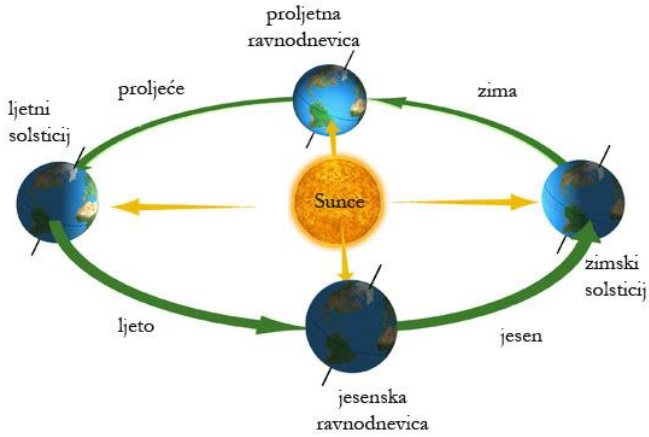

Slika 2.1. *Kretanje Zemlje oko Sunca [3]*

Osa vlastite (jednodnevne) rotacije Zemlje pravi ugao 66,55 ° sa ekliptičkom ravninom u kojoj se Zemlja jednom godišnje okrene oko Sunca koje se nalazi u jednom fokusu elipse. Time ugao ekvatorijalne ravnine Zemlje i ekliptike iznosi 23,45 °. Oko 21. decembra sjeverni pol Zemlje maksimalno je otklonjen na suprotnu stranu od Sunca za ugao 23,45 ° pa sve tačke koje leže na površini Zemlje sjevernije od geografske širine arktičkog kruga (ϕ> 66,55 ° SZŠ) imaju 24 sata noć, dok tačke južne polovine koje leže na površini Zemlje južnije od antarktičkog kruga (ϕ> 66,55 ° JZŠ), imaju 24 sata dan. Te uloge postaju suprotne 22. juna, kada je nagib osi Zemlje prema Suncu maksimalan i kada iznad arktičkog kruga nastaje trajni polarni dan, a ispod antarktičkog kruga traje polarna noć.

Prividno je za stanovnika na ekvatoru Sunce oko 21. decembra nagnuto južnije, do tzv. jarčeve obratnice (ϕ= 23,45 ° JZŠ), a deklinacija Sunca je u tom trenutku minimalna i iznosi δ = -23,45 ° . Tada započinje zima na sjevernoj polutki, a ljeto na južnoj. Iz toga proizilazi kako će ljeti, kada je putanja Sunca najviša i Sunčevo zračenje najstrmije pada na površinu Zemlje (minimalna $AM=AM_0$), direktna komponenta Sunčevog zračenja oko podne na vanjskim jadranskim ostrvima sa vedrim vremenom i s vidljivošću većom od 20 km imati trenutnu vrijednost od 800 W/m^2, dok će u isto vrijeme raspršeno (difuzno) zračenje biti oko 140 W/m^2. Ukupne dnevne ljetne vrijednosti u Junu i Julu iznose:

- za direktno zračenje oko 6,5 kWh/(m^{2}d)
- za difuzno zračenje oko 1,4 kWh/(m^{2}d).

Zimi je putanja Sunca položenija pa relativna atmosferska masa (AM) postaje u dnevnom prosjeku gotovo tri puta veća pa će se direktna komponenta već samo po toj osnovi zimi svesti na trećinu. Time će se trenutna vrijednost direktnog zračenja na jadranskim ostrvima zimi smanjiti na oko 260 W/m^2, dok će doprinos difuzne komponente u odnosu na direktnu porasti i biti oko 80 W/m^2. Ukupne dnevne zimske vrijednosti u decembru i januaru iznose:

- za direktno zračenje oko 1,5 kWh/(m^{2}d)
- za difuzno zračenje oko 0,6 kWh/(m^{2}d).

Stvarne vrijednosti ukupnog (globalnog) dnevnog zračenja na vodoravnu plohu u decembru i januaru biće oko 30% manje zbog udjela oblačnog vremena i iznosiće oko 1,6 kWh/(m2d). [1]

2.2 Difuzno i globalno terestičko zračenje

U razmatranje se uzima opšti slučaj satne insolacije na nagnute površine pod uglom β prema vodoravnoj plohi, ali i dodatno za ugao γ zakrenute u odnosu na smjer sjever-jug. Na takvu plohu u svakom trenutku pada dio oslabljenog **direktnog zračenja** (E_n), uvećanog za ukupno, u zadanom trenutku raspršeno i reflektovano zračenje (E_d), koje se naziva **difuznim zračenjem**. Tada je **ukupno** ili **globalno terestičko** zračenje (E_g) u svakom trenutku je zbir ta dva zračenja:

$$E_g(t)= E_n(t)+ E_d(t),$$

pri čemu su:

E_g – ukupno (globalno) terestičko zračenje kao funkcija vremena, W/m^2

E_n – direktno (usmjereno) zračenje kao funkcija vremena, W/m^2

E_d – raspršeno i reflektovano (difuzno) zračenje kao funkcija vremena, W/m2.

Ukupno zračenje koje pada na plohu nagnutu pod uglom β – γ tada je dato izrazom:

$$E_{\beta\gamma}=E_n \frac{cos\theta}{sin\, A} + E_d\, cos^2\frac{\beta}{2} + \rho_r E_g sin^2\frac{\beta}{2}$$

pri čemu je:

ρ_r – albedo (refleksivnost) okolnih predmeta i ploha (tablica 2.1).

Pri tome prvi član daje osunčanost od usmjerenog (direktnog) zračenja i zavisi od visine Sunca (A) i uglu između normale na površinu nagnute plohe i smjera Zemlja – Sunce. Doprinos drugog člana u osunčanosti kose plohe zavisi od prostornog ugla pod kojim kosa ploha vidi dio nebeskog svoda kao izvor difuznog zračenja. Doprinosi trećeg člana posljedica su refleksija usmjerenog i difuznog zračenja na okolnim predmetima, na onima u neposrednoj blizini i na onima daljima u bližoj okolici, pri čemu je ρ_r tzv. **albedo** ili **refleksivnost** okolnih predmeta i površina. Generalno valja primjetiti kako za okolinu s većim albedom, difuzno zračenje uopšte nije izotropno, već upravo suprotno tome.

Satne vrijednosti osunčanosti površine mogu se izračunati odmah, ako je za svaki sat poznato ukupno globalno i usmjereno (direktno) terestičko zračenje, npr. na osnovu mjerenja piranometrom kojim se mjeri ukupno globalno zračenje, odnosno pirheliometrom kojim se dvoosno prati kretanje Sunca i mjeri samo usmjerena direktna komponenta zračenja. [1]

Ako na zadanoj lokaciji ne postoje mjerenja usmjerenog terestičkog zračenja, već samo mjerenja globalnog zračenja, usmjereno se zračenje mora procjenjivati. Uobičajeno je procijeniti tzv. **satni postotak osunčanosti** ili **indeks propusnosti**, odnosno **čistoće atmosfere** koji se dobija jednačinom:

$$K_t = \frac{Eg}{Eo},$$

pri čemu su:

K_t – indeks propusnosti

E_g – terestičko zračenje na vodoravnu plohu, W/m^2

E_o – ekstraterestičko (nebesko) zračenje na vodoravnu plohu, W/m^2.

Indeks propusnosti atmosfere u velikoj mjeri zavisi od stepena oblačnosti, a i o svim drugim faktorima (npr. o stepenu onečišćenosti atmosfere u urbanim i industrijskim sredinama ili o magli u zimskim uslovima itd.). Jedna od vrlo jednostavnih korelacija između indeksa propusnosti atmosfere i usmjerenog zračenja može se napisati u obliku:

- za $0,3 < K_t < 0,085$:
  $E_n = - 520 + 1800\ K_t$
- za $K_t < 0,3$:
  $E_n = 0$.

površina	albedo ρ_r
svježi snijeg	0,75 - 0,95
stari snijeg	0,4 - 0,6
svijetli pijesak	0,3 - 0,4
suha zemlja	0,15 - 0,3
vlažna zemlja	0,1 - 0,2
morska površina	0,5 - 0,6
trava	0,2 - 0,3
bjelogorična šuma	0,1 - 0,2
crnogorična šuma	0,1 - 0,15
beton	0,25 - 0,35
asfalt	0,1 - 0,2
avionski aluminij	0,85 - 0,95

Slika 2.2. *Albedo nekih važnijih površina [5]*

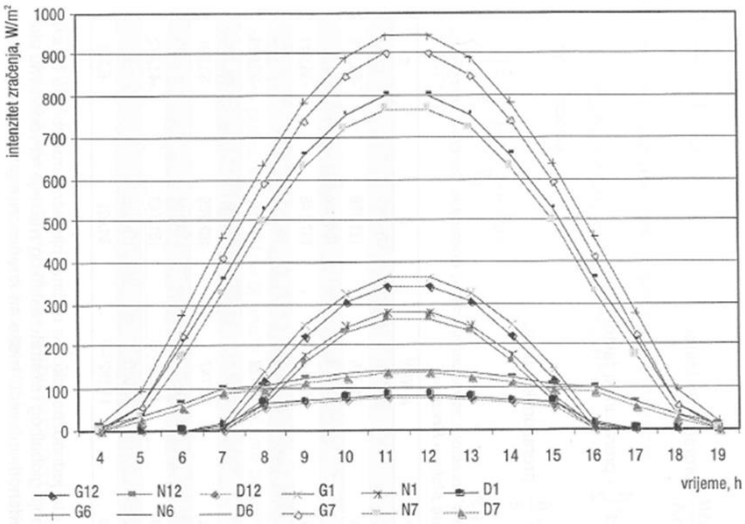

Slika 2.3. *Poređenje udjela satnih vrijednosti normalnog i difuznog zračenja u decembru i januaru (N12, D12 i N1, D1) sa vrijednostima u junu i julu (N6, D6 i N7, D7) na području Dalmacije [6]*

2.3 Pretvarači Sunčeve u električnu energiju

Solarni fotonaponski pretvarači služe za direktno pretvaranje (Sunčeve) svjetlosti u električnu energiju, a izvode se kao **fotonaponske ćelije** (eng. photovoltaic cells) koje mogu biti od:

- monokristalnog i polikristalnog silicijuma
- amorfnog silicijuma
- kadmijum – telurida ili bakar – indijum – diselenida

Najveći dio FN ćelija danas se zasniva na **monokristalnom** i **polikristalnom** silicijumu. Ćelija debljine 0,20 do 0,25 mm oblikuje se od kristala silicijuma vrlo visoke čistoće tako da joj se jedna strana obogaćuje atomima bora čime nastaje tzv, p strana, dok se s druge strane difuzijom fosfora stvara tzv. n strana pa se takve ćelije nazivaju **n-p fotonaponskim ćelijama**. Silicijum je na Zemlji prisutan u vrlo velikim količinama i prirodni je poluprovodnik kome je električna provodljivost između one za dobre provodnike (bakar) i one za loše provodnike, izolatore (npr. plastika ili guma). Veliki električni otpor vrlo čistog kristalnog silicijuma smanjuje se u proizvodnji tehnološkim procesima dopinga i difuzije na potrebnu poluprovodničku vrijednost. Svjetlost koja pada na tako oblikovanu poluprovodničku ćeliju stvara parove negativnih i pozitivnih naboja (elektrona i rupa) koje se odvajaju električnim poljem koje nastaje na granici n-p spoja pa negativni elektroni putuju do n elektrode, a pozitivne rupe do p elektrode (slika 2.2). [1].

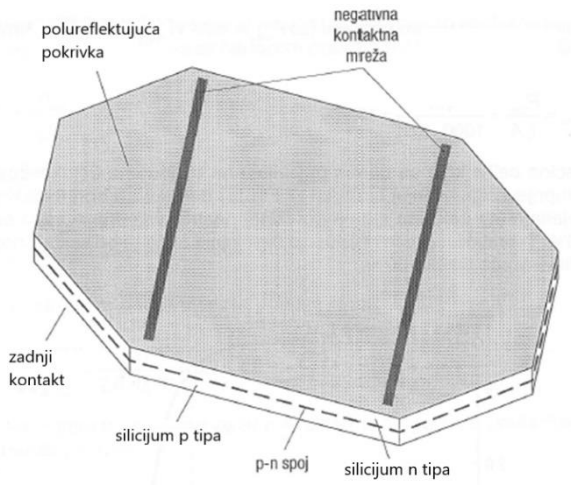

Slika 2.4. *n-p solarna ćelija od kristalnog silicijuma [3]*

2.4 Osnovna podjela

Zavisno od načina rada, postoje sljedeće vrste FN sistema [1]:

1. samostalni (autonomni), za čiji rad mreža nije potrebna
2. hibridni, koji su zapravo samostalni povezani s drugim (obnovljivim) izvorima
3. mrežni, spojeni na električnu mrežu:
    - pasivni, kod kojih mreža služi (samo) kao primarni izvor

- aktivni (interaktivni), kod kojih mreža može prikrivati manjke, ali i preuzimati višak električne energije iz FN modula.

2.4.1 Samostalni (autonomni) sistemi

Samostalni (autonomni) sistemi za svoj rad ne zahtijevaju spajanje na električnu mrežu. Kada kod njihove primjene električnu energiju treba isporučivati tokom noći ili u razdobljima s malim intezitetom Sunčevog zračenja neophodan je akumulator (baterija) koji služi kao skladište električne energije. Tom se sklopu mora dodati regulator za kontrolisano punjenje i pražnjenje baterije, a dodavanjem istosmjerno-naizmjeničnog pretvarača (=12 V/230 V) autonomni sistemi mogu zadovoljiti i sve vrste tipičnih mrežnih potrošača, kao što su veš mašine, hladnjaci, pumpe, hidrofori, motori, televizori, radioaparati, računari, usisivači, mali kućni aparati i drugi potrošači (slika 2.7).

Takvi su sistemi pogodni za osiguravanje potrebnih količina električne energije za udaljene (izolovane) potrošače kao što su ruralna (izolovana) ili primorska vikend – naselja te za brojne pojedinačne objekte različitih namjena (npr. razne vrste signalizacija i upozorenja, rasvjetu, elektrokomunikacijske releje, svjetionike, sisteme nadgledanja itd). [1]

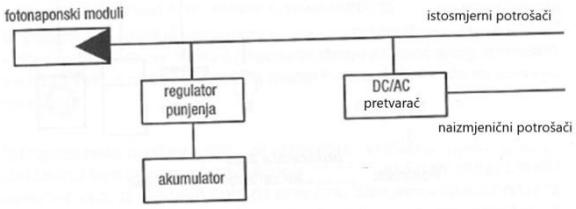

Slika 2.5. *Samostalni FN sistem [3]*

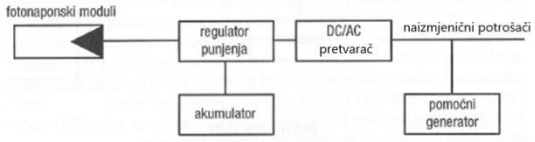

Slika 2.6. *Hibridni FN sistem [3]*

2.4.2 Hibridni FN sistemi

Hibridni FN sistemi nastaju povezivanjem samostalnih (posebno većih) s drugim alternativnim izvorima električne energije, kao što su vjetroturbine, hidrogeneratori, pomoćni plinski i dizelski agregati. Takva rješenja daju veću sigurnost i raspoloživost isporuke električne energije te omogućavaju manje kapacitete akumulatora kao skladišta za električnu energiju (slika 2.8). Kod rješenja koja koriste plinske i dizelske agregate sistemi se dimenzionišu tako da se agregati koriste malo sati u godini čime se štedi gorivo, smanjuju troškovi održavanja i produžuje vijek trajanja.

2.4.3 Pasivni i aktivni mrežni sistemi

Pasivni mrežni FN sistemi električnu mrežu koriste samo uslovno, u razdobljima kada FN moduli ne mogu proizvesti dovoljne količine električne energije, npr. noću kada su istovremeno akumulatori električne energije prazni (slika 2.9).

Aktivni, odnosno interaktivni mrežni FN sistemi mrežu koriste interaktivno, uzimajući je u slučaju većih potreba ili vraćajući je u slučaju viška električne energije proizvedene u FN modulima (slika 2.10).

Oba mrežna FN sistema na izlazu iz modula mogu koristiti i jednosmjerno-jednosmjerne pretvarače napona kojima se mogu podešavati naponski nivoi za potrebe jednosmjernih potrošača koji rade na naponima koji su različiti od 12 V ili 24 V ili se mogu podesiti na napon baterija koje rade na većim jednosmjernim naponima. Često se koriste i posebni pretvarači koji su kod nekih proizvođača integrisani u osnovni jednosmjerno-naizmjenični pretvarač, a koriste se za tzv. MPPT (eng. Maximum Power Point Tracking) kojim se osigurava to da moduli u svim radnim uslovima, bez obzira na intenzitet Sunčevog zračenja ili njihovu radnu temperaturu, uvijek rade na istom maksimalnom naponu. [1]

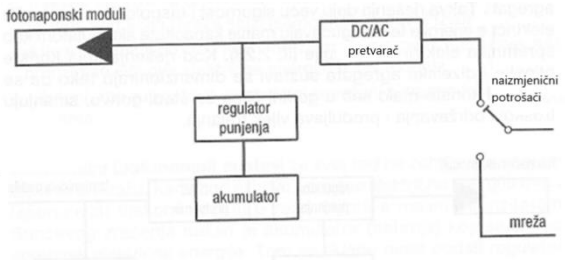

Slika 2.7. *Pasivni mrežni FN sistem [4]*

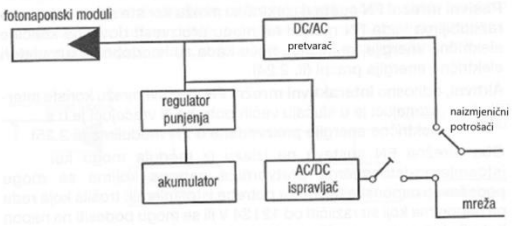

Slika 2.8. *Aktivni mrežni FN sistem [4]*

3 ZAKLJUČAK

Na kraju, kada se uzmu u obzir pozitivne i negativne činjenice u vezi sa FN sistemima, ipak dobijamo rezultat koji govori da je ovo itekako isplativa i čista tehnologija čija primjena nas čeka u budućnosti. Samo je potrebno pratiti određene smjernice i racionalno razmišljanje i FN sistemi će biti na strani čovjeka i prirode.

Trenutno živimo u vremenu kada je potražnja za električnom energijom sve veća jer tehnologija napreduje svakog dana, sve je veća potrošnja, a proizvodnja se ne povećava srazmjerno potrošnji. Ovo daje nagovještaje da može doći i do energetske krize i zato je potrebno racionalno razmišljati i ići u smjeru povećanja proizvodnje

električne energije, ali iz izvora koji ne zagađuju okolinu u kojoj živimo kako ne bismo ugrozili život na planeti Zemlji.

Zaključujemo da je ovo tehnologija u razvoju i da postaje sve raširenija. Sve je veća potražnja za električnom energijom i sve češće srećemo solarne module kao izvor napajanja, a čak i postoje pokušaji da se koriste u transportu (u Australiji se svake godine održavaju trke solarnih automobila). Kako vrijeme odmiče i tehnologija napreduje, zastupljenost FN sistema će biti sve veća, jer je to izvor energije koji ne zagađuje niti utiče na životnu sredinu. Benefiti su definitivno veliki i ovo je energija budućnosti, uz ostale obnovljive izvore energije.

LITERATURA

[1] Labudović B., (2002), Obnovljivi izvori energije, Mašinski fakultet, Zagreb.
[2] Lambić M., (1998), Termotehnika sa energetikom, Tehnička knjiga Zrenjanin.
[3] Golubović D.,(2021), Obnovljivi izvori energije - predavanja na osnovnim studijama Mašinskog fakulteta, Istočno Sarajevo.
[4] Korištenje energije sunca, Solarni-kolektori-i-fotonaponski-sistemi.pdf (ekologija.ba) (Pristupljeno 07.04.2022)
[5] Solarna energija i fotonaponski sistemi, Solarna energija i fotonaponski sistemi (bg.ac.rs) (Pristupljeno 07.04.2022)
[6] Wikipedia Solarna fotonaponska energija - Wikipedia (Pristupljeno 09.04.2022

COMETα 2022
6th INTERNATIONAL SCIENTIFIC CONFERENCE
17th - 19th November 2022
Jahorina, B&H, Republic of Srpska
University of East Sarajevo
Faculty of Mechanical Engineering
Conference on Mechanical Engineering Technologies and Applications

PRORAČUN I PRIMJENA HARMONIJSKIH PRENOSNIKA

Samardzic Srdjan[1]

Rezime: Primarni cilj ovog rada je upoznavanje šire stručne javnosti sa tematikom harmonijskih tj. talasnih prenosnika. Kroz rad je obrađen osnovni princip rada, proračun kinematskih parametara harmonijskih prenosnika kao i proračun osnovnih geometrijskih parametara istih. Primjeri primjene ove vrste prenosnika su prikazani kroz konkretne slučajeve aplikacije u savremenim sistemima.

Ključne riječi: Harmonijski prenosnici, proračun, primjena

CALCULATION METHOD AND APPLICATIONS OF HARMONIC DRIVE

Abstract: The primary goal of this paper is, first of all, to present to the general professional public theme of harmonic drive gears. The paper explain basic principle, the calculation of the kinematic parameters of harmonic drive gears, as well as the calculation of their basic geometric parameters. Examples of the application of this type of gear are shown in specific examples of application in modern systems.

Key words: Application, Calculation method, Harmonic drive gears

1 UVOD

Ekspanzija industrije mehaničkih prenosnika snage doživljava svoj vrhunac u XX i XXI vijeku. Masovna proizvodnja mehaničkih prenosnika vrhunskih karakteristika, prije svega u pogledu stepena iskorištenja, visokih prenosnih odnosa te kompaktne konstrukcije obezbjedila je značajno širu primjenu ove vrste prenosnika u industriji u odnosu na ostale vrste prenosnika [1].

Najvažniji predstavnici savremenih mehaničkih prenosnika su svakako harmonijski prenosnici i cikloreduktori [1].

Kroz radove [1-3], prikazan je kratak uvod te objašnjen princip rada harmonijskih prenosnika. U radovima [5-6] su korišteni kao osnovni izvori za pojašnjavanje kinematike i prikaz proračuna geometrijskih parametara harmonijskih

[1] Srđan Samardžić, Mašinski fakultet Istočno Sarajevo, Istočno Sarajevo, Bosna i Hercegovina, samardzicsrdjan20@gmail.com

prenosnika dok su u radu [7] prikazani primjeri aplikacije ove vrste prenosnika u savremenim sistemima.

2 OSNOVNI PRINCIP RADA

Harmonijski prenosnici često se nazivaju i talasni prenosnici. Građeni su iz tri osnovne komponente (slika 1.) [2]:

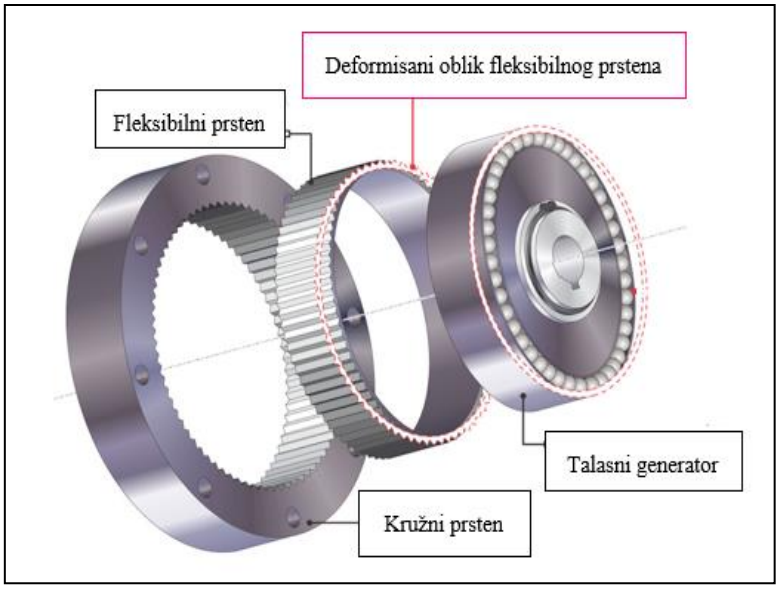

Slika 1. *Struktura harmonijskog prenosnika* [3]

- Talasni generator– elipsoidni dio sa ležajem
- Kružni prsten sa unutrašnjim ozubljenjem i
- Fleksibilni prsten sa spoljašnjim ozubljenjem, koji je spregnut sa kružnim prstenom.

Talasni generator ili deformator predstavlja sklop kugličnog ležaja sa elipsoidnim. Može se vezati na različite načine sa ulaznim ili izlaznim vratilom [4].

Fleksibilni prsten nije ništa drugo do elastična cilindrična ljuska sa spoljašnjim ozubljenjem. Veliki prečnik prstena obezbjeđuje radijalnu savitljivost, istovremeno zadržavajući torzionu krutost. U toku montaže fleksibilni prsten se postavlja na talasni generator i poprima njegov elipsoidni oblik [4].

Obrtanjem generatora talasa dolazi do talasnog kretanja fleksibilnog prstena, što dovodi do sprezanja zubaca fleksibilnog i kružnog prstena. Ovaj proces odvija se u formi kontinualnog kotrljanja. Broj zubaca kružnog prstena veći je od broja zubaca fleksibilnog prstena, pri čemu najčešća razlika iznosi dva zupca. Kao posljedica razlike broja zubaca dolazi do relativnog kretanja između ova dva prstena. Dakle, svaka puna rotacija talasnog generatora uzrokuje pomjeranje fleksibilnog prstena za dva zupca unazad u odnosu na vodeći kružni prsten. Ovo pomjeranje najčešće se odvija u smjeru koji je suprotan smjeru obrtanja generatora talasa. Na ovaj način, talasni prenosnik radi kao reduktor. Princip rada talasnog prenosnika ilustrovan je na slici 2 [4]:

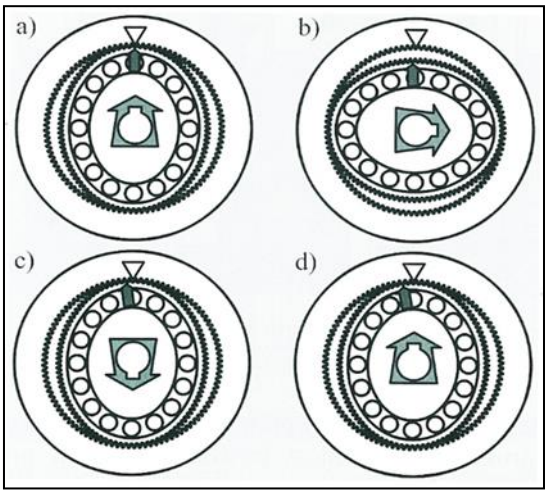

Slika 2. *Princip rada harmonijskog prenosnika* [4]

Talasni prenosnici imaju velike i brojne prednosti [2]: duplo manje dimenzije i trostruko manja težina od drugih prenosnika istih ili sličnih karakteristika, visok nivo obrtnog momenta koji se prenosi, visok prenosni odnos (od 50:1 do 320:1), velika tačnost i ponovljivost pozicioniranja, visok stepen iskorišćenja prenosnika i visok reverzibilitet, visoke brzine sa malom bukom i visoka krutost u odnosu na konvencionalne tipove prenosnika [4].

Najbitniji nedostaci ovih prenosnika ogledaju se, prema [2], u: greškama u pozicioniranju (povezane sa tačnošću izrade pojedinih elemenata prenosnika), mogućnost pojave rezonantnih vibracija, nelinearnosti koja nastaje uslijed fleksibilnosti i trenja tokom prenosa.

Kao jedan od glavnih nedostataka može se smatrati i činjenica da se o ovim prenosnicima jako malo zna.

3 KINEMATIKA HARMONIJSKIH PRENOSNIKA

Sistem sačinjen od tri componente ima dva stepena slobode (u opštem slučaju) kao i planetarni prenosnik. Kinematska šema je prikazana na slici 3 [5]:

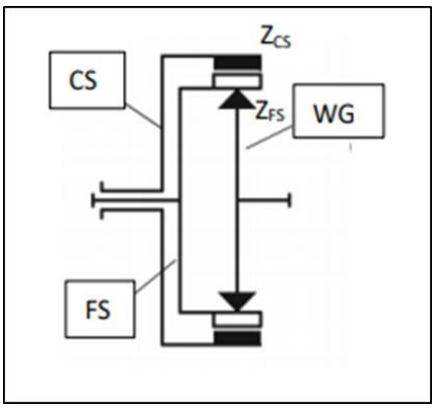

Slika 3. *Kinematska šema harmonijskog prenosnika* [5]

Relacije između ugaonih brzina komponenti su definisane sledećom jednačinom [5]:

$$\frac{\omega_{CS} - \omega_{WG}}{\omega_{FS} - \omega_{WG}} = \frac{Z_{FS}}{Z_{CS}} \tag{1}$$

gdje su: Z_{FS} - broj zubaca fleksibilnog prstena, Z_{CS} - broj zubaca kružnog prstena, ω_{WG} - ugaona brzina deformatora, ω_{CS} - ugaona brzina kružnog prsten, ω_{FS} - ugaona brzina fleksibilnog prstena.

Prenosni odnos se definiše kao:

$$u = \frac{\omega_{ul}}{\omega_{iz}} \tag{2}$$

4 PRORAČUN GEOMETRIJSKIH VELIČINA

Teorija proračuna razvijena je na odjeljenju Teorije mašina i mehanizama, moskovskog Bauman tehničkog instituta a zasniva se na teoriji geometrijske analize evolventnog sprezanja razvijene od strane V.A. Gavrilenka i istraživanja harmonijskih prenosnika njegovih učenika. Teorija se zasniva na pretpostavci da generator talasa obezbjeđuje konstantan radijus zakrivljenja podeonog sloja deformisanog fleksibilnog prstena unutar zone sprezanja ograničene centralnim uglom 2 β (slika 4) [6]:

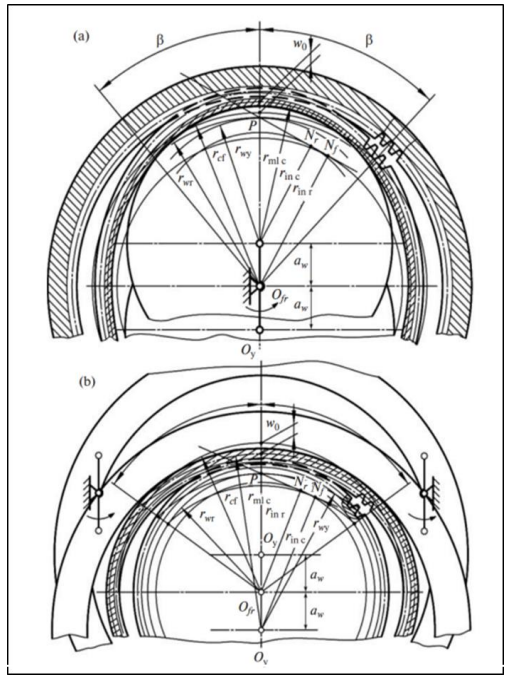

Slika 4. *Sprezanje harmonijskog prenosnika sa a) spoljašnjom i b) unutrašnjom deformacijom* [6]

Ulazni parametri za proračun su [6]: u -prenosni odnos, tip deformacije (unutrašnja/spoljašnja), Z_{FS}, Z_{CS} - broj zubaca fleksibilnog i kružnog prstena, $T, T_{\max}$ - nominalni i maksimalni obrtni moment na izlazu, n_{WG} -broj obrtaja generatora talasa, l_h - projektovani radni vijek, ψ_{ring} - koeficijent širine vrha zuba fleksibilnog prstena, karakteristike materijala fleksibilnog prstena – čvrstoća (HRC), dinamička izržljivost $\sigma_{(-1)}$ materijala, koeficijent torzione krutosti (C - opcionalno).

Proračun geometrije harmonijskog prenosnika podrazumijeva dobijanje prečnika podeone kružnice fleksibilnog prstena u nedeformisanom stanju, u skladu sa sledeća tri kriterijuma [6]:

- kriterijum savojne čvrstoće fleksibilnog prstena:

$$d_{mlf} = 220 \sqrt[3]{k_d \cdot k_{ovl} \cdot \left(\frac{h_{ml}}{d_{mlf}} \right) \cdot \left(k_z - \frac{u}{u+1} \right) \cdot T} \tag{3}$$

gdje je: k_d - dinamički koeficijent, k_{ovl} - koeficijent opterećenja, k_z - koeficijent deformacije, $\frac{h_{mlf}}{d_{mlf}}$ - relativna debljina fleksibilnog prstena ispod vrha zuba

- kriterijum izdržljivosti fleksibilnog prstena:

$$d_{mlf} = 165 \cdot \sqrt[3]{\frac{T}{(0,03 \cdot u - 1) \cdot \sigma_{F0}}} \tag{4}$$

- kriterijum torzione krutosti fleksibilnog prstena:

$$d_{mlf} = (1,12 - \frac{\sqrt{C}}{8000}) \cdot C^{(0,34 + \frac{\sqrt{C}}{35000})} \tag{5}$$

Najveći od ovih prečnika se koristi za izračunavanje modula m' koji se zaokružuje na najbližu standardnu vrijednost:

$$m' = \frac{d_{mlf}}{Z_{FS}} \tag{6}$$

Nakon usvajanja modula izračunava se stvarna vrijednost podeonih prečnika:

$$d_{FS} = m \cdot Z_{FS} \tag{7}$$

$$d_{CS} = m \cdot Z_{CS} \tag{8}$$

5 PRIMJENA HARMONIJSKIH PRENOSNIKA

Harmonijski prenosnici našli su široku primjenu u različitim sistemima u kojima se zahtjevaju mala masa i dimenzije prenosnika, visoki prenosni odnosi, visoka tačnost i mogućnost pozicioniranja, nizak nivo buke itd.

Mala težina i visoka preciznost harmonijskih prenosnika idealni su za primjenu u SCARA robotima. CSF-2UH izvedba omogućuje posebno kompaktan i elegantan dizajn kao što je prikazano na slici 5. Kružni prsten se nalazi u segmentu „nadlaktice“ i fiksan je. Posebno je dizajniran radi lakše integracije u robotski zglob. Talasni generator ima „Oldhamovu“ spojnicu radi kompenzacije radijalnog bacanja vratila motora. Fleksibilni prsten je u ovoj izbedbi izlazni element koji pokreće preko izlazne prirubnice donji segment ruke [7].

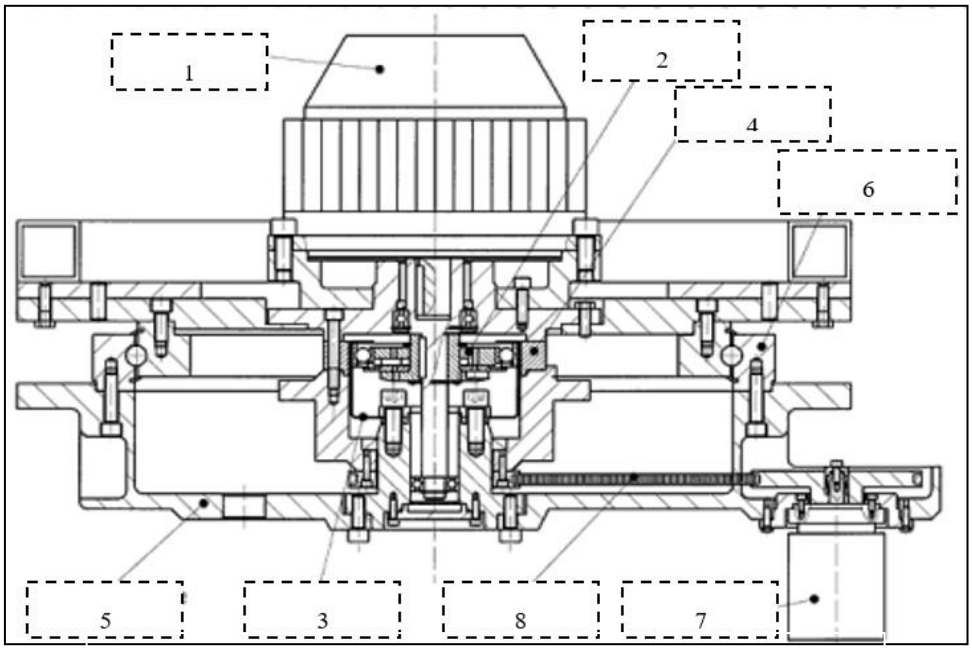

Slika 5. *Izvedba zgloba SCARA robota*
1-motor; 2-talasni generator; 3-fleksibilni prsten; 4-kružni prsten; 5-izlazna prirubnica; 6-ležaj; 7-enkoder; 8-kaišni prenosnik [7]

Harmonijski prenosnici su prevashodno razvijani i projektovani za potrebe aplikacije u složenim sistemima svemirske industrije. Na slici 6. dat je prikaz primjene harmonijskog prenosnika u pogonu rotacionog nosača solarnog panela telekomunikacionog satelita. Aktuator sadrži CSF izvedbu harmonijskog prenosnika postavljenu u kućište unutar kojeg je direktno integrisan i poseban motor. Dizajn je odlikovan i „punim“ talasnim generatorom bez otvora za smanjenje težine. Fleksibilni prsten je povezan sa izlaznom prirubnicom koja je oslonjena preko kugličnih ležajeva. Kružni prsten je takođe modifikovan radi lakše montaže u samo kućište. U ovoj aplikaciji koristi se šuplje vratilo da bi se obezbijedio prolaz kablova do baterije od solarnih panela za napajanje satelita.

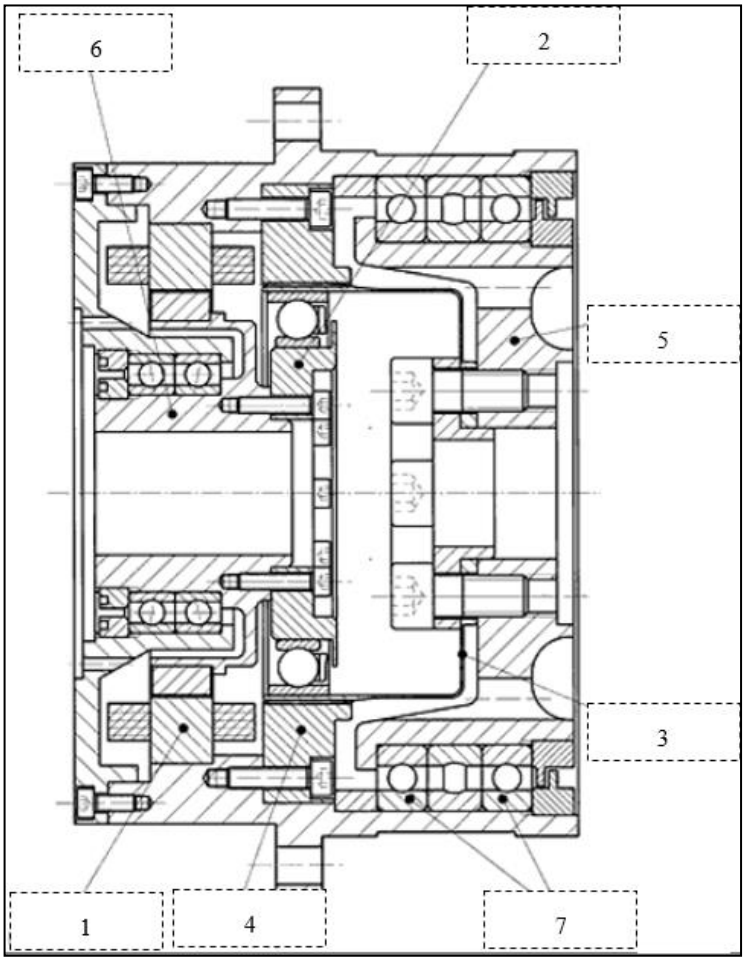

Slika 6. *Aktuator rotacionog nosača solarnog panela telekomunikacionog satelita*
1-motor; 2-talasni generator; 3-fleksibilni prsten; 4-kružni prsten; 5-izlazna prirubnica; 6-šuplje vratiloj; 7-ležajevi [7]

6 ZAKLJUČAK

Primarni cilj rada je analiza trenutnog stanja tehnike iz oblasti proračuna i primjene harmonijskih prenosnika. Na početku su predstavljeni osnovni principi rada harmonijskih prenosnika. Zatim je predstavljena kinematska analiza te dat prikaz proračuna osnovnih geometrijskih parametara navedenih prenosnika.

Doprinos rada se ogleda u približavanju harmonijskih prenosnika široj stručnoj javnosti iz oblasti mašinstva i mehatronike. Trenutno dostupna literatura iz oblasti harmonijskih prenosnika najčešće je na engleskom i ruskom jeziku pa je svaki rad na srpskom jeziku od nemjerljivog značaja za domaću indrustriju, posebno imajući u vidu činjenicu da harmonijski prenosnici zbog brojnih prednosti predstavljaju budućnost u oblasti primjene prenosnika snage.

Na osnovu kinematske analize i prikaza proračuna geometrijskih parametara lako se da zaključiti da je konstruisanje harmonijskih prenosnika veoma složen i

kompleksan proces pa buduća istraživanja trebaju ići u smjeru kreiranja programa za proračun istih.

Shodno prethodnom, cilj budućeg istraživanja je kreiranje algoritma i izrada modela u nekom od programskih paketa za modelovanje. Na osnovu izrađenog modela bilo bi poželjno uraditi MKE analizu prenosnika kao i fizičku proizvodnju ovako dobijenog harmonijskog prenosnika te izvršiti testiranje.

ZAHVALNOST

Na samom kraju, želio bih izraziti zahvalnost svom mentoru, prof. dr Miroslavu Milutinoviću, šefu katedre prof. dr Biljani Marković te doc. dr Aleksiji Đuriću i doc. dr Spasoju Trifkoviću za nesebničnu podršku koju su pružili pri izradi ovog rada ali i mog cjelokupnog školovanja na Mašinskom fakultetu Univerziteta u Istočnom Sarajevu.

LITERATURA

[1] Stojanović, B. i Blagojević, M., Mehanički prenosnici, Kragujevac: Univerzitet u Kragujevcu, Mašinski fakultet Kragujevac, 2015.
[2] Lukić L., Fleksibilni tehnološki sistemi, Kraljevo: Univerzitet u Kragujevcu, Mašinski fakultet Kraljevo, 2008.
[3] "EngineeringClicks," https://www.engineeringclicks.com/harmonic-drive/. [Pristupljeno 26 9 2022].
[4] Čiča Đ. , Mašine alatke, Banja Luka: Univerzitet u Banjoj Luci, Mašinski fakultet, 2016.
[5] Zhiyuan Y., Jiawei G., "Introducing Kinematic Fundamentals of Strain Wave Gear for Robotic Arm Joint," in *ASEE* , Niagara Falls, NY, 2019.
[6] Timofeyev G. A., Kostikov Yu. V., Yaminsky A. V., Podchasov Ye. O.,, "Theory and Practice of Harmonic Drive Mechanisms," in *IOP Conference Series: Materials Science and Engineering*, 2017.
[7] "HarmonicDrive," https://www.harmonicdrive.net/technology/inventor-c-walton-musser. [Pristupljeno 15 8 2022].

COMETa 2022
6th INTERNATIONAL SCIENTIFIC CONFERENCE
17th - 19th November 2022
Jahorina, B&H, Republic of Srpska
University of East Sarajevo
Faculty of Mechanical Engineering
Conference on Mechanical Engineering Technologies and Applications

PRIMJENA CENTRIFUGALNIH VENTILATORA U INDUSTRIJI

Borislav Jović[1]

Rezime: U radu je opisan proces primjene centrifugalnih ventilatora u industriji. Date su osnovne definicije centrifugalnih ventilatora i osnovne jednacine koje se koriste pri proračunu. Opisane su teorijske osnove i nacini na koji se mogu sprezati ventilatori i njihov rad u mreži.

Ključne riječi: centrifugalni ventilator, ventilator u industriji, svojstva ventilatora, sprezanje ventilatora.

APPLICATION OF CENTRIFUGAL FANS IN INDUSTRY

Summary: The paper describes the application process of centrifugal fans in industry. The basic definitions of centrifugal fans and the basic equations used in the calculation are given. The theoretical foundations and ways in which fans can be connected and their operation in the network are described.

Key words: centrifugal fan, industrial fan, fan properties, fan coupling.

1 UVOD

Osnovna namjena ventilatora je potiskivanje vazduha ili drugih gasova, savlađivanje strujnih otpora. Pojavljuju se u mnogim oblastima: u hemijskoj i prehrambenoj industriji, tehnici grijanja, hlađenja, klimatizacije, metalurgiji, rudarstvu, građevinarstvu, poljuprivredi itd.[1]

Zbog velike potrebe za ostvarivanje širokog dijapazona protoka vazduha pri malim ili umjerenim priraštajima pritiska, u različitim oblastima primjene, ventilatori su veoma raširene mašine u savremenom svijetu. Od njih su samo raširenij elektromotori i to pod uslovom da se pri prebrojavanju ventilatora ne broje ventilatorska kola ugrađena, radi obezbbjeđenja hlađenja namotaja, u oklopu motora. Ventilator predstavlja neizostavan element rashladnih tornjeva sa prinudnom promajom. Ventilatori koji se primjenjuju u ovim sistemima mogu biti aksijalni ili centrifugalni.

[1] Dipl. inž. maš. Borislav Jović, Mašinski fakultet, Istočno Sarajevo, borislav1234t@gmail.com

Dosta veću primjenu imaju aksijalni ventilatori koji često rade i u paralelnoj sprezi kako bi ostvarili proračunate uslove rada.

Centrifugalni ventilatori imaju širok dijapazon primjene u industriji. Neki od primjera su hlađenje električnih uređaja, uloga u ventilacijskim sistemima kao i primjena u rashladnoj tehnici. Glavni uslovi koji se stavljaju pred konstruktora ventilatora jesu optimalan rad sa stanovišta iskoristivosti, buke i čvrstoće. Prilikom ugradnje ventilatora neophodno je voditi računa o pojavi mogućih vibracija koje negativno utiču na rad i konstrukciju uopšte. Potreba za prinudnim potiskivanjem vazduha osjetila se još u davna vremena, ali se prvi ventilatori pojavljuju tek oko 1700 godine. Prije toga su za potiskivanje vazduha služili mijehovi.

2 TEORIJSKE OSNOVE CENTRIFUGALNIH VENTILATORA

Ventilator je mehanički uredaj koji pomoću rotacionog kretanja lopatica stvara strujanje gasova (vazduha) i para. Energija se preko lopatica predaje vazduhu i u njemu se stvara prirast pritiska usljed kojega se povećava njegov protok.Ventilatori u ventilacionim jedinicama transportuju vazduh od različitih usisnih mjesta kroz cjevovodni sistem do prostorija koje se ventilišu. Svaki ventilator mora nadvladati otpore strujanju vazduha kroz cjevovod, krivine i druge elemente ventilacionog sistema. U rotoru ventilatora pretvara se mehanička energija rotacije rotora, dobijena od nekog izvora energije, u kinetičku ili potencijalnu energiju strujanja fluida.

Centrifugalni ventilator se sastoji od statora, rotora, konusnog nastavka glavčine i difuzora (slika 1). Osnovni dio je rotor, dok ostali dijelovi služe za poboljšanje korisnosti pa se katkad, radi jednostavnije konstrukcije, mogu i izostaviti. Lopatice rotora oblikovane su tako da sve čestice fluida imaju isti prirast energije. [2]

Slika 1. *Centrifugalni ventilator [1]*

U ventilatoru se odvija sličan proces kao i u turbokompresoru koji služi za komprimiranje gasova na više pritiske od onih koji se postižu kod ventilatora. Klasifikacija ventilatora po obliku kola je od posebnog značaja, iz razloga što je ono elemenat u kojem se ostvaruje prenošenje energije od pogonskog motora na radni fluid. Ventilatorska kola mogu biti: radijalna, dobošasta, osna i poprečno strujna.

2.1 Jednačina kontinuiteta

Jednačina kontinuiteta u stvari predstavlja zakon o održanju mase. Navedena jednačina opisuje izolovanu količinu materije dm gustine ρ i zapremine dV te govori da je moguća promjena zapremine i gustine , ali uz zadovoljenje odgovarajućih uslova. [3]

$$dm = \rho\, dV = const. \tag{2.1}$$

2.2 Ojlerova jednačina kretanja

Ojlerova jednačina kretanja, vezana za strujanje fluida, u suštini predstavlja posljedicu Njutnovog zakona koji daje relaciju između sile i ubrzanja. Prema ovom zakonu važi da je suma zapreminskih i površinskih sila jednaka proizvodu ubrzanja i mase. Ukoliko je riječ o nestišljivom fluidu zapremine V, ograničenom površinom A, moguće je definisat zapreminske i površinske sile u sljedećem obliku: [3]

$$\int_V \rho\, \vec{F}\, dV\ ; \qquad \int_A p\, d\overrightarrow{A}$$

$\vec{F}$ – jedinična zapreminska sila;
p – pritisak po jedinici površine

2.3 Bernulijeva (energetska) jednačina

Ukoliko se ispune odgovarajući uslovi moguće je integraliti Ojlerovu jednačinu obrađenu u prethodnoj cjelini. Jedan od osnovnih uslova, koji moraju biti ispunjeni, jeste da je riječ o barotropnom fluidu (gustina je funkcija pritiska tj. ρ = ρ (p) i ne zavisi od temperature). Nakon što se transformisani oblik Ojlerove jednačine pomnoži sa usmjerenim elementom ds i integrali i dobija se sljedeća jednačina: [3]

$$\frac{c^2}{2} - U + \int \frac{dp}{\rho} = C = const. \tag{2.2}$$

Bernulijeva jednačina predstavlja zakon o održanju energije te se kao takva još naziva i energetskom jednačinom. Kada je riječ konkretno o ventilatorima, članovi koji zavise od visinske kote se mogu zanemariti zbog svoje male vrijednosti i kao takvi neće značajno uticati na sam tok proračuna. Jednostavno objašnjenje za to nalazi se u činjenici da se vazduh prilikom prolaska kroz ventilator ponaša kao nestišljiv fluid male gustine.

3 RADNA SVOJSTVA CENTRIFUGALNIH VENTILATORA

Prilikom težnje za postizanje sličnih radnih uslova dvije mašine neophodno je da se ostvare geometrijska, kinematička i dinamička sličnost. Pod pojmom geometrijske sličnosti podrazumijeva se konstantan odnos odgovarajućih dužina i uglova na samoj mašini i njenom modelu. Kinematička sličnost predstavlja sličnost vezanu za same brzine, tj. sličnost ulaznih i izlaznih trouglova brzina. Konačno, dinamička sličnost podrazumijeva sličnost u polju odnosa sila koje djeluju na model i samu mašinu, respektivno. [3]

Generalno, veza između radnih karakteristika modela i mašine, gledano sa aspekta matematičke interpretacije je jako kompleksna i kao takva nije pogodna za praktičan rad i proračun. Navedena pojava je uticala da se razvije poseban, uprošten,

empirijski pristup koji opisuje korelaciju mašine i modela. Polazna stavka kod teorije sličnosti ventilatora i turbomašina uopšte, jeste korelacija promjenjivih, koje više ili manje utiču na navedeni proces, izraženih funkcijom u sljedećem obliku:

$$F(\eta, Q, \omega, Y, r, \delta, s, w, \rho, \mu, T, c_p, \lambda, \alpha, \varepsilon, R, k, t) = 0 \quad (3.1)$$

3.1 Stepen korisnosti

Uopšteno gledano stepen korisnosti (η) predstavlja odnos izlazne (P_2) i ulazne (P_1) snage tj. :

$$\eta = \frac{P_2}{P_1} \quad (3.2)$$

Ulazna snaga (P1) kod ventilatora jednaka je snazi na vratilu (P), dok izlazna snaga (P2) predstavlja proizvod protoka ($\dot{m}$) i jediničnog rada struje (Y) ili:

$$P_1 = P\ ; \qquad P_2 = \dot{m}\, Y; \quad (3.3)$$

U opštem slučaju postoje zapreminski, mehanički i hidraulički gubici kod ventilatora pa su analogno tome definisani zapreminski (η_v), mehanički (η_m) i hidraulički (η_h) stepeni korisnosti. Veza između navedenih stepeni korisnosti i ukupnog stepena korisnosti u stvari predstavlja proizvod istih, ili :

$$\eta = \eta_v \cdot \eta_h \cdot \eta_m \quad (3.4)$$

4 RAD VENTILATORA U MREŽI

Osnovna namjena ventilatora je da potiskuju ili sisaju gasove kroz ventilaciono postrojenje koje se sastoji od jedne cijevi ili razvodne mreže. Stoga, ventilator u osnovi savlađuje samo strujne otpore, koji se prema svom fizičkom karakteru mogu izraziti na nekoliko načina (slika 2): otpori koji su najčešći i nastaju pri razvijenom turbolentnom strujanju, Otpori gdje je izložilac n manji od 2, a veći od 1, a nastaju pri prelasku laminarnog u turbolentno strujanje ili pri strujanju kroz hidraulički glatke cijevi, otpori koji odgovaraju čisto laminarnom strujanju. Na slici 2. prikazana je radna kriva ventilatora i razne vrste strujnih otpora.

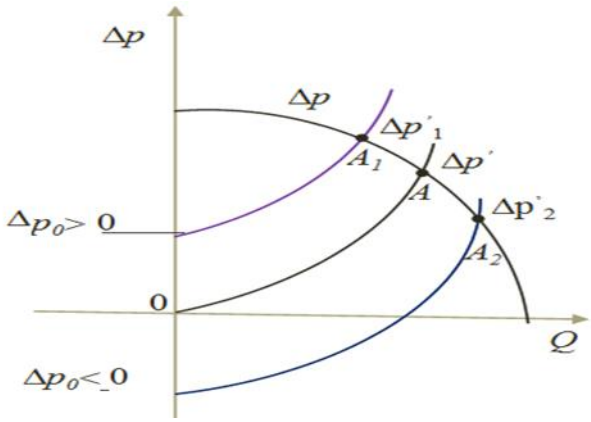

Slika 2. *Radna kriva ventilatora i razne vrste strujnih otpora [4]*

4.1 Otpori mreže

Pod prostim cjevovodom se podrazumijeva ili jedna jedinstvena cijev konstantnog prečnika ili cijev koja se sastoji iz niza dionica različitog prečnika koja se nadovezuje jedna na drugu. Osnovna karakteristika prostog cjevovoda je da se protok ne mijenja cijelom njegovom dužinom i ako se na pojedinim njegovim dužinama mogu mijenjati protočni presjeci odnosno brzine strujanja. Strujanje u ventilacionim sistemima je najčešće turbolentno. Na slici 3 prikazano je grananje cjevovda na usisnoj strani.

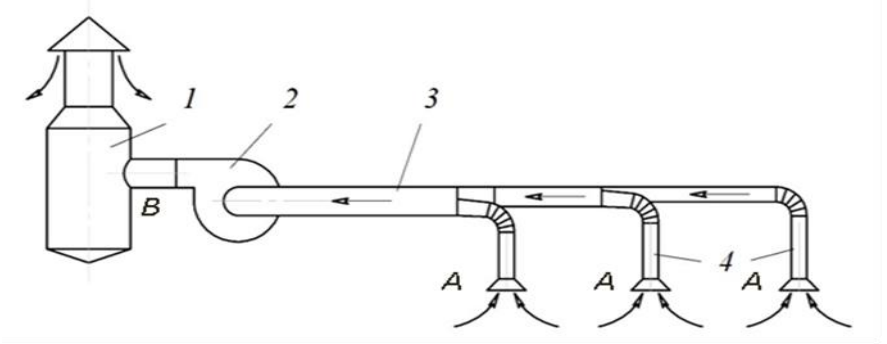

Slika 3. *Grananje cjevovda na usisnoj strani [3]*

5 SPREZANJE VENTILATORA

Da bi bilo moguće zadovoljiti projektne uslove, naročito u većim sistemima, neophodna je sprega više ventilatora. Sprega ventilatora može biti ostvarena na sljedeće načine:

- paralelno
- redno
- kombinovano

Sprezanje mašina vrši se s ciljem povećanja protoka i pritiska i sa jedinicama umjerenih dimenzija i obimnih brzina: u slučajevima kada se potrebni kapacitet mijenja sa vremenom (za vrijeme manje potrebe radi jedna mašina, a druge su u rezervi, a kod povećanja potrošnje uključuju se i druge mašine), u slučaju kada je neophodno savladati velike otpore strujanja, tj. obezbijediti potrebni izlazni pritisak, ako su otpori strujanja u cjevovodu jako veliki, pa se potrebni pritisak ne može ostvariti samo jednom mašinom. U svim takvim slučajevima projektuje se stanica sa više spregnutih mašina koja ima zajedničku energetsku karakteristiku. Načini sprezanja: serijsko (redno) sprezanje, paralelno sprezanje, kombinovano sprezanje.

5.1 Redna sprega

Najprostije rečeno, rednom spregom dva ili više ventilatora ostvaruje se povećanje pritska radnog medija dok protoci ostaju isti. Ukoliko se pomoću redno spregnutih ventilatora distribuira vazduh, prvi ventilator će ga potisnuti kroz drugi i tako redom, pri čemu će svi ventilatori u sprezi raditi sa istim protokom, a pritisci će se sabrati. Naravno, najpogodnija sprega ovoga tipa bi bila sa dva ventilatora identičnih karakteristika, međutim u praksi se nerijetko dešava da se serijski vežu i dva različita

ventilatora, naravno uz ispunjenje odgovarajućih uslova. Na slici 4. prikazana redna sprega ventilatora.

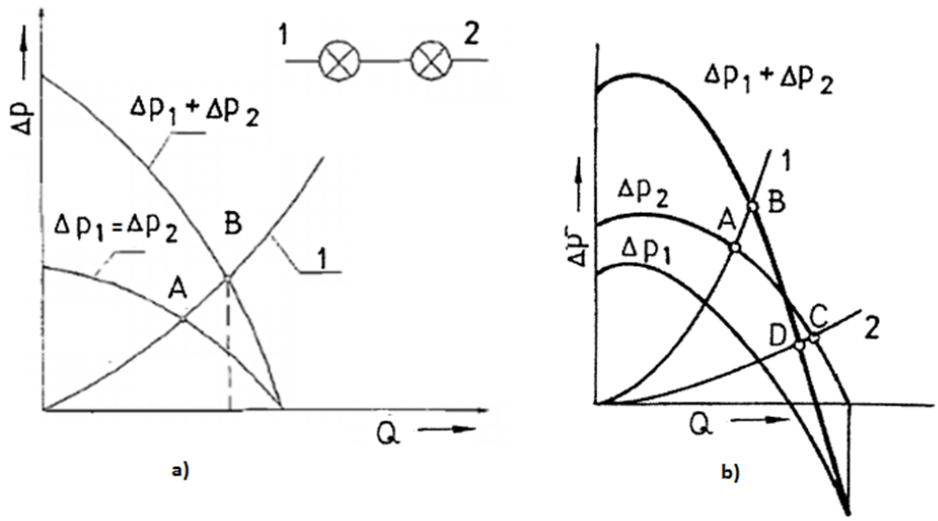

Slika 4. *Redna veza dva a) identična b) različita ventilatora [3]*

5.2 Paralelna sprega

Vrši se s ciljem povećanja ukupnog protoka, slika 5. Karakteristika tako vezanih mašina dobije se sabiranjem pojedinačnih protoka za razne konstantne vrijednosti napora. Poseban vid paralelne sprege ventilatora jeste povezivanje ventilatora identičnih specifikacija i u tome slučaju postiže se simetričan rad. Šema simetrične paralelne veze data je slikom 5.

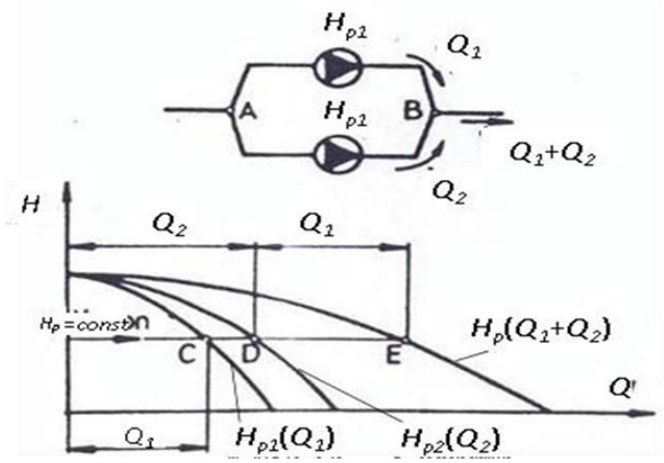

Slika 5. *Primjer paralelne sprege ventilatora [5]*

6 ZAKLJUČAK

Klasični centrifugalni ventilator rezultat je dugogodišnjeg iskustva u dizajniranju i proizvodnji ventilacijske opreme. Ovo nije samo rješenje za industriju, već je i optimalno sredstvo za provjetravanje stambenih i kancelarijskih prostorija. Dakle, radijalni ventilatori mogu biti opremljeni pomoćnim komponentama: podesivi tajmeri i intervalni prekidači, fotosenzori i detektori vlage, regulatori brzine, senzori preopterećenja motora i nedostatka električne energije na mreži, opružni apsorberi ili gumeni izolatori vibracija. Glavni nedostatak ugradnje ventilatora je potreba za napajanjem električnom energijom, koja obično iznosi oko 3-4 kW po proizvedenom MW električne energije. Sastavni dio recirkulacionih rashladnih sistema sa prinudnom promajom je ventilator.

Ventilatori najčešće imaju pogon preko elektromotora i postavljaju se iznad uređaja za raspodjelu bilo da se radi o vodi ili vazduhu. Ispod ventilatora se nalaze i eliminatori kapljica koji odstranjuju kapljice povučene vazdušnom strujom. Upravo, jedna od najvećih prednosti centrifugalnih ventilatora leži u mogućnosti regulacije ventilatorske sekcije, čime se mogu kreirati gotovo isti radni uslovi u svim periodima godine. Regulacija centrifugalnih ventilatora se najčešće obavlja promjenom karakteristike pada pritiska u mreži, promjenom radnih karakteristika ventilatora i kombinovano regulisanje primjenom prethodno navedenih načina regulacije protoka ventilatora.

Ovim radom obrađena je tema „Primjena centrifugalnih ventilatora u industriji“ sa akcentom na centrifugalne ventilatore koji su neizostavan element za rad jednog postrojenja.

LITERATURA

[1] EkoEngineering, Centrifugalni ventilatori.
[2] Pečornik M., (1997). Ventilator. Tehnička enciklopedija, sv. 13, str. 446-454.
[3] Gajić A., Krsmanović Lj., (2000), Turbomašine: ventilatori, Mašinski fakultet, Beograd.
[4] Milovanovic Z., (2014), Pumpe, kompresori i ventilatori, Mašinski fakultet Banjaluka.
[5] Delalić S., (2008), Pumpe, ventilatori i kompresori: skripta, Univerzitet u Tuzli, Mašinski fakultet, Tuzla.

COMETa 2022
6th INTERNATIONAL SCIENTIFIC CONFERENCE
17th - 19th November 2022
Jahorina, B&H, Republic of Srpska
University of East Sarajevo
Faculty of Mechanical Engineering
Conference on Mechanical Engineering Technologies and Applications

PODMAZIVANJE PARNIH TURBINA

Nemanja Vuković[1]

Rezime: U radu su prezentovane osnovne fizičko-hemijske karakteristike ulja koja se koriste za podmazivanje parno-turbinskih postrojenja sa pratećim sistemom podmazivanja. Navedeno je šta sve utiče na period njihove zamjene i kako se može produžiti period zamjene. Razmatrano je podmazivanje parne turbine u Rudniku i Termoelektrani "Gacko" sa njenim sastavnim parametrima koje posjeduje u radu. Takođe, dati su uslovi koje treba da posjeduje turbinsko ulje kako bi moglo da se eksploatiše u Termoelektrani "Gacko".

Ključne riječi: maziva, parna turbina, turbinska ulja, sistem podmazivanja.

LUBRICATION OF STEAM TURBINES

Abstract: The paper presents the basic physico-chemical characteristics of the oil used for the lubrication of steam-turbine plants with the accompanying lubrication system. It is stated that everything affects the period of their replacement and how the replacement period can be extended. Lubrication of the steam turbine in the "Gacko" Mine and Thermal Power Plant was considered with its constituent parameters that it has in operation. Also, the conditions that the turbine oil should possess in order to be able to be exploited in the "Gacko" Thermal Power Plant are given..

Key words: lubricants, steam turbine, turbine oils, lubrication system

1 UVOD

Razvoj tehničkih sistema u svim granama industrije napreduje sve većim intenzitetom. Zajedno sa razvojem tehničkih sistema neophodno je razvijati i maziva koja mogu ispunjavati zahtjeve proizvođača tehničkih sistema. Pojam maziva podrazumijeva gasovite, tečne i čvrste materijale koji se koriste za smanjenje trenja

[1] Nemanja Vuković, Mašinski fakultet Istočno Saarajevo, vukovicn215@gmail.com

između spregnutih radnih površina koje se nalaze u relativnom kretanju. Osim toga, maziva se koriste i za prenos snage, prenos toplote, hlađenje, zaštitu od korozije i dr.

Stalnim usavršavanjem tehničkih sistema oni postaju sve složenijih konstrukcija. Funkcije im bivaju sve raznovrsnije i složenije, a opterećenja sve veća. U skladu sa svakom promjenom konstrukcije i funkcije, konstruktori su tražili poboljšanje kvalitetnog nivoa mazivih ulja i sve duži interval upotrebe.

Turbine odnosno turboagregati predstavljaju jedan od najsloženijih tehničkih sistema sa aspekta zahtjeva za podmazivanje. Osnovni zadatak turbina je da transformišu energiju pare, vode ili gasa u mehanički rad. U zavisnosti od vrste radnog fluida razlikuju se: parne, vodene i gasne turbine. Za njihovo podmazivanje, u početku su se, upotrebljavala čista bazna ulja, međutim sa povećanjem zahtjeva proizvođača turbina, baznim uljima se dodaju aditivi za zaštitu od korozije, EP aditivi i dr. Najčešće su u upotrebi turbinska ulja mineralne osnove. Osnovni zadaci koje treba da ispunjavaju turbinska ulja su: podmazivanje ležajeva i zupčastih prenosnika turbine, odvođenje toplote, zaptivanje sistema, sprečavanje trenja i habanja, zaštita od korozije, prenos snage u regulacionim sistemima turbine i dr. Ova ulja karakteriše: visoka oksidaciona stabilnost, dobra mazivost, izuzetno dobra sposobnost izdvajanja vode, hidrolitička stabilnost, dobra filtrabilnost i niska tendencija na pojavu pjenjenja. Budući da ova ulja često dolaze u kontakt s vodom, moraju imati izuzetno dobra deemulzijska svojstva, sposobnost dobrog odvajanja vode. Osim toga, vrlo je važno da turbinska ulja imaju smanjenu tendenciju stvaranja pjene i visoku sposobnost izdvajanja vazduha.

Razvoj turbinskih ulja je definisan zahtjevima proizvođača turbina. Izbor turbinskog ulja, primjenu i kontrolu u toku rada, treba vršiti u saradnji sa proizvođačem turbine i ulja. Najčešće viskozne gradacije turbinskih ulja su ISO VG 32; 46; 68 i 100. Osnovni parametri za izbor turbinskog ulja su: konstrukcija turbine, uslovi rada, broj obrtaja, opterećenje, radna temperatura i dolivanje ulja. Od ovih parametara zavisi i vijek upotrebe turbinskih ulja.

2 PARNA TURBINA K-300-240

Turbine su uređaji u kojima se vrši pretvaranje energije radnog fluida u mehanički rad i služe za pokretanje neke radne mašine. Turbina zajedno sa radnom mašinom čini turboagregat, a svi elementi od izvora energije, preko turboagregata zajedno sa pripadajućim cjevovodima, pumpama i izmjenjivačima toplote nazivaju se jednim imenom turbinsko postrojenje [1].

Parne turbine imaju najširu primjenu za pogon generatora za proizvodnju električne energije. Kondenzacione turbine su našle primjenu u termoelektranama, mada se koriste i za pogon kompresora i pumpi u hemijskoj i petrohemijskoj industriji. Današnja turbogeneratorska postrojenja rade pri visokim pritiscima i temperaturama pare, što se reflektuje i na zahtjevani kvalitet ulja za podmazivanje [2] . Na slici 1. je prikazana konstrukcija parno-turbinskog postrojenja ruske proizvodnje LMZ (Lenjingradski metalni zavod).

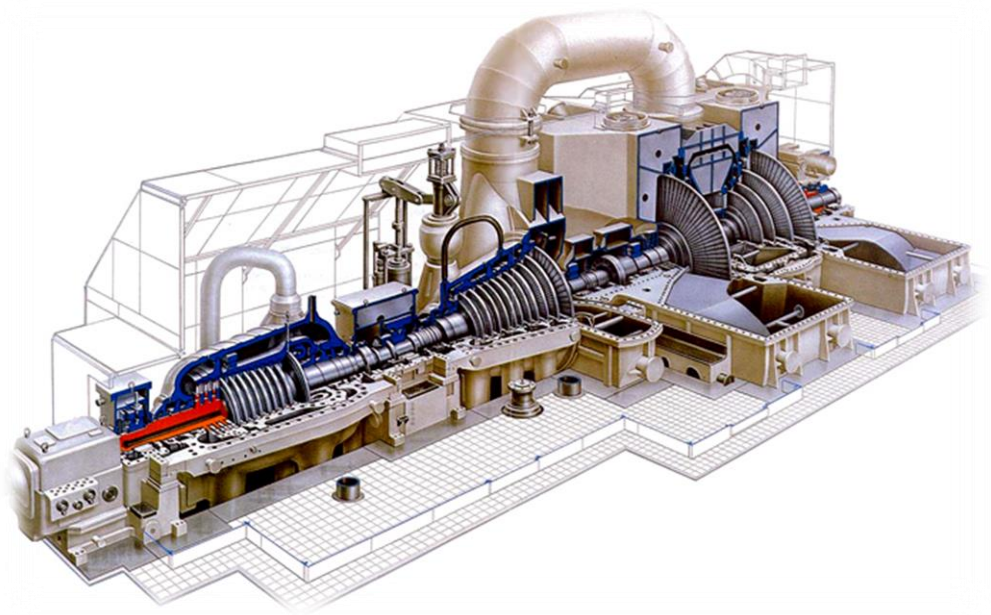

Slika 1. *Parno-turbinsko postrojenje (proizvođač LMZ) [3]*

2.1 Karakteristike turbine K-300-240

Na slici 2. je prikazan uzdužni presjek parne turbine K-300-240 ruske proizvodnje LMZ koja se koristi u Termoelektrani “Gacko”.

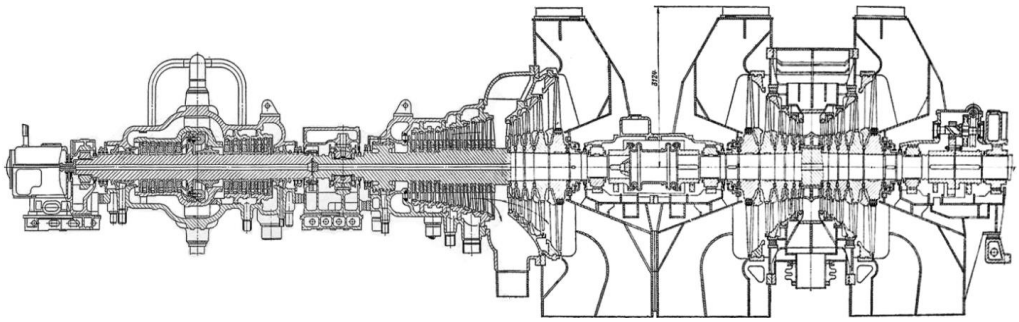

Slika 2. *Uzdužni presjek parne turbine K-300-240 [4]*

Parna turbina K-300-240 je kondenzaciona, jednoosovinska, trocilindrična i namijenjena je za direktan pogon generatora naizmjenične struje. Odlikuje se sljedećim parametrima [4]:

- nazivna snaga turbine: 300 MW;
- nominalni pritisak pare ispred turbine: 240 bar;
- broj obrtaja rotora: n=3000 o/min;

- temperatura primarne pare: T=545 ^{o}C;
- pritisak primarne pare: p=240 bar;
- temperatura pare na izlazu iz cilindra visokog pritiska (CVP): 305 ^{o}C;
- pritisak pare na izlazu cilindra visokog pritiska (CVP): 43,9 bar;
- temperatura međupregrijane pare ispred cilindra srednjeg pritiska (CSP): 545 ^{o}C;
- pritisak međupregrijane pare ispred cilindra srednjeg pritiska (CSP): 39 bar;
- pritisak u kondenzatoru pri proračunskom režimu iznosi: 0,072 bar;
- protok rashladne cirk-vode: 36000 m^3/h;
- nominalni protok svježe pare kroz turbinu iznosi: 930 t/h;
- turbina ima 8 neregulisanih oduzimanja pare, koja su namijenjena za zagrijavanje napojne vode u sistemu regeneracije niskog pritiska (NTZ), u deaeratoru i u sistemu regeneracije visokog pritiska (VTZ) do proračunske temperature 274 ^{o}C.

Na slici 3. je prikazana parna turbina tipa K-300-240 prilikom remonta u jednoj od termoelektrana u Ruskoj Federaciji.

Slika 3. *Remont parne turbine K-300-240 LMZ [5]*

U zavisnosti od parametara pare, parna turbina se dijeli na turbine visokog pritiska (TVP), srednjeg (TSP) i niskog pritiska (TNP) [6].

3 MAZIVA I SISTEM PODMAZIVANJA TURBINE

Osnovna namjena maziva kod turbinskih postrojenja je podmazivanje različitih vrsta pretežno kliznih ležajeva, a zatim kao hidraulički medijum u regulacionim, sigurnosnim i kontrolnim sistemima. Takođe, u termoelektranama služe za zaptivanje generatora hlađenih vodonikom. U zavisnosti od uslova rada, kod turbinskih postrojenja koriste se mineralna i sintetička ulja, kao i teško zapaljive tečnosti [6]. U tabeli 1. dat je pregled maziva primijenjenih za parna turbinska postrojenja.

Tabela 1. *Pregled maziva za parna turbinska postrojenja [2]*

Komponenta	Viskozitetna grupa, VG	Vrsta (familija) maziva
Klizni ležaji turbogeneratora	32, 46 i 68 (100)	Turbinsko ulje
Regulacija i kontrolni sistemi	32 i 46	Turbinsko ulje, teško zapaljive hidrauličke tečnosti
Zaptivanje generatora	32 i 46	Turbinsko ulje
Pumpe		Turbinsko ulje
Hidrodinamičke spojnice		Ulja za hidrodinamičke prenosnike
Hidraulička oprema		Hidrauličko ulje

Svakako, po upotrebi i značaju od posebne su važnosti tečna maziva za podmazivanje ležaja turbine i generatora koja su poznata pod nazivom turbinska ulja. Osnovna njihova funkcija je da [2] :

- podmazuju ležaje i elemente reduktora,
- uspješno prenose impulse u kontrolnim sistemima, podmazujući istovremeno njihove dijelove,
- uspješno vrše hlađenje ležaja i ostalih dijelova, i
- sprečavaju pojavu korozije i taloga u sistemu.

Sistemi za podmazivanje i regulaciju turbinskog postrojenja koriste visoko kvalitetna turbinska ulja gradacije T-22, T-30 ili T-46, proizvedena destilacijom sirove nafte. Da bi turbinsko ulje uspješno obavilo svoju funkciju, potrebno je da posjeduje sljedeća svojstva [6]:

- odgovarajuću viskoznost i indeks viskoznosti,
- da ne sadrži štetne materije i nečistoće,
- da je visoko otporno na oksidaciju,
- da lako otpušta vazduh,
- da ne stvara emulziju sa vodom,
- da ne pjeni, i
- da pruža adekvatnu zaštitu metalnih dijelova od djelovanja korozije.

Radni vijek turbinskih ulja, uz odgovarajuću njegu tokom eksploatacije turbinskog postrojenja, iznosi i 8 do 10 godina (samo u izuzetnim slučajevima moguć je radni vijek od 15 godina). U toku svog radnog vijeka, turbinsko ulje je podložno procesu starenja, pri čemu dolazi do promjene njegovih fizičkih i hemijskih svojstava. U procesu starenja ulja raste njegova gustina i viskoznost, ulje postaje korozivno agresivnim (zbog nastalih topljivih i isparljivih kiselih jedinjenja), a sposobnost deemulgacije se značajno pogoršava. Prisustvo vode i nekih metala, kao i rad sa povišenom temperaturom pogoduju ubrzavanju procesa starenja ulja. U svrhu usporavanja procesa starenja ulja i povećanja pouzdanosti rada regulacionih i sigurnosnokontrolnih sistema koriste se aditivi za smanjenje pjenjenja ulja i sprečavanje njegove oksidacije i korozije [6] .

3.1 Sistem za podmazivanje turbine

Sistem za podmazivanje predstavlja vrlo važnu komponentu turbinskog postrojenja, pa samim tim i zahtjevi za radom ovog sistema su vrlo rigorozni. Nepravilan rad ovog sistema ima za posljedicu nepredviđene situacije, sa veoma teškim posljedicama (pregrijavanje konstrukcionih materijala, njihovo topljenje, pojava požara i slično). Prema nivou pritiska ulja, sistemi za podmazivanje se uslovno dijele u dvije grupe, i to na [6] :

- **sisteme za podmazivanje sa niskim pritiskom,** hlađenje generatora i snabdijevanje hidrauličkih spojnica (pritisak ulja u sistemu za podmazivanje ne prelazi 0,295 MPa, a kod sistema zaptivanja električnog generatora 0,392 MPa), i
- **sisteme za podmazivanje sa visokim pritiskom** (sistemi za regulaciju), zavisno od snage, parametara i konstrukcionih karakteristika turbinskog postrojenja (interval od 0,49 do 0,98 MPa).

Sistem za podmazivanje turbinskih postrojenja mora odgovoriti na tri ključna zahtjeva, koja se postavljaju za njihov rad: visoka sigurnost i pouzdanost u radu (korišćenje dvostrukih ili više rezervnih elemenata, kao i više nezavisnih krugova zaštite), zatim visoka sigurnost protiv požara (najčešće korišćeno organsko ulje ima tačku zapaljenja kod 370 ^{o}C, što zahtijeva da se u uslovima eksploatacije mora spriječiti mogućnost stupanja ulja u kontakt sa vrelim turbinskim dijelovima, parovodima i slično), kao i osiguranje mogućnosti što dugotrajnijeg korišćenja turbinskog ulja (visoka cijena ulja, vrijeme potrebno za njegovu zamjenu, gubici usljed zastoja zbog zamjene ulja i slično). Vrsta, namjena i veličina turboagregata određuje da li će se koristiti jednostavan postupak podmazivanja ili složeni cirkulacioni sistem [6]. Podmazivanje osnovnih elemenata savremenih parnih turbina i generatora vrši se cirkulacionim sistemom. Uopšteno, uljni cirkulacioni sistem uključuje ležišni, visokopritisni, kontrolni, zaptivni i drenažni sistem ili podsistem. Taj sistem odnosno podsistem treba da omogući snabdijevanje kliznih ležaja potrebnom količinom ulja određene temperature i pritiska [2].

3.2 Sistem podmazivanja turbogeneratora Termoelektrane “Gacko”

U sistemu za podmazivanje turbogeneratora ulje se napaja preko dvije glavne pumpe pogonjene elektromotorom naizmjenične struje i dvije havarijske pumpe koje pokreću elektromotori jednosmjerne struje. Jedna od dvije glavne pumpe je rezervna. Tokom rada glavne pumpe pritisak ulja za podmazivanje ležajeva na nivou ose turbine održava se na vrijednosti od 1,2 odgovarajućim odvodnim ventilima. U toku rada havarijske pumpe, ovaj pritisak mora biti 0,7 bara [6] .

Šemu podmazivanja turbogeneratora čine sljedeći elementi: rezervoar za ulje, glavna AC pumpa, sistem cijevi za podmazivanje, hladnjaci ulja, havarijska DC pumpa, odvod rezervoara za ulje, havarijski rezervoari, relej pritiska, separator pjene, odvodni ventili, odvod ulja iz turbogeneratora, pumpe za napajanje, pumpe za podmazivanje i hidro spojnice [6]. Na slici 4. je predstavljena šema za podmazivanje turbogeneratora koji se koristi u Termoelektrani “Gacko”.

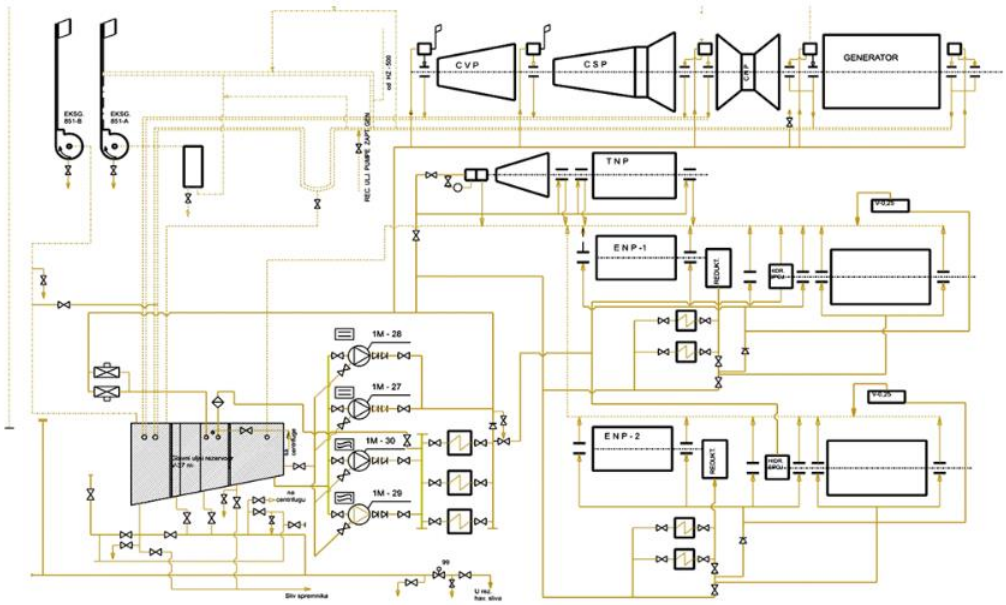

Slika 4. *Šema podmazivanja turbogeneratora [4]*

Pomoćni rezervoari za ulje nalaze se u kućištima ležajeva turbogeneratora i napunjeni su uljem pri normalnom radu turbogeneratora. Ovi rezervoari su namijenjeni da obezbijede snabdjevanje uljem ležajeva turbogeneratora u situacijama kada je redovno podmazivanje poremećeno tokom zaustavljanja od 15 do 20 minuta. To su slučajevi uključivanja pumpi za podmazivanje kao i slučajnog zaustavljanja turbine praćeno gašenjem pumpi za podmazivanje. Havarijsko podmazivanje u slučaju otkazivanja prinudnog podmazivanja trebalo bi da spriječi kvarove rotora turbogeneratora.

Na slici 5. je dat prikaz sistema kontrole podmazivanja turbogeneratora.

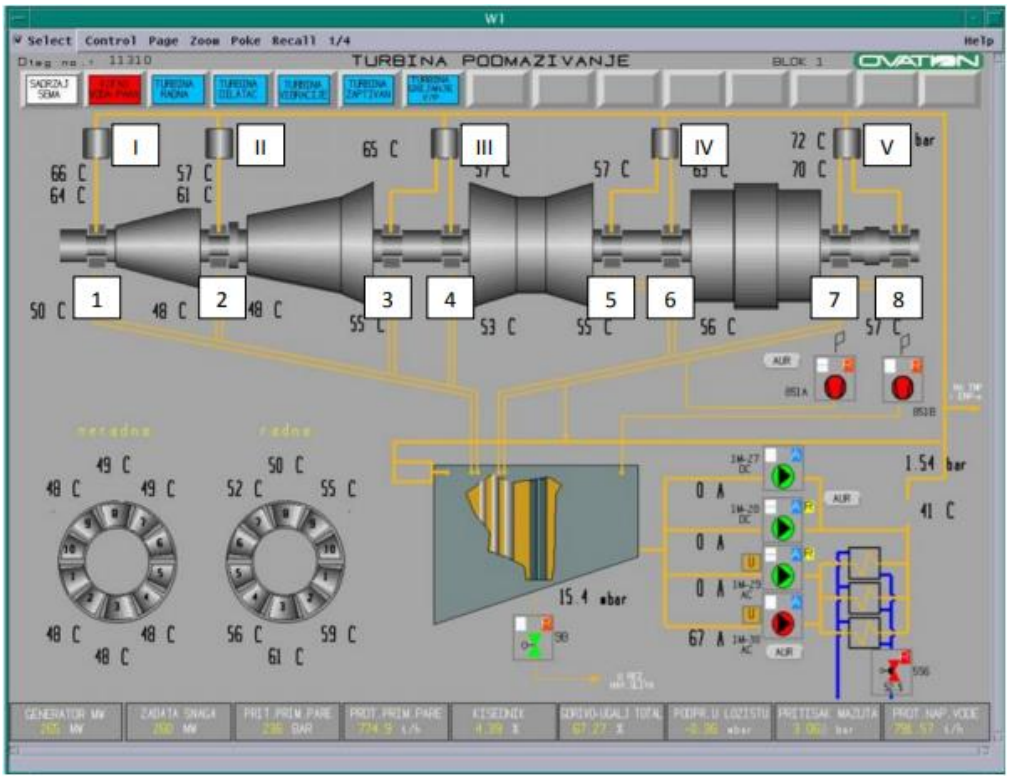

Slika 5. Šema sistema kontrole podmazivanja [6]

Ovaj sistem omogućava praćenje pritiska ulja u sistemu, kao i temperature na pozicijama osam ležajeva turbogeneratora (1-8) i odgovarajućih pet pomoćnih rezervoara za ulje (I-V) za havarijsko podmazivanje. Šest ležajeva (1-6) sa četiri pomoćna rezervoara za ulje (I-IV) pripadaju turbini. Ležajevi 7 i 8 sa pomoćnim razervoarom za ulje V pripadaju generatoru.

Temperatura ulja pri prolasku kroz hladnjak ulja reguliše se količinom rashladne vode koja se dovodi do hladnjaka ulja. Kada je brzina rotacije rotora turbine 3000 o/min, temperatura ulja poslije hladnjaka ulja treba da bude od 40 do 50 ^{0}C.

4 USLOVI PRIMJENE TURBINSKIH ULJA U TERMOELEKTRANI “GACKO”

Pri eksploataciji energetskih ulja treba biti obezbijeđen [4] :

- pouzdan rad tehnoloških sistema sa opremom napunjenom uljem;
- održavanje eksploatacionih svojstava ulja;
- skupljanje i regeneracija eksploatisanih ulja u cilju ponovnog korišćenja u prethodne namjene.

Sva energetska ulja moraju imati sertifikat kvaliteta ili pasoš i moraju se podvrgnuti laboratorijskoj analizi u cilju određivanja njihovih karakteristika prema standardu. Ulja koja ne odgovaraju zahtjevima standarda prema kojima su proizvedena ne smiju se upotrebljavati.

Turbinsko ulje za parne turbine, elektro i turbo napojne pumpe mora zadovoljiti sljedeće norme [4] :

Naftno ulje

- Kiselinski broj – ispod 0,3 mgKOH na 1 g ulja;
- Vode, prljavštine, mehaničkih primjesa – ne smije biti (određuje se vizuelno);
- Rastvorenog taloga ne smije biti (određuje se pri kiselinskom broju ulja 0,1 mgKOH na 1 g ulja i više);
- Termokiselinska stabilnost za ulje Tp-22 S (kiselinski broj ne iznad 0,8 mgKOH na 1 g ulja);
- Uslovi oksidacije ulja: ispitna temperatura 120 ± 5 ^{o}C, vrijeme 14 h i brzina dovođenja kiseonika 200 m^3/min. Termokiselinska stabilnost ulja određuje se jedan put godišnje pred početak jesensko – zimskog maksimuma za ulje (ili njihove smjese) sa kiselinskim brojem 0,1 mgKOH na 1 g ulja i više. Za ulja iz uljnih sistema elektro i turbo napojnih pumpi ovaj pokazatelj se ne određuje.

Regulaciono sintetičko ulje

- Kiselinski broj – ne iznad 0,1 mgKOH na 1 g ulja;
- Sadržaj oksida rastvorljivih u vodi – ne iznad 0,4 mgKOH na 1 g ulja;
- Maseni talog mehaničkih primjesa – ne iznad 0,01 %;
- Promjena viskoziteta – ne iznad 10 % početne vrijednosti za teška ulja;
- Sadržaj rastvorenog taloga (prema procedurama BTI) – promjena optičke prozračnosti – ne iznad 25 % (određuje se pri kiselinskom broju ulja 0,7 mgKOH na 1 g ulja i više).

Regulaciona sintetička ulja, koja su dostigla granične eksploatacione karakteristike kiselinskog broja, moraju biti otpremljena proizvođaču radi regeneracije kvaliteta. Eksploatacija vatrootpornih ulja mora se vršiti u skladu sa zahtjevima specijalne instrukcije.

U toku skladištenja i eksploatacije turbinsko ulje se mora periodično kontrolisati vizuelnim pregledom i skraćenom analizom. Skraćena analiza naftnog ulja obuhvata: određivanje kiselinskog broja, prisustvo mehaničkih primjesa, prljavštine i vode. Skraćena analiza vatrootpornog ulja obuhvata: određivanje kiselinskog broja, sadržaj oksida rastvorljivih u vodi, prisustvo vode, određivanje količinskog sadržaja mehaničkih primjesa ekspres-metodom. Vizuelna kontrola ulja podrazumijeva provjeru ulja po spoljašnjem izgledu na prisustvo vode, prljavštine i mehaničkih primjesa radi donošenja odluke o njegovom prečišćavanju. Vizuelnu kontrolu ulja koja se koriste za parne turbine i turbo-pumpe, treba vršiti jedanput dnevno.

Na elektrani se mora čuvati stalna rezerva naftnog turbinskog ulja u količini jednakoj (ili većoj) od zapremine uljnog sistema agregata i rezerva za dosipanje od 45 dnevnih potreba. Stalna rezerva vatrootpornog turbinskog ulja mora biti veća ili jednaka godišnjoj potrošnji za dosipanje za jedan turbo-agregat.

Kontrolu kvaliteta svježih i eksploatacionih energetskih ulja, davanje podataka o primjeni ulja, kao i formiranje grafikona njihove kontrole, a takođe tehničko rukovođenje tehnologijom obrade, mora vršiti hemijsko-tehnološki pogon.

5 ZAKLJUČAK

Eksploatacija parne turbine kao složenog tehničkog sistema u prvom redu podrazumijeva ostvarenje projektovane funkcije cilja (proizvodnja električne energije, toplote i tehnološke pare) sa što manjim intervalima zastoja. Podizanje vrijednosti stepena korišćenja turbine i njene pomoćne opreme na viši nivo postiže se kvalitetnim i od strane proizvođača opreme propisanim rukovanjem i održavanjem. Osnovni parametar koji karakteriše metode za njihovo održavanje je informacija o njihovom trenutnom stanju.

Od posebnog je značaja primjena maziva za funkcionalan rad i održavanje parne turbine. Za podmazivanje turbina koriste se visokokvalitetna turbinska ulja viskoznih gradacija T-22, T-30 i T-46 koja uz pomoć sistema podmazivanja treba da obave neke veoma vitalne funkcije za pravilan rad i funkcionisanje turbinskog postrojenja kao što su: podmazivanje ležaja, prenošenje impulsa u kontrolnim i regulacionim sistemima, zatim hlađenje ležajeva i ostalih dijelova. Sistem podmazivanja treba da ispuni tri osnovna zahtjeva: visoka sigurnost i pouzdanost u radu, visoka sigurnost protiv požara i osiguranje mogućnosti što dugotrajnijeg korišćenja turbinskog ulja.

U radu su pomenute dvije vrste sistema podmazivanja, sa visokim i sa niskim pritiskom. Da bi se obezbijedilo pravilno funkcionisanje ovog sistema potreban je stalni nadzor radnog osoblja da ne bi došlo do nekih akcidentnih situacija koje bi dovele do oštećenja dijelova turbinskog postrojenja, a samim tim i do povećanih troškova zamjene dijelova. Prezentovan je primjer sistema kontrole podmazivanja u Termoelektrani “Gacko” i prikaz šeme podmazivanja turbogeneratora za istu tu elektranu sa parnom turbinom tipa K-300-240 LMZ. Takođe, navedene su osnovne karakteristike turbine ovog tipa, sa parametrima pare koje posjeduje u radu. Iz toga proizilazi da stalni zahtjevi za gašenjem termoelektrana na fosilna goriva i prelaska na obnovljive izvore energije ne vode u dobrom pravcu, jer su upravo najveće količine energije proizvedene u funkcionalnoj jedinici sa parno-turbinskim postrojenjem.

LITERATURA

[1] Simić, S.: Goriva i maziva, Mašinski fakultet, Istočno Sarajevo, predavanja, 2022. godina.
[2] Perić, S.: Savremene metode analize ulja u tehničkim sistemima, Vojna akademija, Beograd.
[3] http://nizrp.narod.ru/metod/tsuitd/1590157964.pdf, pristupljeno: 21.08.2022.
[4] Gončar, V.A., Ganjžin, N.N., Doder, M., Jeremić, D.: Uputstvo za obuku operativnog osoblja za rad na bloku 300 MW TE Gacko, 2010.
[5] https://thepresentation.ru/uncategorized/konstruktsiya-turboagregata-p-6-355, pristupljeno: 09.09. 2022.
[6] https://www.researchgate.net/, pristupljeno: 05.09. 2022.

COMETa 2022
6th INTERNATIONAL SCIENTIFIC CONFERENCE
17th - 19th November 2022
Jahorina, B&H, Republic of Srpska
University of East Sarajevo
Faculty of Mechanical Engineering
Conference on Mechanical Engineering Technologies and Applications

PRIMJENA AKSIJALNIH VENTILATORA U RECIRKULACIONIM RASHLADNIM POSTROJENJIMA

Nikola Vuković[1]

Rezime: U radu je opisana upotreba i značaj aksijalnih ventilatora u sklopu recirkulacionih rashladnih sistema. Najprije su definisane teorijske osnove aksijalnih ventilatora, a zatim i mogućnost njihovog regulisanja. Posebna pažnja posvećena je recirkulacionim rashladnim sistemima, sa akcentom na one sa prinudnim strujanjem vazduha.

Ključne riječi: Aksijalni ventilatori, regulacija ventilatora, rashladni sistemi, rashladni toranj.

APPLICATION OF AXIAL FANS IN RECIRCULATION COOLING SYSTEMS

Abstract: The paper describes application and the importance of axial fans used in recirculated cooling systems. Basic theoretical principles of axial fans are described, and then the possibility of their control and regulation. The highlight of this work are the recirculated cooling systems, especially ones with forced airflow.

Key words: Axial fans, fan regulation, cooling systems, cooling tower

1 UVOD

Voda kao rashladni medij, u energetici i procesnim postrojenjima, služi za "odvajanje" toplote koja se stvara u postrojenjima. Primjena klasičnih protočnih sistema hlađenja ugrožava slobodne resurse vode. U mnogim zemljama propisi o održavanju čistih voda zabranjuju odvođenje zagrijane rashladne vode u kanalizaciju. U cilju daljeg očuvanja prirodnih izvora vode kao i ekonomske opravdanosti umjesto klasičnih protočnih rashladnih sistema izvode se recirkulacioni sistemi hlađenja tehnoloških voda. Investicija je ekonomski relativno brzo opravdana zavisno od kapaciteta hlađenja i nivoa cijena na tržištu. Osnovni element ovih sistema je vlažni rashladni toranj. [1]

Posljednjih godina sve je veća ekspanzija recirkulacionih rashladnih sistema koji sami po sebi imaju veći broj varijacija. U industriji najznačajniji je takozvani

[1] Nikola Vuković, Mašinski fakultet Istočno Sarajevo, vukovicnikola998@gmail.com

otvoreni recirkulacioni rashladni sistem čiji je neizostavan element rashladni toranj. U zavisnosti od vrste rashladnog tornja moguće je definisati i različite vrste navedenih sistema. Uopšteno gledano svi rashladni tornjevi se klasifikuju u dvije grupe i to u *mokre i suve*. Dalja podjela se vrši prema više kriterijuma, a kako je tema ovoga rada vezana za primjenu aksijalnih ventilatora u recirkulacionim rashladnim sistemima, kao referenti tornjevi uzimaju se oni sa takozvanom prinudnom promajom. Prinudna promaja tj. strujanje vazduha u rashladnim tornjevima ostvaruje se upotrebom ventilatora i to najčešće aksijalnih koji mogu raditi kao posebne jedinice ili pak u sprezi.

Princip rada mokrih recirkulacionih tornjeva sa prinudnom promajom se sastoji u razmjeni toplote rashladne vode sa atmosferskim vazduhom. Zavisno od smjera kretanja vazduha i rashladne vode definišu se tri vrste navedenih rashladnih tornjeva, a to su suprotnosmjerni sa podpritiskom, unakrsni i suprotnosmjerni sa nadpritiskom. Generalno, svaki od navedenih tornjeva sastoji se od sljedećih elemenata: dovoda za zagrijanu vodu, rezervoara za ohlađenu vodu, dovoda dodatne vode, ispune, žaluzina, sistema za distribuciju vode sa mlaznicama, eliminatora kapljica kao i ventilatorske jedinice pogonjene najčešće elektromotorom. Sprega elektromotora sa ventilatorom se čest ostvaruje pomoću klinastog remena ili u kombinaciji vratila i prenosnog mehanizma u vidu reduktora.

Ventilator predstavlja neizostavan element rashladnih tornjeva sa prinudnom promajom. Ventilatori koji se primjenjuju u ovim sistemima mogu biti aksijalni ili centrifugalni. Dosta veću primjenu imaju aksijalni ventilatori koji često rade i u paralelnoj sprezi kako bi ostvarili proračunate uslove rada. Rjeđa primjena je svakako vezana za centrifugalne ventilatore koji se ugrađuju uglavnom u sistemima sa podpritiskom tj. kada se ugrađuju pri dnu rashladnog tornja.

Aksijalni ventilatori imaju širok dijapazon primjene u industriji. Neki od primjera su hlađenje električnih uređaja, uloga u ventilacijskim sistemima kao i primjena u rashladnoj tehnici. Glavni uslovi koji se stavljaju pred konstruktora ventilatora jesu optimalan rad sa stanovišta iskoristivosti, buke i čvrstoće. Kako bi se dobile prave informacije o kvalitetu i specifikacijama jednog ventilatora neophodno je izvršiti ispitivanje istog. Metode za ispitivanje se uglavnom baziraju na eksperimentalnoj analizi, međutim nerijetka je primjena i računarskih softvera kojima je moguće simulirati realne uslove.

2 UOPŠTENO O AKSIJALNIM VENTILATORIMA

Aksijalni ventilator je tip ventilatora kod koga je glavno strujanje vazduha paralelno sa osom rotacije lopatica. Kao posljedica takvog strujanja javlja se i izvjesni prostor u kome će strujanje biti uniformno. Inače, vazduh kod ovog tipa ventilatora dolazi do lopatica u aksijalnom smjeru, a izlazi sa rotacijskom komponentom brzine koja je posljedica rotacije lopatica. Na osnovu izvjesnih pojednostavljenja i pretpostavki, tj. ukoliko se pretpostavi da je protok konstantan i nekompresibilan, aksijalna komponenta brzina na ulazu i izlazu je jednaka, a apsolutna brzina vazduha na izlazu je veća od ulazne apsolutne brzine.

Aksijalni ventilator se sastoji od statora, rotora, konusnog nastavka glavčine i difuzora (slika 1.). Osnovni dio je rotor, dok ostali dijelovi služe za poboljšanje korisnosti pa se katkad, radi jednostavnije konstrukcije, mogu i izostaviti. Lopatice rotora oblikovane su tako da sve čestice fluida imaju isti prirast energije. [2]

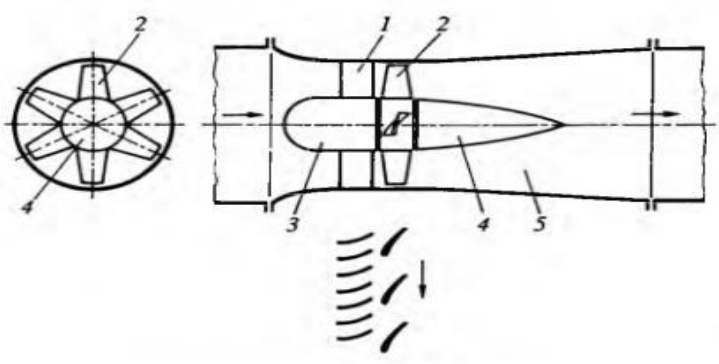

Slika 1. *Aksijalni ventilator. 1. stator 2. rotor 3. glavčina 4. konusni nastavak glavčine 5. difuzor [2]*

2.1 Trouglovi brzina

U svakoj tački radnog prostora definisane su tri brzine: brzina rotacije kola $\vec{u}$, apsolutna brzina fluidne čestice $\vec{c}$ i relativna brzina $\vec{w}$. Veza između ove tri brzine data je sljedećom relacijom:

$$\vec{c} = \vec{u} + \vec{w}$$

Apsolutna brzina predstavlja brzinu u odnosu na neki nepokretni koordinatni sistem npr. vezan za oklop mašine, dok relativna brzina te iste fluidne čestice predstavlja brzinu u odnosu na kolo. Na slici 2. predstavljen je trougao brzina za opšti slučaj:

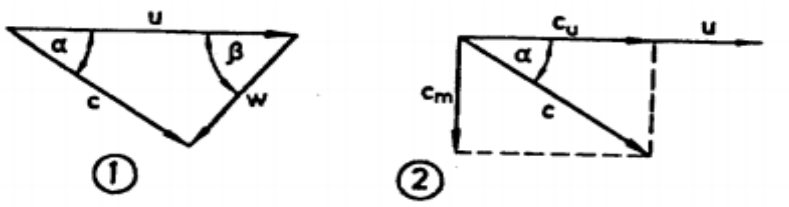

Slika 2. *Trougao brzina [3]*

Sa slike se jasno vidi da projekcija brzine $\vec{c}$ na pravac $\vec{u}$ daje kružnu komponentu brzine predstavljenu kao $\overrightarrow{c_u}$, dok vertikalna komponenta navedene brzine predstavlja meridijansku brzinu te se označava kao $\overrightarrow{c_m}$.

Konačno, trouglovi brzina za aksijalni ventilator dati su na slici 3. sa koje je moguće jasnije objasniti određene komponente:

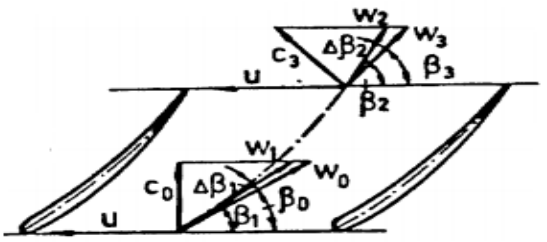

Slika 3. *Trouglovi brzina za aksijalni ventilator [3]*

Ulazni trougao čine brzine u, c_0 i w_0 sa uglovima α_0 i β_0, a izlazne u, c_3 i w_3 sa uglovima α_3 i β_3. Uglovi β_1 i β_2 se razlikuju od uglova β_0 i β_3 a uzrok tome je zanošenje struje na ulazu i izlazu [3].

2.2 Stepen reakcije

Pretvaranje kinetičke energije u potencijalnu, uvijek je praćeno velikim iznosima gubitaka koji se nastoje redukovati na što manju vrijednost. Upravo iz toga razloga uveden je, i definisan, pojam stepena reakcije odnosno reaktivnost (predstavlja odnos statičkog i ukupnog pritiska). Dakle, težnja za što većim stepenom efikasnosti uslovljena je direktno većim stepenom reakcije. Specijalno, za aksijalne ventilatore stepen reakcije je prilično visok i može da iznosi oko jedan pa je i logičan zaključak da su aksijalni ventilatori prilično efikasne mašine sa toga stanovišta. [3]

3 REGULACIJA RADA VENTILATORA

Kako bi se uspostavio odgovarajući protok kroz ventilator u toku eksploatacionih uslova neophodno je vršiti njegovo regulisanje. U opštem sličaju može se govoriti o dva pristupa regulisanja rada ventilatora i to:

- regulisanje promjenom karakteristika cijevnog sistema i
- regulisanje promjnom karakteristika samog ventilatora

Regulisanje uticajem na karakteristike cjevovoda u suštini predstavlja povremeno djelovanje dok je pogon zastuavljen, a smisao se ogleda u dodavanju i oduzimanju cijevnih elemenata (npr. prigušnik) sa ciljem promjene koeficijenata gubitaka čime se u konačnom, utiče i na sam rad ventilatora. Ovakav tip regulacije uglavnom je vezan za ventilacijske sisteme te se neće uzimati u daljnje razmatranje.

Mijenjanje radne krive samog ventilatora se može ostvariti na više načina. Neki od najpodesnijih svakako jesu postavljanjem usmjerenih lopatica, promjenom geometrije kola, mijenjanjem širine protočnog presjeka, produžavanjem ili skraćivanjem lopatica kao i njihovim zakretanjem i sl. Jedan od najpopularnijih načina regulacije jeste mijenjanjem brzine obrtanja. Sve prethodno nabrojane metode regulacije mogu se smatrati kontinualnim i moguće ih je izvoditi u toku rada ventilatora tj. nije potrebno zaustavljati pogon. [3], [4]

U tekstu koji slijedi objašnjen je pojam regulacije rada ventilatora pomoću promjene geometrije kola i brzine obrtanja.

3.1 Promjena geometrije kola

Promjena geometrije kola se ostvaruje na više načina, a neki od njih su zakretanje lopatica, smanjivanje dužine lopatica, promjena širine kola, zakretanje

zakrilaca lopatica kola i slično.

Zakretanje lopatica kola. Ovaj metod se primjenjuje kod srednjih i velikih aksijalnih ventilatora sa pokretnim lopaticama. Prilikom zakretanja lopatica dolazi do promjene karakteristika mašine, a time i do promjene režima rada. Primjena ovoga metoda regulacije je jako efikasna i omogućuje kontinualnu promjenu radne tačke, ali je izvođenje sinhronog zakretanja lopatica radnog kola u toku njegovog obrtanja oko ose jako složeno i neisplativo sa ekonomskog aspekta. Razlog tome je potreba za šupljim vratilom i većim brojem manjih pokretnih dijelova. Stepen korisnosti, pri ovom načinu regulacije, se mijenja jako malo pa je, na osnovu toga, ova regulacija poželjnija nego npr. regulacija pomoću prigušenja. [5]

Promjena dužine lopatica i zakrilca. Kod osnih ventilatora zbog energetske neefikasnosti se ne primjenjuju zakrilca. Promjena dužine lopatica odnosi se na skraćivanje i produživanje lopatica, čime se trajno mijenja radna kriva. Ovaj vid regulacije predstavlja efikasnu i lako izvodljivu metodu kod lopatica od lima. Naime, dodavanjem ravnog lima, lopatica se produžuje čime se prečnik kola povećava. Na ovaj način raste propusna moć i napor kola uz minimalan pad stepena korisnosti. Ukoliko je potrebno smanjiti performanse kola, lopatice kola se podsijecaju čime se i poluprečnik kola redukuje. [3]

Isključivanje nekih međulopatičnih prostora. Jedan od načina privremenog ili trajnog mijenjanja karatkteristika ventilatora jeste sprečavanje tečenja kroz neke od međulopatičnih prostora. Navedeno se postiže prekrivanjem ulaznih ili izlaznih presjeka. Optimalan rad ventilatora bi se postigao kada bi se ulaz i izlaz simultano i simetrično zatvorili. Prilikom takvih uslova, izbjeglo bi se stvaranje vrtloga i neželjenih vibracija. Slika 4. predstavlja primjer potpunog i djelimičnog zatvaranja međulopatičnih prostora.

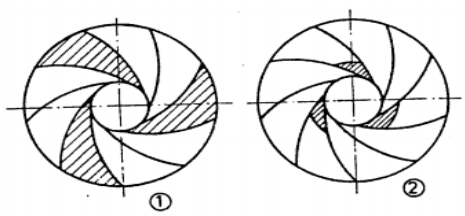

Slika 4. *Potpuno (1) i djelimično (2) prekrivanje međulopatičnih prostora [3]*

3.2 Promjena brzine obrtanja

Regulacija ventilatora promjenom brzine obrtanja predstavlja najekonomičniji vid mijenjanja radnog režima sa energetskog aspekta. Glavni nedostatak ove regulacije jeste što je investiciono skuplja i tehnološki složenija u odnosu na ostale. Ovakav tip regulacije se preporučuje kod ventilatora većih gabarita i snaga i to onda kada je uštedom energije moguće kompenzovati povećane investicione troškove. Za regulisanje rada ventilatora promjenom brzine obrtanja najpovoljnija je kontinualna promjena u relativno uskom rasponu. Za podešavanja radnih područja, promjene obrtanja su skokovite i izvode se najčešće, sa dva ili tri stepena prenosa. Dakle, regulacija promjenom brzine obrtanja se, u opštem slučaju, može izvoditi:

- kontinualno
- skokovito

4 TORNJEVI SA PRINUDNOM PROMAJOM U RECIRKULACIONIM SISTEMIMA

Recirkulacioni sistemi se koriste u mjestima gdje je primjena rashladne vode ograničena. Princip rada je prilično jednostavan, smisao se ogleda u recirkulaciji odnosno stalnoj upotrebi jedne te iste rashladne vode. Recirkulacioni sistemi imaju relativno male gubitke vode i kao takvi koriste prilično male količine vode za kompenzovanje gubitaka. Sve recirkulacione rashladne sisteme moguće je svrstati u dvije opšte grupe i to u:

- zatvorene i
- otvorene

4.1 Tornjevi sa prinudnom promajom

Vlažni rashladni tornjevi sa prinudnom promajom, u pogledu smjera strujanja vazduha, se klasifikuju u tri opšte grupe. Ovakvi tornjevi pogodni su za promjenjive režime rada, a nepovoljni su za opterećenja pri većim snagama. Snaga za pogon ventilatora je relativno mala u odnosu na toplotni protok ali za veća postrojenja je ipak osjetno velika, tako da se u tom slučaju pribjegava upotrebi rashladnih tornjeva sa prirodnom promajom. Neke od osnovnih prednosti ovakvih tornjava jesu da im orijentacija ne zavisi od pravca vjetra i da je visina dizanja pumpe prilično niska. Svakako, jedan od nedostataka jesu mogući kvarovi mašinske opreme čime se performanse tornja jako redukuju.

Kako se u vlažnim rashladnim tornjevima voda hladi direktnim kontaktom sa vazduhom jasno je da intenzitet hlađenja zavisi od više faktora: raspršivanja vode, ravnomjernosti protoka vode po poprečnom presjeku tornja, termičkih karakteristika i visine ispune, gabaritnih dimenzija tornja ali i od ravnomjernosti strujanja vazduha. Osnovni zadatak pri projektovanju vlažnih ventilatorskih rashladnih tornjeva je postizanje ravnomjernog toka vode i strujanja vazduha uz maksimalno povećanje površine između vode i vazduha. Današnje izvedbe navedenih konstrukcija se odlikuju većom efikasnošću hlađenja po jedinici zapremine. [6]

4.1.1 Suprotnosmjerni rashladni tornjevi sa nadpritisnim strujanjem

Glavna razlika ovog rashladnog tornja u odnosu na klasični tip suprotnosmjernog rashladnog tornja jeste u poziciji na kojoj je smješten ventilator. U ovom slučaju ventilator (najčešće radijalni) je smješten pri dnu tornja gdje usisava, a zatim potiskuje vazduh kroz ispunu tornja. Ovakvi tornjevi primjenu nalaze uglavnom kod manjih i srednje velikih postrojenja. Jedan od razloga za ugradnju ventilatora na navedeno mjesto jeste smanjene vibracija. Zbog toga što ventilator potiskuje hladniji ulazni vazduh on ubacuje veću količinu vazduha po jedinici zapremine nego u slučaju potpritisnog strujanja. Glavni nedostaci ovog sistema ogledaju se u mogućnosti hvatanja leda na ventilatoru i blokiranju ulaznog presjeka za vazduh. Neki tipovi mogu biti skloni da recirkulišu korišćeni vazduh što se izbjegava povećavanjem izlazne brzine vazduha. Tipičan primjer rashladnog tornja sa prinudnim nadpritisnim strujanjem vazduha prikazan je na slici 5. [7]

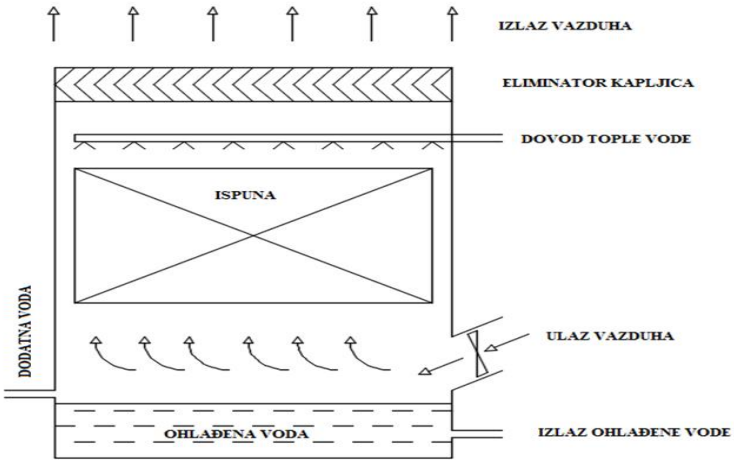

Slika 5. *Rashladni toranj sa prinudnom cirkulacijom vazduha (nadpritisni tip)*

4.1.2 Suprotnosmjerni rashladni tornjevi sa podpritisnim strujanjem

Kod ovakve izvedbe tornja (slika 6.) aksijalni ventilator je smješten na vrhu tornja. Princip rada ogleda se u sljedećem, ventilator uvlači vazduh pri dnu tornja koji dalje struji kroz ispunu ka vrhu. Voda se preko sistema distribucije pomoću mlaznica raspršuje i vertikalno sliva niz ispunu tornja pa se na ovaj način ostvaruje protivsmjerno strujanje.

Ovakvi sistemi dozvoljavaju ugradnju većih aksijalnih ventilatora, što omogućuje nizak stepen buke usljed većih brzina. Visoke ulazne brzine vazduha mogu uvlačiti prljavštinu što se rješava ugradnjom filterskih sekcija. Za razliku od nadpritisnih tornjeva, ovdje je šansa za pojavu recirkulacije jako mala, međutim ovakvi tornjevi su skloniji vibracijama zbog pozicije ventilatora. [7] Prethodno opisan sistem daje najbolje performanse pa se iz toga razloga često primjenjuje u praksi.

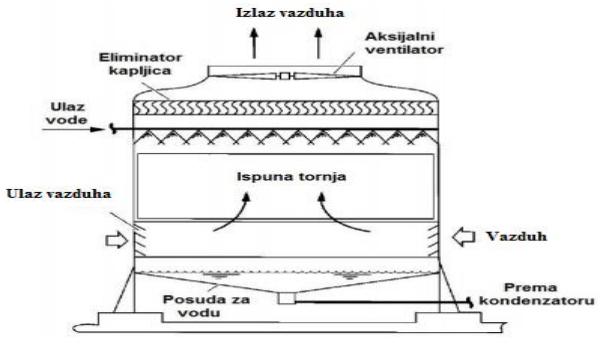

Slika 6. *Suprotnosmjerni rashladni toranj sa prinudnom cirkulacijom vazduha [7]*

4.1.3 Suprotnosmjerni rashladni tornjevi sa podpritisnim strujanjem

Kod tornjeva sa unakrsnim strujanjem (slika 7.) vazduh poprečno struji u odnosu na vodu. Vazduh ulazi u toranj kroz bočne žaluzine i horizontalno struji kroz ispunu i eliminator kapi. Vazduh se zatim usmjerava prema vrhu tornja. Kao i kod

ostalih sistema voda se raspršuje pomoću mlaznica i pada preko ispune čime se izaziva unakrsno strujanje. Usljed unakrsnog strujanja visina toranja može biti znatno niža. Ukoliko je ovakav sistem smješten u zatvorenom prostoru postoji opasnost od pojave recirkulacije vazduha. [7]

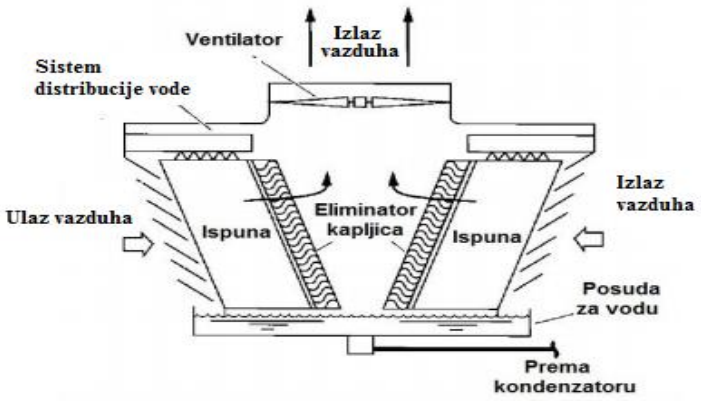

Slika 7. *Rashladni toranj sa unakrsnim strujanjem [7]*

5 ZAKLJUČAK

Kod recirkulacionih rashladnih sistema jedna te ista količina vode obavlja veći broj kružnih tokova u sistemu. Voda koja se koristi u recirkulacionim sistemima mora imati takav sastav koji će osigurati normalan rad u svim radnim uslovima. Izvjesna količina rashladne recirkulacione vode se gubi u procesu, tako da je neophodno nadomjestiti gubitke dodavanjem dodatne vode, koja mora biti prethodno obrađena i mora imati nominalan sastav za upotrebu u navedenom sistemu hlađenja. Prednost ovakvih sistema u odnosu na klasične protočne jeste u racionalizaciji potrošnje vode, zbog čega se mogu primjenjivati na lokacijama oskudnim sa vodom, kao i bolji tretman prema vodi sa aspekta zaštite životne sredine.

Rashladni tornjevi sa vještačkom (prinudnom) promajom se primjenjuju kod recirkulacionih sistema. Prinudnu promaju obezbjeđuje, najčešće aksijalni ventilator velikih dimenzija. Glavni nedostatak ugradnje ventilatora je potreba za napajanjem električnom energijom, koje obično iznosi oko 3-4 kW po proizvedenom MW električne energije. Osnovna prednost rashladnih tornjeva sa prinudnom promajom ogleda se u mogućnosti postizanja nižih temperatura vode u odnosu na tornjeve sa prirodnom promajom, posebno za vrijeme vrućih sušnih dana. Tornjevi sa prinudnom promajom pružaju bolje regulisanje radnih performansi za razne vremenske uslove.

Sastavni dio recirkulacionih rashladnih sistema sa prinudnom promajom je ventilator. Dva najzastupljenija tipa ventilatora, koja se ugrađuju, su aksijalni i centrifugalni. Centrifugalni ventilatori se primjenjuju u tornjevima sa nadpritisnim strujanjem, dok aksijalni ventilatori imaju širu primjenu. Ventilatori najčešće imaju pogon preko elektromotora i postavljaju se iznad uređaja za raspodjelu vode i ispune tornja. Ispod ventilatora se nalaze i eliminatori kapljica koji odstranjuju kapljice povučene vazdušnom strujom. Rashladni tornjevi sa ventilatorima su dosta niži i investiciono jeftiniji u odnosu na tornjeve sa prirodnim strujanjem vazduha. U odnosu na tornjeve sa prirodnom promajom, kod ovih tornjeva je jednostavnija regulacija protoka vazduha i temperature ohlađene vode. Iz razloga što je moguće ostavriti konstantan protok u različitim vremenskim uslovima, uticaj relativne vlažnosti je

neznatan na karakteristike tornja. Jedan od nedostataka tornjeva sa prinudnom promajom je pojava čestih mehaničkih kvarova što utiče na njihovu pouzdanost. Neki od problema koji se mogu javiti u navedenim tornjevima jesu mogućnost recirkulacije vazduha kao i gubici vode usljed isparavanja, što pri nižim temperaturama može izazvati stvaranje leda na dijelovima opreme tornja i samom ventilatoru.

LITERATURA

[1] EkoEngineering, Rashladni tornjevi: Recirkulacioni sistemi hlađenja.
[2] Pečornik M., (1997). Ventilator. Tehnička enciklopedija, sv. 13, str. 454-461.
[3] Krsmanović Lj., (2000), Turbomašine: ventilatori, Mašinski fakultet, Beograd.
[4] Golubović D.,(2020), Pumpe, ventilatori i kompresori- predavanja na osnovnim studijama Mašinskog fakulteta, Istočno Sarajevo.
[5] Delalić S., (2008), Pumpe, ventilatori i kompresori: skripta, Univerzitet u Tuzli, Mašinski fakultet, Tuzla.
[6] Sensorex, https://sensorex.com/blog/2018/02/21/how-cooling-towers-work, (Pristupljeno 15.9.2021)
[7] Wikipedia https://hr.wikipedia.org/wiki/Rashladni_toranj, (Pristupljeno 15.9.2021)

COMETa 2022
6th INTERNATIONAL SCIENTIFIC CONFERENCE
17th - 19th November 2022
Jahorina, B&H, Republic of Srpska
University of East Sarajevo
Faculty of Mechanical Engineering
Conference on Mechanical Engineering Technologies and Applications

OPTIMALNI IZBOR ODVAJAČA KONDENZATA ZA INDUSTRIJSKE SUŠARE

Srđan Suknović[1], Peko Ninković[2], Anđela Suknović[3]

Rezime: Bitan element sigurnog i ekonomičnog rada parnog postrojenja je oprema za odvajanje kondenzata. Za pravilno funkcionisanje sistema važan je odabir odvajača kondenzata prema tipu i uslovima rada procesne opreme. Izbor se bazira na proračunu radnih parametara odvajača kondenzata, potrebnog diferencijalnog pritiska i protoka kondenzata, radnim uslovima i parametrima procesa kao što su maksimalni i radni pritisak pare i temperature. Postoje tri osnovna tipa odvajača kondenzata u koje spadaju sve varijacije. Sve tri su klasifikovane prema međunarodnom standardu ISO6704:1982. Naučni rad obuhvata izbor odvajača kondenzata prema iskustvenim preporukama vodećih kompanija u oblasti procesne industrije.

Ključne riječi: odvajači kondenzata, procesna industrija, razmjenjivači toplote, termodinamika.

OPTIMAL SELECTION OF STEAM TRAPS FOR INDUSTRIAL DRYERS

Abstract: An important element of safe and economical operation of the steam plant is the equipment for steam trap. For the proper functioning of the system, it is important to select the steam trap according to the type and operating conditions of the process equipment. The selection is based on the calculation of the operating parameters of the steam trap, the required differential pressure and flow, operating conditions and process parameters such as maximum and operating steam pressure and temperature. There are three basic types of steam trap that include all variations. All of that are classified according to the international standard ISO 6704: 1982. The paper includes the selection of steam trap according to the experienced recommendations of leading companies in the field of process industry.

Key words: heat exchanger, process industry, steam traps, thermodynamics.

1 Dipl. inž. energetike, Srđan Suknović, Mašinski fakultet Istočno Sarajevo, BiH, suknovic.srdjan@gmail.com (CA)
2 Dipl. inž. energetike, Peko Ninković, Mašinski fakultet Istočno Sarajevo, BiH, pninka093@gmail.com
3 Anđela Suknović, Mašinski fakultet Istočno Sarajevo, BiH, suknovic.a25@gmail.com

1 UVOD

Odvod kondenzata je bitan dio svakog parnog sistema. To je važna veza između dobrog upravljanja parom i kondenzatom, zadržavajući paru unutar procesa radi maksimalnog iskorištenja toplote, ali pritom oslobađajući kondenzat i nekondenzovane gasove u odgovarajuće vrijeme. Imperativ je izbor odgovarajuće opreme za obavljanje funkcije pod traženim uslovima rada. Ovo može uključivati varijacije radnog pritiska, toplotnog opterećenja ili pritiska kondenzata. Odvajači kondenzata moraju biti otporni na koroziju i prljavštinu. Ispravan izbor odvajača kondenzata je važan za efikasnost sistema. Dimenzija odvajača je uslovljena parametrima procesa i zahtijevima sisitema, kao što su: maksimalni i radni pritisci, temperatura i protok pare i kondenzata. [1] [2]

2 TIPOVI ODVAJAČA KONDENZATA

Prema međunarodnom standardu ISO 6704:1982 postoje tri osnovna tipa odvajača kondenzata [2]:

- termostatski (upravlja se promjenama temperature fluida);
- mehanički (koji se pokreće promjenom gustine fluida);
- termodinamički (upravljaju se promjenama u dinamici fluida).

Ova podjela obuhvata i odvajače kondenzata sa fiksnim otvorom, koji se ne mogu jasno definisati kao automatski uređaji. Razlog je propuštanje određene količine kondenzata kroz fiksni prečnik otvora. Navedeno se temelji na činjenicu da se vruć kondenzat, oslobođen pod dinamičkim pritiskom, propusti kroz otvore. [2]

3 PREPORUČENE INSTALACIJE ZA ODVAJAČE KONDENZATA

Pri izboru odvajača kondezata mora se obratiti pažnja na sljedeće [2]:

- izbor odgovarajućeg tip odvajača, jer pogrešan može izazvati loš rad aparata, pa i potpuni prekid rada;
- Dimenzionisanje izabranog tipa odvajača kondenzata, odnosno u zavisnosti od potrebnog kapaciteta bira se odgovarajući nazivni otvor. Podimenzionisan odvajač neće ispustiti dovoljno kondenzata iz aparata i tako će raditi sa smanjenom snagom, dok predimenzionisan odvajač predstavlja nepotreban trošak za kupovinu opreme.

U skladu sa šemama (Slika 1), mogu se definisati opšte napomene za projektovanje instalacije i dimenzionisanje odvajača kondenzata za potrošače pare.

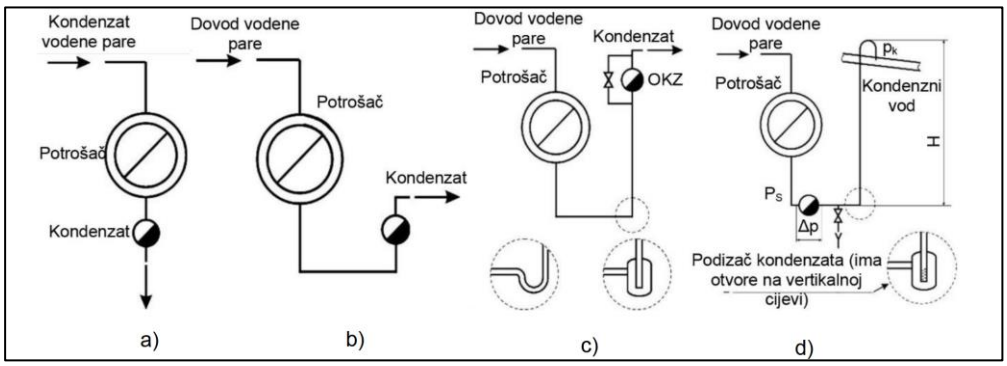

Slika 1. *Moguće šeme za povezivanja potrošača sa odvajačima kondenzata [1] [2]*

Najpovoljnije mjesto za pozicioniranje odvajača je ispod izmjenjivača toplote, tako da kondenzat gravitaciono može isticati (Slika 1,a). U praksi je teško ovo izvesti, zbog same konstukcije aparata i pozicije unutar postrojenja. Kompletna instalacija za odvajanje kondenzata mora da bude lako dostupna zbog održavanja i kontrole ispravnosti. U praksi se pokazalo da cjevovod između odvajača i aparata u "U" obliku (Slika 1,b) treba izbjegavati jer je to najnepovoljniji položaj odvajača i nalazi se ispod aparata. Za razliku od ovog slučaja, prikazana je povoljnija pozicija odvajača (Slika 1,c). Iznad aparata i na cjevovodu je formiran sifon. Za cijevi manjeg prečnika, sifon se može formirati jednostavnim savijanjem cijevi. Kod većih prečnika, potrebno je ugraditi veću cijev koja je za barem dvije dimenzije većeg promjera. Takođe, prikazan je obilazni vod oko odvajača koji služi za odzračivanje opreme prilikom početka rada. Kod nekih tipova odvajača potrebno je da se propušta kondenzat do 1% njegovog kapaciteta. Slika 1(d) prikazuje podizanje kondenzata na kondenzni vod, relativne visine H u odnosu na odvajač. Kondenzni vodovi se postavljaju na veće visine zbog potencijalne energije kondenzata. Tako se olakšava montaža i održavanje cjevovoda, te nema potrebe za ugradnjom mehaničkih pumpi (ako sistem to dozvoljava). Uglavnom, polaganje cjevovoda kondenzata se izvodi po podu pogona, odnosno u kanalima gdje su nepristupačni. Obično je izolacija nakvašena i tako dolazi do pojave korozije. Zbog potrebe izrade kanala za trasiranje cjevovoda povećava se investicija. Na vertikalnim dionicama preporučuje se ugradnja podizača kondenzata. Podizač kondenzata je običan proširen dio cjevovoda u kome se nalazi početak vertikalnog dijela dionice (Slika1,d). Početak dionice treba da bude perforiran sa otvorima ne većim od 3mm. Pored podizača kondenzata, kada je kondenzni vod iznad nivoa odvajača, povoljno je da se iza odvajača postave nepovratni ventili kako bi bilo sprečeno povratno strujanje iz kondenznog voda u aparat. Nepovratni ventili se obavezno primjenjuju ako postoji regulacija temperature na strani pare [1] [2].

Slika 2(a) prikazuje primjer drenaže više potrošača sa jednim zajedničkim odvajačem. Potrošač koji se nalazi najdalje od odvajača ima najlošiju drenažu. Ovaj potrošač može biti potopljen kondenzatom. Na svaki cjevovod poslije potrošača obavezan je nepovratni ventil. Ako se primjenjuje ovakav princip, potreban je veliki promjer cjevovoda od potrošača do odvajača. Generalno, ovakve instalacije treba izbjegavati u praksi. Redna veza potrošača nije preporučljiva (Slika 2,b), jer dovodi do deficita količine pare za naredni potrošač. Prednosti ove šeme su u iskorištenju toplote kondenzata. [1] [2].

Optimalno izvedena drenaža sadrži zaseban odvajač kondenzata za svakog od njih (Slika 2,c). U tom slučaju je potrebno obratiti pažnju na dimenzionisanje zajedničkog kondenznog voda, da ne bi došlo do prigušenja i preplavljivanja potrošača (tzv. *stall* efekat). Postoji mogućnost zadržavanja kondenzata iznad zatvorenog zapornog ventila, nastalog zaostanjem pare u cjevovodu iznad (Slika 2,d). Na poziciji iznad zapornog ventila pogodno je postaviti odvajač kondezata. U praksi, ovaj dio se drenažira prije puštanja sistema u pogon, postepenim blagim otvaranjem zapornog ventila. Preporuka je da se kod elektromagnetih ili elektromotornih venitila primijeni odvajač kondezat, zbog mogućih naglih otvaranja istog. Kada su potrošači 1 i 2 na većoj udaljenosti u odnosu na potrošača 3 (Slika 2,e), kondenzat iz prva dva potrošača se hladi u cjevovodu do potrošača 3. Kao posljedica mješanja kondenzata različitih temperatura, javlja se hidraulički udar u cjevovodu. Redna veza odvajača kondenzata

(Slika 2,f) nije preporučljiva jer izaziva blokadu krajnjeg odvajača zbog nedovoljnog diferencijalnog pritiska. [1] [2]

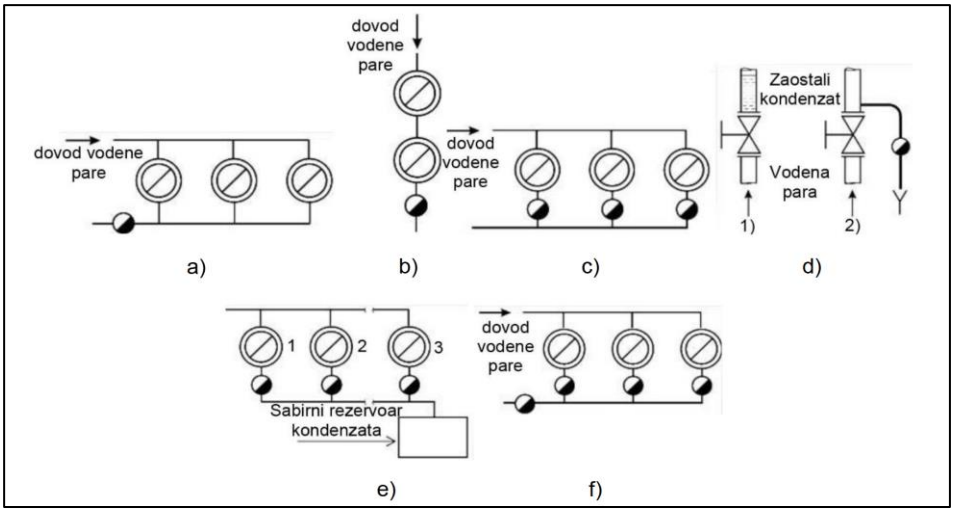

Slika 2. *Šema za paralelno i redno vezivanja potrošača [1] [2]*

4 PREPORUKA ZA PRIMJENU ODVAJAČA

Kompanija *Spirax Sarco* je svjetski lider u proizvodnji procesne opreme za parne sisteme. Domen njihovog poslovanja je podstakao kreiranje standarda u oblasti procesne industrije. S toga, naredna tabela (Tabela 1) definiše preporučene vrste odvajača kondenzata za različite aplikacije u procesnoj industriji.

Tabela 1. *Preporuke za izbor odvajača kondezata u industriji (A-najbolji izbor, B-prihvatljiva alternativa, 1-paralelna odzraka, 2-sa 1m cijevi za podhlađivanje, 4-potrebno predvidjeti mehaničku pumpu, 6-disk za uklanjanje vazduha) [2]*

Aplikacija	*Termostatski odvajač sa plovkom*	*Odvajač sa plovkom*	*Termodinamički odvajač*	*Termostatički odvajač sa mjehom*	*Bimetalni odvajač*	*Odvajač sa zvonom*
Parni kotlovi	*A*	*B*	*B1*	*B*		
Posude za kuhanje	*B*	*A*				
Industrijski autoklav	*A*					*B1*
Digestor	*A1*		*B1*			
Isparivači	*A1*	*B*				*B1*
Oprema za vulkanizaciju gume	*A*		*B1*			*B1*
Kaloriferi	*A4*					
Panelni grijači	*A*	*B1*	*B1*			*B1*
Cijevni izmjenjivači	*B*			*A*		*B1*

Toplovazdušni sušač	*A*		*B1*	*B1*		
Višeredni cijevni sušač	*A*		*B1*	*B1*		*B1*
Cilindri za sušenje	*B*	*A*				*B1*

5 OPTIMALNI IZBOR ODVAJAČA KONDENZATA

Industrijski sušač ima za cilj da smanji količinu vlažnosti skroba, koji se dalje, kao sirovina, primjenjuje u pripremi konditorskih proizvoda. Na uređaju je instaliran ventilator, koji prisilnom ventilacijom uvlači vazduh kroz razmjenjivače toplote preko filtera i dovodi u komoru za sušenje skroba. Uređaj se nalazi na udaljenosti 45m od kotlovnice. Pritisak pare iz kotlovnice na magistalnom parovodu je p_K=8bar (manometarski pritisak). Potrošač posjeduje dva razmjenjivača toplote (toplovazdušni grijači) snage Q_{R1}=Q_{R2}=218kW u nominalnom režimu rada, sa pritiskom suvozasićene pare p_r=4bar. Pritisak se reguliše preko regulacione stanice prije razmjenjivača. Povrat kondenzata u kotlovnicu se odvija energijom pritiska pare do p_{C1}=1,2bar i p_{C2}=1,4bar, u kondenznom vodu (uzima se u obzir visinska razlika H_1 i H_2, linijski i lokalni otpori cjevovoda Δp_{CE}, a krajnji pritisak na cjevovodu prije ulaska u posudu za kondenzat ne smije preći p_{PSK}=0,5bar). Smatra se da oba razmjenjivača toplote dobijaju jednaku količinu pare m_{R1}=m_{R2}. Toplovazdušni grijači imaju dva reda lamelnih izmjenjivača sa jednim krugom cirkulacije pare [1] [2] [4] [5].

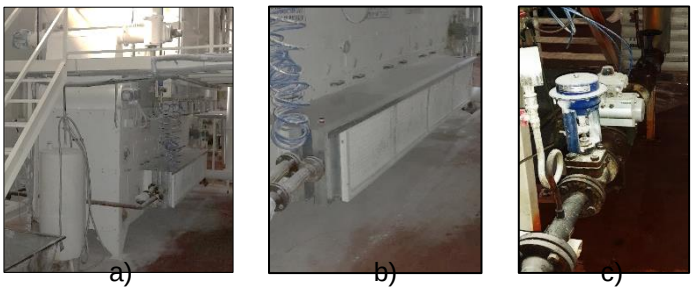

a) b) c)

Slika 3. *Oprema za sušenje skroba u industrijskom pogonu "Swislion" u Trebinju - a) sušač skroba, b) dvoredni toplovazdušni sušač sa filterima, c) stanica za regulaciju pritiska*

Za proračun odvajača kondenzata navedene opreme potrebno je definisati protok G_k i raspoloživi diferencijalni pritisak Δp_g sa šeme ispod (Slika 4).

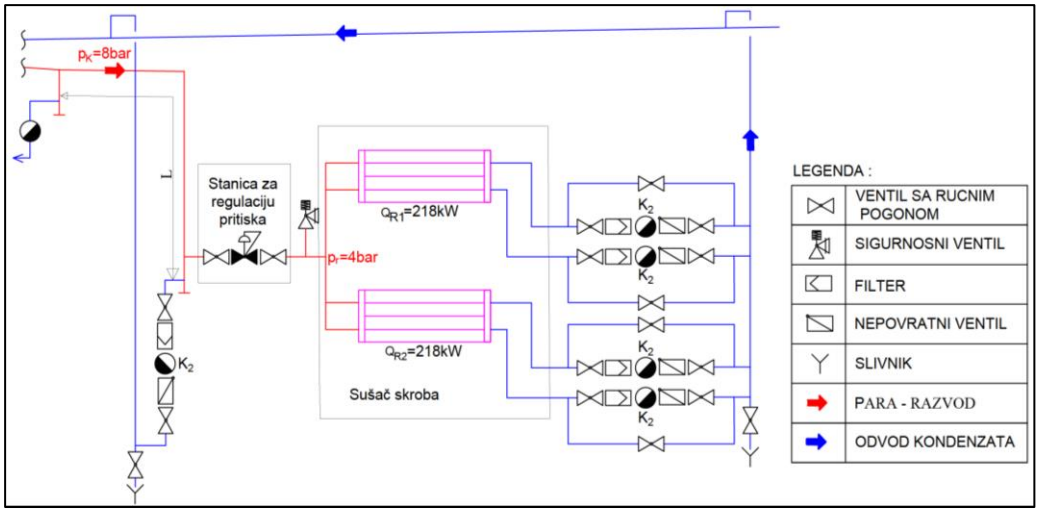

Slika 4. *Šema postrojenja (PI&D) za sušenje skroba [5]*

Prilikom proračuna potrebno je uzeti u obzir odvodnjavanje kondenzata za parovode pri startu iz hladnog stanja sistema i kondenzacije pare tokom rada odvajača kondenzata K_1. Količina nastalog kondenzata se u toku grijanja parovoda, kao najnepovoljni uslov, računa prema izrazu [1] [2]:

$$G_{K1} = \frac{Q_C}{r_1} = \frac{M \cdot L \cdot c \cdot (t_2 - t_1) \cdot A}{r_1} = \frac{17{,}5 \cdot 18{,}5 \cdot 0{,}425 \cdot (175{,}5 - 15) \cdot 1{,}4}{2029} \approx 15 \frac{\text{kg}}{\text{h}} \tag{1}$$

gdje su: Q_c [kJ] - potrebna toplota za grijanje parovoda; r_1 [kJ/kg] - latenta toplota kondenzacije p_k=8bar, M [kg/m] -masa jednog dužnog metra cjevovoda, L [m] - dužina parovoda koji pokriva odvajač kondenzata, c [kJ/kgK] - specifična toplota materijala cjevovoda, t_1 [°C] - temperatura okoline; t_2 [°C] - radna temepratura parovoda; A - koeficijent koji uzima u obzir uticaj izolacije (A=1,1 - za dobro izolovane; A = 1,4 za loše izolovane; A = 2,5÷3 za neizolovane cjevovode;).

Iskustveno se parovodi ove dužine trebaju grijati najmanje 10min (T=0,16h) i prema preporukama vodećih kompanija u ovoj oblasti, odvajač kondenzata treba da je od 2÷2,5 puta veći (usvojeno F_1=2,5). Uzimajući stepen sigurnosti u obzir, dobija se da je potrebni protok [1] [2]:

$$G_{K1S} = \frac{G_{K1}}{T} \cdot F_1 = \frac{15}{0{,}16} \cdot 2{,}5 \approx 234 \frac{\text{kg}}{\text{h}} \tag{2}$$

Raspoloživi diferencijalni pritisak se računa prema obrascu [1] [2]:

$$\Delta p_{K1} = p_K - p_C = 8 - 1{,}2 = 6{,}8\text{bar} \tag{3}$$

Na uređaju je potrebno predvidjeti po dva odvajača za toplovazdušne grijače. Razlog je broj redova razmjenjivača toplote. Svaki red razmjenjivača mora da ima minimalno po jedan odvajač kondenzata. Potreban protok za jedan odvajač kondenzata i jedan red grijača, se računa prema obrascu [1] [2]:

$$G_{K2S} = \frac{Q_{R1}}{2 \cdot r_2} \cdot F_2 = \frac{Q_{R2}}{2 \cdot r_2} \cdot F_2 = \frac{218}{2 \cdot 2017} \cdot 2 \approx 389 \frac{\text{kg}}{\text{h}} \quad (4)$$

Zbog starta iz hladnog stanja mjerodavno je da protok na odvajaču kondenzata bude za 1,5÷2 puta veći (usvojeno F_2=2).

Raspoloživi diferencijalni pritisak se računa prema obrascu [1] [2]:

$$\Delta p_{K2} = p_K - p_C = 4 - 1{,}4 = 2{,}6 \text{ bar} \quad (5)$$

Termostatski odvajač sa plovkom se smatra najboljom opcijom kao preporuka na osnovu Tabele 1. Već je navedeno da se priprema vazduha za sušenje skroba, odvija preko toplovazdušnih sušača. Prema dobijenim rezultatima bira se odvajač kondezata sa plovkom prema dijagramu na kojem je izbor odvajača kondenzata K_1 naznačen plavom bojom, a odvajač kondenzata K_2 crvenom bojom. Usvojen je sljedeći izbor [3]:

- za K1 (G_{K1S}=234kg/h, Δp_{K1}=6,8bar) => FT14-10 - 3/4“ … 1 komad,
- za K2 (G_{K2S}=389kg/h, Δp_{K1}=2,6bar) => FT14-4.5 - 1“ … 4 komada.

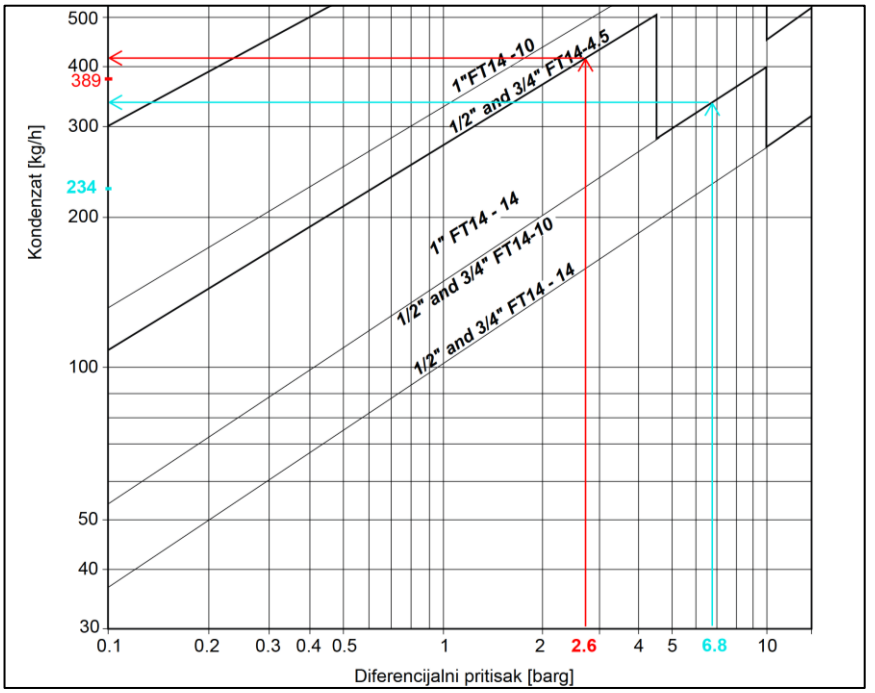

Slika 5. *Dijagram za izbor odvajača kondenzata proizvođača Spirax Sarco* [3]

Sa dijagrama se može primjetiti da, izabrani odvajači kondenzata, daju veći protok nego što je proračunom dobijen za nominalne uslove rada razmjenjivača toplote.

6 TERMOSTATSKI ODVAJAČ KONDENZATA SA PLOVKOM

Odvajač kondenazata s kugličnim plovkom radi tako što prepoznaje razliku u gustini između pare i kondenzata. U slučaju odvajača sa odzrakom (Slika 6,a), kondenzat koji dospijeva u odvajač uzrokovaće podizanje plovka kugle, podizanje ventila sa njegovog sjedišta i oslobađanje kondenzata [2].

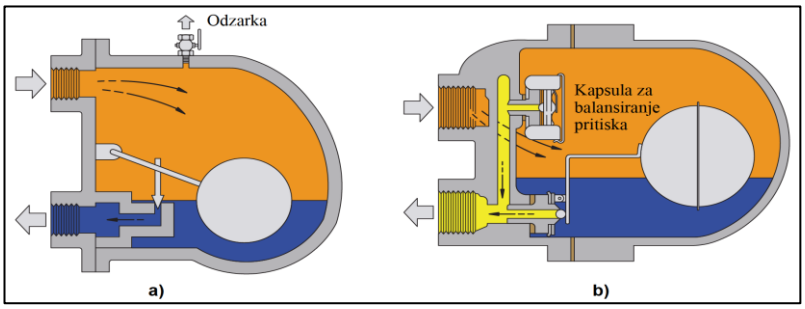

Slika 6. *Odvajači kondenzata sa plovkom* [2]

Kao što se može vidjeti, ventil je uvijek preplavljen i kroz njega neće prolaziti ni para ni vazduh, pa su odvajači ove vrste odzračivani pomoću ručno upravljane odzrake na vrhu tijela. Moderni odvajači ove vrste koriste termostatski ventilacioni otvor (Slika 5,b). Ovo omogućava prolazak početnog vazduha dok odvajač rukuje kondenzatom.

Automatski ventilacioni otvor koristi isti balansirani element kapsule pod pritiskom kao termostatski odvajač kondenzata, a nalazi se u prostoru za paru iznad nivoa kondenzata. Nakon ispuštanja početnog vazduha, ostaje zatvoren sve dok se vazduh ili drugi nekondenzirajući gasovi ne akumuliraju tokom normalnog rada i uzrokuju otvaranje smanjenjem temperature mješavine vazduha i pare. Termostatski ventilacioni otvor nudi dodatnu prednost značajnog povećanja kapaciteta kondenzata pri hladnom pokretanju [2].

Prednosti termostatskog odvajača kondenzata sa plovkom [2]:

- kontinualno ispušta kondenzat na temperaturi pare, što ga čini prvim izborom za primjene gdje je brzina prenosa toplote velika;
- jednako dobro podnosi teška ili lagana opterećenja kondenzata i na njega ne utiču velike i nagle fluktuacije pritiska ili protoka;
- sve dok je ugrađen automatski ventil za ventilaciju, odvajač može slobodno ispuštati vazduh;
- ima veliki kapacitet za svoju veličinu;
- verzije koje imaju ventil za otpuštanje pare su jedini tip odvajača koji je u potpunosti prikladan za upotrebu gdje može doći do blokiranja pare;
- otporan je na hidraulični udar.

Mane termostatskog odvajača kondenzata sa plovkom [2]:

- može se oštetiti jakim smrzavanjem, a tijelo treba biti dopunjeno malim dodatnim termostatskim odvajačem, ako se postavlja na izloženo mjesto;
- potrebne su različite unutrašnje komponente kako bi se omogućio rad u različitim rasponima pritiska.

7 ZAKLJUČAK

U prošlosti je termostatski ventil sa odzrakom bio slaba tačka ako je u sistemu bio prisutan hidraulički udar. Prije izbora odvajača kondenzata, potrebno je razmotriti potrebe procesa. Ovo će presudno djelovati na izbor vrste potrebnog odvajača kondenzata. Način na koji je proces povezan sa sistemom za paru i kondenzat može uticati na odabir istog. Kod odvajača sa plovkom bi moglo doći do oštećenja ako je hidraulični udar bio intenzivan. Međutim, u modernim odvajačima kondenzata ovog tipa, otvor za vazduh je kompaktna, vrlo robusna kapsula od nerđajućeg čelika. Moderne tehnike zavarivanja, koje se koriste na tijelu plovka, čine odvajač kompaktnim i pouzdanim u situacijama hidrauličkog udara. Takođe, najpouzdaniji su jer ispuštaju kondenzat bez obzira na promjenu pritiska.

LITERATURA

[1] Đorđević, R. (2014). “Projektovanje i proračun kondenznih instalacija“, “Procesna tehnika“, SMEITS Beograd.

[2] „The steam and condensate loop book“, Spirax Sarco, 2011, ISBN-10:0955069157.

[3] ***prospektna dokumentacija proizvođača odvajača kondenzata.

[4] Bogner M. „Projektovanje termotehničkih i procesnih sistema“, Eta, Beograd, 2007.

[5] Glavni mašinski projekat “Swislion” a.d. Trebinje, Plenum d.o.o. Subotica 2015.

ISBN 978-99976-947-6-8